Tianfeng Wan

The Tectonics of China

Data, Maps and Evolution

高等教育出版社
HIGHER EDUCATION PRESS

Springer

Tianfeng Wan

The Tectonics of China

Data, Maps and Evolution

Tianfeng Wan

The Tectonics of China

Data, Maps and Evolution

With 156 figures, 52 of them in color

高等教育出版社
HIGHER EDUCATION PRESS

Springer

Author
Prof. Tianfeng Wan
School of Earth Sciences & Resources
China University of Geosciences (Beijing)
Beijing 100083, China

ISBN 978-7-040-29534-4

Higher Education Press, Beijing

ISBN 978-3-642-11866-1 e-ISBN 978-3-642-11868-5

Springer Heidelberg Dordrecht London New York

Library of Congress Control Number: 2009943830

Cover design: Frido Steinen-Broo, EStudio Calamar, Spain

Printed on acid-free paper

Springer is part of Springer Science+Business Media (www.springer.com)

Preface

The theory of plate tectonics was introduced to China in the early 1970s. During the last thirty years, both Chinese and foreign geoscientists have undertaken many studies which contributed to our understanding of the tectonics of the Chinese continent, by systematically analysing and summarising considerable amount of data accumulated by regional geological surveys, and by improvements in the methods of research. These studies concerned not only the distribution and geometry of tectono-stratigraphic units and their deformation, but also the kinematics, dynamics and causes of rock deformation and movement of the lithospheric plates. As a result of these studies, many new and surprising phenomena have been discovered, and many new concepts have also been developed. Research has progressed from purely qualitative assessments of the amount of deformation, with the forces and rates of movement involved, to numerical calculations providing more quantitative estimates. Concepts have also evolved from the presumption that the Earth's crust is essentially stable to an appreciation that it is in constant movement. These aspects will be discussed in this book.

Tectonics is now an essential component of studies in Earth Sciences, providing the scientific basis for the discovery and exploitation of new mineral deposits and energy resources, the protection of the environment and the prediction and reduction of the effects of natural hazards. There is an urgent need to summarise systematically the abundant recently acquired tectonic data for scientific research, exploitation of mineral deposits and energy resources and the protection of the environment.

The factual and theoretical basis for studies in tectonics is provided by developments in: (1) Regional geological studies; (2) Tectonic models; (3) Methods of tectonic analysis; (4) Concepts of tectonic evolution.

Regional geological studies provide the foundation for the study of tectonics and have been conducted in China since 1930s. Regional geological maps at $1:1{,}000{,}000$ scale were compiled for the main part of Chinese continental area during 1930s–1940s and at $1:200{,}000$ scale from 1950s to 1980s (Published as provincial geological maps of China, 1984–1993). Based on these data, tectonic units have been identified, discussed and analysed carefully in each region (Huang JQ (1904–1995), also known as Huang TK, 1945, 1960, 1964, 1965, 1977, 1984, 1987; Group of Regional Geology, Beijing College of Geology, 1963; Ren JS et al., 1980, 1990, 1996, 2000; Yang and Yang, 1985; Cheng YQ, 1994; Che ZC et al., 2002). Local and regional tectonic characteristics are now well understood, but Chinese geoscientists recognized larger scale tectonic features and integrated the regional pictures into the tectonic development of the Chinese continent comparatively later than the geoscientists abroad as a whole. However, the use of fixed tectonic units does not provide an appropriate basis for the description of the tectonics of China, as during the course of geological evolution the effective tectonic units have changed throughout.

Tectonic models have provided important concepts for understanding tectonics. Li SG (1889–1971, also known as Lee JS, 1926, 1947, 1976) proposed a structural system based on a combination of the features of rock deformation and the different types of stress: $\in$ (epsilon) type; ξ (en echelon) type;

shear structural system; parallel structural system; longitudinal structural system; latitudinal structural system, etc. However, this classification will not be used in the following chapters.

Most recent monographs and textbooks on tectonics (e.g. Condie, 1982, 1997; Kearey and Vine, 1996; Van der Pluijm and Marshak, 1997; Oreskes, 2001; Erickson, 2001) used the same tectonic models: Convergent tectonics (subduction, collision, indentation and thrust belts); Divergent tectonics (oceanic ridges, rifts, extensional basins, detachments and metamorphic core complexes); Transform tectonics (transform and strike-slip faults); Inversion tectonics, acting on earlier tectonic systems. This theoretical system emphasizes the mechanisms and the geometry of each tectonic model, and is easy to be understood. However, this system does not place much emphasis on tectonic history. The system emphasizes the tectonic analysis of specific geological situations, but it is important to realize that geology or geosciences is essentially a historical science, and that many changes and many different tectonic events have affected the lithosphere for more than four billion years of Earth history.

It is really important for us to research the methods of tectonic analysis. However, only emphasizing the methods but never discussing the tectonic evolution in detail, as Ma WP (1992) did, has been proved ineffective.

Many monographs and papers emphasizing the historical aspects of the tectonics of China have been published by Huang JQ (1945, 1960, 1964, 1965, 1977, 1984, 1987), Li CY (1904–1988) (1982, 1984), Wang HZ (1982, 1985, 1990, 1994), Ren JS (1980, 1990, 2000) and Khain and Borhko (1996). These studies are concerned with "Historical Tectonics". On one hand, researchers engaged in historical tectonics pay more attention to stratigraphy and the characteristics of geological formations and their origins, and analyze their lithological and paleontological characteristics, their provenance, environments of formation and the origins of the sedimentary or igneous units, with emphasis on their historical evolution. On the other hand, tectonic modelers pay more attention to the transformation of rock bodies, i.e. rock deformation, structural geometry, kinematics and dynamics, with emphasis on the mechanisms of deformation. Although most researchers engaged in tectonics agree that both geological formation and transformation should be studied, and that historical and mechanical analyses should be combined, due to the differences in training, experience and the focus of their interests, these different approaches may produce different results. Zhang WY (1909–1984) et al. (1959, 1983) advocated that these approaches should be integrated in the study of the tectonics of China. The author considered that it is really important for us to follow these precepts in the present volume, though it is very difficult.

In this book, the author did his utmost to combine the studies of formation and transformation using the plate tectonic theory, together with historical and mechanical analyses. Abundant and recently acquired, geological, geochemical and geophysical research data are applied to describing and discussing the sequence of tectonic events which have affected the Chinese continental lithosphere from the Archean to the Recent. Until the present time, it is difficult to achieve this aim because of the scarcity of data on kinematics and dynamics.

In this volume, for understanding the tectonics of China, the author puts forward many new views: calculating the thickness of the continental crust of the Sino-Korean plate during the Archean and Paleoproterozoic; determining the periods during which the Supercontinent of Rodinia broke up and the continental blocks were amalgamated to form the Chinese continent; establishing the stages during the Neoproterozoic in which tillites were deposited on the Sino-Korean and Yangtze plates respectively; following the changes in the latitudinal and longitudinal distribution of the Chinese continental blocks during the Paleozoic. During the Late Paleozoic and Triassic, most of the continental blocks which constitute China collided and were amalgamated with the Eurasian Plate. Subsequently China continent was affected by intraplate deformation, with three periods of shortening in a near N-S orientation: Indosinian Period (260–200 Ma); Sichuanian Period (135–56 Ma); Himalayan Period (23–0.78 Ma); two periods of shortening with a near E-W orientation: Yanshanian Period (200–135 Ma); North Sinian Period (56–23 Ma). Since 0.78 Ma (Neotectonics Period), the state of stress among the plates which constitute the Chinese continent has been nearly in equilibrium.

In this volume, the characteristics of many collision zones in the Chinese continent are analysed in 3 dimensions and discussed in terms of the thickness of the crust and the lithosphere; a new hypothesis

is proposed for the "thinning" of the lithosphere beneath the eastern China continent, which is possibly induced by the counterclockwise rotation of the continental crust extending across onto oceanic mantle; the control of the environment by tectonics is recognized; the influence of intraplate extension during the Mesozoic-Cenozoic on periods of major mineralization in China is made understood; finally, hypotheses about the dynamic mechanisms that control global tectonics are evaluated.

This book was originally written by the author in Chinese and published by the Geological Publishing House in Beijing in 2004. After incorporating many useful comments, the book was translated into English, with a reduction of local terms and the removal of discussions which were not necessary to the foreign readers. Throughout, the emphasis has been placed on large scale features and the major tectonic events which have affected the Chinese continent. Some errors in the initial version have been corrected following the suggestions of experts in specified fields. For the sake of the foreign readers, the latitudes and longitudes of critical localities have been inserted. Original data are recorded in Appendices, and a large number of references are cited, particularly from the Chinese literature, to facilitate further research in Chinese tectonics.

Tianfeng Wan
Beijing October 2010

Acknowledgements

Academician Hongzhen Wang, an academic leader in the field of tectonics of China at China University of Geosciences, has encouraged me to write this book, and his scientific example influenced people's conception and realization of tectonics of China.

The publications and lectures by many leading authors provided information for this book, including Academicians Chongwen Yu, Xuchang Xiao, Tingdong Li, Qi Yang, Guoyu Ding, Yusheng Zhai, Benren Zhang, Zongjin Ma, Dalai Zhong, Jishun Ren, Guowei Zhang, Guangding Liu, and Jiwen Teng; Professors Peiren Zhuang, Jin Bai, Xiufu Qiao, Zhendong You, Benpei Liu, Fengxiang Lu, Chonghe Zhao, Xianglin Qian, Guoqi He, Wenpu Ma, Xiaohong Ge, Xianghua Meng, Ming Ge, Huahui Chen, Lei Zhao, Hongwen Ma, Hefu Liu, Weixiang Wang, Dongxu Li, Hualin Zeng, Yadong Zheng, Shanchi Peng, Dingyi Liang, Weiran Yang, Honglin Song, Tieying Guo, Lifang Ma, Zhengwen Wu, Hong Zhu, Zhihe Ren, Mingguo Zhai, Jinyi Li, Chongqi Wang, Yue Zhao, Yu Wang, Shaofeng Liu, Zhaohua Luo and Dr. Yang Wang. I would like to thank Prof. Kent C. Condie (University of New Mexico, USA), Jin Bai, Xiufu Qiao, Xianghua Meng and Dr. Jinhua Ye for providing figures and original data.

I am also grateful to the following people for their assistance to the parts of initial translation of this book: Dr. Zhongyi Zhang for Chapters 2 and 3, Shouren Zhang for Chapters 4 and 5, Mingming Wang for Chapters 8 and 9, Hongyan Wang for Chapters 10 and 11, Weijun Jin for Chapters 12 and 13, and Chunguang Wei for Chapter 15.

I am especially grateful to Dr. A.J. Barber (University of London, UK), who revised and polished the whole text. Without his kind help I couldn't have completed the manuscript in English.

Prof. M.H.P. Bott, Prof. Guangrong Shi, Prof. B. Windley, Dr. L.R.M. Cocks, and Dr. J. R. Ali made many important comments on and suggestions for this English edition. I would like to thank them all here.

Although the preparation of this book is the responsibility of the author, it really represents the collective literary and scientific creation of many researchers, colleagues and friends. I would like to express my heartfelt gratitude for their invaluable help and guidance.

Contents

Chapter 1
Introduction

Tectonics is a comprehensive subject area involved in Earth Sciences concerning the historical development, evolution and origin of the Earth. The aims of this study are to determine the composition, the structure, the movement (including deformation and displacement) and the evolution of the outer sphere of the solid Earth, the lithosphere, and its relationship to activity in the interior, in the lower mantle and the core. This subject area is encompassed in the Theory of Plate Tectonics originating from the investigation of the ocean floors during 1960s, and combined with the theory of continental drift, which was until then not universally accepted, evolving into a comprehensive theory of global tectonics. Results

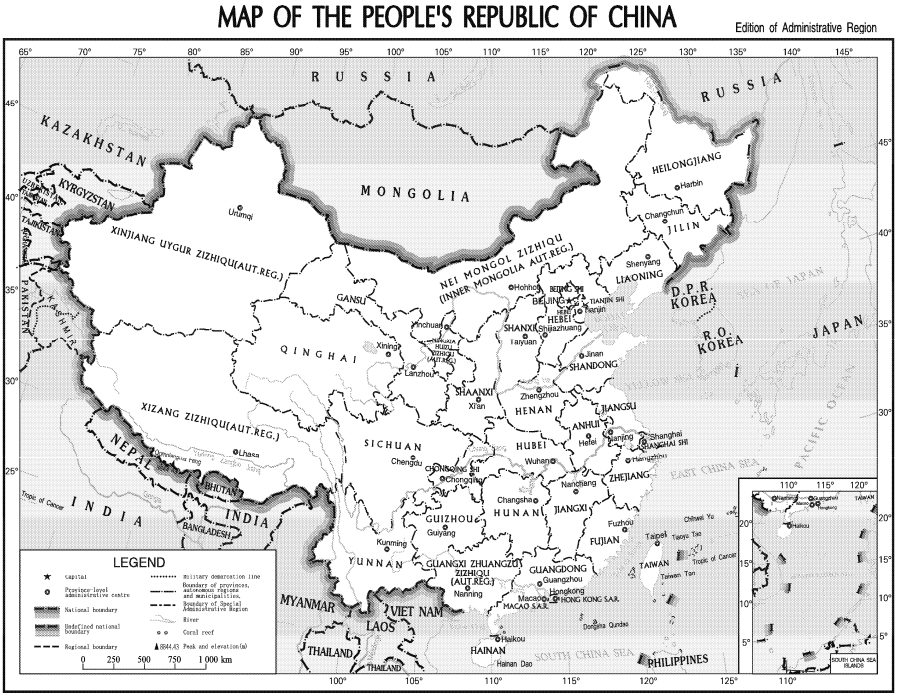

Fig. 1.1 The geography of China (http://www.sbsm.gov.cn, with permission of State Bureau of Surveying and Mapping, China).

from all branches of the geology, geophysics, and geochemistry, including isotope geochemistry, petrology, stratigraphical paleontology, paleoecology, paleoclimatology and paleogeography contribute to the

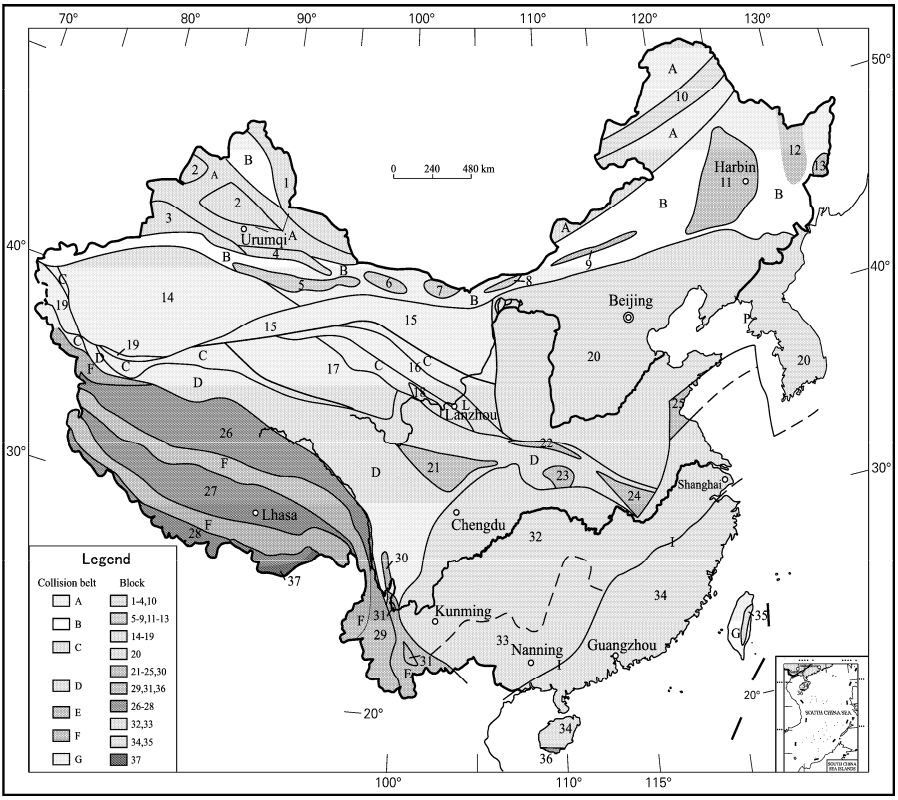

Fig. 1.2 Tectonic units of China during the Paleozoic.

Blocks in the Peri-Siberian Tectonic Domain: 1. Altay; 2. Junggar–East Kazakhstan; 3. Ili–Balchas; 4. Turpan–Xingxingxia; 5. Kuruktag; 6. Hongshishan; 7. Yagan; 8. North Bayannur; 9. Tuotuoshang–Xilinhot (Abagnar); 10. Ergun (close to Gondwana during the Neoproterozoic–Early Cambrian); 11. Harbin (Songhuajiang–Nenjiang); 12. Jiamusi–Bureinsky (close to Gondwana during the Neoproterozoic–Early Cambrian); 13. Xingkai (i.e. Wandashan, close to Gondwana during Neoproterozoic–Early Cambrian).

Sino-Korean plate (20).

Blocks of the Yangtze Tectonic Domain: 32. North Yangtze Plate; 33. South Yangtze Plate; 21. Songpan–Garze (west Sichuan); 22. Middle Qinling; 23. Wudang; 24. Dabie; 25. Jiaonan (Sulu); 30. Zhongdian; 31. Lanping–Simao–Indochina Plate; 34. Cathaysian Plate; 35. Taiwan (eastern Cathaysian Plate); 36. Sanya (northeast Indochina Plate).

Blocks of the Xiyu Tectonic Domain (transition type): 14. Tarim Plate; 15. Altun–Dunhuang–Alxa; 16. Middle Qilian; 17. Qaidam; 18. Hualong; 19. central West Kunlun.

Blocks in the Peri-Gondwanan Tectonic Domain: 26. Qiangtang; 27. Gangdise (Lhasa); 28. Himalaya; 29. Baoshan–Sibumasu (Sino–Burma–Malay–Sumatra); 37. Indian Plate.

Collision Belts: A. Altay–Junggar–Ergun Early Paleozoic Collision Belt; B. Tianshan–South Hingganling Late Paleozoic Collision (eastern part of the Central Asian orogenic) Belt; C. Qilian–Altun Early Paleozoic collision belts in the Xiyu Plate; D. Shuanghu–Lancangjiang (Changning–Menglian), Lazhulong–Jinshajiang, and Qinling–Dabie–Jiaonan Triassic Collision Belt; E. Lanping–Simao Palaeogene Collision Belt; F. Bangong–Nujiang and Yarlung Zangbo River Cretaceous–Paleogene Collision Belt; G. West Pacific Palaeogene subduction zone (trench-arc zone). The Shaoxing–Shiwandashan Triassic Collision Belt is shown as a line between Yangtze Plate and Cathaysian Plate.

development of this subject area, encouraging cooperation of specialists engaged in all the geosciences disciplines in the construction of a comprehensive Earth Sciences system.

In this book, the tectonics of China (Figs. 1.1 and 1.2) is dealt with as a sequence of tectonic events through geological time. A comprehensive analysis of these events is based on the integration of records preserved in the rocks, which provides the evidence of the deformation produced by the movement of continental blocks during processes of the subduction, collision and intraplate compression and extension.

The tectonic systems developed during these events are described in terms of rates of movement, orientation of tectonic stresses, magnitudes of stress, and the timing and rate of deformation. These tectonic and structural aspects are integrated together with the paleo-sedimentary record, paleo-biogeography and tectonic reconstructions of the distribution of continental blocks at different geological periods, based on paleomagnetism, rock deformation and paleo-biogeographical data. As far as possible all these aspects are dealt with in a quantitative and a purely qualitative manner.

The Chinese continent is located in Eastern Asia (Fig. 1.1), composed of the Qinghai-Xizang (Tibet) Plateau, the Inner Mongolia-Ordos-Yunnan-Guizhou Plateau, the Tarim Basin and Junggar Basin and their surrounding mountains, and the eastern plains and hills. Tectonically, the Chinese continent consists of many continental nuclei and small blocks, which were gradually amalgamated to form the present Chinese continent. Until the Paleozoic, 37 tectonic blocks had been identified in the Chinese continent (Fig. 1.2) and classified into five tectonic domains, which will be discussed in detail in later chapters. The evolution of the Chinese continent was very different from the evolution of the North American, South American, Eurasian, African and Australian continental plates.

1.1 Tectonic Events

Concept: Before discussing tectonic events it is necessary to introduce the concept of the tectono-stratigraphic unit (структурный этаж) first proposed by geologists of the Soviet Union in the 1940s, and introduced in the study of the tectonics of China by Zhang WY (1959). American geologists have also used a similar concept, the "tectonosynthem", more recently (Muehlberger and Tauyers, 1989).

A tectono-stratigraphic unit encompasses all the tectono-stratigraphic features of a tectonic unit, distinguished by a particular type of deformation developed during a particular tectonic period. In terms of time, a tectono-stratigraphic unit represents a period in the tectonic evolution of the Earth; in space, it covers the area affected by a specific tectonic event (Fig. 1.3).

The boundary of a tectono-stratigraphic unit is taken at a break in sedimentation, marked by a regional angular unconformity which separates two tectono-stratigraphic units (Fig. 1.3). The tectono-stratigraphic unit lies between two angular regional unconformities. An angular regional unconformity is formed when an older rock unit deformed by either compression or extension is then uplifted, eroded and buried by younger rocks. The boundaries of tectono-stratigraphic unit should not be taken at "parallel" unconformities or disconformities, as these do not represent significant tectonic events.

Different tectono-stratigraphic units are characterized by different types, styles and degrees of rock deformation, with different intensity, resulting from different stress orientations in different tectonic environments (Fig. 1.3). The geological time occupied by a tectono-stratigraphic unit is a "tectonic period". Each tectonic period can be divided into a stable (or "uniform") period, which lasted for a relatively long period of time, and an active (or "catastrophic") period which occupied a much shorter period of time at the end of the tectonic period (Table 1.1). Each tectonic period commences with a long, and stable period and ends with a short, and active period. Movement of plates, rock deformation and the related metamorphism and magmatism mainly constitute a tectonic event during the shorter and active tectonic period. By convention, these tectonic events are named after the area in which the tectonism was first recognized. However, if these events are named after their geological or isotopic age, to make

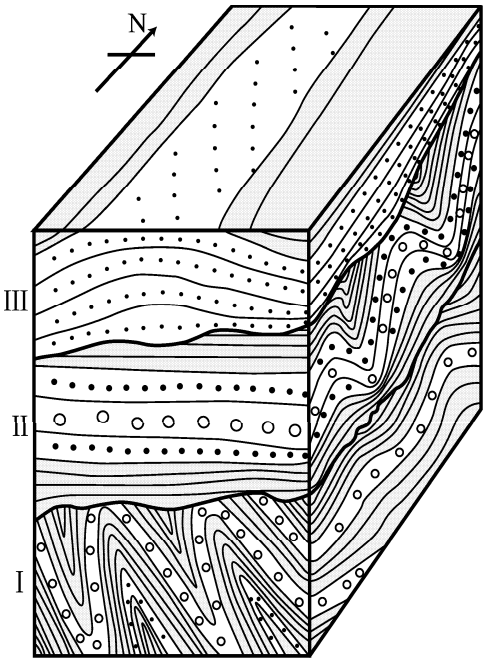

Fig. 1.3 Changes of folding styles and orientation of folding axis in different tectono-stratigraphic units.

Ⅰ. Holomorphic and linear type folds developed in the oldest tectono-stratigraphic unit, in a near north-south direction, slightly influenced by folding with an E-W orientation formed at a later period;
Ⅱ. Transition or Jura-type folds developed in intermediate tectono-stratigraphic unit, on E-W axes;
Ⅲ. Drape or Germano-type folds developed in the youngest tectono-stratigraphic unit, on N-S axes.

international comparison becomes easier. Conventional terms, derived from local tectonic periods or local events, are therefore used as little as possible in this book.

The degree and style of tectonism are different in the stable and active periods, but there is usually some connection and inheritance, for example, the orientation of tectonic stresses and the direction of plate movement may be the same in both periods. However, the styles and rates of rock deformation are very different, the magnitudes of the stresses are different and the types of magmatic activity and metamorphism are also very different (Table 1.1).

1.2 Universal Tectonic Events?

Stille (1876–1966) proposed that there was a rhythm in the tectonic evolution of the Earth and that geological history was punctuated periodically by “orogenic phases”, which occurred at the same time in different parts of the world. In the 20th century this principle exerted a great influence on the development of tectonics, but has generated continual controversy since it was first put forward. By contrast, Soviet structural geologists in 1930s considered that rock deformation occurred continuously, with changes taking place over long periods of geological time (e.g. Vasilievsky, 1964), and some American geologists (e.g. Gilluly, 1949) not only disagreed with the concept of phases of universal orogeny, but

Table 1.1 Stable and active periods in Earth's evolution (in the period of several ten million years)

Type	Stable or uniformity period	Active or catastrophic period
Period of time	$\geqslant n \cdot 10^7$ years	$\leqslant n \cdot 10^4 - 10^6$ years
Atmosphere	Stable change of climatic zone and air temperature	Giant change of climate and climatic zone
Hydrosphere	Stable sea level, water quality and water temperature	Giant change of sea level, water quality and water temperature
Biosphere	Stable propagation and resuscitation	Bio-catastrophe
Paleomagnetism	Stable poles and minor motion	Pole reversal
Sedimentation and erosion	Continuous sedimentation, partial erosion	Partial sedimentation, hiatus, seismite, strong erosion
Strata boundary	Conformity or partial geographic conformity	Regional angular unconformity
Geothermal	Stable accumulation, weak geothermal action	Giant geothermal release and reactions
Magmatism	Magma gradually cooling, minor intrusion	Violent intrusion and volcanism
Metamorphism	Burial metamorphism, weak hydrothermal effects	Regional and dynamo-metamorphism, violent hydrothermal effects
Tectonic stress	Gradual accumulation and revision, small differential stress	Stress increase and release, giant differential stress
Vertical motion of plate	Stable depression and uplift, $\leqslant 0.1$ mm/yr	Strong depression and uplift, $\geqslant 1.0$ mm/yr
Horizontal motion of plate	Weak, $\leqslant n$ mm/yr	Strong, $\geqslant n$ cm/yr
Rock deformation	Slight or bending folds, small fracture	Strong, every type of fold and fault developed
Astronomy	Solar system deviate galaxy disk	Solar system just across the galaxy disk
Meteorite Impact	Small and weak impacts	Major impact

supposed that tectonism had occurred continuously throughout the whole evolution of the Earth (Wang HZ, 1990). In the 1970s–1980s, based on the recognition that sea-floor spreading was a continuous process, the appreciation that syn-sedimentary structures had developed over long periods of time, and the scarcity of unconformities in thrust zones or within orogenic belts, fewer geologists were willing to accept Stille's (1924) proposition. At present, the consensus view is that the Earth is a rheomorphic solid and is able to flow continuously under differential pressure, so that tectonism and orogeny have occurred uniformly, throughout geological time and that there has been no periodicity or rhythm during the tectonic evolution of the Earth (e.g. Gretener, 1981; Sengör, 1982; Hsu, 1989; Li JL, 1991; Zhu ZC, 1996).

Wang HZ (1982, 1985, 1990) advocated the concept of "mobilism" for the tectonic evolution of China, in which deformation had occurred during episodes of tectonic activity, periodically in different areas and at different time. From a comprehensive assessment of a large volume of tectonic data, Wan TF (1997) concluded that there is no evidence that important tectonic events occurred at the same time in different parts of the Earth. However, it is evident that tectonism has occurred over very large areas at approximately the same time in subduction zones, in collision zones and in areas of intraplate deformation. For example, Caledonian tectonic events occurred at almost the same time (429–425 Ma) in a zone extending all the way from the Appalachian Mountains in eastern America to Scotland and the western margins of the Scandinavia (Rogers and Dunning, 1991; Bally et al., 1989; Trewin, 2002). Similar extensive tectonic events have occurred in China, which will be detailed in the following chapters.

According to Hsu (1989) and Sengör (1982), if the Earth is a rheomorphic solid, periodicity would not appear in tectonic evolution on the scale of the Earth. According to the concept of mobilism, orogeny is a continuous and uniform process. When the plate tectonic theory was first proposed and data on sea-floor spreading was limited, this opinion seemed to be sustained. The original map showing the pattern of magnetic anomalies on the floors of the oceans implied that sea-floor spreading was a continuous process, in which the floors of the oceans expanded continuously in the same direction, only varying slightly in their velocity and direction of movement with time (Wilson, 1970; Le Pichon et al., 1973; Press and Siever, 1974). Given the relationship between the expansion of the oceans at mid-ocean ridges

and their destruction in subduction zones along the margins of the oceans, it could easily be assumed that the processes of subduction and collision were also continuous processes. However, Hsu (1989) and Sengör's (1982) hypotheses contradicted many discovered tectonic facts before 1980's. When the much more detailed third edition of the magnetic anomaly map was published at the end of the 1980s (Cande et al., 1989; Cande and Kent, 1992; Ma ZJ et al., 1996), analysis showed that since the Middle Jurassic (156.6 Ma), the Pacific, Atlantic and Indian Oceans had all expanded during the same six periods, with movements in different directions and at different velocities (Table 1.2; Fig. 1.4). Sea-floor spreading at velocities of several cm/yr shows that the Earth has the properties of a rheologic solid, while the process shows some periodicity. It seems that both arguments are to some extent correct with general continuity, and a superimposed element of periodicity.

Evidence compiled in this volume shows that the tectonic evolution of the Earth has not become linear, with a uniform rate of change, but non-linear, with periodic variations in the rate of change. From our present evidence it appears that the processes continue over a period of time at a more or less constant rate, but are then interrupted by sudden and catastrophic changes. Such qualitative and quantitative changes are characteristic of all evolutionary processes. As Yu CW (2003) has explained, tectonism, like all other geological processes, should be considered in terms of non-linear dynamics in an unstable system. The evolution of the Earth systems should be studied using the complexity——"Chaos" theory.

In the past two hundred years, there has been a lively geological debate between proponents of uniformitarianism, who argue that geological processes have continued in much the same way and at the same rate throughout geological time (Hutton, 1785; Lyell, 1830–1833) and proponents of catastrophism, who argue that geological processes proceed by infrequent but catastrophic events (Cuvier et al. , 1817). At present, most Earth scientists agree that these concepts can be reconciled. It is recognized that there are stable periods (or periods of uniformity) lasting over a long time span, which alternate with active (or catastrophic) periods, occupying a much shorter time span (Tao SL et al., 1999); tectonic events represent this catastrophic period (Table 1.1).

Tectonic events are difficult to resolve, as their complete history is rarely preserved in the geological record. The evidence is never complete. Strong deformation, block displacement, violent magmatism and large-scale uplift of the Earth's surface have resulted in widespread erosion, forming unconformities, where the geological record has been destroyed. For this reason the study of tectonics did not advance very rapidly in many parts of the world. In many areas, facts are few, tectonic and geodynamic data are scarce; the geological literature demonstrates that these deficiencies do not deter geologists from engaging in much speculation and guesswork.

Table 1.2 Periods in the accretion of the ocean floor for the Pacific, Atlantic and Indian Oceans

0 Ma	6 stage
10 Ma	5 stage
37 Ma	4 stage
58 Ma	3 stage
97 Ma	2 stage
138 Ma	1 stage
156.6 Ma	

After Cande and Kent, 1992; Ma ZJ et al., 1996.

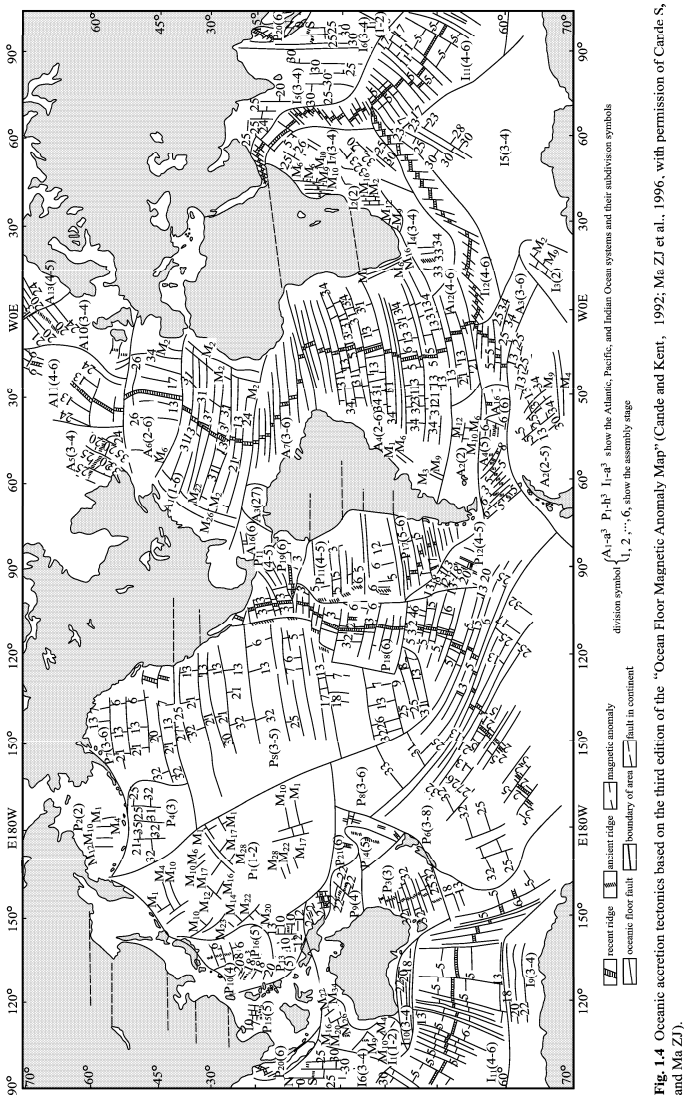

Fig. 1.4 Oceanic accretion tectonics based on the third edition of the "Ocean Floor Magnetic Anomaly Map" (Cande and Kent, 1992; Ma ZJ et al., 1996, with permission of Carde S, and Ma ZJ).

1.3 Determination of Tectonic Events in the Chinese Continent

Geological data from whole China included in the Bureau of Geology and Mineral Resources of the Provinces (1984–1993), the *Introduction on Regional Geology of China* (Cheng YQ et al., 1994) and the earlier researches of the author (1994), are referred to the international stratigraphic chart (Remane et al., 2000; International Commission on Stratigraphy, 2004), and compiled as a table of the tectonic periods and tectonic events in China (Table 1.3).

The former practice of referring the tectonic periods in China to world-wide tectonic periods is incorrect. A division into tectonic periods and events has been devised purely for the Chinese continent,

Table 1.3 Tectonic periods and events in Chinese continent

Age of period Ma	symbol	Geological time	Isotopic age of tectonism (Ma)	Local tectonic period and event
	Q_2-Q_4	Middle Pleistocene–Holocene	Since 0.78	Neotectonic
0.78				
	$N-Q_1$	Miocene–Early Pleistocene	23–0.78	Himalayan
23				
	E_2-E_3	Eocene–Oligocene	56–23	North Sinian
56				
	$K_1^2-E_1$	Middle stage of Early Cretaceous–Paleocene	135–56	Sichuanian
135				
	$J-K_1^1$	Jurassic–Early stage of Early Cretaceous	200–135	Yanshanian
200				
	P_3-T_3	Late Permian–Late Triassic	260–200	Indosinian
260				
	D_2-P_2	Middle Devonian–Middle Permian	397–260	Tianshanian
397				
	$\in_2-D_1$	Middle Cambrian–Early Devonian	513–397	Qilianian
513				
	$NP_3-\in_1$	Ediacaran–Early Cambrian	680–513	Sinian
680				
	NP_2	Cryogenian (Nanhua)	800–680	Nanhua
800				
	NP_1	Tonian	1,000–800	Qingbaikou (Jinning)
1,000				
	MP_{2-3}	Ectasian–Stenian	1,400–1,000	Jixian
1,400				
	PP_4-MP_1	Statherian–Calymmian	1,800–1,400	Changcheng
1,800				
	PP_{1-3}	Siderian–Orosirian	2,500–1,800	Lüliang (Hutuo)
2,500				
	NA	Neoarchean	2,800–2,500	Wutai
2,800				
	MA	Mesoarchean	3,200–2,800	Fuping
3,200				
	PA	Paleoarchean	3,600–3,200	Qianxi
3,600				
	EA	Eoarchean		

and these have been given local names (Table 1.3). However, in order to simplify the terms, and for ease of international comparison, the periods and events in this book are named directly after their geological or isotopic age; and local names for tectonic periods or events are used as little as possible.

As shown in Table 1.3, seventeen tectonic periods and events are identified. The extent of our knowledge concerning these tectonic periods and events is very variable. In general, much less is known about earlier periods compared with the more recent ones. Tectonic periods and events in the Archean and Proterozoic are known only broadly, and periods and events in the Paleozoic can only be discussed generally, and although a series of events can be recognized, the geological data is not very detailed, and only two periods can be distinguished. The eight tectonic periods and events since the Paleozoic have been researched in much more detail, and as geological data is more abundant and more accurately known, one chapter is devoted to each of these periods.

In the Archean and Proterozoic, in the absence of detailed biostratigraphic divisions, geological stages are defined in terms of tectono-magmatism, and the divisions are based on the tectono-magmatic evolution of the continental crust. In the period since the Paleozoic, geological and isotopic ages of the commencement and close of each tectonic period do not coincide with the beginning and end of eras and periods based on biostratigraphy, and the time spans occupied by each tectonic event may be very different (Table 1.3). This is because the climax and end of tectonic periods in China did not occur at

the same time as the extinction events indicated by the biostratigraphy; the climax of a tectonic period is always later than the major catastrophic extinctions.

For example, according to isotopic data from syntectonic magmatism in most areas of China, as shown in Table 1.3, 135 Ma is the most suitable age for the boundary between the Yanshanian and Sichuanian tectonic periods. In the international stratigraphic chart (Remane et al., 2000; International Commission on Stratigraphy, 2004), there are different opinions on the age of the boundary between the Jurassic and Cretaceous, ranging from 135 Ma to 145.5 Ma. From recent studies, most Chinese researchers recognize the boundary between Jurassic and Cretaceous at either 137 Ma or 144 Ma (Li PX et al., 2000). For the age of the boundary between Jurassic and Cretaceous, the author agrees with the opinion of Li PX et al. (2000), that is, the boundary between the Yanshanian and Sichuanian tectonic periods lies between early and middle epoches of Early Cretaceous. Wan TF (1994) originally chose 135 Ma as the age of the boundary between the Jurassic and Cretaceous, but this decision is now reconsidered.

1.4 Research Principles and Methods for Interpreting Tectonic Events

1.4.1 The Rock Record

The study of tectonic events in the active and stable periods of tectonic evolution requires different research methods. Evidence for the active period of tectonic events is commonly preserved in the rocks as structural features such as folds, faults, thrusts, joints, foliations and lineations, which may be accompanied by recrystallization in a process of metamorphism. The internal changes in a rock body or in a hand specimen can be expressed in terms of the amount of deformation or strain it has undergone, i.e. reduction or expansion in volume, shortening or extension. Strain can be determined with respect to changes in the length of three mutually perpendicular principal axes of strain (ε_1, maximum compression = shortest strain axis; ε_2, intermediate; ε_3, minimum compression = the longest extensional strain axis), ε_2 may be equal to or have any value intermediate between ε_1 and ε_3. Strain can be measured if the rock contains "strain markers", objects whose original size, shape, distribution and orientation are known and can be compared with their present size or shape (Ramsay and Huber, 1991).

Tectonic events may also be recorded indirectly by syn-tectonic sedimentation. Tectonic events are commonly accompanied by uplift with accelerated erosion, so that the sedimentary record is destroyed. However, the products of erosion may be deposited in marginal depressions or basins around highly deformed areas as molasse or flysch (bathyal) turbidites, providing a record of episodes of uplift and erosion. Tectonic events may also be accompanied by the intrusion of magmatic rocks with syn-tectonic mineralization and pneumatolitic/hydrothermal metamorphism.

The study of sedimentary strata can be used to solve many problems in tectonics, using the sedimentary facies and the sequence of formations in stable period, for the recognition of unconformities and of episodes of strong deformation in the active tectonic period. These studies are part of a complete study of tectonics.

Methods used in the analysis of sedimentation and paleogeography are more appropriate to the stable period of a tectono-stratigraphic unit. A stable tectonic period is represented by the deposition of a continuous sequence of sedimentary strata in a sedimentary basin. During the stable period, variations in the thickness and rates of deposition of sedimentary strata, and changes in the rate of vertical motion of the Earth's crust, with depression or uplift, can be recognized. By determining the sequence of strata and the facies of each sedimentary unit, it is possible to place these periods of uplift and depression in a changing paleogeographic environment. The statistical methods of measuring the thickness of sedimentary strata and determining rates of deposition since the Mesoproterozoic, as shown in Appendix 2, are very approximate. There is no method of measuring the effects of alternating depression and uplift,

although great thicknesses of sedimentary strata are most likely to be the results of multiple phases of depression-sedimentation and uplift-erosion. Also no allowances have been made for the effects of compaction and diagenesis, or for the thickening or thinning strata caused by later tectonic events. The study of syn-sedimentary faults is helpful to determining the history of development of sedimentary basins during a stable tectonic period. A complete calculation, taking account of all these factors, involves an enormous amount of systematic field and laboratory study.

Although a cover of sedimentary rocks, amounting to several tens of thousands meters, extends over the majar part of the Chinese continent, the greater part of the sediment originally deposited on the continent has been eroded away and is no longer preserved. According to statistical calculations by Ronov et al. (1984, after Qian XL, 1996), based on the thickness and extent of sediments and their geological age, at present day sediments are being deposited throughout the world at a rate of 50×10^8 m^3 per year. Most Mesozoic–Cenozoic sediments have been preserved on the Earth surface, of which ~70% is from the Paleozoic, ~20%–10% from the Proterozoic, and less than 10% from the Archean.

The accumulation of paleobiogeographical data and especially the recognition of ecosystems are important for distinguishing different paleoplates and smaller crustal blocks. The reconstruction of paleobiogeographies demonstrates the continual movement of blocks through out and supports the mobilistic concept of tectonics.

1.4.2 The Geometry of Rock Deformation

The foundation of the study of tectonics is the determination of the distribution and mutual relationships of rock units as seen in the field, together with their internal structural features such as folds, faults, lineations and foliations. Tectonics involves rock deformation on all scales from the megascopic to the microscopic, from the lithospheric plate to the individual mineral crystal and its crystal lattice; this information can then be integrated into a comprehensive tectonic system (Fig. 1.5). Tectonics is also concerned with the intrusion and extrusion of magmatic rocks and the metamorphism and the recrystallisation of rock bodies with the formation of new minerals and new textures, and the relationship of these events to phases of deformation. These relationships must initially be established in the field by detailed geological mapping and regional geological surveys, complemented by drilling and by deep structural studies using geophysical methods and by the study of rocks under the optical and electron microscopes.

The deformation and the displacement of the lithosphere are the major concerns of the study of tectonics. Although comprehensive methods should be used in the study of tectonics, and research should encompass all branches of the geosciences, the study of rock deformation should be made on the major preoccupation of tectonics, which has been neglected in some recent studies.

Contributions to the knowledge and understanding of rock deformation in China during the last fifty years have been immense. This can be attributed to the extent and success of regional geological surveys. The plan for an outline geological survey covering the whole Chinese continent, totalling about 9.6 million square kilometers at the scale of 1 : 1,000,000, commenced, but was not completed before 1949; a reconnaissance survey of regional petroleum geology at the scale of 1 : 200,000 was completed in the 1960s (unpublished report); a regional geological survey at the scale of 1 : 200,000 was completed for most areas of China before the end of the 1980s (Bureau of Geology and Mineral Resources of Provinces, 1984–1993); new regional geological survey at the scale of 1 : 250,000 (more than 100 sheets) has been completed recently over whole Qinghai-Xizang (Tibet) plateau; the results will be published shortly. These surveys raised the extent and precision of geological information substantially. Classification and comparison of regional strata, with the description of types, styles, attitudes and the distribution of folds and faults at the macro-and meso-scale, and of magmatism and metamorphism, build up the foundation for studying the tectonics of China in this book.

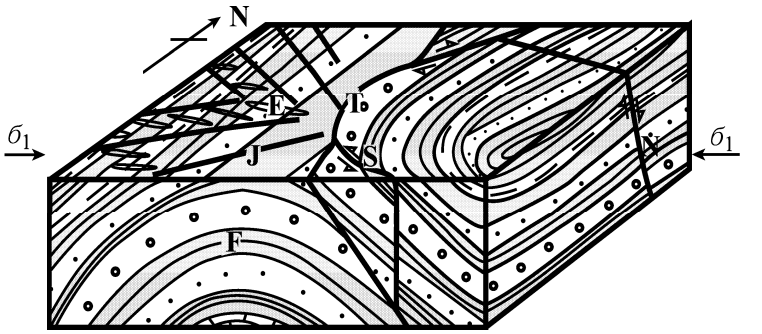

Fig. 1.5 Sketch of a tectonic system affected by deformation in different orientations.

σ_1 = E-W orientated regional horizontal compression and shortening; F. N-S orientated folds; T. N-S orientated reverse faults or thrusts; N. near E-W orientated extension faults; E. near E-W orientation extensional joint system; S. NW or NE orientated strike-slip faults; J. NW or NE orientated shear joint system.

Data concerning the geometry and attitudes of 11,723 macro-and meso-scale folds (Fig. 1.6; Appendix 3) have been collected and analyzed to determine regional tectonic stress orientations. In the area to the west of 105° where regional geological surveys at the scale 1 : 200,000 have not yet been completed and folds are not shown in considerable detail, geological surveys at scales of 1 : 500,000 or 1 : 1,000,000 have been used and the statistics relates to anticlinoria and synclinoria. From these data, it can be seen that rock deformation is widespread throughout the Chinese continental lithosphere. Joint systems, the weakest type of rock deformation, can be found even in the youngest rocks throughout China; it is difficult to find an area not affected by rock deformation.

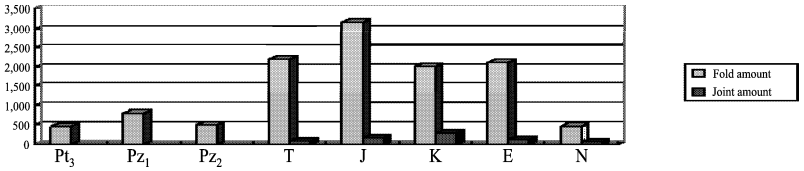

Fig. 1.6 Number of folds/Number of joint observation points: Neoproterozoic (Pt_3) 463/0, Early Paleozoic (Pz_1) 801/0, Late Paleozoic (Pz_2) 492/0, Indosinian (T) 2,195/83, Yanshanian (J) 3,169/168, Sichuanian (K) 2,008/281, North Sinian (E) 2,126/115, Himalayan (N) 469/58.

In collision zones, rock deformation is mainly linear, with Alpino-type folds and nappes with high and intermediate angles of dip for the limbs, associated with many thrusts. In intraplate areas covering half the area of China, there is widespread deformation with intermediate strength, in which the angles of dip fold limbs are usually greater than 20°, and the folds are accompanied by faults. The main types of deformation are transition types, belonging to the sedimentary cover detachment type, and may be called Jura-type folding. Even in stable tectonic areas covering one third of China which appear to have only horizontal sedimentary strata, there are Germano-type folds with limbs with very low angles of dip, and normal faults with high angles of dip and complex joint systems.

1.4.3 The Kinematics of Blocks

The aim of tectonic studies is to examine rock deformation quantitatively, with the determination of the amounts of dilation (changes in volume), distortion (changes in shape) and translation (movements of the rock body as a whole) and the orientation of the stresses responsible for this deformation (Fig. 1.5), together with the determination of the rates of deformation (rates of shortening, extension and/or horizontal and vertical displacement). It may be necessary to manifest the effects of multiple phases of deformation, where the orientation of the stresses may have been different in each phase. This is relatively easy if the orientation of the stresses in each tectonic period was very different, but may be difficult or even impossible if these stresses were in the same, or nearly the same direction.

Research into the kinematics of the lithosphere aims at determining vertical movements of uplift and depression and horizontal movements of compression, extension and strike-slip movement, and the rates at which these movements occurred.

Close attention has been concentrated on vertical movements of the lithosphere with the uplift and depression of Earth surface. The determination of vertical movements during a stable tectonic period makes use of data on variations in sediment thickness, changes in lithology and facies; magmatism may also contribute to vertical movements. Vertical movements can be determined through the study of sedimentation and erosion, transgression and regression, the up-rise of magma or changes in the thickness of the lithosphere over long periods of time. During the last one hundred years, while these methods were being perfected, it seemed that vertical movements were the most important feature of the kinematics of the lithosphere.

This hypothesis laid the theoretical foundation for concepts of global expansion, limited global expansion, pulsation, etc. More recently, hypotheses of opening and closing (Yang WR et al., 1984, 1993; Jiang CF, 1992, 1997), uplift of the Mohorovĭcíc discontinuity (Chen FJ et al., 1992), uplift due to mantle plumes and lithosphere re-rooting or underplating (Deng JF et al., 1992, 1996, 1997, 1998), which have their bases in this earlier tectonic thought, have exerted important influences over the development of tectonics in China. In these concepts, the tectonic evolution of continents takes place essentially *in situ*, with vertical movements being the driving force for deformation and displacement, horizontal movements being secondary and limited in their extent. In these hypotheses, the importance of vertical movements has been more fully emphasized, without account for the possibility of great horizontal displacements over distances of several thousand kilometers. In these models, no explanation is offered at all for such great horizontal displacements.

The importance of horizontal deformation and displacement was much more difficult to realize, and it took a long time to recognize it. In 1912, Wegener (1924, republished in 1966) first proposed the Theory of Continental Drift, based on the distribution of fossils and indications of paleo-climatic zones. However, due to unexplained problems and some errors (e.g. "Is it possible for the lighter sialic continents to drift at velocities of several meters per year through the denser simatic ocean crust?") and after detailed discussion at the International Geological Congress in 1922, the theory of continental drift was rejected. However, Wegener's hypothesis was fundamentally correct and formed one of the foundations for the development of the theory of plate tectonics in the 1960s. This example demonstrates the difficulty of changing entrenched scientific thought.

Methods for determining vertical and horizontal movements of the lithospheric plates are summarized in Table 1.4.

The boundaries of the lithospheric plates differ according to the movements of the plates: high angle normal and reverse faults indicate vertical movements; intermediate and low angle thrusts or overthrusts are characteristics of subduction or collision boundary zones and indicate horizontal crustal shortening; wrench (strike-slip) faults or transform faults indicate horizontal shearing of the plates; intermediate and low angle detachments and listric growth, or syn-sedimentary faults are characteristic of continental rift zones and oceanic ridges and indicate horizontal extension of the plate.

Table 1.4 Research methods for recognizing movements of the lithosphere plates

Vertical movement	Horizontal movement
	Paleomagnetic drift, changes in paleolatitude, changes in paleomagnetic declination
	Horizontal changes in oceanic magnetic anomalies and other geophysical anomalies
Changes in sedimentary thickness	
Transgression and regression, changes in sedimentary facies	Horizontal migration of sedimentary facies and formations
Habitat depth changes of plants and animals	Horizontal migration of plants and animals Anomalous paleo-climatic zones
Magmatism and accompanying uplift or depression of the crust	Horizontal drift of magmatic centers
Progressive and retrogressive metamorphism (*P-T-t* path)	Horizontal drift of metamorphic facies and zones
Bending folds	Buckling folds
High angle faulting	Thrust, strike-slip faulting and folding at plate boundaries
Height change of planation surfaces, valley terraces and buildings on the Earth's surface	Horizontal dislocation of landforms

Ramsay (1985), Ramsay and Huber (1991) proposed a series of methods for determining the strain involved in folding and fracturing, and made significant progress in this field, but parameters and methods for determining regional strain fields have not yet been developed, and it is difficult to determine rates of compression and extension using conventional methods of structural geology.

Sugisaki (1976) first suggested that there was a relationship between velocities of plate movement and the chemical content [K_2O (W_B%), Na_2O (W_B%) and silica index (θ)= w (SiO_2) $-47\times n$ (Na_2O + K_2O) / n (Al_2O_3)] of volcanic rocks near the subduction zone. In the formula above, the unit of w (SiO_2) is the percentage of weight, the units of n (Na_2O), n (K_2O), n (Al_2O_3) are the percentage of molecules (Fig. 1.7). Using these parameters, Sugisaki (1976) discovered that the silica index increases with more rapid rates of shortening, while Na_2O and K_2O decrease (Fig. 1.7).

This relationship is not linear but has an exponential function. These relationships are due to the relative ionic radii of silica and potassium and sodium. The ionic radius of silica is very small, while the ionic radii of potassium and sodium are relatively large. When the velocity of plate movement increases and tectonic activity is enhanced, silica ions are enriched, while the ions of potassium and sodium decrease relatively (Sun Y, 1982; 1998). On the assumption that the velocities of movement involved in marginal and intra-plate deformation are similar, the author (Wan TF, 1994) has used the relationships derived from the study of plate margins to quantify intraplate movements; in general, velocities of movement during intra-plate deformation should be less than the rates for marginal deformation. When the velocities of plate movement for the whole Chinese continent are discussed, on the basis of velocities calculated from plate margins, these velocities may be slightly exaggerated. However, all the data has been treated by the same method, so that the relative magnitudes of movement velocities for different areas are plausible.

Sugisaki (1976) used only the relationship between the chemical content of volcanic rocks and velocity of plate movement. The author has used not only the chemical composition of volcanic rocks, but also that of intrusive rocks to estimate the velocities of plate movement. while volcanic and intrusive rocks were formed at the same time in the same tectonic period, the content of major elements in intrusive rocks, especially SiO_2, Na_2O, K_2O, Al_2O_3, is not likely to differ greatly from that of associated volcanic rocks. Wan TF (1994) has made such comparison many times and found that estimated values of plate movement velocity are almost the same no matter using volcanic or intrusive rocks. Chi JS et al. (1988), Chi JS and Lu FX et al. (1996), Mo XX (1991), and Mo XX et al. (1993, 1998) used Sugisaki's method to estimate velocities of extension and compression of blocks in the Cenozoic volcanic areas of eastern China and of the Latest Paleozoic volcanics in the Hengduanshan area. Using this method the

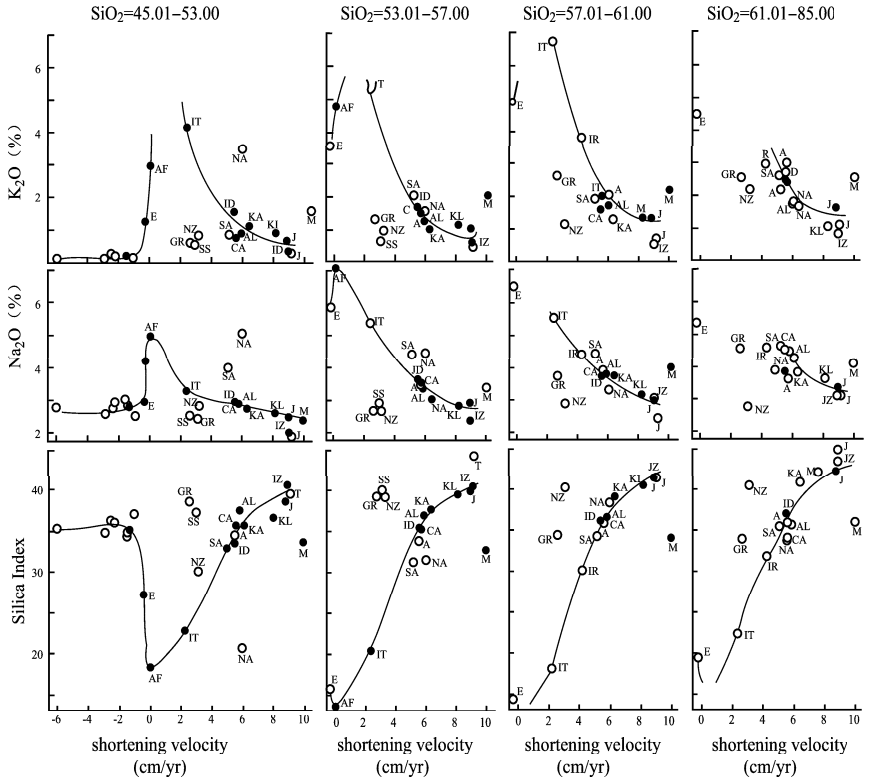

Fig. 1.7 Relationship between the chemical content of volcanic rocks and rates of plate movement (Sugisaki, 1976).

curve for basic magmatic rocks becomes so steep (SiO_2 is about 45%–53%) that it is easy to make mistakes, so that precision in the estimated velocities of movement is low. This is a difficult but unavoidable problem.

The author has collected systematically a total of 18,422 major element chemical analyses of magmatic rocks, formed in different tectonic periods in China, taken from reports of regional geology surveys $(1:200{,}000)$, provincial, municipal and Central Government geological reports, and articles written during the last 20 years (Fig. 1.8). These data has been used to prepare diagrams and to estimate the velocities of intraplate shortening and extension for regional tectonic events (Appendix 5).

The amount of shortening or extension can be determined from balanced geological cross-sections (Woodward et al., 1989). However, over vast areas, where there is insufficient data, the angle of dip of fold limbs can be used to estimate the shortening ratio approximately: shortening ratio $(\%) = 1 - \cos\theta$, where θ is a representative dip angle of the fold limbs in the region, calculated from regional statistics.

By selecting a representative section perpendicular to the regional lineation, the amount of shortening can be obtained by multiplying the shortening ratio by the length of the section. The shortening ratio obtained by this method is a minimum value, because shortening caused by thrusts is not taken into account. However, the shortening taken up by most thrusts in the Mesozoic–Cenozoic is generally between a few kilometers and dozens of kilometers, and has a significant influence on estimations of total shortening. At present, there is very little precise data concerning the effects of thrusting, therefore,

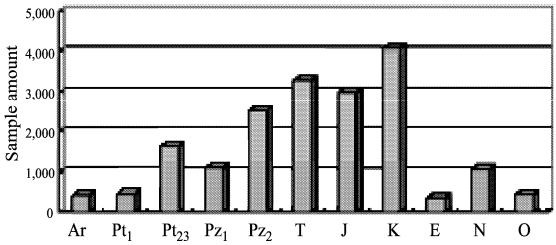

Fig. 1.8 Total number of chemical analyses for major elements in magmatic rocks formed during different tectonic periods.

Archean (Ar) 417, Paleoproterozoic (Pt_1) 469, Meso-Neoproterozoic (Pt_{23}) 1,652, Early Paleozoic (Pz_1) 1,124, Late Paleozoic (Pz_2) 2,548, Triassic (T) 3,284, Jurassic (J) 2,985, Cretaceous (K) 4,076, Paleogene (E) 353, Neogene (N) 1,059, Neotectonic (Middle Pleistocene–Holocene, Q) 455.

more precise methods of calculating shortening using balanced geological cross-sections have not been adopted in this book.

The amount of time over which deformation occurred can be calculated roughly by dividing the amount of shortening into sections by the intraplate shortening ratio, as explained earlier in this chapter. And then by dividing the shortening ratio by the time over which deformation took place, a strain rate ($\dot{\varepsilon}$), which is the strain rate of the minimum principal strain, can be calculated. Estimations of the amount and rates of extension in rift systems can be obtained by reversing the movement on syn-sedimentary faults to determine the amount of extension and using the stratigraphy of the infilling sediments to determine the period of time over which extension took place.

Using the methods outlined above, the amounts and rates of movement during shortening or extension, and the time of deformation and the strain rate ($\dot{\varepsilon}$) can be determined approximately, providing a preliminary model for the kinematics of continental plates.

Studies on paleomagnetism allow the determination of the location of continental block at different geological periods, which can then be used to make paleotectonic reconstructions. During the crystallization of igneous rocks, magnetic minerals cooled through their Curie point take up the magnetic orientation of the Earth's magnetic field at that time. Magnetic sedimentary particles settled through water may also take up the same orientation. By measuring the magnetic vectors in an oriented rock sample, dated isotopically or paleontologically, it is possible to determine the latitude and longitude of past geomagnetic poles, and from the paleomagnetic declination to determine the paleolatitude of a crustal block at the time of cooling of an igneous body or the deposition of sediment. It is, however, not possible to determine the paleolongitude of blocks. Paleomagnetic data cannot generally be used to identify tectonic events in the active period directly. In regions of strong tectonic deformation or with high heat flow, the reliability of paleomagnetic measurements is commonly reduced, or the original magnetism may have been destroyed completely and replaced by a new magnetic orientation.

With reliable paleomagnetic data it is possible to construct a palaeotectonic map and to reconstruct the paleogeography of earlier geological periods. Reliability of reconstructions may be improved by using paleobiology to identify related and unrelated blocks. By comparing the change in paleolatitude and the paleomagnetic declination for a block, before and after a tectonic event, the displacement of a block can be determined by its change in palaeolatitude, and by using age constraints, the rate of latitudinal movement of the block may be determined. It has so far proved impossible to determine the paleolongitudes of crustal blocks, except for the avoidance of overlap. Paleomagnetic studies provide the more convincing evidence for mobilistic tectonics. However, the data may be ambiguous as paleomagmatism does not always provide unique solutions.

In order to understand the kinematics and displacement histories of the crustal blocks making up the Chinese continent and its adjacent areas, only to study and determine intraplate deformation is not

sufficient. It is necessary to collate and carry out a comprehensive analysis of paleomagnetic data, and to prepare paleotectonic reconstructions for determining the distribution of lithospheric plates during each tectonic period. However, there are many difficulties in paleomagnetic research. Paleomagnetic measurements are not very precise and particularly paleolongitude cannot be determined. There are often problems of paleomagnetic overprinting by later events, and it is often difficult to determine the age of sedimentary strata where fossils are absent.

Given the enormous length of geological time, even if the displacement of a continental block is only a very small amount each year, over long periods of time, a block may move over vast distances. To take a very low extension rate of 1 cm/yr for the movement of the oceanic floor during sea-floor spreading, if this movement continued for 100 million years, a block will have moved 1,000 km. For a high spreading rate of 10 cm/yr, a block will move 20,000 km in 200 million years, meaning that a block could have traveled halfway round the Earth!

Over the last twenty years, paleomagnetic measurements, drilling in the oceanic floors and isotopic chronology have demonstrated that continental blocks have undergone dramatic displacements since the Paleozoic. The major parameters have been determined and re-examined repeatedly, so that there is now a general consensus. Maps reconstructing the movements of the continental blocks since the Paleozoic, made by different researchers on a worldwide scale, now differ only in minor details (cf. Scotese et al., 1979, 1986, 1994 and recently on the net; McElhinny & Valencio, 1981; Tarling, 1985; Van der Voo, 1988, 1993; Gordienko, 1999).

Although many paleomagnetic results of the Proterozoic have been published, no consensus has yet been achieved, with each researcher putting forward his(her) own particular model. Particularly, the history of the formation and breakup of the Rodinia supercontinent at about 1 Ga is lively disputed (cf. Powell et al., 1993; Li ZX, 1993; Zhang SH et al., 2000; Condie, 2001; Lu SH, 2001). However, due to the 1300 million-year length of Meso-and Neo-Proterozoic period and the lack of precision in isotopic age dating, it is difficult to correlate the paleomagnetic determinations from different blocks. Even after thorough demagnetization, and using superconducting magnetometers with very high precision, it is difficult to make sure whether the remanent magnetic field has been correctly identified. These problems form an impediment to the reconstruction of paleotectonic maps for the Meso-and Neo-Proterozoic. This is the frontier of paleotectonic reconstruction at present. The use of paleomagnetic data and reconstructions of the distribution of the continental blocks forming the Chinese continent are restricted in this book to periods after the Paleozoic, where results are more plausible (Zhu RX et al., 1998; 2001). Paleomagnetic results of the Proterozoic from previous publications are reported and discussed, but new reconstructions are not attempted.

Research into paleomagnetism in China has not reached the same level of coverage as paleomagnetic research in other regions did. In the 1980–1990s, close attention was first paid to paleomagnetism in the three major blocks forming the Chinese continent (Sino-Korean, Yangtze and Tarim), and many valuable results were obtained. The most controversial problem is whereabouts in the southern hemisphere the Sino-Korean and Yangtze blocks were located during Early Paleozoic, and the Sino-Korean Block was situated to the north or the south of the Yangtze Block. A southern position was first proposed by Lin JL et al. (1985), but many Chinese and overseas researchers have considered that the Sino-Korean Block has always been situated to the north of the Yangtze Block (Wang HZ et al., 1990; Yang WR et al., 1993; Scotese, 1994; Yin A and Nie SY, 1996).

What is the reason for this divergence of views? First, although the area of the Chinese continent is very great, it is composed of many small blocks amalgamated over a long period of time. Some Chinese and overseas paleomagnetic researchers have not fully understood the nature of Chinese continental geology. It is common for data from different blocks to be treated as though they had come from a single block. During the 1980s, this mistake was made many times and in many areas. Second, in the absence of fossils, methods for the determination of isotopic ages in sedimentary strata are inadequate, so that sometimes paleomagnetic data of different ages has been mis-correlated. The third reason may be the effect of specialization. Some geophysicists believe only their own paleomagnetic data and do not consider, or pay less attention on paleobiography and evidence from geological evolution. Since

the paleolongitude of blocks cannot be determined, blocks with very similar features are sometimes placed at a distance from each other, and some reconstructions require the rapid movement of blocks over a very short period of time, "flying" from one side of the map to the other. These phenomena are commonly observed in Neoproterozoic reconstruction maps, and also in some Paleozoic maps (Scotese et al., 1979; Scotese, 1986, 1994; Tarling, 1985; Powell et al., 1993; Li et al., 1993; Condie, 2001; Zhu RX and Tschu KK, 2001). On the other hand, some geologists do not believe the paleomagnetic data, or in its absence, use evidence from paleobiography following their own interpretation of geological evolution, sometimes leading to implausible results (Wang HZ et al., 1990; Windley, 1995; Sengör, 1996; Yin A and Nie SY, 1996; Ziegler et al., 1996; Gordienko, 1999).

When the methods of paleomagnetic research are followed correctly, and the stratigraphic position of the samples has been established reliably, the mean paleomagnetic declination (D°) and the mean paleolatitude (P°) of a continental block can be determined (Appendix 6). Theoretically paleomagnetic declination and paleolatitude can be determined within 1°, but in fact the uncertainty extends to several degrees, equal to a distance of several hundred kilometers, and at present, it is not possible to determine the paleolongitude of a crustal block. Thus ambiguities arise if paleomagnetism only is used to reconstruct the position of paleo-continents. Paleobiographic similarities in the geological evolution of two blocks may provide further important constraints, however the same paleobiographic zone may extend to over 30°–40° of latitude, so that this constraint may not be very precise.

Facing these difficulties, the author has used four principles in assessing the reliability of paleomagnetic results and paleotectonic reconstructions of the Chinese continent:

(1) Only high precision paleomagnetic data is acceptable. Because the content of ferromagnetic minerals in some rocks is very low and the remanent magnetic field is very weak, samples may have to undergo thermal demagnetization many times. Use of the general magnetometer may not be satisfactory, and a superconducting magnetometer may be required to give more satisfactory results. Results from samples collected in areas of folding should be corrected for the dip of the beds, giving an increasing possibility of error. For more certain results, samples should be collected from a stable block in areas of horizontal strata. Highly dispersed paleomagnetic results should also be used as little as possible. Data with a radius of the circle of 95% confidence in the mean direction (α_{95}) of less than 10° should be used.

Where more precise data is not available, the author has been obliged to use data with a larger radius of uncertainty. From the 255 determinations given in Appendix 6, 36 % have α_{95} of more than 10°. In reconstructing the positions of paleocontinents, paleomagnetic data, especially paleomagnetic declination and paleolatitude, should be respected.

(2) Similarities in paleobiography and geological evolution, the concordance of the orientation of deformation in different plates, and of the principal stress orientations of intraplate deformation, and movement characteristics of plates should also be considered and respected. Taking these factors into account will enable plates to be placed in their most probable relative positions, at least in an E-W direction.

(3) Movement of lithospheric plates takes place by plastic deformation and flow of the asthenosphere. It is only possible for a plate or block to move for a certain distance in a particular direction and they cannot leapfrog over adjacent blocks. From plate movements at the present day, reasonable rates of movements of a plate or block are from a few centimeters to dozens of centimeters per year. Suggestion of more rapid rates of movement should be treated with the greatest suspicion.

(4) China and its adjacent areas are composed of a very large number of small continental blocks which developed over their long geological history. It is very difficult to reconstruct the positions of each of these paleocontinental blocks throughout geological time. In reconstructing the history of China the following principle is adopted: first to establish the paleo-positions of the largest blocks surrounding the East Asian continent, Siberia, Australia and India, and then to determine the position of the larger blocks within the Chinese continent, Sino-Korea, Yangtze, Cathaysian and Tarim, and finally to fit in with dozens of smaller blocks. This approach forms a sound basis for reconstructing the positions of the paleocontinental blocks through out.

Prof. Zhu H helped the author for two years, and selected 81 studies on the Chinese continent and its adjacent areas and collected 255 high precision paleomagnetic data from different blocks and different tectonic periods (Appendix 6) to compile a series of paleotectonic reconstructions (see Chapters 4 to 10). Although the original data were collected with care, the results are still not entirely satisfactory. The kinematics of the development of the Chinese continent and its adjacent areas will be discussed in later chapters.

Though the above four principles are used to select paleomagnetic data to reconstruct the positions of the paleocontinents, the results may still be ambiguous, and it is evident that further research is required. Research in paleotectonic reconstruction is a purely technical process, and breakthroughs in the techniques of paleomagnetism and methods of paleogeographic reconstruction are required, in order to make improvements in results.

1.4.4 The Dynamics of Block Deformation

The study of the mechanisms which have affected the continental blocks is based on the collection of data on rock deformation and the establishment of the relationships between magmatism, metamorphism and the kinematics of surrounding plates. It may be possible to determine the original dynamics of deformation by identifying the orientation and magnitude of the tectonic stress, the temperatures, pressures, depths and geothermal gradients at the time the rock was deformed, dating the time of the episode of deformation, and then proceeding to discuss deformation mechanisms and dynamics.

Stress can be determined with respect to three mutually perpendicular principal stress axes (σ_1, maximum compression = shortening stress axis; σ_2, intermediate; σ_3, minimum compression = the extension stress axis), σ_2 may be equal to or have any value intermediate between σ_1 and σ_3. The method of using conjugate shear joint system to calculate the orientation of the three principal axes of stress was first proposed by Bucher (1920–1921) and popularized in the U.K. by Anderson (1951) and in Russia by Gzovsky (1957, 1975). Now many different types of rock deformation (folds, faults, lineations, foliations and some microstructures) can be used to determine the attitudes of the axes of principal stress (Wan TF, 1988).

Commonly, stress has been analyzed on the assumption that a block is homogeneous. Although this is rarely the case,no matter whatever the original tectonic features are, even if there are faults or other zones of weakness in the basement, the strike of syn-sedimentary extension faults or joint systems in the overlying cover will be sub-parallel to the axis of principal compressive stress in the newer tectonic stress field. Extensional features are favorable conduits for the movement, accumulation and leakage of the oil and gas commonly found in sedimentary basins. If faults or shear joint systems are developed in a homogeneous basement and cover, the strike of syn-sedimentary structures will have an angle of 30° to 45° to the axis of principal compressive stress. Even if the basement and cover are inhomogeneous, the axis of maximum principal compressive stress and the strike of the syn-sedimentary extension and shear faults and extension joint systems will usually be almost parallel. Actual tectonic systems are often more complex. If a simple tectonic model is considered only, tectono-chronology may be overlooked, as rock deformation may have occurred at several different periods in response to different stress fields. The consideration of homogeneous materials is not a realistic way to resolve structural problems.

In recent tectonic research in the Chinese continent, different tectonic systems have been recognized in different tectono-stratigraphic units, influenced by different tectonic stress fields (Wan TF, 1988, 1994). It is important to divide the deformation history into separate tectonic periods and tectonic events, and to clarify the kinematics and dynamics of each tectonic event. By comparing the attitude of principal stress axes in each of the tectono-stratigraphic units in the Chinese continent, the orientation of the principal compressive stress axes has been determined for each tectonic period since the Neoproterozoic (Fig. 1.5) (Appendix 3).

Outcrops of rocks after the Paleozoic are widespread on the continental blocks which make up China, so that data is abundant and the orientations of regional stress and the tectonic stress fields can be reconstructed, as presented in this book. However, outcrops of rocks before the Paleozoic are much less extensive. It is difficult to recognize the tectonic significance of different stress orientations in scattered and limited outcrops. Also the crustal blocks have been subject to displacement and rotation, so that it is more difficult to reconstruct the paleotectonic stress field; much more research is needed into this aspect of tectonics.

For the determination of the present day orientation of tectonic stress vectors, seismic data from earthquake shocks is used to find fault plane solutions (or called earthquake focal mechanism solution). The principles and methods for these determinations will be discussed in Chapter 11.

In tectonic dynamics, it is not sufficient to determine the orientation of tectonic stress only, it is also necessary to estimate the strength of the stress. The value of tectonic stress is usually expressed in terms of differential stress, namely, the difference between the values of the maximum and minimum principal compressive stress. From experiments in rock mechanics and the transmission electron microscope (TEM) observations, many researchers have recognized a relationship between ultra-microstructures and magnitude of differential stress. Over the last thirty years, using TEM, Wan TF (1988) has recognized that the examination of ultra-microstructures provides a satisfactory method of estimating values of tectonic stress, although the precision of this estimation is so far only semi-quantitative. The ratio of dynamically recrystallized grains, sub-grains, or dislocation density shows a stable relationship to the magnitude of differential stress, determined experimentally on natural rock specimens (Durham et al., 1977; Nuttal and Nutting, 1978; White, 1979; Ross et al., 1980). Gueguen and Darot (1980) investigated the ultra-microstructure of olivine experimentally and concluded that intra-crystal free dislocation density structure is most reliable to determine the magnitude of paleotectonic stress. Their conclusions were confirmed by Durham et al. (1977), Nuttal and Nutting (1978) and Wan TF (1988, 1989, 1992, 1994, 1997).

Wan TF and Cao XH (1997) conducted research on several hundred samples of magmatic rocks, mylonites, and vein quartz from Chinese continent, ranging in ages from the Triassic to Early Pleistocene. They found that the method of determining the intra-crystal free dislocation density structure (Fig. 1.9) is equally suitable for the study of ductile and brittle deformation. In many weakly deformed sedimentary, magmatic and metamorphic rocks, it is possible to determine the differential stress and an accurate isotopic age at the same time. Differential stress values of known isotopic age provide the most useful data for tectonic research. Quartz and olivine in magmatic and metamorphic rocks formed during a syntectonic period are used to estimate differential stress. Dislocations occur very readily in calcite, and the dislocation density is observed easily using TEM, but is not usually used to estimate differential stress values. Clastic quartz from sedimentary quartz sandstones should not be used for the estimation of the magnitude differential stress, as any dislocations may have been inherited from the source rock, but it is possible to use secondary quartz in sandstone formed during diagenesis.

The intra-crystal free dislocation density structures are usually formed during the first tectonic event following crystallization and diagenesis, and the amount of displacement increases along existing dislocations during later tectonic events, without an increase in the density of dislocations (Guo TY and Wan TF, 1988). Dislocation structures only disappear or change their densities when the mineral is affected by later strong metamorphism or partial re-melting, and the original minerals re-crystallize or change into new minerals. During multiple tectonic events, where the change in the tectonic setting is not obvious, the intra-crystal free dislocation density structures are not increased by later stages of deformation. This observation has been confirmed many times in the Mesozoic–Cenozoic rocks in many intraplate areas of China (Wan TF, 1988, 1994, 1995, 1997). Where deformed rocks have yielded isotopic or geological ages, the intra-crystal free dislocation density provides a suitable method of determining the strength of plate tectonic stress, especially for intraplate deformation. However, in subduction or collision zones, especially those of younger ages, where the rocks may be re-metamorphosed or partially melted in a major subduction or collision stage, new dislocations are formed in the mineral, and old dislocations may be re-activated, and in this case, it is very difficult to distinguish new dislocations from old ones.

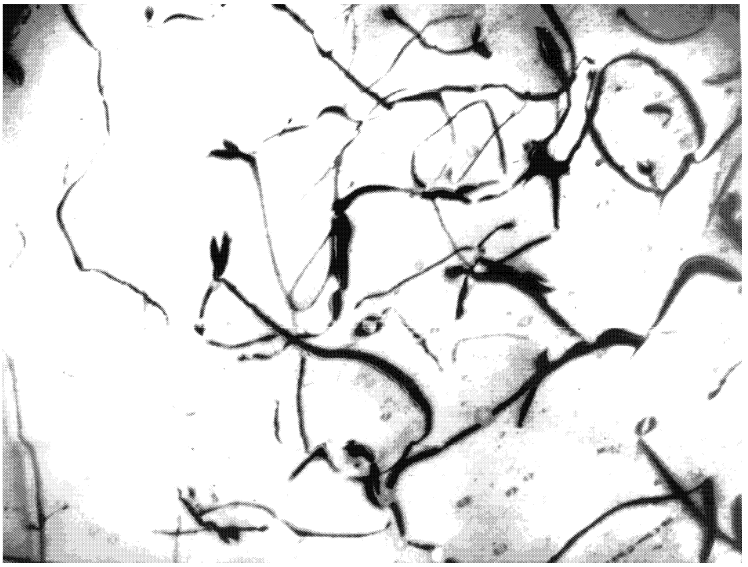

Fig. 1.9 Intra-crystal free dislocation of quartz, collected on TEM (1 cm on photo equals 1 μm).

When using the dislocation density (ρ) in quartz to estimate differential stress ($\Delta\sigma$), the experimental formula, proposed by McCormick (1980), is similar to that of actual geological examples, the formula was obtained by experiments in quartz with water, abundant and widespread in the Earth's crust. Using different methods, Christie and Ord (1980) concluded that the experimental formula of McCormick (1980) was reliable, and Wan TF (1988) has confirmed these results.

Because of the limitations of research projects and financial constraints, the author and his colleagues have determined only 478 samples of differential stress from different tectonic periods of the Mesozoic–Cenozoic in China during the last twenty years. The results of these experiments carried out in China and abroad are compiled in Appendix 4.

The magnitude of differential stress is very little influenced by formation temperature, strain rate, rock characteristics, etc., thus, it settles the difficult problem in using data from rock mechanic experiments to estimate tectonic strength, but it cannot define the time over which the stress operated, i.e. the strain rate problem. In contrast with determination of differential stress, the magnitude of strain depends not only on the strength of tectonism, but also on the lithology, thickness of strata, position on fold structures. Local rock deformation can be studied by taking account of these features, but it is difficult to extrapolate the results to determine regional strain data with not only local significance.

The magnitude of tectonic stress is an important and suitable quantitative parameter for determining tectonic strength. A program to estimate the magnitude of tectonic stress for whole China has only just commenced. Earlier research has been directed at the choice of methods and regional reconnaissance. A lot of further research and experiments will be necessary to determine tectonic stress magnitudes and their orientations in different areas and stages for Chinese continent.

The principles and methods for determining recent quantitative tectonic stress magnitude, using hydraulic fracturing, will be discussed in Chapter 11.

1.4.5 The Chronology of Deformation

The major method for establishing the chronology of deformation is still the recognition of unconformities, where un-deformed rocks of known age are seen to overlie, or are adjacent to deformed rocks. The age of deformation may be determined more exactly by dating methods using isotope chronology. It is possible to determine isotopically the age of intrusion or extrusion of igneous rocks, or the age of crystallization of metamorphic rocks (including the ages of hydrothermal alteration), using single mineral crystals. However, the dating of fault rocks is much more difficult, because faulted rocks are commonly mixed up, and formed from rocks of many different ages from both sides of the fault, therefore,"whole rock" methods of determining the age of fault rocks are usually unreliable. What is more satisfactory is to make determination by Ar-Ar, Rb-Sr, Sm-Nb, U-Pb, Re-Os methods of the age of newly crystallized minerals (e.g. amphibole, illite, mica, feldspar or quartz) formed during the faulting process. However, one has to take care to select those minerals which actually crystallized during the faulting, but this is rather difficult.

To sum up, it is necessary to study tectonics, not only by using traditional geological methods but by using comprehensive data derived from studies on biostratigraphy, biogeography, geochemistry, geophysics and using new technology.

References

Anderson EM (1951) The dynamics of faulting, 2nd edn. Oiver and Boyd, Edinburgh.

Bally AW, Scotese CR, Ross MI (1989) North America: Plate tectonic setting and tectonic elements. In: Bally AW, Palmer AR (eds) The Geology of North America—An Overview. A: pp. 1–15. GSA.

Bucher WH (1920–1921) The mechanical interpretation of joint. J. Geology 28: 707–730; 29: 1–28.

Bureau of Geology and Mineral Resources of Anhui Province (1987) Regional Geology of Anhui Province. Geological Publishing House, Beijing (in Chinese with English abstract).

Bureau of Geology and Mineral Resources of Fujian Province (1985) Regional Geology of Fujian Province. Geological Publishing House, Beijing (in Chinese with English abstract).

Bureau of Geology and Mineral Resources of Fujian Province (1992) Regional Geology of Taiwan Province. Geological Publishing House, Beijing (in Chinese with English abstract).

Bureau of Geology and Mineral Resources of Gansu Province (1989) Regional Geology of Gansu Province. Geological Publishing House, Beijing (in Chinese with English abstract).

Bureau of Geology and Mineral Resources of Guangdong Province (1988) Regional Geology of Guangdong Province. Geological Publishing House, Beijing (in Chinese with English abstract).

Bureau of Geology and Mineral Resources of Guangxi Zhuang Autonomous Region (1985) Regional Geology of Guangxi Zhuang Autonomous Region. Geological Publishing House, Beijing (in Chinese with English abstract).

Bureau of Geology and Mineral Resources of Guizhou Province (1987) Regional Geology of Guizhou Province. Geological Publishing House, Beijing (in Chinese with English abstract).

Bureau of Geology and Mineral Resources of Hebei Province (1989) Regional Geology of Hebei Province, Beijing and Tianjin Municipality. Geological Publishing House, Beijing (in Chinese with English abstract).

Bureau of Geology and Mineral Resources of Heilongjiang Province (1993) Regional Geology of Heilongjiang Province. Geological Publishing House, Beijing (in Chinese with English abstract).

Bureau of Geology and Mineral Resources of Henan Province (1989) Regional Geology of Province Henan. Geological Publishing House, Beijing (in Chinese with English abstract).

Bureau of Geology and Mineral Resources of Hubei Province (1990) Regional Geology of Hubei Province. Geological Publishing House, Beijing (in Chinese with English abstract).

Bureau of Geology and Mineral Resources of Hunan Province (1988) Regional Geology of Hunan Province. Geological Publishing House, Beijing (in Chinese with English abstract).
Bureau of Geology and Mineral Resources of Inner Mongolia Autonomous Region (1991) Regional Geology of Inner Mongolia Autonomous Region. Geological Publishing House, Beijing (in Chinese with English abstract).
Bureau of Geology and Mineral Resources of Jiangsu Province (1984) Regional Geology of Jiangsu Province and Shanghai Municipality. Geological Publishing House, Beijing (in Chinese with English abstract).
Bureau of Geology and Mineral Resources of Jiangxi Province (1984) Regional Geology of Jiangxi Province. Geological Publishing House, Beijing (in Chinese with English abstract).
Bureau of Geology and Mineral Resources of Jilin Province (1988) Regional Geology of Jilin Province. Geological Publishing House, Beijing (in Chinese with English abstract).
Bureau of Geology and Mineral Resources of Liaoning Province (1989) Regional Geology of Liaoning Province. Geological Publishing House, Beijing (in Chinese with English abstract).
Bureau of Geology and Mineral Resources of Ningxia Hui Autonomous Region (1990) Regional Geology of Ningxia Hui Autonomous Region. Geological Publishing House, Beijing (in Chinese with English abstract).
Bureau of Geology and Mineral Resources of Qinghai Province (1991) Regional Geology of Qinghai Province. Geological Publishing House, Beijing (in Chinese with English abstract).
Bureau of Geology and Mineral Resources of Shaanxi Province (1988) Regional Geology of Shaanxi Province. Geological Publishing House, Beijing (in Chinese with English abstract).
Bureau of Geology and Mineral Resources of Shandong Province (1991) Regional Geology of Shandong Province. Geological Publishing House, Beijing (in Chinese with English abstract).
Bureau of Geology and Mineral Resources of Shanxi Province (1989) Regional Geology of Shanxi Province. Geological Publishing House, Beijing (in Chinese with English abstract).
Bureau of Geology and Mineral Resources of Sichuan Province (1991) Regional Geology of Sichuan Province. Geological Publishing House, Beijing (in Chinese with English abstract).
Bureau of Geology and Mineral Resources of Xinjiang Uygur Autonomous Region (1993) Regional Geology of Xinjiang Uygur Autonomous Region. Geological Publishing House, Beijing (in Chinese with English abstract).
Bureau of Geology and Mineral Resources of Xizang (Tibet) Autonomous Region (1993) Regional Geology of Xizang Autonomous Region. Geological Publishing House, Beijing (in Chinese with English abstract).
Bureau of Geology and Mineral Resources of Yunnan Province (1990) Regional Geology of Yunnan Province. Geological Publishing House, Beijing (in Chinese with English abstract).
Bureau of Geology and Mineral Resources of Zhejiang Province (1989) Regional Geology of Zhejiang Province. Geological Publishing House, Beijing (in Chinese with English abstract).
Cande SC, La Brecque JL, Larson RL et al (1989) Magnetic lineations of the world's ocean basins. AAPG, Tulsa, Oklahoma.
Cande SC, Kent DV (1992) A new geomagnetic polarity time scale for the Late Cretaceous and Cenozoic. J. Geophys. Res. B 97(10): 13917–13951.
Chen FJ, Wang XW, Zhang GY et al (1992) Structure and geodynamic setting of oil and gas basins in the People's Republic of China. Geoscience 6(3): 317–327 (in Chinese with English abstract).
Cheng YQ (1994) An Introduction to Regional Geology of China. Geological Publishing House, Beijing (in Chinese).
Chi JS (1988) The Study of Cenozoic Basalts and Upper Mantle Beneath Eastern China (Attachment Kimberlites). China University of Geosciences Press, Wuhan (in Chinese with English abstract).
Chi JS, Lu FX, Zhao L et al (1996) The Kimberlites and Paleozoic Features of Lithospheric Mantle of North China Platform. Science Press, Beijing (in Chinese).
Christie JM, Ord A (1980) Flow stress from microstructures of mylonites: example and current assessment. J. Geophy. Res. 85(B11): 6253–6262.

Condie KC (2001) Mantle Plumes and Their Record in Earth History. Cambridge University Press, Cambridge.

Cuvier G, Latreille PA (1817) Le Rène Animal Distribué d'après son Organisation, pour Servir de Base à l'Histoire Naturelle des Animaux et d'Introduction à l'Anatomie Comparée. Tome I. L'Introduction, Les Mammifères et Les Oiseaux. Paris: Deterville. 540pp. A.T.: comparative anatomy

Deng JF, Mo XX, Zhao HL et al (1997) Geotectonic units of China continent on a lithospheric scale since Cenozoic. Earth Science 22(3): 227–232.

Deng JF, Zhao HL, Wu ZX et al (1992) A mantle plume beneath the north part of China continent and lithosphere motion. Geoscience 6(3): 267–274 (in Chinese with English abstract).

Deng JF, Zhao HL, Mo XX et al (1996) Continental Roots—Plume tectonics of China. Geological Publishing House, Beijing.

Durham WB, Geotze C, Blake B (1977) Plastic flow of oriented single crystals of olivine. Part ll, Observations and interpretations of the dislocation structures. Jour. Geophys. Res. 82(36): 5755–5770.

Gilluly J (1949) Distribution of mountain building in geologic time. Geol. Soc. Am. Bull. 60: 561–590.

Gordienko IV, Kuz'min MI (1999) Geodynamics and metallogeny of the Mongolo-Transbaikalian region. Russian Geology and Geophysics 40(11): 1522–1538.

Gretener PE (1981) Pore pressure discontinuities, isostasy and overthrusts. In: McClay KR, Price NJ (eds) Thrust and Nappe Tectonics. Blackwell Scientific Publication, London.

Gueguen Y, Darot M (1980) Microstructures and stresses in naturally deformed peridotites. Rock Mechanics 9(Suppl.): 159–172.

Guo TY, Wan TF (1988) Estimations of paleotectonic stress magnitude in Rutog-Burang area, Western Xizang-Qinghai Plateau, China. Geoscience 12(1): 57–66 (in Chinese with English abstract).

Gzovsky MB (1957) Tectonic Stress Field. In: Structural Geology Special Collection of Geology, vol 6. Geological Publishing House, Beijing.

Гэовский MB (1975) Основы Тектонофиэики. (Introduction to Tectonophysics) Издательство (Hayka), Moscow (in Russian).

Hsu KJ (1989) Time and place in Alpine orogenesis. Geol. Soc. London Spec. Pub. 45: 421–443.

Hutton J (1785) Theory of the Earth. F.R.S. Edinburg and Members of the Royal Academy of Agriculture at Paris.

International Commission on Stratigraphy (2004) International Stratigraphic Chart. 32th IGC, Florence, Italy.

Jiang CF, Yang JS, Feng BG et al (1992) The Open and Close Structure of Kunlun. Geological Publishing House, Beijing.

Jiang CF (1997) Opening-closing tectonics of Tarim platform. Xinjiang Geology 15(3): 193–202.

Li JL (1991) Time and special problems of lithospheric tectonic evolution in orogenic belts. In: Annual Reports (1989—1990) of Open Laboratory of Lithosphere Tectonic Evolution, Institute of Geology, Chinese Academy of Sciences. China Science and Technology Press, Beijing.

Le Pichon S, Francheteau J, Bonin J (1973) Plate Tectonics. Elsevier Publishing Company, New York.

Li PX, Pang QQ, Cheng ZW, 2000. The continental Jurassic–Cretaceous boundary and critical stage in northern China. In: Proceedings of the Third National Stratigraphical Conference of China. Geological Publishing House, Beijing.

Li ZX, Powell CM, Trench A (1993) Palaeozoic global reconstructions. In: Long JA (ed) Palaeozoic Vertebrate Biostratigraphy and Biogeography. Belhaven Press, London.

Lin JL, Fuller M, Zhang WY (1985) Preliminary Phanerozoic polar wander paths for the north and south China blocks. Nature 313: 444–449.

Lu SN, Li HK, Yu HF (2001) Geological events, event sequence and event group. Geological Review 47(5): 521–526 (in Chinese with English abstract).

Lyell C (1830—1833) Principles of Geology, vols. 1–3c. 1st edn. John Murray, London.

Ma ZJ, Gao XL (1996) Three global-scale seismotectonics systems and geoid. Journal of Southeast Asian Earth Sciences 13(3–5): 337–340.

McCormick JW (1980) Transmission electron microscopy of experimentally deformed synthetic quartz. Dissertation, University of California, Los Angles.
McElhinny MW, Valencio DA (1981) Paleoconstruction of the Continents. Geodynamic Series. Geological Society of America, Boulder, Colorado.
Mo XX (1991) Volcanism and the evolution of Tethys in Sanjiang area, southwestern China. In: Proceedings of the 1st International Symposium on Gondwana Dispersion and Asian Accretion. Kunming, China.
Mo XX, Lu FX, Sheng SY et al (1993) Sanjiang Tethyan volcanism and related mineralization. Geological Memoirs 20: 267. Geological Publishing House, Beijing.
Mo XX, Sheng SY, Zhu QW et al (1998). Volcanic-ophiolite and Mineralization of Middle-southern Part in Sanjiang Area of Southeast China. Geological Publishing House, Beijing.
Muehlberger WR, Tauyers PR (1989) Tectonosynthems and new tectonic map of North America. In: Abstracts of the 28th International Geological Congress. Washington DC, USA.
Nuttal J, Nutting J (1978) Structure and properties of heavily coldworked for metals and alloys. Met. Sci. 12: 430–437.
Powell CM, Li ZX, McElhinny MW et al (1993) Paleomagnetic constraints on timing of the Neoproterozoic breakup of Rodinia and the Cambrian formation of Gondwana. Geology 21: 889–892.
Press F, Siever R (1974) Earth. 1st edn. W. H. Freeman and Company, San Francisco.
Qian XL (1996) The nature of the Early Pre-cambrian continental crust and its tectonic evolution model. Acta Petrologica Sinica 12(2): 169–178 (in Chinese with English abstract).
Ramsay JG (1985) Folding and Fracturing of Rocks. The Blackburn Press, Caldwell.
Ramsay JG, Huber MI (1991) The techniques of modern structural geology. vol 1: Strain Analysis; vol 2: Folds and Fractures. Academic Press, New York.
Remane J et al (2000) International Stratigraphic Chart. International Commission on Stratigraphy.
Rogers G, Dunning GR (1991) Geochronology of appinitic and related granitic magmatism in the West Highlands of Scotland: constraints on the timing of transcurrent fault movement. J. Geol. Soc. London 148, part 1: 17–27.
Ross JV, Ave LHG, Carter NL (1980) Stress dependence of recrystallized-grain and subgrain size in olivine. Tectonophysics 70(1–2): 39–61.
Scotese CR, Bambach RK, Barton C et al (1979) Paleozoic base maps. Journal of Geology (University of Chicago) 87(3): 217–277.
Scotese CR (1986) Phanerozoic reconstructions: a new look at the assembly of Asia. University of Texas, Institute for Geophysics Technical Report, no.66, 54pp.
Scotese CR (1994) Continental Drift, 6th edn. The PALEOMAP Project, University of Texas at Arlington.
Sengör AMC (1982) Edward Suess' relations to the pre-1950 schools of thought in global tectonics. Geol. Rundsch. 71(2): 381–420.
Sengör AMC, Natal'in BA (1996) Paleotectonics of Asia: fragments of a synthesis. In: Yin A, Harrison TM (eds) The Tectonic Evolution of Asia. Cambridge University Press, Cambridge.
State Bureau of Surveying and Mapping (2008) Map of the People's Republic of China. http://www.sbsm.gov.cn. Accessed on 10 Mar 2010.
Sugisaki R (1976) Chemical characteristics of volcanic rocks: relation to plate movements. Lithos 9(1): 17–30.
Sun Y, Shen XZ, Liu SH (1982) Preliminary analysis of some chemical determined by comprehensive fault zone at Dayu, Jiangxi Province. Geochemica (4): 348–356 (in Chinese with English abstract).
Sun Y, Xu SJ, Liu DL et al (1998) An Introduction of Tectono-geochemistry in Fault Zones. Science Press, Beijing.
Tao SL, Wan TF, Cheng J (1999) Introduction to earth science. Geological Publishing House, Beijing.
Tarling DH (1985) Problems in Paleozoic paleomagnetism. Journal of Geodynamics 3(1–2): 87–103.
Trewin NH (2002) The Geology of Scotland, 4th edn. The Geology Society of London, London.

Van der Voo R (1988) Paleozoic paleogeography of North Ameriacan, Gondwana and intervening displaced terranes: comparisons of paleomagnetism with paleoclimatology and biogeographical patterns. GSA Bulletin 100(3): 311–324.
Van der Voo R (1993) Paleomagnetism of the Atlantic, Tethys and Iapetus Oceans. Cambridge University Press, Cambridge.
Vasilivsky HP (1964) Argument about tectonic development and genesis. Translation Collection on Geology (5): 17–22.
Wan TF (1988) Paleo-tectonic Stress Field. Geological Publishing House, Beijing.
Wan TF, Zhu H (1989) Cretaceous–Early Eocene tectonic stress field in China. Acta Geologica Sinica 2(3): 227–239.
Wan TF (1992) Tectonic evolution and stress fields of Shandong Province. Geology of Shandong 8(2): 70–101 (in Chinese with English abstract).
Wan TF, Cao RP (1992) Tectonic events and stress fields of Middle Eocene–Early Pleistocene in China. Geoscience 6(3): 275–285 (in Chinese with English abstract).
Wan TF (1994) Intraplate Deformation, Tectonic Stress and Their Application for Eastern China in Meso-Cenozoic. China University of Geosciences Press, Wuhan.
Wan TF, Cao XH (1997) Estimation of differential stress magnitude in Middle–Late Triassic to Early Pleistocene for China. Earth Science 22(2): 145–152 (in Chinese with English abstract).
Wang HZ (1982) The main stages of crustal development of China. Earth Sciences—Journal of Wuhan College of Geology (3): 155–177 (in Chinese with English abstract).
Wang HZ (1985) Atlas of Paleogeography of China. SinoMaps Press, Beijing.
Wang HZ, Li GC (1990) Comparative Table of International Strata Ages. Geological Publishing House, Beijing.
Wang HZ, Yang SN, Liu BP et al (1990) Tectonopaleogeography and Paleobiogeography of China and Adjacent Regions. China University of Geosciences Press, Wuhan.
Wegener A (1966) The origin of continents and oceans. Dover Publications, New York (first published at 1924).
White S (1979) Difficulties associated with paleo-stress estimates. Bull. Mineral. 102: 210–215.
Wilson JT (1970) Continents Adrift: Readings from Scientific American. W. H. Freeman and Company, San Francisco.
Windley BF (1995) The Evolving Continent, 3rd edn. John Wiley Sons, Chichester, New York.
Woodward NB, Boyer SE, Suppe J (1989) Balaced geological cross-sections. American Geophysical Union.
Yang WR, Guo TY, Lu YL et al (1984) "Opening" and "closing" in the tectonic evolution of China. Earth Sciences (3): 39–56 (in Chinese with English abstract).
Yang WR, Liu YY, Yang ZH et al (1993) Probing into the open and close of Asian continent from the new results of paleomagnetism from Qinling orogenic belt and the paleoland on both sides. In: China Working Group on International Geological Comparison Program. Project 321. Growth of Asia. Seismological Press, Beijing.
Yin A, Nie SY (1996) A Phanerozoic palinspastic reconstruction of China and its neighboring regions. In: Yin A, Harrison TM (eds) The Tectonic Evolution of Asia. Cambridge University Press, Cambridge.
Yu CW (2003) The Complexity of Geosystems. Geological Publishing House, Beijing.
Zhang SH, Li ZX, Wu HC et al (2000) New paleomagnetic results in Neoproterozoic of the north China block and their paleogeographic implications. Science in China D 43(7): 233–244.
Zhang WY et al (1959) An Outline of Tectonics of China. Science Press, Beijing.
Zhu RX, Yang ZY, Wu HN (1998) Magnetic APWP and block moving of China main blocks in Phanerozoic. Science in China D 28: 1–16.
Zhu RX, Tschu K-K (2001) Studies on Paleomagnetism and Reversals of Geomagnetic Field in China. Science Press,Beijing.

Zhu ZC (1996) Thinking on some important geotectonic problems. Geological Science & Technology Information 15(4): 1–7 (in Chinese with English abstract).

Ziegler AM, Rees PM, Rowley DB et al (1996) Mesozoic assembly of Asia: constraints from fossil floras, tectonics and paleomagnetism. In: Yin A, Harrison TM (eds) The Tectonic Evolution of Asia. Cambridge University Press, Cambridge.

Chapter 2
Tectonics of Archean and Paleoproterozoic (Before 1.8 Ga)

It is considered that the continental crust began to form between 4.2 and 3.6 Ga ago. The Archean (4.6–2.5 Ga) and Paleoproterozoic (2.5–1.8 Ga) periods account for more than 60% of the whole of the Earth history. It is therefore not surprising that the greater part of the present continental crust, 70%–80% or more, was developed during the Neoarchean (2.8–2.5 Ga) and Paleoproterozoic (2.5–1.8 Ga). The processes for the formation of the continental crust of China were similar to those for the other continents on the Earth. Rocks formed during the Archean and Paleoproterozoic occur mainly in the lower crust, and their outcrops form between 5% and 8% of the surface area of the Chinese continent.

2.1 The Eoarchean (EA, 4.6–3.6 Ga)

—planetesimal theory, allumulation model of the Earth and the formation of proto-continental nuclei

The study of the origin of the Earth is related closely to the study of the evolution of the solar system as a whole. It is believed that the Earth was produced by the accumulation and accretion of planetesimals, composed largely of the heavier elements, which had previously condensed from the solar nebula (Safranov, 1972; Dai WS, 1979). On the other hand, the sun is composed of the lighter elements, mainly hydrogen (70%), helium (27%) and small proportions of more than 100 other elements (3%), with a similar composition to the original solar nebula.

Therefore the Earth's composition is very different from that of the sun, containing a much higher proportion of the heavier elements. The Earth's composition has been compared to that of chondritic meteorites, considered to be material originally condensed from the solar nebula, the remnants of which now reside in the asteroid belt. The internal structure of the Earth has been determined from the velocity of deep seismic waves passing through the Earth, compared with laboratory experiments on probable Earth materials at high temperatures and pressures. The Earth, with a similar composition to the other terrestrial planets, is composed of Fe (34.6%), O (29.5%), Si (15.2%), Mg (12.7%), Ni (2.4%), Ca (2.2%), Al (2.2%), S (1.9%) and more than 100 other elements (1.5%). From Rb-Sr isotopic chronology it has been found that the Earth and most chondrites were formed at 4.55 Ga, more recently Re-Os isotopic chronology has given an age of 4.57 Ga (Stassen, 2005).

According to the accumulation hypothesis for the origin of the primordial Earth, it is considered that the solid Earth was formed by the aggregation of planetesimals*, mainly with the composition of

* Planetesimals are classified in the same way as meteorites: M-group are iron meteorites; chondrites, i.e. stony meteorites, are made up of chondrules with olivine and pyroxene, surrounded by iron-nickel facies, troilite, and their chemical composition is similar to ultrabasic rock. According to the proportion of metallic iron and ferric oxide, chondrites can be classified into: (1) Enstatite chondrites (E-group); (2) Ordinary chondrites (H-, L-, LL-group), in which H-group is high ferrous chondrites; L-group is low ferrous chondrites; LL-group is the least ferrous chondrites. (3) Carbonaceous chondrites (C-group), which can also be subdivided into three types, C-Ⅰ, C-Ⅱ, C-Ⅲ.

chondritic meteorites, but icy planetismals may have contributed components of the atmosphere and hydrosphere. By analogy with the evolution of the moon, the growth of the terrestrial mass and volume resulting from meteorite impact and accretion occurred exponentially over a period of about 50 million years (Ouyang ZY et al., 2002). After 4.0 Ga the number of meteorite impacts decreased very rapidly, and the augmentation of the Earth's mass since that time, caused by the impacts, has been only 10^{25} grams, 1/600 of its total mass. This implies that accretion of the Earth effectively ceased at about 4.0 Ga, and the mass and volume of the Earth has since remained essentially unchanged. Today the Earth has a total mass of approximately 5.976×10^{27} grams (Allègre, 1985). Recent studies indicate that the process of planetesimal accretion was inhomogeneous, rather than homogeneous (Turekian and Clark, 1969). Based on the results of earlier studies, Ouyang ZY et al. (1995, 2002) proposed recently that the process of accumulation of the planet Earth could be divided into two periods, a period of inhomogeneous accretion and multi-period of accumulation:

1. Proto-Earth was formed by the accumulation of "gaintstars", with a diameter of more than 3, 000 km, accreting to about 70%–90% of the present Earth mass. The gaintstars were composed of M-group planetesimals, mainly iron, and L-group planetesimals whose composition was similar to that of the moon. During the accretion and accumulation process the heavier materials sank towards the center of the Earth under the influence of gravity. As material was continually added to the exterior the pressure increased, heating the materials diabatically, until the interior of the Earth became largely or completely molten. Continual differentiation, with the sinking of denser materials towards the centre, and the rise of lighter materials towards the surface, has led to the development of the present sphere structure of the Earth.

Due to its high density, iron was segregated towards the center of the Earth to form an iron and nickel-rich core, which now accounts for about one third of the mass of the Earth's interior. Towards the surface, lighter silicates formed the proto-crust and proto-mantle. Mg-rich silicates, with a perovskite crystal structure and a higher density, sank and condensed to form the lower mantle. Low-density silicates, with a composition similar to lunar rock and rich in rare earth elements (REE), potassium, phosphorus, uranium and thorium, moved upwards to form a proto-crust, equivalent to the present transition layer of the mantle at a depth of 400–670 km. The crust, mantle and core of proto-Earth have subsequently undergone fractional melting, emphasizing the layered structure. On the whole, the Earth has maintained a stable gravitational equilibrium and a spherical structure, since it was formed at 4.5 Ga.

2. Because the upper mantle and crust are laterally inhomogeneous at the present time, it is proposed that smaller C-group or L-group planetesimals, with an average diameter of 400 km, were accumulated at a late period in the accretion process to form the outer layers of the Earth. These planetismals were partially melted and differentiated after they accumulated on the surface of the cooling proto-Earth. The proto-crust was formed from the partial melting of this proto-upper mantle layer and the process of differentiation of the upper mantle and crust continued since 4.46 Ga.

In Allègre's (1985) model the aggregative process of planetesimals or meteorites was a homogeneous process and layering of the Earth was formed by gravitational differentiation. This model does not account for the present lateral inhomogeneity of the crust and upper mantle, but the inhomogeneity is accounted for in the accretion-multiperiod accumulation model (Ouyang ZY et al., 1995, 2002), according to the Pb, Nb and O isotopic data from Gondwana and Laurentia and their affiliated continents (Turekian and Clark, 1969; Chou et al., 1983; Newsom, 1990; Jacobsen and Wasserburg, 1984). Many other explanations have been offered to resolve this problem, but these will not be discussed here.

From his study of oxygen isotopes, Clayton et al. (1973, 1976, 1983) found that all samples collected from the Earth or the moon lay on the same straight line, with a slope (i.e. the ratio of $\delta^{17}O / \delta^{18}O$) of about 0.52 on a $\delta^{17}O - \delta^{18}O$ diagram. The Earth, the moon and meteorites derived from the solar system show a parallel evolution of their oxygen isotopes, with the same slope, but with different intercepts. On the basis of differences in the characteristics of their oxygen isotopic evolution, meteorites can be divided into six types (chondrite L, LL, H, E, C2 and C3), and it is believed that this represents a primary inhomogeneity in their chemical composition (Fig. 2.1).

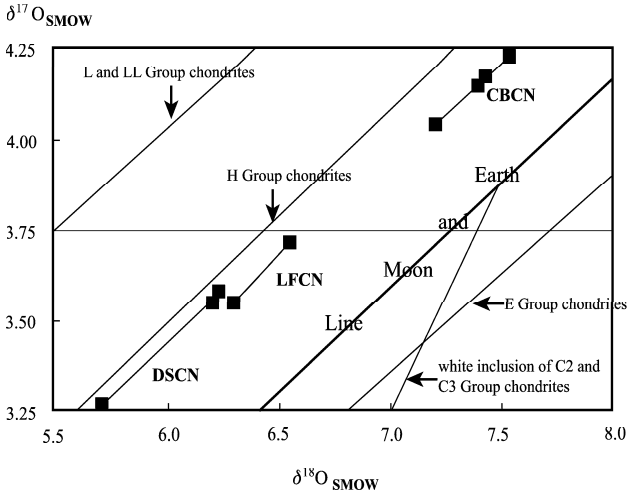

Fig. 2.1 Oxygen isotopic composition of three nuclei of Sino-Korean continental proto-block (after Ouyang ZY et al., 2002, original diagram from Clayton et al., 1973, with permission of Ouyang ZY).

DSCN (Dongsheng nucleus): slope = 0.5886, intercept = 0.0918; CBCN (Circum-Bohai continental nucleus): slope = 0.5617, intercept = 0.0103; LFCN (Linfen nucleus): slope = 0.6431, intercept = 0.4988.

Ouyang ZY et al. (2002) plotted the oxygen isotopic composition of the various nuclei of the Sino-Korean protoblock on a $\delta^{17}O-\delta^{18}O$ diagram (Fig. 2.1) and found that despite the great difference in their isotopic ages, sometimes as many as 800 Ma, the evolutionary trends of the samples are almost all parallel to the trends given by the Earth and the moon. The similarity in their slopes implies that all these materials originated in the solar system. However, the oxygen isotopic intercepts of Dongsheng, Circum-Bohai and Linfen nuclei (Figs. 2.1 and 2.3) are different. It is reasonable to infer that differences in oxygen isotopic evolution reflect inhomogeneities in the isotopic composition of their proto-mantle source, and were not made during the evolution of crust-mantle system. After their formation, the lithospheric plates containing these nuclei have been affected by multiphase horizontal movements, so that their oxygen isotopic characteristics are not related to those of the mantle that lies immediately beneath them at present. In addition, samples from North China and H-group chondrites show similar oxygen isotopic evolutionary trends, which indicate that the primitive composition of Sino-Korean Protoblock was similar to that of H-group chondrites. In future the oxygen isotope composition of the other Chinese continental blocks will also be studied.

In the Eoarchean, the Earth was still frequently impacted by meteorites, which repeatedly fractured the brittle protocrust, forming many large craters and causing the uprise of the mantle, with the generation of intense volcanic eruptions, accompanied by the escape of volatiles. The volatiles were composed mainly of CO_2, helium and water vapor and formed the proto-atmosphere. Below the critical temperature, the water vapor condensed into liquid water to form the primitive ocean (hydrosphere).

Allègre (1985) estimated that by 4.3 Ga, approximately three quarters of the core had been formed, and the mantle was almost thoroughly solidified, although thermal convection was still intense. The atmosphere had also been formed by 4.4 Ga, with the original mass of about 85% of the present atmosphere, and composed mainly of CO_2 and CH_4, but with a temperature as high as 500–600℃and an atmospheric pressure being about 300 times the present day pressure, similar to that of Venus.

In the 1970s, rocks with an age of 3.65 Ga were found among gneisses in the western part of Greenland. Subsequently, the composition and structure of a metamorphosed conglomerate indicated that it

was once a continental sedimentary rock and was collected in the neighboring area (Isua) with pebbles giving an isotopic age of 3.77 Ga (Allègre, 1985). Wilde et al. (2001) reported that detrital zircons with an age of 4.4–4.2 Ga from Archean sedimentary rocks in northern Australia and organic carbon, formed by the metamorphism of carbonaceous organisms, were found in the neighboring area. Liu DY (1991, 1992) obtained an age of 3804±5Ma, using the zircon U-Pb method, from a granitic protocrustal remnant in the Anshan area of Liaoning Province (123°E, 41°N), and a U-Pb age of 3.72–3.65 Ga from a detrital zircon within gaebhardite (rich chromium mica) quartzite in the Qianxi Group of northeastern Hebei Province (118.3°E, 40.2°N), which implies that continental crust existed in north China during the Archean. Proto-crust with an age of 3.8 Ga has now been found in many continents (Greenland, North U.S., Canada, East Antarctica, North China and France) (Qian XL et al., 1994).

By contrast, no protocrustal ultrabasic and basic rocks which could represent the floors of Archean oceans have been found anywhere in the world. Presumably any oceanic protocrustal material which once existed has long been subducted and absorbed back into the mantle. It is presumed that oceanic protocrustal rocks formed before 4 Ga would have been similar to the plagioclasites of the lunar highlands and may be possibly represented by massive anorthosites which occur in many cratons (e.g. the Superior Province, Canada).

It is believed that the global protocrust had formed by 3.8 Ga. By that time the differences between continental crust and oceanic crust had been established, and the surface geological processes of erosion, transportation and sedimentation had commenced. Initially, the temperature of the ocean was very high, nearly at boiling point, and the sea water was highly acid and strongly corrosive. In that early period of the Earth's history weathering and erosion were much more intense than at present. In these extreme conditions thallophytes began to develop (Allègre, 1985; Bai J et al. 1996; Qian XL, 1996). In the Witwatersland, South Africa, the minerals pyrite and uraninite have been found as clastic grains in sedimentary deposits, formed at 3.4 Ga. These minerals are highly unstable in an oxidising environment, indicating that both the atmosphere and the hydrosphere were completely devoid of oxygen at that time.

2.2 Tectonics from Paleoarchean to Neoarchean (PA–NA, 3.6–2.5 Ga)

—formation of proto-continental blocks and continental cratonization

In the 1970s, great progress was made in Paleo-Neoarchean tectonic research by using unstable isotopic geochemistry to determine the ages of tectono-thermal events. This made it possible to identify groups of rocks affected by particular tectono-thermal events and to arrange them into a series of tectono-stratigraphic periods according to age (Kröner and Greiling, 1984).

Following the suggestion of Cheng YQ (1994), the tectonic periods and tectono-thermal events in China during the Archean in this volume, are named after the areas in which these periods and events were first recognized. These periods are correlated with the international stratigraphic chart (Remane, 2000; International Commission on Stratigraphy, 2004): Paleoarchean tectonic era (PA, 3.6−3.2 Ga) = Qianxi Period; Mesoarchean tectonic era (MA, 3.2−2.8 Ga) = Fuping Period; Neoarchean tectonic era (NA, 2.8−2.5 Ga) = Wutai Period (Appendix 1.1).

The average chemical composition of the present day crust (Holland and Turekian, 2004) differs greatly from the average composition of the whole Earth. The average crust is composed of SiO_2(60.6%), TiO_2 (0.72%), Al_2O_3 (15.9%), FeO_{total} (6.71%), MnO (0.1%), MgO (4.66%), CaO (6.41%), Na_2O (3.07%), K_2O (1.81%), P_2O_5(0.13%)(on web). Mineralogically the continental crust is composed principally of aluminosilicates containing oxygen, silicon and aluminium in tectosilicate or inosilicate structures, and compared with the mantle, is characterized by a low iron and manganese content. Continental crust is made up of low density granitic and low femic (Fe and Mg) rocks, pri-

marily granulite, composed mainly of granitoids of the tonalite–trondhjemite–granite (TTG) suite, the dominant rock types at the lower crust today, and presumably also in the past.

The general rock distribution (Fig. 2.2), lithological features and isotopic dating in the Chinese continental crust are shown in Appendix 1 (partial isotopic dating data*). Figs. 2.3 and 2.4. show that Archean rocks occur in the Sino-Korean Block (N), Tarim Block (T), western and northeastern areas of the Yangtze Block (Y), in addition, hidden Archean basement may be present in the Jiamusi area.

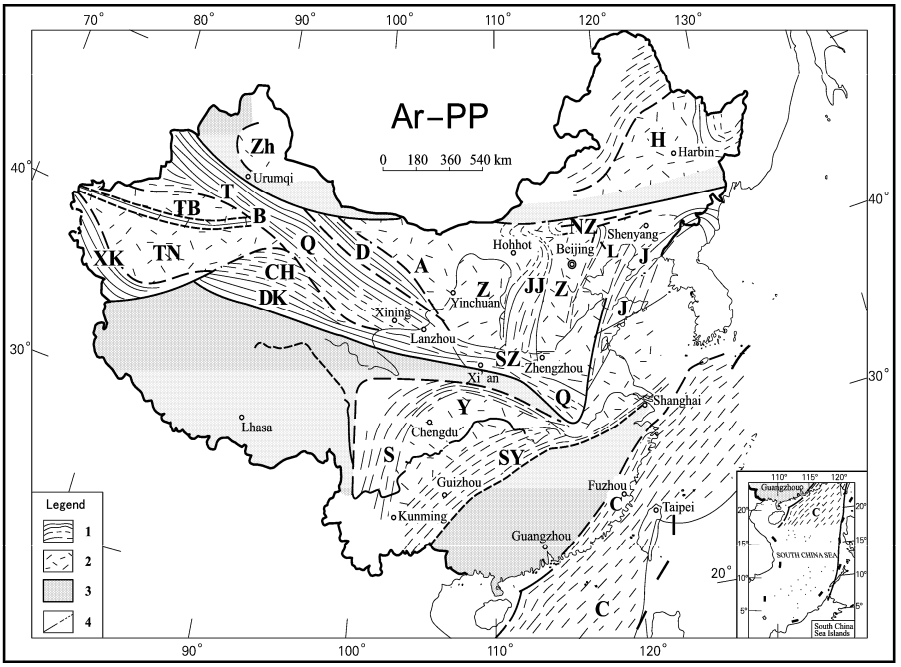

Fig. 2.2 Archean and Paleoproterozoic tectonic framework of China (modified after Bai J et al., 1996, with permission of Bai J).

Legend: 1. Belt of tectonic activity or collision zone in the Paleoproterozoic; 2. Archean craton; 3. Inferred oceanic crust; 4. Boundary of tectonic area.

Name of continental plate: Main part of Sino-Korean block (Z); Alxa continental block (A); Tarim continental block (T); main part of Yangtze continental block (Y); Qinling-Dabie-Jiaonan continental block (Q); Cathaysian continental block (C); Harbin continental block (H); Junggar continental block (Zh).

Belts of tectonic activity: East Shandong and Liaoning active tectonic belt (J); Qinglong-Luanxian active tectonic belt (L); Shanxi-Hebei rift zone (JJ); Northern Sino-Korean accretion zone (NZ); Southern Sino-Korean accretion zone (SZ); Dunhuang-Longshoushan Collision Zone (D); Tianshan-Beishan-Qilianshan Collision Zone (TBQ); Qaidam Collision Zone (CH); West Kunlun-Altun Collision Zone (XK); East Kunlun marginal accretion zone (DK); South Sichuan-East Yunnan marginal accretion zone (S); Southern Yangtze marginal accretion zone (SY).

Bai J et al. (1996) have successfully carried out research on the formation of the Archean continental nuclei and their movement history. They believe that two types of assemblages can be distinguished in the Paleoarchean to Neoarchean rocks of China: (i) Granulite-gneiss, with granulite and amphibolite

* Where a source is not specified, all isotope ages are cited from relevant geological monographs of the provinces or districts (1984–1993).

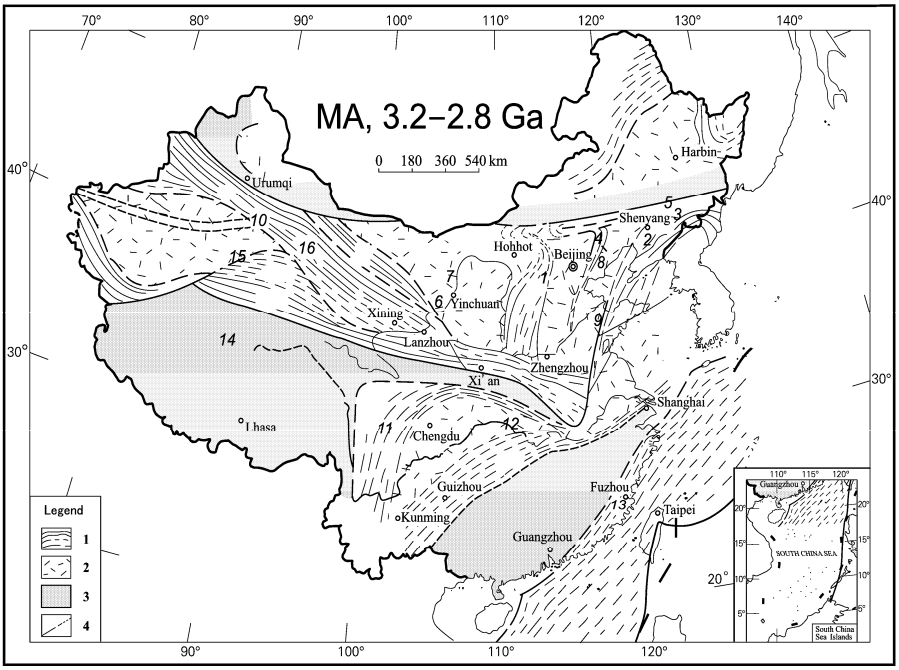

Fig. 2.3 Outcrops of Mesoarchean metamorphic rocks in the Chinese continent (modified after Bai J et al., 1996, with permission of Bai J).

Legend: 1. Belt of tectonic activity or collision zone in the Paleoproterozoic; 2. Archean craton; 3. Inferred oceanic crust; 4. Boundary of tectonic area.

1. Daliushu biotite-plagioclase gneiss of the Fuping Group in Hebei Province (standard section at ~114.1°E, 38.8°N), the lower part of the original Fuping Group, with a zircon U-Pb age of 2, 800±190 Ma (Wu CH et al., 2000); 2. Granulite and amphibolite rock systems in the lower part of Anshan Group at Anshan, Liaoning, with isotopic age of 3.186–2.819 Ga; 3. Granulite and amphibolite rock systems at Qingyuan, Liaoning, with isotopic age > 2.819 Ga; 4. Lower part of Jianping Group, west Liaoning (119.8°E, 41.4°N) with isotopic age >2.97 Ga; 5. Longgang Group isotopic age of 2.97 Ga, south Jilin (126.2°E , 42.2°N); 6. Lower part of Alxa Group (> 2.9 Ga), Ningxia (105.8°E , 39°N); 7. Diebusg Group, with Rb-Sr age of 3.22 Ga, Sm-Nd age of 3.018±0.05 Ga at Ningxia; 8. Upper part of Shuichang Complex, Qianxi Group >3.0 Ga, Hebei (118.3°E, 40.2°N); 9. Yishui Group, with Sm-Rd total rock isochron age of 2.997 Ga, located in middle Shandong 118.7°E, 35.8°N; 10. Kuruktag Group, with age of 3.218 Ga, Xinjiang (88–92°E, 41.6–41.8°N) (Cheng YQ, 1994); 11. Kangting Complex Group, with Pb-Pb total rock isochron age of 2.957 Ga, western Sichuan (standard section ~102°E, 29–31°N); 12. Biotite-plagioclase granulite and amphibolite in the lower part of the Kongling Group, with western Hubei Province zircon U-Pb age of 2.891 Ga (standard section 111°E, 30.8°N) (Li FX et al., 1987); 13. Nine isotopic ages between 3.4 and 2.5 Ga identified by using Sm-Nd or U-Pb methods obtained in Fujian (Gao TJ et al., 1999); 14. Gemuri Group at the base of metamorphosed crystalline rocks of Qiangtang in Tibet, with single grain zircon Pb isotopic age of 3.2 Ga, perhaps related to an indicated earlier phase of metamorphism (Wang GZ, 2001).

lithofacies; (ii) Greenstone belts and TTG rock suites, which have greenschist to amphibolite lithofacies. These assemblages are also found in the other continents throughout the world (Windley, 1995).

Granitic gneiss is the main rock type in granulite-gneiss areas, including Paleo-and Meso-archean deep intrusions, metamorphosed supracrustal rocks and the remains of greenstone belts, including TTG rock suites. The supracrustal rocks are mainly amphibolite and pyroxene granulite, formed from the metamorphism of basic volcanic rocks, gneiss and leptite, mainly metamorphosed from dacititic and rhyolitic protoliths, and biotite plagiogneiss, granulite and aimantine (= magnetite) quartzite. In the

supracrustal rocks of western Yinshan, Inner Mongolia, khondalites, composed mainly of sillimanite, garnet and aplitic gneiss, granulite, quartzite, marble and metamorphosed sedimentary rocks rich in

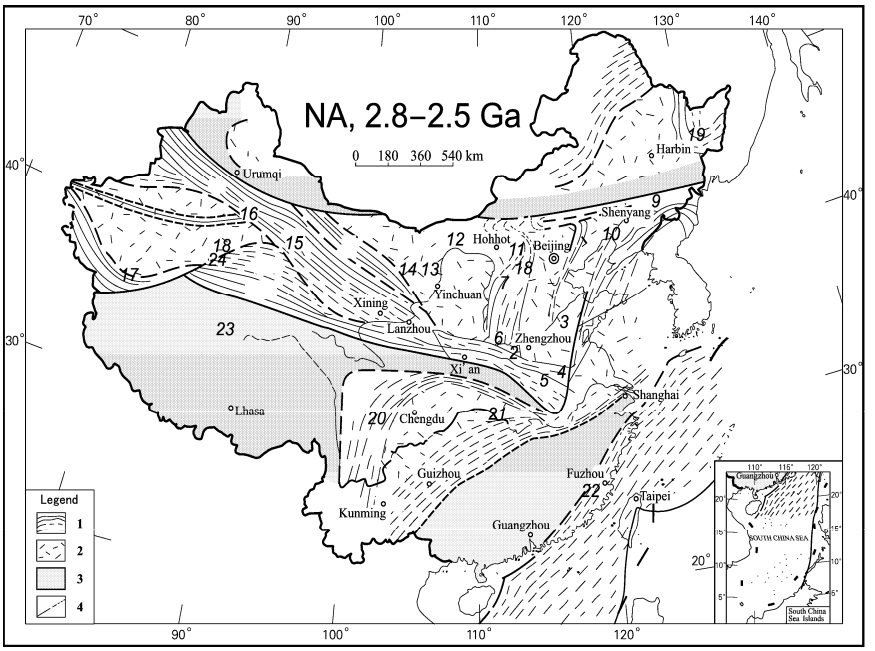

Fig. 2.4 Outcrops of Neoarchean metamorphic rocks in the Chinese continent (modified after Bai J et al., 1996, with permission of Bai J).

Legend: 1. Belt of tectonic activity or collision zone in the Paleoproterozoic; 2. Archean craton; 3. Inferred oceanic crust; 4. Boundary of tectonic area.

1. Quartzite, biotite granulite and amphibolite of the Wutai Group in Shanxi Province formed before 2.55 Ga (standard section 113.3°E, 38.9°N); 2. Taihua, Dengfeng and Songyang groups isotopic age of 2.84–2.4 Ga, Henan Province (standard section 112–113°E, 34–34.5°N); 3. Taishan Group, Shandong Province (>2.5 Ga) (117–117.6°E, 36.2–36.5°N); 4. Wuhe Group (2.65 Ga), northern Anhui Province (118°E, 33°N); 5. Huoqiu Group (2.7 Ga), western Anhui Province (116.2°E, 32°N); 6. Jiangxian–Sushiu, Zhongtiaoshan Group on the border between Shanxi and Henan provinces (111–112°E, 34.8–35.3°N) (Wu CH et al., 2000); 7. Lüliang Group, western Shanxi Province (111–111.8°E, 37–38°N); 8. Upper part of Fuping Group, Taihangshan, western Hebei Province (2.48 Ga) (113.8–114.4°E, 38.3–39°N) (Wu CH et al., 2000); 9. Jiapigou Group, Jilin Province (2.5–2.48 Ga) (126–126.7°E, 42–43°N); 10. Upper part of the Anshan and Jianping groups in Liaoning Province located at 120–123°E, 41°N); 11. Jining Group (2.65 Ga) (112–114°E, 41°N); 12. Wulashan Group (2.52 Ga), Inner Mongolia (108–110°E, 41–41.5°N); 13. Alxa Group (2.6–2.5 Ga), Helanshan (106°E, 38–39°N); 14. Qianlishan Group (2.6–2.5 Ga), Ningxia; 15. Hongliuxia System (Khondalite system, 2.67 Ga) (Yu HF et al., 1998) Dunhuang, Gansu Province, Dakandaban Group, with zircon age of 2, 412±14 Ma, northern Qaidam (Lu SN, et al., 2002); 16. TTG system, Kuruktag, north Tarim Block, with U-Pb and Sm-Nd isotopic ages of 3.2–2.58 Ga (89°E, 41.5°N) (Bai J et al., 1996); 17. Tekiliktag Gneiss, south Tarim, with U-Pb and Sm-Nd isotopic ages 2.78–2.58 Ga; 18. Milan Group, east Tarim (89°E, 39°N) and the Huangyuan Group, north Qaidam, with U-Pb age of 2.46 Ga, (101.2°E, 37°N) (Wang YS et al., 1987); 19. Metamorphic tholeiite, Mashan Group, Jiamusi Block, Heilongjiang Province, metamorphic age Ar-Ar method on pyroxene 2.539 Ga (standard section 130.5°E, 45.3°N); 20. Kangting Complex, western Sichuan zircon U-Pb age of 2.451 Ga; Rb-Sr total rock isochron age of 2.404 Ga, suggesting that the group may have been affected by a later tectono-thermal event (standard section 102°E, 29–31°N); 21. Granulite and migmatite, lower Kongling Group, western Hubei Province, zircon U-Th-Pb age of 2.820–2.165 Ga (111°E, 30.8°N); 22. Fujian, Cathaysian continental block, Sm-Nd or U-Pb ages between 2.8 and 2.5 Ga (Gao TJ et al., 1999); 23. Gemuri Group at the base of metamorphosed crystalline rocks of Qiangtang, Tibet, gave a single grain zircon lead isotopic age of 2.762 Ga, indicating an earlier phase of metamorphism (Wang GZ, 2001).

aluminium, have been described (Bai J et al., 1996). In the Chinese continent, 8 continental blocks and 12 active belts have been recognized which have been formed during the Archean and Paleoproterozoic (Fig. 2.2).

Paleoarchean (3.6–3.2 Ga) metamorphic rocks (Appendix 1.1) are represented by the lowest rock system of the Qianxi Group (Caozhuang Complex, standard section ~118.3°E, 40.2°N). They are composed mainly of plagiogranulite with two-pyroxene, hypersthene granulite in the lower part and plagioamphibolite in the upper part. In the Qian'an area the Sm-Nd isochron age of the amphibolite is ~3.5 Ga (Cheng YQ, 1994). However, Paleoarchean metamorphic rocks have not been observed widely in China.

Mesoarchean (3.2–2.8 Ga) metamorphic rocks are represented by the biotite-plagioclase gneiss, granulite and amphibolite rock systems on 14 sites (Fig. 2.3; Appendix 1.1).

Neoarchean (2.8–2.5 Ga) metamorphic rocks are metamorphic quartzite, biotite granulite, amphibolite and clastic rocks in turbidite facies (Fig. 2.4; Appendix 1.1). Greenstone belts show a stratigraphic sequence from basic volcanics, through intermediate-acid volcanics to unmetamorphosed sediments. Komatiite, with an MgO content greater than 18%, can sometimes be found at the base of the basic volcanics, which are calc-alkaline volcanic rocks, similar to those formed above subduction zones at convergent plate margins, with an MgO content below 14%. The intermediate-acid volcanic rocks are also primarily calc-alkaline volcanics. The sediments in the upper part of the succession are mostly immature turbidites and neritic sediments formed in an active continental marginal tectonic environment. Intrusive rocks in these greenstone belts are granitoids of the TTG rock suite.

The Archean rock system in North China area forms a protoplate with a high degree of sedimentary maturity in crustal evolution. Geochemically the rocks show a relative abundance of the large radius, positive ion, lithophile elements. In this respect, they are similar to the Siberian Plate but differ from the North American and Gondwanan paleo-plates. The ε_{Nd} values of the basic rocks range from +2.2 to +4.3, indicating derivation from a depleted mantle. On the other hand, the volcanics show enrichment in Sr, K, Rb, Ba, Th, Ce and P, indicating that the magmas were affected by metasomatism, so that trace element diagrams resemble those of island arc volcanics. These features demonstrate that the formation of the continental crust was the result of the subduction processes between ancient oceanic crust and an ancient continental plate (Sun DZ, 1990). Metamorphism in the Archean usually reached the hornblende and granulite facies, the temperature of metamorphism was above 700°C and pressure up to 0.6 GPa, and the rocks had a flat-lying layering or foliation (Dong SB et al., 1986).

Bai J et al. (1996) divided the North China part of the China-Korean protoplate into six continental nuclei: Dongsheng (A), Chifeng (B), Liaoning-Jilin (C), Linfen (D), Jining (E) and Bohai (F) (Fig. 2.5). The center of each continental nucleus is an area of Archean granulite-gneiss, and corresponds to an uplifted area of the deep magnetic interface, which was estimated by continuation and filtering of magnetic anomaly (depth 10–18 km; Guan ZN et al. 1987). Archean greenstone belts surround each of the continental nuclei, corresponding to zones of depression of the deep magnetic interface (depth 16–24 km; Guan ZN et al. 1987) and represent paleo-collision zones at the margins of the continental nuclei (Fig. 2.5). The foliation of the gneisses and that of ductile shear zones in the continental and the subcontinental nuclei have circular or arcuate patterns, suggesting that the nuclei rotated at the time of collision and accretion (Bai J et al., 1996). The mechanism of continental growth is depicted by subduction of oceanic crust, leading to collision, accretion and amalgamation of the continental nuclei. The age of formation of the granulite-hornblende lithofacies of the continental nuclei is the Fuping Period (before 3.0–2.8 Ga) and the greenstone belts around it were formed in the Wutai Period (2.7–2.5 Ga). Reymer et al. (1987) estimated that the rate of accretion of continental crust along the active margins of the Archean continents was 1 km^3/yr; the rate of accretion for Chinese continent had a similar value.

Fig. 2.5 shows that the paleocontinental segments are not perfectly circular. In all the paleo-continents in the world the pattern of lineations is truncated at the margins of the continental nuclei, indicating that they are separated fragments of earlier paleocontinents. These nuclei subsequently collided and amalgamated to form the present continents (Condie, 1982, 1994).

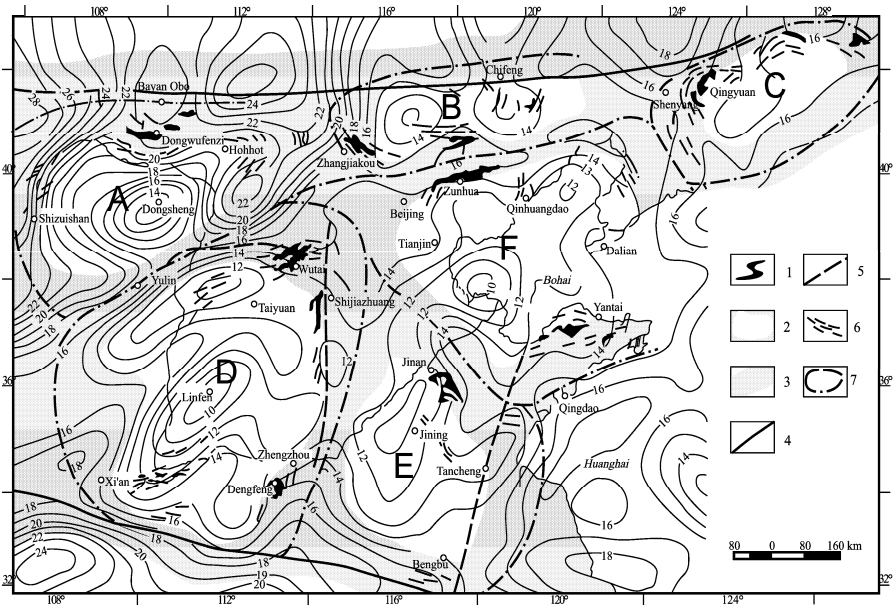

Fig. 2.5 The distribution of Archean continental nuclei in the Sino-Korean Plate in North China and average depth contours of the deep magnetic interface (after Bai J et al., 1996, with permission of Bai J). Data for the deep magnetic interface of the aeromagnetic survey, with the filtering magnetic anomaly, are from Guan ZN et al. (1987).

Legend: 1. Archean greenstone belt; 2. Uplift area of the deep magnetic interface, i.e Archean continental nuclei; 3. Depression zone of the deep magnetic interface, i.e. collision and amalgamation zone; 4. Border of Sino-Korean Plate; 5. Inferred fault zone; 6. Archean rift; 7. Border of Archean continental nuclei.

Continental nuclei: A. Dongsheng; B. Chifeng; C. Liaoning-Jilin; D. Linfen; E. Jining; F. Bohai.

It is probable that in addition to accretion, growth of the continental crust occurs by the thickening of the crust. The widespread occurrence of high grade Archean metamorphic rocks at the Earth's surface, although they have undergone intense erosion over a very long period of time, suggests that they are continually being uplifted by thickening due to the addition of material to the continental crust, either internally or at its base (Dong SB, 1986). This may occur by intrusion, by shearing, by overthrusting and underplating of the crust during horizontal movements, and also by thickening in transpressional shear zones. By these mechanisms the granitic crust expands vertically, bringing high grade metamorphic rocks to the surface (Hunter, 1981; Sun DZ, 1990; Qian XL, 1994). This interpretation is supported by the results of the Global Geoscience Transect (GGT) (Editorial Board of Geoscience Transect, China Seismological Bureau 1991, 1992; Yuan XC, 1990; Wu GJ et al., 1991, 1998), which showed that the lower crust is dominated by horizontal layered structures, in contrast to the complexity of deformation seen in outcrop and in seismic sections of the upper crust.

In early studies of the Archean, the continental nuclei were identified as uplifted "mantled gneiss domes" (Eskola, 1949). Gneiss domes were described in Dabieshan (Ma XY and Cai XL, 1965; Cai 1965, 1979) and at Fuping in the Taihang area (Tan et al., 1993) in China. Many of these gneiss domes are now interpreted as layered structures related to ductile shear deformation and crustal vertical accretion by underplating in zones of extension (Qian XL, 1996).

From studies of strontium, neodymium and lead isotopes**,** it is now considered that the Archean continents were constructed by accretion at the margins of the paleo-continental nuclei. However, the present-day continents show evidence of the continual recycling since the Proterozoic of older continen-

tal materials (Reymer et al., 1987; Allègre, 1989; Veizer, 2005). Although more than 70%–80% of the area of present-day continents was formed initially during the Archean, this material has been reworked during younger collision cycles (Goodwin, 1991; Qian XL, 1994). By contrast, only a minor amount of new material has been added to the continents since the Archean.

From Paleoarchean to Neoarchean, the Chinese continental crust had its own terrestrial thermal regime. According to Grambling (1981), over 4 billion years ago, global heat production was 5 times its present value, and at the end of Archean it doubled the present value. The temperature of formation of Archean granulite globally was over 750°C, and the pressure was 0.41 GPa (this estimated value of pressure may be too low), the depth of formation was 14 km, and the geothermal gradient was therefore 54°C/km. However, in the Chinese continental crust, the average formation temperature of granulite, mainly from the Mesoarchean, was 827°C, the pressure was 0.95 GPa, and the average depth of formation was 32 km (Appendix 1.1). If the Earth's surface temperature was 130°C, then the average geothermal gradient was 22.2°C/km (Appendix 1.1). The above average values were calculated from 11 measurements. If the temperature at the Earth's surface was 0°C at that time, then the average geothermal gradient was 25.8°C/km.

In the Neoarchean the maximum temperature for the formation of hornblende was 714°C, average pressure was 0.81 GPa, and average depth of formation was 27.5 km. If the inferred surface temperature of the Earth was 100°C at the end of Neoarchean, the average geothermal gradient was 24.2°C/km. These average values were calculated from 47 measurements (Appendix 1.1). If the temperature at the Earth's surface was 0°C at that time, then the average geothermal gradient was 26°C/km.

These results all show that the geothermal gradient of Chinese continent in the Archean was only half the global value estimated by Grambling (1981), and close to the geothermal gradient in recent continental crust. The Chinese continental crust (mainly the Sino-Korean protoplate) in comparison with the global thermal gradient was somewhat "cold" during the Archean. These data do not support the suggestion that there was an active mantle plume beneath the Chinese continental crust or that oceanic mantle processes operated at that time, as suggested by Kusky et al. (2001) and Li JH et al. (2002).

From recent studies, it is considered that ultrabasic komatiites, found in the lower part of the sequence in greenstone belts, came from high temperature mantle plumes (Condie, 2001), and were not formed by the partial melting of depleted mantle, as suggested previously. Condie (1997, 2001) suggested that Archean mantle plumes can be distinguished by the following features:

(1) Mantle plumes are related to the formation of oceanic plateaus and flood basalts, and have no relationship to ocean floor, oceanic island or island arc basalts;

(2) Basalts related to mantle plumes have a distinctive chemical composition which can be recognized in the $w(\mathrm{TFeO})_8$ versus $[w(\mathrm{CaO}) / w(\mathrm{Al_2O_3})]_8$ diagram, when $w(\mathrm{MgO}) = 8\ \%$. Mantle plume basalts are characterized by high $w(\mathrm{TFeO})_8$and low $[w(\mathrm{CaO})/w(\mathrm{Al_2O_3})_8]$. On the other hand, in the $w(\mathrm{Th})/w(\mathrm{Ta})$ versus $w(\mathrm{La})/w(\mathrm{Yb})$ diagram, basalts related to mantle plumes have been developed only in special areas such as the Superior Province of Canada, Australia, Siberia.

(3) The distribution and components of komatiite formed from mantle plumes give information concerning the changes in the depth and temperature of the magma source with time. Condie (2001) discovered that from 4.0 Ga to 2.5 Ga, komatiites show that in the Archean the temperature of the mantle decreased from 2,000°C to 1,600℃, and has remained at about 1, 600°C since the Proterozoic. The depth at which komatiites originated in the Archean mantle was 400–300 km, but since the Proterozoic they have originated at 200 km. The solidus of komatiite has also changed with time; the solidus decreased from 14 GPa to 5 GPa, during the Archean, and in the last 100 Ma the pressure has been only 3 GPa. Changes in the pressure of the solidus can change the composition of the solidus of komatiite from low aluminium ($\mathrm{Al_2O_3}$, 5%–10%) and high $w(\mathrm{CaO})/w(\mathrm{Al_2O_3})$ (about 3–1) to high aluminium ($\mathrm{Al_2O_3}$, 10%–15%) and low $w(\mathrm{CaO})/w(\mathrm{Al_2O_3})$ (nearly 1).

Did the Chinese continental greenstone belts originate from mantle plumes? This is a question to answer in future study. No one has yet presented any convincing evidence for mantle plumes in Archean. Research into this problem only just began in China.

The Archean was the main period for the formation of banded ironstone formations, which form large-scale iron ore fields in Anshan, Liaoning and Qian'an, eastern Hebei. In China banded ironstones were formed during the Archean; elsewhere in the world they were formed commonly during the Paleoproterozoic.

Study of Archean oceanic crust also only just begins in China. It is presumed that the most of Archean oceanic crust has been subducted and absorbed back into the mantle, so that only small remnants, resembling ophiolites, remain in the greenstone belts. Archean oceanic crust has been discovered in the Slave Province in Canada, the Bampton greenstone belt in South Africa and in Wyoming in United States, but these occurrences lack the sheeted dykes and layered gabbros characteristic of typical ophiolite suites. Although some researchers (Kusky et al., 2001; Li JH et al., 2002) have reported Archean ophiolitic, and oceanic crust and podiform chromitites with a nodular texture giving an age of 2.5 Ga in Dongwanzi, Hebei, this evidence is not yet conclusive and is still contested. Many geological researchers (Zhai MG et al., 2002; Zhang Q, et al., 2003) have pointed out that: (i) the mantle peridotite and harzbourgite tectonite, described by Kusky et al. (2001) and Li JH et al. (2002), are not recognizable as oceanic mantle. These rocks are virtually composed of Fe-rich pyroxenite and amphibolite, and are not in direct contact with a gabbro unit. Zhang CH et al. discovered that the gabbro intruded into the Mesoproterozoic system of that area, and formed in Triassic (personal communication); (ii) primary biotite rarely occurs in gabbros in ophiolite sections; (iii) the reported sheeted dyke swarms are not actually sheeted dyke swarms, because they do not show either symmetrical or asymmetrical chilled borders. The dykes are composed of pyroxenite and amphibolite, which do not represent a mafic magma; the geochemistry indicates that they are probably formed in an intraplate tectonic setting, and are not related to an ophiolite; (iv) unlike podiform chromitites in ophiolite sections, the chromitites associated with the ultra-mafic rocks are enriched in Fe and Cr, similar to chromitites from Fe-rich ultramafic rocks in the continental nuclei, and (v) there is no comprehensive geochemical data to demonstrate that the rocks in the Dongwanzi area are ophiolitic.

The best evidence against the interpretations of Kusky et al. (2001) and Li JH et al. (2002) is basic geological data. The "sheeted dykes" are only a few 10 cm wide dykelets, spaced every 5–10 m apart intruding into a gabbro dated as Mesozoic (Zhang CH's personal communication), which also intruded into Mesoproterozoic system. But the Re-Os dating of the chromitites as Archaean probably means that a few chromite-layered serpentinites may be of Archaean age, but not adding up to a complete ophiolite suite.

Normally it is considered that life, represented by the cyanophyta and chlorophyta, developed in the Paleoarchean (3.5 Ga) in oceans which were at a high temperature, in conditions which are found today only in submarine "black smokers". At this time it is supposed that volcanic activity released large quantities of CO_2 into the atmosphere which formed an anoxic reducing environment near the Earth's surface.

Cratonization of Archean continental crust in northern China is considered to have occurred about 3–2.7 Ga (Fig. 2.5). In Datong, Jining and Xinghe, Neoarchean or Paleoproterozoic sedimentary rocks, now represented by khondalites and are inferred to have been deposited unconformably on a TTG granulite complex, formed at 2.8 Ga (Qian XL, 1996, 1997). After cratonization, basic diabase dyke swarms intruded into fractured brittle crust. No deformation or metamorphism has occurred subsequently and the Archean continental crust has remained stable over a very long period of time.

Unmetamorphosed and undeformed Mesoproterozoic dyke swarms are widespread in the Sino-Korean continental block, indicating that cratonization was completed during the Neoarchean-Paleoproterozoic. It seems that for many geological phenomena in the world, such as the Kaapvaal Craton in South Africa, the Zimbabwe Craton, the Baltic shield in northern Europe, the Superior Province in the Canadian Shield in North America, and the West Australian shield, cratonization occurred much earlier than in North China. These cratons became cratonized between 3 and 2.6 Ga. The isotopic age of the dyke swarms in the Superior Province is 2.6–2.7 Ga, earlier than the dyke swarms (1, 700–1, 100 Ma) in China.

According to Sugisaki (1976) the rate of movement of crustal blocks can be calculated from the chemical composition of magmatic rocks which were intruded or extruded at times. The rates of movement of the Chinese Archean continental blocks have been calculated mainly for the North Chinese blocks (Appendix 1.2). Extension velocities indicated by the composition of basic and ultrabasic rocks is 0.7–0.88 cm/yr in the Early-Middle Neoarchean periods, and about 0.5 cm/yr in the Late Neoarchean. Rates of shortening reflected by intermediate-acid magmatic rocks are 4.1–5.9 cm/yr at the end of the Neoarchean. Because of the scarcity of data, we cannot define exactly the time at which extension was replaced by shortening.

2.3 Tectonics of the Paleoproterozoic (PP, 2.5–1.8 Ga, Lüliang Period)

—rifting-depression, amalgamation and formation of the unified crystalline basement of Sino-Korean Continental Protoplate

In the inner and marginal zones of the Archean granulite blocks and greenstone belts, intense erosion occurred during the Paleoproterozoic period, and thick deposits of volcanic-sedimentary supracrustal rocks were formed. Compared with the Archean, in the Paleoproterozoic, rocks were formed in a different diagenetic environment and were deformed in a different tectonic style.

In the Sino-Korean continental protoplate there is an angular unconformity between the Archean system and the overlying Paleoproterozoic system. The Lüliangshan in Shanxi Province (111.5°E, 37–38°N; 1 in Fig. 2.6) is the standard area for the Paleoproterozoic of China. This tectonic event is called the Lüliang Tectonic Event, and the period is called the Lüliang Period (Cheng YQ, 1994). This is not the same as the "Lüliang movement", described earlier by Lee JS (1929) and Ma XY (1957). In the Wutai area there is another famous tectonic event, perhaps equal to Lüliang Tectonic Event, called the Hutuo Tectonic Event (Ma XY, 1956; Cheng YQ, 1994; 2 in Fig. 2.6). The Lüliang Tectonic Period is sometimes known as the Hutuo Period (2.3–1.8 Ga; National Commission on Stratigraphy of China, 2001).

According to International Commission on Stratigraphy (Remane et al., 2000; International Commission on Stratigraphy, 2004), the Paleoproterozoic can be divided into 4 periods: Siderian, PP_1, 2.5–2.3 Ga; Rhyacian, PP_2, 2.3–2.05 Ga; Orosirian, PP_3, 2.05–1.8 Ga; Statherian, PP_4, 1.8–1.6 Ga. However, in China the ages of the protoplates have not been determined in sufficient detail to divide the Paleoproterozoic into four periods. The Siderian (PP_1, 2.5–2.3 Ga) is the period in which super large iron ore deposits were developed worldwide, but at that time bedded ironstone deposits were not developed in China.

The unified Sino-Korean and Tarim cratons were finally consolidated to form a unified metamorphic crystalline basement at 1.8 Ga (~1.9–1.75 Ga, Zhai MG, 2004). The Changcheng System is the first system to be formed from supracrustal sedimentary rocks and was deposited after 1.8 Ga. A clear distinction can be made between the crystalline basement and its sedimentary cover, so that 1.8 Ga is taken as an important time boundary, separating the latest Paleoproterozoic from the Mesoproterozoic. Internationally the Statherian (PP_4, 1.8–1.6 Ga) is used as the equivalent of the Changchengian Period in China. A time boundary at 1.6 Ga, recognized internationally, has not been identified in North China, but a similar boundary can be recognized in the Yangtze and Cathaysian protoplates (Bai, et al., 1996) (Fig. 2.6; Appendix 1.3).

As in other protoplates worldwide, the Paleoproterozoic in China includes three types of rock assemblage (Condie, 1982; Windley, 1995):

(1) Low maturity flysch formations with feldspar-quartz, sandstone-shale and magnesian carbonates containing stromatolites, accompanied by continental tholeiites with a total thickness of about ten kilometers. This type of assemblage occurs in the North Hebei–Shanxi rift-depression belt (JJ), in the main

part of Sino-Korean continental block (Z) and in the Jiaodong–East Liaoning active belt (J) (Fig. 2.6). Super large magnesite, ascharite and ludwigite ore deposits, rare elsewhere in the world, occur in East Liaoning. These deposits were formed in a typical intertidal flat sedimentary environment, the materials originated from the erosion of magnesium-rich Archean volcanic rocks.

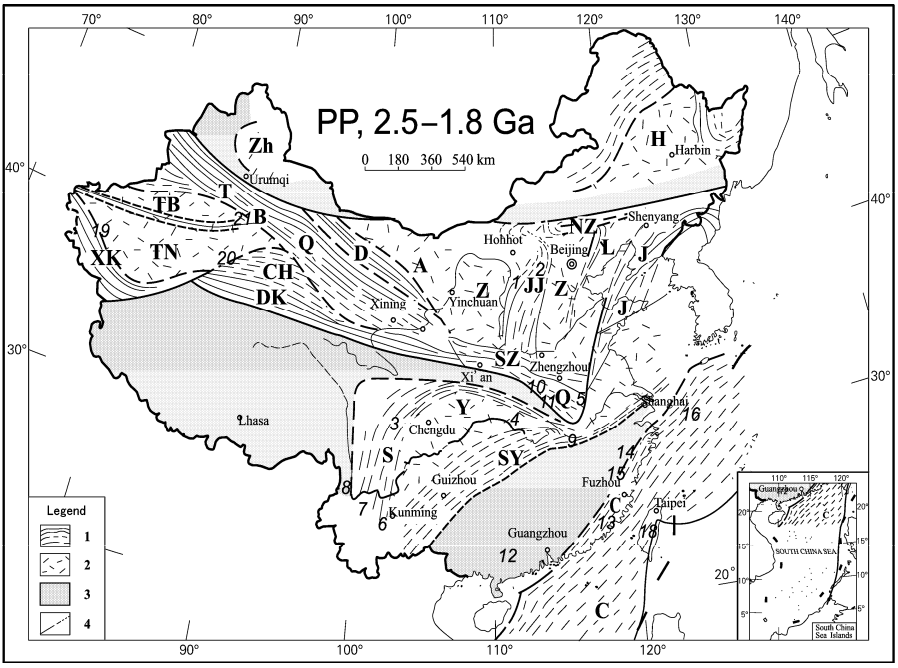

Fig. 2.6 Tectonic framework of the Paleoproterozoic of China (modified after Bai J et al., 1996, with permission of Bai J).

Legend: 1. Belt of tectonic activity or collision zone in the Paleoproterozoic; 2. Archean craton; 3. Inferred oceanic crust; 4. Boundary of tectonic area.

Continental plates: The main part of the Sino-Korean (Z); Alxa continental block (A); Tarim continental block (T); main part of the Yangtze continental block (Y); Qinling-Dabie-Jiaonan continental block (Q); Cathaysian continental block (C); Harbin continental block (H); Junggar continental block (Zh).

Belts of tectonic activity: East Shandong and Liaoning active tectonic belt (J); Qingxian-Luanxian active tectonic belt (L); Shanxi-Hebei rift zone (JJ); Northern Sino-Korean accretion zone (NZ); Southern Sino-Korean accretion zone (SZ); Dunhuang–Longshoushan collision zone (D); Tianshan-Beishan-Qilianshan collision zone (TBQ); Qaidam collision zone (CH); West Kunlun-Altun collision zone (XK); East Kunlun marginal accretion zone (DK); South Sichuan-East Yunnan marginal accretion zone (S); Southern Yangtze marginal accretion zone (SY).

1. Lüliangshan in Shanxi; 2. Hutuo Group in Wutaishan, NE Shanxi; 3. Kangding Group in western Sichuan Province (~102°E, 30°N); 4. Kongling Group, Huanglin, western Hubei Province, age 2.37 Ga (~111°E, 30.8°N); 5. Feidong Group, Anhui Province, age 1.99 Ga (~117.5°E, 31.8°N); 6. Dahongshan Group, Yunnan Province, Sm-Nd model age 2.0–1.9 Ga (Wu MD, 1988); 7. Diancangshan Group, Yunnan Province, age 2.037 Ga; 8. Gaoligongshan Gneiss, western Yunnan Province, Nd model age 2.218 Ga (Zhong DL et al., 1999); 9. Xingzi Group, Lushan, Jiangxi Province, zircon U-Pb dilution age 2.2–2.0 Ga (~115.9°E, 29.5°N); 10. Kuanpin and Taowan groups, Middle Qinling; 11. Tongbai Complex, age 2.418 Ga; 12. Yunkai Group, Luoding, Guangdong Province; 13. Longhai-Shen'ao area, east Fujian Province; 14. Badu Group, SW Zhejiang Province; 15. Mayuan Group, NW Fujian Province; 16. Hupiqiao granite gneiss, Donghai (East China Sea); 17. Well XY 1, Xisha (Paracel) Islands, Nanhai Islands (South China Sea); 18. Tailuge granite, zircon U-Pb age, 1.668 Ga, Yushan, Taiwan Province.

(2) Calc-alkaline volcanic-turbidite series, with some banded ironstone formation, occurring in the eastern part of the northern margin of the Sino-Korean protoplate and on the margins of the Tarim protoplate. The thickness of this series is up to 5 kilometers.

(3) Bimodal volcanic-turbidite series is composed mainly of basic and acid volcanic rocks, with pelitic-arenaceous turbidites and carbonates in the upper part of the sequence. This assemblage occurs on the southern margin of Sino-Korean protoplate (SZ), in the Jiaodong–East Liaoning active belt, and forms the spilite-keratophyre series of the Dahongshan Group in the southwestern part of the Yangtze protoplate (S) (Bai J et al., 1996; Fig. 2.6). In the North Hebei-Shanxi rift-depression belt this assemblage includes feldspathic quartzite, purple or grey-purple phyllite and slate.

These sedimentary assemblages indicate that the global atmosphere was transformed from an oxygen-poor to an oxygen-rich environment during the Paleoproterozoic. The rare earth elements (REE) in fine clastic rocks are also different in the Paleoproterozoic from those in Archean, a negative Eu anomaly appears, and there was a gradual increase in total REE. Otherwise the trace and REE elements in metamorphic, volcanic and sedimentary rocks in the Archean and the Paleoproterozoic are almost the same. The composition of basic volcanic rocks plotted on w(Cr)-w(Y), w(Ti)-w(Zr), [w(Ti)/100-w(Zr)-w(Y)×3] and [w(Ti)/w(Y)-w(Nb)/w(Y)] diagrams indicates formation in arc and intraplate environments. Values of ε_{Nd} range from +2.1 to +3.0, indicating that the volcanic rocks originated from a depleted mantle (Bai J et al., 1996).

The structure of metamorphic rocks in the Paleoproterozoic is very different from the planar layered pattern in the Archean. Metamorphism in the Paleoproterozoic ranges from middle-high temperature regional metamorphism to low temperature regional dynamo-metamorphism (low greenschist to low amphibolite facies). The temperature and the areal extent of metamorphism gradually decreased with time, indicating that the rate of terrestrial heat flow was being reduced irreversibly (Zhang SG, 1990). As this metamorphism occurred in collision belts, marginal accretion belts and in rift-depression zones within the craton, metamorphic facies zones are linear, similar to those in the Archean tectonic belts (Fig. 2.2). High amphibolite facies metamorphism appears in collision and marginal accretion belts, with a lower grade of metamorphism than in nearby Archean plates, indicating that the regions of high heat flow became concentrated in the center of the active belts. Due to the reduced thickness of the crust and low heat flow, low greenschist facies metamorphism occurred in rift-depressions in the craton (Bai J et al., 1996).

In the Paleoproterozoic, tectonism, like metamorphism, is concentrated in linear collision and marginal accretion belts and rift-depressions in the cratons. At the end of Archean the protoplate assumed a rigid character, and the craton was not subsequently involved in large scale tectonism, ductile deformation or tectonic overprinting. Within the craton, inverted fan-shaped and linear folds with overthrusts developed in rift-depressions. Collision and marginal accretion belts form linear fold belts with horizontal fold axes in some places, penetrated by ductile shear belts, reflecting kinematic mechanisms of horizontal shortening and transpression at depth.

Bai J et al. (1996) suggested that after the Paleoproterozoic tectonic events, the Chinese continental protoplate was divided into five protoplates (Fig. 2.6): Sino-Korean Protoplate, Yangtze Protoplate; Cathaysian Protoplate; Harbin Protoplate; and Junggar Protoplate. At present, 28 representative isotopic ages have been obtained on samples from these protoplates (Appendix 1.3).

The Sino-Korean Protoplate is the largest protoplate incorporated in the Chinese continent. Stable plates formed during the Archean include the main part of Sino-Korean Plate [from Erdos, North China to the Korean Peninsula (Z in Fig. 2.6), Alxa (A), Qaidam (CH) and Tarim (T) plates]. Between these plates are active tectonic belts which were formed by Paleoproterozoic events, such as the Dunhuang-Longshoushan Collision Belt (D; 1.94–2.06 Ga), in the Tianshan–Beishan–Qilianshan (TBQ) Collision Belt, the U-Pb isotopic age of zircons in some blocks within the Tianshan Belt is 2.0–2.3 Ga, in the Qilianshan Belt 2.2 Ga, in the marginal accretion belt of east Kunlun (DK) 1.85 Ga; and in the West Kunlun-Altun Collision Belt (XK in Fig. 2.6) 2.46–2.13 Ga.

Crystalline metamorphic basement, formed in the Lüliang Tectonic Event (2.5–1.8 Ga), is found all round the Tarim Protoplate, in the Kuruktag in the northeast (1.92–1.8 Ga), the Altun in the southeast, the

Tekiliktag in the southwest (2.13 Ga) and the Kalpin in the northwest. In the Sino-Korean Plate and its adjacent areas crystalline basement is also developed in the Jiaoliao active belt, i.e. in eastern Shandong and eastern Liaoning (J), the Qingxian-Luanxian (L) active belt in northern Hebei, the Shanxi–north Hebei rift (JJ), the northern marginal accretion belt of the Sino-Korean Plate (NZ), and the southern marginal accretion belt of the Sino-Korean Plate (SZ) (Fig. 2.6), all of which were formed during the Paleoproterozoic tectonic event. After further fractures the Sino-Korean Protoplate was reconstructed from crystalline basement by collisions during the Lüliang Period. At the end of the Paleoproterozoic (1.8 Ga) the Sino-Korean Protoplate extended from the Tarim Plate in the west to the Korean Peninsula in the east, and survived until the end of the Mesoproterozoic (1.0 Ga).

Zhao GC et al. (1998, 2001, 2004) and Wilde et al. (2002, 2004) considered that original Sino-Korean Plate was formed by the amalgamation of the eastern and western parts of the plate along the Hengshan–Wutaishan–Taihangshan Collision Zone as first proposed by Bai J et al. (1996). From the isotopic age of this tectonothermal event and the degree of metamorphism, Zhao GC et al. (1998, 2001, 2004) and Wilde et al. (2002, 2004) believed that the collision in the Hengshan–Wutaishan–Taihangshan belt was connected to the Kola-Karelian Orogenic Belt in the Baltic Shield at the end of Paleoproterozoic. At that time these two continents are thought to have been adjacent to each other. However, these authors paid attention only to the formation of the Hengshan–Wutaishan–Taihangshan Collision Zone, which is well exposed, but they did not recognize many small stable plates and collision zones with not very good outcrop, or the differences between the northern and southern parts of the original Sino-Korean Plate, consequently, their conclusion, recognizing only one collision zone, may be incorrect, and their recognition is rare in evidence to compare with Kola–Karelian Orogenic Belt, which is just a hypothesis.

Most researchers accept the existence of an original Sino-Korean Plate, but use different terms depending on their approaches, e.g. “Asian central axial continental plate” or “North China continental plate tectonic domain” (Wang HZ, 1981; Asian Geological Map Edition Group, China Geological Science Institute, 1975), or Tarim–Sino-Korean Plate (Li CY, 1982, 1984).

The major part of the Yangtze Protoplate was some stable blocks formed during the Paleoproterozoic, of which many outcrops are found, such as Huanglin, western Hubei Province (Kongling Group, 4 in Fig. 2.6), Feidong, Anhui Province (Feidong Group, 5 in Fig. 2.6), the southern Sichuan–eastern Yunnan marginal accretion belt in the southwest of the Yangtze Protoplate (6–8 in Fig. 2.6) and the marginal accretion belt to the southeast of the Yangtze Plate (Xingzi Group), Lushan, Jiangxi Province (9 in Fig. 2.6). Other paleo-blocks have been discovered in western Sichuan Province (Kangding Group, 3 in Fig. 2.6). To the northeast of the Yangtze Plate, there are also the Qinling, Wudangshan, Dabieshan, Jiaonan proto-blocks, formed during the Archean and Paleoproterozoic, including Central Qinling (lower age limit of the Qinling protolith is 2.267–1.987 Ga); the Sm-Nd model ages of the Kuanpin and Taowan groups (10 in Fig. 2.6) are all about 2.0 Ga (Liu GH et al., 1993); Wudangshan with a single zircon age of 2.442–1.967 Ga (data from Tianjin Geological and Resource Institute personal communication); Dabieshan where the lower age limit of rocks of the Dabie Complex is 2.424 Ga; the age of the protolith of the Tongbai complex (11 in Fig. 2.6) is 2.418 Ga; the U-Pb age of the Susong-Hong’an Group (Q in Fig. 2.6) is 2.343–1.85 Ga (Suo ST et al., 1993). Although the Qinling, Wudangshan, Dabieshan and Jiaonan blocks are all regarded as independent, their geochemistry shows that they are related to the Yangtze Plate. The Yangtze Plate and the Qinling, Wudangshan, Dabieshan and Jiaonan blocks were finally amalgamated to form a uniform crystalline basement in the Jinning Period of the Neoproterozoic (Fig. 2.7).

In the last two decades, some zircon samples collected from Yunkaidashan (12 in Fig.2.6) in the Yunkai Group at Luoding, Guangdong Province in the western part of the Cathaysian Plate gave an Rb-Sr age of 1.94 Ga (Chen HJ et al., 1993; Zhang BY et al., 1994). Some Paleoproterozoic ages (2.415–1.831 Ga) were obtained from zircons in magmatic and metamorphic rocks in Fujian Province (Gao TJ et al., 1999). There are many outcrops of Paleoproterozoic rocks (1.73 Ga) in Longhai-Shen’ao area, east Fujian Province (13 in Fig. 2.6) (Huang H et al., 1990), in southwest Zhejiang Province, Badu Group (14 in Fig. 2.6), with zircon U-Pb age of 1.975–1.878 Ga, in northwest Fujian Province, Mayuan Group (15 in Fig. 2.6) with Rb-Sr isochron of 1.93 Ga. Geological surveying and drilling have proved

the existence of a paleoplate, affected by a Paleoproterozoic tectonic event (Guan SC et al., 1999; Qiao XF et al., 1990) in the Donghai(East China Sea), Hupiqiao granite gneiss (16 in Fig. 2.6) and Nanhai (South China Sea) islands, where gneiss was found in well XY 1, Xisha (Paracel) Islands (17 in Fig. 2.6), forming part of the Cathaysian Plate. From the Tailuge Granite Yushan, Taiwan Province (18 in Fig. 2.6), with zircon U-Pb age of 1.668 Ga, and in the southern part of South China Sea, there are also remnants of a paleo-metamorphic crystalline basement. These occurrences show that the original Cathaysian continental block was very extensive (Fig. 2.7), and formed a uniform crystalline basement at the end of the Early Paleozoic (~390 Ma).

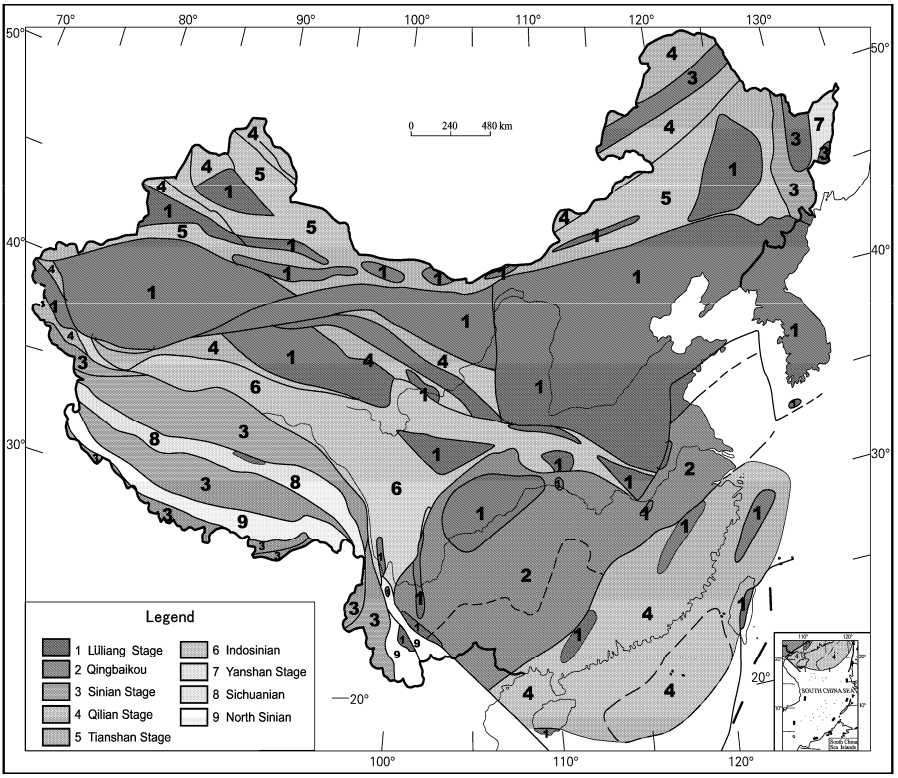

Fig. 2.7 Periods in the formation of uniform crystalline basement in the Chinese continental blocks.

1. Final period of formation in the Paleoproterozoic (before 1.8 Ga): Sino-Korean, Tarim, Alxa-Dunhuang, Middle Qilian, Qaidam, Altay, Ili-Balchas, Turpan-Xingxingxia, Kuruktag, Hongshishan, Yagan, North Bayannur, Tuotuoshang-Xilingol, Songpan-Garze, south Sichuan-east Yunnan, Ailaoshan, Lincang, Zhongdian, Lanping-Simao, South of Hainan, Chengdu, Huangling, Lushan, Feidong, Yunkai-dashan, Southwest Zhejiang-north Fujian, Hubijiao-Yushan uplift, Yushan, Taiwan, North of Gangdise, part of the Himalayan; 2. End of Qingbaikou Period (800 Ma): Yangtze Plate; 3. Sinian Period (Pan-Africa Event, 680–513 Ma): Himalayan, Qiangtang and Gangdise, Ergun, Jiamusi–Bureinskij and Xingkai continental block; 4. Late Period of Early Paleozoic (~390 Ma): Altay, Ili-north of Balchas, North Qilian, South Qilian, Altun, West Kunlun, Qimantag and Cathaysian, etc.; 5. The end of Late Paleozoic (260 Ma): Tianshan–South Dahinggan-ling; 6. Late Triassic (205 Ma): Qinling–Dabie, Bayanhar–Western Sichuan–Eastern Yunnan; 7. Late Jurassic (135 Ma): Wandashan; 8. Cretaceous Period–Late Paleocene (80–52 Ma): Bangongco–Nujiang; 9. Oligocene (~30 Ma): Yarlung Zangbo.

The Harbin (H in Fig. 2.6, Songnen–Jiamusi–Bulia) and Junggar plates (Zh in Fig. 2.6, Junggar–East Kazakstan) show evidence of existance of Archean continental nuclei, and around them, are marginal accretion belts of Paleoproterozoic age, e.g. the Jiamusi Greenstone Belt with a Sm-Nd model age of 2.29–1.99 Ga (Zhao CJ et al., 1996), and in Kuruktag on the southern margin of the Junggar Plate a U-Pb age of 1.92–1.912 Ga was obtained.

The Yangtze, Cathaysian, Harbin and Junggar plates did not form a uniform crystalline basement as the result of the Lüliang Tectonic Event, which extends from the Neoproterozoic into the Paleozoic (Fig. 2.7). If this was the case, it should be possible to find some oceanic crust in these plates and in the adjacent areas (Fig. 2.2). But evidence is scarce and the situation needs to be clarified by future research.

In addition, there are many small continental blocks in China (Fig. 2.7), such as the Altay (~90°E, 47.9°N), Ili–Balchas (~82°E, 43.9°N), Turpan–Xingxingxia (~94°E, 42.2°N), Hongshishan (~98°E, 42°N), Yagan (~102°E, 42°N), North Bayannur (~108°E, 42.2°N), Tuotuoshang–Xilingol (~115°E, 43°N), Ergun (~121°E, 51°N), Xingkai (~134°E, 46°N), Songpan–Garze (~103.5°E, 33°N), north of Gangdise (~86°E, 30.2°N), Himalayan (~86°E, 29°N), Lincang (~100.5°E, 22.5°N), Zhongdian (~99.8°E, 27.7°N), Lanping-Simao (~102°E, 23°N) and south of Hainan (~109.2°E, 18.5°N) blocks (Fig. 2.7). Many Archean and Paleoproterozoic isotopic ages have been obtained from these continental blocks. In later geological periods, perhaps in the Paleozoic, Mesozoic and Cenozoic, these blocks and their adjacent areas were amalgamated to form part of the uniform crystalline basement of China.

The development of the Earth was profoundly influenced by tectonic events in the Paleoproterozoic. Hoffman (1988) has suggested that six cratons were amalgamated to form Laurentia, the North American Paleo-continent, during a super-continental tectonic event at the end of Paleoproterozoic (2.0–1.8 Ga). The Baltic Craton was shaped after the Kola-Karelian collision at 2.0–1.9 Ga. The Yilgarn and Pilbara continental blocks of Australia also collided and were amalgamated to form the West Australian craton at the end of Paleoproterozoic, (Hoffman, 1988). However, there is still insufficient data concerning this Paleoproterozoic global tectonic event.

According to present data on the temperatures, pressures, depths and geothermal gradients for the formation of Paleoproterozoic metamorphic rocks (Appendix 1.3), from samples in 28 areas of China, the average temperature was 681°C, average pressure was 0.78 GPa, average depth was 28.5 km. If average surface temperature is assumed to have been 70°C at that time, the geothermal gradient was 21.4°C/km. If the average surface temperature is assumed to have been 0°C [Frakes (1979) suggested that global glaciation first appeared at 2.3 Ga], the average geothermal gradient of China continental crust was 24°C/km. This value for the geothermal gradient in the Paleoproterozoic is similar to the value calculated for the Neoarchean, but somewhat lower than the average geothermal gradient in recent continental crust, and only half the global Archean average geothermal gradient of 54°C/km suggested by Grambling (1981). From the existing data, one can see that there were no large scale geothermal anomalies over most of the Chinese continental plate during the Paleoproterozoic, and no evidence for mantle plumes according to recent data.

However, data in Appendix 1.3 also shows that there was a geothermal gradient of 50–67°C/km in the Mashan Group in Heilongjiang Province (Cheng YQ et al., 1994; Jiang JS et al., 1993). Cheng YQ (1994) studied Songshan greenschist in Henan Province on the southern margin of Sino-Korean Plate, and concluded that the geothermal gradient was 49.5°C/km and in Dabieshan it was 48.5°C/km. By studying an amphibolite from the southwestern margin of Qaidam, Bureau of Geology and Resource of Qinghai (1991) obtained a geothermal gradient of 47°C/km. If these results are reliable, it seems that there were geothermal anomalies during the Protopaleozoic in four areas: the eastern Heilongjiang Province, the southern part of the Sino-Korean Plate, Dabieshan and southern Qaidam. However, this data may still be questionable.

Rates of movement have been calculated for the Chinese continent in the Paleoproterozoic, using the chemical components of magmatic rocks to calculate the rates of plate movement (Sugisaki, 1976; Appendix 1.4). According to the chemical components of ultrabasic and basic rock samples, the rate of extension was less than 1.0 cm/yr. Based on all granitic samples from the Chinese continental crust in Paleoproterozoic, the calculated rate of shortening for all plates was between 4.6–6 cm/yr. It can be

seen that the rates of plate movement in the Paleoproterozoic are similar to rates of movement since the Paleozoic; evidently the same mechanisms of lithosphere plate motion have operated since the Paleoproterozoic. Chemical analyses used in these calculations are taken from the reports of the 1 : 200,000 regional geological surveys and the regional geology of the provinces (Bureau of Geology and Mineral Resources of Provinces, 1984–1993).

2.4 Discussion of the Thickness of Continental Crust in the Archean and Paleoproterozoic

As has been described above, the continental crust was formed mainly during the Archean and Paleoproterozoic. Accretion of material along the margins of the continental crust and the emplacement of magmatic rocks into the crust depends on the subduction of the oceanic crust beneath the continents. Condie (1982) suggested that the thickness of the continental crust could be calculated from the chemical composition of magmatic rocks occurring at the margins of paleocontinents. Potassium (K) content is low in basalts forming the oceanic crust, and high in continental crust. When subduction and collision occur, the K content of the continental crust is increased. To calculate the thickness of the crust, Condie (1982) suggested the "K60 method": the K content of the rocks should be determined by assuming that the SiO_2 content = 60%.

Condie's (1982) empirical formula for determining the original thickness of the continental crust is:

$$C\ (\text{thickness of continental crust, km}) = 18.2 \times w\ (\text{K60}) + 0.45$$

where w(K60) is the K_2O content, SiO_2 is 60% of crustal rocks. Continental crust formed since the Paleoproterozoic was mainly recycled earlier crust, so that the relationship between the K content and the thickness of the crust for these later periods is uncertain. The "K60 method" may therefore not be applicable to Mesoproterozoic and younger continental crust.

In this volume the chemical composition of samples from representative Archean and Paleoproterozoic areas has been used to calculate the thickness of the Chinese continental crust (Appendix 1.5). Unfortunately, there are very few outcrops of Paleo- and Meso-Archean magmatic rocks in China, therefore, data from samples has been obtained from only three areas; this data is not sufficient to draw any significant conclusions. Neoarchean data from granitic samples of 9 areas represents the later periods of magmatism, the average thickness of continental crust was calculated as 66.2 km. Based on the average composition of Archean magmatic rocks in China provided by Cheng YQ (1994), the average thickness of the continental crust was 64.89 km (Appendix 1.5).

Based on the average chemical composition of Proterozoic (mainly Paleoproterozoic) granites provided by Cheng YQ (1994), the average thickness of the Paleoproterozoic Chinese continental crust was 62.33 km. Data from basic rocks in the early period of the Paleoproterozoic from 11 areas gives an average continental thickness of 30.2 km, while data from granite in the late period of the Paleoproterozoic gives an average thickness of continental crust of 55.9 km. In terms of the analyses presented in Appendix 1.5, although there is insufficient data, it seems that the average thickness of the Chinese continental crust was about 60 km in the Archean and the later periods of the Paleoproterozoic. These thickness is comparable to those obtained for other Archean and Proterozoic continents throughout the world, which doubles the average thickness of 33 km of the continental crust at the present day.

According to the mineralogical composition of samples from 11 areas of Mesoarchean rocks their average depth of formation was 32 km; calculated from 47 areas of Neoarchean rocks the average depth of formation was 27.5 km (Appendix 1.1); and from 28 areas of Paleoproterozoic rocks the average depth of formation was 28.5 km (Appendix 1.3). The Archean and Paleopro terozoic rocks exposed at the surface during the present day were all formed at depths of about 30 km. This means that on average about 30 km has been eroded from the upper part of the Chinese continental crust since the late

periods of the Paleoproterozoic. In other words, half the thickness of continental crust formed during the Archean and Paleoproterozoic has now been eroded away, only half of the original thickness remains. This value is the same as the average thickness of the present day continental crust.

Evidently, the average thickness of continental crust, formed before the end of the Paleoproterozoic, has been gradually reduced to its present value since 1.8 Ga and the area of the continents has not changed over that period of time (Fig. 2.6). Continental crust formed before the Paleoproterozoic has remained essentially stable for the last 1.8 billion years, continually uplifted and eroded, progressively decreasing the thickness of continental crust. The average rate of erosion is exceedingly slow, only 0.0167 mm/yr. The other half of the continental thickness has been eroded away and deposited as sediments on the continental margins and on the ocean floors since the Paleoproterozoic, to be incorporated back into the continent during later tectonic events, forming the more extensive continents of the present day, i.e. the original thick continental crust is now spread more evenly across the Earth.

However, it does not mean that the thickness of all of the continental crust has decreased since the Paleoproterozoic. In areas of subduction and collision, or in the areas affected by intense intraplate deformation, the thickness of the continental crust may have temporarily been increased, but have been isostatically uplifted and eroded back to the stable thickness of 30 km over periods of tens of millions of years.

Rb-Sr isotopic analyses of Paleoarchean-Neoarchean granitic rocks from North China showed that their original $^{87}Sr/^{86}Sr$ ratio was 0.7022–0.7060, indicating that the greater part of the granitic material originated in the mantle (Zhang DQ et al., 1988). All the original materials which form the continental crust have originated in the mantle. However, this value is slightly higher than the original $^{87}Sr/^{86}Sr$ ratio of 0.7005–0.7020 measured by laboratories abroad for the Archean in other continents.

In summary, tectonics in Eoarchean (4.5–3.6 Ga) were characterized by planetesimal accumulation and the accretion and formation of the paleo-continental nuclei. In the Paleoarchean–Neoarchean (3.6–2.5 Ga), protoplates were formed and the continental crust was cratonized. In the Paleoproterozoic (2.5–1.8 Ga), rifting and depression occurred within the paleo-continental blocks, forming the main part of Chinese continental crust. Processes of subduction, accretion and collision reunited, reconstituted and amalgamated the continental blocks to form the unified crystalline basement of the Sino-Korean continental protoplate, and the other protoplates of Chinese continental crust.

References

Allègre CJ (1985) De la Pierre àÍ Etoile. Librairie Arthème Fayard.

Asian Geological Map Editing Group, Chinese Academy of Geological Sciences (1975) Asian Geological Map. Geological Publishing House, Beijing (in Chinese).

Bai J, Huang XG, Wang HC et al (1996) The Precambrian Crustal Evolution of China, 2nd edn. Geological Publishing House, Beijing (in Chinese with English abstract).

Bureau of Geology and Mineral Resources of Provinces (1987–1993) Regional Geology of Provinces. Geological Publishing House, Beijing (in Chinese with English abstract).

Cai XL (1965) The geological structure of Pre-Sinian in Dabieshan area—also discussing the structural features of gneiss arch. In: Beijing College of Geology. Papers on Scientific Research 4 (Special of Structure Geology and Regional Geology): 15–26 (in Chinese).

Cai XL (1979) Preliminary research on early structure behaviors during crustal development. In: Teaching Group of Exploring Geology, Chengdu College of Geology. Papers on Structure Geology, pp.69–84. Geological Society of China (in Chinese).

Chen HJ, Ji X (1993) Preliminary research on the time of Yunkai Group and thrust at Luoxiahe, south to Fenjiezhen, Luoding, Guangxi. In: Collection of Structural Geology in Yunkaidashan and Its Adjacent Area, pp.22–28. Geological Publishing House, Beijing (in Chinese).

Cheng YQ (1994) An Introduction to Regional Geology of China. Geological Publishing House, Beijing (in Chinese).
China National Commission on Stratigraphy (2001) Chart of regional stratigraphy (geological age) of China. Journal of Stratigraphy 25(suppl.): 359–360 (in Chinese).
Chou CL, Shaw DM (1983) Siderophile trace elements in the earth's oceanic crust and upper mantle. Proc. 13th Lunar Planet. Sci. Conf., J.Geophy. Res. 88A:507–518
Clayton RN, Grossman L, Mayeda TK (1973) A component of primitive nuclear composition in carbonaceous meteorites. Science (182): 485–488.
Clayton RN, Onuma N, Mayeda TK(1976) A classification of meteorites based on oxygen isotopes. Earth and Planetary Science Letters 30 (1): 10–18.
Clayton RN, Mayeda T K (1983) Oxygen isotopes in eucrites, shergottites, nakhlites, and chassignites. Earth and Planetary Science Letters (62): 1–6.
Condie KC (1982) Plate Tectonics and Crustal Evolution, 2th edn. Pergamon Press, New York.
Condie KC (1994) Archean Crustal Evolution. Elsevier Scientific Publishing Company, Amsterdam.
Condie KC (1997) Plate Tectonics and Crustal Evolution, 4th edn. 282pp. Butterwoth-Heinemann, Oxford.
Condie KC (1997) Contrasting sources for upper and lower continental crust: the greenstone connection. J. Geol. 105: 729–736.
Condie KC (2001) Mantle Plumes and Their Record in Earth History. Cambridge University Press, Cambridge.
Dai WS (1979) The Evolution of Solar System (part Ⅰ). Shanghai Science & Technology Press, Shanghai (in Chinese).
Dong SB (1986) Metamorphism of China and Its Relationship with Crustal Evolution. Geological Publishing House, Beijing (in Chinese with English abstract).
Eskola PE (1949) The problem of mantled gneiss dome. Q. J.G. S. London, V. CIV. 4.
Frakes LA (1979) Climates Throughout Geologic Time. Elsevier, Amsterdam.
Gao TJ, Wang ZM, Wu KL et al (1999) Tectono-magmatic Evolution and Metallogeny of Taiwan Strait and Its Adjacent Areas. Geological Publishing House, Beijing (in Chinese).
Editorial Board of Geoscience Transect, Seismic Bureau of China (1991) Geoscience Transect from Xiangshui, Jiangsu to Mandalt, Inner Mongolia (1: 1,000,000, attached explanation). Geological Publishing House, Beijing (in Chinese).
Editorial Board of Geoscience Transect, Seismic Bureau of China (1992) Geoscience Transect from Dong Ujimqin, Inner Mongolia to Donggou, Liaoning (1: 1,000,000, attached explanation). Seismological Press, Beijing (in Chinese).
Editorial Board of Geoscience Transect, Siesmic Bureau of China (1992) Geoscience Transect from Zhefang to Malong in Yunnan (1: 1,000,000, attached explanation). Seismological Press, Beijing (in Chinese).
Editorial Board of Geoscience Transect, Siesmic Bureau of China (1992) Geoscience Transect from Suizhou, Hubei to Kalaqinqi, Inner Mongolia (1: 1,000,000, attached explanation). Seismological Press, Beijing (in Chinese).
Editorial Board of Geoscience Transect, Siesmic Bureau of China (1992) Geoscience Transect from Menyuan, Qinghai to Ningde, Fujian (1: 1,000,000, attached explanation). Seismological Press, Beijing (in Chinese).
Editorial Board of Geoscience Transect, Siesmic Bureau of China (1992) Geoscience Transect From Fengxian, Shanghai to Alxa Zuoqi, Inner Mongolia (1: 1,000,000, attached explanation). Seismological Press, Beijing (in Chinese).
Goodwin AM (1991) Precambrian Geology. Academic Press, London.
Grambling JA (1981) Pressure and temperature in Precambrian metamorphic rocks. Earth Planet. Sci. Lett. 53: 63–68.
Guan SC (1999) Marine-facies, Terrestrial and Offshore Petroleum Geology of China. Geological Publishing House, Beijing (in Chinese).

Guan ZN, An YL, Wu CJ (1987) Inversion of magnetic boundaries and investigation into deep-seated geological structures of north China. In: Wang MJ, Cheng JY (eds) Contributions to the Exploration Geophysics and Geochemistry, no.6: Regional Geophysical Features of Eastern China, pp.80–101. Geological Publishing House, Beijing (in Chinese).

Hoffman PF (1988) United plates of America, the birth of a craton: Early Proterozoic assembly and growth of Laurentia. Ame. Rev. Earth Planet Sci. 16: 543–603.

Huang H, Li RA, Yang CX (1990) Geochronologic study for the metamorphic belt along the coast of Fujian province and its tectonic significance. Chinese Science Bulletin 35(9): 751–754.

Hunter DR (1981) Precambrian of the Southern Hemisphere. Elsevier, Amsterdam.

International Commission on Stratigraphy (2004) International stratigraphic chart. 32th IGC, Florence, Italy.

Jacobsen SB, Wasserburg GJ (1984) Sm-Nd isotopic evolution of chondrites and achondrites (Ⅱ). Earth and Planetary Science Letters 67(2): 137–150

Jiang JS, Chen YQ (1993) Cordierite gneisses in Mashan khondalite series, Northeast China. Acta Petrologica Sinica 9(4): 401–410 (in Chinese with English abstract).

Kröner A, Greiling R (1984) Precambrian tectonics illustrated: International Union of Geological Science Commission on Tectonics, Subcommission on Precambrian Structural Type. Lubrecht & Cramer Ltd., Stuttgart.

Kusky T, Li JH, Tucker RD (2001) The Archean Dongwanzi ophiolite complex, North China craton: 2.505 billion year-oil oceanic crust and mantle. Science 292: 1142–1145.

Lee JS(Li Siguang) (1939) The Geology of China. Thomas Murby & Co., London.

Li CY, Wang Q, Liu XY, Tang YQ (1982) Tectonic Map of Asia (1: 8,000,000) and Its Specialties. Geological Publishing House, Beijing (in Chinese).

Li CY, Wang Q, Liu XY, Tang YQ (1984) The evolution of Asian tectonics. Bulletin of the Chinese Academy of Geological Sciences (10): 3–12. Geological Publishing House, Beijing (in Chinese).

Li FX, Nie XW (1987) The geological age and stratigraphic division of Kongling Group in northern part of Huangling faulted up warping. Hubei Geology 1(1): 28–41 (in Chinese with English abstract).

Li JH, Kusky T, Huang XN (2002) Archean podiform chromitites and mantle tectonites in ophiolitic mélange, North China Craton: a record of early oceanic processes. GSA Today, 12(7): 4–11.

Liu DY (1991) Discovery of the palaeocontinental crust before 3,800 Ma in China. Chinese Geology (Geology in China) (5): 30 (in Chinese with English abstract).

Liu DY, Nutman AP, Compston W et al (1992) Remnant of >3,800 Ma crust in the Chinese part of the Sino-Korean Craton. Geology 20: 339–342.

Liu GH, Zhang SG, You ZD et al (1993) Main Metamorphic Rock Groups and Metamorphic Evolution of Qinling Orogenic Belt. Geological Publishing House, Beijing (in Chinese).

Lu SN (2002) From Rodinia to Gondwanaland supercontinents—thinking about problems of researching Neoproterozoic supercontinents. Earth Science Frontiers 8(4): 441–448 (in Chinese with English abstract).

Ma XY, Wei BH (1956) Sinian system of Wutaishan area and Sinian paleogeography in Hebei and Northwestern Shanxi. Acta Geologica Sinica 36(3): 299–314 (in Chinese with Russian abstract).

Ma XY (1957) On the Precambrian stratigraphy of the Songshan area, Henan and its correlation problems. Acta Geologica Sinica 37(1): 11–32 (in Chinese with Russian abstract).

Ma XY, Cai XL (1965) Features of structure changes in Early Archean in east China. In: Problems About Tectonics of China. Science Press, Beijing (in Chinese).

Newsom HE (1990) Accretion and core formation in the Earth evidence from siderophile elements. In: Newsom HE, Jones JH (eds) Origin of the Earth. Oxford University Press, London.

Ouyang ZY (1995) Formation and evolution of planetary earth. Geology and Geochemistry (5): 1–105 (in Chinese).

Ouyang ZY, Liu JZ, Zhang FQ et al (2002) A preliminary study on the origin and evolution of the planetary Earth's heterogeneity. Earth Science Frontiers 9(3): 23–30 (in Chinese with English abstract).

Qian XL, Wang RM (1994) Geological Evolution of Granulite Belt in North Part of North China. Seismological Press, Beijing (in Chinese).

Qian XL (1996) The nature of the Early Pre-cambrian continental crust and its tectonic evolution model. Acta Petrologica Sinica 12(2): 169–178 (in Chinese with English abstract).

Qiao XF, Ma LF, Zhang HM (1990) Terminal Precambrian palaeogeographic framework of China. Bulletin of the Chinese Academy of Geological Sciences 20: 4–5 (in Chinese with English abstract).

Remane J et al (2000) International stratigraphic chart. International Commission on Stratigraphy.

Reymer APS, Schubert G (1987) Phanerozoic and Precambrian crustal growth. In: Kröner A (ed) Proterozoic lithosphere evolution. Geodynamics Series 17: 1–9. American Geophysical Union, Washington DC.

Rudnick RL, Gao S (2003) Composition of the continental crust. In: Rudnick RL (ed) The Crust. vol.3, pp.1–64 of Treatise on Geochemistry (Holland HD, Turekian (eds)) Elsevier Pergamon, Oxford.

Safranov VS (1972) Evolution of the Protoplanetatry Cloud and Formation of the Earth and Planets. Nauka, Moscow (Translated by the Israel program for scientific translation).

Stassen C (1996—2005) The age of the earth. htp: // www. talkorigins. orgl faqs/ faq-age-of-earth. html. Accessed on 20 Mar 2010.

Sugisaki R (1976) Chemical characteristics of volcanic rocks: relation to plate movements. Lithos 9(1): 17–30.

Sun DZ (1990) Tectonic and geochemical development of Archaean and Proterozoic mobile belts in eastern China. Bulletin of the Chinese Academy of Geological Sciences 20: 105–107 (in Chinese with English abstract).

Suo ST, Sang LK, Han YJ et al (1993) The Petrology and Tectonics in Dabie Precambrian Metamorphic Terranes, Central China. China University of Geosciences Press, Wuhan (in Chinese with English abstract).

Tan YJ, Wang FZ, Zhao WX (1993) The Early Precambrian Geology in the South of the Fuping Uplift on the Taihang Mountains, Discussion of a Few Basic Problems and the Research Methods of the Archean Geology. China University of Geosciences Press, Wuhan (in Chinese).

Turekian KK, Clark SP (1969) Inhomogeneous accumulation of the earth from the primitive Solar nebula. Earth Planet Sci. Lett. 6(5): 346–348.

Veizer J (2005) Celestial climate driver: a perspective from four billion years of the carbon cycle. Geoscience Canada 32: 13–28.

Wang GZ, Wang CS (2001) Disintegration age of basement metamorphic rocks in Qiangtang, Tibet, China. Science in China D 44 (suppl.): 86–93.

Wang HZ (1981) Geotectonic units of China from the view-point of mobilism. Earth Sciences—Journal of Wuhan College of Geology (1): 42–66 (in Chinese with English abstract).

Wilde SA, Valley JW, Peck WH et al (2001) Evidence from detrial zircons for the existence of continental crust and oceans on the Earth 4.4 Gyr ago. Nature 409: 175–178.

Wilde SA, Zhao GC, Sun M (2002) Development of the North China Craton during the Late Archaean and its final amalgamation at 1.8 Ga: some speculations on its position within a global Paleoproterozoic supercon-tinent. Gondwana Research 5: 85–94.

Wilde SA, Cawood PA, Wang K et al (2004) Determining Precambrian crustal evolution in China: a case-study from Wutaishan, Shanxi Province, demonstrating the application of precise SHRIMP U-Pb geochronology. In: Malpas J et al (eds) Aspects of the tectonic evolution of China. 5–26. London: The Geological Society, Special Publication 226.

Windley BF (1995) The Evolving Continent, 3rd edn. John Wiley and Sons, Chichester.

Wu CH, Li HM, Zhong CT et al (2000) Timing U-Pb single zircon ages for the orthogneiss and the paragneiss of Fuping complex: implications for existence of the Palaeoproterozoic supracristal rocks in the central basement of north China craton. Progress in Precambrian Research 23(3): 129–139 (in Chinese with English abstract).

Wu GJ, Gao R, Yu QF et al (1991) Integrated investigations of the Qinghai-Tibet Plateau along the Yadong-Golmud Geoscience transect. Acta Geophysica Sinica 34(5): 552–562 (in Chinese with English abstract).

Wu GJ (1998) Integrated Study of the Golmud-Ejin geoscience transect. Acta Geologica Sinica 72(4): 289–300 (in Chinese with English abstract).

Wu MD (1988) The main metallogenesis of pre-Sinian system on the Xikang–Yunnan axis. Geology of Jiangxi 2 (2): 251–254 (in Chinese with English abstract).

Yu HF, Mei HL, Li Q (1998) The characteristics of Archean khondalite series in Dunhuang, Gansu Province. Progress in Precambrian Research 21(1): 19–25 (in Chinese with English abstract).

Yuan XC (1990) Geoscience Transect of Taiwan–Heishui (1: 1,000,000, attached with specialities). Seismological Press, Beijing (in Chinese).

Zhai MG, Zhao GC, Zhang Q et al (2002) Is the Dongwanzi complex an Archean ophiolite? Science 295: 923.

Zhai MG (2004) Precambrian tectonic evolution of the North China Craton. In: Malpas J et al (eds) Aspects of the Tectonic Evolution of China. London: The Geological Society. Special Publication 226.

Zhang BY, Yu HN (1994) Deep-seated Nappe Structure of Hercynian-Indochina Collisional Zone in West Guangdong. Geological Publishing House, Beijing (in Chinese).

Zhang DQ, Sun GY (1988) Granites of Eastern China. China University of Geosciences Press, Wuhan (in Chinese with English abstract).

Zhang Q, Ni ZY, Zhai MG (2003) Comment on Archean ophiolite in eastern Hebei. Earth Science Frontiers 10(4): 429–436 (in Chinese with English abstract).

Zhang SG (1990) Discussion on some features of metamorphism in China. Bulletin of the Chinese Academy of Geological Sciences 20: 67–69 (in Chinese with English abstract).

Zhao GC, Wilde SA, Cawwod PA et al (1998) Thermal evolution of Archaean basement rocks from the eastern part of the North China Craton and its bearing on tectonic setting. International Geological Review 40: 706–721.

Zhao GC (2001) Paleoproterozoic assembly of the North China craton. Geological Magazine 138: 87–91.

Zhao GC, Sun M, Widle SA et al (2004) Late Archaean to Paleoproterozoic evolution of the Trans-North China Orogen: In slights from synthesis of existing data of the Hengshan–Wutai–Fuping belt. In: Malpas J et al (eds) Aspects of the Tectonic Evolution of China. London: The Geological Society. Special Publication 226.

Zhong DL, Ji JQ, Hu SL (1999) Subduction age of Neo-Tethys oceanic crust in southwest Yunnan, China: the laser micro-area ^{40}Ar-^{39}Ar dating. Chinese Science Bulletin 44(23): 2196–2199 (in Chinese).

Chapter 3
Tectonics of the Mesoproterozoic, Neoproterozoic and Early Cambrian (1.8 Ga–513 Ma)

Five tectonic periods can be distinguished in the tectonic evolution of Chinese continent during the Meso-Neoproterozoic and Early Cambrian: (1) the Changcheng Tectonic Period (Latest Paleoproterozoic–Early Mesoproterozoic, equal to the Statherian and Calymmian periods, 1, 800–1, 400 Ma); (2) the Jixian Tectonic Period (Middle–Late Mesoproterozoic, equal to the Ectasian and Stenian periods, 1, 400–1, 000 Ma); (3) the Qingbaikou Tectonic Period (or Jinning Period as it is called in South China, equal to the global Tonian Period, 1, 000–800 Ma); (4) the Nanhua Tectonic Period (Cryogenian Period, 800–680 Ma); (5) the Sinian Tectonic Period (Latest Neoproterozoic–Early Cambrian Epoch, 680–513 Ma) (National Commission on Stratigraphy of China, 2001; International Commission on Stratigraphy, 2004).

As the isotope ages obtained so far are not sufficiently precise, the division of the Proterozoic rocks into tectonic periods depends mainly on their sedimentary features and their tectono-magmatic history. In general there is no correspondence between the boundaries of the tectonic periods and the faunal-floral epochs. However, it is at present impossible to classify the strata in more detail. In recent years it has been demonstrated that there is continuity in sedimentation between the Sinian and Cambrian Systems (the time boundary is about 543 Ma) in many areas of the Chinese continent, with a hiatus in deposition between the Early and Middle epochs of Cambrian. The Sinian Tectonic Period is therefore defined to include both the Sinian and Early Cambrian Periods (i.e. 680–513 Ma).

Thickness data has been compiled for all the sedimentary systems in China, taken from the regional geological reports about the 75 administrative provinces. It is found that the average thickness of sedimentary systems is reduced from 24,000 m in the Mesoproterozoic to 600 m in the Neoproterozoic, and that the rate of deposition of sedimentary strata was also radically decreased (Appendix 2; Fig. 3.1).

In the South China Blocks the Early Mesoproterozoic is represented only by high grade metamorphic rocks, in which the history of rock deformation is not yet properly understood, consequently it is impossible to calculate the thickness of the strata. Recent statistical data providing evidence of changes in sedimentary environments and structure during the Proterozoic are derived mainly from the northern Chinese continental blocks. Data from South China Blocks reflect mainly sedimentary and structural characteristics during the Middle–Late Periods of Meso-Neoproterozoic. Changes in sediment thickness (Appendix 2) will be discussed in the following section.

Using the method of Sugisaki (1976; given in Chapter 1), the velocities of extension or shortening within the continental plates in the Meso-Neoproterozoic have been estimated, using data from 552 chemical analyses of magmatic rocks (Appendices 5.1 and 5.2). The tectonic evolution of the Meso-Neoproterozoic rocks will be discussed in the following sections, bearing in mind the limitations in the data.

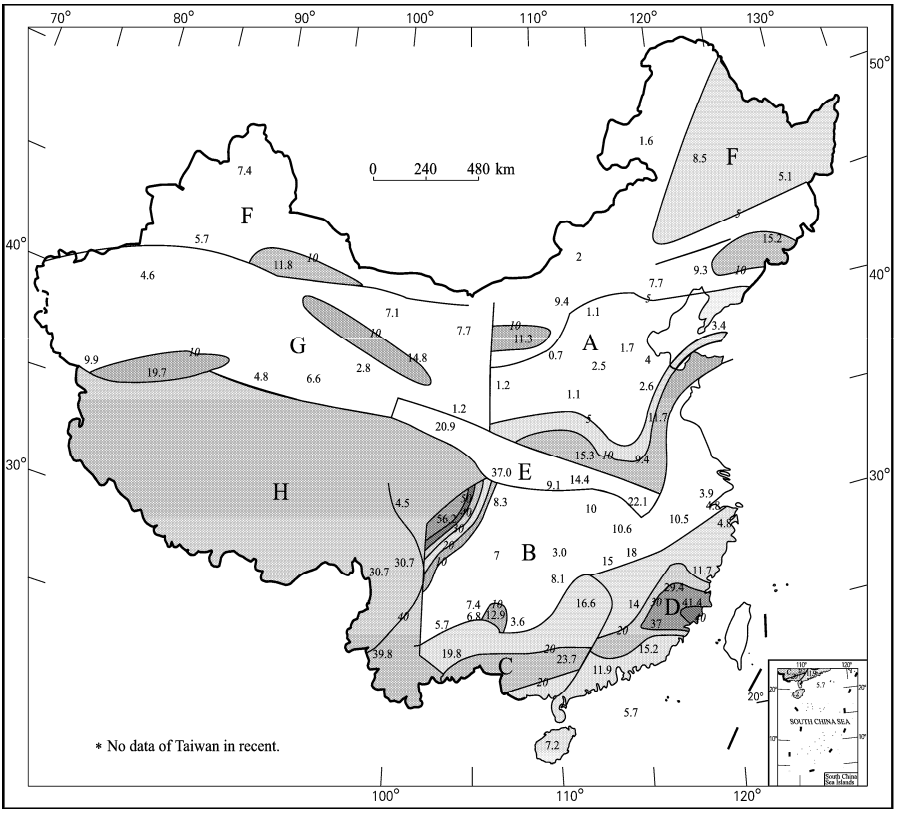

Fig. 3.1 Rates of sedimentation in sedimentary strata of Meso-Neoproterozoic in the Chinese continent (unit: m/Myr).

A. Eastern part of Sino-Korean Protoplate; B. Northern Yangtze Plate; C. Southern Yangtze Plate; D. Cathaysian Plate; E. Dabie–Qinling Block; F. Harbin-Kazakhstan Block; G. Western part of Sino-Korean Protoplate (Tarim, Qaidam, Qilianshan and Alxa Blocks). H. Peri-Gondwanan Blocks.

3.1 Tectonics of the Mesoproterozoic (1, 800–1, 000 Ma, Changcheng Period–Jixianian Period)

—depression and formation of the sedimentary cover of Sino-Korean Protoplate, amalgamation of Yangtze Plate

During the Paleoproterozoic the Sino-Korean Protoplate developed a unified crystalline basement extending westwards to Tarim and eastwards to the Korean Peninsula. The first important angular unconformity occurs between the Paleoproterozoic and Mesoproterozoic. In the Changcheng Period (1, 800–1, 400 Ma) rift basins developed in many places on the Sino-Korean Protoplate, leading to the deposition of the earliest sedimentary cover to rest on the crystalline basement (Fig. 3.2). The sediments at the base of Changcheng System are separated from the basement by a deeply weathered denudation surface, which had been developed over a long period of time. At the beginning of Mesoproterozoic extensional rift basins were developed, although Sino-Korean Protoplate remained a single plate.

Fig. 3.2 Angular unconformity (shown by red line) between the Archean metamorphic system (Ar, amphibolite) with foliation dipping to the left and the Mesoproterozoic sedimentary series (MP, quartz sandstone) which is the earliest sedimentary sequence at Yesanpo, Laishui County, Hebei Province (Wang Y, 2006, personal communication, with permission of Wang Y).

These rift basins were invaded by shallow seas which extended between the Tarim and Qaidam Blocks, as well onto the Sino-Korean Protoplate. Extension adjacent to the Qilianshan Paleoblock probably led to the formation of oceanic crust in this area (Fig. 3.3).

During the Jixian Period the Chinese continental blocks inherited the basic tectonic characteristics which had been developed during the Changcheng Period. Because the data is very limited, these two tectonic periods will be discussed together.

Sediments of the Changcheng and Jixian Systems are widespread over the whole Sino-Korean Protoplate, from Tarim in the west to the Korean Peninsula in the east. The standard section for the Changcheng System is at Jixian, Tianjin in north China (117.4°E, 40.2°N), forming a typical transgressive sequence and including the Changzhougou, Chuanlinggou, Tuanshanzi, Dahongyu and Gaoyuzhuang Formations. The lower part of the sequence consists of conglomerate, sandstone and shale, while the upper part consists mainly of dolomitic carbonates. The Jixian System, which includes the Yangzhuang, Wumishan, Hongshuizhuang and Tieling Formations, is composed mainly of shallow marine deposits, with alternating layers of clastic sediment and siliceous dolomitic carbonate.

In the main part of Sino-Korean Protoplate, from eastern Liaoning, Yanshan, Taihangshan, Shandong, Hebei Plain, Shanxi to east Ningxia (102–127°E, 34–43°N), the thickness of Meso-Neoproterozoic strata reduced from 4, 000 m to 600 m in 400 million years. The average rate of sedimentary deposition was less than 0.01 mm per year. This shows a very little amount of tectonic activity, as rates of sedimentation are normally 1-5 m/Myr (Appendix 2, Fig. 3.1, A). In the Jixian, Tianjin–Chaoyang–Liaoning and adjacent areas, tidal flat to shallow marine facies was deposited in the NE-NNE trending Yanshan–western Liaoning Rift Basin. The center of this rift system is at Qinglong–Ruanxian (118.8–119°E, 39.7–40.5°N), in northern Hebei Province (Figs. 3.3, 3.4 and 3.5), where the thickness of the Mesoproterozoic–Neoproterozoic sediments is ~10,000 m.

Bai J et al. (1996) took samples of siliceous dolomite from the second member of Dahongyu Formation deposited in the rift basin, overlying the products of a volcanic eruption. He used the homogenization of fluid inclusions within the minerals to determine the paleo-temperature, and found a paleotemperature of 260°C in the center of the rift basin, while in Chicheng–Yanqing to the NW, the paleotemperature decreased to 150°C. He inferred that in this period hot water springs erupted onto the sea floor from the Qinglong–Ruanxian Fault.

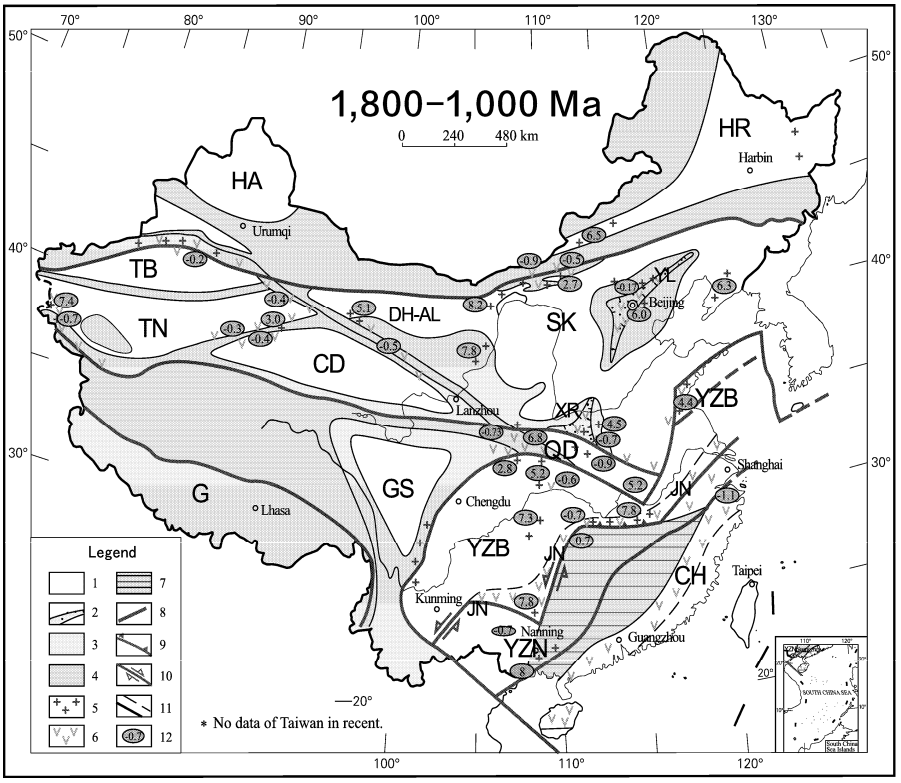

Fig. 3.3 Paleotectonic sketch for the Mesoproterozoic of China (1, 800–1, 000 Ma) (data after Bai J et al., 1996; Liu BJ et al., 1994, and completed by the author).

1. Area of erosion on paleocontinental plate; 2.Rift system; 3. Shallow seas with sedimentation; 4, Oceanic crust; 5. Granitic intrusions; 6. Island arcs with intermediate-acid volcanic rocks; 7. Continental slope with turbidite sedimentation; 8. Collision zone or boundaries of plates; 9. Subduction zone including ophiolite belt; 10. Strike-slip fault; 11. Boundary of tectonic province; 12. Rate of plate movement; "-" is rate of extension; "+" is rate of shortening (cm/yr). See Appendices 5.1 and 5.2.

JN marks the Jiangnan subduction and collision zone, formed at about 1000 Ma.

Divisions of tectonic domains: Peri-Siberian Tectonic Domain (HA= Paleo-Kazakhstan Plate; HR= Paleo-Harbin Plate); Proto-Sino-Korean Plate Tectonic Domain (TR= Paleo-Tarim Plate; CD= Paleo-Qaidam Plate; SK= Paleo-Sino-Korean Plate which included the North China area, the Korean Peninsula and the Alxa Block); Peri-Yangtze Plate Tectonic Domain (YZ= Paleo-Yangtze Plate; also included the Qinling-Dabie Block; GS= Paleo-Songpan-Garze Block; CH= Cathaysian Paleo-Plate); Peri-Gondwanan Tectonic Domain (G).

In this figure, the eastern part of Paleo-Yangtze Plate is shown to be indented into Sino-Korean Plate in the southern Yellow Sea area. This tectonic event occurred in the Triassic. In a tectonic reconstruction, part of the Yellow Sea in this map should be shown to belong to the Sino-Korean Plate.

N.B. No reconstruction of the positions of the plates and their boundaries are attempted in these maps.

The Yanshan–Western Liaoning Rift Basin developed on the Sino-Korean Paleoplate in the Mesoproterozoic along an earlier suture zone which formed an easily deformed zone of weakness in the Archean–Paleoproterozoic crystalline basement. The rift basin had a very low rate of extension. At Tangshan of Hebei, Jixian of Tianjin and Damiao of Hebei (117.8–118.3°E, 39.6–41.2°N), the rate of extension is calculated to be only 0.12–0.23 cm/yr, with an average rate of 0.2 cm/yr (Bai J et al., 1996).

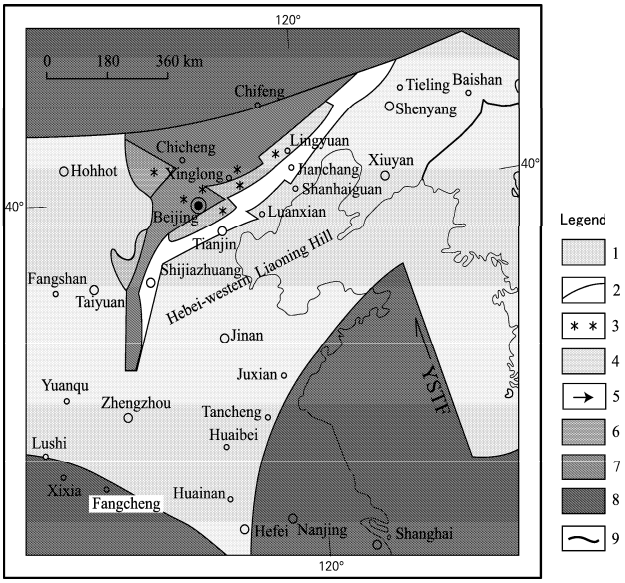

Fig. 3.4 Paleogeographic map of the Sino-Korean Plate in the Early Changcheng Period (1, 800–1, 600 Ma) (after Qiao XF, 2002, with permission of Qiao XF).

1. Area of erosion; 2. Synsedimentary fault; 3. Earthquake event accompanied by synsedimentary faulting (distribution of seismites); 4. Fluviatile sediments (feldspathic quartz sandstone); 5. Direction of river flow; 6. Area with littoral ferruginous sediments (stromatolite hematite of Xuanlong type); 7. Area of marine transgression (inter bedded shales and thin sandstones); 8. Open sea, with deep water sediments; 9. Border of country. ①Yanshan–west Liaoning Rift Basin; YSTF, East Yellow Sea Transform Fault (formed in the Triassic).

If extension had continued at this rate for 100 million years, then plate would have been extended by 200 km. However, the length of time over which extension of the plate continued is unknown.

In Shanxi Province, the northwestern part of Hebei Province and at Jining (113°E, 41°N), Inner Mongolia, during the Proterozoic a basic dyke swarm on a very large scale intruded the Archean crystalline basement and the weakly metamorphosed Early Proterozoic sediments. The dominant direction of strike of the dykes is NNW-SSE (in present day coordinates). About 20 samples from this dyke swarm have been dated isotopically and gave ages ranging from 1, 700 to 1, 100 Ma (Zhang C et al., 1996, 1998; Zhao GC, 2004). The lengths of the dykes range from several thousand meters to dozens of kilometers, and the width from several meters to dozens of meters. The density of dykes in the swarm is normally about 2–3 per kilometer. Based on a study of the magnetic fabric of the dyke swarm, Zhang C et al. (1998) suggested that the source of swarm lay to the east of the Yanshan–west Liaoning Rift Basin. The appearance of a dyke swarm on such a large scale shows that the main body of Sino-Korean Protoplate already formed a unified crystalline basement before the Mesoproterozoic. The dykes are due to ENE-WSW extension along an NNW-trending zone of weakness within the crystalline basement (these rocks should not be used in paleomagnetic reconstructions). At the end of the Changcheng Period, i.e. in the late tectonic period of formation of the Yanshan–west Liaoning Rift Basin, the Sino-Korean Protoplate was shortened in the NNW direction (also unsuitable for paleomagnetism). From the chemical composition of the granites in Liaoning (isotopic age 1, 565–1, 305 Ma) and Shachang, Miyun in Beijing (110–118°E, 40°N; with isotopic age of 1, 588 Ma), it is found that the rate of shortening was about 6 cm/yr, estimated by the method explained in Chapter 1 (data shown in Appendix 5.1).

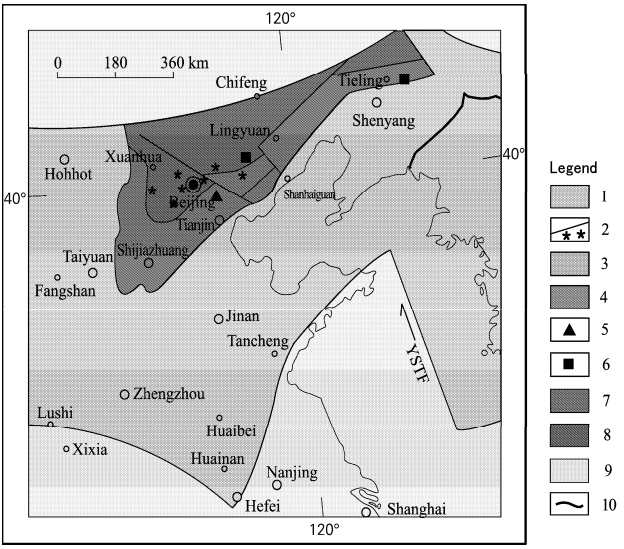

Fig. 3.5 Paleogeographic map of the Sino-Korean Plate in the Late Changcheng and Jixian periods (1, 600–1, 000 Ma) (after Qiao XF, 2002, with permission of Qiao XF).

1. Area of erosion; 2. Syn-sedimentary faults with accompanying earthquake events (seismites in the Dahongyu, Gaoyuzhuang and Wumishan formations); 3. Volcanic eruption (potassium-rich trachyte in the Dahongyu Formation); 4. Basalt, Erdaogou Formation; 5. Volcanic fumarole in limestone of the Tieling Formation; 6. Lead, zinc, sulphur and iron ore belt; 7. Tidal flats (stromatolites, laminated algal limestone, dolomite); 8. Open marine sediments; 9. Land; 10. Border of country. ①Yanshan–west Liaoning Rift Basin; YSTF= East Yellow Sea Transform Fault (formed in Triassic).

The Xiong'er Group, with a thickness of 19,200 m (not sure), was deposited in the Xiong'ershan Rift Basin (aulacogen) between 1, 870 and 1, 459 Ma, in northern and western Henan, north Jiangsu and north Anhui (110–118°E, 32–35°N), along the southern margin of Sino-Korean Paleoplate. A bimodal volcanic rock system was developed, possibly related to intraplate extensional faults, with a rate of plate extension, estimated from the chemical composition of basic volcanic rocks of 0.7 cm/yr. At the end of Changchengian Period, shortening occurred at a rate, estimated from granite compositions, of 4.5 cm/yr (Appendix 5.1).

In the Changcheng and Jixian periods shallow marine sediments were deposited extensively on the southwestern margin of the Sino-Korean Paleoplate. In the southern part of Erdos (106–110°E, 34–36°N), the thickness of the Meso-Neoproterozoic sedimentary strata is about 14,156 m, at Dunhuang, south of Alxa (95°E, 40°N) is 14,525 m, and 9,662 m at Alxa -Longshoushan (100–105°E, 37–38°N). These sediments were deposited in a wide marginal belt of subsidence, with a rate of plate extension, estimated from the chemical composition of basic volcanic rocks, of 0.5 cm/yr. At the end of Changcheng Period, the rate of shortening in the Erdos area was 7.8–8.2 cm/yr, estimated from the chemical composition of granites at Alxa Zuoqi. The Xiaomashi granite (1, 079 Ma isotopic age) around Dunhuang indicates a rate of plate shortening of 5.1 cm/yr (Appendix 5.1, Fig. 3.3).

In the Mesoproterozoic Cha'ertai (106°E, 40.3°N) and Bayan Obo (110°E, 42°N) Inner Mongolia, Beishan (94–97°E, 41–41.8°N) and Tianshan (78–92°E, 42–43°N) were located on the northern margin of the Sino-Korean Protoplate, here the sediment thickness is about 7, 000–9, 000 m. In the Cha'ertai–Langshan zone of subsidence (>1, 600 Ma) the transgressive sedimentary sequence is composed of coarse and fine grained clastic rocks, black shales and carbonates. Coarse clastic rocks near the base of the sequence have a low maturity, indicating rapid sedimentation during subsidence. The clastic

sediments become finer and more mature upwards, representing a change from littoral to shallow marine conditions.

The earliest sediments of the Bayan Obo Group in the north marginal Bayan Obo Rift Basin in the Sino-Korean Plate are immature terrestrial clastic rocks, and the group is composed mainly of clastic rocks and claystones. Being higher in the sequence the sediments are mainly lutites and turbidites, with slide and slump structures, believed to be formed during the active phase of rifting. The uppermost sediments are mature clastics and carbonates. The deposits in the Bayan Obo Rift Basin reflect rapid sedimentation at the margin of the protoplate. The rift basin was also the site of intermediate, alkaline intrusion and hydrothermal activity, followed by the formation of super-large deposits of rare earth elements, rare metals and iron ore. The mechanism for the formation of these ore deposits is not very clear. A popular view is that hydrothermal fluids originating in the mantle moved upwards along faults into a marine basin, via reacting with sea water, precipitating niobium, rare earth elements and iron ore deposits. These deposits are interpreted as the result of sedimentary, hydrothermal and metasomatic processes (Chen H et al., 1987; Wang J and Li SQ, 1987; Zhai YS et al., 1999).

The Bainaimiao Group was deposited in the Bainaimiao–Wenduermiao area (111°E, 42.1°N) on the northern margin of Bayan Obo Rift Basin. The sediments are of continental margin rift type in which the Dongshengmiao sedimentary lead-zinc, sulphur hydrothermal ore-deposits were formed. At the time of rifting, the rate of extension was 0.4–0.5 cm/yr. After extension ceased, shortening occurred at the rate of 2.7 cm/yr. On the basis of the chemical composition of the Sandaoqiao, Dengkou and Wuhai granites in Inner Mongolia (centered on 107°E, 40.2°N; isotopic age of 1, 717–1, 500 Ma), and a diorite of the Jixian Period in the Balunbieli and Bayan Obo basins (isotopic age of 1, 696–1, 681 Ma), at the end of Mesoproterozoic the rate of plate shortening in Inner Mongolia ranged between 2.7 and 6.5 cm/yr (Appendix 5.1).

Recently Qiao XF et al. (1997) found trilobite detritus at the base of the Yusailin-hudong Group in the Baiyan Obo area, and separated Ordovician acritarchs and chitinozoan fossils from the deposit. They concluded that the group was of Early Paleozoic age. It is probable that some of the Bayan Obo super-large scale ore-deposits may have been formed in the Early Paleozoic, rather than in the Proterozoic; this probability requires further investigation.

In the Changcheng Period, the rates of extension in the rift basins around the Sino-Korean Protoplate, in Liaoning Province, Bayan Obo, Fangcheng in Henan Province (113°E, 33.3°N), the Kuangping Group in Shaanxi -Henan (108°E, 34.3°N–114°E, 32.2°N), western Qingling in Gansu (100°E, 36°N–106°E, 34°N) and Qilianshan (96°E, 39.6°N–103°E, 37°N) have been estimated from the composition of basic volcanic rocks to be 0.45–0.7 cm/yr. In the Jixian Period, the rate of extension in the rift basin on the northern margin of the Sino-Korean Protoplate increased to 0.9 cm/yr (Fig. 3.3). In the rift basins on the northern and southern margins of eastern Sino-Korean Protoplate, rates of sedimentation were 5–15 m/Myr, greater than those in the basins in the central part of the plate (Appendix 2; Fig. 3.1, A).

In earlier periods the Qaidam and Tarim blocks formed the western part of Sino-Korean Protoplate. In the Mesoproterozoic rift systems formed around these blocks and they became separated from the Sino-Korean-Alxa Plate by the Qilian Paleo-Ocean. At Qilian -Tianshan, Altun (88°E, 38°N–94°E, 39.5°N), in the northern part of West Kunlun, north of the Middle Kunlunshan Fault (76°E, 37.5°N to 82°E, 35.8°N), thick shallow marine to bathyal sediments were deposited. At Qilianshan in Gansu, a series of bathyal volcanic rock, carbonates and flysch sediments, with a thickness of 18,543 m, were deposited. These rocks have been metamorphosed in the amphibolite and greenschist facies. In the Tielike area on the northern slopes of West Kunlun, a shallow marine sequence up to 24,871 m thick accumulated. Rates of sedimentation in the Qilianshan and Kunlunshan are very high, between 10 m/Myr and 19 m/Myr. On the Qaidam and Tarim Blocks the Mesoproterozoic sediments are thinner. On the northern margin of the Qaidam Block the sediments are 3, 547 m thick, in the center 8, 354 m and on the southern margin (in the Xiaomiao Group, isotopic age 1, 666–1, 549 Ma) of East Kunlun (87°E, 36.2°N–96°E, 35.8°N) 6,073 m. On the Tarim Block sediment thickness is 5,879 m. Rates of sedimentation in all these areas are less than 10 m/Myr (Fig. 3.1 G; Appendix 2).

Rates of extension around the Tarim Paleoplate in the Changcheng Period have been estimated from the composition of basic volcanic rocks, and were found to be 0.2–0.4 cm/yr, very similar to rates of extension in the rift basins in the Sino-Korean Protoplate. The highest rate of extension in West Kunlun was 0.7 cm/yr. Basic volcanic eruptions in Changcheng Period, in Tielike and Suliman in the Tarim Block, gave an isotopic age of 1, 764 Ma. In Altun, where bimodal volcanic rocks were extruded in association with extensional faulting, the rate of extension was 0.3–0.34 cm/yr. During the Jixian Period, rates of extension in the Tarim Block were similar to those in the Sino-Korean Paleoplate. In West Kunlun the rate of plate shortening at a late period in the Mesoproterozoic, estimated from the composition of granites, was 7.6 cm/yr, but only 3 cm/yr in Altunshan (Appendix 5.1).

The Harbin Protoplate (centered on 127°E, 46°N) was relatively stable in the Mesopro-terozoic. In the western part of the Hinggan Ling area, the thickness of the Mesoproterozoic sedimentary strata is only 2, 064 m. In the Jiamusi area in the eastern part of Harbin and in the southern part of the Harbin Plate, southeast Jilin Province, the sediments reach 6,000–19,000 m in thickness. In the Changcheng Period basic volcanic eruptions (1,376 Ma, Rb-Sr method) were controlled by extensional fractures. Granitic intrusions, such as the Jiamusi granite, occur in the Harbin Protoplate. Recently zircon grains were found in north of Dunhua -Mishan (132°E, 45.5°N) granite, giving an Ar-Ar isotopic age of 1,134 Ma (Li JY et al., 1999).

The Kazakhstan–Junggar Plate shows evidence of a moderate amount of tectonic activity in the Mesoproterozoic, with sedimentary strata being only 9,240 m thick. Rates of sedimentary deposition on the Harbin and Kazakhstan–Junggar paleoplates were less than 10 m/Myr (Fig. 3.1 F). By contrast, there was a large amount of tectonic activity in the Dabie–Qinling Block (116°E, 31°N to 104°E, 35°N), during the Mesoproterozoic and the thickness of the slight metamorphosed sedimentary strata is between 11,400 m and 27,700 m, with rates of deposition being more than 9–37 m/Myr. In the Changcheng Period, the rate of extension in the Dabie-Qinling Block was 0.9 cm/yr and in West Qinling was 0.75 cm/yr. The velocity of shortening of the Dabie Block in Late Mesoproterozoic was 5.2 cm/yr, and that of the Qinling Block 6.8–7.9 cm/yr.

During the last ten years 30 isotopic ages have been obtained from metamorphic and granitic rocks, in the Qinling and Kuangping groups. The peak of metamorphic and magmatic activity was in the Jixian Period, between 1,200 Ma and 920 Ma (Li JH et al., 1998). A tectonic event at ~1,000 Ma in the Dabie–Qinling Block caused re-metamorphism and deformation of the Qinling Group and metamorphism of the Kuanping Group, together with the emplacement of a series of basic and granitic intrusions. In the Wudang (centered on 120.5°E, 32.5°N) and the Hong'an groups in Dabie, the age of the metamorphism was also ~1,000 Ma (Appendix 7). It can be concluded that in the Early Mesoproterozoic, the whole Dabie–Qinling Block first experienced extensional fracturing, followed by collision and shortening in the last period of Mesoproterozoic. But, because of the limited amount of data, much more work will be required to reconstruct completely the tectonic evolution of the Qinling–Dabie area during the Meso-proterozoic.

In South China the history of deformation and metamorphism in the Mesoproterozoic metamorphic system (1,800–1,000 Ma) has not been determined, and the rocks have not yet been divided satisfacto-rily. There is still much discussion concerning the age and classification of the rocks, as Paleozoic strata, and even Triassic blocks have been found (Zhao CH et al., 1995). The reconstruction of paleotectonics and paleogeography of the Mesoproterozoic of South China will require a great deal of further research.

Metamorphic rocks, formed during the Changcheng Period (1,700–1,200 Ma) in South China, belong to the Kunyang Group (centered on 102.7°E, 24.7°N) of Middle Yunnan, the Damenglong Group in the Ailaoshan (101.3°E, 24°N; isotopic age of 1,436–1,367Ma, Sm-Nd method), the Diancangshan Group (100.1°E, 25.8°N; isotopic age of 1,402–1,492 Ma, Sm-Nd method) (Zhong DL et al., 1998), the Huili Group (102.2°E, 26.7°N) in southwest Sichuan, and the Lower Shennongjia Group in Hubei (110.3°E, 31.4°N). Meta-sedimentary schist from a clastic protolith, and gneiss formed from intermediate to acid volcanic rocks of the Baoban Group (109°E, 19.2°N) in Hainan gave metamorphic ages of 1,800–1,400 Ma (Wang KF, 1991).

Metamorphic rocks in South China formed during the Jixian Period (1,200–1,000 Ma), belong to the Dongchuan Group (103.3°E, 26°N) of central Yunnan and southwest Sichuan, and the Upper Shennongjia Group of Hubei. Metamorphic rock systems, formed during the Changcheng and Jixian periods, which cannot be divided temporally, are the Fanjingshan Group (108.8°E, 27.9°N) to the northeast of Guizhou, the Shuangqiaoshan Group (centered on 117°E, 29.3°N) and the Jiuling Group (115°E, 29°N) of northern of Jiangxi and Hunan, most of the Shennongjia Group in Hubei, the Lengjiaxi Group (centered on 111.5°E, 28.5°N) of Hunan, the Shangxi Group (117.8°E, 29.8°N) of south Anhui, the Shuangxiwu Group (118.6°E, 28.8°N) to the west of Zhejiang, the Sibao Group (the standard section at 108.9°E, 24.8°N) southeast of Guizhou, north of Guangxi, and the Shenshan Group (116°E, 28°N) in central Jiangxi.

At the end of Jixian Period the most important tectonic event in South China was the Sibao Tectonic Event, which reached a peak at ~1,050 Ma. The angular unconformity, corresponding to the Sibao Tectonic Event, is seen clearly in northern Guangxi, northeast of Guizhou, Hunan, northern Jiangxi and southern Anhui.

Most of the Yangtze Plate was tectonically stable in the Mesoproterozoic, including Jiangsu, northwest Zhejiang, western Hunan, eastern Sichuan, Guizhou and eastern Yunnan. The sediments are not very thick (600–4,000 m), and velocities of the sedimentation were usually below 10 m/Myr (Fig. 3.1B; Appendix 2). On the other hand, strata are much thicker in the active tectonic belts, 10,490 m at Dabashan and 14,436 m at Chengdu-Xichang. The highest rate of sedimentation in the active belt was 56.2 m/Myr (i.e. 0.056 mm/yr). Rates of plate shortening on the western and northern margins of the Yangtze Plate during the Jixian Period, estimated from the chemical composition of granites, were 4.4 cm/yr in Haizhou of Jiangsu, only 2.8 cm/yr in north Sichuan and 5.2 cm/yr in Huangling, Hubei (Appendix 5.1). During the Mesoproterozoic this area was the most tectonically active of all the Chinese continental plates.

In the Sibao Tectonic Event at the end of Mesoproterozoic, the South Yangtze Plate was subducted and collided with the North Yangtze Plate to form the present Yangtze Plate (Fig. 3.3). The Jiangnan subduction and collision belt (*JN* in Fig. 3.3) extends to the south of the Yangtze River from southern Anhui, northeastern Jiangxi, northern Hunan and central Hunan to the border of Guizhou–Guangxi, and then to eastern Yunnan. Different sections of the belt have different tectonic characteristics. The section in southern Anhui and northeast of Jiangxi, has been regarded as a continent-continent collision belt, but is mainly a subduction zone, in which the rock units have dip angles of ~45°towards northwest down to a depth of 200 km, steepening at greater depths (Xu Y, 2006). In Dexing of Jiangxi, southern Anhui, cold ultramafic rocks were thrust over the collision belt at the end of Mesoproterozoic (Xu B et al., 1992; Shen WC et al., 1992; Zhao JX et al., 1995). From northern Jiangxi to northern Hunan, the suture zone trends E-W, and seismic tomography shows that the oceanic crust subducted towards the northwest (Xu Y, 2006), although this is not clear in the outcrop. In southeast Guizhou, north of Guangxi, it again appears to be a continent-continent collision zone. In western Hunan and eastern Yunnan, the suture is a sinistral strike-slip fault (transform fault; Liu BJ et al., 1993; 1994).

There is evidence for tectonic activity adjacent to the Jiangnan subduction and collision belt in the Mesoproterozoic, with thick sedimentation: 22,778 m in northern Jiangxi; 16,261 m in north Guangxi; and 5,092 m in southeast Yunnan. In Late Mesoproterozoic rates of shortening adjacent to the Jiangnan subduction and collision belt were 7.9–6.6 cm/yr, in northern Hunan and northern Jiangxi, Guangxi up to 8.0–7.8 cm/yr, at Motianling (108.5°E, 25.5°N) on the border of Guizhou -Guangxi, 7.8 cm/yr. Even in the Fanjingshan area (108.7°E, 27.9°N) of Guizhou, which is several hundred kilometers to the northwest of the Jiangnan subduction-collision belt, the rates of shortening were 7.3–4.7 cm/yr. In the Early Jixian Period (Early Sibao Tectonic Period), rates of plate extension in the northern Hunan, Hubei and the Guangxi areas, estimated from the composition of basic volcanic rocks, were 0.6–0.7 cm/yr.

The eastern part of the Cathaysian Plate, including southeast Zhejiang, the East China Sea (Donghai), southern Jiangxi, northern and central Guangdong, and the Nanhai Islands in South China Sea area, was relatively stable tectonically. Sedimentary thickness is 1,800–6,000 m (4,277 m in southeast Hunan, and 5,501 m in northern Guangdong). Rates of sedimentation in most areas were 15–20 m/Myr. Sedimentary

thickness is greater in Fujian, (13,453 m in eastern Fujian and 18,929 m in western Fujian) with the highest rate of sedimentation being 41.4 m/Myr. The greatest rate of extension, up to 1.1 cm/yr (Fig. 3.3; Appendix 5.1), is found in Zhuji, Zhejiang (120.2°E, 29.7°N) on the northern margin of the Cathaysian Plate.

The South Yangtze Plate is characterized by an abundance of tin; the Cathaysian Plate is characterized by an abundance of tungsten. The South Yangtze Plate contains the largest deposits of tin ore in the world. Tin deposits are located in eastern Yunnan, northern Guangxi, and on the borders of Hunan, Guangdong and Jiangxi. Only small tin deposits occur in the North Yangtze Plate. On the other hand, the Cathaysian Plate has the largest tungsten ore deposits in the world, concentrated in south Jiangxi, northern Guangdong and southwestern Fujian. However, the main period in the formation of these tin and tungsten ore deposits occurred during the Mesozoic, and the source rocks were formed in Mesoproterozoic–Early Paleozoic. Although there are geochemical similarities between tin and tungsten, their areas of distribution are rather different. The South Yangtze Plate could be called the "tin-rich plate", and the Cathaysian Plate the "tungsten-rich plate". It is suggested that this may be due to differences in the original compositions of the planetismals, which formed these regions of the Earth.

In the Mesoproterozoic (1,800–1,000 Ma), there must have been an ocean between the Cathaysian and Yangtze plates, although no ophiolite complexes have yet been identified in the Shiwandashan–Shaoxing Collision Belt, which was formed along the boundary between two plates at the end of the Qingbaikou Tectonic Period. Continental slope and bathyal turbidite deposits occurred on the margins of the Cathaysian and Yangtze plates and metamorphosed Mesoproterozoic volcanic rocks are common in adjacent areas.

There is no data concerning the nature and distribution of rocks of Mesoproterozoic age in the Qinghai -Xizang (Tibet) area. It is inferred that shallow marine sediments were widespread around the Garze-Songpan Plate (100–104°E, 31.8–32.3°N) and in southern Gangdise (centered on 80°E, 32°N–86°E, 30°N) which form part of the peri-Gondwanan blocks (Fig. 3.3). The thickness of Mesoproterozoic strata in the Henduan Mountains (97°E, 31.5°N–100°E, 27°N) is 11,651 m at Kangding-Zoige (102°E, 30°N–103°E, 33.3°N), more than 7,900 m in Zhongdian (100°E, 28°N) and Lanping-Simao (from 99.5°E, 26.4°N to 101.2°E, 22.7°N) and more than 10,230 m in the Baoshan (99°E, 25°N) to Lancang (100°E, 24°N) area. Rates of deposition of these sediments were 30–40 m/Myr. Recently a single zircon lead isotope age of 1,111 Ma was obtained from the Guoganjia'nianri Group in the metamorphic crystalline basement of Qiangtang in Xizang (from 81°E, 34°N to 92°E, 32°N). This may be the age of formation of the basaltic protolith before metamorphism (Wang GZ et al., 2001).

Geothermal gradients during the Mesoproterozoic have been estimated by using rather incomplete data from 34 areas on formation temperatures and pressures of the metamorphic rocks and granites (Appendix 7). Only 4 estimates of geothermal gradients have been collected from metamorphic rocks formed in the Changcheng Period from the Sino-Korean Plate with an average value of 22.15℃/km. In Jixian Period (12 values) the average geothermal gradient in the Sino-Korean Protoplate (4 values) was 16.3℃/km, in the Qinling -Dabie Block (7 values) was 26℃/km; the highest value of 37℃/km was obtained from the Sibao Group (1 value), in the south of the Yangtze River (Appendix 7). Using data from Mesoproterozoic magmatic rocks, the average geothermal gradient given by the Shanxi kimberlite (2 values) was 10.4–15℃/km (Chi JS et al., 1996), from Wendu'ermiao, in Inner Mongolia (1 value) 17℃/km and in Jiangxi (3 values) 20–25℃/km (Appendix 7).

Data from Mesoproterozoic rocks obtained so far does not suggest that the geothermal gradients were in any way abnormal, although geothermal gradients were lower than the average for present day continental crust. Only the value from the south of the Yangtze River area is somewhat higher than normal for the continental crust. This high gradient may be due to volcanic activity related to the formation of the Jiangnan subduction and collision belt, but the possibility of a Mesoproterozoic paleo-mantle plume cannot be excluded.

The incomplete data presented above shows that there was only relatively weak tectonic activity during the Changcheng and Jixian periods in the Chinese continent blocks, although the blocks were moving and were affected by intraplate rifting and plate collisions.

The main characteristics of the tectonic evolution of Chinese continent in the Mesopro terozoic are that a sedimentary cover was beginning to develop on the Sino-Korean protoplate, which was broken up and divided to three blocks: the main Sino-Korean Plate (including Alxa block), and the Tarim and Qaidam blocks. The Jiangnan subduction and collision belt formed between the northern and southern Yangtze plates, completing the amalgamation of these two blocks. Compression and collision also occurred between the Qinling-Dabie and Yangtze blocks at the end of Mesoproterozoic; the other blocks show only weak tectonic activity.

After the Mesoproterozoic four tectonic domains can be distinguished in the Chinese continent: (1) Peri-Siberian Tectonic Domain (Paleo-Kazakhstan Plate; Paleo-Harbin Plate); (2) Sino-Korean Tectonic Domain (Paleo-Tarim Plate; Paleo-Qaidam Plate; Sino-Korean Paleoplate, which includes the North China area, Korean Peninsula and the Alxa Block); (3) Peri-Yangtze Tectonic Domain (Yangtze Plate; also including the Qinling-Dabie Block; paleo-Songpan-Garze Block; Cathaysian Plate); (4) Peri-Gondwanan Tectonic Domain (Fig. 3.3).

3.2 Tectonics of the Qingbaikou Period (1,000–800 Ma)

—amalgamation and collision of continental blocks, formation of the unified crystalline basement of Yangtze Plate

The China National Commission on Stratigraphy (2001) named the period between 1,000 Ma and 800 Ma (Early Neoproterozoic) the Qingbaikou Period in North China. This division is almost equal to the Tonian Period (1,000–850 Ma) in the International Stratigraphic Chart (Remane, 2000; International Commission on Stratigraphy, 2004). However, the typical and strongest tectonic events in this period occurred in South China, and the standard section is located at Jinning, Yunnan; many researchers, especially in South China, refer to this period as the "Jinning Tectonic Period".

In the Qingbaikou Period, the main tectonic characteristics of Sino-Korean, Tarim and Qaidam paleoplates, including small blocks, such as the Hualong, Middle Qilian and northern West Kunlun blocks, were similar to those in the Mesoproterozoic, although the area of sedimentation was more extensive (Figs. 3.6 and 3.7). The main sedimentary lithologies belonging to the Qingbaikou Period near Beijing in north China are black shales of the Xiamaling Formation, sandstones of Longshan Formation and micritic limestones of the Jing'eryu Formation, with a Pb-Pb isotopic age of 879–853 Ma (Qiao Xiufu, 1997), equivalent to a late period of Qingbaikou Period. However, in Recent the zircon SHRIMP isotopic age (1,327 Ma) of diabase sill, intruded into Xiamaling Formation, was got (Wang Tieguan, 2009, personal communication), if that isotopic age is correct, which means that Xiamaling Formation should be put under the Mesoproterozoic.

In the Taizihe area (123.5°E, 41.3°N) of Liaoning, sandstones and shales, and in western Henan sandstones, shales and stromatolitic limestones of the Heyao Formation were deposited in a tidal flat sedimentary environment. The Liaoning–Shandong Rift Basin developed in the eastern Sino-Korean Plate. The southern part of this fault-depression basin is located to the west of the Triassic Tancheng–Lujiang (Tanlu) fault zone, while the northern part is located in the northern Korean Peninsula, to the east of that. The Neoproterozoic Liaoning–Shandong fault depression basin was superimposed on the Paleoproterozoic Liaoning–Shandong Rift Basin, where the crystalline basement was already weakened and was easily extended and subsided, permitting the accumulation of sedimentary deposits. In contrast to the Yangtze and Cathaysian plates there is no obvious rock deformation in the whole Sino-Korean Plate.

The Sino-Korean Plate underwent weak extension at the rate of only 0.49 cm/yr. Compression and collision occurred on the southern margin of the Sino-Korean Plate, while magmatism developed at

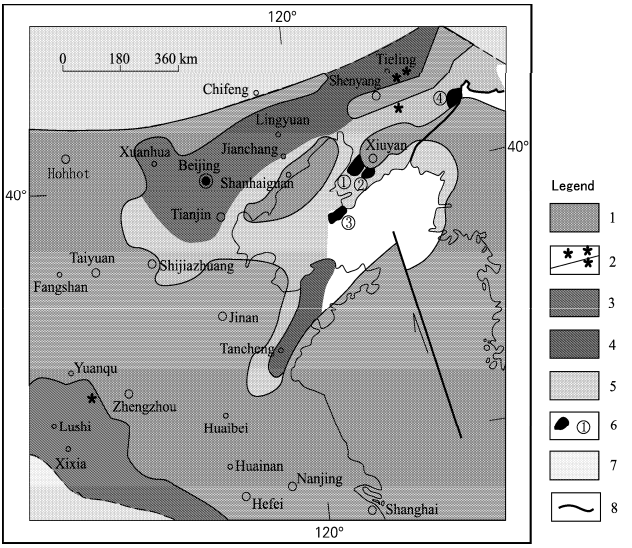

Fig. 3.6 Paleogeographic map of the Sino-Korean Plate in the Qingbaikou Period (1,000–800 Ma) (after Qiao XF, 2002, with permission of Qiao XF).

1. Area of erosion; 2. Synsedimentary faults and accompanying earthquake events (seismites); 3. Main tidal flat sedimentary area (stromatolites, algal laminated limestone and sandstone); 4. Littoral and shallow marine sedimentary area in the Late Qingbaikou Period (shales of the Xiamaling Formation, quartz sandstones of the Longshan Formation and bedded limestones of the Jing'eryu Formation); 5. Area of shallow marine sedimentation in the Late Qingbaikou Period; 6. Terrestrial basin formed in early period of Late Qingbaikou Period, including ①Yongning Basin, ②Buyunshan Basin, ③Lüshun-Dalian Basin, ④Weishahe Basin; 7. Broad area of shallow marine sedimentation; 8. Border of country. YSTF= Yellow Sea Transform Fault (formed in Triassic).

Zhongtiaoshan (centered on 111.3°E, 35°N), where the rate of shortening, estimated from the chemical composition of granite, was 5.8–6.4 cm/yr.

The most important tectonic events in the Meso-Neoproterozoic were the formation of the Qilianshan and Altunshan rift basins between the Tarim, Qaidam and Sino-Korean paleoplates, and shortening and collision in the middle-late epoch of the Qingbaikou Period. Recently, a lot of data has been obtained in these rift systems: a U-Pb zircon age of 880±31 Ma was obtained in the Liuyuan (95.7°E, 41°N) granitic gneiss, in southern Beishan (Mei HL et al., 1999); many U-Pb zircon ages (between 950 Ma and 870 Ma) were abtained from granitic gneiss on the northern border of the Qaidam Plate (97°E, 38°N; Lu Songnian, 1998) and an Sm-Nd isochron age of 829±60 Ma was found from gabbro near Aksay, at Altunshan (94°E, 37.6°N; Guo ZJ et al., 1999). In recent years, from the interpretation of deep seismic experiments, wedging or crocodile tectonics between the Dunhuang–Tarim and Qaidam plates has been recognized in Altunshan. The crust of Dunhuang–Tarim Plate has been inserted into the middle crust of the Qaidam Plate (Xu ZQ et al., 1999), but this collision was not very intense, as no strong deformation is seen in the Neoproterozoic rocks.

However, the northern and southern margins of the Tarim Plate, i.e. Kuruktag (centered on 90°E, 41.6°N), Tianshan (centered on 82°E, 42°N) and Kunlunshan (centered on 80°E, 36°N), all experienced compression, folding and metamorphism in the Qingbaikou Period. Rates of shortening were between 4 cm/yr and 6.5 cm/yr, with an average value of 6 cm/yr. At this time the Sino-Korean, Tarim and Qaidam plates collided and were amalgamated to form a single plate, similar to the original Sino-Korean Protoplate (Fig. 3.7).

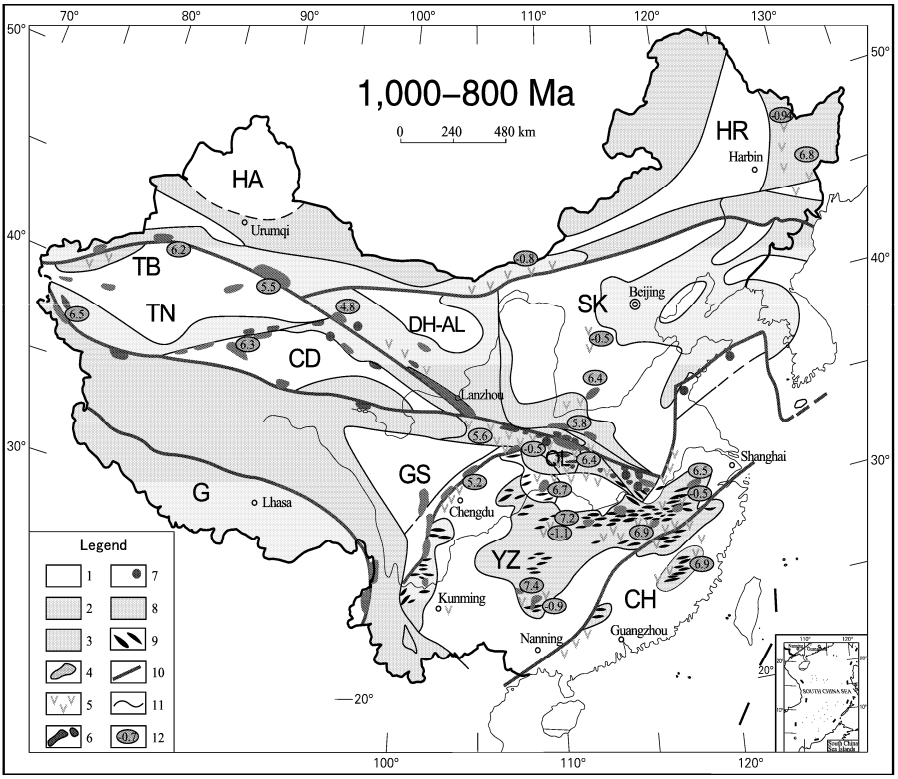

Fig. 3.7 Paleotectonics of the Qingbaikou Period (1,000–800 Ma).

Legend: 1. Area of erosion on the paleo-plate; 2, Shallow marine depression and belt of sedimentation; 3. Low grade metamorphic rocks. 4. Granitic intrusions. 5. Island arcs with intermediate-acid volcanic rocks; 6. Ophiolite suite; 7. Eclogites; 8. Ocean crust; 9. Folds (only anticlines); 10. Subduction zone (including ophiolites); 11. Boundary of tectonic province; 12. Rate of plate movement; "-" is rate of extension, others are rates of shortening (cm/yr) (data in Appendix 5.2).

Divisions of tectonic domains: 1. Peri-Siberian Tectonic Domain (HA= Paleo-Kazakstan Plate; HR= Paleo-Harbin Plate); 2. Sino-Korean Plate Tectonic Domain (TR= Tarim Paleoplate; CD= Qaidam Paleoplate; SK= Sino-Korean Paleoplate, including North China, Korean Peninsula and Alxa Block); 3. Peri-Yangtze Plate Tectonic Domain (YZ= Yangtze Paleoplate; GS= Garze-Songpan Paleoplate; CH= Cathaysian Plate; Qinling-Dabie Plate); 4. Peri-Gondwanan Tectonic Domain (G).

In this figure, the eastern part of Yangtze Paleoplate is shown indenting the Sino-Korean Plate in the southern Yellow Sea area; this tectonic event occurred in the Triassic. In a tectonic reconstruction, part of the Yellow Sea on this map should be shown as part of the Sino-Korean Plate.

The strongest tectonic events in the Qingbaikou Period affected the Yangtze and Cathaysian plates (Fig. 3.7). The earliest sedimentary cover deposited on the crystalline basement of western Yangtze Plate was the Jinning System, called the Dayingpan or Shuanshuijing formation in the middle Yunnan and southwest Sichuan areas, and the Huashan or Machaoyuan groups in Hubei Province. However, in most part of the Yangtze Plate, a greenschist metamorphic series was formed, which during the Nanhua Period was overlain with clear unconformity by the Liantuo Formation, seen especially in Hubei Province. In the Qingbaikou Period metamorphic systems in the Yangtze and Cathaysian plates were derived from

shallow to bathyal clastic sedimentary protoliths, and are classified into several groups: the Baxi Group in Hunan and northeast Guizhou; the Danzhou Group in the southeast Guizhou to north Guangxi areas; the Luokedong or Dengshan Group in north Jiangxi; the Shuanxiwu Group and the Shangsu Formation in west Zhejiang. Equivalent rocks in the Cathaysian Plate are the Longquan Formation in southwest Zhejiang and the upper part of the Longbeixi Group in west Fujian.

In the Qingbaikou Period metamorphic and sedimentary systems in the Yangtze and Cathaysian plates developed strong folding, commonly isoclinal, on E-W trending axes (Fig. 3.7). As during the Proterozoic the orientation of these plates, determined from palaeomagnetism, is uncertain, in this discussion the directions refer to present day co-ordinates. The attitudes of 463 folds (234 anticlines and 229 synclines), with predominantly E-W trending axes, have been collected from 76 regional geological survey sheets (scale 1: 200,000) (Wan TF and Zhu H, 1990; Appendix 3.1). N-S shortening occurred throughout the Yangtze and Cathaysian plates. The preferred orientation and attitude of the maximum principal compressive stress (σ_1) were N-S trending and near horizontal ($\angle 0^\circ - \angle 2^\circ$), the intermediate principal compressive stress (σ_2) which is parallel to the fold axes, trends E-W, and was also almost horizontal (NE $88^\circ \angle 8^\circ$), and the minimum principal compressive stress (σ_3) was near vertical (SW $265^\circ \angle 87^\circ$). At the same time the Yangtze Plate developed a unified crystalline basement.

From the evidence of similar intraplate tectonic characteristics in the Yangtze and Cathaysian plates, it is found that both plates were affected by almost the same tectonic stress field in the Qingbaikou Period. During this period the two plates were very close to each other, or had collided and were amalgamated. However, no ophiolite complexes or other clear structural evidence of collision have been recognized in the Shaoxing -Shiwandashan Collision Zone (from 120.5°E, 30°N to 108°E, 21.9°N) along the boundary between the Yangtze and Cathaysian plates. Shui T (1986, 1987) first proposed that the collision between Yangtze and Cathaysian plates occurred in the Jinning (i.e. Qingbaikou) Period in the Shaoxing–Jiangshan Zone in Zhejiang Province.

In the last twenty years, the rocks and isotopic age records of the Shaoxing–Shiwandashan Collision Zone and adjacent areas have been studied intensively (Zhou XM et al., 1989; Cheng H, 1991; Yang MG, 1994; Liu BG et al., 1995; Tang HF et al., 1997). These authors used Sm-Nd isochron or U-Pb zircon methods to determine the isotopic age of magmatic rocks giving results from 1,034 Ma to 806 Ma and concluded that collision and the first periods of amalgamation in the Shaoxing–Shiwandashan belt occurred during the Qingbaikou Period. Gilder et al. (1996) and Chen JF et al. (1998) first recognized a zone of high ε_{Nd} values in a granitic zone in the Shaoxing–Shiwandashan belt and its adjacent area. Hong DW et al. (2002) considered that the granite zone with high ε_{Nd} and low T_{DM} values, indicating mantle influence, provided evidence for collision between the Yangtze and Cathaysian plates along the Shaoxing–Shiwandashan Zone.

Magmatism occurred in the Qingbaikou Period in the Yangtze and Cathaysian plates (chemical analyses of 718 igneous samples, Fig. 3.7, Appendix 5.2). Basic volcanism occurred during the Early Qingbaikou Period at Fanjingshan in northeast Guizhou with a rate of plate extension of 1.1 cm/yr. Many basic rock bodies with isotopic ages of around 823 Ma were developed in Longmenshan–Panzhihua, western Sichuan; intrusive ultrabasic and basic bodies in Sanmen, north Guizhou gave an isotopic age of 837 Ma with a rate of plate extension of 0.59–0.93 cm/yr; basic volcanic eruption on the border between Anhui and Jiangxi showed a rate of extension of 0.55 cm/yr.

Acid magmatism in the Late Qingbaikouan Period shows that the Yangtze and Cathaysian plates were undergoing shortening at rates between 5 cm/yr and 7.6 cm/yr, which is rather rapid. In modern coordinates the Yangtze Plate underwent N-S shortening, with E-W extension along the western margin of the Yangtze Plate, creating conditions favorable for granitic intrusion. From the chemical composition of granites with isotopic ages of 1,043–818 Ma in Pengcheng and Guanxian (103.5°E, 31°N) in Sichuan, the rate of plate shortening was 5.2 cm/yr; the Rb-Sr isotopic ages of granite at Dukou (101.9°E, 26.5°N) in Sichuan are 867–833 Ma. Zhou MF et al. (2002) used the SHRIMP zircon U-Pb method to determine the ages of the Kangding Complex (102°E, 30°N) on the western margin of the Yangtze Plate, those of the Gongcai Complex near Danba (101.9°E, 30.9°N) and the related granites, and discovered that the cores of many zircon grains were formed in Late Qingbaikouan Period (824–796 Ma), whereas the rims

of some zircon grains gave a Jurassic age of 177±3 Ma. This study resolved the controversial problem of the isotopic ages of the intrusions in those areas.

The Jiangnan Collision Zone (*JN* in Fig.3.3) and its adjacent areas of the Yangtze Plate formed during the Late Qingbaikou period, with the widespread emplacement of granitic magmas, giving rates of plate shortening in southeast Guizhou and north Guangxi of 5.9–7.6 cm/yr, and in Huangling, Hubei of 6.7 cm/yr (Rb-Sr isotopic age of 846 Ma; 111.1°E, 30.8°N). The Rb-Sr isotopic ages of granitic intrusions in Jiuling, Jiangxi (115°E, 29°N) are 838–844 Ma, and the rate of shortening in that area was 6.9 cm/yr; on the border among Zhejiang, Anhui and Jiangxi (118.1°E, 29.5°N) the isotopic age of rhyolite is 818 Ma, with a rate of shortening of only 3.2 cm/yr; in Xiuning in Anhui (118.2°E, 29.8°N) the isotopic age of the granite is 913 Ma, with a rate of shortening of 7.1 cm/yr; a granite in northwest Zhejiang gave a rate of shortening of 6.5 cm/yr.

Only a few data have been collected from the Cathaysian Plate. The rate of plate shortening of 6.9 cm/yr indicated by rhyolite of Mayuan Group (standard section 118.3°E, 27.7°N) in Fujian is similar to that in the Yangtze Plate.

Evidence of a tectono-thermal event in the crystalline basement of the Qiangtang Block during the Qingbaikou Period is indicated by a zircon lead isotopic age of 1,016–929 Ma found recently in the Gomori Group (85.9°E, 34°N) (Wang GZ et al., 2001).

Many researchers have studied the tectonism of Qinling-Dabie Block in the Qingbaikou Period, where its effects are very obvious. The rates of extension in Early Qingbaikou Period in that area were not very great, around 0.5 cm/yr. The Songshugou Ophiolite Suite (from 110°E, 33.8°N to 116.9°E, 31.5°N) with isotopic age of 983 Ma (Li SG et al., 1991) and 914 Ma (Yang WR et al., 2000); incorporated in the Shangdan–Shangnan–Xinyang–Shucheng Collision Zone, is generally considered to be the residue of Qingbaikou palaeo-mantle and paleo-oceanic crust. In the Qinling–Dabie Block extensive metamorphism and magmatic intrusion occurred during the Qingbaikou Period. In recent years, more than one hundred isotopic ages between 987 Ma and 796 Ma have been determined, using Rb-Sr whole-rock, U-Pb zircon and Sm-Nd isochron methods (Liu GH et al., 1993; Suo ST et al., 1993; Zhang GW et al., 1996; Zhang SG et al., 1991, 1998).

In addition, many basic igneous bodies in the Qinling–Dabie Block have been metamor-phosed under ultra-high pressure to form eclogite. There have been many studies by Chinese and foreign researchers aiming at determining the age and mechanism of formation of the eclogites (Cong BL and Wang QC, 1994, 1999; Xu ST et al., 1992). Li SG et al. (1993, 1996, 1997) used the Sm-Nd method to determine the age of formation of the eclogites, and concluded that they were formed mainly in the Triassic, between 221 Ma and 244 Ma, precluding the possibility that they were formed in the Precambrian. Other authors have maintained that geological evidence for the age of the eclogites is more important than the isotopic age. High pressure metamorphic rocks have never been found in the Dengying Formation of the Sinian Period within the Dabie collision zone and in its overlying units. Zhang SY et al. (1989, 1990) therefore concluded that the eclogites were formed earlier than the Sinian Period. An Rb-Sr whole-rock isochron age of 744 Ma was obtained from blueschists in northern Hubei and a K-Ar dilution age of 845 Ma was obtained from eclogite. The conclusion of them is that high pressure rocks in the Dabie Collision Zone were formed during the Qingbiakou Period, other than in the Triassic, with the younger age resulting from the effects of later thermal events. With improvement in methods of isotopic age determination and a better understanding of the application and limitations of the various methods it is hoped that this controversy will soon be resolved.

In recent years, the opinion that Qinling–Dabie high pressure metamorphic belt is composite, formed during several periods of tectonic activity, has gained the support of many researchers (Zhang GW et al., 1996, 2001; Suo ST et al., 1993; Bai J et al., 1996; Yang WR et al., 2000). It is suggested that the first important tectonic process in the Qinling–Dabie Zone was subduction and shortening, beginning from the Qingbaikou Period (about 800 Ma); at the end of the Early Paleozoic (about 400 Ma) arc-continent subduction occurred between the plates; then the main period of continent-continent collision occurred in the Triassic (250–200 Ma). This interpretation may not be the final conclusion, although there is general agreement that multiple tectonic events have led to the formation of Qinling–Dabie Tectonic

Zone. However, the most important tectonic period occurred during the Qingbaikou Period when the Qinling–Dabie Tectonic Zone began to form as a result of plate subduction. Depending on the chemical composition of acidic magmatic rocks intruded during the Qinbaikou Period, the rate of plate shortening in the zone is estimated to be between 5.6 cm/yr and 6.4 cm/yr (Appendix 5.2).

The eclogites, together with the adjacent strata, formed under conditions of plate compression and ultra-high pressure metamorphism during the Qingbaikou Period. However, sometimes eclogites are found as inclusions in gneiss or marble, which crystallized under low pressure metamorphic conditions.

In recent years, besides the Triassic age, the eclogites have yielded many younger ages using the Sm-Nd method. Isotopic ages of 329.68 Ma, 265 Ma, 176.5 Ma, 57.1 Ma and 55.5 Ma (quoted from Suo ST et al., 1993) have been obtained and interpreted as the age of the high pressure metamorphism. It is possible that the Sm-Nd isotopic ratios in eclogite may be changed easily due to subsequent tectonothermal events. Besides, when it is agreed that the Qinling–Dabie eclogites formed under ultra-high pressure conditions during Qingbaikou Period, the mechanism of emplacement of the eclogites in their present position is not a problem, if the eclogite and its surrounding strata are regarded as constituting a "tectonic mélange" formed by multi-period tectonic processes (Suo ST et al., 1993). Over a period of 800 million years, even if the eclogite was formed at a depth of about 100–200 km in the lithosphere, as suggested by some researchers, there has been ample time to denude the overlying rocks and to allow the high pressure rocks to rise to the surface, with an average rate of uplift of only 0.25 mm/yr.

It is generally considered that the Qinling–Dabie Tectonic Zone was formed in a subduction zone between the Sino-Korean and Yangtze plates during the Qingbaikou Period. The Qinling–Dabie Tectonic Zone had a similar tectonic history to the Yangtze Plate during the Qingbaikou Period, with approximately the same types of rock deformation, metamorphism and magmatism, and with parallel lineations and tectonic zones, but these characteristics are not found in the Sino-Korean Plate. Therefore, it is reasonable to suppose that Qinling–Dabie Tectonic Zone is related to the Yangtze Plate, and may actually be part of that plate.

The Sino-Korean and Yangtze plates show distinctive characteristics (Wan TF and Zeng HL, 2002). The effects of the Qingbaikou Event are important tectonic features of the Qinling–Dabie Zone and the Yangtze Plate (Fig. 3.7), but why there is no intraplate deformation, magmatism and metamorphism related to the Qingbaikou Event in Sino–Korean Plate? The eclogites formed under ultra-high pressure conditions indicate the subduction of the lithosphere to a depth of 100–200 km in the mantle. If ancient oceanic crust and lithosphere belonging to the Qinling–Dabie Plate were subducted beneath the Sino-Korean Plate, it would be expected to have a great influence on the Sino-Korean Plate, with strong rock deformation, magmatism and metamorphism, and to build up a trench-arc system. Palaeomagnetic evidence for the distribution of the paleocontinents in Proterozoic era is not very satisfactory. On the basis of present data it cannot be established whether the Sino-Korean Plate was located to the north or to the south of the Qinling–Dabie Plate. With the current evidence it is impossible to say that a unified "ancient China platform (or plate)", including the Sino-Korean, Yangtze, Cathaysian, Qaidam and Tarim blocks, as Ren JS (1980, 2000) recognized, was formed during the Qingbaikou Period. It is also impossible to make certain that the Qingbaikou Period was a phase of convergence which resulted in the formation of a "Super Cathaysian Continental Group" as suggested by Zhang GW et al. (2001). Consequently it is not certain that the Qinling–Dabie oceanic crust was subducted beneath the Sino-Korean Plate; it is possible that during the Qingbaikou Period the Qinling–Dabie Plate was subducted beneath some unknown ocean crust. All these possibilities require further consideration.

According to lead isotopic studies by Zhang LG (1995) on the Yangtze Plate and surrounding blocks (including the Qinling–Dabie), the lead isotopes in the central part of the Yangtze Plate show similar features to those of the Sino-Korean Plate, but the surrounding blocks, including Qinling–Dabie Block, show mixed oceanic and continental crustal features. Zhang LG's (1995) results confirm that oceanic crust was subducted together with the Qinling–Dabie Block, it means that the Sino-Korean and Yangtze Plates were not a unified continental plate, and that in between was the Qinling–Dabie Block with oceanic crust attached.

In other parts of the Chinese continent, geological evidence for tectonic events during the Qingbaikou Period is rather sparse. During the Early Qingbaikou Period the Harbin Paleoplate was extended and fragmented. According to data from the ophiolite at Yilan and Zhangguangcailing (128.5°E, 45°N) in Heilongjiang, the rate of extension in that area was 0.94 cm/yr. Granitoids formed in Qingbaikou Period, with a U-Pb isotopic age of 908 Ma, are found in Daluomi town, Mudanjiang, Shuanghe, Shuangyazitun and Xingkai, in Heilongjiang Province, the plate shortening velocities here were between 4.6 cm/yr and 7.1 cm/yr. The rate of extension reflected by andesite with isotopic ages of 1,056–899 Ma in Altan Obo (centered on 116.5°E, 48.8°N) in Inner Mongolia is 0.8 cm/yr, similar to that of Heilongjiang area. Ocean is considered to have surrounded the ancient Harbin and Kazakhstan plates (Fig. 3.7).

From temperatures and pressures of formation of metamorphic rocks from 21 areas, and of magmatic rocks from 3 areas during the Qingbaikou Period, it is possible to estimate the geothermal gradient (Appendix 7). The current data shows that the geothermal gradient of the crust and upper mantle of Chinese continent in the Qingbaikou Period was lower than that of the present average value for the whole world (<30°C/km), only on the Cathaysian Plate can we find evidence of a higher geothermal gradient.

The tectonic domains in the Chinese continent during the Qingbaikou Period were similar to those in the Mesoproterozoic: the Peri-Siberian, Sino-Korean, Peri-Yangtze, and Peri-Gondwanan plates (Fig. 3.7).

The tectonic events of the Qingbaikou Period in the Chinese continent occurred after the formation of Rodinia Supercontinent, at the when time when Rodinia passed from a period of relative stability to the breakup period (Hoffman et al., 1999). It is not appropriate to regard the Qingbaikou Tectonic Event as a manifestation of the accretion and amalgamation in China. Globally, the period of amalgamation of Rodinia is called the Tonion Period. However, the events on the Chinese continent in the Qingbaikou Period were very different from events in Rodinia. When the Rodinia supercontinent began to break up there was widespread amalgamation and collision in China, with only limited extensional fracturing. It seems that the Chinese continental blocks did not form part of Rodinia at this time.

3.3 Tectonics of the Nanhua Period (800–680 Ma)

—widespread extension and rifting of continental blocks, glaciation developing tillites of the Nantuo Formation on the Yangtze–Tarim plates

In South China the typical sediments of the Nanhua Period are feldspathic sandstones of the Liantuo Formation and tillites (glacial deposit) of the Nantuo Formation. Formerly these rocks were classified in the Lower Sinian System, and were named the Nanhua System at the 3rd China National Symposium on Stratigraphy (China National Commission on Stratigraphy, 2001). This period corresponds to the Cryogenian Period, 850–680 Ma, as recently defined on the International Stratigraphic Chart (Remane et al., 2000; International Commission on Stratigraphy, 2004).

The Nanhua Period was a period of widespread extension in the Chinese continent in which a sedimentary cover was first deposited on the crystalline basement of the Yangtze Plate, and tillites were deposited on the Yangtze and Tarim–Qaidam plates. This glacial period, at about 720 Ma, is equivalent to the global Sturtian glacial period (Fig. 3.8). The Nanhua sedimentary system was deposited on the Yangtze Plate where it shows an angular unconformable contact with the underlying metamorphic strata, but is overlain by rocks of the Sinian System with a disconformable contact.

In the early Nanhua Period, the major part of the Yangtze Plate formed a land area with terrestrial fluviatile sedimentation (Liantuo Formation) in the interior and on the margins of the paleocontinent, passing in the northern Guizhou–Hunan–Hubei area and in the southeast into transitional continental margin and oceanic sediments. In the Lower Yangtze River area sediments were deposited in a coastal

tidal flat sedimentary environment. A volcanic rock series was developed in the western Sichuan -middle Yunnan rift basin.

In the Late Nanhua Period, the Yangtze Plate was covered largely by tillites, deposited from valley glaciers or continental ice sheets (Nantuo Formation). Glacio-marine sediments in the eastern part of Yangtze Plate belong to the Leigongwu Formation. The standard section in the eastern Three Gorges, in Hubei (111.2°E, 30.8°N) shows a dark grayish-green and purplish-red color glacial boulder clay, deposited from a continental glacier. Glacial conglomerates and clays were deposited on the western part of the Yangtze Plate, with some tuffites and other pyroclastic rocks. The glacial deposits of the Nantuo Formation can be compared with those of southern Australia and the Lubumbashi area in Zaire of Africa, it means that the above areas had a similar ancient latitude.

Rates of plate extension, estimated from the chemical composition of basalts, are 0.9 cm/yr in Hunan, and 0.55 cm/yr in southern Shaanxi and western Hubei (Yaolinghe Formation). In the Late Nanhua Period, from the composition of the Sanfang and Rongshui granites in Guangxi (isotopic age of 730–712 Ma; 109°E, 25.1°N), the rate of plate shortening was 6.1 cm/yr, from a granitoid in north Zhejiang (isotopic age of 844–766 Ma; 120°E, 30.5°N) that was 6.9 cm/yr and in the Qinling area in the northern part of the Yangtze Plate (isotopic age of 747–606 Ma; 108°E, 33.8°N) that was 5.8 cm/yr (Appendix 5.2).

In the Nanhua Period, the greater part of the Sino-Korean Plate was a land area and subject to erosion, including the fault-depression basins formed during the Qingbaikou Period in the eastern part of the Sino-Korean Plate. The characteristic sedimentation in the Sino-Korean Plate in the Nanhua period was very different from that in the Yangtze Plate, with a stable assemblage of sandstone, shale and carbonate restricted to narrow fault-depression basins along the southern and western margins. In the south the Huangliantuo and Dongjia Formations, consisting of conglomerates, sandstones and carbonates, with each forming a complete transgressive sedimentary cycle, were deposited in a narrow zone in western Henan (112°E, 33.1°N), and have yielded a K-Ar isotopic age of 665–669 Ma from glauconite (Guan BD et al., 1986). On the western margin of the Sino-Korean Plate near Yinchuan (106°E, 38.5°N), Nanhua sediments are not restricted to a fault-depression basin, but were much more widely deposited. The area from Alax to Beishan (106°E, 38.5°N to 95°E, 41°N) was exposed to erosion and the Nanhua System is not preserved.

By the Nanhua Period the Tarim and Qaidam blocks already formed a unified plate. Sedimentation on these blocks was similar to that on the Yangtze Plate. Glacial deposits, formed either in the sea or on the land, are widespread. Marine glacial deposits of the Tery'eken Formation were deposited in the northern Tarim, Tianshan and Kuruktag areas; continental glacial deposits were deposited to form the You'rmeinak Formation in northwest Tarim and the Quanji Formation in Qaidam. These deposits can all be compared with the glacial deposits of the Nantuo Formation on the Yangtze Plate (Gao ZJ et al., 1983).

From similarities in sedimentation and structural evolution it can be inferred that the Tarim–Qaidam Plate was very close to Yangtze Plate during the Nanhua Period. In the Mesoproterozoic, and in earlier times, the Tarim–Qaidam Plate had been part of the Sino-Korean Protoplate, but in the Nanhua Period and later, they were closer to the Yangtze Plate. During the Nanhua Period the Chinese continent was still divided into four tectonic domains: the Peri-Siberian, Sino-Korean, Peri-Yangtze and Peri-Gondwanan Tectonic Domains. However, the Tarim and Qaidam paleo-plates should be included in the Yangtze Tectonic Domain, rather than in the Sino-Korean Tectonic Domain (Fig. 3.8).

In central and southern Tianshan the Beiyixi Formation of Nanhua System, which consists mainly of acid volcanic lavas and pyroclastic rocks, was deposited on a folded basement of the Qingbaikou and older systems. Volcanic rocks have the widest distribution and were associated with plate extension and faulting. The Beiyixi Formation also includes polymict conglomerates, pebbly sandstones and greywackes. Some researchers think that these are glacial deposits, but Gao ZJ et al. (1983) considered that Beiyixi Formation and equivalent rock series are the product of turbidite sedimentation, and quite possibly include gravity flows. However, Bureau of Geology and Mineral Resources of Xinjiang (1993)

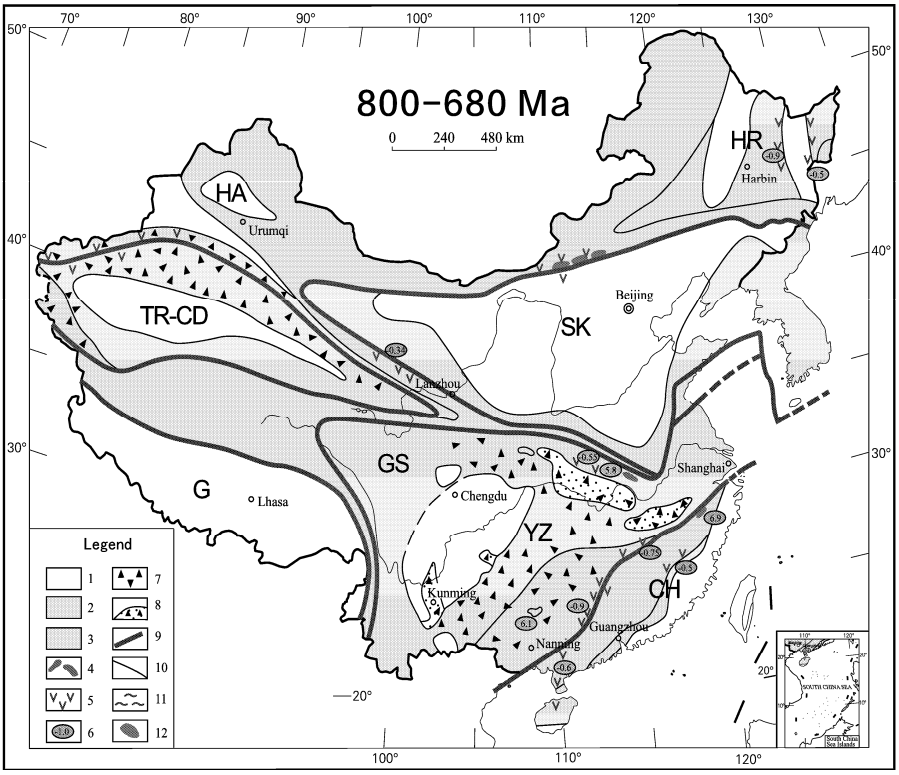

Fig. 3.8 Paleotectonic sketch of the Chinese continent in Nanhua Period (800–680 Ma) (data from Bai J et al., 1996; Liu BJ et al., 1994; Meng XH et al., 1993 and then completed).

Legend: 1. Area of erosion; 2. Shallow marine basin, sedimentation zone or continental marginal extension zone; 3. Bathyal oceanic region; 4. Ophiolite suite; 5. Volcanic rocks; 6. Rate of plate deformation, "-"= extension, and "+"=shortening (unit in cm/yr) (data as seen in Appendix 5.2); 7. Glacial marine deposit (Nantuo Formation and other equivalent rock series); 8. Continental tillite (Nantuo Formation and equivalent rock series); 9. Boundaries between plates, possibly oceans; 10. Boundary between tectonic or sedimentary units; 11. Area of metamorphism; 12. Granitic intrusions. Tectonic reconstruction has not been attempted.

Divisions of tectonic domains: 1. Peri-Siberian Tectonic Domain (HA = Kazakhstan Paleoplate; HR = Harbin Paleoplate); 2. Sino-Korean Tectonic Domain (SK = Sino-Korean Paleoplate, including North China, Korean peninsula and Alax, etc.); 3. Peri-Yangtze Plate Tectonic Domain (YZ = Yangtze Paleoplate; TR = Tarim Paleoplate, CD = Qaidam Paleoplate, GS = Ganzi-Songpan Paleoplate, CH = Cathaysian Paleoplate and Qinling–Dabie Plate); 4. Peri-Gondwanan Tectonic Domain (G).

prefers to regard the conglomerates of the Beiyixi Formation as glacial deposits of the Early Nanhua Period, but this interpretation is still controversial.

The Qilianshan region (96°E, 40°N to 102°E, 37.5°N), between the Alax area in the western Sino-Korean Plate and the Tarim–Qaidam Plate, shows sedimentary features and glacial deposits which belong exclusively to Nanhua Period. At that time, most of the Chinese continent was a stable block, except the Qilianshan region, which underwent active subsidence with the deposition of the 5,000 m Duoruonur Group. This group consists of a suite of low grade metamorphic rocks (chlorite schist, metamorphosed basic-intermediate volcanic rocks, slates and crystalline limestones). The rate of plate extension in that

area was not very rapid during the Nanhua Period, only 0.34 cm/yr estimated from the composition of the Subei basalt.

Basic magma was extruded in Heilongjiang area on both sides of the Jiamusi Block. The rate of extension is estimated to be 0.45 cm/yr on the eastern side (around Huma and Jixi; 131°E, 45.3°N), and 0.88 cm/yr on the western side (near Zhangguangcailing; 128.7°E, 45°N).

From the temperatures and pressures of formation for the metamorphic rocks of the Nanhua Period in the two areas (Dong SW, 2002; Zhang C et al., 1998; Appendix 7) the paleogeothermal gradients are estimated to be 20.6°C/km in east Dabieshan, and 17°C/km at Wendu'rmiao (111°E, 42°N) in Inner Mongolia, lower than the average thermal gradient in the present day continents. This subject requires further study.

3.4 Tectonics of the Sinian Period–Early Cambrian Epoch (680–513 Ma)

—developing the tillite of Luoquan Formation on the southern margin of Sino-Korea Plate, widespread influence of the Pan-African Tectonic Event

The Sinian Tectonic Period is almost equivalent to the late Neoproterozoic Period (Ediacaran or Neoproterozoic Ⅲ Period) in the newly approved stratigraphic chart (Remane, 2000; International Commission on Stratigraphy, 2004). The Sinian Period in China is defined by isotopic ages of 680–543 Ma, equivalent to the Late Sinian age in older classifications, i.e. the period during which the limestone of the Doushantuo and Dengying Formations was deposited in South China (National Commission on Stratigraphy of China, 2001). The Sinian Tectonic Period continued into the Early Cambrian epoch (543–513 Ma) in many areas. In the most Chinese continent this was a period of tectonic stability; it was also the period in which the Pan-African Tectonic Event influenced the northeastern and southwestern China continental blocks

In South China, in the Liuchapo Formation in Hunan and east Guizhou and the Laobu Formation in North Guangxi (109.5°E, 25.7°N), deposition was continuous from the Late Sinian Period to the Early Cambrian Epoch. In those areas, it is appropriate to extend the Sinian Tectonic Event of the Sinian Period into the Early Cambrian age. However, in other areas of South China, such as eastern Yunnan, Sichuan, Hubei, lower-Yangtze River area of Yangtze Plate and Cathaysian Plate, a major sedimentary discontinuity occurs between the Sinian and Cambrian systems, and the Sinian Tectonic Period should be limited to the Sinian Period. In most areas of the Sino-Korean and Tarim -Qaidam plates there is a disconformity between the Sinian and Cambrian systems, but within the Cambrian system there was essentially continuous sedimentation; again it is appropriate to limit the Sinian Tectonic Period to the Sinian Period. It may be acceptable to regard the Sinian Tectonic Period as being diachronous occurring at different times in different areas.

The standard section of Sinian System is in the eastern Three Gorges, Hubei (111.1°E, 30.8°N) on the Yangtze Plate, where the lowest unit is the Doushantuo Formation, composed of siliceous dolomite and manganese shale, deposited in a restricted reducing environment. The upper unit is the Dengying Formation, composed of dolomite which was deposited in a vast epicontinental sea. In the Sinian Period, following the glaciation of the Nanhua Period and a long period of denudation, a marine transgression took place from east to west, forming a shallow marine carbonate platform which covered a very large area. These sediments extended into the south Qinling area (from Zheng'an and Shanyang in Shaanxi to the borders of Shaanxi, Henan and Hubei; from 109.1°E, 33.4°N to 111°E, 33.2°N). This indicates that after the collision and amalgamation of the Qinling Block and Yangtze Plate in the Qingbaikou Period, the south Qinling area and Yangtze Plate were united into a single plate, and both were covered by Sinian sediments (Fig. 3.9). In the northern Qinling area, the plate was extended and split during the Sinian Period, and the Taowan Group, composed originally of sandstone, mudstone and impure

carbonate rocks of marine facies (Liu GH et al., 1993), now a series of metamorphic rocks in the low greenschist facies, was deposited. Studies of micro-fossils and isotopic dating (660–570 Ma) show that the main part of Taowan Group belongs to the Sinian System. In the Dabieshan area the main part of Foziling Formation is a similar rock series, which may also belong to the Sinian System.

The Sinian System in North China is distributed over only a limited area. Most of the area was uplifted and was being eroded. In the eastern part of Sino-Korean Plate, to the east of Tancheng–Lujiang Fault Zone, shallow marine sediments were deposited. The lower part of the system is composed of clastic rocks and the upper part of the system is composed of carbonate rocks, distributing mainly in Shandong (Tumen Formation, 118°E, 36.3°N), Xuzhou–Huaihe area (Xuhuai Formation, 117°E, 34°N; Fengtai Formation, 116.7°E, 32.7°N), east Liaoning (Jinxian Formation, 122°E, 39.6°N) and the Gyeonggi massif, adjacent to Seoul in the southern Korean Peninsula (Fig. 3.10). On the southern margin of the Sino-Korean Plate, the Sinian System is composed of tillite belonging to the Luoquan Formation (glacial conglomerate and aqueo-glacial conglomerates and siltstones) and Dongpu Formation (standard section in western Henan, 110.8°E, 34.1°N). The Luoquan Formation and its equivalent strata are distributed over a very large area, from west Henan, south Shaanxi and Ningxia to Beishan in the Gansu area (96°E, 41.5°N). The thickness varies from 0.3 to 288 m, thinner in the north and thicker towards the south. They are regarded as having been deposited from mountain glaciers, passing into glacio -marine sediments, on the southern margin of Sino-Korean continent. Further to the northwest, tillites of the Luoquan Formation are found in Tianshan and Karatal in Central Asia (Fig. 3.9).

This Luoquan glacial period is equal to Varangian glacial period around 590 Ma. The distribution of glacial deposits and the other sediments of the Luoquan Formation shows that the main part of Sino-Korean Plate, i.e. Edos (north Shaanxi–Southern Inner Mongolia)–North China–Korean Peninsula and the Alax Block must all have been connected in Sinian Period, and separated from the Tarim–Qaidam and Yangtze plates, which have a significantly different tectonic history.

In the Sinian, sedimentation and the environments of deposition on the Tarim–Qaidam and Yangtze plates were similar. The sediments are mainly dolomite, deposited in an open epicontinental sea, with a comparable combination of stromatolites and other microflora. However, in some areas of the north Tarim and north Qaidam blocks, such as Tianshan, Kuruktag and the northern margin of Qaidam, there are glacial deposits, similar to those of the Luoquan Formation in the upper part of Sinian System, (e.g. the Hangerqiaoke Formation in the upper Kuruktag Group and the Hongtiegou Formation in the Quanji Group (Fig. 3.9)). These glacial deposits indicate that although Sino-Korean Plate was already separated from Tarim–Qaidam Plate by a sea or ocean in the Qilian Aulacogen, the distance between the two plates was not very long, so that the similar marine glacial sediments are found also on the northern margins of the Tarim and Qaidam blocks. The Qilian Aulacogen, between Tarim–Qaidam and Sino-Korean paleoplates, was in a state of extension in the Sinian Period, and controlled emplacement of super large copper-polymetallic ore deposits at Baiyinchang and Guomisi in the Qilian area.

According to the data from Chinese continental blocks, by comparing Figs. 3.8 with 3.9, it can be seen that tillites were deposited in different areas at different times. In the Nanhua Period tillites were deposited on the Yangtze and Tarim–Qaidam plates, but any tillites were never found on Sino-Korean plate; in the Sinian Period the tillites were deposited on the southern margins of the Sino-Korean Plate, but never occurred on the main part of Yangtze and Tarim–Qaidam plates. This shows that tillites never covered the whole Earth at one time, but were limited to specific areas. It means that the "Snow Ball Earth" (Kirschvink, 1992) hypothesis about Neoproterozoic period for whole globe has some mistakes.

In a late epoch of Sinian Tectonic Period (i.e. in the late Early Cambrian Epoch), violent tectonothermal events affected the Jiamusi–Xingkai Block (130–132°E, 45–47°N); these were formerly called the Xingkai movements (Huang JQ, 1960, 1965; Ren JS et al., 1980, 1990, 2000; Zhao CJ et al., 1996). The clastic-carbonate rocks formed in the Sinian -Early Cambrian were metamorphosed in the greenschist facies. An Ar-Ar age of 645–599.6 Ma has been obtained from glaucophane schists around Yilan (Zhang XZ et al., 1992), accompanied by adjacent collision-type granitic magmatic intrusions, showing that blocks had collided and were amalgamated during this period. On the Jiamusi Block, tholeiite in the Mashan rock series has been metamorphosed into amphibolite and granulite. In recent years, through ac-

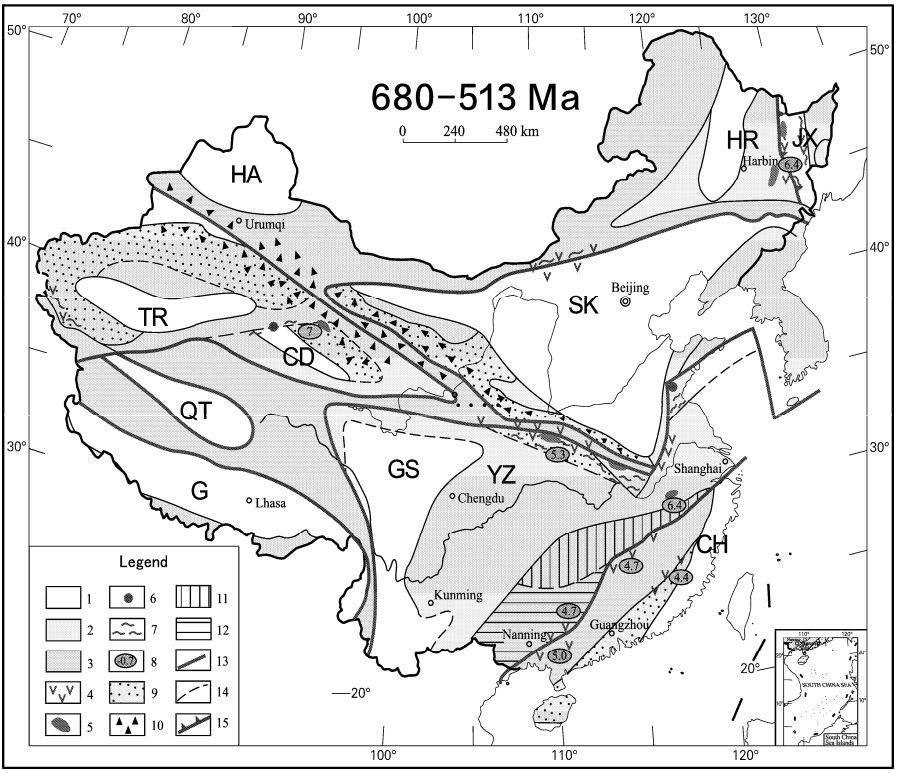

Fig. 3.9 Paleotectonic sketch of China in the Sinian Period (680–513 Ma) (data from Bai J et al., 1996; Liu BJ et al., 1994; Meng XH et al., 1993).

Legend: 1.Area of erosion; 2. Shallow marine sedimentation or epicontinental basin; 3. Bathyal oceanic region; 4. Volcanic rocks; 5. Granitic intrusions; 6. Eclogites; 7. Area of intermediate and low grade metamorphism; 8. Rate of plate deformation, "-"= extension, others are rate of shortening, in cm/yr (data in Appendix 5.2); 9. Continental margin clastic deposits; 10. Continental margin glacial deposits (Luoquan Formation and its equivalents); 11. Bathyal siliceous shale; 12. Bathyal volcanic flysch; 13. Plate boundaries; 14. Boundaries between tectonic or depositional units. 15. Collision belt.

Divisions of tectonic domains: 1. Peri-Siberian Tectonic Domain (HA= Ancient Kazakhstan Plate; HR= Ancient Harbin Plate); 2. Sino-Korean Tectonic Domain (SK= Sino-Korean Paleoplate, including North China, Korean Peninsula and Alxa blocks, etc.); 3. Peri-Yangtze Tectonic Domain (YZ= Yangtze Plate; TR= Tarim Plate; CD= Qaidam Plate; GS= Ancient Garze-Songpan plate; CH= Cathaysian Plate, also including the Qinling–Dabie Block); 4. Peri-Gondwanan Tectonic Domain (G), including QT= Qiangtang Plate. A Paleotectonic reconstruction has not been attempted.

curate chronology with zircon, it has been shown that this rock series was formed in the Early Cambrian (527.5 Ma, Song B et al., 1997; Li JY et al., 1999). Dorsett-Bain et al. (1996) employed the SHRIMP method of U-Pb determination on zircon from granulite of the Jaimusi Block and obtained an age for the zircon rims of 502±10 Ma. Other Paleozoic strata on the Jiamusi–Xingkai Block overlie the Sinian–Early Cambrian metamorphic system unconformably. Therefore, the unified crystalline basement of the Jiamusi–Xingkai Block was formed at the end of Early Cambrian Epoch, it is therefore appropriate that the Sinian Tectonic Period includes rocks formed in the Sinian–Early Cambrian. Correspondingly, in north Heilongjiang, the Jiagada Group–Erguna River Group, a greenschist facies metamorphic rock series of Neoproterozoic–Early Cambrian age and in the People's Republic of Mongolia the Wendu'rmiao ophiolite and metamorphic rock suite of Neoproterozoic–Early Cambrian age (551–519 Ma) were de-

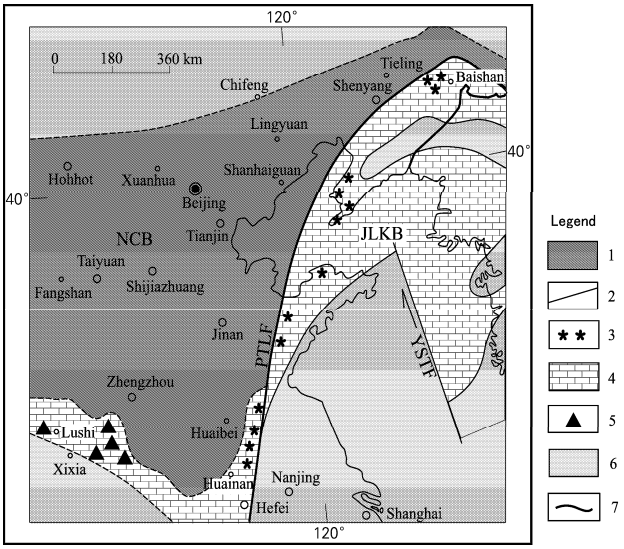

Fig. 3.10 Paleogeographic map of the Sino-Korean Plate in the Sinian Period (630–543 Ma) (Qiao XF, 2002, with permission of Qiao XF).

1. Area of erosion; 2. Syn-sedimentary faults; 3. Distribution of seismites indicating earthquake activity; 4. Shallow marine sediments (clastic rocks in the lower part, transgressive carbonates in the upper part); 5. Mountain glaciers and marine glacial sediments (Luoquan Formation in the upper Sinian); 6. Vast open sea marine sediments; 7. Border of country.

PTLF= Paleo-Tancheng-Lujiang zone of weakness; NCB= North China Block; JLKB= Jiaodong–Liaodong -Korean Block; YSTF= Yellow Sea transform fault (formed in the Triassic Period).

veloped (Ren JS et al., 1980, 1990). This tectonic event affected the blocks of northeast of China and Mongolia, but is not seen in most central part of the Chinese continent. This tectonic event occurred almost simultaneously with the Pan-African Tectonic Event on the Gondwana, and may have been an expression of that event in Northeast China.

In the Himalayan, Gangdise, Qiangtang and Sibumasu (including Baoshan) Blocks of western Yunnan, Shan States of Burma, west of Chiang Rai and Tak of Western Thailand, Western Malay Peninsula, the pre-Ordovician rocks are all metamorphic. The tectonic evolution of the Jiamusi -Xingkai Plate, where the Rouqiecun, Guqin and Qiwugongba Groups are equivalent to the Sinian and Early Cambrian series, is similar to that of the Himalayan Plate. In the metamorphic Namunani Group in the Ngari area of western Tibet (Xizang), the earliest intrusive rock has an isotope age of 645 Ma (Guo TY et al., 1991). In the Nyalam-Tingri area (86°E, 28.5°N) of the Central Himalaya, the ages of metamorphic rocks are between 1,250 and 536 Ma. In mica quartz schist of the Guqin Group to the south of Nyingchi-Tongmai (94.5°E, 29.5°N) in southeastern Tibet, a zircon U-Pb age of 564 Ma has been determined. Around Amdo (92°E, 32.1°N) in the Qiangtang Plate, a U-Pb zircon age of 530–519 Ma was obtained from gneiss (Bureau of Geology and Mineral Resources of Xizang, 1993). Recently, zircon isotopic ages of 1,016–929 Ma and 548–509 Ma were obtained from the Gemuri Group in the crystalline basement of the Qiantang Plate, showing two tectono-thermal events (Wang GZ et al., 2001). An Rb-Sr whole-rock isochron age of 519 Ma, marking the early metamorphic-deformation event, is associated with an east-west trending foliation in the Lancang Metamorphic Zone of western Yunnan (Zhao J et al., 1992, 1994; centered on 100°E, 24°N). Pre-Cambrian–Early Cambrian rocks, metamorphosed at a low grade during the Sinian–Early Cambrian, are overlain by the Upper Ordovician sedimentary system with

angular unconformity (Fig. 3.11). The above geological data prove the widespread occurrence of a Pan-African collision (also called the "East Gondwana collision") in the Yunnan–Tibet area. This tectonic event led to the formation of a unified crystalline basement in the Himalayan, Gangdise, Qiangtang and Sibumasu blocks of southwestern China, and separately in the Jiamusi–Xingkai Block, Jiagada–Erguna River Blocks of Northeastern China.

Fig. 3.11 Unconformity between Ordovician dark yellow-grey limestone (upper) and Pre-Cambrian siliceous marble of the Laguigangri Group (whitish gray in photo, lower), photo orientation looking towards the NW in the Kangmar area of the Central Himalayas (89.9°E, 28.5°N). Siliceous breccia and metamorphic quartz sandstone occur at the base of the Ordovician System, (photo by Zhou ZG and Liang DY, 2005 and details via personal communication, with permission of Zhou ZG).

Granitic intrusions of the Sinian Period have been found in the West Kunlun Block, and to the southwest in Tarim, giving Rb-Sr isotopic ages of 644–517 Ma (Bi H et al., 1999), showing that the Tarim and west Kunlun blocks had converged and had been shortened. This episode of tectono-magmatism is closely related to the Pan-African Tectono-thermal Event. In recent years, in further studies on the West Kunlun Block, Jin XC et al. (1999) found the Kudi ophiolite suite (centered on 76°E, 37.6°N) in the area to the south of the West Kunlun central fault, and to the north of the Kangxiwar Fault Zone (centered on 79°E, 36°N), there is a metamorphic rock series of Neoproterozoic–Early Cambrian age, possibly representing the Pan-African Tectonic Event. The times of formation of the metamorphic crystalline basements of the southern and northern West Kunlun Block are very different. The basement of the northern block composed of an amphibolite facies metamorphic rock series was formed in the Archean-Paleoproterozoic, and the basement of the southern block was formed in the Pan-African Tectonic Event.

Zhu YF and Ogasawara (2002) discovered a super high pressure metamorphic assemblage in the Kokchetav Subduction Zone in Central Asia, formed at 530 Ma, with dolomite, aragonite and garnets with diamond inclusions indicating a depth of formation of at least 250 km, presumably forming part of the Pan-African Tectonic Event. On the Chinese continent, in the Jiaonan Block (southern Shandong; centered on 119.5°E, 35.7°N) and Qiemo -Mang'ai, Altun (centered on 90°E, 38°N), and the northern

edge of Qaidam (centered on 96°E, 38°N), Sinian isotopic ages of 550–504 Ma were discovered in eclogite, also possibly related to the Pan-African Tectonic Event (Lu SN et al., 2001). Recently, Shi Rendeng et al. (2004) using the U-Pb SHRIMP dating method found an isotopic age of 550±17 Ma in the Yushigou ophiolite in Qilianshan (centered on 100°E, 38.4°N). The formation of this oceanic crust was also related to the Pan-African Tectonic Period. The influence of this event evidently extended into Central Asia, Altun and the northern margins of the Qaidam, Qilianshan and Jaionan blocks.

Using 169 chemical analyses of the composition of intermediate and acid magmatic rocks, the rate of plate shortening in the whole Chinese continent in the Sinian Period is estimated to be between 4.7 and 7 cm/yr (Appendix 4.2), with an average value of 5.5 cm/yr. The rates of shortening in Altun Mountain, Hutieling, eastern Heilongjiang (centered on 132°E, 46°N) and Xiuning, Anhui (centered on 118.2°E, 29.8°N) are higher, between 6.4-7 cm/yr, but were generally lower than 5.5 cm/yr in other areas. The initial strontium isotope ratio of the Zhuguangshan granite (isotopic age 591 Ma; centered on 114°E, 35.7°N) on the western Cathaysian Plate is 0.7048, showing that much mantle material was intruded into this area.

According to the temperature, pressure and depth of formation of rocks metamorphosed in the Sinian Period from 8 different areas (Appendix 6.1), calculated ancient geothermal gradients were 8.2–18.8°C/km. These geothermal gradients are very low, about half or 1/4 of the average geothermal gradient in the continents at the present day. One exception is the rough temperature and pressure estimation formed by Zhang C et al. (1996) on the Wulawusu Amphibolite (isotopic age of 638–607 Ma) in Inner Mongolia, where the formation temperature was 670°C, the pressure 0.3 GPa, the depth 11 km giving a geothermal gradient of 61°C/km. In this estimation, the author believes that the value for estimated pressure is so low that the geothermal gradient in this area is far higher than all the other determinations, although there may be other possibilities.

In the Sinian Period, most areas of the Chinese continent were tectonically stable. Deposition of the tillite of the Luoquan Formation around 590 Ma, equivalent to the Varangian glacial period all over the world, occurred on the southern margin of Sino-Korean Plate and the northern margin of Tarim–Qaidam Plate, whereas the greater part of the South China blocks and the Tarim–Qaidam Block were covered by shallow warm water carbonate sedimentation. The Jiamusi–Xingkai, Himalayan, Gangdise and Qiangtang blocks formed a unified crystalline basement, whose structural evolution occurred during the Pan-African Tectonic Event during which the Gondwana was formed. It is possible for these blocks to constitute part of the Gondwana at that time. The four tectonic domains forming the Chinese continent in the Sinian Period were similar to those of the Nanhua Period, with the Tarim and Qaidam paleoplates still belonging to the Yangtze Tectonic Domain (Fig. 3.9).

3.5 Chinese Continental Blocks in Mesoproterozoic and Neoproterozoic Global Evolution

The global tectonic evolution in Mesoproterozoic and Neoproterozoic was characterized by the formation and breakup of the Columbia and Rodinia supercontinents, the occurrence of the Pan-African Tectonic Event, and the formation of the Gondwana.

Several hypotheses have been put forward for global tectonic evolution during Early Mesoproterozoic, but none of these are entirely believable. Particularly, many researchers have attempted tectonic reconstructions of the Rodinia supercontinent (1,100 Ma). This concept was first proposed by McMenamin et al. (1990), who considered that Rodinia was a global supercontinent formed by the collision of many continental blocks. They proposed that the margins of this supercontinent provided the cradle for the earliest animals. On the basis of analysis of the rock formations of the Grenville Collision Zone and correlations on a global scale, Hoffman (1991) proposed a restoration of the ancient Rodinia supercon-

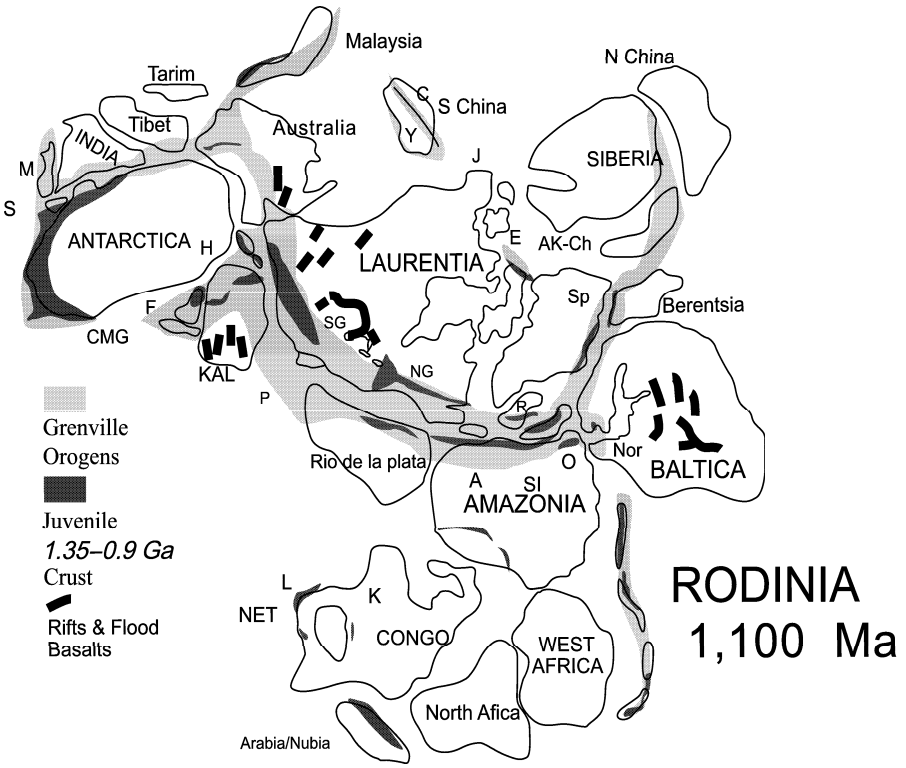

Fig. 3.12 Reconstruction of the Rodinian supercontinent at 1,100 Ma (Condie, 2001, personal communication, with permission).

Light gray color shows the Grenville Collision Zone (orogenic zone); dark gray shows the continental crust formed by Juvenile collision (1,350–900 Ma); short black heavy line indicates the distribution of rifts and flood basalts.

Note by the authors: In this figure the Yangtze and Cathaysian plates are included in the South China Block. According to Condie the Yangtze and Cathaysian plates were amalgamated with the South China Plate at this period. There is a large amount of geological data to show that these collisions and amalgamations occurred in the late Qingbaikouan Period (Jinning) at ~800 Ma, and not at this period.

tinent. Powell et al. (1993) and Li ZX et al. (1996; 1998) added paleogeomagnetic data and provided many supporting arguments.

In recent years, Condie (2001) has improved the previous reconstructions and brought a new understanding to the formation and evolution of the Rodinia supercontinent (Fig. 3.12). He carried out comparative geotectonic studies on the front and rear of the Grenvillian collision zones, including Juvenile zones, using them as the main control over the reconstruction of the Rodinia supercontinent. He considered the ancient Sino-Korean Plate (N China in Fig. 3.12) to be adjacent to the Siberian Plate, and included the South China blocks among the Laurentian, Australian, Siberian and Malaysian Plates. On the Chinese continental blocks in the Late Mesoproterozoic only the Sibao Tectonic Event in the Yangtze Plate was contemporaneous with the formation of the Rodinia supercontinent throughout the world. Li ZX et al. (1996) suggested that the collision between the Yangtze and Cathaysian plates occurred during the Sibao Period (1,100–1,000 Ma), forming part of the worldwide Grenvillian Orogeny. However, as described above, the Jiangnan Collision Zone (*JN* in Fig. 3.3) formed between the North

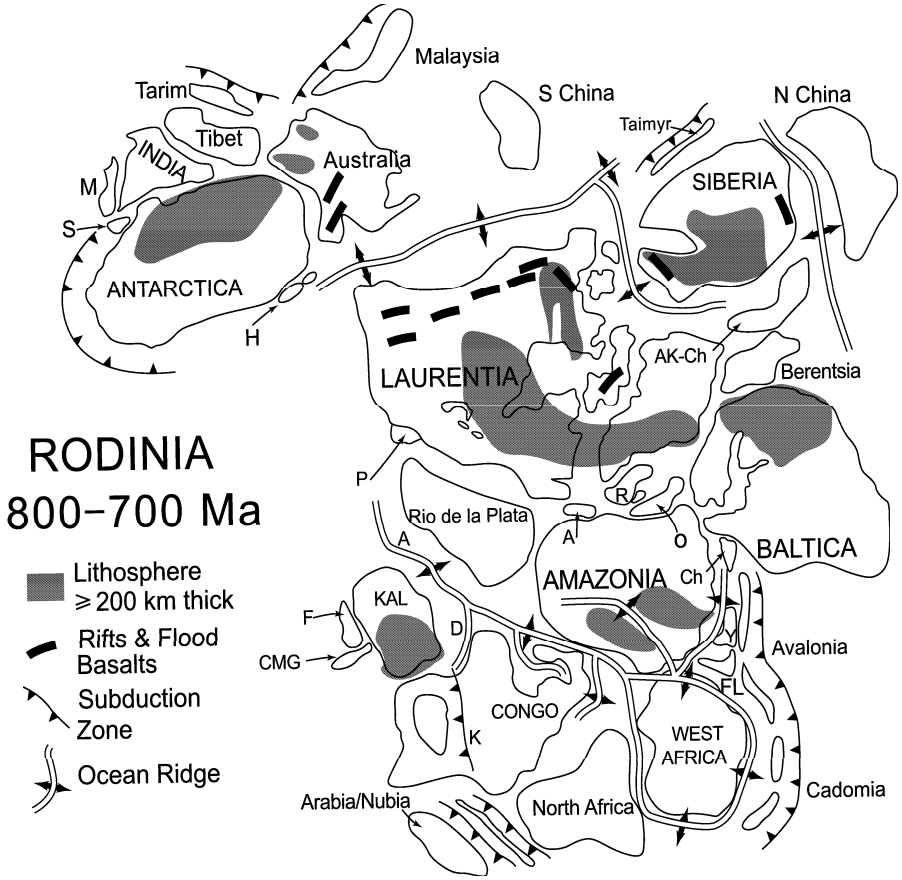

Fig. 3.13 Reconstruction of the Rodinia supercontinent (800–700 Ma) (Condie, 2001, personal communication, with permission).

Gray indicates a lithosphere thickness $\geqslant$ 200 km; the short heavy black lines show the locations of rifts and flood basalts; light line with teeth shows the subduction zone; double lines with opposed arrows show oceanic ridges.

and South Yangtze plates during the Sibao Period (Liu BJ et al., 1994), and not between the Cathaysian and Yangtze plates. The collision between the Cathaysian and Yangtze plates must have occurred later, at the end of the Qingbaikou Period (1,000–800 Ma), at the time when the Rodinia supercontinent began to break up. The Shaoxing–Shiwandashan Collision Zone between Cathaysian and Yangtze plates does not show any of the characteristics of the Grenvillian Orogeny; Li ZX et al. (1996) possibly made this mistake because it is easy to confuse the two adjacent sutures.

According to the model of Condie (2001) the central radiating extensional area of rifts and flood basalts within Rodinia supercontinent, with Laurentia, Australia and Antarctica, was due to the rise of a mantle plume at a late period; there was possibly a second plume beneath the Baltica Plate (Fig. 3.12).

The Rodinia supercontinent broke up between 800 and 700 Ma (Fig. 3.13). In large plates such as Australia, Siberia, Laurentia, Amazonia, and Baltica, the thickness of the lithosphere was 200 km or more. Rifts and flood basalts obviously related to extension occur between Laurentia and South

China, Australia, Antarctica, Siberia and between Siberia and North China, between Rio de la Plata and Amazonia, Congo, and North Africa and around West Africa. Data concerning the breakup with the formation of oceanic crust comes mainly from Laurentia, Australia and Siberia. Subduction zones were developed on the margins of Malaysia, Tarim, Taimyr, Antarctica, West Africa, Congo and Amazonia.

The breakup and fragmentation of the Rodinia supercontinent between 800–700 Ma, affected mainly Laurentia and South China, Australia, Antarctica and Siberia (the upper part of Fig. 3.13) and Rio de la Plata, Amazonia, West Africa and Congo, North Africa (the lower part of Fig. 3.13). The breakup of the Chinese continent during the Nanhua Period was related to the breakup of the former assemblage.

By virtue of tectonic features in south China and the large number of granitic intrusions, Li ZX et al. (1998) proposed that the breakup of the Rodinia supercontinent was related to the development of a mantle plume beneath South China. This proposal is not supported by the evidence and is in contradiction to the data indicating low geothermal gradients during the Nanhua Period in China (Appendix 7).

From the reconstruction of the ancient continents between 700 and 550 Ma (Fig. 3.14), tectonic collisions between the African, South American, Indian and Antarctic plates (the lower part of Fig. 3.14) at that time formed part of the Pan-African Tectonic Event and led to the formation of the Gondwana

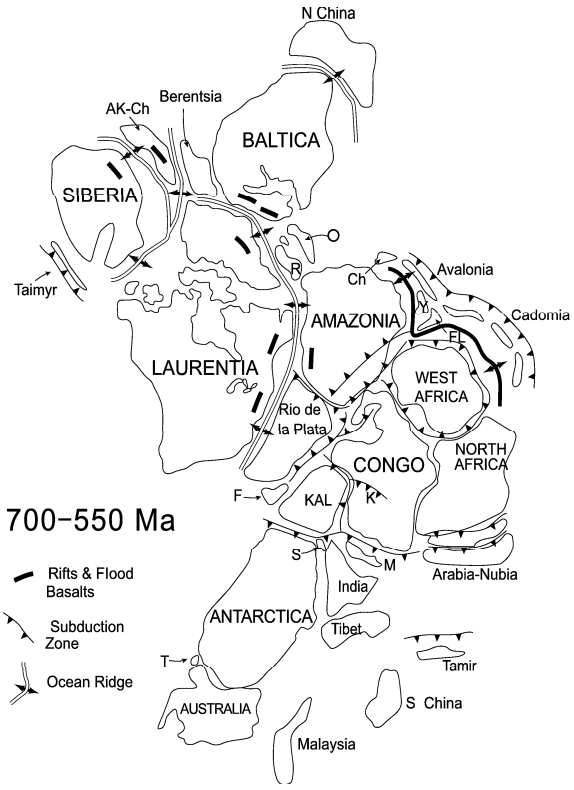

Fig. 3.14 Reconstruction of global tectonics between 700 and 550 Ma (Condie, 2001, personal communication, with permission).

Black short heavy lines= rifts and flood basalts; light line with black teeth= subduction zone; double line with opposed arrows= oceanic ridges.

(Unrug, 1996) with associated extensive metamorphism and deformation. This tectonic event continued until ~500 Ma.

Deformation and metamorphism in the Himalayan, Gangdise, Qiangtang, Sibumasu, and Jiamusi–Xingkai, Jiagada -Erguna River blocks in Chinese continent and their adjacent areas were also related to forming the part of Gondwana. However, Condie's (2001 (personal communication)) (Fig. 3.14) reconstruction allows no space for the Himalayan, Gangdise, Qiangtang, Sibumasu and Jiamusi-Xingkai, Jiagada-Erguna River blocks. The locations of these blocks during this period will be the subject of future research.

Extension and breakup between Amazonia -Baltica and Siberia -Laurentia, was preceded by rifting and extrusion of flood basalts, leading to the formation of oceanic ridges. At that time, the Sino-Korean and Yangtze Plates were not connected, and were in similar state of extension and subsidence. How to revise Condie's (2001) reconstruction in accordance with our knowledge of the tectonic evolution of the Chinese continental blocks will be a matter for future study.

During the tectonic evolution of the plates during the Meso-and Neoproterozoic, the characteristics of sediments and their chemical compositions were also changing. The initial ratio of the strontium isotopes ($^{87}Sr / {}^{86}Sr)_i$ may reflect the ratio of the contributions of the mantle and crustal source rocks to the sediments (Fig. 3.15). During a late period in the formation of the Rodinia continent, the initial ratio of $^{87}Sr / {}^{86}Sr$ increased from 0.7055 to 0.7071 showing that at that period, sediments from crustal sources were being supplied in large quantities, with a relative decrease in material from mantle sources, whereas at the climax of the breakup of Rodinia (around 800 Ma), the initial ratio of $^{87}Sr/^{86}Sr$ decreased to around 0.7057, indicating the supply of large quantities of sediment derived from mantle sources and the reduction of material from crustal sources. With the accretion of the Gondwana during the Pan-African collisions, the initial ratio of $^{87}Sr/^{86}Sr$ again increased from 0.7067 to 0.710 indicating the influx of large quantities of material from crustal sources and the reduction of material from mantle sources.

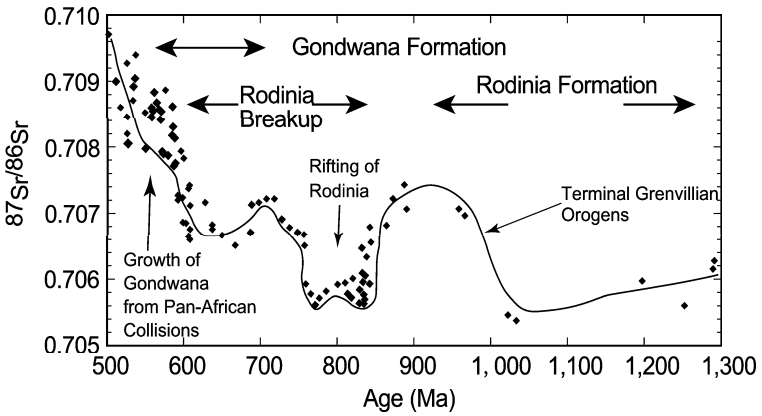

Fig. 3.15 Evolution of ancient continents and the initial ratio of $^{87}Sr / {}^{86}Sr$ (Condie, 2001, personal communication, with permission).

The abscissa shows isotopic age, and ordinate shows the initial of $^{87}Sr / {}^{86}Sr$ ratio.

There were four periods during the breakup of Rodinia (850–600 Ma), when the deposition of black shale became common (Fig. 3.16). The number of phosphorite deposits also changed during the process of continental evolution. Phosphorites are rare in the Mesoproterozoic, and only became common in the late Neoproterozoic, apart from the two glacial periods, at 720 Ma and 590 Ma (Fig. 3.17). After 680

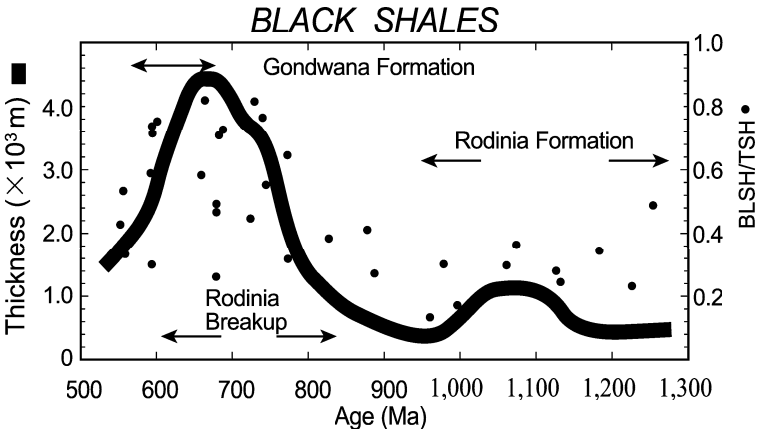

Fig. 3.16 Evolution of ancient continents and the increase in black shales (Condie, 2001, personal communication, with permissions).

The abscissa shows isotopic age; the left ordinate shows the thickness of the strata; the right ordinate shows the ratio between black shales and the total amount of shale.

Ma, during the accretion of the Gondwana, at ~550 Ma the deposition of phosphorite increased, reaching ten times the background value. The appearance and the increase in black shale and phosphorite indicate a rapid increase in the quantity of living material. Zhang TG et al. (2002) suggested that following the two Neoproterozoic glacial periods there was a significant bio-radiation event, with evolution from protozoan eucaryotes to multi-cellular metazoans, leading to a rapid increase in the quantity of in biogenetic material (Zhu MY and Steiner, 2004).

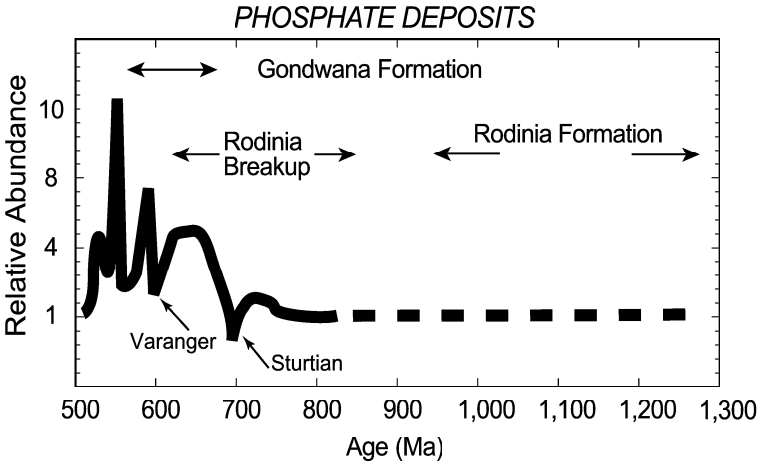

Fig. 3.17 The relationship between phosphate deposits and the evolution of ancient continents (Condie, 2001, personal communication, with permission).

The abscissa shows isotopic age; the left ordinate shows the relative abundance of phosphate deposits; The Sturtian glacial period occurred at ~720 Ma; the Varangian glacial period occurred at ~590 Ma.

The relationship between significant tectonic events and the cosmic year, i.e. the time it takes for the solar system to rotate around the galactic disc (265±60 Ma), is the subject of lively discussion at the present time. The breakup of the Rodinia supercontinent, the accretion of the Gondwana continent, the two large-scale low latitude glacial events, and the bio-radiation event in the Neoproterozoic occurred during the third and second cosmic years before the present.

In the Mesoproterozoic and Neoproterozoic the tectonic evolution of Chinese continental blocks shows some similarities to and differences from the tectonic evolution of the other global continental blocks. The main tectonic events in the evolution of China in the Mesoproterozoic (1,800–1,000 Ma) were the deposition of a sedimentary cover on the Sino-Korean Protoplate and then its breakup into three continental blocks. Using the age of formation of the Jiangnan subduction and collision zone as a marker, the Yangtze Plate completed its amalgamation around 1,000 Ma. During the period of global convergence and formation of the Columbia and Rodinia supercontinents (1,900–950 Ma), the Chinese continent was still mainly in a separate state. Convergence and collision, with associated magmatic activity in the Yangtze and Qinling–Dabie blocks, occurred at 800 Ma, but the Rodinia supercontinent began to break up. It means that the evolution of Chinese continental blocks was not synchronism with global blocks during the Mesoproterozoic and Neoproterozoic.

Widespread convergence and collision of the Chinese continental blocks took place in the Late Neoproterozoic, at the end of the Qingbaikou Period, while Rodinia appears to have changed from stability to the breaking up period, around 800 Ma, three cosmic years before the present.

The most important tectonic events in the Chinese continent during the Nanhua Period (800–630 Ma) were widespread extension and separate, similar to the events elsewhere in the world. The first sedimentary cover was deposited on the Yangtze Plate; at around 720 Ma the Yangtze and Tarim–Qaidam Plates entered the Nantuo glacial zone, equivalent to the Sturtian glacial period. In the Sinian Period (630–513 Ma), most areas of the Chinese continent were tectonically stable. Around 590 Ma, equivalent to Varangian glacial period, the southern margin of Sino-Korean Plate and the northern margin of the Tarim–Qaidam Plate also entered the glacial zone with the deposition of the tillites of the Luoquan Formation. At this time shallow warm water carbonate sediments were deposited over vast areas of South China, North China and the Tarim–Qaidam Plates. From the evidence of the distribution of the glacial deposits during the Nanhua and Sinian periods, the Sino-Korean Plate and South China–Tarim–Qaidam plates must have been widely separated, providing evidence against the hypothesis of a "Snow Ball Earth" during these periods; although the glacial deposits are widespread at these times, glaciation did not cover the whole Earth.

Major events in the tectonic evolution of China in the Meso-Neoproterozoic and Early Cambrian are: the commencement of the breakup Sino-Korean Protoplate with the deposition of a sedimentary cover; the amalgamation of blocks originating in Gondwana to form the Jiamusi–Xingkai, Jiagada–Erguna, Himalaya, Gangdise and Qiangtang blocks with a unified crystalline basement; the protoplates forming the Chinese continent underwent multiple breakups, displacements and collisions and were then reunited; the Tarim–Qaidam Block was separated from Sino-Korean Protoplate, and gradually developed characteristics similar to those of the Yangtze Plate.

During the whole Meso-and Neoproterozoic the Sino-Korean and Yangtze plates were always entirely separate and developed different tectonic features. During the Qingbaikouan Period in the Mesoproterozoic the Tarim–Qaidam blocks formed part of the Sino-Korean Plate, but since the Nanhua Period they developed features, suggesting that they were more closely related to the Yangtze Block, but were still not at great distance from the Sino-Korean Plate. During the Sinian Period, the Jiamusi and Xingkai blocks, now in northeast China, formed a unified crystalline basement belonging to Gondwana. This was the period when the Himalayan, Gangdise and Qiangtang blocks also formed a unified crystalline basement and were accreted to Gondwana.

After the formation of a unified crystalline basement, in the Mesoproterozoic, the Chinese continental blocks began to break up and became dispersed. The breakup into separate blocks occurred during different times in different plates: 1,800–260 Ma in the Sino-Korean, Alax, Qaidam, Tarim and Tianshan–South Hingganling blocks; 1,800–400 Ma in the Altay-Ergun Block; 1,000 or 800–200 Ma

in the Yangtze Plate; 400–220 Ma in the Cathaysian Plate; 513–200 Ma in the Qiangtang Plate; 513–56 Ma in the Gangdise Plate; 513–34 Ma in the Himalayan Plate.

References

Bai J, Huang XG, Wang HC et al (1996) The Precambrian Crustal Evolution of China, 2nd edn. Geological Publishing House, Beijing (in Chinese with English abstract).

Bi H, Wang ZG, Wang YL et al (1999) History of tectono-magmatic evolution in the Western Kunlun Orogen. Science in China D 42(6): 604–619.

Bureau of Geology and Mineral Resources of Xinjiang Uygur Autonomous Region (1993) Regional Geology of Xinjiang Uygur Autonomous Region. Geological Publishing House, Beijing (in Chinese with English abstract).

Chen H, Shao JA (1987) Formation pattern and tectonic background of carbonate in Bayan'obo. In: Contributions to the Project of Plate Tectonic in Northern China. no.2, pp.73–79. Geological Publishing House, Beijing (in Chinese with English abstract).

Chen JF, Jahn BM (1998) Crust evolution of southeastern China: evidence from Nd and Sr isotopic compositions of rocks. Tectonophysics 284: 101–133.

Cheng H (1991) The Neoproterozoic collision orogen in northwestern Zhejiang Province. Geological Review 37(3): 203–213 (in Chinese).

China National Commission on Stratigraphy (2001) Chart of regional stratigraphy (geological age) of China. Journal of Stratigraphy 25(suppl.): 359–360 (in Chinese).

Condie KC (2001) Mantle Plumes and Their Record in Earth History. Cambridge University Press, Cambridge.

Cong BL, Wang QC (1994) Review of researches on ultrahigh-pressure metamorphic rocks in China. Chinese Science Bulletin 39(24): 2068–2075 (in Chinese).

Cong BL, Wang QC (1999) The Dabie-Sulu UHP rocks belt: review and prospect. Chinese Science Bulletin 44(12): 1074–1086.

Dong SW, Liu XC (2002) Zercon U-Pb ages in granitic gneiss of eastern Dabieshan. Geologica Scientica 37(2)： 165–173 (in Chinese with English abstract).

Dorsett BH, Wilde SA, Liu JL (1996) A Pan-African granulite facies event in northeastern China: SHRIMP U-Pb zircon dating of the Mashan Group of Liumao, Heilongjiang Province. 30th IGC, Abstracts, 2: 552.

Gao ZJ, Wu SZ. 1983. Tectonic evolution of Tarim paleocontinent in Xinjiang. Chinese Science Bulletin 28(23): 1448–1450 (in Chinese).

Gilder SA, Zhao XX, Coe R et al (1996) Paleomagnetism and tectonics of the southern Tarim basin, northwestern China. J. Geophys. Res. 101 (B10): 22015–22031.

Guan BD, Wu RT, Hambrey MJ et al (1986) Glacial sediments and erosional pavement near the Cambrian-Precambrian boundary in western Henan province, China. Journal of the Geological Society, London 143: 311–323.

Guo TY, Liang DY, Zhang YZ et al (1991) Geology of Ngari Tibet (Xizang). China University of Geosciences Press, Wuhan (in Chinese with English abstract).

Guo ZJ, Zhang ZC, Wang JJ (1999) Sm-Nd isochron age of ophiolite along northern margin of Altun Tagh Mountains and its tectonic significance. Chinese Science Bulletin 44(5): 456–458.

Hoffman PF (1991) Did the breakout of Laurentia turn Gondwanaland inside-out? Science 252: 1409–1412.

Hoffman PF et al (1998) A Neoproterozoic snowball Earth. Science 281: 1342.

Hoffman PF et al (1999) The breakup of Rodinia, birth of Gondwana, true polar wander and snowball Earth. J. African Earth Sci. 28: 17–33.

Hong DW, Xie XL, Zhang JS (2002) Geological significance of the Hangzhou–Zhuguangshan–Huashan high-ε_{Nd} granite belt. Geological Bulletin of China 21 (6): 348–354 (in Chinese with English abstract).

Huang TK (Jiqing) (1960) The main characteristics of the geological structure of China: preliminary conclusions. Acta Geologica Sinica 40(1): 1–37 (in Chinese with English abstract).

Huang JQ, Xiao XC, Ren JS et al (1964) Basic Features of Tectonics of China—Specialties for One Three Million Tectonic Map of China. Industry Publishing House of China, Beijing (in Chinese).

Huang JQ, Yin ZX (1965) Several suggestions about denominations of crustal movement of China (draft). Geological Review 23(suppl.): 2–4 (in Chinese).

International Commission on Stratigraphy (2004) International Stratigraphic Chart. 32th IGC, Florence, Italy.

Jin XC, Wang Jun, Ren LD et al (1999) Problems concerning the tectonics of the west Kunlun orogen. In: Ma Z et al (eds) Advances in Structural Geology and Geophysics in China—In Honor of Academian Xingyuan Ma's 80th Birthday, pp.105–113. Seismological Press, Beijing (in Chinese with English abstract).

Kirschvink, J (1992). Late Proterozoic low-latitude global glaciation: the Snowball Earth. In: Schopf JW, Klein C (eds) The Proterozoic Biosphere: A Multidisciplinary Study. Cambridge University Press, Cambridge.

Li JH, Zhai MG, Li YG et al (1998) The discovery of Mesoarchean high-pressure granulites in Luanping-Chengde area, Northern Hebei, and their tectonic implication. Acta Petrologica Sinica 14(1): 34–41 (in Chinese with English abstract).

Li JY, Niu BG, Song B et al (1999) Crustal Formation and Evolution of Northern Changbai Mountains, Northeast China. Geological Publishing House, Beijing (in Chinese with English abstract).

Li SG, Chen YZ, Zhang GW et al (1991) A 1Ga Alpine peridotite body emplaced into the Qinling group: evidence for the existence of the Neoproterozoic plate tectonics in the north Qinling area. Geological Review 37(3): 235–242 (in Chinese with English abstract).

Li SG, Zhang ZM, Zhang QD et al (1993) The zircon U-Pb ages of Qingdao eclogite and gneiss in Jiaonan Group–evidence of magmatic event of Jinning stage in Jiaonan Group. Chinese Science Bulletin 38(19): 1773–1777.

Li SG, Jagoutz E, Xiao YL et al (1996) Ultrahigh pressure metamorphic chronology in Dabieshan–Sulu terrane–I. Sm-Nd isotopic system. Science in China D 26(3): 249–257 (in Chinese).

Li SG, Li HM, Chen YZ et al (1997) Ultrahigh pressure metamorphic chronology in Dabieshan–Sulu terrane–Ⅱ. zircon U-Pb isotopic system. Science in China D 27(3): 200–206 (in Chinese).

Li ZX, Zhang L, Powell CM (1996) South China in Rodinia: part of the missing link between Australia-East Antarctic and Laurentia? Geology 23: 407–410.

Li ZX (1998) Tectonic history of the major East Asia lithospheric blocks since the mid–Proterozoic: A synthesis. In: Flower MFJ et al (eds) Mantle dynamics and plate interactions in East Asia, Geodynamics Series, vol. 27, pp.221–243, AGU, Washington DC.

Liu BJ, Xu XS, Pan XN et al (1993) Sedimentation, Crustal Evolution and Metallogenesis of Paleocontinent in South China. Science Press, Beijing (in Chinese).

Liu BJ, Xu XS, Xia WJ et al (1994) Atlas of Petrological Phase Paleogeography of South China (Sinian to Triassic). Science Press, Beijing (in Chinese).

Liu BG, Zheng GC, Chen SM et al (1995) The zircon U-Pb isotopic dating and its significance for pre-Cambrian volcanic rocks, western Zhejiang. Chinese Science Bulletin 40(21): 2015–2016 (in Chinese).

Liu GH, Zhang SG, You ZD et al (1993) Main Metamorphic Rock Groups and Metamorphic Evolution of Qinling Orogenic Belt. Geological Publishing House, Beijing (in Chinese).

Lu SN (1998) A review on subdivision of Proterozoic eon in China. Progress in Precambrian Research 21(4): 1–9 (in Chinese with English abstract).

McMenamin MAS, McMenamin DLS (1990) The Emergence of Animals—The Cambrian Breakthrough. Columbia University Press, New York.

Mei HL, Li HM, Lu SN et al (1999) The age and origin of the Liuyuan granitoid, northwestern, Gansu. Acta Petrological et Mineralogical 18(1): 14–17 (in Chinese with English abstract).
Meng XH et al (1993) Sedimentary Basin and Formation Sequence. Geological Publishing House, Beijing (in Chinese with English abstract).
Powell CM, Li ZX, McElhinny MW et al (1993) Paleomagnetic constraints on timing of the Neoproterozoic breakup of Rodinia and the Cambrian formation of Gondwana. Geology 21: 889–892.
Qiao XF, Song TR, Li HB et al (1996) Genetic Stratigraphy of the Sinian and Lower Cambrian Strata in South Liaoning Province. Science Press, Beijing (in Chinese).
Qiao XF, Gao LZ, Peng Y, 2001. Neoproterozoic in Paleo-Tanlu Fault Zone—Catastrophe Sequence Biostratigraphy. Geological Publishing House, Beijing (in Chinese).
Qiao XF, Gao LZ, Peng Y et al (2002) Seismic event, sequence and tectonic significance in Canglangpu Stage in Paleo-Tanlu fault zone. Science in China D 45(9): 781–791.
Remane J et al (2000) International stratigraphic chart. International Commission on Stratigraphy.
Ren JS, Jiang CF, Zhang ZK et al (1980) The Geotectonic Evolution of China. Science Press, Beijing (in Chinese).
Ren JS, Chen TY, Niu BG et al (1990) Tectonic Evolution of the continental lithosphere and metallogeny in Eastern China and Adjacent Areas. Science Press, Beijing (in Chinese).
Ren JS, Wang ZX, Chen BW et al (2000) China Tectonics, Outlooked by the Globe—Brief Direction of Tectonic Map of China and Its Adjacent Areas. Geological Publishing House, Beijing.
Shi RD, Yang JS, Wu CL et al (2004) First SHRIMP dating for formation of Late Sinian at Yushigou ophiolite, North Qilian Mountains. Acta Geologica Sinica 78(5): 649–657 (in Chinese).
Shui T, Xu BT, Liang RH et al (1986) Shaoxing-Jiangshan deep-seated fault zone, Zhejiang Province. Chinese Science Bulletin 31(18): 1250–1255.
Shui T (1987) Basement tectonic framework in southeast China continent. Science in China B (4): 414–422 (in Chinese).
Song B, Li JY, Niu BG et al (1997) Single-grain zircon ages and its implications in biotite-plagioclase gneiss in Mashan group in the eastern Heilongjiang. Acta Geoscientia Sinica 18(3): 306–312 (in Chinese with English abstract).
Sugisaki R (1976) Chemical characteristics of volcanic rocks: relation to plate movements. Lithos 9(1): 17–30.
Suo ST, Sang LK, Han YJ et al (1993) The Petrology and Tectonics in Dabie Precambrian Metamorphic Terranes, Central China. China University of Geosciences Press, Wuhan (in Chinese with English abstract).
Tang HF, Zhou XM (1997) Geochemical constraints on the petrogenesis of basalts from eastern Jiangnan orogen, South China. Science in China D 40(6): 627–633.
Wan TF, Zeng HL (2002) The distinctive characteristics of the Sino-Korean and the Yangtze plates. Journal of Asian Earth Sciences 20(8): 881–888.
Wan TF, Zhu H (1991) Tectonic events of Late Proterozoic–Triassic in South China. Journal of Southeastern Asian Earth Sciences 6(2): 147–157.
Wang J, Li SQ (1987) The Langshan-Bayanobo rifting and its metallogenesis. In: Contributions on the Project of Plate Tectonic in Northern China, no.2. 59–72. Geological Publishing House, Beijing (in Chinese with English abstract).
Wang GZ, Wang CS (2001) Disintegration age of basement metamorphic rocks in Qiangtang, Tibet, China. Science in China D 44 (suppl.): 86–93.
Wang KF (1991) Metamorphic event research of gold-bearing metamorphic rocks of Baoban Group in Hainan Province. Hainan Geology and Geography (1): 9–12 (in Chinese).
Xu ST, Su W, Liu YC et al (1992) Diamonds from high-pressure metamorphic rocks in Eastern Dabie Mountains. Chinese Science Bulletin 37(2): 140–145.
Xu Y, Liu JH, Hao TY et al (2006) P wave velocity structure and tectonic analysis of lithospheric mantle in eastern China seas and adjacent regions. Chinese J. Geophys. 49(4): 1053–1061 (in Chinese).

Xu ZQ, Yang JS, Zhang JX et al (1999) A comparison between the tectonic units on the two sides of the Altun sinistral strike-slip fault and the mechanism of lithospheric shearing. Acta Geologica Sinica 73 (3): 193–205 (in Chinese with English abstract).

Yang MG, Wang YG, Li L et al (1994) Regional geological features of South China. In: Cheng YQ (ed) An Introduction to Regional Geology of China. Geological Publishing House, Beijing (in Chinese).

Yang WR, Wang GC, Jian P (2000) Research on the Tectono-chronology of the Dabie Orogenic Belt. China University of Geosciences Press, Wuhan (in Chinese with English abstract).

Zhai YS, Deng J, Li XB (1999) Essentials of Metallogeny. Geological Publishing House, Beijing (in Chinese with English abstract).

Zhang C, Li MS, He GQ et al (1996) Age of Sm-Nd isotopic isochron of amphibolite facies metamorphic zone and its significance in Wulawusu-Deyanqimiao area of Inner Mongolia. Scientia Geologica Sinica 31(1): 65–70 (in Chinese with English abstract).

Zhang C, Wu TR (1998) Sm-Nd, Rb-Sr isotopic isochron of metamorphic volcanic rocks of Ondor sum Group, Inner Mongolia. Scientia Geologica Sinica 33(1): 25–30 (in Chinese with English abstract).

Zhang GW, Zhang BR, Yuan XC (1996) Orogenic Process of Qinling Orogenic Belt and Three Dimensional Structural Map Series of Lithosphere. Science Press, Beijing (in Chinese).

Zhang GW, Zhang BR, Yuan XC et al (2001) Qinling Orogenic Belt and Continental Dynamics. Science Press, Beijing (in Chinese).

Zhang LG et al (1995) Block-geology of Eastern Asia lithosphere—Isotope Geochemistry and Dynamics of Upper Mantle, Basement and Granite. Science Press, Beijing (in Chinese with English abstract).

Zhang SG, Wan YS, Liu GH et al (1991) Metamorphic Geology of the Kuanping Group in the Northern Qinling Mountains. Beijing Science and Technology Press, Beijing (in Chinese with English abstract).

Zhang SG, Wei CY, Yang CH (1998) Metamorphism of east part of South Qinling orogenic belt. Earth Science Frontiers 5(4): 210 (in Chinese).

Zhang SY, Hu K, Liu XC (1989) The glaucophane-mica schist-eclogite zone of Proterozoic at central China. Journal of Changchun College of Geology, Monography of glaucophane zone at Hubei and Anhui, 158–162 (in Chinese).

Zhang SY, Hu K, Liu XC (1990) The rock sequences and origins of highpressure metamorphic zone at central China. Collections of Qinling–Dabie Geology (1): 221–229, Beijing Science and Technology Press, Beijing (in Chinese).

Zhang TG, Chu XL, Chen ME et al (2002) The effect of the Neoproterozoic global glaciation on the early biological evolution. Earth Science Frontiers 9(3): 49–56 (in Chinese with English abstract).

Zhang XZ (1992) Heilongjiang Group–the evidences of Caledonia collision zone in Jamusi block. Journal of Changchun College of Geology, Proceedings of PhD., 94–101 (in Chinese).

Zhao CH, He KZ, Mo XX et al (1995) Discovery Radiolaria siliceous rock of Late Paleozoic in ophiolite melange of Northeast fault zone. Chinese Science Bulletin 40(23): 2161–2163 (in Chinese).

Zhao CJ, Peng YJ, Dang ZX et al (1996) Structure Framework of East Part of Both Jilin and Heilongjiang Provinces and Their Crustal Evolution. Liaoning University Press, Shenyang (in Chinese).

Zhao GC, Sun M, Widle SA et al (2004) Late Archaean to Paleoproterozoic evolution of the Trans-North China Orogen: In slights from synthesis of existing data of the Hengshan–Wutai–Fuping belt. In: Malpas J et al (eds) Aspects of the tectonic evolution of China. London: The Geological Society, Special Publication 226.

Zhao J, Zhong DL, Wang Y (1992) Disaggregation of Lanchang Group in West Yunnan and its tectonic significance. In: Contribution to Geology Research by Post Doctors of Peking University (1): 12–24. Seismological Press, Beijing (in Chinese with English abstract).

Zhao J, Zhong DL, Wang Y (1994) Metamorphism of Lanchang metamorphic belt, the western Yunnan and its relation to deformation. Acta Petrologica Sinica 10(1): 27–40 (in Chinese with English abstract).

Zhong DL (1998) Paleo-Tethyan Orogenic Belt in Western Yunnan and Sichuan. Science Press, Beijing (in Chinese).

Zhou MF, Yan DP, Kennedy AK et al (2002) SHRIMP U-Pb zircon geochronological and geochemical evidence for Neoproterozoic arc-magmatism along the western margin of the Yangtze Block, South China. Earth Planet. Scie. Lett. 196: 51–67.

Zhou XM, Zhou HB, Yang JD et al (1989) Sm-Nd isochron age of ophiolite suite and its geological significance in Fuchuan, Xixian, Anhui Province. Chinese Science Bulletin 34(16): 1243–1245 (in Chinese).

Zhu MY, Steiner M (2004) Biological and geological processes of the Cambrian Explosion. Progress in Natural Science (special report): 1–158.

Zhu YF, Ogasawara Y (2002) Carbon recycled into deep earth: evidence from dolomite dissociation in subduction-zone rocks. Geology 30(10): 947–950.

Chapter 4
Tectonics of Middle Cambrian–Early Devonian (The Qilian Tectonic Period, 513–397 Ma)

—amalgamation of Xiyu (Western China) Plate
—forming the collission zone of Altay-Ergun
—forming the unified crystalline basement in the Cathaysian Plate
—intraplate deformation in the South Yangtze Plate
—many continental blocks migration

The Early Paleozoic Tectonic Period (Middle Cambrian–Early Devonian, 513–397 Ma) was formerly called the Caledonian Orogenic Period* in China. However, the Caledonian Orogeny was defined in northwest Europe and northeast America (Rogers and Dunning, 1991; Bally et al., 1989; Trewin, 2002), but in East Asia. Recently Li Tingdong (personal communication, 2003) has proposed that it should be replaced by the local term "Qilian Tectonic Period", as first suggested by Li K et al. (1962).

During Early Paleozoic Tectonic Period in China, most of continental blocks migrated and became dispersed. However, also during this period separate continental blocks were amalgamated to form the Xiyu Plate (called the West China Plate). The Altay–Middle Mongolia–Ergun collision belt was formed, a unified crystalline basement was formed in the Cathaysian Plate, and intraplate folding occurred in the South Yangtze Plate. In this chapter the following topics will be discussed: sedimentation, palaeogeography, paleobiological distribution, palaeomagnetism, paleo-continental reconstructions during tectonically stable periods; rock deformation, tectonic stress fields, metamorphism, magmatism and rates of plate movement during periods of tectonic activity.

* A distinctive tectonic terminology has been developed in China, however the Paleozoic "Caledonian" and "Variscan" (or "Hercynian") tectonic periods were taken directly from European terminology (Huang JQ and Yin ZX, 1965; Yin ZX et al., 1965). These two tectonic periods (~400 Ma and 397–260 Ma) are roughly coincident with the European Caledonian and Variscan orogenic periods and can be compared with them in their relationship to biological evolution. This terminology has been used for a long time in China. It is now well established that global tectonic events occur at different times in different areas so that it is not appropriate to use the European tectonic terminology for East Asian tectonic periods. It is therefore necessary to choose a local tectonic terminology for these tectonic periods in China. However the style and timing of rock deformation, metamorphism and magmatism in these two tectonic periods are so different in the different continental blocks which compose the Chinese continent, that it is difficult to choose a single term which could be used to cover the whole of China. What names should be used? At the end of Early Paleozoic, they were called the Guangxi (Ding WJ, 1929), Qilian (Li K et al., 1962), Jiangnan (Li SG, 1931), and Qujing (Guo WK, 1941) Movements. At the end of the Late Paleozoic, they were called the Tianshan (Mushketov DJ, 1928), Kunlun (Huang JQ, 1945), Nanshan (Wang HZ, 1955), Vietnam (Ding WJ, 1929), Qinling (Weng WH, 1927) and Dongwu (Li SG, 1931) Movements (N.B. the above terminology and references are taken from the thesis of Yin ZX, 1965). Tectonic periods and tectonic events should be named after the area where major tectonism occurred at that time. According to this principle, the author has named the Early Paleozoic event the "Qilian Tectonic Period" (513–397 Ma) and the Late Paleozoic event the "Tianshan Tectonic Period" (397–260 Ma).

4.1 Sedimentation, Paleogeography and Paleontology

The Early Paleozoic tectonic period can be defined as commencing at the beginning of the Early Cambrian (543 Ma) or the Middle Cambrian (513 Ma), and terminating at the end of the Silurian (416 Ma) or Early Devonian (397 Ma), covering about 120 million years, or half a cosmic year (the length of time it takes for the solar system to rotate around the galaxy). The periods and systems of the Early Paleozoic, according to the National Commission on Stratigraphy of China (2001), Remane (2000) and the International Commission on Stratigraphy (2004), are shown in Table 4.1.

Table 4.1 Periods and systems in the Early Paleozoic

Epoch	Age	Isotopic age	Area of distribution
Early Devonian and Middle–Late Silurian	Sipain, Yujiangian, Nagaolingian	428–397 Ma	Mainly in South China
Middle Silurian	Ankangian	428–423 Ma	Mainly in South China
Early Silurian	Ziyangian, Dazhongban, Longmaxian	444–428 Ma	Mainly in South China
Late Ordovician	Qiantangjiangian, Aijiashanian	461–444 Ma	Mainly in South China
Middle Ordovician	Darriwilian, Dawanian	472–461 Ma	Mainly in South China
Early Ordovician	Daobaowanian, Xinchangian	488–472 Ma	Almost the whole of China
Late Cambrian	Fengshanian, Changshanian, Gushanian	501–488 Ma	Almost the whole of China
Middle Cambrian	Zhangxian, Xuzhuangian, Maozhuangian	513–501 Ma	Almost the whole of China
Early Cambrian	Longwangmiaoan, Canglangpuan, Qiongzhusian, Meishucunian	543–513 Ma	Mainly in South China

In the Chinese continent the Early Paleozoic Tectonic Period comprises many tectonic events which occurred at different times in different areas of China. There is at present insufficient data to subdivide these events into separate tectonic periods, but the main tectonic event occurred at about 400 Ma.

Because of the abundance of fossils in Paleozoic rocks, stratigraphic correlation between the different areas of China is very straight forward, so that many local stratigraphic terminologies used previously have lost their importance. On this account national and international terminologies for stratigraphic units and ages will be used to facilitate correlation (Table 4.1).

During stable periods in tectonic evolution, the tectonics can be most easily discussed in terms of paleogeography, using palaeontology and the distribution of fossils. Generally, the effects of tectonic activity were more profound in areas where the sedimentary formations were thickest and rates of sedimentation were relatively high.

The thickness of sedimentary formations and their rates of sedimentation are given in Appendix 2 and illustrated in Fig. 4.1. In stable tectonic regions of China the thickness of Palaeozoic sedimentary formations is very different from that in the tectonically active regions. On the relatively stable central part of the Sino-Korean Plate (mainly North China), the thickness of Paleozoic sedimentary formations is 800–2,000 m, and rates of sedimentation are 3–7 m/Myr (i.e. 0.003–0.007 mm/yr), while on the margins of the plate in Jilin, Liaoning, and North Anhui provinces and in the East Ningxia Hui Autonomous Region, thickness of 4,000–5,000 m is reached, and rates of sedimentation are 9–17 m/Myr. From seismic profiling in the West Sino-Korean Plate in Shanxi and Shaanxi provinces, Wang TH (1995) found that the thickness of the Lower Paleozoic systems was controlled by N-S trending uplifts, alternating with depressions, with sediment thickness ranging from zero on the Ulad uplift to 1,400 m in the Hebei-Shandong depression, while in the southern and western marginal depressions of the Sino-Korean Plate, the Lower Palaeozoic system is more than 4,000 m thick (Fig. 4.1, A).

The thickness of Paleozoic strata in the centre of the stable Yangtze Plate is 3,000–4,000 m, and rates of sedimentation are about 15 m/Myr. However, in regions of active tectonics on the margins of

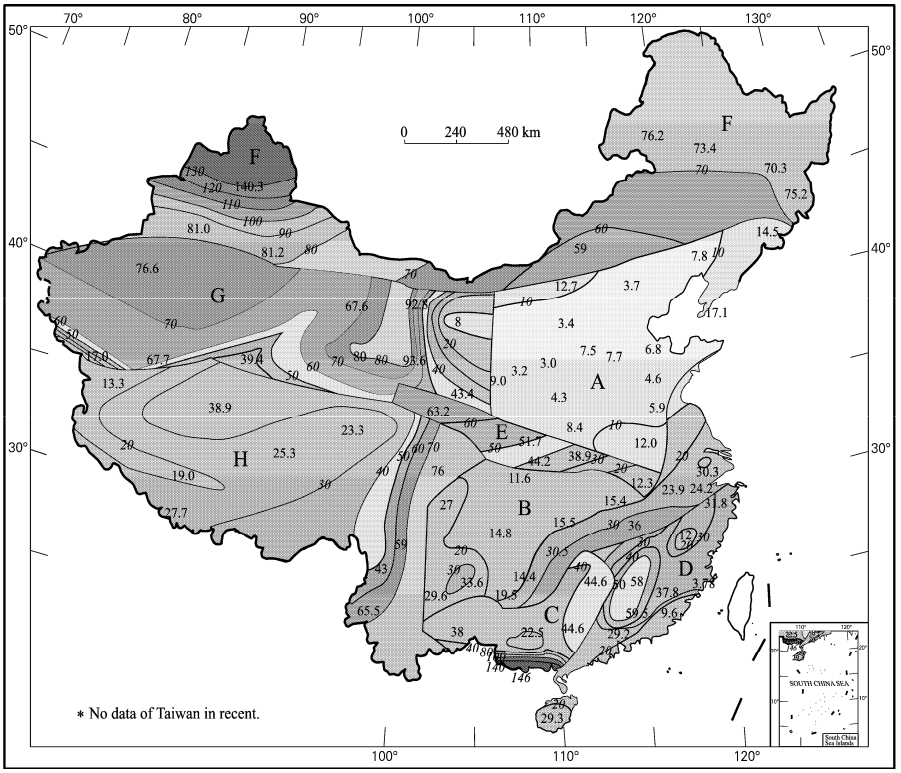

Fig. 4.1 Rates of sedimentation of Paleozoic strata in China (m/Myr).

A. Sino-Korean Plate; B. Main part of Yangtze Plate; C. Hunan–Guangxi area in Southern Yangtze Plate (distinguished because of obvious strong tectonic activity); D. Cathaysian Plate; E. Qinling–Dabie Belt; F. Tianshan–Hingganling Belt; G. Xiyu Plate (including Tarim, Qaidam, and Alxa blocks); H. Yunnan–Xizang blocks. There is no information from Taiwan Province.

the Yangtze Plate, in Jiangsu and Zhejiang, North Jiangxi, Southeast Guangxi, Guizhou and Yunnan provinces, the thickness reaches 10,000 m, with rates of sedimentation of 30–146 m/Myr (Fig. 4.1, B). Tectonic activity was also strong in the Cathaysian Plate during the Paleozoic. In East Fujian and NE Guangdong provinces, the thickness of the Paleozoic strata is 3,000 m and the rate of sedimentation was about 10 m/yr. In West and North Guangdong, South Jiangxi and SE Hunan provinces the thickness of the Paleozoic strata is 13–17 km and the sedimentation rate was 45–60 m/Myr (Fig. 4.1, D). In the western Yunnan and Xizang blocks where tectonic activity was very strong (Fig. 4.1, H) Paleozoic strata are 3–11 km thick and the sedimentation rates were between 13 and 76 m/Myr. Tectonic activity was the strongest in the western part of the Qinling–Dabie Belt and the weakest in the east, the thickness of the Paleozoic strata ranged from 3 to 18 km with rates of sedimentation of 12–63 m/Myr. In the Tianshan–South Hingganling Belt (Fig. 4.1, F), tectonic activity was the strongest in the western Altay region, where Paleozoic strata are about 41,000 m thick and the rate of sedimentation was close to 140 m/Myr (i.e. 0.14 mm/yr). In the main part of Tianshan–South Hingganling Belt and in the Xiyu Plate

(Tarim, Qaidam, and Alxa blocks (Fig. 4.1, G)), the thickness of the Paleozoic strata is about 20,000 m, and the rate of sedimentation was 60–70 m/Myr, although activity was weaker in the Alxa Block.

Although tectonic activity in most of the blocks* in the Chinese continent was not very intense during the Early Paleozoic, which is characterized primarily by the dispersion and subsidence of the blocks, paleogeographical and paleontological evidence shows that there were important changes in the sedimentary and paleoecological environments.

After long-term erosion during the Neoproterozoic and Early Cambrian, a marine transgression occurred on the Sino-Korean Plate in the late Early Cambrian from east to west and from south to north (Fig. 4.2). Only the youngest Lower Cambrian, Xiaweidian and Changping limestone formations occur on the Sino-Korean Plate near Beijing, comparable to the Canglangpu and Longwangmiao formations in South China. There are possibly older Cambrian formations, comparable to the Qiongzhushi Formation, in East Liaoning Province on the East Sino-Korean Plate and in the Xuzhou-Huaihe region (from 117.1°E, 34.2°N to 117°E, 32.6°N) on the southern margin of the Sino-Korean Plate.

Middle and Upper Cambrian deposits occur over most of the Sino-Korean Plate and consist of argillaceous carbonate rocks. In the southern Sino-Korean Plate, from northern Anhui to southern Henan Province, the sediments were formed in sabkha tidal flats (sabkha = salt flat in Arabic), representing a supratidal sedimentary environment in an arid to semi-arid climate. The Middle Cambrian is found only in the central Sino-Korean Plate and is composed mainly of littoral deposits, including oolitic carbonate rocks. By careful correlation, Meng XH et al. (2002) demonstrated that the Middle Cambrian Zhangxian oolitic beach deposits are characterized by cyclic sedimentation, repeated at ~0.40 Ma, perhaps the sedimentary response to the period of the eccentricity of the Earth's orbit around the sun.

Late Cambrian sediments are shallow marine argillites, inter-bedded with limestones and often including carbonate conglomerates deposited as storm beach deposits under warm climatic conditions (Yin HF et al., 1988).

During the Early Ordovician, a broad marine carbonate sedimentary basin covered the Sino-Korean Plate, with gypsum deposits formed in shallower water on the south-central part of the plate. As there are no deposits of Middle Ordovician to Early Carboniferous age on the Sino-Korean Plate, the plate was evidently uplifted towards the end of the Early Ordovician, and was subject to erosion during this time interval.

Beneath the Middle Carboniferous disconformity, in the central part of Sino-Korean Plate, An TX and Ma WP (1984, 1993) recognized a facies boundary in the Early Ordovician, extending from Hohhot City (111.8°E, 41°N) to Qikou in Tianjin City (117.7°E, 38.5°N) and to Jinxian County, Liaoning Province (121.8°E, 39.1°N). North of this boundary the Early Ordovician Majiagou carbonate formation occurs immediately below the Carboniferous, while to the south the Majiagou Formation is overlain by the clastic Middle Ordovician Fengfeng Formation. The facies boundary has been displaced along the Late Triassic Tancheng–Lujiang Fault; to the west the boundary occurs to the south of Tianjin City, while to the east it occurs in Jinxian County, Liaoning Province, indicating a sinistral strike-slip displacement of ~160 km across the fault (Wan TF and Zhu H, 1996; Wan TF et al., 1996).

* "Block" is a neutral term used for a relatively stable tectonic unit, regardless of size, including its area and depth. "Plate" is used for large, stable tectonic units, such as a lithospheric plate, underlain by the asthenosphere, with a lower boundary marked by a high-conductivity and low seismic velocity layer, indicating partial fusion or rich ness in fluid. "Micro-plate" means a small lithospheric plate. The authors suggest that small plates without a clearly defined base marked by a high conductivity or low seismic velocity layer should be termed a "block", rather than a "terrane". The term "Terrane" is not clearly defined and is not necessary. Wan Tianfeng and his colleagues have discussed the terminology of "terrane", in 1988, with Howell DG (USGS), the originator of the term. Howell considered that a "terrane" is a separate tectonic unit which has been displaced over a long distance. It is neither a micro-plate nor a thrust sheet, and does not show a clearly defined basal detachment surface. Since the basal detachment surface of a micro-plate is a layer with high-conductivity and low-velocity, and of a thrust sheet is a low angle reverse fault, a terrane can be described as either a microplate or a thrust sheet. The term "terrane" is therefore superfluous and has recently been used less frequently in the international literature.

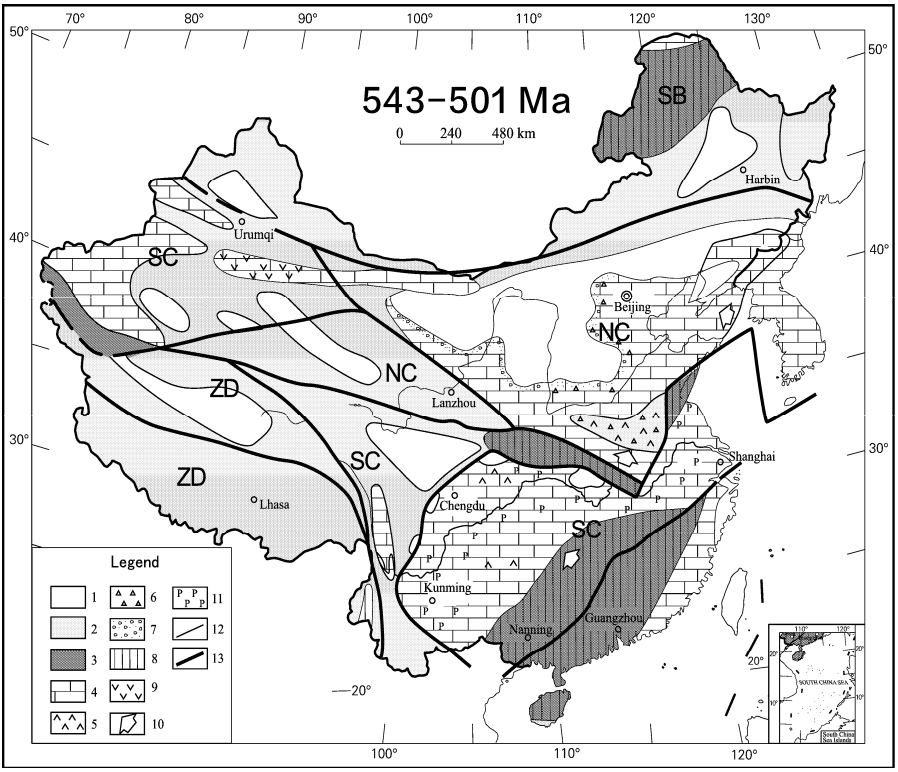

Fig. 4.2 Palaeogeographic sketch map of the Early and Middle Cambrian (543–501 Ma) in the Chinese continent (Data compiled from Wang HZ et al., 1985; Yang JL, 1988; Liu BJ et al., 1994; Meng XH et al., 2003).

Legend: 1. Area of erosion; 2. Littoral and shallow marine, and continental shelf deposits; 3. Shallow marine and continental slope deposits; 4. Carbonate; 5. Gypsum, tidal flat deposits; 6. Karstic breccia; 7. Conglomerate and sandstone; 8. Sandy mudstone; 9. Volcanic rocks; 10. Direction of marine transgression; 11. Phosphatic deposits; 12. Boundary of sediments or geological units; 13. Plate boundary, perhaps with residual oceanic crust.

NC. North China Biogeographical Province; SC. South China Biogeographical Province; SB. Peri-Siberian Biogeographical Province; ZD. Yunnan-Xizang Biogeographical Province.

On the margins of the Sino-Korean Plate Ordovician deposits are sands and argillaceous deposits laid down in a shallow marine environment, passing into bathyal flysch on the northern margin of the plate (Fig. 4.3). During the Silurian, most of Sino-Korean Plate was uplifted to form part of the continent and was subject to erosion, but again residual bathyal deposits occur along the northern margin of the plate. During the Ordovician-Silurian aulacogens were developed locally at Imjingang (127°E, 38.1°N) and Ogcheon (127.5°E, 36.5°N) in the Korean Peninsula (Fig. 4.4), and similar aulacogens of Early Paleozoic age are found in North China at Taizihe, Liaoning (centered on 123.5°E, 41.8°N), north Qilian (centered on 108.5°E, 34°N) and Baoji, west Shaanxi–Ningxia Hui Autonomous Region (106–107°E, 34.3–37°N).

The Early Palaeozoic history of the relatively stable Sino-Korean Plate may be summarized by the deposition of shallow marine sediments on the plate which underwent both uplift and subsidence, and was subject to a series of marine transgressions and regressions, with the local development of aulacogens.

Standard sections for the Cambrian formations of China were defined in the South China blocks. The similar Early Cambrian sediments are developed on the Yangtze Plate in the eastern Yunnan, Sichuan and Hubei provinces, in the Lower Yangtze region, and on the Cathaysian Plate. The sedimentary-tectonic environment of the Yangtze Plate during the Early Cambrian was inherited from the situation in the Sinian. In most areas of Yangtze Plate shallow marine sediments were deposited, with phosphatic, argillaceous carbonates at the base, (Fig. 4.2), while bathyal flysch was deposited in middle Jiangxi and Hunan regions of the South Yangtze. In many regions (for example, in south Hanzhong (107°E, 33°N), from East Sichuan to West Hunan provinces, after the earliest transgression, there was a rise in sea level, but in Guangxi Province palaeontological and sedimentary evidence indicates shallowing (Yang JL, 1988).

Perhaps shallowing was caused by uplift of the Yangtze Plate during the latest period of the Early Cambrian, which shows that the Early Cambrian should be considered as part of the Sinian Tectonic Period. According to the evidence of small *Archaeocyatha* reefs in west Hubei, North Guizhou, North Sichuan and South Shaanxi provinces in the Early Cambrian, the depth of the seawater was 20–30m (Liu BJ et al., 1994). During the Middle Cambrian, shallow marine sandy mudstones and carbonates with abundant fossils were deposited on the Yangtze Plate. Late Cambrian dolostones and gypsum deposits indicate that the Yangtze Plate had a hot dry climate at that time (Yang JL, 1988).

During the Ordovician, the sedimentary environment became relatively tectonically stable but with gradually deepening water (Fig. 4.3); from ecological evidence seawater depths are estimated to be 100–150 m. However, by the Silurian, after the Fentou Formation (~428 Ma, Liu BJ et al., 1994), a marine regression occurred (Fig. 4.4), with seawater depths of less than 50 m. During the Middle Cambrian and Silurian the Yangtze Plate suffered both marine transgression and regression.

According to the distribution, diversity and the ecological characteristics of the fossils, there were almost no differences between the paleo-biology of the Sino-Korean and Yangtze plates during the Early Cambrian, however, after the Middle Cambrian obvious differences arose.

The biogeographical area of the Sino-Korean Plate is generally called the North China Biogeographical Province, characterized in the Cambrian by a few trilobites and some small shells, without *Archaeocyatha* and *Bradoria*, and in the Ordovician by *Actinocerida* and a few trilobites (Yang JL, 1988; Li ZM, 1988).

In the Early Palaeozoic the Yangtze Plate belonged to the South China Biogeographical Province, characterized in the Cambrian by abundant trilobites, small shells and *Bradoria*, in the Ordovician by *Endocerida-Orthocerida*, the most abundant trilobites, *Graptolithina*, *Brachiopoda* and *Agetolites*, and in Silurian by typical fossils, such as *Brachiopoda* (*Nalivkinia, Xinanospirifer*), *Spiriferida, Atrypa,* and corals, *Tetracoralla*, *Heliolites,* and *Nautilida* (Lu YH, 1976; Mu EZ, 1983; Yang JL, 1988; He XY, 1988). Palaeontologists considered that the West Sichuan Province i.e. Garze-Litang-Aba area (in the west of the Yangtze Plate and eastwards to the Lancangjiang River) belonged to the South China Biogeographic Province, however there are few outcrops of Lower Paleozoic systems, and the area has a complex structure which has not yet been properly investigated. The West Cathaysian Plate, i.e. Middle Zhejiang, South Jiangxi, most of Guangdong, southeast Guangxi and Hainan provinces, also belonged to the South China Biogeographical Province, where from the Cambrian to the Ordovician, the deposits were mainly shallow marine sediments. The area was then subject to regression and uplifted to form a land area, except for the Qinzhou–Fangcheng region (centered on 108.5°E, 22°N) in Guangxi, where there was a residual bathyal marine environment, with continuous sedimentation from the Silurian to the Devonian.

The Early Paleozoic evolution of northwest China is very distinctive. The Alxa Block had very similar sedimentary and palaeontological characteristics to the Sino-Korean Plate in the Early and Middle

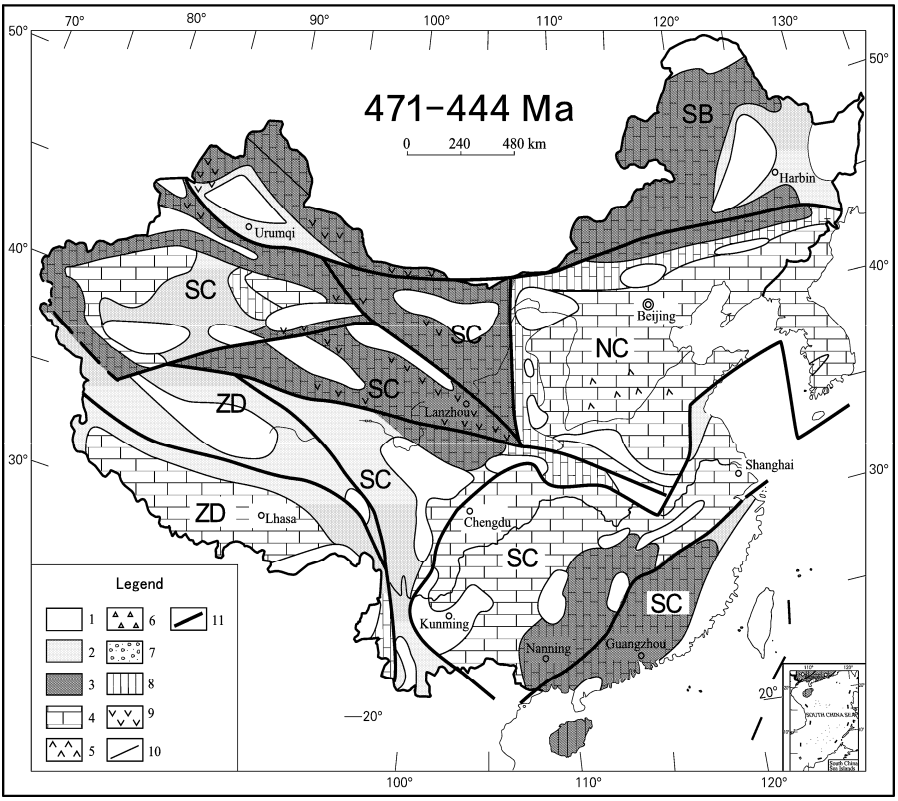

Fig. 4.3 Sketch map of tectonic units and biostratigraphic provinces in the Chinese continent during the Middle and Late Ordovician (471–444 Ma) (compiled from Lu YH, 1976; Mu EZ, 1983; Wang HZ et al., 1985; Liu BJ et al., 1994; Meng XH et al., 2003).

Legend: 1. Area of erosion; 2. Littoral to shallow marine and continental shelf deposits; 3. Shallow marine and continental slope deposits; 4. Carbonates; 5. Gypsum, tidal flat deposits; 6. Karstic breccia; 7. Conglomerate and sandstone; 8. Sandy mudstone; 9. Volcanic rocks; 10. Boundary of sedimentary units; 11. Plate boundary, perhaps with residual ocean crust.

NC. North China Biogeographical Province; SC. South China Biogeographical Province; SB. Peri-Siberian Biogeographical Province; ZD. Yunnan–Xizang Biogeographical Province.

Cambrian*. However, from the Late Cambrian to Silurian, the Alxa biological assemblages are similar

* There are many opinions concerning the location of Alxa Block, at the time of the formation of the Xiyu Plate in the Cambrian. Wang HZ (1985) and Yang JL (1988) believe that Alxa Block was part of Sino-Korean Plate. Due to the presence of the Sinian glacial series, the Lower Cambrian phosphatic layer and a fauna similar to that of the Yangtze Plate, Duan JY et al. (1992) think that the Alxa Block was part of the Xiyu Plate from the Sinian to the Cambrian. However, in recent years the Sinian Luoquan glacial series and the Lower Cambrian phosphatic layer have also been discovered on the southern margin of the Sino-Korean Plate (in Henan, Shaanxi and Gansu provinces), which were not found on the Yangtze Plate. The author has discussed the significance of the Cambrian fossils discovered by Duan JY (1992), with Professor Peng SC of the Nanjing Geology and Palaeontology Institute of China Science Academy in 2003. Prof. Peng (personal Communication, 2003) considers that the Lower and Middle Cambrian fossils (*Xystridura, Galahetes, Erbia, Pagetia*) on the northern margin of Alxa Block belong typically to the Peri-Siberian Biogeographical Province, the Middle Cambrian fossils (*Crepicephalina, Ampoton, Kootenia*) in the centre of the Alax Block belong to the North China Biogeographical Province, and only a few dozen Upper Cambrian fossils belong to the South China Biogeographical Province. Professor Peng's opinion has been adopted in this account.

to those of South China, with the bathyal marine flysch deposits and basic volcanics related to rifting around the margins of the block (Lu YH, 1976; Mu EZ, 1983). These features suggest that Alxa Block belonged to Sino-Korean plate before Late Cambrian, separated from the Sino-Korean Plate during Late Cambrian, whose paleomagnetic and palaeontological evidence indicates that it was located in the same paleolatitude as the Yangtze Plate.

There is not sufficient geological evidence to establish whether the Qaidam Block, like Alxa Block, was part of the Sino-Korean Plate during the Cambrian (Yang JL, 1988). However, during the Ordovician and Silurian, the Qaidam Block, with its extensive bathyal marine deposits, formed part of the South China Biogeographical Province (He XY, 1988). Since the Cambrian the Tarim Block, unlike the Alxa and Qaidam blocks, was covered by shallow marine deposits, with a marginal faulted depression, which developed more rapidly in the Ordovician. In the Early Paleozoic, from the time of the Sinian Tectonic Period, the Tarim Block formed part of the South China Biogeographical Province, but the faunas are not completely identical (Lu YH, 1976; Mu EZ, 1983; Gao ZJ et al., 1983; Yang JL, 1988; He XY, 1988). It is probable that the Tarim Block was located in the same paleolatitude as the Yangtze Plate, but was not in contact with it. Sedimentary and palaeogeographic data show clearly that during the Early Paleozoic the three blocks in northwest China had a similar history to the Yangtze Plate, and had become part of the South China Biogeographical Province (Figs. 4.2, 4.3 and 4.4), and in the Ordovician and Silurian were located in the same paleolatitude as the Yangtze Plate.

Throughout Early Paleozoic the Qiangtang, Gangdise, Himalayan and West Yunnan Blocks (Lincang and Baoshan region, i.e. the North Sibumasu Plate, centered on 99°E, 24.5°N), were covered by relatively stable shallow marine carbonate deposits in which Cambrian fossils are rare. The Ordovician cephalopod fauna is similar to that of the Sino-Korean or Yangtze plate except for the presence of *Georgina*. However, the Silurian planktonic fauna, characterized by cephalopods and conodonts, is similar to that of western Europe. This paleontological assemblage is intermediate between that of the North and South China Biogeographical provinces, but can be recognized clearly, so that it has been distinguished by Chinese geologists as the Yunnan-Xizang Biogeographical Province (Li ZM, 1988; He XY, 1988).

A marine transgression occurred in Northeast China and the Junggar-Altay region of northwest China from the Middle Cambrian to Silurian. With the marine area increasing and the continental area decreasing, bathyal marine flysch was deposited in the Junggar, Ergun, Songhuajiang–Nenjiang (around the Harbin block), Jiamusi-Bureinskiy and Xingkai regions, where there were more and more intense volcanic activities during the Ordovician and Silurian. These two regions belonged mainly to the Peri-Siberian Biogeographical Province. The Ordovician palaeontological assemblage is characterized by the tabulate and tetracorals *Amsassia* and *Favistella*, and some distinctive trilobites. The Silurian assemblage is characterized by *Tuvaella* (He GQ and Li MS, 2001). These palaeontologic characteristics are completely different from those of the other regions of the Chinese continent. The Jiamusi–Bureinskiy Block (Figs. 3.9, 4.15) had a similar geological history to the Gondwanan crystalline basement during the Sinian and Early Cambrian, and from the Middle Cambrian to the Silurian the biota was similar to that of the Siberian Biogeographical Province. So it seems that had a great migration for Jiamusi-Bureinskiy Block in Cambrian.

In the Early Paleozoic Tectonic Period, sedimentary and paleontological data (Figs. 4.2, 4.3 and 4.4) show that different marine transgressions, regressions, and vertical movements affected all the blocks in Chinese continent. In addition, horizontal migrations occurred, with the drift of the Qaidam and Alxa blocks from the North China into the South China Biogeographical Province (i.e. from the neighborhood of the Sino-Korean Plate towards the Yangtze Plate). During Ordovician and Silurian, the Yangtze, Cathaysian, West Sichuan, Qaidam, Alxa, and Tarim blocks belonged to South China Biogeographical Province. They were all located close to the same paleolatitude. However, the continental blocks belonging to Peri-Siberian, North China and Yunnan–Xizang Biogeographical Provinces had a different tectonic evolution, so that they should be placed separately in paleogeographical reconstructions, with some distance between them.

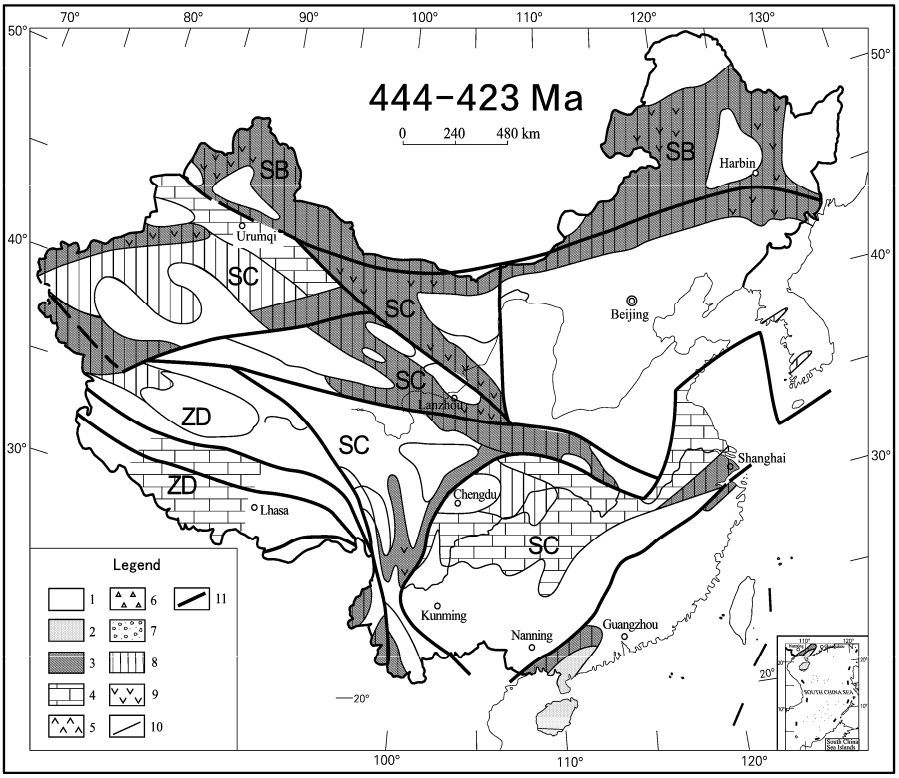

Fig. 4.4 Sketch map of the distribution of Early and Middle Silurian series (444–423 Ma) in the Chinese continent (compiled from Wang HZ et al., 1985; He XY, 1988; Liu BJ et al., 1994; Meng XH et al., 2003).

Legend: 1. Area of erosion; 2. Littoral to shallow marine continental shelf deposits; 3. Bathyal marine and, continental slope deposits; 4. Carbonates; 5. Gypsum, tidal flat deposits; 6. Karstic breccia; 7. Conglomerate and sandstone; 8. Sandy mudstone; 9. Volcanic rocks; 10. Boundary of sedimentary units; 11. Plate boundary, perhaps with residual ocean crust.

NC. North China Biogeographical Province; SC. South China Biogeographical Province; SB. Peri-Siberian Biogeographical Province; ZD. Yunnan-Xizang Biogeographical Province.

4.2 Palaeomagnetism and Palaeotectonic Reconstruction

Palaeomagnetism from the Chinese continent has been compiled according to the methods and treatment of paleomagnetic data, as described in Chapter 1, using the data which had been collected carefully and tested precisely in terms of international standards (Appendix 6). Since 1998, paleomagnetic data from different laboratories all over the world has become more and more agreeable to the correct methods for the collection of data and for the preparation of palaeotectonic reconstructions.

Using the palaeomagnetic data collected and analyzed properly (Appendix 6), the palaeomagnetic characteristics and the palaeotectonic reconstruction of three major continental blocks, Siberia, India and Australia, surrounding the Chinese continent during the Early Paleozoic are first discussed (Fig. 4.5).

From Early Cambrian to Silurian the Siberian (Angaran) Plate rotated 12° clockwise with respect to a central reference point and the paleolatitude changed from latitude 31.4° south to latitude 18.4° north

(Khramov et al., 1981). Over this period the position of the plate changed through latitude 49.8° (about 5,000 km of displacement), the average movement velocity was 4.53 cm/yr, perhaps more, if changes in the longitude were considered. The latitude of Indian Plate changed only slightly from latitude 25.3° to 28.7° south during the Early Paleozoic, but first rotated 25° clockwise during the Cambrian, and then rotated 78° counterclockwise during the Ordovician and Silurian (Klootwijk and Radhakriehnamurty, 1981). The Australian Plate rotated 60.8° counterclockwise during the Early Paleozoic, but remained latitude 11°–13° south (Van der Voo, 1993). Although the Australian and Indian plates all belong to Gondwana domain, they have different characteristics of movement.

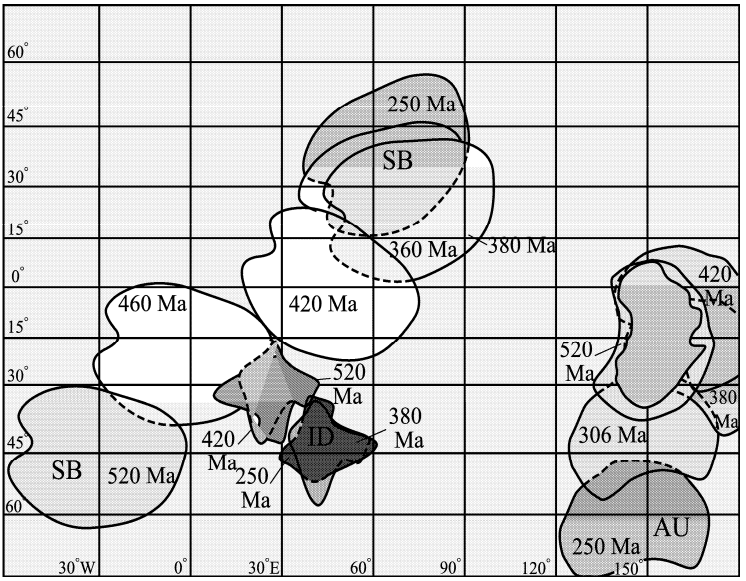

Fig. 4.5 Palaeotectonic reconstruction and displacement of the Siberian (SB), Indian (ID), and Australian (AU) plates during the Paleozoic, data is showed in Appendix 6.

Therefore, during the Early Paleozoic the horizontal displacement of the Indian and Australian plates was very small, but the displacement of the Siberian Plate was much greater. Many Chinese geologists thought incorrectly that because of its huge area the Siberian Plate would have been very stable, in fact, according to palaeomagnetic and geological data the plate migrated over a great distance and suffered a substantial amount of tectono-thermal activity during the Early Paleozoic.

During the last thirty years, the Chinese and international researchers have made many determinations of the palaeomagnetism of the Sino-Korean, Yangtze and Tarim blocks, which make up the Chinese continent, and have reconstructed their paleogeographical relationships. There are two opinions about the locations of Sino-Korean and Yangtze plates in the Early Paleozoic: in one model both plates lay in the southern hemisphere, with the Sino-Korean Plate to the south of the Yangtze Plate (Lin JL et al., 1985); in the other model the Sino-Korean Plate has always lain in the northern hemisphere, and always to the north of the Yangtze Plate (Wang HZ et al., 1990; Yang WR et al., 1993; Scotese, 1994; Yin A and Nie SY, 1996).

The dispute is whether during Cambrian and Ordovician the Sino-Korean Plate was located in the northern or southern hemisphere. According to data from recent palaeomagnetic studies of the Paleozoic in North China (Yang ZY et al., 1998; Yang ZY et al., 1998; Huang BC et al., 1999), the Early and

Middle Ordovician magnetization direction (north pole) recorded from rocks of the Sino-Korean craton, when converted to a normal polarization direction, is oriented NNW and downward dipping (λ=32. 9°N, Φ=314.2°E, A_{95}=9.6°), similar to that of Laurasia at that time. These results show that the Sino-Korean Plate was located at a low latitude in the southern hemisphere during the Early and Middle Ordovician. However, Cambrian palaeomagnetic results for the Sino-Korean Plate from different authors differ from each other (Zhao J et al., 1992; Huang BC et al., 1999; Lin JL et al., 1985; Yang ZY et al., 1998; Yang ZY et al., 1998). The results of Huang BC et al. (1999) are preferred because of their high precision, and because they are relatively close to the average value, and also close to the Ordovician data. Therefore it is most probable that during the Cambrian the Sino-Korean Plate was also located in the southern hemisphere at a low latitude. The conclusion of some researchers that the Sino-Korean Plate has always been located in the northern hemisphere was perhaps based on the random selection of south/north magnetic poles or re-magnetization of the analyzed samples.

Palaeomagnetic data in the Early Paleozoic from the blocks forming the Chinese continent is listed in Appendix 6, and palaeotectonic reconstructions are shown in Figs. 4.6–4.12. Considering the many more believable paleomagnetic data for Chinese blocks and the world reconstruction maps, proposed by Scotese, had some mistakes especially in the parts data of Chinese blocks, Wan TF and Zhu H (2007) combined the believable Chinese paleomagnetic data with the others according to Scotese's data, and redrew the Paleocontinental reconstruction map of the globe in Paleozoic (showed in Figs. 4.8, 4.10, 4.12, 5.5, 5.7 and 5.9).

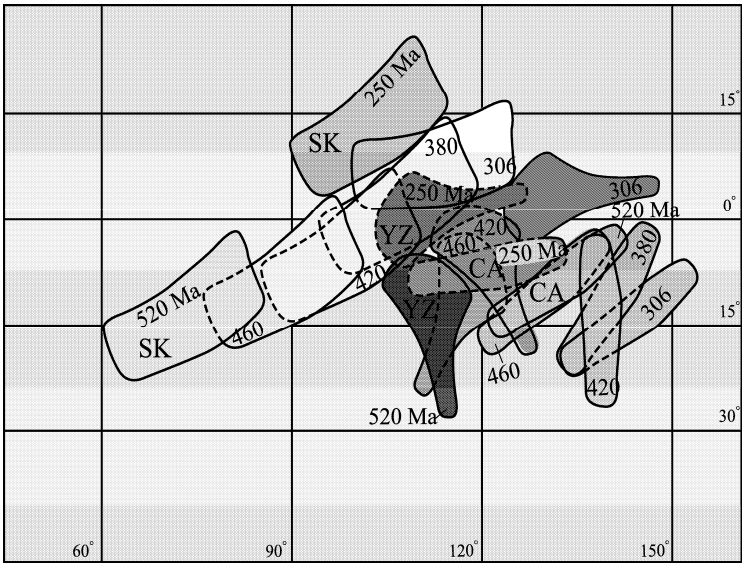

Fig. 4.6 Palaeotectonic reconstruction and displacement of the Sino-Korean (SK), Yangtze (YZ) and Cathaysian (CA) plates during the Paleozoic, data is showed in Appendix 6.

The Sino-Korean Plate rotated 13.8° clockwise in the Early Paleozoic and migrated from latitude 20.2° to 12.9° south with a rate of movement of only 0.8 cm/yr. From the Cambrian to the Early Silurian the Yangtze Plate rotated 24.4° clockwise, and during the Middle and Late Silurian 70° counterclockwise, and migrated from latitude 11.7° south to latitude 2.8° north, with a rate of northward movement of 0.7 cm/yr. Some credible palaeo-magnetic data from the Cambrian and Devonian showed that the Cathaysian Plate rotated during the Early Paleozoic, however with only a slight change in paleo-

latitude. Palaeomagnetic data shows that in the Early Paleozoic the Tarim and Alxa blocks were both located at a low latitude in the southern hemisphere, but moved towards the north and underwent considerable rotation. However these data are not very precise. During the Early Paleozoic, India, Australia and other small blocks in Chinese continent rotated, and only changed their paleolatitude slightly.

In the Early Paleozoic the Sino-Korean and Yangtze plates migrated towards the north and simultaneously rotated, and were perhaps influenced by the large-scale movement of Siberian Plate. Rotations given for these larger blocks are plausible, because many different studies have produced similar results. However, the details of the location and movement of the smaller blocks are uncertain because there is no sufficient data.

Conclusions derived from palaeomagnetism concerning palaeotectonic reconstructions and the migration of the crustal blocks, which now form the Chinese continent and its the adjacent areas, are in accordance with the palaeogeographic and palaeontological evidence. In the Early Paleozoic most of these blocks were distributed to the south of the equator in a tropical to subtropical environment, and underwent slight northward migration. The palaeotectonic reconstruction of the Siberian, Mongolian, and Ochotsk blocks made by Gordienko (1994) is valuable. His conclusions concerning the location and movements of the Siberian Plate are acceptable, but his conclusion that the Sino-Korean and Yangtze plates were located in middle latitudes of the northern hemisphere during the Early Paleozoic must be reconsidered in the light of more recent data.

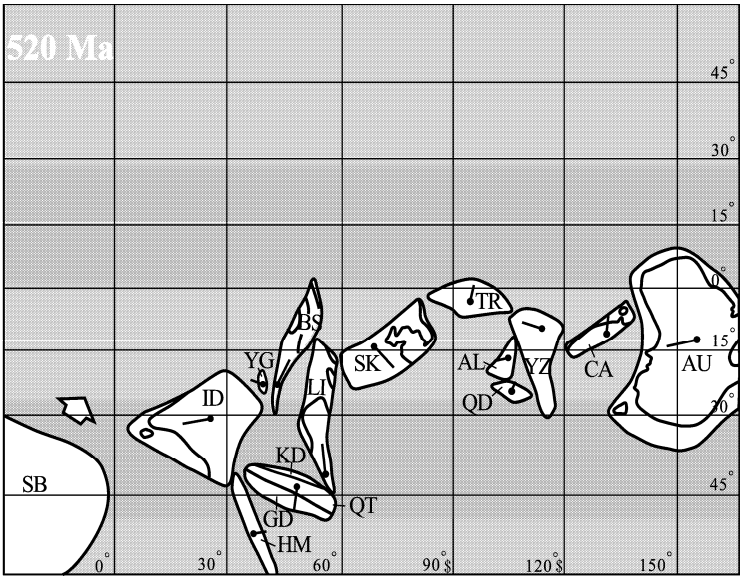

Fig. 4.7 Palaeotectonic reconstruction of the distribution of the Chinese blocks and their adjacent continental plates in the Cambrian (520 Ma). Black dots show the reference point for the blocks, and black lines indicate the direction of palaeomagnetic north, data is showed in Appendix 6.

Blocks: AL. Alxa; AU. Australian; BS. Baoshan-Sibumasu; CA. Cathaysian; GD. Gangdise; HM. Himalayan; ID. Indian; JG. Junggar; JP. Japan; KD. East Kunlun; KZ. Kazakhstan; LI. Lingcang-Indochina; ND. Wandashan; QD. Qaidam; QT. Qiangtang; SB.Siberian; SK. Sino-Korean; TR. Tarim; YG. Yagan; YZ. Yangtze; XM. Hingganling; XY. Xiyu (The same symbols have the same meaning in the other illustrations in Chapters 4 and 5, and Appendix 6).

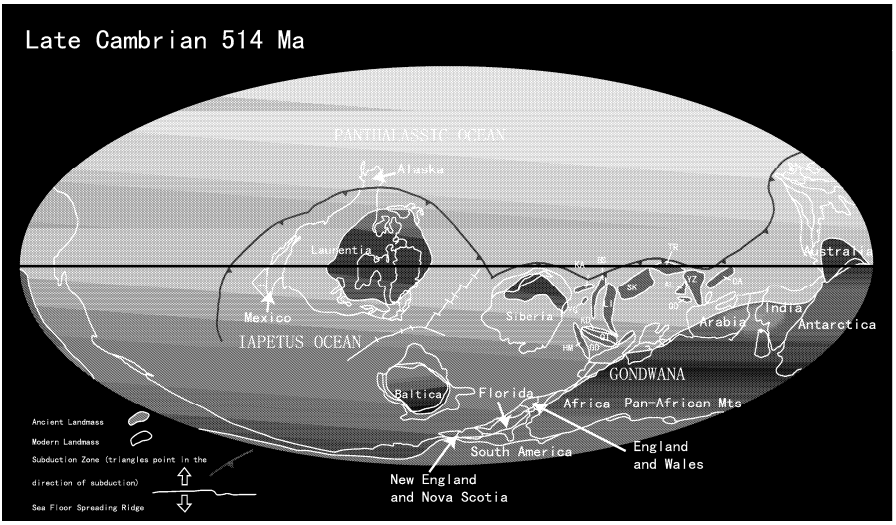

Fig. 4.8 Paleocontinental reconstruction of the globe during the Late Cambrian (514 Ma) (Wan TF and Zhu H, 2007; Data of Chinese blocks and their adjacent areas from Appendix 6, others from Scotese's web).

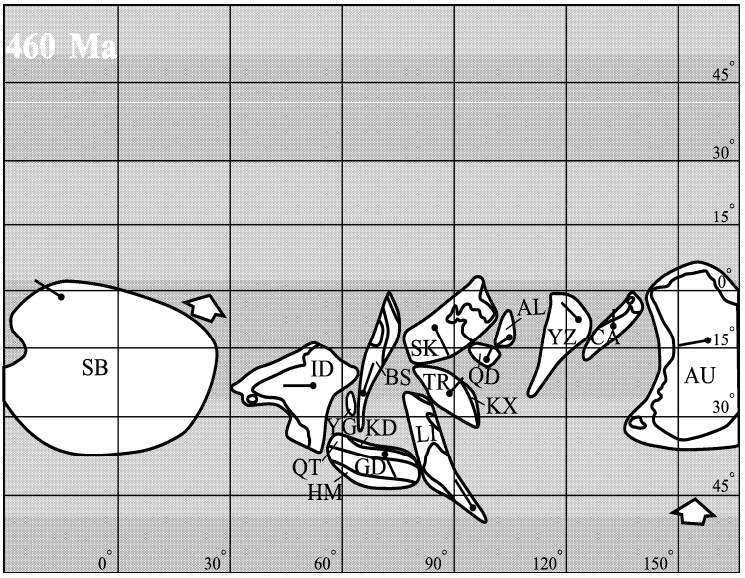

Fig. 4.9 Palaeotectonic reconstruction of the distribution of Chinese and adjacent blocks in the Ordovician (460 Ma), data is showed in Appendix 6.

In compiling Figs. 4.7–4.12, due to the inadequacy of the palaeomagnetic data, the locations of smaller blocks had been estimated by interpolation or extrapolation. Relative paleo-latitudes and paleo-longitudes were estimated by using similarities in the paleontology and paleotectonics of different

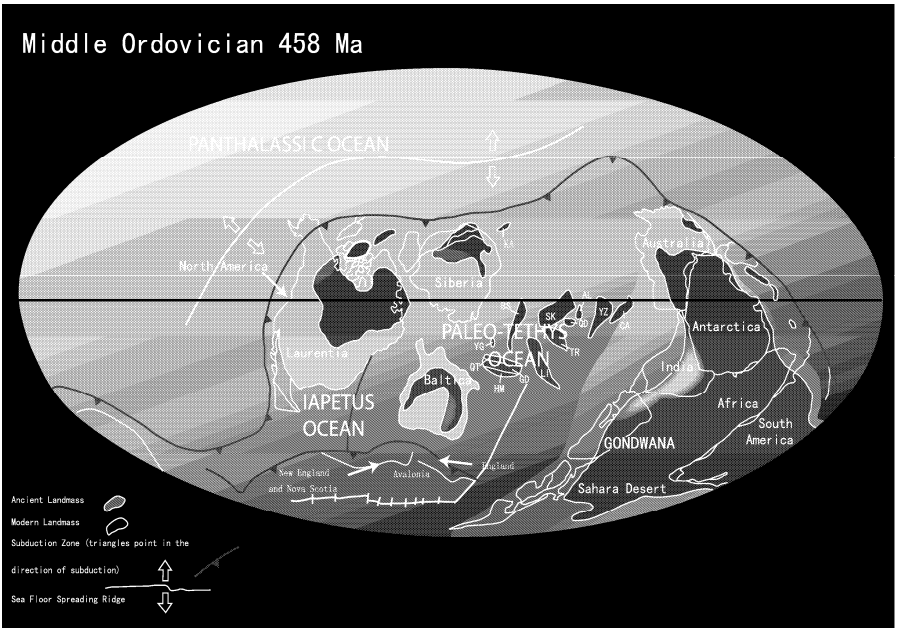

Fig. 4.10 Paleocontinental reconstruction of the globe during the Middle Ordovician (458 Ma) (Wan TF and Zhu H, 2007; Data of Chinese blocks and their adjacent areas from Appendix 6, others from Scotese's web).

blocks. Some constraint on the distribution and migration of the smaller blocks is provided by the more reliable data obtained from the six larger plates, but these palaeotectonic reconstructions are still extremely sketchy.

4.3 Rock Deformation, Metamorphism and Stress Field

The tectonic event which occurred at the end of the Early Paleozoic is marked by an angular unconformity at the contact between the Lower and Upper Paleozoic systems (Fig. 4.13). The age of this unconformity can be used to define five tectonic regions (yellow in Fig. 4.13):

(1) In the Tarim, Qaidam and Dunhuang–Alxa blocks, there are commonly clear angular unconformities between the Middle and Upper Silurian and the Lower and Middle Devonian systems. These three blocks had been amalgamated by the end of the Silurian along the Qilian–Altun Collision Zone to form the Xiyu Plate, accompanied by widespread deformation and low-grade greenschist facies metamorphism of the Lower Paleozoic systems. However, in the central part of the Tarim Block there are only disconformities between the Lower Silurian and the Lower Devonian systems, so this event did not affect the central part of this block.

(2) In the Tianshan–South Hingganling Tectonic Belt, which includes a series of small blocks in the marginal fault belts of the Junggar Block, the Yiliekede-Jagdaqi Fault Belt (from 122°E, 49°N to 123.8°E, 50.5°N) (1 in Fig. 4.13), the Ertix-Derbugan Fault Belt (from 85.5°E, 48°N to 91°E, 45.5°N) (3 in Fig. 4.13), the Karameili-Erenhot Fault Belt (from 91°E, 45°N to 112°E, 43.8°N) (2 in Fig. 4.13) and the Nilak-Xar Moron He Thrust Fault Belt (from 113°E, 42.5°N to 119°E, 43°N) (5 in Fig. 4.13), there are clear angular unconformities between the Silurian and Lower or Middle Devonian sediments.

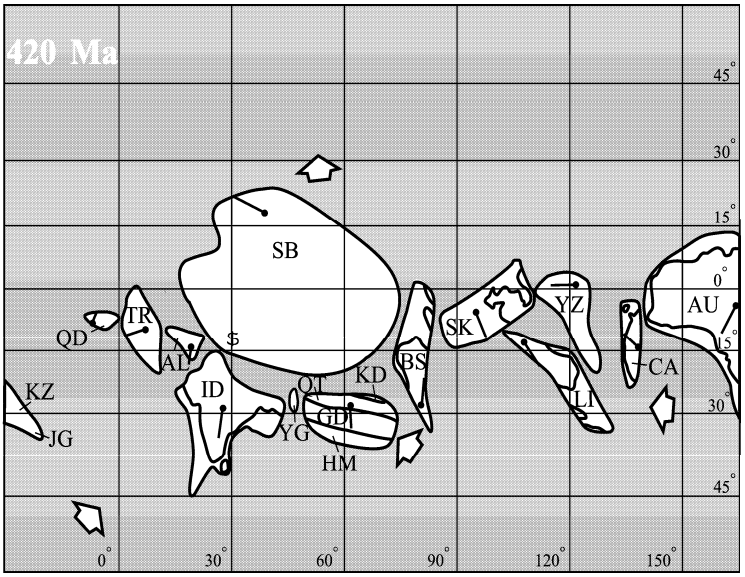

Fig. 4.11 Palaeotectonic reconstruction of the distribution of Chinese and adjacent blocks in the Silurian (420 Ma), data is showed in Appendix 6.

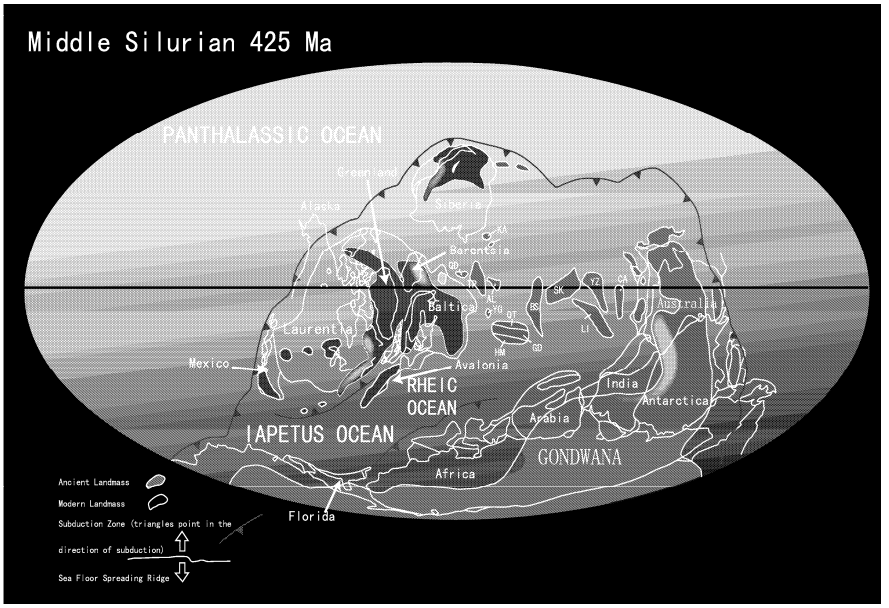

Fig. 4.12 Paleocontinental reconstruction of the globe during the Middle Silurian (425 Ma) (Wan TF and Zhu H, 2007; Data of Chinese blocks and their adjacent areas from Appendix 6, others from Scotese's web).

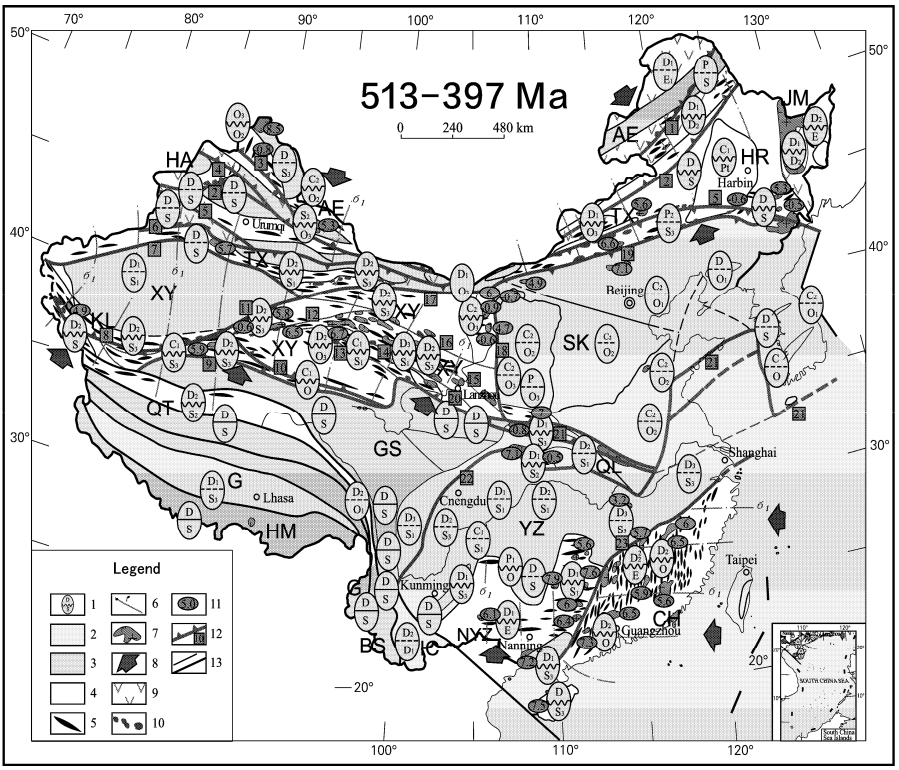

Fig. 4.13 Sketch map showing tectonic events of the Qilian Period (513–397 Ma) in China.

1. Strata relationship in international stratum code; angular unconformity with a wavy line; disconformity with broken line; conformity with continuous line; 2. Area with disconformity; 3. Area with conformable strata; 4. Area with angular unconformity; 5. Anticlinal fold axis (data in Appendix 3.2); 6. Trace of maximum principal stress axis (σ_1); 7. Granite intrusions during the Qilian Period (513–397 Ma); 8. Direction of block movement; 9. Volcanic rocks extruded during the Qilian Period (513–397 Ma); 10. Ophiolites and ultramafic rocks formed during the Qilian Period (513–397 Ma); 11. Rate of intraplate deformation estimated from litho-chemical data, "-" implies spreading rate, others imply shortening rate, cm/a (data in Appendix 5.3); 12. Plate boundary, collision and fault belts and their serial numbers; 13. Activity not clearly related to block boundary or faults.

Serial numbers of plate boundaries, collision or fault belts: [1] Yiliekede–Jagdaqi Fault Belt; [2] Karameili–Erenhot Fault Belt; [3] Ertix–Derbugan Fault Belt; [4] Narmand Collision Belt; [5] Nilak–Xar Moron He Thrust Fault Belt; [6] Hariktao Thrust Fault Belt; [7] Wuqia–Korla block boundary; [8] Kangxiwa Collision Belt; [9] Northern boundary of East Kunlun Block [10] Qimantag–Golmud Collision Belt (southern boundary of Qaidam Block); [11] Ruoqiang–Dunhuang Collision Belt; [12] Altun Collision Belt; [13] Junulshan–southern boundary of Qinghai Lake Collision Belt; [14] Southern boundary collision belt of the Middle Qilian Mountains; [15] Northern boundary collision belt of the North Qilian Mountains; [16] Longshoushan Collision Belt; [17] Northern boundary of the Alxa Block; [18] Western boundary of the Sino-Korean Plate; [19] Northern boundary of the Sino-Korean Plate; [20] Boundary collision belt of Wushan–Baoji Block; [21] Shangdan–Tongbo–Zhucheng–Cheju Island Collision Belt; [22] Northern boundary of Yangtze Plate Collision Belt; [23] Shiwandashan–Shaoxing plate boundary (between Yangtze and Cathaysian plates).

Meanwhile, in the Altay region(centred on 88°E, 48°N) of northwest China, and the Ergun(centered on 120°E, 50°N) region of northeast China, a hiatus in sedimentation occurred earlier, as there is an angular unconformity between the Middle and Upper Ordovician, so that more strata are missing. In other segments of the Tianshan–South Hangganling Tectonic Belt, the strata beneath the unconformity

are generally the Lower and Middle Ordovician, and in the Ergun region even the Lower Cambrian, while the overlying strata are of Devonian, Carboniferous or Permian ages. In the Bainaimiao region and the Ondor Sum–Ongniud Qi Collision Belt (from 113°E, 42.5°N to 119°E, 43°N) in the centre of the Inner Mongolia there is an angular unconformity between the Silurian and Lower and Middle Devonian sediments (Tang KD et al., 1993).

(3) In the Cathaysian Plate (SE China) the Cambro-Ordovician is folded on ~N-S axes accompanied by greenschist facies metamorphism and overlain with angular unconformity by Middle Devonian system. The unified crystalline basement of the Cathaysian Plate was formed during this Qilian Tectonic Event.

(4) In the southern part of the Yangtze Plate, there is a widespread angular unconformity between the Upper and Lower Paleozoic systems. The underlying strata are Cambrian, Ordovician or Silurian systems, and the overlying strata are mainly Lower Devonian sediments with E-W trending fold structures. On the northern margin of the Yangtze Plate and in the western Qinling Mountains there is an angular unconformity between the Middle Silurian and Lower Devonian systems, indicating strong tectonic activity at that time. In the Yunkaidashan region (centered on 111°E, 22.6°N) east to Shiwandashan (centered on 108°E, 21.8°N) in Guangxi, there are angular unconformities between the folded and metamorphosed Neoproterozoic Yunkai Group and the Devonian, or between the Cambrian and Ordovician; this has been termed the "Yu'nan Tectonic Event", which is associated with a series of northward-directed upthrusts with E-W trending (Qiu YX et al., 1993, 1996). This type of deformation is similar to that in the South Yangtze Plate, so at the end of Early Paleozoic, the boundary between Yangtze and Cathaysian plates was located along the Wuchuan–Sihui Fault Belt to the east of the Yunkaidashan region, and at that time the Qinzhou–Fangcheng and Yunkaidashan regions formed parts of the South Yangtze Plate. However, the Qinzhou–Fangcheng region (centered on 108.4°E, 21.8°N) was a marginal rift belt in the South Yangtze Plate, where continuous sedimentation from the Upper Silurian into the Lower Devonian shows that no tectonic events occurred at that time.

(5) In the Guanzhong region, Shaanxi Province (from 107°E, 34.8°N to 110°E, 34.8°N), in the southwestern part of the Sino-Korean Plate there is an angular unconformity between the Upper Ordovician and Permian systems, indicating compression and folding at the end of the Early Paleozoic (Tan YJ, 1992). However, most of Sino-Korean Plate was tectonically stable, and was not affected by deformation at the end of Early Paleozoic.

At the end of Early Paleozoic a disconformity occurs in four regions (light green areas in Fig. 4.13):

(1) Several disconformities occur in the Sino-Korean Plate. To the north of Hohhot-Tianjin City-Jinxian, Liaoning, there is a disconformity between the Lower Ordovician Majiagou Formation and the Middle Carboniferous, and to the south of this boundary there is a disconformity between the Middle or Upper Ordovician and the Middle or Upper Carboniferous. However, in several aulacogens there were shorter sedimentary lacunae. For example in the Taizi River region(centered on 124°E, 41.3°N) in Liaoning Province and the Imjingang(centered on 127°E, 38.2°N) and Ogcheon(centered on 127.5°E, 36.2°N) areas in the Korean Peninsula, the underlying strata are Middle, Upper Ordovician, or Silurian, and the overlying strata are Devonian (Wan TF and Zeng HL, 2002). An erosion residual of Devonian rocks was found in the northern part of the Shandong Peninsula perhaps indicating a disconformity in that area.

(2) In the main part of Yangtze Plate, there are disconformities, with only short breaks in sedimentation. In the central part of the Yangtze Plate, i.e. East Sichuan and North Guizhou Provinces, there is a disconformity between the Lower Silurian and the Devonian or Lower Carboniferous. There was almost continuous sedimentation on the margins of Yangtze Plate, with only a short lacuna, forming a disconformity between the Upper Silurian and Lower or Middle Devonian. Evidently the central part of the Yangtze Plate was uplifted relatively at the end of Silurian and the beginning of Devonian. In South Qinling and the West Longmenshan-Panzhihua region of western Sichuan, as in the Yangtze Plate, there is a disconformity between the Lower Silurian and Middle or Upper Devonian. However, in the southern Lanping-Simao region, there is a disconformity between the Lower and Middle Devonian.

(3) In the Gangdise Block, a disconformity occurs between the Lower Silurian and the Lower Devonian.

(4) In the central Tarim Block, there is a disconformity between the Upper Ordovician and the Lower Silurian, in which up to 800–1,100 m of strata were eroded, however on the northern and southern margins of the Tarim Block only about 200 m of strata were eroded (Zhang YW et al., 2000). On the margins of many small blocks in the Tianshan-Hingganling Tectonic Belt, there are generally disconformities between the Silurian and Devonian.

Regions of continuous sedimentation at the end of Early Paleozoic (dark green in Fig. 4.13) include the Himalayan, Qiangtang, Hohxil–Garze–Litang regions, West Yunnan Province, East Yunnan aulacogen and the Qinzhou–Fangcheng marginal rift areas. These regions did not undergo any significant tectono-thermal activity between the Early and Late Paleozoic.

The data shows that in the Early Paleozoic the blocks forming the Chinese continent had different histories of sedimentation and erosion, Fig. 4.13 demonstrates that even between adjacent blocks the history may be completely different. Evidently Early Paleozoic tectonic events were limited in their extents, the main blocks were not connected, but were separated from each other at some distance, so that tectonic activity in one block did not affect other blocks. The most important tectonic event in the Early Paleozoic was the formation of the Xiyu Plate with the most intense episode of deformation occurring in the Qilianshan region. So it is appropriate to name the Early Paleozoic tectonic event the "Qilian Event".

The Xiyu Plate is made up of the Tarim, Qaidam, Alxa-Dunhuang, Middle Qilian, Hualong (in northeast Qinghai Province, centered on 102.1°E, 36.2°N) and West Kunlun blocks (Figs. 4.13 and 4.15). As already mentioned, these blocks were amalgamated into a unified crystalline basement at the end of the Paleoproterozoic (~1,800 Ma) and formed the western part of the Sino-Korean Protoplate (Fig. 2.2). They began to break up in the Mesoproterozoic (Fig. 3.3), but went together in the Qingbaikou Period (1,000–800 Ma) to form the western part of the Sino-Korean Paleoplate (Fig. 3.7). A rift system was formed in the Qilian region during the Nanhua–Sinian Period (800–513 Ma), with the development of oceanic crust, separating the Tarim–Qaidam Block from the Alxa-North China Block which formed the main part of the Sino-Korean Plate. The occurrence of two tillites in the Neoproterozoic succession on the Tarim-Qaidam Block showed that it had a similar history to the Yangtze Plate (Figs. 3.8 and 3.9). During the Cambrian the Tarim Block was still associated with the and Yangtze Plate, and its paleobiological assemblages belong to the South China Biogeographical Province. However the Qaidam and Alxa-North China blocks belong to the North China Biogeographical Province (Fig. 4.2). During Ordovician the Tarim, Qaidam and Alxa blocks suffered extension and subsidence, with the deposition of bathyal marine deposits (Wang HZ et al., 1985). From the Late Cambrian to the Silurian the paleobiological assemblages in these blocks belong to the South China Biogeographical Province (Yin HF et al., 1988). In the Cambro-Ordovician extensive magmatic activity occurred between the blocks in the Qilian and Altun regions, and ophiolite suites, remnants of Ordovician oceanic crust have been reported (Feng YM et al., 1995; Xia LX et al., 1995; Xu ZQ et al., 1994, 1999; Zhang JX et al., 1997, 1999; Guo ZJ et al., 1999; Liu L et al., 1998; Zhang Q et al., 1998) (Figs. 4.3 and 4.13). Marine regression began during the Silurian, and the collisions between the continents formed the Qilian-Altun Collision Belt during the Late Silurian (Xu ZQ et al., 1999) (Figs. 4.4 and 4.13). Consequently, the Tarim, Qaidam, Alxa and other surrounding small blocks were amalgamated to form the Xiyu Plate. The times of collision and amalgamation are indicated by the isotopic ages of granulite, eclogite and amphibolite in the metamorphic rocks of the Qilian-Altun Belt (Appendix 7): 460–400 Ma in the North Qilian Belt (Cheng YQ et al., 1994; Zhang JX et al., 1998); 465 Ma along the northern margin of Qaidam (Lai SC et al., 1996; Yang JS et al., 1998), 503–462 Ma for the western Altun Belt (Zhang JX et al., 1999, 2002), forming the independent Xiyu Plate.

The term "Xiyu Plate" was firstly proposed by Gao ZJ et al. (1983) of the Bureau of Geology and Mineral Resources of the Xinjiang Uygur Autonomous Region. Yang WR et al. (1984) named it the "Huaxi" (meaning "West China") Plate. Wang YS and Chen JN (1987) agreed with Xiyu's suggestion, and it has been adopted by many researchers (Ge XH et al., 1998).

A deep seismic profile of the collision belt in the Qilian Mountains (Wang ZJ et al., 1997) showed that the crust of Alxa–Dunhuang Block forms a wedge in the middle crust of the Qilian Mountains, and that the fault belt shows the characteristics of ramp-thrusting. At a shallow depth the thrust plane dips southwards, however, in the lower crust the thrust plane dips to the north.

It is well established that collisions occurred in the Qilian–Altun Belt in the Neoproterozoic Qingbaikou Period and at the end of the Early Paleozoic. However the period of the major amalgamation of the Xiyu Plate is uncertain. The author considers that the Xiyu Plate was finally amalgamated to form a single plate by the end of the Early Paleozoic. However Ge XH et al. (1998, 2000) and Duan JY et al. (1992) believe that the amalgamation occurred during Jinning Period (i.e. Qingbaikou Period) in the Neoproterozoic. The disagreement does not lie in the interpretation of the isotopic age data, because the isotopic age data indicates that there were two collision events, nor does it lie in the affinities of the Tarim Block, because the Tarim Block has been closely associated with the Yangtze Plate since the Neoproterozoic. The key point of the argument is the status of the Alxa Block. If the Alxa Block formed part of Sino-Korean Plate during the Nanhua, Sinian and Early-Middle Cambrian, then the Neoproterozoic (Qingbaikou or Jinning period) collision, represented by the Qilian-Altun Belt, marks the amalgamation between the Sino-Korean Plate (including the Korean, North China, and Alxa blocks) and the Tarim-Qaidam Plate, and the Xiyu Plate was not completely formed at this period. If the Alxa Block was associated with the Yangtze Plate from the Nanhua and the Sinian periods to the Cambrian, as Ge XH et al. (1998, 2000) have proposed, then the collision represented by the Qilian–Altun Belt marks the amalgamation of the components of the Xiyu Plate, which has therefore existed since the Neoproterozoic. However, the author considers that the evidence indicates that the amalgamation of blocks to form an independent Xiyu Plate took place only at the end of the Early Paleozoic, and not in the Neoproterozoic.

Folds occur in the Early Paleozoic systems and in the underlying strata around the Xiyu Plate, and in the Qilian–Altun Belt. The folding was accompanied by intense regional metamorphism and magmatism. The angle of dip of the fold limbs is between 60° and 70° and the fold axes trend WNW-ESE in Qilian, and ENE in Altun. A statistical analysis has been made of the attitudes of 126 anticlinoria and 119 synclinoria formed during the Qilian Period (Appendix 3.2). In present coordinates, the preferred attitude of maximum principal compressive stress axis (σ_1) was NE 20° plunging at 6°, of the intermediate principal stress axis (σ_2) NW 287° plunging at 7°, and of the minimum principal stress axis (σ_3) SW 197° plunging at 83° (Fig. 4.13). The plate suffered almost horizontal compression and convergence in an NE 20°-SW 200° direction in present coordinates. Under the influence of this tectonic stress field, the Qilian Collision Belt was formed almost at right angles to the shortening direction and suffered major compression. However, the Altun Collision Belt lay at an angle of 60°–70° to the main shortening direction, and suffered not only compression, but also a component of sinistral strike-slip movement. During this intense tectonic activity, the rocks in the Qilian, the northern margin of the Qaidam, and the Altun collision belts were affected by widespread granulite-amphibolite facies metamorphism, and in some regions by high-ultrahigh pressure blueschist and eclogite facies metamorphism (Lai SC et al., 1996; Zhang JX et al., 1999, 2002). On the northern margin of the Tarim Block and in the South Tianshan Mountains, the rocks were also affected by granulite-blueschist facies metamorphism as the result of subduction and collision (Shu LS et al., 1996; Gao J et al., 1996).

In the Cathaysian Plate, east of the Wuchuan–Sihui Fault and Yunkaidashan in Guangdong Province, southeast of the Shaoxing–Jiangshan Fault, Early Paleozoic systems are affected by folding, accompanied by widespread regional greenschist facies metamorphism, rising to amphibolite and granulite facies metamorphism in some regions and followed by magmatism (Bureau of Geology and Mineral Resources of Fujian Province, 1985; Chen B et al., 1994). The angles of dip of the fold limbs are between 30° and 80°, and directions of the fold axes and lineations are nearly N-S. Sm-Nd isotopic ages of amphibolite are about 509 Ma and 463 Ma respectively in Jinjiang (118.5°E, 24.8°N), East Fujian Province and in the Zhongmen Peninsula (119.2°E, 25.2°N), Putian (Huang H et al., 1990).

In present day coordinates, statistical analysis of the attitude of 154 anticlines and 133 synclines affecting Early Paleozoic systems in the Cathaysian Plate (Appendix 3.2) shows that the preferred attitude

of the maximum principal compressive stress axis (σ_1) was SE 97° plunging at 9°, the intermediate principal stress axis (σ_2) NE 8° plunging at 6°, and the minimum principal stress axis (σ_3) NW 285° plunging at 85° (Fig. 4.14), indicating that the Cathaysian Plate suffered nearly E-W compression and shortening. The amount of shortening has been calculated along latitudes 27° and 25° north, based on data from the 1:200,000 regional geological survey map. The estimated amounts of shortening in the Cathaysian Plate on these two E-W profiles with a length of about 1,000 km were 34.2% and 41.4%, amounting to plate shortening of 342 km and 414 km respectively.

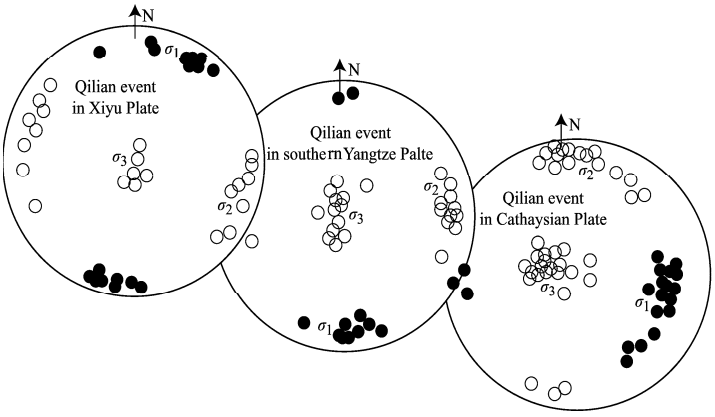

Fig. 4.14 Attitude of the principal stress axes in the Early Paleozoic(data in Appendix 3.2).

Folds are widely developed in the Early Paleozoic systems on the southern Yangtze Plate, at Shiwandashan in Guangxi and Yunkaidashan in western Guangdong Province, due to intraplate deformation. The angles of dip of the fold limbs are generally between 30° and 70°, with folding becoming more intense to the south, and both deformation and metamorphism are more intense in the Yunkaidashan region. Greenschists and granulites in Yunkaidashan have given an Rb-Sr isochron age of 487 Ma, and are accompanied by isoclinal folds and thrust systems (Qiu YX et al., 1993, 1996). The intensity of deformation drops off towards the north, and in Middle Guizhou Province the fold limbs dip at angles of only a few degrees. Statistical analysis of the attitude of 130 anticlines and 114 synclines formed during the Qilian Period in the South Yangtze region shows that the preferred orientation of the maximum principal compressive stress axis (σ_1) was SE 178° plunging at 8°, the intermediate principal stress axis (σ_2) NE 88° plunging at 6°, and the minimum principal stress axis (σ_3) NW355° plunging at 80° in present day coordinates (Fig. 4.14). At that time, the plate suffered ~N-S horizontal compression and shortening, evidently the dynamics for the deformation came from the south, quite a different direction from the compression of the Cathaysian Plate. Calculated on a 500 km N-S profile along 109.5°E longitude in the Hunan–Guangxi region, the amount of crustal shortening is estimated to be 42.16 %, showing that the South Yangtze Plate was shortened by ~210 km in the Early Paleozoic.

Why did folding occur in the southern part of the Yangtze Plate, but only weak deformation to the north? The explanation may be found in the relative strengths of the crystalline basement. In Chapter 3, it has been suggested that the amalgamation of the South Yangtze and the North Yangtze plates, accompanied by greenschist facies metamorphism, occurred at the end of the Mesoproterozoic (1,000 Ma). In contrast to the pre-Mesoproterozoic crystalline basement in the northern Yangtze Plate, the southern Yangtze Plate had a lower strength as there was no relatively rigid crystalline basement in the upper part of the plate. In the Early Paleozoic under slight tectonic compression, the overlying sedimentary cover of southern Yangtze plate was easily deformed. As the compression was not very

strong at that time, folding occurred mainly in the cover and did not result in metamorphism, and there was only a small amount of magmatic activity.

Previously the Yangtze Plate was distinguished from Cathaysian Plate using the stratigraphic position of angular unconformities. This is difficult, especially in the Middle Hunan, Guangxi, and the East Yunnan provinces on the South Yangtze Plate, because in both the South Yangtze and Cathaysian plates the Lower Paleozoic systems are folded, with angular unconformities between the Early and Late Paleozoic systems. However, it is possible to distinguish the Yangtze and Cathaysian plates by the very different directions of the fold axes and lineations, and their styles of deformation, and whether or not they were accompanied by regional metamorphism during the Early Paleozoic (Table 4.2).

As the South Yangtze and Cathaysian plates have very different styles of deformation, metamorphism and magmatism, they cannot have been connected in Early Paleozoic time. This has been confirmed by the results of studies in palaeomagnetism. As suggested by Liu BJ (1993) and Zhong ZQ et al. (1996) the Cathaysian Plate is considered to extend eastwards to the boundary of Shaoxing-Yunkaidashan, including the Wuchuan-Sihui area in west Guangdong and the Wuyishan region in west Fujian. In the Early Paleozoic the Yunkaidashan region either was an independent island arc block (Zhang BY et al., 1994; Wu HR et al., 2001) or belonged to the southeastern part of the Yangtze Plate (Wang HZ and Mo XX, 1995). In the Jiangxi-Hunan region it is difficult to define the location of Shaoxing-Yunkaidashan Tectonic Belt, because it is overlain by a Cretaceous sedimentary cover. Nevertheless because of the very different directions of the fold axes, different deformation styles and metamorphism of the Early Paleozoic systems, the problem can be solved. The Shaoxing-Yunkaidashan Tectonic Belt is considered to extend from Shaoxing (120.6°E, 30°N) to Jiangshan, Zhejiang to the southeastern side of Wugongshan (114.5°E, 27.5°N), southwestward to Chenzhou (113°E, 25.8°N), Hunan and then to Sihui-Wuchuan (110.9°E, 21.5°N) in Guangdong.

In addition, in the Jianglang (101.8°E, 28.7°N) region on the western margin of Yangtze Plate, to the west of the Longmenshan, Early Paleozoic amphibolite facies metamorphism has been discovered in recent years (Yan DP et al., 1997), this metamorphism also occurred on the northern margin of the Yangtze Plate and in the Qinling-Dabie Tectonic Belt (North Qinling-Tongbai Collision Belt, (Liu GH et al., 1993; Zhang GW et al., 2001)).

Recently, Yang WR et al. (2000, 2002) have suggested that the high and ultrahigh pressure eclogite metamorphism in the Dabie Collision Belt occurred in the Early Paleozoic (519–403 Ma), based on results of isotopic dating using Sm-Nb, zircon U-Pb, Pb-Pb, Ar-Ar and SHRIMP methods, and from the work of Zhai MG et al. (1998) and Che ZC et al. (2002) also suggested that the collision and orogeny in North Qinling occurred in the Early Paleozoic. The reason is that the final disappearance of oceanic crust, marked by an ophiolite suite, occurred at the end of Early Paleozoic. Recently, Suo ST et al. (2003) recognized that the ultrahigh pressure metamorphic belt in North Qinling and North Dabie was also formed in the Early Paleozoic from the isotopic age of the ophiolite. It is evident that a major collisional tectono-thermal event occurred mainly in the North Qinling Collision Belt. However, due to the superposition of later tectonic events, more research is required to reconstruct the overall characteristics, scale and effects of Early Paleozoic tectonics on the western and northern margins of the Yangtze Plate and in the Qinling-Dabie Belt.

At present, it is not possible to prove conclusively that the collision period in the formation of the Qinling-Dabie Belt occurred mainly in the Early Paleozoic (Zhang GW et al., 2001). The slight regional deformation in the Sino-Korean and Yangtze plates cannot be used to support the viewpoint that a major collision occurred between the two plates in the Early Paleozoic. If collision in the Qinling-Dabie Belt was completed at the end of the Early Paleozoic, evidence of intense deformation should be seen in the marginal regions of the Sino-Korean and Yangtze plates. In addition, palaeomagnetic, palaeogeographic, and palaeontologic data does not support the view that collision in the Qinling-Dabie Belt was completed at the end of Early Paleozoic. The author has proposed that plate underthrusting occurred in the North Qinling-Tongbai Belt at the end of the Early Paleozoic, but this event did not constitute the collision and amalgamation of the Sino-Korean and Yangtze plates. Because the characteristics of the neighboring blocks are unknown, and some of them may have been subducted beneath the crust,

the marginal intraplate deformations of those two plates were never formed in Late Paleozoic, but in Triassic. The detailed understanding of these events requires a much more research.

Mild tectonism occurred during Qilian Period in all the blocks in Hingganling–Laoyeling (130°E, 44.3°N) region of Northeast China, but the trends of the tectonic lineations are not consistent. Analysis of the attitude of 12 anticlines and 16 synclines (Appendix 3.2), in present day coordinates, showed that the preferred attitude of the maximum principal compressive stress axis (σ_1) was NE 50° plunging at 5°, that of the intermediate principal stress axis (σ_2) was NW 320° plunging at 4°, and that of the minimum principal stress axis (σ_3) was SW 231° plunging at 85°. At that time, the blocks suffered nearly horizontal compression and shortening in an NE 50°-SW 230°direction. The direction of compression of these blocks was different from all the other blocks in China. Low-grade greenschist facies metamorphism accompanied deformation in central Inner Mongolia and parts of Northeast China. In the Yilan region (129.7°E, 46.3°N) in Heilongjiang Province, Early Paleozoic systems (445–415 Ma) have been discovered with intensely deformed blueschists (Ye HW et al., 1994; Zhao CJ et al., 1996).

Table 4.2 Tectonic characteristics contrasts among Northern Yangtze, Southern Yangtze and Cathaysian Plates in the Early Paleozoic

Plate	Northern Yangtze	Southern Yangtze	Cathaysian
Biogeographical province	South China	South China	South China
Formation age of unified crystalline basement	800 Ma	800 Ma	400 Ma
mean paleomagnetic declination	129.1°–83.8° in Early Paleozoic	129.1°–83.8° in Early Paleozoic	205.4°–201.3° in Cambrian
mean paleolatitude	From 11.7° S to 2.8° N	From 11.7° S to 2.8° N	From 10.8° to 11°
Stratal boundary between Upper and Lower Paleozoic	Disconformity	Unconformity	Unconformity
Folding axies trending	No folding	Near E-W	Near N-S
Shortening orientation	No	Near N-S	Near E-W
Regional metamorphism	No	No	Green schist
Magmatism	Almost no	weak	strong

Data of paleomagnetism shown in Appendix 6 and folding data in Appendix 5.3

The analyses of deformation data show evidently that the Xiyu Plate was situated near the Tianshan Tectonic Belt, as their tectonic lineations and the paleostress orientations are similar. However, some small blocks in Hingganling-Laoyeling region in Northeast China suffered compression in an NE-SW direction, suggesting that during the movements the smaller blocks were extruded between the Sino-Korean Plate and the northern Mongolian and Siberian Plates. The orientation of rock deformation, the magmatism and the metamorphism in the Cathaysian Plate (Appendix 7) in the Early Paleozoic are very different from those of Yangtze Plate, which provides powerful evidence that the two plates could not have been connected and amalgamated with each other at that time. During the Silurian, the South Yangtze and the main Cathaysian plates formed continental areas, but it cannot be demonstrated that they were united. Indeed palaeomagnetic data shows different paleomagnetic north directions and indicates that these two plates were located at different latitudes (shown in Table 4.2).

4.4 Magmatism and Rates of Plate Movement

Compared with other geological periods, magmatism was not very extensive, the area covered by Early Paleozoic magmatic rocks is 67,500 km^2, accounting for only ~7% of the total area of China occupied by magmatic rocks.

Magmatic activity occurred in Xiyu, Cathaysian Plates and Qinling–Dabie, Tianshan–South Hingganling zones. At the beginning of each tectonic event basic or ultrabasic magmatic activity, caused by extension, occurs between or on the margins of plates. However, intermediate-acidic magmatism occurs mainly at the end of each tectonic event, caused by marginal or intraplate compression and shortening.

Early Paleozoic ophiolites are found in the Tianshan–South Hingganling, Qilian–Altun-East Kunlun-West Kunlun-Pamir and Qinling-Dabie belts (Xiao XC, 1984; Li JY, 1996) (Fig. 4.13), indicating that oceanic crust separated the continental blocks. There are Ordovician ophiolites in the Zhaheba-Baytikshan region (91°E, 45.5°N), East Junggar, in the Tianshan-South Hingganling Belt (Li JY, 1995) and at Hoglen (86°E, 46°N) in the West Junggar region, on the northeastern margin of the Kazakhstan Plate (Bei WJ, et al., 1995). There are Early Paleozoic ophiolites at Mayla-Tangbal (84°E, 46°N) on the northwestern margin of Junggar block (Xiao XC et al., 1992). The presence of Early Paleozoic ophiolite suites between the Junggar Block and the Kazakhstan Plate indicates that they were initially two independent blocks amalgamated in the Late Paleozoic. There is the Ondor Sum-Ongniud Qi-Xar Moronhe Cambrian Ophiolite Belt (from 113°E, 42.5°N to 120°E, 43.4°N) on the southern side of the Hingganling Tectonic Belt in the north of the Sino-Korean Plate (Li CY, 1982; Peng LH, 1984; Wang Q et al., 1991), and the Erdaojing-Hongger Horsefield-Kedanshan Cambrian-Ordovician Ophiolite Belt (from 112.2°E, 43.3°N to 118°E, 44°N) on the northern side of that belt (He GQ, 1983; Li JY, 1987; Wang Q et al., 1991).

In the Qilian-Altun-East Kunlun Belt, three Early Paleozoic ophiolite belts and more than one hundred ultrabasic and basic rock bodies have been discovered. These are: (1) The North Qilian Belt (Xiao XC, 1978, 1984; Feng YM et al., 1995; Xia LX et al., 1995; Zhang Q et al., 1998); (2) The Late Ordovician ophiolite and oceanic tholeiite belt on the northern margin of the Qaidam Basin (from 94°E, 38.2°N to 98°E, 37.5°N), in which the rate of oceanic extension, estimated by the chemical components of basic rocks, was about 2.5 cm/yr (Lai SC et al., 1996); (3) The Qingshuiquan Belt (from 92°E, 36°N to 96°E, 35°N) in East Kunlun, to the south of the Qaidam Basin (Gao YL et al., 1988).

There are many Cambrian-Ordovician ophiolite melanges (Guo ZJ et al., 1999; Liu L et al., 1998) in both the E-W Hongliugou-Lapeiquan region (from 91°E, 38.7°N to 92°E, 38.8°N) and the Altun Belt (508–512 Ma, using the Sm-Nd method). This ophiolite is perhaps the western extension of the North Qilian Ophiolite Belt, displaced by a fault. In the Mang'ai–Aba region (from 90.5°E, 38.3°N to 88°E, 38°N) in the southwestern segment of the Altun Fault there are 71 mafic blocks, with isotopic ages, using the Sm-Nd method, ranging from 481 to 493 Ma.

The West Kunlun-Pamir Ophiolite Belt (i.e. Kudi-Subaz, centered on 79°E, 36.3°N) has generally been considered to represent a segment of the Sinian-Early Ordovician oceanic crust (Deng WM, 1995). However, it has been also considered to have been formed in the Carboniferous (359 Ma, Rb-Sr whole-rock on basalt (Jiang CF et al., 1992)). According to the opinion of Jin XC et al. (1999), the West Kunlun Central Fault Belt (Kudi-Subaz Ophiolite Belt) was formed by collision at the end of the Devonian, and was covered unconformably by the Carboniferous system. But it is most likely that the Kudi-Subaz Ophiolite Belt was developed in the Sinian-Early Ordovician.

The Early Paleozoic ophiolites in the Qinling-Dabie Belt have been carefully studied in recent years (Zhang GW et al., 2001). The Shangdan Belt (Shang County-Danfeng, in Shaanxi Province; centered on 110.2°E, 33.7°N) is composed of oceanic island arc rocks and residual blocks of ophiolitic oceanic crust. It is the main suture zone between the Qinling Block and the Sino-Korean Plate. To the east of the Shangdan Belt is the Erlangping Ophiolite Belt (Xixia of Henan Province, centered on 111.4°E, 33.4°N), which is composed of blocky basalt, pillow basalt, and sheeted dykes or sills, accompanied by siliceous rocks with Ordovician-Silurian radiolaria. These rocks represent residual sheets of the upper parts of oceanic crust, and provide evidence for the presence of an Early Paleozoic ocean between the Qinling Block and the Sino-Korean Plate.

Rates of plate extension and shortening in the Early Paleozoic have been estimated from the chemical composition of 1,124 magmatic rocks (data from the geology of provinces and the 1:200,000 regional geological surveys of the whole of China) (Appendix 5.3, the preferred data in Fig. 4.13).

In the early periods of the Early Paleozoic (Middle–Late Cambrian, 513–500 Ma), all the continental blocks had generally extension. Basic and ultrabasic magmatism often led to the opening of oceans, now represented by ophiolite suites, between the blocks. The rates of plate extension, calculated from basic and ultrabasic rocks in Kedanshan and Xiaosongshan, Inner Mongolia (106.5°E, 39.5°N) was the most rapid, with an average value calculated from 11 analyses reaching 1.1 cm/yr. At Qingshankou and Xinglonggou (128°E, 47.5°N) in Heilongjiang Province, the average rates of extension calculated from 22 analyses were 0.72 cm/yr, and 0.75 cm/yr from 35 analyses in the Qilian Mountains.

According to Song SG and Su L (1998), dunite in the Middle and Late Cambrian ophiolite suite in Yushigou (100°E, 38.6°N), North Qilian, was formed in the mantle environment at high temperature (1,025°C–1,093°C), ultrahigh pressure (3.0–4.28 GPa), low differential stress (28–32 MPa), and low strain rate (0.2×10^{-14}–2.13×10^{-14}), at depths of 95–132 km. The chemical composition of basic rocks showed that the rate of plate extension was 1–3 cm/yr. The rate of extension in Qinling Mountains was the slowest, with an average value from 18 analyses being only 0.2–0.28 cm/yr.

Rates of plate extension calculated from the chemical compositions of Ordovician (500–435 Ma) basic and ultrabasic rocks gave an average value of 0.88 cm/yr from 38 analyses in the rift belt in the northeastern margin of Qaidam and Qilian. The average value, estimated from 19 analyses in Fengxian, Shaanxi Province, and Donghe, Hubei Province, in the Qinling Belt (from 106.5°E, 33.9°N to 111°E, 32.5°N), was 0.5 cm/yr. The average rate of extension from 27 analyses in A'nyemaqenshan and Qingshuiquan, Qinghai Province (from 92°E, 36.3°N to 100°E, 34.6°N) was 0.7 cm/yr. Three analyses from the South Yangtze Plate at Damingshan (108.5°E, 23.3°N) of Guangxi, and Dexing (117.5°E, 28.9°N) of Jiangxi Province gave 0.4–0.84 cm/yr, and the average value from 29 analyses in Cathaysian Plate was 0.8cm/yr (Appendix 5.3; Fig. 4.13).

Rates of plate-shortening were calculated from the chemical composition of Ordovician (500–435 Ma) intermediate-acidic magmatic rocks. The average value obtained from 81 analyses from the Yichun-Jiling region (129°E, 47.8°N), Heilongjiang Province was 6.2 cm/yr, and that obtained from 15 analyses from Baoqing-Mishan (132°E, 46°N), Heilongjiang Province was 5 cm/yr. The average rate of shortening from 88 analyses in Xiao Hingganling (127.9°E, 48.2°N), Heilongjiang Province was 5.3 cm/yr. The average rate of shortening from 20 analyses from the Bainaimiao-Bat Obo region (111°E, 42°N) was the most rapid in Inner Mongolia, i.e. 9.2 cm/yr. The average rate of shortening from 17 analyses in the Qinling-Dabie Belt was 4.5 cm/yr. The average rate of shortening from 19 analyses in the Baoji region (107°E, 34.4°N) in the West Qinling Belt was more rapid, i.e. 7.1 cm/yr. The average rate of shortening from 46 analyses in the northern margin of Qaidam in Xiyu Plate was 5.5 cm/yr. The average rate of shortening in North Qilian, Gansu Province was 4.4 cm/yr, and the average rate of shortening in Beishan (96°E, 41.2°N), Gansu Province was 7.5 cm/yr.

In conclusion, all the tectonic blocks in North China began to be compressed and shortened after extension and dispersion during the middle period of Early Paleozoic. The rate of shortening was the most rapid (9.2 cm/yr) in the Bainaimiao-Bat Obo region, Inner Mongolia. The rate of amalgamation of the blocks in the Xiyu Plate, and the shortening rate at Hingganling in the Qinling-Dabie Tectonic Belt were of medium values (4–7 cm/yr).

Rates of plate extension were calculated from the chemical composition of late period of Early Paleozoic (Silurian–Early Devonian, 444–397 Ma) basic and ultrabasic rocks. The average rate of extension from 20 analyses in Altan Obo, Dengkou, and Xiaosongshan in Wuhai City (107°E, 39.7°N) in central Inner Mongolia was 0.84 cm/yr. The average rate of extension from 16 analyses in the Altay Mountains (89°E, 48°N), Xinjiang was 0.84 cm/yr. The average rate of extension from 13 analyses in Jilin Province was 0.6 cm/yr. The average rate of extension from 12 analyses in Alxa Zuoqi (105.7°E, 39°N) was 0.6 cm/yr. The average rate of extension in the Altun Belt in southeast Xinjiang region was about 0.62 cm/yr. The average rate of extension from 55 analyses in East Qinling was 0.8cm/yr. However, the average extension velocity from 9 analyses in West Qinling was relatively slow (0.45 cm/yr).

Rates of plate shortening were calculated from the chemical composition of intermediate-acidic rocks were intruded at a late period in the Early Paleozoic (Silurian, 444–397 Ma), at the peak of a series of tectono-thermal events. The average rate of shortening from 40 analyses in central Inner Mongolia was

6 cm/yr. The average rate of shortening from 34 analyses in Jilin Province was 5.3 cm/yr. The average rate of shortening from 19 analyses in south Alxa was only 4.7 cm/yr. The average rate of shortening at Kangbao, northern Hebei Province was 7.1 cm/yr. The average rate of shortening from 34 analyses in the Altay in the Xinjiang region was 8.5 cm/yr. The average rate of shortening from 12 analyses in East Junggar, Xinjiang region was 5.3 cm/yr. The average rate of shortening from 44 analyses in the West Qinling Belt, South Shaanxi Province was 6.6 cm/yr. The average rate of shortening from 23 analyses in the East Qinling is 7 cm/yr. The average rate of shortening in the Dabie Belt was 4.7 cm/yr.

There was a major phase of granitic magmatism at a late period of the Early Paleozoic (416–400 Ma) in the Qilian and Zhangye (Hexizoulang) (from 97°E, 39.5°N to 103°E, 37.5°N) regions in the Xiyu Plate. The average rate of shortening from 20 analyses in South Qilian, northern Qinghai Province was 6.7 cm/yr. The average rate of shortening from 18 analyses in Dangjinshan and Sertengshan (94.3°E, 39.4°N to 95°E, 38.5°N) in the Altun Belt in northwest Qinghai Province was 6.2 cm/yr. The average rate of shortening from 12 analyses from the Tianshan Mountains of the Xinjiang region was 5.7 cm/yr. The average rate of shortening from 7 analyses in the West Kunlun of Xinjiang region was 4.9 cm/yr. The average rate of shortening from 5 analyses in East Kunlun in the Xinjiang region was 5.9 cm/yr (Appendix 5.3).

Large number of granitic intrusions were emplaced in the Cathaysian Plate during the Early Paleozoic. These are mainly crust-mantle syntactic (I-type) granitoids in areas of bathyal flysch deposits in the west Cathaysian Plate (Middle Jiangxi–South Hunan provinces), in which the initial value of the strontium isotope ratio is generally less than 0.709 (Bureau of Geology and Mineral Resources of Jiangxi Province, 1984; Bureau of Geology and Mineral Resources of Hunan Province, 1988). But other granitoids were formed mainly by crustal melting of granite and migmatite in the continental margin deposits of the central Cathaysian Plate (west Zhejiang, Fujian, and middle and west Guangdong provinces), in which initial values of strontium isotope ratios are usually greater than 0.710 (Sun MZ and Xu KQ, 1990). It is considered that on the western margin of the Cathaysian Plate magma came from a deep crust-mantle boundary, but that in the central part of the Cathaysian Plate the magma came from a shallower depth in the crust (Appendix 7). In the early Paleozoic the Cathaysian Plate suffered intense tectonic compression and collision. Oceanic crust was subducted westwards beneath the western margin of the Cathaysian Plate, while intraplate magmatism occurred in the central part of the Cathaysian Plate.

In line with the style of rock deformation, metamorphism and granitic magmatism, the author does not consider that compression and shortening were caused by the collision and amalgamation of the Yangtze and Cathaysian plates at the end of Early Paleozoic, as Sun MZ et al. pointed (1990), because the tectonics of the two plates has quite different orientations, N-S in the Cathaysian Plate and E-W in the southern Yangtze Plate, and there was no any regional metamorphism in the Yangtze Plate.

In the Cathaysian Plate, the average rate of shortening from 16 analyses of granitic rocks from Fujian Province was 6.1 cm/yr, from 20 analyses in central and southern Jiangxi Province, 5.6 cm/yr, from 37 analyses in Guangdong Province, 6.5 cm/yr, from 18 analyses on the western margin of Guangdong Province, 7.7 cm/yr, from 21 analyses in Hainan Province, 7.8 cm/yr, from 15 analyses of the north of Yangtze Plate in Hubei Province, only 3.2 cm/yr. There are also some granitic intrusions (400 Ma) in the southern Yangtze Plate, caused by the N-S compression and collision. In Hunan Province from 34 analyses the average values of rates of shortening were 7.7 cm/yr, and from 41 analyses in Guangxi, 6.1 cm/yr (Appendix 5.3).

During the Silurian, the rate of plate shortening in the Altay region, Xinjiang was the most rapid (8.5 cm/yr) in China. The rate of plate shortening in Hainan Province and on the western border of Guangdong Province (Yunkaidashan) was about 8.0 cm/yr; in the other regions, rates of shortening were between 5 and 7 cm/yr. However, in the relatively stable blocks of South Alxa, the Dabie Belt and the North Yangtze Plate, rates of plate shortening were generally less than 5 cm/yr.

Because the periods of time of over which extension of the continents and shortening of paleo-oceans between the blocks occurring are difficult to determine, it is not possible to calculate the total amount of extension and shortening from the rates of plate extension and shortening. Gao CL (1992) calculated the width of "Paleo-Asian Ocean" in the Ordovician to be 5,805 km. But this result is not credible. From

the available palaeomagnetic data (Figs. 4.9, 4.10), one can see that the Siberian Plate was located at almost the same latitude as the Sino-Korean Plate during the Ordovician, but it is not clear which plate lay to the north of the Sino-Korean Plate. Posed this problem is it sensible to call the ocean to the north of Sino-Korean Plate, the "Paleo-Asian Ocean", let alone to attempt to calculate its width?

4.5 Division of Tectonic Units in Early Paleozoic

During the Early Paleozoic, most of the continental blocks which form China were dispersed and were not involved in collision and amalgamation. The geological history, paleomagnetism and paleogeography of these blocks are all very different, so that it is easy to distinguish the tectonic divisions. Tectonic units recognized during the Early Paleozoic in the Chinese continent are shown in Fig. 4.15 and Fig. 1.2. Five major domains can be distinguished: the Peri-Siberian, Sino-Korean, Yangtze, Xiyu and Peri-Gondwanan tectonic domains.

Peri-Siberian Tectonic Domain (N.B. blocks are indicated by the numbers in brackets in Fig. 1.2 and Fig. 4.15): Altay (1), Junggar-East Kazakhstan (2), Ili-Balchas (3), Turpan-Xingxingxia (4), Kuruktag (5), Hongshishan (6), Yagan (7), North Bayannur (8), Tuotuoshan-Xilinhot (Abagnar, 9), Ergun (10), Harbin (Songhuajiang-Nenjiang, 11), Jiamusi-Bureinskiy (12), Xingkai (Wandashan, 13). These blocks were all separated from the Middle Cambrian to Silurian. A marine transgression occurred in each block, with the marine areas becoming gradually more extensive and the water gradually deepening. The palaeon-tological assemblages in these blocks are similar to those of the Siberian Plate. The crystalline basement of Jiamusi-Bureinskiy block was similar to that of the Gondwana Plate from the Sinian to Early Cambrian, but after the Middle Cambrian was similar to that of the Siberian Plate. During the Ordovician a collision commenced in the Altay–Central Mongolia-Ergun belt, which formed Altay–Junggar-Central Mongolian-Ergun Early Paleozoic Collision Belt. The other blocks remained separate during the Early Paleozoic, but were amalgamated during the Late Paleozoic.

Sino-Korean Tectonic Domain is the Sino-Korean Plate (20), which formed the crystalline basement during 1,800 Ma and moved northwards to near the equator during the Early Paleozoic, possibly influenced by the great northwards migration of the Siberian Plate, simultaneously progressing from an episode of marine transgression to one of regression. From the Middle Ordovician to the Silurian the plate was uplifted to form an extensive continental area. Only the southwestern part was affected by deformation. The plate constituted an independent biogeographic province in a warm tropical environment. Subsidence occurred along the plate margins or in aulacogens within the plate, which showed that it was not in direct connection with the other plates.

Yangtze Tectonic Domain includes: North Yangtze Plate (32), South Yangtze Plate (33), Cathaysian Plate (34), Taiwan (East Cathaysian) block (35), Songpan-Garze (21), Middle Qinling (22), Wudang (23), Dabie (24), Jiaonan (25), Zhongdian (30), Lanping–Simao-Indochina Plate (31), Sanya (Northeast Indochina) block (36). The Yangtze Plate formed the crystalline basement during 800 Ma and moved slowly northwards to a position near the equator during the Early Paleozoic, perhaps influenced by the northwards migration of the Siberian Plate. It formed an independent biogeographical province within the tropical zone. Between the Middle Cambrian and Silurian the plate progressed from a marine transgression to a regression, but with continual deposition of bathyal sediments in whole Paleozoic at the Qinzhou-Fangcheng marginal depression. Only the northern margin of the Yangtze Plate was affected by deformation. However, the sedimentary cover of the South Yangtze Plate was affected by intraplate folding on E-W axes. In the Cathaysian Plate, from the Cambrian to the Ordovician, deposition was mainly bathyal, and the fauna belongs to the South China Paleobiogeographical Province. A marine regression occurred during the Silurian, and most of the Cathaysian Plate formed a land area. At the end of the Early Paleozoic the plate was affected by deformation on N-S trending axes, associated with greenschist facies metamorphism, and developed a unified crystalline basement. Shallow marine sediments were deposited during the whole of the Early Paleozoic in the Songpan-Garze, Lanping-

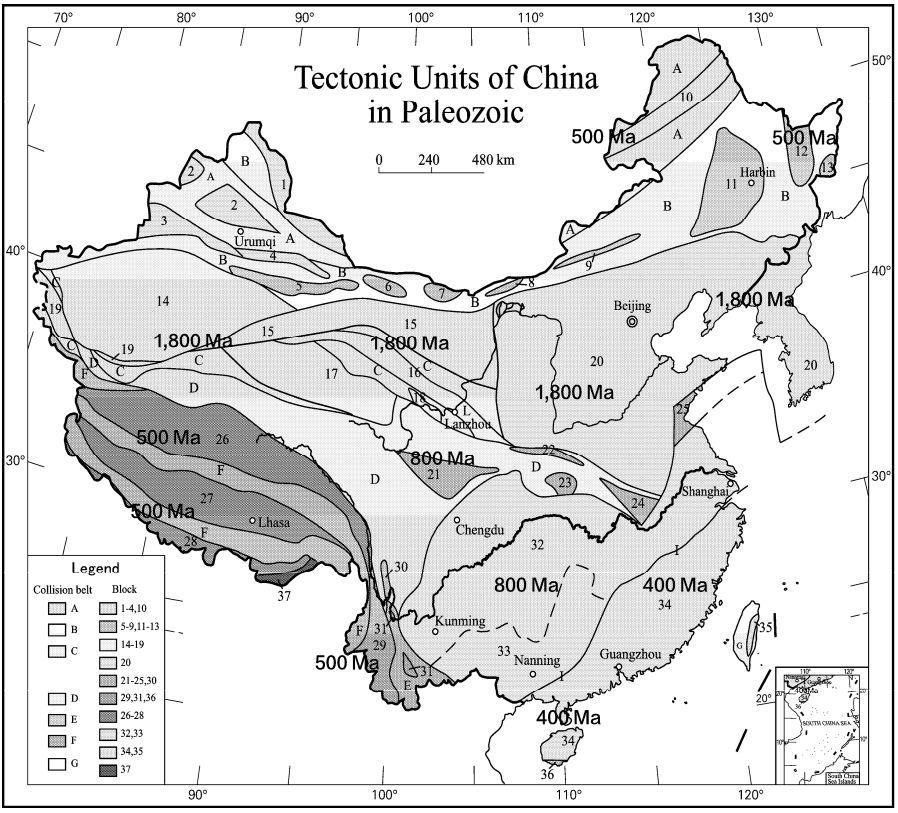

Fig. 4.15 Tectonic units in China during the Early Paleozoic.

Peri-Siberian Tectonic Domain: 1. Altay; 2. Junggar-East Kazakhstan; 3. Ili-Balchas; 4. Turpan-Xingxingxia; 5. Kuruktag; 6. Hongshishan; 7. Yagan; 8. North Bayannur; 9. Tuotuoshang-Xilinhot (Abagnar); 10. Ergun; 11. Harbin (Songhuajiang-Nenjiang); 12. Jiamusi-Bureinskiy; 13. Xingkai (Wandashan). **Sino-Korean Tectonic Domain** (20). **Peri-Yangtze Tectonic Domain**: 32. North Yangtze Plate; 33. South Yangtze Plate; 21. Songpan-Garze (west Sichuan); 22. Middle Qinling; 23. Wudang; 24. Dabie; 25. Jiaonan (Sulu); 30. Zhongdian; 31. Lanping-Simao-Indochina Plate; 34. Cathaysian Plate; 35. Taiwan (East Cathaysian Plate); 36. Sanya (northeast Indochina Plate). **Xiyu Tectonic Domain** (transition type): 14. Tarim Plate; 15. Altun–Dunhuang-Alxa; 16. Middle Qilian; 17. Qaidam; 18. Hualong; 19. central West Kunlun. **Peri-Gondwanan Tectonic Domain**: 26. Qiangtang; 27. Gangdise (Lhasa); 28. Himalayan; 29. Baoshan–Sibumasu (Baoshan–Burma–Malay-Sumatra); 37. Indian Plate.

Collision belts (folded zones or orogenic belts): A. Altay–Junggar–Ergun Early Paleozoic Collision Belt; B. Tianshan-Hingganling Late Paleozoic Collision Belt (eastern extension of the Central Asian Orogenic Belt); C. Qilian-Altun Early Paleozoic collision belts in the Xiyu Plate; D. Shuanghu-Lancangjiang (Changning-Menglian), Lazhulong-Jinshajiang and Qinling–Dabie–Jiaonan Triassic collision belts; E. Lanping-Simao Palaeogene Collision Belt; F. Bangong-Nujiang and Yarlung Zangbo River Cretaceous-Oligocene collision belts; G. Subduction zone (trench-arc zone) of the West Pacific since the Palaeogene. The Shaoxing-Shiwandashan Triassic Collision Belt between the Yangtze and Cathaysian plates is shown as a boundary line.

The isotopic ages in the figure are the forming ages of crystalline basements for main blocks.

Simao and east Yunnan aulacogens, and their paleobiotic assemblages are similar to those of the South China Biogeographical Province. In the Qinling-Dabie Belt sediments were deposited in marginal to oceanic environments during the Early Paleozoic, and the palaeobiotic assemblages belong to the South

China Biogeographical Province. Subduction and amalgamation occurred in the Qinling-Dabie Belt during the Early Paleozoic. Nevertheless the areas affected are not clear, because local deformation occurred only in the southwestern part of the Sino-Korean Plate and on the northern margin of the Yangtze Plate. During this period there is no obvious deformation over most Sino-Korean and Yangtze plates.

To sum up, there are so different tectonic characteristics between the Yangtze and Cathaysian plates (Table 4.2), they are separately never amalgamated and can not to be a unified continental plate in Early Paleozoic, although they are located in the same biogeographical province. The Cathaysian plate formed the unified crystalline basement during 400 Ma. The differences between Northern and Southern Yangtze Plate are only in characteristics of rock deformation and strata boundary, and they are in the same plate.

Yan MC et al. (1997) analyzed the upper-crustal chemical components from 2,718 samples collected over 3,300,000 km^2 in the three major tectonic domains of East China, using 15 chemical and physical analytical methods. In the Sino-Korean Tectonic Domain, the samples are Al-poor, and rich in Fe, Mg and Ca, with high oxidation [$w(Fe_2O_3)$ / $w(FeO)$ = 1.12] , rich in platinum group elements, rich in Cr, Ni, Co, Cu but poor in Li, Rb, Cs, U, Th, Zr, Hf, Ti, Mn, V and HREE. Samples from the Peri-Siberian Tectonic Domain are Al-rich, high in $w(Na_2O)$ / $w(K_2O)$ = 1.32, with low oxidation [$w(Fe_2O_3)$ / $w(FeO)$ = 0.63], rather rich in As, Be, Li, Mn, Ti, V and HREE, but poor in Cu, Ni, F, Se, Ba, the platinum group elements and LREE, and low in $w(La)$ / $w(Yb)$. Samples from the Yangtze Tectonic Domain are rich in Si and K, poor in Fe, Mg and Ca, with low $w(Na_2O)$ / $w(K_2O)$ and with high incompatible trace elements, such as Rb, Cs, Nb, Ta, U, Th, W, Sn, Sb, Bi and REE. The Qinling-Dabie Belt is an important boundary; to the north the rocks are rich in Na, with low $w(Rb)$ / $w(Sr)$ and low LREE, while to the south they are rich in Si and K, with high $w(Rb)$ / $w(Sr)$, and rich in the LREE and incompatible elements. These data prove that the different tectonic domains are composed of chemically distinct types of continental crust.

Xiyu Tectonic Domain is a transitional tectonic domain. Its formation age of crystalline basement is 1,800 Ma. During the Mesoproterozoic, Tarim (14), Altun-Dunhuang-Alxa (15), Middle Qilian (16), Qaidam (17), Hualong (18), and the centre of the West Kunlun (19) blocks all belonged to the Sino-Korean Plate. In the Neoproterozoic the Tarim Block was separated from the Sino-Korean Plate and approached the Yangtze Plate. Before the Middle Cambrian the Alxa-Dunhuang-Altun, Middle Qianlian, Hualong and Qaidam blocks still belonged to the western part of Sino-Korean Plate, but in the Late Cambrian they became related to the Yangtze Plate. At the end of the Early Paleozoic, these blocks were amalgamated to form the independent Xiyu Plate. The Qilain-Altun Belt was the main collision belt in the Xiyu Plate. Sedimentary, paleogeographic, paleobiotic and palaeomagnetic data all show that the Xiyu Plate was related to the Yangtze Plate. Although the Xiyu Plate was not connected to the Yangtze Plate at that time, they were both located in the South China Biogeographical Province and lay in the same latitude.

Peri-Gondwanan Tectonic Domain includes the Qiangtang (26), East Kunlun, Gangdise (Lhasa) (27), Himalayan (28), Baoshan-Sibumasu (29) blocks and the Indian Plate (37), whose formation ages of crystalline basement are about 500Ma. The Himalayan, Qiangtang, east Kunlun and Hoh Xil-Litang blocks were stable and were not affected by any tectono-thermal events from the Middle Cambrian to the Silurian. In the Peri-Gondwanan Tectonic Domain shallow marine carbonate sediments accumulated during the most part of the Early Paleozoic. There was a short cessation of deposition at the end of the Early Paleozoic in the Gangdise Block. The paleobiotic assemblages of the Peri-Gondwana Tectonic Domain, although they have some similarity to those of the South China Paleobiogeographical Province, can still be distinguished, and are related to those of Gondwana. This has been called the Yunnan-Xizang Paleobiogeographical Province by Chinese scholars. In the Early Paleozoic these blocks were dispersed at low latitudes in the southern hemisphere.

The summary of the Early Paleozoic tectonic evolution of the Chinese continent. The amalgamation of the Xiyu Plate was completed, the Altay-Ergun Collision Belt formed, the Cathaysian Plate developed a unified crystalline basement, intraplate folding occurred in the South Yangtze Plate, and most of the crustal blocks in China were dispersed but in the process of migration.

References

An TX (1984) The advanced research on Ordovician statigraphic area in North China. In: Collected Papers for Commemorating Professor Le Senxun Worked on Geological Scientific Education for 60 Years, Geological Publishing House, Beijing (in Chinese).

An TX, Ma WP (1993) Middle Ordovician–Lower Carboniferous of Sino-Korean platform and its paleogeography and tectonic significance. Earth Science 18(6): 777–793 (in Chinese).

Bai WJ, Robinson P, Yang JS et al (1995) The Ophiolites in different stages and its tectonic evolution of the western Junggar, Xinjiang. Acta Petrologica Sinica 11(suppl.): 62–72 (in Chinese with English abstract).

Bally AW, Scotese CR, Ross MI (1989) North America: plate tectonic setting and tectonic elements. In: Bally AW, Palmer AR (eds) The geology of North America–an overview, A: pp.1–15. GSA.

Bureau of Geology and Mineral Resources of Fujian Province (1985) Regional Geology of Fujian Province. Geological Publishing House, Beijing (in Chinese with English abstract).

Bureau of Geology and Mineral Resources of Hunan Province (1988) Regional Geology of Hunan Province. Geological Publishing House, Beijing (in Chinese with English abstract).

Bureau of Geology and Mineral Resources of Jiangxi Province (1984) Regional Geology of Jiangxi Province. Geological Publishing House, Beijing (in Chinese with English abstract).

Che ZC, Liu L, Luo JH (2002) Regional Tectonics of China and Its Adjacent Areas. Science Press, Beijing (in Chinese).

Chen B, Zhuang YX (1994) The petrology and petrogenesis of Yunlu chamockite and its granulite inclusion, west Guangdong, South China. Acta Petrologica Sinica 10(2): 139–150 (in Chinese with English abstract).

Cheng YQ (1994) An Introduction to Regional Geology of China. Geological Publishing House, Beijing (in Chinese).

Commission on Stratigraphy of China (2001) Chart of regional stratigraphy (geological age) of China. Journal of Stratigraphy 25(suppl.): 359–360 (in Chinese).

Deng WM (1995) Geological features of ophiolite and tectonic significance in the Karakorum-west Kunlun Mts. Acta Petrologica Sinica 11(suppl.): 98–111 (in Chinese with English abstract).

Duan JY, Ge XH (1992) Tarim-Yangtze Plate and its palaeogeographic pattern. Journal of Changchun College of Earth Sciences 22(3): 260–268 (in Chinese with English abstract).

Feng YM, He SP (1995) Research for geology and geochemistry of several in the north Qilian Mountains, China. Acta Petrologica Sinica 11(suppl.): 125–146 (in Chinese with English abstract).

Gao CL (1992) Wirth of the Paleo-Asian Ocean (Mongolia district). Geoscience 6(2): 209–216 (in Chinese with English abstract).

Gao J, He GQ, Li MS et al (1996) Uplift mechanism of high–pressure metamorphic rocks, South Tianshan, Xinjiang. Scientia Geologica Sinica 31(4): 365–374 (in Chinese with English abstract).

Gao YL, Wu XN, Zuo GC (1988) Ophiolitic features of Qingshuiquan in east Kunlun and their tectonic significances. Journal of Xi'an Institute of Geology and Mineral Resources, Chinese Academy of Geological Sciences (21): 17–28 (in Chinese).

Gao ZJ, Wu SZ (1983) Tectonic evolution of Tarim paleocontinent in Xijiang. Chinese Science Bulletin 28(23): 1448–1450 (in Chinese).

Ge XH, Zhang MS, Liu YJ (1998) Scientific problems and thought for research of the Altun fault. Geoscience 12(3): 295–301 (in Chinese with English abstract).

Ge XH, Liu JL (2000) Be broken "Western China Craton" . Acta Petrologica Sinica 16(1): 59–66 (in Chinese with English abstract).

Gordienko IV (1994) Paleozoic geodynamic evolution of the Mongol-Okhotsk fold belt. Journal of Southeast Asian Earth Sciences 9(4): 429–433.

Guo ZJ, Zhang ZC, Wang JJ (1999) Sm-Nd isochron age of ophiolite along northern margin of Altun Tagh Mountains and its tectonic significance. Chinese Science Bulletin 44(5): 456–458.

He GQ, Shao JA (1983) Determination of Early Paleozoic ophiolite in southeastern Nei Mongol and their geotectonic significance. In: Contributions to the Project of Plate Tectonic in Northern China. no.1, pp.243–250. Geological Publishing House, Beijing (in Chinese with English abstract).

He GQ, Li MS (2001) Significance of paleostructure and paleogeograpy of Ordovician-Silurian rock associations in Northern Xinjiang, China. Acta Scientiarum Naturalium Universitatis Pekinensis 37(1): 99–110 (in Chinese with English abstract).

He XY (1988) Silurian. In: Yin HF et al (eds) Paleobiogeography of China. China University of Geosciences Press, Wuhan (in Chinese).

Huang BC, Zhu RX, Yang ZY (1999) Study of Paleozoic kinematics features of the North China block. Geoscience 13(suppl.): 1–7 (in Chinese with English abstract).

Huang H, Li RA, Yang CX (1990) Geochronologic study for the metamorphic belt along the coast of Fujian province and its tectonic significance. Chinese Science Bulletin 35(9): 751–754.

International Commission on Stratigraphy (2004) International Stratigraphic Chart. 32th IGC, Florence, Italy.

Jiang CF, Yang JS, Feng BG et al (1992) The Open and Close Structure of Kunlun. Geological Publishing House, Beijing (in Chinese).

Jin XC, Wang J, Ren LD et al (1999) Problems concerning the tectonics of the west Kunlun orogen. In: Ma ZJ et al (eds) Advances in Structural Geology and Geophysics in China—In Honor of Academian Xingyuan Ma's 80th Birthday, pp.105–113. Seismological Press, Beijing (in Chinese with English abstract).

Khramov AN, Petrova GN, Peckersky DM (1981) Paleomagnetism of Soviet Union. In: McElhinny MW, Valencio DA (eds) Paleoconstruction of the Continents, Geodynamic Series, pp.177–194. Geological Society of America, Boulder, Colorado.

Klootwijk CT, Radhakrishnamurty C (1981) Phanerozoic paleomagnetism of the Indian plate and India-Asia collision. In: McElhinny MW, Valencio DA (eds) Paleoconstruction of the Continents, Geodynamics Series, pp.93–105. Geological Society of America, Boulder, Colorado.

Lai SC, Deng JF, Zhao HL (1996) Paleozoic ophiolites and its tectonic significance on the north margin of Qaidam basin. Geoscience 10(1): 18–28 (in Chinese with English abstract).

Li CY, Wang Q, Liu XY, Tang YQ (1982) Tectonic Map of Asia (1: 8,000,000) and Its Specialties. Geological Publishing House, Beijing (in Chinese).

Li JY (1987) Essential characteristics of Early Paleozoic ophiolites to north of Xar Moron River, eastern Nei Mongol and their plate tectonic significance. In: Contributions to the Project of Plate Tectonic in Northern China. no.2, pp.136–150. Geological Publishing House, Beijing (in Chinese with English abstract).

Li JY (1995) Main characteristics and emplacement processes of the east Junggar ophiolites, Xinjiang, China. Acta Petrologica Sinica 11(suppl.): 73–84 (in Chinese with English abstract).

Li JY (1996) The timing and special distribution of ophiolites in China. In: Zhang Q (ed) Study on the Ophiolites and Geodynamics. Geological Publishing House, Beijing (in Chinese with English abstract).

Li K et al (1962) Geology of Qilian Mountains. vol. 2, part II, pp.171–192. Science Press, Beijing (in Chinese).

Lin JL, Fuller M, Zhang WY (1985) Preliminary Phanerozoic polar wander paths for the North and South China blocks. Nature 313: 444–449.

Liu BJ, Xu XS, Xia WJ et al (1994) Atlas of Petrological Phase Paleogeography of South China (Sinian to Triassic). Science Press, Beijing (in Chinese).

Liu GH, Zhang SG, You ZD et al (1993) Main Metamorphic Rock Groups and Metamorphic Evolution of Qinling Orogenic Belt. Geological Publishing House, Beijing (in Chinese).

Liu L, Che ZC, Wang Y et al (1998) The evidence of Sm-Nd isochron age for the Early Paleozoic ophiolite in Mangya area, Altun Mountains. Chinese Science Bulletin 43(9): 754–756.

Lu YH (1976) Biologic strata and paleo-biogeography of Ordovician in China. Journal of Nanjing Institute of Geological Paleontology, no.7.

Meng XH, Ge M (2002) The sedimentary features of Proterozoic microspar (Molar-tooth) carbonates in China and their significance. Episodes 25(3): 185–195.
Meng XH, Ge M (2005) Sequences, Events and Evolution of the Sino-Korean Plate. Science Press, Beijing (in Chinese with English abstract).
Mu EZ (1983) Ordovician biostratigraphical types and biogeographical regions of China. In: The editorial of paleontology theory. Paleobiographic Provinces of China, Science Press, Beijing (in Chinese).
Peng LH (1984) Geological time of Ophiolite suite at south zone of Udormiao Group, Inner Mongolia and its tectonic significance. Chinese Science Bulletin 29: 104–107 (in Chinese).
Qiu YX, Chen HJ (1993) Professional Papers for the Geological Structure of Yunkaidashan and Its Adjacent Areas. Geological Publishing House, Beijing (in Chinese).
Qiu YX, Peng SM, Zhou YZ et al (1996) The geological features and evolution of metamorphism in Yunka—the Guidebook of Geology of T391 field trip for the 30th International Geologcial Conference, 63pp. Editorial Department of Acta of Zhongshan University, Guangzhou (in Chinese).
Remane J et al (2000) International Stratigraphic Chart. International Commission on Stratigraphy.
Rogers G, Dunning GR (1991) Geochronology of appinitic and related granitic magmatism in the West Highlands of Scotland: Constraints on the timing of transcurrent fault movement. J. Geol. Soc. London, 148, part 1: 17–27.
Scotese CR (1994) Continental Drift, 6th edn. The PALEOMAP Project, University of Texas at Arlington
Shu LS, Wang CY, Ma RS (1996) Granulite relics and pyroxene-facies ductile deformation in the northern boundary of the southern Tianshan. Scientia Geologica Sinica 31(4): 375–383 (in Chinese with English abstract).
Song SG, Su L (1998) Rheological properties of mantle peridotites at Yushigou in North Qilian Mountains and their implications for plate dynamics. Acta Geologica Sinica 72(2): 131–141.
Sun MZ, Xu KQ (1990) On the Caledonian granitoids and their geotectonic environments of south China. Journal of Nanjing University (4): 10–22 (in Chinese with English abstract).
Suo ST, Zhong ZQ, Zhou HW et al (2003) Kanfenggou UHP metamorphic fragment in eastern Qinling orogen and its relationship to Dabie-Sulu UHP and HP metamorphic belts, Central China. Journal of China University of Geosciences 14(2): 95–102.
Tan YJ (1992) The tectonic deformation and its evolution in the Southern Margin of Ordos Basin, China. Dissertation, China University of Mining & Technology, Beijing.
Tang KD, Yan ZY (1993) Regional metamorphism and tectonic evolution of the Inner Mongolian suture zone. J. Metamorphic Geol. 11(4): 511–522.
Trewin NH (2002) The Geology of Scotland, 4th edn. The Geology Society of London, London.
Van der Voo R (1993) Paleomagnetism of the Atlantic, Tethys and Iapetus Oceans. Cambridge University Press, Cambridge.
Wan TF, Zhu H, Zhao L et al (1996) Formation and Evolution of the Tancheng–Lujiang Fault Zone. China University of Geosciences Press, Wuhan.
Wan TF, Zeng HL (2002) The distinctive characteristics of the Sino-Korean and the Yangtze plates. Journal of Asian Earth Sciences 20(8): 881–888.
Wan TF, Zhu H (2007) Positions and kinematics features of Chinese blocks in global paleocontinental reconstruction during Paleozoic and Triassic. Geosciences 21(1): 1–13.
Wang HZ (1985) Atlas of Paleogeography of China. SinoMaps Press, Beijing (in Chinese).
Wang HZ, Li GC (1990) Comparative Table of International Strata Ages. Geological Publishing House, Beijing (in Chinese).
Wang HZ, Mo XX (1995) An outline of the tectonic evolution of China. Episodes 18(1–2): 6–16.
Wang Q, Liu XY, Li JY (1991) Plate Tectonics Between Chathaysian and Angaraland in China. Peking University Press, Beijing (in Chinese with English abstract).
Wang TH (1995) Evolutionary characteristics of geological structure and oil-gas accumulation in Shanxi-Shaanxi area. Jour. Geol. & Min. Res. North China 10(3): 283–398 (in Chinese with English abstract).

Wang YS, Chen JN (1987) Metamorphic belts and metamorphism of Qinghai Province and adjacent areas. Geological Memoirs, no.6. Geological Publishing House, Beijing (in Chinese).

Wang ZJ, Wu GJ, Xiao XC et al (1997) Explanatory Notes for Global Geoscience Transect, Golmud-Ejin Transect, China. pp.21–54. Geological Publishing House, Beijing (in Chinese).

Wu HR, Kuang GD, Wang ZC (2001) The Yunkai block since Silurian. Journal of Palaeogeography 3(3): 32–40 (in Chinese with English abstract).

Xia LQ, Xia ZC, Xu XY (1995) Dynamics of tectono-volcano-magmatic evolution from North Qilian Mountains, China. Northwest Geoscience 16(1): 1–28 (in Chinese with English abstract).

Xiao XC, Chen GM, Zhu ZZ (1978) A preliminary study on the tectonics of ancient ophiolites in the Qilian Mountain, northwest China. Acta Geologica Sinica 52(4): 281–295 (in Chinese with English abstract).

Xiao XC, Wang FG (1984) An Introduction to the Ophiolite of China. Bulletin of the Chinese Academy of Geological Sciences, 9: 19–30. Geology Publishing House, Beijing (in Chinese with English abstract).

Xiao XC, Tang YQ, Feng YM et al (1992) Tectonic Evolution of Northern Xinjiang and Its Adjacent Regions. Geological Publishing House, Beijing (in Chinese with English abstract).

Xu ZQ, Xu HF, Zhang JX et al (1994) The Zhoulangnanshan Caledonian subductive complex in the northern Qilian Mountains and its dynamics. Acta Geologica Sinica 68(1): 1–15 (in Chinese with English abstract).

Xu ZQ, Yang JS, Zhang JX et al (1999) A comparison between the tectonic units on the two sides of the Altun sinistral strike-slip fault and the mechanism of lithospheric shearing. Acta Geologica Sinica 73(3): 193–205 (in Chinese with English abstract).

Yan DP, Song HL, Fu ZR et al (1997) Metamorphic Core Complexes in the Western Margin of Yangtze Platform. Geological Publishing House, Beijing (in Chinese with English abstract).

Yan MC, Chi QH, Gu TX et al (1997) Chemical composition of upper crust in eastern China . Science in China, D 40(5): 530–539 (in Chinese).

Yang JL (1988) Cambrian. In: Yin HF et al (eds) Paleobiogeography of China. China University of Geosciences Press, Wuhan (in Chinese).

Yang JS, Xu ZQ, Li HB et al (1998) Discovery of eclogite at northern margin of Qaidam Basin, NW China. Chinese Science Bulletin 43(20): 1755–1760.

Yang WR, Guo TY, Lu YL et al (1984) "Opening" and "closing" in the tectonic evolution of China. Earth Sciences (3): 39–56 (in Chinese with English abstract).

Yang WR, Liu YY, Yang ZH et al (1993) Probing into the open and close of Asian continent from the new results of paleomagnetism from Qinling orogenic belt and the paleoland on both sides. In: China Working Group on International Geological Comparison Program. Project 321. Growth of Asia. Seismological Press, Beijing (in Chinese).

Yang WR, Wang GC, Jian P (2000) Research on the Tectono-Chronology of the Dabie Orogenic Belt. China University of Geosciences Press, Wuhan (in Chinese with English abstract).

Yang WR, Jian P, Han YJ (2002) Determination and significance of Caledonian high-pressure and ultrahigh-pressure metamorphism in Dabie orogen. Earth Science Frontiers 9(4): 273–283 (in Chinese with English abstract).

Yang ZY, Ma XH, Huang BC et al (1998) Polar wander paths of magnetism and block migration of north China in Phanerozoic. Science in China B 28(suppl.): 44–56 (in Chinese).

Yang ZY, Otofuji Y, Sun ZM et al (1998) Geomagnetic pole series of boundary between Cambrian and Ordovician in Tangshan, Hebei. Chinese Science Bulletin 43(17): 1881–1885 (in Chinese).

Ye HW, Zhang XZ, Zhou YW (1994) ^{40}Ar-^{39}Ar age and its geologic significance of vein crossite in glaucophane-schist, Mudanjiang area. Journal of Changchun University of Earth Sciences 24(4): 369–372 (in Chinese with English abstract).

Yin A, Nie SY (1996) A Phanerozoic palinspastic reconstruction of China and its neighboring regions. In: Yin A, Harrison M (eds) The Tectonic Evolution of Asia. Cambridge University Press, Cambridge.

Yin HF et al (1988) Paleobiogeography of China. China University of Geosciences Press, Wuhan (in Chinese).
Yin ZX, Xu DY, Pu QY (1965) Collection of denominations of China crustal movement. Geological Review 23(suppl.): 20–81 (in Chinese).
Zhai MG (1998) Three important high-pressure and high-temperature metamorphic zones in China and their geotectonic significance. Acta Petrologica Sinica 14(4): 419–429 (in Chinese with English abstract).
Zhang BY, Yu HN (1994) Deep-seated Nappe Structure of Hercynian-Indochina Collisional Zone in West Guangdong. Geological Publishing House, Beijing (in Chinese).
Zhang GW, Zhang BR, Yuan XC et al (2001) Qinling Orogenic Belt and Continental Dynamics. Science Press, Beijing (in Chinese).
Zhang JX, Xu ZQ, Chen W et al (1997) A tentative discussion on the ages of the subduction-accretionary complex/volcanic arcs in the middle sector of north Qilian Mountains. Acta Petrological et Mineralogical 16(2): 112–119 (in Chinese with English abstract).
Zhang JX, Xu ZQ, Xu HF et al (1998) Framework of North Qilian Caledonian subduction-accretionary wedge and its deformation dynamics. Scientia Geologica Sinica 33(3): 290–299 (in Chinese with English abstract).
Zhang JX, Zhang ZM, Xu ZQ et al (1999) The age of U-Pb and Sm-Nd for eclogite from the western segment of Altun Tagh tectonic belt-Evidence for existence of Caledonian orogenic root. Chinese Science Bulletin 44(24): 2256–2259.
Zhang JX, Zhang ZM, Xu ZQ et al (2000) Discovery of khondalite series from the western segment of Altun Tagh and their petrological and geochronological studies. Science in China D 43(3): 308–316.
Zhang JX, Meng FC, Qi XX (2002) Comparison of garnet zoning between edlogites in Da Qaidam and Xitieshan on the northern margin of the Qaidam basin. Geological Bulletin of China 21(3): 123–129 (in Chinese with English abstract).
Zhang Q, Chen Y, Zhou DJ et al (1998) Geochemical characteristics and genesis of Dachadaban ophiolite in North Qilian area. Science in China D 41(3): 277–281 (in Chinese).
Zhang YW, Jin ZJ, Liu GC et al (2000) Study on the formation of unconformaties and the amount of eroded sedimentation in Tarim basin. Earth Science Frontiers 7(4): 449–457 (in Chinese with English abstract).
Zhao J, Zhong DL, Wang Y (1992) Disaggregation of Lanchang Group in West Yunnan and its tectonic significance. In: Contribution to Geology Research by Post Doctors of Peking University, (1): 12–24. Seismological Press, Beijing (in Chinese with English abstract).
Zhao CJ, Peng YJ, Dang ZX et al (1996) Structure Framework of East Part of Both Jilin and Heilongjiang Provinces and Their Crustal Evolution. Liaoning University Press, Shenyang (in Chinese).
Zhong ZQ, You ZD, Zhou HW et al (1996) The evolution and basic structural framework of the basement of the Yunkai uplift in Gunagdong and Guangxi. Regional Geology of China (1): 36–43 (in Chinese with English abstract).

Chapter 5
Tectonics of Middle Devonian–Middle Permian (The Tianshan Tectonic Period, 397–260 Ma)

—formation of Tianshan–South Hingganling Collision Belt, development of the Emeishan Mantle Plume

In China the tectonic period from Middle Devonian to Middle Permian (397–260 Ma) has previously been called the Variscian or Hercynian Period, following the terms used for Late Carboniferous to Early Permian tectonic movements in Europe, but it is more appropriate that this period should be re-defined from China.

Mushketov (1928) first used the term "Tianshan Movement" on geological maps of Central Asia. Xie JR (1936) subdivided the Tianshan movements into two periods, the first at the end of the Devonian or Early Carboniferous, and the second at the end of the Late Carboniferous. Since that time the term has been commonly used in China. Li TD (2003, personal communication) has suggested that the entire Late Paleozoic tectonic period should be named the "Tianshan Period" and this usage is followed on this account. The Tianshan Tectonic Period extended over a period of 130 million years, nearly half a cosmic year.

The Tianshan–South Hingganling Tectonic Period commenced in the Middle Devonian and closed at the end of the Middle Permian. At this period most of the blocks which compose the Chinese continent were dispersed and in the process of migration. The main tectonic events were the formation of Tianshan-South Hingganling Collision Belt between the Xiyu (including the Tarim–Alxa–Qaidam Blocks)–Sino-Korean plates and the Middle Mongolia Block (southern margin of Siberian Plate), and the development of the Emeishan Mantle Plume. Over most of Chinese continent sedimentation was continuous, with no major tectonic activity at the end of the Permian (251 Ma) and no break or almost say no unconformity between the Permian and Triassic systems.

5.1 Sedimentation, Paleogeography and Paleontology

The thickness of the Late Paleozoic strata in China has not been specifically calculated, but the characteristics of Late Paleozoic sedimentation are broadly the same as those described in Chapter 4 for the Paleozoic as a whole.

Early Devonian deposits are absent over most of the Chinese continent (Fig. 5.1). In the Tianshan-South Hingganling region, Middle and Late Devonian (397–359 Ma) deposits are mainly bathyal flysch (turbidite), and the included fauna and flora belong to the temperate Siberian Biogeographic Province. Volcanic activity occurred in the Altay, Junggar and Tianshan regions. Terrestrial clastic sediments were deposited in sedimentary basins on the northern margin of the Dunhuang-Alxa Block, and in the Beishan and Qilian areas. On the southwestern margin of the Tarim Plate, sandy mudstones were deposited

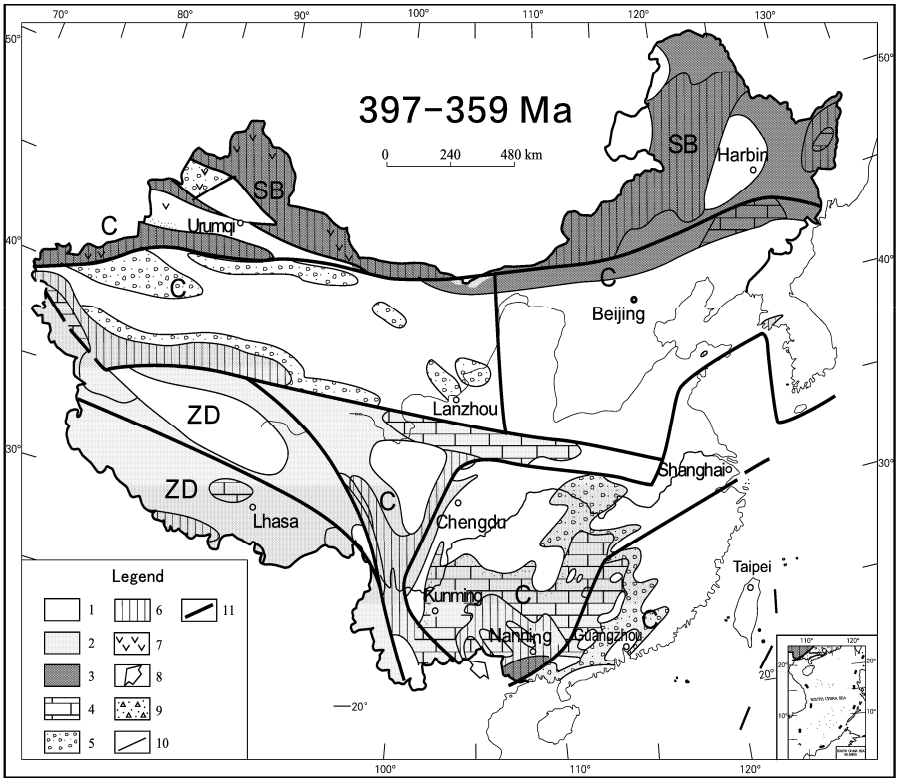

Fig. 5.1 Paleogeographic sketch map of the Chinese continent in the Middle and Late Devonian (397–359 Ma) (Data after Wang HZ et al., 1985; Zhao XW, 1988; Liu BJ et al., 1994 and recompiled).

Legend: 1. Land or area of erosion; 2. Shallow marine, continental shelf; 3. Bathyal, continental slope; 4. Carbonate deposits; 5. Conglomerate and sandstone deposits; 6. Sandy mudstone deposits; 7. Volcanics area; 8. Direction of marine transgression; 9. Glacial clastic-mud group; 10. Border of sedimentary facies or geological units; 11. Plate boundaries, perhaps with residual oceanic crust

C. Central China Biogeographic Province; SB. Peri-Siberian Biogeographic Province; ZD. Peri-Gondwanan (Yunnan–Tibet) Biogeographic Province.

in a shallow sea. The fauna and flora in shelf to bathyal deposits on the Xiyu Plate, and on the northern margins of the Sino-Korean Plate all belong to the Central Chinese Biogeographic Province (Zhao XW, 1988). There are no Devonian deposits over most of the Sino-Korean Plate, but they do occur in the east Shandong (Jiaodong) Peninsula and at Imjingang in the Korean Peninsula. In the Early Devonian (416–397 Ma) clastic deposits lay down on the South Yangtze Plate, and in the Middle Devonian a marine transgression progressed across the plate from southwest to northeast, with the deposition of shelf carbonates. In Hubei and NW Jiangxi provinces clastic shelf sediments were deposited, but the Devonian system is absent in the Lower and Upper Yangtze (Sichuan Province) regions. In the Qinling area, the deposits are mainly shelf carbonates. In west Sichuan and middle Yunnan provinces, the deposits are sandy shelf mudstones. In the western Cathaysian Plate carbonate shelf sediments are interrupted by areas of erosion which were islands during the Devonian. The Devonian fauna and flora in the areas from west Sichuan to middle Yunnan, from the Yangtze to the Cathaysian Plate, all belong to the Central China Biogeographic Province. In the Devonian North China and South China both belonged

to the tropical Central China Biogeographic Province (Zhao XW, 1988). There is very little difference between the faunas and floras of the Sino-Korean, Yangtze and Xiyu plates, showing that these were neighboring plates occupying the same tropical environment.

Because of limited information, the nature and extent of Devonian sediments in the Qinghai-Tibet region are not very clear. Perhaps there were ancient land areas in the Qiangtang region. Marine shelf carbonates occur in the Gangdise region and clastic shelf deposits in the central Himalayan Mountains. All these deposits contain a tropical fauna and flora, similar to Peri-Gondwanan (Yunnan-Tibet) Biogeographic Province. Devonian fauna and flora in China define three biogeographic provinces: the Peri-Siberian; Central China and Peri-Gondwanan (Yunnan-Tibet) Biogeographic Provinces (Zhao XW, 1988) (Fig. 5.1).

During the Carboniferous (359–299 Ma), deposition on the Chinese continent was more extensive (Fig. 5.2). In the central Sino-Korean Plate, after a period of denudation and planation, which lasted from the Middle Ordovician to the Early Carboniferous, the early epoch of Late Carboniferous clastic shelf sediments of the Hutian and Benxi formations were deposited, characterized by rich bauxitic shales, followed by the Jinci Formation, characterized by alternating marine and terrestrial deposits, including coals, in a series of sedimentary cycles (China National Commission on Stratigraphy, 2001).

Seismic exploration of the Carboniferous system in North China has shown that the thickness of the sediments is relatively uniform, ranging from 50m in the Qingyang region (~108°E, 36°N) to 100m in the Hebei-Shandong depression (Wang TH, 1995). Carboniferous fauna and flora in the Sino-Korean Plate belong to the subtropical-tropical North China Biogeographic Province, with the typical fossil land plants: *Neuropteris gigantea, Linopteris neuropteroides, Eleutherophyllum mirabile, Pecopteris aspera*, etc. Marine fossils, anthozoans, fusulinids and brachiopods, are very similar to those in the South China Biogeographic Province. Bathyal flysch was deposited in faulted depressions in southern Inner Mongolia on the northern margin of the Sino-Korean Plate, together with the products of volcanic eruptions. During the Late Carboniferous important deposits of bauxite and sedimentary iron ore were formed on the Sino-Korean Plate (Wang HZ et al., 1991).

Marine regression commenced during the Carboniferous in the Tianshan–South Hingganling and the Altay-Junggar zones and the Xiaohingganling–Songhuajiang–Nenjiang areas were subjected to tectonic compression and were uplifted to form part of the continent. The deposits are mainly clastic and carbonate sediments with volcanics, while locally in depressions bathyal sediments continued to be deposited. Typical fossils are: small single corals (*Hapsiphyllum, Amplexizaphrentis, Zaphrentites, Kinkaidia, Cyathaxonia*), brachiopods (*Rotaia, Syringothyris, Pseudosyrinx*) and an Angara flora (*Caenodendron primaevum, Chacassopteris consinna, Cardioneura microphylla*), being characteristics of the northern cool-temperate Peri-Siberian Biogeographic Province.

Because of abundant fossils and its distinctive sedimentary characteristics, the Carboniferous System can be defined easily in South China. The Lower Carboniferous is made up of the Yan'guan and Datang periods and the Upper Carboniferous of the Weining and Maping periods. Apart from areas of uplift in the center and on the western margins, shelf carbonates were deposited over most of the Yangtze Plate. Carbonate shelf sediments were also deposited on the Cathaysian Plate. Most of the Xiyu Plate was uplifted during Carboniferous to form a continental area, except for the Dunhuang-Altun Zone where bathyal turbidites were deposited. A rift depression formed in the west Sichuan-middle Yunnan area, in which bathyal carbonates and clastics were deposited, associated with basic volcanics. Typical fossils in South China are: anthozoans with local characteristics (*Cystophrentis, Chuanshanophyllum, Pseudouralinia, Fuchungopora, Huangongophyllum, Donetzites, Jintingophyllum, Kueichouphyllum, Yuanophyllum, Qinglongshanophyllum*), brachiopods (*Yanguania, Eochoristites, Martiniella*), a distinctive flora of *Lycopsida* and *Sphenopsida* (*Lepidodendron gaolishanense, Sublepidodendron mirabile, Cardiopteridium spitsbergense, Triphyllopteris collombiana*), and during the Late Carboniferous, fusulinids (*Profusulina, Fusulina, Fusulinella, Pseudostaffella, Triticites*). These fossils show that the South China Biogeographic Province lay in a warm humid tropical environment during the Carboniferous.

Fauna and flora in the Yangtze, Cathaysian and west Sichuan-middle Yunnan areas belong to the subtropical-tropical South China Biogeographic Province, and the fauna and flora of the Xiyu Plate are also similar to those of the South China Province. Clastic shelf sediments were deposited in the Alxa and Qilian regions, and shallow marine carbonates on the western and northeastern margins of the Tarim Plate. During the Early Carboniferous, widespread bauxite, gypsum, iron and manganese deposits were formed on the Yangtze, Cathaysian and Xiyu plates (Wang HZ et al., 1991).

Glacial pebbly mudstones were deposited in the Qiangtang, Gangdise, and Himalayan regions in the Carboniferous, associated with a Gondwana coldwater fauna. Typical fossils are small single corals (*Ekvasophylloides, Rhopalolasma*, *Parahumboldtia*) and brachiopods (*Unispirifer, Spirifer, Fusella, Tylothyris, Pseudosyrinx, Syringothyris*) (Yang FQ, 1988; Wang HZ et al., 1991; Fig. 5.2).

It is very obvious that the blocks making up the Chinese continent were subject to different climatic conditions during the Carboniferous (Yang Fengqing, 1988): the Tianshan-Hingganling Zone be-

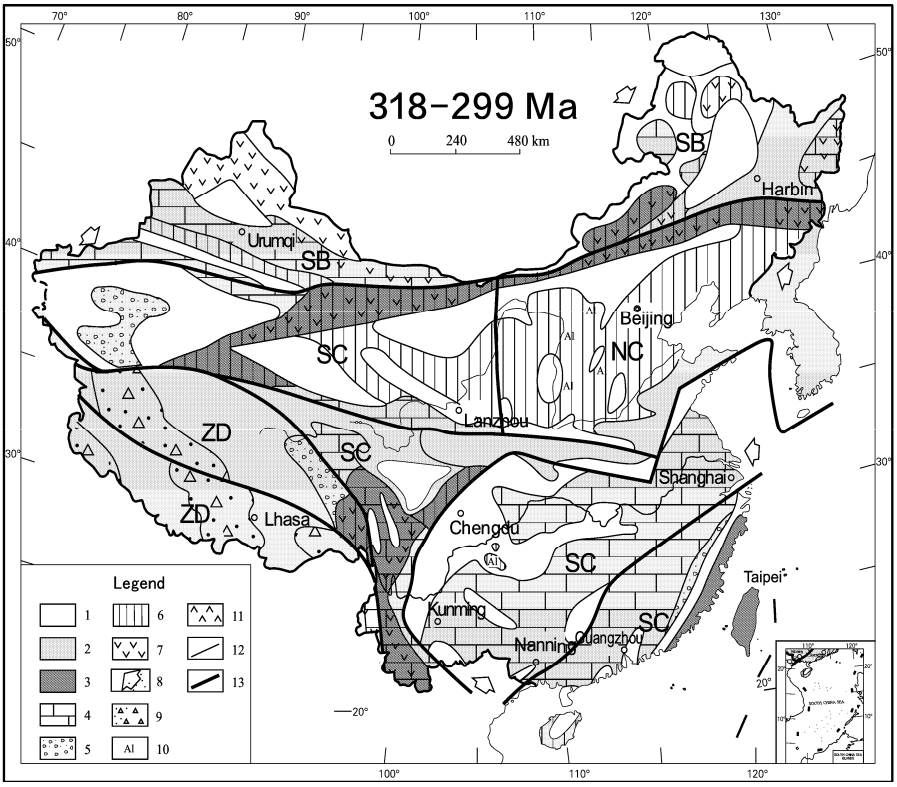

Fig. 5.2 Paleogeographic sketch of the Chinese continent in the Late Carboniferous (318–299 Ma) (Data after Wang HZ et al., 1985, 1991; Yang FQ, 1988; Liu BJ et al., 1994; Meng XH et al., 2002 and recompiled).

Legend: 1. Land or area of erosion; 2. Shallow sea, continental shelf; 3. Bathyal, continental slope; 4. Carbonate deposits; 5. Conglomerate and sandstone deposits; 6. Sandy mudstone deposits; 7. Areas of volcanic rock; 8. Direction of marine transgression; 9. Glacial clastic-mud group; 10. Bauxitic formation; 11. Gypsum and saline, tide flat deposits; 12. Boundaries of sedimentary facies or geology; 13. Plate boundaries, perhaps with residual oceanic crust.

NC. North China Subtropical-Tropical Biogeographic Province; SC. South China Subtropical-Tropical Biogeographic Province; SB. Peri-Siberian Subtemperate Biogeographic Province; ZD. Yunnan–Tibet Cold Biogeographic Province.

longs to the cool-temperate Peri-Siberian Biogeographic Province; the Sino-Korean Plate belongs to the subtropical-tropical North China Biogeographic Province; the South China blocks (including the Yangtze, Cathaysian, west Sichuan and Xiyu plates) also belonged to the subtropical-tropical South China Biogeographic Province, but have a very different fauna and flora from the North China area; the Yunnan-Tibet blocks belong to the Gondwana Biogeographic Province in a cold-cool climatic zone with glaciers on a continental margin (Fig. 5.2).

The climate on the blocks making up the Chinese continent during the Carboniferous ranged from cold in the north and south to warm in the middle firstly. The blocks in the Chinese continent extended across the world's climatic zones; the Peri-Siberian blocks migrated into the northern temperate zone; the Sino-Korean, Yangtze, Cathaysian, west Sichuan and Xiyu plates remained near the equator, while the Peri-Gondwanan blocks migrated southwards to the margins of the glacial zone.

During the Early and Middle Permian (299–260 Ma), the Sino-Korean Plate was still covered by broad sedimentary basins (Fig. 5.3). The sediments were mainly clastic with alternating marine and terrestrial facies (Taiyuan and Lower Shihezi periods), with the lower part containing coal-bearing strata (China National Commission on Stratigraphy, 2001). So the sedimentary environment was very different from that in the Carboniferous. Coarse clastic marine molasse was deposited on the northern margin of the Sino-Korean Plate, while shallow marine shelf carbonates and coal-bearing sandy mudstones were deposited on the southern Sino-Korean Plate. The water in this sedimentary basin became gradually deeper, and the grain size of the sediments became gradually finer from north to south (Meng XH et al., 2005).

The pattern of sedimentation indicates that the Sino-Korean Plate migrated northwards during the Permian and collided with the South Hingganling-Inner Mongolia–Tianshan blocks forming the Yinshan-Xar Moron He Collision Zone with the development of high mountains along the northern border of the plate. However, it is not certain that a foreland basin developed on the Sino-Korean Plate (Meng XH et al., 2005). It is not possible to demonstrate by seismic profiling whether the Sino-Korean Plate was subducted beneath the Yinshan-Xar Moron He Collision Zone. But the subduction must have occurred, although there is little evidence, otherwise it is difficult to explain the formation of a foreland basin on the Sino-Korean Plate. Carbonates were deposited on the southern part of the Sino-Korean Plate (Fig.5.3), during the Permian; there is no evidence that there are mountains in this area and there are no signs of a collision.

Permian sediments reach a thickness of 700–1,000 m at Yinchuan (~106°E, 38°N), Qingyang-Yan'an (~108°E, 36°N), Suide-Yulin (~110°E, 38°N) and in the Hebei-Shandong (~114–119°E, 36–41°N) faulted depression, but only 300–600 m in the N-S trending uplifted zones of Xinzhao–Uxin qi (~109°E, 38.5°N) and Huoshan (~112°E, 36.5°N) (Wang TH, 1995). Typical fossils in the Permian sediments are: flora (*Gigantopteris*, *Gigantonoclea*, *Emplectopteris triangularia*, *Cathaysiopteris whitei*, *Sphenophyllum*), brachiopoda (*Lingula* sp.) (Xu GR et al., 1988). The center of the Xiyu Plate was uplifted and became a land area, with a fauna and flora similar to those of the North China Biogeographic Province, but shelf carbonates and bathyal sandy mudstones were deposited on the northern and southern parts of the plate, characterized by the mixing of forms from the North and South Chinese Biogeographic Provinces (Xu GR et al., 1988; Shi GR et al., 1995; Shi GR, 2006; Fig. 5.3).

During the Early and Middle Permian a bathyal sedimentary environment continued in the South Hingganling-Inner Mongolian zone (Fig. 5.3), with the deposition of sandy mudstones and carbonates, together with volcanic rocks. At the end of the Carboniferous the Tianshan Block had completed its northward migration and became amalgamated with the Junggar Block, and in the Permian it was uplifted into a land area. Typical fossils include an Angaran flora (*Zamiopteris, Crassinervia, Nephropsis, Walchia*), gymnosperm pollen, cold water brachiopods (*Spiriferella, Kochiproductus, Yakovlevia*), anthozoans (*Tahylasm, Calophyllum*), fusulinids (*Pseudodoliolina*、*Monodiexodina*) (Xu GR et al., 1988), belonging to the Peri-Siberian Biogeographic Province.

During the Early and Middle Permian, shelf carbonates were deposited in South China, including most part of the Yangtze Plate, and in the Aba-Litang area in West Sichuan (Fig. 5.3). The Lower Permian (299–270 Ma) includes the Zisong and Longlin periods, the Middle Permian (270–260 Ma), the

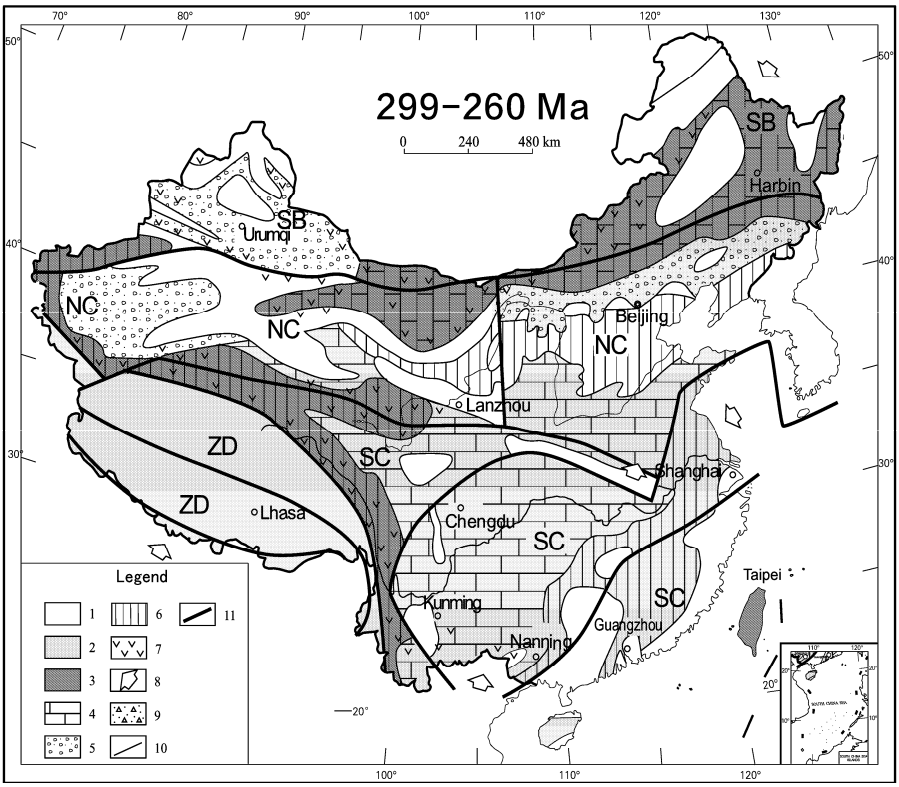

Fig. 5.3 Paleogeographic sketch of the Chinese continent in the Early and Middle Permian (299–260 Ma) (Data compiled from Wang HZ et al., 1985; Xu GR et al., 1988; Liu BJ et al., 1994; Meng XH et al., 2002).

Legend: 1. Land or area of erosion; 2. Shallow marine, continental shelf; 3. Bathyal, continental slope; 4. Carbonate deposits; 5. Conglomerate and sandstone deposits; 6. Sandy mudstone deposits; 7. Area of volcanic activity; 8. Marine transgression direction; 9. Glacial pebbly mudstone; 10. Borders of sedimentary facies or geological units; 11. Plate boundaries, perhaps with residual oceanic crust.

NC. Temperate North China Biogeographic Province; SC. Subtropical-tropical South China Biogeographic Province; SB. Cool temperate Peri-Siberian Biogeographic Province; ZD. Cool temperate Yunnan-Tibet Biogeographic Province.

Qixia, Xiangbo, Maokou and Lengwu periods, and the Upper Permian (260–251 Ma), the Wujiaping period, in which the Longtan coal-bearing formation was developed, and the Changxing period (China National Commission on Stratigraphy, 2001; International Commission on Stratigraphy, 2004). However, in the eastern Yangtze and Cathaysian plates shallow marine sandy mudstones were deposited. Typical fossils are: anthozoans (*Wentzelloophyllum volzi*, *Hayasakaia elegentula, Polythecalis yangtzeens*, *Cystommichelina*), fusulinids (*Schwagerina tschernyschewi, Parafusulina, Neoschwagerina*), ammonoids (*Rotodiscoceras*, *Pseudotirolites*, *Pleuronodoceras*) and brachiopods (*Monticu-lifera, Cryptspirifer*). These forms all belong to the tropical Tethyan Biogeographic Province, or to the South China Biogeographic Province (Xu GR et al., 1988).

The Yunnan-Tibet area was characterized by the deposition of shelf carbonates (Fig. 5.3), which extended to the northern border of the Karakorum and East Kunlun regions, with the eastern border along the Lancangjiang Zone. The boundary of the Yunnan-Tibet and the South China Biogeographic

Provinces was also the boundary between the Gondwana and Eurasian continents. The segment of the boundary in the Changning-Menglian area of China represents the site of the Lancangjiang Ocean, as first proposed by Liu BP et al. (1991, 1993). The boundary then extends southwards across Thailand through Chiangmei (~99°E, 19°N) and Tak (~99°E, 17°N), through the Gulf of Thailand and the centre of the Malay Peninsula (~102°E, 4°N) to Bangka island, south of Sumatra (Barber et al. 2005). The border extends westwards through East Kunlun (83–86°E, 36°N), Karakoram (78°E, 35°N to 75°E, 37°N), along the southern Caspian Sea and northern Turkey, as far as the Alps and Pyrenees.

Gondwanan glacial sediments occur in the Yunnan-Tibet region to the south of the Yarlung Zangbo River zone, associated with a cold-water fauna, such as solitary corals (*Lytvolasma, Wannerophyllum*), ammoniods (*Uraloceras*), large thick-shelled brachiopods (*Taeniothaerus*), and a Gondwanan flora (*Glossopteris, Sphenophyllum*) (Xu GR et al., 1988). However in the Qiangtang and Gangdise blocks this cool water fauna is mixed with forms belonging to the South China warm-water fauna, indicating that during the Permian the Qiangtang and Gangdise blocks are separated from the Gondwanan super-continent and migrated northwards into the temperate zone (Xu GR et al., 1988; Shi GR et al., 1995).

In the Early and Middle Permian, the blocks which now form the Chinese continent were distributed through the paleoclimatic zones and belonged to different biogeographic provinces, but during the Late Permian these relationships changed (Fig. 5.3). The fauna and flora of the Xiyu Plate were similar to those of North China, and they were both in the temperate climatic zone. The fauna and flora in the Yangtze, Cathaysian and west Sichuan regions still belonged to the South China tropical warm-water climatic zone. Although North China and South China both belonged to Chinese-Tethyan Biogeographic Domains, and differences can be found in their fossil faunas and floras. The fauna and flora in the Tianshan–South Hingganling region are similar to those of the Siberian Biogeographic Province, belonging to the northern cool temperate zone, with a typical Angaran flora, and a mixed fauna of cold- and warm-water forms (Xu GR et al., 1988; Shi GR, 2006). However, the Yunnan-Tibet Biogeographic Province still belonged to the southern Gondwana cold and temperate zone (Xu GR et al., 1988).

In the Chinese continent the Peri Siberian Biogeographic and the Peri Gondwanan (Yunnan-Tibet) Biogeographic Provinces can be defined easily, as they had distinctive faunas and floras during the Late Paleozoic. There were almost no differences in the faunas and floras of the Sino-Korean, Xiyu and Yangtze plates, during the Devonian, but they became distinct during the Carboniferous and Permian. During the Carboniferous the faunas and floras of the Xiyu Plate were similar to those of the South China Biogeographic Province, but during Permian they were closer to the North China Biogeographic Province. These changes can be easily explained using evidence from paleomagnetism (Figs. 5.4–5.9). During the Devonian the Chinese continental blocks were all nearly at the same latitude and were arranged with an E-W trend, so that they had similar faunas and floras. In the Carboniferous some of these blocks migrated northwards, so that the blocks were re-arranged with an NW-SE trend and extended across different latitudes and climatic zones, so that their faunas and floras were different. However, the Xiyu and Yangtze plates had a similar paleo-latitude, and both plates belonged to South China Biogeographic Province. During the Permian, the paleo-latitudes of most of the Chinese blocks were still very different, so that their faunas and floras are also distinctive. However, the Xiyu and Sino-Korean plates collided with the southern side of the Tianshan–South Hingganling Collision Belt and became amalgamated with the Siberian continent, so that they became part of the same biogeographic province.

5.2 Paleomagnetism and Paleotectonic Reconstruction

The paleotectonic reconstruction of the blocks forming the Chinese continent during the Late Paleozoic is discussed using the methods of paleomagnetic research and paleotectonic reconstruction, already described in Chapter 4 for the Early Paleozoic, and the paleomagnetic data all plotted in Appendix 6.

Paleomagnetism and paleotectonic reconstructions for the Siberian, Indian, and Australian plates, surrounding the Chinese continent during the Late Paleozoic, will be first discussed (Fig. 4.5). From the Devonian to the Early Permian, using a central reference point to represent each of continental blocks, one can find the Siberian (Angaran) Plate migrated from 33.4°N to 37.5°N latitude, a paleolatitude change of 4.1°, the rate of latitudinal displacement was only 0.34 cm/yr, much lower than its rate of movement during the Early Paleozoic. The measurements of paleomagnetic declination show that the Siberian Plate rotated counter-clockwise through a rather small angle of 13.9° (Khramov et al., 1981; Appendix 6). During the same period the Indian Plate migrated southwards from 28.4°S to 37.3°S, a change of 8.9° in latitude, at a rate of 0.74 cm/yr. During the Devonian the Indian Plate rotated 40° counterclockwise, and then during the Carboniferous and Permian rotated 67° clockwise (Klootwijk and Radhakriehnamurty, 1981; Appendix 6). In the Late Paleozoic the Australian Plate rotated ~20° counterclockwise and migrated southwards from 4.4°S to 56.3°S paleolatitude, at a rate of movement of 4.3 cm/yr (Van der Voo, 1993; Appendix 6). While the Siberian and Indian plates migrated slowly over only a short distance during the Late Paleozoic, the Australian Plate moved very rapidly southwards, while rotations of the Siberian and Australian plates were small compared with those of the Indian Plate, although Both Australia and India Plates were the parts of Gondwana Supercontinent, which was caused by rapid opening of east part of Paleo-Tethys Ocean (Figs. 5.4–5.9).

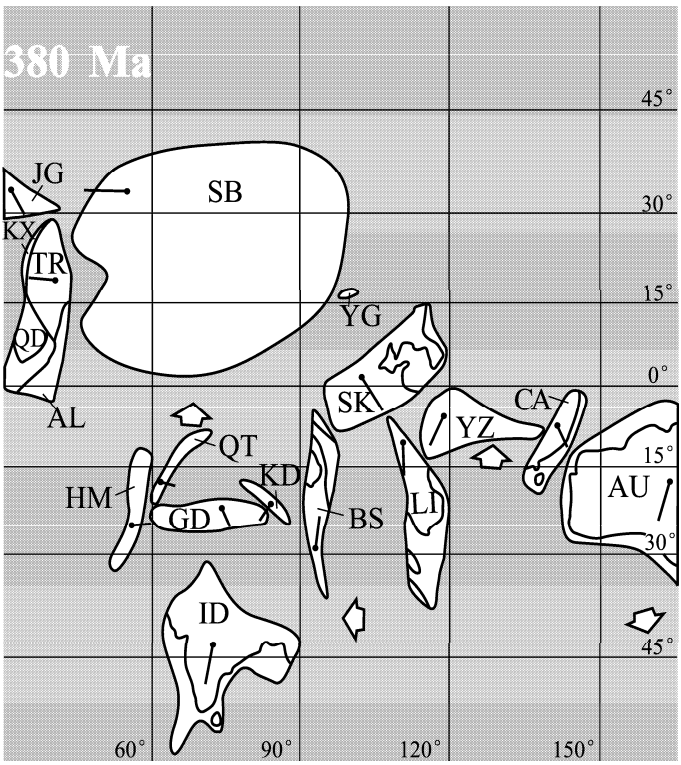

Fig. 5.4 Paleotectonic reconstruction of the Chinese continent and its adjacent blocks in the Devonian (380 Ma) (Data showed in Appendix 6)

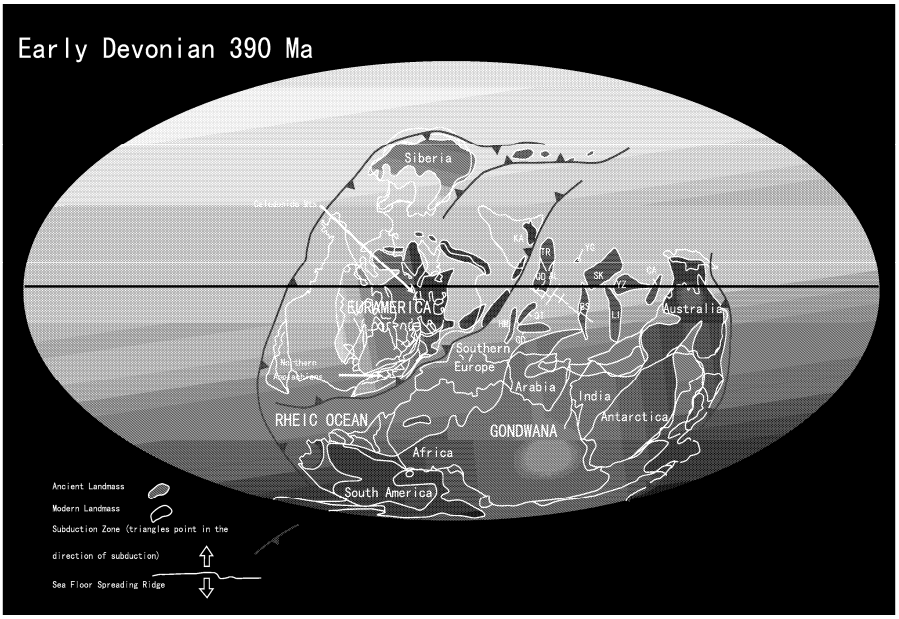

Fig. 5.5 Paleo-continental reconstruction of the globe during the Early Devonian (390 Ma) (Wan TF and Zhu H, 2007) (Data of Chinese blocks from Appendix 6, others from Scotese's web).

Paleogeomagnetic determinations show that in the Paleozoic the three major plates surrounding the Chinese continental blocks became dispersed (Fig. 4.5): the Siberian Plate moved directly northwards across 71° of latitude (~7,000 km); the Australian Plate moved southwards across 42° of latitude (~4,100 km); at first the Indian Plate was relatively stable, but during the Late Paleozoic moved rapidly southwards over a total distance of 27° of latitude (~2,600 km) (Figs. 5.4–5.9). These paleogeomagnetic data (Appendix 6), indicating dispersion of the major continental blocks throughout the Paleozoic, suggested that the continental blocks forming the Chinese continent migrated similarly and became more dispersed over this period.

There are no deposits of Silurian and Devonian ages on the Sino-Korean Plate, but it is postulated that the plate moved from 12.9°S to 10.8°N, about 23.7° of latitude change, with little change declination during these periods. Paleomagnetic determinations on Carboniferous and Permian strata in the Sino-Korean Plate show that from the Middle Carboniferous to the Permian, the plate moved northwards through 3.1° of latitude (~310 km), at a rate of movement of little more than 1 cm/yr, and that it rotated 18.5° counterclockwise from 338.2° to 319.7°. The Yangtze Plate migrated from 6.9°S to 3.3°N (~1,000 km) from the Devonian to the Early Permian, with a rate of movement of 0.84 cm/yr, more slowly than the Sino-Korea Plate, and rotated counterclockwise through 7.6°. The Cathaysian Plate remained in the southern hemisphere during the Devonian and Early Carboniferous, moving only 1.5° (~150 km), from 11.8°S to 10.3°S latitude, but rotated counterclockwise through 52.3° from 111.2° to 58.9 ° (Figs. 4.6, 5.4–5.9; Appendix 6).

The Junggar Block remained in the northern hemisphere during the Late Paleozoic moving only from 29.7°N to 28.3°N latitude, but rotated clockwise through 77° from 342.4° to 59.4°. The Tarim Block which formed part of the Xiyu Plate moved through 10° of latitude (~1,000 km) northwards from 21.2°N to 31.3°N between the Devonian and the Permian, at a rate of more than 0.84 cm/a, and rotated counterclockwise through 73.4°, from 94.5° to 21.1° (Figs. 5.4–5.9; Appendix 6). Paleomagnetic data

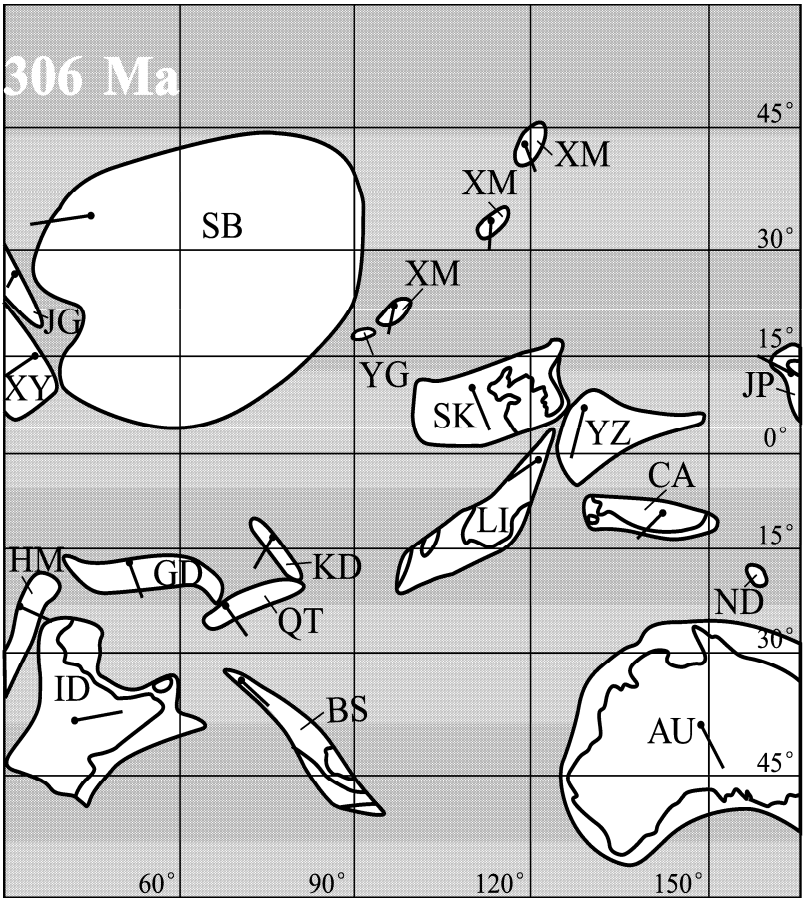

Fig. 5.6 Paleotectonic reconstruction of the Chinese continent and its adjacent blocks in Carboniferous (306 Ma) (Data showed in Appendix 6).

from the Alxa-Dunhuang and Qaidam blocks shows that both blocks were located at a low latitude in the northern hemisphere, but the data is not well constrained and may have rather large errors.

Late Paleozoic paleomagnetic data from the East Kunlun, Qiangtang, Gangdise and Himalayan blocks show that they were all located between 20°S and 30°S latitudes, in a similar position to the Indian Plate and adjacent to the Gondwana (Figs. 5.4–5.9).

Paleomagnetic data from the East Kunlun Block shows that it was close to the Gondwana in the Late Paleozoic, and did not form any part of the Xiyu Plate. A cold-water fauna has recently been found in the Qixia period of the Early Permian in the Muztag region (87.9°E, 36.1°N) in the East Kunlun Block, confirming this interpretation (Sun QL et al., 2002). On the other hand, the West Kunlun (Kudi) Block was part of the Xiyu Plate. From the collision history and paleomagnetic data from the Xiyu Plate, the East Kunlun and West Kunlun blocks did not belong to the same tectonic unit and the locations of these

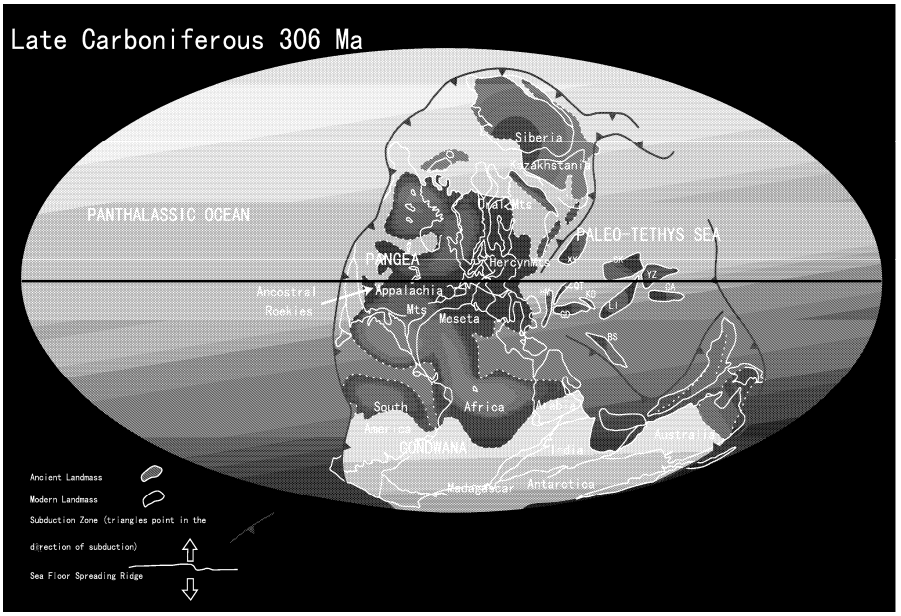

Fig. 5.7 Paleo-continental reconstruction of the globe during the Late Carboniferous (306 Ma) (Wan TF and Zhu H, 2007; Data of Chinese blocks from Appendix 6, others from Scotese's web).

plates were completely different during the Late Paleozoic*. Reliable paleogeomagnetic data from the Late Paleozoic of the Baoshan-Sibumasu Block is scarce, so that its position can only be suggested from paleontological, sedimentary and paleogeographic evidence (Figs. 5.4–5.9).

Paleomagnetic data shows that the Siberian Plate migrated a great distance northwards during the Paleozoic, while during the Late Paleozoic the Gondwana and Indian plates migrated southwards. The continental blocks forming the Chinese continent remained dispersed, migrated gradually northwards by different degrees during the whole of the Paleozoic. At particular times, blocks collided and amalgamated, for example the Altay–Junggar-Ergun Collision Belt was formed in Early Paleozoic, the blocks forming the Xiyu Plate were amalgamated together in the end of Early Paleozoic, and the Tianshan–South Hingganling Collision Belt occurred during the Carboniferous and Early Permian.

The Chinese continental blocks were arranged along the equator during the Early Paleozoic, however in the process of gradual movement arrived at an N-S arrangement in the Carboniferous. This was an important turning point in the assembly of the Chinese paleo-continent.

* The tectonic evolution of the West Kunlun, East Kunlun, and Qinling-Dabie blocks were very different. Geographically, they consist of similar E-W trending mountain belts. The Kunlun–Qinling–Dabie region has therefore been regarded as a single tectonic belt, and named the "Central Orogenic Belt". This is correct, if "Central Orogenic Belt" is used only as a geographic term for an E-W trending mountain belt in the center of China recently, but is incorrect geologically, because the parts of West Kunlun–East Kunlun–Qinling–Dabie Belt had different tectonic evolutionary histories.

The West Kunlun and Tarim blocks were amalgamated at the end of the Early Paleozoic and became part of the Xiyu Plate. The East Kunlun Block was an isolated block within Paleo-Tethys to the north of the Gondwanan Supercontinent during the Late Paleozoic, and amalgamated with the southern margin of the Qaidam Block at the end of the Triassic. The Qinling -Dabie Collision Belt lies between the Sino-Korean and Yangtze plates, and was finally completed at the end of the Triassic. From the Triassic to the Neogene the East Kunlun and Qinling-Dabie blocks were located in different latitudes and had different tectonic positions. However, they collided and became amalgamated with the Eurasian continent, by the end of Triassic. In the Middle to Late Quaternary these blocks moved to almost the same latitude.

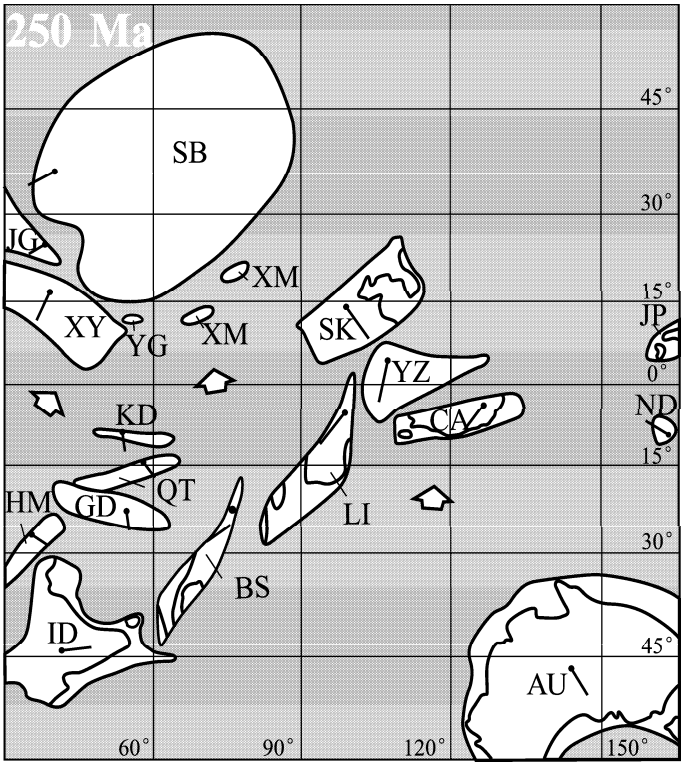

Fig. 5.8 Paleotectonic reconstruction of the Chinese continent and its adjacent blocks in Permian (250 Ma) (Data showed in Appendix 6).

In that the above Chinese continental blocks are located at northern parts of Paleo-Tethys Ocean, when Paleo-Tethys Ocean expanded and Siberian Plate moved to north greatly and fast in Paleozoic, these blocks all moved to the north in different degrees, the Sino-Korean and Xiyu Plates maybe following the Siberian Plate moved to north faster, and others did slower (Wan TF and Zhu H, 2007). But till now no researcher explained why the Siberian Plate moved to north greatly and fast and the Paleo-Tethys Ocean expanded during Paleozoic. Although the causes and mechanisms of plate migration are not clear enough, the evidence for the existence of plates, continental blocks, and continual movement during their geological and tectonic evolution cannot be denied.

5.3 Rock Deformation, Metamorphism and Stress Field

The nature of stratigraphic contacts defines the importance and intensity of tectonic activity in different areas at different periods. The distinctive character of stratigraphic contact relationships in the blocks of Chinese continent at the end of Late Paleozoic can be used to elucidate the history of tectonic activity (Fig. 5.10). Angular unconformities, indicating major tectonic activity at the end of the Late Paleozoic, are found in five regions: (1) Altay–Junggar–Ergun Belt, (2) Tianshan–South Hingganling Belt and its

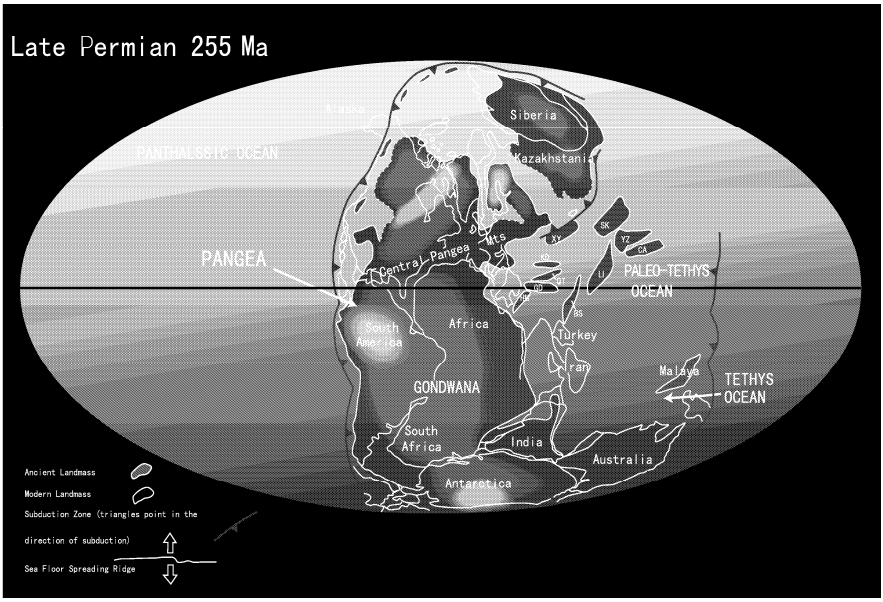

Fig. 5.9 Paleo-continental reconstruction of the globe during the Late Permian (255 Ma) (Wan TF and Zhu H, 2007) (Data of Chinese blocks from Appendix 6, others from Scotese website).

southern margin, (3) West Kunlun–Altun–Beishan, (4) Qaidam Basin, and its northern and southern margins (5) Bayanhar (southern Qinghai)–West Qinling (yellow in Fig. 5.10).

In the Junggar-Ergun Belt and the Tianshan region (i.e. West Tianshan–South Hing-ganling Belt), there are two angular unconformities, one between the Devonian and Carboniferous, generally regarded as marking the subduction of oceanic crust with plate collision at the end of the Early Carboniferous (Coleman, 1989; Xiao XC et al., 1992; He GQ et al., 1994), and one between the Carboniferous and Permian, generally recognized as representing a later collision event. Both above were tectono-thermal events, accompanied by regional metamorphism. The tectonic activity was most intense in the Tianshan region, so it is reasonable to name the period of tectonic activity in the Chinese continent near the end of the Late Paleozoic the "Tianshan Event".

In west Junggar an unconformity occurred earlier between the Early and Middle Devonian. In Xilin Gol region an angular unconformity occurred between the Devonian and Carboniferous (Tang KD et al., 1993), while in the South Hingganling area an angular unconformity occurred between the Early and Late Carboniferous. In Inner Mongolia the Late Paleozoic collision occurred at the end of Early Permian, along the Sonidyouqi (Mandalt)–Xar Moron River and Erenhot-Xi Ujimqinqi lines. The collision, marked by tectonic activity, occurred a little bit earlier in the western (Junggar–Tianshan) and central (Inner Mongolia) parts of the Junggar–Tianshan–South Hingganling Collision Belt, than in the southeastern part.

In the Tianshan-South Hingganling and its adjacent regions to the south, tectonic activity occurred earlier in the west than in the east, earlier in the north than in the south, and was stronger in the north than in the south. An angular unconformity occurs between the Devonian and Carboniferous in the West Kunlun area (Jin XC et al., 1999). In the Altun-Beishan region an angular unconformity occurs between the Lower-Middle and Upper Permian. Angular unconformities between the Lower-Middle Permian and Lower Triassic occur on the northern and southern sides of the Qaidam Block and in the Bayanhar–West

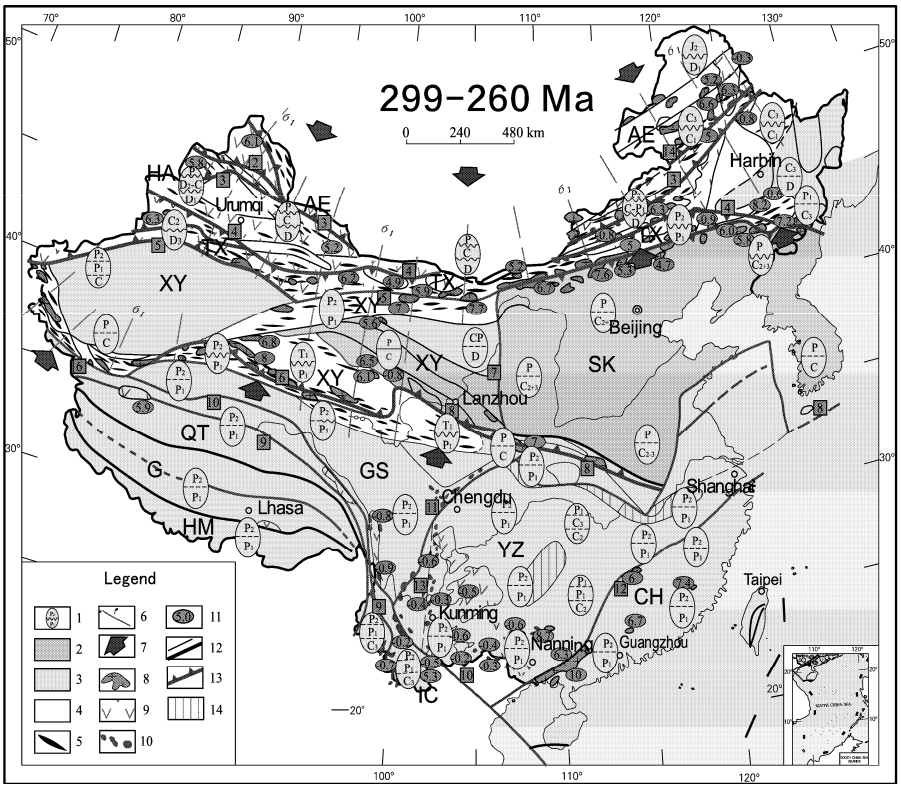

Fig. 5.10 Tectonic sketch map of the Chinese continent (299–260 Ma) in the Tianshan Period.

Legend: 1. Strata contacts, named as in international stratum code, angular unconformities in wavy lines, disconformities in dashed line, conformities in continuous line; 2. Area of strata conformity; 3. Area of disconformity; 4. Area of angular unconformity; 5. Anticlinal fold axis, (data in Appendix 3.3); 6. Trace of maximum principal compression (σ_1); 7. Direction of block movement; 8. Granite intruded during the Tianshan Period (299–260 Ma); 9. Volcanism during the Tianshan Period (299–260 Ma); 10. Ophiolite and ultramafic emplaced during the Tianshan Period (299–260 Ma); 11. Rate of intraplate deformation estimated from litho-chemistry data, "-", rate of extension, others, rate of shortening (cm/yr) (data in Appendix 5.4); 12. Plate boundary; 13. Collision belt and fault belt and their serial numbers; 14. Intraplate faulted-depression. N.B. In this figure the Lower Permian (P_1) includes the former Lower and Middle Permian (299–260 Ma), the Upper Permian (P_2) is the same as the former Upper Permian (260–251 Ma).

Plate boundaries, collision or fault belts and their serial numbers:

[1] Kurt-Narmand Collision Belt; [2] Tagtai-Derbugan Collision Belt; [3] Radbut-Karameili-Xilinhot Collision Belt; [4] Nilak–Yilinxbierga-Xar Moron He Collision Belt; [5] Wuqia–Korla–northern border of the Alxa Block Thrust Belt; [6] Kangxiwa–southern border of the Qaidam Thrust Belt; [7] Western border of the Sino-Korean Plate (Helanshan-Liupanshan); [8] Plate boundary of Tianshui–Shangdan–Tongbo–Zhucheng–Cheju Island; [9] Plate boundary of Shuanghu–Lancangjiang; [10] Plate boundary of Lazhulung–Jinshajiang–Honghe; [11] Plate boundary of Longmenshan; [12] Plate boundary of Shiwandashan–Shaoxing (between Yangtze and Cathaysian plates); [13] Penzhihua–Xichang extension zone; [14] Erenhot–Heihe Collision Belt.

Qinling regions. So there are two angular unconformities in the Tianshan–South Hingganling region, occurring earlier in the north than to the south of the Tianshan–South Hingganling Belt. However, to the south of the Tianshan–South Hingganling Belt, no angular unconformities are seen between the Devo-

nian and Carboniferous, except in the West Kunlun region, but angular unconformities do occur between the Lower-Middle and the Upper Permian. In most of the area to the south of Tianshan–South Hingganling Belt there are disconformities and conformable contacts in the Upper Paleozoic systems, but no angular unconformities (shown on the left of Fig. 5.10). So during the Late Paleozoic tectonic activity occurred mainly on or near the Tianshan–South Hingganling Belt, but gradually faded out towards the south.

Disconformities occur at the end of the Upper Paleozoic in six regions: (1) the Alxa Block, (2) the Tarim Block, (3) the Qiangtang–Gangdise–Himalayan Block, (4) the Aba–Garze-Litang region in West Sichuan, (5) the Yangtze Plate and (6) the Cathaysian Plate (light green color in Fig. 5.10).

In the Alxa region the earliest disconformity occurs between the Devonian and Carboniferous. In South Tianshan and northern Tarim, disconformity occurs between the Lower-Middle and Upper Permian systems. However, there are conformable contacts between the Lower-Middle and Upper Permian systems in most of the Tarim area. In central Tarim, there are disconformities at the base of the Upper Devonian (representing the erosion of 200–1,000 m), and between the Permian and Triassic (erosion of 100–1,000 m) (Zhang YW et al., 2000). In southern Tarim disconformities occur only between the Permian and Triassic systems. In the Qiangtang, Gangdise and Himalayan blocks, in the Aba–Garze-Litang region of West Sichuan and in the Cathaysian Plate, there is a disconformity between the Lower-Middle and Upper Permian, which has been called the "Dongwu Tectonic Event" (Li SG , 1932). In the central Yangtze Plate (West Hunan and West Hubei), there are two disconformities, one between the Middle and Upper Carboniferous (or the Lower Permian), and the other between the Lower-Middle and Upper Permian (cf. Dongwu Tectonic Event).

If the attitude of the strata alone is considered, there is a disconformity between the Lower-Middle and Upper Permian systems in the Yangtze Plate. However, the underlying plate was undergoing extensional tectonic activity with the development of growth faults and the occurrence of seismites generated by paleo-earthquakes. This type of unconformity commonly occurs in extensional basins and can be called a "seismic-extensional unconformity" (Liang DY et al., 1991, 1994; Plaziat et al., 1990, 1993). Seismic-extensional unconformities are widespread on the southern margin of the Yangtze Plate (southern Anhui, Hunan, Guangxi, Guizou, and Yunnan provinces), and in most of Sichuan Province, especially in the West Sichuan-Middle Yunnan region (Songpan-Garze, Yanyuan-Lijiang, Panzhihua-Xichang, Yanbian) (Liang DY et al., 1994), demonstrating that extensional activity occurred on a large-scale in the Yangtze Plate during the Late Paleozoic, especially on its western margin, which was formerly called the Panzhihua-Xichang (Panxi) Rift Belt by former researchers (Luo YN, 1985), however, in light of recent research that is not a rift belt, but three paleo-oceanic basins (Mo XX, 1991, 1993, 1998; Zhong DL et al., 1998; Liu BP et al., 2002). This extensional faulting marks the initiation and opening of the Lancangjiang and Jinshajiang Paleo-Ocean.

In the Sino-Korean Plate and the Qilian region contact relations in the Upper Paleozoic are mainly conformable (dark green color in Fig. 5.10). However, because the sediments were deposited in a terrestrial environment, where breaks in sedimentation are very likely to occur, it is difficult to make sure that all the contacts are conformable. However, these two regions were relatively stable tectonically, and were not greatly affected either by the Tianshan–South Hingganling collision, or by the extension of the Yangtze Plate.

Data from folds and the principal compressive stress axes of the Tianshan Tectonic Period (397–260 Ma) have been compiled from 250 anticlinoria and 242 synclinoria (Appendix 3.3). The angles of dip of the fold limbs are mainly 40°–60°. The trend of the fold axes, the intermediate principal stress axis (σ_2), are: NW-trending in the Altay–Junggar–Ergun Belt; near E-W-trerding in the middle Inner Mongolia region; NE-trending in the Tianshan–South Hingganling Belt, and the area to the south, on a large scale defining an arcuate fold belt; the maximum principal compressive stress radiate from the center of the Siberian Plate and trend nearly N-S; the minimum principal compressive stress axis (σ_3) are nearly vertical (Figs. 5.10 and 5.11).

These data show that a single integrated stress field was developed in the northern part of the Chinese continent at the end of the Paleozoic. This resulted from the northward migration of the Sino-Korean

and Xiyu plates and their collision and amalgamation with the central Mongolian and Siberian Plates in the Tianshan–South Hingganling Collision Belt, the largest scale arcuated tectonic belt in China. In terms of modern coordinates the movement of the blocks was broadly N-S, the palaeogeomagnetic data is not sufficiently accurate to give the precise direction of convergence, and is near to NW trend.

There was no obvious tectonism in the Qilian region during the Late Paleozoic, perhaps because of the welding of the continental blocks, during intense tectono-thermal activity in the Early Paleozoic. However, in the regions of collision which were not securely amalgamated during Early Paleozoic, for example West Kunlun, Altun, the northern and southern margins of the Qaidam and Bayanhar-West Qinling blocks, there was no deformation during the Tianshan Event of Late Paleozoic. Although no deformation occurred in the Sino-Korean Plate to the south of the Tianshan-South Hingganling Collision Belt, there was subsidence on the northern margin of the plate, with the deposition of marine molasse in a sedimentary basin, with a gradual decrease in grain size towards the south (Meng XH et al., 2002; Fig. 5.3).

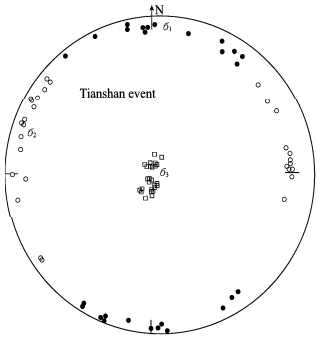

Fig. 5.11 Attitude of the principal stress axes in the Late Paleozoic.

Recently, Wu HR et al. (2001) have suggested that there was a unified Yunkai Block in the South Guangxi and west Guangdong regions, including also the northern South China Sea and the Nansha Islands. This is a reasonable proposal, but this block existed during the Late Paleozoic for only a short time. As discussed in Chapter 4, perhaps the Yunkai Block formed the southern part of Yangtze Plate during the Early Paleozoic. During the breakup of the Yangtze Plate at the end of Late Paleozoic, the Yunkai Block was separated from the Yangtze Plate and shows distinctive sedimentary and tectonic features. From the Devonian to the Early Permian, a deep faulted depression was formed in Qinzhou-Luoding between the Yunkai Block and the Yangtze Plate, and a deep marine depression developed along the Wuchuan–Sihui-Qiongzhou Zone to the east of the Yunkai Block, but an ophiolite suite has not yet been found (Qiu YX et al., 1993). During collision and compression at the end of Early Permian (Rb-Sr age of 265 Ma, Fang QH et al., 1987), recumbent folds and northward directed thrust systems, associated with granitic migmatization and regional metamorphism, were formed in Late Paleozoic strata on the Yunkai Block. The deformed rocks are overlain unconformably by Upper Permian and Middle Triassic strata. Collision and amalgamation of the Yunkai Block, with the Yangtze and Cathaysian plates, were completed during the Indosinian Tectonic Event at the end of Middle Triassic (Wang QQ et al., 1989; Liao QK, 1991; Qiu YX et al., 1993).

5.4 Magmatism and Rates of Plate Movement

Large scale magmatism occurred in Chinese continent during Late Paleozoic. The areas of outcrop of the magmatic rocks formed at that period extend over 278,900 km^2, mainly adjacent to the Tianshan–

South Hingganling Collision Belt (Cheng YQ, 1994; Appendix 7). They constitute nearly one third of the total outcrop area of magmatic rocks in the Chinese continent.

From chemical analyses of 2,548 samples of magmatic rock the rates of plate movement during Late Paleozoic have been calculated (Fig. 5.10; Appendix 5.4): in the eastern Tianshan-South Hingganling Belt, from Heilongjiang to Hegenshan in Inner Mongolia, rates of plate extension were 0.3–0.8 cm/yr during the Early Tianshan Period (Middle and Late Devonian, 397–359 Ma), estimated from the chemical composition of 52 ultrabasic and basic rocks; during the Middle Tianshan Period (Carboniferous, 359–299 Ma) rates of plate extension, determined from 38 ultrabasic and basic rocks, were 0.5–0.7 cm/yr; and during the Late Tianshan Period (Early and Middle Permian, 299–260 Ma) the rate of plate extension determined from 12 ultrabasic and basic rocks was 0.8 cm/yr.

In the western Tianshan–South Hingganling Collision Belt, formed at the end of the Devonian, in Altay and Tianshan–Xingxingxia, Xinjiang, rates of plate shortening of 6.1–7.3 cm/yr in the Early Tianshan Tectonic Event have been calculated from the chemical composition of 284 granite samples. The Tianshan Collision Belt was formed mainly in the Early Carboniferous, when magmatism resulted in the lateral growth of the continent. In the processes of subduction and collision were formed blueschists and high-pressure granulites and eclogites in the Tianshan–Junggar region, however the geothermal gradient was normal (<33 °C/km) for continental areas (Zhao ZY, 1993; Gao J, et al., 1996; Wang RS, et al., 1999; Zhang LF, et al., 1998, 2001) (Appendix 6.1). In the Tianshan–Xingxingxia region, Xinjiang, the rate of plate shortening during the Carboniferous was estimated to be 6.2 cm/yr from the chemical composition of 174 granite samples; in Altay, Xinjiang, 6.1 cm/yr from 160 granite samples; in northern Tianshan, Xinjiang, 6.3 cm/yr from 238 granite samples; around Junggar, Xinjiang, 5.5 cm/yr from 338 granite samples.

Extensive post-collisional magmatism of mantle origin occurred in northern Tianshan during the Carboniferous and Permian (359–260 Ma), characterized by high $\varepsilon_{Nd(t)}$ (+2.6±9), relative low $(^{87}Sr/^{86}Sr)_i$ (0.702–0.710) and new model Nd and Pb ages (Han BF et al., 1998, 1999). The magma evidently came from depleted mantle mixed with some crustal material. Abundant magma of mantle origin may have caused underplating near the crust-mantle boundary, generating granitic fluids in the lower crust by partial melting. The thickened continental crust became an important part of the Junggar basement (Han BF et al., 1999; Jahn BM et al., 2000). The Paleozoic continental crust in that region is due to the recycling of Archean continental crust, and also includes substantial juvenile components. The data does not support the view that the Junggar basement is composed of oceanic crust as suggested by Coleman (1989).

In the east part of Tianshan–South Hingganling Belt, from south Heilongjiang to Inner Mongolia, the rate of plate shortening during the Devonian was 5–7.6 cm/yr, estimated from the chemical composition of 56 granite samples, however the rate of shortening in Jilin Province was only 3.9 cm/yr. Rates of plate–shortening in tectonically active areas in Inner Mongolia were 6.5–7 cm/yr, and about 4.5–5 cm/yr in tectonically stable areas from 118 granite samples. During the Late Tianshan Period (Early and Middle Permian) when the collision and amalgamation in the Tianshan-South Hingganling Belt were finally completed, the rate of plate-shortening in the East Tianshan–South Hingganling Belt was about 5.9 cm/yr, estimated from 945 granite samples.

In West Qinling–Beishan, Gansu Province, and the northern margin of Qaidam, Qinghai Province, the rate of plate shortening during the Devonian was 4.7–5.8 cm/yr from the chemical composition of 7 granite samples. In the Foping region of south Qinling, shortening may have resulted in folding and amphibolite metamorphism, with a geothermal gradient in the normal range for continental crust (18–34 °C/km) (Zhang SG et al., 1998). In the Beishan–Qilian region, the rate of plate shortening was about 5.6 cm/yr, estimated from the chemical composition of 3 granite samples. In the Qilian region, the rate of plate extension during the Early Permian was 0.79 cm/yr, estimated from 12 basic and ultrabasic samples, and the rate of plate shortening was about 6.4 cm/yr from 15 granite samples. On the southern margin of Qaidam, Qinghai Province and East Kunlun, the rates of plate shortening during the Devonian were 5.5–6.9 cm/yr from 92 granite samples, and during Early Permian, was ~7 cm/yr from 15 granite samples.

In the Dabieshan region, only two Devonian granite samples have been analyzed, gaving a rate of plate-shortening of 4.1 cm/yr. In Guangxi Province on the southwestern margin of the Yangtze Plate, the rate of plate shortening during the Carboniferous was 6.4 cm/yr from the analysis of 8 granite samples, and in the Early Permian $\sim$ 6.3 cm/yr from 91 granite samples.

In the Cathaysian Plate, the rate of dispersion during the Devonian was 0.5 cm/yr, estimated from two basic samples from Jian'ou-Dakang, northern Fujian Province, and during the Carboniferous 0.4 cm/yr, from 6 basic samples. In southeast Guangxi and west Guangdong on the southwestern margin of the Cathaysian Plate, collision-type granitic intrusions were emplaced. The Rb-Sr isochron age of the granite in Darongshan and Liuwandashan region is 265 ± 5 Ma, and many Ar-Ar, K-Ar, and Rb-Sr isotopic studies have given ages of 290–265 Ma. It has been suggested that the collision event between the Cathaysian and Yunkai blocks occurred during the Middle and Late Permian. There also exhibited an Indosinian Tectonic Event at the end of the Middle Triassic (Fang QH et al., 1987; Wang QQ et al., 1989; Liao QK, 1991; Qiu YX et al., 1993; Zhang BY et al., 1994). The rate of plate shortening in Guangdong, on the Cathaysian Plate during the Carboniferous was 6.7 cm/yr, estimated from the chemical composition of 5 granite samples. In the Piaotang region of south Jiangxi Province the rate of plate-shortening was 5.9 cm/yr during the Carboniferous, estimated from the chemical composition of only one granite sample, and during the Permian was about 7.5 cm/yr, estimated from 8 granite samples from the Cathaysian Plate.

Three Late Paleozoic ophiolite belts occur in the Hengduanshan region, West Sichuan-Yunnan (Liu ZQ et al., 1993; Mo XX et al., 1998). These were the earliest to be recognized and are best known in China (Appendix 5.4).

From west to east, they are:

(1) In the Early-Middle Carboniferous ophiolite belt of the Changning–Menglian Zone near the Lancangjiang River (Liu BP, et al., 1991; 1993), according to a plate-dispersion velocity of 0.67 cm/yr, estimated from basalt compositions (Mo XX et al., 1991), the width of the Lancangjiang paleo-ocean was $\sim$1,200 km. Recently a complete ophiolite suite was found in the Jiaomeri area, on the southwestern side of Shuanghu(centered on 89°E, 33.5°N), central Qiangtang, representing the northwestern extension of the Lancangjiang Paleo-ocean (Zhai QG et al., 2004).

(2) The Middle Carboniferous–Early Permian ophiolite belt in the middle Jinshajiang Zone (Shen SY et al., 1994; Sun XM et al., 1994, 1997), gave a rate of plate extension of 0.9 cm/yr, estimated from basalts (Mo XX et al., 1991). The Xijin'ulan Group formed during the Early Carboniferous-Early Permian shows that this zone extends northwestwards into the northern Jinshajiang area, Qinghai Province (Bian QT et al., 1997). The Early Carboniferous (359–318 Ma) Ailaoshan Ophiolite Belt occurs to the southeast of the Jinshajiang Belt (Tian N et al., 1991). Subduction of the oceanic crust and shortening occurred in the Jinshajiang Belt at the end of Early Permian, with a continental collision during a late period of the early Middle Triassic (Wang LQ et al., 1999). According to the well-known data, the width of Early Carboniferous-Early Permian Jinshajiang Paleo-Ocean has been estimated to be 1,800 km. It is unreasonable to regard this as a small ocean basin (Chen BW et al., 1991; Zhang Q, 1992; Zhong DL et al., 1993), or a back-arc basin (Pan GT et al., 1997; Hsu KJ et al., 1995; Wang XF et al., 2000); this is a major ocean basin (Mo XX, 1991, 1993, 1998; Liu ZQ et al., 1993).

(3) Generally, it is considered that tholeiitic basalts and Upper Permian radiolarian cherts along the Garze–Litang Zone, to the east of the Jinshajiang Belt, represent an ocean basin, but a complete ophiolite suite has not been found. According to basalt compositions, the rate of plate dispersion was 0.8 cm/yr (Mo XX et al., 1991), and the width of the ocean basin was about 400 km.

In southern China the Carboniferous and Early Permian are characterized by extension and large scale basic volcanism. During the Late Permian continuous extension, with the eruption of the Emeishan flood-basalt (Large Igneous Province), occurred on the western margin of the Yangtze and Qiangtang plates. The basalts extend over an area of 2.5×10^5 km^2, and are 250–2000 m thick (Bureau of Geology of Sichuan, 1991; Liu BJ et al., 1994). The rate of plate-dispersion in the Late Permian was between 0.3 and 0.6 cm/yr estimated from 89 samples from the Emeishan basalt.

The Eurasian (including the Yangtze Plate) and the Gondwana (including the Qiangtang Plate) continents can be distinguished clearly by the chemical analyses of tholeiites from either side of the Lancangjiang Paleo-Ocean (Yang KH, 1998) (Table 5.1). In the Gondwana w (CaO) / w (TiO_2) and w (Al_2O_3) / w (TiO_2) are much higher than in the Eurasian continent, however, w (La) / w (Yb), w (Ce) / w (Y), w (Zr) / w (Yb), and $^{87}Sr/^{86}Sr_{(av.)}$ are lower; the reasons for these differences are not clear.

Table 5.1 Element chemical characteristics of tholeiites in the Gondwanan and Eurasian continents (Yang KH, 1998).

Element chemical characteristics	Gondwana	Eurasia
w(CaO) / w (TiO_2)	4.63–5.26	2.1–3.94
w (Al_2O_3) / w (TiO_2)	7.75–10.73	3.42–5.84
w (La) / w (Yb)	1.9–4.63	5.43–11.24
w (Ce) / w (Y)	0.78–1.54	1.75–2.02
w (Zr) / w (Y)	3.84–5.81	6.85–15.84
w (Zr) / w (Yb)	32–58	72–176
^{87}Sr / $^{86}Sr_{(av.)}$	0.7054	0.7074

Geothermal gradients during the Carboniferous and Permian have been estimated from the temperatures, pressures and depths of formation of regional metamorphic and magmatic rocks (Appendices 7.1 and 7.2). Most of the blocks in the Chinese continent still had normal geothermal gradients during the Carboniferous and Permian periods, apart from the abnormal geothermal gradient related to the Emeishan extrusions in the Jinshajiang and Lacangjiang areas and the southwestern part of the Yangtze Plate.

Normal geothermal gradients were rare during the tectonic evolution of the Chinese continent. The geothermal gradient is estimated to be 37°C/km from amphibolites in the Jinshajiang region, Sichuan Province (Bureau of Geology of Sichuan, 1991), 44°C/km from amphibolites in the Lancangjiang Group (Zhong DL et al., 1998), 36.4–38.5°C/km from gabbro in West Mojiang, West Yunnan Province (Zhou DJ et al., 1992), 52.6°C/km from granites in Darongshan, Guangxi Zhuang Autonomous Region (Wang QQ et al., 1990) and 49°C/km from granite-porphyries in Shiwandashan, Guangxi Zhuang Autonomous Region, between the Yangtze and Cathaysian plates (Xu HL et al., 2001).

During the whole of the tectonic evolution of the Chinese continent, very large-scale basalt eruptions occurred only during the Permian on the western Yangtze and eastern-northern Qiangtang plates. It has been proposed that the Emeishan large igneous province (LIP) represents the site of an underlying mantle plume which developed between the Yangtze and Qiangtang plates (Huang KN et al., 1988, 1992; Chung SL et al., 1995, 1998), and was responsible for the formation of the Jinshajiang and Lancangjiang Paleo-Ocean. This mantle plume may be called the Emeishan Plume. However, the center of the plume was not at Emeishan, but beneath the Jinshajiang and Lancangjiang Paleo-Ocean. The development of the Emeishan Plume initiated the extension and dispersion of the surrounding plates, including the Yangtze, Xiyu and many Gondwana blocks to distances of up to 1,000 km, generating the Jingshajiang and Lancangjiang Paleo-Ocean in the central part of the Tethys Paleo-Ocean. The plume may be the primary dynamic cause of the dispersion of the South China continents and their surrounding blocks.

Recently, a newly discovered eclogite belt, i.e. a Carboniferous-Permian collision zone at Gyaxing and Sumdo in eastern part of Lhasa (i.e. Gangdise) block of Xizang (Tibet), is about 500–1,000 m wide and at least 60 km long in an E-W direction. The eclogites result tectonic slices in garnet-bearing mica-quartz schist, whose peak metamorphic conditions of 2.7 GPa and 730℃and SHRIMP U-Pb dating of zircons from the eclogite yielded metamorphic ages ranging from 242±15 to 292±13 Ma. The MORB eclogite is interpreted as remnants of Paleo-Tethyan oceanic lithosphere (Yang JS et al., 2009; Chen SY et al., 2009). It means that the Gangdise (Lhasa) plate comprised North and South Lhasa blocks during Carboniferous–Permian Periods.

5.5 Tectonics and Plate Movement from the Mesoproterozoic to the Paleozoic

Tectonic, paleomagnetic and paleogeographic information shows that the tectonic units and the tectonic evolution of the blocks forming the Chinese continent were very different from their situation from the beginning of the Mesoproterozoic to the end of the Middle Permian (1,800–260 Ma), because throughout this period, the blocks were separate and in a process of movement, leading to collision and amalgamation.

From the Changcheng and Jixian Periods (1,800–1,000 Ma) to the end of the Paleozoic (260 Ma), the Chinese continent can be considered to comprise four tectonic domains: Peri-Siberian, Sino-Korean (North China-Korean Block), Yangtze (Yangtze, West Sichuan, Qinling-Dabie, and Cathaysian blocks) and Peri-Gondwana (Qiangtang, Gangdise, Himalayan and Sibumasu blocks) (Figs. 1.2, 4.15). Although this basic tectonic framework continued through to the end of the Paleozoic, the blocks included in these tectonic domains changed through out.

The Tarim, Qaidam and Alxa blocks belonged to the Sino-Korean Tectonic Domain during the Archean-Mesoproterozoic, but after the Neoproterozoic they gradually became more closely associated with the Yangtze Tectonic Domain.

Blocks in Peri-Siberian Tectonic Domain (including Altay, Junggar-East Kazakhstan, Ili-Balchas, Turpan–Xingxingxia, Kuruktag, Hongshishan, Yagan, North Bayannur, Tuotuo–shang–Xilin Hot, Ergun, Songhuajiang–Nenjiang–Harbin, Jiamusi–Bureinskiy and Xingkai), all with an Archean–Paleoproterozoic crystalline basement, were separated and migrated from the southern to the northern hemisphere, together with the Siberian Plate, during the Mesoproterozoic to Early Paleozoic. The crystalline basement of Jiamusi-Bureinskiy and Xingkai blocks was formed in the Early Cambrian, influenced by the Pan-African Tectonic Event. The Altay, Junggar–East Kazakhstan and Ergun blocks accompanied the Central Mongolia Block northwards, where during the Ordovician they collided and were amalgamated in the Baykal Belt around the Siberian (Angaran) Plate, and with the northern Chinese continent to form the Early Paleozoic Altay–Junggar–Central Mongolia-Ergun Collision Belt. From the Early Carboniferous to the end of the Middle Permian, all the dispersed blocks of the Peri-Siberian Tectonic Domain collided and were amalgamated to form the Tianshan–South Hingganling Collision Belt, the eastern part of the Central Asian Collision Belt, in the Tianshan Tectonic Event.

In the Archean-Mesoproterozoic the Sino-Korea Tectonic Domain included the North China-Korean, Tarim, Qaidam and Alxa blocks. The main Sino-Korean Plate (North China-Korean Peninsula block) remained stable from the Mesoproterozoic to the end of the Paleozoic. Then the Liaoning–Shandong–Xuzhou–Huaihe depression belt developed in the east of the block, accompanied by many paleoearthquakes. During the Sinian period (680–513 Ma), glacial sediments of the Luoquan Formation were deposited on the southern margin of the Sino-Korean Plate showing that the plate had moved into the glacial zone. During the Paleozoic, the Sino-Korean Plate moved from 15°S to 15°N latitudes, and was covered by shallow marine pelite and shelf carbonate deposits. Collision and amalgamation occurred between the blocks in the Peri-Siberian Tectonic Domain at the end of the Middle Permian. All these blocks then became part of the Pangea Super-Continental Plate.

The tectonic evolution of the three blocks in the west of the original Sino-Korean tectonic domain was more complicated. During the Mesoproterozoic, the Qilian and Altun rift-faulted belts developed, separating and dispersing the Tarim, Qaidam and Sino-Korean (including the Alxa Block) plates. But during the Middle and Late Qingbaikou Period (900–800 Ma), collision and compression in the Qilian and Altun belts, brought the Tarim, Qaidam, and the main Sino-Korean Plate back together again to reconstruct the original framework of the Sino-Korean Tectonic Domain. During the Nanhua-Sinian periods (800–513 Ma), the Qilian faulted depression was formed, so that the Tarim and Qaidam blocks developed very different sedimentary characteristics from the main Sino-Korean Plate (including the Alxa Block), and moved nearer to the Yangtze Plate, so that during Nanhua–Sinian Period the Tarim and Qaidam blocks became part of the Yangtze Tectonic Domain. From the Nanhua period to the Carboniferous, the Tarim Block was attached to the Yangtze Plate. From the Archean to the Middle Cambrian

(2,500–501 Ma) the Alxa block was always attached to the west Sino-Korean Plate, however fossils show that from the Late Cambrian to the Carboniferous they belonged to the Yangtze Tectonic Domain. During the Ordovician and Silurian, faulted depressions were formed on the eastern margin of the Alxa Block and in the Qilian–Altun Belt, and the Tarim, Qaidam, Alxa, West Kunlun and Hualong blocks became gradually more related to the Yangtze Tectonic Domain. However they remained separate until their amalgamation in the Qilian–Altun Collision Belt to form the independent Xiyu Plate at the end of the Silurian. The Xiyu Plate existed for only a very short time during the end of Silurian and Devonian. From the Early Carboniferous to the Middle Permian the Xiyu Plate moved gradually northeastwards until it collided with the Peri-Siberian Tectonic Domain in the Tianshan–Hingganling Collision Belt; the Xiyu Plate, together with Sino-Korea Plate, was then incorporated into the Pangea Super-Continental Plate.

The Yangtze Tectonic Domain including the Yangtze, middle Qinling-Dabie, West Sichuan and Cathaysian blocks were gradually joined by the Tarim, Qaidam, Alxa-Dunhuang, West Kunlun and Hualong blocks. The Yangtze Plate was formed by the collision and amalgamation of the north and south Yangtze plates at the end of the Mesoproterozoic (Sibao Tectonic Period (1,000 Ma)), forming a unified crystalline basement at the end of the Qingbaikou Period (800 Ma). During the Nanhua Period (800–680 Ma), widespread glacial deposits of the Nantuo Formation were deposited on the Yangtze Plate, indicating that they had migrated into the glacial zone. However, during the following Sinian Period, the Yangtze Plate was overlain by carbonate shelf deposits showing that it had migrated into a warm water environment, which is so different to Sino-Korean Plate. During the Paleozoic, the Yangtze Plate migrated northwards from latitude 15°S to near the equator. Although the plate did not move very far, it rotated by about 90°, and shelf carbonates and sandy mudstones were deposited. At the end of the Early Paleozoic, intraplate folding occurred in the South Yangtze Plate, but the causes of this deformation are not known. At the end of the Late Paleozoic large scale extension occurred in the southwestern part of the plate under the influence of the rising Emeishan Plume.

At the end of the Qingbaikou Period (800 Ma), the ocean separating the Yangtze Plate and the central blocks of the Qinling–Dabie Belt was subducted, and the ocean separating the Yangtze and Cathaysian plates may also have been subducted, leading to the collision of these plates. At the end of the Early Paleozoic (~400 Ma), there was convergence and compression in the Qinling–Dabie Belt, perhaps as the result of oceanic subduction, because the main continent-continent collision in this belt occurred only at the end of Triassic.

During the Paleozoic the Cathaysian Plate was always located at a low latitude in the southern hemisphere and its latitude did not change greatly, but the plate rotated significantly, as indicated by the change in its paleomagnetic declination. In the Cathaysian Plate at the end of the Early Paleozoic (~400 Ma), deformation in an independent stress field, with greenschist facies regional metamorphism, and magmatic activity, occurred, forming a unified crystalline basement. Collision between the Cathaysian and Yangtze plates did not occur at the end of the Paleozoic, but in the Triassic.

The tectonic evolution of the Peri-Gondwanan Tectonic Domain, including the Qiangtang, Gangdise, Himalayan and Sibumasu blocks, during the Meso-and Neoproterozoic is not very clear. During the Neoproterozoic and Early Cambrian (1,000–513 Ma), regional metamorphism and deformation occurred, forming a unified crystalline basement under the influence of Pan-African tectonic events. During the Paleozoic, these blocks were always located in the southern hemisphere at mid to low latitudes, with shelf sedimentation in a cold-temperate climate. At this period they occurred as dispersed blocks along the northern margin of the Gondwana.

At the end of the Early Paleozoic, the North American and the European Avalonian and Baltic plates collided to form the Caledonian Collision Belt, extending from the Appalachians through New England, Greenland, Ireland and Scotland to Norway (Trewin, 2002). At the end of Late Paleozoic the North American, Baltic and African plates were amalgamated to form the Hercynian (Variscan) Collision Belt. From the Carboniferous to the end of the Middle Permian, the Baltic (East European) and Siberian plates were amalgamated in the Ural Collision Belt. At this period the Laurasian Super-continental Plate, including the North America and Eurasian plates, and the Gondwana, including South America,

Africa, Antarctica, India and Australia, were amalgamated together in the western hemisphere to form the global super-continent, Pangea. However, many blocks in and around the Chinese continent were still dispersed within the Eastern Tethys Paleo-Ocean (Smith et al., 1981; Sengör, 1989; Yang, 1998; Liu BP et al., 2002 (Fig. 5.12)).

Blocks in the Yangtze Tectonic Domain including the Yangtze, Cathaysian and West Sichuan blocks, and the Qiangtang Block were gradually incorporated into the Eurasian super-continent during the Triassic. The Xingkai (Wandashan) Block (upper right of Fig. 4.15) collided and was amalgamated with the northeastern Chinese continent during the Jurassic. The Gangdise Block was amalgamated with the southern border of the Qiangtang Block at the end of Cretaceous and the Paleocene. Finally, the Himalayan Block and the Indian Plate collided and were amalgamated with the southern margin of the Eurasian super-continent at the Late Paleogene (Fig. 4.15). The amalgamation of whole of the Chinese continent and its adjacent areas was then completed.

To sum up, the tectonic domains and tectonic units which make up the Chinese continent have changed through out. What is more a tectonic block may belong to different tectonic domains at different times during its geological history. A single map of the tectonic units cannot represent the tectonic evolution of the blocks and their changing relationships during whole tectonic periods.

If the regional tectonic evolution in China were to be discussed only in terms of local tectonic units, it would be easy to overlook the differences in the characteristics of the various blocks, the causes of

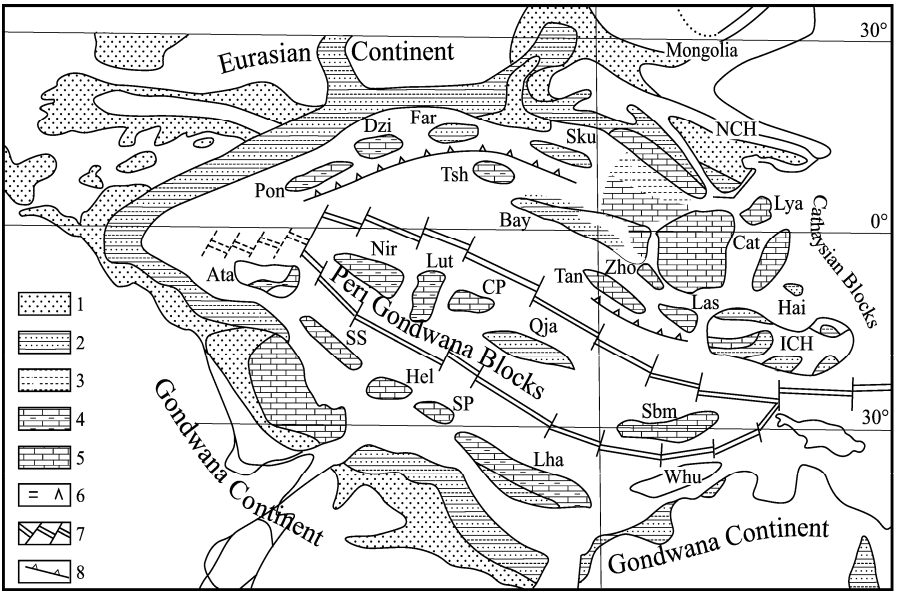

Fig. 5.12 Distribution of ocean basins in the East Tethys Ocean (during the Qixia Period in the Middle Permian; after Liu BP et al., 2002, with permission of Liu BP).

Legend: 1. Fluviatile-lacustrine deposits; 2. Marine sandy mudstone deposits; 3. Turbidite deposits; 4. Carbonate shelf; 5. Dolomite and dolomitic carbonate; 6. Gypsum and halite; 7. Oceanic spreading ridges and transform faults; 8. Subduction zone.

Blocks: NCH-North China; Sku-South Kunlun; Far-Farah; Dzi-Dogobayazit; Pon-Pontide; YAN-Yangtze; ICH-Indochina; Cat-Cathaysian; Lya-Lower Yangtze; Hai-Hainan; Las-Lanping-Simao; Zho-Zhongza; Tan-Tanggula-Qamdo; Bay-Bayanar; Tsh-Tianshuihai; Sbm-Sibumasu; Qia-West Qiangtang; CP-central Pamir; Lut-Lut; Nir-Northwest Iran; Whu-West Burma; Lha-Lhasa; SP-South Pamir; Hel-Helmand; SS-Sanandaj-Sirjan; Ata-Anatolide-Tauride.

these differences and the changing relationships of the blocks through out. This is the major reason that the regional tectonics of the Chinese continent is not described in a map of tectonic units for whole geological history in this book. In order to understand tectonics on the larger scale it is necessary to strengthen comparative research on the different tectonic blocks.

References

Bian QT, Zheng XS, Li HS et al (1997) Age and tectonic setting of ophiolite in the Hoh Xil region, Qinghai Province. Geological Review 43(4): 347–355 (in Chinese with English abstract).

Bureau of Geology and Mineral Resources of Sichuan Province (1991) Regional Geology of Sichuan Province. Geological Publishing House, Beijing (in Chinese with English abstract).

Chen BW, Li YS, Qu JC et al (1991) Main tectonic problems of Sanjiang area and their relations to metallogenesis. Geological Memoirs, no.11, pp110. Geological Publishing House, Beijing (in Chinese).

Chen SY, Yang JS, Li Y et al (2009) Ultramafic blocks in Sumdo region, Lhasa Block, Eastern Tibet Plateau : a ophiolite unit. Journal of Earth Science 20(2): 332–347.

Cheng YQ (1994) An Introduction to Regional Geology of China. Geological Publishing House, Beijing (in Chinese).

Chung SL, Jahn BM (1995) Plume–lithosphere interaction in generation of the Emeishan flood basalts at the Permian-Triassic boundary. Geology 23: 889–892.

Chung SL, Jahn BM, Wu G et al (1998) The Emeishan flood basalt in SW China: a mantle plume initiation model and its connection with continental breakup and mass extinction at the Permian-Triassic boundary. In: Flower MFJ et al (eds) Mantle dynamics and plate interactions in East Asia, Geodynamics Series, vol 27, pp.47–58, AGU, Washington DC.

Coleman RG (1989) Continental growth of Northwest China. Tectonics 8(3): 621–635.

China National Commission on Stratigraphy (2001) Chart of regional stratigraphy (geological age) of China. Journal of Stratigraphy 25(suppl.): 359–360 (in Chinese).

Fang QH et al (1987) S-type granitic suite in Darongshan, Guangxi. Acta Petrologica Sinica 3: 23–34.

Gao J, He GQ, Li MS et al (1996) Uplift mechanism of high–pressure metamorphic rocks, South Tianshan, Xinjiang. Scientia Geologica Sinica 31(4): 365–374 (in Chinese with English abstract).

Han BF, He GQ, Wang SG et al (1998) Postcollisional mantle-derived magmatism and vertical growth of the continental crust in north Xinjiang. Geological Review 44(4): 396–406 (in Chinese with English abstract).

Han BF, He GQ, Wang SG (1999) Postcollisional mantle-derived magmatism, underplating and implications for basement of the Junggar Basin. Science in China D 42(2): 113–119 (in Chinese).

He GQ, Li MS, Liu DQ et al (1994) Paleozoic Crustal Evolution and Mineralization in Xinjiang of China. Xinjiang People's Publishing House, Urumchi & Culture and Education Press, Hongkong (in Chinese with English abstract).

Hsu KJ, Pan GT, Sengor AM et al (1995) Tectonic evolution of the Tibetan Plateau: a working hypothesis based on the archipelago model of orogenesis. International Geological Review 37: 473–508.

Huang KN, Yang RY, Wang XC et al (1988) Preliminary research on trace element geochemistry of basalts in Emei Mountain, southwestern China. Acta Petrologica Sinica 4(1): 49–60 (in Chinese).

Huang KN, Opdyke ND, Peng XJ et al (1992) Paleomagnetic results from the Upper Permian of the eastern Qiangtang Terrane of Tibet and their tectonic implications. Earth Planet. Sci. Lett. 111: 1–10.

International Commission on Stratigraphy (2004) International Stratigraphic Chart. 32th IGC, Florence, Italy.

Jahn BM, Wu FY, Chen B (2000) Massive granitoid generation in Central Asia: Nd isotopic evidence and implication for continental growth in the Phanerozoic. Episodes 23(2): 82–92.

Jin XC, Wang J, Ren LD et al (1999) Problems concerning the tectonics of the west Kunlun orogen. In: Ma ZJ et al (eds) Advances in Structural Geology and Geophysics in China—In Honor of Academian Ma Xingyuan Ma's 80th Birthday, pp.105–113. Seismological Press, Beijing (in Chinese with English abstract).

Khramov AN, Petrova GN, Peckersky DM (1981) Paleomagnetism of Soviet Union. In: McElhinny MW, Valencio DA (eds) Paleoconstruction of the Continents, Geodynamic Series, pp.177–194. Geological Society of America, Boulder, Colorado.

Klootwijk CT, Radhakrishnamurty C (1981) Phanerozoic paleomagnetism of the Indian plate and India-Asia collision. In: McElhinny MW, Valencio DA (eds) Paleoconstruction of the Continents. Geodynamics Series. pp.93–105. Geological Society of America, Boulder, Colorado.

Li SG (Lee JS) (1932) Orogenic movements in post Paleozoic in southeastern China. Journal of Geological Society of China 11(2): 209–216.

Liang DY, Nie ZT, Wan XQ et al (1991) On the seismite and seismo-disconformity: as an example for West Sichuan and West Yunnan regions. Geoscience 5(2): 138–146 (in Chinese with English abstract).

Liang DY, Nie ZT, Song ZM (1994) Extensional Dongwu movement in western margin of Yangtze region. Earth Science 19(4): 443–453 (in Chinese with English abstract).

Liang DY, Nie ZT, Song ZM (1994) A re-study on seismite and seismo-unconformity: as an example for western Sichuan and western Yunnan. Earth Science 19(6): 845–850 (in Chinese with English abstract).

Liao QK (1991) Formation time of Darongshan-Shiwandashan granite batholith in Guangxi. Geology of Guangxi 4(4): 59–68 (in Chinese with English abstract).

Liu BJ, Xu XS, Xia WJ et al (1994) Atlas of Petrological Phase Paleogeography of South China (Sinian to Triassic). Science Press, Beijing (in Chinese).

Liu BP, Feng QL, Fang NQ (1991) Tectonic evolution of the Paleo-Tethys in Changning–Menglian and Lancangjiang belts, Western Yunnan. In: Proceedings of 1st International Symposium on Gondwana Dispersion and Asian Accretion (IGCP Project 321), pp.189–192. Kunming, China. Geological Publishing House, Beijing.

Liu BP, Feng QL, Fang NQ et al (1993) Tectonic evolution of Paleo-Tethys-Ocean in Changning–Menglian and Lancangjiang belts, Southwestern Yunnan, China. Earth Science 18(5): 529–539 (in Chinese with English abstract).

Liu BP, Feng QL, Chonglakmain C et al (2002) Framework of paleotethyan archipelago ocean of western Yunnan and its elongation towards north and south. Earth Science Frontiers 9(3): 161–171 (in Chinese with English abstract).

Liu ZQ, Li XZ, Ye QT et al (1993) Division of Tectonic Magma Belt in Sanjiang Area (Hengduanshan) and Its Distribution of Mineral Resources. Geological Publishing House, Beijing (in Chinese).

Luo YN (1985) Panzhihua-Xichang Paleo-rift zone, China. In: Zhang YX (ed) Contribution to Panzhihua-Xichang Rift, China. no.1, pp.1–25. Geological Publishing House, Beijing (in Chinese with English abstract).

Meng XH, Ge M (2002) The sedimentary features of Proterozoic microspar (Molar-tooth) carbonates in China and their significance. Episodes 25(3): 185–195.

Meng XH, Ge M (2005) Sequences, Events and Evolution of the Sino-Korean Plate. Science Press, Beijing (in Chinese with English abstract).

Mo XX (1991) Volcanism and the evolution of Tethys in Sanjiang area, southwestern China. In: Proceedings of 1st International Symposium on Gondwana Dispersion and Asian Accretion, pp.51–56. Kunming, China.

Mo XX, Lu FX, Sheng SY et al (1993) Sanjiang Tethyan volcanism and related mineralization. Geological Memoirs, no.20. pp.267 Geological Publishing House, Beijing (in Chinese).

Mo XX, Sheng SY, Zhu QW et al (1998) Volcanic-ophiolite and Mineralization of Middle-southern Part in Sanjiang Area of Southeast China. Geological Publishing House, Beijing (in Chinese with English abstract).

Mushketov DJ (1928) Geological map of Central Asia (in Russian).

Pan GT, Chen ZL, Li XZ et al (1997) Geological-tectonic Evolution in the Eastern Tethys. Geological Publishing House, Beijing (in Chinese with English abstract).

Plaziat JC, Purser BH, Philobbos ER (1990) Seismic deformation structures (seismites) in the syn-rift sediments of the NW Red Sea (Egypt). Bull. Soc. Geol. France 6(3): 419–439.

Plaziat JC, Ahmed EA (1993) Diversity of the sedimentary expressions of major earthquakes: an example from the Pliocene sandy seismites of the Egyptian Red Sea Coast. Geol. Soc. Egypt. Spec. Publ. (1): 277–294.

Qiu YX, Chen HJ (1993). Professional Papers for the Geological Structure of Yunkaidashan and Its Adjacent Areas. Geological Publishing House, Beijing (in Chinese).

Sengör AMC (1989) Tectonic Evolution of the Tethyan Region. Kluwer Academic Publishers, Berlin.

Sheng SY, Zhang BM et al (1994) Research on the volcanic characteristics of oceanic ridge-quasi ridge of Jinshajiang. Tethys Geology (18). Geological Publishing House, Beijing (in Chinese).

Shi GR, Archbold NW, Zhan LP (1995) Distribution and characteristics of mid-Permian (Late Artinskian-Ufimian) mixed/transitional marine faunas in the Asian region and their palaeogeographical implications. Palaeogeography, Palaeoclimatology, Palaeoecology 114: 241–271.

Shi GR (2006) Marine Permian of East and NE Asia: an overview of biostratigraphy, palaeobiogeography and implications for palaeogeography and plate tectonics. Journal of Asian Earth Sciences 26(3–4) (Special Issue): 175–206.

Smith AG, Hurley AM, Briden JC (1981) Phanerozoic Paleocontinental World Maps. Cambridge University Press, Cambridge.

Sun QL, Ma HD (2002) Discovery of monodiexodina in the vicinity of Muztag, east Kunlun, Xinjiang. Geological Bulletin of China 21(1): 48 (in Chinese with English abstract).

Sun XM, Nie ZT, Liang DY (1994) On the time and tectonic significance of ophiolite melange in Jinsha River belt, northwest Yunnan. Geoscience 8(3): 241–245 (in Chinese with English abstract).

Sun XM, Zhang BM, Nie ZT et al (1997) Formation age and environment of ophiolite and ophiolitic mélange in the Jinshajiang belt, northwestern Yunnan. Geological Review 43(2): 113–120 (in Chinese with English abstract).

Tang KD, Yan ZY (1993) Regional metamorphism and tectonic evolution of the Inner Mongolian suture zone. J. Metamorphic Geol. 11(4): 511–522.

Tian N, Yang YQ (1991) Geology, Geochemistry and genesis of gold deposits in ophiolitic mélange in northern Ailao Mountain, Yunnan. In: Contribution to the Geology of the Qinghai-Xizang (Tibet) Plateau. no.21. pp.84–97. Geological Publishing House, Beijing (in Chinese with English abstract).

Trewin N H (2002) The Geology of Scotland, 4th edn. The Geology Society of London, London.

Van der Voo R (1993) Paleomagnetism of the Atlantic, Tethys and Iapetus Oceans. Cambridge University Press, Cambridge.

Wan TF, Zhu H (2007) Positions and kinematics features of Chinese blocks in global paleocontinental reconstruction during Paleozoic and Triassic. Geosciences 21(1): 1–13.

Wang HZ (1985) Atlas of Paleogeography of China. SinoMaps Press, Beijing (in Chinese).

Wang HZ, Zheng LR, Wang XL (1991) Tectono-paleogeography and biogeography of China and adjacent regions in the Carboniferous period. 11th International de Stratigraphie et de Geologie du Carbonifere, Beijing, 1987, Compte. Rendu. 1: 97–116.

Wang LQ, Pan GT, Li DM et al (1999) The Spatio-temporal framework and geological evolution of the Jinsha Jiang arc-basin systems. Acta Geologica Sinica 73(3): 206–218 (in Chinese with English abstract).

Wang Q, Liu XY, Li JY (1991) Plate Tectonics Between Chathaysian and Angaraland in China. Peking University Press, Beijing (in Chinese with English abstract).

Wang QQ, Wang LK (1989) Physicochemical conditions for the formation of peraluminous granites at Darongshan Guangxi, China. Geochenica (4): 287–296 (in Chinese with English abstract).

Wang RS, Zhou DW, Wang JL et al (1999) Variscan terrane of deep-crustal granulite facies in Yushugou area, southern Tianshan. Science in China D 42(5): 306–313.

Wang TH (1995) Evolutionary characteristics of geological structure and oil-gas accumulation in Shanxi-Shaanxi area. Jour. Geol. Min. Res. North China 10(3): 283–398 (in Chinese with English abstract).

Wang XF, I Metcalfe, Jian P et al (2000) The Jinshajiang suture zone: tectono-stratigraphic subdivision and revision of age. Science in China D 43(1): 10–22.

Wu HR, Kuang GD, Wang ZC (2001) The Yunkai block since Silurian. Journal of Palaeogeography 3(3): 32–40 (in Chinese with English abstract).

Xiao XC, Tang YQ, Feng YM et al (1992) Tectonic Evolution of Northern Xinjiang and Its Adjacent Regions. Geological Publishing House, Beijing (in Chinese with English abstract).

Xie JR (1936) The formation age and distribution area of Chinese mineral resources. Geological Review 1(3): 363–380 (in Chinese).

Xu GR, Yang WP (1988) Permian. In: Yin HF et al (eds) Paleobiogeography of China. China University of Geosciences Press, Wuhan (in Chinese).

Xu HL, Yang YN, Shen Y et al (2001) New knowledge on structural features of Shiwandashan basin, Guangxi. Scientia Geologica Sinica 36(3): 359–363 (in Chinese with English abstract).

Yang FQ (1988) Carboniferous. In: Yin HF et al (eds) Paleobiogeography of China. China University of Geosciences Press, Wuhan (in Chinese).

Yang JS, Xu ZQ, Li ZL et al (2009) Discovery of an eclogite belt in Lhasa block, Tibet : a new border for Paleo-Tethys? Journal of Asian Earth Sciences 34: 76–89.

Yang KH (1998) A plate reconstruction of the eastern Tethyan orogen in southwestern China. In: Flower MFJ et al (eds) Mantle dynamics and plate interactions in East Asia, Geodynamics Series, 27, pp.269–288, Washington DC: AGU.

Zhai QG, Li C, Cheng LR et al (2004) Geological features of Permian ophiolite in the Jiaomuri area, Qiangtang, Tibet, and its tectonic significance. Geological Bulletin of China 23(12): 1228–1230 (in Chinese with English abstract).

Zhang BY, Yu HN (1994) Deep-seated Nappe Structure of Hercynian-Indochina Collisional Zone in West Guangdong. Geological Publishing House, Beijing (in Chinese).

Zhang LF, Sun M, Xian WS (1998) The discovering of charnockites and their granulite xenoliths in west Junggar, Xinjiang. Earth Science Frontiers 5(3): 132 (in Chinese with English abstract).

Zhang LF, Gao J, Ekebair S et al (2001) Low temperature eclogite facies metamorphism in Western Tianshan, Xinjiang. Science in China D 44(1): 85–96 (in Chinese with English abstract).

Zhang Q (1992) The Mafic-Ultramafic Rocks in Hengduan Mountains. In: Comprehensive Geological Bregade of Qinghai-Tibet Plateau, Chinese Acadamy of Science, Zhang KW, Li DZ (eds) The Series of the Scientific Expedition to the Hengduan Mountains of the Qinghai-Xizang Plateau. Science Press, Beijing (in Chinese).

Zhang SG, Wei CY, Yang CH (1998) Metamorphism of east part of South Qinling orogenic belt. Earth Science Frontiers 5(4): 210 (in Chinese).

Zhang YW, Jin ZJ, Liu GC et al (2000) Study on the formation of unconformaties and the amount of eroded sedimentation in Tarim basin. Earth Science Frontiers 7(4): 449–457 (in Chinese with English abstract).

Zhao XW (1988) Devonian. In: Yin HF et al (eds) Paleobiogeography of China. China University of Geosciences Press, Wuhan (in Chinese).

Zhao ZY (1993) Dislocation structures in olivine from spinel lherzolite of Sartokay ophiolite and their significance in upper mantle rheology. Scientia Geologica Sinica 28(3): 279–282 (in Chinese with English abstract).

Zhong DL, Ding L, 1993. Analyzed dispersion of Gondwana continent and accretion of Asia from the evolution of Tethys belt in Sanjiang and adjacent areas. In: China Working Group on International Geological Comparison Program. Project 321. Growth of Asia. Seismological Press, Beijing (in Chinese).

Zhong DL (1998) Paleo-Tethyan Orogenic belt in Western Yunnan and Sichuan. Science Press, Beijing (in Chinese).

Zhou DJ, Zhou YS, Xu P (1992) Carboniferous and Late Permian volcanic rocks of western Mojiang, Yunnan. Scientia Geologica Sinica (3): 249–259 (in Chinese with English abstract).

Chapter 6
Tectonics of Late Permian–Triassic (The Indosinian Tectonic Period, 260–200 Ma)

—forming the Lancangjiang, Jinshajiang, Qinling–Dabie and Shaoxing–Shiwandashan Collision Zones
—widespread intraplate deformation and formation of the Indosinian Tectonic System

Major collision and amalgamation of continental fragments occurred in the Chinese continent during the Indosinian Tectonic Event; the Lancangjiang (i.e. Lazhulung–Shuanghu–Changning–Menglian–Dak of Thailand–central Malaya Peninsula, 1 in Fig. 6.3), Jinshajiang (18 in Fig. 6.3), Qinling–Dabie (6,10 and 11 in Fig. 6.3) and Shaoxing–Shiwandashan (19 in Fig. 6.3) Collision Zones were formed during this period. More than three quarters of the Chinese continental area became amalgamated to the Pangean Super Continent in the areas to the north and east of the Bangongco –Nujiang zone. At the same time, widespread intraplate folding and faulting developed in the Indosinian Tectonic System affecting the sedimentary cover over a large part of the Chinese continent.

Indosinian movement was first recognized in the Triassic of Vietnam by the French geologist, Fromaget (1934); this term was popularized in China by Huang TK (Huang JQ, 1945). Many Chinese geologists regard the Indosinian Tectonic Event as the most important event in the formation of the Chinese continent (Wang HZ, 1981, 1982; Zhao ZP, 1986; Zhang WY 1984; Huang JQ et al., 1987).

In the Indochina Peninsula and in South China the Indosinian Tectonic Event is represented by an angular unconformity between the Middle and Upper Triassic systems. But recently the Indosinian Tectonic Period has been extended to cover all tectonic events from the Late Permian to the end of the Triassic. On the Chinese continent major collisions and deformations occurred both at the end of the Middle Triassic and at the end of the Late Triassic. There is generally a continuous sequence between the Permian and Triassic systems, with successive transitional lithologies, deposited in a tectonically stable environment, although a catastrophic faunal and floral extinction event occurred between the Permian and Triassic, with a rate of extinction of more than 90% of species (Peng YQ and Yin HF, 2002; Benson, 2003).

Molnar and Tapponnier (1975), Tapponnier and Molnar (1977), using remote sensing imagery to study active faults, first proposed an indentation model for the collision between Indian and Asian Plates in the Cenozoic, influencing the eastward displacement (escape) of crustal blocks in Asian continent. Later, Tapponnier et al. (1982, 1986) had extended the indentation model to all the earlier collisions since the Triassic (Fig. 6.1). This model is regarded as the classic model of tectonics by the international tectonic community and has greatly influenced the tectonic studies of Eastern Asian. However, since their study was based on movements along active faults, their tectonic model is strictly only applicable to the tectonic evolution of Asia during a late period in the Cenozoic. If this model is used to explain tectonic evolution during earlier tectonic periods, for example, in the Indosinian Period, it would encounter a great deal of controversy and it may not be at all applicable. According to the data presented in this volume, the Tapponnier model may be applicable to the Eastern Asian continent following the Late Cenozoic (since 34 Ma), but cannot be applied to earlier tectonic periods.

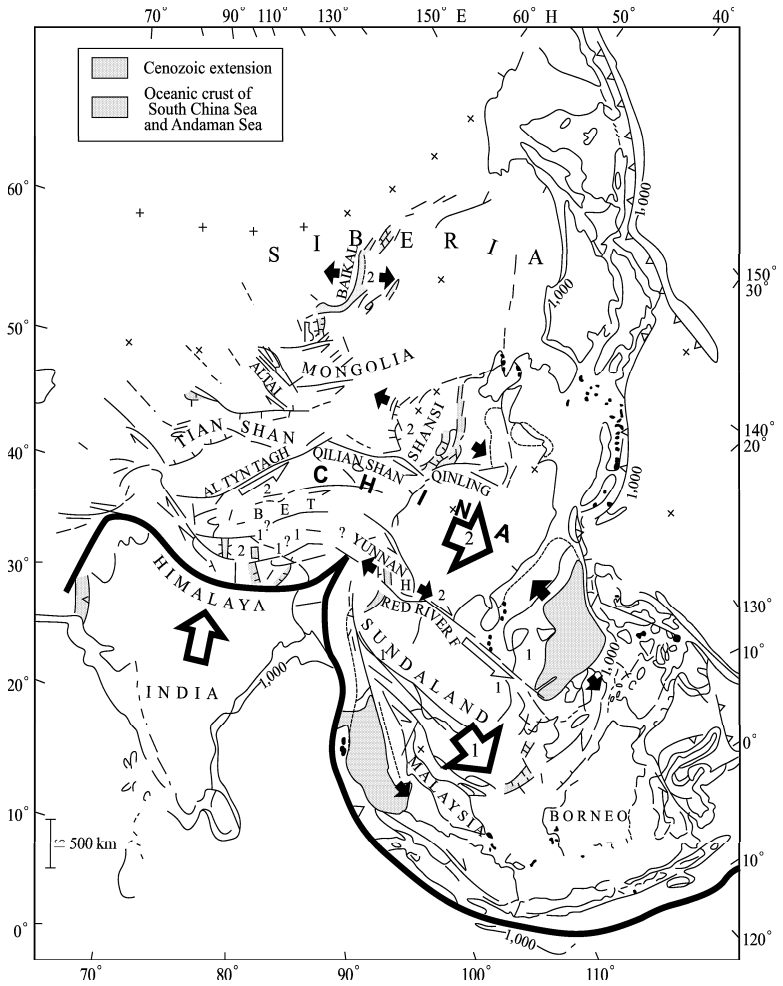

Fig. 6.1 Indentation tectonics in the East Asian continent (Tapponnier et al., 1982, with permission of Tapponnier P).

6.1 Sedimentary Paleogeography

In order to discuss the Triassic tectonic evolution of China, it is necessary to establish the Late Permian and Triassic paleogeography and biogeography. As in the Early to Middle Permian, China continent during the Triassic can be divided into four biogeographical provinces (Yin HF et al., 1988 (Fig. 6.2)): the Altay–Hingganling, Northern and Northwest China, Southern China–Tethys and Gondwana–Tethys Biogeographical Provinces. These biogeographical divisions are based on the distribution of the paleoflora (Sun KQ, 2002) confirmed by evidence from paleomagnetism (Appendix 6; Fig. 6.8).

The Altay–Hingganling Biogeographical Province (i.e. Angara (north Eurasian) cold temperate biogeographical province; AX in Fig. 6.2), has a fauna and flora in the Late Permian to Late Triassic which is transitional between those of Angara and North China. In this area clastic sedimentation occurred

in scattered basins. The Northern and Northwest China Biogeographical Province, extending from Kunlunshan–Qinling–Dabieshan in the north to Altay–Yinshan in the south, was located in the north temperate climate zone. At this time Northern and Northwest China were amalgamated to the Pangean Super-continent. Terrestrial clastic sediments in sedimentary basins are coarser grained in north and become finer towards south. In North China, northern Tarim and Junggar (NC in Fig. 6.2), large scale intra-continental basins formed in an arid climate and fossils are scarce.

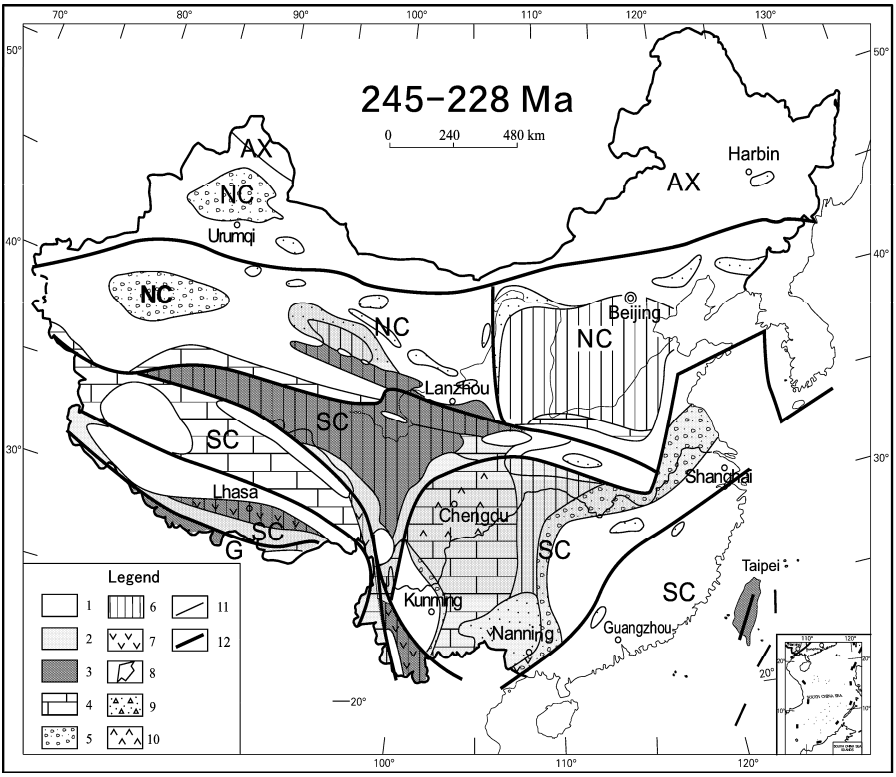

Fig. 6.2 Paleogeographic sketch map of the Chinese continent in the Middle Triassic (245–228 Ma) (Compiled from Wang HZ et al., 1985; Yin HF et al., 1988; Liu BJ et al., 1994; Yang SR et al., 2001).

1. Land or area of denudation; 2. Shallow marine continental shelf; 3. Bathyal, continental slope; 4. Carbonate deposits; 5. Conglomerate and sandstone deposits; 6. Sandy mudstone deposits or flysch ; 7. Volcanic rocks; 8. Direction of marine transgression; 9. Glacial clastic-mud group; 10. Gypsum and saline, tidal flat deposits; 11. Boundaries of sedimentary facies or geology; 12. Plate boundaries, perhaps with residual oceanic crust.

AX. Altay–Hingganling Biogeographical Province; NC. Northern and Northwest China Biogeographical Province; SC. South China–Tethyan Biogeographical Province; G. Gondwanan–Tethyan Biogeographical Province.

Denudation occurred in the Tarim Basin (western most NC in Fig.6.2) at the end of Triassic. In northern Tarim, there is a disconformity between the Triassic and Jurassic systems, but in eastern and central Tarim an angular unconformity occurs between the Jurassic and the underlying strata. The unconformity may have been due to collision between the Qiangtang and Tarim blocks which caused deformation, uplift and erosion in the Tarim Basin. The amount of denudation represented by the unconformity is

estimated to be about 100m, reaching ~2,000 m in the Luntai–Ruoqiang area (middle Tarim, western NC in Fig. 6.2) towards the east.

The South China–Tethyan Biogeographical Province (SC in Fig. 6.2), including the South China, Western Sichuan, Qiangtang and Gangdise blocks, was located in a tropical environment. In South China the Wujiaping Formation forms the lower part of the Upper Permian, including the Longtan coal system, characterized by clastic sedimentation, with alternating marine and terrestrial facies. The Changxing or Dalong Formation forms the upper part of the Upper Permian. The Changxing Formation occurs in the central part of the Yangtze Plate as a shallow marine platform carbonate, and the Dalong Formation, composed of bathyal sandstones and clay, with radiolarian chert, is distributed around its margins, indicating uplift of the central part of the Yangtze Plate, while its margins were depressed. The Emeishan basalts were erupted on the western part of the Yangtze Plate, above the head of the Emeishan mantle plume. Clastic littoral sediments were deposited over more part of the Cathaysian Plate, except for the Yunkai, eastern Fujian and eastern Guangdong areas, which were uplifted to form land areas.

In the Early Triassic and the early epoch of the Middle Triassic shallow marine carbonates were deposited on the Yangtze Plate, and shallow marine clastic carbonates on the Cathaysian Plate. In the later periods of the Middle Triassic, the southeastern parts of the Yangtze and Cathaysian plates were uplifted to form land areas, due to the collision between the Yangtze and Cathaysian plates, while shallow marine sedimentation continued on the western part of the Yangtze Plate. During the Late Triassic, after the complete amalgamation of the Yangtze and Cathaysian plates, fluviatile and lacustrine clastic sedimentary deposition was widespread in the Hunan, Guangdong, Sichuan, Guizhou and Yunnan areas. The Anyuan coal system was formed in northern Hunan and Jiangxi. Other areas of South China were covered by low mountains or hills (Liu BJ et al., 1994). Intensive erosion occurred in a tropical rain forest environment after the collision between Yangtze and Cathaysian plates.

In the Gondwanan–Tethyan Biogeographical Province (G in Fig. 6.2), shallow marine carbonate sedimentation was established on the Himalayan Block in the southern temperate zone.

6.2 Collision Tectonics

Four collision zones were formed in China during the Triassic: the Lancangjiang, Jinshajiang, Qinling–Dabie and Shaoxing–Shiwandashan collision zones. The stronger Indosinian collision period occurred during Middle–Late Triassic at 228–200 Ma (Fig. 6.3).

The Lancangjiang Collision Zone (i.e. Lazhulung–Shuanghu–Changning–Menglian–Dak, Thailand–central Malay Peninsula (1 in Fig. 6.3)) was a collision and amalgamation zone, located between the south Kunlun–northern Qiangtang–Ningjingshan–Lanping–Simao-Indochina blocks and the southern Qiangtang–Tanggulashan–Taniantawengshan–Baoshan–Sibumasu blocks. This collision zone marks the boundary between Gondwanan continental blocks with Late Paleozoic glacial deposits and cold water faunas, and Chinese continental blocks with warm water faunas (Figs. 5.2, 5.3). The Changning–Menglian area in Yunnan has been the most carefully studied part of the collision zone and here the collision is marked by the occurrence of mélange, accretionary thrust slices and fold-and thrust-zones, (Liu BP et al., 1991; Zhong DL et al., 1998). These rocks belong mainly to Late Paleozoic systems and include ophiolitic suites and crystalline basement rocks affected by greenschist and amphibolite facies metamorphism. Foliation is steeply dipping, and the main fault planes dip to the west at high to intermediate angles. Glaucophane from the Changning–Menglian zone gave Ar-Ar isotopic ages of 279 and 214 Ma, and muscovite ages of 238–215 Ma. The Lincang Granite which was intruded into the collision zone syntectonically has yielded zircon U-Pb ages of 254–213 Ma (Zhong DL et al., 1998). The Shuanghu Collision Zone has yielded an isotopic age of 275–287 Ma from the Gangmari glaucophane schist (Deng XG, 2000), and that of 222.5 Ma from the Naru glaucophane schist (Li C, 1997). According to general and regional relationships, the collision began in the Late Permian and continued into the Late Triassic, climaxing at the end of the Middle Triassic. In light of the chemical composition

of magmatic rocks, the rate of plate shortening near Lancangjiang is calculated to be 6.1 cm/yr and in northwestern Qiangtang, 6.8 cm/yr (Appendix 5.5).

The Jinshajiang (i.e. Lazhulung–Jinshajiang–Mojiang–Red River) collision zone (18 in Fig. 6.3) marked by ophiolite-mélange, accretionary slices and fold-and thrust-zones is the zone of amalgamation between the north Qiangtang–Ningjingshan–Simao–Indochina blocks and the Hohxilshan–Garze–Litang–Yangtze blocks. Triassic and pre-Triassic systems show extreme deformation and metamorphism, with steeply dipping foliations. Due to overprinting by later periods of movement (Paleogene and Neogene) along the multi-phase Jinshajiang–Red River strike-slip fault, an isotopic age for the phase of metamorphism which represents the major period of collision, is difficult to determine. Molasse deposits of Upper Triassic, which rest unconformably on the rocks of the collision zone, closure of the Jinshajiang Paleo-Ocean commenced during the Late Permian with subduction, and sinistral transpression and the collision was completed by the end of the Middle Triassic (Gu XD et al., 1988; Liu ZQ et al., 1993). A syn-collision granite gave isotopic ages of 255–227 Ma (Wang XF et al., 2000). The evidence from geological relationships and from isotopic dating gave similar results. From the chemical composition of magmatic rocks, the estimated rate of plate shortening in the Jinshajiang collision zone was about 6 cm/yr, 7.2 cm/yr at Yidun and 6.9 cm/yr at Karakorum (Appendix 5.5). The Lancangjiang, Jinshajiang collision zones and their adjacent areas show the most rapid rates of plate shortening.

According to deep seismic data from the Jinshajiang Collision Zone in Yunnan, fault planes dip to the east at intermediate angles at shallow depths, but in the lower crust they dip to the west. This relationship has been termed indentation tectonics, crocodile tectonics (Meissner et al. 1989) or wedge tectonics (Quinlan et al., 1993). The seismic profile shows that the upper crust of Yangtze Plate was obducted towards the west, while the lower crust and upper mantle of the Yangtze Plate were subducted westwards to a depth of 250 km (Zhao YG, et al., 1992; Zhong DL et al., 1998 (Fig. 12.3)).

Based on surface geological expression, the Lancangjiang Collision Zone is the most important, as it represents the boundary between Eurasian blocks and dispersed blocks from the Gondwana continent. However, with respect to lithospheric tectonics, the Jinshajiang Collision Zone is the most important, as it affects the whole lithosphere, while the Lancangjiang Thrust Zone affects only the shallowest part of the lithosphere, and is cut off by the Jinshajiang Thrust Zone. This was the first study of the deep structure of a collision zone in China. Subsequently, similar tectonic structures have been discovered in other collision zones, such as the Tianshan (Shao XZ et al., 1996), Himalayan (Teng JW et al., 1996), Longmenshan (Cai XL et al., 1995, 1997, Fig. 12.4), Qinling (Yuan XC et al., 1997, Fig. 12.5), Qilianshan (Wang ZJ et al., 1997) and Altunshan (Cai XL et al., 1998; Xu ZQ et al., 1999) collision zones. It appears that indentation or crocodile tectonics occurs rather commonly in continental collision zones.

The Qinling–Dabie Collision Zone, between the Sino-Korean and Yangtze plates, is composed of a series of thrusts. The Wushan–Baoji Collision Zone (6 in Fig. 6.3) occurs along the northern border of the Qinling–Dabie Collision Zone; the Luonan–Fangchang Collision Zone (10 in Fig. 6.3) occurs in the western section, but is cut off to the east by the Tancheng–Lujiang sinistral strike-slip fault zone (12 in Fig. 6.3), continuing as the Zhucheng–Qingdao-Rongcheng Collision Zone (11 in Fig. 6.3) as far as the Yellow Sea, where it is cut off along the eastern margin by a dextral strike-slip fault (13 in Fig. 6.3) (Hao Tianyao et al., 2002). To the south of the Korean Peninsula it continues as the Cheju Do Collision Zone (14 in Fig. 6.3). The Shandan–Tongbo Collision Zone (9 in Fig. 6.3) occurs in the central part of the Qinling–Dabie Collision Zone. The Mianxian–Lueyang–Dabashan–Fangxian–Xiangfan–Guangji Thrust Belt (8 in Fig. 6.3) along the southern border of the Qinling–Dabie Collision Zone also forms the northern border of the Yangtze Plate. Again this zone is cut off along the Tancheng–Lujiang Fault and transposed to northern Jiangsu. The eastward extension of this thrust belt is covered by the southern Yellow Sea, and is cut off by the dextral strike-slip fault along its eastern margin.

Collision and amalgamation in the Qinling–Dabie Zone were completed at the end of Triassic, and the residual marginal seas were destroyed. Isotopic data from many syn-collision metamorphic and magmatic rocks gives ages of 240–210 Ma (Ames, 1993; Maruyama, 1994; Cong BL and Wang QC, 1994, 1995; Li SG et al., 1997; Webb et al., 1999; Suo ST et al., 2000; Zhang GW et al., 2001; Liu

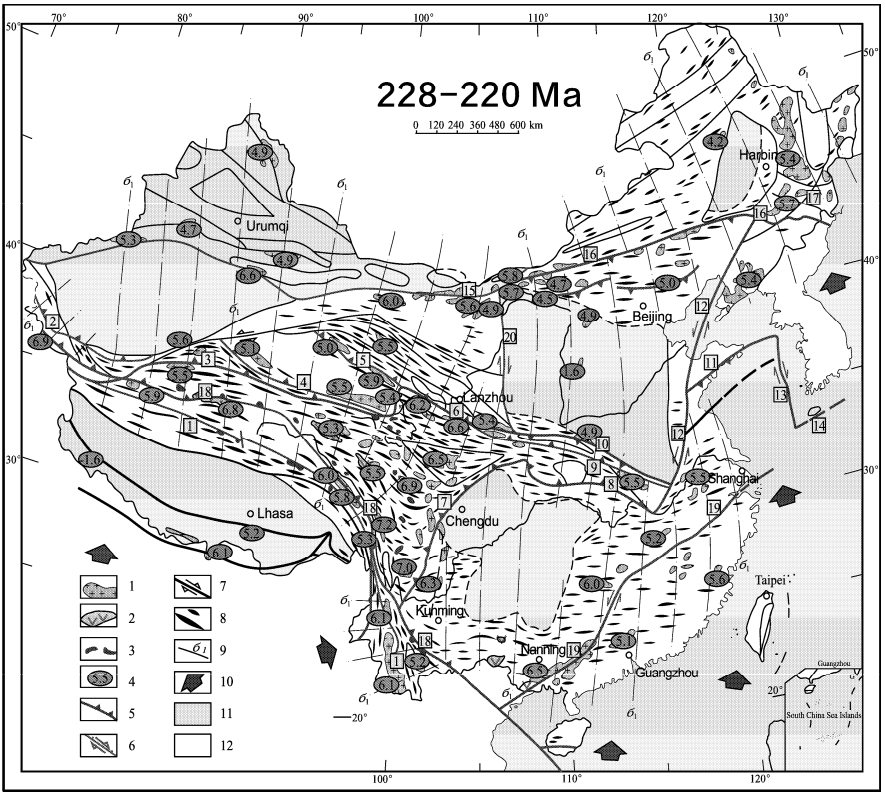

Fig. 6.3 Tectonic map of the Chinese continent in the Indosinian Tectonic Period (228–200 Ma).

1. Indosinian granite; 2. Indosinian volcanic rocks; 3. Indosinian ultramafic rocks in ophiolite suites; 4. Rates of intraplate deformation, estimated from the chemical compositions of magmatic rocks, "-", rate of extension, others, rates of shortening, units: cm/a, (data in Appendix 5.5); 5. Numbered collision zones or thrust belts; 6. Numbered normal and strike-slip faults; 7. Boundaries or strike-slip faults with weak activity not numbered; 8. Fold axes, only anticlines are shown (data in Appendix 3.4); 9.Trace of maximum principal compressive stress (σ_1); 10. Direction of plate movement; 11. Areas with angular unconformity; 12. Areas with parallel disconformity.

Names of numbered plate boundaries, collision zones and fault belts: [1] Lazhulung–Shuanghu–Lancangjiang–Changning–Menglian–Dak, Thailand–central Malay Peninsula Collision Zone; [2] Kangxiwa–southern border of Tarim Thrust Belt; [3] Southern border of Kunlun; [4] Central East Kunlun thrust belt; [5] Junulshan–Qinghainanshan Thrust Belt; [6] Wushan–Baoji Collision Zone; [7] Longmenshan Collision Zone; [8] Mianxian–Lueyang–Dabashan–Fangxian–Xiangfan–Guangji (northern border of Yangtze Plate) Thrust Belt; [9] Shandan–Tongbo Collision Zone; [10] Luonan–Fangchang (southern border of Sino-Korean Plate) Collision Zone; [11] Zhucheng–Qingdao–Rongcheng Collision Zone; [12] Tancheng–Lujiang sinistral strike-slip fault zone; [13] Eastern border of Yellow Sea dextral strike-slip fault; [14] Cheju Do Collision Zone; [15] Northern border of Alxa Thrust Zone; [16] Northern Yinshan–Xar Moron He (northern border of Sino-Korean Plate) Thrust Zone; [17] Dunhua–Mishan sinistral strike-slip fault zone; [18] Jinshajiang–Honghe (Red River) Collision Zone; [19] Shaoxing–Shiwandashan Collision Zone (sinistral strike-slip fault zone); [20] Helanshan–Liupanshan (western border of Sino-Korean Plate) dextral strike-slip fault zone.

YC et al., 2003), indicating that amalgamation occurred during the Late Triassic. An ophiolite suite ranging in age from the Late Paleozoic to the Early Triassic has been discovered at Huashan along the Mianxian-Lueyang segment of Shaanxi-Suizhou of Hubei Collision Zone (Dong YP et al., 1999; Zhang GW et al., 2001). This suite represents residual oceanic crust, which was deformed by collision at the

end of the Middle Triassic. This interpretation is accepted by most geoscientists as it is fully supported by the geological evidence.

The evidence shows that the collision between Sino-Korean and Yangtze plates had been completed, and the two plates were amalgamated by the end of the Triassic. There is no evidence to suggest that collision continued into the Jurassic or Cretaceous as suggested by Wang QC et al. (1998), Yang ZY et al. (1998) and Ren JS et al., 2000. Tectonism in the Qinling–Dabie Zone after the Triassic was due to intraplate deformation. During the Jurassic period, the Qinling–Dabie Collision Zone underwent N-S extension and subsidence to form sedimentary basins in which terrestrial sediments were deposited. There is no difference between these basins and other intraplate basins, which formed throughout China in response to the same N-S trending extensional stress at the Jurassic.

Based on 549 chemical analyses of samples of magmatic rocks, the rates of plate shortening in the Qinling–Dabie Collision Zone during the Indosinian period were between 5.4–6.6 cm/yr in northern Qinling, 5.5 cm/yr in central Qinling, 5.3 cm/yr in southern Qinling and 6.2–6.8 cm/yr in western Qinling (Appendix 5.5). The rate of plate shortening was more rapid in western Qinling, suggesting that compression and convergence were stronger here, due to the northwards migration of the South Qiangtang Plate. The magnitudes of differential stress determined from the Qinling–Dabie Collision Zone during the Triassic are the highest values which have been obtained in that period: 147 MPa in the northern Huaiyang area (Xiong CY, 1992), and 142 MPa in Fengxian of Shaanxi (Wang GH, 1993). The deformation was more intense in the Qinling-Dabie Collision Zone than in the other collision zones.

The high to ultra-high pressure metamorphic rocks, including eclogite with quartz, coesite, microdiamonds and glaucophane schist in mélange in the Qinling–Dabie Collision Zone, may be residual sheets of upper mantle lithosphere belonging to the Yangtze Plate, which were subducted, but have been uplifted, and are now exposed at the earth's surface. Isotopic ages obtained from these high-ultrahigh pressure metamorphic rocks are concentrated in three periods: about 800 Ma (Neoproterozoic) (Liu GH et al., 1993; Suo ST et al., 1993; Li SG et al., 1993; Zhang GW et al., 1996; Zhang SG et al., 1991, 1998); 400 Ma (end of the Early Paleozoic) (Liu GH et al., 1993; Zhai XM et al., 1998; Yang WR et al., 2000, 2002; Xu B et al., 2000; Zhang GW et al., 2001; Che ZC et al., 2002), and 221–244 Ma (Triassic). It is probable that major tectonic events occurred in each of these periods. In the Qingbaikou Period (about 800 Ma) and at the end of Early Paleozoic, there were ocean-continent subduction, convergence and shortening events. But these events did not cause deformation in the Sino-Korean Plate and did not result in intraplate deformation in the plates on either side of the collision zone. The final continent-continent collision between the Sino-Korean and Yangtze plates with obvious intrapalte deformations occurred in the Late Triassic.

Webb et al. (1999) obtained many isotopic ages from the high to ultra-high pressure metamorphic rocks in the Qinling–Dabie Collision Zone using U-Pb, Sm-Nd and Ar-Ar methods. They concluded that these rocks were formed deep in the mantle, between 245 and 240 Ma, they were uplifted between 240 and 230 Ma through a distance of 75–375 km from the mantle into the middle crust, at a rate of 5–25 mm/yr, reaching the upper crust in the Jurassic (200–190 Ma). At that period muscovite mica re-crystallized at a temperature of 300°C. More recently Liu YC et al. (2003) reached the similar conclusions.

From regional research in Chenmagang and Hejiawan, Macheng in Hubei, Donghe chong, Yingshan, Bixiling, Yuexi in Anhui and Maobei, Donghai in Jiangsu Province, Zhong ZQ et al. (1999) and Suo ST et al. (2000) concluded that residual high to ultra-high pressure metamorphic minerals and deformation are preserved only in large blocks of eclogite and ultra-high pressure metamorphic rocks, which were formed during oblique collision between Sino-Korean and Yangtze plates during the Triassic (240–210 Ma). The uplift of the high pressure Dabie-Jiaonan blocks in mélange, with retrograde metamorphism under amphibolite facies conditions, occurred as a result of N-S extension during the Early Jurassic (200–170 Ma). These recent interpretations of the origin and subsequent evolution of the high to ultra-high pressure metamorphic rocks in Qinling–Dabie Collision Zone are not identical, but each may contain elements based on which a complete account could be constructed.

A deep seismic profile across the Qinling–Dabie Collision Zone shows the characteristic features of "crocodile" tectonics (Yuan XC, 1994, 1996, 1997) with the middle and lower crust of the Qinling Block penetrating the middle crust of Sino-Korean Plate to the north, and the middle and lower crust of Yangtze Plate penetrating the middle crust of the Qinling Block also to the north (Fig. 12.5). Using seismic tomography, Xu PF et al. (2002) also identified crocodile tectonics in the Jiaonan Collision Zone, the eastwards extension of the Dabie Collision Zone (Fig. 12.6). They found that at a depth between 16 and 25 km the crust of Sino-Korean plate penetrated the crust and mantle of the lithosphere of the Yangtze Plate towards south, for a distance of more than 80 km.

There has been much discussion concerning the eastward extension of the Qinling-Dabie Collision Zone. If the whole of the Korean Peninsula forms part of the Sino-Korean Plate (Chang KH, 1997, 2000; Wan TF and Zeng HL, 2002), it was predicted that the Qinling-Dabie Collision Zone would extend eastwards to the Cheju Do area, and further east to form the southern margin of Hida Block in northern Honshu, Japan. Recently Japanese geologists (Tsujimori et al., 2000; Kunugiza et al., 2001) have discovered glaucophane in a rock sample with partial eclogitic mineralogy in the Hida Marginal Belt. Three groups of metamorphic ages (350–300 Ma, 270–210 Ma and 210–180 Ma) were determined from single grains of zircon, monazite and pitchblende using SHRIMP and U-Th-Pb me- thods, and from amphibole, mica and whole rock, using Rb-Sr and K-Ar methods. These researchers suggest that the 270–210 Ma tectono-thermal event can be correlated with events of the same age in the Dabie Collision Zone. If this interpretation is correct, the Hida Block is part of the Sino-Korean Plate, the Hida Marginal Belt is equivalent to the Dabie Collision Zone, and the "interior belt" of northern Southwest Japan can be correlated with the Yangtze Plate. To further east the Yangtze Plate would become very narrow and terminate near Tokyo at the Tanakura Tectonic Line; to the east of the Tanakura Line Japan belongs to the Okhotsk Plate (western part of North American Plate).

Recently, high temperature and high pressure laboratory experiments to determine the rheological strength of the crust under the differential stress during continental collision (Hobbs, 1968; Hirth et al., 1994; Zhou YS et al., 2004, 2005) found that the transition between quartz and coesite occurred in rather low conditions of differential stress (550–950 MPa), at a strain rate of 10^{-14}–10^{-13} /s. This means that ultra-high pressure metamorphic (UHPM) rocks could form between 20 and 60 km below the surface. If this is correct, it does not require subduction to depths of 200–300 km to form UHPM rocks, followed by rapid uplift as supposed by Cong BL et al. (1999) and Liu YJ et al. (2001).

In South China the Shaoxing–Shiwandashan Collision Zone (19 in Fig. 6.3) between the Yangtze and Cathaysian plates was formed during the Indosinian Tectonic Event, mainly at the end of the Middle Triassic. However, there is some evidence for convergence and compression in the Jinning period ($\sim$800 Ma) of the Neoproterozoic and at the end of Early Paleozoic. Shui T et al. (1986, 1987) suggested that collision occurred gradually after the Jinning Tectonic Period. Sun MZ et al. (1990) proposed that different sections of the collision zone developed step by step in different periods, the Shaoxing-Jiangshan section colliding in the Jinning Period, the middle section, to the southeast of Wugongshan, colliding at the end of the Early Paleozoic, and the southwestern section (near Shiwandashan) in the Indosinian Period. Hsu (1980, 1987) first suggested that Shaoxing–Jiangshan–Shiwandashan Collision Zone had formed during the Indosinian Period and proposed new models of tectonic movement. For example, he suggested that the Jiuling–South Anhui Block was subducted beneath the Lower Yangtze Block along the boundary between the Precambrian greenschist system and the Paleozoic sedimentary systems; he recognized Triassic metamorphic rocks, but not the Meso- and Neoproterozoic systems. He and his colleagues described the South China area as an orogenic zone and interpreted the Lantian in south Anhui as a window in a nappe structure, and concluded that collision was continuous from the Triassic to the Cretaceous (Hsu et al., 1988, 1989, 1990).

However, many Hsu et al.'s (1988, 1989, 1990) opinions are not in accord with the geological facts, so that many geologists do not agree with their interpretations (Gupta, 1989; Rodgers, 1989). Most Chinese geologists consider that the Yangtze and Cathaysian plates collided along the Shaoxing –Jiangshan–Shiwandashan Collision Zone at the end of Middle Triassic, but do not accept all the opinions of Hsu and his colleagues. As shown in earlier chapters of this book, convergence occurred in the eastern sec-

tion of Shaoxing–Jiangshan–Shiwandashan Zone at ~800 Ma, but there is no evidence to indicate that continent–continent collision occurred in the Early Paleozoic. There may have been ocean–continent subduction, but the directions of convergence and shortening in the Yangtze and Cathaysian plates at the end of Early Paleozoic were very different (Table 4.2). There is a great deal of evidence from sedimentation, paleogeography and the occurrence of intraplate deformation for the Shaoxing–Jiangshan–Shiwandashan Collision Zone, but perhaps because of the extent of the Cretaceous sedimentary cover and the scarcity of outcrops no paleo-oceanic crust has yet been found in this zone.

New seismic tomography from the eastern part of Shaoxing–Jiangshan Collision Zone (Xu Y et al., 2006) shows that the Cathaysian Plate was subducted northwards at an intermediate angle of dip beneath the Yangtze Plate to a depth of 400 km, and that in the middle part of the collision zone the Yangtze Plate was subducted southeastwards to the depth of 400 km at an intermediate angle beneath the Cathaysian Plate (Cai XL et al., 1998, 2002).

There was a large amount of shortening along the Shaoxing–Jiangshan–southeast Wugongshan Collision Zone during the N-S convergence and collision between the Yangtze and Cathaysian plates, with transpression from southeast of Wugongshan to Siwandashan, the development of near N-S extensional faults along the margins, and the intrusion of syn-collisional granites (19 in Fig. 6.3; T in Fig. 7.8). As a result of the collision strong folding and faulting occurred in the Upper Permian–Middle Triassic systems in the Yunkai Block in western Guangdong Province, and the collision between Yangtze and Cathaysian plates was completed (Qiu YX et al., 1993). The Upper Triassic rests unconformably on folded Middle Triassic and older systems. K-Ar and U-Pb isotopic ages obtained from 43 samples of syn-collisional granites are concentrated between 221 and 290 Ma; Early–Middle Triassic geological ages were obtained for volcanic rocks in the same period (Fang QH et al., 1988; Wang QQ et al., 1989; Liao QK, 1991). From chemical analyses of magmatic rocks, the rates of shortening in the Shaoxing–Siwandashan Collision Zone in the Indosinian Tectonic Period were 4.9 cm/yr from analysis of 12 samples from western Zhejiang, and about 6.0 cm/yr from 98 samples near Siwandashan (Appendix 5.5).

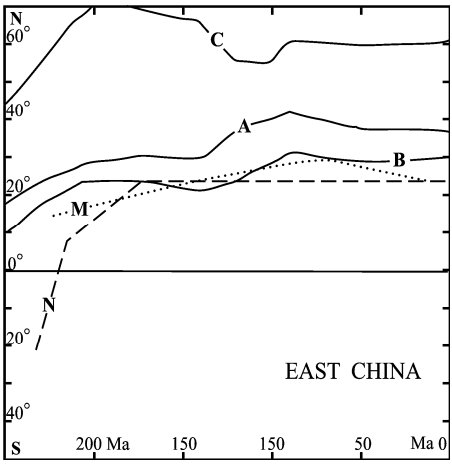

Fig. 6.4 Paleo-latitudinal change of the eastern blocks of Chinese continent and its adjacent areas from the Triassic to the present.

A. Sino-Korean Plate; B. South China Plate (mainly Yangtze); C. Siberian Plate; M. Simao-Indochina Plate; N. Baoshan–Sibumasu Plate.

Granitic bodies related to collision during the Indosinian Tectonic Period, outcrop over more than 54,000 km^2, equalling one sixth of the total area of granitic rocks in China (Cheng YQ et al., 1994).

In summary, the Indosinian Tectonic Period (260–200 Ma) was the main tectonic period for the formation of the Chinese continent. As a result of collisions along the four collision zones, Lancangjiang, Jinshajiang, Qinling–Dabie and Shaoxing–Shiwandashan, blocks composing three quarters of the Chinese continent were amalgamated with the Pangean Super-continent; the Chinese continent built its southeastern extension, like a peninsula. Paleomagnetic data also supports this conclusion (Appendix 6). During the last 200 million years, the blocks forming the eastern Chinese continent have remained in the same latitudes and have maintained the same relationships, moving together synchronously (Fig. 6.4), showing that the collision and amalgamation of the blocks in eastern Chinese continent were completed by the end of the Triassic.

6.3 Intraplate Deformation

The sedimentary cover of the Chinese continent underwent widespread intraplate folding and faulting forming the Indosinian Tectonic System during the Indosinian Tectonic Event. The deformation was very strong near collision zones, for example, to the north of the Qinling Collision Zone (2 in Fig. 6.5), on the northern margin of the Sino-Korean Plate (3 in Fig. 6.5), on the western margin of the Yangtze Plate (7 in Fig. 6.5) and to the north of the Shaoxing–Shiwandashan Collision Zone (8 in Fig. 6.5). However, there is only weak deformation in other intraplate areas, such as Junggar in Xinjiang, Jinyuan in Gansu, Huaining in Anhui and Rutog in Tibet (Xizang) (1, 4, 5 and 6 in Fig. 6.5).

Data from 2,195 macro-and meso-scale folds (including 1,109 anticlines and 1,086 synclines) formed during the Indosinian Tectonic Period, and taken from the 1: 200,000 regional geological survey of the whole of China is shown in Appendix 3.4. Folds with a near E-W trend are widespread, occurring from north Heilongjiang to south Guangdong. Isoclines and overturned folds occur in the vicinity of the collision zones or paleo-faults, and are accompanied by magmatism and metamorphism. In the smaller paleo-blocks or on the margins of large plates, such as the Sino-Korean, Yangtze, Tarim and Songhuajiang–Nengjiang plates, Jurano-type box folds are commonly found. However, there are almost no folds in the center of the large blocks, for example, in the Erdos (western Sino-Korea) and Western Yangtze (Figs. 6.3 and 6.5). There is no folding in the Tarim Block and its adjacent area to the north. This may be due to strain-hardening, as these areas were affected by strong folding and magmatism during the Late Paleozoic. The Gangdise and Himalayan blocks also show no folding. These blocks were located in the Tethys Ocean in the southern hemisphere during the Triassic and were not amalgamated with the Chinese continent until a later period.

In most areas of the Sino-Korean and Yangtze plates the earliest and most widespread folding of the sedimentary cover occurred during the Indosinian Tectonic Period. On the margins of Sino-Korean Plate, the Mesoproterozoic, Neoproterozoic, Paleozoic and Triassic systems were all folded during this period. In the northern and eastern areas of the Yangtze Plate, rocks from the Jinning and Nanhua up to the Middle or Late Triassic systems were also folded during this period. Detachment occurred in incompetent units, such as the shale of the Silurian Fentou Formation, Longtai coal formation of Permian and the Middle Triassic evaporites, so that strata above and below show very different styles of folding. In the southern part of the Yangtze Plate, where E-W trending folds were formed at the end of Early Paleozoic, strata of the Upper Permian and Lower-Middle Triassic systems were folded during the Indosinian Period. The orientations of the fold axes and the maximum principal stress were very similar during these two separate tectonic events, so that the unconformity between Middle and Upper Triassic systems is not easily distinguished.

From the study of more than ten sections in southern China, Guo FX (1998) concluded that the Indosinian Tectonic Event was relatively weak, so that the sedimentary cover on the South China blocks was not extensively folded. When the orientations of the strike and the fold axes in different tectono-str-

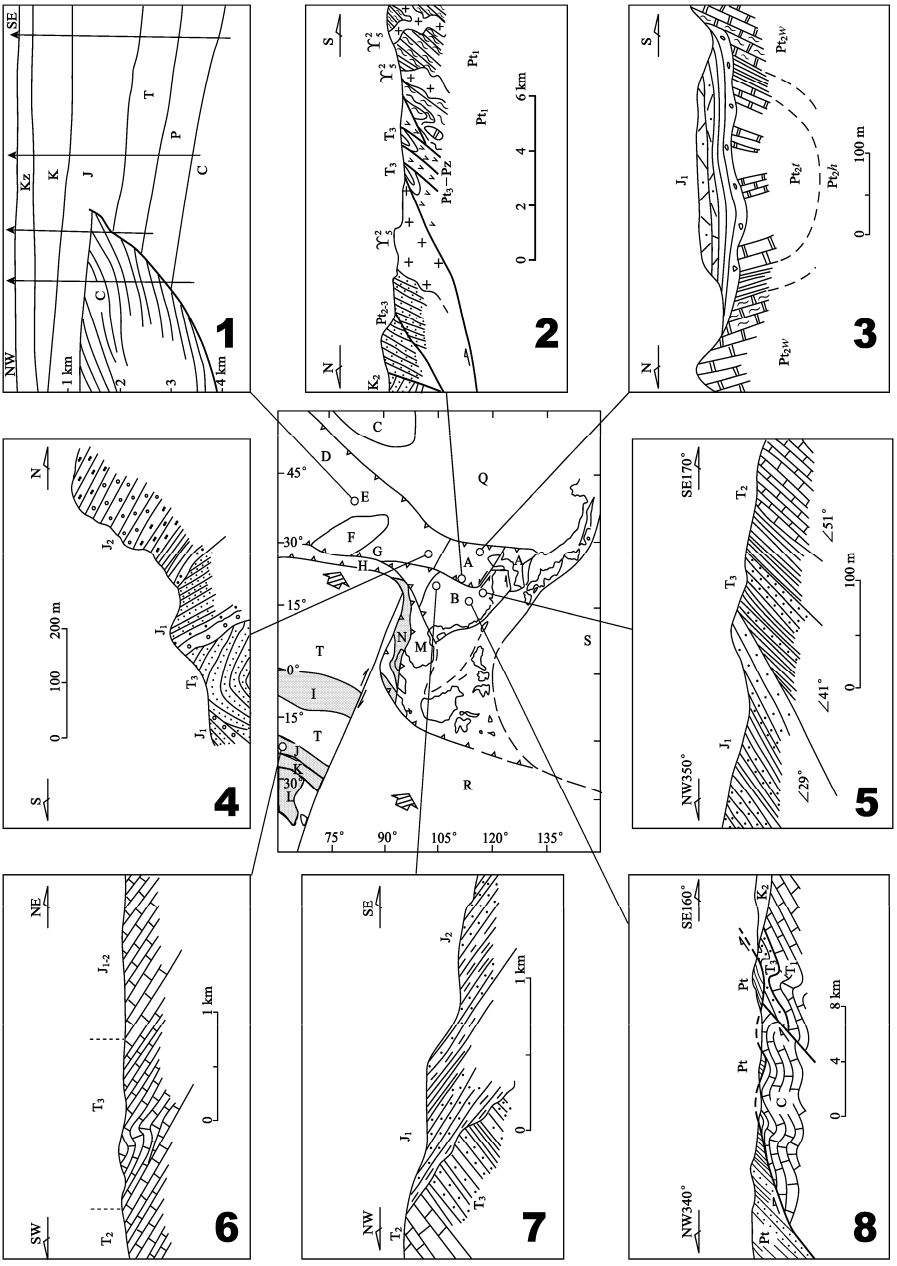

Fig. 6.5 Examples of deformation during the Indosinian Tectonic Period.

1. A slight angular unconformity between the Triassic and Jurassic in the Junggar basin, Xinjiang; there was almost no deformation during the Indosinian. The Karamay-Ulhuy fault movement between the Middle and Late Jurassic belongs to the Yanshanian Period; 2. In North Qinling thrust system, the Triassic and the underlying systems underwent metamorphism and deformation during the Indosinian Period, γ_5^2 is a Jurassic granitic intrusion, and the underlying thrust was formed in the Sichuanian Tectonic Period; 3. In the Boluoshu Dongshancun in Chengde City, Hebei, the Early Jurassic

Xingshikou Formation rests unconformably on the Tieling (Pt_2t), Hongshuizhuang (Pt_2h) and Wumishan (Pt_2w) formations (Bureau of Geology and Mineral Resources of Hebei Province, 1989); 4. The unconformity between the Early Jurassic and Late Triassic at Sidaogou, in Jinyuan, Gansu (Bureau of Geology and Mineral Resources of Gansu Province, 1989); 5. An unconformity between the Early Jurassic and Middle and Late Triassic at Lalijian in Yueshan, Huaining, Anhui province (Wan TF's personal record); 6. Conformity between the Early and Middle Jurassic and Middle and Late Triassic systems at Linjitang, Rutog, Xizang (Bureau of Geology and Mineral Resources of Xizang, 1993); 7. Angular unconformity between the Early Jurassic Baitianba Formation and Middle and Late Triassic near Erlangmiao, in Jiangyou, Sichuan (Bureau of Geology and Mineral Resources of Sichuan, 1991); 8. Xishan Thrust in Xinjian, Nanchang City, Jiangxi, the Proterozoic system thrust over Triassic and Carboniferous systems (Zhu ZC, 1989).

Symbols: A. Sino-Korean Plate; B. South China Plate (including Yangtze and Cathaysian plates); C. Siberian Plate; D. Kazakhstan Plate; E. Junggar Block; F. Tarim Block; G. Qaidam Block; H. Kunlun Block; I. Qiangtang Block; J. Gandise Block; K. Himalayan Block; L. Indian Plate; M. Simao-Indochina Plate; N. Baoshan-Sibumasu Block; O. Pacific Plate; P. Philippines Sea Plate; Q. Hingganling–Mongolia-Tianshan Collision Zone; R. Australian Plate; S. Izanagi Plate; T. Tethys Oceanic Plate.

The above symbols are used in the figures of deformation, stress magnitude and tectono-paleogeographic reconstruction in Chapters 6 to11.

atigraphic units are very similar, and there is only a small angle between them, the unconformity may not be very obvious. Where fold systems intersect each other at right angles or at a large angle, unconformities can be distinguished more easily (Fig. 6.5). In the South China area these relationships are demonstrated clearly by thousands of folds, shown on 1: 200,000 regional geological maps. On the Cathaysian Plate, including the East and South China Sea areas, Upper Paleozoic and Early and Middle Triassic systems were affected by folding during the Indosinian Event.

In Northeast China the Permian and Triassic systems were affected by Indosinian folding. An understanding of these tectonic relationships is important in the exploration for oil and gas in buried pre-Mesozoic systems in basins.

An important characteristic of the Indosinian Tectonic Period was the formation of arcuate tectonic zones with linear folds and faults, for example, the famous Guangxi (in northern Guangxi) and Huaiyang (along the lower Yangtze River, from Hubei to Jiangsu) tectonic zones. In the sedimentary cover of the Sino-Korean and Yangtze plates the lithological characters are rather homogeneous. When folding occurs in areas with inhomogeneous lithological characters, arcuate folds and faults may occur at different scales. In present day coordinates nearly all the axes of the Indosinian folds trend E-W. This system of folding was termed "latitude trending tectonics" by Lee JS (1929, 1939), as he considered that their formation was related to their latitude and the effects of velocity change of the Earth's rotation. But the formation of these folds bears no relation to latitude or rotation of the Earth. Paleomagnetic studies show that during the Indosinian Tectonic Period the declination of blocks forming the eastern part of the Chinese continent was about 30°to the east of their present declination (Appendix 6; Figs. 6.8 and 6.9), so that on a paleogeographic map Indosinian fold axes would have an NW-SE trend, which occurred, having nothing to do with latitude and effects of velocity change of the Earth's rotation.

Along N-S longitudes (103.5°E, 112.5°E, 115°E and 124°E) in the eastern parts of the Chinese continent, the shortening ratio, shortening magnitude, shortening rate, deformation time and linear strain rate for intraplate folds have been calculated (methods of calculation shown in Chapter 1; Table 6.1). It is found that the greatest shortening ratio, up to 50%, occurred in eastern South China along longitude 115°E, with lesser amounts of shortening in Northeast China (36.69%), middle China (20.18 %) and western South China (14.13%). In North China, folding was rather weak with a much smaller amount of shortening. The length of time over which deformation occurred, calculated from the four sections above, is between 2.1 and 8.6 million years, meaning that intense deformation occupied only between 5 and 17% of the total length of the Indosinian Tectonic Period. Linear strain rates were very small (1.39–2.13)$\times 10^{-15}$/s , indicating that deformation took place while the rocks were in a rheological state.

In addition to the collision zones and widespread intraplate folding, a series of near E-W trending thrust zones were formed under the influence of the tectonic stress field during the Indosinian Period, originating in weakened zones or paleo-faults, e.g. the Kanxiwa–southern border of the Tarim Thrust Zone (2 in Fig. 6.3), the Central East Kunlun Thrust Belt (4 in Fig. 6.3), the Junulshan–Qinghainanshan

Table 6.1 Shortening ratio, shortening magnitude, deformation time and strain rate during Indosinian Period

Area	Western South China	Middle South China	Eastern South China	Northeast China
Longitude	103.5°E	112.5°E	115°E	124°E
Length (km)	1,000	1,000	1,000	1,125
Mean limb angle of folds	30.8°	37°	60°	50.7°
(amount of data)	(352)	(402)	(628)	(200)
Shortening ratio (%)	14.13	20.18	50.0	36.69
Shortening magnitude (km)	141.3	201.8	500	413
Shortening velocity (cm/yr)	6.7	6.7	5.8	4.9
Time of Deformation (Myr)	2.1	3.0	8.6	8.4
Strain rate (ε, 1/s)	2.13×10^{-15}	2.13×10^{-15}	1.84×10^{-15}	1.39×10^{-15}

Thrust Belt (5 in Fig. 6.3), the Yushigou-Chuncigou, northern Qilian Overthrust (Feng YM, 1998), the Longmenshan Collision Zone (7 in Fig. 6.3), the northern border of the Alxa Thrust Zone (15 in Fig. 6.3) and the north Yinshan–Xar Moron He (northern border of the Sino-Korean Plate) Thrust Zone (16 in Fig. 6.3). These thrusts were developed by the re-activation of paleo-faults, and are accompanied commonly by S or A type granitic intrusions. Intraplate intrusions of the Indosinian Period are distributed around Laoyeling in Northeast China, the northern Yinshan–Xar Moron He Thrust Zone, the northern border of the Qiadam, eastern Kunlun and the Aba–Garze–Litang–Hengduanshan areas (Fig. 6.3).

Under the influence of N-S shortening, near N-S trending weakened zones easily form strike-slip faults, such as the Tancheng–Lujiang sinistral strike-slip fault, which extends from south of Guangji in Hubei to the north of Siping in Jilin (12 in Fig. 6.3), the sinistral Dunhua–Mishan strike-slip fault (17 in Fig. 6.3), the eastern margin of the Yellow Sea dextral strike-slip fault (13 in Fig. 6.3) (Hao TY et al., 2002) and the dextral Helanshan-Liupanshan strike-slip fault (20 in Fig. 6.3).

The formation and evolution of Tancheng–Lujiang fault zone is of great interest to geoscientists in China and abroad (Wan TF, 1995, 1996). Xu JW (1957) first suggested that there had been a large displacement along the Tancheng–Lujiang sinistral strike-slip fault. Zhang WY (1959, 1964) recognized that collision and shortening in the Qinling–Dabie zone were connected with strike-slip movements along the Tancheng–Lujiang Fault. He considered that collision and strike-slip represented two types of deformation which were developed during the same tectonic period. Although in the last forty years no Triassic isotopic ages have been obtained from the fault rocks in Tancheng–Lujiang Fault Zone, the structural and sedimentary evidence indicates that the fault zone formed after the Paleozoic and before the Jurassic. The greatest sinistral strike-slip displacement of 300–400 km is found in the southern section of the fault (Zhang YX et al., 1984; Weng SJ, 1984; Guo ZY, 1987; Wan TF et al., 1995, 1996; Wang XF et al., 2000). Most geoscientists agree with this interpretation. However, there are many different opinions about the time of formation and amount of strike-slip displacement along the Tancheng–Lujiang Fault Zone. Xue JS (1982), Zhang JS, (1983) and Qiao XF et al. (2001) suggested that the earliest movement along the fault zone occurred during the Archean or Meso-Neoproterozoic, Zhu G et al. (2001) suggested that movement occurred mainly during the Jurassic (190 Ma), while Xu JW et al. (1987) suggested the Cretaceous (about 130 Ma), however recently Zhang Q, Zhu G et al. (2008) recognized that first moving happened during Triassic (236–238 Ma), turning back to the former consideration. Xu JW (1980, 1994) and Xu JW et al. (1993) considered that the greatest strike-slip displacement was more than 700 km, while Qiao XF et al. (2001) thought that there was no evidence of strike-slip at all. Although on the face of it these opinions are extremely different, it is possible that a consensus view can be reached.

Some basic facts are generally verified: in the Archean-Paleoproterozoic weakened zones and faulted-depressions, with NE-trending foliations, were formed along the fault zone; there is much evidence for paleo-earthquakes; the fault zone was re-activated after the Triassic, and isotopic ages obtained so far are mainly Triassic, Jurassic, Cretaceous and so on. Most structural geologists do not agree with neither the estimate of 700 km for the maximum amount of displacement, nor the viewpoint of the complete absence

of displacement. From the displacement of the Qinling–Dabie–Jiaonan Collision Zone the maximum amount of strike-slip displacement is 430 km at its southern end, if the rotation of crustal blocks is considered to be about 350 km (Weng SJ, 1984). In Hebei and Liaoning provinces the boundary of Ordovician lithofacies is displaced by about 160 km along the fault zone (An TX and Ma WP, 1993); the outcrops of the Archean–Paleoproterozoic metamorphic systems and a zone of high normal aeromagnetic anomalies are cut off and displaced by about 120 km. All these pieces of evidence are certainly correct (Wan TF et al., 1995, 1996).

Recently, using gravity anomaly data, a dextral strike-slip fault zone was found on the eastern margin of the Yellow Sea (Hao TY et al., 2002). The boundary between the Sino-Korean and Yangtze plates is an example of indentation tectonics*. The Southern Yellow Sea area of the Yangtze Plate has clearly indented the Sino-Korean Plate, the western margin of the indenting block is the Tancheng–Lujiang sinistral strike-slip fault zone and the eastern margin is the eastern Yellow Sea dextral strike-slip fault zone (Fig. 6.3).

Although the Tancheng–Lujiang Fault Zone cuts through the Sino-Korean Plate from north to south, over a distance of 1,100 km, no Triassic granitic intrusions are found along the fault. This could be explained if the fault was an intra-crustal fault not extending to a depth of more than 20 km, so that the fault zone extended into the crust only as far as a detachment zone between the upper and lower crust (Wan TF et al., 1996). Recently Xu PF et al. (2002) discovered that at a depth of 16–25 km the crust of Sino-Korean Plate has penetrated between the upper crust and the lithospheric mantle as a sheet or wedge, extending for a distance of more than 80 km into the Yangtze Plate (Fig. 12.6). It is possible that the Tancheng–Lujiang Fault Zone penetrated only as far as a detachment zone in the middle crust at a depth of 16–25 km, allowing the upper crust of the Yangtze Plate in the southern Yellow Sea area to thrust northwards over the Sino-Korean crust for a distance of 300–400 km, as indicated by the amount of displacement on the bounding strike-slip faults. The upper crust of the Yangtze Plate, to a depth of 16 km in the south Yellow Sea area, could be called the South Yellow Sea Nappe. Between 15 and 25 km depths the crust of the Sino-Korean Plate has penetrated the middle crust of Yangtze Plate, below 25 km depth the lower crust and the upper mantle belong to the Yangtze lithospheric plate. In addition, from the distribution of areas of intraplate deformation in the Chinese continent and the limited number of granitic intrusions belonging to the Indosinian Period, it is suggested that intraplate deformation throughout China was controlled mainly by a detachment between the upper and lower crust.

Data from Indosinian folds presented in Appendix 3.4 shows that the preferred attitude of the maximum principal compressive stress axis (σ_1), relative to the present day geographical coordinates, is SE174°∠4°, the intermediate principal stress axis (σ_2) (i.e. the average orientation of the fold axes) is NE86°∠2°, with intermediate angles of dip of the fold limbs (40°–60°), and the minimum principal stress axis (σ_3) is NW355°∠87° (Fig. 6.6). Although the fold axes have a generally E-W trend, in the arcuate tectonic systems there is sometimes a very great variation up to 40° in the orientation of the fold axes. In western Yunnan and Eastern Xizang in southwest China, the variation in the trend of the fold

* The indentation tectonic model between Sino-Korean and Yangtze plates was first proposed in Chinese by Zhang WY et al. (1983), and then re-proposed by Yin A and Nie SY (1993, 1996) in English. However, Yin A and Nie SY considered that northern border (Zhucheng–Qingdao Fault) of the Qinling–Dabie–Jiaonnan (Sulu) Collision Zone continues into the Imjingang area in the central Korean Peninsula. The eastern margin of the area of indentation tectonics is not very clear, but may be marked by the NNE-trending Hunan faults. According to Yan A and Nie SY (1993, 1996), the Gyeonggi Massif and the area to the south belong to the Yangtze Plate. However, they did not undertake any field work in the Korean Peninsula before publishing their paper (Yin A and Nie SY, 1993). In 1994, during the geological field excursion for the IGCP 321 Symposium, many Korean and Chinese geologists agreed that the Gyeonggi Massif and the areas to the south belong to the Sino-Korean Plate, because the geological evolution and characteristics of the whole Korean Peninsula, from the Archean to the Paleozoic are similar to those of the Sino-Korean Plate. Since the Hunan faults do not form a continuous marginal fault zone (Chang KH, 1995, 1997, 2000; Wan TF, 2001; Wan TF and Zeng HL, 2002), it is predicted that there is a dextral strike-slip fault located in the southern Yellow Sea, as suggested by Zhang WY (1983), but there is no evidence for this fault zone. However, during 2001–2002, Korean and Chinese geophysicists cooperated in a gravity survey in the Yellow Sea and discovered that there is a dextral strike-slip fault zone along its eastern margin (Hao TY et al., 2002). Indentation tectonics provides a reasonable interpretation of the relationships between Sino-Korean and Yangtze plates as firstly predicted by Zhang WY et al. (1983).

axes is very great, sometimes as great as 90°, due to later compression and deformation caused by the northward movement of the Indian Plate, so that the fold axes trend N-S.

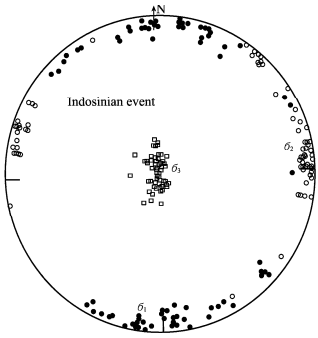

Fig. 6.6 Attitude of principal stress axes during the Indosinian Period. σ_1. Maximum principal stress axis; σ_2. Intermediate principal stress axis; σ_3. Minimum principal stress axis.

The Indosinian Tectonic System includes a series of near E-W trending folds and thrusts, arcuate tectonic zones and a series of N-S, NNE or NNW-trending normal and strike-slip faults and extension joints (Fig. 6.3). The development of a unified tectonic stress field in the Indosinian Tectonic System across many paleo-blocks shows that all the continental blocks forming the eastern part of the Chinese continent were amalgamated to form a single tectonic unit by the end of the Indosinian Tectonic Period.

Based on 111 samples dated isotopically, data on the tectonic stress (i.e. differential stress) magnitude for the Indosinian Period was collected from 12 sample points and estimated. The average magnitude of differential stress was calculated as 105.5 MPa (Fig. 6.7; Appendix 4), it means that tectonism was stronger during Indosinian Period. In the areas of folding from the middle and lower Yangtze, Shandong and the western area of Altun and Burang of Xizang, the magnitude of differential stress was between 100 and 125 MPa. The highest value of 147 MPa occurs in north Huaiyang (Xiong CY, 1992), there is also a high value of 142 MPa at Fengxian, Shaanxi (Wang GH, 1993), indicating the strength of the collision in the Qinling-Dabie zone. In areas of pre-Cambrian crystalline systems or granite intrusions (Jiuling of Jiangxi, Hetai of Guangdong, Ailaoshan and east Kunlun), there is almost no Indosinian folding, and the magnitudes of differential stress for samples collected at the Earth's surface are much lower, commonly <90 MPa (Fig. 6.7), indicating that there was very little stress on the sedimentary cover. Because there are insufficient determinations of paleo-stress magnitude, the general characteristics of the tectonic stress field during the Indosinian Period have not been established completely; further research is necessary.

Magmatism was not very extensive during the Indosinian Tectonic Period; the outcrop area of magmatic rock is 129, 000 km^2, about one seventh of the area of magmatic rocks in China (Cheng YQ, 1994).

From the chemical composition of 3,284 samples of magmatic rocks, from 73 areas (Appendix 5.5) taken from the regional geological surveys, the average rate of intraplate N-S shortening was 5.6 cm/yr during the Indosinian Tectonic Period. Fig. 6.3 shows rates of shortening in the Songhuajiang–Liaohe, north China, upper Yangtze and Tarim stable areas were rather small, all less than 4 cm/yr, the rates of shortening in north Qiangtang, Kunlun, Qaidam, Qilian, Henduanshan, Hunan and Guangxi areas were more rapid, all more than 6 cm/yr. Collision and amalgamation in the Hohxil–Lancangjiang areas were most intense at that time; other areas, including Shaoxing–Shiwandashan, Qinling–Dabie and their adjacent areas, show intermediate rates of shortening at 4–6 cm/yr. The Tethys Ocean, to the south of Qiangtang, shows a slow and steady extension rate of 0.2–0.4 cm/yr, less than one tenth of the rate of extension in the present Atlantic Ocean. Only in the western Himalayan areas of Ngari and Burang was the rate of extension more rapid, at 1.6 cm/yr, estimated from the chemical composition of ophiolites, a value similar to that of the present Atlantic Ocean.

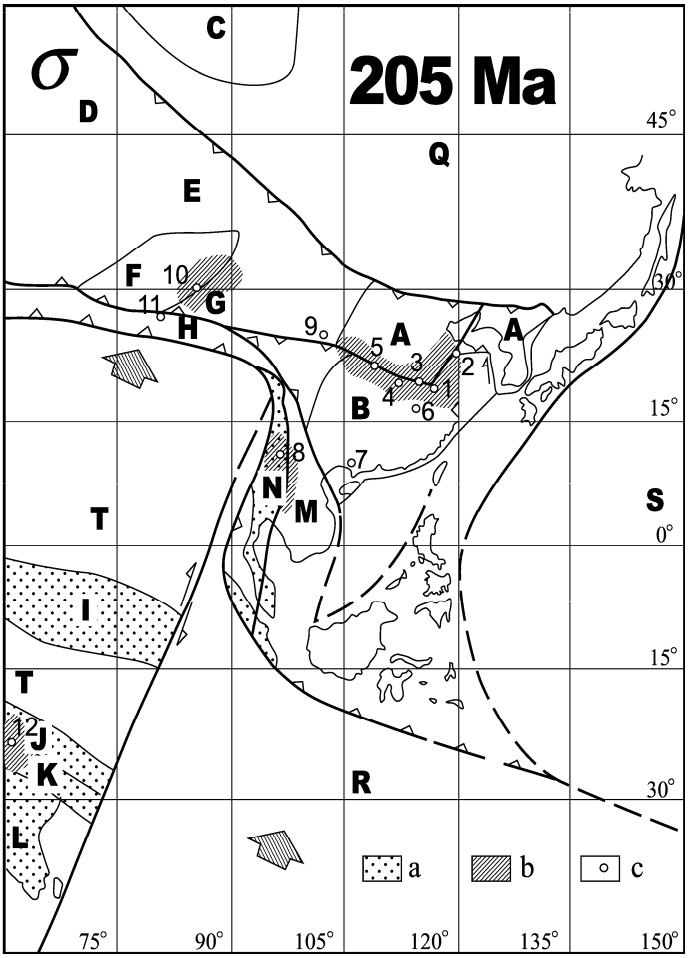

Fig. 6.7 Magnitude of tectonic stress in the Indosinian Period (~205Ma).

a. Gondwana continental blocks before the Indosinian Period; b. Areas with differential stress >90 MPa; c. Sample locations for differential stress estimations; differential stress < 90 MPa or not determined in areas left blank. The data is presented in Appendix 4. The symbols used for the tectonic blocks are the same as in Fig. 6.3.

The block symbols are the same as in Fin.6.5.

1. Middle and Lower Yangtze; 2. Jiaonan, Shandong; 3. northern Huaiyang; 4. Xincheng-Huangpi; 5. Fengxian, Shaanxi; 6. Jiuling, Jiangxi; 7. Hetai, Guangdong; 8. Ailaoshan-Cangyuan, Yunnan; 9. eastern Gansu; 10. Altunshan; 11. eastern Kunlun, Qinghai; 12. Burang, Tibet (Xizang).

A tectono-paleogeographic reconstruction of the Chinese continent and its adjacent areas during the Late Indosinian Period (208 Ma) has been compiled, controlled by paleomagnetic data (Appendix 6), supported by tectonic, sedimentary, paleontological and paleogeographic evidence (Figs. 6.8 and 6.9). These paleogeographic reconstructions emphasize the importance of the Indosinian Tectonic Period in the formation of the major part of the Chinese continent. At this period most of the Chinese continental blocks were amalgamated with the Pangean Super-continent, and their sedimentary cover was

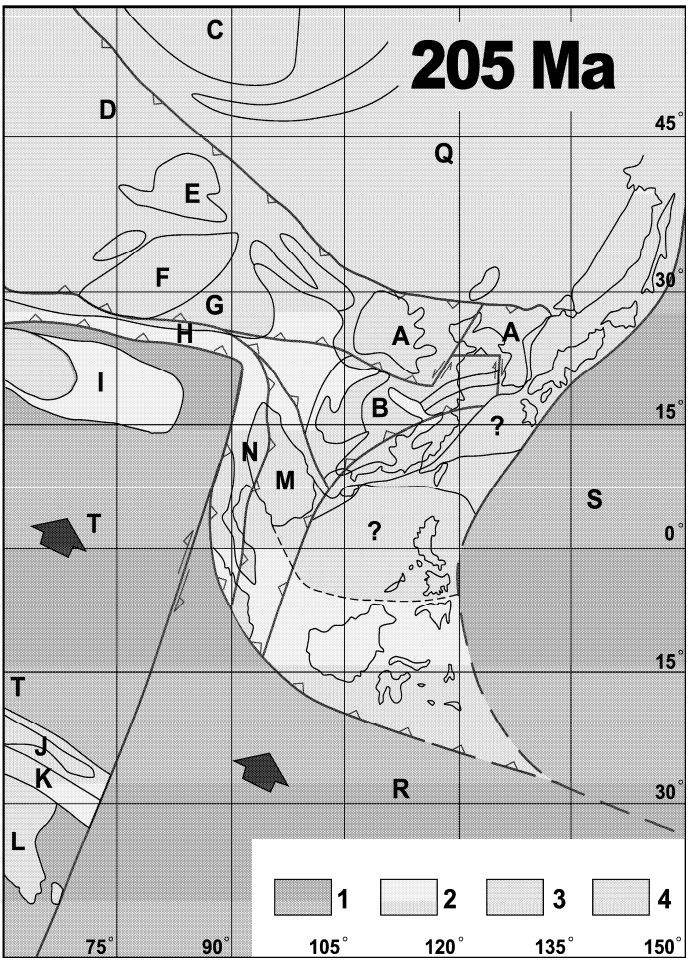

Fig. 6.8 Paleo-tectonogeographic reconstruction of the Chinese continent and its adjacent areas in the Triassic (205 Ma) (based on the paleomagnetic data, showed in Appendix 6).

1. Ocean; 2. Shallow seas; 3. Sedimentary basins; 4. Lowland with hills.

Symbols: A. Sino-Korean Plate; B. South China Plate (including Yangtze and Cathaysian); C. Siberian Plate; D. Kazakhstan Plate; E. Junggar Plate; F. Tarim Plate; G. Qaidam Plate, H. Kunlun Block; I. Qiangtang Block; J. Gangdise Block; K. Himalayan Block; L. Indian Plate; M. Simao–Indochina Plate; N. Baoshan–Sibumasu Block; Q. Hingganling–Mongolia–Tianshan Collision Zone; R. Australian Plate; S. Izanagi Plate; T. Tethys Oceanic Plate.

The block symbols are the same as in Fig.6.5.

The above symbols are used for maps of deformation, stress magnitude and reconstruction in Chapters 6 to11. Paleomagnetic data is presented in Appendix 6.

affected by widespread intraplate deformation, with the formation of a series of near E-W (in present co-ordinates) trending folds and thrusts. However, paleomagnetic determinations of declination show that the continents have rotated through 30°compared with their declination in the Indosinian (Fig. 6.8). When the folds were formed the trends of folds and fault zones were about NW 300°–SE 120°, as shown

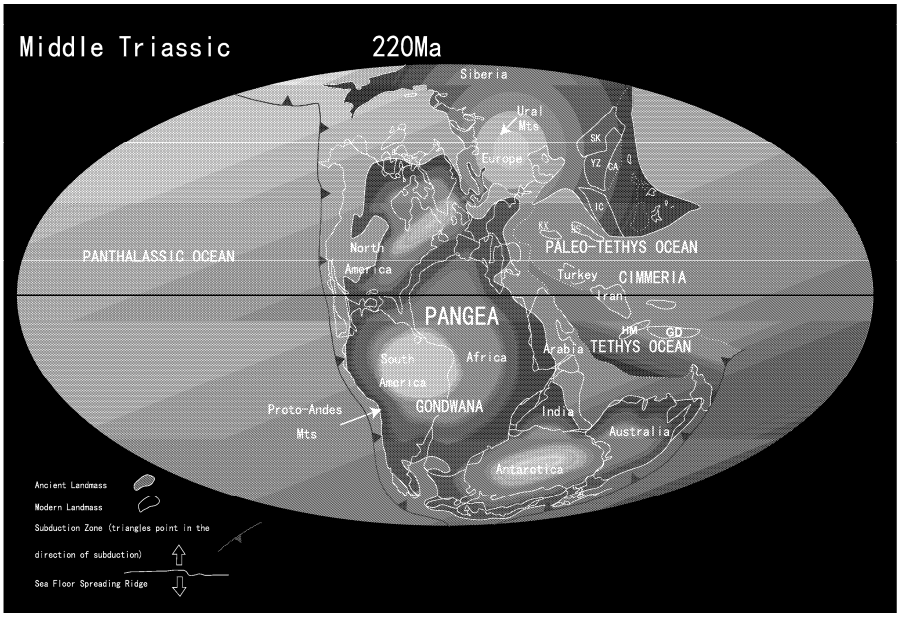

Fig. 6.9 Paleo-continents reconstruction of globe during Middle Triassic (220 Ma) (Wan TF and Zhu H, 2007) (Data of Chinese blocks and their adjacent areas from Appendix 6, others from Scotese website).

in the tectono-paleogeographic reconstruction (Fig. 6.8). Throughout the whole of the Triassic period, a large part of the southern Chinese continent was covered by shallow shelf seas in a hot, and moist climate. In the North China, Tarim and western Yangtze areas, large terrestrial sedimentary basins were developed in a hot and dry climate. The elevation of the four mountain belts formed as the result of intercontinental collision is estimated to be less than 3,000 m, and they were being denuded rapidly in a hot and moist climate.

The Indosinian Tectonic Period was the key period for the formation of the Chinese paleo-continent. Continental blocks to the north and east of the Bangongco–Nujiang zone including the Yangtze, Cathaysian, Qiangtang, Baoshan–Sibumasu and Indochina blocks migrated northeastwards, and became amalgamated with the Pangean Super-continent. The Indosinian was the period in which dispersed blocks in the eastern Tethys Ocean converged and collided. However, the situation was very different in the western hemisphere, where the North American, South American and African continental plates were extended, broken up and separated since the end of Triassic to form the Paleo-Atlantic Ocean. There is evidence for uplift, with the development of a mantle plume between these three plates (Fig. 15.4) (Condie, 2001). In the eastern hemisphere the Triassic was a period of major collisions and amalgamations among continental blocks which had been separated from Gondwana, while in the western hemisphere this was the period of the breakup of the Pangean Super Continent. The tectonic evolution of the eastern and western hemispheres was certainly not synchronous.

References

Ames L, Tilton GR, Zhou G (1993) Timing of collision of the Sino-Korean and Yangtze cratons: U-Pb zircon dating of coesite-bearing eclogites. Geology 21: 339–342.

An TX, Ma WP (1993) Middle Ordovician-Lower Carboniferous of Sino-Korean platform and its paleogeography and tectonic significance. Earth Science 18(6): 777–793 (in Chinese with English abstract).

Benson MJ (2003) When Life Nearly Died: The Greatest Mass Extinction of All Time. Thames & Hudson, London.

Bureau of Geology and Mineral Resources of Gansu Province (1989) Regional Geology of Gansu Province. Geological Publishing House, Beijing (in Chinese with English abstract).

Bureau of Geology and Mineral Resources of Hebei Province (1989) Regional Geology of Hebei Province, Beijing and Tianjin Municipality. Geological Publishing House, Beijing (in Chinese with English abstract).

Bureau of Geology and Mineral Resources of Sichuan Province (1991) Regional Geology of Sichuan Province. Geological Publishing House, Beijing (in Chinese with English abstract).

Bureau of Geology and Mineral Resources of Xinjiang Uygur Autonomous Region (1993) Regional Geology of Xinjiang Uygur Autonomous Region. Geological Publishing House, Beijing (in Chinese with English abstract).

Cai XL, Shi SQ, Wu DC et al (1995) Formation and Tectonic Evolution of the Wudangshan Nappe Structure. Chengdu University of Science and Technology Press, Chengdu (in Chinese with English abstract).

Cai XL et al (1997) On the wedging in orogenesis. In: Progress in Geology of China (1993—1996)–Papers to 30th IGC. pp.315–320. China Ocean Press, Beijing.

Cai XL, Wei XG, Li YC et al (1998) Geodynamic analysis on the orogenic process of intracon-tinental orogenic belts of China. Journal of Mineralogy and Petrology 18(suppl.): 1–7 (in Chinese with English abstract).

Cai XL, Zhu JS, Cao JM et al (2002) Structure and dynamics of lithosphere and asthenosphere in the gigantic East Asian-West Pacific rift system. Geology in China 29(3): 234–245 (in Chinese with English abstract).

Chang KH (1997) Korean Peninsula. In: Moores EM, Fairbridge RW (eds) Encyclopedia of European and Asian Regional Geology. Champman and Hall, London.

Chang KH (2000) Paleozoic Yellow-Sea transform fault and Mesozoic Korea. Geosciences Journal (Korea) 4(special edition): 4–6.

Che ZC, Liu L, LuoJH (2002) Regional Tectonics of China and Its Adjacent Areas. Science Press, Beijing (in Chinese).

Cheng YQ (1994) An Introduction to Regional Geology of China. Geological Publishing House, Beijing (in Chinese).

Condie KC (2001) Mantle Plumes and Their Record in Earth History. Cambridge University Press, Cambridge.

Cong BL, Wang QC (1994) Review of researches on ultrahigh-pressure metamorphic rocks in China. Chinese Science Bulletin 39(24): 2068–2075 (in Chinese).

Cong BL, Wang QC (1995) Ultra-high-pressure metamorphic rocks in China. Episodes 18(1–2): 91–94.

Cong BL, Wang QC (1999) The Dabie–Sulu UHP rocks belt: review and prospect. Chinese Science Bulletin 44(12): 1074–1086.

Deng XG, Ting L, Liu XH et al (2000) Blueschist and its $^{40}Ar/^{39}Ar$ chronology in Gangmuri area, Middle Qiangtang, Qingzang Plateau. Chinese Science Bulletin, 45(21): 2322–2326 (in Chinese).

Dong YP, Zhang GW, Lai SC et al (1999) An ophiolitic tectonic melange first discovered in Huashan area, south margin of Qinling orogenic belt and its tectonic implications. Science in China D 42(3): 292–302.

Fang QH, He SY (1988) Rare-earth elements geochemistry of granitic suite in Darongshan, Guangxi. Journal of Guilin College of Metallurgical Geology 8(3): 255–262 (in Chinese).

Fromaget JI (1934) Observations et reflexions Sur La geologic stratigraphique et Indochina. Bull. Soc. Geol. France, Ve str. t.4.

Gu XD, Zhao YN (1988) On the Indosinian movement on the Qinghai-Xizang (Tibet) plateau. Regional Geology of China (2): 137–144, 125 (in Chinese with English abstract).

Guo FX (1998) Meso-Cenozoic Nanhua (South China) orogenic belt-Subaerial tridirectional orogen . Acta Geologica Sinica 72(1): 22–33 (in Chinese with English abstract).

Guo ZY (1987) Formation and evolution of the Tan–Lu fault zone and its kinematics analysis. Geology of Shandong 3(1): 51–62 (in Chinese with English abstract).

Gupta S (1989) Comments and reply on "Mesozoic overthrust tectonics in South China". Geology 17: 669–671.

Hao TY, Mancheol S, Wang QS et al (2002) A study on the extension of fault zones in Yellow Sea and its adjacent areas based on gravity data. Acta Geophysica Sinica 45(3): 385–397 (in Chinese with English abstract).

Hirth G, Tullis J (1994) The brittle–plastic transition in experimentally deformed quartz aggregates. J. Geophys. Res. 99(B6): 11731–11747.

Hobbs BE (1968) Recrystallization of single crystals of quartz. Tectonophysics 6: 353–401.

Hsu KJ (1980) Terrestrial catastrophe caused by cometary impact at the end of Cretaceous. Nature 285: 201–203

Hsu KJ (1981) Thin-skinned plate-tectonic model for collision-type orogenesis. Scientia Sinica 24 (1): 100–110.

Hsu KJ, Sun S, Li JL (1987) Been South China orogenic zone, but not South China platform. Science in China, B 10: 1107–1115 (in Chinese).

Hsu KJ, Sun S, Li JL et al (1988) Mesozoic overthrust tectonics in South China. Geology 16: 418–427.

Hsu KJ (1989) Time and place in Alpine orogenesis. Geol. Soc. London Spec. Pub. 45: 421–443.

Hsu KJ, Li JL, Chen H et al (1990) Tectonics of South China: key to understanding West Pacific geology. Tectonophysics 183: 9–39.

Huang TK (Jiqing) (1945) On the major structural forms of China. Geological Memoirs, ser. A, no. 20, 165pp.

Huang JQ, Chen BW (1987) The Evolution of the Tethys in China and Adjacent Regions. Geological Publishing House, Beijing (both in Chinese and English).

Kunugiza K, Tsujimori T, Kano T (2001) Evolution of the Hida and Hida marginal belt. In: ISRGA Field Workshop (FW-A), Geotraverse across the Major Geologic Unit of SW Japan. pp.75–131.

Li C (1997) The $^{40}Ar/^{39}Ar$ age and its significance of the crosstie from blueschists in the mid-Qiangtang Area, Tibet. Chinese Science Bulletin 42(1): 88 (in Chinese).

Lee JS (Li Siguang) (1939) The Geology of China. Thomas Murby & Co., London.

Li SG (Lee JS) (1929) Some characteristic structural types in Eastern Asia and their bearing upon the problem of continental movement. Geological Magazine 96 (782): 358–375; 96 (784): 457–473; 96(785): 501–526. Reprinted in 1976, Geological Mechanics Methods. Science Press, Beijing (in Chinese).

Li SG, Zhang ZM, Zhang QD et al (1993) The zircon U-Pb ages of Qingdao eclogite and gneiss in Jiaonan Group—evidence of magmatic event of Jinning stage in Jiaonan Group. Chinese Science Bulletin 38(19): 1773–1777.

Li SG, Li HM, Chen YZ et al (1997) Ultrahigh pressure metamorphic chronology in Dabieshan–Sulu terrane– Ⅱ. zircon U-Pb isotopic system. Science in China D 27(3): 200–206 (in Chinese).

Liao QK (1991) Formation time of Darongshan–Shiwandashan granite batholith in Guangxi. Geology of Guangxi 4(4): 59–68 (in Chinese with English abstract).

Liu BJ, Xu XS, Xia WJ et al (1994) Atlas of Petrological Phase Paleogeography of South China (Sinian to Triassic). Science Press, Beijing (in Chinese).

Liu BP, Feng QL, Fang NQ (1991) Tectonic evolution of the Paleo-Tethys in Changning–Menglian and Lancangjiang belts, Western Yunnan. In: Proceedings of 1st International Symposium on Gondwana Dispersion and Asian Accretion (IGCP Project 321), pp.189–192. Kunming, China. Geological Publishing House, Beijing.

Liu GH, Zhang SG, You ZD et al (1993) Main Metamorphic Rock Groups and Metamorphic Evolution of Qinling Orogenic Belt. Geological Publishing House, Beijing (in Chinese).

Liu YC, Xu ST, Li SG et al (2003) Tectonic setting and cooling history of eclogites from Northern Dabie Mountains. Earth Science 28(1): 11–16 (in Chinese with English abstract).

Liu YJ, Ye HW, Ge XH et al (2001) Laser probe $^{40}Ar/^{39}Ar$ dating of mica on the deformed rocks from Altun fault and its tectonic implication, western China. Chinese Science Bulletin 46(4): 322–325.

Liu ZQ, Li XZ, Ye QT et al (1993) Division of Tectonic Magma Belt in Sanjiang Area (Hengduanshan) and Its Distribution of Mineral Resources. Geological Publishing House, Beijing (in Chinese).

Maruyama S (1994) Plume tectonics. Journal of the Geological Society of Japan 100(1): 24–49.

Meissner R, Reston T (1989) The three-dimensional structure of the Oberpfalz: an alternative interpretation of DEKORP–KTB data. Tectonophysics 157(1–3): 1–11.

Molnar P, Tapponnier P (1975) Cenozoic tectonics of Asia: effects of a continental collision. Science 89(4,201): 419–426.

Peng YQ, Yin HF (2002) The global changes and bio-effects across the Paleozoic–Mesozoic transition. Earth Science Frontiers 9(3): 85–93 (in Chinese with English abstract).

Qiao XF, Gao LZ, Peng Y (2001) Neoproterozoic in Paleo-Tanlu Fault Zone—Catastrophe Sequence Biostratigraphy. Geological Publishing House, Beijing (in Chinese).

Qiu YX, Chen HJ (1993) Professional Papers for the Geological Structure of Yunkaidashan and Its Adjacent Areas. Geological Publishing House, Beijing (in Chinese).

Quinlan G, Beaumont C, Hall T (1993) Tectonic model for crustal seismic reflextivity patterns in compression orogens. Geology (Boulder) 21(7): 663–666.

Ren JS, Wang ZX, Chen BW et al (2000) China Tectonics, Outlooked by the Globe—Brief Direction of Tectonic Map of China and Its Adjacent Areas. Geological Publishing House, Beijing.

Rodgers J (1989) Comments and reply on "Mesozoic overthrust tectonics in South China". Comment. Geology 7: 671–672.

Shao XZ, Zhang JR, Fan HJ et al (1996) The crust structure of Tianshan orogenic belt: a deep sounding work by converted waves of earthquakes along Urumqi-Korla profile. Acta Geophysica Sinica 39(3): 336–346 (in Chinese with English abstract).

Shui T, Xu BT, Liang RH et al (1986) Shaoxing–Jiangshan deep-seated fault zone, Zhejiang Province. Chinese Science Bulletin 31(18): 1,250–1,255.

Shui T (1987) Basement tectonic framework in southeast China continent. Science in China, B (4): 414–422 (in Chinese with English abstract).

Sun KQ (2002) The Chathaysia flora and its comparison with global contemporaneous floras. Earth Science Frontier 9(3): 73–84 (in Chinese with English abstract).

Sun MZ, Xu KQ (1990) On the Caledonian granitoids and their geotectonic environments of south China. Journal of Nanjing University (4): 10–22 (in Chinese with English abstract).

Suo ST, Sang LK, Han YJ et al (1993) The Petrology and Tectonics in Dabie Precambrian Metamorphic Terranes, Central China. China University of Geosciences Press, Wuhan (in Chinese with English abstract).

Suo ST, Zhong ZQ, Zhang HF et al (2000) Relic UHP structures in Dabie-Sulu region, China: structures expression and geodynamic significance. Earth Science 25(6): 557–563 (in Chinese with English abstract).

Tapponnier P, Molnar P (1977) Active faulting and tectonics in China. J. Geophys. Res. 82(20): 2905–2930.

Tapponnier P, Mercier JL, Proust F et al (1981) The Tibetian side of the India-Eurasia collision. Nature 294(5,840): 405–410.

Tapponnier P, Peltzer G, Le Dain AY et al (1982) Propagating extrusion tectonics in Asia: new insights from simple experiments with plastic line. Geology 10: 611–616.

Tapponnier P, Peltzer G, Armijo R (1986) On the mechanics of the collision between India and Asia. In: Coward MP, Ries AC (eds) Collision tectonics. Geological Society Special Publications, 19: 115–157. Geological Society of London, London.

Teng JW, Zhang ZJ, Hu JF et al (1996) Physical-mechanical mechanism for the whole uplifting of the Qinghai-Xizang plateau and the lateral shortening and vertical thickening of the crust. Geological Journal of China Universities 2(2): 121–133; 2(3): 307–323 (in Chinese with English abstract).

Tsujimori T, Ishiwatari A, Banno S (2000) Ecologic glaucophane schist from the Yunotani Vally in Omi town, the Range metamorphic belt, the inner zone of southwest Japan. J. Geol. Soc. Japan 106(5): 353–362.

Wan TF (1995) Evolution of Tancheng–Lujiang fault zone and paleostress fields. Earth Science 20(5): 526–534 (in Chinese with English abstract).

Wan TF, Zhu H, Zhao L et al (1996) Formation and Evolution of the Tancheng—Lujiang Fault Zone. China University of Geosciences Press, Wuhan.

Wan TF, Teyssier C, Zeng HL et al (2001) Emplacement mechanism of Linglong granitoid complex, Shandong Peninsula, China. Science in China D 44(6): 535–544.

Wan TF, Zeng HL (2002) The distinctive characteristics of the Sino-Korean and the Yangtze plates. Journal of Asian Earth Sciences 20(8): 881–888.

Wan TF, Zhu H(2007) Positions and kinematics features of Chinese blocks in global paleocontinental reconstruction during Paleozoic and Triassic. Geosciences 21(1): 1–13.

Wang GH (1993) Research on Tangzang–Huangboyuan ductile shear zone of Fengxian-Taibai area, Shaanxi Province. Dissertation, China University of Geosciences(Beijing).

Wang HZ (1981) Geotectonic units of China from the view-point of mobilism. Earth Sciences—Journal of Wuhan College of Geology (1): 42–66 (in Chinese with English abstract).

Wang HZ (1982) The main stages of crustal development of China. Earth Sciences—Journal of Wuhan College of Geology (3): 155–177 (in Chinese with English abstract).

Wang HZ (1985) Atlas of Paleogeography of China. SinoMaps Press, Beijing (in Chinese).

Wang QC, Cong BL, Zhu RX (1998) Geodynamics of UHP-rock-bearing continental collision zone in central China. In: Flower MFJ et al (eds) Mantle dynamics and plate interactions in East Asia, Geodynamics Series, 27, pp.259–267, AGU, Washington DC.

Wang QQ, Wang LK (1989) Physicochemical conditions for the formation of peraluminous granites at Darongshan Guangxi, China. Geochenica (4): 287–296 (in Chinese with English abstract).

Wang XF, Ian Metcalfe, Jian P et al (2000) The Jinshajiang suture zone: tectono-stratigraphic subdivision and revision of age. Science in China D 43(1): 10–22.

Wang ZJ, Wu GJ, Xiao XC et al (1997) Explanatory Notes for Global Geoscience Transect, Golmud-Ejin Transect, China. Geological Publishing House, Beijing (in Chinese).

Webb LE, Hacker BR, Ratschbacher L et al (1999) Thermo-chronologic constraints on deformation and cooling history of high-and ultrahigh-pressure rocks in the Qinling–Dabie orogen, Eastern China. Tectonics 18(4): 621–638.

Weng SJ (1984) Several Geological Problems about Tanlu Fault Zone. Collection of Structural Geology (3): 66–71. Geological Publishing House, Beijing (in Chinese).

Xiong CY, Zhang YM, Wei CS et al (1992) Structural evolution of Tongbai–Dabie area and its influences on mineral deposits. Research Report of Yichang Institute of Geological Minerals Product (unpublished report, in Chinese).

Xu B, Grove M, Wang CQ et al (2000) $^{40}Ar/^{39}Ar$ thermochronology from the northwestern Dabie Shan: constrains on the evolution of Qinling-Dabie orogenic belt, east-central China. Tectonophysics 322 (3–4): 279–301.

Xu JW (1957) The preliminary analysis for the tectonics on southeastern of Sino-Korean platform and its marginal area. Hefei Mining College, 32pp (in Chinese).

Xu JW (1980) Parallel movement of Tanlu fault zone and its geological significance.In: Contribution to International Geological Communication, (1) 129–142. Geological Publishing House, Beijing.
Xu JW, Zhu G, Tong WX et al (1987) Formation and Evolution of the Tancheng–Lujiang wrench fault system: a major shear system to the northwest of the Pacific Ocean. Tectonophysics 134(4): 273–310.
Xu JW (1993) The Tancheng–Lujiang Wrench Fault System. John Wiley & Sons, New York.
Xu JW (1994) Rediscussion on the maximum horizontal displacement of Tancheng–Lujiang fault zone—comparison between west Shandong and north Liaoning blocks. Journal of Shenyang Institute of Geology, Chinese Academy of Geological Sciences 3: 43–55 (in Chinese with English abstract).
Xu PF, Liu F, Ye K et al (2002) Flake tectonics in the Sulu orogen in eastern China as revealed by seismic tomography. Geophysical Research Letters 29(10): 23 (1–4).
Xu Y, Liu JH, Hao TY et al (2006) P wave velocity structure and tectonic analysis of lithospheric mantle in eastern China seas and adjacent regions. Chinese J. Geophys. 49(4): 1053–1061 (in Chinese).
Xu ZQ, Yang JS, Zhang JX et al (1999) A comparison between the tectonic units on the two sides of the Altun sinistral strike-slip fault and the mechanism of lithospheric shearing. Acta Geologica Sinica 73(3): 193–205 (in Chinese with English abstract).
Xue JS, Li ST (1982) A discussion on the forming time of Shandong Yishu fault belt. Journal of Shandong College of Oceanology 12(4): 51–59 (in Chinese with English abstract).
Yang SR, Hao WC, Jiang DY (2001) Provincialism of Triassic conodonts in China. Journal of Palaeogeography 3(3): 1–10 (in Chinese with English abstract).
Yang WR, Wang GC, Jian P (2000) Research on the Tectono-Chronology of the Dabie Orogenic Belt. China University of Geosciences Press, Wuhan (in Chinese with English abstract).
Yang WR, Jian P, Han YJ (2002) Determination and significance of Caledonian high-pressure and ultrahigh-pressure metamorphism in Dabie orogen. Earth Science Frontiers 9(4): 273–283 (in Chinese with English abstract).
Yang ZY, Otofuji Y, Sun ZM et al (1998) Geomagnetic pole series of boundary between Cambrian and Ordovician in Tangshan, Hebei. Chinese Science Bulletin 43(17): 1881–1885 (in Chinese).
Yin A, Nie SY (1993) An indentation model for North and South China collision and the development of the Tanlu and Honam fault system, Eastern Asia. Tectonics 12(4): 801–813.
Yin A, Nie SY (1996) A Phanerozoic palinspastic reconstruction of China and its neighboring regions. In: Yin A, Harrison M (eds) The Tectonic Evolution of Asia. Cambridge University Press, Cambridge.
Yin HF et al (1988) Paleobiogeography of China. China University of Geosciences Press, Wuhan (in Chinese).
Yuan XC, Xu MC, Tang WB et al (1994) Seismic reflection profiling of crust in Eastern Qinling. Acta Geophysica Sinica 37(6): 749–758 (in Chinese with English abstract).
Yuan XC (1996) Atlas of Geophysics in China. Geological Publishing House, Beijing (in Chinese).
Yuan XC, Zuo Y (1996) Geophysical Lithospheric Transect of Qinling Orogenic Belt. Science Press, Beijing (in Chinese).
Yuan XC (1997) The crustal structure of the Qinling orogen and wedging mountain building. Acta Geologica Sinica 71(3): 227–235 (in Chinese with English abstract).
Zhai XM, Day HW, Hacker BR et al (1998) Paleozoic metamorphism in the Qinling orogen, Tongbai Mountains, Central China. Geology 26(4): 371–374.
Zhang GW, Zhang BR, Yuan XC (1996) Orogenic Process of Qinling Orogenic Belt and Three Dimensional Structural Map Series of Lithosphere. Science Press, Beijing (in Chinese).
Zhang GW, Zhang BR, Yuan XC et al (2001) Qinling Orogenic Belt and Continental Dynamics. Science Press, Beijing (in Chinese).
Zhang JS (1983) The basement ductile shear zone of the middle Yihe-Shuhe fault belt. Seismology and Geology 5(2): 11–23 (in Chinese with English abstract).
Zhang Q, Zhu G, Liu GS et al (2008) Sinistral transpressive deformation in the northern part of Zhangbaling uplift in the Tan-Lu fault zone and its ^{40}Ar-^{39}Ar dating. Earth Science Frontiers 15(3): 234–249 (in Chinese with English abstract).

Zhang SG, Wan YS, Liu GH et al (1991) Metamorphic Geology of the Kuanping Group in the Northern Qinling Mountains. Beijing Science and Technology Press, Beijing (in Chinese with English abstract).
Zhang SG, Wei CY, Yang CH (1998) Metamorphism of east part of South Qinling orogenic belt. Earth Science Frontiers 5(4): 210 (in Chinese).
Zhang WY et al (1959) An Outline of Tectonics of China. Science Press, Beijing (in Chinese).
Zhang WY (1964) Stress analysis of major fracture systems in China. Chinese Science Bulletin 15(19): 604–608 (in Chinese).
Zhang WY (1983) Sea and Continental Tectonic Map of China and Adjacent Areas. Science Press, Beijing (in Chinese).
Zhang WY (1984) An Introduction to Fault-block Tectonics. Petroleum Industry Press, Beijing (in Chinese).
Zhang YX, Li LL (1984) The giant strike-slip along Tancheng-Lujiang fault zone and its influence on the nearby structures. Collection of Structural Geology (3): 1–8. Geological Publishing House, Beijing (in Chinese with English abstract).
Zhao YG, Zhong DL, Liu JH et al (1992) Fundamental of geological interpretation for seismic tomography and its application to studying of west Yunnan's deep structure. Scientia Geologica Sinica (2): 105–113 (in Chinese with English abstract).
Zhao ZP (1986) Review of the 50th anniversary of the Indosinian Movement. Scientia Geologica Sinica (1): 7–15 (in Chinese with English abstract).
Zhong DL (1998) Paleo-Tethyan Orogenic Belt in Western Yunnan and Sichuan. Science Press, Beijing (in Chinese).
Zhong ZQ, Suo Shutian, You ZD (1998) Extentional tectonic framework of post high and ultrahigh pressure metamorphism in Dabieshan, China. Earth Science 23(3): 225–229 (in Chinese with English abstract).
Zhou YS, Zhong DL, He CR (2004) Upper limit for rheological strength of crust in continental subduction zone: Constrains imposed by laboratory experiments. Journal of China University of Geosciences 15(2): 167–174.
Zhou YS, He CR, Song Q et al (2005) Experimental research for the transmutation from quartz to coesite under the condition of differential stress. Chinese Science Bulletin 50(6): 565–570 (in Chinese).
Zhu G, Song CZ, Wang DX et al (2001) Studies on $^{40}Ar/^{39}Ar$ thermochronology or strike-slip time of the Tan–Lu fault zone and their tectonic implications. Science in China D 44 (11): 1002–1009 (in Chinese).
Zhu ZC (1989) Structure Geology. China University of Geosciences Press, Wuhan (in Chinese).
Zhu ZC (1989) Thrust Nappe Structure. China University of Geosciences Press, Wuhan (in Chinese).

Chapter 7
Tectonics of Jurassic–Early Epoch of Early Cretaceous (The Yanshanian Tectonic Period, 200–135 Ma)

—counterclockwise rotation of Chinese continent, westwards subduction and compression of Okhotsk and Izanagi Plate.
—forming Neocathaysian Tectonic System and the Wandashan Collision Zone
—violent detachments and tectono-magmatism in the crust of Eastern China

The Yanshanian movements were first recognized by Weng WH (1927, 1929) in Yanshan area, 116°–119.5°N, 40°–42°E. Since then the Yanshanian has been used as a local term in China for tectonic events which occurred mainly during the Jurassic Period. Later, Ding WJ (1929), Huang JQ (1945, 1960) and Zhao ZF (1959) extended the term to cover tectonic events which occurred throughout China during the Jurassic and Cretaceous tectonic periods. However, it was soon realized that tectonic and magmatic events in the Jurassic and Cretaceous were very different. In the Jurassic there are NNE-NE trending folds and thrusts related to transpressional tectonics, and WNW trending normal faults with some strike-slip movement and widespread calc-alkaline magmatism, while the Cretaceous is characterized predominantly by extensional tectonics with NE-NNE trending normal faults, WNW trending folds and thrusts and highly alkaline acid magmatism located along faults, or at fault intersections.

In the regional geological survey of China, the Yanshanian Period has been divided into "Early Yanshanian" (200–135 Ma) and "Late Yanshanian" (135–65 Ma) Periods (Bureaus of Geology and Mineral Resources of Provinces, 1984–1993). (Wan TF(1994) considers that it is best to revert to Weng WH's (1927, 1929) original terminology and define the Yanshanian Tectonic Period as extending from the Jurassic to the earliest epoch of the Early Cretaceous (200–135 Ma). However south of the Shaoxing-Shiwandashan Collision Zone in Southeast China, the Yanshanian Tectonic Period began from the Late Triassic and extended to the early period of the Early Cretaceous (228–135 Ma). The following tectonic period from middle period of the Early Cretaceous to the Eocene (135–56 Ma) is called the Sichuanian Tectonic Period (Wan TF and Zhu H, 1989; Wan TF, 1994).

Sedimentation in the Yanshanian Tectonic Period included: the Lower Jurassic, Badaowan and Sangonghe formations, mainly coal-bearing sediments; the Middle Jurassic Xishanyao and Doutunhe formations; the Upper Jurassic Tuchengzi and Dabeigou formations, mainly terrestrial clastic rocks; the Yixian Formation, mainly acidic volcanic rocks forming the base of the Lower Cretaceous. The standard sections for all these formations are located in the Yanshan area.

The definition of the boundary between Jurassic and Cretaceous deposits in China has been controversial for a long time because sedimentation was continuous, without any obvious tectonic breaks (Li PX et al., 2000). Most researchers have followed the proposal of Hao YC (1986) that the occurrence of *Eosestheria* is diagnostic of the top of the Upper Jurassic, while the fauna and flora of the base of the Cretaceous are characterized by *Yanjiestheria Nakamuranaia*, *Cypridea, Darwinula* and *Classopollis.* In recent years, the boundary between Jurassic and Cretaceous has been recognized at Zhangjiagou, Luanping in northern Hebei, defined by abundant fossils in the Upper Jurassic Dabeigou Formation (first

biozone, *Luanpingella–Eoparacypris–Pseudopara–Cypridopsis*) and the Lower Cretaceous Dadianzi Formation (second biozone, *Yanshanina–Cypridea–Rhinocypris*, equal to the Yixian Formation) (Pang QQ and Li PX et al., 2002). The Jurassic in China consists mainly of terrestrial clastic rocks, shallow marine sediments are found only in middle Hunan, Guangdong, southwestern Tarim and Xizang areas, but there is evidence of residual oceanic deposits at Wandashan (132°–134°E, 45.5°–47.5°N), Northeast China and along the Banggongco–Nujiang and Yarlung–Zangbojiang zones in Xizang (Tibet).

Most of the continental blocks which make up the Chinese continent were amalgamated in the Triassic. Since the Jurassic the whole of China has behaved as a single tectonic unit, and moved as a single

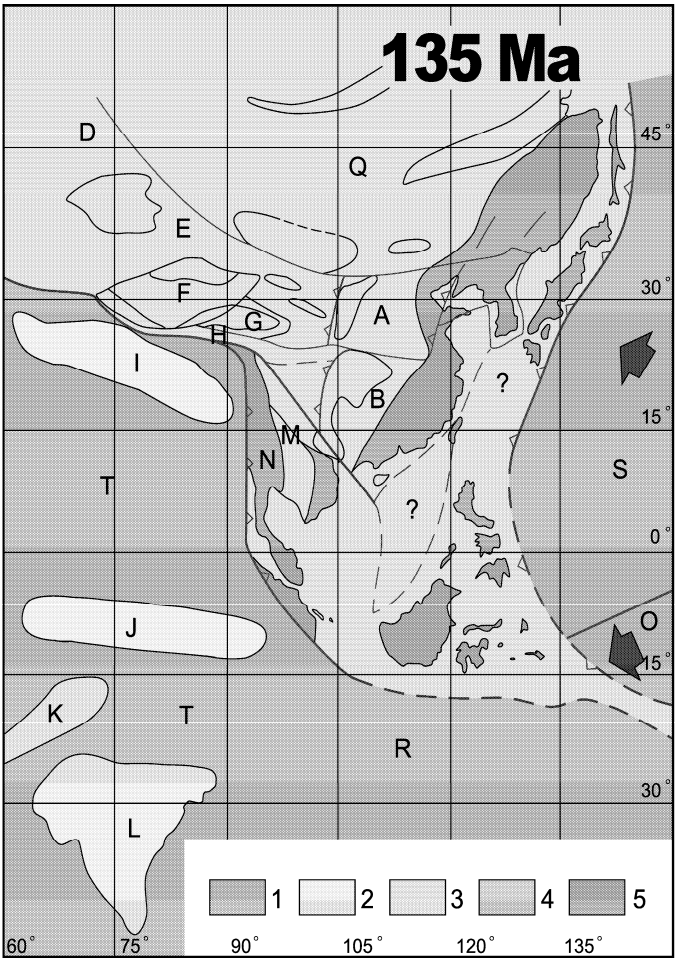

Fig. 7.1 Paleo-tectonogeographic reconstruction of China and its adjacent blocks in the Late Yanshanian Tectonic Period (135 Ma). The paleomagnetic data is given in Appendix 6.

1. Oceans; 2. Shelf seas; 3. Terrestrial sedimentary basins; 4. Subdued topography; 5. Mountains. The block symbols are the same as in Fig. 6.5.

continental plate. Subsequently China has formed a single sedimentary and biogeographical province so that these aspects are discussed only in outline in the following chapters.

In the Jurassic Period, the most of the Chinese continental blocks occupied an intraplate situation, and were located in the eastern part of the Asian Continent. The eastern boundary of the East Asian Continent was the collision zone along the border of Siberia-Far East Russia, the Wandashan zone of NE China and the Tanakura Tectonic Line in the Japanese Islands. The East Asian Continent was connected to the Russian–Baltic (Northern Europe) and the North American Continents, and formed the northeast part of the Pangean Super Continent. The southern boundary of the East Asian Continent was formed by a passive continental margin against the Tethys Ocean (Figs. 7.1 and 7.2).

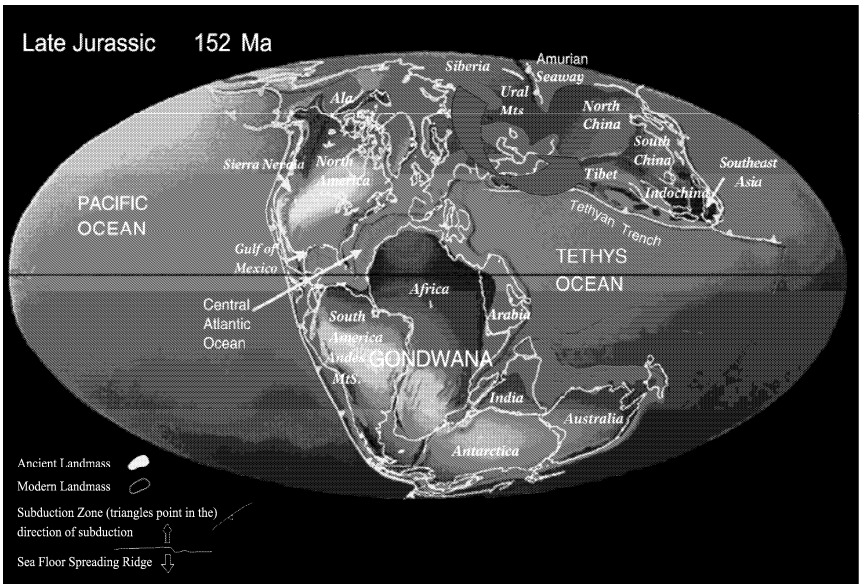

Fig. 7.2 Paleo-continental reconstruction of the globe during the Late Jurassic (152 Ma) (Data of Chinese blocks and their adjacent areas from Appendix 6, others from Scotese's web).

The red arrow shows Eastern Asian continental plate with counterclockwise rotation, due to the collision and compression of the North American Plate (including the Okhotsk Block) against the Siberian–Chinese continent.

7.1 Movement and Rotation of Chinese Continent

Using accumulated paleomagnetic data (Appendix 6) it is possible to reconstruct the kinematics of the Chinese continent. Although, the results from different researchers are not always consistent, nevertheless it is clear that there is a great difference of mean paleomagnetic declination in paleomagnetic results for periods prior to the Jurassic, but that since the end of the Jurassic the paleomagnetic declination has been similar to that of today.

During the Triassic and earlier periods the mean paleomagnetic declination for the Sino-Korean Plate varied from NW 319° to NW 338° (Huang BC et al., 1999; Ma XH et al., 1993; Fang DJ et al., 1988), but in the Late Triassic the mean paleomagnetic declination rotated to NE 30°, then during the Early Jurassic rotated to NE 0.9° similar to the present declination; during Middle Jurassic changed only a

little to NE 3.6° (Ma XH et al., 1993). The above rotations of the declination can be seen by comparing Figs. 6.8 and 7.1. Fang DJ et al. (1988) determined the mean paleomagnetic declination during Late Jurassic to be NE 22.2° but this result may be in error. From the Triassic to Jurassic periods there was a counterclockwise rotation of 20°–30°in the mean paleomagnetic declination, and then at the end of Jurassic period the declination rotated to nearly its present orientation on Sino-Korean Plate. From the Cretaceous to Recent, the mean paleomagnetic declination was around 17° and has varied only slightly. From the Triassic to Jurassic periods the southern Korean Peninsula rotated 20°counterclockwise (Kim and Van der Voo, 1990) and the Yangtze Plate also rotated counterclockwise through almost 20° (Liang QZ, 1990; Zhu ZW et al., 1988, Enkin et al., 1992； Huang KN et al., 1993). The mean paleomagnetic declination of the Siberian Plate rotated from 77.3°in the Late Triassic to 41.1°in the Late Jurassic, a counterclockwise rotation of 36.2°. Data on the paleomagnetic declination of the smaller continental blocks in China is not discussed here, as it is at present scarce and unreliable. The counterclockwise rotation of many areas in Chinese continent and its adjacent areas is important for its effects on the intraplate deformation of the East Asian continent during the Yanshanian Period (Fig.7.2).

Apart from paleomagnetic data, counterclockwise rotation of the blocks forming the Chinese continent is also indicated by biostratigraphic and paleo-climatic evidence. Gu ZW (1982) has pointed out that there is a 30°–40°counterclockwise difference in the angle between the northern limit, of the *Pachyodonta* fauna, representing a moist and warm climate during the Middle Jurassic along the Altay-

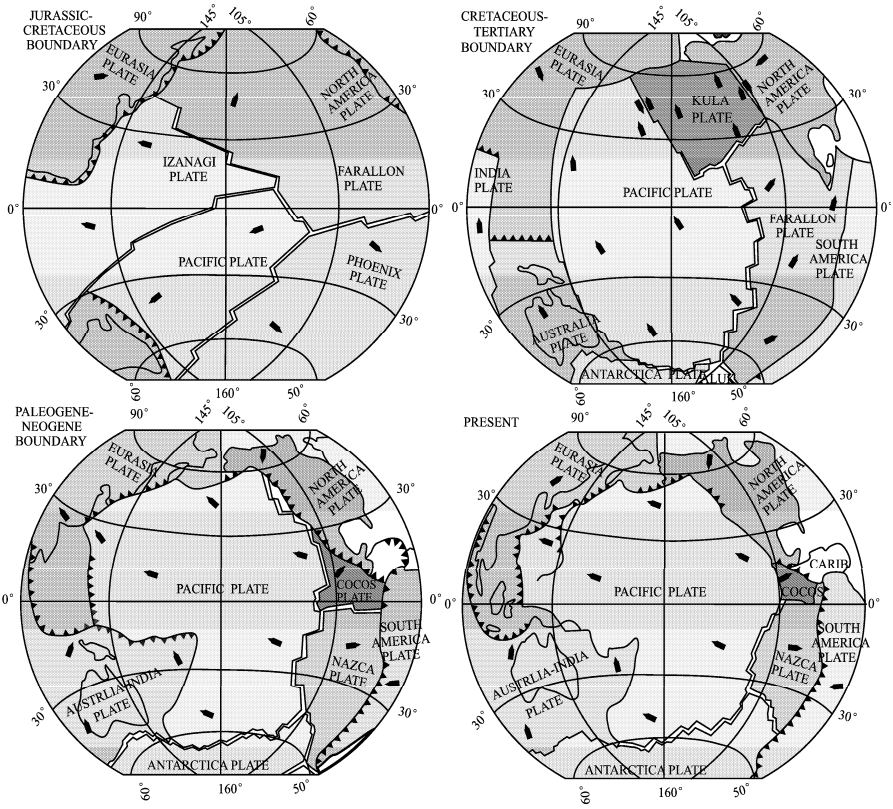

Fig. 7.3 Paleotectonic reconstruction of tectonic plates in the Pacific area since the Jurassic (Moore, 1988).

Shanghai line, and the present latitude. Liu BP and Chen F (1995) revised the limit of the *Pachyodonta* fauna (*Lamprotula, Psilunio*) to determine the northern border of the warm climatic zone and concluded that there was only 15°of counterclockwise rotation. Although there is some controversy there is general agreement that counterclockwise rotation has occurred, coinciding with the paleomagnetic results.

The counterclockwise rotation of East Asian continent (Fig. 7.2), which occurred during the Jurassic period, was influenced directly by the collision and westward movement of the North American Plate (including the Okhotsk Block) and more weakly by the northwestward subduction of the Izanagi Plate (Moore, 1988; Maruyama et al. 1986, 1997). Westward collision and compression by the North American Plate caused very strong deformation in the eastern Siberian continent, the formation of the Wandashan Collision Zone in Northeast China, movement along the Tanakura Tectonic Line in the Japanese Islands, and also the 20°–30°of counterclockwise rotation of the East Asian continent, resulting in the westward movement of Siberia, northern Asia, the southward migration of Junggar and Tarim blocks (Appendix 6), and the eastward movement of southern Asia, including South China (Fig. 7.2). It seems that rotation of East Asian continent did not influence the Russian and north Europe continents.

One important result of the third attempt at reconstructing the magnetic anomalies on floor of the Pacific Ocean was the reconsideration of the movement of tectonic plates in the Paleo-Pacific area (Moore, 1988). At the end of the Jurassic (top left diagram in Fig. 7.3), there was a radial migration of the plates, the Izanagi Plate moved northwestwards, the Farallon Plate moved northeastwards, the Phoenix Plate moved southeastwards and Pacific Plate moved southwestwards. It has been suggested that the radial movement of these plates was due to the up-rise of a super-mantle plume (Pavoni, 1997; Condie, 2001). However, there is no satisfactory explanation why uplift of a super-mantle plume occurred in that particular area.

7.2 Intraplate Deformation and the Stress Field

The greater part of the thickness of Mesozoic sedimentary rocks in China is composed of Jurassic strata. Variations in the thickness of Mesozoic sediments (Appendix 2, Fig. 7.4) can therefore be used to recognize vertical crustal movements during the Yanshanian Tectonic Period.

The greatest sedimentary thicknesses and rates of deposition in the Mesozoic of China are located in Yanshan (35,435 m, 191.5 m/Myr = 0.191,5 mm/yr) and southern Guangxi (33,342 m). Areas in which the thickness of strata is more than 20,000 m occur at Jiamusi, Heilongjiang (20,286 m), Dahingganling, Heilongjiang (22,479 m), southern Anhui (20,093 m) and Kangding–Zoige (23,362 m) (Fig. 7.4). These were the most important areas of sedimentation in the Mesozoic, and show the greatest evidence of deformation, with tectonic activity during the Yanshanian and Sichuanian tectonic periods. In other areas the thickness of the strata is mostly between 20,000 and 3,000 m. Areas, in which the thickness of the Mesozoic strata is equal to or less than 2,000 m, such as the Qinling–Dabie Zone, Taihangshan and Hainan, were areas of denudation or non-deposition during this period.

The total sedimentary thickness >35 km was not measured at a single location, but is a composite of thickness measurements from several different locations, indicating that the deposit centre moved to different locations at different periods during the Mesozoic. If the complete 35 km thickness of the Mesozoic had accumulated at one location the rate of sedimentation would have been 184 m/Myr, or only 0.184 mm/yr, still not very fast but continuous.

Strata thickness and rates of sedimentation for intraplate sedimentary basins, such as Yanshan (A in Fig. 7.4), and western Shandong (B in Fig. 7.4), are very different, but are not related to distance from the margin of the continental plate, as the distance from the margin of the oceanic plate is almost the same. In the Yanshan and western Liaoning areas where the thickness of Mesozoic sediments reaches 35,435 m and the rate of sedimentation was about 191 m/Myr, strong macro scale folds and thrusts occur in the sedimentary cover (3 in Fig. 7.5). When being subjected to deformation the thick sedimentary pile is weaker than the underlying crystalline basement. However, detachments occur in the crust or between

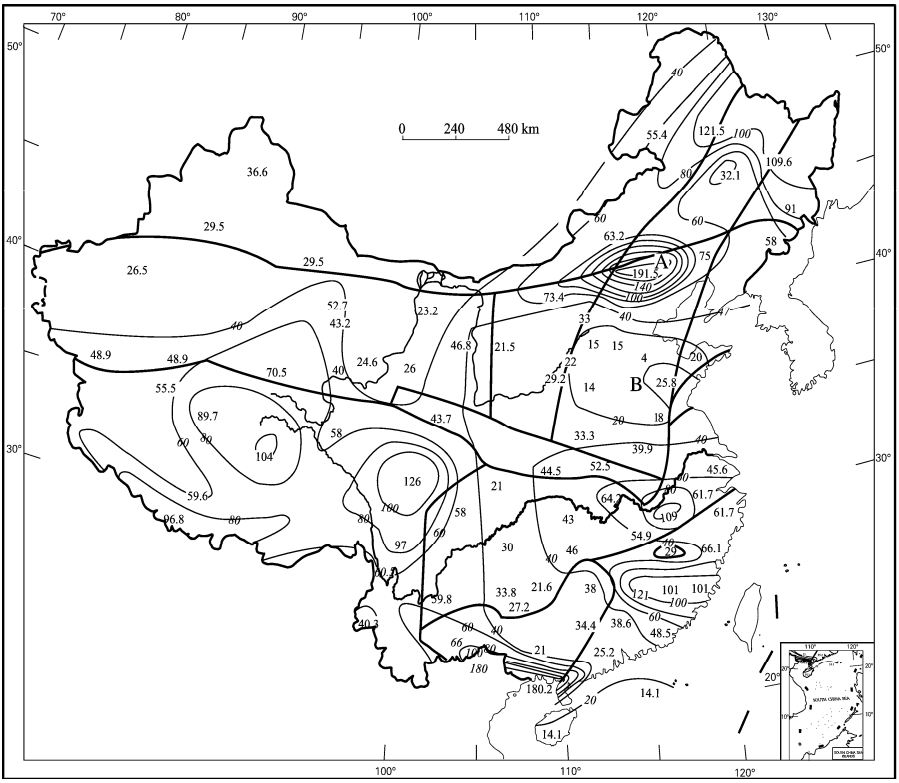

Fig. 7.4 Average rates of deposition (m/Myr) of Mesozoic sediments for each stratigraphic subdivision on the Chinese continent. A. Yanshan area; B. western Shandong.

the crust and mantle or in the middle crust, and the Yanshanian intraplate tectono-thermal events are well known internationally. In the western Shandong area, where the Mesozoic sediments are only several hundred meters thick and the rate of sedimentation was ~10 m/Myr, only one nineteenth of that in the Yanshan area, the sediments rest on the Pre-Cambrian crystalline basement. Although the tectonic stress was almost equally strong in both areas, only very weak deformation occurred in the sedimentary cover, with a ~10° dip angle in the limbs of open folds (5 in Fig. 7.5), evidently the crystalline basement with greater strength supported most of the tectonic stress. The tectonism was very weak in later periods, similar to the Ordos on the western Sino-Korean Plate, eastern Guangxi, Sichuan Basin and southeast Guizhou on the western Yangtze Plate (4, 5 and 7 in Fig. 7.5). In all these areas the sedimentary strata are very thin, the basement is strong and intraplate deformation was weak.

Thick sedimentation in the Yanshan area is related to the intersection of three major basement faults: the near E-W trending northern marginal fault zone of the Sino-Korean Plate; the NNE trending Dahingganling–Taihangshan Fault; the NNE trending Tancheng–Lujiang Fault. A zone of Paleoproterozoic collision and amalgamation, a Meso-Neo-Proterozoic sedimentary faulted depression, the low strength of the sedimentary cover and the crystalline basement all contributed to the concentration of tectonic activity in this area. However, western Shandong is located on a stable part of the Sino-Korean Plate.

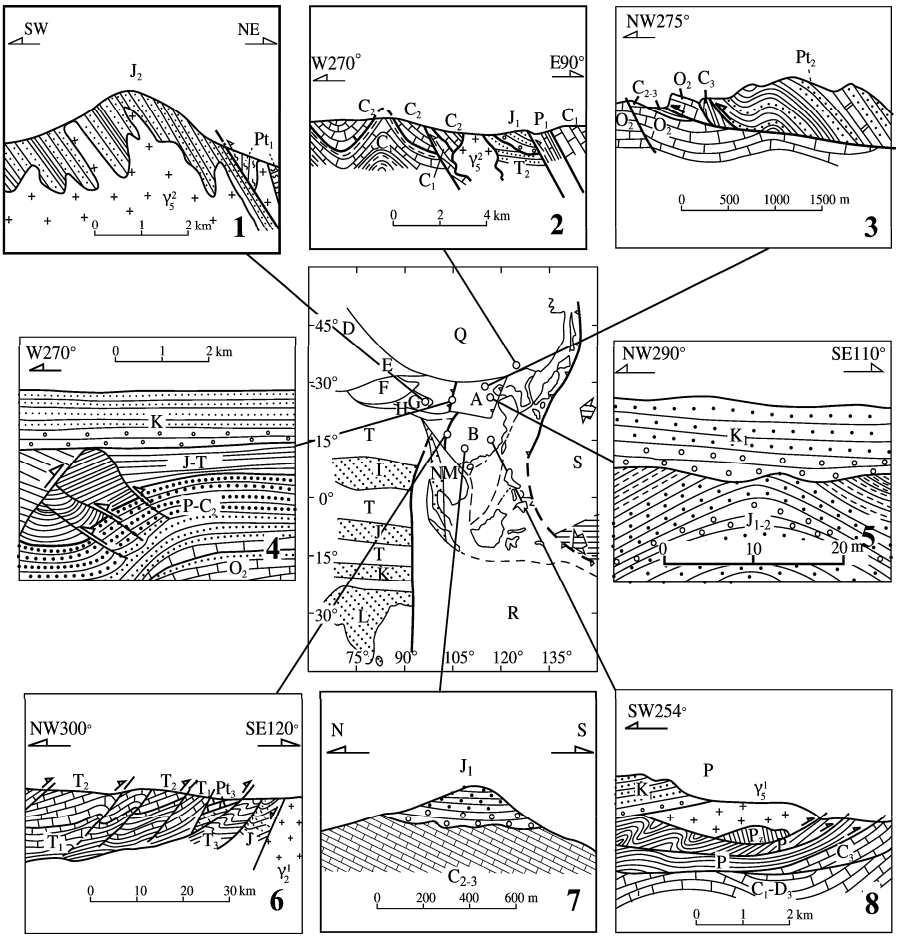

Fig. 7.5 Deformation in the Yanshanian Tectonic Period.

1. Structural section in eastern Qaidam: Middle Jurassic system was intruded by a Late Jurassic granite (Bureau of Geology and Mineral Resources of Qinghai Province, 1991); 2. Geological section at Panshi in Jilin: Jurassic system covering Triassic system with unconformity (Bureau of Geology and Mineral Resources of Jilin Province, 1988); 3. Structural section of Tuoli, in the Western Hills, Beijing, showing the Late Jurassic, NE trending Nandazhai–Babaoshan Thrust (Wan TF, 1981); 4. Seismic profile of western Ordos, showing ramp thrust formed by E-W orientation compression and shortening during the Late Jurassic, overlain unconformably by the Cretaceous system, (Wang TH, 1995); 5. Geological section of the unconformity between the Jurassic and Cretaceous, west of Mengyin in Shandong: Jurassic system forming an open fold with an angle of dip of the fold limbs of about 10° (Wan Tianfeng personal record, 1982) ; 6. Structural section of Yanyuan, imbricated Sichuan, Jurassic and Triassic systems are underlain by a thrust plane, the orientation of the faults is NNE (Bureau of Geology and Mineral Resources of Sichuan Province, 1991); 7. Geological section of eastern Guangxi, the near horizontal Jurassic system rests unconformably on the Carboniferous system (Bureau of Geology and Mineral Resources of Guangxi Province, 1985); 8. Geological section of coalfield in middle Fujian, the granite body formed in the Indosinian Period, thrusted over the Permian coal-bearing system, the age of thrusting was Late Jurassic (unpublished data of Bureau of Geology and Mineral Resources of Fujian Province).

Intraplate deformation is generally stronger near the margins of the paleo-plates. However, intraplate deformation during the Yanshanian Tectonic Period in China does not conform to this pattern. For example, in eastern Qaidam, Panshi County in Jilin, the Western Hills of Beijing, Yanyuan in Sichuan and the coalfields of central Fujian (1, 2, 3, 6 and 8 in Fig. 7.5), there are regions of strong intraplate deformation and major tectono-thermal events, which are all right away from the plate margins, but related to regions of thick sedimentation, zones of paleo-weakness and the presence of faults in the basement.

The major features of the intraplate deformation which occurred during the Yanshanian Tectonic Period were recognized seventy years ago. Almost at the same time, as Weng WH (1927, 1929) proposed the Yanshanian movements, defined by a distinctive combination of styles of deformation, Li SG (1929) proposed the Neocathaysian Tectonic System in eastern China, composed of a series of NNE trending folds and thrusts formed since the Late Mesozoic. Although at that time these structures could not be dated correctly, his proposal of the Neocathaysian Tectonic System has strongly influenced the study of deformation in eastern China. More recently it has been recognized that the Neocathaysian Tectonic System is the same as the Yanshanian Tectonic Period, and that deformation occurred mainly in the Jurassic (Wan TF, 1994).

Intraplate deformation in the Yanshanian Tectonic Period, forming the Neocathaysian Tectonic System, mainly formed during 175–135 Ma, is characterized by a series of NNE or NE trending flexural folds and thrusts, and WNW-NW trending extensional or strike-slip faults. Based on data from the regional geological survey of China (bureaus of geology and mineral resources of provinces, 1984–1993 (Fig.7.6)), 1,566 anticlines and 1,603 synclines in macro-or meso-scales with mainly intermediate angles (30°–60°) of dip of the fold limbs (Appendix 3.5) were collected. Adjacent to zones of weakness in the crystalline basement or in large sedimentary basins, Alpino-type and linear folds were formed, and on the stable crystalline basement or in areas with thin sediment, open, germano-type folds or only horizontal sedimentary strata are found, in Sichuan, Ordos and western Shandong. Folds of the Yanshanian Tectonic Period occur mainly in eastern China, e.g. east of Liupanshan (106.5°–107°E, 36°–38°N) and Henduanshan (99°–102°E, 27°–32°N), but in western China folding is rather weak and limited to local areas (Fig. 7.6).

From research in the Yanshan, Henan and Fujian areas, Wan (1994) found that during the Yanshanian Tectonic Period the orientation of the fold axes changed with time. Fold axes formed at the end of the Early Jurassic are usually ENE trending, at the end of Middle Jurassic NE trending, and at the end of the Late Jurassic commonly NNE trending. Fold axes show a counter-clockwise rotation from Early to Late Jurassic period, which may have been influenced by the counterclockwise rotation of the crustal blocks. This is rather similar to the rotation from the Paleocathaysian and Mesocathaysian to the Neocathaysian tectonic systems proposed by Li SG (1929, 1976). This counterclockwise rotation is exhibited most clearly by the change in the direction of maximum principal compressive stress: NNW trending in the Early Jurassic; NW trending in the Middle Jurassic; WNW trending in the Late Jurassic. In many areas of the eastern Chinese continent where the strongest deformation occurred in the Late Jurassic, NNE trending fold axes are dominant. In southern China NE trending fold axes were formed as deformation was constrained by NE trending lineaments in the basement. Although some fold axes are NNE trending, and some are NE trending, they are all considered to belong to the Neocathaysian Tectonic System. The Neocathaysian Tectonic System is not defined by any distinctive orientation of the fold axes.

Data from 3,169 folds and 168 points of joint observation (Appendix 3.5) was divided into 37 areas for statistical purposes, and the orientation of the principal stress axes was determined for the end of the Yanshanian Tectonic Period. In the present day coordinates the preferred attitude of the maximum principal compressive stress axis (σ_1) for Yanshanian Tectonic Period was SE116°∠7°, the intermediate principal stress axis (σ_2) (equal to the average orientation of fold axis) were NE26°∠3°, and the minimum principal compressive stress axis (σ_3) were 297°∠80° (Figs. 7.6 and 7.7). The tectonic stress field during the Yanshanian Tectonic Period in China was characterized mainly by near horizontal WNW-ESE shortening, and near horizontal NNE-SSW extension. During the Yanshanian Period the crust of the eastern Chinese continent based on formation of many thrusts was slightly thickened. From the

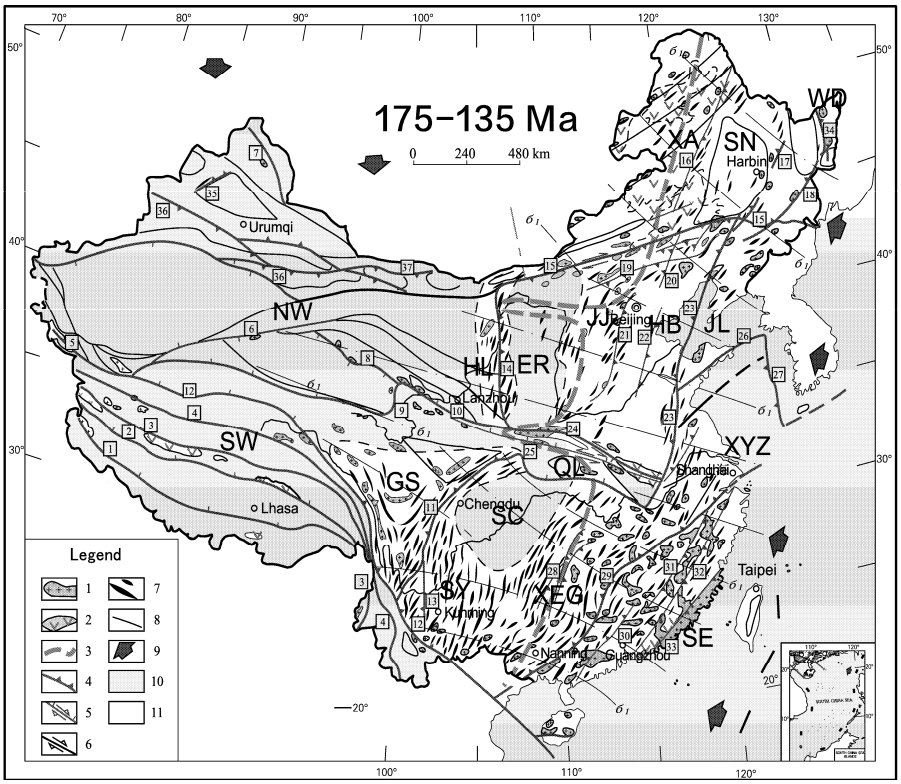

Fig. 7.6 Tectonic sketch of the effects of the Yanshanian Tectonic Period in China (175–135 Ma).

1. Granite of Yanshanian Period; 2. Volcanic rocks of the Yanshanian Period; 3. Rate of intraplate deformation, estimated from the chemical composition of magmatic rocks, "-" is rate of extension, others are rates of shortening (unit: cm/a), (data shown in Appendix 5.6); 4. Numbered collision zones or thrust belts; 5. Numbered normal and strike-slip faults; 6. Boundaries of blocks with weak activity or faults, no number; 7. Fold axes, anticlines only are shown (data in Appendix 3.5); 8. Trace of maximum principal compressive stress (σ_1); 9. Direction of plate movement; 10. Areas with conformity or disconformity; 11. Areas with angular unconformity. Name and number of plate boundaries, collision zones or fault belts are listed in Table 7.1.

determination of 70 values of paleo-differential stress (method shown in Chapter 1), the magnitude of tectonic stress was found to be stronger in eastern China than in western China. The locations from which the data was obtained, the rock types, minerals, numbers of samples and the magnitude of the average differential stress are all shown in Appendix 4. The average magnitude of differential stress over the whole Chinese continent is 99.4 MPa. The areas with the greatest differential stress (>80 MPa) are concentrated in eastern China, i.e. east to the Ordos and Sichuan basins (Fig. 7.8). Around some fault zones, for example the Nandazhai Thrust Zone of the Western Hills (Beijing) differential stress reached 161.8 MPa. It was commonly <80 MPa at the Gansu–Qinghai-Altun and in the western Kunlun areas of western China. According to incomplete data, there is an area with a high value differential stress in Gangdise, southeastern Xizang, where values reached 130–135 MPa. This may be due to a concentration of tectonic stress, according to westwards compression by the Izanagi and Pacific plates (Fig. 7.3). At that period, the Gangdise Block and the Pacific Plate were located at low latitudes in the southern hemisphere.

Table 7.1 List of major boundaries or faults moving during the Yanshanian Tectonic Period

Boundaries or fault type	Name of boundaries or fault zones	Shown in Fig 7.6
Boundaries	Boundary of plates along Yalung Zangbojiang Tectonic Zone (with oceanic crust)	1
	Boundary of plates along the Bangongco–Nujiang Tectonic Zone (with oceanic crust)	3
	Wandashan Collision Zone	34
NNE or NE trending thrust zone or reverse fault	Longmenshan	11
	Panzihua–Xichang reverse fault with strike-slip	13
	Liupanshan–Helanshan	14
	East of Dahingganling	16
	Yilan–Yitong	17
	Dunhua–Mishan	18
	Fuxin–Jinzhou (western Liaoning)	20
	East of the Taihangshan	21
	East of the Cangzhou–Liaocheng	22
	Tancheng–Lujiang reverse fault	23
	Eastern border of Yellow Sea reverse fault	27
	Xuefengshan	28
	Shaoxing–Shiwandashan reverse fault	29
	Wuchuan–Sihui reverse	30
	Chong'an–Heyuan	31
	Lishui–Lianhuashan	32
	Changle–Nan'ao	33
	Karamay buried thrust during Mid-Late Jurassic	35
	NorthYagan Thrust during Early-Mid Jurassic	37
E-W or WNW trending normal faults with strike-slip	Gegyal–Nyainqentangulha Fault	2
	Shuanghu–Lancangjiang	4
	Kangxiwa–southern border of Tarim strike-slip fault belt	5
	Altun dextral strike-slip fault	6
	Kurt–Narmande strike-slip fault	7
	Junulshan–Qinghainanshan strike-slip fault belt	8
	Southern border of Qaidam (Wenquan–Chaka) Fault Zone	9
	Wushan–Baoji strike-slip fault zone	10
	Jinshajiang–Red River (Honghe) sinistral strike-slip fault zone	12
	Yinshan-Xar Moron He dextral strike-slip zone (former northern border of the Sino-Korean Plate)	15
	Shangyi–Gubeikou–Pingquan dextral strike-slip fault	19
	Luonan–Fangcheng sinistral strike-slip fault zone (former southern border of the Sino-Korean Plate)	24
	Shandan–Tongbo sinistral strike-slip fault zone	25
	Zhucheng–Qingdao–Rongcheng dextral strike-slip fault zone	26
	North Tianshan (Bruknu–Aqigkuduk)	36
	North Yagan extension detachment fault after Middle Jurassic	37

Shortening ratio, shortening magnitude, length of time of deformation and linear strain rate for folds developing during the Yanshanian Tectonic Period have been estimated roughly (using the methods in Chapter 1) for four E-W profiles along latitudes (45°N, 40°N, 33°–31°N and 25°N) in the present coordinates (Table 7.2). The area with greatest shortening ratio (23.4%) is located along the Qinling–Dabie Zone; smaller ratios are found in South China (21.6%), North China (11%) and Northeast China (11.5%). The time of formation of the folds was between 2.25 and 7.59 million years, meaning that episodes of strong deformation occupied only 3.2%–10.8% of the whole Yanshanian Tectonic Period. Linear strain rates are between 0.9×10^{-15}/s and 1.6×10^{-15}/s, indicating a process of flow deformation.

A series of reverse faults and thrusts with an NNE to NE trend were formed together with the folds during the Yanshanian Period (Fig. 7.6; Table 7.1). Most of these faults developed along zones of paleo-

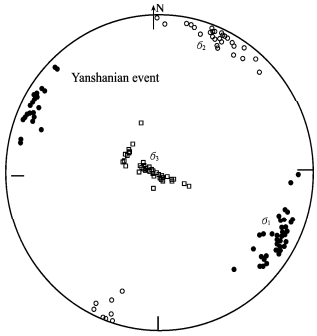

Fig. 7.7 Attitudes of axes of principal stress during Yanshanian Tectonic Period. σ_1. maximum principal stress axis; σ_2. intermediate principal stress axis; σ_3. minimum principal stress axis.

Table 7.2 Shortening ratio, shortening magnitude, deformation time and strain rate during the Yanshanian Tectonic Period

Area	Northeast China	North part of North China	Qinling–Dabie zone	South China
Latitude	45°N	40°N	33°–31°N	25°N
Length (km)	1,000	1,500	1,500	2,000
Mean limb angle	27.7°	27.1°	40.04°	38.4°
(amount of data)	(166)	(301)	(354)	(262)
Shortening ratio (%)	11.5	11.0	23.4	21.6
Shortening magnitude (km)	114.6	164.9	351.6	432.8
Shortening velocity (cm/yr)	5.1	4.5	4.9	5.7
Deformation time (Myr)	2.25	3.66	7.18	7.59
Linear strain rate (ε, 1/s)	1.6×10^{-15}	9.5×10^{-16}	1.04×10^{-15}	9.0×10^{-16}

weakness, or from the combination of many small faults. Some strike-slip faults formed during the Indosinian Period were converted into reverse faults during the Yanshanian Period. In areas where strong deformation had occurred earlier, due to work-hardening, it was evidently difficult for superposed folds to form during the Yanshanian Period, so faults were formed, cutting across folds formed during earlier tectonic periods.

E-W trending thrusts (Table 7.1) formed in the Indosinian Tectonic Period were converted to normal and strike-slip faults in the Yanshanian Period. Zhang CH et al. (2001) studied the Shangyi–Gubeikou–Pingquan Fault in northern Hebei in detail, and found a great deal of evidence for dextral strike-slip faulting in that zone during the Yanshanian Period; similar evidence is also found in many E-W trending faults (Table 7.1).

To sum up, near E-W trending faults were almost parallel to the regional maximum principal compression stress axes in the Yanshanian Period, but were influenced by WNW-ESE shortening and by NNE-SSW extension, and all appeared to be normal faults with strike-slip features. Intermediate-basic volcanic rocks were erupted on the northern border of the Qinling–Dabie Zone, influenced by the NNE-SSW extension along an E-W trending fault. Recently, Lu FX et al. (2003) discovered inclusions of granulite and eclogite derived from a deep source in andesites and basalts at Minggang (Henan), with an isotopic age of 178±3.7 Ma, the trace elements and lead isotopes were similar to those of south Qinling. Volcanism during the Yanshanian Period transported material subducted beneath the Sino-Korean Plate during the Indosinian Tectonic Period from the lower crust of south Qinling to the surface. Near E-W trending faulted–depression basins in the western Liaoning and Hefei were controlled by near E-W trending normal–strike-slip faults. In the Hefei Basin denudation contours of the Jurassic system are also shown to be nearly N-S trending, influenced by E-W shortening and N-S extension (Xue AM et al., 1999).

E-W trending normal faults in the western Chinese continent were all influenced by N-S trending extension, but were not highly active during the Yanshanian Tectonic Period. Deformation was limited

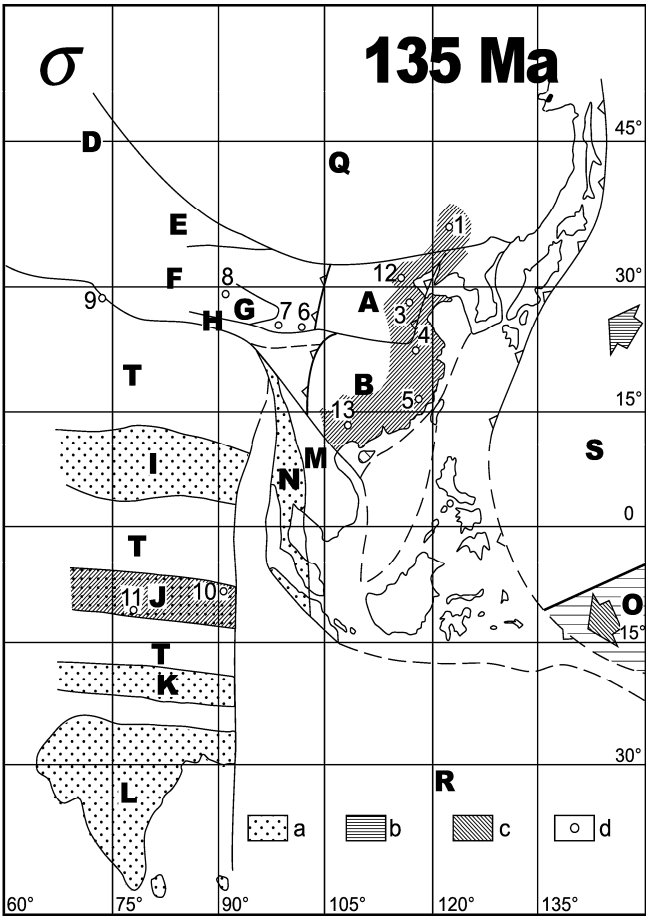

Fig. 7.8 Magnitude of differential stress (σ) in the Yanshanian Period.

a. Gondwanan continental blocks before the Indosinian Period; b. Pacific Plate; c. Area with > 80 MPa differential stress; d. Locations of samples collected for the determination of differential stress. Areas shown to be white have less than 80 MPa stress or have no data. The data is shown in Appendix 4. Symbols for the blocks are the same as in Fig. 6.5.

Locations of stress determinations: 1. Daheishan, Jilin; 2. Zhaoyuan-Laizhou, Shandong; 3. Mengyin, Shandong; 4. Middle and lower Yangtze; 5. Eastern Fujian; 6. Eastern Gansu; 7. Eastern Qinghai; 8. Altun; 9. Western Kunlun; 10. Eastern Xizang; 11. Southern Xizang; 12. Nandazhai, Western Hill, Beijing; 13. Nandan, Guangxi.

to areas in the proximity of the faults. In areas distant from the faults, strata of the Upper and Lower Jurassic systems are all conformable and do not show any deformation.

With the influence of near E-W shortening and near N-S extension, a series of E-W trending sedimentary depressions were formed in the Chinese continent during the Jurassic: e.g. the Junggar, Turpan–Hami, Tarim, Dunhuang–Chaoshui, Alxa, Qaidam, Mohe of Heilongjiang, Hailar–Baicheng, Erenhot, Yin'gen, Dengkou in Inner Mongolia, Shangyi, Xiahuayuan–Houcheng in Hebei, Nanpu of Hebei, mouth of Yellow River–Zibo of Shandong, southern Zhoukou of Henan, Ordos, Qilian–Minhe of Qinghai and northern Sichuan basins. Huge hydrocarbon accumulations and coals were formed in those

basins, mainly during the Early Jurassic, including many important oil-gas fields and the largest coalfield in China.

Recently, Feng YM (1998) carried out detailed tectonic research on the later periods of deformation in the North Qilian Collision Zone and recognized detachment sheets in the western part of the North Qilian Domain. The Zhulongguan and Beidahe detachments, with a displacement of 50km, occurred during the Late Jurassic. These structures were formed under the influence of E-W shortening and N-S extension. The hanging walls of these detachments are composed of Paleoproterozoic and Mesoproterozoic rocks. The detachments cut across and overlie closed folds in the footwall formed during the Indosinian Tectonic Period, and the whole assemblage is covered unconformably by the Lower Cretaceous system.

However, around Junggar and Inner Mongolia, E-W trending thrusts were formed during N-S shortening and compression, perhaps due to the southward movement of the Siberian Plate. The Karamay–Ulhuy buried thrust (35 in Fig. 7.6 and 1 in Fig. 6.5) was formed during the Middle–Late Jurassic, penetrating all the systems below the Upper Jurassic and leading to the accumulation of oil and gas in depth. A similar fault is the Bruknu–Aqigkuduk reverse fault zone (36 in Fig. 7.6) on the northern border of the Tianshan. Zheng YD et al. (1990, 1991, 1993) studied the E-W trending thrust zone, north of the Yagan Block near the border between China and Mongolia and considered that the thrust was formed during a late period of the Early Jurassic. The observed separation along the thrust is 60–70 km, but the estimated separation due to the thrust may be as many as 120 km, since the Middle Jurassic the thrust was converted into an extension detachment fault (37 in Fig. 7.6). Since the Middle Jurassic this area was influenced by the tectonic stress field of eastern China, and was also controlled by near E-W shortening and N-S extension, forming a low angle detachment fault.

The only collision during the Yanshanian Tectonic Period in Chinese continent occurred in the Wandashan Collision Zone of Northeast China (Shao JA et al., 1992, 1995; Zhao CJ et al., 1996) (34 in Fig. 7.6). Mizutani et al.(1986) and Kojima (1989) have called this collision zone the Nadanhada Collision Zone, but this name is not appropriate. In the Raohe area of Wandashan an Early Jurassic ophiolite suite has given isotopic ages between 188 and 173 Ma. The lower part of the ophiolite is composed of ultra-mafic and mafic magmatic rocks; the middle part is basalt with pillow structures and the upper part siliceous radiolarian chert, interbedded with clay of abyssal facies. The ophiolitic rocks occur as tectonic slices near the major collision zone, and all the rocks are mylonitized. The Wandashan–West Sikhote–Alin Block which lies to the east of this collision zone may be part of Okhotsk Block (including the Okhotsk Sea, northeast Japan and the Far East of Russian), belonging to the North American Plate. The North American Plate, including the Okhotsk Block and their adjacent micro-plates, migrated rapidly westwards during the Jurassic, to collide with the Siberian Block of the northern Eurasian Plate, forming the Wandashan Collision Zone in Chinese continent.

The series of NNE-NE trending folds and thrusts, WNW trending normal faults with strike-slip and NNW or ENE trending strike-slip faults, influenced by the tectonic stress field during Yanshanian Tectonic Period, comprise the Neocathaysian Tectonic System. Some authors consider that only the NNE trending folds and thrusts constitute the Neocathaysian Tectonic System; this usage does not conform to the original terminology of Li SG (1962).

7.3 Tectono-magmatism in Crust

The Yanshanian Tectonic Period was a period of major magmatic activity in eastern China, where the magmatic rocks outcrop over an area of more than 229,000 km^2, 25% of the outcrops of magmatic rocks in China formed during its whole geological history (Cheng YQ, 1994).

Before the Jurassic, magmatism always occurred near subduction or collision zones on the margins of the Chinese continental blocks. There were only a few intraplate magmatic intrusions. However, during the Jurassic, granitic intrusions and volcanic rocks were distributed widely throughout eastern China

(Appendix 7). Magmatic intrusions were emplaced at least 600 km away from the nearest subduction zone and sometimes at a distance of 1,000–2,000 km. Since the 1970's, the mechanism of magmatism during Yanshanian Period has been hotly disputed. If magmatism occurred within 100–400 km of a subduction zone, it would be reasonable to suppose that the magmatism was connected with subduction. But during the Jurassic, magmatism in the Chinese continent occurred in an intraplate environment, far away from any subduction zone.

Magmatism in the Yanshanian Period was mainly of intermediate-acid type of the calc-alkaline series. Most of the granitoids are of S-type re-melted crust, with a magma source in the middle or lower crust, or of A-type syntactic crust and mantle, with a magma source near the Mohorovǐcíc discontinuity. The volcanic rocks have a bimodal basalt and rhyolite-trachyte composition (Appendix 7).

Data has been collected from 409 magmatic intrusions, of which 62.8% are S-type granitoids with obvious foliation, distributed as sheets, together with volcanic rocks along NNE and NE trending thrust zones, formed under NW–SE compression and originating in crust, 35% are A-type granitoids which, together with volcanic rocks, occur along WNW–ESE trending normal fault zones, nearly parallel to the maximum principal compressional stress axis during the Yanshanian Period, and formed near Moho discontinuity, only 2.2% of the magmatic intrusions contain ultra-mafic inclusions, indicating that the magma originated from a source at the base of the lithosphere and rose along deep lithosphere faults (Appendix 7; Figs. 7.9 and 7.10). The evidence indicates that the Yanshanian magmatic rocks originated in the crust or near the Mohorovǐcíc discontinuity, only a few originated from the base of the lithosphere, but were not related to subduction or collision (Wan TF, 1994; Wan TF et al., 2008).

Volcanic rocks are widespread across the whole of Northeast China. In the central area of the Songhuajiang–Linghe Basin, east of Northeast China, they are mainly intermediate–basic volcanic rocks bounded by the Duhua–Mishan Fault (18 in Fig. 7.6), Yanbian-Suifenhe, Laoyeling and the Yilan–Yitong faults (17 in Fig. 7.6) where they were erupted during the Early and Middle Jurassic (171–191 Ma). From the basin of Songhuajiang–Nenjiang (Daqing Oil Field) to Dahingganling, i.e. in the middle part of Northeast China, the volcanism mainly occurred in the Late Jurassic-Early Cretaceous (about 160–120 Ma). The migration of volcanic zone was westward, i.e. counterclockwise rotation (Fig.7.11) (Xu WL et al., 2008; Lei MS, 2009 (personal communication)). The granitoids were commonly intruded in the Middle to Late Jurassic (160–135 Ma). Granodiorite occurs near the Nenjiang Fault in northern Dahingganling, and there are major granites in other areas of Northeast China. Recently, in the basement of Daqing oil basin, the Middle Jurassic (160 Ma) granites were found (Lei MS, 2009 (personal communication)). The distribution of granitoid zones was also shown to be westward migration, i.e. counterclockwise rotating a little bit in Northeast China,

Magmatism of the Yanshanian Period was extremely active in the Yanshan–west Liaoning–Taihangshan areas of North China. In the eastern area Early Jurassic volcanic rocks of the Nandaling and Xinglonggou formations (185–170 Ma), consisting mainly of basalts and andesites. occurred in rather narrow zones along ENE trending faults. In the western area Middle Jurassic volcanic rocks, mainly andesites, of the Diaojishan and Lanqi formations (170–155 Ma), are distributed widely along NE trending faults. In northern Taihangshan Late Jurassic rhyolites of the Baiqi and Zhangjiakou formations (155–135 Ma) are distributed mainly along NNE trending faults. At different periods in the Jurassic, volcanism erupted along transpressional faults with different orientations, corresponding to the change in the orientation of the fold axes in North China. From the Early to Late Jurassic the fold axes and volcanic eruption zones all trend ENE, NE or NNE, showing the counterclockwise rotation (Bao YG et al., 1995). Granitoids intruded during the Yanshanian Period in the Yanshan–west Liaoning–Taihangshan areas had a similar distribution to the volcanic rocks, however intrusive activity was not continuous. Also during the Yanshanian Tectonic Period, intermediate–acid magmatism occurred separately along the northern boundary fault of the former Sino-Korean Plate.

Intermediate-acid intrusions were emplaced in eastern Shandong and eastern Liaoning in the Middle and Late Jurassic. Recently, Wan TF et al. (2001) studied the Linglong granitoid complex, the largest in North China, and recognized that although it is mixed with many pre-Cambrian metamorphic inclusions, the major body was intruded during the Middle Jurassic (170–153 Ma). The intrusion forms a sheet-like

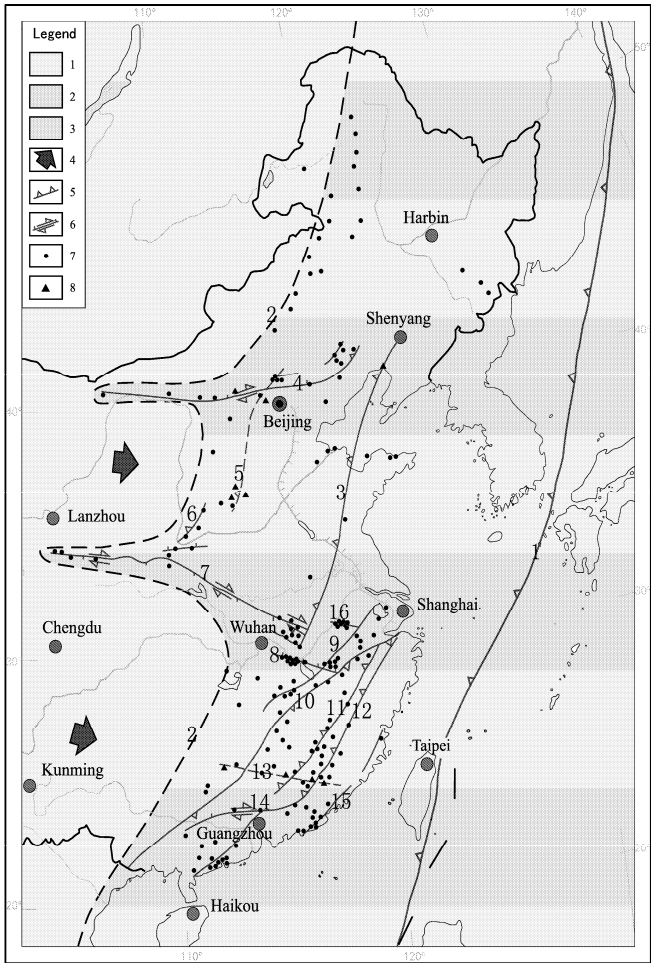

Fig. 7.9 Distribution of magmatic source areas and faults near the Mohorovĭcíc discontinuity and bottom of lithosphere during Yanshanian Stage (205–135 Ma) in eastern China (Wan TF et al., 2008).

Numbers of legend: 1. continental crust almost without magmatism; 2. continental crust with obvious magmatism; 3. oceanic crust; 4. compression orientation in crust; 5. subduction zone, thrust or reverse fault; 6. normal fault with strike-slip; 7. magmatic source depth data near Mohorovĭcíc discontinuity (data shown in Appendix 7); 8. magmatic source depth data near bottom of lithosphere (data shown in Appendix 7).

Numbers of faults: 1. inferred subduction zone between continental and oceanic crusts of eastern China during Yanshanian stage (Japan Islands were located west to the zone, which due to rare data can never be reconstructed); 2. boundary between obvious and weak magmatism during Yanshanian stage; 3. Tancheng–Lujiang reverse fault zone; 4. Yanshan (Shangyi-Gubeikou-Pingquan)–Yinshan normal fault with dextral strike-slip; 5. East Taihangshan lithosphric reverse fault; 6. southwestern Shanxi reverse fault; 7. North Dabie–Qinling normal fault with dextral strike-slip; 8. Ruichang–Jiujiang–Dexing normal crust fault; 9. northeast Jiangxi reverse fault; 10. Shaoxing–Shiwandashan reverse fault zone; 11. Dayuling–North Wuyishan thrust zone; 12. Shaowu–Heyuan thrust; 13. Nanling lithosphric fault; 14. Heyuan–Fugang–Darongshan normal fault with dextral strike-slip; 15. Changle–Nan'ao thrust; 16. Tonglin WNW trending normal fault.

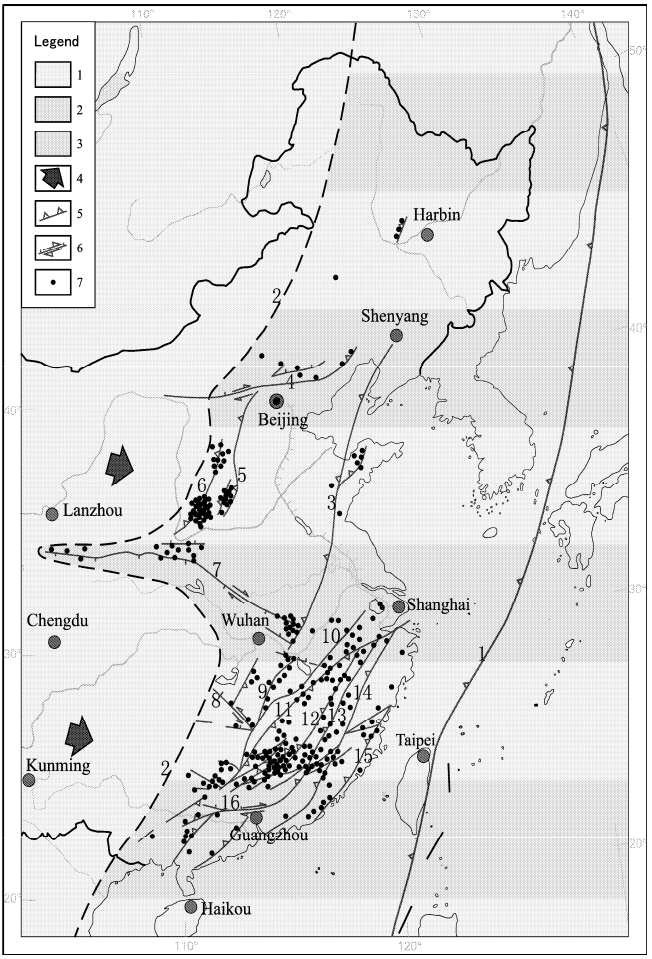

Fig. 7.10 Distribution of magmatic source areas and faults in crust during Yanshanian Stage (205–135 Ma) in eastern China (Wan TF et al., 2008).

Numbers of legend: 1. continental crust almost without magmatism; 2. continental crust with obvious magmatism; 3. oceanic crust; 4. compression orientation in crust; 5. subduction zone, thrust or reverse fault; 6. normal fault with strike-slip; 7. magmatic source depth data in crust (data shown in Appendix 7).

Numbers of faults: 1. inferred subduction zone between continental and oceanic crusts of eastern China during Yanshanian stage (Japan Islands were located west to the zone, which due to rare data can never be reconstructed); 2. boundary between obvious and weak magmatism during Yanshanian stage; 3. Tancheng–Lujiang reverse fault zone; 4. Yanshan (Shangyi-Gubeikou-Pingquan)–Yinshan normal fault with dextral strike-slip; 5. East Taihangshan lithosphric reverse fault; 6. southwestern Shanxi–Middle Shanxi reverse fault; 7. North Dabie–Qinling normal fault with dextral strike-slip; 8. Mufushan–Hengshan fault; 9. Jiuling–Hengdong reverse fault; 10. northeast Jiangxi reverse fault; 11. Shaoxing–Shiwandashan reverse fault; 12. Dayuling–North Wuyishan thrust zone; 13. Shaowu–Heyuan thrust; 14. Zhenghe–Dapu–Lianhuashan thrust; 15. Changle–Nan'ao thrust; 16. Heyuan–Fugang–Darongshan normal fault with dextral strike-slip.

batholith less than 10 km thick, covering an area of more than 3,000 km^2, which has been exposed by the erosion of about 3 km of overburden since the Jurassic. The magma was intruded at the intersection

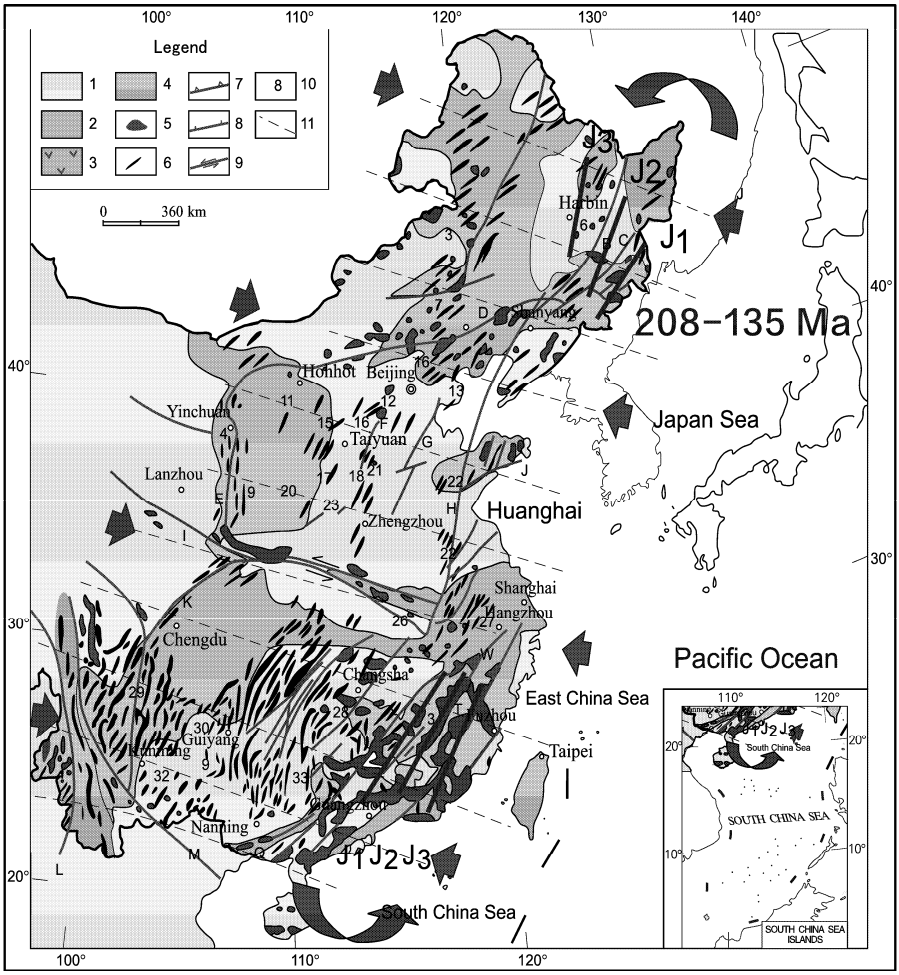

Fig. 7.11 Rotation of magmatic zone in Jurassic.

J_1, Early Jurassic magmatic zone; J_2, Jurassic magmatic zone; J_3, Jurassic magmatic zone. Big red rotation arrow shows the rotation direction of magmatic zone.

1. Jurassic basin; 2. Mountains; 3. Volcanic rock; 4. Shallow sea; 5. Granite; 6. Fold axes, anticlines; 7. Reverse fault or thrust belts; 8. Normal fault; 9. Strike-slip fault; 10. Number of areas; 11. Trace of maximum principal compressive stress (σ_1).

of a main strand of the Tancheng–Lujiang Fault Zone and a low angle thrust, at a depth of about 20 km. At this intersection, crustal rocks were partially melted to form granitic magma, which was intruded eastwards and upwards along the thrust plane.

In South China volcanic rocks erupted in the southern Jiangxi, southwest Fujian and eastern Guangdong areas in the Early and Middle Jurassic. The rocks are mainly bimodal intermediate-basic rocks, with about 70% basalt, forming an east-west trending volcanic belt, with isotopic age of around 170 Ma (Lai ZZ et al., 1996; Tao KY et al., 1998; Zhang BT et al., 2002). The basaltic magma may have

been intruded along a partial detachment near the Mohorovĭcíc discontinuity, caused by underplating in the lower crust, and then erupted to the Earth's surface, together with a slight admixture of crustal materials, along E-W trending extensional faults (Chen PR et al., 1999). Granites in South China are commonly highly acid, with an average SiO_2 content of 73.25%, higher than Precambrian granites which have an average SiO_2 content of 62.1%, and a higher total alkali and rare earth element content. The granites are mainly of S-type remelted crust and secondary A-type syntactic crust and mantle. Their essential and accessory mineral contents, SiO_2, K_2O+Na_2O, the characteristics of $[Fe^{3+}/(Fe^{3+}+Fe^{2+})]$, $[Al_2O_3/(K_2O+Na_2O+CaO)]$, corundum standard mineral, trace elements, rare earth elements and isotopes (Sr_i, $\delta^{18}O$) for different types of granites are given in the related references (see Gilder et al., 1996).

In South China the granites show clear zoning. Zhan MG (1994) synthesised earlier studies to show that from the Triassic to the Cretaceous granitic intrusions migrated gradually eastward, volcanic zones also migrated similar to granitic zone (Figs. 7.11 and 7.12). Triassic granites occur mainly in the Shiwandashan–Changsha area, i.e. the southwest section of Shaoxing–Shiwandashan Collision Zone. Apart from syn-collision granites, there are many small granitic bodies intruded along N-S extensional faults. Early Jurassic S-type granites are located mainly in central and southwestern Jiangxi, Middle Jurassic granites extend mainly to the north and east of Jiangxi, Late Jurassic granites occur to the west of Zhejiang, west Fujian and east and central Guangdong. The granitoids are all formed in the middle crust or near Mohorovĭcíc discontinuity (Appendix 7) and influenced by counterclockwise rotation of crust (Fig. 7.11)

However, A -or I-type granites of Jurassic age are located mainly along WNW extensional faults, such as Tongling of Anhui, southeast Hubei–northeast Jiangxi, central Hunan and west Guangdong; there is only one intrusion along the NNE Zhenghe–Dapu–Lianhuashan Fault Zone. Cretaceous granites are developed only in the coastal areas of Zhejiang, Fujian and Guangdong. Li Wuxian and Zhou XM (1999) also found that the ages of the magmatic rocks become gradually younger from west to east, and that their composition varies from calc-alkaline to calc-alkaline with high potassium content. Zhan MG (1994) proposed that the emplacement of the granitic intrusions was controlled by a series of NE trending thrusts and detachments in the crust. His suggestion provides a convincing explanation for the distribution of granitic rocks in South China.

Zhan MG (1994) found that from Triassic to Cretaceous the centre of granitic intrusion rotated and migrated eastwards for about 420 km, with an average rate of displacement of 0.24 cm/yr (Fig. 7.9). During the Yanshanian Period the zone of granitic intrusion gradually migrated eastwards for about 180 km at an average rate of 0.26 cm/yr. The depth of formation of the S-type (remelted crust) granitic magma in South China was 15–22 km, i.e. about the depth of the low seismic velocity layer of the middle crust (Zeng HL, 1995 (Appendix 7)) and the original depth of formation of A-or I-type granitic magma was at 32–42 km, i.e. near that of the Mohorovĭcíc discontinuity (Teng JW, 2002 (Appendix 7)). In the light of the discussion above concerning the rotation of eastern China, the eastward migration of granitic intrusion in South China could be the result of counterclockwise rotation of the East Asian continent crust (Figs. 7.2 and 7.11).

Where no tectonism occurs in the lithosphere, the lithosphere remains stable and solid under the control of gravity and magmatic chambers cannot form. Where tectonism, rock deformation and migration, or any other patterns of deformation, including extension, compression or shearing, occur, rock fractures or ductile shears can develop, resulting in the formation of tectonic weakness zone, detachment and the release of pressure. In a deep and enclosed environment, release of pressure causes an increase of temperature. When the temperature exceeds the melting point of rocks, the magmatic source areas occur with the partial melting to form magma. Thus, based on the data of the depth of magmatic sources from different areas during particular tectonic periods, the inversion of space position of local tectonic detachment and sphere interaction could be realized (Appendix 7). Magmatic source areas do not form in continental lithosphere with a great thickness and low thermal gradients, although tectonic detachment within the lithosphere or at the base of the lithosphere may have occurred.

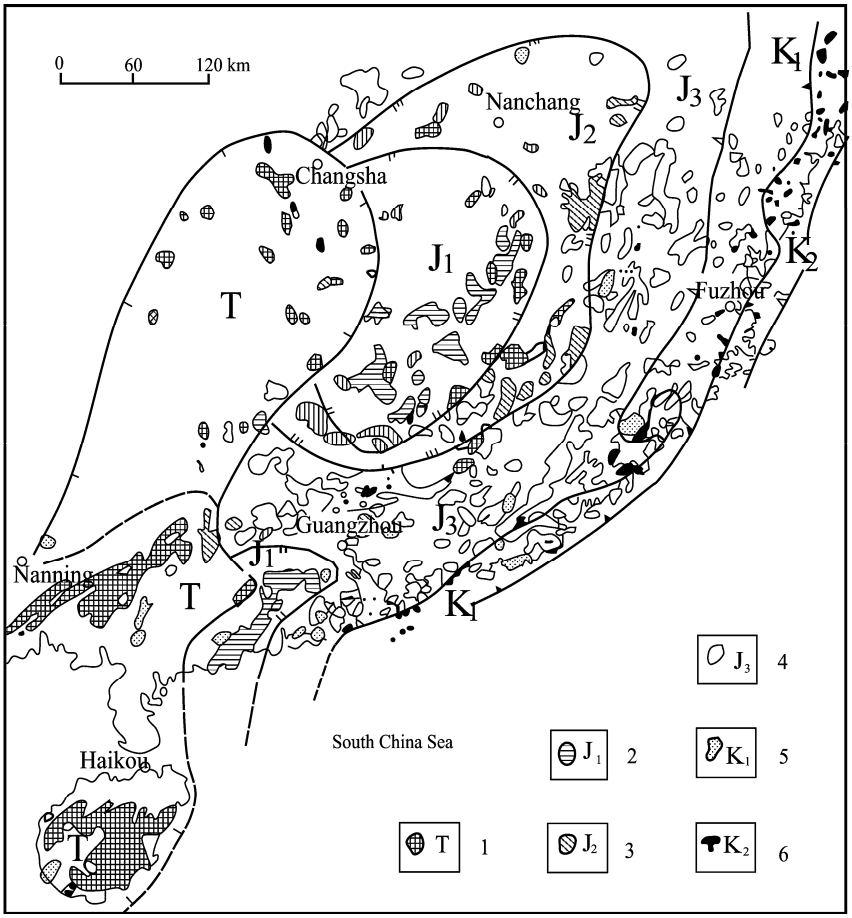

Fig. 7.12 Spatial distribution of Triassic–Cretaceous granitic intrusions in South China.

1. T-Triassic intrusions; 2. J_1-Early Jurassic intrusions; 3. J_2-Middle Jurassic intrusions; 4. J_3-Late Jurassic intrusions; 5. K_1-Early Cretaceous intrusions; 6. K_2-Late Cretaceous intrusions.

The author proposed that the eastward migration of the zone of granitic intrusion in South China was controlled mainly by detachments in the low seismic velocity layer in the middle crust, and by the eastward propagation of piggyback thrusts (Fig. 7.13). These are the largest thrusts known in eastern China. The flat-lying thrust planes are closely parallel to the maximum principal compressive stress (almost horizontal) with a small amount of vertical extension at that period. Steep thrust planes are obviously compressive and granitic intrusions in these areas often show strong foliation. The intersection of high angle fault planes with major thrusts or ductile shear zones in the middle crust or at the Mohorovicíc discontinuity would have the effect of partially decreasing the pressure and then increasing the temperature, thus causing the formation of granitic magma and its upward movement. Controlled by propagating thrusts, magmatism migrated gradually eastwards in South China with time, influenced during the Yanshanian Tectonic Period by the counterclockwise rotation of the East Asian continent and WNW trending compression. The source area for the formation of granitic magma was located near the

middle crust or Mohorovĭcíc discontinuity, where the temperature is usually 700–900°C. At the earth's surface this temperature is sufficient to cause the melting of rocks, but with increasing pressure at the depth, this temperature is not sufficient, so that when the crust is stable, melting is impossible. The implication is that magma sources were localised at the intersections between regional branch faults and detachments in the middle crust or at the Mohorovĭcíc discontinuity, where magma was formed with the reduction of pressure.

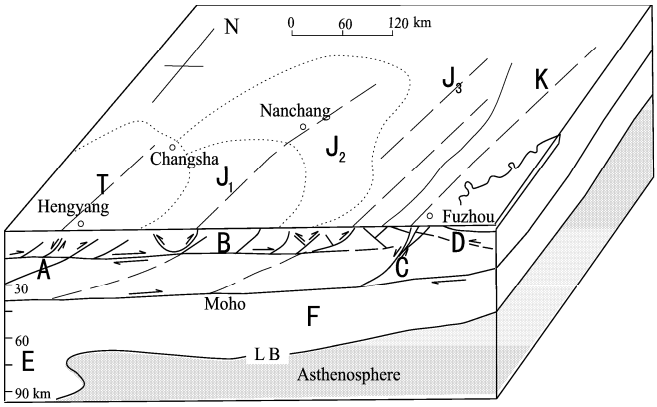

Fig. 7.13 Detachments in the crust, location of granites and the thickness of the lithosphere in South China.

T. Area of Triassic granites; J_1. Area of Early Jurassic granites; J_2. Area of Middle Jurassic granites; J_3. Area of Late Jurassic granites; K. Area of Cretaceous granites.

A. Shaoxing-Shiwandashan Collision Zone, Triassic crustal fault; B. Jurassic middle crustal detachment and overthrust with piggyback propagation; C. Cretaceous crustal fault along the Fujian coast; D. Recent Fujian-Taiwan thrust system; E. Thicker lithospheric mantle (continental type), west of Hengyang; F. Thinner lithospheric mantle (oceanic type), east of Hengyang; Moho. Mohorovĭcíc discontinuity; LB. Base of lithosphere. The transition zone of lithosphere type is near Hengyang, east to it is the thin lithosphere with continental crust and oceanic lithospheric mantle, and west to it is the typical continental and thick lithosphere.

Another important reason for the localization is the variation in the thickness of the lithospheric mantle. Areas of magmatism in eastern China during Yanshanian Period extended eastwards to Dahingganling, western Shanxi, Wulingshan and Shiwandashan. However, to west of that line the magmatic activity was very weak (Wan TF et al., 2008) (Figs. 7.9 and 7.10). This boundary is close to the present zone of high gravity gradient which extends from Dahingganling to Taihangshan and Wulingshan. The present high gravity gradient marks not only a change in crustal thickness, but also a change in the thickness of the lithosphere, where the mantle passes from a western continental-type lithospheric mantle (continental mantle) with a thickness of 60–120 km to an eastern oceanic-type lithospheric mantle (oceanic mantle) (Chi JS, 1988) with a thickness of about 40 km, that is, from a western continental lithosphere composed of continental crust and continental mantle to an eastern transitional lithosphere composed of continental crust overlying oceanic mantle (Figs. 7.9, 7.10 and 7.13) (Wan TF, 2004; Wan et al., 2008). Thus, the author has proposed that during the Jurassic there was a continental lithosphere, showing rare magmatic activity as far west as the Dahingganling-western Shanxi-Wulingshan-Shiwandashan line, with a transitional lithosphere and strong magmatic activity to the east of this line. In this type of thinner transitional lithosphere, the depth of the base of the lithosphere, with a temperature of 1,200°C, is only 70–80 km. Both the temperature and the geothermal gradient will be higher than those in continental lithosphere. When local tectonic detachment occurs within a lithospheric plate, a magmatic source area is easily formed. Local tectonic detachments can also have occurred in the continental lithosphere to the

west of the Dahingganling–western Shanxi –Wulingshan–Shiwandashan line, but due to thickness of lithosphere of more than 100–120 km, the temperature and the geothermal gradient are relatively low, and a magmatic source area is not easily formed.

It seems that counterclockwise rotation of China, with the eastward movement of continental crust over thin, hot, oceanic lithospheric mantle, may have combined to cause widespread granitic magmatism in eastern China during the Jurassic.

Recently, facing the same facts, Li WX and Zhou XM (1999) proposed another explanation. They considered that the widespread magmatism in eastern China during the Jurassic was caused by a change in the angle of subduction in the subduction zone on the eastern margin of the Chinese continent. From the relationship of the angle of subduction to the position of the magmatic arc, they calculateed that the angle of subduction of the paleo-oceanic plate beneath Chinese continent increased from 10°to 50°between 180 and 85 Ma. Based on their hypothesis, magmatic activity during the Jurassic represents a paleo-arc in South China, like the Andes on the eastern margin of South American continental plate. However, in South China the granites are largely acid, with no andesites at all; most volcanic rocks have a bimodal pattern, formed by crustal melting, casting doubt on this hypothesis.

Later, Zhou XM et al. (2000) proposed that magmatism in South China was due to underplating of the crust by mafic magma. However, this underplating hypothesis is not supported by any reasonable evidence. Although some lower crustal inclusions have been found (Du YS et al., 2003), mantle inclusions have never been reported from any of the granites in South China. Basic magmatism occurred along E-W trending extensional fault zones in the south Jiangxi, southwest Fujian and east Guangdong areas, during the Jurassic period. If underplating by mafic magmas did occur, it is not the main mechanism for the formation of the widespread granitic intrusions in South China.

In western China magmatism was not very important during the Yanshanian Period. In Qinghai area, there are four N-S trending tectono-magmatic zones. The typical magmatic zone is the Ngolashan Zone (centered on 99°E, 36°N) in which many separate Yanshanian granitoids occur along an N-S trending reverse fault (Bureau of Geology and Mineral Resources of Qinghai Province, 1991). In Xinjiang most granitoid magmatism occurred in the Late Paleozoic and Triassic, however, a large number of Jurassic K-Ar isotopic ages (190–140 Ma) have been obtained, and show that there was a tectono-thermal event during the Jurassic (Bureau of Geology and Mineral Resources of Xinjiang Uygur Autonomous Region, 1993). There was also extensive granitoid magmatism in the Qiangtang, Gangdise and Himalayan areas (Bureau of Geology and Mineral Resources of Xizang (Tibet) Autonomous Region, 1993). In southwestern China, Jurassic ophiolitic rocks along the Bangongco–Nujiang (3 in Fig. 7.6) and Yalung-Zangbo (1 in Fig. 7.6) zones represent subducted paleo-oceanic crust, indicating that the Gangdise and Himalayan micro-plates lay within the Tethys Ocean in the southern hemisphere (J and K in Fig. 7.1) and were not connected to the Eurasian continent at that time.

Based on the chemical composition of 2984 samples of magmatic rocks (Appendix 5.6), the rates of movement have been estimated for 75 areas throughout the Chinese continent. The average rate of WNW intraplate shortening during the Yanshanian Tectonic Period was 5.6 cm/yr. The average rate of N-S extension in Tethys Ocean, south of the Qiangtang Block, was 1.6 cm/yr. In the Yanshan, Jiangxi, East Hunan, Guangdong and Guangxi areas the average rate of WNW shortening was 6.0 cm/yr, and more than 6.0 cm/yr in the Kunlun, Qaidam, Henduanshan, Qiangtang, Gangdise and Himalayan areas (Fig. 7.6). The regional distribution of rates of shortening higher than average ones suggests that the combined effects of the northwestward subduction of the Izanagi Plate and the southwestward subduction of the Pacific Plate produced a region being of relatively high stress and strong deformation in the Kunlun, Qaidam, Henduanshan, Qiangtang, Gangdise and Himalayan blocks. In the stable crystalline basement of Ordos, Sichuan, Tarim and Inner Mongolia the average rate of WNW shortening was less than 4.0 cm/yr.

The most important tectonic event during the Yanshanian Tectonic Period was the 20°–30° counterclockwise rotation of the Chinese continent crust, influenced by the westward migration, subduction and compression of the Okhotsk (a part of American Plate) and Izanagi plates, formation of the Wandashan Collision Zone, development of detachments and thrusts in the middle and lower crust underneath the

Neocathaysian Tectonic System, followed by widespread tectono–magmatism in the above transitional lithosphere of eastern China.

References

Bureau of Geology and Mineral Resources of Provinces (1984–1993) Regional Geology of Provinces. Geological Publishing House, Beijing (in Chinese with English abstract).

Cheng YQ (1994) An Introduction to Regional Geology of China. Geological Publishing House, Beijing (in Chinese with English abstract).

Chi JS (1988) The Stuby of Cenozoic Basalts and Upper Mantle Beneath Eastern China (Attachment Kimberlites). China University of Geosciences Press, Wuhan.

Condie KC (2001) Mantle Plumes and Their Record in Earth History. Cambridge University Press, Cambridge.

Ding WJ (1929) Orogenic movements of China. Journal of Geological Society of China 8(2): 151–170.

Du YS. Liu JH, Qin XL et al (2003) Resrarch on the Magmatic underplating. Progress on Nature Science 13(3): 237–242.

Du YS, Che QJ, Qin XL et al (2003) A review of progresses in research of xenoliths in granitoids Bulletin of Mineralogy Petrology & Geochemistry 22(4): 334–339.

Enkin RJ, Yang ZY, Chen Y et al (1992) Paleomagnetic constrains on the geodynamic history of the major blocks of China from the Permian to the present. J. Geophys. Res. 97: 13953–13989.

Enkin RJ, Courtilot V, Letoup P et al (1992) The Upper Permian record of Uppermost Permian, Lower Triassic rocks from the South China block. Geophys. Res. Lett. 19: 2147–2150.

Fang DJ, Guo YB, Wang ZL et al (1988) Tectonic significance of paleomagnetic study on the Triassic and Jurassic systems in Ningwu basin, Shanxi. Chinese Science Bulletin 33(24): 2057–2059.

Feng YM (1998) Allochthones along the west section of the north Qilian orogenic belt. Geological Review 44(4): 365–371 (in Chinese with English abstract).

Gu ZW (1982) Mesozoic unmarine branchiopoda, stratigraphic distribution and development in China. Science in China B 4: 438–452 (in Chinese).

HaoYC et al (1986) Cretaceous System in China. Geological Publishing House, Beijing (in Chinese).

Huang TK (Jiqing) (1945) On the major structural forms of China. Geological Memoirs, ser. A, no. 20, p.165.

Huang JQ, Zhang ZK, Zhang ZM et al (1965) Eugeosynclines and miogeosynclines of China and their development of multi-gyration. In: Professional papers of Chinese Academy of Geological Sciences, Section C: Regional Geology and Structure Geology, no.1. China Industry Press, Beijing (in Chinese).

Huang KN, Opdyke ND (1993) Paleomagnetic results from Cretaceous and Jurassic rocks of South and Southwest Yunnan: evidence for large clockwise rotations in the Indochina and Shan-Thai-Malay terranes. Earth Planet. Sci. Lett. 117: 507–524.

Huang BC, Zhu RX, Yang ZY (1999) Study of Paleozoic kinematics features of the North China block. Geoscience 13(suppl.): 1–7 (in Chinese with English abstract).

Kim KH, Van der Voo R (1990) Jurassic and Triassic paleomagnetism of South Korea. Tectonics 9(4): 699–717.

Kojima S (1989) Mesozoic terrane accretion in Northeast China, Sikhote-Alin and Japan regions. Palaeogeo-graphy, Palaeoclimatology, Palaeoecology 69: 213–232.

Li PX, Pang QQ, Cheng ZW (2000) The continental Jurassic-Cretaceous boundary and critical stage in northern China. In: Proceedings of the Third National Stratigraphical Conferences of China. Geological Publishing House, Beijing (in Chinese).

Li SG (Lee JS) (1929) Some characteristic structural types in Eastern Asia and their bearing upon the problem of continental movement. Geological Magazine 96(782): 358–375; 96(784): 457–473;

96(785): 501–526. Reprinted in 1976, Geological Mechanics Methods, pp.65–112. Science Press, Beijing (in Chinese).
Li SG (1962) An Introduction to Geomechanics. Geological Publishing House, Beijing (in Chinese).
Li SG (1976) Orogenic history and structural contours of China. In: Geological Mechanics Methods. pp.215–228. Science Press, Beijing (in Chinese)(Originally published in "Contribution to the 7th Pacific Science Conference in New Zealand. vol. 2, pp. 26–44." in 1949).
Li WX, Zhou XM (1999) Late Mesozoic subduction zone of southeastern China. Geological Journal of China Universities 5(2): 164–169.
Liang QZ (1990) Paleo-magnetic research on petrological phase paleogeography and sedimentation. Unpublished report of Institute of Scientific Research, Geological Bureau of Yunnan (in Chinese).
Liu BP, Chen F (1995) Mid-Jurassic bio-climate events and their dynamic significance of the spheres of the Earth. In: Annual Report of the Laboratory of Lithosphere Tectonics and Its Dynamics (MGMR), 1994. Seismological Press, Beijing.
Lu FX, Wang CY, Zheng JP et al (2004) Lithospheric composition and structure beneath the northern margin of the Qinling orogenic belt–On deep-seated xenoliths in Mingguang region of Henan province. Science in China D 47(1): 13–22.
Ma XH, Yang ZY (1993) The collision and suturing of the three major blocks in China and the reconstruction of the Paleo-Eurasian continent. Acta Geophysica Sinica 36(4): 476–488 (in Chinese with English abstract).
Maruyama S, Seno T (1986) Orogeny and relative plate motions: example of the Japanese Islands. Tectonophysics 127: 305–329.
Maruyama S, Isozaki Y, Kimura G et al (1997) Paleogeographic map of the Japanese Islands: Plate tectonic synthesis from 750 Ma to the present. The Island Arc 6: 121–142.
Mizutani S, Kojima S, Shao JA et al (1986) Mesozoic radiolarians from the Nadanhada area, Northeast China. Proc. Japan Acad. 62(B): 337–340.
Moore GW (1989) Mesozoic and Cenozoic paleogeographic development of the Pacific region. Abstracts of 28th International Geological Congress, 2: 455–456. Washington DC, USA.
Pang QQ, Li PX, Tian SG et al (2002) Discovery of ostracods in the Dabeigou and Dadianzi formations at Zhangjiagou, Luanping county, northern Hebei Province of China and new progress in the biostratigraphic boundary study. Geological Bulletin of China 21(6): 329–338 (in Chinese with English abstract).
Pavoni N (1997) Geotectonic bipolarity: evidence of bicellular convection in the Earth's mantle. S. Afr. J. Geol. 100(4): 291–299
Shao JA, Wang CY, Tang KD (1992) A new approach to the tectonics in the Ussuri (Wusuli) region. Geological Review 3(1): 33–39 (in Chinese with English abstract).
Shao JA Tang KD et al (1995) Terranes in Northeast China and Evolution of Northeast Asia Continental Margin. Seismological Press, Beijing (in Chinese).
Wan TF (1981) Research on the structural features and mechanism of Nandazhai-Babaoshan fault zone, the Western Mountains, Beijing. Collection of Structural Geology (1): 152–164 (in Chinese with English abstract).
Wan TF, Zhu H (1989). Cretaceous-Early Eocene tectonic stress field in China. Acta Geologica Sinica 2(3): 227–239.
Wan TF (1994) Intraplate Deformation, Tectonic Stress and Their Application for Eastern China in Meso-Cenozoic. China University of Geosciences Press, Wuhan.
Wan TF (2004) Rotation of Jurassic crust and transformation of the Lithosphere in eastern China. Geological Bulletin of China 23(9–10): 966–672.
Wan TF, Teyssier C, Zeng HL et al (2001) Emplacement mechanism of Linglong granitoid complex, Shandong Peninsula, China. Science in China D 44(6): 535–544.
Wan TF, Wang YM, Liu JL (2008) Detachment and magmatic source depth in lithosphere of Eastern China during Yanshanian and Sichuanian stages. Earth Science Frontiers 15(3): 1-35.

Wang TH (1995) Evolutionary characteristics of geological structure and oil-gas accumulation in Shanxi-Shaanxi area. Jour. Geol. & Min. Res. North China 10(3): 283–398 (in Chinese with English abstract).

Weng WH (1927) Crustal movements and volcanic activities of east China since Mesozoic. Journal of Geological Society of China 6(1): 9–36.

Weng WH (1929) Mesozoic orogenic movement of east China. Journal of Geological Society of China 8(1): 33–44.

Xue AM, Jin WJ, Yuan XC (1999) Tectonic evolution of Hefei basin, northern Dabie Mountains in the Mesozoic and the Cenozoic. Geological Journal of China Universities, 5(2): 157–163 (in Chinese with English abstract).

Zhan MG (1994) Research on Tectono-Magmatism-Mineralization and Regional Metallogenic Principles for the Mesozoic of South China. Dissertation, Yichang Institute of Geology and Mineral Resources.

Zhang CH, Song HL, Wang GH et al (2001) Mesozoic dextral strike-slip structural system in middle segment of intraplate Yanshan orogenic belt, Northern China. Earth Science 26(5): 464–472 (in Chinese with English abstract).

Zhao CJ, Peng YJ, Dang ZX et al (1996) Structure Framework of East Part of Both Jilin and Heilongjiang Provinces and Their Crustal Evolution. Liaoning University Press, Shenyang (in Chinese).

Zhao ZP (1995) An intracontinental-type orogeny–evidence from Qinling–Dabie orogenic belt, China. Scientia Geologica Sinica 30(1): 19–28 (in Chinese with English abstract).

Zheng YD, Wang SZ, Wang YF (1990) New discovery macro-thrust and extension metamorphic core complex, at the boundary area between China and Mongolia. Science in China (12): 1300–1305 (in Chinese).

Zheng YD, Wang SZ, Wang YF (1991) An enormous thrust nappe and extensional metamorphic core complex newly discovered in Sino-Mongolian boundary area. Science in China B 34(9): 1145–1152.

Zheng YD, Zhang Q (1993) The Yagan metamorphic core complex and extensional detachment fault in Inner Mongolia. Acta Geologica Sinica 67(4): 301–309.

Zhou XM, Li WX (2000) Origin of Late Mesozoic igneous rocks in southeastern China: implications for lithosphere subduction and underplating of mafic magmas. Tectonophysics 326(3–4):269–287 (in Chinese with English abstract).

Zhu ZW, Hao TY, Zhao HS (1988) Paleomagnetism and its implication of Pan–Xi region in Mesozoic. In: Zhang YX, Yuan XC (eds) Collection of Pan–Xi Rift, China, (3): 199–211. Geological Publishing House, Beijing (in Chinese with English abstract).

Chapter 8
Tectonics of Middle Epoch of Early Cretaceous–Paleocene (The Sichuanian Tectonic Period, 135–56 Ma)

—formation of the Sichuanian Tectonic System
—development of the basin and range tectonics in eastern China
—clockwise rotation of the principal stress orientation
—formation of the Banggongco-Nujiang Collision Zone

The Sichuanian movement or tectonic event was first identified by Tan XC and Li CY (1948), while conducting geological survey in the Xikang area, western Sichuan Province. They recognized the distinctive tectonic characteristics of this period, and appreciated that they were different from the Yanshanian and Himalayan Periods. They considered that the main tectonic event occurred in the Late Cretaceous or at the end of the Cretaceous, because in the middle of last century the stratigraphy was not very well established.

Many subsequent researchers came to the same conclusion, supposing that there was a continuous tectonic evolution from the Jurassic to the Cretaceous, and regarding the NNE trending structures relating to compression in the Jurassic, and those relating to extension in the Cretaceous as part of a single tectonic cycle (Huang JQ, 1945; Huang JQ, 1960; Zhao ZP, 1959). In the last 50 years, it has been established by regional geological survey and detailed study that the contacts between the Cretaceous and Paleocene are conformable in most areas of China, with no evidence of any tectonic event. Concerning the Sichuanian Tectonic Event represented by a small angular extensional unconformity, according to the older stratigraphic divisions, between the Kongdian and Shahejie formations, or between the Shasi and Shasan members of Shahejie formation in northern China (2, 3, 5 in Fig. 8.1), recently, most researchers recognized that it occurred mainly at the end of the Paleocene. These angular unconformities were first noticed by Tang Z (1979), who appreciated that these tectonic events were not related to Himalayan tectonism, but related to the first epoch of the "North Sinian" movements. However, as shown in Chapter 7, Wan TF and Zhu H (1989) suggested that in accordance with the principle of priority, the term "Sichuanian Tectonic Event" or "Sichuanian Tectonic Period" should be used for tectonic events which occurred mainly during the Cretaceous and Paleocene. The China National Commission on Stratigraphy (2001) has defined the Sichuanian Tectonic Period as commencing in the middle period of the Early Cretaceous and continuing to the end of the Paleocene, i.e. between 135 Ma and 56 Ma from recent isotopic data.

Events of the Sichuanian Period occurred over most of China during the Cretaceous-Paleocene. The deposits are mainly red clastic sediments of alluvial fan and fluvial-lacustrine facies, with some volcanic rocks. They represent deposition in hot continental and arid environments in which gypsum and halite were formed. Relict marine deposits occur in the southwestern part of the Tarim Basin and in southern Xizang (Tibet). In Northeast China, Inner Mongolia and northern Xinjiang, there are massive accumulations of organic material, formed in warm, humid climatic conditions. There was very little tectonic activity in northwest China during the Sichuanian Period, the Jurassic, Cretaceous and Paleogene se-

dimentary systems are largely conformable, with weak deformation and break in deposition occurring only near fault zones.

8.1 Intraplate Deformation and the Stress Field

Deformation in the Sichuanian Period consisted of open folds on WNW trending axes, WNW trending overthrusts, NNE trending normal faults and NE or NW trending strike-slip faults, formed under the influence of a tectonic stress field comprising the Sichuanian Tectonic System.

In the Sichuanian Period, open folds formed on WNW trending axes are widespread. The broad, gently undulating strata appear to have been irregularly deformed, but the trend of fold axes within basins is relatively constant, and only on the margins can strata dip towards the center of the basins. Thousands of folds with curvilinear axes on a macro-to meso-scale have been identified during regional geological and petroleum geology surveys (Appendix 3.6). Dips of fold limbs are mainly at low or intermediate angles (1°–30°) (1, 2, 3, 5, 8 in Fig. 8.1; Fig. 8.2). Axial traces of folds range in length from several to hundreds of kilometers, and most fold axial planes are almost vertical, especially in the southern Sichuan Basin (6 in Fig. 8.1) which is a reason why the tectonic system is called the Sichuanian. On the Qinghai-Xizang Plateau in the vicinity of the Banggongco–Nujiang Collision Belt, the folds are close, and the axial traces of the folds are either parallel to the trend of the collision belt, or intersecting it at low angles. In the middle and western Yunnan and Hengduan Mountains (25°–32°N, 99°–103°E) the folds are very close and fold limbs dip at intermediate to high angles (30°–70°). In that area the trending of fold traces trends NNW-SSE, influenced by strong later tectonism. In most of Southern and Northern China, fold limbs dip at intermediate to low angles, but in NE China, fold limbs dip only at low angles (<5°). Evidently tectonic stresses in the Sichuanian Period were stronger in SW China than in NE China.

Table 8.1 Shortening ratio, shortening magnitude, folding deformation time and linear strain rate in the Sichuanian Period

Area	Helanshan–East Yunnan	Hingganling–West Guangdong	Laoyeling–Coast of Fujian
Longitude	105°E	110°–120°E	120°–135°E
Statistical length (km)	2,130	3,600	3,100
Mean limb angle of folds	20.6°	27.7°	20.4°
(amount of data)	(490)	(768)	(313)
Shortening ratio (%)	6.39	11.46	6.27
Shortening magnitude (km)	136	413	194
Rate of shortening (cm/yr)	5.1	5.0	5.2
Folding deformation time (Myr)	2.7	8.2	3.7
Linear strain rate (ε, 1/s)	7.5×10^{-16}	4.4×10^{-16}	5.4×10^{-16}

Using the fold data and the rate of plate shortening, the shortening ratio, the shortening magnitude, the folding deformation time and the linear strain rate during the Sichuanian Period have all been estimated (Table 8.1). Because the trend of the fold axes formed during the Sichuanian Period is mainly E-W, the amount of shortening was calculated in an N-S direction. Therefore, the following three sections, Helanshan–East Yunnan (105°E), Hingganling–west Guangdong (110°–120°E) and Laoyeling–Coast of Fujian (120°–135°E), were chosen, and regional shortening ratios were estimated separately. The shortening ratio in the Hingganling–west Guangdong section was the greatest (11.46%); the shortening ratio in Helanshan–East Yunnan and Laoyeling–Coastal Fujian sections is only half that amount (6.27%–6.39%). It demonstrates that in the Sichuanian Period the shortening ratio in every area was significantly lower than during the Indosinian and Yanshanian Periods. In the Sichuanian Period the length of time over which intraplate deformation and folding took place was between 2.7 and 8.2 million years,

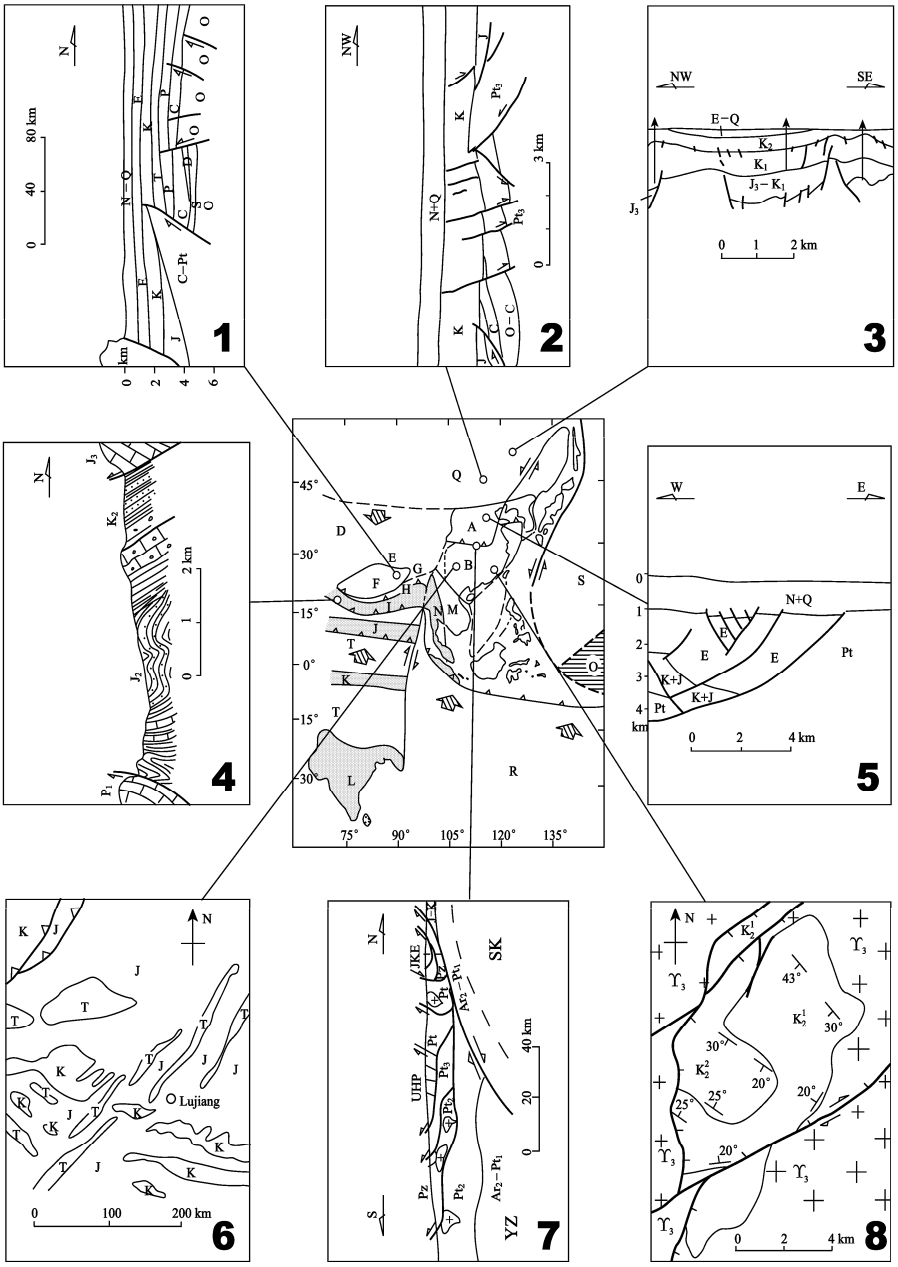

Fig. 8.1 Deformation in the Sichuanian Period.

1. Sketch of a seismic profile from the east Tarim Oilfield (Xinjiang), faults penetrate all the systems below the Pale-

ogene (unpublished data of Xinjiang Petroleum Bureau); 2. Seismic profile from Bayanhot (Inner Mongolia), with two angular unconformities, reverse faults occur below the Cretaceous System, and normal faults penetrate the Cretaceous and the older systems (Wang TH, 1995); 3. Sketch of the Song 1 seismic profile in the Songliao Basin, Jurassic and Cretaceous systems form a continuous sedimentary succession (unpublished data of Exploration and Development Institute of the Daqing Oil Field); 4. Geological profile from Domar, northern Rutog, Tibet, the contact of Jurassic and Cretaceous systems are either disconformable or faulted (Guo TY et al. 1991); 5. Geological profile near Ningjin, central Hebei, North China. The Jurassic and Cretaceous systems are not distinguished as sedimentation was continuous (unpublished data from Zhongyuan Oilfield); 6. WNW trending folds of the Sichuanian Period are superposed on NE trending folds of the North Sinian Period at southern Luzhou, Sichuan (Chinese Academy of Geological Sciences, 1973); 7. Sketch of a telluric electromagnetic sounding profile (MT) in the Dabie Mountains, UHP = ultrahigh pressure metamorphic zone; thrusts were formed after the Cretaceous (Zhang GW et al. 2001); 8. The Shuiqian Basin, west of Fujian, a fault depression basin controlled by normal faults extends to both north and south, the axis of folding of the Cretaceous in the basin trends WNW.

3%–10% of the length of time of the whole Sichuanian Tectonic Period. The linear strain rate was between 7.5×10^{-16}/s and 4.4×10^{-16}/s, indicating that the deformation process was rheological (Table 8.1).

Data from 2,008 folds (1,032 anticlines and 976 synclines) taken from the regional geological surveys, and data from 281 joint observation points, measured by the author and his colleagues were divided into 50 areas and analyzed statistically (Appendix 3.6). In the present coordinates the preferred attitude of the maximum principal compressive stress axis (σ_1) during the Sichuanian Period in the China was NE24°∠3°, that of the intermediate principal compressive stress axis (i.e. trend of fold axis, σ_2) was NW296°∠3° and that of the minimum principal compressive stress axis (σ_3) was SW203°∠80°, being nearly vertical (Figs. 8.2 and 8.3). The result of the applied tectonic stress field in China continent during the Sichuanian Period was mainly NNE-SSW shortening and ESE-WNW extension.

Data from 176 calculations of the magnitude of tectonic stress during the Sichuanian Period, tested by the author and his colleagues, were collected from 19 areas (N.B. the area of collection, rock types tested, minerals tested, number of samples and the average value of differential stress are shown in Appendix 4 (Fig. 8.4)). The amount of tectonic stress calculated experimentally for the Sichuanian Period is greater than for any of the periods tested. The average value of differential stress was calculated as 107.4 MPa. The variation in the value of differential stress from one area to another is gradational. Differential stress was stronger in the southwest and weaker in the northeast, reaching 183.5 MPa in the Ngari–Yarlung Zangbo area of Tibet, and was about 145 MPa in the Qinling–Dabie area. In northern and northeastern China, differential stress values are about 90–100 MPa, exceeding 100 MPa only near fault zones, such as the Tancheng–Lujiang Fault Zone (Appendix 4).

The calculated values of differential stress decrease from southwest to northeast, showing that tectonic stress during the Sichuanian Period originated in the southwest, presumably due to the rapid northeastward migration of the Indian Plate and the subduction of the Tethys Ocean. When plotted on tectonic reconstructions (Figs. 8.4 and 8.7), the value of differential stress decreases over a distance of ~5,000 km from 183.5 MPa in the Ngari area, to only 90 MPa in the northeastern China (Wan TF et al., 2002). The value of tectonic stress decreased gradually at a rate of ~1.8 MPa per 100 km, when the stress was transmitted through a continental crust.

Reverse faults or overthrusts with the same WNW-ESE trend as the folds cut the folds and penetrate the Paleocene, Cretaceous and the underlying systems. Earlier WNW-trending normal faults have been converted into reverse faults or thrusts. The most important fault zones in China are the fan-type thrust zone, marginal to the Qinling–Dabie Tectonic Belt (7 in Fig. 8.1) (Zhang GW et al., 2001), on the southern side of the Wudangshan–southern frontal Dabieshan overthrust, south of the Dabashan–Fangxian–Guangji overthrust (18 in Fig. 8.2) (Cai XL, 1995), and the north frontal Qinling overthrust (Wushan–Baoji–Luonan–Fangcheng Thrust Zone) (20 in Fig. 8.2); the Shangdan-Tongbai overthrust zone (19 in Fig. 8.2); the Zhucheng–Rongcheng Thrust Zone (21 in Fig. 8.2) (Zhang GW ei al., 2001).

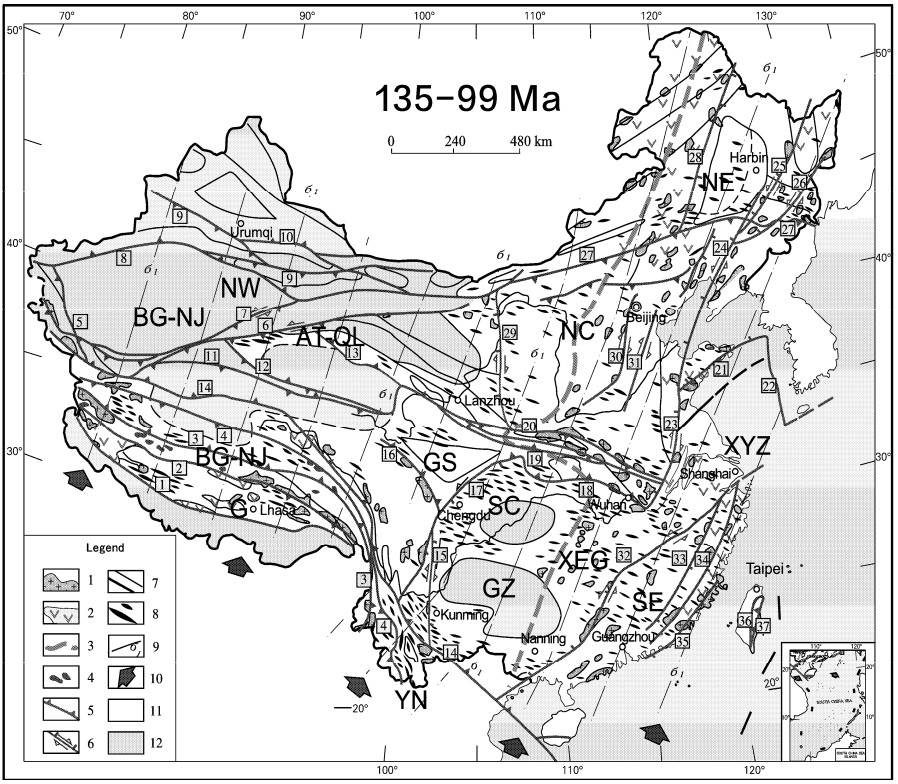

Fig. 8.2 Tectonic sketch of the Chinese continent in the Late Sichuanian Period (135–99 Ma).

1. Granite of the Sichuanian Period; 2. Volcanic of the Sichuanian Period; 3. Rate of intraplate deformation, estimated from the chemical composition of magmatic rocks, "-" is rate of extension, others are rates of shortening (unit: cm/yr) (data in Appendix 5.7); 4. Ophiolite and ultramafic rocks of the Sichuanian Period; 5. Numbered collision zones or thrust belts; 6. Numbered normal and strike-slip faults; 7. Block boundaries or faults with weak activity, unnumbered; 8. Anticline fold axes (data in Appendix 3.6); 9. Trace of maximum principal compressive stress (σ_1); 10. Direction of plate movement; 11. Areas with angular unconformity; 12. Areas with conformity or disconformity.

The names of numbered plate boundaries, collision belts and fault zones: [1] Yalungzangbo Suture Zone, with oceanic crust; [2] Gerze–Nyainqentanglha reverse fault; [3] Banggongco–Nujiang Collision Belt; [4] Shuanghu–Lancangjiang reverse fault; [5] Kangxiwa–southernmost Tarim strike-slip and reverse fault zone; [6] Altun sinistral strike-slip fault zone; [7] Ruoqiang–Dunhuang reverse and sinistral strike-slip fault; [8] Korla–Wuqia overthrust zone; [9] Nilek–Yilinhabirga reverse fault zone; [10] Bogda reverse fault; [11] East Kunlun reverse fault or central Kunlun fault; [12] Northern Kunlun (southmost Qaidam zone) reverse fault; [13] Junulshan–southernmost Qinghai Lake (northernmost Qaidam) reverse fault zone; [14] Jinshajiang–Honghe dextral strike-slip and reverse fault zone; [15] Anninghe dextral strike-slip and reverse fault zone; [16] Daofu–Kangding dextral strike-slip and reverse fault zone; [17] Longmenshan sinistral strike-slip and normal fault zone; [18] Southern Dabashan–Fangxian–Guangji overthrust zone; [19] Shangdan–Tongbai overthrust zone; [20] Wushan–Baoji–Luonan–Fangcheng reverse fault zone; [21] Zhucheng–Rongcheng reverse fault zone; [22] East marginal Huanghai (Yellow Sea) dextral strike-slip fault zone; [23] Southern section of Tancheng-Lujiang dextral strike-slip and normal fault zone; [24] Middle section (Liaohe–Siping) of Tancheng–Lujiang sinistral strike-slip and normal fault zone; [25] Yilan–Yitong sinistral strike-slip and normal fault zone; [26] Dunhua–Mishan sinistral strike-slip fault zone; [27] Xarmoronhe reverse fault zone; [28] Eastern frontal Dahingganling dextral strike-slip and normal fault zone; [29] Liupanshan–Helanshan dextral strike-slip and normal fault zone; [30] Eastern frontal Taihangshan dextral strike-slip and normal fault zone; [31] Eastern Cangzhou dextral strike-slip and normal fault zone; [32] Shiwandashan–Shaoxing sinistral strike-slip and normal fault; [33] Chong'an–Heyuan normal fault; [34] Lishui–Lianhuashan normal fault; [35] Changle–Nan'ao normal fault; [36] Shoufeng Fault; [37] Yuli sinistral strike-slip fault zone.

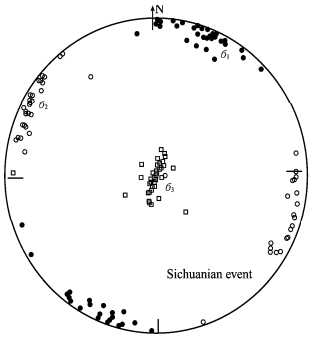

Fig. 8.3 Stereogram of the attitude of the principal stress axes in the Sichuanian Period. σ_1. maximum principal stress axis; σ_2. intermediate principal stress axis; σ_3. minimum principal stress axis.

Many E-W and WNW-trending fault zones in western China were re-activated during the Sichuanian Period, with reverse faults developed along existing fracture surfaces, such as the Gerze-Nyainqentanglha reverse fault (2 in Fig. 8.2), the Kongkela–Shuanghu–Lancang-jiang Thrust (4 in Fig. 8.2), Kangxiwa–south marginal Tarim Thrust Zone with strike-slip (5 in Fig. 8.2), the Ruoqiang–Dunhuang reverse fault (7 in Fig. 8.2), the Korla–Wuqia overthrust zone (8 in Fig. 8.2), the Nilek-Yilinhabirga reverse fault zone (9 in Fig. 8.2), the Bogda Thrust (10 in Fig. 8.2), the East Kunlun or Central Kunlun Thrust (11 in Fig. 8.2), the North Kunlun Thrust in southern marginal Qaidam (12 in Fig. 8.2) and the Qinghainanshan–Junulshan Thrust Zone on the northern margin of Qaidam (13 in Fig. 8.2).

In the Sichuanian Period, existing NE-trending faults moved as strike-slip or normal faults, because they intersected the regional maximum principal compressive stress at a low angle, such as Altun sinistral strike-slip fault zone (Ge XH et al., 2001) (6 in Fig. 8.2) and Longmenshan sinistral strike-slip and normal fault zone (17 in Fig. 8.2). However, NW-trending faults are dextral strike-slip and reverse faults, such as Anninghe dextral strike-slip and reverse fault zone (15 in Fig. 8.2), the Daofu-Kangding dextral strike-slip and reverse fault zone (16 in Fig. 8.2) and the Jinshajiang-Honghe dextral strike-slip and reverse fault zone (14 in Fig. 8.2).

A series of NNE-trending faults in eastern China were formed as thrust or reverse faults during the Yanshanian Period, but under NNE shortening and WNW extension during the Sichuanian Period were converted into normal faults, with some strike-slip. Some researchers have argued that this reactivation was due to elastic rebound following compression. This is a basic misunderstanding of a mechanical concept applied to geology. the term of elastic rebound after compression is very short, for example, it occurs during the transmission of a seismic wave, when the rock returns to its original state after the wave has passed. Deformation in rocks is plastic deformation, where after the removal of the deforming forces the rock is permanently deformed. The climaxes of deformation events in the Yanshanian and Sichuanian tectonic Periods are separated by tens of millions of years; it is impossible for elastic deformation to be preserved over such a long period of time.

The main NNE-trending normal faults in the eastern Chinese continent are: the southern section of the Tancheng–Lujiang normal fault zone, with dextral strike-slip (23 in Fig. 8.2); the middle section of the Tancheng–Lujiang (Liaohe–Siping) normal fault zone, with sinistral strike-slip (24 in Fig. 8.2); the Yilan–Yitong normal fault zone, with sinistral strike-slip (25 in Fig. 8.2); the Dunhua–Mishan sinistral strike-slip fault zone (26 in Fig. 8.2); the Dahingganling east marginal normal fault zone, with dextral strike-slip (28 in Fig. 8.2); the Liupanshan-Helanshan normal fault zone, with dextral strike-slip (29 in Fig. 8.2); the Taihangshan east marginal normal fault zone, with dextral strike-slip (30 in Fig. 8.2); the Cangdong normal fault zone, with dextral strike-slip (31 in Fig. 8.2); the Shiwandashan-Shaoxing normal fault with sinistral strike-slip (32 in Fig. 8.2); the Chong'an-Heyuan normal fault (33 in Fig. 8.2); the Lianhuashan-Lishui normal fault (34 in Fig. 8.2); the Changle-Nanao normal fault (35 in Fig. 8.2); the Shoufeng Fault (36 in Fig. 8.2) in Taiwan. When they were oriented almost parallel to the regional axis of maximum principal compressive stress these fault zones operated as normal faults and as normal

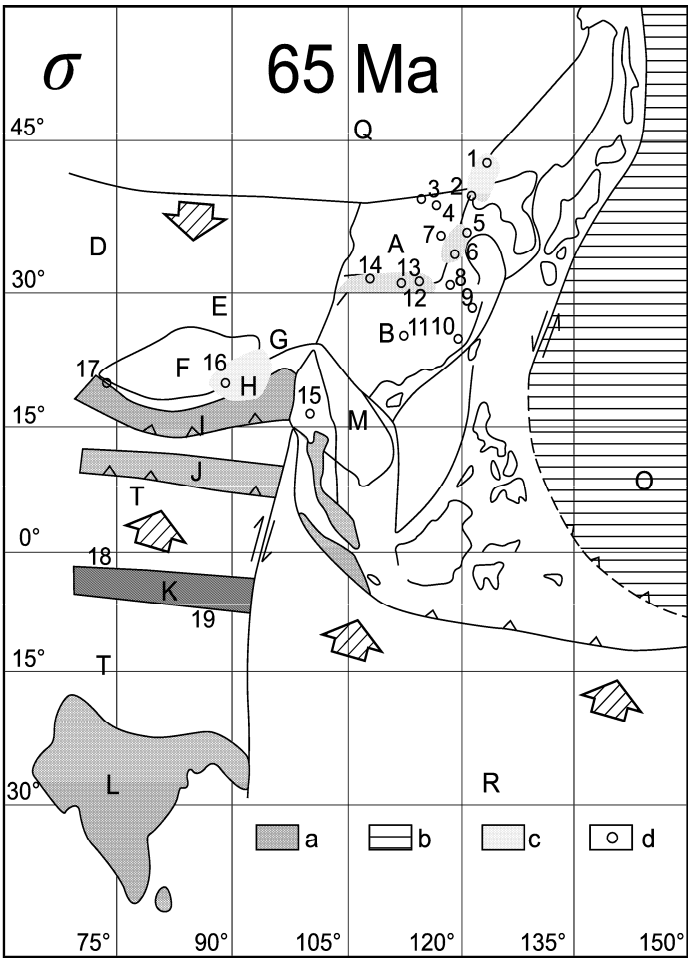

Fig. 8.4 Values of differential stress during the Sichuanian Period (data showed in Appendix 4).

a. Gondwanan continental blocks before the Indosinian Period; b. Pacific Plate; c. Areas with values of differential stress >100 MPa; d. Locations where differential stress values were measured. Areas with values of differential stress <100 MPa, or without measured data are left white. Index letters of blocks are the same as in Fig. 6.5; the data are given in Appendix 4.

Locations of collected samples: 1. Daheishan, Jilin; 2. Fuxin, Liaoning; 3. North Hebei; 4. Nandazai, western Beijing; 5. East Shandong; 6. Tancheng–Lujiang Fault Zone; 7. West Shandong; 8. Middle and lower Yangtze area; 9. Linhai, Zhejiang; 10. Fujian; 11. Xikuangshan, Hunan; 12. Tongbaishan; 13. Xuong'ershan; 14. Mangling, Qinling; 15. West Yunnan; 16. Altun; 17. Western Kunlun; 18. Ngari–Yalung Zangbo; 19. Southeastern Tibet.

faults with strike-slip, when they intersected the trace of the maximum principal compressive stress at a small angle (Wan TF et al., 1981, 1989, 1992, 1995, 1996; Lin JP et al., 1990, 1994; Liu MQ et al., 1993; Tao KY et al., 1998).

The present-day landscape of eastern China was originally formed during the Sichuanian Tectonic Period, that is, formation of a basin-and-range structure by E-W extension along NNE-trending listric and

detachment boundary faults. Basins formed during the Cretaceous have remained sedimentary basins until the present day. Cretaceous sediments were the first to be deposited in most of the sedimentary basins in eastern China. Sedimentary basins were formed in areas where the crystalline basement contained many high density mafic and basic rocks relatively depressed under the influence of gravity. Most of these sedimentary basins are half grabens, bounded by normal faults on one side, but were controlled by step faults near surface. Areas affected by tectonic activity since the Paleozoic, and including lower density granitoid intrusions were relatively uplifted to form horst mountain blocks (Xu SD et al., 2001). Some researchers have regarded the period in which the basins were formed as the period of rift development. The period of rifting was relatively short-lived so that the basin-and-range does not have the characteristics of rift system; it is more appropriate to refer to the basins as extensional or fault-depression basins.

The formation of large fault-depression basins in eastern China was controlled by E-W extension and SSW-NNE shortening: e.g. Songliao (Songhuajiang–Liaohe) (centered on 125°E, 46°N); Sanjiang (Heilongjiang–Songhuajiang–Wusulijiang) (centered on 133°E, 47°N); Hailar–Erenhot (centered on 119°E, 49°N), Hegang in Heilongjiang Province; Yanji (centered on 129°E, 43°N), Bohai Bay including central Hebei, Huanghua and Liaodong Bay–lower region of Liaohe; Jiaozhou–Laizhou (centered on 119.4°E, 36.2°N); north Jiangsu-southern Yellow Sea (centered on 121°E, 32.5°N); Jianghan–Dongting(centered on 122.5°E, 30°N), Sanshui in Guangdong (centered on 113°E, 23°N); Dunhuang–Jiuquan–Minle (centered on 95°–101°E, 38°–40°N); Tarim; Qaidam; Junggar. In addition, there are thousands of medium to small sedimentary basins in South China in which red beds were deposited. Larger basins are equivalent in area to a city and its suburbs, medium-sized basins are equivalent to a town and its suburbs, while smaller basins are equivalent to a village. The basins are surrounded by lower mountains or hills.

Large fault-depression basins developed in northern and northeastern China, but medium-sized or small fault-depression basins developed in South China. In the crystalline basement of North China, the weakness zones are separately and widely spaced (300–400 km), while in South China the crystalline basement is more highly fragmented by a large number of NE-trending faults in the upper crust, formed during Yanshanian Period. Distances between faults here range from several kilometers to hundreds of kilometers, controlling the formation of a large number of small or medium-sized basins.

Recently, amounts and rates of E-W extension have been estimated for many basins formed in East China during the Sichuanian Period. Zhang JS et al. (2002) investigated detachment faults along the front of Taihang Mountains. They found that the surface of detachment extended over a distance of 70 km, with a maximum amount of displacement of 17 km; the width of North China basin increased in an E-W direction by 24%. This detachment occurred before 68 Ma, at the end of the Cretaceous.

Chen QH et al. (1998) investigated the effects of deformation during the Sichuanian Tectonic Period in the eastern part of South China. They found that NNE trending extension faults were concentrated in nine belts in this region: (1) Southeastern Coastal Fault Zone; (2) Shaowu-Heyuan (Sm-Nd ages of 119-106 Ma were obtained from fault rocks), the amount of extensive movement on the Huichang Fault was 1.36 km, with an extension of 19.4 %; (3) from Nancheng (Jiangxi) to Shanshui (Guangdong) (Rb-Sr and Sm-Nd ages between 102 and 94 Ma were obtained from an NE-trending basic dike swarm at Nanxiong), the amount of extension on NNE-trending listric faults was about 4 km, with an extension of 24%); (4) Jiangshan-Ji'an of Jiangxi Province (a basic vein in Qianshan gave isotopic ages of 131–102 Ma, and the age of uranium mineralization was 120–75 Ma), the amount of extension on NE trending faults was 2.8–3.48 km, with an extension of 19%–16.4%; (5) from Pingxiang of Jiangxi-Chenzhou of Hunan to Maoming of Guangdong; (6) Changsha-Hengyang of Hunan (fault rocks gave K-Ar ages of 121–85 Ma), the amount of extension on the fault was ~5.8 km; (7) the Yueyang–Shaoyang Fault, the amount of extension of faults on the margins of the Zhiyuan Basin of Guangxi is between 2.8 and 3.48 km, with an extension of 36%; (8) Changde -Huaihua; (9) Wuzhou-Yulin of Guangxi fault zones. The formation of these belts was controlled by regional NW-SE extension and NE-SW shortening, by means of utilizing existing fractures, and developing detachments and sometimes exposing metamorphic core

complexes. In addition, the extension faults controlled the emplacement of deposits of uranium and other important metal ore deposits.

High mountains, uplands and basins formed in eastern China during the Sichuanian Period changed the geological environment greatly compared with the preceding Yanshanian Tectonic Period, providing sites for the accumulation of hydrocarbons and mineral resources. The largest accumulation of petroleum resources found during the last half century is the Daqing Oil field in the Songhuajiang–Nenjiang Basin, NE China. This hydrocarbon-bearing system was formed in the Early Cretaceous with warm and moist climate. Because the climate was hot and dry during the later Cretaceous, gypsum and halite deposits were formed in red-bed basins in many parts of middle and south China, such as the Zigong Basin in the Sichuan, Hubei and Jiangxi provinces.

NNE trending detachment faults, formed on the margins of many basins during the Sichuanian Period, controlled the formation of hydrothermal deposits, such as the Shuikoushan lead-zinc deposit in Hunan, the Wubu lead-zinc deposit in Zhejiang, the Dalingkou native silver deposit and many hydrothermal uranium ore deposits. Cretaceous red-bed basins, large or small, are the main sites of residential and agricultural development in southern China at the present day.

In western China, from western Hunan to the west of the Taihangshan–Wulingshan, the Jurassic, Cretaceous and Paleogene systems were deposited conformably. Deformation of the rocks, with the development of unconformities, occurred only in the vicinity of fault zones. During the Sichuanian Tectonic Period, most of western China was a region of relative tectonic stability, with the deposition of sediments in rivers and lakes.

8.2 Tectono-magmatism

There was also strong magmatic activity in the Sichuanian Period (called the "Late Yanshanian Period" in reports of many Chinese regional geological surveys). However, the area of outcrop of magmatic rocks formed during Sichuanian Period covers only 43, 864 km^2, equal to 5% of the total outcrop area of magmatic rocks in China, and only one fifth of the outcrop area of the magmatic rocks formed in the Yanshanian Period (Cheng YQ, 1994). Outcrops of magmatic rocks of the Sichuanian Period arranged in linear patterns or as scattered intrusions, very different from the distribution of S-type granites in the Yanshanian Period. Although the magmatic rocks belong to the calc-alkaline series, with a high SiO_2 content (averaging 71.43%), a high alkali content (8.45 %) and lower total mafic content (3.15%), magmatic activity in the Sichuanian Period had its own individual character (Cheng YQ, 1994).

Magmatic rocks intruded during the Sichuanian Period in eastern China are distributed mainly along four NNE trending transtensional fault belts: the Hengduanshan, Dahingganling–Taihangshan, Tancheng–Lujiang Fault Zone and the coastal zone of southeast China (Lishui–Dapu–Lianhuashan and the Changle–Nanao zones). Of the 379 magmatic bodies of Sichuanian Period which have been studied and collected (Figs. 8.5 and 8.6; Appendix 7), the main granitic rocks are of A-type (236 bodies, 62.4% of total), where the original source magma formed at the intersection of NNE trending faults or ductile shear zones and the Mohorovĭcíc discontinuity (Fig. 8.5); less than one third of the intrusions are of S-type (113 bodies, 29.6% of total), with a source of the original magma in the crust (Fig. 8.6), often caused at the intersection of NNE trending faults and low velocity layer of middle crust, while only 30 basaltic dykes or ultrabasic xenoliths inclusions (8% of total) had a deep source at the base of the lithosphere (Fig. 8.5). The formation of original source magmas was usually located near the intersection between NNE trending extensional fault belts and Mohorovĭcíc discontinuity or in the middle crust; it is suggested that magmas originated from local detachment or fracturing parts at these levels.

During the Sichuanian Period (138–102 Ma) bimodal volcanic rocks were extruded along NNE trending fault zones, including the Lishui–Dapu–Lianhuashan normal fault zone and the eastern coastal fault zone of Zhejiang–Fujian–Guangdong. Acid rhyolites make up more than 50% of these volcanic rocks, while basalts make up less than 30% (Mao JR, 1994; Yu YW, 1993; Gao TJ et al., 1999 (Fig. 7.9). The

magma consisted of material of both crustal and mantle origin, including A-type granites with a Sr_i content of 0.7036–0.7090. Basaltic magma was highly contaminated by crustal material during intrusion. This suggests that the NNE-SSW trending faults controlling the magmatism were deeply penetrating transtensional faults within the continental crust tapping a magmatic source near the Mohorovĭcíc discontinuity.

A distinctive A-type alkali granite with a SiO_2 content of 76% and with a miarolitic structure, indicating that the magma was emplaced at shallow depth and had a high volatile gas content, was intruded during the middle and late epochs of the Sichuanian Period in the granitic zone of the southeastern coastal region of China. This granite originated from depth and has a Sr_i content of 0.706–0.708, including 70% of mantle material (Gao TJ et al., 1999). This granitic zone extends northeastwards to the Yeongnam area of South Korea and southwestwards to Hainan Island and the coastal area of eastern Vietnam. This type of rock is also found in the Laoshan of Qingdao (Shandong), Gangshan (Jilin) and Dahingganling zones. These types of granites originated from near the Mohorovĭcíc discontinuity by partial re-melting of A-or I-type granites under conditions of continental extension, facilitated by the addition of fluorine-rich fluids. They are F-rich, with W, Sn and B, and reach the upper part of the crust along deep penetrating faults.

In Qinghai-Xizang Plateau, Late Cretaceous (about 80–90 Ma) granites, adjacent to the Banggongco–Nujiang Collision Belt, were intruded. In the Altun Mountains, Xiaoqinling of western Henan, and the middle-lower Yangtze River areas, in addition to intermediate-acidic granitoids, there are many small and hypabyssal porphyries (phenocrysts usually alkali feldspar) or porphyrites (phenocrysts usually andesine and rich calcium plagioclase) intruded from 135 to 87 Ma, associated with metal ore deposits; porphyry copper deposits in the Yangtze area and W-Sn deposits in the Nanling area of southern China. These intrusions usually originated from the crust/mantle boundary and were intruded at fault intersections.

In Kunlun, Qinling–Dabie and middle–lower Yangtze River areas, the dominant strike direction of the basement structures is broadly E-W (usually ENE or WNW), however, during the Sichuanian Period, under the influence of the tectonic stress field, N-S trending transverse extension faults were formed. Intrusions are often localised at the intersection of E-W and N-S faults.

Dike swarms and veins with steep angles of dip intruded during the Sichuanian Period have been studied intensively over the past ten years and have been used to determine the orientation of the axes of principal tectonic stress and the distribution of the regional stress field. Wan TF et al. (2000) recorded >50 basic dykes, giving isotopic ages of 130–120 Ma, in the Linglong granitoid complex in Shandong, filling tension joints and fissures trending NE 20°. This means that the direction of extension was NW-SE at that time and the orientation of the maximum principal compressive stress was nearly NE 20°. At about 100 Ma, hundreds of gold-bearing quartz veins (such as in Linglong gold ore deposit) were formed in a conjugate shear joint system, indicating that the maximum principal compressive stress was orientated at ~NE 40° during that time. Between 120 Ma and 100 Ma the maximum principal compressive stress had rotated clockwise through 20°.

In the study of Qiyugou goldfield in Henan, Qi JZ (2001) found that in the Early Cretaceous (135–122 Ma) the orientation of the maximum principal compressive stress, indicated by a conjugate shear joint and vein system, was near N-S, in the mid-Cretaceous (122–107 Ma) the orientation of the maximum principal compressive stress, indicated by tension joints filled by quartz veins, was NE 40°, but in the Late Cretaceous (104–80 Ma) the orientation of the maximum principal compressive stress, indicated by zones of small intrusions and veins, was ENE. This study showed that during the Cretaceous the orientation of the maximum principal compressive stress rotated clockwise through 45°. A similar clockwise rotation is shown by zones of volcanic rocks erupted during the Cretaceous in the eastern areas of Fujian and Zhejiang; in the Early Cretaceous (135–120 Ma) these zones trend NNE, while in the Late Cretaceous they trend ENE (Lin JP et al., 1990).

Although there is still insufficient evidence, it has been demonstrated clearly that in eastern China, from Early to Late Cretaceous, the orientation of the maximum principal compressive stress rotated clockwise from NNE to ENE. The clockwise rotation of the axes of principal stress during the Sichua-

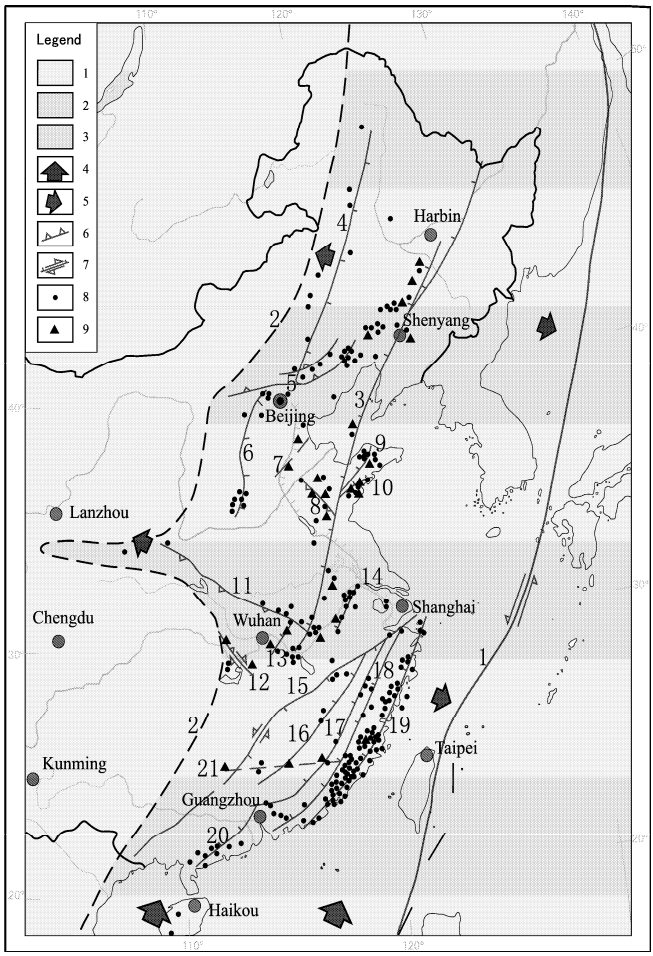

Fig. 8.5 Distribution of magmatic source areas and faults near the Mohorovičíc discontinuity and bottom of lithosphere during the Sichuanian Period (135–56Ma) in eastern China (Wan TF et al., 2008)

Numbers of legend: 1. Continental crust almost without magmatism; 2. Continental crust with obvious magmatism; 3. Oceanic crust; 4. compression orientation in crust; 5. extension orientation in crust; 6. subduction zone, thrust or reverse fault; 7. normal fault with strike-slip; 8. magmatic source depth data near the Mohorovičíc discontinuity (data shown in Appendix 7); 9. magmatic source depth data near the bottom of lithosphere (data shown in Appendix 7).

Numbers of faults: 1. inferred subduction zone, between continental and oceanic crusts of east China during Sichuanian Period (Japan Islands were located west to the zone, on account of rare data, here never to be reconstructed); 2. boundary between obvious and weak magmatism during the Sichuanian Period; 3. Tancheng–Lujiang normal fault zone; 4. East Taihangshan normal fault; 5. Yanshan (Shangyi-Gubeikou-Pingquan)–Yinshan reverse fault; 6. East Taihangshan normal fault; 7. Huanghua–Puyang normal fault group; 8. West Shandong NW trending reverse fault group; 9. Zhaoyuan–Pingdu normal fault; 10. Zhucheng–Qindao normal fault with sinistral strike-slip; 11. North Dabie–Qinling normal reverse fault; 12. Yuan'an–Linxiang reverse fault with dextral strike-slip; 13. Macheng–Xianning normal fault; 14. Nanjing–Wuhu normal fault; 15. Shaoxing–Shiwandashan normal fault with sinistral strike-slip; 16. Ganzhou–Nanfeng –Shangrao normal fault; 17. Shaowu–Heyuan normal fault; 18. Zhenghe–Dapu–Lianhuashan normal fault; 19. Zhejiang–Fujian coastal (Changle-Nan'ao) normal fault; 20. Foshan–Dianbai normal fault; 21. Nanling lithosphric fault.

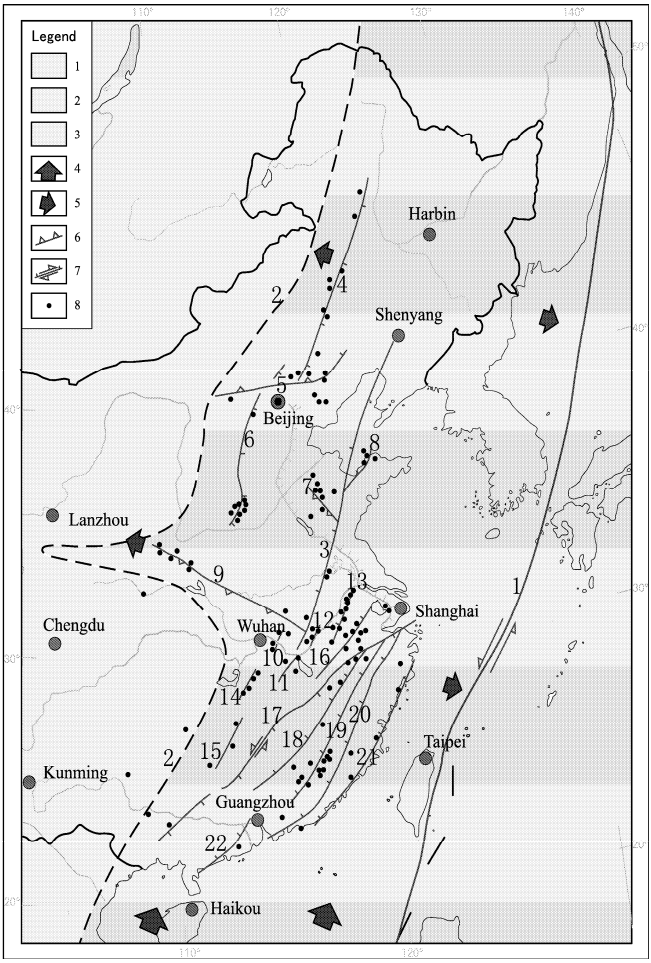

Fig. 8.6 Distribution of magmatic source areas and faults in the crust during the Sichuanian Period (135–56 Ma) in eastern China (Wan TF et al., 2008)

Numbers of Legend: 1. continental crust almost without magmatism; 2. continental crust with obvious magmatism; 3. oceanic crust; 4. compression orientation in crust; 5. extension orientation in crust; 6. subduction zone, thrust or reverse fault; 7. normal fault with strike-slip; 8. magmatic source depth data in crust (data shown in Appendix 7).

Numbers of faults: 1. inferred subduction zone, between continental and oceanic crusts of east China during the Sichuanian Period (Japan Islands were located west to the zone, on account of rare data, here never to be reconstructed); 2. boundary between obvious and weak magmatism during the Sichuanian Period; 3. Tancheng–Lujiang normal fault zone; 4. East Taihangshan normal fault; 5. Yanshan (Shangyi-Gubeikou-Pingquan)–Yinshan reverse fault; 6. East Taihangshan normal fault; 7. West Shandong NW trending reverse fault group; 8. Zhaoyuan–Pingdu normal fault; 9. North Dabie–Qinling normal reverse fault; 10. Macheng–Echeng–Xianning normal fault; 11. Yongxiu–Wanzhai normal fault; 12. Anqing–Wangjiang normal fault; 13. Nanjing–Wuhu normal fault; 14 Tongcheng–Xiangyin normal fault; 15. Zhuzhou–Hengyang normal fault; 16. Northeast Jiangxi normal fault; 17. Shaoxing–Shiwandashan normal fault with sinistral strike-slip; 18 Ganzhou–Nanfeng–Shangrao normal fault; 19. Shaowu–Heyuan normal fault; 20. Zhenghe–Dapu–Lianhuashan normal fault; 21. Zhejiang–Fujian coastal (Changle–Nan'ao) normal fault; 22. Foshan–Dianbai normal fault.

nian Period was the opposite of the crust counter-clockwise rotation in the Yanshanian Period. Also, in contrast to the Yanshanian Period, the rotation of the stress axes in the Sichuanian Period did not coincide with the rotation of the crust or plate, as indicated by changes in the paleomagnetic declination. In fact the declination of the continental plates shows virtually no rotation during the Sichuanian Period.

It is suggested that the clockwise rotation of the orientation of the maximum principal compressive stress in Sichuanian Period resulted from the continuous northeastward movement of the Indian and Gangdesi plates and their collision with Eurasia in the Banggongco–Nujiang Belt. This collision resulted in the compression of the area to the north in a SW-NE direction. At the beginning of Cretaceous, with the continuation of this northward movement, the eastern part of China was compressed in an NNE-SSW direction, which changed gradually to the ENE-WSW direction in the Late Cretaceous. The change in the orientation of the maximum principal stress did not result in the formation of fold systems with different orientations over large areas. This suggests that in the Middle and Late Cretaceous, tectonic forces were not very strong, resulting in deformation in weaker zones only, with the formation of extensional and shear joints or the re-opening of pre-existing fault planes.

Shao JA et al. (2001) found a bimodal dyke swarm, comprised of alkali-basalt and granitic rocks, extending for an distance of 40 km in an NNW direction, which gave K-Ar ages of 114-120 Ma, and a Rb-Sr age of 128 Ma at Nankou, Cangping–Guyaju, Yanqing of north Beijing. The trend of this dyke swarm is close to the orientation of the maximum principal compressive stress in that area during Early Cretaceous. It also indicates that N-S shortening and E-W extension controlled the development of the main structural features in that area. Dike swarms of different composition, but with the same trend, are final products of magmatic differentiation. Their attitude is controlled by the orientation of the horizontal regional maximum principal compressive stress; there is no evidence of uplift by a mantle plume or of underplating, as recognized by Li XH and McCulloch (1998) and Shao JA et al. (2001).

Data from whole rock chemical analyses of 4,081 samples of magmatic rocks divided into 67 petrographic areas were used in calculation and statistical analysis, and in the estimation of the rates of plate deformation during the Sichuanian Period (Fig. 8.2; Appendix 5.7). During that time, the average rate of NE-SW intraplate shortening in the Chinese continent was 5.4 cm/yr, the average rate of extension in the Tethys Ocean (Banggongco–Nujiang Ocean) to the southwest was 1.2 cm/yr, the average rate of intraplate shortening was about 6.0 cm/yr in the centre of Gangdise, west Qiangtang, Karakorum, West Kunlun, southwestern Tarim, Hunan, Hengduanshan zone, Guizhou, Fujian, Dabie-Qinling, as well as Laoyeling in NE China. However, in Erdos, Sichuan and Tarim the average rate of intraplate shortening was usually less than 4.0 cm/yr, and in other areas between 6.0 cm/yr and 4.0 cm/yr. In the Sichuanian Period, areas which show rapid intraplate shortening are small and scattered. Rates of intraplate deformation during the Sichuanian Period were of the same order of magnitude as in the earlier Indosinian and Yanshanian Periods. The differences in rates of shortening in different areas are due to differences in the direction and intensity of compression caused by the rate of movement of adjacent plates.

The rates of intraplate shortening indicate the northeastward movement of the entire crust and lithosphere. Limited magmatic activity during the Sichuanian Period was often related to fault zones or ductile shear zones in depth in the Chinese continent. At the intersection among the N-S or NNE trending tensile faults, E-W structure lineation and the middle crust or Mohorovĭcíc discontinuity, the rocks in depth were easy to fracture partially and cause decompression, magma composed of mixed crustal and mantle material was formed. This shows that the magmatic activity was due to happening of partial fracture or ductile shear zone at the Mohorovĭcíc discontinuity or in the low velocity layer in the middle crust, only a few formed at the base of the lithosphere. Evidently the partial tectonic fractures in the Sichuanian Period were not as great as in Yanshanian Period, so that less magma was formed and there were fewer intrusions.

8.3 Formation of the Banggongco–Nujiang Collision Zone and Northward Movement of the Plates

The Banggongco–Nujiang Collision Belt resulted from the only collision which occurred in China from the end of the Cretaceous to the Early Paleogene, formed during the amalgamation between the Qiangtang–Taniantaweng–Indochina and Gangdise (i.e. Lhasa)–Baoshan–Sibumasu Blocks (3 in Fig. 8.2). This collision belt extends from Banggongco eastwards, through Gerze–Dengqen (from 84.1°E, 32.5°N to 95.8°E, 31.6°N), to Kangsha-Shizika on the southwest side of Taniantaweng (98°E, 29.7°N), east of Xizang, and southwards along Nujiang to Burma. Rocks in the collision belt have a high dip angle and are folded and overthrust, with thrust ramps, forming a fan shape in section. The major overthrust surfaces dip to the north or east, with an intermediate angle of dip. The collision belt was formed by subduction, with northeastward underthrusting of the footwall and southwest-ward overthrusting of the hanging wall. Faults in the collision belt cut the Jurassic, Cretaceous and part of the Paleogene system, ophiolite suites occur along the belt. The ophiolite suite of Banggongco formed as part of the oceanic crust in the Early Cretaceous (Guo TY, 1991), and part of Gerze–Dengqen in the Middle Jurassic, according to the recent isotopic dating (Bureau of Geology and Mineral Resources of Xizang (Tibet) Autonomous Region, 1993); at Kangsha-Shizika, they were thrust with "cold-emplacement" into the Early Cretaceous system (Wang GH et al., 1996); at Nujiang on the eastern side of Gaoligong, western Yunnan, they were thrust with "cold-emplacement" into the Lower Jurassic system (Zhong DL et al., 1998).

The rate of extension in the ocean basins in Cretaceous to Paleocene times was about 1.2 cm/yr (Appendix 5.7, Fig. 8.2), being equal to or less than the rate of extension of the Atlantic Ocean at the present day. From reliable data, the Banggongco-Nujiang collision, already amalgamated with the Eurasian Plate, occarred at the end of the Cretaceous or in the Early Paleogene. The time of intrusion of syn-and post-collision granite near Banggongco was between 126 Ma and 55 Ma (Guo TY et al., 1991). The ophiolite suites of Kangsha-Shizika were formed between 75 and 86.4 Ma (Wang GH et al., 1996). It means that the collision time of different sections of Banggongco-Nujiang collision zone may change from Jurassic to the end of Cretaceous.

There has not yet been a detailed tectonic study of the whole of the Banggongco-Nujiang Collision Belt. However, Wang GH et al. (1996) studied deformations on the southwest side of Taniantaweng and discovered that mylonites in the Kangsha-Shizika Fault Zone indicate a major sinistral strike-slip movement at 75-86.4 Ma, and weaker dextral strike-slip at about 30 Ma, related to compression and collision. It is reasonable that the sinistral strike-slip indicates that the regional maximum principal compressive stress was WSW-ENE in eastern China during the Late Cretaceous Period. Under the influence of this stress field, the E-W trending Banggongco–Nujiang Collision Belt developed a sinistral strike-slip component. This stress direction is related to the migration of Indian Plate towards NE 40°–50° during the period from 70 to 80 Ma (Figs. 8.8 and 8.9).

In the Sichuanian Period, the high degree of folding and high values of differential stress in southwestern China, becoming weaker towards the northeast, indicates that the main dynamic source, which caused the extensive intraplate deformation in the Banggongco–Nujiang Collision Belt and in the east of China, was the rapid northeastward displacement of the Indian Plate.

Tectonic reconstruction through paleomagnetism (Fig. 8.7, Appendix 6) shows that during the Cretaceous the declination of every part of the Chinese continent changed by only 10° and was not very different from the present declination. But, the palaeolatitude of the whole of China did change, with the whole continent moving gradually northwards: the paleolatitude of Sino-Korea block has changed through 8° from 34.3°N to 42.3°N, a northward displacement of about 800 km; the palaeolatitude of the Yangtze area changed from 23.9° to 31.3° north latitude, a northward displacement of 7.4° or ~740 km; the paleolatitude of Siberia changed from 55.7° to 61.1° north latitude, a northward displacement of 5.4° or about 530 km; the palaeolatitude of Tarim changed from 22.9° to 25.4° north latitude, a 2.5° or ~250 km northward displacement; the palaeolatitude of the Indian Plate changed from 43.8° to 35.1°

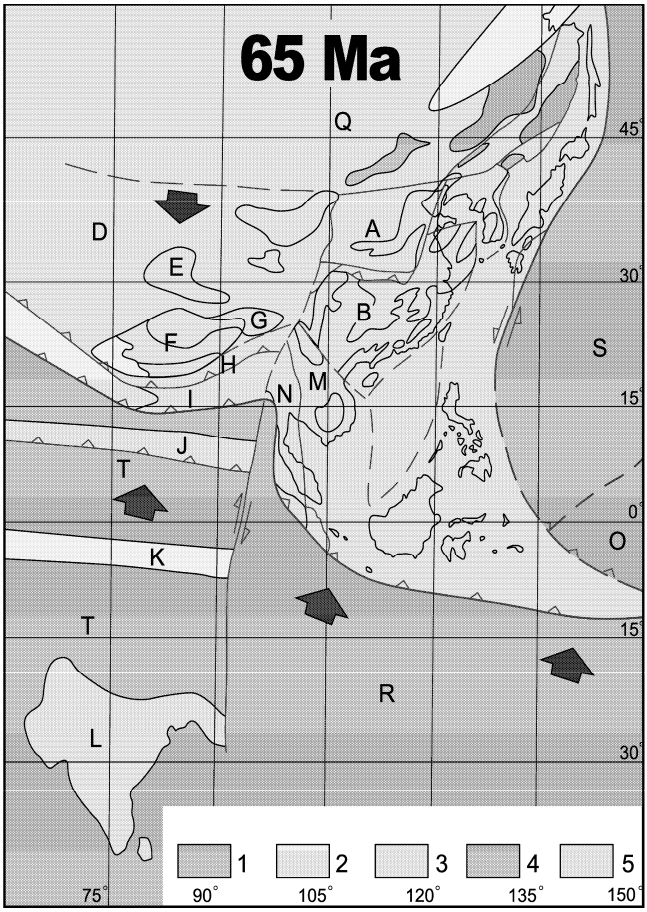

Fig. 8.7 Paleo-tectonogeographic reconstruction of China and its adjacent blocks in the Late Sichuanian Period (about 65 Ma).

1. Oceans; 2. Shallow seas; 3. Terrestrial facies in arid basins; 4. Terrestrial facies in humid basins; 5. Lowlands and hills (letters for blocks are the same as in Fig. 6.5). Paleomagnetic data and central reference points for the blocks are listed in Appendix 6.

south latitude, 8.7° or about 860 km northward displacement, with the most rapid movement reaching 17 cm/yr at the end of the Cretaceous (Figs. 8.8 and 8.9); the palaeolatitude of the Australian Plate changed from 65.1° to 58.9° south latitude, 6.2° or about 620 km northward displacement (Appendix 6). All plates in the region of the Chinese continent moved northwards nearly synchronously. Any difference in amount of movement of the blocks may be due to either the inaccuracy in the methods of measurement, or the deformation within or between blocks.

At that time, the Indian Plate was still far away from the Eurasian Plate, separated by a wide segment of the Tethys Ocean, reducing the resistance to the northward movement of the Indian Plate, permitting the rapid displacement. At the end of Sichuanian Period, the Gangdise, Baoshan and Sibumasu block

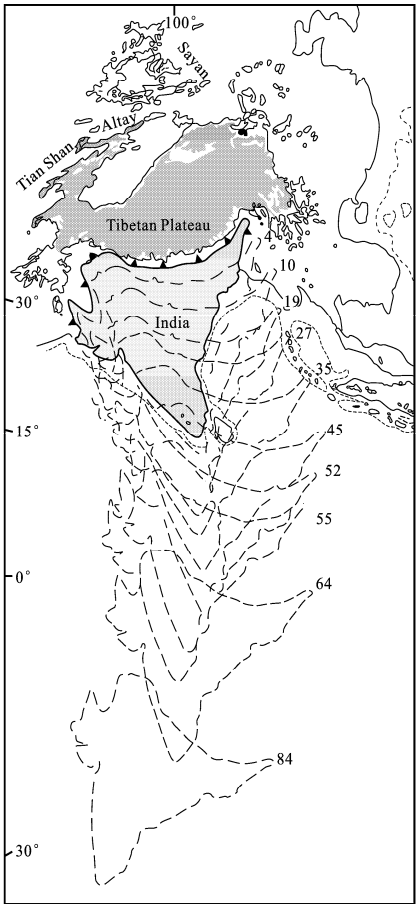

Fig. 8.8 Displacement of the Indian Plate since 84 Ma (after Lee TY and Lawer, 1995, with permission of Lee TY).

The numbers on the right hand side of the India Plate are isotopic ages in Ma. The figure illustrates the gradual slowing rate of movement of the Indian Plate, and the changes in the direction of movement, as indicated by paleomagnetic north.

separated from Gondwana collided with the Chinese–Indochina part of the Eurasian Plate, and the Indian Ocean Plate subducted to the north.

The movement of the Chinese continent and its adjacent plates corresponds with the general global plate movements during the Cretaceous (upper right, Fig. 7.7), in which all the continents and oceans on the Earth moved northwards (including NE or NW). But, the rates of displacement of the different plates were not the same. The rates of northward displacement of the Chinese continent and its adjacent plates were only about 5–6 cm/yr. However, the rate of northward displacement of the Indian Plate was 17 cm/yr in the Late Cretaceous, which is the highest known rate of plate movement. This is a very strange phenomenon, which will be discussed in a future chapter.

At end of Cretaceous, all the plates on the Earth were displaced northwards (upper right, Fig. 7.7). It actually illustrates a radiative plate displacement, centered near Antarctica. Another similar example of radiative displacement occurred in the Jurassic (upper left, Fig. 7.7). These displacements might be

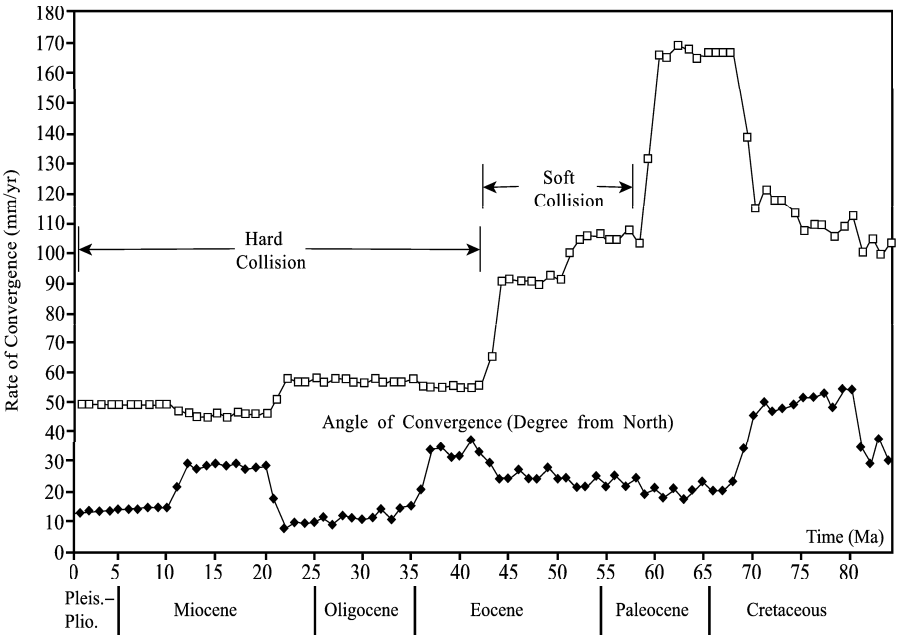

Fig. 8.9 The changes of velocity and angle of convergence between the Indian Plate and Eurasia since 84 Ma (Lee TY and Lawver, 1995, with permission of Lee TY).

The ordinate shows the rate of convergence of plates in mm/yr. The numbers in the lower part of left ordinate refer to the angles of convergence indicated by the black dots on the lower curve. The abscissa shows the age in Ma. In the Eocene and Oligocene, relict fragments of Tethys lay between the Indian Plate and Eurasia.

caused by mantle plume uplift or by a giant meteorite impact. These possibilities will be discussed in detail in Chapter 15.

During the Cretaceous, Taiwan Island was located on the eastern margin of Eurasia. In the Mid-Cretaceous (115–100 Ma) there was an N-S sinistral strike-slip fault zone with about 2,500 km in length, between the Pacific Plate and eastern Japan, Taiwan Island and the Philippines (Osozawa, 1998) (Fig. 8.7). In southwest Japan the Median Tectonic Line and the Kurosegawa Tectonic Zone were both formed at this time. By careful study, the Median Tectonic Line has been shown to be a major sinistral strike-slip tectonic zone during the Middle and Late Cretaceous (Yoshikura et al., 1990). In addition, a series of Cretaceous pull-apart basins were formed along the line of the tectonic zone. The Pacific Plate was formerly located to the south of the equator and extended rapidly northwards and southwards. It then moved rapidly northwards, faster than the Eurasian Plate, so that sinistral strike-slip tectonic zones developed between the Pacific Plate and the East Asian continent.

Gneiss, amphibolites and migmatites occur at Su'ao-Nan'ao in the Tailuge tectonic zone of Taiwan Island, and there are amphibolite facies metamorphic rocks in the Ruishui faulted block giving isotopic ages between 87 and 60 Ma. The formation of these metamorphic rocks and associated magmatism was not related to subduction but to regional thermal metamorphism (Bureau of Geology and Mineral Resources of Fujian Province, 1992). Therefore, there was no subduction zone between Taiwan and the Pacific Plate during the Cretaceous and Paleocene, although Faure and Natal'in (1992), Isozaki et al. (1992), Li WX and Zhou XM (1999), Zhou XM and Li WX (2000) have suggested that since the Jurassic there has been either a subduction zone or a low angle overthrust belt between the oceanic and

Eurasian plates to the east of Japan and Taiwan Island. It is an important result that a subduction zone between Pacific and Eurasian plates did develop in the Jurassic and Eocene–Oligocene (described in Chapters 7 and 9), but not in the Cretaceous.

In conclusion, the tectonics in Sichuanian Period (135–56 Ma) was characterized by deformation within continental plates, forming the Sichuanian Tectonic System, developing basin and range tectonics in eastern China, the rotation of the maximum principal compressive stress in a clockwise direction, extension with detachments at the Mohorovičíc discontinuity or the low velocity layer in the middle crust caused the magmatism, formation of the Banggongco–Nujiang Collision Belt and the northward movement of most of the tectonic plates on the Earth. It was the period when the general features of the present landscape of eastern Chinese continent were formed preliminarily, and the period when many endogenetic and exogenous economic hydrocarbon and metallic deposits were also accumulated.

References

Bureau of Geology and Mineral Resources of Fujian Province (1985) Regional Geology of Fujian Province. Geological Publishing House, Beijing (in Chinese with English abstract).

Bureau of Geology and Mineral Resources of Xizang (Tibet) Autonomous Region (1993) Regional Geology of Xizang Autonomous Region. Geological Publishing House, Beijing (in Chinese with English abstract).

Cai XL, Shi SQ, Wu DH et al (1995) Formation and Tectonic Evolution of the Wudangshan Nappe Structure. Chengdu University of Science and Technology Press, Chengdu (in Chinese with English abstract).

Chen QH, Chen ZB, Chen ZY et al (1998) Mesozoic Extension Tectonics and Uranium Mineralization in Southeastern China. Geological Publishing House, Beijing (in Chinese).

Cheng YQ (1994)An Introduction to Regional Geology of China. Geological Publishing House, Beijing (in Chinese).

China National Commission on Stratigraphy (2001) Chart of regional stratigraphy (geological age) of China. Journal of Stratigraphy 25(suppl.): 359–360 (in Chinese).

Chinese Academy of Geological Sciences (1973) Geological Atlas of People's Republic of China (in Chinese).

Faure M and Natal in Boris (1992) The geodynamic evolution of the eastern Eurasian margin in Mesozoic times. Tectonophysics 208:397–411.

Gao TJ, Wang ZM, Wu KL et al (1999)Tectono-magmatic Evolution and Metallogeny of Taiwan Strait and Its Adjacent Areas. Geological Publishing House, Beijing (in Chinese).

Ge XH, Liu YJ, Ren SM et al (2001)Re-understanding on some academic problems of the Altun fault. Chinese Journal of Geology 36(3): 319–325 (in Chinese with English abstract).

Guo TY, Liang DY, Zhang YZ et al (1991) Geology of Ngari Tibet (Xizang). China University of Geosciences Press, Wuhan (in Chinese with English abstract).

Huang TK (Jiqing) (1945) On the major structural forms of China. Geological Memoirs, ser. A, no. 20, pp.165.

Huang TK (Jiqing) (1960) The main characteristics of the geological structure of China: preliminary conclusions Acta Geologica Sinica 40(1): 1–37 (in Chinese with English abstract).

Isozaki Y, Hashiguchi T, Itaya T (1992) The Kurosegawa klippe: an examination. Geological Society of Japan Journal 98: 917–941.

Lee TY, Lawver LA (1995) Cenozoic plate reconstruction of Southeast Asia. Tectonophysics 251 (1–4): 85–138.

Li CY (1950) Sichuan movement and its distribution in China. Journal of Geological Society of China, 30: 1–8

Li WX, Zhou XM (1999) Late Mesozoic subduction zone of southeastern China Geological Journal of China Universities of Geosciences 5(2): 164–169 (in Chinese with English abstract).
Li XH, McCulloch MT (1998) Geochemical characteristics of Cretaceous mafic dikes from northern Guangdong, SE China: Age, origin and tectonic significance. In: Flower MFJ et al (ed) Mantle dynamics and plate interactions in East Asia, Geodynamics Series, vol. 27, pp.405–419, AGU, Washington DC.
Lin JP, Wan TF, Chu MJ (1990) Semi-quantitative research on tectonic stress field of Mesozoic–Cenozoic in Fujian province. In: Division of Structural Geology and Tectonics, Geological Society of China. Proceedings of International Continental Lithosphere Tectonic Evolution and Dynamics (1): 160–166. Geological Publishing House, Beijing (in Chinese).
Lin JP, Wan TF, Feng M (1994) Tectonic evolution of Late Paleozoic-Mesozoic in the southern Daheishan horst, Jilin province. Geoscience 8(4): 467–473 (in Chinese with English abstract).
Liu MQ, Yang BZ, Deng JG et al (1993) Tectonic Features and Evolution of Yitong–Shulan Graben. Geological Publishing House, Beijing (in Chinese with English abstract).
Mao JR, Tao KY, Li Jiyu et al (2002) Mesozoic grano-diorite characteristics and its tectonic evolution in Southwest Fujian. Journal of Petrology and Mineralogy 21(2): 135–142 (in Chinese with English abstract).
Osozawa S (1998) Major transform duplexing along the eastern margin of Cretaceous Eurasia. In: Flower MFJ et al (eds) Mantle Dynamics and Plate Interactions in East Asia, Geodynamics Series vol 27, pp.245–257, Washington DC: AGU.
Qi JZ (2001) Metallogenesis Research on Gold Deposit at Qiyugou, Henan Province. Dissertation, China University of Geosciences, Beijing (in Chinese with English abstract).
Shao JA, Li XH, Zhang LQ (2001) Geochemical condition for genetic mechanism of the Mesozoic bimodal dike swarms in Nankou-Guyaju. Geochimica 30(6): 517–524 (in Chinese with English abstract).
Tan XC, Li CY (1948) Geology of Xikang, Sichuan Province. In: Central Geological Survey. Geological Memoirs. ser. A no.15 (reprinted by Geological Publishing House in 1959, in Chinese).
Tang Z (1979) Structural features of oil-gas-bearing basins of eastern China. Petroleum Exploration and Exploitation (1): 30–37 (in Chinese).
Tao GY, Gao TJ, Lu ZG et al (1998) Basement Tectonics of Volcanic Rock and Volcanic-intrusion Related to Mineralization of Coastal Area in Southeast China. Geological Publishing House, Beijing (in Chinese with English abstract).
Wan TF (1981) Research on the structural features and mechanism of Nandazhai–Babaoshan fault zone, the Western Mountains, Beijing. Collection of Structural Geology (1): 152–164 (in Chinese with English abstract).
Wan TF, Zhu H (1989) Cretaceous–Early Eocene tectonic stress field in China. Acta Geologica Sinica 2(3): 227–239.
Wan TF (1992) Tectonic evolution and stress fields of Shandong Province Geology of Shandong 8(2): 70–101 (in Chinese with English abstract).
Wan TF (1994) Intraplate Deformation, Tectonic Stress and Their Application for Eastern China in Meso-Cenozoic. China University of Geosciences Press, Wuhan.
Wan TF (1995) Evolution of Tancheng–Lujiang fault zone and paleostress fields. Earth Science 20(5): 526–534 (in Chinese with English abstract).
Wan TF, Zhu H, Zhao L et al (1996) Formation and Evolution of the Tancheng–Lujiang Fault Zone. China University of Geosciences Press, Wuhan.
Wan TF, Zhu H (1996) The maximum sinistral strike-slip and its forming age of Tancheng–Lujiang fault zone. Geological Journal of China Universities 2(1): 14–27 (in Chinese with English abstract).
Wan TF (2000) Preliminary study of complexity of the tectonic stress-strain system. Earth Science Frontiers 7(1): 161–168 (in Chinese with English abstract).
Wan TF (2002) Tectonics of Sino-Korean Plate and prediction of oil-gas field near western coast of Korean peninsula. In: Cheong DK, Lee JM (eds) Tectonics of east Asia. Proceedings of International

Symposium Celebrating 55th Anniversary of the Geological Society of Korea, p.2–3. The Geological Society of Korea.

Wan TF, Zhao WM (2002) On the mechanism of intraplate deformation in Chinese continent. Earth Science Frontiers 9(2): 451–463 (in Chinese with English abstract).

Wan TF, Wang YM, Liu JL (2008) Detachment and magmatic source depth in lithosphere of Eastern China during Yanshanian and Sichuanian stages. Earth Science Frontiers 15(3):1–35 (in Chinese with English abstract).

Wang GH, Zhou X, Pubuciren, Zeng QG (1996) Structures and Its Evolution of Taniantaweng Mountain Chain in Xizang. Geological Publishing House, Beijing (in Chinese).

Wang TH (1995) Evolutionary characteristics of geological structure and oil-gas accumulation in Shanxi-Shaanxi area. Jour. Geol. & Min. Res. North China 10(3): 283–398 (in Chinese with English abstract).

Xu SD, Zeng HL, Wan TF (2001) Apparent density mapping and tectonic of China. Earth Science Frontiers 8(2): 407–413 (in Chinese with English abstract).

Yoshikura S, Hada S, Isozaki Y (1990) Kurosegawa terrane. In: Ichikawa K, Mizutani S, Hara I (eds) Pre-Cretaceous Terranes in Japan. Publication of IGCP Project No. 224, Osaka.

Yu YW, Zhou TX, Chen JF (1993) The characteristics and origin of the Xuantandi Bimodal volcanic rocks of the late stage of Early Cretaceous, Zhejiang. Journal of Nanjing University 5(4): 420–429 (in Chinese with English abstract).

Zhang GW, Zhang BR, Yuan XC, Xiao QH et al (2001) Qinling Orogenic Belt and Continental Dynamics. Science Press, Beijing (in Chinese).

Zhang JS, Xu J, Wan JL et al (2002) Meso-Cenozoic detachment zones in the front of the Taihang Mountains and their fission-track ages. Geological Bulletin of China 21(4–5): 207–210 (in Chinese with English abstract).

Zhao ZP (1959) On the Yanshan movement. Geological Review 19(8): 339–346.

Zhong DL (1998) Paleo-Tethyan Orogenic Belt in Western Yunnan and Sichuan. Science Press, Beijing (in Chinese).

Zhou XM, Li WX (2000) Origin of Late Mesozoic igneous rocks in southeastern China: implications for lithosphere subduction and underplating of mafic magmas. Tectonophysics 326 (3–4): 269–287.

Chapter 9
Tectonics of Eocene–Oligocene (The North Sinian Tectonic Period, 56–23 Ma)

—the formation of the North Sinian Tectonic System, first westward subduction of Pacific Plate, appearance of four drainage basins, the formation of the Yarlung Zangbo Collision Zone

Tang Z (1979) first recognized that tectonic events in China during the Eocene and Oligocene were not caused by the collision marked by the Himalaya. Previously all tectonic events during the Cenozoic had been attributed to Himalayan tectonic movements (Huang JQ, 1945, 1965). Tang Z named the tectonic event represented by the unconformity between the Paleocene Kongdian and the Eocene Shahejie Formations, the "first epoch" of the North Sinian Tectonic Event, and the tectonic event represented by the unconformity between the Oligocene and Miocene the "second epoch". These two unconformities are widespread throughout eastern China. The "Sichuanian Tectonic Event" related in Chapter 8 was first named by Tan XC and Li CY (1948), and is equivalent to the "first epoch" of the North Sinian Tectonic Event proposed by Tang Z (1979). The "North Sinian Tectonic Period" is used here only for the "second epoch", covering the Eocene and Oligocene (56–23 Ma), as proposed by Wan TF and Cao RP (1992) and terminating in the North Sinian Tectonic Event at the end of this period.

The North Sinian Period includes the Shahejie and Dongying formations which contain the main petroleum source beds of eastern China. The North Sinian Tectonic Event at the end of the North Sinian Period, marked by the unconformity at the top of the North Sinian tectono-stratigraphic unit, occurred at different times in different parts of China: in the Mid-Oligocene (27–25 Ma) in the East China Sea; at the end of the Oligocene (~23 Ma) in eastern China; during the Middle Miocene (20–15 Ma) in western Yunnan, Tibet and Xinjiang (Wan TF and Cao RP, 1992; Wan TF, 1994).

The sedimentary thickness and rates of sedimentation in the Cenozoic systems (Appendix 2, Fig. 9.1) reflect Cenozoic intracontinental tectonic activity, especially during the Paleogene. In general, Paleogene sediments are the thickest in northern China and west Taiwan Island, and the thinnest in southern China. The thickest Cenozoic sediments are found in the Hebei Plain (13,000 m), west Taiwan Island (14,600 m) and the Tarim Basin (13,782 m), where rates of sedimentation were 224.8–200 m/Myr (i.e. 0.22–0.2 mm/yr). Cenozoic sediments between 4,000 and 10,000 m in thickness occur on the southern side of the Yinshan in Inner Mongolia (4,957 m), Junggar (4,224 m), west Liaoning (5,453 m), north Henan (4,607 m), north Jiangsu and the southern Yellow Sea (4,746 m), the southern front of the Dabashan (4,035 m), southeast Guangxi (6,315 m), east Taiwan (7,350 m), Zhongdian, Yunnan (5,256 m), Lanping-Simao (7,953 m), the front of the Qilian Mountains and Qaidam, Qinghai (6,803–5,308 m), the northern front of the Kunlun Mountains (8,046 m), the southern front of the Tanggula Mountains (5,383 m) and Qiangtang-Changdu (6,230 m), where rates of sedimentation were 105–62 m/Myr (0.1–0.06 mm/yr). In other areas of the Chinese continent the thickness of Cenozoic sediments is <3,200 m, and the rate of sedimentation was <49 m/Myr (0.049 mm/yr).

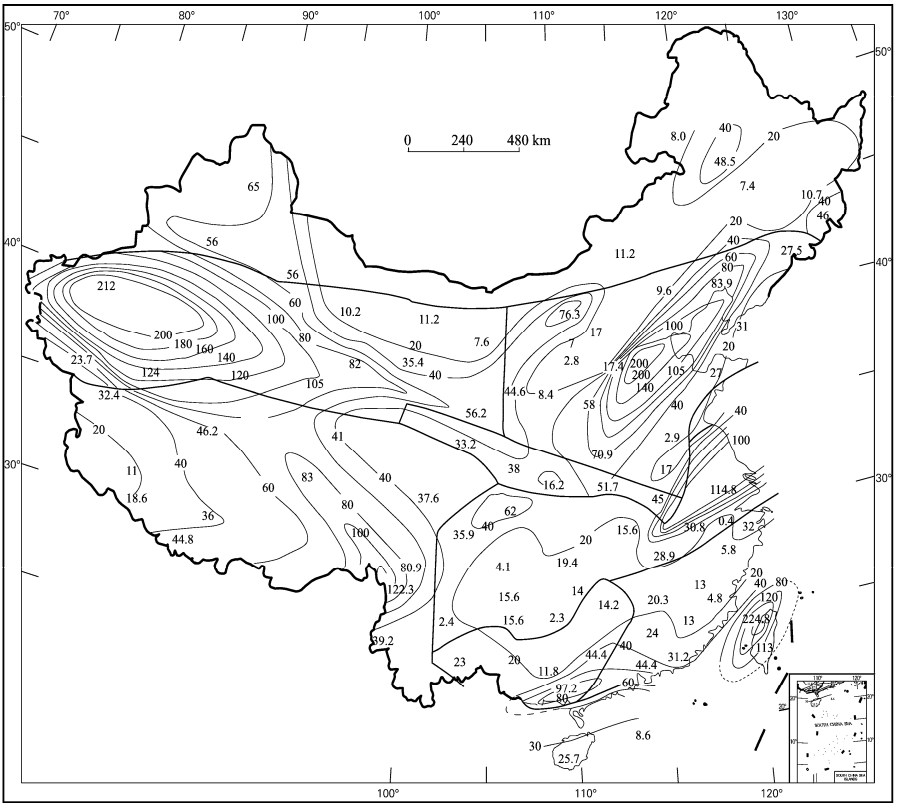

Fig. 9.1 Rates of sedimentation in the Cenozoic system in the Chinese continent (unit: m/Myr).

9.1 Intraplate Deformation, Stress Field and Magmatism

Deformation during the North Sinian Period has generally been ignored in most areas of the Chinese continent, because their effects are considered to be very weak. But deformation at this period was really a little bit strong, with the formation of NNE or N-S trending folds and reverse fault zones, NE trending dextral strike-slip faults, NW trending sinistral strike-slip faults and WNW or E-W trending extension detachment (listric) fault zones, comprising the North Sinian Tectonic System.

The NNE or N-S trending folds formed during the North Sinian Period are open folds, in which the angles of dip of both limbs are usually $<10°$. Oligocene and underlying formations are involved in the folds, which formed at the end of the Oligocene. Anticlinal folds found in the exploration of oilfields provide many oil and gas traps, such as the famous drape fold in the Daqing Oil field (3 in Fig. 9.2) and many small N-S anticlines in the lower reaches of the Liaohe River, near Liaodong Bay (5 in Fig. 9.2), the central Hebei Plain, northern Jiangsu and the southern Yellow Sea Basin. high angle normal and of Ningxia, 1990);

Many folds were formed in the southwestern part of the Chinese continent in the North Sinian Period. There has been a great deal of discussion concerning the period, during which the NNE-trending ejective folds in East Sichuan with $\sim 30°$ dipping fold limbs were formed (4 in Fig. 9.2). In that area the Triassic, Jurassic and Cretaceous systems all have conformable contacts and all are involved in the folding. Many researchers have considered these NNE-trending folds are related to the Neocathaysian Tectonic System,

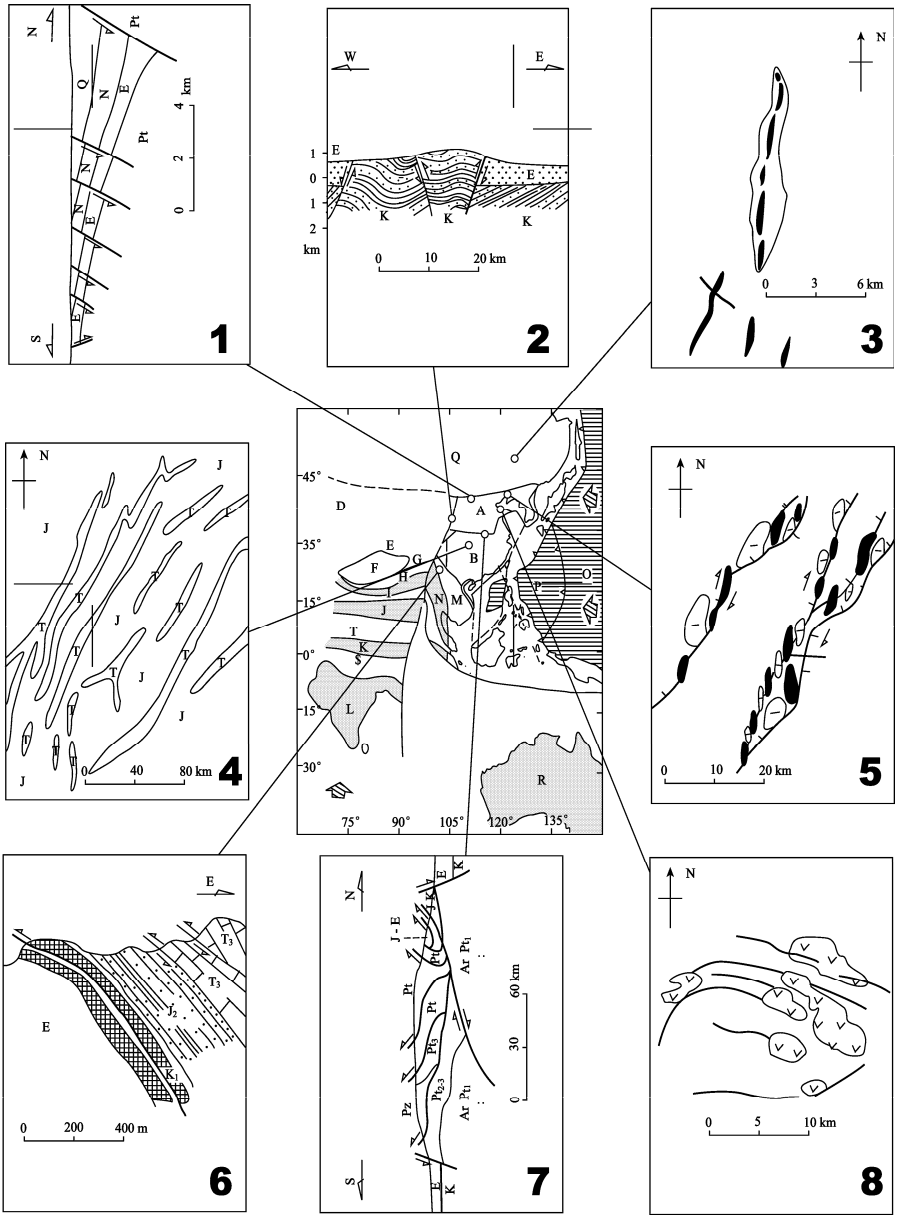

Fig. 9.2 Deformation in the North Sinian Period.

1. A step-faulted, half-graben basin due to N-S extension has formed on the southern side of the Daqingshan, Hetao, since the Paleogene (Changqing Oil Field); 2. Cretaceous and Paleogene systems cut by post-Paleogene high angle normal

and reverse faults at Liupanshan, Ningxia (Bureau of Geology and Mineral Resources 3. Distribution of NNE-trending Daqing drape anticline (black lens) is shown. Cretaceous and Paleogene systems were folded at the end of the Paleogene (Daqing Oil Field); 4. The distribution of ejective fold systems in the East Sichuan basin. Triassic, Jurassic and Cretaceous systems were folded at the end of the Oligocene (Bureau of Geology and Mineral Resources of Sichuan Province, 1991). "T" is outcropping of Triassic system and "J" is outcropping of Jurassic system; 5. Eocene and Oligocene systems in the Liaohe Oil Field form en echelon traps (anticlines, black lens) and synclines ("-" white lens) caused by dextral strike-slip and reverse faults (Li Hongwei et al., 2001); 6. Jinding lead-zinc deposit of Yunnan, located in a reverse fault system between the Lower Cretaceous (K_1) and Paleogene (E) systems, formed at the end of the Oligocene (data from the Third Brigade of Bureau of Geology and Mineral Resources of Yunnan, 1989); 7. Extension faults on the northern and southern margins of the Dabie Mountains formed by N-S extension, the Dabie Mountain has formed a horst block since the end of the Paleogene (Zhang GW, 2001); 8. Huiming sag of the Shengli Oil Field, Shandong. The WNW-trending normal faults controlled basalt eruptions in the Eocene and Oligocene (data from Shengli Oil Field).

Index letters for blocks or plates in the central figure are also presented in Fig. 6.5.

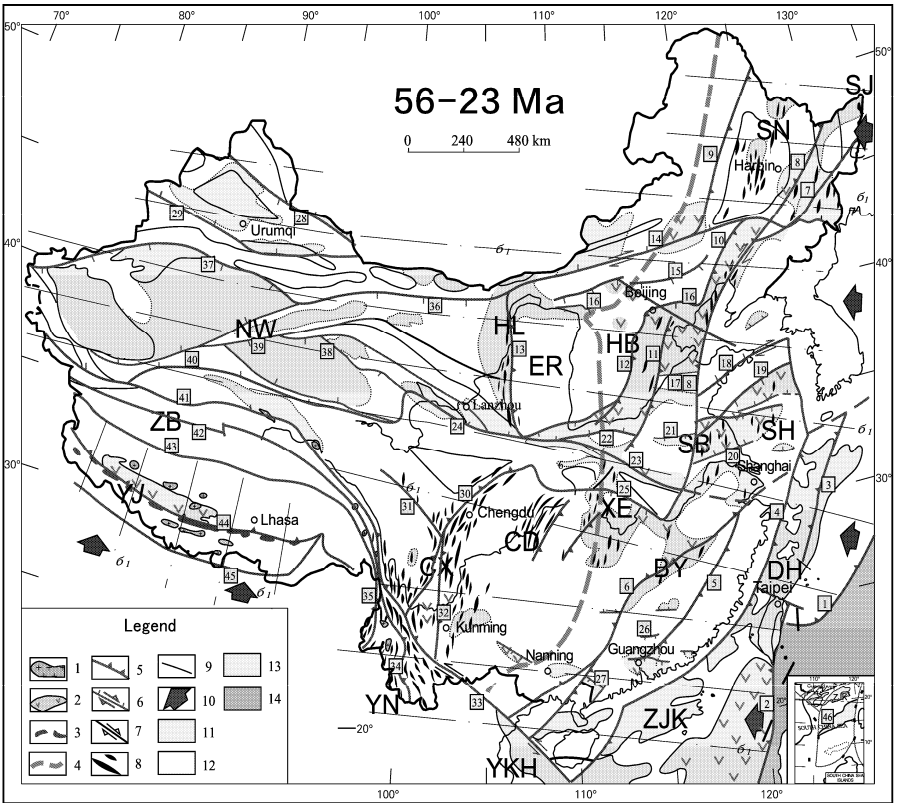

Fig. 9.3 Tectonic sketch of Chinese continent in the North Sinian Period (56–23Ma).

1. Granitic intrusions in the North Sinian Period; 2. Volcanic rocks (mainly tholeiite) in the North Sinian Period; 3. Ophiolitic and ultramafic rocks in the North Sinian Period; 4. Rate of intraplate deformation calculated from litho-chemical data. "-" is rate of extension, others are rate of shortening (Unit: cm/yr) (Data in Appendix 5.8); 5. Numbered plate collision belts, reverse fault zones; 6. Numbered normal and strike-slip faults; 7. Unnumbered block margins or faults with weak activity in the North Sinian Period; 8. Axial traces of anticlinal folds (Data in Appendix 3.7); 9. Traces of maximum principal compressive stress axes (σ_1); 10. Direction of plate movement; 11. Basins with terrestrial sedimentation; 12. Eroding land areas; 13. Shallow seas; 14. Oceans.

Names of numbered subduction, collision and fault zones: [1] Ryukyu subduction belt; [2] Eastern Taiwan-western Philippines subduction belt; [3] Reverse fault on the western side of the Diaoyudao uplift; [4] Reverse fault of off-shore (~50 m isobath) Fujian–Guangdong; [5] Chong'an–Heyuan reverse fault; [6] Shiwandashan–Shaoxing reverse fault; [7] Dunhua–Mishan dextral strike-slip and reverse fault zone; [8] Northern section (Yilan–Yitong) of the Tancheng–Lujiang dextral strike-slip and reverse fault zone; [9] Eastern side of Dahingganling reverse fault zone; [10] Beipiao–Jianchang reverse fault zone; [11] Cangdong reverse fault; [12] Eastern side of Taihangshan reverse fault zone; [13] Liupanshan–Helanshan reverse fault zone; [14] Xar Moron River dextral strike-slip and normal fault zone; [15] Jining–Gubeikou normal fault zone; [16] Southernmost Yinshan–Daqingshan–Yanshan normal fault; [17] Guangrao–Jiyang normal fault; [18] Zhucheng–Rongcheng dextral strike-slip and normal fault; [19] Guanyun-southern Yellow Sea dextral strike-slip and normal fault; [20] Jiangdu–Hai'an dextral strike-slip and normal fault; [21] Wuhe–Huaiyuan normal fault; [22] Luoning–Luoyang normal fault; [23] Luonan–Fangcheng sinistral strike-slip and normal fault; [24] Baoji–Tianshui normal fault zone; [25] Fangxian–Xiangfan-Guangji normal fault zone; [26] E-W trending Nanling normal fault group; [27] Maoming Graben; [28] Derbugan–Kelameili normal fault zone; [29] Southernmost Nilek–Turpan–Hami normal fault; [30] Longmenshan dextral strike-slip and reverse fault zone; [31] Daofu–Kangding sinistral strike-slip fault; [32] Anninghe reverse fault; [33] Honghe (Red River) sinistral strike-slip fault; [34] Lancangjiang reverse fault; [35] Nujiang reverse fault; [36] The northernmost part of Alxa normal fault; [37] Korla–Wuqia normal fault; [38] The southernmost part of the Junulshan–Qinghai Lake normal fault zone (northernmost Qaidam zone); [39] Altun dextral strike-slip and normal fault; [40] Northern Kunlun (southernmost Qaidam zone) normal fault; [41] Jinshajiang sinistral strike-slip fault; [42] Kongkela–Tanggula–Wenquan normal fault; [43] Bangongco–Dongqiao normal fault; [44] Yarlung Zangbo Collision Belt; [45] Southernmost relic of Himalayan (Tethys) Ocean; [46] E-W trending extensional fracture zone of the South China Sea (new oceanic crust).

and were formed, during the Yanshanian Period, mainly in the Jurassic; this mistake was also made by Wan TF (1989). Gan ZG (1988) first proposed that the "ejective" fold systems were formed during the Tertiary, by comparing characteristics of the sediments, the folds and planation surfaces in the Sichuan Basin. The Bureau of Geology and Mineral Resources of Sichuan Province (1991) concluded that the folds in East Sichuan were formed during the Cenozoic by comparing the tectonic systems over a wide area, and especially from the study of the N-S trending folds and reverse faults in the Cretaceous and Paleogene systems of West Sichuan and its adjacent areas. According to the present understanding, the formation time of the NNE-trending ejective fold system in East Sichuan was at the end of the Oligocene. The reason for the development of strong fold systems is that the folds are linked to three deep detachments, a Triassic gypsum-salt layer, the Middle Permian coal system and Silurian shales. These detachments could have been formed under quite weak tectonic stress. When the applied force and the rock materials are inhomogeneous, local folds and small-scale thrusts formed at depth may lead to the formation of "ejective" folds near the surface. Close and overturned folds, accompanied by thrusts, occur in western Yunnan (6 in Fig. 9.2), where Early Miocene folds, also formed during the North Sinian Tectonic Period, are best developed.

Using data from 2,126 macro-and meso-scale folds (1,043 anticlines and 1,083 synclines) from the North Sinian Period, taken from the results of the regional geological survey, and data from the measurement of joints from 115 locations by the author and his colleagues, the Chinese continent was divided into 29 districts and the results were analyzed statistically (Appendix 3.7). The orientation of the principal stress axes was calculated from the analysis of this data. In present day coordinates, the preferred attitude of the maximum principal compressive stress axis (σ_1) during North Sinian Period was SE114°∠4°; that of the intermediate principal compressive stress axis (σ_2, i.e. fold axes) was SW186°∠2°; that of the minimum principal compressive stress axis (σ_3) was NW293°∠86°, nearly vertical (Figs. 9.3 and 9.4). The tectonic stress field in the Chinese continent was controlled by WNW-ESE horizontal compression and NNE-SSW horizontal extension during the North Sinian Period.

The author and his colleague have recently determined the average magnitude of differential stress in eastern China. Data from 47 determinations of tectonic stress have been gathered from the research areas, with rock type, mineral tested, number of samples and the magnitude of average differential stress in the North Sinian Period (56–23 Ma) (Appendix 4). The average magnitude of differential stress was found to be 76.7 MPa: with 77.3 MPa from 6 samples of the Daqing Oil Field (Chen ZD et al., 2002);

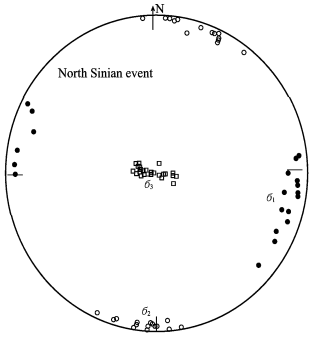

Fig. 9.4 Attitude of the principal stress axes in the North Sinian Period. σ_1. maximum principal stress axis; σ_2. intermediate principal stress axis; σ_3. minimum principal stress axis.

74.4 MPa from 4 samples of the Nanpu sag in the east of Hebei; 73.6 MPa from 5 samples of the Liaohe Oil Field (Wang MM, 2003); 45.7 MPa from 17 samples of Guacangshan, Zhejiang (Wan TF and Cao XH, 1997). In recent years, the author has also obtained some data from western China: 77.3 MPa from 4 samples of western Yunnan; 71.7 MPa from 2 samples of western Kunlun, Qinghai and Hohxilshan; 115.5 MPa from 3 samples of eastern Xizang (Tibet); 81.9 MPa from 12 samples of the southern Xizang (Tibet); 118 MPa from 3 samples of the Burang, southwest Xizang (Tibet) (Wan TF and Cao XH, 1997) (Fig. 9.5; Appendix 4).

Differential stress magnitudes of more than 80 MPa have so far been found only in Tibet. This was probably an area of intraplate stress concentration at latitude $\sim 15°$N, caused by the westward subduction of the Pacific Plate. However, there is insufficient data to confirm this suggestion; more research will be required.

Due to E-W shortening an NNE trending fold system was formed in the North Sinian Period, accompanied by NNE trending reverse faults, such as the reverse fault on the western side of the Diaoyudao uplift-folded zone (3 in Fig. 9.3), the reverse fault of off-shore (50 m isobath) Fujian–Guangdong (4 in Fig. 9.3), the Chong'an–Heyuan reverse fault (5 in Fig. 9.3), the Shiwandashan–Shaoxing reverse fault (6 in Fig. 9.3), the southern section of the dextral Tancheng–Lujiang strike-slip and reverse fault zone (8 in Fig. 9.3), the eastern side of Dahingganling reverse fault zone (9 in Fig. 9.3), the Beipiao–Jiancang reverse fault zone (10 in Fig. 9.3), the Cangdong reverse fault (11 in Fig. 9.3), the eastern side of the Taihangshan reverse fault zone (12 in Fig. 9.3), the Liupanshan–Helanshan reverse fault zone (13 in Fig. 9.3), the Anninghe reverse fault (32 in Fig. 9.3), the Lancangjiang reverse fault (34 in Fig. 9.3) and the Nujiang reverse fault (35 in Fig. 9.3).

In the eastern part of the Chinese continent the effects of these reverse faults are usually weak. However, locally in the southern section of the Tancheng–Lujiang Fault Zone, the Paleogene system is overturned (Wan TF et al., 1996). High angle reverse faults on either side of the uplifted Liupanshan–Helanshan block (2 in Fig. 9.2) also cut the Paleogene system. Only minor magmatism is found along the NNE trending reverse faults. It illustrates that those faults were formed during compression.

All the NE-trending faults formed during the North Sinian Period show dextral strike-slip movement: Dunhua–Mishan reverse fault zone with dextral strike-slip (7 in Fig. 9.3); the northern section (Yilan–Yitong) of the Tancheng–Lujiang dextral strike-slip fault zone (8 in Fig. 9.3); the Zhucheng–Rongcheng normal fault with dextral strike-slip (18 in Fig. 9.3); the Guanyun–southern Yellow Sea normal fault with dextral strike-slip (19 in Fig. 9.3); the Jiangdu–Hai'an normal fault with dextral strike-slip (20 in Fig. 9.3); the Longmenshan reverse fault zone with dextral strike-slip (30 in Fig. 9.3); the Altun normal fault with dextral strike-slip (39 in Fig. 9.3). During the Eocene–Oligocene NE-trending pull-apart basins were formed in association with these strike-slip faults, such as the Yilan–Yitong (centered on 127°E, 45°N), Dunhua–Mishan (centered on 129°E, 44°N), lower reaches of Liaohe River–Liaodong Bay (centered on 122°E, 41°N), Huanghua (centered on 117.2°E, 38.5°N), Central Hebei (centered on 116°E, 38.5°N), Linqing (centered on 115.7°E, 36.8°N), northern Jiangsu (centered on 120.3°E,

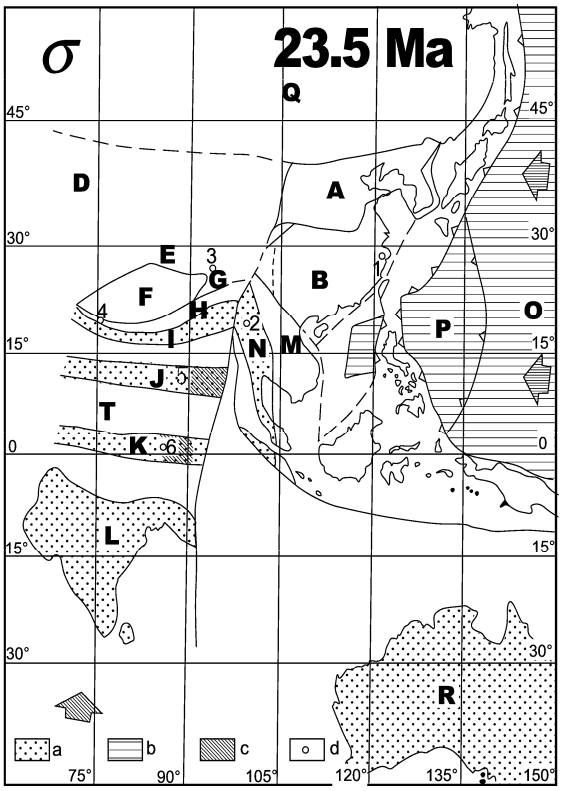

Fig. 9.5 Magnitude of differential stress in the North Sinian Period.

a. Dispersed Gondwanan continental blocks; b. Pacific (O) and Philippine Sea (P) plates and newer oceanic crust; c. Area with >80 MPa differential stress magnitude; d. Locations where differential stress magnitude was measured. Areas with a magnitude of differential stress <80 MPa, or never measured, are left white. Index letters of blocks are the same as in Fig. 6.5 (data in Appendix 4).

Numbers of research areas: 1. Guacangshan, Linhai, Zhejiang; 2. Western Yunnan; 3. Hohxil shan, Qinghai; 4. Western Kunlun; 5. Eastern Tibet; 6. Southern Tibet.

32.2°N), southern Yellow Sea (centered on 122°E, 33°N), Wuwei (centered on 117.9°E, 31.2°N), Qianshan (centered on 116.6°E, 30.6°N), Changzhou (centered on 120°E, 31.8°N) and Jurong (centered on 119.2°E, 32°N) basins.

During the North Sinian Period the NE-trending fault zones show dextral strike-slip displacement of several kilometers, such as 4.5 km displacement of the lower reaches of Liaohe River fault-depression, and the largest displacement, 10 km, in the Liaodong Bay fault-depression. Extension occurred at the same time as dextral strike-slip. Qi JF et al. (1995) estimated that the amount of extension in the Liaodong Bay fault-depression during the North Sinian Period was 7.7–16 km, an average extension ratio of 20%. In the Eocene, the amount of extension was 3.2–9.4 km, and the rate of extension was 0.075 cm/yr. In the Oligocene, the amount of extension was 2.5–6.6 km, and the rate of extension was 0.036 cm/yr.

All the earlier NW-trending faults developed sinistral strike-slip movement during North Sinian Period under the influence of the stress field: the Daofu–Kangding Fault (31 in Fig. 9.3); the Honghe (Red

River) Fault (33 in Fig. 9.3); the Jinshajiang Fault (41 in Fig. 9.3). Wu HW (1989) and Zhong DL et al. (1998) studied a mylonite zone formed by the fault movements along the Jinshajiang–Honghe sinistral strike-slip fault. Isotopic age dating showed that the fault movements occurred between 30 and 20 Ma (Scharer et al., 1990, 1994; Zhong DL et al., 1990). From the amount of shear strain and the width of the shear zone, they calculated the strike-slip movement along the fault to be between 100 and 250 m, with a rate of movement of 0.45 cm/yr. Zhong DL et al. (1993, 1998) determined horizontal displacement of 320 km from the Paleozoic sedimentary system that occurs on both sides of the fault. Tapponnier et al. (1990) used the displacement of an ophiolitic-mélange suite at Jingshajiang and Mojiang to indicate a movement of 500 km, a rate of movement of 5 cm/yr. Harrison et al. (1996) considered that during 26–17 Ma, the Red River sinistral strike-slip ductile shear belt was displaced by 400 km, with a rate of movement of 4.5 cm/yr. It appears that calculations through the amount of shear strain in the mylonite zone for the amount of displacement along the fault give a too much small amount of movement. Pull-apart basins, such as the Honghe–Yinggehai (west to Hainan Island), and Baise (middle Guangxi) basins, were formed during strike-slip movements along the NW-trending fault zones.

Due to the subduction of Pacific Plate, E-W trending shortening of the eastern China continent was not very strong and many detachments in crust and at Mohorovǐcíc discontinuity were sealed by solidified magma during the Jurassic and Cretaceous; magmatism in the Paleogene was rather weak depending on recent data. The main magmatism was tholeiite eruption along E-W or NW trending deep fault zones during the North Sinian Period, for example, at northern Shandong (Shengli Oil Field)–western Bohai Bay (Dagang Oil Field)–Beijing–Hannoba of Hebei, lower Liaohe area, northern Jiangsu, eastern Jilin and Liaoning (Fig. 9.3). These tholeiites often originated from oceanic type mantle (Chi, 1988). However, granitoids were intruded in the Gangdise Zone (west of Lhasa) and the Yulong Zone of eastern Tibet, and western Yunnan, related to collision between the Indian and Asian Plates during Eocene and Oligocene (Appendix 7).

To determine the average rate of E-W shortening of the blocks in the Chinese continent, China was divided into 32 areas for statistical analysis. Data from the chemical analyses of 377 samples of volcanic rocks from the North Sinian Period, together with ocean floor magnetic anomalies, were used to calculate an average rate of shortening of 4.5 cm/yr (Fig. 9.3; Appendix 5.8). This is slightly less than the rates of shortening in the Indosinian, Yanshanian and Sichuanian Periods. In some areas the rate of intraplate shortening was >5 cm/yr: Baitoushan, east of Liaoning and Jilin (5.4 cm/yr); Northern China and Huanghuai (between Yellow River and Huai River) (6.4 cm/yr); Taiwan (7.1 cm/yr); Jiangxi (5.4 cm/yr); western Yunnan (6.6 cm/yr); Gangdise (5.8 cm/yr); Himalayan (6.3 cm/yr). In the most of the Chinese continent and in areas surrounding the Tarim Basin the rate of shortening was 3–5 cm/yr. Because of the lack of data from magmatic rocks, shortening rates in Erdos, Sichuan and the areas to the north and west and in the central Tarim Basin, are difficult to evaluate, but are estimated to be less than 3 cm/yr.

Table 9.1 Amount of shortening ratio, shortening rate, fold deformation time and linear strain rate in the North Sinian Period.

Area	Northeastern China	Northern China	Yangtze area	Southern China	South China Sea
Latitude	45°N	38°N	30°N	25°N	15°N
Statistics length (km)	1,250	1,375	2,125	2,000	2,000
Mean fold limb angle (amount of data)	6.2° (302)	11.7° (188)	30.2° (1,336)	36.5° (878)	Based on magnetic anomaly
Shortening ratio (%)	0.58	2.08	13.57	19.61	−25
Shortening magnitude (km)	7.3	28.6	288	392.2	−500
Shortening rate (cm/yr)	4.3	5.6	4.3	4.2	−4.86
Fold deformation time (yr)	0.17	0.51	6.7	9.3	10.3
Linear strain rate (ε, 1/s)	1.09×10^{-15}	1.29×10^{-15}	6.4×10^{-16}	6.7×10^{-16}	7.7×10^{-16}

The shortening rate, the amount of shortening, the length of time for fold deformation and the intraplate linear strain rate during the North Sinian Period can be estimated from the folds as measured on four E-W profiles (the method of calculation is described in Chapter 1), along latitudes 45°N, 38°N, 30°N and 24°N (Table 9.1). The greatest ratio of regional shortening is found in southern China (19.6%), with lesser ratio in the Yangtze area (13.57%), in North China (2.08%) and in Northeast China (0.58%). The differences in the amount of shortening ratio represent the effects of a strong regional stress field in the south, but a weaker field in the north. In the North Sinian Period, South China formed a southeastern peninsula of the Eurasian continent, and was located to the west of the Pacific Plate (Figs. 9.5 and 9.10). Differences in the magnitude of regional stress are due to the westward movement of the Pacific Plate with the strong compression of southern China.

The South China Sea was formed by N-S trending extension at latitude $\sim 15°$N during the Paleogene. The amount and ratio of extension in the first phase can be calculated as 500 km and 25%, from the extent of the oceanic crust. From magnetic anomaly patterns the rate of extension of the ocean floor was 4.9 cm/yr. Some researchers (e.g. Tapponnier et al., 1990) have suggested that the northward movement and subduction of the Indian Plate caused the southeastward extrusion of the Indochina Peninsula and the extension of the South China Sea (Fig. 6.1). But this suggestion is implausible as the extension of the South China Sea was stronger in the east than in the west. It is considered that extension to form the South China Sea was caused by back-arc N-S spreading due to the westward subduction of the Philippine Sea Plate and formation of the Philippine Island Arc.

In the North Sinian Period, the amount of shortening was greater in south China and weaker in the north. The percentage of deformation time in the North Sinian Period was longer in the south (36%) and shorter (only 0.6%) in the north. Southern China and the South China Sea were affected by much stronger tectonic activity occupying nearly one third of the North Sinian Period, while in the north deformation took place over a much shorter time span, but there are very little difference in the linear strain rates, $1.29\times10^{-15}$and 6.4×10^{-16}, indicating that the deformation in both areas was rheologic.

As to volcanism in Eocene-Oligocene, i.e. North Sinian Tectonic Period, there is mainly eruption of tholeiites (29 in data, shown in Appendix 7), which is usually recognized by the evolution result of oceanic lithosphere mantle (Chi JS, 1988). The tholeiites and some alkali-basalts (6 in data) intruded in faults to form the dykes or small intrusions, and erupted on the surface to form the small lava sheets and flows. There is no large igneous province (LIP), found in eastern China in Cenozoic. So Chi JS (1988) pointed that there is "intraplate type" of Cenozoic magmatism in eastern China.

Depending on the deduced data of original depth from basic magmatic rocks and their mantle xenoliths (Appendix 7), the tectonic detachment in lithosphere during Eocene–Oligocene Periods was discussed (Wang and Wan, 2008). Most of magmatic source depths are estimated by the value of t-$^{86}Sr/^{87}Sr_{i,}$ isotopic ratio of oxygen or lead, ratio of MgO–ΣFeO / (ΣFeO +ΣMgO) for biotite or ratio of TiO_2-Al_2O_3 for amphibolite, rare earth elements assemblage and other litho-chemistry characteristics. Thus, the lithosphere tectonic detachments positions and mechanism of eastern China during Eocene–Oligocene Periods can be preliminarily researched.

According to Appendix 7 and Fig. 9.6, it can be shown that the most of magmatic sources formed near the intersection of branch faults and the bottom of lithosphere, only a few (just two) originated in crust. The Tancheng–Lujiang fault zone (5 in Fig. 9.6) is NNE trending and the most important lithospheric fault in eastern China (Wan TF et al., 1996; Niu ML et al., 2001; Sun XM et al., 2005). However, obvious detachments did not all form and the basaltic magmatic sources did not all occur everywhere in the intersection of that fault zone and bottom of lithosphere. Actually, most of them only originated from fault intersections of NNE, E-W trending faults and bottom of lithosphere, in which near the intersections of Tancheng–Lujiang fault zone and its cross cut extension faults (Xialiaohe–Chifeng and Penglai–Beijing faults) (6 and 7 in Fig. 9.6) the magmatic sources are easy to form. They may be formed by subduction of Pacific Plate first towards the China continent, caused that to form near E-W trending shortening and N-S trending extension, and then resulted in that obvious dextral strike-slip and reverse movements occurred in NE and NNE trending faults and sinistral strike-slip and normal movements happened in NW or E-W trending faults (Wan TF and Zhao WM, 2002; Wan TF, 2004). Usually, NNE

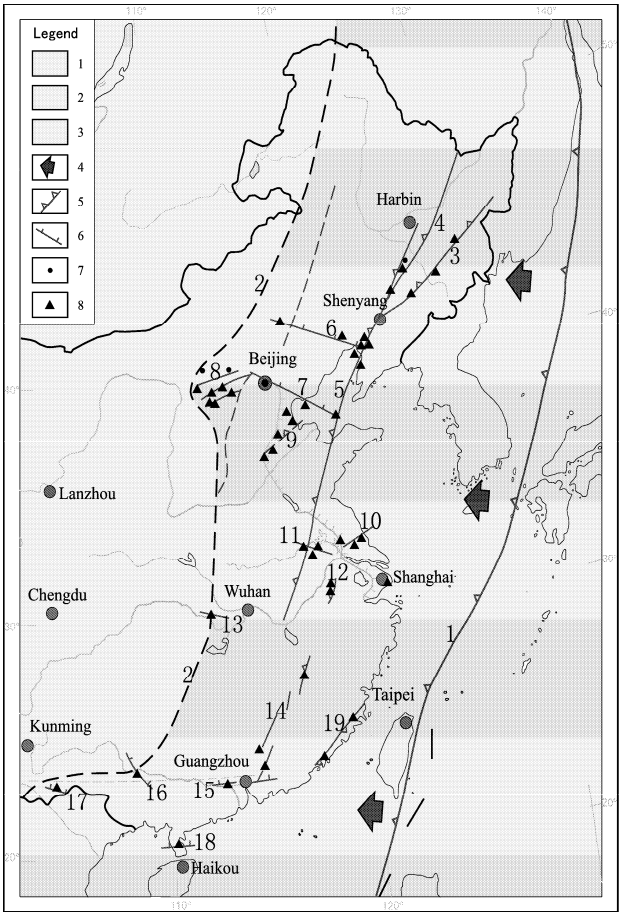

Fig. 9.6 Distribution of magmatic source areas and faults near the bottom of lithosphere during North Sinian Period (52–23 Ma) in eastern China (Wang YM and Wan TF, 2008)

Numbers of legend: 1. continental crust area with weak magmatism; 2. continental crust area with strong magmatism; 3. oceanic crust; 4. plate compression direction; 5. subduction zone or thrust; 6. strick-slip and normal fault; 7. magmatic source depth data in crust(data shown in Appendix 7); 8. magmatic source depth data near the bottom of lithosphere (data shown in Appendix 7).

Numbers of faults: 1. predicted subduction zone between continental and oceanic crusts (Japan Islands should be located west to this zone, here never reconstructed); 2. the border between weak and strong magmatism areas; 3. Dunhua–Mishan reverse fault; 4. Yilan–Yitong reverse fault; 5. Main Tancheng–Lujiang reverse fault zone; 6. Xialiaohe–Chifeng fault; 7. Penglai–Beijing fault; 8. Datong, northern Shanxi NE trending fault zone; 9. Huanghua–Puyang normal fault zone; 10. Northern Jiangsu NE trending normal fault; 11. Jiashan normal fault; 12. Jintan reverse fault; 13. Jianglin normal fault; 14. Nanfeng fault zone; 15. Sanshui–Heyuan–Lianping normal fault; 16. Mashan, Guangxi normal fault; 17.Maguan, Yunnan normal fault; 18. Qiongzhou normal fault; 19. Changle–Nan'ao normal fault.

trending faults are compressed and rather close, only the intersections of NNE lithosphere faults and their cross cut extension faults are easy to form the partial decrease pressure positions, and then brought about the magmatic sources. It may be the reason why the volcanic rocks in Eocene–Oligocene were not very widely distributed in eastern China continent.

9.2 Development of the Eastern Basins and Accumulations of Oil and Gas

E-W shortening and N-S extension in the regional stress field caused major intraplate deformation in the Chinese continent, represented by E-W or WNW normal, extensional and detachment faults: the Xar Moron River dextral strike-slip and normal fault zone (14 in Fig. 9.3); Ji'ning–Gubeikou normal fault zone (15 in Fig. 9.3); the southernmost Yinshan–Daqingshan–Yanshan normal fault (16 in Fig. 9.3); the Guangrao–Jiyang normal fault, i.e. southernmost fault in the Bohai Bay hydrocarbon basin (17 in Fig. 9.3); the Wuhe–Huaiyuan normal fault (21 in Fig. 9.3); the Luoning–Luoyang normal fault (22 in Fig. 9.3); the Luonan–Fangcheng normal fault (23 in Fig. 9.3); Baoji–Tianshui normal fault zone (24 in Fig. 9.3); the Fangxian–Xiangfan–Guangji normal fault zone (26 in Fig. 9.3); the Nanling E-W normal fault system (26 in Fig. 9.3); the Maoming N-S depression (27 in Fig. 9.3); the Derbugan–Kelameili normal fault zone (28 in Fig. 9.3); the southernmost normal fault of the Nilek–Turpan–Hami fault zone (29 in Fig. 9.3); the northern border of the Alxa normal fault zone (36 in Fig. 9.3); the Korla–Wuqia normal fault (37 in Fig. 9.3); the southernmost normal fault of the Junulshan–Qinghai Lake fault zone (northernmost Qaidam zone) (38 in Fig. 9.3); the Northern Kunlun (southernmost Qaidam Zone) normal fault (40 in Fig. 9.3); the Kongkela–Tanggula–Wenquan normal fault (42 in Fig. 9.3); the Bangongco–Dongqiao normal fault (43 in Fig. 9.3); the E-W trending South China Sea extensional fracture zone (46 in Fig. 9.3). These E-W faults sometimes occur as a series of step faults and form the margins of dustpan-shaped basins with great thickness (thousands of meters) of terrestrial clastic deposits of fluvial-lacustrine facies, and sometimes with gypsum-salt beds containing reservoirs of oil and gas.

The Eocene–Oligocene was not only the main period for the formation of petroleum source in China (including the marginal shallow seas), but also the main period of petroleum migration and accumulation. E-W or WNW trending normal faults formed the main conduits for petroleum migration, and adjacent structures (i.e. small reverse drag anticlines, growth faults, dense fissure belts and so on) formed traps favourable to the accumulation of petroleum. The unconformity at the top of the Paleogene tectonostratigraphic unit represents a phase of very weak deformation before the deposition of the overlying Neogene system, which includes caprocks favourable to the formation and preservation of petroleum reservoirs, e.g. the Shengli Oil Field in the Jiyang fault-depression of Shandong and the Bohai oil fields in the fault-depression of central Bohai Bay.

Xu J (1994) estimated the amount of N-S extension in the North China Plain during the Paleogene to be 25–29 km. Tian ZY et al. (1996) estimate the amount of N-S extension in Bohai Bay during the Paleogene to be 25–70 km, with an extension ratio of 15%–40%, 70% of this extension occurred along a detachment (décollement) forming the margin of the basin. From the preparation of seismic profiles Lu KZ et al. (1997) estimated that the amount of extension in the Bohai Basin during the Paleogene was 15–25 km, with an extension ratio of 30%. The amount of vertical displacement on the faults in the Bohai Basin during the Cenozoic is up to 8–10 km. This basin has the largest amount of depression and extension in the eastern Chinese continent.

During the North Sinian Period basalts were commonly intruded along E-W and WNW trending normal faults, such as the Huimin sag of Shandong (forming ~40.7 Ma) (Fig. 9.7), the Beijing plain (66.1–29.9 Ma), north of Jiangsu (55.9–34.6 Ma), Qianjiang of Hubei (52–46.5 Ma), and Maoming of Guangdong (49–45 Ma). Basalts injected into E-W or WNW faults commonly give rise to high positive magnetic anomalies, which can be traced across unexposed areas with the same orientation. The basalt is a distinctive tholeiitic basalt, with a bimodal character, composed mainly of oceanic mantle material, with an $^{87}Sr/^{86}Sr$ initial ratio between 0.703 and 0.705, but may not contain peridotite inclusions from the base of the lithosphere. Although many of the features of the chemical composition of this kind of basalt are analogous to ocean-floor basalt, it is generally considered that they are related to the formation of continental extensional fracture systems (Wu LR et al., 1984: Chi JS et al., 1988).

In eastern China there are three E-W extensional fault zones: (1) the southern footwall of the Yinshan–Daqingshan–Yanshan normal fault (Figs. 9.8 and 9.9; 16 in Fig. 9.3); (2) the normal fault zones at the southern and northern fronts of the Qinling–Dabie Mountains (7 in Fig. 9.2) including the

Wuhe–Huaiyuan normal fault (21 in Fig. 9.3); the Luoning–Luoyang normal fault (22 in Fig. 9.3); the Baoji–Tianshui normal fault zone (24 in Fig. 9.3); the Fangxian–Xiangfan–Guangji normal fault (25 in Fig. 9.3); (3) the E-W trending Nanling normal fault zone (26 in Fig. 9.3). Three mountain ranges were formed by N-S trending extension: Yinshan–Yanshan, Qinling–Dabieshan and Nanling (Fig. 9.8). These ranges are bounded along one or both sides of normal faults. The Yinshan–Yanshan (Y in Fig. 9.8) and Qinling–Dabieshan (Q in Fig. 9.8) ranges are great metamorphic core complexes in China, uplifted as the result of N-S extension, while the Nanling (N in Fig. 9.8) area includes large outcrop of granite bodies.

Differences in crustal density were probably responsible for the uplift of the Yinshan–Yanshan, Qinling–Dabieshan and Nanling mountain ranges and the depression of the surrounding basins under the influence of N-S extension (Fig. 9.8). The Yinshan–Yanshan, Qinling–Dabieshan and Nanling uplifted blocks underwent strong tectonism during their geological history, and they include many highly fractured rocks and many granite intrusions, giving them a low density. These three zones are the "latitudinal tectonic zones", defined by Li SG (1929, 1947, 1962) and related to variations in the rotation velocity of the Earth. However, Shi YL (1976) calculated by stress analysis that changes in the rate of the Earth's rotation velocity are not strong enough to cause deformation of the Earth's crust. However, in 1940's isotopic dating was not available, demonstrating that it is not sensible to study tectonic belts unless they could be related to a reliable time frame. E-W trending mountain belts occur only in the eastern part of the Chinese continent, resulting from N-S extension and E-W compression due to the westward subduction of the Pacific Plate; however in the western part of the Chinese continent these effects are very weak.

The three E-W mountain ranges divide the eastern part of the Chinese continent into four drainage basins: (1) the Songhuajiang–Nenjiang, Yanji, Liaohe and Erlianhot basins north of the Yinshan–Yanshan (A of Fig. 9.8); (2) the Yellow River drainage basin between the Yinshan–Yanshan and Qinling–Dabieshan ranges, forming the Hetao and Guyang (Inner Mongolia), the Weihe of Shaanxi, Jiyang, Huimin, Dongying and Laiwu of Shandong, Qikou of Tianjin, Nanbu of Eastern Hebei and central Hebei, the Kaifeng, Zhoukou, Nanyang of Henan Province, and the Suxian and Hefei basins of An-

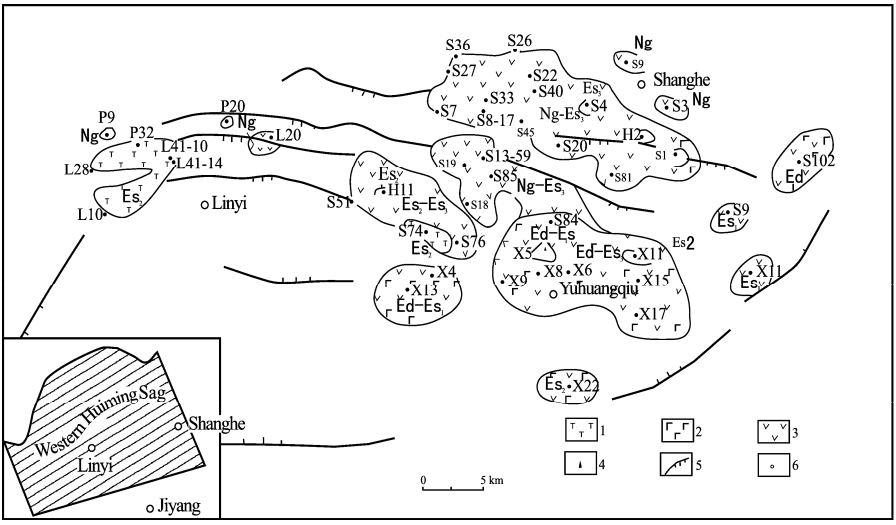

Fig. 9.7 WNW trending faults and the distribution of tholeiites in the Paleogene at Huimin sag of Shandong (Liu ZR et al., 1988, with permission of Liu ZR). The eroded tholeiites form oil reservoirs.

Legend: 1. basalt-porphyrite; 2. pyroxenite; 3. basalt; 4. volcanic breccia; 5. fault; 6. well position.

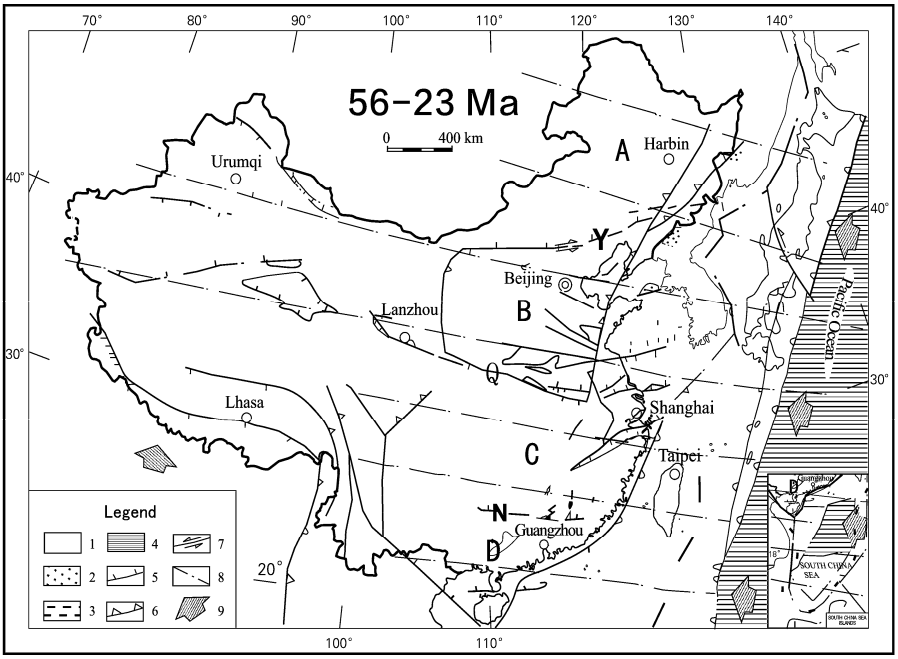

Fig. 9.8 Tectonics and landforms in the North Sinian Period.

1. Mountainous areas; 2. Sedimentary basins; 3. Shallow seas; 4. Ocean; 5. Normal fault; 6. Reverse fault; 7. Strike-slip fault; 8. Trace of axes of maximum principal compression stress; 9. Direction of plate movement.

A. Songhuajiang–Liaohe drainage basins and interior drainage basin of Inner Mongolia; B. Yellow River drainage basin; C. Yangtze River drainage basin; D. Zhujiang River drainage basin. Y. Yinshan-Yanshan Mountains; Q. Qinling–Dabie Mountains; N. Nanling Mountains.

hui (B in Fig. 9.8); (3) the Yangtze River drainage basin, between the Qinling–Dabieshan and Nanling ranges, forming the Jianghan, Lake of Dongting, Lake of Poyang, the northern Jiangsu, southern Yellow Sea and the mouth of the Yangtze River basins (C in Fig. 9.8); (4) the Zhujiang River drainage basin, south of the Nanling range, forming the Sanshui, the mouth of Zhujiang, Nanning, and the Guangxi basins (D in Fig. 9.8). In the North Sinian Period coherent drainage systems did not develop throughout the area, these basins formed a series of separate lake basins, with scattering independent drainage systems (Wan TF, 1994).

During the North Sinian Period there were no high mountains or plateaus in the whole of the Chinese continent, including the western part. The sites of the present Tianshan and Qilianshan Mountains were occupied only by low mountains and hills. At this time the Tarim and Qaidam basins formed a broad continuous area of sedimentation, as they were not yet separated by the Altun Mountains, which were uplifted later by movements along a large scale strike-slip fault (Ge XH et al., 1990). There was a relict sea in the southwestern part of the Tarim area, connected to the Neo-Tethys and the Paleo-Mediterranean Sea. The Eocene and Oligocene system contains abundant fossils and according to geological records of the fauna and flora all the provinces of China were deposited in a similar ecological environment with warm and moist climate.

After the eastern part of the Chinese continent developed a pattern of E-W mountain ranges and basins in the North Sinian Period, the moist monsoon derived from Pacific Ocean was able to travel

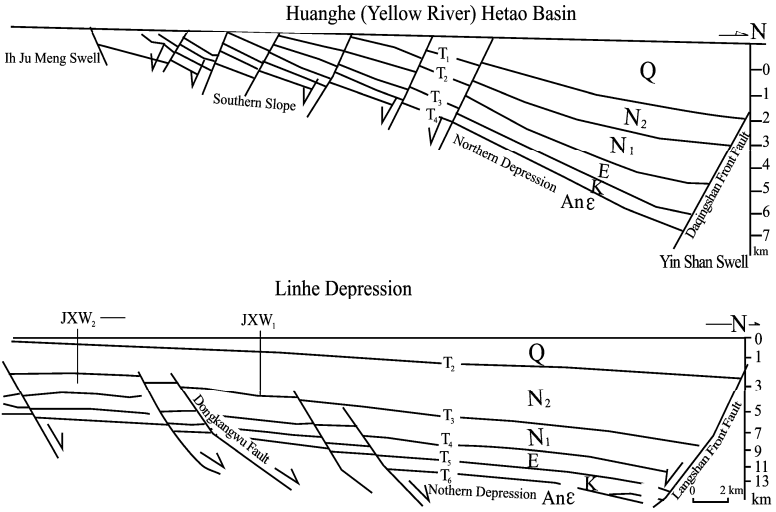

Fig. 9.9 Seismic profiles in the Hohhot and Linhe sags of Hetao area on the southern side of the Daqingshan in Inner Mongolia (Bureau of Geology and Mineral Resources of Inner Mongolia, 1991).

from east to west across the whole of China. The hot and arid environment, which occupied most of the Chinese continent in the Cretaceous, was changed during the Eocene-Oligocene Period to a warm and damp climate, favorable to the proliferation of animals and plants. In the North Sinian Period the Chinese continent enjoyed the most favorable ecological environment in its geological history. This was the major epoch for the generation and accumulation of petroleum in China and also one of the main periods for the formation of coal deposits. In the exploration and exploitation of fossil fuel resources an understanding of tectonic developments during the North Sinian Period is of vital economic importance.

9.3 Formation of the Western Pacific Subduction Zone and Yarlung Zangbo Collision Zone

The Western Pacific subduction zone, a system of trenches and island arcs extending from the Aleutians through Kuril, Japan, Ryukyu and Taiwan to the Philippines, forming a major feature of global tectonics at the present day, initiated in the Middle Oligocene. This was the second period in which an oceanic plate occupying the Pacific Basin was subducted beneath eastern Eurasia, compressing eastern Chinese continent. Relics of oceanic lithosphere and tectonic mélanges of Eocene–Middle Oligocene age are observed in the accretion complex of the Shimanto Belt in the southern part of the Japanese Islands (Okamura, 2001). This accretionary belt extends southwards into the Yuli–Shoufeng Subduction Zone in Taiwan. Some researchers recognized that the subduction probably commenced at 87–60 Ma, but intense tectono-magmatism and metamorphism in Taiwan is dated isotopically as occurring between 40 and 30 Ma. Rb-Sr and K-Ar isotopic ages of metamorphic minerals in the Tailuko Belt on the western side of the Yuli–Shoufeng Subduction Zone show that metamorphism took place between 35 and 40 Ma (Chen Z, 1984; Jahn et al., 1986). Andesites in the eastern Coastal Mountain Range of Taiwan, interpreted as the volcanic arc related to subduction have been dated at 29.7 Ma (Stephan et al., 1986), indicating that subduction continued until the mid-Oligocene. Because of this subduction, the rate of E-W shortening in eastern Taiwan was ~7 cm/yr, the most rapid in the Chinese continent.

Initiation of the trench-arc system from the Aleutians to the Philippines in the Western Pacific was related to a sudden change in the direction of movement of the Pacific Plate. From isotopic dating and the study of ocean floor magnetic anomalies around the Hawaii–Emperor Seamount Ridge (Clague et al., 1972; Uyeda et al., 1974; Seno et al., 1977, 1984; Maruyama et al., 1986; Stephan et al., 1986), it has been established that between 40 and 36 Ma the direction of movement of the Pacific Plate changed from the NNW to the WNW (Figs. 7.7 and 15.1). The rate of westward movement of the Pacific Plate was up to 9 cm/yr. The subduction of the Pacific Plate led to the formation of the Aleutian–Kuril–Japanese–Ryukyu–Taiwan–Philippine arc-trench system and Izu–Bonin–Mariana (IBM) arc-trench system, with the Philippine Sea Plate lying between them.

At the same time the western part of the Chinese continent was affected by the northward movement of the Indian Plate, with subduction of the intervening oceans leading to the collision of India with Eurasia (Figs. 8.6, 9.5 and 9.10). Lee TY and Lawver (1995) and Royden and Burchfiel et al. (1997) used data from ocean floor magnetic lineation and ocean drilling to trace the northward movement of the Indian Plate. Oceanic lithosphere was subducted continuously beneath Eurasia, but the process of subduction gradually slowed. The rate of northeastward movement of the Indian Plate reduced from an initial 17 cm/yr to about 10 cm/yr between 60 and 45 Ma, Lee TY and Lawver (1995) named this process "soft collision". Since 45 Ma, the northeastward rate of movement of the Indian Plate decreased further to 6 cm/yr, they named this process "hard collision" (Figs. 8.8 and 8.9). During the Paleogene the Indian Plate moved northwards about 1,100 km, from near the equator to about latitude 11°N (Klootwijk and Radhakriehnamurty, 1981).

In the period between 60 and 45 Ma the oceanic lithosphere to the north of the Indian Plate was subducted beneath the Eurasian Plate at a reduced rate of 10 cm/yr, but without continent-continent collision. From 45 to 22 Ma with a reduced rate of movement (6 cm/yr), the period of really "hard collision", the oceanic lithosphere was gradually subducted completely leading to continent-continent collision in the Late Eocene–Early Oligocene (about 34 Ma) (Aitchison et al., 2001, 2004, 2007).

The Yarlung Zangbo River–Indus River Collision Belt is the major boundary between the Indian and Eurasian plates. The collision belt includes ophiolite suites, Triassic flysch and Cretaceous–Oligocene mélange. Outcrops of the Yarlung Zangbo River ophiolite suite are distributed over a very wide area near Xigaze and extend E-W as a ribbon of 170 km long and 2–20 km wide (Tapponnier et al., 1981; Allègre et al., 1984). Within the collision belt bedding, schistosity and fault planes dip steeply either to the north or south on the earth surface. The former consensus was that collision between Indian and Eurasian continents occurred during the Paleocene (Tapponnier et al., 1981; Allegre et al., 1984; Besse et al., 1984). However, Aitchison et al.(2001, 2004, 2007) and Wang CS et al.(2002) found Late Oligocene radiolaria in pelagic cherts associated with the ophiolite suite of Yarlung Zangbo River, showing that oceanic crust survived to the north of India until the Late Oligocene (~34 Ma), and that the final collision did not occur until this date.

The Indian Plate finally collided with Eurasia (Gangdise or Lhasa block) at a late period of the Eocene (i.e. about 34 Ma) in the Yarlung Zangbo River Collision Zone (Aitchison et al., 2007). However, on the basis of paleomagnetic data from the 90°E Ridge, Klootwijk et al. (1991) considered that the Indian Plate collided with the Kohistan Block (i.e. equal to Gangdise Block of Tibet), in the western Himalayan syntaxis in northern Pakistan at ~ 50 Ma, and this date is not very well constrained. Searle (1991) suggested that this collision occurred before 37 Ma. Ding L et al. (1999; 2001) found that the main metamorphic period for the formation of garnet, kyanite and high pressure granulite in the eastern Himalayan syntaxis (Namjagbarwa area) was 69–40 Ma, he did not show CL images of the zircon grains used for U/Pb dating, it is difficult to evaluate Ding et al.'s data. However, recently, Liu Yan et al. (2007) discovered the age of 30–33 Ma at the rim domains of zircon crystals in recrystallizing high pressure felsic granulites by SHRIMP U/Pb analyses (at the mantle domains of zircons, got 515±35 Ma of U/Pb isotopic age, which is the metamorphic age derived from Proterozoic sedimentary rocks). Depending on the above recent isotopic data, it can be seen that the Yarlung Zangbo River Collision Zone formed at 30–37 Ma.

There is a swarm of WNW trending diabase dykes at southern Yamzhoyumco in the Himalayan Block. Their chemical composition indicates a rate of N-S extension of 1.1 cm/yr in that area.

The Paleogene continent-continent collision between the Indian and Eurasian plates affected the adjacent areas. Because in the Indosinian, Sichuanian and North Sinian Periods the directions of maximum principal compressive stress in Qinghai–Tibet were all approximately N-S trending, during later tectonic events earlier folds were more intensely compressed, and movement occurred readily along earlier fault planes, with little change in orientation. In this case, in order to separate the tectonic results at different periods, it is necessary to make careful, thorough, detailed structural studies. At present, the data is not sufficient to resolve this problem. Nevertheless it is possible to put forward some propositions.

Broad open folds in Cretaceous–Paleocene strata, with near E-W or WNW trending axes are the result of N-S shortening. Guo TY et al. (1991) first pointed out that in the Ngari area of Xizang, weak folds with an N-S axial trend are superimposed on these folds. Because Cretaceous and Paleocene systems are involved in the later folding, it is supposed that these folds were formed during the Middle Miocene. Similar phenomena occur in the Turpan and Hami oil fields in the Xinjiang Uygur Autonomous Region (Zheng YD, 1989, personal communication). It is evident that in western China deformation due to E-W compression and shortening during the North Sinian Period was weaker and later than in eastern China.

In the Taniantaweng area, adjacent to the Nujiang Fault Zone, movements along the fault zone changed from sinistral to dextral, with a reverse component, between 42.5 and 30 Ma. The western side of the fault moved northward under the influence of the collision, and the continued northward movement of the Indian Plate (Wang GH et al., 1996).

There are a large number of collision-related igneous intrusions on both sides of the Yarlung Zangbo River Collision Belt and in Gangdise–Nyainqentanglha Zone, north of the Himalaya. Some of these intrusions are small stocks or diapirs originating from remelted continental basement by compression, with the assimilation of migmatite and gneissose migmatitic granite. The isotopic ages of all these intrusions are between 50 and 20 Ma (Bureau of Geology and Mineral Resources of Xizang (Tibet) Autonomous Region, 1993). During the same period bimodal volcanic rocks of the Linzizong Group and the Nadingco and Dazuka formations, inter-bedded with alternating clastic sediments of marine and terrestrial facies, were erupted. Rates of intraplate shortening, determined from the composition of the igneous rocks, were most rapid in western Yunnan (6.6 cm/yr), Gangdise (5.8 cm/yr) and the Himalayas (6.3 cm/yr).

Because of compression due to the northward movement of the Yarlung Zangbo River Collision Belt, there was little magmatic activity in north Qiangtang. Volcanic rocks of the calc-alkaline series, with a high potassium content, were erupted between 44.66–35 Ma and there were high potassium granite intrusions between 29 and 24 Ma (Chi XG et al., 1999). It means that there was an intraplate magmatism at north Qiangtang during those epochs. The effects of the collision of India and Eurasia were weaker in the more northerly and easterly areas of the Chinese continent.

In recent years, Liu ZF et al. (2000) restudied the Feng Volcanic Group (56–33.2 Ma) and the Yaxico Group (33.2–30 Ma) covering an area of 100,000 km^2 in the Hohxil continental sedimentary basin between the Tanggula and Kunlun Mountains. The balanced cross section method was used to calculate the magnitude and ratio of N-S shortening at the Paleogene (equivalent to North Sinian Tectonic Period) as 53.1 km and 42.8%.

Tapponnier et al. (1986, 1990) suggested that the southeastward movement of the Indochina Plate was due to the northward movement of the Indian Plate, with its collision and indentation of the southern margin of the Eurasian Plate. As reported above, the rate of northeastward movement of the Indian Plate had decreased to 6 cm/yr during the period of 45–22 Ma. According to Tapponnier et al. (1986, 1990), between 30 and 20 Ma the sinistral Red River–Jinshajing strike-slip fault zone was generated by this movement, with a displacement of 500 km at a rate of 5 cm/yr. If movement along the zone was controlled only by the northward migration of the Indian Plate, it should have had a dextral strike-slip movement, similar to the Nujiang Fault. However, the Red River–Jinshajiang Fault certainly behaved as a sinistral strike-slip fault at that time, so that the explanation of Tapponnier et al. (1986, 1990) is incorrect. In recent years there has been a tendency between both Chinese and foreign scientists to

attribute all the deformation in the Chinese continent to the effects of the collision and the continued northward movement of the Indian Plate, and to ignore other possible causes. The author considers that movements along the Red River–Jinshajing Fault Zone in the North Sinian Period were controlled by the tectonic system which affected the eastern Chinese continent, where E-W compression generated NW-trending sinistral strike-slip faults.

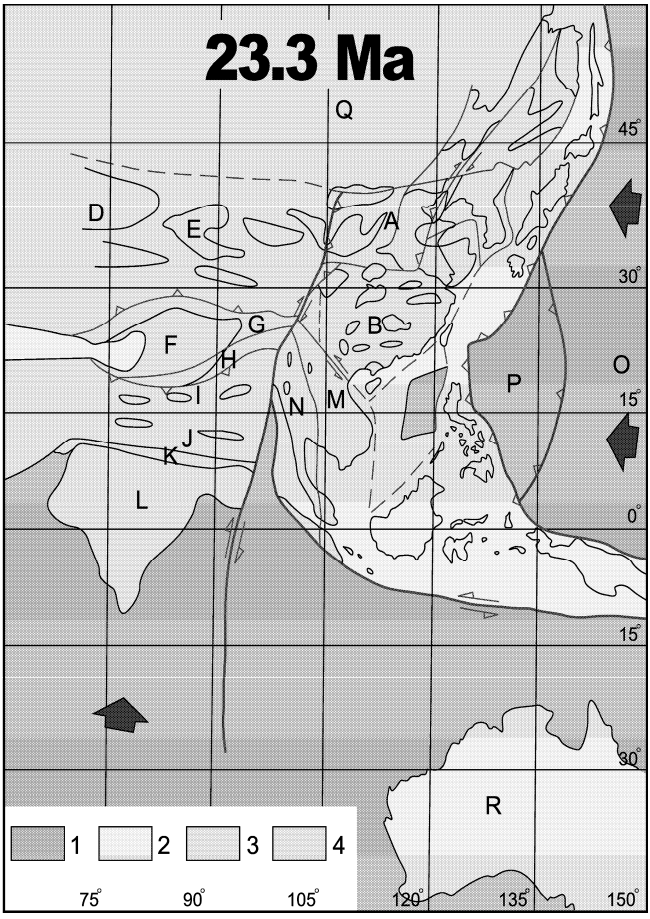

Fig. 9.10 Paleo-tectonogeographic reconstruction of China and its adjacent blocks in the Late North Sinian Period (23 Ma).

1. Ocean: 2. Shallow and inland seas; 3. Humid basin with terrestrial facies; 4. Hills and low mountains (Index letters are the same as in Fig. 6.5). The paleomagnetic data and central reference points of the blocks are listed in Appendix 6.

A paleogeographic reconstruction has been prepared from paleomagnetic data (Fig. 9.10; Appendix 6). From the Jurassic to the present day the paleomagnetic declination in the eastern Chinese continent has not varied by more than 10°, and it is possible that some of the apparent variations are due to errors in measurement. During the late North Sinian Period there was little change in the latitude of the eastern Chinese continent, but there were obvious changes in the position of Qinghai–Xizang (Tibet).

The direction of magnetic north in the Qiangtang, Gangdise and Himalayan blocks and Indian Plate was about NW340°–350° and these blocks continued to move in an NE10°–20°direction. The Gangdise and Qiangtang blocks moved northward for only a few degrees, but the Himalayan Block, the northern continental margin of India, was at 4.3°S in the Late Cretaceous, but moved to 3°N in the Paleogene and to 25°N in Pliocene. At the same time the Indian Plate moved northward 1,200 km at the rate of 6 cm/yr.

In addition, the formation periods of strong rock deformation areas induced by westward migration of Pacific Plate with nearly N-S trending folding are gradually transmitted in Paleogene and Neogene: beginning of westward migration of Pacific Plate is 34 Ma, formation epoch of western Pacific subduction zone and island arc is about 30 Ma, stronger deformation epoch in Eastern China continent is 23 Ma, and slight deformation epoch in western China (Yunnan, Tibet and Xinjiang) is about 10–15 Ma. It means that westward horizontal migration velocity of strong deformation from Pacific to western China is about 0.65 m/yr. It is a suitable evidence for explanation of quasi-synchronous tectonism.

In the North Sinian Period (56–23 Ma) the tectonics of Chinese continent was first influenced by westward subduction of the Pacific Plate, causing the compression in eastern China and the intraplate deformation of the North Sinian Tectonic System. This resulted in the uplift of three E-W trending mountain ranges and the formation of four large drainage basins in eastern China. However, in western China rock deformations formed during this period record the influence of the northward movement of the Indian Plate and the formation of the Yarlung Zangbo Collision Belt.

References

Aitchison JC, Davis AM (2001) When did the India–Asia collision really happen? In: International Symposium and Field Workshop on the Assembly and Breakup of Rodinia and Gondwana and Growth of Asia. Osaka City University, Japan. Gondwana Research 4: 560–561.

Aitchison JC, Davis AM (2004) Evidence for the multiphase nature of the India-Asia collision from the Yarlung Tsangpo suture zone, Tibet. In Malpas J et al (eds) Aspects of the tectonic evolution of China. London: The Geological Society. Special Publication 226.

Aitchison JC, Jason RA, Davis AM (2007) When and where did India and Asia collide? JGR 112: B05423

Allègre CJ, Courtillot V, Tapponnier P et al (1984) Structure and evolution of the Himalaya-Tibet orogenic belt. Nature 307: 17–22.

Besse J, Courtillot V, Pozzi JP et al (1984) Palaeomagnetic estimates of crustal shortening in the Himalayan thrusts and Yarlung Zangbo suture. Nature 311 (5,987): 621–626.

Bureau of Geology and Mineral Resources of Inner Mongolia Autonomous Region (1991) Regional Geology of Inner Mongolia Autonomous Region. Geological Publishing House, Beijing (in Chinese with English abstract).

Bureau of Geology and Mineral Resources of Ningxia Hui Autonomous Region (1990) Regional Geology of Ningxia Hui Autonomous Region. Geological Publishing House, Beijing (in Chinese with English abstract).

Bureau of Geology and Mineral Resources of Sichuan Province (1991) Regional Geology of Sichuan Province. Geological Publishing House, Beijing (in Chinese with English abstract).

Bureau of Geology and Mineral Resources of Xizang (Tibet) Autonomous Region (1993) Regional Geology of Xizang Autonomous Region. Geological Publishing House, Beijing (in Chinese with English abstract).

Chen Z (1984) Preliminary analysis of terrene characteristics in Taiwan, China. Oceanic Science and Technology of South China Sea 6: 7–15.

Chi JS (1988) The Study of Cenozoic Basalts and Upper Mantle Beneath Eastern China (Attachment Kimberlites). China University of Geosciences Press, Wuhan (in Chinese with English abstract).
Chi XG, Li C, Jin W et al (1999) Cenozoic volcanic evolution and plateau uplift in northern Xizang. Geological Review 45(Suppl.): 978–986 (in Chinese).
Clague DA, Jarrard RD (1972) Tertiary Pacific plate motion deduced from the Hawaiian-Emperor China. Geol. Soc. Amer. Bull. 84: 1135–1154.
Ding L, Zhong DL (1999) Metamorphic characteristics and geotectonic implications of the high-pressure granulites from Namjagbarwa, eastern Tibet. Science in China D 42 (5): 491–505.
Ding L, Zhong DL, Yin A et al (2001) Cenozoic structural and metamorphic evolution of the eastern Himalayan syntaxis (Namche Barwa). Earth and Planetary Science Letters 192: 423–438.
Gan ZG, Liang EY (1988) Folding formation period in Sichuan Basin and controlling the oil-gas reservoirs. Gas Industry 8(4): 1–6 (in Chinese).
Ge XH, Duan JY, Li C et al (1990) Formation and evolution of Qaidam Basin. Petroleum Bureau of Qinghai & Changchun College of Geology (unpublished reports, in Chinese).
Guo TY, Liang DY, Zhang YZ et al (1991) Geology of Ngari Tibet (Xizang). China University of Geosciences Press, Wuhan (in Chinese with English abstract).
Harrison TM, Leloup PH, Ryerson FJ et al (1996) Diachronous initiation of transtension along the Ailao Shan–Red River shear zone, Yunnan and Vietnam. In: Yin A, Harrison TM (eds) The Tectonic Evolution of Asia. Cambridge University Press, Cambridge.
Huang TK (Jiqing) (1945) On the major structural forms of China. Geological Memoirs, ser. A, no. 20, 165pp.
Huang TK (Jiqing) (1960) The main characteristics of the geological structure of China: preliminary conclusions. Acta Geologica Sinica 40(1): 1–37 (in Chinese with English abstract).
Jahn BM, Martineau F, Percat JJ et al (1986) Geochronology of the Tananao schist complex, Taiwan and its regional tectonic significance. Tectonophysics 125: 103–124.
Klootwijk CT, Radhakrishnamurty C (1981) Phanerozoic paleomagnetism of the Indian plate and India-Asia collision. In: McElhinny MW, Valencio DA (eds) Paleoconstruction of the Continents. Geodynamics Series. Geological Society of America, Boulder, Colorado.
Klootwijk CT, Gee JS, Pierce JW et al (1991) Constraints on the India–Asia convergence: paleomagnetic results from Ninety East Ridge. In: Weissel J, Pierce J et al (eds) Proceedings of the ocean drilling program, scientific results. Texas A & M University Press, College Station.
Lee TY, Lawver LA (1995) Cenozoic plate reconstruction of Southeast Asia. Tectonophysics 251 (1–4): 85–138.
Li CY (1950) Sichuan movement and its distribution in China. Journal of Geological Society of China 30: 1–8.
Li HW, Xu K (2001) The dextral strike-slip faulting of Tan–Lu fault zone and the structural oil fields distribution in Liaohe basin. Earth Science Frontiers 8(4): 467–470 (in Chinese with English abstract).
Li SG (Lee JS) (1929) Some characteristic structural types in Eastern Asia and their bearing upon the problem of continental movement. Geological Magazine 96 (782): 358–375; 96(784): 457–473; 96(785): 501–526. Reprinted in 1976, Geological Mechanics Methods, pp.65–112. Science Press, Beijing (in Chinese).
Li SG (Lee JS) (1947) Fundaments and methods of geological mechanics. In: Geological Mechanics Methods (reprinted in 1976). Science Press, Beijing (in Chinese).
Li SG (1962) An Introduction to Geomechanics. Geological Publishing House, Beijing (in Chinese).
Liu Y, Yang ZQ, Wang M (2007) History of zircon growth in a high-pressure granulite within the Eastern Himalayan syntaxis and tectonic implications. International Geology Review 49: 861–872.
Liu ZR, Xin QL et al (1988) Formation conditions and distribution regularities of oil-gas pools in Tertiary volcanic rocks in the western part of the Huimin depression. Acta Geologica Sinica (3): 210–222 (in Chinese with English abstract).
Lu KZ, Qi JF et al (1997) Tectonic Model of Cenozoic Petroliferous Basin, Bohai Bay. Geological Publishing House, Beijing (in Chinese with English abstract).

Maruyama S, Seno T (1986) Orogeny and relative plate motions: example of the Japanese Islands. Tectonophysics 127: 305–329.

Niu ML, Zhu G, Song ZZ et al (2001) Mantle characteristis and its evolution of Cenozoic basalt source area at middle and southern sections of Tancheng–Lujiang fault zone. Geosciences 15(4): 383–390 (in Chinese with English abstract).

Okamura M (2001) Geology of the Shimanto belt and Quaternary uplift in cape Muroto. In: Geotraverse Across the Major Geologic Units of Southwest Japan. ISRGA Field Workshop (FW-A), pp.17–36.

Qi JF, Chen FJ (1995) Structural Analyses of Cenozoic Fault Basin in Lower Liaohe–Liaodong Bay. Geological Publishing House, Beijing (in Chinese).

Royden LH, Burchfiel BC (1997) Surface deformation and lower crustal flow in eastern Tibet. Science 276(5,313): 788–790.

Schaerer U, Tapponier P, Lacassin R et al (1990) Intraplate tectonics in Asia: a precise age for large-scale Miocene movement along the Ailaoshan–Red River shear zone, China. Earth Planet. Sci. Lett. 97(1–2): 65–77.

Schaerer U, Zhang LS, Tapponier P (1994) Duration of strike-slip movements in large shear zones: the Red River belt, China. Earth Planet. Sci. Lett. 126(4): 379–397.

Searle MP (1991) Geology and tectonics of the Karakoram Mountains. John Wiley & Sons, New York.

Seno T (1977) The instantaneous rotation vector of the Philippine Sea Plate relative to the Eurasian Plate. Tectonophysics 42(2–4): 209–226.

Seno T, Maruyama S (1984) Paleogeographic reconstruction and origin of the Philippine Sea. Tectonophysics 102(1–4): 53–84.

Shi YL (1976) Preliminary analysis on the ε type tectonic stress field. Geomechanis Communication (1): 39–54 (in Chinese).

Stephan JF, Blanchet R, Rangin C et al (1986) Geodynamic evolution of the Taiwan–Luzon–Mindoro belt since the Late Eocene. Tectonophysics 125(1–3): 245–268.

Sun XM, Wang PJ, Hao FJ et al (2005) Time-space distribution, migration and origin type of Mesozoic–Cenozoic regional fault system at middle area of continental margin of Eastern China. Journal of Jilin University (Geosciences) 35(5): 554–563 (in Chinese with English abstract).

Tan XC, Li CY (1948) Geology of Xikang, Sichuan Province. In: Central Geological Survey. Geological Memoirs. ser.A. no.15. (reprinted by Geological Publishing House in 1959, in Chinese).

Tang Z (1979) The structure characteristics of oil-gas field in Eastern China. Oil Exploration and Exploitation (1): 30–37.

Tapponnier P, Mercier JL, Proust F et al (1981) The Tibetian side of the India-Eurasia collision. Nature 294 (5,840): 405–410.

Tapponnier P, Peltzer G, Armijo R (1986) On the mechanics of the collision between India and Asia. In: Coward MP, Ries AC (eds) Collision Tectonics. Geological Society Special Publications, 19: 115–157. Geological Society of London, London.

Tapponnier P, Lacassin R, Leloup PH et al (1990) The Ailao Shan / Red River metamorphic belt: tertiary left-lateral shear between Indochina and South China. Nature 343 (6,257): 431–437.

Tian ZY, Zhang QC (1996) On Oil-bearing and Gas-bearing Sedimentary Basins of China. Petroleum Industry Press, Beijing (in Chinese).

Uyeda S, Miyashiro a (1974) Plate tectonics and the Japanese Islands: a synthesis. GSA Bulletin 85(7): 1159–1170.

Wan TF, Zhu H (1989) Cretaceous–Early Eocene tectonic stress field in China. Acta Geologica Sinica 2(3): 227–239.

Wan TF, Cao RP (1992) Tectonic events and stress fields of Middle Eocene–Early Pleistocene in China. Geoscience 6(3): 275–285 (in Chinese with English abstract).

Wan TF (1994) Intraplate deformation, tectonic stress and their application for Eastern China in Meso-Cenozoic. 156pp. China University of Geosciences Press, Wuhan.

Wan TF, Zhu H, Zhao L et al (1996) Formation and Evolution of the Tancheng–Lujiang Fault Zone. China University of Geosciences Press, Wuhan.

Wan TF, Zhu H (1996) The maximum sinistral strike-slip and its forming age of Tancheng–Lujiang fault zone. Geological Journal of China Universities, 2(1): 14–27 (in Chinese with English abstract).
Wan TF, Cao XH (1997) Estimation of differential stress magnitude in Middle–Late Triassic to Early Pleistocene for China. Earth Science 22(2): 145–152 (in Chinese with English abstract).
Wan TF, Zhao WM (2002) On the mechanism of intraplate deformation in Chinese continent. Earth Science Frontiers 9(2): 451–463 (in Chinese with English abstract).
Wan TF, Zeng HL (2002) The distinctive characteristics of the Sino-Korean and the Yangtze plates. Journal of Asian Earth Sciences 20(8): 881–888.
Wan TF (2004) An Outline of China Tectonics. Geological Publishing House, Beijing (in Chinese).
Wang CS, Li XH, Hu XM et al (2002) Latest marine horizon north of Qomolangma (Mt. Everest): Implications for closure of Tethys seaway and collision tectonics. Terra Nova 14: 114–120.
Wang GH, Zhou X, Pubuciren et al (1996) Structures and Its Evolution of Taniantaweng Mountain Chain in Xizang. Geological Publishing House, Beijing (in Chinese).
Wang MM et al (2003) Petroleum prospecting region and target assessment around Bohai Bay areas. Unpublished report for Exploration and Research Institute of China National Petroleum Corporation.
Wang YM, Wan TF (2008) Lithosphere tectonic detachments in Eastern china control of Cenozoic magmatism and earthquake. Geoscience 22(2): 207–229 (in Chinese with English abstract).
Wu HW, Zhang LS, Ji SC (1989) The Red River–Ailaoshan fault zone—a Himalayan large sinistral strike-slip intracontinental shear zone. Scientia Geologica Sinica (1): 1–8 (in Chinese with English abstract).
Wu LR (1984) Meso-Cenozoic Volcanic Rocks in East China and Adjacent Areas. Science Press, Beijing (in Chinese).
Xu J, Liu GD, Han ZJ et al (1994) Discussion on the WNW trending Cenozoic fault-depression basin system at North China and East China Sea of eastern Chinese continent. Institute of Geology, National Seismological Bureau: Recent Geodynamic.
Zhang GW, Zhang BR, Yuan XC et al (2001) Qinling Orogenic Belt and Continental Dynamics. Science Press, Beijing (in Chinese).
Zhong DL, Ding L (1993) Analyzed dispersion of Gondwana continent and accretion of Asia from the evolution of Tethys belt in Sanjiang and adjacent areas. In: China Working Group on International Geological Comparison Program, Project 321. Growth of Asia. Seismological Press, Beijing (in Chinese).
Zhong DL (1998) Paleo-Tethyan Orogenic Belt in Western Yunnan and Sichuan. Science Press, Beijing (in Chinese).

Chapter 10
Tectonics of Miocene–Early Pleistocene (The Himalayan Tectonic Period, 23–0.78 Ma)

The Himalayan movements were first recognized by Huang TK (1945) correlated with the New Alpine movements of Europe. At the time of Huang's studies in France during the 1930s, it was considered that the Alpine Orogeny had occurred in two phases, an "Old Alpine" (Mesozoic) phase and a "New Alpine" (Cenozoic) phase, however, he did not think so recently. Huang considered that the Himalayan movements should include all the tectonic events occurring during the Cenozoic. This view has commonly been accepted and applied in China over last sixty years. However, as described in earlier chapters in this volume, both the Sichuanian and North Sinian Tectonic Events occurred within the Cenozoic. In the early Mesozoic the Himalayan and adjacent continental blocks were attached to Gondwana. Subsequently these blocks were separated from Gondwana and moved gradually northwards until they converged and collided with the southern margin of Eurasia in the Banggongco–Nujiang and Yarlung Zangbo Collision Zones. In the Siuchuanian and North Sinian stages the separated blocks still lay within the Tethys Ocean, right to the south of Asia. The collision zones, which resulted in the Himalayan Tectonic Zone and the Himalayan Mountains, did not form until the Neogene.

The "Himalayan Tectonic Period" is properly applied to the strongest deformation, which resulted in the formation of the Himalayan Mountains during the Neogene and Early Pleistocene (Wan TF, 1994), which is really an orogenic period. Because in China the contacts between Neogene and Early Pleistocene systems are conformable, with no evidence of a tectonic event at their boundary, the Neogene and Early Pleistocene epochs are considered to constitute a single tectonic stage. Due to the formation of Himalayan Mountains and the uplift of the Qinghai–Xizang (called Qingzang or Tibet) Plateau, and the consequent erosion, the Siwalik Molasse Group was deposited in the foreland basin to the south of the Himalaya Mountains and similarly the Xiyu (quasi-) Molasse Group was deposited at the foot of the Kunlun and Tianshan Mountains, the Yumen conglomerate formation to the north of the Qilianshan and the Ya'an conglomerate formation in western Sichuan. These coarse molasse groups were formed mainly during a late stage of the Neogene and in the Early Pleistocene. All these molasse formations are folded and are overlain unconformably by Middle Pleistocene sediments.

10.1 Thin-skinned Tectonics, the Formation of the Himalayan Thrust Zone and the Uplift of the Qinghai–Xizang (Tibet) Plateau

At the late epoch of the Paleogene (about 37–30 Ma), collision between the Indian and Eurasian plates occurred, forming the Yarlung Zangbo Collision Zone and making the oceanic crust disappear (Fig. 10.1 and 3 in Fig. 10.4). Further convergence in the Neogene led to the development of the Himalayan Thrust Zone to the south, with shortening in a "thin-skinned" tectonic system. There are three major thrusts from south to north: the Main Boundary Thrust (MBT in Fig. 10.1; 6 in Fig. 10.3; 1 in Fig.

10.4,), the Main Himalaya Thrust (MHT in Fig. 10.1; 6 in Fig. 10.3; 2 in Fig. 10.4), and the Main North Thrust (MNT in Fig. 10.1) or Kangmar (KT) (Tapponnier et al., 1981; Allègre et al., 1984). The Main Boundary Thrust and the Main Himalaya Thrust occur to the south of the watershed of the Himalayan Mountains in Nepal, Bhutan and India, and have rarely been studied by Chinese geoscientists.

The main thrust planes of Himalayan Thrust Zone all dip to the north at low or intermediate angles, with the hanging wall overthrust towards the south. The rocks form an imbricate thrust system striking E-W, which includes zones affected by low and intermediate grade dynamo-metamorphism of greenschist, amphibolite, sillimanite and glaucophane facies. Tight folding and metamorphism occurred during the Miocene and Pliocene (Sinha-Roy, 1982; Allègre et al., 1984). However, Searle (2007) discovered that Main Himalayan Thrusts were changed to low angle normal faults or called detachments at present time. It is very similar to what the author observed at the top of Alps Mountains of Italy in 2004 and at Eastern Himalayan Syntaxis in 2009, where the most of thrusts are changed to normal faults at low or intermediate angle recently.

Over the last twenty years many methods of isotopic chronology have been used to determine the time at which thrusting took place, and ages between 23.5 and 16.8 Ma have been obtained: 23.5 Ma by U/Pb (Tapponnier et al., 1990); 17 Ma by Ar/Ar (Copeland and Harrison, 1990); 18.5 Ma by Ar/Ar and Apatite fission track (AFT) (Copeland et al., 1987); 16.8 Ma by the AFT method (Corrigan and Crowley, 1992). Similar ages were obtained by the Bureau of Geology and Mineral Resources of Xizang (Tibet) Autonomous Region (1993) by isotopic methods and using geological criteria. In northern Pakistan, in the northwestern Himalayan syntaxis, movements of the Main Mantle Thrust occurred earlier, between 45 and 20 Ma (Chamberlain and Zeitler, 1996). In the eastern Himalayan or the Namjagbawa syntaxis, the youngest metamorphic ages are between 23 and 18 Ma (Ding L and Zhong DL, 1999). Isotopic dating shows that movements in the Himalayan Thrust Zone commenced in the Early Neogene.

The amount of displacement along the Main Central Thrust is estimated by several researchers to be 80–115 km using the shear strain method (Sinha-Roy, 1982). However, this may be an underestimate. According to paleomagnetic data, the central reference point for the Indian Plate moved from latitude 11°N to 21°N during the last 22 million years (Appendix 6). From the convergence of the Indian and Eurasian plates, and estimations of the amounts of movement along the Himalayan thrust zones the displacement of India has been estimated to be ~1,000 km (Klootwijk and Radhakriehnamurty, 1981; Lee TY and Lawver, 1995), with an average rate of movement of 4.8 cm/yr. Besse et al. (1984) estimated that the amount of convergence between the Indian and Eurasian plates was 550±650 km, and displacement along the thrusts was 400±400 km. The last two estimated values are similar. However, Besse et al., (1984) considered that the collision occurred before 50 Ma.

Paleomagnetic data (Appendix 6) from crustal blocks in western China and its adjacent areas (Fig. 10.2) support the above interpretation. The blocks, which make up western China, were widely separated over a very long period of time, but during the last 40 million years, these continental blocks came together, until at 22 Ma they reached positions similar to those they occupy at the present day.

Recently, convincing results were obtained by deep seismic profiling across the Main Himalayan Thrust Zone. Results from the cooperative China-USA INDEPTH project, make clear that the footwall of the thrust zone has been subducted northwards for more than 200 km, reaching a depth of ~15 km. At the deepest level the fault plane dips to the north at only 5°, the depth of Mohorovĭcíc Discontinuity is around 23 km (Fig. 10.1), and a zone of partial melting (STD in Fig. 10.1) is recognized beneath the Yarlung Zangbo Fault Zone (Zhao WJ, et al., 1993, 1997). The above results provide important evidence for the structure of the Himalayan Thrust Zone and the northward subduction of the Indian Plate, increasing thickness of the Xizang-Qinghai crust to 60–74 km (Zeng RS et al., 1995; Zhao WJ et al., 1997; Teng JW et al., 2003).

In the last few years, seismic tomographic studies of the western Himalayas to a depth of 1,000 km have shown that the cool Indian Plate with high velocity has been subducted to a depth of 600 km almost vertically, and then the depth between 600 and 800 km has been turned over towards the south (Van der Voo et al., 1999; Bigwaard et al., 1998). This shows that the subduction of Indian Plate did not extend

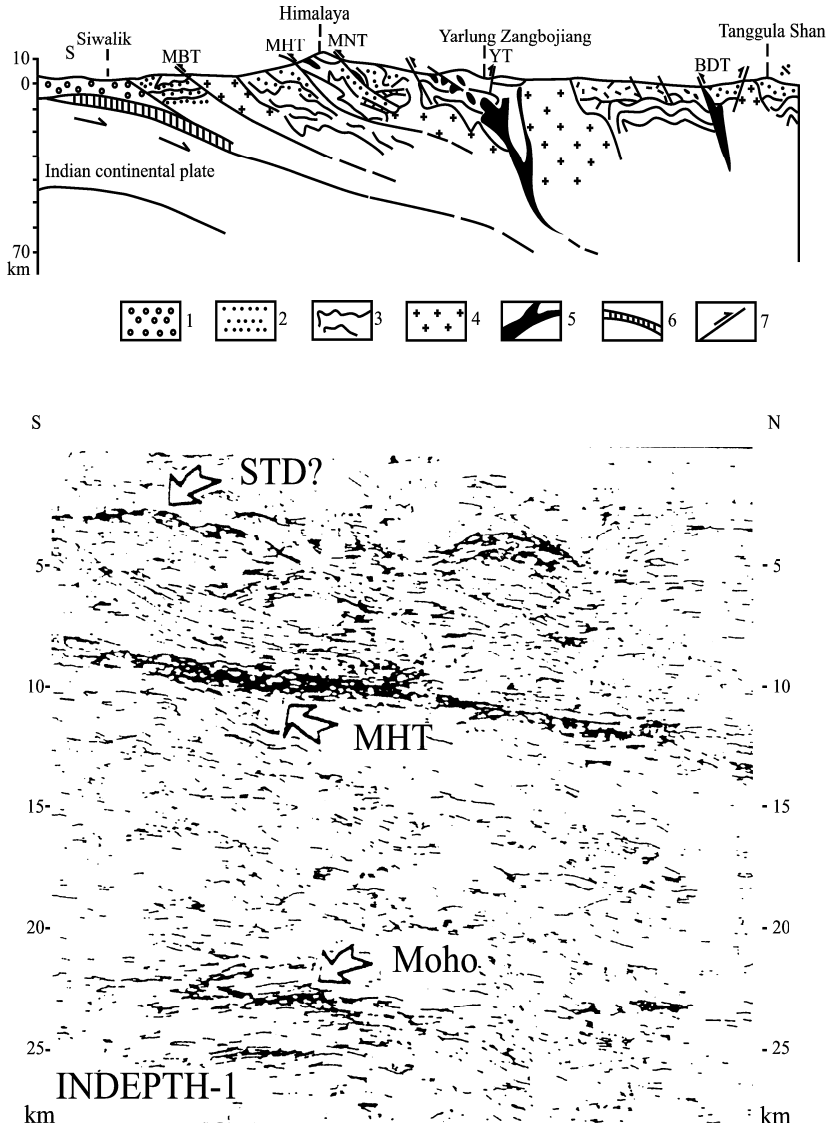

Fig. 10.1 Geological section and INDEPTH seismic profile across the Himalayan Collision Zone.

Upper section: 1. Cenozoic molasse formation; 2. Sedimentary cover; 3. Crystalline basement; 4. Granite; 5. Ultramafic rocks; 6. Subduction zone; 7. Thrust zone; MBT, Main Boundary Thrust; MHT, Main Himalayan Thrust; MNT, Main Northern Thrust; YT, Yarlung Zangbo Fault Zone; BDT, Banggongco–Dengqen Thrust.

Lower section: MHT, Main Himalayan Thrust; Moho, Mohorovĭcíc Discontinuity (Zhao WJ et al., 1993, 1997, with permission of Zhao WJ).

northwards for a long distance, as has been suggested by some researchers (Argand, 1924； Powell and Conagham, 1973; Seeber et al., 1981; Klootwijk et al., 1985; Houseman et al., 1996).

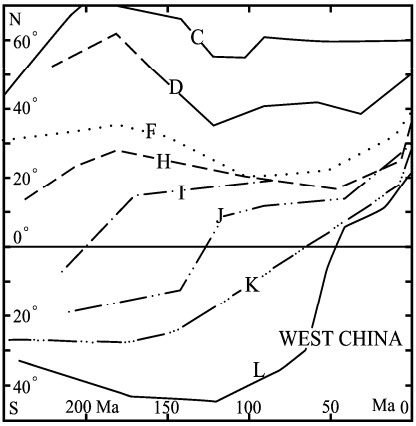

Fig. 10.2 Change in paleolatitude for blocks in western China and its adjacent areas.

C. Siberian Plate; D. Kazakhstan–Junggar Plate; F. Tarim Block; H. Kunlun Block; I. Qiangtang Block; J. Gangdise Block; K. Himalayan Block; L. Indian Plate.

Deformation in the Himalayan Stage produced a large-scale, thin–skinned thrust zone in western China. According to Burchfiel et al. (1989, 1992) and Royden et al. (1997), the thrusts of the Himalayan Period constitute a large-scale thin–skinned tectonic system, not only forming the Himalayan Mountains (6 in Fig.10.3; 1, 2 and 3 in Fig. 10.4), but also extending for over 1,000 km northeastwards, covering the area of the Qinghai–Xizang (hereinafter called Qingzang) Plateau as far as the Longshoushan–Haiyuan Thrust Zone (17 in Fig. 10.4). The western margin of this system is formed by the Altun sinistral strike-slip fault (13 in Fig. 10.4), and the eastern margin lies in the Daxueshan–Xiaojiang foothills, along a dextral strike-slip and normal fault zone (20 and 22 in Fig. 10.4). Within this area a series of WNW trending faults form imbricate thrust systems, such as the Banggongco–Nujiang Thrust (4 in Fig. 10.4), the Kongela–Wenquan Tanggula Thrust (5 in Fig. 10.4), the Jinshajiang–Honghe (Red River) Thrust (6 in Fig. 10.4), the Kunlun Thrust (i.e. Central Kunlun Thrust) (7 in Fig. 10.4), the southern margin of the Qaidam Thrust Zone (12 in Fig. 10.4), the Junulshan –southern margin of the Qinghaihu Thrust Zone (14 in Fig. 10.4), the southern margin of the Central Qilianshan Thrust Zone (15 in Fig. 10.4) and the northern margin of the north Qilianshan Thrust (16 in Fig. 10.4). Burchfiel et al. (1989, 1992) and Royden et al. (1997) considered that this thin-skinned tectonic system, with a displacement of tens to hundreds of kilometers, was developed mainly in the upper crust, with a major detachment at a depth of ~30 km along the low velocity layer in the lower crust.

There are still several opinions concerning the amount and rate of sinistral strike-slip displacement in the Altun Fault Zone during the Miocene–Early Pleistocene. From a systematic study of geomorphology and sedimentation, the Altun Active Fault Zone Research Group of the Seismic Bureau of China (1992) estimated a sinistral strike-slip displacement of ~75 km, with an average rate of movement of 0.58 cm/yr. Based on the sedimentation and deformation in the basin in the middle section of the Altun Fault Zone during the Neogene, Chen ZL (2001) proposed that the amount of sinistral strike-slip displacement was 80–100 km. From the process of formation of the Qingzang Plateau, Meyer et al. (1998) suggested that the sinistral strike-slip displacement in the Altun Fault Zone reached 156±40 km. Of course, some researchers have proposed greater displacements, choosing different markers for the determination of the amount of strike-slip, but at present there is no consensus view.

The Qingzang thin-skinned tectonic system developed in the tectonic stress field caused by northeastwards subduction and compression by the Indian Plate, making use of pre-existing faults. A series

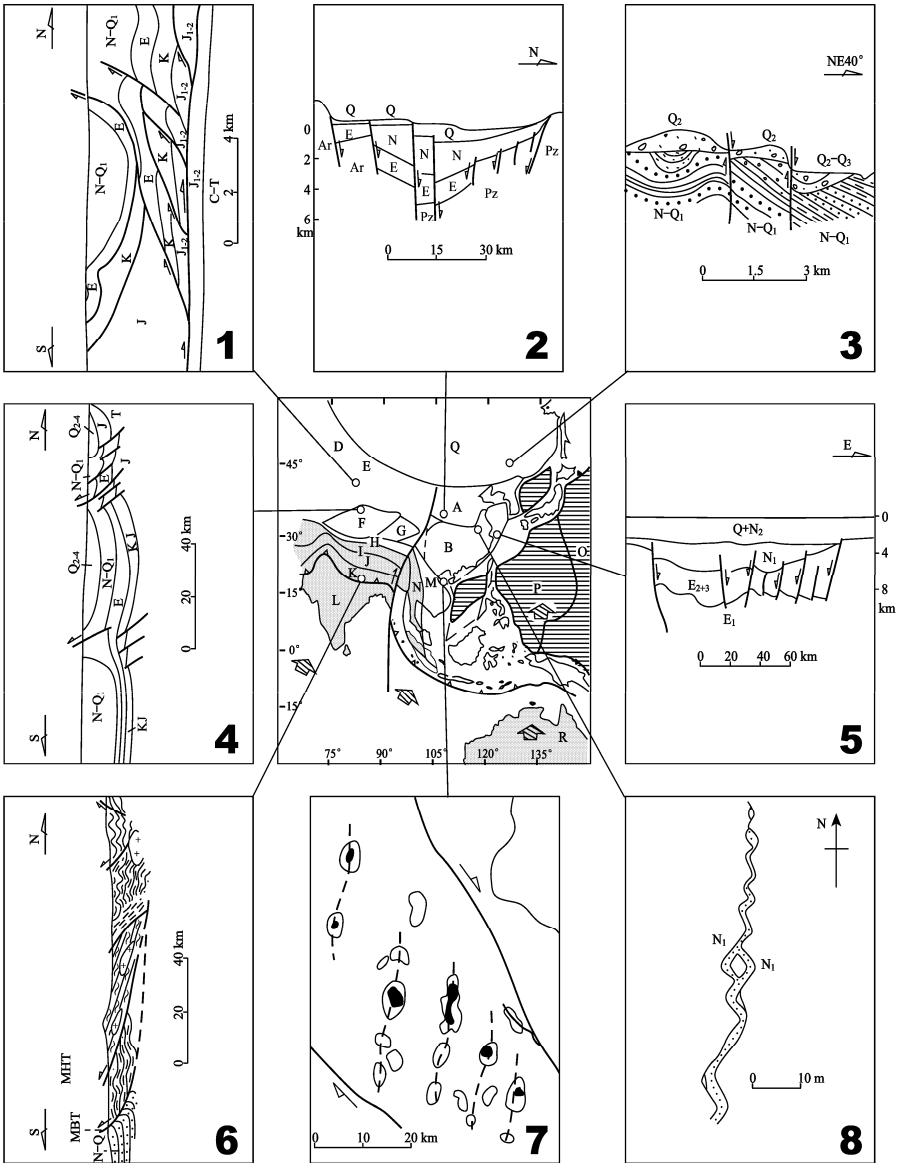

Fig. 10.3 Rock deformation in the Himalayan Tectonic Period.

1. Tugulu anticlines in Junggar, Xinjiang. Thrusting and folding occurred in the Early Pleistocene and affect all the older strata (N8724 profile, Bureau of Petroleum of Xinjiang (unpublished data)); 2. Seismic profile of Weihe–Pucheng. Normal faulting occurred in the Pleistocene, forming the Fen-Wei graben (Yang KC et al., 1989); 3. Yitong fault-depression in Jilin. Dahuanshan structural section. Normal faults and folds were formed during the Early Pleistocene and are overlain unconformably by the Middle Pleistocene (Liu MQ et al., 1993); 4. Kuche fold zone in southern Xinjiang. Faulting and

folding occurred in the Early Pleistocene, overlain unconformably by unfolded Middle Pleistocene-Holocene (Jia JH, 2000); 5. Seismic profile of the Xihu fault-depression, Donghai (East China Sea), Deformation occurred in the Miocene. The Pliocene and Quaternary systems are almost undeformed (Yang KC et al., 1989); 6. Cross-section of the Himalayas (Tapponnier et al., 1981), MBT–Main Boundary Thrust, BHT –Main Himalaya Thrust. The thrusts affect Neogene and Quaternary systems; 7. Yingehai Neogene fault-depression basin, southwest of Hainan Island, influenced by the Honghe (Red River) Fault Zone with horizontal dextral strike-slip, N-S extension faults and diapir structures (Zhang QM et al., 1996); 8. Vertical conjugate shear joints in horizontal Miocene sandstone north of Jiashan, Anhui, followed by an N-S trending extensional joint system, caused by N-S shortening (Ding GY, 1989).

Initial letters for blocks and plates are the same as in Fig. 6.5.

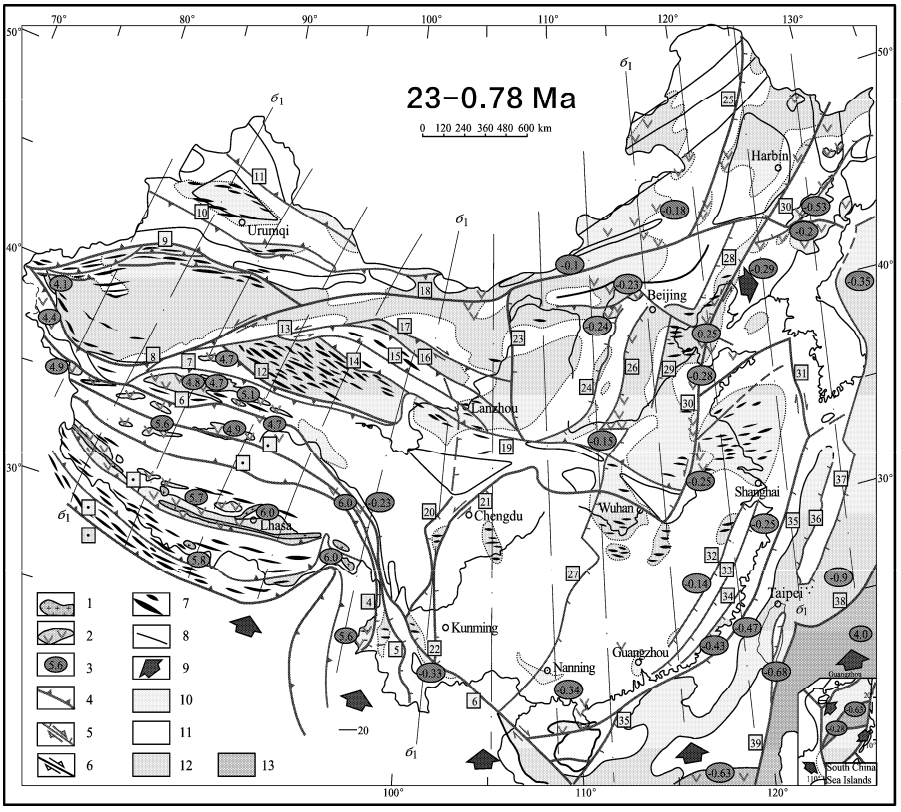

Fig. 10.4 Tectonic sketch of the Chinese continent in the Himalayan Period (23–0.78 Ma).

Legend: 1. Granites of the Himalayan Period; 2. Volcanic rocks of the Himalayan Period; 3. Rates of intraplate deformation, estimated from the chemical composition of magmatic rocks: "-" is rate of extension, other values are rates of shortening in cm/yr (Appendix 5.9); 4. Numbered collision zones or thrust belts; 5. Numbered normal and strike-slip faults; 6. Boundaries of blocks or faults with weak activity during the Himalayan Period; 7. Fold axes, only anticlines are shown (Appendix 3.8); 8. Trace of axes of maximum principal compressive stress (σ_1); 9. Direction of plate movement; 10. Areas of terrestrial sedimentation; 11. Land areas subject to erosion; 12. Areas of shallow sea; 13. Oceanic areas.

Numbered plate boundaries, collision belts and fault zones:

[1] Main Boundary Thrust of the Himalayas (MBT, boundary between the Indian and Eurasian plates); [2] Main Himalaya Thrust (MHT); [3] Yalung Zangbo Thrust; [4] Banggongco-Dongqiao Collision Belt; [5] Kongela-Wenquan Tanggula Thrust; [6] Jinshajiang–Honghe (Red River) Thrust Zone, with dextral strike-slip on the Honghe section; [7] Kunlun Thrust (i.e. Central Kunlun Thrust); [8] Kangxiwa–Ruoqiang-Dunhuang reverse fault zone with strike-slip; [9] Korla-Wuqia thrust zone; [10] Nile–Yilinhabirga–Yagan Thrust Zone [11] Debuga-Kramali Thrust Zone; [12] Southern margin

of the Qaidam Thrust; [13] Altun sinistral strike-slip fault zone; [14] Junulshan–southern margin of the Qinghaihu Thrust; [15] Southern margin of the Central Qilianshan Thrust; [16] Northern margin of the north Qilianshan Thrust; [17] Longshoushan Thrust; [18] Northern margin of the Alxa Thrust; [19] Wushan–Baoji–Luonan-Fangcheng Thrust Zone; [20] Eastern margin of the Daxueshan normal fault zone; [21] Longmenshan sinistral strike-slip fault zone; [22] Xiaojiang dextral strike-slip and normal fault zone; [23] Liupanshan–Helanshan normal fault zone; [24] Fenhe Graben Zone; [25] Eastern frontal Dahingganling normal fault zone; [26] Eastern frontal Taihangshan dextral strike-slip and listric fault zone; [27] Wulingshan–Damingshan normal fault; [28] Beipiao–Jianchang normal fault zone; [29] Eastern Cangzhou normal fault zone; [30] Tancheng-Lujiang sinistral strike-slip and normal fault zone; [31] Eastern marginal Huanghai (Yellow Sea) dextral strike-slip fault zone; [32] Chong'an-Heyuan normal fault; [33] Lishui-Lianhuashan normal fault; [34] Changle-Nan'ao normal fault; [35] Coastal fault zone of Fujian and Guangdong; [36] Western marginal normal fault of Diaoyu Island; [37] East marginal normal fault of Diaoyu Island; [38] Ryukyu Subduction Zone; [39] Western Philippine–east Taiwan longitudinal valley sinistral strike-slip fault zone.

of folds were developed, especially in the southern Xizang and Qaidam areas, in addition to the thrusts.

In the western part of the thin-skinned tectonic system E-W or WNW trending thrust zones were developed to the north of Kunlun, in which the mountains were thrust over their marginal basins, accompanied by folding and the formation of near N-S trending extensional faults, e.g., the Kangxiwa–Ruoqiang–Dunhuang sinistral strike-slip and reverse fault (8 in Fig. 10.4), the Korla–Wuqia Thrust Zone (9 in Fig. 10.4) and the Nilek–Yilinhabilg–Yagan Thrust Zone (10 in Fig. 10.4) on the margins of the Tianshan. During the Early Pleistocene the Xiyu and Yumen conglomerate formations and their underlying strata were folded and faulted. The Neogene and Early Pleistocene basins, located in the northern foothills of the Kunlunshan, and on the margins of Qilianshan and Tianshan, such as the northern and southern marginal basins of Tarim (4 in Fig. 10.3), the northern and southern marginal basins of Qaidam, the southern marginal basin of Junggar (1 in Fig. 10.3) and the Yumen Basin in Gansu, could be called foreland basins. Only sedimentary basins formed in front of subduction zones and intra-continental underthrust zone are properly called "foreland" basins. The Tarim, Qaidam and Junggar basins were formed before the Neogene, so that before the thrust zones developed, i.e. before the Neogene, it is not appropriate to call them foreland basins. Many sedimentological researchers have expanded the use of the term "foreland basin" to cover all the basins which occur in front of mountain ranges (Liu HF, 1995); however, this is not the correct use of the term.

Great progress has been made in recent years in determining the history of uplift of the Qingzang Plateau. Studies of the relationship between the vegetation and changes in the height of the plateau have shown that since the Paleogene the plateau has changed from an area of forested lowlands in the torrid zone to highland forests and bush grasslands in the subtropical zone. The Qingzang Plateau was affected by periodic uplift, and by the end of Miocene, had reached a height of more than 3000 m above sea level (Wei MJ et al., 1998). In the Early Neogene ($\sim$23 Ma) a planation surface was developed across the plateau. In Hohxilshan the lacustrine facies of the Wudaoliang Group was deposited extensively across this planation surface (Li TD, 2002). Recently other researchers have concluded that the Qingzang Plateau was uplifted rather later (Ge XH et al., 2002). Although uplift of the Qingzang area continued throughout the Neogene, at the end of Neogene the plateau area was not more than 2000 m above sea level.

Researchers from Lanzhou University studied the relationship between the height of the plateau and the grain size of the sediments in the foothills along the northern margin of the Qingzang Plateau, using the sediment grain size to determine the history of uplift. They considered that the rate of uplift of the northern Qingzang Plateau was 0.13mm/yr during the middle epoch of the Neogene (12.18–8.26 Ma) (Song CH et al., 2001). At 8.35 Ma the height of the plateau was only 900 m above sea level, during 8.35–3.1 Ma it was uplifted by only 420 m, at a rate of 0.11 mm/yr. The major period of uplift occurred in the Early Pleistocene, at 3.1–0.9 Ma, when the plateau was uplifted from 1,320 m to $\sim$3,700 m, the rate of uplift reached 1.075 mm/yr, almost 9 times the rate during the Neogene; since the Middle Pleistocene, the rate of uplift has been very slow (Fu KD et al., 2001).

From 3.1 to 0.9 Ma the plateau was affected by a period of strong erosion and sedimentation, which was prevalent throughout the globe, due to the change from a stable to a more turbulent climatic environment (Zhang PZ and Molnar, 2001). This probably relates to the Early Pleistocene global glacial epoch, when large amounts of water were frozen in the Arctic and Antarctic ice sheets, causing a fall in global sea level, an increase in the rate of erosion of the continents and an increase in the grain size of sediments. However the increase in grain size was not entirely due to the fall in sea level. In the Early Pleistocene the plateau was uplifted by ~ 2,400 m, while the drop in sea level was only ~100 m. So the increasing grain size of sediments in the northern foothills of the Qingzang Plateau reflects mainly the uplift of the plateau.

From a study of the sedimentary sequences and the subsidence history of the Yinggehai Basin (108.1°E, 18.2°N) and some intra-continental pull-apart basins to the southeast of the Qingzang Plateau in western Yunnan, Wang GZ et al. (2001) established that the initial stage of uplift in the western Yunnan Plateau occurred between 23 Ma and 11 Ma, while the main stage of erosion and planation stage occurred between 11 Ma and 5.3 Ma. The most rapid rate of uplift, to form the framework of the western Yunnan Plateau, occurred between 5.3 and 1.6 Ma. This plateau reached a height of 1,700–2,100 m, at a rate of uplift between 0.5 and 0.57 mm/yr.

From a comprehensive analysis of large amounts of data from Cenozoic tectonics, sedimentation, fission track dating and a precise leveling survey, Xiao XC et al. (1998) proposed that the Qiangzang Plateau underwent a slow rate of uplift from the Paleocene to a late stage in the Miocene (60–11 Ma), during which rates of uplift were between 0.07 and 0.6 mm/yr; from the Late Miocene to Late Pliocene (10–3 Ma), the rate of uplift had intermediate values between 0.3 and 2.05 mm/yr; from Early Pleistocene to an early epoch of the Middle Pleistocene (~2–0.5 Ma) was the period with the highest rates of uplift between 5.35 and 1.6 mm/yr.

Ma ZJ et al. (1998) pointed out that the deformation of the Qingzang Plateau was three dimensional. From a comprehensive analysis of fission track, paleoclimatic, paleogeo-graphic and paleoplanation data, the three dimensional kinematics of the deformation of the Qingzang Plateau was reconstructed. Their results are very similar to those of Xiao XC et al. (1998), although there are some differences. Ma ZJ et al. (1998) emphasized that there was a large-scale N-S shortening from the end of the Neogene, and in the Early Pleistocene there was vertical thickening, with uplift of the ground surface and E-W extension, especially during the last 3 Ma.

Harrison et al. (1992) obtained an ^{40}Ar / ^{39}Ar isotopic age of 21 Ma for the Qushui intrusion in the Gangdise Zone, and considered that this marked the time of the initial uplift of the Qingzang Plateau. At 8 Ma the plateau reached its greatest height, followed by E-W extension. Different authorities have different opinions concerning the time at which N-S compression was replaced by E-W extension. Molnar et al. (1993) concluded that the uplift of the Qingzang Plateau at 10 Ma was controlled by mantle dynamics, and was also greatly influenced by rapid erosion caused by the establishment of the Indian monsoon. Coleman and Hodges (1995) and Searle (1995) determined an ^{40}Ar / ^{39}Ar isotopic age of 14 Ma for hydrothermal muscovite in a N-S trending normal fault in northern Nepal, and considered that this dated the change from N-S shortening to E-W extension. Subsequently the Himalayan Mountains began to subside and the height of the Qingzang Plateau also decreased. However, Burchfiel et al. (1987) proposed that E-W detachment and extension occurred when the Qingzang Plateau had reached its greatest height at ~4 Ma.

Burbank et al. (1996) studied the Siwalik Group in the foreland basin to the south of the Himalayan Mountains and found that the basin contains no Paleogene sediments; the oldest sediments being of Early Miocene age were deposited between 16.8 and 14.6 Ma. Between 14.6 and 10.8 Ma (mid-Miocene) the average rate of sedimentation was 0.3–0.2 km/Myr (i.e. 0.3–0.2 mm/yr); the most rapid rates of sedimentation, from 1.0 to 0.3 km/Myr occurred between 10.8 and 7.8 Ma, decreasing to 0.4–0.2 km/Myr between 7.8 and 0.7 Ma (i.e. Pliocene–Early Pleistocene). Based on the rates of sedimentation in the Himalayan foreland basin, the greatest rate of erosion and the highest rate of sedimentation, and also the most rapid rate of uplift of the Himalayan Mountains occurred between 10.8 and 7.8 Ma.

There is general agreement that the Qingzang Plateau has been uplifted since the Miocene or a little earlier. It is well known that compression was accompanied by thrusting, shortening and uplift of the plateau, followed by extension and collapse. However, there is still discussion concerning the timing of this change. Many overseas researchers (Harrison et al., 1992; Molnar et al., 1993; Coleman and Hodges, 1995; Searle, 1995; Burbank et al., 1996) recognized that the climax of uplift of the Qingzang Plateau occurred between 10.8 and 7.8 Ma or earlier. However, most Chinese researchers (Xiao XC et al., 1998; Ma ZJ et al., 1998; Song CH et al., 2001; Fu KD et al., 2001; Wang GZ et al., 2001) and some overseas researchers (Burchfiel et al., 1987) consider that the uplift occurred mainly at the end of Neogene and in the Early Pleistocene (3–1 Ma). It is possible that the final epoch of uplift of the Qingzang Plateau occurred between 3 and 1 Ma and that the most rapid period of uplift of the Himalayan Mountains occurred earlier. It seems unlikely that the N-S rifts are evidence of plateau collapse.

Crustal shortening was accompanied by magmatism: there are intraplate potassium-rich volcanic rocks and muscovite granites formed by crustal re-melting, which give isotopic ages younger than 20 Ma (Bureau of Geology and Mineral Resources of Xizang (Tibet) Autonomous Region, 1993). In western Kunlun and Yumen of Gansu, intra-continental volcanic rocks, including shoshonite, erupted in the central Kunlun–Hohlxil zone at 19–7 Ma and at ~5 Ma.

The dynamics and mechanics responsible for the uplift of the Qingzang Plateau are the subjects of controversy, and at present there is no general agreement. From field observations, geological mapping, the use of mathematics and tectonophysical modelling, a great many hypotheses have been proposed, for example, the hypothesis of continuous uplift, the effects of multiple subduction and collision in different directions, causing the thickening of the crust and lithosphere, and the influence of isostasy (Xu ZQ et al., 1996; Houseman et al., 1996; Cai XL et al., 1998; Ma ZJ et al., 1998). The main dynamics of surface uplift and extension was the detachment between the crust and the mantle among the geological effects was uplift of the asthenosphere with partial melting and gravitational collapse (Cui JW, 1992, 1997; Molnar et al., 1993; Zhao WJ et al., 1993; Gao R et al., 1998; Yin A et al., 2000; Xiao XC et al. 1998).

At present there are not sufficient constraints to distinguish between the many hypotheses which have been proposed to account for the uplift of the Qingzang Plateau. Because many data are imprecise, many of these hypotheses appear to be reasonable. The author recognizes that it may not be established easily that melting of the crust was caused by uplift and extension of plateau. Beneath the Qingzang Plateau the asthenospheric mantle is depressed. Partial melting of the crust and mantle is not sufficient to cause the regional uplift of the crust to form the plateau. Many processes were responsible for the three dimensional deformation of the lithosphere of the Qingzang Plateau, including subduction and N-S shortening between plates, which caused the thickening of the crust and lithosphere, the uplift of the plateau, its isostatic collapse and E-W extension under the influence of gravity.

10.2 Intraplate Deformation, Extension and Dispersion in Eastern China

During the Himalayan Period, while the Himalayan Mountains were being formed in southwestern China, the weak intraplate deformation was occurring in eastern China, causing widespread subsidence and sedimentation. At this period more than a thousand meters thick sediments were deposited, showing no obvious signs of deformation, (2 and 5 in Fig. 10.3). However, in local areas, especially near regional faults, E-W trending open folds were formed, with dip angles usually $<10°$(Fig. 10.4). Also in many areas, near N-S extensional joint systems were formed (8 in Fig. 10.3).

The main type of deformation in eastern China during the Himalayan Period was extension, with the formation of normal faults based on pre-existing near N-S faults, such as the eastern margin of the Daxueshan normal fault zone (20 in Fig. 10.4), the Xiaojiang dextral strike-slip and normal fault zone (22 in Fig. 10.4), the Fenhe Graben Zone (24 in Fig. 10.4), the eastern Dahingganling frontal normal fault zone (25 in Fig. 10.4), the eastern Taihangshan listric frontal dextral strike-slip fault zone (26 in Fig. 10.4), the Wulingshan–Damingshan normal fault (27 in Fig. 10.4), the Beipiao–Jianchang normal

fault zone (28 in Fig. 10.4), the eastern Cangzhou normal fault zone (29 in Fig. 10.4), the Tancheng-Lujiang sinistral strike-slip and normal fault zone (30 in Fig. 10.4), the Chong'an-Heyuan normal fault (32 in Fig. 10.4), the Lishui-Lianhuashan normal fault (33 in Fig. 10.4), the Changle-Nan'ao normal fault (34 in Fig. 10.4), the coastal fault zone of Fujian and Guangdong, with ~50 meters contour below sea level (35 in Fig. 10.4), and the eastern and western marginal normal faults of Diaoyu Island (36 and 37 in Fig. 10.4). These faults controlled the locations of the N-S fault-depression basins formed during the Neogene-Early Pleistocene as the result of E-W extension, for example, the Songhuajiang–Nengjiang, Yilan–Yitong, Mishan–Dunhua, around Bohai Bay (including central Hebei), Yinchuan of Ningxia, Fenhe of Shanxi, northern Jiangsu–southern Yellow Sea, Eastern East Sea, Ryukyu Trench and many zig-zag basins in Xizang.

NNE trending faults in eastern China often show dozens of kilometers of sinistral strike-slip displacement. These faults penetrated the crust and the mantle of lithosphere, and alkali-basalts erupted along them during the Neogene and Early Pleistocene. The $^{87}Sr/^{86}Sr$ initial values of these rocks are usually lower than 0.705, and they often contain mantle xenoliths of dunite and lherzolite, indicating that the faults penetrated the lithosphere (Chi JS et al., 1988, 1996; Appendix 7). From the occurrence of xenoliths of mantle peridotite, the eastern frontal Dahingganling–east frontal Taihangshan–Wulingshan–Damingshan normal fault zone, the Tancheng–Lujiang normal fault zone with sinistral strike-slip and the coastal normal fault zone of Fujian and Guangdong formed during Neogene and Early Pleistocene were lithospheric faults. These faults were sealed at the end of the Early Pleistocene after the basalts had been intruded into them (Wang YM and Wan TF, 2008).

A basic dyke swarm was intruded into extensional joint systems associated with these faults. In the basins the dike swarm is marked by high positive magnetic anomalies. The N-S to NNE Neogene and Early Pleistocene basic dyke swarm should not be confused with the E-W to NW trending Eocene and Oligocene dyke swarm described already in Chapter 9. The Paleogene and Neogene dyke swarms were separated by a time span of ~20 million years and their orientations are quite different; they cannot be used as evidence for the presence of a mantle plume beneath eastern China.

From the isotopic ages of the basalts the normal faults were active at different time (E ML and Zhao DS, 1987; Chi JS et al., 1988; Liu RX et al., 1992). Time of movement on the fault zones are: ~14 Ma for the eastern frontal Dahingganling–eastern frontal Taihangshan–Wulingshan –Damingshan normal fault zone; 19.79–1.14 Ma for the Tancheng–Lujiang normal fault zone with sinistral strike-slip; 5.1–1 Ma for the eastern margin of the Daxueshan normal fault zone; 2.2–1.8 Ma for the coastal normal fault zone of Fujian and Guangdong, which was also the main epoch of extension of the Taiwan Straits, separating Taiwan from the continent.

The eastern margin of the Daxueshan and Xiaojiang normal fault zones is the intra-continental expression of the 90°E Ridge Fault Zone in the Indian Ocean, an important dextral strike-slip fault, which has separated the Indian plate from Australian plate since the Cretaceous (Klootwijk et al., 1991, 1992). During the Himalayan Tectonic Period the Indian Plate was still migrating northwards at a rapid rate of 4.8 cm/yr, while the Australian Plate was moving more slowly, at a rate of 0.43 cm/yr. As a result there was very strong shortening in western China, but only weak deformation in eastern China. The eastern margin of the Daxueshan and Xiaojiang normal fault zones, and their northward extension in the Liupanshan Fault Zone formed the boundary between different types of tectonic activities in China during the Cenozoic. In eastern China, a series of long narrow NNE trending blocks were separated by the eastern margin of the Daxueshan and Xiaojiang, the east frontal Dahingganling, the east frontal Taihangshan–Wulingshan–Damingshan, the Tancheng–Lujiang and the coastal Fujian and Guangdong normal fault zones. During the Himalayan Period the major tectonic zones of eastern China have a near N-S orientation rather than an E-W orientation; zones with a near N-S orientation are also seen in the deep seismic data.

Activity was weak on near E-W trending high angle faults, which were closed under compression, while pre-existing NE trending faults show sinistral strike-slip movement, with only small amounts of displacement. Qi JF and Chen FJ (1995) studied the fault kinematics in the Xialiaohe–Liaodong Bay oil fields, controlled by 45° NE trending faults. They estimated that in the Neogene the average

amount of E-W extension was only 0.88 km, with a ratio of extension of 1.4%, an extension rate of 0.036 mm/yr, and an average rate of subsidence of 0.014 mm/yr. The rate of sinistral strike-slip was 0.55 mm/yr, with very weak deformation. However, strike-slip movement along NW-trending faults, for example, the Red River Fault Zone, was mainly sinistral in the Paleogene (Zhong DL et al., 1993, 1998), changing to dextral during Neogene (Zhang QM et al., 1996; Gong ZS et al., 1997). As the result of these movements a series of N-S trending secondary en echelon normal faults were developed, which controlled the development of mud diapiric structures and formed reservoirs in the giant Yingehai gas field (7 in Fig. 10.3).

Data on 469 macro-or meso-folds (including 247 anticlines and 222 synclines) obtained from regional geological surveys (bureaus of geology and mineral resources of the provinces, 1984–1993) formed in China during the Himalayan Tectonic Period (23–0.78 Ma), and joint data from 58 observation points were divided into 39 areas (Appendices 3–8) for statistical analysis. In the Himalayan Period in China the preferred attitude of maximum principal compressive stress axis (σ_1) was 184° SW ∠2°, that of intermediate principal compressive stress axis (i.e. fold axial trend, σ_2) was 94° SE ∠4° and that of the minimum principal compressive stress axis (σ_3) was 4°∠87° NE, being nearly vertical in the present day geographical coordinates (Figs. 10.4 and 10.5). The controlling features of the tectonic stress field in the Chinese continent during the Himalayan Period were near N-S horizontal compression and near E-W horizontal extension.

So far insufficient data have been obtained for the complete determination of the tectonic stress during the Himalayan Period (Appendix 4 and Fig. 10.6); only 18 determinations have been made in quartz-bearing rocks, using the dislocation density method. Average differential stress was found to be 92.6 MPa, with most areas giving results between 80 and 90 MPa. Higher values of 105.3–109.8 MPa were measured at Malanshan, Qinghai and Ngari, Xizang, which may be due to the northward movement of the Indian Plate.

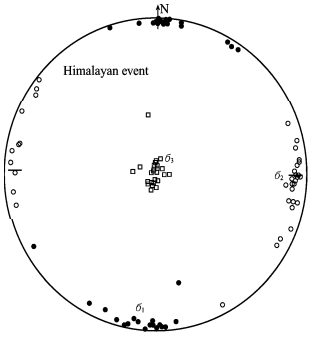

Fig. 10.5 Attitude of principal stress axes during the Himalayan Period.

Olivine from mantle-derived xenoliths was used to determine 24 differential stress values from the lithospheric mantle (at depths ~55–62 km, according to the estimated depth of the original magmatism) (Appendix 4 and Fig. 10.6). The average value of differential stress was 21.5 MPa (Appendix 4), similar to that of the global lithospheric mantle (Mercier, 1980). Usually, the value of differential stress at the base of the lithosphere is less than values near the surface of the crust by an order of magnitude.

Rates of intraplate deformation during the Himalayan Period have been calculated from the statistical analysis of the whole-rock composition of 1,079 samples of magmatic rocks (Appendix 5.9), divided into 41 petrographic areas (Fig. 10.4). The average rate of N-S intraplate shortening in China during the Himalayan Period was 5.2 cm/yr, and the shortening rate was usually greater than 4 cm/yr. These values may be an overestimate, because these values were calculated according to the values of plate margins. From data on rates of active horizontal fault movement since the Neogene, Ding GY et al. (1991) calculated that the northward movement of the Xizang area was 2.8 cm/yr and in the Qaidam

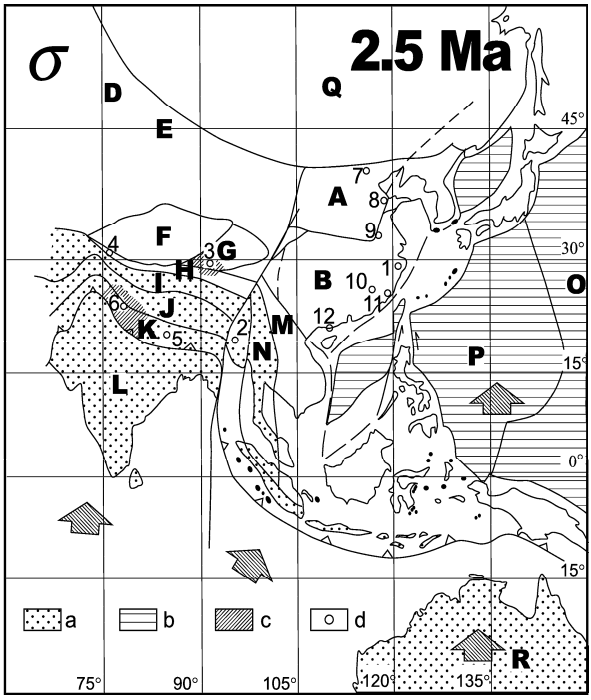

Fig. 10.6 Differential stress magnitudes during the Himalayan Period.

a. Gondwanan continental blocks; b. Oceanic and younger plates; c. Areas with values of differential stress >90 MPa; d. Locations of measurements of differential stress values. The white areas are areas of differential stress values <80 MPa or with no data. The index letters for blocks are the same in Fig. 6.5; data are shown in Appendix 4.

Numbered areas for data collection: 1. Guacangshan, Linhai, Zhejiang; 2. Tengchong, Yunnan; 3. Malanshan, Qinghai; 4. Western Kunlun; 5. Southern Xizang; 6. Ngari, southwestern Xizang, reflecting the stress magnitude in upper mantle; 7. Damaping, northern Hebei; 8. Shanwang, Shandong; 9. Nüshan, Anhui; 10. Mingxi, Fujian; 11. Changle, Fujian; 12. Leizhou Peninsula, Guangdong.

area the rate of movement was 1.5 cm/yr in a 25° NE direction. The average rate of E-W extension calculated for 12 areas in eastern China was 0.33 cm/yr and the rate of N-S shortening was ~0.6 cm/yr. Rates of E-W extension in the marginal sea areas of the Eastern Asian continent were much greater, reaching 0.35–0.9 cm/yr; this was the main period for the formation of the marginal seas of Eastern Asia and the western Pacific.

Amounts and rates of shortening and extension, the duration of episodes of folding and linear strain rates have been estimated for the Himalayan Period, using the data from folds and the rates of plate movement (Table 10.1). From statistics on E-W trending folds formed during the Himalayan Period, rates of N-S shortening can be calculated relatively easily. The ratio of shortening in Tancheng–Lujiang was 0.56%, shortening ratio was greater than 1.77% in Hingganling–Taihangshan, and was greatest in Henduanshan, reaching 2.59%. Generally, the ratio and rates of shortening or extension in eastern China during the Himalayan Period are rather small, less than those in the Paleogene or earlier periods. In eastern China the length of time over which intraplate deformation in the Himalayan Period occurred was 1.54–6.98 million years, equal to 7%–30% of the duration of the Himalayan Period. Linear strain rates were between 8.0×10^{-17}/s and 3.8×10^{-16}/s, the deformation processes were also rheological.

In the marine areas of eastern China, the amount of extension was estimated from the outcrop width of the oceanic crust or from the sea floor magnetic anomalies, and rates of extension were estimated from the chemical composition of ocean floor volcanic rocks. It can be seen that in the zone of marginal extension in the East Asian continent, the amount of extension was greatest in the Japan Sea, ~50%, in the Taiwan Straits and the South China Sea it was between 10% and 15%, however there is no oceanic crust in the Taiwan Straits. The extension duration of the Neogene–Early Pleistocene is estimated to have lasted between 14.3 and 21.5 million years, throughout almost all of the Himalayan Period and still belongs to rheology, with linear strain rates between 1.1×10^{-15}/s and 2.2×10^{-16}/s.

Table 10.1 Amount and ratio of shortening, ratio and rates of extension, time of deformation and linear strain rate in eastern China during the Himalayan Stage

Area	Hengduan Mountains	Hingganling –Taihangshan	Tancheng–Lujiang	Taiwan Straits	South China Sea	Japan Sea
Statistical length (km)	800	2,250	2,500	1,000	1,000	1,000
Average dip angle of fold	13.08°	10.8°	6.05°			
limbs (amount of data)	(50)	(41)	(106)			
Ratio of shortening (%)	2.59	1.77	0.56			
Amount of shortening (km)	20.7	39.8	13.9			
Amount of extension (km)	6.9	13.2	4.6	100	140	500
Rates of extension (cm/yr)	−0.32	−0.19	−0.30	−0.47	−0.65	−3.5
Ratio of extension (%)				10	15	50
Deformation time (Myr)	2.16	6.98	1.54	21.3	21.5	14.3
Linear strain rate (ε, 1/s)	3.8×10^{-16}	8.0×10^{-17}	1.15×10^{-16}	1.49×10^{-16}	2.2×10^{-16}	1.1×10^{-15}

It is found that while the rates of extension in eastern China are small, those in western China are large. Because shortening in western China during the Early Paleozoic, Late Paleozoic, Triassic, Cretaceous and Neogene-Early Pleistocene Periods was superimposed in almost the same orientation, distinguishing the amounts of shortening for these various stages will require a great deal of further detailed geological and structural research.

During the Himalayan Period N-S shortening and E-W extension caused the migration of the deposit-centers in some of the sedimentary basins in China, especially near NW-trending fault zones. For example, in the WNW-trending Qaidam Basin, in the western part of the basin affected by greater tectonic stress, there was no obvious migration in the Paleogene, but during the Neogene the sedimentary deposit-center migrated about 160 km southeastwards, at an average rate of 0.73 cm/yr (Yang YL, unpublished paper of the Institute of Geology, Bureau of Petroleum of Qinghai Province; Zhang ML, 1998). In the Yingehai Basin (centered on 108.2°E, 18.8°N), where the Red River dextral strike-slip fault zone extends out into the South China Sea, the deposit-center of the basin migrated 300 km southeastwards at about 1 cm/yr from the end of the Oligocene to the Pliocene (32–5 Ma) (Gong ZS et al., 1997). In these two areas, the distances and rates of migration of the deposit-centers are similar, influenced by strong compression at the western end of the faults, leading to uplift in the northwest, so that the sedimentary deposit-centers migrated gradually southeastwards. However, it should be pointed out that the migration of sedimentary centers and the movement of the blocks are so different, that these data could not be used to deduce that the continental blocks had moved southeastwards over a great distance, as suggested by Tapponnier et al. (1990).

The volcanism is the strongest and more widespread distribution along the NNE trending faults in eastern China during Neogene–Early Pleistocene, i.e. Himalayan Tectonic Period (Fig.10.7). Due to the influence of N-S shortening and E-W extension of Himalayan tectonic stress field, these NNE trending lithosphere faults are all extension, so they are easy to make decrease pressure positions in the depth, and then present the magmatism. It is also the result of E-W extension in eastern China continent.

271 volcanic rock samples of data are collected, including 264 basalt data originating near the intersections of bottom of lithosphere and NNE faults, 7 rock samples originating in crust. In the research

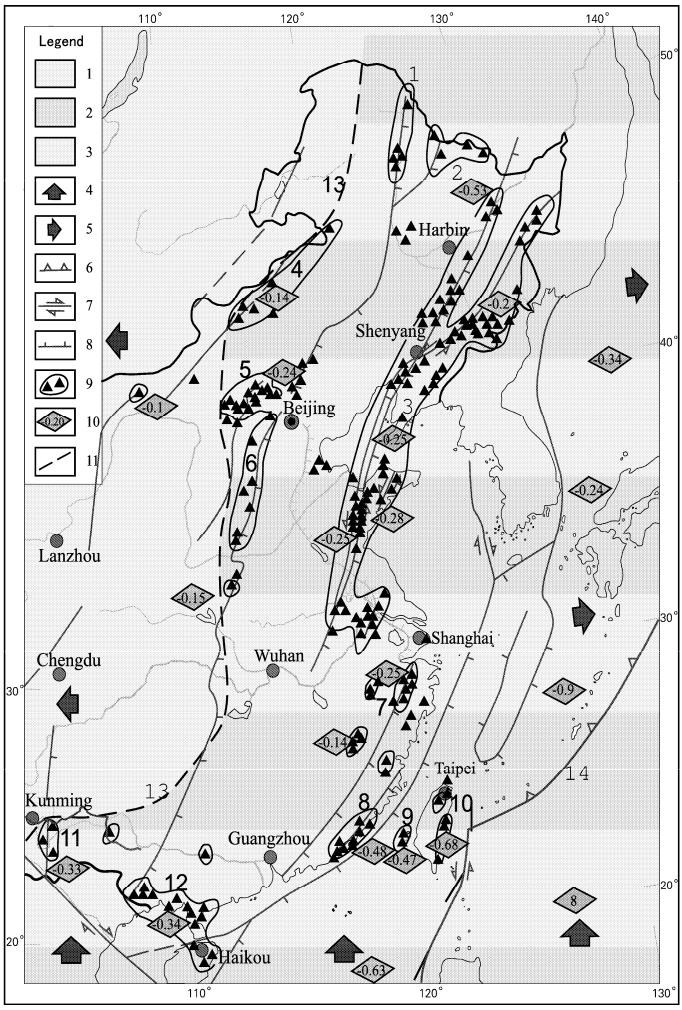

Fig. 10.7 Distribution of magmatic source areas and faults near the bottom of lithosphere during Himalayan Period (23–0.78 Ma) in eastern China (Wang YM and Wan TF, 2008)

Numbers of legend: 1. continental crust area with weak magmatism; 2. continental crust area with strong magmatism; 3. oceanic crust; 4. plate compression direction; 5. plate extension direction; 6. subduction zone or thrust; 7. strike-slip fault; 8. normal fault; 9. magmatic source depth data near the bottom of lithosphere (data shown in Appendix 7); 10. negative value is plate extension velocity, positive value is plate shortening velocity (cm/yr); 11. the border between weak and strong magmatism areas.

Numbers of faults: 1. northern section of Dahingganling fault; 2. Xiaohingganling fault; 3. Tancheng–Lujiang lithosphere fault zone; 4. Xilin Gol fault; 5. Zhangbei–Datong fault; 6. east border of Taihangshan fault; 7. middle part of Zhejiang and Fujian (Xinchang–Mingxi) fault zone; 8. Longhai–Santou fault; 9. Penhu fault; 10. East and North Taiwan fault zone; 11. southeast Yunnan fault; 12. southern Guangxi–Leizhou Peninsula–Wenchang fault; 13. border between weak and strong magmatism areas; 14. subduction zone between continental and oceanic crusts.

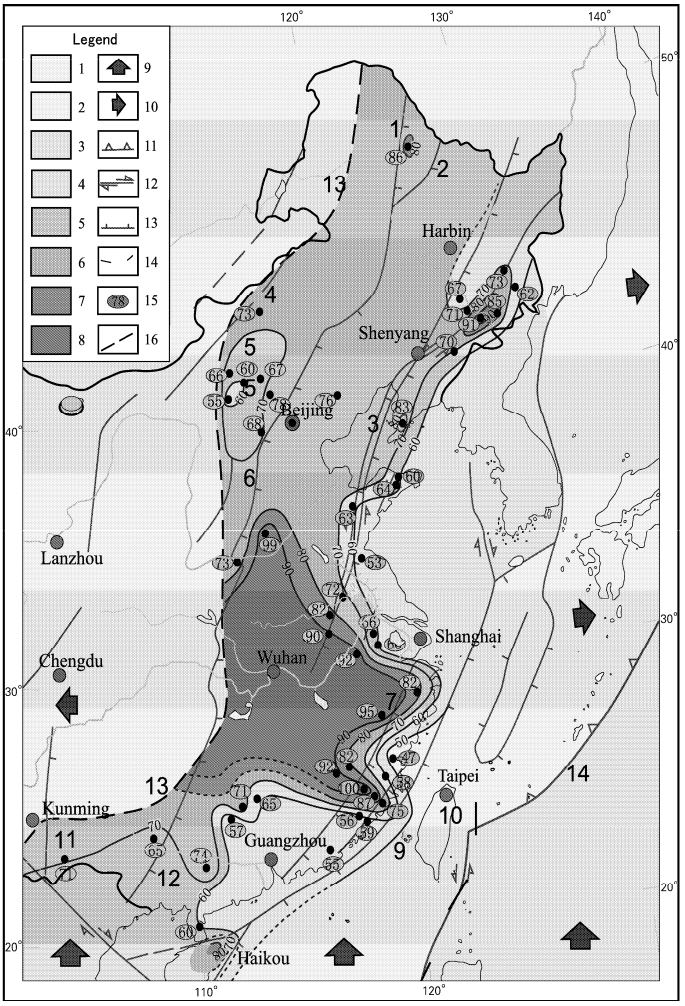

Fig. 10.8 Thickness of the lithosphere during Himalayan Period (23–0.78 Ma) in eastern China (Wang YM and Wan TF, 2008)

Numbers of legend: 1. continental crust area with weak magmatism; 2. continental crust area with strong magmatism; 3–8. continental crust with strong magmatism, lithosphere thickness is respectively: 3. <50 km, 4. 50–60 km, 5. 60–70 km, 6. 70–80 km, 7. 80–90 km, 8. >90 km; 9. plate compression direction; 10. plate extension direction; 11. subduction zone or thrust; 12. strike-slip fault; 13. normal fault; 14. isobaths of lithosphere bottom; 15. depth of data point of lithosphere bottom; 16. the border between weak and strong magmatism areas.

Numbers of faults: the same as in Fig. 10.7.

samples, there are mainly alkali-basalts (236 data), 11 data of tholeiites, 15 data of basanite, 7 data of mixed alkali basalts and tholeiites; 2 data of dolerite (Appendix 7) (Wang YM and Wan TF, 2008). The magmatic source depths are estimated by the value of t-$^{86}Sr/^{87}Sr_{0,}$isotopic ratio of oxygen or lead, ratio of MgO–ΣFeO / (ΣFeO +ΣMgO) for biotite, or ratio of TiO_2-Al_2O_3 for amphibolite, rare earth elements assemblage, geothermobarometer and other litho-chemistry characteristics. Thus, depending on the de-

duced data of original depth from basic magmatic rocks and their mantle xenoliths (Appendix 7), the tectonic detachment in lithosphere during Miocene–Early Pleistocene Period can be discussed.

In the Himalayan Tectonic Period (Miocene–Early Pleistocene), detachments widely occurred at the intersection in between the bottom of lithosphere and four NE and NNE trending lithospheric faults, namely, Xilin Gol fault (4 in Fig.10.7), Dahingganling–Taihangshan fault (1, 2 and 6 in Fig.10.7), Tancheng –Lujiang fault (3 in Fig.10.7) and fault of southeast coast of China (8 in Fig.10.7) on eastern China continent (Wang YM and Wan TF, 2008). After Early Pleistocene, the above four NNE faults, filling the basic magma, are almost fixed, and the activities of faults decrease a lot.

According to original depths of magmatism, which are nearly at the bottom of lithosphere, the sketch of the lithosphere thickness during the Himalayan Period (23–0.78 Ma) in eastern China is compiled (Fig.10.8). It shows that the thickness of lithosphere on eastern China continent is mainly 70–80 km, at the middle part of eastern China the thickness of lithosphere can be more than 90 km. However, west to the border between weak and strong magmatism areas (west to the fault number 13 in Fig. 10.8), i.e. west to the line form western Dahingganling, Middle Shanxi, Wulingshan to Kunming, the thickness of lithosphere is about 100–200 km (discussed in Chapter 13), which is the typical thickness of continental lithosphere. The above result is rather similar to the data of inversion of transverse wave tomography (Cai XL et al., 2002). It is really a thin continental lithosphere in eastern China. The mechanism of thin lithosphere of eastern China will be discussed in Chapter13.

10.3 Formation of Giant Step in Landscape and Extension Basins in Continental Margin

Under the influence of the N-S shortening and E-W extension tectonic stress field during the Himalayan Tectonic Period, all N-S trending fault zones were converted into normal faults, and E-W trending fault zones were converted into reverse faults or thrusts, causing major changes in the geomorphology and topography on the Chinese continent.

During horizontal extension, areas of lower density thick crust and lithosphere, with mass depletion of the lithosphere, are compensated by deep mantle material, causing isostatic uplift of the surface. Conversely, in areas of thinned crust and lithosphere, high density asthenospheric mantle approaches the surface producing a high positive gravity anomaly, which causes isostatic subsidence at the surface. These principles can be used to interpret changes in the landscape of the Chinese continent.

Five major fault zones divide the landscape of China into six giant steps from western China to the Pacific Ocean: (1) The eastern margin of the Daxueshan–Xiaojiang Fault Zone; (2) The eastern front of the Dahingganling–eastern frontal Taihangshan–Wulingshan–Damingshan Fault Zone; (3) The coastal fault zone of Fujian and Guangdong; (4) The eastern marginal Diaoyu Island fault; (5) The Ryukyu Subduction Zone–East Taiwan longitudinal valley–West Philippine Fault Zone (Figs. 10.9, 10.10 and 10.11).

The giant steps are: (1) The Qingzang Plateau (average 4,000 m above sea level); (2) Northwest China-Inner Mongolia–Loess–Yunnan-Guizhou Plateau (average 2,000 m above sea level); (3) Plains, hills and lower mountains of eastern China (average less than 1,000 m above sea level, down to 50 m below sea level, including Bohai Bay and the Yellow Sea); (4) Continental shelf shallow sea (average 50–200 m below sea level); (5) Japan –Ryukyu-Taiwan Islands; (6) Pacific Ocean basin (average 4,000 m below sea level) (Figs. 10.9 and 10.11). Since that time, China continent has been characterized by a topography higher in the west than in the east (Wan TF, 1994; Jiang FZ et al., 1993).

The giant steps in the landscape and areas of steep gravity anomaly gradients coincide with changes in crustal thickness. In the section showing crustal thicknesses for Eastern Asia and its adjacent areas in Fig. 13.1, the crustal thickness of the Qingzang Plateau is shown to be 60–74 km, that of Northwest China-Inner Mongolia–Loess–Yunnan-Guizhou Plateau to be 40–48 km, that of the eastern plains, hills

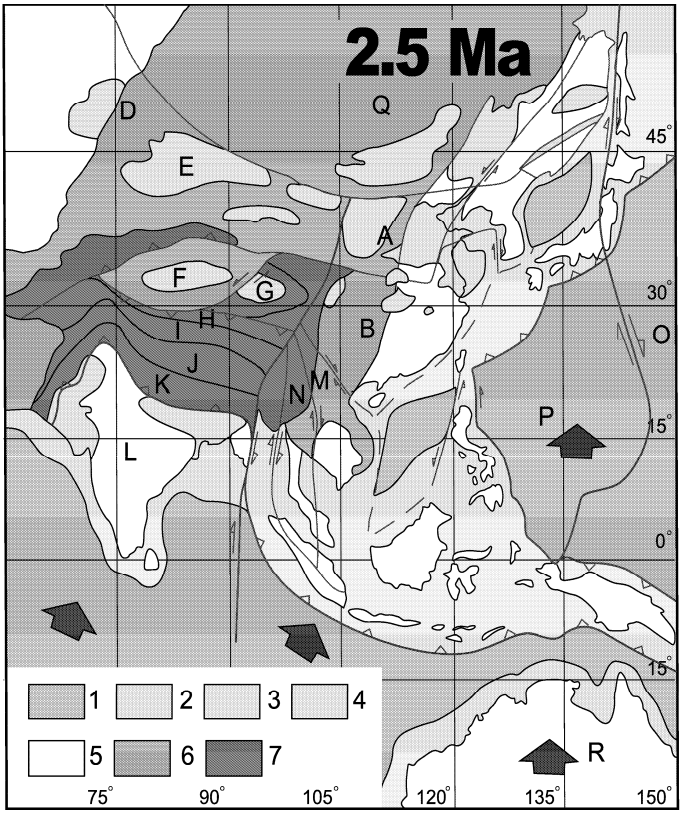

Fig. 10.9 Paleo-tectonogeographic reconstruction of China and its adjacent blocks in the Late Himalayan Stage (2.5 Ma).

1. Ocean (average depth 4,000 m below sea level); 2. Shallow marine continental shelf and islands (average depth 50–200 m below sea level); 3. Plains and hills (average height less than 200 m above sea level and down to 50 m below sea level); 4. Inland basins and deserts (average height 500–1,000 m above sea level); 5. Lower mountains (average height 200–1,000 m above sea level); 6. Northwest China-Inner Mongolia–Loess–Yunnan-Guizhou Plateau (average height 2,000 m above sea level); 7. Qingzang Plateau (average height 4,000 m above sea level).

The index letters for blocks and plates are the same as in Fig. 6.5.

and lower mountains to be 30–36 km (which is normal and average thickness of crust on the Earth), that of shallow marine continental shelf to be 28–24 km and that of the Pacific Ocean to be 10–20 km (Teng JW et al., 2003). These relationships show that the giant landscape steps, gravity anomalies and crustal thicknesses are the result of tectonism and gravitational isostatic compensation during the Neogene and Early Pleistocene.

In the Chinese continent, E-W trending tectonic zones were formed gradually during the last 2,000 million years, and especially in the last 250 million years. However, the N-S trending tectonic zones, gravity anomalies and crustal thicknesses in eastern China were formed during just the last 20 million years. The present day tectono-physical framework, which coincides with the gravity anomalies, were formed during the Cenozoic; gravity anomalies cannot, however, be used to explain deformation in earlier geological periods.

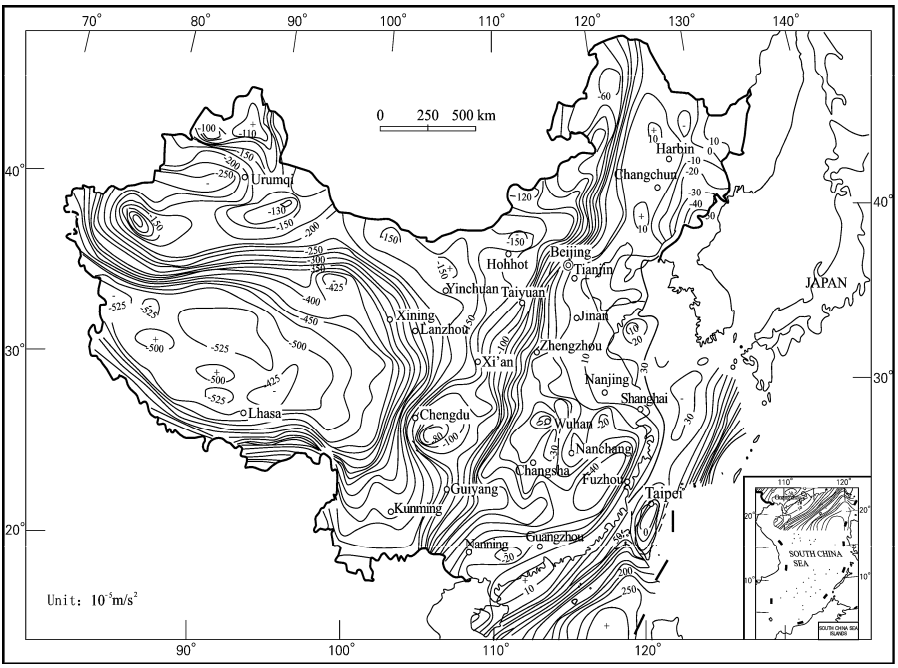

Fig. 10.10 Average Bouguer gravity anomaly (1°×1°) in China (Yin XH et al., 1988, with permission of Yin XH).

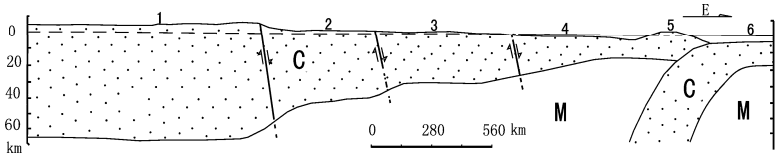

Fig. 10.11 Profile of the Chinese continent during the Himalayan Stage.

1. Qingzang Plateau (average height 4,000 m above sea level); 2. Northwest China-Inner Mongolia–Loess–Yunnan-Guizhou Plateau (average height 2,000 m above sea level); 3. Eastern plains, hills and lower mountains (average height less than 1,000 m above sea level and down to 50 m below sea level); 4. Shallow marine continental shelf (average depth 50–200 m below sea level); 5. Japan–Ryukyu–Taiwan Islands; 6. Ocean (average depth 4,000 m below sea level). C–crust; M–mantle.

A few decades ago, when there was insufficient data, it was considered, incorrectly, that the Yangtze (Changjiang) and Yellow (Huanghe) Rivers had been formed in Paleogene or even earlier times (Li CY, 1934; Li CS, 1956; Ren ME, 1959; Shen YC, 1980). From paleogeographic data Wang HZ et al. (1985) and Chen HH (1985) have shown that the Yangtze and Yellow Rivers did not form completely integrated drainage systems during the Paleogene or Neogene, or even in the earliest Early Pleistocene. At these times the rivers were represented only by a series of isolated lakes and small drainage systems (Fig. 10.4). The formation of the giant steps in the Chinese landscape led to the amalgamation of these separate systems to form the present drainage systems of the Yangtze and Yellow Rivers.

The Three Gorges provide the key to understand the development of the Yangtze drainage system. From systematic study of the river terraces in the Three Gorges area, Yang DY et al. (1988, 1992)

considered that the whole Yangtze drainage became integrated at 1.0±0.2 Ma. The most controversial aspect of the historical development of the Yellow River drainage has been the time at which the stretch of the river bed between the Shaanxi and Shanxi Provinces was formed. From a compilation of the paleo-geomorphology of the middle reaches of the Yellow River in the Pliocene and Early Pleistocene, Zhu ZY (1989) proposed that the river bed between the Shaanxi and Shanxi provinces was formed at 0.9 Ma. Evidently the whole of the Yellow River was connected up to form an integrated drainage system in the Early Pleistocene.

The sources of the Yangtze and Yellow Rivers are located in western China in the middle of the Qingzang Plateau. The rivers ran eastwards to connect up with pre-existing small drainage systems to form the two great drainage systems in the Chinese continent. The linking of the Yangtze and Yellow Rivers to form coherent drainage systems occurred in the latest epoch of the Early Pleistocene (1.0–0.9 Ma), i.e. at the peak of the Himalayan Tectonic Event. After the formation of the giant landscape steps and the rapid uplift of the Qingzang Plateau, as the difference in height between eastern and western China increased, river gradients increased, enhancing retrogressive erosion, so that the Yangtze River carved out the Three Gorges and the Yellow River carved out the Hukou Gorge, linking up the separate drainage systems.

During the Himalayan Period, the Central Asian monsoon developed due to the rapid uplift of the Qingzang Plateau and the formation of the Loess Plateau (eastern Gansu, Ningxia, Shaanxi and Shanxi). The influence of moist air masses from the Indian Ocean is restricted to the Hengduan Mountains area and the southern side of the Himalayan Mountains. Because of the gradual uplift of the Northwest China–Inner Mongolia–Loess–Yunnan-Guizhou Plateau, moist air masses from the Pacific Ocean are barely able to reach the northwest plateau in the summer, while in winter the Siberian monsoon is able to drive straight into China, gradually causing deterioration of the ecological environment and converting Northwest China into a desert. Thus the Himalayan Tectonic Event was responsible for the serious deterioration of the ecological environment of northwestern China.

The Himalayan Tectonic Event, not only resulted in a series of geological and geomorpho-logical features, such as strong deformation in western China, giant landscape steps, and the extension of the Yangtze and Yellow Rivers, but also formed a series of extensional marginal seas in the eastern part of the Chinese continent, for example, the Japan Sea (or East Korean Sea), East China Sea, the Taiwan Straits and the South China Sea. These marginal seas have been interpreted previously as back-arc basins, forming part of the western Pacific trench–arc–basin system (Uyeda, 1977; Uyeda and Kanamori, 1979).

The western Pacific trench–arc–basin system has provided the type model for all trench–arc–basin systems globally, and has provided a model for the relationships between tectonics and sedimentation in this system. According to the ideal model of a trench–arc–basin system, in the back-arc region plate subduction causes extension with the rise of the mantle and the formation of a high heat flow anomaly, parallel to the arc and the trench, leading to the formation of a back-arc basin. In this model all the components of the parallel trench–arc–basin system were forming at the same time. However, in the western Pacific the Japan–Ryukyu–Taiwan–Philippine trench–arc system was formed between 40 and 30 Ma, at a late epoch in the Paleogene, while recent paleomagnetic results, oceanic drilling and isotopic chronology for Japan and South China Sea show that these basins were formed much later, from 23-1 Ma in the Neogene to Early Pleistocene.

According to Yoon (2001), there was no extension in the Japan Sea area during the Paleogene (58–30 Ma) and shallow marine sediments were deposited in the Far East of Russia and on the eastern margin of the Korean Peninsula. Extension occurred in the middle of the Japan Sea at the end of the Oligocene and the earliest epoch of Miocene (26–18 Ma) with the formation of graben structures. Further extension, forming oceanic crust with the deposition of sediments of abyssal facies, occurred in the northeastern part of the Japan Sea during the middle and late epochs of the Miocene (18–7 Ma) with NE trending. By the late epoch of the Miocene (7 Ma) the Japan Sea, limited by polygonal faults, had been formed. Using ODP data, Tamaki et al. (1992), Jolivet and Tamaki (1992, 1994) proposed a dynamic mechanism for the origin of the Japan Sea. They proposed that extension of the Japan Sea was related to major dextral

strike-slip displacement of the eastern marginal fault. Extension, with the formation of the oceanic crust, occurred during the Early Miocene (21–18 Ma), and ceased at ~10 Ma.

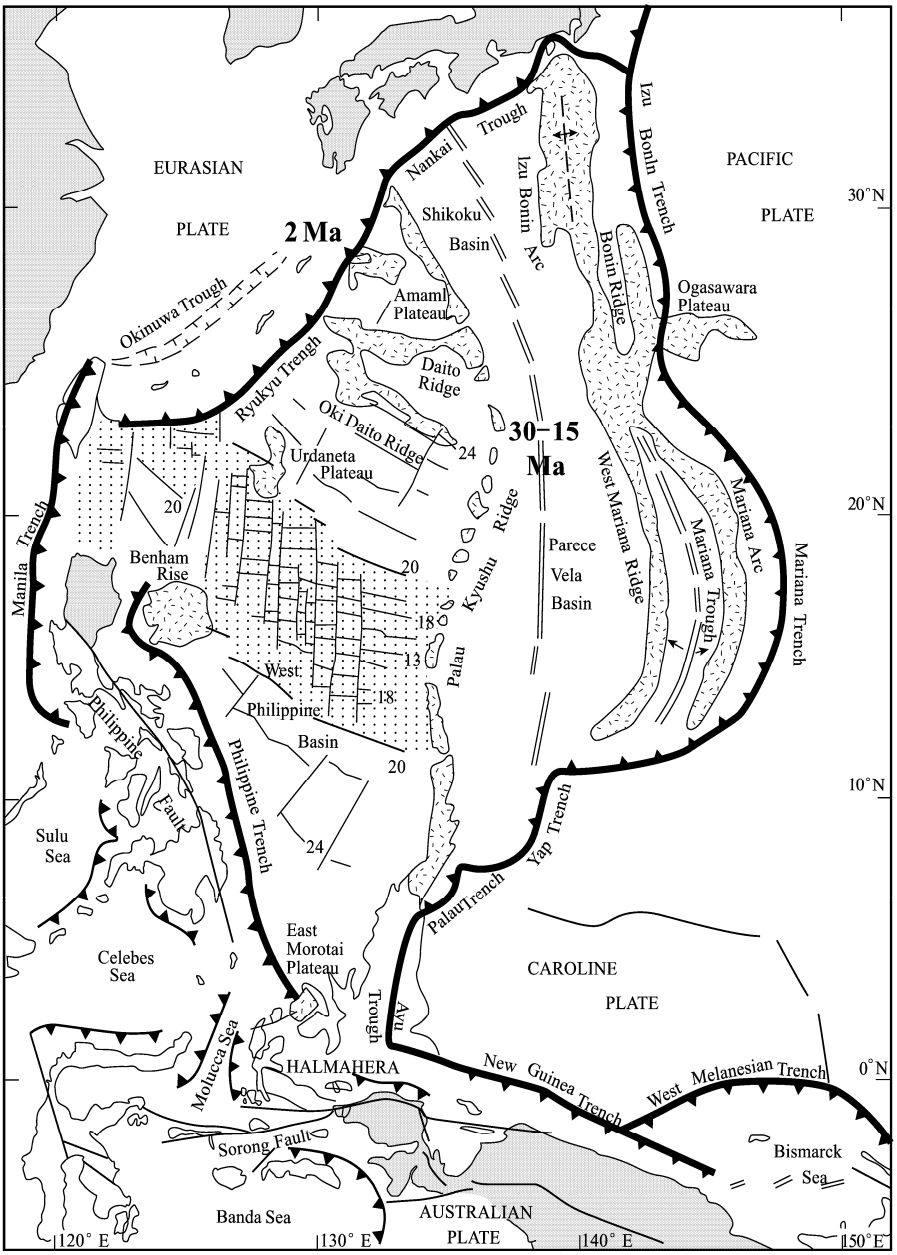

Fig. 10.12 Tectonics of the Philippine Sea Plate (Hall et al., 1995, with permission of Hall R).

In the east central part of the South China Sea an ocean with depths of 3,000–4,000 m is underlain by typical oceanic crust, with a thickness of only 4.4–8.75 km. E-W trending sea floor magnetic anomalies in that area indicate that initial N-S extension occurred during the Oligocene (32–20 Ma); there was no volcanic arc along the eastern margin of that area at that time. Wedge-shaped oceanic crust was formed in the southwestern part of the South China Sea during the Early Miocene (20–15 Ma). Basalts forming the seafloor in that area are not of back-arc type, but are of alkali and alkali-tholeiite transition type (Taylor et al., 1980, 1983; Briais et al., 1993). N-S extension in South China Sea was caused by regional E-W compression and shortening of the Pacific Plate in the Oligocene, and the NE trending wedge-shaped extension in the southwestern South China Sea could be due to northeastward compression related to the subduction of the Australian Plate. The framework of South China Sea was established in the Middle Miocene, and at the same time the Taiwan Straits and southern East China Sea changed gradually into shallow seas. The northern East China Sea became a shallow sea at the end of the Pliocene, at ~2 Ma (Xu H, 1997).

It is concluded that the dynamic mechanism for the formation of the Japan and South China Seas was not related to back-arc extension of western Pacific Plate. These marginal sea basins were formed 10–20 million years later than the formation of the trench–arc system, and the sea floor basalts are not of back-arc type. Therefore the South China and Japan Seas are not back-arc basins. If these two important marginal basins of the western Pacific Ocean are not back–arc basins, where are typical back–arc basins? The Tectonics Group of Institute of South China Sea, Chinese Academy of Sciences (1988) first recognized that the South China Sea was not a back-arc basin and proposed that it should properly be called a continental marginal extensional basin.

In the discussion of the tectonic evolution of the Chinese continent in the Himalayan Period, it is necessary to pay attention to the influence of both the Indian and Australian Plates, however, the influence of the Philippine Sea Plate should not be ignored.

The ocean floor of the Philippine Sea Plate has been systematically surveyed over the last ten years. Hall et al. (1995) using paleomagnetic data pointed out that during the Neogene the Philippine Sea Plate moved northwards at a rate of 8 cm/a. From 30 to 15 Ma the eastern basin extended E-W at a rate of 2.8 cm/yr, to form the Shikoku and Parece Vela Basins, to the south of the Japanese Islands (Fig. 10.12). In the Late Neogene and the Early Pleistocene (4–2 Ma), the Philippine Sea Plate was subducted to the north along the Ryukyu Trench and the Nankai Trough, at a rate of 4 cm/yr (Seno and Maruyama, 1984). In the Neogene, between 14 and 2.6 Ma, the west Philippine–Batan–Babuyan–East Taiwan longitudinal valley fault zone changed to a normal fault with sinistral strike-slip (39 of Fig. 10.3). The rate of extension of the East Taiwan longitudinal valley fault zone is 0.68 cm/yr (original data after E ML et al., 1987). The rate of extension in the Ryukyu Trench was 0.9 cm/yr between 11 and 1 Ma (Liu CB, 1987). The northward movement and subduction of the Philippine Sea Plate caused sinistral strike-slip translation and E-W extension along N-S trending faults in the East Asian continent, especially along its eastern margin.

The tectonic evolution of eastern China and the western Pacific during the Neogene in the Himalayan Tectonic Period was influenced by the northward migration and subduction of the Philippine Sea and Australian plates (Barber et al., 1986; Simandjuntak and Barber, 1996; Hall, 2002) and the collision of India with the southern margin of Asia. This resulted in strong deformation in western China, with thin-skinned tectonics to form the Himalaya Mountains and lithosphere shortening and thickening in Qingzang, causing the uplift of the Qingzang Plateau, followed by E-W extension and collapse. On the other hand, deformation in eastern China was very weak, with the main intraplate deformation occurring on near N-S trending faults caused by E-W extension, associated with sinistral strike-slip movement, resulting in the formation of the marginal seas of the East Asian continent. These basins should be called continental marginal extensional basins formed by N-S compression and E-W extension, rather than "back-arc" basins. The geomorphological and climatic effects of this deformation were the formation of the giant landscape steps, the full development of the Yangtze and Yellow Rivers drainage systems, the development of the Asian monsoon and the deterioration of the ecological environment of northwestern China.

References

Allègre CJ, Courtillot V, Tapponnier P et al (1984) Structure and evolution of the Himalaya–Tibet orogenic belt. Nature 307: 17–22.

Argand E (1924) La tectoniue de I'Asie. In: Proceedings of the Thirteenth International Geological Congress, pp.171–172. Brussels.

Barber AJ, Tjokrosapoetro S, Charlton TR (1986) Mud volcanoes, shale diapers, wrench faults and mélanges in accretionary complexes, Eastern Indonesia. The American Association of Petroleum Geologists Bulletin 70(11): 1729–1741.

Besse J, Courtillot V, Pozzi JP et al (1984) Palaeomagnetic estimates of crustal shortening in the Himalayan thrusts and Yarlung Zangbo suture. Nature 311 (5,987): 621–626.

Bigwaard H, Spakman W, Engdahl E (1998) Closing the gap between regional and global travel tomography. J. Geophys. Res., B 103: 30055–30078.

Briais A, Patriat P, Tapponnier P (1993) Updated interpretation of magnetic anomalies and seafloor spreading stages in the South China Sea: Implications for the Tertiary tectonics of Southeast Asia. J. Geophys. Res. 98: 6299–6328.

Burbank DW, Beck RA, Mulder T (1996) The Himalayan foreland basin. In: Yin A, Harrison TM (eds) The Tectonic Evolution of Asia. Cambridge University Press, Cambridge.

Burchfiel BC, Hodges KV, Royden LH et al (1987) East-west striking Miocene–Pliocene normal faults within the high Himalaya, south-central Tibet. Abstracts with Programs-GSA, 19(7): 605.

Burchfiel BC, Deng QD, Molnar P et al (1989) Intracrustal detachment within zones of continental deformation. Geology (Boulder) 17(8): 748–752.

Burchfiel BC, Chen ZL, Hodges KV et al (1992) The south Tibetan detachment system, Himalayan Orogen: extension contemporaneous with and parallel to shortening in a collisional mountain belt. Special Paper-GSA, 269: 41.

Bureau of Geology and Mineral Resources of Provinces (1984-1993) Regional Geology of Provinces. Geological Publishing House, Beijing (in Chinese with English abstract).

Cai XL, Zhu JS, Cao JM et al (2002) Structure and dynamics of lithosphere and asthenosphere in the gigantic East Asian–West Pacific rift system. Geology in China 29(3): 234–245 (in Chinese with English abstract).

Chamberlain CP, Zeitler PK (1996) Assembly of the crystalline terranes of the northwestern Himalaya and Karakoram, northwestern Pakistan. In: Yin A, Harrison TM (eds) The Tectonic Evolution of Asia. Cambridge University Press, Cambridge.

Chen HH, Min LR (1985) The paleogeography map of Early Pleistocene and Middle–Late Pleistocene. In: Wang HZ (ed) Paleogeography Atlas of China. SinoMaps Press, Beijing (in Chinese).

Chen ZL, Zhang YQ, Chen XH et al (2001) Late Cenozoic sedimentary process and its response to the slip history of the central Altyn Tagh fault, NW China. Science in China D 44(suppl.): 103–111 (in Chinese).

Chi JS (1988) The Study of Cenozoic Basalts and Upper Mantle Beneath Eastern China (Attachment Kimberlites). China University of Geosciences Press, Wuhan (in Chinese with English abstract).

Chi JS, Lu FX, Zhao L et al (1996) The Kimberlites and Paleozoic Features of Lithospheric Mantle of North China Platform. Science Press, Beijing (in Chinese).

Coleman RG, Wang X (1995) Overview of geology and tectonics of UHPM. In: Coleman RG, Wang X (eds) Ultrahigh Pressure Metamorphism. Cambridge University Press, Cambridge.

Copeland P, Harrison TM, Parrish RR et al (1987) Constraints on the age of normal faulting, north face of Mt. Everest: implications for Oligo–Miocene uplift. Eos Transactions 68(44): 1444. A G U, Washington DC, USA.

Copeland P, Harrison TM (1990) Episodic rapid uplift in the Himalaya revealed by ^{40}Ar/ ^{39}Ar analysis of detrital K-feldspar and muscovite, Bengal Fan. Geology (Boulder) 18(4): 354–357.

Corrigan JD, Crowley KD (1992) Unroofing of the Himalayas: a view from apatite fission-track analysis of Bengal Fan sediments. Geophysical Research Letters 19(23): 2345–2348.
Ding GY (1989) Atlas of Active Faults of China. Seismological Press, Beijing & Xi'an Map Press, Xi'an (in Chinese).
Ding GY (1991) Lithospheric Dynamic of China—Explanatory Notes for the Atlas of Lithospheric Dynamics of China. Seismological Press, Beijing (in Chinese).
Ding L, Zhong DL (1999) Metamorphic characteristics and geotectonic implications of the high-pressure granulites from Namjagbarwa, eastern Tibet. Science in China D 42(5): 491–505.
E ML, Zhao DS (1987) The Cenozoic Basalts and Deep-derived Rock Xenoliths of Eastern China. Science Press, Beijing (in Chinese).
Fu KD, Gao JP, Fang XM et al (2001) Relationship model of sediment grain size and Tibetan Plateau uplift in middle-west parts of Qilian Mountains. Science in China D 44(suppl.): 210–217.
Gong ZS, Li ST et al (1997) Continental Marginal Basins and Oil-gas Accumulation for Northern Nanhai. Science Press, Beijing (in Chinese).
Hall R, Blundell DJ (1995) Reconstructing Cenozoic SE Asia. Geological Society Special Publications 106: 153–184.
Hall R (2002) Cenozoic geological and plate tectonic evolution of SE Asia and the SW Pacific: computer based reconstructions, models and animations. Journal of Asian Earth Sciences 20(4): 353–431.
Harrison TM, Copeland P, Kidd WSF et al (1992) Raising tibet. Science 255: 1663–1670.
Houseman G, England P (1996) A lithospheric-thickening model for the Indo-Asian collision. In: Yin A, Harrison TM (eds) The Tectonic Evolution of Asia. Cambridge University Press, Cambridge.
Huang TK (Jiqing) (1945) On the major structural forms of China. Geological Memoirs, ser. A, no. 20, 165pp.
Huang JQ, Zhang ZK, Zhang ZM et al (1965) Eugeosynclines and miogeosynclines of China and their development of multi-gyration. In: Professional Papers of Academy of Geological Sciences, Section C: Regional Geology and Structure Geology. China Industry Press, Beijing (in Chinese).
Jia JH (2000) Depositional sequence and reservoir of Cretaceous Bashijiqike formation in Kuqa foreland basin. Earth Science Frontiers 7(3): 133–143 (in Chinese with English abstract).
Jiang FC, Wu XH (1993) Fundamental characteristics of the stepped landform in China continent. Marine Geology & Quaternary Geology 13(3): 15–24 (in Chinese with English abstract).
Jolivet L, Tamaki K (1992) Neocene kinematics in the Japan Sea region and the volcanic activity of the northeast Japan arc. Proc. Ocean Drill. Program Sci. Results 127–128: 1311–1331.
Jolivet L (1994) Japan Sea, opening history and mechanism: a synthesis. J. Geophys. Res. 99: 22237–22259.
Klootwijk CT, Radhakrishnamurty C (1981) Phanerozoic paleomagnetism of the Indian plate and India-Asia collision. In: McElhinny MW, Valencio DA (eds) Paleoconstruction of the continents. Geodynamics series, 93–105. Geological Society of America, Boulder, Colorado.
Klootwijk CT, Conaghan PJ, Powell CM (1985) The Hiamlayan arc: large–scale continental subduction, oroclinal bending and back-arc spreading. Earth Planet. Sci. Lett. 75: 167–183.
Klootwijk CT, Gee JS, Pierce JW et al (1991) Constraints on the India-Asia convergence: paleomagnetic results from Ninety East Ridge. In: Weissel J, Pierce J et al (eds) Proceedings of the ocean drilling program, scientific results, pp.777–884. Texas A & M University Press, College Station.
Klootwijk CT, Gee JS, Peirce JW et al (1992) An early India-Asia contact: paleomagnetic constraints from Ninety east ridge, ODP leg 121. Geology 20: 395–398.
Lee TY, Lawver LA, (1995) Cenozoic plate reconstruction of southeast Asia. Tectonophysics 251(1–4): 85–138.
Li CS (1956) The developmental history of Yangtze River. Yangtze River, Oct (in Chinese).
Li CY (1934) The genesis of the river valleys in upper Yangtze River. Journal of Geological Society of China 13(1): 107–118.
Liu CB (1989) The pumice in Okinawa trough. Acta Petrological et Mineralogical 8(3): 193–202 (in Chinese with English abstract).

Liu HF (1995) Classification of foreland basins and fold thrust style. Earth Science Frontiers 2(3): 59–68 (in Chinese with English abstract).

Liu MQ, Yang BZ, Deng JG et al (1993) Tectonic Features and Evolution of Yitong–Shulan Graben. Geological Publishing House, Beijing (in Chinese with English abstract).

Liu RX Chen WJ, Xie GX et al (1992) The Chronology and Geochemistry of Cenozoic Volcanic Rock in China. Seismological Press, Beijing (in Chinese).

Ma ZJ, Zhang JS, Wang YP (1998) The 3-D deformational movement episodes and neotectonic domains in the Qinghai-Tibet plateau. Acta Geologica Sinica 72(3): 211–227 (in Chinese with English abstract).

Mercier JCC (1980) Magnitude of the continental lithospheric stresses inferred from rheomorphic petrology. Jour. Geophys. Res. B 85(11): 6293–6303.

Meyer B, Tapponnier P, Bourjot L et al (1998) Crustal thickening in Gansu-Qinghai, lithospheric mantle subduction and oblique strike-slip controlled growth of the Tibet Plateau. Geophysical Journal International 135(1): 1–47.

Molnar P, England P, Martinod J (1993) Mantle dynamics, uplift of the Tibetan Plateau and the Indian monsoon. Rev. Geophys. 34(4): 357–396.

Powell CM, Conagham PJ (1973) Plate tectonics and the Himalayas. Earth Planet. Sci. Lett. 20: 1–12.

Qi JF, Chen FJ (1995) Structural Analyses of Cenozoic Fault Basin in Lower Liaohe–Liaodong Bay. Geological Publishing House, Beijing (in Chinese).

Ren ME (1959) River valley geomorphology and river capturing problems of Jinshajiang, northwestern Yunnan. Acta Geographica Sinica 25(2): 135–155 (in Chinese).

Research Group of Altun Active Fault Zone, Seismic Bureau of China (1992) Altun Active Fault Zone. Seismological Press, Beijing.

Royden LH, Burchfiel BC (1997) Surface deformation and lower crustal flow in eastern Tibet. Science 276(5,313): 788–790.

Searle MP (1995) Plate tectonics: the rise and fall of Tibet. Nature (London) 374 (6,517): 17–18.

Searle MP (2007) Geological map of the Mount Everest-Makalu Region Nepal-South Tibet Himalaya, Scale 1: 100,000. University of Oxford, Allan Hochreiter.

Seeber L, Armbruster JG, Quittmeyer RC (1981) Seismicity and continental subduction in the Himalayan Arc. In: Gupta HK, Delany FM (eds) Zagros, Hindu Kush, Himalaya, geodynamic evolution, geodynamics series, 3: 215–242. American Geophysical Union, Washington DC.

Seno T, Maruyama S (1984) Paleogeographic reconstruction and origin of the Philippine Sea. Tectonophysics 102 (1–4): 53–84.

Shen YC (1980) River geomorphology. In: Editorial Committee of Physical Geography, Chinese Academy of Science, Physical Geography of China (Geomorphology). Science Press, Beijing (in Chinese).

Simandjuntak TO, Barber AJ (1996) Constant tectonic styles in the Neogene orogenic belts of Indonesia. In: Hall R, Blundell D (eds) Tectonic Evolution of Southeast Asia. Geological Society Special Publication, 106: 185–201.

Sinha-Roy S (1982) Hamalayan main central thrust and its implications for Himalayan inverted metamorphism. Tectonophysics 84(2–4): 197–224.

Song CH, Fang XM, Li Jijun et al (2001) Tectonic uplift and sedimentary evolution of Jiuxi basin in the northern margin of the Tibetan Plateau since 13Ma BP. Science in China D 44(suppl.): 192–202.

Tamaki K, Suyehiro K, Allan J et al (1992) Tectonic synthesis and implications of Japan Sea ODP drilling. Proc. Ocean Drill. Program Sci. Results 127–128: 1333–1348.

Tapponnier P, Mercier JL, Proust F et al (1981) The Tibetian side of the Indian-Eurasian collision. Nature, 294 (5840): 405–410.

Tapponnier P, Lacassin R, Leloup PH et al (1990) The Ailao Shan / Red River metamorphic belt: tertiary left-lateral shear between Indochina and South China. Nature 343 (6,257): 431–437.

Taylor B, Hayes DE (1980) The tectonic evolution of the South China Basin. In: Hayes DE (ed) The tectonic and geologic evolution of Southeast Asian Seas and Islands, Geophy. Monogr. 23: 89–104. American Geophysical Union, Washangton DC.

Taylor B, Hayes DE (1983) Origin and history of the South China Basin. In: Hayes DE (ed) The tectonic and geologic evolution of Southeast Asian Seas and Islands. Geophy. Monogr. 27(Part 2): 23–56. American Geophysical Union, Washangton DC.

Teng JW, Zeng RS, Yan YF et al (2003) Depth distribution of Moho and tectonic framework in Eastern Asian continent and its adjacent ocean areas. Science in China D 46(5): 428–446.

Tectonics Group of Institute of South China Sea, Chinese Academy of Sciences (Liu ZS et al) (1988) Geological Structure in South China Sea and Spreading of Continental Margin. Science Press, Beijing (in Chinese).

Uyeda S (1977) Some basic problems in the trench-arc-back arc basin system. In: Talwani M and Pitman WC (eds) Island arc, deep sea trenches and back-arc-basin, 1–14. American Geophysical Union, Washangton DC.

Uyeda S, Kanamori H (1979) Back-arc opening and the mode of subduction. J.G.R. 84: 1049–1062.

Van der Voo R (1990) The reliability of Paleomagnetic data. Tectonophysics 184(1): 1–9.

Wan TF (1994) Intraplate deformation, tectonic stress and their application for Eastern China in Meso-Cenozoic. China University of Geosciences Press, Wuhan.

Wang GZ, Wang CS (2001) Disintegration age of basement metamorphic rocks in Qiangtang, Tibet, China. Science in China D 44(suppl.): 86–93.

Wang HZ (1985) Atlas of Paleogeography of China. SinoMaps Press, Beijing (in Chinese).

Wang YM, Wan TF (2008) Lithosphere tectonic detachments in Eastern China control of Cenozoic magmatism and earthquake. Geoscience, 22(2): 207–229 (in Chinese with English abstract).

Xiao XC, Li TD, Li GC et al (1998) Lithospheric Tectonic Evolution of Himalaya. Geological Publishing House, Beijing (in Chinese).

Xu H (1997) Changing in Chinese seas and continents. Marine Geology Letters (7): 4–7 (in Chinese).

Yang DY, Lü Guonian (1992) Study on the through time and its geological implication of the Three Gorges along the Changjiang (Yangtze) River. In: Liu DS, An ZS (eds) Loess, Quaternary Geology and Global Change. vol. 3. Science Press, Beijing (in Chinese).

Yang KC (1989) Skip-Type Fault-depression mechanism and its oil bearing for China basins, discussed from regional seismic profile. unpublishing report, Explanation Center, Petroleum Geophysical Bureau (in Chinese).

Yin XH, Liu ZP, Wu JX et al (1988) The features of bouguer gravity field and structures of crust-upper mantle in the transition zone on the eastern border of Qinghai-Xizang-Mongolian Plateau. Seismology and Geology 10(4): 143–150 (in Chinese with English abstract).

Yoon S (2001) Tectonic history of the Japan Sea region and its implications for the formation of the Japan Sea. Journal of Himalayan Geology 22(1): 153–184.

Zeng RS, Sun WG, Mao TE et al (1995) Depth map of Moho interface of China continent. Acta Seismologica Sinica 17(3): 322–327 (in Chinese with English abstract).

Zhang ML (1998) Studies on the tectonic evolution and the stress field of the Qaidam Basin in Meso-Cenozoic Era. Dissertation, China University of Geosciences, Beijing (in Chinese with English abstract).

Zhang PZ, Molnar P (2001) Reponse of sedimentary and erosion rate to climate change. In: Lu YC et al (eds) Neotectonics and Environment. Seismological Press, Beijing.

Zhang QM, Liu FN, Yang JH (1996) Overpressure system and hydrocarbon accumulation in the Yinggehai basin. China Offshore Oil and Gas (Geology) 10(2): 65–75 (in Chinese with English abstract).

Zhao WJ, Nelson KD and Project INDEPTH Team (1993) Deep seismic reflection evidence for continental underthrusting beneath southern Tibet. Nature 366 (6,455): 557–559.

Zhao WJ, Nelson KD, Xu ZX et al (1997) Double intracontinental underthrusting structure of the Yarlung Zangbo suture and different molten layers-A comprehensive study of INDEPTH's results. Acta Geophysica Sinica 40(3): 325–336 (in Chinese with English abstract).

Zhong DL, Ding L (1993) Analyzed dispersion of Gondwana continent and accretion of Asia from the evolution of Tethys belt in Sanjiang and adjacent areas. In: China Working Group on International Geological Comparison Program. Project 321. Growth of Asia. Seismological Press, Beijing (in Chinese).

Zhong DL (1998) Paleo-Tethyan Orogenic Belt in western Yunnan and Sichuan. Science Press, Beijing (in Chinese).

Zhu ZY (1989) The formation of river terraces and evolution of drainage system in the middle Yellow River. Acta Geographica Sinica 44(4): 429–440 (in Chinese with English abstract).

Chapter 11
Tectonics of Middle Pleistocene–Holocene (The Neotectonic Period, since 0.78 Ma)

The Neotectonic Period during which the present day landforms were developed was proposed by the Soviet Russian geologist Obruchef in 1948. Using this criterion, his student, Niglayf, considered that the Neotectonic Period commenced during the Miocene or Pliocene Period. However, it was later found that it was not appropriate to define the period only in terms of landform evolution (Ding GY, 2003 (personal communication)). As explained in Chapter 10, the main period for the formation of the present landforms of the Chinese continent mainly formed in the Miocene–Early Pleistocene. However, if the rules of priority are followed, it was unnecessary to introduce a "Neotectonic Period", as Huang JQ (1945) had already defined the Himalayan Tectonic Period to cover the same period, and this usage was widely applied in China.

During the past 40 years, with the development of large-scale engineering projects, geologists have paid more attention to seismic activity, geomorphology and environmental geology, and the term "Neotectonics" has been used more universally. Ding GY (1995), who first pioneered the study of Neotectonics in China, considered that the recognition of a Neotectonic Period was necessary as applied to ground stability studies on major engineering projects, and recognized that the Neotectonic Period Commenced from Quaternary. Now Neotectonics is taken to comprise recent active tectonics.

According to author's present understanding of the tectonics of China, there was a notable change in the tectonic stress field between the Early and Middle Pleistocene. It has been suggested by Wan TF (1993) that the Neotectonic period should be defined to extend from the Middle Pleistocene to the present day on the Chinese continent, because in China there is generally an angular unconformity between the Early and Middle Pleistocene systems, but since the Middle Pleistocene the continent has been consistently stable. However, after the Middle Pleistocene the situation was quite different from the Neogene and Early Pleistocene epoch in the Himalayan Tectonic Period (23–0.78 Ma). As defined by Wan TF (1993), the Neotectonic Period commenced only 780 thousand years ago, marking the commencement of a new period in the tectonic evolution of China. In the Neotectonic Period the orientation and magnitude of the principal stresses have new characteristics, but tectonic activity is very weak compared with the Mesozoic era and earlier Cenozoic era.

At the present time, although Neotectonic tectonic activity is the youngest and weakest, because of its importance for major engineering projects and its obvious applications in the exploration for mineral and energy resources, research on earthquakes, changes in the environment and for the prediction and mitigation of geological disasters, it is the most intensively and quantitatively studied aspect of tectonics in China.

11.1 Intraplate Deformation and Recent Tectonic Stress Field

(1) Deformation During the Neotectonic Period

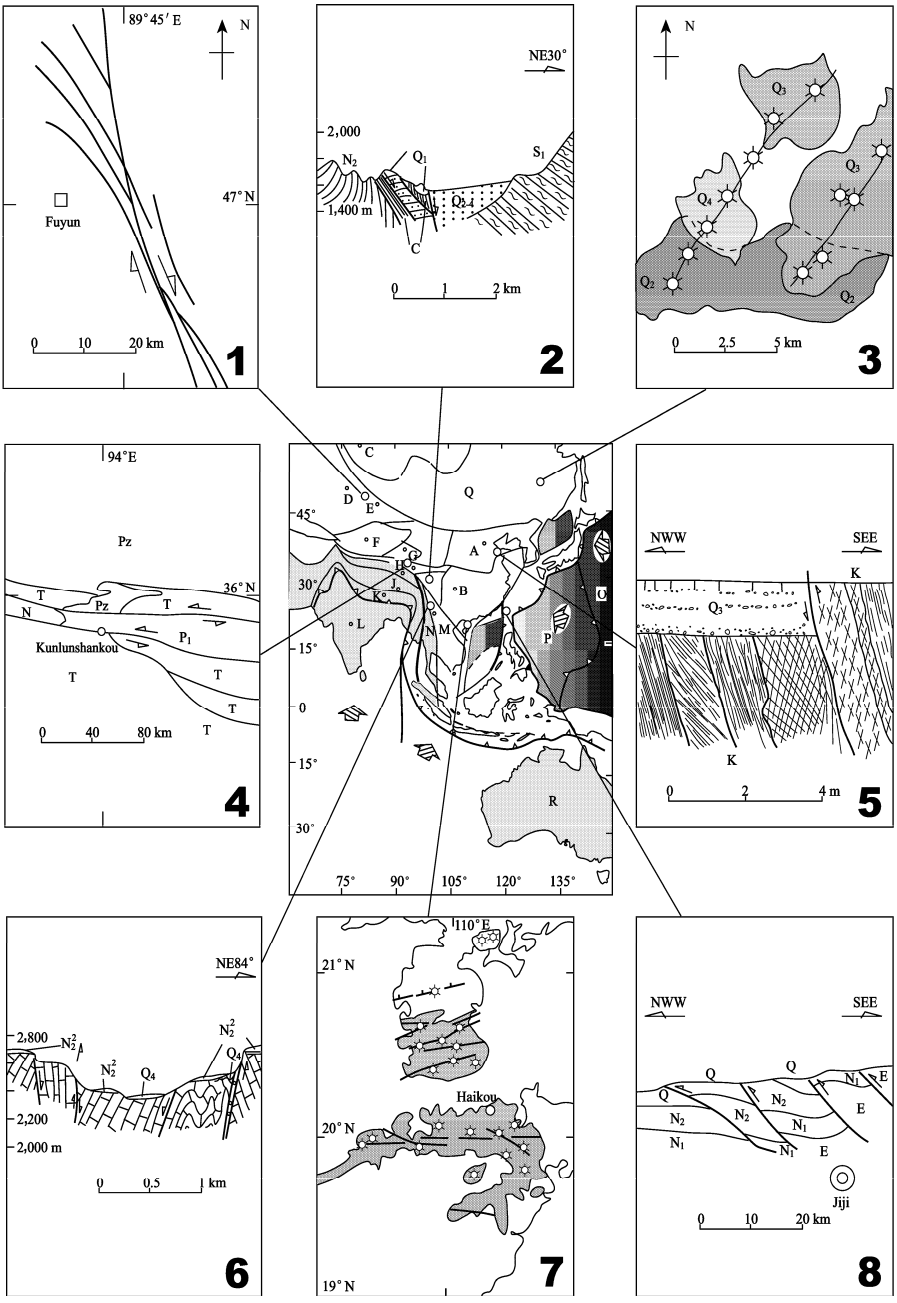

Fig. 11.1 Deformation in China during the Neotectonic Period.

1. The Fuyun earthquake fault, an earthquake of Ms = 8 occurred in 1931, due to movement along a dextral fault of 180 km long with a maximum horizontal displacement of 14m (Seismic Bureau of Xinjiang, 1985); 2. The active Haiyuan Fault, trending NW 290° with a maximum sinistral horizontal displacement of 600 m since the Late Pleistocene (Deng QD et al., 1987); 3. The distribution of Middle Pleistocene to Holocene Wudalianchi volcanoes, controlled by active faults trending NE 45° (Bureau of Geology and Mineral Resources of Heilongjiang Province, 1993); 4. The rate of horizontal displacement of the East Kunlun sinistral strike-slip fault is 10–15 mm/yr, with a vertical displacement of 1 mm/yr since Late Pleistocene (Ren JW, et al., 1999); 5. Since the Late Pleistocene the F1 active fault in Tancheng–Lujiang Fault Zone has a vertical displacement of 2–3 m and a horizontal dextral strike-slip displacement of ~100 m (Wan TF et al., 1996; Lin AM et al., 1998), and the dextral strike-slip displacement is about 200 m on its northward extension in Bohai Bay (Sea Oil Exploration Institute (unpublished data)); 6. In an active Quaternary fault near Lijiang-Baoshan, Western Yunnan; the planation surface of the Neogene is cut off about 800–1,000 m to the north (Zhongdian), vertical displacement of the active fault is about 2,000 m, and only 300 m to the south at Lianghe area; Sinistral strike-slip displacement on this fault is more than 1 km since Middle Pleistocene (He KZ et al., 2001); 7. Volcanic craters and controlling active E-W faults in the Leizhou-Qiongzhou district. The volcanoes have been active since 7.5 Ma (Chen WJ et al., 1992); 8. An earthquake fault at Jiji, Taiwan; an earthquake of Ms=7.3 occurred along this fault on November 21st, 1999, in which the hanging wall was uplifted for 2.2–4.5 m with a horizontal sinistral slip of 7.1 m to the northwest; the footwall subsided 0.3 m with a horizontal sinistral slip of 1.1 m. The depth of the epicenter was 7–10 km, indicated by the circles (Wang Y et al., 2001).

Note: All the symbols are the same as those used in Fig. 6.5.

Deformations have been very weak on the Chinese continent during the Neotectonic Period. In most areas there are no records of folding since Middle Pleistocene. The Neotectonic has been a stable tectonic period in Chinese continent, especially during Middle Pleistocene the weathering has formed "terra rossa" soils over the most of areas. However, since the Late Pleistocene, tectonic activity has increased.

Since the Middle Pleistocene 105 folds have developed in the Neogene and Quaternary systems in western Taiwan and its adjacent sea floor. These folds are several kilometers long, and have NNE trending axes with fold limbs dipping at various angles, from steep to gentle. Nearly half the folds are sheared by reversed faults, and some form oil and gas-bearing structural reservoirs. These reversed faults, such as Ji-Ji earthquake fault, Taiwan (8 in Fig. 11.1) also have a sinistral displacement. Folds and reversed faults indicate that at present these areas are undergoing ESE-WNW shortening. The Taiwan area shows the most obvious Quaternary tectonism in China.

Faults activities since the Late Pleistocene are distributed throughout the Chinese continent. Most of this activity is due to the reactivation of old faults, but may show a different style of displacement. For instance, volcanic craters in Leizhou-Qiongzhou, between Guangdong and Hainan Island are distributed along active E-W faults, but have been erupting from 7.5 Ma to the present day (7 in Fig. 11.1) (Chen WJ et al., 1992). This area is undergoing near E-W shortening. In the Neotectonic Period the F1 active fault in the eastern part of the Tancheng-Lujiang Fault Zone has changed to a transpressional fault with dextral strike-slip, which is rather closed, influenced by E-W shortening, very different from the Neogene-Early Pleistocene normal fault displacement due to E-W extension. Since the Late Pleistocene, vertical displacement on the F1 active Tancheng-Lujiang Fault Zone has been 2–3m and the horizontal dextral strike-slip displacement 100–200 m (5 in Fig. 11.1) (Wan et al., 1996; Lin et al., 1998 (personal communication of CNOOC)). Recently, a macro gas and oil reservoir (PL19-3 in Bohai area) has been discovered along the fault (F1) due to closing the fault zone, which had been explored and exploited by ConocoPhillips China Inc. and CNOOC (personal communication, 2008). The Wudalianchi volcanic craters formed in Heilongjiang Province during the Middle Pleistocene-Holocene are controlled by NE 45° trending active faults. These faults are tension fractures, showing that the area has been shortened in an NE-SW direction since the Middle Pleistocene (3 in Fig. 11.1) (Bureau of Geology and Mineral Resources of Heilongjiang Province, 1993).

In western China violent earthquakes have occurred along active faults. In 1931 during the Ms = 8 NNW Fuyun earthquake in north Xinjiang, a fault developed over a distance of 180 km, with a maximum dextral displacement of 14 m, indicating N-S shortening (1 in Fig. 11.1) (Seismic Bureau of Xinjiang, 1985). In the frontal faults of the thin-skinned thrust structure in northeast Qinghai-Xizang, the NW 290° strike of the active transpressional Haiyuan Fault, Ninxia, is controlled by NE-SW shortening, with a maximum sinistral strike-slip displacement of 600 m since the Late Pleistocene (2 in Fig. 11.1) (Deng QD et al., 1987). Since the Late Pleistocene the sinistral displacement of the E-W trending East Kunlun

Fault in the Qinghai-Xizang thin-skinned structure has reached 1,000–1,500 m, at a rate of horizontal movement of 10–15 mm/yr and a rate of vertical movement of 1 mm/yr (4 in Fig. 11.1) (Ren JW et al., 1999). In an active Quaternary fault near Lijiang-Baoshan, Yunnan on the eastern front of Qinghai-Xizang thin-skinned thrust structure, the Neogene planation surface is cut off about 800–1,000 m, to the north (Zhongdian) vertical displacement across the fault is about 2,000 m, but only 300 m to the south, at Lianghe area. The amount of sinistral strike-slip displacement has been more than 1 km since the Middle Pleistocene in this district (6 in Fig. 11.1) (He KZ et al., 2001).

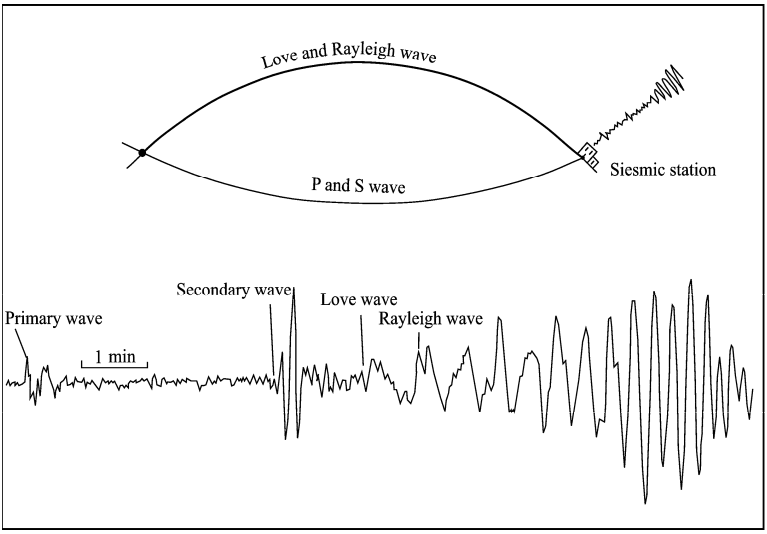

Fig. 11.2 Transmission of earthquake waves.

(2) The Recent Tectonic Stress Field

The active faults described above are controlled completely by the Neotectonic stress field. It is difficult to determine the Recent tectonic stress field using rare data from deformation during the Neotectonic Period, but it is possible to determine the principal stress directions of the Recent tectonic stress field by using fault plane solutions from seismic data (Byerly, 1926; "seismic focus mechanism solution" in Russia). The method uses the positive or negative (up or down) symbols of the P-wave (longitudinal wave) first motions of seismic wave transmissions from the same earthquake, as recorded by adjacent seismic stations, this data is then plotted on a stereogram as two fault planes dividing positive or negative quadrants of the P-wave first motion (Figs. 11.2 and 11.3). The angular bisector within the positive quadrant of the P-wave initial motion is equal to the extension axis (T axis, namely minimum principal compressive stress axis $=\sigma_3$), the angular bisector within the negative quadrant of P-wave initial motion is equal to the compression axis(P axis, namely the maximum principal compressive stress axis $=\sigma_1$), and the intersection of the two fault planes defines the intermediate principal stress axis ($=\sigma_2$) (Fig. 11.3).

In 1973, the Chinese National Seismic Bureau organized a fault plane solution research group, which has studied earthquake data since 1933 systemically for the whole of China. The research group recognized that most earthquakes which occurred beneath the Chinese continent are intraplate shallow-focus earthquakes, controlled by the horizontal principal stress direction. Using data from 173 shallow-focus tectonic earthquakes, recorded between 1937 and 1977, Yan JQ et al. (1979) calculated fault plane

solutions, selecting earthquakes stronger than Ms=6, and using the principal earthquake, but not the aftershocks. The results were compiled from earthquake data for China and its adjacent areas on a distribution map of principal compressive stress axes. Continuing research during the last 30 years has verified these results, although researchers have used different earthquake data to determine the fault plane solutions (Li QZ, 1973; Kan RJ, 1977; Lin JC, 1980; Group of Earthquake Focal Mechanism of Six Provinces and Cities, 1981; Zhang SC, 1981; Xu ZH, 1983, 1989; Wang SY, 1985). These results have once again shown that the orientation of the principal compressive stress axes have been determined correctly from earthquake data, and are applicable to local conditions. The author has used these data to show the distribution of the maximum principal compressive stress axes for the Recent tectonic stress field on the Neotectonic map (Wan TF, 1984, 1988, 1994) (Fig. 11.4).

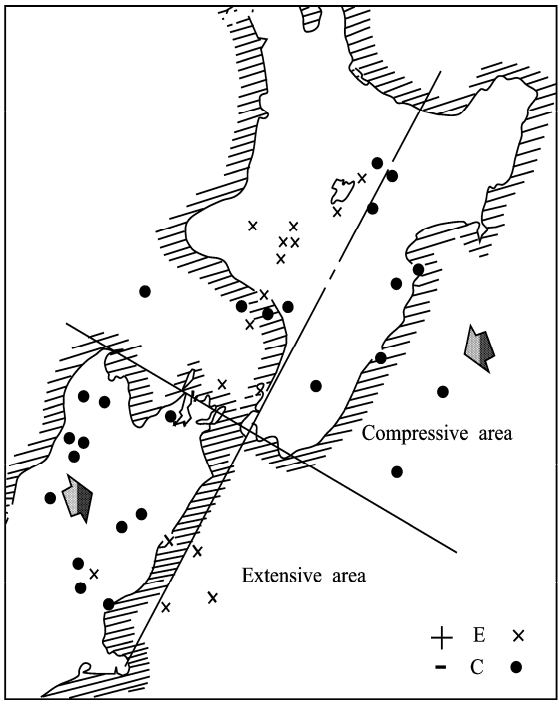

Fig. 11.3 The distribution of earthquake first motion P-wave determinations (black dots–negative, in the compression quadrant; crosses–positive, in the extension quadrant) and the fault plane solution (lines), an example from an earthquake in middle New Zealand (Eiby, 1980).

As shown in Fig.11.4, the direction of the maximum principal compressive stress axes (σ_1) for the Recent tectonic stress field is different in the areas of Chinese continent. In northeastern China the maximum compressive stress axis has an NE orientation, in North China an ENE orientation, in the Shandong–Henan–southern Shaanxi area, a near E-W orientation, in South China an NW orientation, in Hainan Island, an E-W orientation, south of the Qinghai-Xizang area, an N-S orientation, the same as in the Neogene period, and changes to an NE orientation in the northern Qaidam area, however in the western Xinjiang area it has an NNW orientation. In general, the maximum principal compressive stress axes are mainly nearly E-W in the eastern Chinese continent, radiating and gradually spreading out eastwards. In western China the maximum compressive stress axes have a near N-S orientation radiating

and gradually spreading northwards. The present tectonic stress field did not appear in the geological record before the Middle Pleistocene Epoch. The orientation of recent maximum principal compressive stress traces and their variation throughout China is most important for understanding active tectonics and for resolving problems in the distribution of resources, changes in geological environments and in the prediction and mitigation of natural disasters.

In the Neotectonic Period the value of tectonic stress, obtained from reliable "*in situ*" testing during the past forty years, is much more precise than the estimated magnitude of paleo-tectonic stress for earlier geological periods. The method used to measure the value of recent tectonic stress is the hydraulic fracturing method (Hubbert and Willis, 1957; Haimson, 1975; Zoback et al., 1977, 1979, 1980; Zhang JH et al., 2001). Hydraulic fracturing data is obtained easily from oil and gas fields, as the method is used to increase the permeability of the reservoir rocks to enhance recovery. Rubber packers are used to line a section of the drill hole where rocks are un-fractured and a hydraulic fluid is pumped into this section of the well. Under the action of original fracture pressure (Pr), the rock ruptures around the well. When pressure increase is stopped, maintaining the hydraulic pressure, the pressure gradually decreases until it reaches an equilibrium. The value of the pressure is then measured and is termed the "instant closing pressure" (Pc is equal to the value of horizontal minimum principal compression stress σ_3). The value of horizontal maximum principal stress(σ_1) can be calculated using the following formula:

$$\sigma_1 = 3Pc + St - Pr - P_0$$

where St is the tensile strength of the rock, obtained from well samples measured in the laboratory, or by calculating the difference between the original fracture pressure and secondary tensile pressure. P_0 is the fluid pore pressure, and could be represented by the hydrostatic pressure at the point of measurement. The differential stress between the maximum horizontal principal stress and minimum horizontal principal stress is represented as $\Delta\sigma(=\sigma_1-\sigma_3)$.

According to the report of China National Committee, International Union of Geodesy and Geophysics (IUGG, 1983) and data collected more recently (Appendix 4), the mean value of recent tectonic stress (differential stress) in the Chinese continent is 20.9 MPa, which is equivalent to 1/4–1/5 of the value of the paleo-differential stress during tectonically active periods in geological history. It shows that Recent tectonic stress field does not represent a period of high tectonic activity, but a period of relative stability. At depth of 2,000 m in sedimentary basins on the Chinese continent, the value of maximum horizontal principal stress is 1.1–2.2 times that of vertical principal stress, which shows that the horizontal principal stress is greater than vertical principal stress at present in the basins. This data does not support the hypothesis that the basins are the result of mantle uplift. The value of maximum horizontal principal stress is 1.2–1.7 times greater than that of minimum horizontal principal stress.

In 9 areas in North China the value of mean differential stress was found to be 18.5 MPa, and in South China 29 MPa in 6 areas (Appendix 4). As estimated by Wan TF and Chu MJ (1987) the value of differential stress is 38.2 MPa at 5 km depth in the Fujian-Taiwan active reverse fault system, similar to the value at 2 km depth in the Shanshui Basin, Guangdong (Appendix 4). The difference in the value of tectonic stress between North and South China may be related to the presence, in North China, of many active faults and detachments, especially in the middle crust, which have not healed, so that the stress is easily released and difficult to accumulate and to maintain in the present tectonic stress field. By contrast, in South China, deep faults and detachments in the middle crust were sealed during the Mesozoic by granitic magma, so that the crust is more coherent and has a higher strength. Therefore tectonic stress is more easily accumulated but not easily released.

In the Recent tectonic stress field, pre-existing faults have often been reactivated in the Neotectonic Period. Most pre-existing faults with a high angle of dip in the upper crust, both in eastern and western China, are nearly perpendicular to the direction of maximum principal compressive stress, or intersect this direction at a high angle, so that most of these fault planes are closed under compression. In faults which have other angles to the axis of maximum compressive stress, movement along the fault plane is

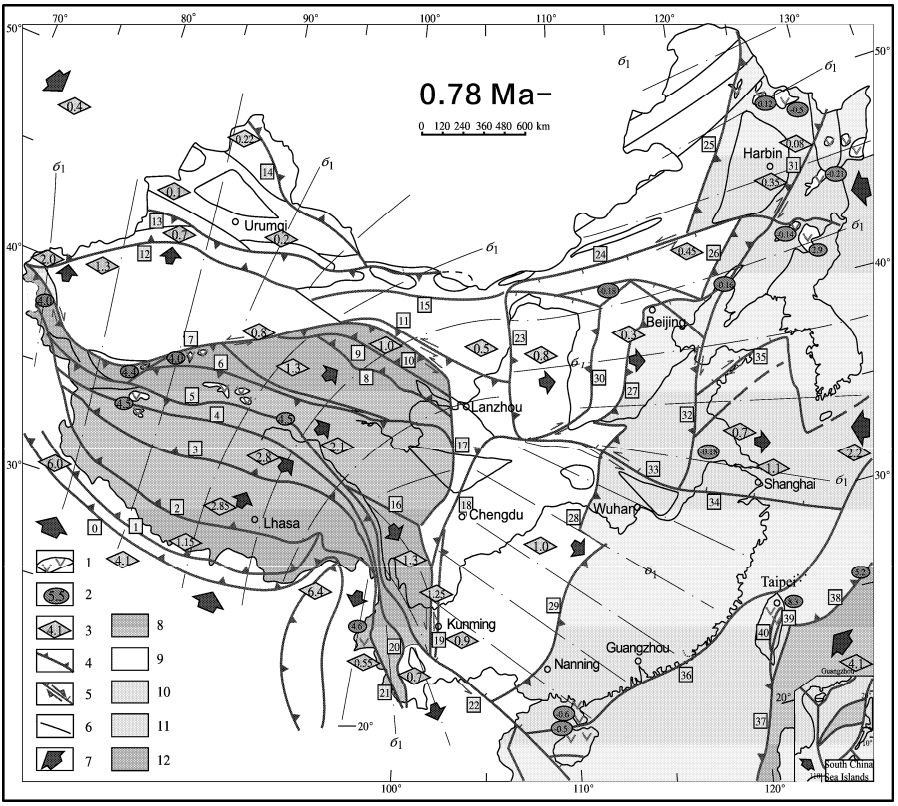

Fig. 11.4 Tectonic sketch of the Chinese continent in the Neotectonic Period (since 0.78 Ma).

1. Neotectonic volcanic rocks; 2. Rates of plate movement obtained from petrochemical data, "-", the velocity of extension, others, the velocity of shortening (unit: cm/yr) (Appendix 5.10); 3. Rates of in-plate movement, calculated from GPS and seismic moment data (Appendix 5.11); 4. Numbered recent plate boundaries or active large-scale reverse faults; 5. Numbered active strike-slip or normal faults; 6. Maximum principal compressive stress trace (according to earthquake fault plane solutions); 7. Directions of plate movement; 8. Qinghai-Xizang Plateau, mean height above sea level 4,000 m; 9. Inner Mongolia-Loess-Yunnan-Guizhou Plateau, mean height above sea level 2,000 m; 10. Lower mountains, hills and plains in eastern China, mean height above sea level 1,000–0 m; 11. Shallow marine area; 12. Oceans.

Numbered subduction, collision and fault zones:

Fault Number: [0] Himalayan Main Boundary Thrust (MBT); [1] Himalayan Main Central Thrust (MCT); [2] The Yarlung Zangbo River Thrust; [3] Bangonco–Nujiang Thrust Belt; [4] Shuanghu–Tanggula reversed fault zone; [5] Lazhulong–Jinshajiang reversed fault zone; [6] Kangxiwa–Kunlun Mountains reversed fault zone; [7] Southern frontal Tarim (Keziletao–Kuyake–Altun) Thrust with sinistral displacement; [8] Southern frontal Junulshan–Qinghai Hu (northern frontal Qaidam) reversed fault; [9] Southern frontal Mid-Qilian overthrust; [10] North frontal North Qilian overthrust; [11] Longshoushan reversed fault; [12] Korla–Wuqia Thrust; [13] Yilin Habirga–Yagan Thrust; [14] Ertis–Klamali Thrust; [15] Northern frontal Alxa reversed fault; [16] Yidun–Litang Thrust; [17] Eastern frontal Daxueshan reversed fault; [18] Jiajinshan reversed fault; [19] Xiaojiang normal-sinistral strike-slip fault; [20] Lancangjiang normal fault zone; [21] Luxi–Menglian normal fault; [22] Honghe sinistral strike-slip fault; [23] Liupanshan–Helanshan reversed fault; [24] Xar Moron He sinistral strike-slip-normal fault; [25] Eastern frontal Dahingganling Thrust; [26] Beipiao–Jianchang reversed fault; [27] Eastern frontal Taihangshan Thrust; [28] Eastern frontal Funiushan–Wulingshan reversed fault; [29] Xuefengshan–Damingshan reversed fault; [30] Fenhe–Weihe reversed fault zone (dextral strike–slip at the southern end); [31] Yilan–Yitong dextral strike-slip-reversed fault; [32] Tancheng–Lujiang dextral strike-slip-reversed fault; [33] Baoji–Luonan–Fangcheng sinistral strike-slip normal fault; [34] Fanchang–Ningbo hidden active normal fault zone; [35] Zhucheng–Rongcheng sinistral strike-slip-normal fault; [36] Coastal Fujian–Guangdong reversed fault; [37] West Philippine–eastern Taiwan sinistral strike-slip fault zone; [38] Ryukyu subduction belt; [39] Eastern Taiwan longitudinal valley (sinistral strike-slip); [40] Western Yushan Thrust.

strike-slip, either sinistral or dextral. First motion studies show that most shallow-focus earthquakes in the Chinese continental crust have a strike-slip mechanism.

(3) Earthquake Activity and Neotectonics

From the analysis of all Ms≥7 earthquakes between 1900 and 1980 and all Ms≥4 earthquakes between 1970 and 1980 in the Chinese continent, it is found that 90 percent of the seismic foci of Ms≥6 earthquakes and their aftershocks are concentrated at depths between 10 and 25 km (Xue F et al., 1989). Most continental earthquakes in China are shallow intra-crustal earthquakes, occurring especially in the unhealed middle crust, i.e. in the low velocity and high conductivity layer, and at the Mohorovĭcíc discontinuity at the base of the crust. In the Qinghai-Xizang Plateau a few seismic foci occur at depths over 70 km, and in the Taiwan area most seismic foci are shallow focus earthquakes occurring at depths of less than 70 km. Intermediate depth earthquakes with foci between 100 and 280 km occur only in the Pamir in the far west of China, and in oceanic areas to the northeast and southeast of Taiwan. These earthquakes occur within the mantle, below the base of the lithosphere. The East Longitudinal Valley of Taiwan has not acted as a subduction zone since the Neogene, but was converted into a high angle reverse fault with small amount of sinistral strike-slip. In China continental deep foci earthquakes, at depths of 500–590 km, occur only in Jilin and eastern Heilongjiang provinces (Xue F et al., 1989), due to the westward subduction of the Pacific Plate. At present there is no evidence of subduction in other areas beneath the Chinese continent.

Liang HG (1989) counted 757 great earthquakes before 1900 and Feng H (1989) analyzed statistically 1,300 great earthquakes in 1900–1985. These studies showed that seismic centers are concentrated mainly in the Qinghai-Xizang thin-skinned tectonic area, and in the Fujian–Taiwan area, related to the listric fault system (Wan TF and Chu MJ, 1987). The eastern boundary of the Fujian–Taiwan reverse fault system in the East Longitudinal Valley of Taiwan is a high angle lithospheric fault. To the west there are a series of low angle thrusts, extending as far as the Zhenhe–Dapu Fault in middle Fujian. This can also be termed an active thin-skinned tectonic system (dipping to east with low angle) with seismic foci at depths between 5 and 70 km. According to statistics, earthquakes are very frequent in the Fujian-Taiwan listric fault system; one third of the Ms≥6 great earthquakes throughout the China occurred in the eastern part of this system, accounting for 16 % of the total earthquake energy released. The earthquake activity in the Fujian–Taiwan thrust system is the result of the northwestward movement of the Philippine Sea Plate and southeastward movement of the Chinese continent.

Earthquakes are also very frequent in the thin-skinned Qinghai-Xizang tectonic system (Burchfiel et al., 1989, 1992; Royden et al., 1997), accounting for 47% of all the Ms≥4.7 earthquakes in China. The recurrence period of the earthquakes is short, and the intensity very great; the energy released by these earthquakes accounts for 78% of that for the whole of China. Earthquake activity in the Qingzang thin-skinned tectonic system is the result of the continuous northward movement of the Indian Plate.

Strong earthquakes with a longer recurrence period occur in Northeast and North China areas. Hebei Province is the most earthquake-prone district, in which the frequency and released energy account for 2% of the earthquakes for the whole country (Feng H, 1989). The Tancheng–Lujiang Fault Zone alone is responsible for 68% of the energy released by earthquakes in North China (Tang FT, 2003). This is the most obvious intra-continental effect of the compression caused by the westward movement of the Pacific Plate.

Earthquakes in other areas are scattered and rather weak. Earthquakes occur along other fault zones, for example the Tianshan, Altay and the eastern margins of Jilin and Heilongjiang provinces. Many of the collision zones formed in the interior of the Chinese continent and in South China during its earlier geological history have not been reactivated during the Neotectonic Period, as the fractures were intruded and sealed by granitic magma. There is some relationship between active tectonics and geological historical tectonics, with considerable differences.

(4) Intraplate Kinematics During the Neotectonic Period

The average rates of displacement along recent active faults can be determined by using the major element composition of volcanic rocks, from sea floor magnetic anomalies, or by calculation of seismic moment and the area affected by a seismic fault (Appendix 5.10) (Brune, 1968). Rates of movement of the present crustal blocks can be confirmed by precise measurements using the Global Position System (GPS) (Appendix 5.11). Comparing the results presented in Appendices 5.10 and 5.11 shows that the rates of deformation during intraplate shortening, estimated from major element whole-rock analysis of volcanic rocks, are generally slightly greater than by other methods, however the rates of extension, estimated from major element analyses, are very close to results obtained by the other three methods (Fig. 11.4).

The average rate of extension in intraplate deformation in North China is 0.26 cm/yr, estimated from the total chemical analyses of 455 volcanic rock samples, and the average rate of displacement along recent active faults is 0.32 cm/yr calculated from the seismic moment. According to GPS data, eastern China as a whole is moving southeastwards at a rate of 0.1–0.12 cm/yr. Rates of deformation in the Qinghai–Xizang Plateau in southwestern China are 2–2.85 cm/yr, and in Northwest China are 0.7–1.3 cm/yr, Junggar–Altay 0.1–0.22 cm/yr, Erdos 0.8 cm/yr, eastern North China 0.1–0.3 cm/yr, Northeast China 0.08–0.35 cm/yr and in South China 0.7–1.1 cm/yr (Wang Q et al., 2002; Zhang PZ et al., 2002). The rate of slip movement along the East Longitudinal Valley of Taiwan is 4.5 cm/yr (Wan TF and Chu MJ, 1987), with a sinistral strike slip movement of 25 km since the Pleistocene (Biq Chingchang, 1971). The average rate of movement along the fault system of West Taiwan is 1.22 cm/yr, however, the average rate of movement of the fault system in the coastal areas of Fujian and Guangdong is only about 0.1 cm/yr (Wan TF and Chu MJ, 1987). The direction of extension in intraplate deformation is perpendicular to maximum principal compressive stress trace (Fig. 11.4) at each area.

The rates of movement of the neighboring tectonic plates are greater than in the interior of Chinese continent. The average rate of shortening in the Indian Plate is 4.0–4.2 cm/yr in a 20° NE direction, and the rate of shortening of the Philippine Sea Plate is 3.7–4.5 cm/yr in northwest direction (Wang Q et al., 2002; Zhang PZ et al., 2002), which indicates extension in an NE-SW direction in the western Philippine Sea Plate (Appendix 5.11 and Fig. 10.10). The current rate of movement of the Pacific Plate is estimated by Maruyama et al. (1986) to be 9–10 cm/yr from magnetic anomalies. Using GPS data, Ma ZJ (2003) measured the current rate of movement of the Pacific Plate and found it was 7 cm/yr in a WNW direction. During the Neotectonic Period, since 0.78 Ma, it is estimated that the Indian Plate has moved 31.2–33 km northwards, the Philippine Sea Plate has moved 28.9–35 km northwestwards, and the Pacific Plate has moved 55–74 km westwards.

The rates of deformation in the interior of the continent during the Neotectonic Period are only 1/2 to 1/10 of the rates of deformation during the Mesozoic. As shown in Fig. 11.4, the intraplate movement directions at present are similar to the movement model proposed by Molnar and Tapponnier (1975) and Tapponnier et al. (1977, 1981, 1982) (Fig. 6.1). This model, based on active strike-slip fault movements, as indicated on satellite imagery, is the only reasonable model for the analysis of tectonic movements in China during the Neotectonic Period (Fig. 6.1). However, it is unreasonable to extend this model further back in time to interpret the tectonics of the Eastern Asian continent since the Triassic period (Tapponnier, 1982).

11.2 The Influence of Recent Tectonic Stress Field on the Earthquakes, Resources and Environment

(1) Influence of the Recent Stress Field on Earthquakes

The recent tectonic stress field influences the distribution of earthquakes and earthquake belts. For example, in the Qinghai-Xizang thin-skinned tectonic system, active earthquake belts do not occur along E-W trending thrusts, but along N-S trending trans-tensional faults (Fig. 11.5). It shows that under the

influence of the present stress field, E-W trending overthrusts are under compression and are closed by N-S shortening, becoming active under extremely high stress, so that earthquakes occur with a low frequency. However, where the N-S traces of the recent maximum principal compressive stress are parallel to existing extensional faults, earthquakes occur with a high frequency and migrate along the earthquake belt in an S-N direction (Fig. 11.5).

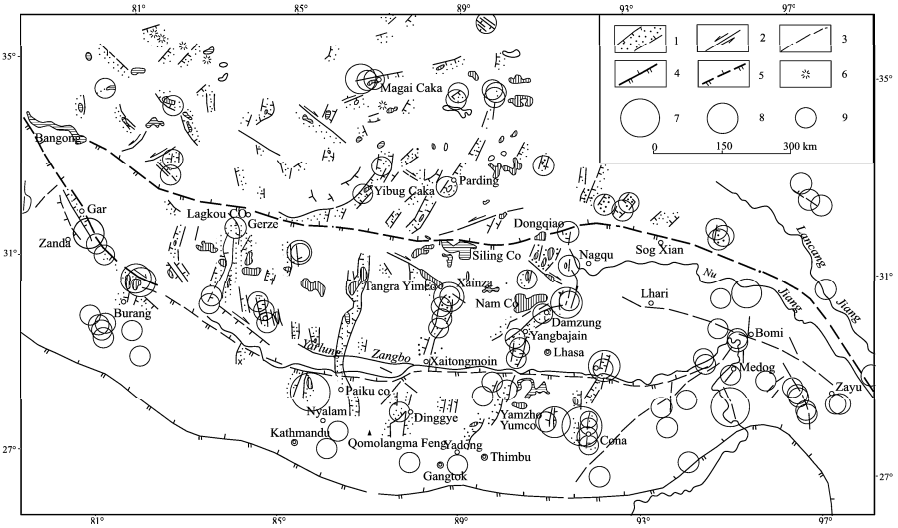

Fig. 11.5 Distribution of seismic epicenters in Xizang (Tibet) and zone of geothermal anomaly (Ma XY, 1989).

1. Fault-depression zone; 2. Strike-slip fault; 3. Inferred fault; 4. Thrust; 5. Inferred thrust; 6. Volcanic crater; 7. Epicenters, Ms≥8; 8. Epicenters, Ms = 6–8; 9. Epicenters, Ms≤6.

Geothermal anomalies and earthquake epicenters are all concentrated N-S trending fault-depressions.

Similarly, during 1966–1976 a series of earthquakes occurred in North China, although in this district the main bedrock fractures have NNE and NW orientations, strong shocks migrated along an ENE-WSW direction from Xingtai and Hejian in 1966 to the Bohai Sea in 1969, and from Haicheng in 1975 to Tangshan in 1976 (Fig. 11.6). The earthquake shocks migrated along the direction of maximum principal compressive stress, with many foci concentrated in the low velocity layer of the middle crust, but they were not controlled by faults in the bedrock or by lineaments formed during the earlier geological history of the area.

Summarizing periods of earthquake activity in the Chinese continent over the last century, according to the division principle of earthquake periods, first proposed by Ma ZJ and Jiang M (1987), to add the present data, the author (Wan TF, 2008) divides earthquakes (Ms≥6.5) into six earthquake periods: A.D. 1897–1916, A.D.1917–1940, A.D.1941–1961, A.D.1962–1980, A.D.1981–1999 and since A.D.2000 (Fig. 11.7). Earlier three periods (A.D.1897–1916, A.D.1917–1940, A.D.1941–1961) and last two periods (A.D.1981–1999, since A.D.2000) occurred mainly in western China. This is probably due to the northward movement of the Indian Plate, which causes adjustments in the intraplate stress field, resulting in strong earthquakes. The distributions of earthquake zones are so similar between A.D.1897–1916 and A.D.1981–1999, and between A.D.1917–1940 and since A.D.2000. Only one period (A.D.1966–1980) of earthquake activity affected North China and the Hengduanshan area, caused by Pacific Plate westward subduction and compression, whereas these earthquakes affected densely populated regions of eastern China and were highly destructive of life and property. Based on the characteristics of above

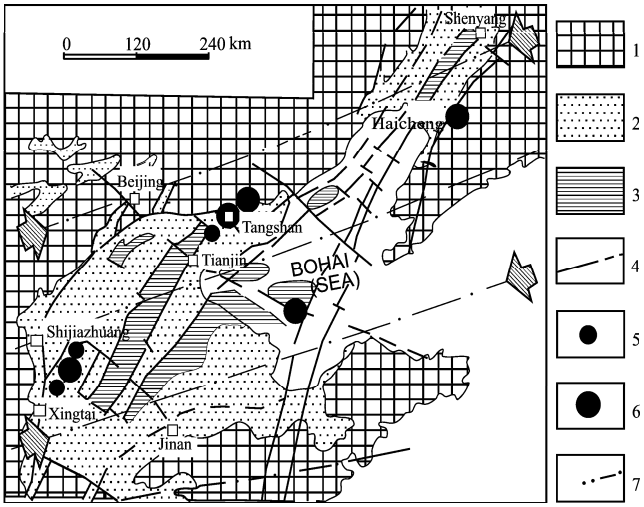

Fig. 11.6 Distribution of seismic epicenters during 1966–1976 in North China.

1. Continental basement; 2. Post-Cretaceous sedimentary basin; 3. Areas of uplift within the sedimentary basin; 4. Regional or inferred faults; 5. Epicenters, Ms$\leqslant$6; 6. Epicenters, Ms >6; 7. Direction of maximum principal compressive stress trace.

earthquake periodicity, it could be predicted that strong earthquake activities in the areas of Longmen–Hengduanshan–Eastern Kunlun Mountains will be continually from A.D.2000 to about A.D.2020. As to the North China area, the strong earthquakes (Ms$\geqslant$6.5) could occur 32–52 years later.

According to historical records (Historical Working Group of Earthquake Committee, Chinese Academy of Sciences, 1956) and many authors' (Mei SR, 1960; Shi ZQ et al., 1974; Zhang HL et al., 1989) research, violent shocks (about Ms=7−8) have occurred in North China at four periods: A.D.1038–1057; A.D.1303–1307; A.D.1668–1695; A.D.1966–1976, with a periodicity of 300±30 years. It is supposed that these phases of earthquake activity were related to compression caused by the westward movement of the Pacific Plate. The last episode of violent earthquakes occurred between Xingtai and Tangshan, Hebei in 1966–1976. This means that for the next 240 years there will not likely be any dangerous earthquakes (about Ms = 7−8) in North China. However, the reason for this 300 years periodicity is not clear and maybe it is the period of stress accumulation. These episodes of earthquake activity did not affect the Fujian-Taiwan area, where the earthquakes are due to the convergence of the SE movement of China and the NW movement of the Philippine Sea Plate shown above.

Although the determination of the tectonic stress field can explain some of the features of the distribution and causes of earthquake activity, at present, the stress field can not be used to precisely predict the timing of earthquakes in any way. The precise prediction of earthquakes depends to some degree on recognizing the repeated periodicity of the earthquake activity and using empirical methods, such as premonitory symptoms, till now it has not been found any quantitative relationship between a lot of geophysical symptoms and occurrence of earthquake. This problem is very complex as earthquake activity depends on so many factors. Because of the destructive effects of earthquakes on property and infrastructure and the frequent great loss of life, determined efforts must be made to predict their occurrence and to mitigate their effects.

(2) The Recent Tectonic Stress Field and the Accumulation and Migration of Fluid Resources

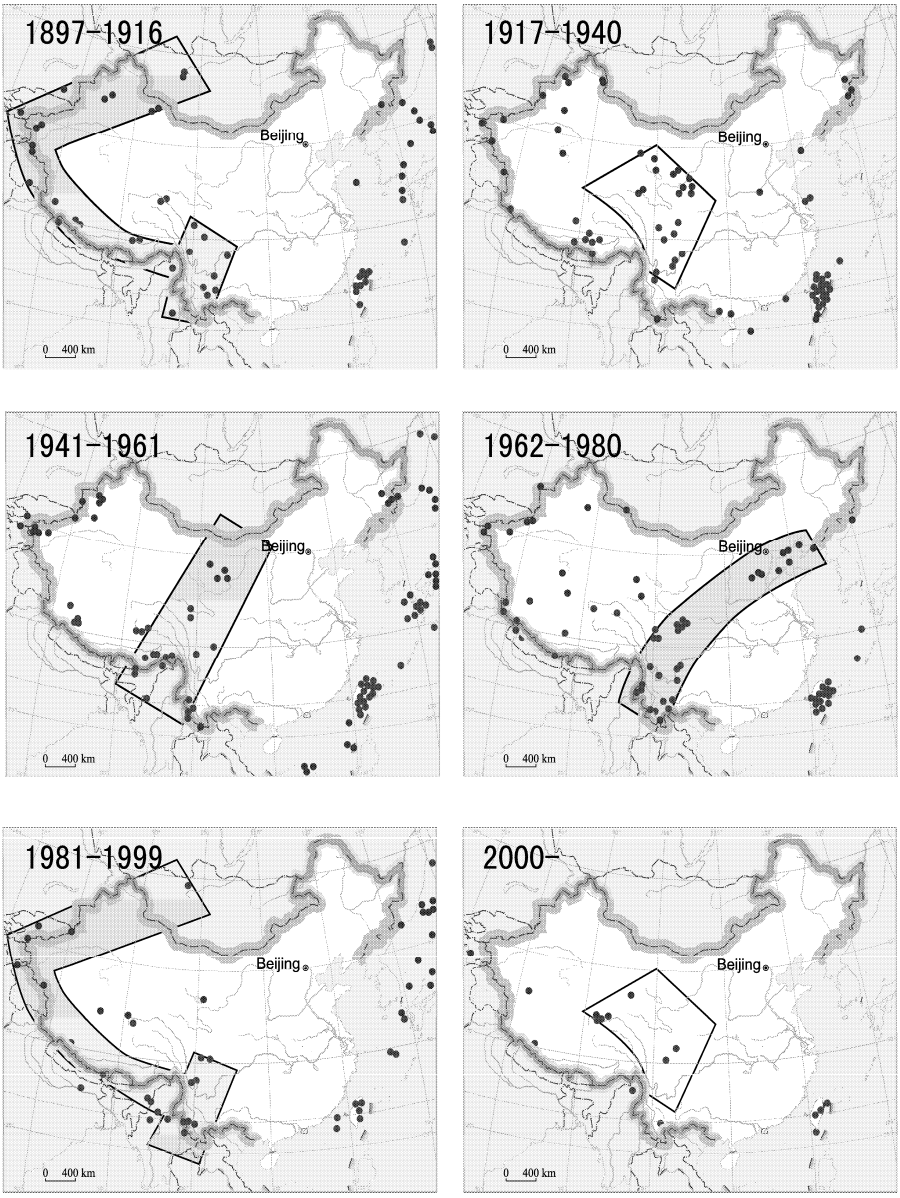

Fig. 11.7 Locations of earthquakes in the Chinese continent during six periods between 1897 and 2008 (Wan TF, 2008; revised from Ma ZJ et al., 1987).

Red dots: Epicenters, Ms>6.5; The color frame shows different earthquake zones.

The recent tectonic stress field plays an important role in controlling the movement and concentration of fluids such as oil, gas and ground water in fracture zones, including the deep circulation of hydrother-

mal water. During its geological history the Chinese continent has undergone many multi-period and multi-directional tectonic events. Large number of fractures are distributed throughout the rocks. It is impossible to find rocks without any fractures, in the range from several centimeters to hundreds of meters, anywhere in the bedrock of the Chinese continent.

As fractures are distributed throughout the rocks in many different orientations, the direction in which fractures are most easily opened is most important in controlling the flow of fluids. The distribution of fractures and fissures in the rocks depends on the tectonic forces to affect the rocks in the past and their mechanical properties throughout their geological history. Fault planes may form conduits filled with permeable breccia or gouge, but in general, few of the fissures developed during the evolution of the rock are open. Fissures, perpendicular to, or at a high angle to the direction of maximum principal compressive stress, are closed and the rock is impermeable to the movement of fluids in this direction. However, fissures parallel to, or at a small angle to the direction of the maximum principal compressive stress are more easily opened and may form zones of high permeability, allowing the flow of fluids through the rock. The permeability of rock may differ by 5 to 10 times depending on the relationship of the fractures to the direction of maximum principal compressive stress.

Wan TF (1984) studied the relationships between active controlling faults and the orientation of the recent maximum principal compressive stress in 89 areas in China famous for their geothermal waters and hot springs, and found that in 74 of the fields, accounting for 83.2 % of the total, the controlling active faults were almost parallel to, or have angles of less than 45° to the direction of recent maximum principal compressive stress. In Fujian Province, Wan TF et al. (1986) studied the relationship between active controlling faults of 171 fields of geothermal water and the recent direction of the maximum principal compressive stress. They found that in 116 geothermal fields, accounting for of 67.8% of the total, the active controlling faults are parallel to the recent maximum principal compressive stress, or intersect this direction at an angle of less than 45°. In most cases, the flow and accumulation of geothermal waters are favored when the interior angle between the active controlling faults of the geothermal fields and the recent maximum principal compressive stress is less than 45°.

The controlling factor in the occurrence of ground water in fractures in shallow bedrock is consistent with that of geothermal waters. Extensional faults forming water-bearing fracture belts are usually parallel to the direction of recent maximum principal compressive stress. There are many examples of the successful use of this principle in search of water-bearing fracture belts in China (Shen ZL et al., 1985; Coal Mining College of Huainan et al., 1979; Xiao NS et al., 1986).

Xiao NS et al. (1986), Yin Shuren et al. (1989) suggested that most water-bearing fractures in China are WNW trending, and gave many examples. If only the Jiangsu, Anhui and Henan provinces in which they worked are considered, their conclusion is certainly correct, because in those areas at present the maximum principal compressive stress is oriented WNW, and fractures in this direction show extension and are water-bearing. However, they concluded that WNW trending fractures provide the optimum direction for water-filled fractures throughout the whole of China. They did not understand that the direction of recent maximum principal compressive stress is different in other parts of China. Experience gained in local areas cannot be extrapolated directly to cover all the regions of China.

This objective lesson should be borne in mind in search of water supplies. Local variations in the direction of the maximum principal compressive stress in China should be considered in locating water-bearing fracture belts. This direction is NE in northeastern China, ENE in North China, near E-W trending along the Shandong–Henan–southern Shaanxi belt, WNW in Jiangsu-Anhui, mainly NW in South China (including Taiwan Island), E-W in Hainan Island, N-S in south Qinghai-Xizang, changing in Qaidam to the north into NE, and gradually changing to NNW-trending in western Xinjiang. If these variations in direction are recognized, the probability of successfully locating water-bearing fracture belts may be 70%–80%.

Similar relationships occur in oil and gas fields. Faults or fissure system, parallel to the direction of maximum principal compressive stress often provide migration paths for oil and gas, and if the fault or fracture system is sealed by a cap rock to form a trap, a fracture belt may form a reservoir for oil and gas. When searching for, or forecasting the location of deep seated oil and gas reservoirs and if both

the length and depth of the fracture zone or fissure belt are less than the depth of burial, the position of blind faults and fracture zones is the position of oil-gas fracture reservoir. Recently, it has been found that a numerical simulation of the tectonic stress field, according to the above principle, can be used to predict the locations of deep fracture reservoirs of oil and gas (Chen ZD et al., 2002; Zhang SR et al., 2003; Wang MM et al., 2003), as explained in detail by Wan TF (1988) and Wan TF et al., (2004). This principle can also be used in oil and gas reservoirs to select the most effective location and direction for the injection of water for secondary recovery. The most effective direction for injection is related to the recent tectonic stress field and not to paleo-lineations or to the intensity of earlier deformation. Water injection wells should not be necessarily drilled along the direction of the recent maximum principal compressive stress but the local angle of intersection of fissures with this direction should be taken into account, and the appropriate depth is selected for water injection to drive the oil and gas towards the surface.

(3) Influence of the Recent Stress Field on the Environment and Geological Hazards

Pre-existing fault and fissure (joint) zones, parallel to the current maximum principal compressive stress direction, are more easily affected by recent tectonic activity, to cause that rocks adjacent to the fissure zone weakened, and new movements may give rise to a major geological disaster, such as the massive eruption of geothermal waters or the influx of water or gas into mining galleries, leading to flooding or explosions. Fractures and fissure zones often constitute hidden dangers for the stability of the foundations of large-scale construction projects (irrigation work, nuclear power station, etc.), and if water gains access to fracture and fissure zones, the foundations may become unstable. It is important to establish the local relationships between the recent maximum principal compressive stress orientation and pre-existing faults or fissure zones to prevent geological disasters and to ensure the stability of the foundations before commencing any major construction project.

(4) Geomorphical Changes in the Neotectonic Period

The geomorphical framework of the Chinese continent was basically shaped during the Himalayan Tectonic Period and has changed only a little during the Neotectonic Period. The macroscopic geomorphical features during the Neotectonic Period are very similar to those at the present day (Fig. 11.8), but some important differences should be noted.

Since the Middle Pleistocene, under the influence of the recent tectonic stress field, horizontal displacement along the sinistral strike-slip western Altun Fault Zone was 5000–6500 m, but vertical displacement was only 1/10 of horizontal displacement (Research Group of Altun Active Fault Zone, Seismological Bureau of China, 1992). If the average horizontal displacement was 10 m for each of the earthquakes along this zone, it would have required 650 violent earthquakes, with a major earthquake occurring once every 1200 years since the Middle Pleistocene, to account for this amount of displacement.

In the Middle Kunlun an Ms=8.1 earthquake occurred in 2001, forming a fracture zone of 400 km long with a maximum horizontal displacement of 16.3 m at the earth's surface. This is the most violent earthquake with the maximum horizontal displacement along a fracture zone recorded from the Chinese continent (Lin AM et al., 2002). The amounts of horizontal displacement recorded for individual earthquakes are generally less than 10 m. The Qomolangma district of southern Xizang was geodetically surveyed 35 times between 1975 and 1992. It was found that this district is moving horizontally in a NE 54° direction at a rate of 6–7 cm/yr, with an average rate of uplift of 3 mm/yr (Chen JY et al., 2001).

Under the influences of the Neotectonic stress field, NNE-trending active faults in North and Northeast China generally have dextral displacement, and rivers which cross the faults are diverted mostly to the right. One of these faults, the frontal fault zone of the Taihangshan, shows a dextral horizontal displacement of ~600 m since the Late Pleistocene. Rivers crossing WNW-trending faults are displaced mainly to the left, for example, the Tieluzi Fault, north of Qinling, has a sinistral displacement of 500

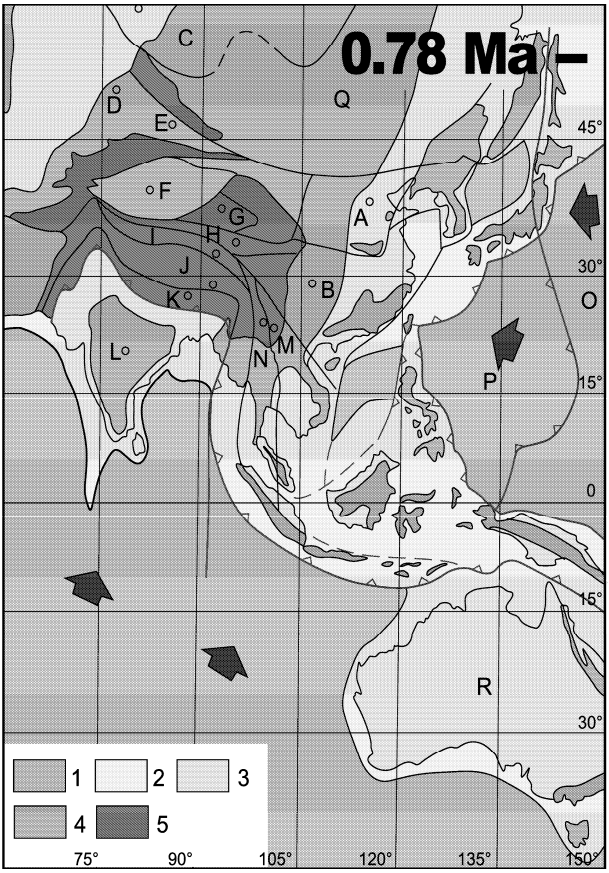

Fig. 11.8 Paleo-tectonogeographic sketch reconstruction of China and its adjacent blocks in the Neotectonic Period (since 0.78 Ma).

1. Oceans; 2. Shallow seas; 3. Hills and plains; 4. Plateaux and mountains with average elevation of 2,000 m; 5. Plateaux and mountains with average elevation above 4,000 m;

Small circles represent central reference point for paleomagnetism in each block. Positional data for the paleomagnetic reference point for each block is shown in Appendix 6. Initial letters for each block are the same as in Fig. 11.1.

m (Yang JQ, 1983; Han MK, 1983). During the Neotectonic Period, the landscape of eastern China has been much less modified geomorphologically than western China.

In the southeastern coastal areas of China, under the influence of the NW-SE recent maximum principal compressive stress, the landscape has been affected by a series of conjugate shear fractures controlling the recent drainage system. The tectonic stress direction indicated by this drainage system is the same as the direction determined from earthquake fault plane solutions (Ai NS, 1982).

Research on rates of vertical uplift and depression of the ground surface during the Neotectonic Period has encountered difficulties by giving different results during repeated leveling, due to disturbance in the landscape elevation in rainy and dry seasons, so that there is uncertainty regarding the reliability of the data. Between 1951 and 1982, Zhang ZS et al. (1989) used data from two national leveling surveys and many precise regional surveys to make an overall assessment. Taking the average value of

rates of vertical motion as being equal to zero, they concluded that the basins and plains of South China were undergoing uplift, while North China was being depressed, with a boundary along the Kunlun–Qinling–northern front of the Huaihe plain. The most rapid rate of uplift, 2 cm/yr, is occurring in the Himalayan Mountains; in the North Xizang Plateau uplift is 0.4–0.5 cm/yr, in the East Kunlun Mountains is 0.5–0.7 cm/yr, and in the Altun, West Tianshan, Qilian and in the Qinling mountains is about 0.1 cm/yr. A rate of depression of 0.3–0.4 cm/yr occurs in the Tarim Basin, in the Qaidam Basin the rate is 0.2–0.3 cm/yr, and in most of eastern China the rate is between 0.2 and 0.1 cm/yr; the highest rate of depression of 1 cm/yr occurs near Tianjin. Rates of vertical movement are much less than rates of horizontal movements.

A landscape deformation survey across earthquake faults carried out by the Seismic Survey, Seismological Bureau of China (1975, 1977) (Zhao JR (1981), Chen YT et al. (1979), Deng QD (1980) Wang CY (1978)), showed that in North China the ratio between horizontal and vertical displacement is 2, while in West China it is between 6 and10. These results are similar to those obtained from seismic fault plane solutions, as measured by macro-seismogeological survey (Ren JW et al., 1999; Wang Y et al., 2001). At depths between 1,000–4,000 m in oil and gas-bearing sedimentary basins, as measured from hydraulic fracturing, the horizontal principal stress is generally greater than the vertical one, (China National Committee, IUGG, 1983). All these results show that horizontal stress and horizontal motion are the predominant factors in landscape modification.

(5) The Change of Coast During the Neotectonic Period

Because there are only several meters to several kilometers of total horizontal movement and several meters to hundred meters of vertical movement, there were no great changes in the landscape of the Chinese continent during the Neotectonic Period and their influence is limited. However, the effects were much greater in coastal areas. It is commonly recognized that at the end of the Neogene the floors of the Yellow Sea and Bohai Bay were land areas, forming plains with many rivers and lakes. Recently, before 15,000 years BP, near the end of the Late Pleistocene, after several transgressions, the present Yellow Sea and Bohai Bay formed the youngest of the marginal seas of eastern China (Fig. 11.9) (Xu Hong, 1997). During the last transgression in the Holocene, Hainan Island became isolated from the mainland.

According to the records of the National Ocean Bureau, from 1891 to 1990 the average rise in sea level in Chinese coastal areas was 1.4 mm per year, and since 1960 has risen by 2.1–2.3 mm per year (Huang CJ et al., 2000), corresponding with a global sea level rise of 180 mm (the most optimal evaluation) in the last 100 years (IPCC Working Group, 1996). Based on the statistical result of the annual bench mark survey, Yang HT (1999) found that the sea level around China has recently risen by 1.0–4.5 mm/yr. The difference between these results may be caused by: a) a rise in global sea level (at an average rate of 1.8 mm/yr); or b) by local tectonic uplift or depression.

A rough calculation of the local rates of crustal uplift or depression along the coast of China can be worked out, by deducting the rise in global sea level from the apparent rate of sea level rise suggested by Yang HT (1999) (Table 11.1).

Table 11.1 Rates of sea level rise in coastal areas of China (mm/yr) (data from Yang HT, 1999 and IPCC Working Group, 1996)

Area	Apparent rate of sea level rise	Rate of crustal rise or depression	Area	Apparent rate of sea level rise	Rate of crustal rise or depression
Bohai	2.0	0.2 depression	Shanghai	4.5	2.7 depression
Yellow sea	1.0	0.8 rise	Zhejiang	3.4	1.6 depression
East china sea	2.7	0.9 depression	Fujian	1.9	0.1 depression
South china sea	2.1	0.3 depression	East Guangdong	2.1	0.3 depression
East Liaoning	2.6	0.8 depression	West Guangdong	2.8	1.0 depression
Tianjin-Tanggu	2.2	0.4 depression	Hainan Island	1.7	0.1 rise

This calculation is more reliable where the difference in the apparent rise in sea level and the global rise in sea level is greater, as shown in Table 11.1. For example, it is found that the rate of depression in the Shanghai area is 2.7 mm/yr, in the Zhejiang area is 1.6 mm/yr, and in western Guangdong is 1.0 mm/yr. These data correspond very closely with areas of enhanced sedimentation. In coastal areas, where the apparent rate of the rise in sea level is almost equal to global sea level rise, as in Bohai Bay, Nanhai Sea (South China), Fujian, east Guangdong and Hainan Island, there is evidently very little crustal movement.

Comparison of the geological hazard distribution map (1:5, 000, 000, Zhang MS, 1997) of the Chinese coastline during the Late-Quaternary, the bedrock geological map for each area (1:500, 000, Provincial geological survey maps), and the recent tectonic stress field shows that zones of tectonic weakness in the bedrock and the recent maximum principal compressive stress direction control the distribution of areas of crustal uplift or subsidence, and determine whether the coast is subject to erosion or is being extended by sedimentation (Fig. 11.9). Zones of tectonic weakness in the bedrock are regional tectonic lineaments, including the strike of major fault zones and fold axes.

Where regional tectonic lineaments near the coastline are parallel to, or intersect the directions of recent maximum principal compressive stress at a small angle, crustal weakness and fault zones are more extensive, consequently there are greater subsidence and more sedimentation. Four areas of sedimentation along Chinese coastline have the following characteristics (Zhang MS, 1997): (A) From Tanggu, Tianjin City to Laizhou Bay, south Bohai Bay, lineaments near the coastline trend E-W, and the present maximum principal compressive stress direction trends 70°–80° NE; since the angle of intersection is small, this is a zone of extension and subsidence, forming an area of coastal sedimentation; (B) The Rizhao–Lianyungang coastline of northern Jiangsu, where the angle of intersection between regional lineaments and the present maximum principal compressive stress direction is also very small; the orientation of lineaments and maximum principal stress are E-W trending; (C) Shanghai–mouth of Yangtze River area, the angle of intersection between two regional lineaments and the present maximum principal compressive stress direction is rather small, orientations of the lineaments and the maximum principal stress are nearly WNW-NW trending; (D) The coastline of the Leizhou Peninsula-Beibuwan (Northern Bay), southwestern Guangdong, the present direction of maximum principal compressive stress and the main faults active since the Middle Pleistocene both lie E-W (Fig. 11.9).

Along the greater part of Chinese coastline, regional lineaments and fault zones commonly trend NNE, intersecting the E-W trending direction of present maximum principal compressive stress, at a high angle, fault zones are closed under compression and it is impossible for large-scale zones of extension to form. Where intermediate-acidic magmatic rocks have been intruded along faults, the crust is relatively light, and easily uplifted to re-establish isostatic equilibrium. Here, along the coastline the seafloor is very shallow, enhancing marine erosion and the removal of beach sediments. Most of the Chinese coastline, such as the eastern Liaoning Peninsula, the northern Bohai Bay, the Shandong Peninsula, Jiangsu, Fujian, Guangdong, and Hainan and Taiwan islands, is undergoing uplift and requires protection from marine erosion, particularly along sandy shores.

The state of gravitational equilibrium of the crust is an important geophysical property, greatly influenced by Neotectonics. The lithosphere is always tending to adjust towards equilibrium, however, tectonic activity often disturbs this gravitational equilibrium. If tectonic activity is weak, it maybe take thousands or hundred of thousands of years for isostasy to re-establish the equilibrium. According to the nationwide $1^\circ \times 1^\circ$ isostatic gravity anomaly data (Jia MY et al., 1989, precision 10 mgal), areas where the absolute isostatic gravity anomaly is less than ± 40 mgal, have almost reached gravitational equilibrium, in fact most of China (89%) is nearly at gravitational equilibrium. Areas where the absolute value of the isostatic gravity anomaly is greater than ± 40 mgal, accounting for 11% of China, are not in equilibrium. Areas with positive isostatic gravity anomalies are underlain by light, low density lithosphere and are subject to crustal uplift, and areas with negative isostatic gravity anomalies are underlain by heavy, high density lithosphere and are subject to crustal subsidence (Zeng HL, 2005). Isostatic anomalies vary greatly in West China, from 120 mgal to –100 mgal, with steep gravity gradients. Isostatic anomalies occur in ENE-or WNW-trending belts with alternating positive and negative anomalies.

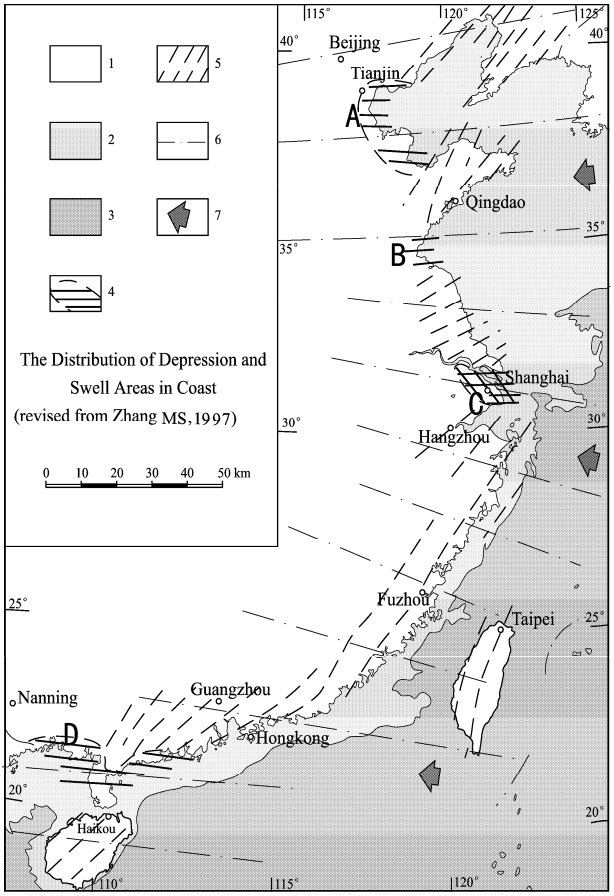

Fig. 11.9 The Recent tectonic stress field and uplift and subsidence of the Chinese coastline in the Late Quaternary (original data according to Zhang MS, 1997).

1. Land; 2. Recent NW extension of the marginal seas; 3. Marginal seas before 15,000 BP; 4. Areas of subsidence and the strike of fault zones; 5. Areas of uplift and the strike of fault zones; 6. Recent maximum principal compressive stress traces; 7. Directions of compression.

A. Tianjin-Tanggu; B. Rizhao-Lianyungang; C. Shanghai–Mouth of Yangtze River; D. Southwestern Guangdong.

Mountain belts such as the Altay, Tianshan, Qilian, Kunlun and Himalaya show positive isostatic anomalies, and coincide with paleo-tectonic lineaments. There are fewer zones of positive isostatic anomaly in East China, but they occur at Dahingganling (120–123°E, 44–52°N), north Taihangshan (114–115°E, 37–40°N), middle Qinling (107–110°E, 34–34.5°N), middle Wuling (109–111°E, 27.5–29°N), Changbaishan (~128°E, 42°N) and the eastern Shandong Peninsula. Most of East China has reached a state of equilibrium.

There are two rather different maps showing isostatic gravity anomalies in China. One is the 1°×1°isostatic gravity anomaly map of Jia MY et al. (1989) quoted above, the other was compiled by Zuo Y et al. (1996). In West China the two maps show great differences in isostatic gravity anomaly values, reaching 100–220 mgal; although the values for East China shown on both maps are similar,

there is a great difference in the pattern of the contours (Zeng HL and Wan TF, 1999). It is not clear why these two maps are different, but the precision of gravitational measurement requires improvement to resolve this problem. Judging from the relationship between isostatic gravity anomaly values and areas of recent vertical crustal uplift and subsidence, the map compiled by Jia MY et al. (1989) appears to be closer to reality (Zeng HL and Wan TF, 1999).

11.3 Dynamic Mechanism of the Recent Tectonic Stress Field

Although the nature and distribution of the present tectonic stress field are characteristic, distinctive, important, and have been deeply studied, their dynamic mechanism is not properly understood. From Chapter 4 to Chapter 10 of this volume, the author has interpreted the tectonic stress field in each period since the Paleozoic as resulting from the interactions of lithosphere plates. In each period of geological history the tectonics was determined by the stress concentration in the last episode of each tectonic

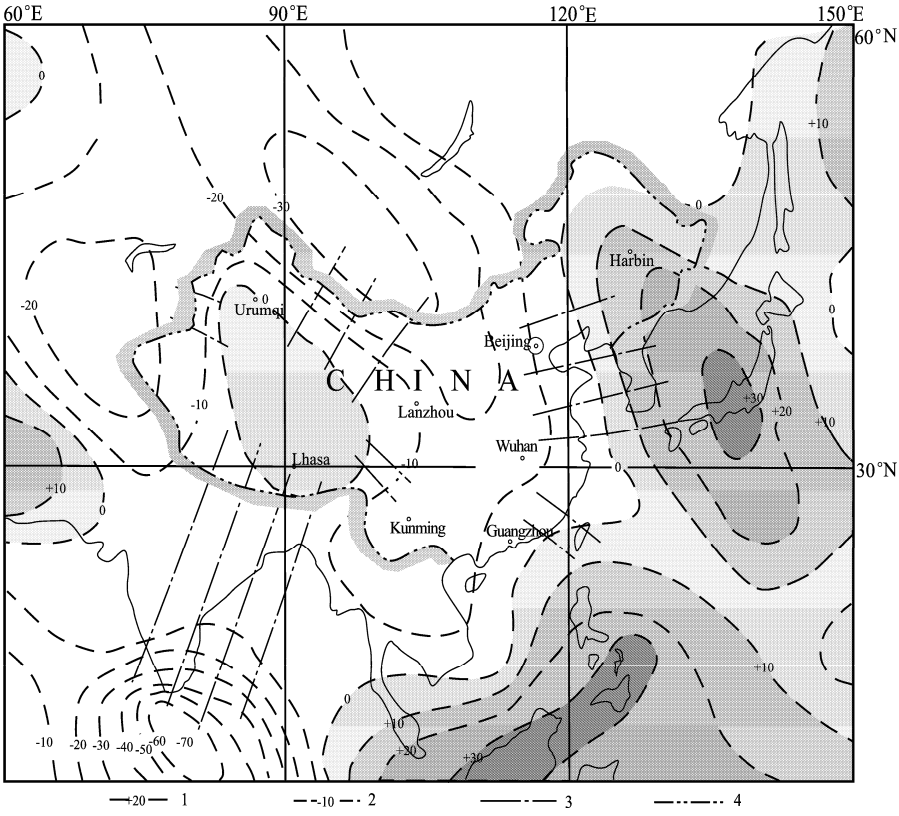

Fig. 11.10 The free air gravity anomaly, measured from satellites, and the directions of the maximum principal compression stress for the Chinese continent and its adjacent areas (revised from Gaposchkin and Lambeck, 1971).

1. Contours of positive gravity anomalies; 2. Contours of negative gravity anomalies;
3. Normals to gravity gradients; 4. Border of China.

period, when the stress exceeded the fracture strength of rocks and deformation occurred, releasing the stress, it was then possible to determine the stress fields for the different periods. However, the Neotectonic Period, where the tectonic stress field is weak and has operated only for the past 780,000 years, with a very small amount of differential stress, and where the directions of principal stress have changed, is different. The Neotectonic Period represents the beginning of new period in tectonic evolution; the accumulation of stress is just beginning. There are outstanding problems in understanding the accumulation of stress. What is the tectonic factor which plays the leading role during the process of the stress accumulation? Stress accumulation occurs as a series of pulses and shows periodicity. What are the factors which control this periodicity in the accumulation of stress?

Two dynamic mechanisms are suggested to control the formation of the present tectonic stress field: (1) Isostatic gravitational compensation; (2) Plates interaction.

The effect of gravitational isostatic compensation of the lithosphere is evident in the recent tectonic stress field of Chinese continent (Wan TF, 1988). On the free air gravity anomaly map of the Chinese continent and its adjacent areas measured from satellites (Fig. 11.10), contours showing variations in the value of gravity represent differences in the density of the mantle. Directions down the gravity gradient, normal to the contours, indicate either the direction of the mass movements of the lithospheric mantle due to lateral isostatic compensation, or the direction of the relative movement of the tectonic plates. This is given most attention to by many geophysical scientists (Artyushkov, 1973; Turcotte and Oxburgh, 1976; Lago and Cazenave, 1981; Bott and Kusznir, 1984). If the free air gravity anomaly map of the Chinese continent and its adjacent areas (Fig. 11.10) is compared with the map showing the maximum principal compressive stress traces, it may be seen that directions normal to the free air gravity anomaly gradient correlate well with the traces of maximum principal compressive stress during the Neotectonic Period (Fig. 11.4). Consistency over wide areas shows that the origin of the recent tectonic stress field in Chinese continent may be related to the movement of lithospheric material in order to establish gravitational isostatic compensation. Bott and Kusznir (1991) estimated that if the Qinghai–Tibet Plateau, with a mean altitude of more than 4,000 m above sea level, is entirely elastic, the differential stress in the deep part of plateau is about 100 MPa, but the estimated amount of stress at different depths is not shown as that. Many researchers would agree with the hypothesis that a large ground load is one of the causes of tectonic stress.

Most authors would accept that the dynamic mechanism mainly responsible for the recent tectonic stress field is the interaction between the tectonic plates (Ma XY, 1989; Ma ZJ, 1990; Ding GY, 1991). This mechanism also provides a reasonable explanation for the origin of the stress field.

Which mechanism, isostasy or plate moving, is most responsible for the stress field, or do both mechanisms operate together? If both mechanisms operate, what percentage of the stress field can be attributed to each of these mechanisms? This problem should be considered seriously; it is not sensible to dismiss either of these possible mechanisms.

The Recent stress field of the Neotectonic Period is the geophysical field which currently controls the present tectonic activity on Earth. Although this stress is very weak, yet it have important consequences in the location of earthquakes, the search for fluid mineral resources and changes in the environment. Neotectonic research must be an important aspect of future studies in tectonics.

References

Ai NS, Liang GZ, Scheidegger AE (1982) The valley trends and neotectonic stress field of southeast China. Acta Geographica Sinica 37(2): 111–122 (in Chinese with English abstract).

Artyushkov FV (1973) Stress in the lithosphere caused by crustal thickness inhomogeneities. J. Geophys. Res. 78: 7675–7708.

Biq CC (1971) Some aspects of post-orogenic block tectonics in Taiwan: recent crustal movement. Royal Society of New Zealand Bulletin 9: 19–24.

Bott MHP, Kusznir NJ (1984) The origin of tectonic stress in the lithosphere. Tectonophysics 105: 1–13.
Bott MHP, Kusznir NJ (1991) Sublithospheric loading and plate-boundary forces. Phil. Trans. R. Soc. Lond. A: 337: 83–93.
Brune JN (1968) Seismic moment, seismicity and rate of slip of major fault zones. J. Geophys. Res. 73: 777–784.
Burchfiel BC, Deng QD, Molnar P et al (1989) Intracrustal detachment within zones of continental deformation. Geology (Boulder) 17(8): 748–752.
Burchfiel BC, Chen ZL, Hodges KV et al (1992) The south Tibetan detachment system, Himalayan Orogen: extension contemporaneous with and parallel to shortening in a collisional mountain belt. Special Paper-GSA 269: 41.
Bureau of Geology and Mineral Resources of Heilongjiang Province (1993) Regional Geology of Heilongjiang Province. Geological Publishing House, Beijing (in Chinese with English abstract).
Bureau of Seismology of Xinjiang (1985) Fuyun Earthquake Fault Zone. Seismological Press, Beijing (in Chinese with English abstract).
Byerly P (1926) The Montane earthquake of June 28, 1925. G. M.C.T., Bull. Seismol. Soc. Ame. 16(4): 209–232.
Chen JY, Wang JY, Pang SY et al (2001) On the earth crust movement of Qomolangma area. Science in China 31(4): 265–271 (in Chinese).
Chen WJ, Ge TM, Li DM et al (1992) The K-Ar magnetostratigraphic chronology of Cenozoic basalt in Hainan Island and Leizhou Peninsula. In: Liu RX (ed) The Age and Geochemistry of Cenozoic Volcanic Rock in China. Seismological Press, Beijing (in Chinese).
Chen YT, Huang LR, Lin BH et al (1979) A dislocation model of the Tangshan earthquake of 1976 from the inversion of geodetic data. Acta Geophysica Sinica 22(3): 201–207 (in Chinese with English abstract).
Chen ZD, Meng QA, Wan TF et al (2002) Numerical simulation of tectonic stress field in Gulong depression in Songliao basin using elastic-plastic increment method. Earth Science Frontiers 9(2): 483–492 (in Chinese with English abstract).
China National Committee, IUGG (1983) National Report on Seismology and Physics of the Earth Interior.
Coal Mining College of Huainan et al (1979) Mining Geology and Mining Hydrogeology. China Coal Industry Publishing House, Beijing (in Chinese).
Deng QD (1980) Main characteristics of Cenozoic fault-block tectonics in China. In: Scientific Papers on Geology for International Exchange. (I) Tectonics and Geological Mechanics. 101–108. Geological Publishing House, Beijing (in Chinese).
Deng QD, Zhang WQ, Wang YP et al (1987) Main features of Haiyuan fault zone and 1920 Haiyuan earthquake faults and their formationmechanism. In: Institute of Geology, State Seismological Bureau. Research on Recent Crustal Movement (3): 9–25. Seismological Press, Beijing (in Chinese).
Ding GY (1991) Lithospheric Dynamic of China—Explanatory Notes for the Atlas of Lithospheric Dynamics of China. Seismological Press, Beijing (in Chinese).
Ding GY (1995) Neotectonics. In: Cheng YQ (ed) Great Encyclopedia in China, Geology, 567–568. Encyclopedia of China Publishing House, Shanghai.
Eiby CA (1980) Earthquakes. Heinemann.
Feng H (1989) Recent epicenter distribution of strong earthquake (1900–1985). In: Ma XY (ed) Lithospheric Dynamics Atlas of China. SinoMaps Press, Beijing (in Chinese).
Gaposchkin EM, Lambeck K (1971) Earth's gravity field to the sixteen degrees and station coordinated from satellite and terrestrial data. J. Geophys. Res. 76(20): 4855–4883.
Group of Earthquake Focal Mechanism of Six Provinces and Cities (1981) Recent tectonic stress field, referred by earthquake focal mechanism in Jiangsu, Shandong, Anhui and Henan areas. Seismology and Geology 3(1): 19–28 (in Chinese).

Haimson BC (1975) Crust stress in the continental United States as derived from hydrofracturing test. In: Heacock JG (ed) The earth's crust, its nature and physical properties. Geophysical Monograph 20, pp.576–592, AGU.

Han MK, Zhu SL, Zhao JZ et al (1983) Geomorphic expressions of Quaternary tectonic stress field in the southern section of the eastern piedmont fault zone of Taihangshan Mountains. Acta Geographica Sinica 38(4): 348–357 (in Chinese with English abstract).

He KZ, Zhang XJ, Qin ZL (2001) Cenozoic tectonic movements and environmental change of western Yunnan. In: Lu YC et al (eds) Neotectonics and Environment. Seismological Press, Beijing (in Chinese).

Historical Working Group of Earthquake Committee, Chinese Academy of Sciences (1956) Annual Tables of China Earthquake. Science Press, Beijing (in Chinese).

Huang CJ, Dong QX, Lin JD et al (2000) Global warming and rising of sea level. Journal of Nature 22(4): 225–232 (in Chinese).

Huang TK (Jiqing) (1945) On the Major Structural Forms of China. Geological Memoirs, ser. A, no. 20, 165pp.

Hubbert MK, Willis DG (1957) Mechanics of fracturing. J. Petrol. Technol. 9: 153–168.

IPCC Working Group (1996) Climate Change 1995. In: The Second Assessment Report of the Intergovernment Plan on Climate Change, pp.289–405. Cambridge University Press, London.

Jia MY, Yuan GT, Xiang AM (1989) Isostatic gravity anomalies in grid $1^{\circ} \times 1^{\circ}$. In: Ma XY (ed) Lithospheric Dynamics Atlas of China. SinoMaps Press, Beijing (in Chinese).

Kan RJ, Zhang SC, Yan FT et al (1977) Present tectonic stress field and its relation to the characteristics of recent tectonic activity in southwestern China. Acta Geophysica Sinica 20(2): 96–109 (in Chinese with English abstract).

Lago B, Cazenave A (1981) State of stress in the oceanic lithosphere in response to loading. Geophysical Journal of the Royal Astronomical Society 64(3): 785–799.

Li QZ et al (1973) The stress field of two regions inferred from the micro-earthquake data on an observation station. Acta Geophysica Sinica 16(1): 45–61 (in Chinese with English abstract).

Liang HG (1989) Distribution of history earthquake epicenters(before1900A.D). In: Ma XY (ed) Lithospheric Dynamics Atlas of China. SinoMaps Press, Beijing (in Chinese).

Lin AM, Miyata TK, Wan TF (1998) Tectonic characteristics of the central segment of the Tancheng-Lujiang fault zone, Shandong Peninsula, eastern China. Tectonophysics 293(1–2): 85–104.

Lin AM, Fu BH, Guo JM et al (2002) Co-Seismic strike-slip and rupture length produced by the 2001 M_S 8.1 Central Kunlun Earthquake. Science 296(5,575): 2015–2017.

Lin JZ, Liang GZ, Zhao Y et al (1980) Earthquake focal mechanism and tectonic stress field of coastal southeast China. Acta Seismologica Sinica 2(3): 245–257 (in Chinese).

Ma XY (chief editor, Editorial Board for Lithospheric Dynamics Atlas of China, State Seismological Bureau) (1989) Lithospheric Dynamics Atlas of China. SinoMaps Press, Beijing (in Chinese with English abstract).

Ma ZJ, Jiang M (1987) Strong earthquake periods and episodes in China. Earthquake Research in China 3(1): 47–51 (in Chinese with English abstract).

Ma ZJ (1990) Subareas of continental earthquakes of China and their analysis on dynamics. In: International Conference of Analysis on Tectonic Evolution of Continental Lithosphere and Its Dynamics, 3th Conference of Structure Geology, pp.86–95. Geological Publishing House, Beijing (in Chinese).

Ma ZJ, Ren JW, Zhang J (2003) The present plate movements shown by GPS vector fields and the model of the combined latitudinal and longitudinal mantle flow. Earth Science Frontiers 10(1): 5–13 (in Chinese with English abstract).

Maruyama S, Seno T (1986) Orogeny and relative plate motions: example of the Japanese Islands. Tectonophysics 127: 305–329.

Mei SR (1960) Seismic activities of China. Acta Gephysica Sinica 9(1): 1–19 (in Chinese with English abstract).

Molnar P and Tapponnier P (1975) Cenozoic tectonics of Asia: effects of a continental collision. Science 189(4,201): 419–426.

Ren JW, Wang YP, Wu ZM et al (1999) Quaternary active features and slip rate of east Kunlun fault belt in northern Tibetan Plateau. In: Editorial Board of Research on Active Faults. Research on Active Faults, no.7, pp.147–164. Seismological Press, Beijing (in Chinese).

Research Group of Altun Active Fault Zone, Seismic Bureau of China (1992) Altun Active Fault Zone. Seismological Press, Beijing.

Royden LH, Burchfiel BC (1997) Surface deformation and lower crustal flow in eastern Tibet. Science 276(5,313): 788–790.

Seismic Survey, Seismological Bureau of China (1975) Landform deformation at Xingtai earthquake, in 1966. Acta Geophysica Sinica 18(3): 153–163.

Seismic Survey, Seismological Bureau of China (1977) Landform deformation at Haicheng earthquake M_S=7.3 . Acta Geophysica Sinica 20(4): 251–263.

Shen ZL et al (1985) Hydrogeology. Science Press, Beijing (in Chinese).

Shi ZL, Huan WL, Cao HL et al (1974) Some characteristics of seismic activity in China . Acta Geophysica Sinica 17(1): 1–13 (in Chinese with English abstract).

Tang FT (2003) Research on Recent Structural Deformation of North China Block and its Active Features of Strong Earthquakes . Dissertation, Institute of Geology, China Seismic Bureau (in Chinese with English abstract).

Tapponnier P, Molnar P (1977) Active faulting and tectonics in China. J. Geophys. Res. 82(20): 2905–2930.

Tapponnier P, Mercier JL, Proust F et al (1981) The Tibetian side of the India-Eurasia collision. Nature 294 (5,840): 405–410.

Tapponnier P, Peltzer G, Le Dain AY et al (1982) Propagating extrusion tectonics in Asia: new insights from simple experiments with plastic line. Geology 10: 611–616.

Turcotte DL, Oxburgh ER (1976) Stress accumulation in the lithosphere. Tectonophysics 35(1–3): 183–199.

Wan TF (1984) Recent tectonic stress field, active faults and geothermal fields (hot water type) in China. Journal of Volcanology and Geothermal Research 22(3–4): 287–300.

Wan TF, Chu MJ (1987) Active detachment in Fujian and Taiwan. Earth Science 12(1): 21–29 (in Chinese with English abstract).

Wan TF (1988) Paleo-tectonic Stress Field. Geological Publishing House, Beijing (in Chinese).

Wan TF (1994) Intraplate Deformation, Tectonic Stress and Their Application for Eastern China in Meso-Cenozoic. China University of Geosciences Press, Wuhan.

Wan TF (1994) Tectonic event and stress field of Quaternary in China. Quaternary Sciences (1): 48–55 (in Chinese with English abstract).

Wan TF, Zhu H, Zhao L et al (1996) Formation and Evolution of the Tancheng–Lujiang Fault Zone. China University of Geosciences Press, Wuhan.

Wan TF (2004) An Outline of China Tectonics. Geological Publishing House, Beijing (in Chinese).

Wan TF (2008) Mechanism of Wenchuan Earthquake (M_S=8.0) and recent situation of Earthquake in China. Chinese Journal of Nature 30(3): 125–127 (in Chinese with English abstract).

Wang CY, Zhu CN, Liu YQ (1978) Determination of earthquake fault parameter for the Tonghai earthquake form ground deformation data. Acta Geophysica Sinica 21(3): 191–198 (in Chinese with English abstract).

Wang MM et al (2003) Petroleum prospecting region and target assessment around Bohai Bay areas(No. 010107–9–4). Unpublished report for Exploration and Research Institute of China National Petroleum Corporation.

Wang Q, Zhang PZ, Ma ZJ (2002) GPS datebase and velocity field of contemporary tectonic deformation in continental China . Earth Science Frontiers 9(2): 415–429 (in Chinese with English abstract).

Wang SY, Xu ZH (1985) Seismo-tectonic stress field in east China. Acta Seismologica Sinica 7(1): 17–32 (in Chinese with English abstract).

Wang Y, Zhang YZ, Niu ZS (2001) Global volcanic earthquake activities and coastal-oceanic environmental effects . In: Lu YC et al (eds) Neotectonics and Environment. Seismological Press, Beijing (in Chinese).

Xiao NS et al (1986) Neotectonic Analysis and Its Application for Underground Water Exploration . Geological Publishing House, Beijing (in Chinese with English abstract).

Xu H (1997) Changing in Chinese seas and continents . Marine Geology Letters (7): 4–7 (in Chinese).

Xu ZH, Yan M, Zhao ZH (1983) Evaluation of the direction of tectonic stresses in north China from recorded data of a large number of small earthquakes . Acta Seismologica Sinica 5(3): 268–279 (in Chinese with English abstract).

Xu ZH, Wang SY, Huang YR et al (1989) The tectonic stress field of Chinese continent deduced from a great number of earthquakes. Acta Geophysica Sinica 32(6): 636–647 (in Chinese with English abstract).

Xue F, Huang JW (1989) Distribution of earthquake focal depths. In: Ma XY (ed) Lithospheric Dynamics Atlas of China. SinoMaps Press, Beijing (in Chinese).

Yan JQ, Shi ZL, Wang SY et al (1979) Regional features of recent tectonic stress field for China and adjacent areas. Acta Seismoloigca Sinica 1(1): 9–24 (in Chinese with English abstract).

Yang HT (1999) Sea level rise and coastal disasters in China's coast. Quaternary Sciences (5): 456–465 (in Chinese with English abstract).

Yang JC (1983) Relationship between morphotectonic evolution and Quaternary tectonic stress state in north and northeast China. Acta Geographica Sinica 38(3): 218–228 (in Chinese with English abstract).

Yin SR, Xiao YQ (1988) The hydrogeologic significance of Neotectonic fractures. J. Nanjing University (Natural Sciences) 24(3): 401–405 (in Chinese with English abstract).

Zeng HL, Wan TF (1999) Gross differences between two isostatic gravity anomaly maps of China. Tectonophysics 306(2): 253–257.

Zeng HL (2005) Gravity Field and Gravity Exploration. Geological Publishing House, Beijing (in Chinese).

Zhang HL, He SY (1989) Periodic analysis on historical earthquake sequence in North China. In: Research on Recent Strong Earthquakes. Seismological Press, Beijing (in Chinese).

Zhang JH, Sun ZX (2001) Determine Technique of Earth's Stress and Fissures in Application of Oil Exploration and Exploitation. Petroleum Industry Press, Beijing (in Chinese).

Zhang MS (1997) Some comments on the map of distributions of types of Late Quaternary geologic hazards along China coast. Marine Geology & Quaternary Geology, 17(1): 101–104 (in Chinese with English abstract).

Zhang PZ, Wang Q, Ma ZJ (2002) GPS velocity field and active crustal blocks of contemporary tectonic deformation in continental China. Earth Science Frontiers 9(2): 430–441 (in Chinese with English abstract).

Zhang SS (1981) Active features of earthquakes in Fujian and their mean stress field. Fujian Geology 2(1): 23–36 (in Chinese with English abstract).

Zhang SR, Wan TF (2003) Research on tectonic stress field and prediction of fissure zone at upper Triassic system, in Xiaoquan-Xinchang, Sichuan. China University of Geosciences, (an unpublished report in Chinese).

Zhang ZS, Gen SC, Chen DM et al (1989) Rate of recent vertical crustal deformation. In: Ma XY (ed) Lithospheric Dynamics Atlas of China. SinoMaps Press, Beijing (in Chinese).

Zhao JR (1981) On the strain field and recent crustal movement of central and south Shandong province. Acta Seismologica Sinica 3(2): 126–134 (in Chinese with English abstract).

Zoback MD, Healy JH, Roller JC (1977) Preliminary stress measurements in central California using the hydraulic fracturing technique. Pure and Applied Geophysics 115(1–2): 135–152.

Zoback MD, Roller JC (1979) Magnitude of shear stress on the San Andreas Fault: implication of a stress measurement profile at shallow depth. Science 206(4,417): 445–447.

Zoback ML, Zoback MD (1980) State of stress in the conterminous United States. J. Geophys. Res. B 85(11): 6113–6156.

Zuo Y, Liu LY, Li YQ (1996) Map of abnormity of equilibrium gravity. In: Yuan XC (ed) Atlas of Geophysics of China. Geological Publishing House, Beijing (in Chinese).

Chapter 12
Characteristics and Mechanisms of Chinese Continental Tectonics

12.1 Characteristics, Influence Factor and Mechanism of Intraplate Deformation

The intraplate deformation is the most important characteristic in China tectonics. At the present time the Chinese continent forms part of the Eurasian continental plate, this plate appears to be a coherent and unified lithospheric plate. However, China, from the point of view of its geological evolution, does not form a single solid, stable continental block. During the last one hundred years, Chinese and foreign geologists have discovered that large areas of the Chinese continent have been affected by intense folding, thrusting, with variously orientated linear and foliar structures and widespread magmatism and metamorphism, as described in Chapters 2 to11 of this volume. Recognizing structural evidence for repeated strong tectonic activity in the Chinese continent in the past, the deformation has been described as polycyclic (Huang JQ, 1945, 1960; Huang JQ et al., 1965). The tectonic activity has included the formation of geodepressions (Diwa), the activation of platforms (Chen GD, 1960, 1998), the activation of para-platforms and platform margins (Ren JS et al., 1980, 1990, 2000), the formation of platformal fold belts (Li DX, 1959; Ma XY et al., 1961; Group of Teaching and Research of Regional Geology, Beijing College of Geology, 1963) and intraplate or intra-continental orogenic zones (Ge XH, 1989; Cui SQ, 1999; Zhao ZP, 1995; Song HL, 1999; Wu ZW and Zhang CH,1999; Zhang CH, 1999).

All of the above descriptive terms have some justification and are supported by academic arguments. It appears, at first, that these terms represent different points of view, however, they attempt to represent the same phenomena, but with differences in emphasis and approached from different points of view. Since the Mesoproterozoic, parts of the Chinese continental plate have suffered from collision, with strong deformation, at different geological periods. The author considers that proposing new terms to describe tectonic phenomena is neither useful nor helpful. It is more profitable to recognize the characteristics of the evolution, the mechanisms of rock deformation and the displacements of the continental lithospheric plates, and to use this information for the location of economic resources, the preservation of the environment and the amelioration of geological hazards.

Many accounts have already been published describing intraplate deformation, the changes in the tectonic stress field and the influence of adjacent plates on the tectonic development of Chinese continent during the Mesozoic and Cenozoic (Wan TF, 1994, 1997; Wan TF and Zhu H, 1996; Wan TF and Cao XH, 1997; Wan TF and Ren ZH, 1999, Wan TF, 2004), and these have been summarized in the earlier chapters of this volume. In this chapter the causes and the dynamic mechanisms responsible for strong intraplate deformation in China will be described. The author considers that the causes of intraplate deformation in China are: (1) The occurrence of many small unstable continental blocks; (2) The deposition of huge thickness of sedimentary cover; (3) The multi-period collision and amalgamation

of blocks; (4) Active movement of the adjacent plates resulting in frequent changes in the tectonic stress field within China since the Mesoproterozoic.

(1) Unstable and Small Blocks

Researches by Chinese and foreign geologists over the last 30 years, have led to the recognition that the Chinese continent has been constructed by the amalgamation of many plates or micro-plates, generally called "blocks" (Huang TK, 1945; Ren JS et al., 1980, 1990; 2000; Wang HZ and Mo XX, 1995). Recently, Ren JS et al. (2000) divided the Chinese continent and its adjacent areas into 53 "para-platforms" or blocks. From discussion with many colleagues, and according to results from recent research, especially from the isotopic dating of metamorphic crystalline basement, the author considers that some of these small blocks, previously considered to be separate, belong together. According to our interpretation, in the Proterozoic, before collisions and amalgamations occurred, the Chinese continent was divided originally into 37 separate blocks or microplates. In Fig. 4.15 a new tectonic map of China has been prepared showing the tectonic units of China during the Paleozoic.

The largest paleo-plate in Chinese continent, the Sino-Korean Plate (20 in Fig. 4.15), occupying less than 18% of the whole of China, is about 1.7 million km^2, almost 1/12 of the North American Plate or 1/5 of the Russian (Baltic) Plate (Ren JS et al., 1990). Smaller blocks, for example, the Yagan (7 in Fig. 4.15), Northern Bayannur (8 in Fig. 4.15), Hualong (18 in Fig. 4.15) and Zhongdian (30 in Fig. 4.15) blocks occupy only several thousand or hundred km^2. Very small blocks are too small to be represented on small-scale tectonic maps. Collision belts (A-G in Fig. 4.15), formerly called orogenic belts, which have suffered strong compression and have developed complex folding and faulting, occur between the blocks. Only the larger collision belts are shown in Fig. 4.15. In these belts the rocks are always foliated, providing zones of weakness which were easily deformed during later tectonic periods. This is similar to the situation in experiments in rock mechanics, where the strength of a jointed rock is always lower than that of an intact rock, devoid of joints. The Chinese continent, made up of many small blocks and many collision belts, is weaker than an intact continent, so that the continent is unstable and plastic deformation occurs easily.

Even in the larger plates, like the Sino-Korean and Yangtze plates, almost undeformed areas or areas with low deformation are limited, the greater part of these plates show evidence of intraplate deformation. Almost undeformed areas include the Ordos area in the western Sino-Korean Plate (western part of 20 in Fig. 4.15) and the area between Huayingshan and Longmenshan in the Sichuan basin, western Yangtze Plate (western part of 32 in Fig. 4.15).

(2) Huge Thickness of Sedimentary Cover

In the regional geology of China (bureaus of geology and mineral resources of provinces or autonomous regions, 1984–1993), China was divided into 86 sub-regions. The total thickness of sedimentary strata from the Meso- or Neo-Proterozoic to Quaternary systems was found to be 23,356 m (Appendix 2). On the relatively stable blocks (49 sub-regions), the average thickness of the sedimentary cover is 16,985 m. The average thickness of sediments on the Sino-Korean Plate is 12,584 m; the thinnest sediments, only 5,987 m, occur in the stable Ordos area on the western Sino-Korean Plate. The average thickness of sediments on the Yangtze Plate is 17,488 m; the thinnest sediments, 8,373 m, occur in southeastern Guizhou, the most stable area on the central Yangtze Plate.

In paleo-collision belts and their adjacent areas (37 sub-regions) (Appendix 2), the average total thickness of the sediments is 42,036 m, thickest in the Altun–Kunlun Collision Belt with 61,712 m (Fig. 4.15, western part of C, between western part of 15 and 17). The thickness of the sediments in the Qinling (eastern D in Fig. 4.15), northern Hingganling (Fig. 4.15, northeastern A and B, west to 11) and Qilianshan (Fig. 4.15, 16 and eastern part of C) are between 55, 000 and 58, 000 m. Dozens of kilometers of sediment indicate that uplift and depression have occurred over a great vertical range in the Chinese continent since the Meso- or Neo-Proterozoic, controlled and accompanied by the horizontal

migration of all the blocks in China over thousands of kilometers during the same period. As discussed in Chapter 1 these sedimentary thickness estimates are only approximate.

A cover of sediments of dozens of kilometers in thickness is widespread over most areas of China. These great thickness of sediment is relatively weak compared with the underlying crystalline basement. Sediments on small blocks, or on the margins of plates, have generally been affected by intraplate deformation during later tectonic events (Ren JS et al., 1990, 2000; Wan TF, 1994).

A good example, showing how sedimentary thickness influences intraplate deformation, occurs in the Yanshan (A in Fig. 7.1; 3 in Fig. 7.2; Fig. 7.3) and western Shandong (B in Fig. 7.1; 5 in Fig. 7.2; Fig. 7.3) areas of the eastern Sino-Korean Plate. In the Yanshan area in the north of Hebei Province and in its adjacent area of southwestern Liaoning Province, the thickness of Jurassic and Cretaceous sediments reaches 35,435 m. These sediments were deposited at a rate of 191 m/yr (i.e. 0.191 mm/yr). This area was affected by strong folding, faulting and thrusting (3 in Fig.7.2) with detachments either between the sedimentary cover and the crystalline basement or in the middle crust, together with magmatism and metamorphism. According to results from geoscience transects and from geodynamics (Ma XY, 1989; Geoscience Transect Compilation Committee, China Seismological Bureau, 1991, 1992), there has been no uplift due to a mantle plume or to the swelling of the asthenosphere in the Yanshan area.

However, in western Shandong, only hundreds of meters of Jurassic and Cretaceous sediments cover the Pre-Cambrian crystalline basement, and the rate of sedimentation was about 10 m/myr, only 1/19 of the rate in the Yanshan area. Although a similar strong tectonic stress acted on both the western Shandong and Yanshan areas at the same time, the sedimentary cover of western Shandong is only weakly deformed, with fold limbs dipping only at 10°–20° angles (5 in Fig.7.2). It is evident that the main part of the tectonic stress was supported by the crystalline basement so that deformation in the thin sedimentary cover was very weak. Why was such great thickness of sediments deposited in Yanshan and only thin sediments in the western Shandong area? The Yanshan area is located at the intersection of the E-W trending northern boundary fault zone of Sino-Korean Plate and the Hingganling–Taihangshan and Tancheng-Lujiang NNE-trending basement fault zones (Fig. 7.3), so here the basement was rather weak and the influence of later tectonic events more profound. The western Shandong area, however, is located in the interior of the more stable and intact Sino-Korean Plate, so that later tectonic events had much less influence.

In the areas where the sediments are thin, as in the Ordos area of the western Sino-Korean Plate (Fig. 4.15, western part of 20), the area between Huayingshan and Longmenshan, western Yangtze Plate (Fig. 4.15, western part of 32) and southeastern Guizhou area, i.e. in the centre of the Yangtze Plate, intraplate deformation was very weak, similar to the situation in the western Shandong area.

(3) Multi-period Collision and Amalgamation

The thirty-seven plates or blocks which make up Chinese continent and its adjacent areas were formed during the Proterozoic, and have since suffered complex processes of multi-period collision and amalgamation. The author considers that since the Proterozoic there have been eight collisions affecting different areas, on different scales and with different directions of movement:

① Some small blocks (1–4, and 10 in Fig. 4.15) in the Altay–Junggar–Ergun Collision Belt (A in Fig. 4.15) collided in the middle to late period of Early Paleozoic (435 Ma) (He GQ and Li MS, 2001; Li JY, 1998) (Fig. 4.13).

② At the end of the Early Paleozoic (~400 Ma), blocks belonging to the Xiyu tectonic regime, including the Tarim, Altun–Dunhuang–Alxa, middle Qilian, Hualong, Qaidam, middle Kunlun and northern Qiangtang blocks (C and 14–19 in Fig. 4.15; Fig. 4.13) collided to form the Xiyu Plate (Gao ZJ and Wu SZ, 1983; Yang WR et al. 1984).

③ In the late period in the Late Paleozoic (300–260 Ma), 8 small blocks (5–9 and 11–13 in Fig. 4.15) in the South Hingganling–Tianshan Collision Belt (B in Fig. 4.15) were gradually amalgamated with the Altay–Junggar–Ergun Collision Belt, the Xiyu Plate and the Sino-Korean Plate (He GQ and Li MS, 2001; Li JY, 1998) (Fig. 5.10) to become part of the Eurasian or the Pangean Super-continental plate.

④ In the Indosinian Tectonic Period many collisions occurred in the Chinese continent, mainly in the Triassic (260–200 Ma). The Shuanghu–Lancangjiang–Changning–Menglian (western border in D in Fig. 4.15), Jinshajiang–Honghe (Red River) and Qinling–Dabie–Jiaonan (Sulu) collision belts (eastern D in Fig. 4.15) and the Shaoxing-Shiwandashan collision zones were formed between the Yangtze and Cathaysian plates (32, 33 and 34 in Fig. 4.15; Fig. 6.3). At this period the main Chinese blocks, to the north of the Qiangtang Block and east of the Nujiang Fault Zone (Fig. 4.15) composed the southeastern part of the Eurasian Continental Plate.

⑤ The Wandashan Collision Zone (34 in Fig. 7.3) was formed, and during the Late Jurassic (Yanshanian Tectonic Period) the Wandashan Block was amalgamated with the main Eurasian Plate.

⑥ The Gangdise Block moved northwards and, between the Cretaceous and Early Paleogene (Sichuanian Tectonic Period), was amalgamated with the Qiangtang Block to form the Banggongco-Nujiang Collision Zone (Fig. 8.2).

⑦ The Pacific Plate moved WNW-wards and was subducted beneath the Eurasian Plate, forming the western Pacific trench and island arc system (Japan–Ryukyu–Taiwan-Philippines) (G and 35 in Fig. 4.15; Fig. 9.9) and after the Late Oligocene (North Sinian Period, 30–23 Ma) induced intraplate deformation in the eastern Chinese continent. However, the Gangdise Block, Himalayan Block and the Indian Plate (27, 28 and 37 in Fig. 4.15) formed the Yarlun Zangbo Collision Belt and became amalgamated completely with the Eurasian Continental Plate during Oligocene (30–37 Ma)(F in Fig. 4.15; Fig. 10.4).

⑧ In the Neogene and Early Pleistocene (23–0.78 Ma, Himalayan Tectonic Period), the strongest deformations occurred in Hamalayan and Qingzang areas to uplift and form the Qingzang Plateau.

These multi-period amalgamations resulted in the formation of the Chinese continent. Later collisions caused intraplate deformation in the blocks which had already been amalgamated, and multi-period or polycyclic deformation in the intervening collision belts.

(4) Movements of Adjacent Plates and Changes in the Tectonic Stress Field

It is now recognized by geoscientists that there have been 5–6 phases of plate movement, with changes of the tectonic stress field in the continents and oceans since the Mesozoic (Cande et al., 1989; Cande and Kent, 1992; Burchfiel et al., 1993; Wan TF, 1994; Hibsch et al., 1995; Ma ZJ and Mo XX, 1997). The hypothesis of uniformitarianism that continuous processes form collision or orogenic belts (Vacilivsky, 1964; Sengör, 1982; Hsu, 1989; Li JL, 1991; Zhu ZC, 1996) contradicts many facts. Since the main phase of formation of the Chinese continent, including the period of major collision (Indosinian Period) and related intraplate deformation, the Chinese continent has undergone compression and shortening in different directions at different times (Wan TF, 1994,1997; Wan TF et al., 1996; Wan TF and Ren ZH, 1999). Three times intraplate deformation was caused by blocks derived from the breakup of Gondwana, moving northwards to collide with the southern margin of the Eurasian continent in the Indosinian (260–200 Ma) (Fig. 6.3), Sichuanian (135–56 Ma) (Fig. 8.2) and Himalayan Tectonic Periods (23–0.78 Ma (Fig.10.4); in Himalayan area the collision since 37–30 Ma, i.e. Oligocene). In each of those periods intraplate deformation caused by the collision was stronger in the south and weaker in the north. Twice intraplate deformation was caused by the westward movement of oceanic plates occupying the Pacific Basin, with the subduction of the Izanagi Plate in Yanshanian Period (200–135 Ma) (Fig. 7.3) and the Pacific Plate in the North Sinian Period (56–23 Ma) (Fig. 9.3). In these two Periods intraplate deformation was stronger in the east than in the west. Finally, in the Neotectonic Period (since 0.78 Ma) (Fig. 11.4) a quasi-balance has been maintained between the Eurasian, Indian-Australian, Pacific plates and Philippine Sea. Intraplate deformation was super-imposed upon pre-existing deformation to varying degrees.

Changes in the direction of plate movements induced tectonic reactions near the plate boundaries, along paleo-faults and zones of weakness, or in extensive sedimentary basins. This has resulted in many episodes of rock deformation and has caused widespread inversion tectonics. Because of these changes in plate movement the multi-period intraplate deformation occurred in different orientations many times.

In intraplate deformation, stress at the margins is stronger than in central parts of the plates. The effects of intraplate deformation are controlled by the size of the continental blocks, the thickness and strength of the sedimentary cover, and the strength of the crystalline basement. For these reasons the effects of intraplate deformation have been very complex in the Chinese continent.

(5) Discussion about Mechanisms

Three models have been proposed as dynamic mechanisms which control intraplate deformation and the associated magmatism:

① Subduction model (Burchfiel and Davis, 1975; Livacari et al., 1981) and plate collision (Dunlap and Teyssier, 1995);

② Mantle plume model, with uplift and delamination of the crust and mantle, inducing intracontinental subduction (Martin, 1983; Deng JF et al., 1996);

③ Far-field model, due to the transmission of the effects of subduction or collision over a long distance through the plates (Ben et al., 1997; England, 1987).

In the marginal areas of the continental plates, over a width of less than 500–600 km, it is clear that deformation and magmatism are related to subduction or the collision between plates, as proposed in the first model. However, to account for intraplate deformation thousands of kilometers away from the plate boundary, the case has been argued for either model 2 or 3. Martin (1983) and his colleagues believed that the rise of mantle plumes cause delamination between the crust and mantle, inducing strong deformation and magmatism. In China recent years, the results from the geosciences transect and from seismology (Ma XY, 1989; Yuan XC, 1990; Wu GJ et al., 1991; Geoscience Transect Compilation Committee, China Seismological Bureau, 1991, 1992 a-e; Geological Group of M-SGT, 1994; Gao R et al., 1995, 1998; Zeng RS et al., 1995) in the Chinese continent have shown that strong deformation and magmatism are not related to mantle plumes, or to the uplift of the Mohorovĭcíc discontinuity, or the uplift of the base of the lithosphere. It is not clear whether some mantle plumes have occurred in the Chinese continent during the Phanerozoic, apart from the Emeishan plume at the end of Paleozoic. Evidence from geology and geophysics does not support the hypothesis that deformation and magmatism during the Mesozoic were due to the rise of mantle plumes, the uplift of the Mohorovĭcíc discontinuity, or uplift of the base of the lithosphere.

The effects of intraplate deformation are widespread in the Chinese continent, with distances as many as 2,000–5,000 km between areas of obvious intraplate deformation, and recent or paleo-plate boundaries. In this case most geoscientists naturally consider that this is due to far-field effects, transmitted through the plates from the sites of subduction or of collision between plates. Ben et al. (1997) studied deformation in the eastern and western North America systematically, and considered that the activity at the boundary between plates could be transmitted over distance of ~2,000 km. However, in intraplate areas at distance of 300 km from the plate boundary, differential stress decreases rapidly from 100 MPa to 20–30 MPa. In most intraplate areas the differential stress would be too small to cause any obvious deformation. Due to the completeness of the data from the North American continental plate, Ben et al.'s (1997) research results must be taken seriously. Intraplate deformation is probably limited to the marginal areas, at distances of less than 1,000 km from the plate boundary (Burchfiel and Davis, 1975; Burchfiel et al., 1993). Over most of the North American continental plate the sedimentary cover shows only horizontal layering, being almost completely undeformed.

However, the Chinese continent is very different from the North American continent. The lithosphere of the Chinese continent is rather weak. It is easily deformed by plastic (brittle or ductile) deformation, with the differential stress decreasing rather slowly with transmission in crust, so that tectonic stress may be transmitted over long distances, which is very different to the transmission of earthquake wave. Wan TF (1994) and Wan TF and Cao XL (1997) took 176 measurements of stress magnitude for the Sichuanian Tectonic Period (135–56 Ma) by the dislocation density method in quartz and olivine using the transmission electron microscope. This deformation was caused by the northward movement and collision of dispersed blocks from the Gondwana (Figs. 8.2 and 8.4). In the Ngari area, southwestern

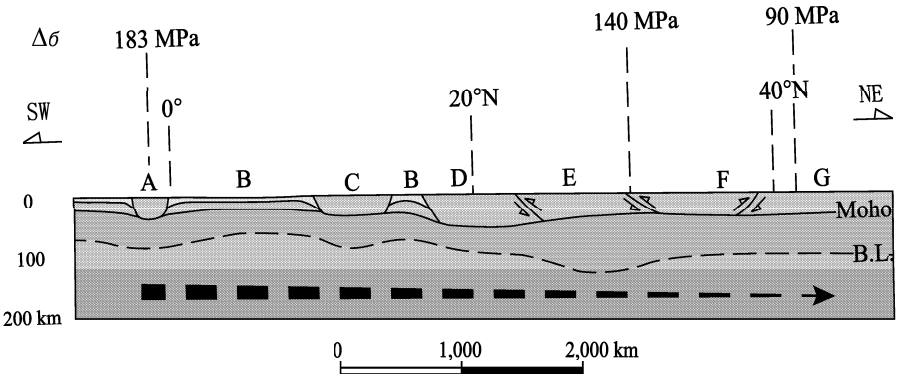

Fig. 12.1 Far-field effects of the collision between plates during Cretaceous in the Chinese continent.

A. Ngari region, Himalayan Block; B. Neo-Tethys Ocean; C. Gangdise Block; D. original Qiangtang and Indochina block; E. original Yangtze Plate; F. original Sino-Korean Plate; G. original Central Asian Fold Belt.

D-G were already amalgamated into Eurasian continental plate by the Cretaceous period.

Moho. Mohorovĭcíc discontinuity; B.L. base of the lithosphere; the depths of the Moho and the B.L. are shown at their present depths.

The $\Delta\sigma$ is the magnitude of the differential stress; the arrow represents the decrease in stress from SW to NE in crust and upper mantle.

China, the differential magnitude of stress reached 183 MPa; further northeast, in the Qinling-Dabie area, central China, ~140 MPa; in northern and northeastern China is still 90–100 MPa (Fig. 12.1), only half the differential magnitude of stress in the Ngari area. The magnitude of differential stress decreased during transmission through 5,000 km by almost 90 MPa, with an average rate of decrease of 1.8 MPa per hundred kilometers. This shows that far-field effects resulting from the subduction or collision between plates can be transmitted through the Chinese continent and are sufficient to account for widespread intraplate deformation.

A series of detachments may develop under the influences of the far-field effects transmitted by subduction or collision between plates, due to the different strength of layers in the lithosphere, allowing differential movement between the sedimentary layers, between the sedimentary cover and the crystalline basement, between the upper and lower crust, between the crust and mantle and between the lithosphere and asthenosphere, leading to the development of folds, faults, thrusts and ductile shear zones. A decrease in pressure at depth may lead locally to partial melting, causing the rise of magmas. Far-field effects, caused by horizontal reactions between plates, are considered to be the main geodynamic mechanism for intraplate deformation in the Chinese continent.

It should be mentioned that the influences of rock strength and the mechanisms of transfer of stress by processes of plastic deformation and of seismic waves by elastic deformation are completely different.

Dislocation within and between crystals is the main mechanism for penetrative rock deformation (White, 1977). This is a process of plastic deformation, taking place over a long time span and transmitted through the rock at the very slow rate, characteristic of rheological materials. As stress is transferred through the rock, energy is consumed, decreasing the differential stress. The greater the rock strength, the more competent the rock, the more energy is consumed in deformation. When the differential tectonic stress rises to a level sufficient to cause crystal dislocation, the rock fails and differential stress decreases rapidly, so that tectonic stress cannot be transferred easily through the rock. When rock strength is low, less energy is consumed in the process of stress transfer, differential stress decreases more slowly and tectonic stress can be transferred farther, as occurred in the Chinese continent.

However, the dispersion of earthquake waves through the Earth takes place by the different processes of elastic deformation. Crystal cells in the rock vibrate parallel and transversely to the direction of propagation of earthquake waves, with each crystal cell recovering its original position after the wave has passed. As in the case of plastic deformation, when the density of the rock is higher, rock strength is higher, the particle interval of crystal cells is smaller, seismic wave is transmitted more easily and transferred over greater distances. Where the rock is loose or has low strength, the density of rock is lower, the particle interval of crystal cells is larger, seismic waves are not easily transferred, the velocity of seismic waves is lower and waves are transferred over shorter distances, or are absorbed more quickly. When the rock is liquid in a molten state, the particle intervals of crystal cell are even greater, cells cannot maintain a fixed structure, the velocity of longitudinal (P) wave decreases very rapidly and transverse waves are absorbed completely.

12.2 Extension Tectonics and Mechanism of Basin Forming

Evidence of intraplate extension can be found in the Chinese continent since the Archaean. The trend of extension zones is almost parallel to the direction of the maximum principal compressive stress, because they usually accorded with the existing weakness zone. Extension zones can be formed on the margins of continental plates and also internally within plates. Most extensional fracture zones are formed by the re-activation of older zones of weakness. Normal faults, caused by extension, are syn-sedimentary faults or growth faults, controlling the formation of sedimentary basins. These faults have often a high angle of dip near the Earth's surface, but connect to low angle detachments at 15–20 km depth at low velocity, in high conductivity layer between the sedimentary cover and the crystalline basement in the middle crust. These are listric faults, steep in upper part and flattening at depth (Fig. 12.2). Only multi-period extension faults penetrate to the base of the lithosphere, causing lithospheric extension tectonics, during Neogene Period, for example, the Taihangshan–Dahingganling fault, the Tancheng–Lujiang Fault and the southeast coastal margin fault along China Sea, often forming fault–depression basins, controlled by parallel step faults near the Earth's surface.

Because the Chinese continent has undergone stress in several different directions at different times, zones of extension do not maintain the same direction over a long period. The extension faults are frequently affected by compression and show the effects of inversion tectonics. At different periods extension belts have been formed in different directions. The life cycle of an extension zone is relatively short, with only limited displacement, for example, in the basins surrounding the Bohai Basin, including the Central Bohai, Huanghua and Central Hebei basins, the amount of extension was less than 10% (Fig. 12.2). According to descriptions given in earlier chapters of this volume, WNW-trending extensional basins with near N-S extension were formed during the Jurassic (Fig. 7.3), NNE-trending extensional basins, with near E-W extension, were formed during the Cretaceous-Paleocene (Fig. 8.2), WNW or near E-W trending extensional basins, with N-S extension, were formed during the Eocene–Oligocene (Fig. 9.3), while NNE-trending wide extensional basins, with near E-W extension, developed during the Neogene–Early Pleistocene (Fig. 10.4). Extension did not proceed to a rift period, leading to the formation of oceanic crust within the Chinese continent, so that rifting came to a premature end, and most faulted basins are affected by inversion tectonics. While the faults operated as normal faults, the basins showed depression with sedimentation; when the basins were compressed, normal faults were converted to thrusts or reverse faults, the basins were uplifted and there was a hiatus in sedimentation. Multi-period inversion is one of the major characteristics of Chinese continental basins.

Taking the NNE-trending Songhuajiang-Nengjiang basin as an example, in Cretaceous-Paleocene, i.e. during the Sichuanian Tectonic Period (135–56 Ma), a maximum principal compressive stress oriented NNE trending, induced E-W extension, developing the original sedimentary basin (Fig. 8.2); during the North Sinian Tectonic Period (56–23 Ma) with a maximum principal compressive stress oriented E-W orientation, the area showed E-W shortening, the basin was inverted and uplifted, forming

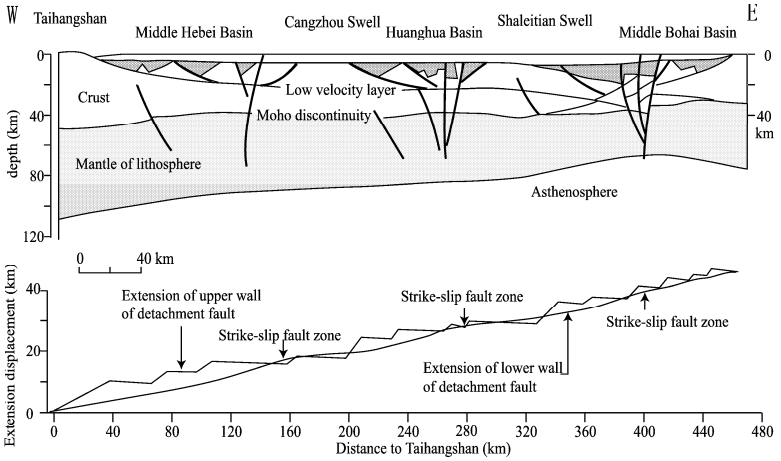

Fig. 12.2 Extension tectonics and mechanisms of basin development taking the Bohai Bay Basin as an example (modified after Lu KZ et al., 1997, with permission of Lu KZ).

the Daqing "plain-type" anticline with the main oil-gas reservoir; so during the Eocene-Oligocene there was no sedimentation (Fig. 9.3). During the Himalayan Tectonic Period (23–0.78 Ma) (Fig. 10.4) the area underwent N-S shortening and E-W extension, the basin was extended with further subsidence and sedimentation. During the Neotectonic Period (since 0.78 Ma) the basin was slightly inverted, uplifted and eroded, under the influence of NE-SW shortening and NW-SE extension (Fig. 11.4).

Syn-sedimentary or growth faults are commonly developed during the formation of sedimentary basins. Depending on recent three dimensional seismic research, the horizontal displacements of syn-sedimentary or growth faults are usually bigger than vertical displacement. Growth faults are frequently based on earlier faults and zones of weakness. According to statistical analysis of the strike directions of faults, most growth faults are found to be almost parallel to the orientation of maximum principal compressive stress. Using the above principle, the orientation of the maximum principal compressive stress can be determined, based on statistical analysis of the strike of growth faults at any period. In homogeneous media, faults usually develop at an angle of $\sim 45^\circ$ to the maximum principal compressive stress (Fig. 1.4).

The classification of sedimentary basins is commonly based on their plate tectonic (Dickinson, 1976; Ingersoll, 1988) or geodynamic environment (Allen and Allen, 1990; Chen FJ et al., 1992; Liu HF, 1993, 1995). Using these classifications it is necessary to know the tectonic features of the basin. However, there are some problems in relating these classifications to regional tectonics. As described above the Songhuajiang-Nengjiang basin underwent different phases of evolution during a complex geological history. It is difficult to summarize the different plate tectonic backgrounds and different geodynamic environments using only a single model. In compiling a synthetic tectonic unit map to represent regional tectonics, it is also difficult to represent a long and complex evolutionary history. To classify basins using their tectonic background or geodynamic environment excluding a time concept is inappropriate for the Chinese continent, for its multi-period tectonic evolutionary history. All basins originated in an extensional situation, but then experienced various tectonic events, sometimes extension, sometimes compression and sometimes with horizontal shearing. In discussing basin-forming mechanisms in terms of plate tectonics or the geodynamic environment, it is necessary to add a historical dimension. For example, since the Cretaceous the Songhuajiang-Nengjiang basin has experienced twice E-W extension with subsidence (Figs. 8.2 and 10.4), and twice E-W compression and uplift (Figs. 9.3 and 11.4). Because the basin experienced a great deal of depression and subsidence, the dominant features

in basin are due to extension tectonics. However, in the Songhuajiang-Nengjiang basin, if the periods of compression and inversion with uplift were not taken into account, but only the effects of extension tectonics were emphasized, the formation of an oil reservoir during the North Sinian Period (Fig. 9.3) and the re-migration of the hydrocarbons during the Neotectonic Period (Fig. 11.4) would not have been recognized.

The Yanqi and Kuche basins, located on the southern margin of the Tianshan in the northern Tarim Basin of western China, provide other examples. During the Himalayan Tectonic Period (23–0.78 Ma) (Fig. 10.4) they formed as foreland basins, located in front of the Tarim Block, subducted beneath the Tianshan. However, during the Paleogene and earlier periods there were no thrusts or subduction zones in the basin. Prior to the Neogene these basins were not foreland basins, but in the Mesozoic and Paleogene sedimentation consisted of extensive fluvial and lacustrine facies. In addition to the plate tectonic background and geodynamics, basin classification also requires a time concept. It is necessary to take time and the history of the evolution of a basin into consideration in any geodynamic classification of sedimentary basins. It is important to consider the complete sedimentation history and processes of inversion in the classification of sedimentary basins.

There is discussion concerning the foreland basin mechanism for the formation of sedimentary basins, no matter whether they are related to plate subduction or intra-continental subduction, this is of marginal importance. There is no dispute about the mechanism responsible for the formation of strike-slip, pull-apart basins, controlled by movements along strike slip faults (Li ST, 1988; Xia BD et al., 1994 b). The main arguments concern the mechanism for the formation of extensional basins.

Many hypotheses have been proposed for the formation of extensional basins in the Chinese continent, such as mantle uplift (Li DS, 1980), subduction-related back-arc basins (Gao MX 1983), plate subduction and mantle delamination (Zhao HL et al., 1996; Deng JF, 1996) and post-orogenic extensional collapse (Zhang JS et al., 2002).

In China the mantle uplift hypothesis has been supported by many geoscientists. It seems reasonable to use gravity data to explain basin tectonics. Most basins have a high positive gravity anomaly due to a high density upward mantle bulge. Many researchers thought that the hollow basin and the uplifted mantle have mirror symmetry. If the mantle has a noticeable bulge there should be radial and ring fault systems near the Earth's surface, but this type of fault system does not occur in association with any of the Chinese continental basins. Seismic reflection profiles frequently show no mantle uplift, the amount of uplift is not very great and may be within the margin of error. Mantle uplift is often seen on one side of a basin, but not obviously on the other (for detailed data see Chapter 13). The clearest example of mantle uplift of 8–10 km occurs on the margins of the Tarim Basin. However, this does not prove that the Tarim Basin was formed by mantle uplift. At present the mantle uplift hypothesis is becoming less popular.

As for back-arc basin hypothesis, as stated in Chapter 10, the marginal seas of the western Pacific Ocean were formerly regarded as typical "back-arc basins", but recent research suggests that they are not back-arc basins at all (Tamaki, 1992; Jolivet and Tamaki, 1992, 1994; Tayler, 1980, 1983; Tectonics Group of Institute of South China Sea, Chinese Academy of Sciences 1988; Briais, 1993). Where are the back-arc basins on the margins of Chinese continent? The Chinese continental basins are more than 600 km from an island arc. How could these basins possibly have been formed as back-arc basins?

In the post-orogenic extensional collapse hypothesis it is considered that compression, shortening and mountain building occurred earlier, and that subsequent extension, subsidence and collapse were the main mechanisms for the formation of the basin: mountain building first; basin formation later. Recently, sedimentary research in foreland basins has shown that mountain building and basin formation occur simultaneously, with no priority in their time sequence (Burbank et al., 1996; Wang GZ et al., 2000; Song CH et al., 2001; Fu KD et al., 2001).

The "plate-subduction with mantle-delamination" hypothesis has been very influential in recent years. In this hypothesis the sedimentary basins of the eastern Chinese continent are interpreted as being related to subduction zones in the Pacific Ocean, which have caused delamination in the deep mantle. Hot mantle, uplifted as a result of mantle delamination, then caused the formation of extensional basins.

This hypothesis is a variant of the mantle uplift hypothesis, but can not explain why there are no radial or ring fractures around any basins in China. In the search for evidence to support the delamination hypothesis, some researchers have combined fractures formed in different directions and at different times. It is argued that radial fault systems, caused by mantle uplift, have the leading role in basin formation. The key problem lies in determining whether radial fractures were formed contemporaneously or not. If they were formed during the "Mesozoic" or "Cenozoic", it might appear that they were approximately simultaneous, using crude methods of timing. At the present time, it is not too difficult, using three-dimensional seismic exploration, to identify the time of formation of faults in different directions. As described in the previous few chapters in this volume, during the formation of the Chinese continental basins the preferred directions of syn-sedimentary or growth faults were different at different times. However, many researchers are content with the present delamination interpretation and do not wish to consider the matter further.

According to the data presented in the earlier chapters of this book, the author has considered that multi-period, multi-directional tectonic stress fields, with horizontal compression and extension, were the dominant mechanisms controlling the formation of the Chinese continental extensional basins and their surrounding mountains. In every tectonic period there are distinct preferred fault trends, but ring and radial fault systems do not occur in the same period. The amount of horizontal displacement on faults, related to internal basins and nearby areas, is many times greater than their vertical displacement. Evidently the amount of horizontal stress is greater than the amount of vertical stress. The subsidence of basins and the associated mountain uplift are controlled mainly by isostatic compensation under the influence of gravity. Since the Paleozoic Era, lithosphere consisting of ancient crystalline basement rich in intermediate-basic rocks with a high density, subject to extension, has subsided under the influence of isostasy to form sedimentary basins. On the other hand, lithosphere consisting largely of granitoid rocks, with a low density, has been relatively uplifted to form mountains (Xu DS et al., 2001; Zhang L, 2005). The major controlling factor for the distribution of basins and mountains is the tectonic stress field, while subsidence and uplift to form basins and mountains are controlled by isostatic gravitational compensation.

12.3 Characteristics of Collision Tectonics

There are many examples of continent-continent collision belts in the Chinese continent, characterized by:

(1) Tectonic Thrust Sheets and Mélange Belts

Collision zones consist of mixed crust and mantle derived from separate tectonic plates, including relics of oceanic crust and mantle which once separated two continental plates. The results of mixing of materials from different plates during plate collision are mélange and tectonic thrust sheets on a macro- and meso-scale, and mylonites and cataclasites on a microscopic scale. Collisions result in the mixing of rock types and of chemical elements, which does not lead to the enrichment of particular elements or the formation of mineral ore deposits. The correct recognition of the characteristics of collision zones has important implications in the search for new solid mineral resources. This lesson has been learned over many years from many disappointing attempts at mineral exploration in eastern China.

(2) Fan Folds and Ramp Thrust System

Fan folds and ramp-thrust systems are often formed in collision belts (Xiao XC et al., 1991, 1992, 1998; Zhong DL et al., 1998; Zhang GW et al., 1996, 2001). Because in the final period of continent-continent collision, rock composition and strength of the two colliding plates are very similar, in contrast to oceanic and continental subduction, conjugate shear fractures are easily developed, forming ramped

thrust systems, accompanied by fan folds. Ramp thrust systems do not show the same features throughout the whole section. Faults with a dominant direction of dip may be associated with faults with the opposite direction of dip. This is possibly connected with the difference of rock strength for plates.

(3) Three-dimensional Wedge Tectonics (Crocodile Tectonics)

Collision belts universally exhibit on a large scale and three-dimensionally, "wedge" tectonics (Quinlan et al., 1993), "crocodile" tectonics (Meissner et al., 1989) or "indentation" tectonics. The first study in deep tectonics carried out by Chinese scientists using seismic tomography was in the Jinshajiang–Lancangjiang Collision Belt. In the Yunnan segment the Jinshajiang Collision Zone is inclined eastwards, with a medium angle of dip near the surface, but in the lower crust and mantle is inclined westwards, showing a ramp and indentation thrust system. The upper crust of the Yangtze Plate was obducted onto the Lanping–Simao Block, while the lower crust and lithospheric mantle were subducted westwards to a depth of 250 km beneath the Lanping–Simao Block (Zhao YG, Zhong DL et al., 1992; Zhong DL et al., 1998) (Fig. 12.3). On the basis of its surface geological expression the Lancangjiang Collision Belt is the most important, as it marks the boundary between the Eurasian continent and accreted Gondwana continental fragments. However, if lithospheric tectonics is considered, the Jinshajiang Collision Belt is most important as it affects the whole of the lithosphere. The Lancangjiang Collision Zone affects only the shallow lithosphere, and is cut off at depth by the Jinshajiang Collision Belt. Later, many Chinese scientists have reported similar wedge or indentation tectonics in Tianshan (Shao XZ et al., 1996), Himalaya (Teng JW et al., 1996), Longmenshan (Cai XL et al., 1995, 1997) (Fig. 12.4), Qinling (Yuan XC, 1997) (Fig. 12.5), Qilianshan (Wang ZJ et al., 1997) and the Altun Mountains (Cai XL, 1998; Xu ZQ et al., 1999).

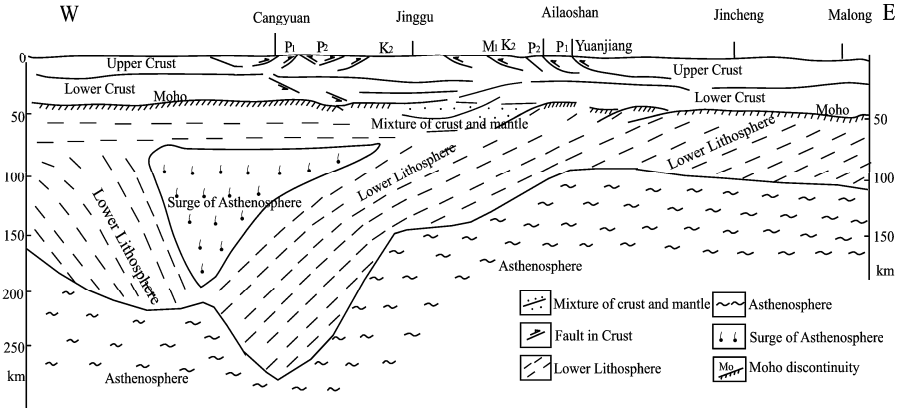

Fig. 12.3 Lithospheric tectonics in western Yunnan (Zhong DL et al., 1998, with permission of Zhong DL).

The Qinling–Dabie Collision Belt has been studied in detail. From deep seismic sounding in eastern Qinling from Fangcheng to Henan-Xiangfan, Hubei, Yuan XC et al. (1994, 1996, 1997) discovered that the Qinling crust, with a close affinity to the Yangtze Plate, was obducted northwards over the Sino-Korean Plate. The main fault plane dips to the south. The Yangtze crust penetrated the Qinling Block as a wedge between the upper and lower crust (Fig. 12.5).

In the Dabie Collision Belt Wang XF et al. (2000) found that the Dabie Block (including the southern Dabie, ultrahigh pressure metamorphic, and the Northern Dabie Belt) and the northern Huaiyang Belt are related to the Yangtze Plate, and have penetrated between and indented the upper and lower crust of the Sino-Korean Plate. The dip angles of fault planes are steep, wedging northwards with a rela-

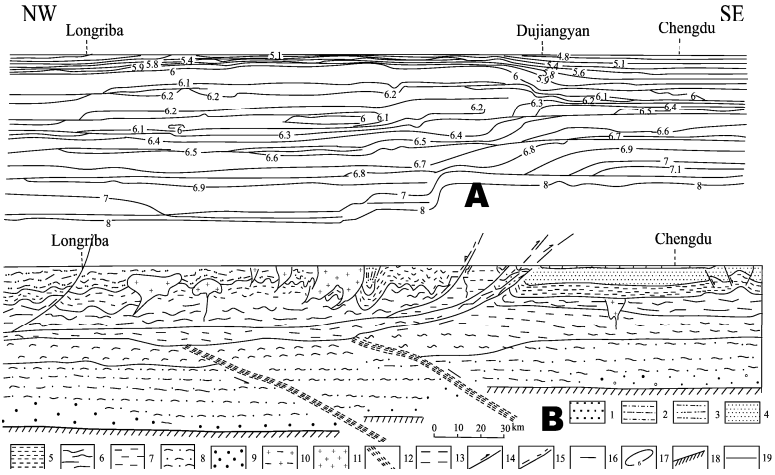

Fig. 12.4 Lithospheric tectonics in the Longmenshan Collision Zone, showing crocodile tectonics (Cai XL et al., 1995, with permission of Cai XL). A. Seismic sounding profile; B. Geological explanation of the seismic section.

1. Cenozoic; 2. Xujiahe Group; 3. Low grade Triassic metamorphic system; 4. Mesozoic; 5. Sinian and Paleozoic systems; 6. Intermediate-low grade Proterozoic metamorphic rock systems; 7. Intermediate-high grade Archaean metamorphic rock system; 8. Metamorphic rocks of the lower crust; 9. Granulite; 10. Pre-Sinian granite intrusion; 11. Mesozoic granite intrusion; 12. Ductile shear zone penetrating crust and mantle; 13. Intra-crustal low velocity zone; 14. Thrust belt; 15. Thrust at an early period, later a normal fault; 16. Direction of block displacement; 17.Velocity contours; 18.Mohorovicíc discontinuity; 19. Velocity discontinuity.

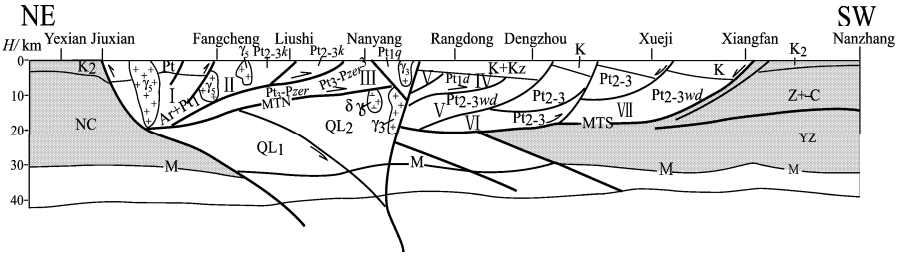

Fig. 12.5 Crust and upper mantle tectonics in Qinling from Jiuxian to Dengzhou, Henan Province (Yuan XC et al., 1996, with permission of Yuan XC).

NC. North China crust; YZ. Yangtze crust; QL_1. Qinliang crust (originally from the North China Block); QL_2. Qinling crust (originally from the Yangtze Block).

North Qinliang thrust system: Ⅰ. Luanchuan Nappe; Ⅱ. Waxuezi Nappe; Ⅲ. Erlangping Nappe.

Southern Qinliang thrust system: Ⅳ. Douling Nappe; Ⅴ. Xinye Nappe; Ⅵ. Zhaoyang Nappe; Ⅶ. Xiangfan Nappe.

Kz. Cenozoic; K. Cretaceous system; Z +ε. Sinian and Cambrian systems; Pt_{3yl}. Neoproterozoic Yaolinghe Group; Pt_{2-3}. Meso-Neoproterozoic Erlangping Group; Pt_{2-3k}. Kuanping Group; Pt_{2-3m}. Maotang Group; Pt_{2-3w}. Wudang Group; Pt_{1d}. Paleoproterozoic Douling Group; Pt_{1q} Qinling Group; Ar_3 + Pt_1. Tiahua Group and Dengfeng Group; γ_3. Early Paleozoic granite; γ_5. Indosinian and Yanshanian Periods granite; $\delta\gamma_5$. Indosinian and Yanshanian Periods granodiorite; M. Moho. MTS. Southern Main Thrust; MTN. Northern Main Thrust.

tively small displacement. The fault plane is inclined northwards near the Earth surface, and inclined southwards at depth. The crystalline basement and lower crust of the Sino-Korean Plate were subducted southwards beneath the Dabie Block, and perhaps also the Yangtze Plate.

Based on seismic tomography, Xu PF et al. (2002) discovered crocodile tectonics (wedge) in the Jiaonan Collision Belt, which is the eastward extension of the Dabie Collision Zone. They pointed out that the Sino-Korean crust was wedged between the crust and lithospheric mantle of Yangtze Plate at a depth of 16–25 km (a and b in Fig. 12.6) and inserted as a flake southwards for a distance of 80 km (c in Fig. 12.6). The main collision fault plane is inclined southwards near the Earth's surface, but dips northwards at depth. The upper crust of Yangtze Plate was obducted northwards over the Sino-Korean crust. From seismic tomography Hao TY et al. (2003, personal communication) also discovered that the main plane of the eastern extension of the Jiaonan Collision Zone near Cheju Island was inclined northwards, as far as the southern end of the Korean Peninsula, i.e. the Yangtze Plate has been subducted beneath the Sino-Korean Plate.

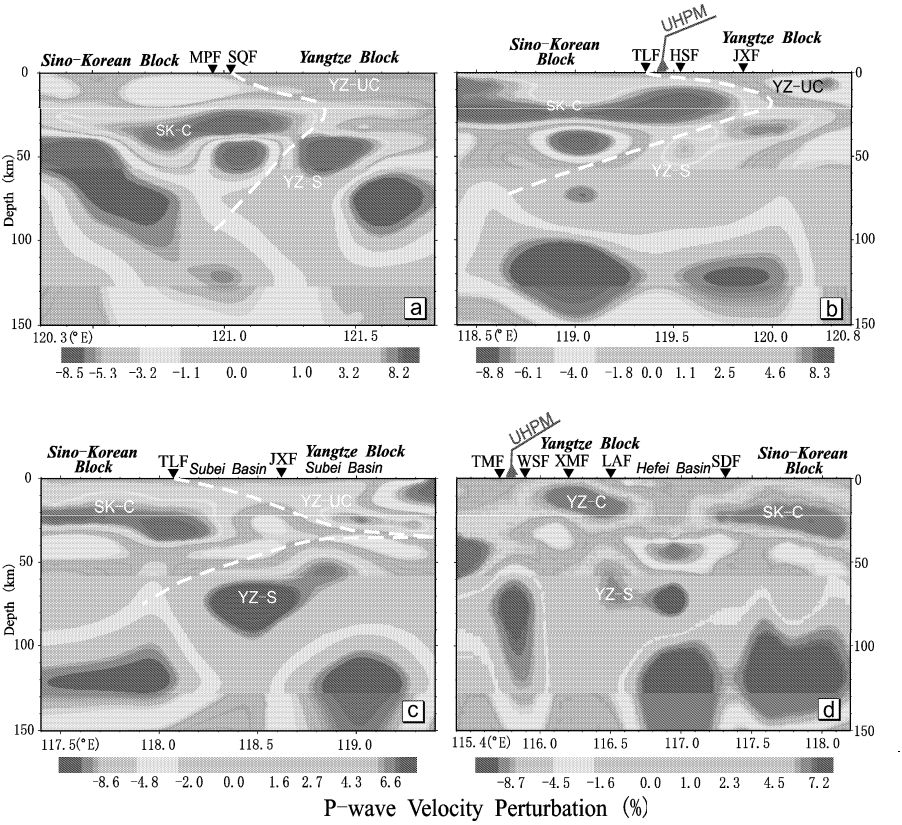

Fig. 12.6 Lithospheric structure of the Jiaonan-southern Yellow Sea region (Xu PF, 2002, with permission of Xu PF).

a. NNW-SSE section of the Jiaodong Peninsula; b. NW-SE section of Lianyuangang; c. NW-SE section across the Tancheng–Lujiang Fault, northern Jiangsu; d. NNE-SSW section cross the Dabieshan. Ordinate is depth; abscissa is longitude, color legend indicates perturbation in the P-wave velocity (%).

HSF. Haizhou–Siyang Fault; JXF. Jiashan–Xiangshui Fault; LAF. Lui'an Fault; MPF. Mouping Fault; SDF. Shaoxian–Dingyuan Fault; SK-C. Crust of the Sino-Korean Block; SQF. Shidao–Qingdao Fault; TLF. Tancheng-Lujiang Fault Zone; TMF. Taihu-Mamiao middle detachment; UHPM. Ultra-High Pressure Metamorphic Belt; WSF. Wuhe-Shuihouling lower detachment; XMF. Xiaotian-Muizitang Fault; YZ-S. Subducted remnants of the paleo-Yangtze Plate; YZ-UC. Upper crust of the Yangtze Plate.

In the Qinling–Dabie-Jiaonan Collision Belt, near the Earth's surface the attitude of the main fault plane varies greatly, sometimes is inclined to the south (in eastern Qinling and Jiaonan), and sometimes to the north (in Dabie and Cheju Island). In the collision zone the dip of the main fault plane near the Earth's surface is often in the opposite direction to the dip at depth. These observations suggest that because the upper and lower crust in the two continental blocks had a similar strength a conjugate fault system developed, in which northward or southward movements on the fault planes were likely equal, producing a complex fault system. These characteristics of collision zones are quite different from those of oceanic subduction systems where movement has occurred in one direction only.

It has been well known for a long time that the Himalayan Collision Zone was formed by the subduction of the Indian Plate beneath the Eurasian Plate. In recent years seismic tomography of the western Himalayas, to a depth of 1,000 km, has shown that in the Qinghai-Xizang Plateau the cold, high density, high velocity lithospheric slab of the Indian Plate has penetrated vertically northwards, but below 600 km this direction is reversed, and between 600 and 800 km the slab dips southwards (Grand et al., 1997; Bigwaard et al., 1998; Van der Voo et al., 1999). Previously it was believed that the Indian Plate was subducted beneath Eurasia for a great distance towards the north (see Chapter 10). It has only recently been discovered, that the lithospheric slab turns southwards and has penetrated the mantle to a depth of 800 km. This situation may explain the vigorous uplift of the Qinghai-Xizang Plateau. The evidence that the lithospheric slab had been subducted into mantle with a very steep attitude to a depth of 800 km precludes the possibility that the Tethys Ocean had been subducted beneath the Eurasian continent for a distance of $\sim$1,000 km. When continent-continent collision occurred since the Oligocene Period, the tectonic mechanism changed from thin-skinned, ramp-thrust tectonics near the surface to wedge tectonics at depth.

In zones of tectonic collision, not only the direction of dip of the fault surface does vary, to form wedge or crocodile tectonics in cross-section, but indentation or zig-zag tectonics also occurs in a horizontal plane. As described in Chapter 6, the Qinling–Dabie–Jiaonan Collision Zone, formed during Indosinian Tectonic Period, was cut by the Tanchang-Lujiang sinistral strike-slip fault zone (Wan TF et al., 1996) and the dextral strike-slip fault zone on the eastern margin of the Yellow Sea (Hao TY et al., 2002). The Jiaonan-southern Yellow Sea area is part of the Yangtze Plate, which has indented the Sino-Korean Plate to the north (Fig. 6.3). The weak Jiaodong (eastern Shandong)–eastern Liaoning crystalline basement of the Sino-Korean Plate occurs at the Earth's surface. During the collision the Yangtze Plate easily developed a detachment in the middle crust and was obducted along a shallow detachment for a great distance northwards, while the crust of the Sino-Korean Plate penetrated a mid-crustal detachment in the Yangtze Plate.

The first example of indentation tectonics to be recognized was the gradual indentation of the Indian Plate into the Eurasian Plate during the Cenozoic (Tapponnier et al., 1982) (Fig. 6.1) (referring to Chapters 6, 8, 10 and 11), which does not need to be discussed further.

Indentation is characteristic of continental collision zones in three dimensions, in both plan and cross-section. This model is very different from the single directional B-subduction or A-subduction models envisaged by many researchers. The concept of indentation has made a major contribution to the theory of global collision tectonics. The contributions of both Chinese and overseas geoscientists to the development of this model should be properly acknowledged.

12.4 Characteristics and Problems of Strike-slip Tectonics

(1) The Geometry and Kinematics of Strike-slip Tectonics

The geometry of strike-slip tectonics is the same in China as elsewhere in the world (Sylvester, 1988). The attitude of the fault planes is steep and fairly straight. At the surface the fault trace is represented by

several parallel faults, which merge to form a single fault plane at depth. In seismic sections this type of structure is described as a structure of "flower" or "palm tree".

The largest scale strike-slip fault zones in China are the Tancheng–Lujiang, Honghe, and Altun fault zones. The greatest amount of sinistral displacement on the Tancheng-Lujiang strike-slip fault, ~350 km, occurred during Triassic period (Wan TF et al., 1995, 1996) (Fig. 6.3). There has been ~500 km of sinistral strike-slip displacement along the Honghe Fault Zone (Fig. 9.3) since the Paleogene (Tapponnier et al., 1990), and during the Late Oligocene–Early Miocene (26–17 Ma) there was a dextral strike-slip displacement of 400 km (Fig. 10.4) (Harrison et al., 1996). The amount of sinistral strike-slip displacement along the Altun Fault Zone (Fig. 10.4) has been 350–400 km (Ge XH et al., 1998, 1999; Xu ZQ in et al., 1999) since the Early Paleozoic. These faults with large-scale horizontal displacements provide the most important evidence for intra-continental rock deformation in China; other strike-slip fault zones have much smaller displacements.

(2) The Origin of Strike-slip Faults

According to our present understanding, strike-slip fault zones do not appear suddenly but are re-activated earlier fractures or zones of weakness. For instance, the Tancheng–Lujiang Fault Zone is located on the western side of the Jiaodong (East Shangdong)–eastern Liaoning aulacogen, formed in the Sino-Korean Plate during Paleoproterozoic (Fig. 2.2). In the Neoprotorozoic earthquakes occurred many times along this margin, forming seismites (Qiao XF et al., 1994, 1996, 2001) (Fig. 3.8). The Tancheng–Lujiang Fault Zone formed along this zone of weakness on the western side of the aulacogen, with great strike-slip displacement and accompanied by paleo-earthquakes, as a result of the collision between the Sino-Korean and Yangtze plates during the Indosinian Tectonic Period (Fig. 6.3). The author does not accept that evidence of ancient earthquakes precludes the possibility of strike-slip fault movements at a later period (Qiao XF et al., 2001, 2002). The evidence for a large displacement along the Tancheng–Lujiang strike-slip fault is reasonably conclusive (Wan TF et al., 1995, 1996).

The Honghe Fault Zone, located on the southwestern boundary of the Yangtze Plate, is related to the Middle Triassic collision between the Yangtze and Lanping–Simao–Indochina Plates (Fig. 6.3). Large sinistral strike-slip movements on this fault zone occurred in the Late Paleogene (Zhong DD et al., 1998) (Fig. 9.3). During the Qinbaikou Period (1,000–800 Ma) the Altun Fault Zone formed the collision zone between the Tarim and Qaidam blocks, and in the Early Paleozoic (500–400 Ma) (Figs. 3.6 and 4.10) began to form the sinistral strike-slip, large-scale sinistral strike-slip occurred possibly during the Cretaceous and Neogene–Early Pleistocene Periods (Ge XH, 1998; Xu ZQ, 1999) (Figs. 8.2, and 10.4). Each strike-slip fault zone has a long history of earlier movement and was not formed as the result of a single tectonic event.

(3) The Limited Strike-slip

According to much recent research, strike-slip faults have limits, either in the history of their evolution or in their distribution. Intra-continental strike-slip faults can extend for thousands of kilometers, and the amount of displacement is of the order of hundreds of kilometers. A displacement of hundreds of kilometers may not require a great deal of time. Faults with displacements of five hundred kilometers would need only ten million years of continuous movement, at an intermediate rate of 5 cm/yr, to cause this amount of displacement.

Strike-slip faults do not always move in the same direction, but the direction of movement, controlled by the tectonic stress, may change with time and may show displacement episodically. For example, the Tancheng–Lujiang Fault Zone was formed during the Indosinian Tectonic Period (260–200 Ma) (Fig. 6.3) with a sinistral strike-slip displacement of ~350 km (Wan TF et al., 1995, 1996). No Indosinian magmatism has been recognized along the fracture, suggesting that the fault zone was restricted into the crust at that time, accompanied with a detachment in the low velocity layer in the middle crust. The fault zone, penetrating to a depth of less than 30 km, can be called a basement fault. In the Yanshanian Tectonic Period (200–135 Ma) the Tancheng-Lujiang Fault Zone underwent compression in a WNW-

ESE direction, there is no obvious slip, but the zone was affected by dynamic metamorphism, with steepening of the strata and the formation of a series of ductile shear zones (Fig. 7.3). No magma was intruded along the main faults at this period, but magma was generated at a depth of 20 km along the intersecting faults (Wan TF et al., 2001). During the Sichuanian Tectonic Period (135–56 Ma), the Tancheng-Lujiang Fault Zone extended northeastwards into Far East of Russia, linking with other faults, such as Duhua–Mishan, Yilan–Yitong and Siping–Dehui faults. In the northeastern segment, to the north of the Bohai area, it behaved as a normal fault, with a little sinistral strike-slip, while in the southern segment of the fault, south of Bohai, there was a small amount, less than 10 km, of dextral strike-slip (Fig. 8.2). Acid-intermediate magma intrusion and eruption occurred along the fault. At this period the fault could be termed a crustal fault, because the fault zone probably penetrated through the crust to the Mohorovĭcíc discontinuity. During the North Sinian Tectonic Period (56–23 Ma) the Tancheng–Lujiang Fault Zone underwent E-W compression and behaved as a reverse fault in the southern segment, south of the Bohai area, but shows dextral strike-slip movement in the northern segment, north of Bohai (Fig. 9.3). Basaltic, usually tholeiitic eruptions occurred often at the intersection between the Tancheng-Lujiang Fault and E-W and northwest trending secondary faults, or along the secondary faults. During the Himalayan Tectonic Period (23–0.78 Ma), the Tancheng-Lujiang Fault Zone was reactivated as a normal fault zone, together with sinistral strike-slip movement of 1–20 km. Many small faults with similar features were developed parallel to the fault zone. Xu JW (1987, 1993) presumed that these faults were part of the main Indosinian Tan-Lu fault system. However, many of these later faults can be distinguished easily by their small sinistral strike-slip displacements. In the Neogene and Early Pleistocene alkaline basalts enclosing peridotitic mantle xenoliths were erupted along the Tancheng-Lujiang Fault Zone, indicating that the fault penetrated the top of the asthenosphere at a depth of 70–80 km. This fault zone is a lithospheric fault, penetrating the whole of the lithosphere. During the Neotectonic Period (since 0.78 Ma), the Tancheng-Lujiang Fault Zone behaved as a reverse fault, with a small dextral strike–slip of 100–200 meters displacement in the Bohai-Shandong segment. Earthquakes are located along the fault with foci in the middle crust at ~20 km in depth; the shallow depth is explained by the sealing of the Tancheng-Lujiang Fault Zone by basaltic magma. At the present day the Tan-Lu Fault is no longer a lithospheric fault (Wan TF et al., 1995, 1996).

Although most geoscientists, have got to a common view on the general history of the Tan-Lu Fault, as given above, there are still a great many problems to be resolved. The key to understand the issue is that according to geological data, the Tancheng-Lujiang fault zone was formed in the Indosinian Tectonic Period, so did the Qinling–Dabie–Jiaonan Collision Zone. However, so far rare evidence of isotopic age has been obtained from fault rocks of the Tancheng–Lujiang Fault to confirm that it was formed during the Indosinian Period.

There is still considerable controversy concerning the amount of displacement along the Altun Fault Zone. Xu ZQ et al. (1999) proposed a sinistral strike-slip movement of ~400 km, from the displacement of corresponding tectonic zones on either side of the fault zone since the Early Paleozoic (500–400 Ma). Ritts and Biffi (2000) considered that sinistral strike-slip displacement on the Altun Fault Zone has reached ~360 km since the Middle Jurassic. If corresponding tectonic zones on either side of the fault zone are correlated the amount of sinistral strike-slip displacement is between 350 and 400 km. Particularly, Ge XH et al. (1998, 2001) identified similar tectono-petrological zones on the southern side of north Qilian and the Bashikaogong Fault, and on the northern side the Heihe–Changma Fault in the middle segment of the Altun Fault. They obtained Ar-Ar ages of 97–89 Ma from syn-tectonic micas from the Altun Fault Zone, and considered that the Altun Fault Zone was formed in Late Cretaceous, and the major sinistral strike-slip movement occurred during the Neogene. The Altun Fault Zone has been displaced by 285 km of sinistral strike-slip movement since the Late Cretaceous–Paleocene, causing isoclinal, vertically plunging folds in the Jurassic coal system and forming a ductile shear zone. Yang JS et al. (2001) did not find any evidence of activity during the Jurassic and Eocene. Meyer et al. (1998) studied the Altun Fault Zone with its relationship to the formation of the Qinghai-Tibet Plateau and considered that the amount of sinistral strike-slip displacement is 156±40 km.

Chen ZL (2001) studied basin sedimentation and deformation features in the middle segment of Altun Fault Zone and concluded that sinistral strike-slip displacement of the fault zone has been 80–100 km since the Neogene. The fault has undergone three periods of strike-slip displacement: (1) Trans-tensional strike-slip faulting formed a pull-apart basin in the Later Miocene–Early Pliocene. (2) Sinistral strike-slip with slight compression during the Late Pliocene caused the atrophy of the strike-slip basin. (3) Continual sinistral strike-slip faulting since the Early Quaternary. Since the Late Pliocene the average rate of strike-slip movement has been only 16–20 mm/yr.

By careful study of the geomorphology, the Quaternary geology and the chronology, the Research Group of the Altun Active Fault Zone, China Seismological Bureau (1992) established that there has been 75 km of sinistral strike-slip displacement along the Altun Fault since the Late Pliocene with an average rate of movement of 5.6 mm/yr. There has been ~16 km of horizontal displacement along the fault during Quaternary, at an average rate of 6.4 mm/yr, with an average rate of vertical movement of 0.56 mm/yr.

(4) The Problems of Strike-slip Tectonics

Arguments about strike-slip tectonics depend mainly on the choice of indicators to demonstrate differential horizontal movement. The best strike-slip indicators are narrow vertical structures at right angles to the fault. These may be steep cross-cutting faults, shear zones or dykes, a steep lithofacies boundary, metamorphic zones, the contact of an igneous intrusion, contours of trace element distributions and boundaries of geochemical or geophysical anomalies. However, it may be necessary to use indicators of lower accuracy, such as basin margins, fossil zones, lithofacies zones, fold belts and paleomagnetic data, to determine the amount of strike-slip displacement.

Because the temperatures of fault rocks caused by friction during fault movement may not exceed the temperatures of formation of the minerals in the rocks adjacent to the fault, especially during strike-slip movements, it is often difficult to determine date of faulting using the isotopic ages of syntectonic minerals from the fault rocks. It is difficult to distinguish between those minerals which were formed syn-tectonically as the direct result of fault movement, and those which formed part of the country rock. This is a great problem in determining the age and duration of fault movements.

12.5 On the Types of Continental Crust

In earlier discussions of tectonics, before the 1960s, only two distinct types of continental crusts were recognized: Orogenic belts (formed in geosynclines) and Platforms. In this classification there is no concept that the crust may have evolved tectonically with time. With the development of plate tectonic theory it was appreciated that this classification was completely inadequate.

In 1997 Marshak, Van der Pluijm and Hamburger et al. (1999) organized a seminar on intra-continental tectonics in USA, at which a new scheme for the classification continental crust was put forward, based on the tectonic evolution of the crust during its history, through multi-period, tectono-thermal processes.

This classification scheme distinguished ten types of continental crust:

(1) Recent active crust at a convergent plate boundary (e.g. subduction zones-Japan)

(2) Recent active crust involved in a collision zone (e.g. Himalaya)

(3) Recent active rift crust (e.g. East African rift)

(4) Recent active transform plate boundaries (e.g. California)

(5) Mesozoic reactive crust, no tectono-thermal event during the Mesozoic, but with low temperature deformation (e.g. the western Sino-Korean and western Yangtze plates; however, there were rather strong tectono-thermal events with high temperature deformation during the Jurassic and Cretaceous in the eastern Sino-Korean and eastern Yangtze plates; this type was not discussed)

(6) Mesozoic convergent margin crust, with no subsequent convergent tectonism (e.g. similar to the Qinling–Dabie, Shaoxing–Shiwandashan, Lancangjiang and Jinshajiang collision zones, but now it is well known that the subsequent convergent or rift tectonism occurred in many parts of these zones).

(7) Mesozoic rift crust, now forming or adjacent to a passive rift margin (e.g. during the Cretaceous–Neogene, Northeast China and North China blocks formed rift crust for a short time with different directions of extension, but they show strong intraplate deformation since the Mesozoic, and are no longer passive margin rift crust).

(8) Paleozoic tectonic and metamorphic crust, with no metamorphism or penetrative deformation after the Paleozoic (e.g. some parts of the Cathaysian and Xiyu plates, but most of these plates have undergone some metamorphism or penetrative deformation after the Paleozoic).

(9) Proterozoic tectono-thermal crust, without metamorphism or penetrative deformation after the Proterozoic (e.g. the western Sino-Korean and western Yangtze plates).

(10) Archaean tectono-thermal crust, with no metamorphism or penetrative deformation after the Archaean (e.g. many areas of Dongsheng, Chifeng, Liaoning-Jilin, Linfen, Jining and Bohai Continental Nuclei in the Sino-Korean Plate).

Compared with the earlier classification, the classification of crustal type in terms of age has certainly advantage. A more detailed classification could be prepared if crustal types were classified by periods. However, if the scheme of classification was too complex, it would not be used. The scheme of classification outlined above is suitable for continental crust which has experienced only a single tectono-thermal event. If the crust has undergone several tectono-thermal events, as is commonly the case in China, then the crust cannot be classified easily in this type of scheme. It is very difficult for a simple classification scheme to describe and distinguish crusts that had undergone a long geological evolution with a complicated tectono-thermal history. Fortunately, no one requires the compilation of comprehensive paleogeographic maps covering billions of years of the Earth's geological history. Palaeogeographic maps are usually prepared to cover paleogeographic environments over only short periods of geological time.

The author recognizes that there is a fundamental shortcoming in the methods used currently in the tectonic classification of the types of continental crust, which ignore the possibility that particular areas of continental crust may have undergone many tectonic events in several different tectonic environments over the course of their geological history. This may be due to a lack of evolution in thought concerning global tectonics. It may be undesirable to attempt a comprehensive division of the continental crust. In discussing the classification of segments of crust, the period of time during which the crust was affected by particular tectonic events needs to be represented more clearly. A tectonic classification which does not take account of the concept of time is not helpful to the solution of tectonic problems. A satisfactory scheme of crustal classification has yet to be devised; further advances in the study of global tectonics and further discussions may be needed to resolve this problem.

References

Allen HA, Allen JR (1990) Basin Analysis, Principles and Applications. Blackwell Scientific Publications, Oxford.

Ben A, Van der Pluijm, John P et al (1997) Paleostress in Cratonic North America: implications for continental interiors. Science 277(8): 794–796.

Bigwaard H, Spakman W, Engdahl E (1998) Closing the gap between regional and global travel tomography. J. Geophys. Res. B 103: 30055–30078.

Briais A, Patriat P, Tapponnier P (1993) Updated interpretation of magnetic anomalies and seafloor spreading stages in the South China Sea: implications for the Tertiary tectonics of Southeast Asia. J. Geophys. Res. 98: 6299–6328.

Burbank DW, Beck RA, Mulder T (1996) The Himalayan foreland basin. In: Yin A, Harrison TM (eds) The Tectonic Evolution of Asia. Cambridge University Press, Cambridge.

Burchfiel BC, Davis GA (1975) Nature and controls of Cordilleran Orogenesis, western United States: extensions of an earlier synthesis. Amer. J. Sci. 275–A: 363–396.

Burchfiel BC, Cowan DS, Davis GA (1992) Tectonic overview of the Cordilleran orogeny in the western United States. In: The Cordilleran Orogeny: Conterminous US. The Geology of North America. G3, Chapter 8: pp.407–479. The Geological Society of America.

Bureau of Geology and Mineral Resources of Provinces (1984-1993) Regional Geology of Provinces. Geological Publishing House, Beijing (in Chinese with English abstract).

Cai XL, Shi SQ, Wu DC et al (1995) Formation and Tectonic Evolution of the Wudangshan Nappe Structure. Chengdu University of Science and Technology Press, Chengdu (in Chinese with English abstract).

Cai XL et al (1997) On the wedging in orogenesis. Progress in Geology of China (1993–1996). Papers to 30th IGC. China Ocean Press, Beijing.

Cai XL, Wei XG, Li YC et al (1998) Geodynamic analysis on the orogenic process of intracontinental orogenic belts of China . Journal of Mineralogy and Petrology 18 (suppl.): 1–7 (in Chinese with English abstract).

Cande SC, La Brecque JL, Larson RL et al (1989) Magnetic lineations of the world's ocean basins. AAPG, Tulsa, Oklahoma.

Cande SC, Kent DV (1992) A new geomagnetic polarity time scale for the Late Cretaceous and Cenozoic. J. Geophys. Res. B 97(10): 13917–13951.

Chen FJ, Wang XW, Zhang GY et al (1992) Structure and geodynamic setting of oil and gas basins in the People's Republic of China. Geoscience 6(3): 317–327 (in Chinese with English abstract).

Chen GD (1960) The Activation of Platforms and Their Significances in Deposits Investigation. Geological Publishing House, Beijing (in Chinese).

Chen GD (1998) Crustobody Geotectonics of Asian Continent and Adjacent Seas. Hunan Education Press, Changsha (in Chinese).

Chen ZL, Zhang YQ, Chen XH et al (2001) Late Cenozoic sedimentary process and its response to the slip history of the central Altyn Tagh fault, NW China. Science in China D44 (suppl.): 103–111 (in Chinese).

Cui SQ (1999) On global Meso-Cenozoic intracontinental orogenesis and orogenic belts. Earth Science Frontiers 6(4): 283–293 (in Chinese with English abstract).

Deng JF, Zhao HL, Mo XX et al (1996) Continental Roots—Plume Tectonics of China. 105pp. Geological Publishing House, Beijing (in Chinese).

Dickinson WR (1976) Plate Tectonic Evolution of Sedimentary Basin. AAPG Continuing Education Course Note, series no.1, 1–56. New Orleans.

Dunlap WJ, Teyssier C (1995) Thermal and structural evolution of the intracratonic Arltunga Nappe Complex, central Australia. Tectonics 14: 1182–1204.

Editorial Board of Geoscience Transect, Seismic Bureau of China (1991) Geoscience Transect From Xiangshui, Jiangsu to Mandalt, Inner Mongolia (1 : 1,000,000, attached explanation). Geological Publishing House, Beijing (in Chinese).

Editorial Board of Geoscience Transect, Seismic Bureau of China (1992) Geoscience Transect From Dong Ujimqin, Inner Mongolia to Donggou, Liaoning (1 : 1,000,000, attached explanation). Seismological Press, Beijing (in Chinese).

Editorial Board of Geoscience Transect, Siesmic Bureau of China (1992) Geoscience Transect From Zhefang to Malong in Yunnan (1 : 1,000,000, attached explanation). Seismological Press, Beijing (in Chinese).

Editorial Board of Geoscience Transect, Siesmic Bureau of China (1992) Geoscience Transect From Suizhou, Hubei to Kalaqinqi, Inner Mongolia (1 : 1,000,000, attached explanation). Seismological Press, Beijing (in Chinese).

Editorial Board of Geoscience Transect, Siesmic Bureau of China (1992) Geoscience Transect From Menyuan, Qinhai to Ningde, Fujian (1 : 1,000,000, attached explanation). Seismological Press, Beijing (in Chinese).

Editorial Board of Geoscience Transect, Siesmic Bureau of China (1992) Geoscience Transect From Fengxian, Shanghai to Alxa Zuoqi, Inner Mongolia (1 : 1,000,000, attached explanation). Seismological Press, Beijing (in Chinese).

England PC (1987) Diffuse continental deformation: length scale, rates and metamorphic evolution. Phil. Trans. R Soc. London A 321: 3–22.

Fu KD, Gao JP, Fang XM et al (2001) Relationship model of sediment grain size and Tibetan Plateau uplift in middle-west parts of Qilian Mountains. Science in China D 44(suppl.): 210–217.

Gao MX (1983) The tectonic comparison of mountains in basin systems of east China and basins of western United States, and researches on their formation mechanism. In: Zhu X (ed) Tectonics and Evolution of Meso-Cenozoic Basins of China. Science Press, Beijing (in Chinese).

Gao R, Cheng XZ, Ding Q (1995) Preliminary geodynamic model of Golmud-Ejin Qi geoscience transect . Acta Geophysica Sinica 38 (suppl. II): 3–14 (in Chinese with English abstract).

Gao R, Li TD, Wu GJ (1998) Lithospheric evolution and geodynamic process of the Qinghai-Tibet plateau: an inspiration from the Yadong-Golmud-Ejin geoscience transect. Geological Review 44(4): 389–395 (in Chinese with English abstract).

Gao ZJ, Wu SZ (1983) Tectonic evolution of Tarim paleocontinent in Xijiang. Chinese Science Bulletin 28(23): 1448–1450 (in Chinese).

Ge XH, Zhang MS, Liu YJ (1998) Scientific problems and thought for research of the Altun fault. Geoscience 12(3): 295–301 (in Chinese with English abstract).

Ge XH, Liu JL (1999) Formation and tectonic background of the northern Qilian orogenic belt. Earth Science Frontiers 6(4): 223–230 (in Chinese with English abstract).

Ge XH, Liu YJ, Ren SM et al (2001) Re-understanding on some academic problems of the Altun fault. Chinese Journal of Geology 36(3): 319–325 (in Chinese with English abstract).

Geological Group of M-SGT (1994) Lithosphere Structure and Its Evolution in Geoscience Transect from Manzhouli to Suifenhe. Seismological Press, Beijing (in Chinese).

Grand SP, Van der Hilst RD, Widiyantoro S (1997) Global seismic tomography: a snapshot of convection in the Earth. GSA Today 7(4): 1–7.

Group of Regional Geology, Beijing College of Geology (1963) Regional Geology in China. 404pp. China Industry Press, Beijing (in Chinese).

Harrison TM, Leloup PH, Ryerson FJ et al (1996) Diachronous initiation of transtension along the Ailao Shan–Red River shear zone, Yunnan and Vietnam. In: Yin A, Harrison TM (eds) The Tectonic Evolution of Asia, pp.208–226. Cambridge University Press, Cambridge.

He GQ, Li MS (2001) Significance of paleostructure and paleogeograpy of Ordovician-Silurian rock associations in Northern Xinjiang, China. Acta Scientiarum Naturalium Universitatis Pekinensis 37(1): 99–110 (in Chinese with English abstract).

Hibsch C, Jarrige JJ, Cushing EM et al (1995) Paleostress analysis, a contribution to the understanding of basin tectonics and geodynamic evolution. Example of the Permian-Cenozoic tectonics of Great Britain and geodynamic implications in Western Europe. Tectonophysics 252: 103–136.

Hsu KJ (1989) Time and place in Alpine orogenesis. Geol. Soc. London Spec. Pub. 45: 421–443.

Huang TK (Jiqing) (1945) On the major structural forms of China. Geological Memoirs, ser. A, no. 20, 165pp.

Huang TK (Jiqing) (1960) The main characteristics of the geological structure of China: preliminary conclusions. Acta Geologica Sinica 40(1): 1–37 (in Chinese with English abstract).

Huang TK, Zhang ZK, Zhang ZM et al (1965) Eugeosynclines and miogeosynclines of China and their development of multi-gyration. In: Professional Papers of Chinese Academy of Geological Sciences, Section C: Regional Geology and Structure Geology. no.1. 71pp. China Industry Press, Beijing (in Chinese).

Ingersoll RV (1988) Tectonics of sedimentary basin. GSA Bulletin, 100: 1704–1719.

Jolivet L, Tamaki K (1992) Neocene kinematics in the Japan Sea region and the volcanic activity of the northeast Japan arc. Proc. Ocean Drill. Program Sci. Results 127–128: 1311–1331.
Jolivet L (1994) Japan Sea, opening history and mechanism: A synthesis. J. Geophys. Res. 99: 22237–22259.
Li DS (1980) Geology and structural characteristics of Bohai Bay, China. Acta Petrolei Sinica 1(1): 6–20 (in Chinese with English abstract).
Li DX (1959) Explanation of Tectonic Map of Hubei Province. Bureau of Geology of Hubei (in Chinese).
Li JL (1991) Time and special problems of lithospheric tectonic evolution in orogenic belts. In: Annual Report (1989–1990) of Open Laboratory of Lithosphere Tectonic Evolution, Institute of Geology, Chinese Academy of Sciences. China Science and Technology Press, Beijing (in Chinese).
Li JY (1998) Some new ideas on tectonics of NE China and its neighboring areas. Geological Review 44(4): 339–347 (in Chinese with English abstract).
Li ST (1988) Fault Basin Analyses and Coal Accumulation. Geological Publishing House, Beijing (in Chinese with English abstract).
Liu HF (1993) Dynamic classification of sedimentary basins and their structural styles. Earth Science 18(6): 699–724 (in Chinese with English abstract).
Liu HF (1995) Classification of foreland basins and fold thrust style. Earth Science Frontiers 2(3): 59–68 (in Chinese with English abstract).
Livaccari RF, Burke K, Sengör AMC (1981) Was the Laramide orogeny related to subduction of an oceanic plateau? Nature 289(5795): 276–278.
Lu KZ, Qi JF et al (1997) Tectonic Model of Cenozoic Petroliferous Basin, Bohai Bay. Geological Publishing House, Beijing (in Chinese with English abstract).
Ma XY, Cai XL (1965) Features of structure changes in Early Archean in east China. In: Problems About Tectonics of China. Science Press, Beijing (in Chinese).
Ma XY (chief editor, Editorial Board for Lithospheric Dynamics Atlas of China, State Seismological Bureau) (1989) Lithospheric Dynamics Atlas of China. SinoMaps Press, Beijing (in Chinese with English abstract).
Ma ZJ, Mo XX (1997) Time-space indications of the Earth's rhythm and its dynamics. Earth Science Frontiers 4(4): 211–221 (in Chinese with English abstract).
Marshak S, Van der Pluijm BA, Hamburger M (1999) Tectonics of continental interiors. Tectonophysics 305(1–3): 1–408.
Martin H (1983) Alternative geodynamic models for the Damara Orogeny: a critical discussion. In: Martin H, Eder FW (eds) Intracontinental fold belts: case studies in the Variscan Belt of Europe and the Damara Belt in Namibia, pp.913–945.
Meissner R, Reston T (1989) The three-dimensional structure of the Oberpfalz: an alternative interpretation of DEKORP-KTB data. Tectonophysics 157 (1–3): 1–11.
Meyer B, Tapponnier P, Bourjot L et al (1998) Crustal thickening in Gansu-Qinghai, lithospheric mantle subduction and oblique strike-slip controlled growth of the Tibet Plateau. Geophysical Journal International 135(1): 1–47.
Qiao XF, Song TR, Gao LZ et al (1994) Seismic sequence in carbonate rocks by vibrational liquefaction. Acta Geologica Sinica 68(1): 16–34 (in Chinese with English abstract).
Qiao XF, Song TR, Li HB et al (1996) Genetic Stratigraphy of the Sinian and Lower Cambrian Strata in South Liaoning Province. Science Press, Beijing (in Chinese).
Qiao XF, Gao LZ, Peng Y (2001) Neoproterozoic in Paleo-Tanlu Fault Zone—Catastrophe Sequence Biostratigraphy. Geological Publishing House, Beijing (in Chinese).
Qiao XF, Gao LZ, Peng Y et al (2002) Seismic event, sequence and tectonic significance in Canglangpu Stage in Paleo-Tanlu fault zone. Science in China D 45(9): 781–791.
Quinlan G, Beaumont C, Hall T (1993) Tectonic model for crustal seismic reflextivity patterns in compression orogens. Geology (Boulder) 21(7): 663–666.

Ren JS, Jiang CF, Zhang ZK et al (1980) The Geotectonic Evolution of China. Science Press, Beijing (in Chinese).
Ren JS, Chen TY, Niu BG et al (1990) Tectonic Evolution of the Continental Lithosphere and Metallogeny in Eastern China and Adjacent Areas. Science Press, Beijing (in Chinese).
Ren JS, Wang ZX, Chen BW et al (2000) China Tectonics, Outlooked by the Globe—Brief Direction of Tectonic Map of China and Its Adjacent Areas. Geological Publishing House, Beijing.
Research Group of Altun Active Fault Zone, Seismic Bureau of China (1992) Altun Active Fault Zone. Seismological Press, Beijing.
Ritts BD, Biffi U (2000) Magnitude of post-Middle Jurassic (Bajocian) displacement on the central Altun Tagh fault system, Northwest China. GSA Bulletin 112(1): 61–74.
Sengör AMC (1982) Edward Suess' relations to the pre-1950 schools of thought in global tectonics. Geol. Rundsch. 71(2): 381–420.
Shao XZ, Zhang JR, Fan HJ et al (1996) The crust structure of Tianshan orogenic belt: a deep sounding work by converted waves of earthquakes along Ürümqi-Korla profile . Acta Geophysica Sinica 39(3): 336–346 (in Chinese with English abstract).
Song CH, Fang XM, Li JJ et al (2001) Tectonic uplift and sedimentary evolution of Jiuxi basin in the northern margin of the Tibetan Plateau since 13Ma BP. Science in China D 44(suppl.): 192–202.
Song HL (1999) Characteristic of Yanshan type intraplate orogenic belts and a discussion on its dynamics. Earth Science Frontiers 6(4): 309–316 (in Chinese with English abstract).
Sylvester AG (1988) Strike-slip faults. GSA Bulletin 100(11): 1666–1703.
Tamaki K, Suyehiro K, Allan J et al (1992) Tectonic synthesis and implications of Japan Sea ODP Drilling. Proc. Ocean Drill. Program Sci. Results 127–128: 1333–1348.
Tapponnier P, Peltzer G, Le Dain AY et al (1982) Propagating extrusion tectonics in Asia: new insights from simple experiments with plastic line. Geology 10: 611–616.
Tapponnier P, Lacassin R, Leloup PH et al (1990) The Ailao Shan / Red River metamorphic belt: tertiary left-lateral shear between Indochina and South China. Nature 343(6,257): 431–437.
Taylor B, Hayes DE (1980) The tectonic evolution of the South China Basin. In: Hayes DE (ed) The tectonic and geologic evolution of Southeast Asian Seas and Islands, Geophy. Monogr. 23: 89–104. American Geophysical Union, Washington DC.
Taylor B, Hayes DE (1983) Origin and history of the South China Basin. In: Hayes DE (ed) The tectonic and geologic evolution of Southeast Asian Seas and Islands, Geophy. Monogr. 27 (Part 2): 23–56. American Geophysical Union, Washington DC.
Tectonics Group of Institute of South China Sea, Chinese Academy of Sciences (Liu ZS et al) (1988) Geological Structure in South China Sea and Spreading of Continental Margin. Science Press, Beijing (in Chinese).
Teng JW, Zhang ZJ, Hu JF et al (1996) Physical-mechanical mechanism for the whole uplifting of the Qinghai-Xizang plateau and the lateral shortening and vertical thickening of the crust . Geological Journal of China Universities 2(2): 121–133; 2(3): 307–323 (in Chinese with English abstract).
Van der Voo R, Spakman W, Bigwaard H (1999) Tethyan subducted slabs under India. Earth Planet. Sci. Lett. 171(1): 7–20.
Van der Voo R, Spakman W, Bijwaard H (1999) Mesozoic subducted slabs under Siberia. Nature 397(6716): 246–249.
Vasilivsky P (1964) Argument about tectonic development and genesis. Translation Collection on Geology (5): 17–22.
Wan TF (1994) Intraplate Deformation, Tectonic Stress and Their Application for Eastern China in Meso-Cenozoic. China University of Geosciences Press, Wuhan.
Wan TF (1995) Evolution of Tancheng-Lujiang fault zone and paleostress fields. Earth Science 20(5): 526–534 (in Chinese with English abstract).
Wan TF (1995) The progress of researches on tectonic stress field. Earth Science Frontiers 2(2): 226–235 (in Chinese with English abstract).

Wan TF, Zhu H, Zhao L et al (1996) Formation and Evolution of the Tancheng-Lujiang Fault Zone. China University of Geosciences Press, Wuhan.
Wan TF, Cao XH (1997) Estimation of differential stress magnitude in Middle-Late Triassic to Early Pleistocene for China. Earth Science 22(2): 145–152 (in Chinese with English abstract).
Wan TF (1997) On the accretion of Eastern Asian continental blocks since Triassic. Journal of China University of Geosciences 8(2): 114–120.
Wan TF, Ren ZH (1999) Research on the intraplate deformation velocity of China in Meso-Cenozoic. Geoscience 13(1): 83–92 (in Chinese with English abstract).
Wan TF, Teyssier C, Zeng HL et al (2001) Emplacement mechanism of Linglong granitoid complex, Shandong Peninsula, China. Science in China D 44(6): 535–544.
Wan TF (2004) An Outline of China Tectonics. Geological Publishing House, Beijing (in Chinese).
Wang GZ, Wang CS (2001) Disintegration age of basement metamorphic rocks in Qiangtang, Tibet, China. Science in China D 44(suppl.): 86–93.
Wang HZ, Mo XX (1995) An outline of the tectonic evolution of China. Episodes 18(1–2): 6–16.
Wang XF, Metcalfe I, Jian P et al (2000) The Jinshajiang suture zone: tectono-stratigraphic subdivision and revision of age. Science in China D 43(1): 10–22.
Wang ZJ, Wu GJ, Xiao XC et al (1997) Explanatory Notes for Global Geoscience Transect, Golmud-Ejin Transect, China. Geological Publishing House, Beijing (in Chinese).
White S (1977) Geological significance of recovery and recrystallization processes in quartz. Tectonophysics 39(1–3): 143–170.
Wu GJ, Gao R, Yu QF et al (1991) Integrated investigations of the Qinghai-Tibet Plateau along the Yadong-Golmud geoscience transect. Acta Geophysica Sinica 34(5): 552–562 (in Chinese with English abstract).
Wu ZW, Zhang CH (1999) Some ideas regarding to the establishment of orogeny theory with Chinese characters. Earth Science Frontiers 6(3): 21–29 (in Chinese with English abstract).
Xia BD, Zhong LR, Fang Z et al (1994) Early Permian Gufengian formation argillized volcanics in the lower Yangtze region. Geological Review 40(1): 64–73 (in Chinese with English abstract).
Xiao XC, Tang YQ (1991) Tectonic Evolution of the Southern Margin of Complex and Very Large Suture Zone in Paleo-Central Asia. Beijing Science and Technology Press, Beijing (in Chinese).
Xiao XC, Tang YQ, Feng YM et al (1992) Tectonic Evolution of Northern Xinjiang and Its Adjacent Regions. Geological Publishing House, Beijing (in Chinese).
Xiao XC, Li TD, Li GC et al (1998) Lithospheric Tectonic Evolution of Himalaya. Geological Publishing House, Beijing (in Chinese).
Xu SD, Zeng HL, Wan TF (2001) Apparent density mapping and tectonic of China. Earth Science Frontiers 8(2): 407–413 (in Chinese with English abstract).
Xu JW, Zhu G, Tong WX et al (1987) Formation and evolution of the Tancheng–Lujiang wrench fault system: a major shear system to the northwest of the Pacific Ocean. Tectonophysics 134(4): 273–310.
Xu JW (1993) The Tancheng–Lujiang Wrench Fault System. John Wiley & Sons, New York.
Xu PF, Liu F, Ye K et al (2002) Flake tectonics in the Sulu orogen in eastern China as revealed by seismic tomography. Geophysical Research Letters 29(10): 23 (1–4).
Xu ZQ, Yang JS, Zhang JX et al (1999) A comparison between the tectonic units on the two sides of the Altun sinistral strike-slip fault and the mechanism of lithospheric shearing. Acta Geologica Sinica 73(3): 193–205 (in Chinese with English abstract).
Yang JS, Meng FC, Zhang JX et al (2001) The shoshonitic volcanic rocks at Hongliuxia: pulses of the Altyn Tagh fault in Cretaceous? Science in China D 44(suppl.): 94–102.
Yang WR, Guo TY, Lu YL et al (1984) "Opening" and "closing" in the tectonic evolution of China. Earth Sciences (3): 39–56 (in Chinese with English abstract).
Yuan XC (1990) Geoscience Transect of Taiwan-Heishui (1: 1,000,000, attached with specialities). Seismological Press, Beijing (in Chinese).
Yuan XC (1996) Atlas of Geophysics in China. Geological Publishing House, Beijing (in Chinese).

Yuan XC, Zuo Y (1996) Geophysical Lithospheric Transect of Qinling Orogenic Belt. Science Press, Beijing (in Chinese).
Yuan XC (1997) The crustal structure of the Qinling orogen and wedging mountain building. Acta Geologica Sinica 71(3): 227–235 (in Chinese with English abstract).
Zeng RS, Sun WG, Mao TE et al (1995) Depth map of Moho interface of China continent. Acta Seismologica Sinica 17(3): 322–327 (in Chinese with English abstract).
Zhang CH (1999) A primary discussion on the intraplate orogenic belt. Earth Science Frontiers 6(4): 295–308 (in Chinese with English abstract).
Zhang GW, Zhang BR, Yuan XC (1996) Orogenic Process of Qinling Orogenic Belt and Three Dimensional Structural Map Series of Lithosphere. Science Press, Beijing (in Chinese).
Zhang GW, Zhang BR, Yuan XC et al (2001) Qinling Orogenic Belt and Continental Dynamics. Science Press, Beijing (in Chinese).
Zhang JS, Xu J, Wan JL et al (2002) Meso-Cenozoic detachment zones in the front of the Taihang Mountains and their fission-track ages. Geological Bulletin of China 21(4–5): 207–210 (in Chinese with English abstract).
Zhang L (2005) Seismic Tomography of Crust and Upper Mantle in Circum-Bohai Region. Dissertation, Institute of Geology and Geophysics, Chinese Academy of Science (in Chinese with English abstract).
Zhao HL, Deng JF, Chen FJ et al (1996) Petrology and tectonic setting of Mesozoic volcanic rocks along southeastern margin of Songliao basin. Earth Science 21(4): 421–427 (in Chinese with English abstract).
Zhao YG, Zhong DL, Liu JH et al (1992) Fundamental of geological interpretation for seismic tomography and its application to studying of west Yunnan's deep structure. Scientia Geologica Sinica (2): 105–113 (in Chinese with English abstract).
Zhao ZP(1995) An intracontinental-type orogeny—evidence from Qinling–Dabie orogenic belt, China. Scientia Geologica Sinica 30(1): 19–28 (in Chinese with English abstract).
Zhong DL (1998) Paleo-Tethyan orogenic belt in Western Yunnan and Sichuan. Science Press, Beijing.
Zhu ZC (1996) Thinking on some important geotectonic problems. Geological Science & Technology Information 15(4): 1–7 (in Chinese with English abstract).

Chapter 13
Tectonics and the Thermal Regime in the Chinese Continental Lithosphere

For a long time, the study of tectonics was based purely on geological data, restricted to research into the upper crust—the sedimentary cover and its crystalline basement. In recent years, more attention has been paid to the structure and composition of the lithosphere, using geophysical and geochemical methods, with particular emphasis on the relationship between the shallow lithosphere and the lithosphere as a whole. The structure and composition of the of Earth's mantle and core (Song XD and Richards, 1996), beneath the lithosphere (Condie KC, 2001； Xu ZQ et al., 2003), are studied by deep geophysical methods using the passage of seismic waves generated by natural earthquakes, and by comparison with the composition of meteorites (meteoritics) and other planetary bodies (astrogeology), accompanied by high temperature and high pressure experiments on possible mantle and core materials. These experiments are still at a preliminary period.

In describing research on continental lithospheric tectonics, first variations in the thickness of the crust and the lithosphere, and then the variations in their composition, physical characteristics and internal tectonics will be considered. Secondly, two contentious issues in research on the continental lithosphere of China will be discussed: the mechanism which caused the thinning of the lithosphere in eastern China in the Jurassic, and whether mantle plumes have had any influence on the tectonic development of China. Arguments are put forward for the apparent thinning of the continental lithosphere in eastern China by the detachment (ductile shear zone) and rotation of the upper crust, rather than by the uplift and delamination of the mantle.

13.1 Characteristics of the Crust of the Chinese Continent and Its Adjacent Area

For many years the depth of Mohorovǐcíc discontinuity and therefore the thickness of the crust were deduced by inverting the Bouguer gravity anomaly (Shi ZH et al., 1989). The results are essentially similar to those obtained by deep seismic sounding using an artificial source, although the latter method gives much greater precision. Gravity data usually give lower precision, but has the advantage that a much larger area can be covered. During the last 30 years, the China Seismological Bureau, the Chinese Academy of Sciences and the Ministry of Land and Resources have completed about 50,000 km deep seismic sounding profiles using artificial sources in China and its surrounding seas, including 2,000 km of high precision seismic reflection profiles. These data are important for determining variations in the depth of the Mohorovǐcíc discontinuity, and therefore crustal thickness. Using this information Li SL and Mooney(1998), Teng JW et al. (2002) and Sun (2003) have compiled a map of crustal thicknesses in Eastern Asia and its adjacent seas (Fig. 13.1). In this compilation 4,000 data points were used. The contours give an error in crustal thickness of ± 2 km, with the greater precision on the Chinese continent.

The crust of Chinese continent and its adjacent areas belongs to different crustal regimes: the thickness of continental-type crust is >30 km; that of quasi-continental type 30–15 km; that of quasi-oceanic type 15–10 km; that of oceanic type <10 km (Teng JW et al. 2002).

The crust of Pacific Ocean to the east of the Chinese continent is of oceanic type; the central part of the Japan Sea (12 km) and the central section of South China Sea (10 km) are of quasi-oceanic type; East Asia and the continental shelf, including Sakhalin Island, the Okhotsk Sea (28–34 km), the Japanese Islands (20–36 km), the Korean Peninsula (28–34 km), the Yellow Sea and East China Sea (18–24 km), the Ryukyu Islands, Taiwan Straits (24 km), Taiwan Island (28 km), the Philippine Islands and the northern part of South China Sea (18–24 km), are all of quasi-continental type; the major part of Chinese continental crust is of continental type. On the eastern margin of China crustal thickness is 30 km, reaching 74 km in the central part of the Qinghai–Xizang (Tibet) Plateau in western China, the greatest crustal thickness on Earth.

Eastern Asia can be divided into 18 crustal blocks within which the thickness varies very little. These crustal blocks correspond to areas of ancient crystalline basement. The boundaries between crustal blocks are zones of abrupt change in crustal thickness, coinciding with ancient collision belts or large-scale fault zones penetrating completely through the crust.

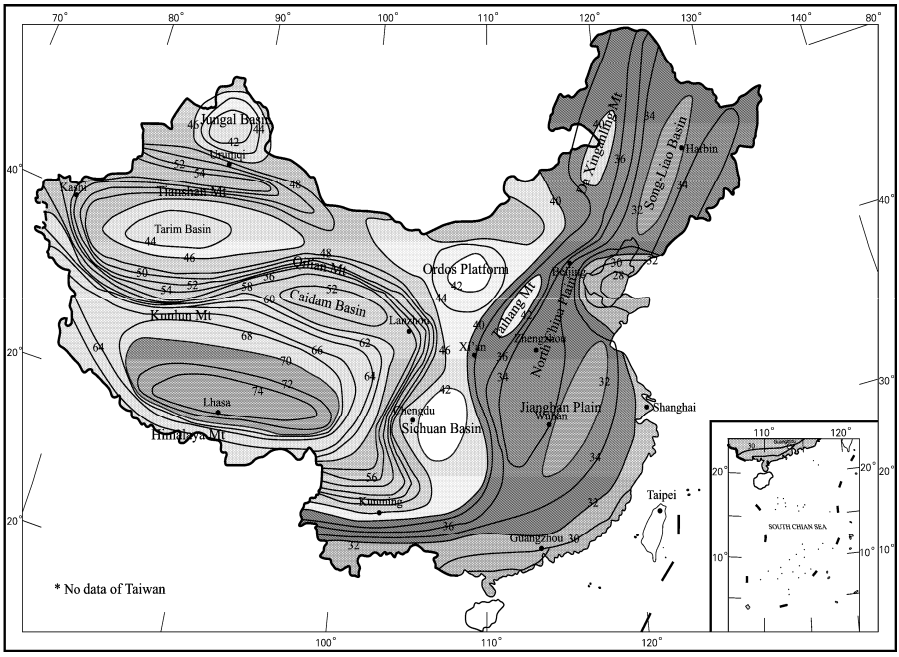

Fig. 13.1 Crustal thickness of Eastern Asia and its adjacent seas (Li SL and Mooney, 1998, with permission of Li SL).

The thickness of the crustal blocks which form Eastern Asia (Li SL and Mooney, 1998; Teng JW et al., 2002) is: (1) Balchash Lake–Junggar Block, 42–44 km, 4–6 km thinner than that of the Altay and Tianshan Mountains on either side; (2) Tarim Block, 44 km, 8–10 km thinner than that of the Tianshan and Kunlun Mountains to the north and south. The southern margin is marked by a steep gravity gradient in the Altun-Kunlun zone, separating the Qinghai-Xizang Block from the Tarim Block; (3) Qinghai-Xizang Plateau Block, 52 km in Qaidam in the north, 68 km in north central Qiangtang,

74 km in south central Gangdise, 56 km in the Himalaya to the south, corresponding to a central E-W trending depression in the Mohorovĭcíc discontinuity; (4) Indian Sub-continental Block, 44 km thick in the centre, thickening to the north and thinning in other directions; (5) Bay of Bengal Block, thinning from 36 km in the north to 18 km in the south; (6) Indochina Peninsula Block, 38 km in the north, gradually thinning to 36–32 km in the south; (7) South China Sea Block, 10–16 km thick in the central part, thickening rapidly in the surrounding areas, producing an uplift of the Mohorovĭcíc discontinuity; (8) Mongolian Plateau Block, varying from 40 to 48 km; (9) Ordos–Fenhe–Weihe Block, 42–44 km in the central part with an E-W trend, in the east thickness contours trend N-S, but E-W towards the west, consistent with the regional tectonic trend; (10) Upper Yangtze Block, varying greatly, from 36 to 52 km, with 40–42 km in the central area, an important south-north zone of steep gradient on the western edge, thinning rapidly from 60 km in Qinghai–Xizang to 44 km in the Yangtze Block; (11) Northeast China Block, 32–34 km, changing gently to form an NNE trending mantle uplift of 2–4 km compared to the western mountains; (12) Japan Sea Block, crust of continental and quasi-continental type, is only 12 km in the central part of the Japan Sea, reaching 38 km in the northern part of Japanese Islands, 36 km in the south, and 20 km in its adjacent regions; (13) Bohai Bay Block is about 32–34 km; (14) Coastal Southeast China Block, 25–34 km, in the central area, the Mohorovĭcíc discontinuity rising to 2 km higher than on the margins, along the SSW-trending south to Tancheng-Lujiang Fault Zone to near South China Sea Islands, the measured uplift is close to the limits of precision, so there may be no uplift; (15) Taiwan Island-East China Sea-Yellow Sea Block, 18–28 km, belonging to the transition from quasi-continental to quasi-oceanic type; (16) Ryukyu Trough Block, 10–14 km in the east, belonging to the transitional type from quasi-oceanic to oceanic type, at the southern end of this block is the Bashi Channel and the Philippine Sea Basin Block; (17) Philippine Sea Basin Block, 10–16 km, rhomboid-shaped, belonging to the oceanic type; (18) Sunda Islands Block, including Sunda Islands, Borneo Island, Sulu Sea, Sulawesi Island, the Java and Banda seas and Zengmu'ansha in the South China Sea Islands to the northwest, thinning from 20 km in the north to 16 km in the south, belonging to the quasi-oceanic type.

In classifying the crustal blocks of the east Asian continent, three zones of steep gradient in the Mohorovĭcíc discontinuity control the structure: (1) around the Qinghai–Xizang Plateau Block of steep gradients such as the Kunlun–Altun, the north-south seismic zone and the Himalayan zone; (2) Dahingganling–Taihangshan–Wulingshan–Damingshan zone of steep gradient, extending along the eastern side of the Indochina Peninsula; (3) Southeastern coastal steep gradient zone of the Chinese continent. These three zones of steep gradient coincide with the three giant landscape steps in the Chinese continent and the zones of steep gradient in average Bouguer gravity anomalies (Yin XH et al., 1988) (see Chapter 10; Fig. 10.8). Steep gradients in the Mohorovĭcíc discontinuity coincide with large scale fault systems, such as the Kunlun–Altun–Haiyuan Thrust Zone—the eastern edge of Daxueshan-Xiaojiang Fault Zone–the Himalayan Thrust Zone surrounding the Qinghai–Xizang Plateau, the eastern Dahingganling–eastern Taihangshan–Wulingshan–Damingshan Normal Fault Zone, the Fujian–Guangdong coastal normal fault zone located below sea level at the 50 meter contour. Variations in the thickness of the Chinese continental crust are related closely to tectonic activity since the Neogene (see Chapter 10).

On the basis of detailed tectonic research (Yuan XC et al., 1996) and the composition of the eastern Chinese continental crust (Gao S et al., 1999), the crust can be divided into four layers:

(1) Upper Crust, 14 km thick, the seismic primary wave velocity is about 6.0 km/s, the average SiO_2 content is 65%, typical rocks are sediments, granites and low grade metamorphic rocks, with a composition comparable to the average global chemical composition of the crust, in strongly deformed areas (Condie, 1993).

(2) Middle Crust, between 14 and 24 km in depth, the seismic primary wave velocity is 6–6.6 km/s below the global average value. In northern China at about 20 km depth there is a layer of high electrical conductivity, with a low seismic velocity, the average SiO_2 content of the middle crust is 62%, the typical rocks are TTG granitic gneiss (90 %) and amphibolite (10%). The chemical composition is consistent with that of the global middle crust, with high SiO_2, K_2O, Ba, Li, Zr, LREE and La_N/Yb_N

with an obvious Eu negative anomaly. The middle crust of eastern China is interpreted as being at a higher degree of evolution, with strong deformation, and many detachments.

(3) Upper part of Lower Crust, between 24–32 km in depth, the seismic primary wave velocity is about 6.8 km/s. The average SiO_2 content, taking the granulites in the North China Block as representative, is 57%–66%.

(4) Lower part of Lower Crust, between 32–37 km in depth, the velocity of seismic primary wave is about 7.0–7.1 km/s (N.B. below the Mohorovĭcíc discontinuity the velocity of seismic primary wave reaches 8.1 km/s), the average SiO_2 content is 50% and the representative rock is mafic granulite.

From the structural features of the crystalline basement and from deep seismic soundings, it can be deduced that structure of the lower crust is relatively simple. From geological, geophysical and geochemical evidence, the overall composition of the lower crust is comparable to intermediate granulite. The primary wave velocity is 0.2–0.5 km/s, lower than the average of global continental lower crust (Gao S et al., 1999) and is different from the global mafic lower crustal model of [$w(SiO_2) < 50\%$] (Taylor and McLennan, 1995; Christensen and Mooney, 1995), but close to the European lower crustal model with a salic upper layer and a mafic lower layer (Wedepohl, 1995). The ratio of the thickness of the upper and lower layers in the lower crust is different in different areas, 0.3 in southern China and Qinling, and 3.0 in northern China and Qilianshan, showing that lower crust in southern China and Qinling has a great thickness, and a basic composition.

The extent of evolution of the composition of the crust in eastern China is higher than the global value, and is characterized by $w(SiO_2) = 62$ %, with an obvious and negative Eu anomaly [$w(Eu) / w(Eu^*) = 0.80$], relative depletion in Sr and transition elements and a higher rate of $w(La) / w(Nb) = 3.0$. This may be explained by an amount of continental crustal growth by intraplate processes smaller than 10% (Rudnick, 1995), the ratio of similar compatible elements is consistent with, or close to, the ratio in the original mantle.

Complete regional geochemical data and geophysical information are still lacking in the western part of the Chinese continent.

13.2 Lithosphere Characteristics of the Chinese Continent and Its Adjacent Area

The lithosphere is primarily a mechanical concept, and is not defined by chemical composition. The lithosphere is defined seismologically and is recognized as the outer layer of the Earth with a strength greater than the interior (Barrell, 1914; Daly, 1940). The lithosphere forms a sphere near the Earth surface distinguished by the transmission of high velocity seismic waves, enclosing a sphere with a lower velocity, the asthenosphere. The average depth of the base of the lithosphere is typically more than 40 kilometers beneath the oceans; but may exceed 150 kilometers beneath the continents, or even 400 km in Russia. In most areas the continental crust is coupled to the continental lithosphere and the oceanic crust to the oceanic lithosphere. However, sometimes the crust and the underlying lithospheric mantle are not coupled permanently together. Especially, in the transitional region between the continental and oceanic lithosphere the crust and lithospheric mantle may become separated along a series of detachments.

Apart from a mechanical or seismological concept, there are three other definitions of the lithosphere and asthenosphere: (1) the lithosphere may be defined thermally as the outer sphere through which a thermal, adiabatic conduction gradient extends to the surface of the solid Earth, while the asthenosphere is an inner sphere with a thermal convection gradient; (2) petrologically, the asthenosphere is composed of fluid-rich intra-crystalline fissures or partially melted peridotite with basaltic magma, while the overlying lithosphere is completely solid (Deng et al., 1984); (3) the lithosphere can also be defined in terms of isotope geochemistry where the lithosphere is enriched mantle (EM) while the asthenosphere is depleted mantle (DM).

"Enriched mantle" is defined relative to "depleted mantle". Sometimes the composition is the same as melted mid-ocean ridge basalt, i.e. MORB, sometimes it is considered to be equivalent to the composition of the whole Earth (or chondrite) or the contaminated reservoir of continental flood basalts, and a thermal boundary layer (TBL), forming the top of the thermal convection system, and is also called the "thermal conductive margin layer" (Anderson, 1995). Although the boundary defined in different ways may be located at a similar level, the mechanical definition of the lithosphere is not equal completely to the geochemical, thermal or petrological definitions. More difficulties are created, if the depleted mantle (DM) reservoir is regarded as the asthenosphere, and the enriched mantle (EM) reservoir is regarded as the lithosphere. Many geoscientists have observed that oceanic peridotites are mantle rocks of enriched or slightly depleted type, however when oceanic mantle peridotites are subducted beneath a continental margin, they are characterized as depleted mantle with an intermediate or high degree of depletion (Johnson et al., 1990; Niu Y, 1997)

The temperature at the boundary between lithosphere and asthenosphere is 1280°C (McKenzie and Bickle, 1988). Arndt and Christensen (1992) considered that a temperature of 1210°C may mark the transition zone between the lithosphere and asthenosphere. In the upper part of lithosphere, based on determinations of tectonic stress, the greatest magnitude of differential stress is 100–200 MPa, but at the base of the lithosphere is only 15–5 MPa (Mercier, 1980). The strength of lower lithosphere notably decreased, it cannot permanently maintain a greater magnitude of differential stress. The viscosity of the lithosphere (equivalent viscosity, $\eta = 10^{23}$–10^{25} poise) is 2–3 orders of magnitude greater than that of asthenosphere, which is 10^{21}–10^{22} poise. Normally, the viscosity and strength of the lithosphere increase with increasing pressure (or depth), and decrease with increasing temperature and fluid content. Thus, the strength and viscosity of asthenosphere are reduced substantially and cannot support a higher differential stress, due mainly to an increase in the fluid content.

From studies based on inversion of transverse wave tomography, the thickness of the lithosphere in the Chinese continent is found to vary considerably (Cai XL et al., 2002) (Fig. 13.2). In western China the lithosphere is typically continental, with a thickness commonly greater than 150 km. The thickest lithosphere in China occurs in the Tarim area, where the average thickness is about 170 km, but can reach 195–210 km, with an average thickness in the southern Qinghai-northwest Sichuan area of more than 170 km. Thicker lithosphere occurs on the northern margin of the Chinese continent, where the Siberian lithosphere reaches 195–205 km. The lithosphere also reaches 160–230 km in northern India-Afghanistan. The average lithospheric thickness in the northeast and northern parts of eastern China is only 70–73 km, and in southern China is 75–79 km, belonging to the transitional type between continental and oceanic lithosphere. In the marginal sea and trench-arc system of the western Pacific the lithosphere is only 55–65 km thick, in the main part of Philippine Sea Plate the thickness of lithosphere is 50–60 km, being of oceanic type.

If the lithospheric thickness for China and its adjacent areas is compared (Fig. 13.2) with crustal thickness (Fig. 13.1), it is found that they have no fixed relationship. Cai XL (1998) suggested that there were three types of relationship between the crust and the lithosphere: (1) A thick crust with a thin lithosphere, an example of a thick crust with a thin lithosphere occurs in the Qilian Mountains where the crust is 64 km thick, while the lithosphere is only 120–150 km thick; (2) A thin crust with a thin lithosphere, an example of a rather thin crust with a thin lithosphere occurs in northern China where the crust is 32–42 km thick and the lithosphere is only 60–80 km thick (Fig. 13.3); (3) A thin crust with a thick lithosphere, an example of a thin crust with a thick lithosphere occurs in the Sichuan Basin where the crust is only 41.5–44 km thick, but the lithosphere has the greatest thickness exceeding 200 km (Fig. 13.3). In the Tarim Block the crust is only 44–50 km thick, but lithospheric thickness reaches 210 km, with the crust being only 1/4 to 1/5 of lithospheric thickness. A fourth type is proposed here, with both a thick crust and a thick lithosphere; in Qinghai-Xizang area the crust is 64–74 km thick and the lithosphere reaches 160–170 km in thickness.

It appears that there is no connection between the thickness of crust and the thickness of the lithosphere (including the lithospheric mantle). The reason is that the crust was formed over a long time-span by the tectonic evolution of crust, so that the crust differs in both composition and tectonic features from

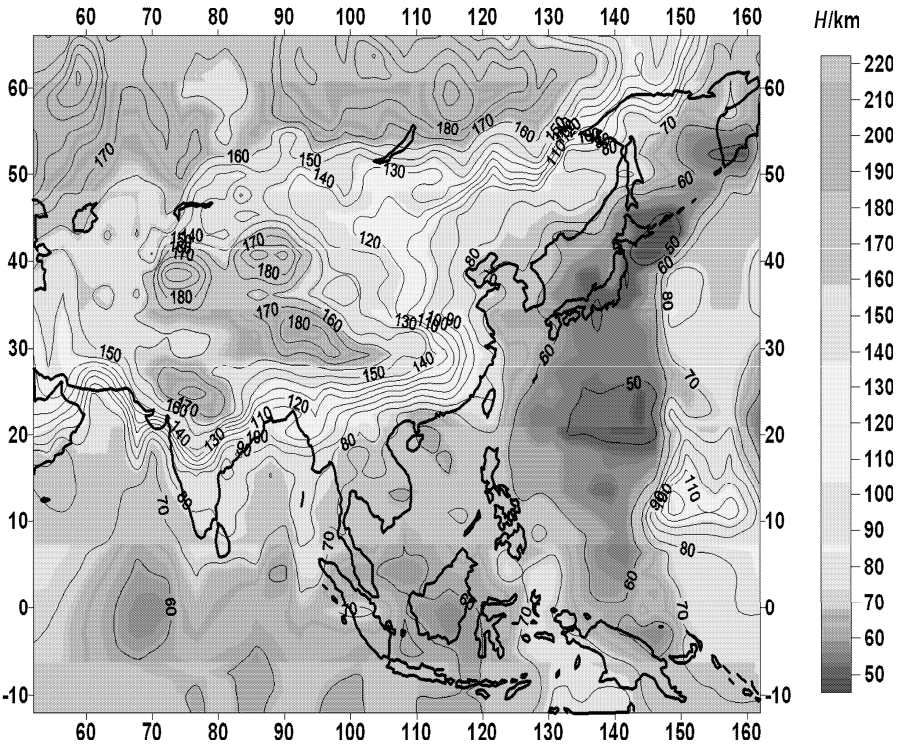

Fig. 13.2 Thickness of the lithosphere in Eastern Asia and the western Pacific Ocean (after Cai XL, 2002, with permission of Cai XL).

the mantle. There is almost no difference in silicate composition between the lithospheric mantle and the asthenosphere; the only difference is that the asthenospheric mantle has probably undergone partial melting and contains more fluid (ultra critical gas and volatiles). However, the most important factor to determine the depth of the interface between the lithosphere and asthenosphere is the mantle thermal regime, as well as the mantle fluid content. In most intraplate areas, the base of the lithosphere is not related to the long-term evolution of the crust; this is only evident near present plate subduction and oceanic ridge zones, and controlled by thermal convection of the mantle.

Because the different methods used to determine the thickness of the lithosphere, such as seismic tomography, artificial source seismology, and telluric electro-magnetic sounding, have different degrees of precision, and are suitable for different conditions determinations of the thickness of the lithosphere obtained by different methods may differ by dozens of kilometers.

As shown in Figs. 13.2, 13.3 and 13.4, there are great differences in determining lithosphere thickness in the Sichuan Basin. At present this problem cannot be solved; in order to determine the lithosphere thickness reliably, improvements in technology and methods are required. However, there is no doubt that there is no relationship between the thickness of the lithosphere and the crust.

A great amount of research has been carried out to determine the composition of the mantle in the eastern Chinese continental lithosphere. Zhang BR et al. (1998) studied mantle source rocks for the Sino-Korean and Yangtze plates on either side of the Qinling Collision Belt during the Archean–Paleoproterozoic. They determined 63 elements using 15 reliable methods of analysis. They found that mantle source rocks on the southern edge of Sino-Korean Plate have relatively high ΣFeO (12.0%–

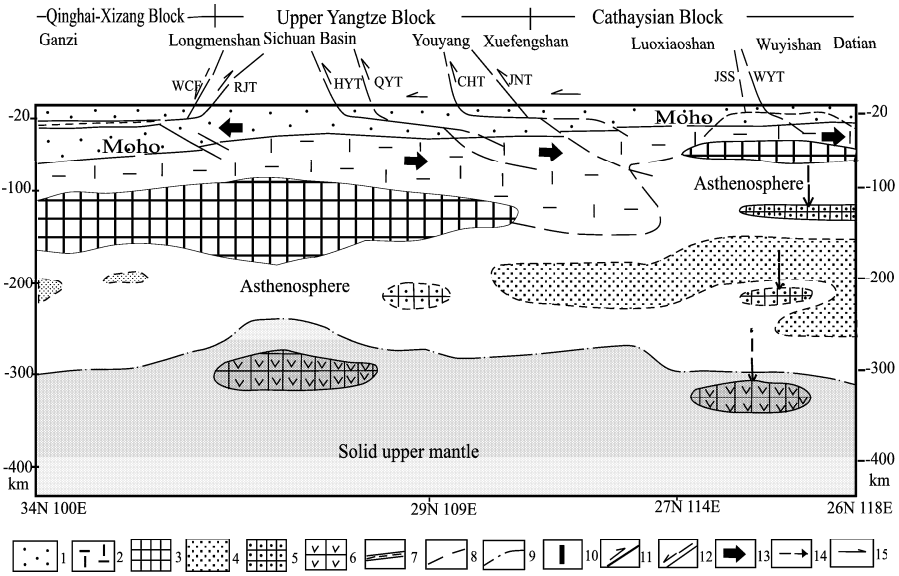

Fig. 13.3 Geological explanation of variations in lithospheric thickness in the Longmenshan of Sichuan–Xuefengshan and the western Hunan–Wuyishan between Jiangxi and Fujian (after Cai XL et al., 2002, with permission of Cai XL).

1. Crust; 2. Lithospheric upper mantle; 3. Lower lithosphere with high velocity; 4. Asthenospheric low velocity zone; 5. Highest velocity within the low velocity asthenospheric zone; 6. High velocity block in the solid mantle; 7. Low velocity layer in the crust; 8. Base of the lithosphere; 9. Base of the asthenosphere; 10. Paleo-plate subduction and collision zone; 11. Large scale thrust; 12. Thrusts in the early period but a normal fault in a later period; 13. Directions of relative movement of lithospheric blocks; 14. Directions of relative sinking of high velocity bodies in the lithosphere and asthenosphere; 15. Directions of relative movement of crust near the surface; M. Mohorovícíc discontinuity.

12.28%), MgO (7.75%–5.84%), Mo [(0.64–0.58)×10^{-6}], a high ratio of *w*(Zr) / *w*(Hf) (54.4–44); on the northern edge of the Yangtze Plate they are relatively rich in Li (26.3×10^{-6}), Rb [(27–30)×10^{-6}], Sc [(34–46.7)×10^{-6}], Cu [(80–126)×10^{-6}], with a high ratio of *w*(Nb)/*w*(Ta) (16–25) and a low ratio of *w*(Zr) / *w*(Hf) (40), poor in ΣFeO (9.14%), MgO (5.19%–6.84%) and Mo [(0.3–0.54)×10^{-6}].

The $\varepsilon_{Nd(t)}$ in metamorphosed basalts from mantle sources in the Sino-Korean Plate during the Archean–Paleoproterozoic was stabilized at about +3, and at the southern end was stabilized at +2.9–+2.2. The $\varepsilon_{Nd(t)}$ values indicate that in which districts the crust-mantle coupling ended comparatively early, and has not changed since the Proterozoic. However, the $\varepsilon_{Nd(t)}$ values increase from +2 to +7 on the $\varepsilon_{Nd(t)}$–t (Ga) diagram in the Yangtze Plate during the Archean-Paleoproterozoic, showing the trend of mantle evolution.

Lead isotopes in the Sino-Korean Plate did not originate from radioactive decay, but in the Yangtze Plate lead isotopes originating from radioactive decay are notably enriched. This feature demonstrates that the Sino-Korean and Yangtze plates have different geochemical characteristics and underwent different processes of geochemical evolution during the Archean–Paleoproterozoic. They are therefore two different plates, and their lithosphere mantle had a completely different origin. Even though the two plates have similar rocks (Zhang SG, 1993), it cannot be concluded that these plates ever formed a single unified plate. It is probable that similar conclusions would be reached concerning other ancient plates, if similar research was carried out. This type of research can also yield positive results as Zhang BR et al. (1998) concluded that mantle geochemical characteristics of the Qinling Collision Belt are related to those of the Yangtze Plate, but quite different from those of the Sino-Korean Plate.

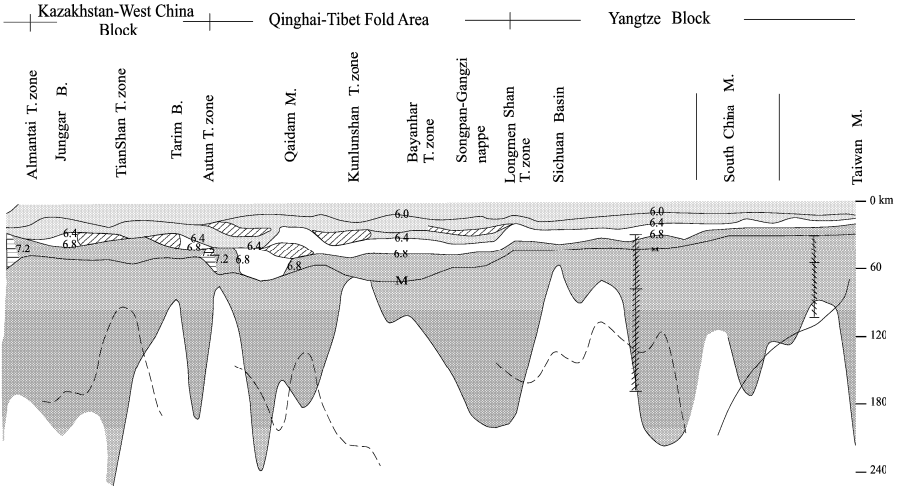

Fig. 13.4 Global Geosciences Transect in Eastern Asia (the eastern section of Europe-Asia profile No.21) (The Development Research Center in Ministry of Land and Resources of China, China Geological Survey and All-Russian Geological Research Institute, 2002, with permission of Yuan XC).

The dark grey shading in the figure is the lithospheric mantle, the base is determined by seismic wave velocity; the light grey layer is the crust, the unshaded zone is the low velocity layer in the middle crust; the dotted line in the lower part of the figure is the base of the lithosphere determined by telluric electro-magnetic sounding. Obviously this does not coincide with the base determined by seismic wave velocity and may differ considerably in some areas.

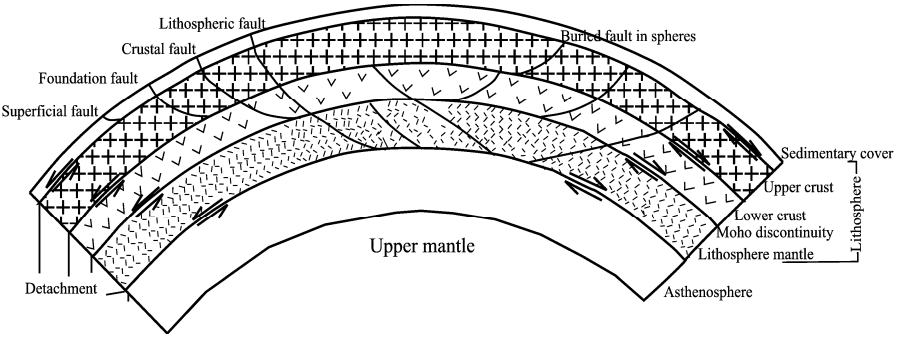

Fig. 13.5 Distribution of faults and detachments in the lithosphere (modified after Zhang WY, 1984).

It is important to recognize the true structure of the lithosphere, especially the continental lithosphere. It does not form a completely homogeneous rigid body, but contains a series of possible levels of detachment. Since the plate tectonic theory was first proposed the main detachment has been considered to occur at the base of the lithosphere. However, detailed studies of the continental lithosphere have recognized many interfaces and detachments in lithosphere at various depths, such as the boundary between sedimentary cover and the basement, the zone of low seismic velocity and high electric conductivity in the middle crust and near the Mohorovĭcíc discontinuity (Fig. 13.5). Evidence from faults and magmatism indicates that the low velocity and high conductivity layer is an important zone of displacement in many areas of Chinese continental lithosphere, while the interface between the sedimentary cover and

the crystalline basement, and the Mohorovĭcíc discontinuity are less frequently zones of displacement. The interfaces of the low velocity and high conductivity layer and Mohorovĭcíc discontinuity are more important for magmatism and endogenic metallization in Chinese continent.

Displasement is most notable in the low velocity and high conductivity layer, where many major shallow earthquakes have been recorded in the Chinese continent by many geoscientists (Ma ZJ, 1987; Xue F, 1989). The low velocity and high conductivity layer in the Chinese continental crust is distributed locally and has a discontinuous interface; it is not the same as the Mohorovĭcíc discontinuity, which is continuous and occurs everywhere. The low velocity and high conductivity layer was previously called the Conrad discontinuity and was considered to be continuous, but now there are abundant data to prove that this is not correct. Xu CF (1996) discovered that the most highly active seismic areas, with the strongest fault and earthquake activity in the crust of northern China, the Tianshan belt, the southeast coastal zone and the Qinghai-Xizang plateau area, are characterized by a layer of low velocity and high conductivity in the middle crust. On the other hand, some areas comparatively lacking in recent tectonic activity and earthquakes, for instance, the Yangtze area, Shandong-northern Jiangsu, the southern Taihangshan, the Yinshan-Yanshan regions, and most of the Tarim and Junggar, do not show a low velocity and high conductivity layer in the middle crust.

In the South China area, as discussed in Chapter 7, during Yanshanian Period the upper crust was moved eastward by almost 200 kilometers along the low velocity and high conductivity layer in the middle crust, and was superimposed on the lower crust and a hot thin oceanic lithosphere mantle (Figs. 7.8 and 7.9). This is the main reason for the large-scale granitic magmatic activity in the eastern part of southern China during the Yanshanian Tectonic Period.

Now in continental tectonic research, geoscientists pay more attention to the possibility of displacements in the low velocity and high conductivity layer of the middle crust. Anderson (1995) pointed out that the isothermal surface of 650±100°C is the interface between upper crust with greater strength, showing brittle deformation and composed of dipole magnetic material, and lower crust with lower strength, showing ductile deformation, composed of non-dipole magnetic material. This surface is close to Curie point interface between the dipole magnetic and non-dipole magnetic materials. From the point of view of deformation of the Earth's surface, this interface is really important, because shallow earthquake foci are concentrated at or above this interface (Xu CF, 1996). Below this surface the crust is composed of distinctly weaker formations, with rare earthquakes deformed by ductile flow. The interface of 650±100°C temperature is equivalent to about half the temperature required to melt mantle rock completely, it is the highest temperature at which serpentinite remains in a brittle state and is also the temperature boundary for a series of important mineral phase changes. In the temperature interval of 500–700°C, α-quartz changes to β-quartz and clinoenstatite changes to enstatite, there are also dehydration reactions, as well as the commencement of partial melting (Table 13.1). In the Chinese continent, the isothermal interface of 650±100°C temperature at a depth of about 20 km coincides with the low velocity and high conductivity layer in the middle crust,.

Table 13.1 The change of features in the low velocity and high conductivity layer in the middle and upper crust (temperature 650±100°C, about 20 km depth) (data after Anderson, 1995)

Crust	Deformation type	Seismic S wave velocity (km/s)	Strength	Dipole magnetism	Quartz mineral phase	Pyroxene mineral
Upper crust	brittle	2.4–3.65	high	yes	α-quartz	clinoenstatite
Lower crust	ductile	3.4–3.6	low	no	β-quartz	enstatite

Melcher et al. (2002) in a study of the tectonics of the Eastern Alps suggested that continental crust might be emplaced over "preoceanic subcontinent mantle" by thrust tectonics. His interpretation is consistent with the suggestion put forward in Chapter 7 of this book, that is, crust and lithosphere mantle are not always coupled together, especially in the transitional region between continental and oceanic lithosphere. Crust and mantle can be detached and moved separately. It has been known for a long time that

oceanic lithosphere may be subducted beneath continental lithosphere, but recently it has been proposed that continental crust might be obducted or overthrust onto oceanic lithospheric mantle.

13.3 Lithosphere Transformation (Thickness Thinning) of East China—Hypothesis of Rotation and Detachment of the Upper Crust

Great advances have been made over the last 30 years in understanding the tectonics of the Chinese continent using the theory of plate tectonics (Li CY et al., 1982, 1984; Zhu X, 1982; Wang HZ, 1981, 1982, 1985, Xiao XC, 1978, 1984, 1988). Mobilism is now accepted by most researchers, and it is not now considered that continental plates are stable rigid blocks, but that they may be affected by strong intraplate deformation with sliding along several layers within the lithosphere, which may even cause violent magmatic activity (Zhang WY, 1984; Ma XY, 1989; Xue F et al., 1989; Burchfiel et al., 1989; Royden et al., 1997).

A vast amount of petrologic and geochemical data has been accumulated in the investigation of the lithosphere tectonics of the eastern Chinese continent. The geological history has been thoroughly researched and original interpretations have been put forward by E ML and Zhao DS (1987), Chi JS et al. (1988; 1996), Deng JF et al. (1992; 1996), Menzies and Xu YG (1998), Lu FX et al. (2000) and Zhou XM et al. (2000). These researchers have determined that in the Archean and Paleoproterozoic the thickness of the lithosphere in the eastern Chinese continent was between 200 and 250 km, in the Meso-Neoproterozoic and Paleozoic about 160–220 km, suddenly thinning in the middle period of the Mesozoic (170–100 Ma) to 60–80 km, and thickening a little in the Cenozoic (Fig. 13.6). Most researchers now recognize that lithospheric thinning and crustal thickening in the eastern Chinese continent occurred during the Middle–Late Jurassic (170–135 Ma), and was related to a violent tectono-magmatic event.

How can thinning of the lithosphere, with thickening of the crust at the same time, be explained? Many hypotheses have been proposed, among them the lithosphere delamination and de-rooting hypothesis (Deng JF et al., 1996) has been accepted by many researchers. It is suggested that areas of lithosphere thinning are regions of continental rifting, underlain by hot mantle plumes; collision zones have deep crustal mountains and lithosphere roots; stable blocks (cratons) have deep continental lithosphere roots. It is inferred that lithosphere thinning of the eastern Chinese continent in the Meso-Cenozoic was due to a deep mantle plume and the effects of isostasy, which caused delamination and de-rooting of the lower lithosphere. This hypothesis was also used by Cai XL et al. (2002) to provide a mechanism for the formation of the giant rift system of western Pacific Ocean underneath the eastern China continent. However, how do we know that there was a hot mantle plume at depth? It is probable that a higher density mantle plume would not be able to cause the delamination and de-rooting of the lower density in lower lithosphere. This problem throws doubt on the delamination hypothesis.

Lu FX et al. (2000) propose that lithospheric thinning was related to regional horizontal extension. They point out that the mantle materials of old lithosphere are mainly peridotite, with a depleted basaltic component, with buoyancy due to a low density. This is the main reason why the stability of a craton is preserved, and that gravity-induced delamination and de-rooting cannot occur. They suggest that the hot mantle materials beneath the lithosphere or crust form upward surges, like “mushroom clouds”, including remnants of paleo-mantle. The surge of mushroom clouds and hot mantle materials would cause strong magmatic activity at the base of the crust. However, the key period for lithosphere thinning in the eastern Chinese continent was during the Jurassic (Menzies and Xu YG, 1998), which was not an epoch of continental extension, but an important period of crustal shortening and thickening, with a crustal thickness of about 40 km, with violent rock deformation and magmatism (Wan TF, 1994, 2004). If the thinning of crust and lithosphere occurred during the Cretaceous it might be reasonably explained by E-W extension, as the Cretaceous Period was an important period of E-W trending extension in the

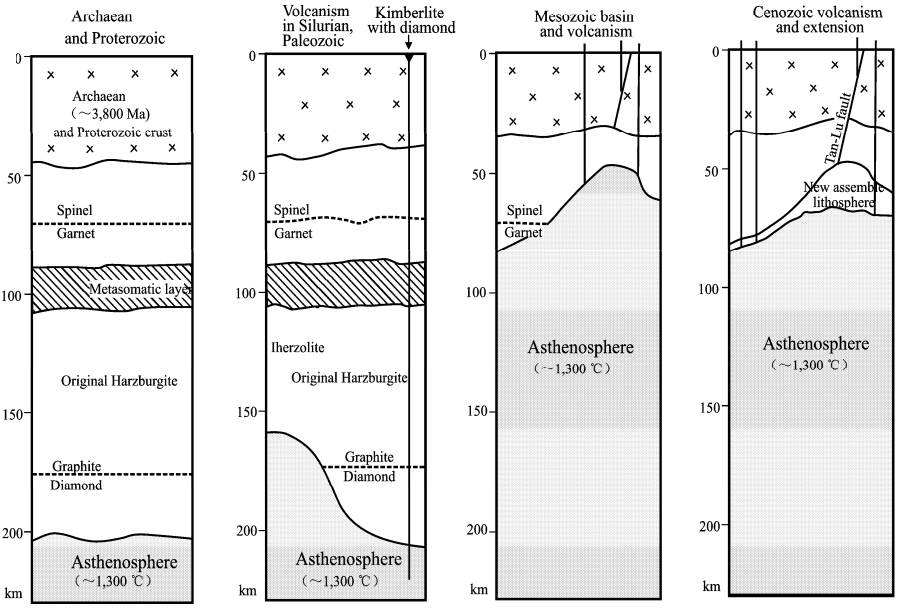

Fig. 13.6 The structure and thickness of lithosphere in different periods of North China (modified from Menzies and Xu YG et al., 1998, with permission of Menzies M).

eastern Chinese continent. Crustal shortening and thickening, and lithospheric thinning occurred in the Jurassic almost at the same time, and this is difficult to explain by continental extension.

In view of the difficulties with the above hypothesis, the author advances a new hypothesis for discussion. It is proposed that upper crustal rotation and the transformation of lithosphere were the main reasons for crustal thickening and lithospheric thinning during the Jurassic (Wan TF, 2004).

(1) Paleomagnetic Evidence of Jurassic Crustal Rotation

By systematically compiling paleomagnetic data from the Chinese continent (Wan TF, 1994) (Appendix 6 and Chapters 4 to 7 in this book), it is possible to reconstruct the paleo continental kinematics of China. As the data are secured by many different authors it is possible that some of these results may be in error. However, it can be still recognized that paleomagnetic orientations of Chinese continental blocks in the Triassic and former geological periods were very different from their present magnetic orientations.

In the Paleozoic the paleomagnetic north in the Sino-Korean Plate was oriented between 319° and 338° NW, relative to its present magnetic orientation (Fang DJ et al., 1988; Ma XH and Yang ZY, 1993; Huang BC et al., 1999). In the Late Triassic the palaeomagnetic north orientation of the Sino-Korean Plate corresponds to 30° NE in the present magnetic orientation. Since the Early Jurassic the paleomagnetic orientation has been very close to the present magnetic orientation; in Middle Jurassic it is equal to the present 0.9° NE and 3.6° NE (Ma XH and Yang ZY, 1993). However, data for the Late Jurassic paleomagnetic north (22.2° NE) is obviously in error (Fang DJ et al., 1988). From Cretaceous to Recent, paleomagnetic north in the Sino-Korean Plate has changed only a little, fluctuating around the present orientation of magnetic north. It is evident that during the Jurassic the continental crust of the Sino-Korean Plate rotated through 30° counterclockwise to reach its present magnetic orientation.

This change is shown clearly in Figs. 6.8 and 7.1. Paleomagnetic data since the Paleozoic are consistent, with high degree of reliability.

Kim and Van der Voo (1990) found a 20° counterclockwise rotation of the south Korean continental crust from Triassic to Early Jurassic. About 20°of counterclockwise rotation is also recorded for the Yangtze continental crust between the Late Triassic and the Middle Jurassic (Zhu ZW et al., 1988; Liang QZ, 1990; Enkin et al., 1992; Huang KN et al., 1993). Khramov et al. (1981) recorded a counterclockwise rotation of 36.2° in the Siberian continental crust between the Late Triassic and Late Jurassic, the paleomagnetic north rotating from 77.3° NE to 41.1° NE.

Counterclockwise rotation of the East Asian crust through 20°–30° had clearly an important influence on Jurassic intraplate deformation and was responsible for changes in the thickness of the lithosphere.

(2) Geological Evidence for Jurassic Crustal Rotation

The Jurassic Period, called the Yanshanian Tectonic Period in China, is a period of strong tectono-magmatism in the eastern Chinese continent (see Chapter 7 of this book). Zhan MG (1994) was the first to recognize that from the Triassic to the Cretaceous, an area of granitic intrusion gradually migrated eastwards over a distance of 420 km (Figs. 7.12 and 7.13), with an average rate of displacement of 0.24 cm/yr. During the Jurassic, the axis of the granitic zone migrated eastwards for a further 180 km, with an average rate of displacement of 0.26 cm/yr (Figs. 7.12 and 7.13). Zhan MG (1994) suggested that the source area of S-type granite magmatism was controlled by the occurrence of thrusts and detachments in the crust. S-type granitic magmas in southern China originated in the middle crust at a depth of 15–22 km, in the low seismic velocity and high electric conductivity layer (Zeng RS et al., 1995), while A-or I-type granitic magmas were formed at a depth of 32–40 km, near the Mohorovĭcíc discontinuity (Zeng RS et al., 1995).

Comparing the distributions of magmatic zones between Northeastern China and South China (Fig. 7.11), it is clearly shown that magmatic zone is counterclockwise rotation from Early Jurassic to Late Jurassic.

In the Jurassic, magmatism was rather strong in the Yanshan-western Liaoning area of North China. In the Early Jurassic (185–170 Ma) volcanic rocks were erupted along an ENE trend; in the Middle Jurassic (170–155 Ma) along an NE trend; in the Late Jurassic (155–135 Ma) along an NNE trend. Volcanic rocks of different ages were erupted along faults with different trends, which changed in the same way as the axes of the regional folds (Bao YG et al., 1995). From Early to Late Jurassic, tectono-volcanic zones all formed during shortening, both the changes in the trend of tectono-volcanic zones and the shortening were caused by the counterclockwise rotation of the continental crust (Wan TF, 2004), but the migrations of magmatic zones are not clear.

If the distributions of magmatic zones in South, North and Northeast China are compared, in Northeast China the amount of volcanic zone westward migration and crustal rotation were clear; in North China the counterclockwise rotation of tectono-magmatic zones is obvious, but the migration of the magmatic zones is not clear; in South China there was not only counterclockwise crustal rotation, but also an eastward displacement of the tectono-magmatic zone. The author recognizes that while westward subduction of North American Plate was mainly influenced by the counterclockwise rotation of the Eastern Asian continental crust in the Jurassic, the thrusts and magmatism mainly occurred in the upper and middle crust of Eastern China. Both thickening of the crust and the rotation of the magmatic zones have occurred to varying degrees.

(3) Mechanism of Crustal Rotation

Counterclockwise rotation of the eastern Chinese continental crust in the Jurassic was influenced by the westward movement of the North American Plate (mainly the western part–the Okhotsk Plate), the northwestward movement of the Izanagi Plate, and the northward movement of the Farallon Plate (Maruyama et al., 1986, 1997; Moore 1989; Scotese, 1994) (upper left in Fig. 7.3). During the westward migration and subduction of the North American Plate, a collision zone with strong deformation

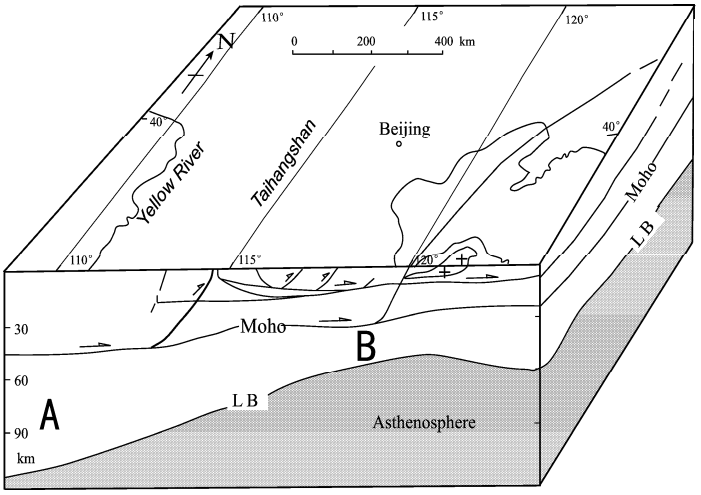

Fig. 13.7 Crustal detachments and lithospheric thinning in North China during the Jurassic.

A. Continental type of lithospheric mantle; B. Oceanic type of lithospheric mantle; Moho. Mohorovĭcíc discontinuity; LB. Base of the lithosphere; the asthenosphere is shown in gray shading.

Arrows show the direction of movement of crustal segments.

was formed on the eastern margin of the Siberian Plate, extending to the Wandashan (someone called Nadanhada) Collision Zone and the Tanakura Tectonic Line (TTL, the boundary between northeast and southwest Japan). These movements caused a 20°–30°counterclockwise rotation of the continental crust of Eastern Asia (Fig. 7.1), leading to the relative westward movement of the northern, and the relative eastward movement of the southern parts of the East Asian continent.

One important result of the third magnetic survey of the oceanic floor was to reassess the directions of plate motion in the paleo-Pacific region (Moore, 1989) (upper left in Fig.7.3). At the end of Jurassic there was a radial movement of the plates in the Pacific region, the Izanagi Plate moved NW, the Pacific Plate moved SW, the Farallon Plate moved NE, and the Phoenix Plate moved SE. The radial movement of the plates is accounted for by the rise of a superplume at the junction of the four plates causing radial horizontal extension (Pavoni, 1997; Condie, 2001) (Fig. 15.5). Since Middle Jurassic the rise of mantle material and magma in this super mantle plume has induced radial extension and the horizontal movement of the plates. This mechanism for long-term plate tectonic dynamics has recently gained much support and would provide a mechanism for the large-scale rotation of the eastern Chinese continental crust.

(4) Lithospheric Transformation of Eastern Chinese Continent

Worldwide seismic data show that the thickness of the oceanic lithosphere is usually about 40 km, and that of the continental lithosphere is 110–200 km. However, according to seismic tomography, the thickness of continental lithosphere is only 70–80 km in eastern China, but in western China reaches 110–200 km (Cai XL et al., 2002) (Fig.13.2). On the other hand, in eastern China the thickness of the crust is only 30–40 km, while in western China is 40–70 km (Teng JW et al., 2002) (Fig. 13.1).

The lithosphere beneath the crust is called the lithospheric mantle. In western China, to the west of the Taihangshan (between Hebei and Shanxi)–Wulingshan (between Hunan and Guizhou), the continental type of lithospheric mantle commonly reaches a thickness of 70–100 km or more. However, in eastern China, east of the Taihangshan-Wulingshan, the thickness of the lithospheric mantle is commonly only

about 40 km, which is very nearly the same as the thickness of oceanic lithosphere mantle (Cai XL et al., 2002; Anderson, 1995) (Figs. 7.10 and 13.7). Usually it is recognized that oceanic mantle could be subducted beneath the continental plate, almost never concerning that the continental crust could be moved and covered onto oceanic mantle. Maybe it is a good example for continental crust covered on oceanic mantle in eastern China.

To account for this anomaly it is suggested that in the Triassic and earlier periods, the crust of eastern China was located on continental lithosphere mantle with a normal thickness of 70–100 km, but in the Jurassic, due to rotation and eastward movement, the crust of eastern China (North and South China) was emplaced onto oceanic lithospheric mantle, less than 40 km thick. Since the Jurassic, the thickness of the crust has remained the same (Figs. 7.10 and 13.7). By this mechanism the lithosphere of eastern China was transformed from a thick continental type of lithosphere to a thin transitional type between continental and oceanic lithosphere. Before the Jurassic the crust of eastern China was underlain by a thick continental lithospheric mantle, but during the Jurassic was transferred to a thinner oceanic lithosphere mantle. As the result of this process the depth to the top of the asthenosphere was reduced from ~100 km to 70–80 km. At this depth the temperature was about 1280°C, causing these higher temperatures to be conducted into the lithosphere, giving rise to melting and the rise of granitic magmas.

Granitic magmas are most easily formed along weak zones in the crust during over thrusting. This model explains why Jurassic granitic magmatism was concentrated in eastern China, to the east of the Taihangshan-Wulingshan, while in most of western China Jurassic magmatism was very rare, although crustal shortening and overthrusting were strongly developed, for example, at Xuefengshan, western Hunan and the western margin of the Ordos area. In north China middle crustal detachments were not commonly developed; crustal movements were localized only near the intersections of crustal faults, such as fault intersections along the Mohorovĭcíc discontinuity, the Tancheng-Lujiang and the frontal faults of the Taihangshan, causing granitic intrusion near these fault intersections.

The major reasons for the widespread tectono-magmatism in eastern China during the Jurassic were the counterclockwise rotation of the upper and middle crust and its emplacement on high temperature oceanic lithosphere mantle.

The westward movement of the Okhotsk Plate and its collision with the Siberian Plate and the NW movement and subduction of the Izanagi Plate caused deformation along the eastern margin of the Siberian Plate. These movements caused the counterclockwise rotation of the whole of the Eastern Asian continental crust through 20°–30°, resulting in the westward movement of the continental crust of northern Asia and the relative eastward movement of southern Asia, including eastern China. Rotation and movement of the crust were responsible for this major tectono-magmatic event, for crustal thickening and for the transfer of the lithosphere of eastern China from a lithospheric mantle of continental type to a mantle of oceanic type. The apparent thinning of the lithosphere of eastern China was due to its transfer from a continental to a continental /oceanic transition type, not to continental extension, or to the rise of a deep mantle plume.

13.4 The Thermal Regime in the Crust and Discussion on the Mantle Plumes

The thermal regime in the crust is an important indicator of the type of tectonic activity. What was the thermal regime in Chinese continent during different geological periods compared with the present day? In understanding tectonic evolution it is important to know the thermal regime. First, the present thermal regime in the crust of the Chinese continent will be discussed, then the thermal regime in earlier geological periods during its evolution, and finally whether mantle plumes ever existed beneath the Chinese continent.

(1) Recent Crustal Thermal Regime

Wang J et al. (1990) of the Geothermal Group, Institute of Geology, Chinese Academy of Sciences systematically studied the present day thermal regime in the continental crust of China. Temperatures and geothermal gradients were measured in 5,954 wells, 76% of these wells provided static thermal measurements with a high degree of reliability. Using these data Wang J et al. (1990) compiled a geothermal map (Fig. 13.8) and a map to show geothermal gradients at a depth of 3,000 meters (Fig. 13.9). The average geothermal gradient in a continental area is 33°C/km, with a global average heat flow value of 63 mW/m^2. Areas with higher values have positive heat flow anomalies, and areas with lower values have negative heat flow anomalies.

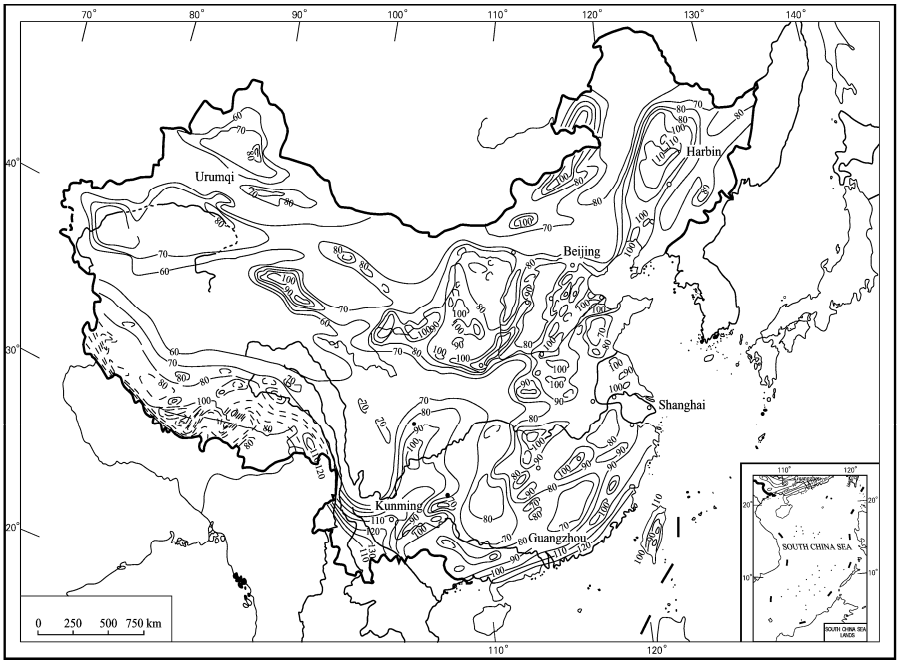

Fig. 13.8 Present temperatures (°C) below 3,000 meters depth in the Chinese continent (after Wang J et al., 1990).

Recent geothermal gradients in the Chinese continent are shown in Table 13.2. Really notable geothermal anomalies occur only in western Yunnan and southern Xizang (Tibet), where the gradient is as high as 40°C/km. In some areas of eastern China, such as the Songhuajiang–Liaohe Basin, the central Hebei Basin, the Jiyang depression, the Nanyang Basin, Leizhou, Guangdong, Beibu Bay (Gulf of Tongking) and Taiwan, the geothermal gradient is only a little higher than the global average, but in most areas of China the gradient is below the global average, showing negative anomalies.

Average heat flow can be obtained by relating the average geothermal gradient to the thermal conductivity of the local rocks. In North China the average heat flow is 61.5 mW/m^2, in the Songhuajiang-Liaohe Basin, 63.92 mW/m^2, in the Fenhe-Weihe Rift Zone, 63.9 mW/m^2, and in the middle and lower reaches of Yangtze River, 51.5 mW/m^2. These are all negative anomalies, or only slightly higher than average global heat flow values; there are no large positive geothermal anomalies. In most areas of western China the average heat flow is low, for instance, in the Sichuan Basin heat flow is 47.6 mW/m^2, in Gansu, 51.6 mW/m^2, in the Qaidam Basin 52.1 mW/m^2, in the Junggar Basin, 43.1 mW/m^2 and in the Tarim Basin, 40.7 mW/m^2 (Wang J et al., 1990).

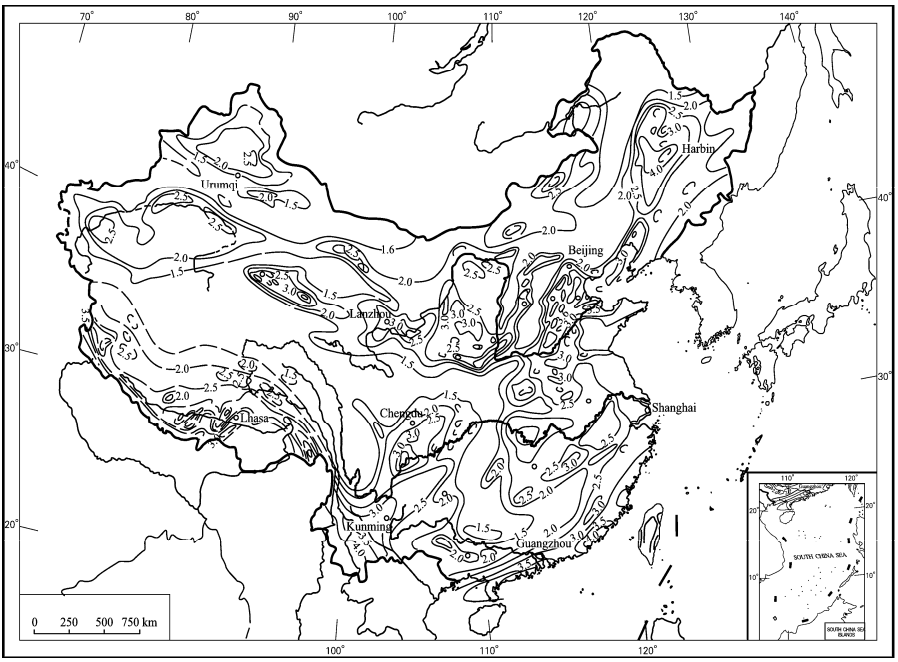

Fig. 13.9 Geothermal gradients in China in mW/m^2 (after Wang J et al., 1990).

An uplift of the mantle occurs beneath each of the larger basins in western China, but there are no positive heat flow anomalies. The most notable positive heat flow anomalies occur in western Yunnan (81 mW/m^2), southern Xizang (80–120 mW/m^2) and Taiwan (78.1 mW/m^2). Eastern China is often regarded as an extension system on the basis of heat flow data. If this were the case, it should show a positive regional geothermal anomaly. Chinese geoscientists often consider the basins of eastern China to be depression basins, and take individual local high geothermal anomalies as representative of the whole basin. But high positive geothermal values are local features, existing for only short periods. There is no obvious mantle uplift, and at different times extension occurred in different directions. Local high positive geothermal anomalies are related to structural features in the basins, i.e. anticlines (such as the Daqing anticline, 40–50°C/km); uplifted faulted blocks (such as the Tianjin geothermal anomaly in the Cangzhou uplifted block, 35–40°C/km, and the southwest Sichuan uplifted block, 30–35°C/km), or to ancient buried hills, such as Central Hebei oil field.

Theoretically, the change in the geothermal gradient and heat flow values in the lithosphere are caused by thermal conduction. Usually, about 60% of conduction heat comes from the mantle and the other 40% is produced by the decay of radioactive elements in the crust.

The lithosphere, defined in terms of heat "has a continuous thermal conduction gradient in the outer sphere of the solid Earth". As previously mentioned, this definition does not include contributions from thermal convection or radiation. Normally the contribution of thermal radiation is too small to be considered, however thermal convection is relatively important. The presence of fluids is essential for thermal convection. Wherever fluids (gas and liquid) are present in the rock, thermal convection will occur. Underground water seeps into the ground in mountainous areas surrounding basins, and accumulates in fissures; confined underground waters converge in basins, absorb heat and form geothermal fluids at depth, which may emerge as geothermal springs. Where a basin includes an anticline, uplifted faulted

Table 13.2 Present geothermal gradients in the Chinese continent (unit: ℃/km)

Area	Geothermal gradient	Area	Geothermal gradient	Area	Geothermal gradient
Songhuajiang -Liaohe Basin	33.75	Ordos Basin	28.8	Southern Sichuan Basin	32.7
Lower Liaohe Basin	31.3	Northern Jiangsu Basin	26.4	Northern Sichuan Basin	18
Central Hebei Depression	34.0	Nanyang Basin, Henan	38.2	Baise Basin, Guangxi	27.3
Huanghua Depression	33.22	Jianghan Basin, Hubei	28.4	Eastern Guizhou	11.33
Jiyang Depression	35.89	Leizhou, Guangdong	35.2	West Guizhou, Eastern Yunnan	22.5
Linqin Depression	29.5	Hainan Island	25.6	Gansu	28.4
Baofeng-Shengqiu	25.27	Beibu Bay (Gulf of Tongking)	34.7	Qaidam Basin	27.29
SE Inner Mongolia	28.7	Taiwan	35.4	Junggar Basin	20.2
Sonit, Inner Mongolia	21.7	Western Yunnan	42.3	Tarim Basin	21.3
NW Inner Mongolia	29.4	Maqiu, southern Xizang (Tibet)	40		

Data simplified after Wang J et al. (1990); the value for southern Xizang is from Zhang ZG (personal communication).

block or ancient buried hill, confined, deep, hot, underground water rises, inducing thermal convection and producing high positive geothermal anomalies along fault zones.

When values of regional heat flow and regional geothermal gradient are discussed, the measured values include heat due to thermal convection, but these data should not be taken into account. This is the major reason why many slightly positive geothermal anomalies are recorded for the basins of eastern China; these are not true regional geothermal anomalies. However, a zone of positive geothermal anomalies provides suitable temperature conditions for the accumulation of oil and gas and for the utilization of geothermal waters. This relationship warrants further attention. This is commonly used as evidence of the geodynamic mechanism for the origin of oil-and gas-bearing sedimentary basins in China (Compiling Group of Petroleum Geology, Daqing Oil Field, 1993; Compiling Group of Petroleum Geology, Liaohe Oil Field, 1993). However, it is not correct to use these geothermal convection anomalies as evidence of basin extension and mantle uplift.

(2) Thermal Regimes in Geological History

Thermal regimes for past geological times cannot be determined by direct *in situ* temperature measurements, but must be obtained from estimated ancient temperatures and pressures from the rocks, combined with accurate isotopic ages. In metamorphic rocks the peak temperatures and pressures can be determined from the stable mineral assemblages, or from mineral or fluid inclusions, and the isotopic age may also be measured in the same rocks (Han YQ, 1993). From the peak temperatures and pressures of metamorphism the geothermal gradient can be calculated at that time. In order to determine geothermal gradients from magmatic rocks, the temperatures and pressures from the magmatic source area should be used, other than the temperatures and pressures at the time of eruption, intrusion or emplacement of the magma, as these are not suitable for the determination of past regional geothermal gradients. In sedimentary rocks, temperatures may be determined by the inversion of vitrinite reflection data, by fission track measurements, and by evidence from fluid inclusions, accompanied by data concerning the depth and the age of deposition of the rocks. From these data it may be possible to determine the geothermal gradients in ancient sedimentary systems.

In order to calculate the average geothermal gradient in 35 km thick continental crust during its geological history, the temperature at a certain point in the crust is divided by its depth. The assumption is that the geothermal gradient in the crust has not changed during geological time, neglecting the lower crustal geothermal gradient change beneath the shallow constant temperature layer.

Data for 309 determinations of pressure, temperature and the depth of formation of the rocks, and ancient geothermal gradients during geological time have been collected from about 300 papers (Appendices 7.1 and 7.2), including 205 estimates of geothermal gradients within the crust. Average geothermal gradients for Chinese continental crust in the geological periods are listed in Table 13.3. Additionally, by contrast, the average values of 86 calculations for Archaean and Paleoproterozoic crust (Appendices 1.1 and 1.3) are also listed in Table 13.3. It should be said that the above data are not yet sufficient, and are presented only in order to put forward some preliminary concepts.

During the Sichuanian and North Sinian Tectonic Periods, the geothermal gradient in the Chinese continent exceeded slightly the global average, and in other tectonic periods the geothermal gradient was less than the recent global average (Table 13.3). The Chinese continent has existed since the Neoarchean. It is reasonable to presume that the geothermal gradient was never very high. From the geothermal gradient data given above it is difficult to judge where and when an ancient mantle plume was developed beneath the continental lithosphere. However, the data for each geological historical period are not sufficiently reliable to draw firm conclusions from the existing data.

Table 13.3 Average geothermal gradient for the Chinese continental crust (°C/km) during geological time

Tectonic period	Isotopic age of tectonic period	Number of determinations	Average geothermal gradient (°C/km)
Archaean	Before 2,500 Ma	58	23.8
Paleoproterozoic	2,500–1,800 Ma	28	24.6
Early Mesoproterozoic	1,800–1,400 Ma	4	23.2
Late Mesoproterozoic	1,400–1,000 Ma	11	28
Early Neoproterozoic	1,000–800 Ma	16	27.8
Late Neoproterozoic	800–513 Ma	3	21
Early Paleozoic	513–397 Ma	28	27.9
Late Paleozoic	397–260 Ma	20	32.9
Indosinian	260–200 Ma	22	29.7
Yanshanian	200–135 Ma	24	30.1
Sichuanian	135–52 Ma	27	34
North Sinian	52–23 Ma	19	33.4
Himalayan	23–0.78 Ma	31	29.3

The detailed data presented in the above table and the references are shown in Appendices 1.1, 1.3 and 7.

The temperatures (T), pressures (P) and geothermal gradients, calculated by many geoscientists (Appendices 1 and 7), give fairly similar results, and perhaps a high degree of confidence can be placed on the original data. Although data are not abundant, these results were obtained from all over China by many geoscientists, using similar methods. The data are objective, but problems still exist in judging the accuracy of the results.

Nearly 100 determinations of ancient crustal* geothermal gradients are based on temperature and pressure data obtained from mantle rocks (Appendices 1 and 7). These values are commonly far lower

* Nearly 100 determinations of ancient crust geothermal gradients listed in Appendix 7 are based on temperature and pressure data from upper mantle inclusions occurring as xenoliths in igneous rocks. When rocks were formed in the mantle, at depths greater than 35 km, the geothermal gradient in crust is calculated by following formula:

$$T_q = [T_x - t_m \times (d_x - d_q)]/d_q$$

where T_q is the average geothermal gradient in the crust (°C/km); T_x is the formation temperature of the rock (°C); t_m is the average geothermal gradient in the mantle (°C/km); d_x is the formation depth of the rock (km); d_q is the average crustal thickness (35 km).

than geothermal gradients based on crustal rocks, the cause of this difference is unknown. These data cannot be included in the calculation of average geothermal gradients (Table 13.3). Additionally, in Appendices 1 and 7, about ten values are still too high or too low, possibly due to the method of calculation, or to mistakes in the estimation of some parameters. These data do not correspond to the average calculation listed in Table 13.3.

According to heat flow values and geothermal gradients in South China (Wan TF, 1988; Wan TF et al., 1989), the average geothermal gradient in the mantle (t_m) has been calculated; the geothermal gradient for the upper mantle is approximately 6–13°C/km. For simplicity, this is taken as an average value of 10°C/km in this book. This is a preliminary estimation as information is scarce. In order to obtain better estimates of the geothermal gradient in the crust or the mantle, using data from mantle rocks, more information will be required.

From existing data, southwest Yangtze or Emeishan area, eastern Xizang and the neighboring trap province show very high positive anomalies in their ancient geothermal gradient during the Late Permian period. It is possible that during this period a hot mantle plume existed at depth beneath the Jinshajiang and Lancangjiang Paleo-Oceans, as discussed in Chapter 5. In other periods or in other areas high positive geothermal gradient anomalies are only local, and do not occur over large areas. These conclusions are based only on the data available at present. It is probable that the acquisition of further data will require modification of these conclusions.

(3) Discussion on Mantle Plumes

In the absence of high positive regional anomalies in the geothermal gradient, it is difficult to believe in mantle plumes at depth. However, some geoscientists have proposed that there were many mantle plumes in the Chinese continent over the period from the Archaean to the Recent, unfortunately these proposals are not supported by sufficient evidence, so these are just hypothetical. For example, it is proposed that whenever komatiites are recognized, from their high magnesium content, it can be deduced that a mantle plume occurred at depth, completely neglecting the strict definition of komatiite and its relationship to mantle plumes (see Chapter 2) (Condie, 2001). Some scholars have also suggested that when a basic dike swarm occurs at the surface, it is indicated that a mantle plume occurs at depth (Storey, 1989; Li ZX, 1996, 1998); this suggestion is not supported by most geoscientists. Similarly some geoscientists have suggested that radial basic dike swarms indicate mantle plumes at depth, but some of these radial swarms are composite, correlating dikes which were not intruded at exactly the same time, but over a period of time, for example, the swarm described from northern Guangdong (Li and McCulloch, 1998). As stated in Chapters 7 and 8, according to the isotopic age and orientation of dikes in the field studied by Li XH and McCulloch, (1998), it was found that WNW trending dikes have isotopic ages >135 Ma (Jurassic), while N-S or NNE trending dikes have isotopic ages <135 Ma (Cretaceous). These dike swarms are parallel to the orientation of the maximum compressive principal stresses during the Yanshanian and Sichuanian Periods respectively. These two sets of dikes result from the extension under the influence of tectonic stress in different orientations. The interval between the two groups of dike swarm is about 30–40 millions years. It is probable that all the dykes in a radial dike swarm, caused by a mantle plume, would be formed virtually simultaneously. The length of time, over which all the dikes in different orientations in a radial dike swarm were formed, is likely to be less than a million years (Condie, 2001). Similar problems are encountered in interpreting the Mesozoic basic dike swarms studied by Shao JA et al. (1998, 2001) in the Dahingganling and Beijing areas, due to mantle plumes, but this hypothesis is also not correct.

Based on the evidence of radial basaltic dike swarms Deng JF et al. (1988, 1992 and 1996) claimed that seven sub-mantle plumes occurred beneath North China during the Paleogene and Neogene-Early Pleistocene. However, in this type of study, pre-existing faults which controlled the intrusion of basalts at various times should be taken into account. There has been no sufficient evidence that all the basalts are of Cenozoic age. There are very few areas with basaltic dikes showing a radial distribution, indicating the occurrence of sub-mantle plumes, as they suggested. However, Deng JF et al. (1988, 1992,

1996) proposed that there are seven basaltic eruptions in North China (Bohai, Shuangliao, Mudanjiang, Changbaishan, Zhangjiakou, Dahingganling and Wudalianchi), during the Paleogene and Neogene–Early Pleistocene. Four of them are located on the western side of the Dahingganling-Taihangshan, and three of them are located along the eastern side of the Tancheng–Lujiang Fault Zone. However, in the western area along the Dahingganling-Taihangshan, the basalts are mainly of Paleogene age, and along the Tancheng–Lujiang Fault Zone they are mainly of Neogene-Early Pleistoceneage. Chi JS et al. (1988) have pointed out that the compositions of the Paleogene and Neogene-Early Pleistocene basalts are notably different. The Neogene-Early Pleistocene intrusions are alkali-basalts containing inclusions indicating a mantle source, while the Paleogene basalts are mainly tholeiitic, indicating oceanic mantle. As discussed in Chapters 9 and 10, the NW or near E-W trending faults controlled Paleogene basalt eruptions and dike swarms, while NNE or N-S trending lithospheric faults controlled Neogene-Early Pleistocene basaltic eruptions and dike swarms. The tectonic background and the tectonic stress field were completely different in the Cenozoic. Certainly, trends of magmatic activity occur in all directions, if the Cenozoic is regarded as a single unit. However, the interval of time between the intrusion of Paleogene and Neogene-Early Pleistocene basalts is more than 20 million years. Radial basic dike swarms have never been found in the locations where all the dikes were intruded at the same time. Needless to say, the seven areas of concentrations of basalt were marked by positive regional geothermal gradients during the Paleogene and Neogene-Early Pleistocene. It is just a coincidence that positive geothermal gradient anomalies are also found in these seven areas at present. It seems that there are still a lot of problems in using these data to deduce the earlier occurrence of mantle plume and this problem will require further research.

The main characteristics of Chinese lithospheric tectonics are: western China has typical continental type crust and lithosphere; eastern China has a crust of continental type and transitional type lithosphere between ocean and continent, the lithospheric mantle in eastern China is of oceanic type; the boundary between eastern and western China is located along the Taihangshan–Wulingshan; in eastern China the lithosphere was thinned since the Jurassic. The thinning of the lithosphere was caused possibly by the counterclockwise rotation of the crust of Eastern Asia, which became detached and thrust eastwards, over oceanic type lithospheric mantle, rather than by large scale extension, rifting, the rise of a mantle plume or lithospheric delamination and removal of its root.

In this book this immature proposal has been put forward in the hope of stimulating readers to pay attention to, and to promote the research into the lithosphere tectonics of the Chinese continent. So far research on the Chinese continental lithosphere is still in a preliminary period. Many improvements in research methods, techniques, theory and philosophy will be required before a consensus can be reached.

References

Anderson DL (1995) Lithosphere, asthenosphere and perisphere. Reviews of Geophysics 33(1): 125–149.

Arndt N, Christensen N (1992) The role of lithospheric mantle in continental flood volcanism: thermal and geochemical constraints. J.Geophys. Res. 97: 10967–10981.

Bao YG, Bai ZM, Ge SW et al (1995) Volcano-geology and Rocks of Beijing in Yanshanian Period. Geological Publishing House, Beijing (in Chinese).

Barrell J (1914) The strength of the Earth's crust. Geology 22: 28–48.

Burchfiel BC, Deng QD, Molnar P et al (1989) Intracrustal detachment within zones of continental deformation. Geology (Boulder) 17(8): 748–752.

Cai XL, Wei XG, Li YC et al (1998) Geodynamic analysis on the orogenic process of intracon-tinental orogenic belts of China. Journal of Mineralogy and Petrology 18(suppl.): 1–7 (in Chinese with English abstract).

Cai XL, Zhu JS, Cao JM et al (2002) Structure and dynamics of lithosphere and asthenosphere in the gigantic East Asian-West Pacific rift system. Geology in China 29(3): 234–245 (in Chinese with English abstract).

Chi JS (1988) The Study of Cenozoic Basalts and Upper Mantle Beneath Eastern China (Attachment Kimberlites). China University of Geosciences Press, Wuhan (in Chinese with English abstract).

Chi JS, Lu FX, Zhao L et al (1996) The Kimberlites and Paleozoic Features of Lithospheric Mantle of North China Platform. Science Press, Beijing (in Chinese).

Christensen NL, Mooney WD (1995) Seismic velocity structure and composition of the continental crust: a global view. J. Geophys. Res. 100: 9761–9788.

Compiling Group of Petroleum Geology (1993) Daqing Oil Field. In: Zhai et al (1993) Petroleum Geology, vol. 4 (A), 34–40. Petroleum Industry Publishing House, Beijing (in Chinese).

Compiling Group of Petroleum Geology (1993) Liaohe Oil Field. In: Zhai et al (1993) Petroleum Geology, vol. 3, 80–83. Petroleum Industry Publishing House, Beijing (in Chinese).

Condie KC (1993) Chemical composition and evolution of the upper continental crust: contrasting results from surface samples and shales. Chem. Geol. 104: 1–37.

Condie KC (2001) Mantle Plumes and Their Record in Earth History. Cambridge University Press, Cambridge.

Daly RA (1940) Strength and Structure of the Earth. Prentice-Hall, Englewood Cliffs, NJ.

Deng Jinfu (1988) The magmatism and deep processes of continental rifts. In: Chi JS (ed) The Study of Cenozoic Basalts and Upper Mantle Beneath Eastern China (Attachment Kimberlites), pp.201–218. China University of Geosciences Press, Wuhan (in Chinese).

Deng JF, Zhao HL, Wu ZX et al (1992) A mantle plume beneath the north part of China continent and lithosphere motion. Geoscience 6(3): 267–274 (in Chinese with English abstract).

Deng JF, Zhao HL, Mo XX et al (1996) Continental Roots—Plume Tectonics of China. Geological Publishing House, Beijing (in Chinese).

Development Research Centre, China Geological Survey and All-Russian Geological Research Institute (2002) Geophysical Characteristics of the Lithosphere along GGT, Arctic Ocean–Eurasia-Pacific Ocean. Global Geoscience Transect 21: Arctic Ocean-Eurasia-Pacific Ocean.

E ML, Zhao DS (1987) The Cenozoic Basalts and Deep-derived Rock Xenoliths of Eastern China. Science Press, Beijing (in Chinese).

Enkin RJ, Yang ZY, Chen Y et al (1992) Paleomagnetic constrains on the geodynamic history of the major blocks of China from the Permian to the present. J. Geophys. Res. 97: 13953–13989.

Fang DJ, Guo YB, Wang ZL et al (1988) Tectonic significance of paleomagnetic study on the Triassic and Jurassic systems in Ningwu basin, Shanxi. Chinese Science Bulletin 33(24): 2057–2059.

Gao S, Luo TC, Zhang BR et al (1999) Structure and composition of the continental crust in East China. Science in China D 42(2): 129–140.

Han Yujing (1993) The p-T-t Trace of Metamorphism. China University of Geosciences Press, Wuhan (in Chinese).

Huang BC, Zhu RX, Yang ZY (1999) Study of Paleozoic kinematics features of the North China block. Geoscience 13(suppl.): 1–7 (in Chinese with English abstract).

Huang KN, Opdyke ND (1993) Paleomagnetic results from Cretaceous and Jurassic rocks of South and Southwest Yunnan: evidence for large clockwise rotations in the Indochina and Shan-Thai-Malay terranes. Earth Planet. Sci. Lett. 117: 507–524.

Johnson KTM, Dich HJB, Shimizu N (1990) Melting in the oceanic upper mantle: an ion microprobe study of diopside in abyssal peridotites. J. Geophys. Res. 95: 2661–2678.

Khramov AN, Petrova GN, Peckersky DM (1981) Paleomagnetism of Soviet Union. In: McElhinny MW, Valencio DA (eds) Paleoconstruction of the continents, geodynamic series. pp.177–194. Geological Society of America, Boulder, Colorado.

Kim Kwang Ho, Van der Voo R (1990) Jurassic and Triassic paleomagnetism of South Korea. Tectonics 9(4): 699–717.

Li CY, Wang Q, Liu XY et al (1982) Tectonic Map of Asia (1: 8,000,000) and Its Specialties. Geological Publishing House, Beijing (in Chinese).

Li CY, Wang Q, Liu XY et al (1984) The evolution of Asian tectonics. Bulletin of the Chinese Academy of Geological Sciences (10): 3–12. Geological Publishing House, Beijing (in Chinese).

Li Songlin, Mooney WD (1998) Crustal structure of China from deep seismic sounding profiles. Tectonophysics 288: 111–113.

Li XH, McCulloch MT (1998) Geochemical characteristics of Cretaceous mafic dikes from northern Guangdong, SE China: age, origin and tectonic significance. In: Flower MFJ et al (eds) Mantle dynamics and plate lnteractions in East Asia, geodynamics series, vol. 27, pp.405–419, American Geophysical Union, Washington DC.

Li ZX, Zhang L, Powell CM (1996) South China in Rodinia: part of the missing link between Australia-East Antarctic and Laurentia? Geology 23: 407–410.

Li ZX (1998) Tectonic history of the major East Asia lithospheric blocks since the mid-Proterozoic: A synthesis. In: Flower MFJ et al (eds) Mantle dynamics and plate interactions in East Asia, geodynamics series, vol. 27, pp.221–243, American Geophysical Union, Washington DC.

Liang QZ (1990) Paleo-magnetic research on petrological phase paleogeography and sedimentation. Unpublished report of Institute of Scientific Research, Geological Bureau of Yunnan (in Chinese).

Lu FX, Zheng JP, Li WP et al (2000) The main evolution pattern of Phanerozoic mantle in the eastern China: the "Mushroom Cloud" Model. Earth Science Frontiers 7(1): 97–107 (in Chinese with English abstract).

Ma XH, Yang ZY (1993) The collision and suturing of the three major blocks in China and the reconstruction of the Paleo-Eurasian continent. Acta Geophysica Sinica 36(4): 476–488 (in Chinese with English abstract).

Ma XY (chief editor, Editorial Board for Lithospheric Dynamics Atlas of China, State Seismological Bureau) (1989) Lithospheric Dynamics Atlas of China. SinoMaps Press, Beijing (in Chinese with English abstract).

Ma ZJ, Jiang M (1987) Strong earthquake periods and episodes in China. Earthquake Research in China 3(1): 47–51 (in Chinese with English abstract).

Maruyama S, Seno T (1986) Orogeny and relative plate motions: example of the Japanese Islands. Tectonophysics 127: 305–329.

Maruyama S, Isozaki Y, Kimura G et al (1997) Paleogeographic map of the Japanese Islands: plate tectonic synthesis from 750 Ma to the present. The Island Arc 6: 121–142.

McKenzie D, Bickle MJ (1988) The volume and composition of melt generated by extension of the lithosphere. J. Petrol. 29(3): 625–679.

Melcher F, Meisel T, Puhl J et al (2002) Petrogenesis and geotectonic setting of ultramafic rocks in the Eastern Alps: constraints from geochemistry. Lithos 65(1–2): 69–112.

Menzies MA, Xu YG 1998) Geodynamics of the North China Craton. In: Flower MFJ et al (eds) mantle dynamics and plate interactions in East Asia, geodynamics series, vol. 27, pp.155–166, American Geophysical Union, Washington DC.

Mercier JCC (1980) Magnitude of the continental lithospheric stresses inferred from rheomorphic petrology. Jour. Geophys. Res. B 85(11): 6293–6303.

Moore GW(1989) Mesozoic and Cenozoic paleogeographic development of the Pacific region. Abstracts of 28th International Geological Congress, 2–455–456, Washington DC, USA.

Niu Y (1997) Mantle melting and melt extraction processes beneath ocean ridge: evidence from abyssal peridotites. Jour. Petrol. 38: 1047–1074.

Pavoni N (1997) Geotectonic bipolarity: evidence of bicellular convection in the Earth's mantle. S. Afr. J. Geol. 100(4): 291–299.

Royden LH, Burchfiel BC (1997) Surface deformation and lower crustal flow in eastern Tibet. Science 276(5,313): 788–790.

Rudnick RL (1995) Making continental crust. Nature 378(6,557): 571–578.

Scotese CR (1994) Continental drift, 6th edn. The PALEOMAP Project, University of Texas at Arlington.

Shao JA, Zhang LQ, Mou BL (1998) Tectono-thermal evolution of middle-south section of the Da Hinggan Mountains . Science in China D 41(6): 570–579.

Shao JA, Zhang LQ, Wei CJ et al (2001) The composition and its characteristics of bimodal dyke swarm of Mesozoic at Nankou, Beijing . Acta Geologica Sinica 75(2): 205–212 (in Chinese with English abstract).

Shi ZH, Liu ZP, Yin XH (1989) Crustal thickness by gravity inversion. In: Ma XY (ed) Lithospheric Dynamics Atlas of China. SinoMaps Press, Beijing (in Chinese).

Song XD, Richards PG (1996) Seismological evidence for differential rotation of the Earth's inner core. Nature 382(6,588): 221–224.

Storey M, Saunders AD, Tarney J et al (1989) Contamination of Indian Ocean asthenosphere by the Kerguelen-Heard mantle plume. Nature 338(6216): 574–576.

Suo ST, Zhong ZQ, Zhou HW et al (2003) Kanfenggou UHP metamorphic fragment in Eastern Qinling orogen and its relationship to Dabie-Sulu UHP and HP metamorphic belts, Central China. J. China University of Geosciences, 14(2): 95–102.

Taylor SR, McLennan SM (1995) The geochemical evolution of the continental crust. Rev. Geophys. 33(2): 241–265.

Teng JW, Zeng RS, Yan YF et al (2003) Depth distribution of Moho and tectonic framework in eastern Asian continent and its adjacent ocean areas. Science in China D 46(5): 428–446.

Wan TF (1988) Silica heat flow in South China. Chinese Science Bulletin 33(8): 655–657.

Wan TF, Tong YF, Zheng WW (1989) Thermal structure of the lithosphere in Fujian, China. Journal of Geophysical Research B 94(2): 1888–1894.

Wan TF (1994) Intraplate Deformation, Tectonic Stress and Their Application for Eastern China in Meso-Cenozoic. China University of Geosciences Press, Wuhan.

Wan TF (2004) An Outline of China Tectonics. Geological Publishing House, Beijing (in Chinese).

Wang HZ (1981) Geotectonic units of China from the view-point of mobilism. Earth Sciences—Journal of Wuhan College of Geology (1): 42–66 (in Chinese with English abstract).

Wang HZ (1982) The main stages of crustal development of China. Earth Sciences—Journal of Wuhan College of Geology (3): 155–177 (in Chinese with English abstract).

Wang HZ (1985) Atlas of Paleogeography of China. SinoMaps Press, Beijing (in Chinese).

Wang J, Huang SY, Huang GS et al (1990) Basic Characteristics of the Earth's Temperature Distribution in China. Seismological Press, Beijing (in Chinese).

Wedepohl KH (1995) The composition of the continental crust. Geochim. Cosmochim. Acta 59(7): 1217–1232.

Xiao XC, Chen GM, Zhu ZZ (1978) A preliminary study on the tectonics of ancient ophiolites in the Qilian Mountain, northwest China. Acta Geologica Sinica 52(4): 281–295 (in Chinese with English abstract).

Xiao XC, Wang FG (1984) An introduction to the ophiolite of China. Bulletin of the Chinese Academy of Geological Sciences 9: 19–30. Geological Publishing House, Beijing (in Chinese).

Xiao XC, Li TD, Li GQ et al (1988) Tectonic Evolution of Himalayan Lithosphere. Geological Publishing House, Beijing (in Chinese).

Xu CF (1996) Electrol structure of crust-upper mantle of China continent and earthquake distribution. Acta Seismologica 18(2): 254–261.

Xu ZQ, Zhao ZX, Yang JS et al (2003) Tectonics beneath plates and mantle dynamics. Geological Bulletin of China 22(3): 149–159 (in Chinese with English abstract).

Xue F, Huang JW (1989) Distribution of earthquake focal depths. In: Ma XY (ed) Lithospheric Dynamics Atlas of China. SinoMaps Press, Beijing (in Chinese).

Yin XH, Liu ZP, Wu JX et al (1988) The features of bouguer gravity field and structures of crust-upper mantle in the transition zone on the eastern border of Qinghai-Xizang-Mongolian Plateau. Seismology and Geology 10(4): 143–150 (in Chinese with English abstract).

Yuan XC (1996) Atlas of Geophysics in China. Geological Publishing House, Beijing (in Chinese).
Zeng RS, Sun WG, Mao TE et al (1995) Depth map of Moho interface of China continent. Acta Seismologica Sinica 17(3): 322–327 (in Chinese with English abstract).
Zhai MG (1998) Three important high-pressure and high-temperature metamorphic zones in China and their geotectonic significance. Acta Petrologica Sinica 14(4): 419–429 (in Chinese with English abstract).
Zhang BR, Han YW, Xu JF et al (1998) Geochemical evidence for north Qinling being a part of Yangtze plate prior to the Neoproterozoic. Geological Journal of China Universities 4(4): 369–382 (in Chinese with English abstract).
Zhang SG (1993) Analysis on the dispersal and convergence of North China block and Yangtze block from features of metamorphic geology in Qinling area. In: China Working Group on International Geological Comparison Program, Project 321. Growth of Asia, pp.99–102. Seismological Press, Beijing (in Chinese).
Zhang WY (1984) An Introduction to Fault-Block Tectonics. 385pp. Petroleum Industry Press, Beijing (in Chinese).
Zhou XM, Li WX (2000) Origin of Late Mesozoic igneous rocks in southeastern China: implications for lithosphere subduction and underplating of mafic magmas. Tectonophysics 326(3–4): 269–287.
Zhu X (1982) Tectonics of continental margin and basin evolution. Petroleum Experiment and Geology (4): 53–60 (in Chinese).
Zhu ZW, Hao TY, Zhao HS (1988) Paleomagnetism and its implication of Pan-Xi region in Mesozoic. In: Zhang YX, Yuan XC (eds) Collections of Pan-Xi Rift, China (3), 199–211. Geological Publishing House, Beijing (in Chinese with English abstract).

Chapter 14
Mineralization and Tectonics in China

Following an account of the main features of the structure and tectonic history of the Chinese continent presented in this volume, the related applied problems, the influence of the environment and geological hazards have been discussed. Particularly, the relationship between tectonics and mineralization will be considered in this chapter; there are very good prospects for the further development of mineral resources in China.

Tectonics provides the context in which the search for strategy of mineral resources in China must be conducted; the tectonic setting must always be taken into account in mineral exploration. During the last century the older generation of geologists in China, such as Weng WH (1920*, 1927, 1929), Xie JR (1936, 1952), Li SG (1947, 1962), Huang TK (Huang JQ, 1945, 1960, 1965), Li CY (1982, 1984), Zhang WY (1959, 1983, 1984), Chen GD (1960, 1978), Guo WK (1987), and Song SH (1989, 1992), used tectonic theory to make great contributions to the exploration for mineral resources in China. The present generation of geoscientists must make research on these foundations.

Recently, many important books and theses on tectonics and mineralization have been published, providing excellent guidance to the exploration for mineral resources. The monograph by Zhai YS et al. (1999) covers tectonics, petrogenesis, mineralization and dynamics, identifies research targets systematically, provides an account of ore deposits, and defines the principles and methods for the study of regional metallogeny. Major aspects are the background to mineralization, metallogenic systems and metallogenic evolution. The book gives an account of the materials, and the genesis of minerals in time and space, discusses the formation and distribution of ore deposits, with the scientific basis for predicting the presence of ore deposits and provides a comprehensive monograph of the relationship between tectonics and metallogenesis.

In this chapter, the major epochs and belts of mineralization in Chinese continent will be described, which are influenced by tectonics of China. The control of deformation on the development of endogenic ore deposits will be explained, the importance of intraplate extension tectonics in metallogenesis and the prospects for the discovery of further mineral resources in China will be discussed, with the addition of some personal opinions.

In the second prospecting project for mineral resources in China, Ye JH (1998) (Group of Regional Planning, Chinese Academy of Geological Sciences) (personal communication) studied 1,573 macro- and meso-scale metallic and nonmetallic mineral deposits systematically, including 52% macro-scale ore deposits, recorded by the Ministry of Land and Resources, and the main characteristics of their metallogeny were discussed. Most metallic minerals have a hydrothermal origin, with those being of exogenic origin having the secondary importance; nonmetallic mineral deposits are mainly of exogenic origin, with hydrothermal deposits being secondary, while metamorphic and magmatic ore deposits

* The article "On the regional mineralization in China" was published by Weng WH in 1920, who first defined the zones of metallic mineral deposits in south China, i.e. the distribution of the tin, lead-zinc-copper, antimony and mercury zones, and also recognized the relationship of magmatic rocks to metallogenesis (after Zhai YS, 1999).

form less than 10% of the ore deposits in China (Fig. 14.1). Although oil, gas and coal are of exogenic origin, they are not included in these statistics.

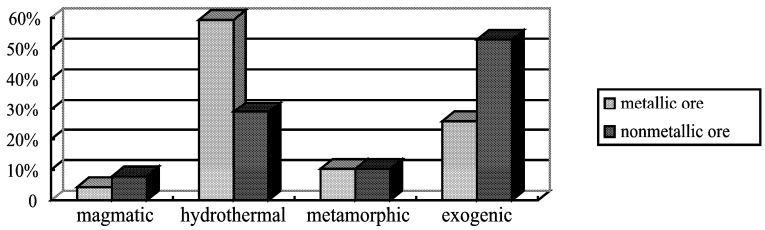

Fig. 14.1 Types of metallic and nonmetallic mineral deposits in China (original data from Ye JH, 1998) (personal communication).

Metallic mineral deposits (number 993): magmatic (44; 4.4%); hydrothermal (590; 59.4%); metamorphic (102; 10.3%); exogenic (257; 25.9%).

Nonmetallic mineral deposits (number 580): magmatic (44; 7.6%); hydrothermal (169; 29.1%); metamorphic (60; 10.3%); exogenic (307; 52.9%).

Hydrothermal types, broadly speaking, include contact-metasomatic, pneumato-hydrothermal and exhalation deposits.

14.1 Main Epochs and Belts of Mineralization

Many different types of ore deposit have been formed in the Chinese continent during its long geological history. According to the statistics gathered by Ye JH (1998), the Mesozoic was the main period for the formation of both metallic and nonmetallic mineral deposits, fewer deposits were formed during the Late Paleozoic, and even fewer in the Cenozoic (Fig. 14.2): 82.4 % of metallic mineral deposits and 73.7 % of nonmetallic mineral deposits have been formed since the Late Paleozoic; 61.6 % of metallic mineral deposits and 49.2 % of the nonmetallic mineral deposits were formed during the Mesozoic and Cenozoic. Deposits bearing the relatively stable elements of the iron group (Fe, Mn, V ,Ti and rare earth elements, etc., i.e. ferrous metals) were formed mainly before the Mesozoic, while deposits bearing relatively active minerals, sulfides with non-ferrous, rare and noble metals, were formed mainly during the Mesozoic and Cenozoic (Zhai YS et al., 1999).

The objective data given above differ from the conclusions reached by some Chinese researchers, and also the main periods for the formation of ore deposits in China differ from those recognized on a global scale (Fig. 14.3), where most ore deposits (38 %) are seen to have been formed during the Precambrian. The main reason for this difference may be that there have been a great many collisions in the Chinese continent since the Late Paleozoic, and intraplate deformation has been very strong, while Precambrian rocks are rarely exposed, forming only less than 10% of the total surface area of China (Cheng YQ, 1994). Tectonism since the Late Paleozoic has resulted in the formation of many ore deposits, but also destroyed and replaced earlier formed ore deposits, thus ore deposits found at or near the Earth's surface were formed mainly since the Late Paleozoic. During the Precambrian there might be just as many ore deposits formed in China as in other parts of the Earth, however they are now buried deeply beneath younger Paleozoic, Mesozoic and Cenozoic systems. But it may be that these ore deposits cannot be exploited economically, even in the distant future.

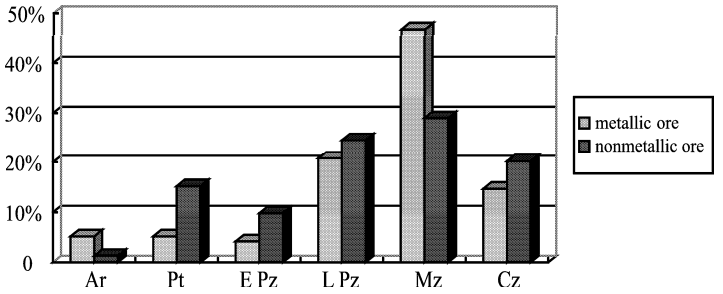

Fig. 14.2 Periods of formation of metallic and nonmetallic mineral deposits in China (original data from Ye JH, 1998).

Metallic mineral deposits (number 993): Archean (52; 5.2%); Proterozoic (82; 8.2%); Early Paleozoic (42; 4.2%); Late Paleozic (207; 20.8%); Mesozoic (466; 46.9%); Ceonozoic (146; 14.7%).

Nonmetallic mineral deposits (number 580): Archean (8; 1.3%); Proterozoic (88; 15.2%); Early Paleozoic (57; 9.8%); Late Paleozic (142; 24.5%); Mesozoic (168; 29%); Ceonozoic (117; 20.2%).

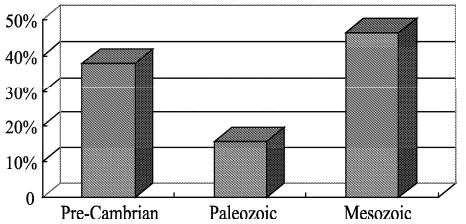

Fig. 14.3 Main periods for the formation of global ore deposits (after Zhai YS et al., 1999). (38 % in Precambrian; 15.7% in Paleozoic; 46.3 % in Mesozoic)

Periods in which oil and gas reservoirs accumulated in China are also extremely unevenly distributed in time: 92% of hydrocarbon reservoirs occur within the Mesozoic and Cenozoic systems; only 8% are found in the Paleozoic systems (Chen RS, 1994). Although more oil and gas reservoirs have been found in Paleozoic systems recently, research shows that 80 % of oil and gas reservoirs occur in Cenozoic rocks (Jia CZ et al., 2003).

Determination of the main episodes of formation of the ore deposits in China is very important, as it will control the direction of exploration programs and strategic mineral supply. During the 1990s there was a lively debate as to whether the emphasis should be concentrated on the exploration for Precambrian ore deposits, or more attention should be paid to ore deposits formed since the Paleozoic. This debate still has immediate practical significance at the present time.

It should be possible to relate the formation of the various metallogenic belts in China to specific metallogenic periods. It is of little use to compile maps showing the distribution of the metallogenic belts without including the concept of time. Because different styles of tectonism were dominant in different tectonic periods, different mineral associations and types of ore deposits were formed. When isotopic dates are not available the classification of metallogenic belts is based upon the tectonic divisions in which they occur. This provides only a rough guide for the exploration of ore deposits. Maps of the distribution of ore deposits, the classification of metallogenic belts, or metallogenic prospects, based on similar principles, should be compiled for each tectonic period. When isotopic ages were difficult to obtain or completely lacking, it was understandable that metallogenic maps were compiled without

including the time concept. More recently, with the development of isotopic dating methods, it has become possible to attribute the formation of the different metallogenic belts to specific tectonic periods.

The characteristics of the main metallogenic belts in the Chinese continent and representative ore deposits formed during each metallogenic period are described based on recent data (Ye JH, 1998; Zhai YS et al., 1999):

Archean and Paleoproterozoic metallogenic periods. Ferruginous quartzite in Anshan of eastern Liaoning and Qian'an of Hebei was formed mainly during these periods. The super-macroscale siderite ore deposit in Dashiqiao and macroscale ascharite and ludwigite ore deposits, which occur in the eastern Liaoning Aulacogen, the Sedex type lead-zinc ore deposit in Qingchengzi and the copper and zinc ore deposits in Hongtoushan were also formed. A deposit rich in Ni, Cu, Pt and Pd was formed in Jinchuan of Gansu, controlled by paleo-fault zones.

Meso- and Neo-proterozoic metallogenic periods. The super-macroscale Sedex type niobium, rare earth elements and iron ore deposits in Baiyun–Ebo, Inner Mongolia, the Sedex type lead, zinc and sulphur deposits in Dongshengmiao, Inner Mongolia, all formed in an aulacogen on the northern margin of the Sino-Korean Plate. Sedex type copper, iron and lead-zinc deposits were formed in an aulacogen on the southwestern margin of the Yangtze Plate. The iron, titanium and vanadium ore deposits at Damiao-Heishan, Hebei formed in a deep fault zone on the northern margin of the Yanshan-western Liaoning depression in the Sino-Korean Plate. The nickel deposit at Dapoling, Guangxi, is located in the collision zone formed during the Qingbaikou Tectonic Period (~1,000 Ma).

Early Paleozoic metallogenic period. The main deposits are the lead-zinc and silver deposits at Baiyinchang, Gansu, the lead-zinc deposits at Xitieshan, Qinghai, the copper, gold and silver deposits at Bainaimiao, Inner Mongolia, uranium, gold and silver deposits at Maqu, Gansu, all developed in an internal continental depression, or in a marginal rift. Sedimentary mineral deposits, formed mainly during this period, are the phosphorus deposits at Kunyang, Yunnan, the phosphorus deposit at Xinhua, Guizhou, and the sulphur deposit at Dalongping, Guangdong; these deposits were all deposited on a continental shelf in a shallow marine environment. Important sedimentary-metamorphic iron, copper and cobalt deposits at Shilu, Hainan Island, formed during this period were also deposited initially on a continental shelf.

Late Paleozoic metallogenic period. The main ore deposits in this period are of porphyry copper type, with gold deposits at Duobaoshan and Xiaoxinancha, Heilongjiang, which developed along an extensional fault zone near a continental margin accretion zone. The gabbro-type nickel and copper ore deposits were also intruded along a deep fault at Hongqiling, Jilin. The copper-zinc ore deposit at Ashile, Xinjiang, the gabbro-type copper and nickel ore deposits at Hami and Kalatongk, Xinjiang, and the lead-zinc deposit at Changba, Gansu, the hydrothermal copper, cobalt and zinc deposits at Delni, Qinghai were formed in local extensional fault zones in or near the Tianshan–Inner Mongolia–Dahingganling Collision Zone. The iron, titanium, vanadium and nickel deposits at Panzhihua and Danba, Sichuan, the tin, lead and zinc deposits at Dachang, Guangxi, manganese deposits at Xialie, Guangxi, the gold deposits at Getang, Guizhou, and the lead-zinc deposits at Laochang, Yunnan were formed as magmatic or hydrothermal deposits in an aulacogen at the margin of the Yangtze Plate. The lead-zinc deposits at Fankou, Guangdong, the gold and silver deposits at Changken, Guangdong, the iron and copper deposits at Dabaoshan, Guangdong, and the bauxite deposits at Gongxian, Henan were formed as sediments in a shallow sea, or by hydrothermal activity beneath a shallow sea. The bauxite deposit at Maochang of Guizhou was formed as a paleo-soil by weathering during the Late Carboniferous. The Carboniferous and Permian were also important coal-forming periods; the coal beds in these systems also supply methane.

Indosinian (Triassic) metallogenic period. This is not one of the main metallogenic periods (Fig. 14.4), although continental collisions and intraplate deformations were widespread, but is a very interesting period for tectonic research. But during this period the eastern migration of magmatic or hydrother-

mal systems caused the mobilization of mineral-bearing fluids to form ore deposits; these movements also destroyed ore deposits and reservoirs. Major metallic deposits are related to collision, as well as intermediate to small-scale chromium and platinum group deposits occurring in ultra-mafic rock bodies, asbestos and blue asbestos deposits are related to serpentinization, and some other endogenic magmatic and hydrothermal deposits were formed in secondary cross extension faults. Some intermediate and small-scale endogenic ore deposits are related to intraplate deformation.

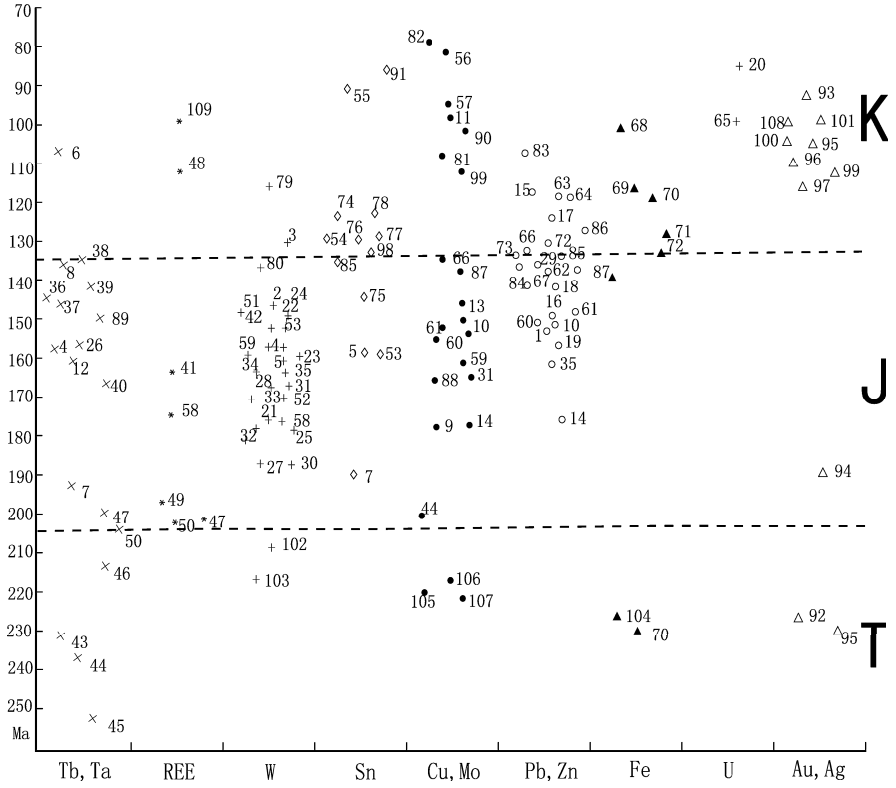

Fig. 14.4 The age of formation of metallic mineral deposits in South China during the Mesozoic (Zhan MG, 1994). T. Triassic metallogenic epoch; J. Jurassic metallogenic epoch; K. Cretaceous metallogenic epoch.

1. Shizhuyuan; 2. Xianglinp; 3. Shanshan; 4. Xianghuapu; 5 and 6.Xianghualing; 7. Limu; 8. Dengfuxian; 9. Dabaoshan; 10 and 11. Qiebaoshan; 12. Yiliu; 13. Dashunlong; 14.Tongshanling; 15. Huangshaping; 16. Shuikoushan; 17. Lianyang; 18. Paojinshan; 19.Dongpo; 20. No.212 ore deposit; 21. Yaogangxian; 22 and 23. Huangsha; 24. Hongling; 25 and 26. Dajishan; 27. Piaotang; 28. Xihuashan; 29. Meiziwo; 30. Yaoling; 31. Jubanken; 32. Guimeishan; 33. Pangushan; 34. Beiyunxian; 35.Qianchang; 36.Jiangkenli; 37. Hailuoling; 38. Hanjiaoshan; 39. No.531 ore deposit; 40. No.430 ore deposit; 41. Zhudong; 42. Xingluoken; 43. Dafan; 44. Deqing; 45. Nanping; 46. Shimaling; 47. No.541 ore deposit; 48. No.414 ore deposit; 49. Henshan; 50. No. 561 ore deposit; 51. Huken; 52. Xushan; 53. Xishan; 54. Xiping; 55. Yinyan; 56. Shilu; 57. Tiantang; 58.Yashan; 59. Tianpaishan; 60. Fuzichong; 61. Sanhe; 62. Zhanggongling; 63. Mang'eling; 64.Lengshuiken; 65. Xiangshan; 66. Zhudi; 67. Tongken; 68. Yangshan; 69. Guashan; 70. Maken; 71. Qianshan; 72. Tieshanzhang; 73. Sutian; 74. Xianwu; 75. Changpu; 76. Xiling; 77. Houpo'ao; 78. Boluo; 79. Jiuquling; 80. Lianhuashan; 81. Zhongteng; 82. Chilu; 83. Yinken; 84. Wubu; 85. Dalingkou; 86. Xiashan; 87. Yinshan; 88. Tongchang; 89. Geyuan; 90. Zijinshan; 91. Tashan; 92. Hongpumenling; 93. Beiniu; 94. Bumo; 95. Hetai; 96. Changken and Fuwan; 97. Babaoshan; 98. Yanbei; 99. Yadai; 100. Yaliang; 101. Anding, Jiusuo; 102. Niumiao; 103. Chuankou; 104. Dajiangping; 105. Fenghuangling; 106. Liannan, 107. Gaotian; 108. Jinshan; 109. Heling.

The main metallogenic period did not occur during the major collision period. This lesson has been learned over the past thirty years, after the expenditure of large-scale funding for scientific research and exploration. However, some researchers have either forgotten or do not know about this experience and still consider that metallogenesis occurred during collision and emphasize the interdependence of metallogenesis and the scale and strength of collision. It is regrettable that this opinion is still held by some researchers studying orogenic collision zones, and also by some policymakers in the government (Qiu XP, 2002). It is necessary to reconsider this opinion.

Yanshanian metallogenic period (200–135 Ma). This period was very short, however the quantity of metallic mineral deposits, formed during this period, comprise a quarter of the total for the whole of China; the quantity of nonmetallic mineral deposits are about 15% of total for the whole of China. It is a major period for the formation of hydrothermal ore deposits of non-ferrous, rare and noble metals, these are controlled by intraplate deformation, especially in extensional faults or joints, and can be divided into three metallogenic zones (Fig. 14.5):

The metallogenic zones of northern margin of north China and Qinling–Dabie-Tongling were all developed in original collision zones or along basement faults and were influenced by the stress field in the Yanshanian Tectonic Period. Earlier near E-W trending foliation and fault zones limited extension, forming conditions for the accumulation of many ore deposits. The main representative ore deposits are the gold deposits at Jiapigou, Jilin, at Paishanlou and Yiwulvshan, Liaoning and Shuanwang and Xiaoqinling, Shaanxi, and the lead, zinc, silver and gold deposits at Caijiaying, Hebei.

The third important metallogenic zone is located in south China, concentrated in the Nanling area. Although regional fault zones of the Yanshanian Tectonic Period are mainly NE-trending, the major metallogenic zones are WNW-trending, nearly parallel to the maximum principal compressive stress during that period. Representative ore deposits are: copper, gold, molybdenum and sulphur at Tongling, Anhui and Tongchang, Jiangxi, and tungsten at Xihuashan, Dajishan, Piaotang and Dahutang.

During the Yanshanian Tectonic Period, mercury deposits at Wanshan, Guizhou, and antimony deposits at Xikuangshan, Hunan were concentrated in the hinge zones of NNE-trending anticlines. The tungsten, tin, molybdenum and bismuth deposits at Shizhuyuan, Hunan, occur at the intersections of faults, forming multi-period hydrothermal super-giant ore deposits. Statistical analysis by Shi MK et al. (1993) showed that the major periods for the formation of copper and lead-zinc ores were in the Middle to Late Jurassic.

Where deformation was rather weak, the Yanshanian Period was also the most important period for the formation of coal deposits in and near Ordos, and the period for the accumulation of oil, gas and uranium in North and Northwest China, in the Ordos, Sichuan, the western part of Northeast China, Inner Mongolia and in the Northwest China basins.

Sichuanian metallogenic period (135–52 Ma). This period was also very short. However, the metallic mineral deposits formed amount to a quarter of the total for the whole of China, and the amount of nonmetallic mineral deposits forms about 20% of the total for the whole of China, similar to the Yanshanian Tectonic Period. This was the major period for the formation of hydrothermal ore deposits of non-ferrous, rare and noble metals, controlled by intraplate deformation and for the formation of four NNE-trending metallogenic zones in East China (Fig. 14.6): the Hengduanshan, Dahingganling–Taihangshan, Tancheng–Lujiang and South China metallogenic zones. About 70%–80% of all ore deposits in China were formed during this period in extensional fault and fissure zones trending NNE, NE and ENE, almost parallel to the maximum principal compressive stress during the Sichuanian Period.

The main representative ore deposits are: lead-zinc at Jiachun, Sichuan, tin at Gejiu, Yunnan, in the Hengduanshan metallogenic zone; lead-zinc at Bayinor; iron and tin at Huanggang, Inner Mongolia; molybdenum at Yangjiazhangzi, Liaoning; gold at Jinchangyu, Hebei; uranium at No.460 Mine, Guyuan, Hebei; the iron at Handan-Xingtai, Hebei; molybdenum at Jinduicheng, Shaanxi; mercury at Gongguan, Shaanxi; molybdenum at Nannihu, Luanchuan, Henan in the Dahingganling-Taihangshan metallogenic zone; gold fields at Zhaoyuan–Laizhou, Muping-Rushan and Guilaizhuang, Shandong in the Tancheng-Lujiang metallogenic zone; the lead-zinc deposit at Wubu, Zhejiang, fluorite, alunite and

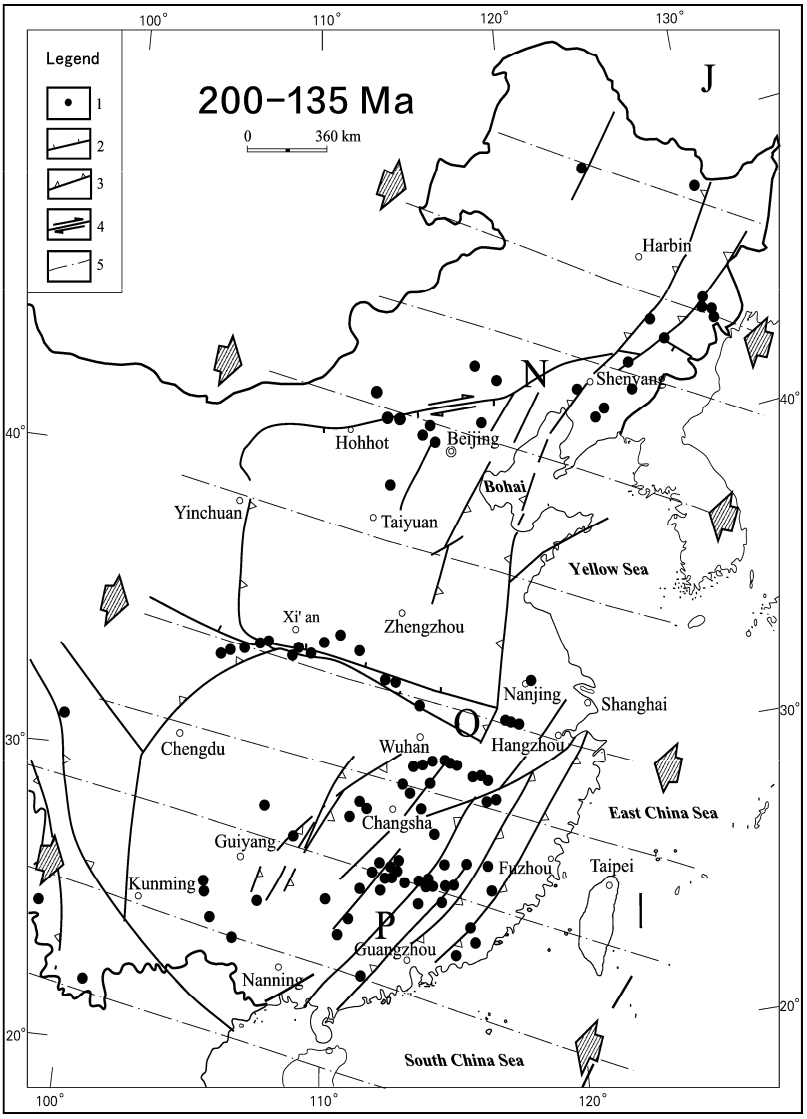

Fig. 14.5 Zones of metallic mineral deposits in eastern China during the Yanshanian Period (200–135 Ma) (Wan TF, 1994).

Legend: 1. Metallic mineral deposit; 2. Normal fault; 3. Thrust; 4. Strike-slip fault; 5. Trace of maximum principle compression stress.

N: Metallogenic zones on the northern margin of north China; O: Metallogenic zone of Qinling–Dabie–Tongling; P: Metallogenic zones of southern China (centered in Nanling).

pyrophyllite deposits in Zhejiang, and tin deposits at Dachang, Changpu and Jishuimen, Guangxi in the

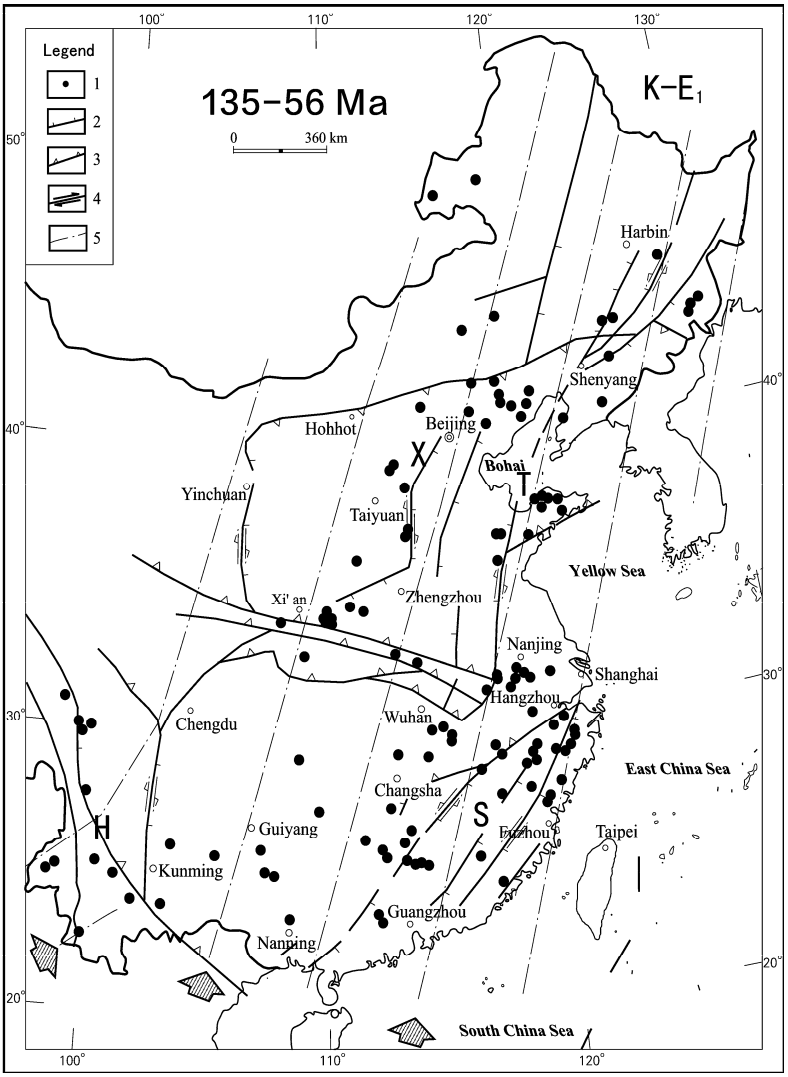

Fig. 14.6 The metallic mineral deposit zones of eastern China during the Sichuanian Tectonic Period (135–56 Ma) (Wan TF, 1994).

Legend: The same to Fig. 14.5.

H: Metallogenic zone of Hengduanshan; X: Metallogenic zone of Dahingganling–Taihangshan; T: Metallogenic zone of Tancheng–Lujiang; S: Metallogenic zone of south China.

South China metallogenic zone. The main period for the formation of tin deposits in the South China metallogenic zone was the Early Cretaceous (Shi MK et al., 1993).

The South China metallogenic zone can be divided into three zones: (1) the southeast coastal epithermal deposit zone with Pb, Zn, Au, Ag, fluorite, alunite and pyrophyllite; (2) the southern Jiangxi–central

Hunan hypothermal and mesothermal deposit zone with W, Sn, Pb, Zn, Nb, Ta and rare elements; (3) the western Hunan-Guizhou epithermal deposit zone with Hg, Sb, As, Au, Tl. This zonal division for south China was first proposed by Weng WH (1920). Recently, mining in South China metallogenic zone has faced a crisis, for most of the minerals have been extracted, so that as a matter of urgency exploration and mining have been extended over a much broader area and to depths of up to 1,500 m.

In the Sichuanian Tectonic Period, most of the sedimentary basins in China had a desert environment with a hot, dry climate with the formation of gypsum and halite deposits; however, in northeastern China and in the Junggar area the climate was warm and moist, favorable to the formation of oil and gas, e.g. the Daqing oil and gas field.

Mineral deposits formed during the Yanshanian and Sichuanian Periods often show evidence of the superposition of several episodes of metallogenesis, so that many useful elements have become highly concentrated, e.g. the copper, iron and gold deposits at Daye–Yangxin, Jiujiang–Ruichang and at Tongling in the lower and middle reaches of the Yangtze River area (Zhai YS et al., 1992; Wan TF, 1994). Ore deposits of the Yanshanian metallogenic period fill mainly WNW-trending extensional fault zones, while those of the Sichuanian metallogenic period fill mainly NNE-trending extension fault zones (Fig. 14.7). The intersection points of faults formed in separate tectonic periods are often provided the positions for the formation of the richest ore bodies. Two metallogenic periods affected the antimony deposit of Xikuangshan, Hunan, in which the main controlling structures for the deposition of ore bodies were the hinge zones of anticlines. Ore bodies of the Yanshanian Period are preserved mainly in the NNE-trending hinge zones of anticlines, and those of the Sichuanian Period are preserved in the WNW-trending hinge zones of superposed secondary anticlines, with the major ore deposits being formed at the intersection of two anticlinal hinge zones.

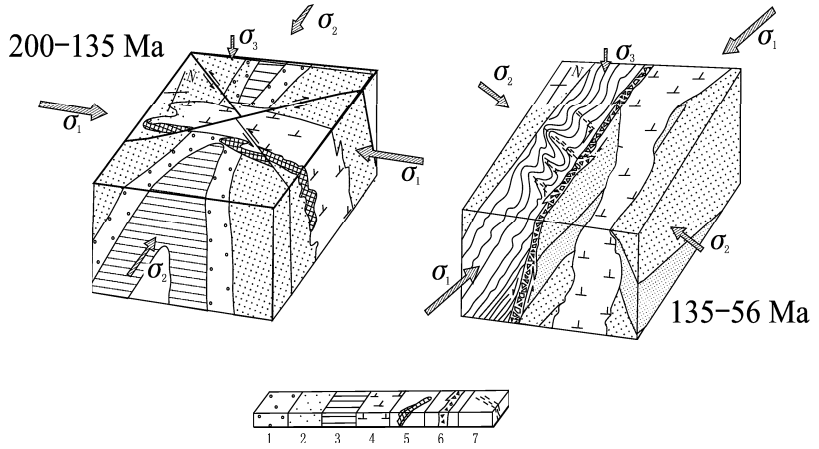

Fig. 14.7 The tectonic stress fields, rock deformation and their influences on metallogenesis during the Yanshanian and Sichuanian Tectonic Periods.

1. Conglomerate; 2. Sandstone; 3. Siltstone and Shale; 4. Diorite; 5. Ore deposit; 6. Breccia Zone; 7. Axial surface of microfold

There are many ring structures outcropping at the surface in the Chinese continent, with some relating to deeply buried igneous intrusions. Hydrothermal ore deposits are commonly associated with these ring structures, but are not developed all around the ring fault, while are often concentrated on either side of the ring structure. In the Yanshanian Tectonic Period, the NE and SW sides of the ring faults were subject to extension, and easy to accumulate ore deposits, due to the WNW orientation of the regional

maximum principal compressive stress, while in the Sichuanian Tectonic Period, the NW and SE sides of ring faults were extended, and easy to accumulate ore deposits, due to the NNE orientation of the regional maximum principal compressive stress. Clearly in these cases the horizontal regional tectonic stress controlled the location of the ore deposits (Wan TF, 1994). The above distribution features are very important for exploration of ore deposits in China.

North Sinian metallogenic period (52–23 Ma). According to recent data, this was the major period for the formation and accumulation of oil and gas resources in eastern China, such as the oil and gas fields around Bohai Bay, north Jiangsu-south Yellow Sea, East China Sea, the Jianghan Plain (south Hubei and north Hunan areas) and the mouth of the Zhujiang. The source rocks of the large Daqing oil and gas field were deposited in the Early Cretaceous, and the structures forming the reservoirs were developed at the end of the Paleogene.

Endogenic metallic mineral deposits formed during the North Sinian period occur in the Hengduanshan and Qinghai–Xizang areas, in the Yunnan–Qinghai–Xizang metallogenic zone. Representative ore deposits are the porphyry copper and molybdenum deposits near Yulong, eastern Xizang formed between 40 and 50 Ma, the gold deposit at Laowangzhai, Yunnan, the lead-zinc deposit at Jinding, Yunnan. Ore deposits formed during this period will be explored and exploited as part of the "Western China Developing Plan". In eastern China the only lead-zinc deposit formed during this period, controlled by a near E-W-trending normal fault, was at Taolin, Hunan.

Himalayan metallogenic period (23–0.78 Ma). This was another important period for the deposition of source rocks and accumulation of oil and gas resources in Chinese continent. The discovery and exploration of two great gas fields have been very successful: Yinggehai, southwest Hainan Island, and PL 19-3 in southern Bohai Bay. Both fields were formed during this epoch, controlled by N-S trending compression, near N-S trending fracture zones and faults opened up with a high permeability, permitting hydrocarbons to rise through the section. After the Early Pleistocene, in the Neotectonic Period, these fractures and faults were closed, influenced by near E-W compression, forming excellent gas reservoirs at Yinggehai and PL 19-3. This discovery was extremely important for exploration oil and gas in China. Before this discovery, geoscientists thought that faults always provide good migration paths for oil-gas, and could not be responsible for the formation of reservoirs.

A great many endogenic ore deposits and porphyry copper deposits (intra-continental type) formed during the Himalayan period have been discovered in the Gangdise metallogenic zone, Xizang, in recent years, giving isotopic ages of 14–15 Ma (Hou ZQ et al., 2003; Rui ZY et al., 2003; Li GM and Rui ZY, 2004), with the largest mineral reserves in China.

Neotectonic metallogenic period (0.78 Ma). Ore deposits, such as placers of gold, monazite, xenotime and rutile, formed along coasts or in rivers also have economic values. Underground water in the crust provides an important water resource, including geothermal vapor and water. Hypothermal systems occur mainly in the Yunnan-Xizang and Taiwan areas; only epithermal systems were developed in the basins of eastern China.

14.2 Rock Deformation Influencing Mineralization

In recent years the major development in research into the geology of ore deposits has been the recognition that metallogenesis is a mobile and changing dynamic process. Petroleum geologists first recognized that research into the formation of oil and gas fields required consideration of the association of source rocks, migration pathways, reservoirs and cap-rocks. The same concepts can be applied to the genesis and accumulation of ore deposits. Research into mineralization should consider the source of the metallogenic materials, the migration paths of the metallogenic elements, reservoir status and con-

ditions of preservation of ore bodies. The tectonic stress field and its influence on the deformation of the rocks may also affect the mineralization process to varying degrees.

Tectonic units and the source of metallogenic materials. As described in Chapters 1, 2 and 4, the different continental blocks making up China continent belong to different tectonic regimes. The original crust and mantle materials, of which each block is composed, were different, and they have undergone very different geological evolution, with each block having developed distinct geochemical characteristics. A continental block, belonging to a particular tectonic unit, will often host similar ore deposits, different from those of other blocks. Regional geochemical characteristics are an essential controlling factor for metallogenesis. It means that particular types of ore deposits may only be found in certain regions, and may not occur in other areas.

On a theoretical basis it might seem that more than one hundred chemical elements could be found in anywhere on the Earth's surface, only the proportions of different elements might be different. Generally, any elements which were originally common in the Earth's crust and mantle can be concentrated by geological processes and accumulated as ore deposits. Of course, different ore deposits may be accumulated to different degrees. Also technical and economic conditions must be considered. It seems probable that any ore deposit could occur in any region. However, when the distribution of ore deposits is studied in detail, it is discovered that different regions have their own distinctive types of ore deposits.

Taking each of the continental blocks before their incorporation into China, the Sino-Korean Plate is characterized by deposits of iron, gold, magnesium, boron, niobium and rare earth elements, deposits of magnesium and boron were formed during the Paleoproterozoic, mainly at the base of the aulacogen in eastern Liaoning-eastern Shandong. In the Mesoproterozoic deposits of niobium and rare earth elements with reserves, making up 70 % of those of the whole globe, were concentrated in the Baiyun-Ebo aulacogen on the northern margin of the Sino-Korean Plate. The North Yangtze Block is characterized by deposits of copper, iron, gold and mercury; the South Yangtze Block is characterized by deposits of tin, lead, zinc and antimony, forming the largest tin metallogenic province, not only in China, but in the whole world. Although tungsten deposits also occur in the South Yangtze Block, the size and reserves of these deposits are very small. The characteristics of element accumulations in the South Yangtze Block are similar to those of the eastern Malay Peninsula, northern Sumatra and parts of Vietnam; however, the Cathaysian Block is very special, reserves of tungsten make up more than half the deposits of the whole globe. There are also many important deposits of lead, zinc, silver, copper, gold, uranium and some nonmetallic minerals.

The Junggar, Tarim, Qaidam, Qiangtang and the other small blocks in China are largely covered by sedimentary basins at the present day and outcrops of the basement are rare, so that there are not sufficient data available for a sensible discussion.

Ore deposits in collision zones are similar to those formed during the Triassic metallogenic period, i.e. mainly intermediate or small-scale chromium and platinum group deposits in ultra-mafic bodies, asbestos and blue asbestos deposits associated with metasomatic serpentinization, and some magmatic or hydrothermal deposits formed in extensional fault zones. A large number of small-scale chromium deposits formed in different periods are found in collision zones, for example, the chromite deposits of Dadorg and Yushigou, Qilianshan were formed in the Neoproterozoic, those of Shartohai in western Junggar in the Devonian and Carboniferous, those of Yilinhabirgar in north Tianshan in the Middle Carboniferous, and those of Lubusha and Dongqia, Anduo, Xizang in the Cretaceous and Paleogene. Following collision, later tectonic processes, related to intraplate deformation, have controlled the form of many deposits. Where two crustal blocks are juxtaposed along zones of weakness ore deposits may show mixed elemental characteristics from both blocks and it may be difficult to determine the contribution of each block to the deposit.

Accumulations of tungsten and tin in the Cathaysian and South Yangtze plates, respectively, are quite unique. It is only a slight simplification to claim that the Cathaysian Plate is rich in tungsten, while the South Yangtze Plate is rich in tin. In the most areas of Chinese continent, these elements are rather rare, however some small-scale tungsten and tin deposits are found at Jiamusi and Dahingganling in

northeastern China, in Gansu and in the Junggar areas. The element accumulations in the various crustal blocks may provide important evidence for plate reconstructions.

The above discussion is preliminary, as it is difficult to establish the distribution of the characteristic elements in each continental block, a great deal of work is necessary. Crustal blocks have been affected by multiple tectonic processes, with large-scale movements and catastrophic collisions. There may have been intra-crustal detachments or detachments between the crust and mantle. After collision there may have been intraplate deformation during several later tectonic periods, so that the original distribution of elements and ore deposits may have been greatly modified by later events. The result may be extremely complex and many researchers have considered that it might be impossible to resolve.

Control of element migration by faults. There is very little element migration in solid rocks, especially in sedimentary or metamorphic rocks. However, during the formation of magmatic rocks and hydrothermal deposits, elements are in a fluid condition, and are able to migrate over considerable distances, behaving in a similar fashion to fluids like oil, gas, underground water or epithermal fluids.

Faults, penetrating to different depths, may provide conduits for the movement of magmas and the deposition of ore deposits of different types (Fig. 14.8). Ultra-mafic rock bodies from the mantle with inclusions containing ore deposits of the iron and platinum groups, and diamonds may have been uplifted along lithospheric faults, caused from athenosphere, and emplaced in a cold state near the Earth's surface.

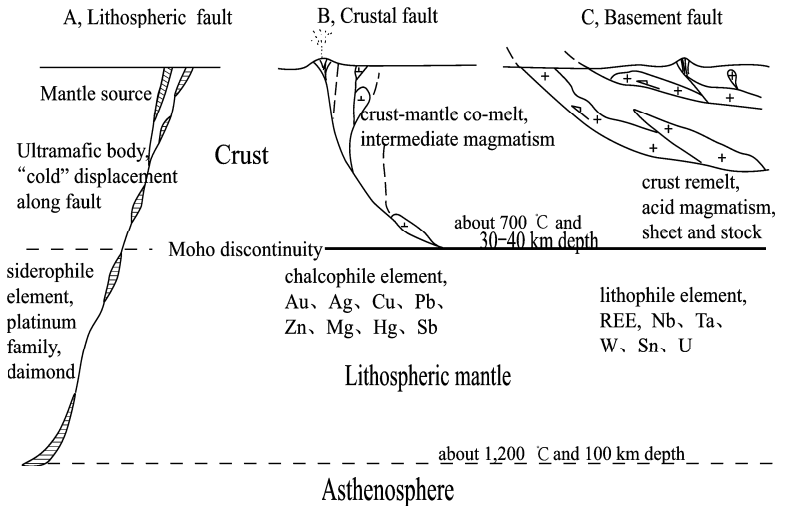

Fig. 14.8 Faults, penetrating to different depths in the crust provide channels for different types of magmatism and metallogenesis.

Crustal faults, penetrating to the Mohoreovĭcíc discontinuity, provide conduits for the rise of magma from mixed crustal and mantle sources. The magmas are mainly of intermediate composition and the associated porphyry copper deposits are characterized by chalcophile elements, noble, non-ferrous and rare metals, such as gold, silver, molybdenum, copper, lead, zinc, mercury, arsenic and antimony.

Basement faults, penetrating to the low velocity and high conductivity layer in the middle crust, provide conduits for S-type acid granitic magmas formed by re-melting of the crust, intruded as sheeted granitoid batholiths and stocks. The associated ore deposits are characterized by lithophile elements, such as tungsten, tin, uranium, niobium, tantalum and rare earth elements.

Faults penetrating to different depths in the crust may cause a decrease in pressure and a rise in temperature, inducing partial melting of the rocks and the mobilization of geothermal fluids, allowing different element associations, formed at different depths, to rise and accumulate nearer to the Earth's surface.

The above relationships between faulting and metallogenesis are proposed by the author; it is hoped that this proposition will be considered and confirmed by future studies. It seems that for most endogenic ore deposits, the controlling faults are mainly basement and crustal faults, indicating that metallogenesis occurs mainly near the base of the crust, and that lithospheric faults give rise to relatively few mineral deposits. Tectonism has been very strong in the Chinese continent and occurred during many periods, with different directions of stress. Slidings and ductile shear zones occur easily in the low velocity layer of the middle crust and at the Mohorovĭcíc discontinuity, in most areas of the Chinese continent, except the Qinghai-Xizang area, crust and mantle have been decoupled. The lower crust or upper mantle, which at present lies beneath the upper crust, is not the same lower crust or upper mantle, as it used to be. There is no close relationship between the lithospheric mantle or the asthenosphere and metallogenesis. Research into lithospheric tectonics is only of limited value as a guide to the exploration for mineral deposits. This is not to say that research into lithospheric tectonics should be discontinued, but the value of this research should be assessed realistically. A greater amount of research into the interior of the Earth is not likely to lead to greater success in the exploration for minerals.

The relationship between rock deformation and reservoir space for metallogeny. This problem is discussed very thoroughly in many textbooks and monographs (Chen GD, 1978; Zhai YS et al., 1993, 1997). If fissures or cavities occur in rocks during deformation, there is always the possibility that minerals may be concentrated in them to form ore bodies. This has been a central concept for the relationship between the structural geology of ore fields and ore deposits over the last fifty years.

Is it possible for ore genesis to become specific to different tectonic environments (extension, compression or strike-slip)? For example, is the formation of lead-zinc deposits related to normal faulting (including extension and detachment types) or gold deposits to the formation of ductile shear zones? Many examples demonstrate that different types of mineral deposits are not related to particular structural environments. However, this is not the case for magmatism; different types of magmatism are related to specific types of mineral deposits. The major influence of deformation on ore deposits is to determine the shape of the ore bodies. In magmatic and hydrothermal deposits, rock deformation opens up pathways for the migration of fluids and opens up spaces for the accumulation of mineral deposits. Deformation does not create new rock types, apart from fault rocks or ductile shear zones, nor does it form new ore deposits. Where fissures are formed in rocks as the result of deformation, any kind mineral-bearing fluid may pass through the rock to form accumulations of ore minerals. It would be a mistake to attribute different types of metallogenesis to specific types of deformation.

Different scales of deformation affect the scale of metallogenesis. Usually, larger scale deformational structures accumulate larger ore deposits. For example, larger sedimentary basins accumulate larger deposits of organic matter or of gypsum and halite. There are always greater accumulations of oil and gas in large-scale anticline reservoirs. Large regional fault zones, hundreds to thousands of kilometres in length and several hundred or thousand meters in width, control the migration of metallogenic fluids, and control the distribution of metallic mineral deposits across a complete metallogenic province. In south China, regional faults and metallogenic belts are NE-trending, however, within the metallogenic belts, a series of ore deposits were accumulated only along secondary WNW-trending extensional faults.

Large-scale regional fault zones have a high permeability due to numerous open fractures, favorable to fluid migration, but unfavorable to the accumulation of mineral material to form ore deposits. Not only are there no large ore deposits, but few ore deposits are found, except some "stone-like coal", i.e. argillaceous quartzite with 5%–10% carbon. When this "coal" is involved in a fault zone, the permeability is increased, and the coal is fractured and can then be used as fuel, for example, in the Yunxi, Hubei stone-like coal deposit. In addition, some large-scale fault zones, when they were compressed and became impermeable in the Neotectonic Period (since 0.78 Ma), have accumulated gas deposits,

such as the newly discovered PL 19-3 gas reservoir in southern Bohai Bay, along the Tancheng-Lujiang Fault Zone.

Meso-scale fault zones often provide fracture zones, dozens to thousands of meters in length, dozens of centimeters to hundreds of meters in width, and thousands of meters in depth in which endogenic ore deposits are accumulated. Most ore deposits occur in meso-scale fault zones.

Small-scale fault zones may form giant or super-giant deposits of copper, molybdenium, gold or uranium where there is a high concentration of micro-fissures or joints, in which ore deposits form finely disseminated vein structures, and there is no requirement for high grade ores. There is no relationship between the type and scale of deformation and the types of ore deposit.

Preservation of ore deposits by late period tectonism with uplift or depression. For ore deposits to be preserved from the time of formation until the present day, they need to remain intact and to remain buried at a suitable depth. These requirements are related closely to their tectonic history.

Ore deposits do not usually survive later tectonism; if they suffer tectonism they are easily destroyed. In the Chinese continent many ore deposits, formed before the Early Paleozoic, have been destroyed with only a few being preserved. Major tectonism in the Mesozoic–Cenozoic was related to the formation of many new ore deposits, but also destroyed many former deposits. It cannot be said that a great many ore deposits were formed in Mesozoic–Cenozoic, and it is really the case that a high proportion of Mesozoic–Cenozoic deposits has been preserved. This has the important result that the Mesozoic–Cenozoic appear to be the main metallogenic epochs, because ore deposits, formed in the Early Paleozoic and earlier periods, are preserved only in areas, such as Northwest China, the western Yangtze area and Inner Mongolia which suffered only weak tectonic deformation at later periods during the Mesozoic–Cenozoic.

The most of structures controlling the formation of ore deposits in the Mesozoic–Cenozoic metallogenic epochs were developed along existing zones of tectonic weakness. The orientation of stress has changed many times, breaking the continental blocks into much smaller pieces, so that the scale of deformation was rather limited. This may be the reason why many small or intermediate scale, but rich, ore deposits are found in the Chinese continent.

Conditions for the formation of economic ore deposits are rather exacting. In addition to favorable geological conditions, economic and technical conditions must also be satisfied. In China, at present, economic and technical considerations limit the depth to which ore deposits can be worked to less than a kilometer beneath the surface, and for fluid resources to less than 6 km. If buried ore deposits are too deep the cost of exploitation will be too high and the deposit cannot be worked economically. Shallow deposits are likely to be weathered and eroded. The depth at which a deposit is now found is unlikely to be the depth at which it was formed. After ore deposits or hydrocarbon deposits have been formed, appropriate uplift is required to make them accessible. Integrated research on the depth of formation of deposits and the geomorphology of ore fields is required to identify the effects of recent vertical movements. So far there has been very little research into these effects.

14.3 Intraplate Extension Mineralization

From research into regional metallogenic epochs, metallogenic belts, the main controlling structures for ore deposits and recent data on large and intermediate scale ore deposits (Ye JH, 1988) (personal communication), it is found that of 1,573 endogenic and exogenic solid ore deposits, 1,255 were controlled by regional extension, forming 79.8% of total; 39 ore deposits were controlled by local extension, forming 2.5% of the total; 123 ore deposits were controlled by compression, forming 7.8% of the total; tectonic influences were unclear in 156 ore deposits, forming 9.9% of the total. The formation of all oil, gas and coal reserves was controlled by regional or local extension.

The data given above demonstrate that the most important endogenic or exogenic phases of mineralization in the Chinese continent were due to intraplate extension, including ore deposits formed on continental shelves and in subsiding rift basins. The formation of these deposits was unrelated to subduction or collision. Ore deposits filling extensional or transtensional faults, controlled by regional extension, include most of the magmatic and hydrothermal deposits. By ore deposits, influenced by local extension, it is found that even in a general compressive regime many extensive cross faults may be formed, which are filled by magmatic and hydrothermal materials. Only the occurrence of a few ore deposits, such as the chromium, platinum and blue asbestos deposits, related to the emplacement of cold ultramafic bodies, and the iron and graphite deposits due to regional metamorphism were formed and emplaced directly by regional compression.

These conclusions differ from the prevailing opinion, according which orogenesis (collision zone) was the cause of the main episodes of mineralization in China, and also from the opinion that the scale of deposits is related to the intensity of collision (Qiu XP, 2002). Collision should not be confused with subduction; there is a great difference between collision and subduction. When ocean crust is subducted beneath a continent to a depth of ~100 km, partial melting of the rocks occurs, producing intermediate volcanism and generating many large and famous super-large porphyry copper, molybdenum and gold deposits of the world, which are related to this magmatism. However, in collision zones, as has been described above, many ramp thrusts, subduction and obduction zones may be formed simultaneously, so that the margins of the continental blocks become indented in three dimensions. In this situation if partial re-melting of rocks occurs at depth, it is difficult for magma to rise towards the surface to be emplaced or erupted. Collision zones are belts in which different types of rocks and elements become mixed, but minerals are not easily concentrated to form mineral deposits in these zones.

Recently, many ore deposits have been found in collision zones. When isotopic chronology for the formation of rocks and ore deposits was less well developed it was presumed that collision zones and the formation of ore deposits occurred simultaneously. Some deposits were formed before the collision, such as the hydrothermal and fumarolic deposits formed during the extension of oceanic floor or in aulacogens. The greater part of the deposits found in collision zones are post-collision deposits, not formed during the collision, and are not different from those formed during intraplate deformation. In collision zones there are foliations, zones of weakness and faults developed during the collision period. When in later tectonic periods, the direction of maximum principal compressive stress is nearly parallel to the strike of these pre-existing foliations, zones of weakness or faults, these undergo extension, providing channels for the migration of ore fluids and the accumulation of ore deposits. A good example is provided by the Qinling–Dabie Zone, where after the collision during the Yanshanian and Sichuanian Tectonic Periods, many ore deposits were formed, but only a few of these deposits were actually formed in the Triassic during the collision period. Many porphyry copper deposits found in the Gangdise Zone were formed in the Miocene (at around 15 Ma), after the main Himalayan collision period (about 34 Ma). In the collision period, deformation not only permitted the migration of ore-fluids, but also allowed their dispersal and disappearance, so that elements and ore minerals were less easily concentrated. However, the highly deformed rocks in the collision zone may provide a suitable environment for mineralization in later tectonic periods.

In western China, since the Himalayan Tectonic Period paleo-collision zones have been uplifted gradually forming mountains. Similarly many endogenic deposits were uplifted nearer to the Earth's surface, where they are more easily explored and exploited. However, stable blocks between collision zones have been subject to subsidence to form sedimentary basins. Endogenic deposits may have been formed in these basins buried beneath sedimentary systems of Mesozoic and Cenozoic, but because they occur at depths of several thousand meters they are much too deep to be exploited economically. Due to the different conditions of preservation, the exploration for mineral deposits in western China has been concentrated in paleo-collision zones and along their margins. But this cannot be used as evidence that collision is the most suitable environment for metallogenesis.

14.4 On the Tectonics and Prospect of Mineral Resources

Recently, the relationship between tectonics and prospects for the occurrence of mineral resources has attracted more attention from tectonic researchers. It is easy to prepare an account of the existing relationships between tectonics and known ore deposits. However, it is much more difficult to forecast the prospects for mineral resources on the basis of tectonic environments. In this book, the several limited and immature proposals for the value of the study of tectonics in prospecting for mineral resources will be discussed. Prospects for the discovery of endogenic deposits in eastern China, prospects for the discovery of ore deposits in western China and the formation of accumulations of oil and gas in depression basins in eastern China during the Cenozoic will be discussed:

Prospect for the exploitation of endogenic deposits in eastern China. During the last one hundred years, especially in the last fifty years, since the establishment of modern geological surveys, exploration for ore deposits has proceeded systematically. Initially many outcrops of endogenic and exogenic deposits were discovered, mainly in eastern China, but subsequently discoveries of buried endogenic deposits have gradually increased. According to the statistics of the 280 large-scale deposits, found before 1965 in the whole of China, only 28 buried endogenic deposits were discovered, accounting for 10% of the total, while between 1965 and 1983, 98 large-scale deposits were found, half of which are buried endogenic deposits (Shi MK, 1993). During the last twenty years, as for oil and gas exploration, all the newly discovered endogenic deposits are buried indicating that the exploration for buried endogenic deposits in eastern China has reached a mature period.

It is not usually necessary to search for buried nonmetallic mineral deposits, apart from some very high value nonmetallic minerals, such as diamonds. So far endogenic deposits in China have not been exploited to depths of more than 500 m. However, nearly half of the endogenic deposits being exploited are facing shortages and the situation is reaching crisis point. It would be technologically and economically feasible to extend the depth of exploitation of endogenic deposits in China to 1,500 m. In China, at the present time, it is urgently necessary to prospect for new buried endogenic deposits, especially in known ore provinces and near old ore fields.

Prospecting adjacent to presently exploited meso-and epi-hydrothermal ore fields for buried ore deposits is very likely to prove successful. At depth it is possible to find mesothermal and epithermal deposits formed at temperatures of 100–300°C, or mesothermal and hypothermal deposits formed at temperatures of 300–500°C. In high permeability fault zones, hydrothermal fluids would be at almost the same temperature and have similar characteristics to the ore deposit (Wan TF, 1994). However, sudden transitions in the temperatures of formation and the typo-morphic characteristics of mineral associations have been discovered near the Earth's surface. For example, in the Shanggong gold deposit, Luoning, west of Xiongershan in western Henan, formed in Cretaceous, there is mesothermal gold deposit extending up to 1,700 meters above sea level, and a mesothermal lead deposit extending down to 1,700 meters above sea level. Eastwards, on the eastern side of Xiongershan, in the Qiyugou gold deposit, Songxian, the height of the transition boundary decreases to about 400 meters above sea level (Wan's personal data). In the Nandaxian ore field, in the Jurassic volcanic system of Hebei, there is a mesothermal gold deposit in sulphide quartz veins up to 750 meters above sea level, there is a gold deposit in an alteration zone, controlled by micro fissures, between 750 and 710 meters above sea level, and there are mainly mesothermal copper, lead-zinc deposits down to 630 meters above sea level (Wei Fuyou, 1991). In addition to the differences in the depth for exploration, metallic elements and types of buried ore deposits may be altered by regional chemical characteristics.

Depending on these examples it can be predicted that copper, lead, zinc and molybdenum deposits, apart from gold, will occur at depth of 1,000–1,500 m below sea level beneath the East Shandong gold fields. In the hypothermal ore fields in the Cathaysian Plate which yield tungsten, niobium, tantalum and rare earth elements, it seems likely that similar deposits and veins would be found vertically beneath these deposits, because of the former 300–400 m exploration depth. In mesothermal and epithermal ore fields, yielding Pb, Zn, Cu, Au, Ag, U, fluorite and pyrophyllite, there are very good prospects of finding

mesothermal and hypothermal ore deposits (W, Nb, Ta, Pb, Zn, Cu, Au, U, and rare earth elements) at depth in those areas. In the south Yangtze Plate, characterized by tin and lead-zinc deposits near the surface, it is probable that tin deposits will be found around the margins of the plate. It should be said that it is a little bit difficult to find further deposits vertically beneath recent hypothermal tin deposits, but below other mesothermal deposits the chances of finding further meso-and hypo-thermal deposits of tin and lead-zinc are rather more. Usually the exploration depth of ore deposits is only less than 500 m of depth in recent China, so even at the deep part of hypothermal tin deposits, the exploration should be undergone to find the buried ore deposits at 1,000–1,500 m deep.

Remote sensing has shown that there are a large number of ring structures in eastern China, in areas in which there is not much limestone, so that the rings are not sinkholes or poljes (karst topography). Only a few ring structures are thought to be meteorite craters. Most of these ring structures are developed in magmatic areas, so that they may be caused by intrusion of a buried magma at depth, formed by collapse along ring faults when the magma is cooled. If in existing ore provinces, such as eastern Shandong, south China, Yanshan, and western Henan, buried magmatic intrusions less than 1–2 kilometers deep are discovered by geophysical exploration, it is hoped that on the top of the intrusion will be found an ore deposit similar to the Olympic Dam deposit of Australia, with ore minerals dependent on the geochemical characteristics of the tectonic blocks. If this type of deposit is required there are many ring structures in eastern China to choose. This project would require high risk, large-scale investment to locate endogenic deposits related to buried shallow intrusions. Such a project could hardly be sponsored by a small mine without the support of the government or a major financial group. If it is thought desirable to develop exploration in eastern China a major effort should be made to find these types of deposits. The author thinks that in the long term it will be necessary to undertake such a project.

In the deep exploration for hydrothermal deposits, the characteristic patterns of arrangement of vein arrays should be appreciated. Because horizontal stress is always greater than the vertical stress, the orientation of stresses controls the development of vein systems throughout their geological history. At depth all ore-bearing veins have an en echelon arrangement in plan and an angle of dip in profile. As vein systems develop, individual veins are initiated at a regular distance from each other so that there will be intervals between adjacent veins in which no ore-bearing veins are present. This distribution of veins is so common and so characteristic of vein systems that it should be possible to construct a quantitative three-dimensional mathematical model of a vein array to predict accurately the size and distribution of the constituent ore bodies (Wan TF, 1988). Before this characteristic arrangement of ore bodies was appreciated, geologists frequently drilled a large number of boreholes along the strike and down the dip of existing ore vein, without locating any further ore bodies, so that mine managers had no alternative but to close the mine.

Prospect for the discovery of endogenic ore deposits in western China. Compared with eastern China there are good prospects for exploration for ore deposits in western China at Earth surface. To the west of the Helanshan–Liupanshan–Hengduanshan Mountains, there are a great many outcrops of ore deposits waiting to be explored. In western China, the Qiangtang, Tarim, Qaidam and Zunggar areas were previously stable blocks, but most of them are now covered by large Mesozoic–Cenozoic sedimentary basins. The exposed areas are former collision zones, thus it is necessary to search and explore for endogenic deposits in these collision zones. According to research on the regional tectonic evolution of western China discussed earlier in this book, this area has been influenced by the near N-S (NNW, S-N, NNE and NE) shortening of plates since the Early Paleozoic, quite different from the situation in eastern China. Due to tectonic activity endogenic metallogenesis occurred during the Paleozoic in the areas to the north of Tarim and Qaidam, and during the Mesozoic and Cenozoic to the south.

The following four types of ore deposit are the main targets in western China:

(1) Magmatic, sea floor hydrothermal, metamorphic or sedimentary deposits, found along near east–west regional tectonic lines, were formed mainly before the collision. After their formation, multi-collision and shortening, the deposits were incorporated into the collision complex and gradually up-

lifted towards the Earth's surface. Typical deposits are copper and lead-zinc fields in Altay, massive hematite and pyrolusite at Motosala, siderite at Wutonggou, Kalatongk, copper and nickel deposits at Huangshan in northern Tianshan Mountains, the Qilic iron deposit in western Kunlun, the lead-zinc and silver deposits at Baiyinchang and the iron deposit at Jingtieshan, Gansu.

(2) Deposits, formed in the collision period, are controlled by compressive or trans-pressive structures, with strikes parallel to the regional tectonic trend. Typical examples are the Luobusha chromite deposit in Xizang and many small chromite deposits in Tianshan and Qilianshan. These are related to ultra-mafic rocks and were emplaced cold, during shortening, at a shallow depth within the collision zone.

(3) Magmatic and hydrothermal deposits formed in syn-collision or post-collision periods are controlled by NE or NW trending trans-tensional fault zones, near N-S extensional faults or E-W reverse faults. These deposits were developed in local extensional positions in a regional compressive environment. Well-known representative deposits are the Hatu and Axi gold deposits in Xinjiang, the Puchang titano-magnetite and coulsonite deposits of magmatic type formed in the post-collision period in south Tianshan, the Kalama copper deposit in western Kunlun, the Tamu lead-zinc deposits, the Hetian jade deposits in south Xinjiang and the Xitieshan lead-zinc deposit in Qinghai. Recently, many porphyry copper deposits (intracontinental type) have been found in the Gangdise Zone, formed between 14 and 15 Ma, after the main Himalayan Collision Period, controlled by N-S trending extensional faults or E-W trending reverse fault (Hou ZQ et al., 2003; Rui ZY et al., 2003; Li GM and Rui ZY, 2004). Many ore bodies in the Yulong porphyry copper field in eastern Xizang always occur at the intersection between NNW-trending main faults and ENE secondary extensional faults. The Mang'ya asbestos deposits of Qinghai were formed in an en echelon extensional system by sinistral strike-slip faulting along the Altun Fault in the Cenozoic, accompanied by widespread serpentinization.

(4) Sedimentary deposits such as sylvine, celestine, borax and gold placer deposits are found in recent valleys and in the sedimentary basins on the stable blocks.

Ring structures, in the Chinese continent, no matter whether caused by meteorite craters or by other processes, are always worthy of investigation. On the global scale there are more than 150 giant meteorite craters, several to hundreds of kilometers in diameter. Metallic ores occur in association with meteorite craters throughout the world, 20% of these deposits are of economic value (Grieve, 1997). For example, the Sudbury nickel, copper and platinum group deposits, the Carswell uranium deposit and the Boltysh oil shale deposit with 4.5 billion tons reserves were all formed in meteorite craters. It is disappointing that no meteorite craters or deposits associated with meteorite craters have yet been found in China. In eastern and southwestern China, meteorite craters would have undergone deformation in later tectonic periods and may not have been preserved, or might be difficult to recognize, and in northwestern China, although there is less deformation, meteorite craters may be buried beneath Mesozoic–Cenozoic sediments. This may explain why meteorite craters have not so far been found on the Chinese continent.

Fault-depression zones and the accumulation of oil and gas in eastern China during the Cenozoic. Fault-depression zones formed sedimentary basins developed with four different orientations in the eastern Chinese continent during the Cenozoic. Although these fault-depression zones occur at the Earth's surface, at depth they are controlled by basement faults, and their development has been influenced by changes in the tectonic stress field. They also have different prospects for the formation of oil and gas fields. These characteristics should be considered in exploration and exploitation.

The four directions are: (1) E-W fault-depression zones; (2) N-S fault-depression zones; (3) NE fault-depression zones; (4) NW fault-depression zones. The four fault orientations which have controlled the formation of the fault-depression basins will be described and the prospects for the occurrence of oil and gas resources in these basins will be discussed, the Bohai Bay provides a good example (Fig. 14.9).

E-W trending fault-depression zones are represented by the Jiyang and Huimin fault-depressions containing the Shengli Oil Field, the Qikou fault-depression with the Dagang Oil Field, the Nanpu fault-depression with the East Hebei Oil Field, and the Bozhong fault-depression in the south central part of Bohai Bay, which is the largest E-W fault-depression in Bohai Bay (Fig. 14.9). These fault-depression

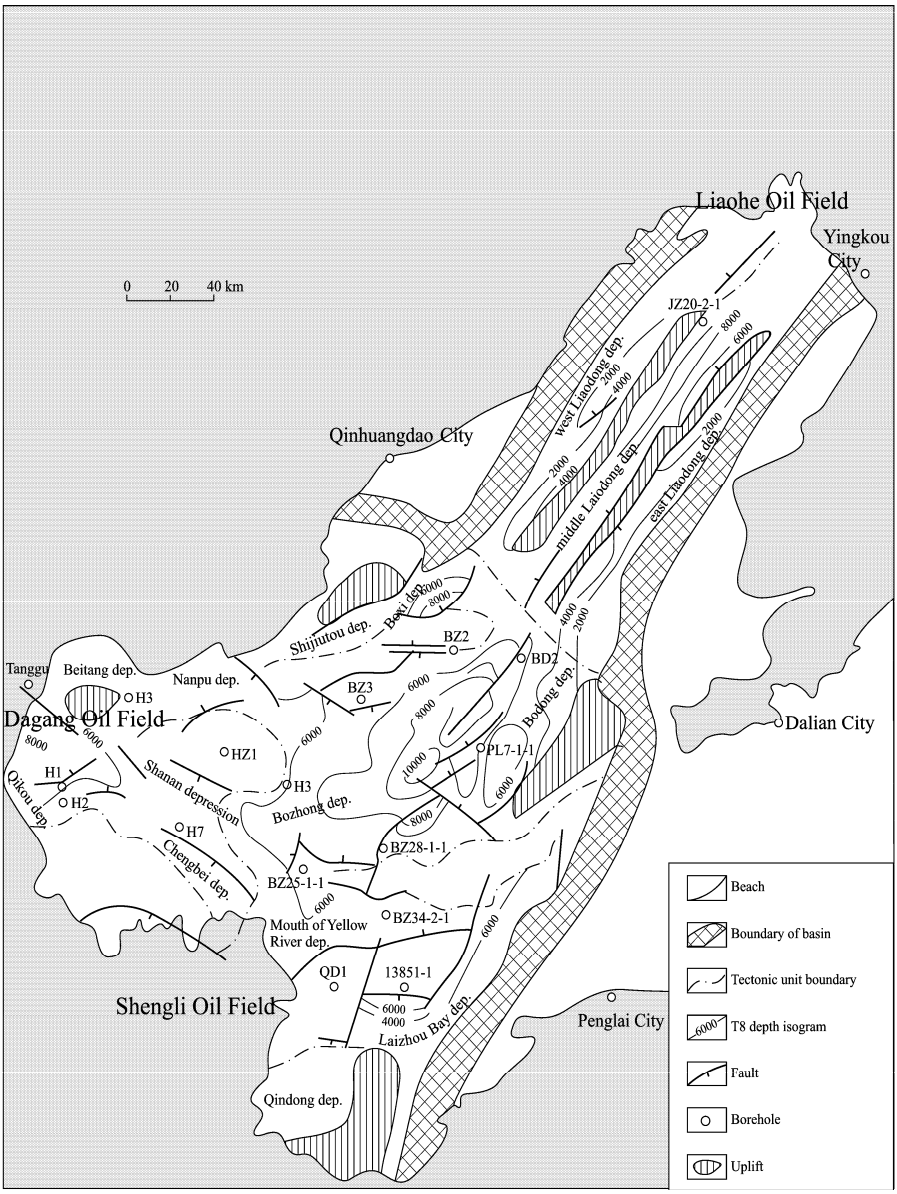

Fig. 14.9 Tectonic sketch of Bohai Bay (Wang MM, 2003, with permission of Wang MM).

zones were developed as the result of E-W shortening during the Eocene and Oligocene, which caused strong N-S extension, to form deep depressions and the deposition of a great thickness of sediments, favorable to the formation and accumulation of hydrocarbons. However, during the Miocene to Early Pleistocene, in response to N-S shortening, the near E-W trending faults tended to be closed. In the

present tectonic stress field, with an ENE-WSW shortening direction in north China, and an NNW-SSE extension direction, E-W trending faults in north China show a small amount of extension, opening the pathways for the secondary migration and further accumulation, or loss, of oil and gas.

Fault-depression basins usually develop by the movement along syn-sedimentary (growth) faults penetrating deep into the basin. Paleogene sediments in the fault-depression show obvious differences in thickness on either side of the faults, with a distinct growth index, but Miocene to Early Pleistocene sediments show no difference in thickness on either side of the faults, but again Middle Pleistocene to Holocene sediments show a difference in thickness, indicating a further syn-sedimentary displacement. These fault-depression basins provide a favorable environment for the formation of large-scale oil and gas reservoirs, as has been found in the oil and gas fields of Bohai Bay. It should also be noticed that WNW trending faults show recent slight opening, and are favorable for the accumulation of oil and gas, while ENE trending faults exhibit a greater amount of recent opening, leading to the major loss of oil and gas. In Bohai Bay the WNW trending faults are most favorable for the formation of oil and gas reservoirs.

Apart from continuously seeking to locate oil and gas reservoirs near existing oil and gas fields (such as Shengli, east of Dagang, and Nanpu, East Hebei), exploration should also be extended into the Bozhong depression, the largest area for possible Cenozoic hydrocarbon accumulation in Bohai Bay, which has not yet been explored and exploited; the prospects for success in this basin are very good. However, exploration in the Bozhong depression should be also extended below the depths reached by recent exploration, as the Paleogene oil and gas reservoirs quite likely lie at greater depths. Where faults were reactivated at a later period, oil and gas may have migrated again along faults, and have accumulated at a shallower level within the Neogene. Therefore the possibility of reservoirs developed within the Neogene related to E-W, N-S NE or NW faults should be also examined during seismic exploration. In the Bohai Bay the sea floor lies at a depth of 40–50 meters below sea level. Exploration and exploitation of oil reserves is always much more difficult beneath the sea than on land.

N-S trending fault-depression zones are represented in Bohai Bay by the PL19-3 oil-gas field in the Miaoxi depression (Fig. 14.9) and in the South China Sea by the Yinggehai gas field, both controlled by N-S or NNE trending faults. Generally, it would seem unlikely that oil and gas reservoirs could be found along major fault zones, such as Fault No.1 of Tancheng-Lujiang Fault Zone, as a high proportion of the hydrocarbons is likely to have been lost. But if conditions for the accumulation of hydrocarbons existed during the Paleogene and Neogene, it is possible that reservoirs have been formed along these major faults. In eastern China N-S faults, formed during E-W shortening, were closed and sealed during the Eocene and Oligocene. During N-S shortening in the Miocene-Early Pleistocene, the faults were commonly opened and became zones of high permeability. This was the main period for upward migration and loss of oil and gas. However, during Neogene the amount of E-W extension in eastern China was not very large, and the period in which the faults were opened was not very long, thus oil and gas reservoirs may have formed near N-S trending faults. Since the Middle Pleistocene the direction of the maximum principal compressive stress in eastern China changed to near E-W, so that the N-S faults were closed and sealed, once again providing conditions for the formation of oil and gas reservoirs.

The thickness of the Paleogene sediments on either side of the N-S growth faults is the same, indicating that there was no displacement during sedimentation, while the thickness of the Neogene sediments is obviously different, indicating displacement, again there has been almost no displacement since the Middle Pleistocene. The discovery of reservoirs along N-S trending faults was the major success in the exploration for oil-gas in Bohai Bay. The discovery of reservoirs, especially found in Miaoxi depression, will encourage exploration in Laizhou Bay, Liaodong Bay, the East China Sea, the southern Yellow Sea, northern Jiangsu Basin, eastern Hefei Basin, Dongting Lake and Boyang Lake. On the eastern margin of the south Yellow Sea, in Korean territorial waters, a gas field similar to the PL19-3 field may be found (Wan TF, 2002) along an N-S trending en echelon fault zone (Hao TY et al., 2002).

The Yinggehai Gas Field is controlled by near N-S trending secondary faults developed in an NW-SE rift zone, due to transtension in the Red River strike-slip fault zone (Fig. 14.10). In view of recent disco-

veries, these faults should be re-examined. The source formations occur in the Paleogene and Neogene systems. The N-S trending faults were opened, and as zones of high permeability in the Neogene and Early Pleistocene, allowed hydrocarbons to migrate and accumulate at shallower levels. It is likely that shallow reservoirs will be found in the Neogene system along N-S trending faults. However influenced by E-W trending compression of Neotectonic Period, N-S trending faults are closing and form the good condition for reservation of gas. So that in exploration, shallow seismic data should be re-examined, paying particular attention to near E-W trending vertical seismic profiles and isochronal surfaces.

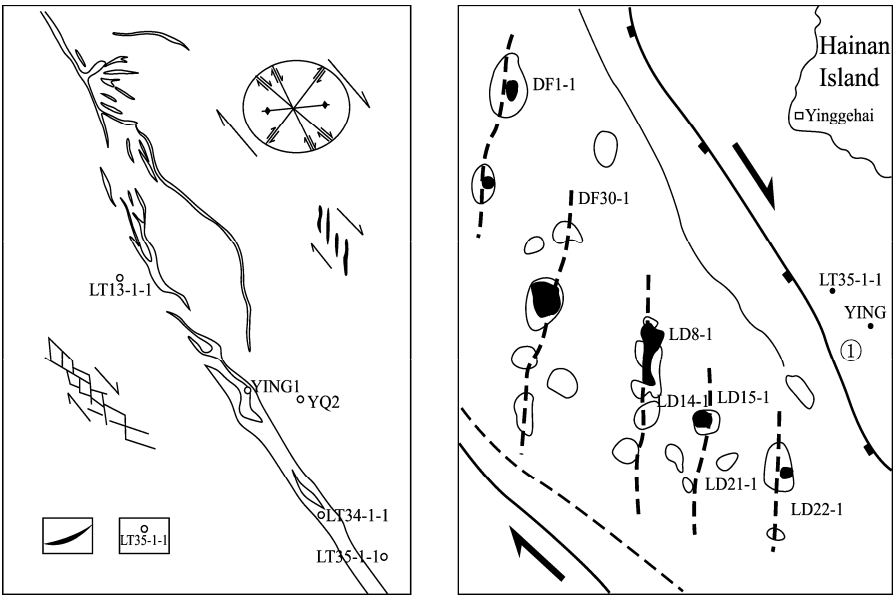

Fig. 14.10 Tectonic sketch of Yinggehai Gas Field, in South China Sea, southwest to Hainan Island (Zhang QM et al., 1996).

NE trending fault-depression basins are well developed around Bohai Bay (Fig. 14.9), in northern Jiangsu and in the south Yellow Sea. However, fault-depression basins in this direction are not very favorable for the accumulation of oil and gas. A series of en echelon, intermediate and small-scale oil and gas reservoirs occur along NE-SW faults. In Bohai Bay the reservoirs are distributed in three zones: the Lower Liaohe (River) and Liaodong Bay; the Huanghua (Yellow Sea) depression, the western on-land part of the Dagang Oil Field; the middle Hebei and Dongpu depressions of North Henan. There are many depressions of this kind in northern Jiangsu and the southern Yellow Sea. In the Paleogene this type of depression was controlled by dextral strike-slip faults with several to dozens of kilometers of displacement. In the Neogene and Early Pleistocene they were controlled by sinistral strike-slip faults with several kilometers of displacement; since Middle Pleistocene by weak dextral strike-slip and normal faults, with only several hundred meters of displacement. The effects of the changing movement directions, with small dextral or sinistral strike-slip displacements, are obvious where there are major differences in the competence of the rocks, especially where there are gypsum-halite formations and mudstone layers, or near abrupt changes in the direction of strike of the faults, where the more competent formations form traps for oil and gas. Because the greatest strike-slip displacements occurred during the Paleogene, the traps are due mainly to the effects of dextral strike-slip faulting. The strike of

a single trap is often N-S and a series of traps form a pattern of NE-trending dextral strike-slip faults, typically seen in the Lower Liaohe Basin (Li HW and Xu K, 2001). Where the rocks are of diverse lithology, or are cut by many other faults, the en echelon pattern may not be clear. The best way to discover these traps is to analyze in detail horizontal isochronal surfaces in three-dimensional seismic data. If only cross sectional seismic profiles are examined, it is easy to miss the trap structures, but difficult to recognize the effects of the strike-slip faulting.

In the southern Yellow Sea and the northern Jiangsu areas, there are many unexplored main E-W and N-S trending faults as exploration of oil and gas is very difficult. Since these areas are located between two major N-S fault zones: the Tancheng–Lujiang Fault and the eastern marginal fault zones of the Yellow Sea, important targets for future oil and gas exploration will be adjacent to secondary N-S and E-W faults (Wan TF, 2010).

NW trending fault-depression basins occur in eastern China. An NW-trending fault-depression basin is located along the seismically active Beijing-Penlai hidden fault zone in Bohai Bay (Fig. 14.9). There are also the Dachang-Wuqing, southeastern Nanpu and Chengbei small fault-depression basins. These NW-trending fault-depression zones were formed mainly by sinistral strike-slip movements during the Paleogene, dextral strike-slip faulting during the Neogene and Early Pleistocene, and sinistral strike-slip faulting again since the Middle Pleistocene. None of these faults systems have yet been examined in detail.

The most important NW-trending fault-depression basin is the Neogene Yinggehai fault-depression system to the southwest of Hainan Island and in Beibu Bay (Fig. 4.10). As the result of dextral strike-slip movements along the Honghe (Red River) Fault Zone during the Neogene, a series of N-S trending extensional faults with mud diapiric structures formed, and subsequently a major fissure gas field developed on top of these diapiric structures (Zhang QM et al., 1996). Since the Middle Pleistocene E-W shortening and compression have closed the N-S faults and fissure zones, so that the gas has been trapped and not dispersed or lost.

Both NW and NE trending fault-depression zones were developed at the same time, only the directions of strike-slip faulting are different, however they can be explored and may give different results. There are different and complex prospects for oil and gas exploration in the four differently trending Cenozoic fault-depression basin systems in eastern China.

These fault-depression basin systems should be systematically researched and explored using different play concepts to provide new breakthroughs in the exploration for oil and gas in China. E-W (or WNW) and N-S (or NNE) trending fault-depressions usually were more favorable for the formation of giant oil-gas fields in East China.

Although the discovery and exploitation of mineral resources in China are at present more difficult than in the past, the prospects for the discovery of new mineral resources are bright. There is long way to go before all the mineral deposits in China will have been exhausted. More exploration is required in eastern China in the search for buried deposits, and in western China in the search for outcrops of new mineral deposits, to meet China's urgent need for additional mineral resources.

In recent years, because the responsibility for exploration has been given to the mining companies themselves, exploration has not been carried out according to government plans. Many mining companies, running short of mineral resources or with low profits, are content to maintain their present situation until their mineral resource is exhausted. There has been no strategic research, no unified planning and no specific plans for the development and use of resources throughout the whole country. Now there is a serious shortage of reserves of most mineral and oil-gas resources in China. A concentrated program of exploration for mineral resources on a national scale is urgently required; this is an economic, social and political problem, beyond the scope of this volume.

In this volume the main metallogenic epochs and zones, and the influence of tectonics on mineralization in China have been discussed, based on the most recent theories about tectonics, the importance of metallogenesis during intraplate extension in the Chinese continent has been emphasized, the prospects for the discovery of new mineral resources in the Chinese continent have been assessed from the view

point of tectonic evolution. It is hoped that the above discussion has strengthened the case for a systematic program of prospecting and exploration for mineral and oil-gas resources in China, as a national priority.

References

Chen GD (1960) The Activation of Platforms and Their Significances in Deposits Investigation. Geological Publishing House, Beijing (in Chinese).

Chen GD (1978) Methods of Metallotectonic Researches. Geological Publishing House, Beijing (in Chinese).

Chen RS (1994) Geology of Petroleum and Natural Gas. China University of Geosciences Press, Wuhan (in Chinese).

Cheng YQ (1994) An Introduction to Regional Geology of China. Geological Publishing House, Beijing (in Chinese).

Grieve RAF (1990) Terrestrial impact: the record in the rocks. Meteoritics 26: 175–194.

Guo WK (1987) Manual of Ingrown Metal Metallomaps (1:4,000,000). Geological Publishing House, Beijing (in Chinese).

Hao TY, Mancheol S, Wang QS et al (2002) A study on the extension of fault zones in Yellow Sea and its adjacent areas based on gravity data. Acta Geophysica Sinica 45(3): 385–397 (in Chinese with English abstract).

Hou ZQ, Qu X, Wang SX et al (2003) Re-Os age of molybdenite in Gangdise porphyry copper zone of Xizang: timing of metallogenesis and dynamic background. Science in China D 33(7): 609–618.

Huang JQ, Zhang ZK, Zhang ZM et al (1965) Eugeosynclines and miogeosynclines of China and their development of multi-gyration. In: Professional Papers of Chinese Academy of Geological Sciences, Section C: Regional Geology and Structure Geology, no.1, 71 China Industry Press, Beijing (in Chinese).

Huang TK (Jiqing) (1945) On the major structural forms of China. Geological Memoirs, ser. A, no. 20, 165.

Huang TK (Jiqing) (1960) The main characteristics of the geological structure of China: preliminary conclusions. Acta Geologica Sinica 40(1): 1–37 (in Chinese with English abstract).

Jia CZ, He DF, Shi X et al (2003) Himalayan movement and reservoir formation in late stage. In: Division of Structural Geology and Tectonics, Geological Society of China et al (eds) Proceedings of Controlling of Sedimentary Basins during Himalayan Stage and Oil and Gas Reservoirs Formation in Late Stage, 11–48. Oct. 10–12, 2003, Huairou, Beijing (in Chinese).

Li CY, Wang Q, Liu XY et al (1982) Tectonic Map of Asia (1: 8,000,000) and Its Specialties. Geological Publishing House, Beijing (in Chinese).

Li CY, Wang Q, Liu XY et al (1984) The evolution of asian tectonics. Bulletin of the Chinese Academy of Geological Sciences (10): 3–12. Geological Publishing House, Beijing (in Chinese).

Li GM, Rui ZY (2004) The ages of metallogenesis and petrogenesis of porphyry copper deposits in Gangdise metallogenic zone of Xizang. Tectonics and Metallogeny 28(2): 165–170 (in Chinese with English abstract).

Li HW, Xu K (2001) The dextral strike-slip faulting of Tan-Lu fault zone and the structural oil fields distribution in Liaohe basin. Earth Science Frontiers 8(4): 467–470 (in Chinese with English abstract).

Li SG (Lee JS) (1947) Fundaments and methods of geological mechanics. In: Geological Mechanics Methods. Science Press, Beijing (in Chinese).

Li SG (1962) An Introduction to Geomechanics. Geological Publishing House, Beijing (in Chinese).

Qiu XP (2002) Collisional orogenic belt and metallogenetic divisions. Geological Bulletin of China 21(10): 675–681 (in Chinese with English abstract).

Rui ZY, Hou ZJ, Qu XM et al (2003) Metallogenic age of porphyry copper deposits in Gangdise and uplift of Qinghai-Xizang Plateau. Deposit Geology 22(3): 218–225.
Shi MK, Xiong CY, Jia DY et al (1993) Comprehensive Research and Prospect on Burial Deposits of Nonferrous Metal in Hunan, Guangxi, Guangdong and Jiangxi Provinces. Geological Publishing House, Beijing (in Chinese).
Song SH (1989) Deposits in China. Geological Publishing House, Beijing (in Chinese).
Song SH (1992) Atlas of Mineral Resources of China (1: 5,000,000). Geological Publishing House, Beijing (in Chinese).
Wan TF (1988) Paleo-tectonic Stress Field. Geological Publishing House, Beijing (in Chinese).
Wan TF (1994) Intraplate Deformation, Tectonic Stress and Their Application for Eastern China in Meso-Cenozoic. China University of Geosciences Press, Wuhan.
Wan TF, Zhao WM (2002) On the mechanism of intraplate deformation in Chinese continent. Earth Science Frontiers 9(2): 451–463 (in Chinese with English abstract).
Wan TF, Hao TY (2010) Mesozoic–Cenozoic tectonics of the Yellow Sea and its oil-gas exploration. Acta Geologica Sinica 84(1): 77–90.
Wang MM et al (2003) Petroleum prospecting region and target assessment around Bohai Bay Areas. An unpublished report for Exploration and Research Institute of China National Petroleum Company.
Wei FY (1991) Discussion on the height of gold deposit of continental volcanic type. Geological Science and Technology for First Brigade of Metallury Geology 4 (total 34): 23–26 (in Chinese).
Weng WH (1927) Crustal movements and volcanic activities of east China since Mesozoic. Journal of Geological Society of China 6(1): 9–36.
Weng WH (1929) Mesozoic orogenic movement of east China. Journal of Geological Society of China 8(1): 33–44.
Xie JR(1936) The formation age and distribution area of Chinese mineral resources. Geological Review 1(3): 363–380 (in Chinese).
Xie JR (1952) Ideas about mining in future proposed from some roles of Chinese mineral resources. Acta Geologica Sinica 32(3): 219–231(in Chinese).
Zhang QM, Liu FN, Yang JH (1996) Overpressure system and hydrocarbon accumulation in the Yinggehai basin. China Offshore Oil and Gas (Geology) 10(2): 65–75 (in Chinese with English abstract).
Zhang WY et al (1959) An Outline of Tectonics of China. Science Press, Beijing (in Chinese).
Zhang WY (1983) Sea and Continental Tectonic Map of China and Adjacent Areas (1: 5,000,000). Science Press, Beijing (in Chinese).
Zhang WY (1984) An Introduction to Fault-block Tectonics. Petroleum Industry Press, Beijing (in Chinese).
Zhai YS, Yao SZ et al (1992) Metallogeny of Ion, Copper and Gold in Lower and Middle Reaches of Yangtze River. Geological Publishing House, Beijing (in Chinese).
Zhai YS, Lin XD (1993) Structure of Mineralization Fields. Geological Publishing House, Beijing (in Chinese).
Zhai YS, Zhang H, Song HL et al (1997) Macroscopic Structures and Superlarge Ore Deposits. Geological Publishing House, Beijing (in Chinese with English abstract).
Zhai YS, Deng J, Li XB (1999) Essentials of Metallogeny. Geological Publishing House, Beijing (in Chinese with English abstract).
Zhan MG (1994) Research on Mesozoic tectono-magmatism-metallogeny and regional minerallization of South China. Dissertation, Yichang Institute of Geology and Mineral Resources (in Chinese with English abstract).

Chapter 15
Discussion on the Dynamic Mechanism of Global Tectonics

After the evolution of the Chinese continent was described, as presented in this volume, many researchers and students frequently pose the problem of the mechanisms which control the movements of the lithosphere plates, and ask why directions of movement and compression have been changed through the Earth's history including the evolution of Chinese continent. These are major problems confronted by all geoscientists. The dynamic mechanisms of global tectonics are generally considered to lie outside the scope of courses on the tectonics of China, so that it would be possible to avoid these difficult problems in this book. However, it is not possible to discuss the dynamic mechanisms which have affected the Chinese continental plate, without considering the whole field of global tectonics. In order that readers may understand the present status of research into global tectonic mechanisms, all the reasonable hypotheses proposed in the past, and those being considered currently are reviewed, analyzed and commented upon.

Many eminent geoscientists have ventured opinions on these problems, which would seem to be resolved easily. In fact, these problems are still very difficult to be settled which are embarrassing the geoscientists, and provide them with the greatest theoretical challenge. It seems that the present day is not the proper time to solve the problems definitively. The study of tectonics is still at the stage of data accumulation. No new theories are proposed in this account, but existing theories of the dynamic mechanisms responsible for driving global tectonics are reviewed. The different hypotheses proposed to explain global plate tectonics, new advances in plate tectonic theory, and the mantle plume and meteorite impact hypotheses, which are the most popular dynamic mechanisms proposed at the present time for driving plate tectonics, will all be discussed.

15.1 Review of Hypotheses about Global Tectonic Dynamics

Over the past century, hypotheses about the dynamic mechanisms which drive the tectonics on the Earth have proliferated. They can be classified into three types: (1) Lithosphere tectonics due to the rotation of the Earth; (2) Effects of thermodynamics and gravity; and (3) Mantle convection. The main arguments for and against these hypotheses will be discussed. During the past thirty years, many geoscientists have emphasized the control of mantle plumes and meteorite impacts on the movements of the lithosphere plates. These hypotheses will be discussed in sections 15.3 and 15.4.

(1) Hypotheses Invoking Earth Rotation and Celestial Mechanics

The tectonic dynamics on the Earth's surface is a part of global geodynamics. Many years ago research in geodynamics was considered to lie within the scope of mathematics and mechanics, but in the last three decades it has also been considered to be a branch of geophysics. Tectonic dynamics is an

intra-disciplinary subject, involving the integration of data from several different sciences. As the Earth rotates, the influence of the moment of inertia on the Earth's rotation, on atmospheric circulation and in controlling the direction of flow of rivers has long been considered. Some geoscientists have also supposed that the deformation of rock layers near the surface of the lithosphere is influenced by the Earth's moment of inertia and is controlled by changes in the velocity of the Earth's rotation (Li SG, 1947, 1962; Scheidegger, 1963, 1982). It may be possible to explain limited horizontal displacements of crustal blocks by this hypothesis. However, at the time that this hypothesis was proposed the amount of stress caused by changes in the velocity of the Earth's rotation had not been calculated. Jeffreys (1929), Shi YL (1976) and Wang R (1979) have calculated that the amount of differential stress due to these effects is only a few Pa. This amount of stress is much too small, less than one millionth of atmospheric pressure, to cause large-scale deformation of the lithosphere. It is possible that under special conditions some conjugate shear joints or earthquakes may be induced by these small differential stresses. This hypothesis has been advocated internationally by a few geoscientists, and is now rarely discussed in the literature. However, some Chinese geoscientists have suggested that small stresses may accumulate over tens of millions of years to more than tens of MPa, to cause rock deformation (Wang R and He GQ, 1979). It seems very unlikely that tiny stresses could accumulate continuously and be preserved over such a long period of time.

Changes in the obliquity of the ecliptic and migration of the Earth's poles may cause the accumulation of stress in the crust. It is commonly agreed that stress induced by changes in the obliquity of ecliptic may amount to ~ 0.003 MPa, hundreds of times the amount of stress caused by changes in the velocity of the Earth's rotation. However, although this is a greater amount of stress, it is much less than the amount necessary to cause rock deformation. A change in the obliquity of the ecliptic might be responsible for causing earthquakes or for precipitating volcanic eruptions, but it is unlikely to be responsible for rock deformation on a large scale.

In summary, the hypotheses that changes in the velocity of the Earth's rotation or changes in the obliquity of the ecliptic may result in the accumulation of stress in crust, and cause large-scale deformation of the lithosphere, are advocated by very few geoscientists and are now rarely mentioned in the geological literature.

(2) Hypotheses invoking thermodynamics and gravity

This hypothesis considers that internal thermodynamics and gravity control rock deformation in the solid Earth. Representative opinions are:

Large-scale expansion of the Earth. According to Glikson (1980), the Earth's radius in the Pre-Cambrian is estimated to have been 40–50 percent of its present radius, and the continental area for globe is obviously smaller than that of recent Earth surface. The Earth is considered to have inflated continuously since the Pre-Cambrian, due to changes in the ratio of the continental and oceanic crust. However, as discussed in Chapter 2, the period persisted for about fifty million years, over which the mass of the Earth increased, and then the rate of increase decayed exponentially. In last four billion years, the amount of the increase in the Earth's mass, due to meteoric impact, has been only one six hundredth of the Earth's volume, because the amount of incoming meteoritic material has declined rapidly (Allègre, 1985).

Finite expansion of the Earth by 15%–20%. Owen (1992) and Wang HZ (1995) proposed that major disasters occurred at key times during Earth history caused a 15%–20% change in the Earth's radius, with pulsating and asymmetrical expansion. They consider that it is difficult to visualize drifting of the continents, as the lithospheric roots of some continents extend to depths of 250–400 km, such as Russian (Baltic) Plate. They point out that the area covered by continents is considerably less than the surface area of the whole globe, and support their hypothesis by appealing to paleo-biogeographic data. However, most geoscientists accept the astronomical results, which suggest a decrease in the Earth's gravitational constant (G) of 5×10^{-11}/a, resulting in a rate of expansion of 0.025 mm/a, a volume increase of 1.18% and a total increase in the Earth's radius of only 100 km during the last 4 billion years

(Dirac, 1974; Hoyle and Narliker, 1971). There is a little possibility that there has been any large-scale expansion of the Earth. After all, the Earth is a fairly stable dynamic system.

Pulsating expansion and contraction. This was a popular and dominant hypothesis when the theory of geosynclines and platforms prevailed (Bucher, 1933; Grabau, 1940; Umbgrove, 1947; Zhang WY, 1959; Milanovsky, 1980). It is natural to presume that uplift and depression of the Earth's surface are related to the expansion and contraction of the Earth. On the other hand, there is no positive evidence for this hypothesis, and particularly, no explanation for large-scale several thousand kilometers of horizontal displacement of the lithosphere.

Isostatic inequilibrium. Gravity influences all types of rock deformation and processes in the lithosphere and asthenosphere which disturb the isostatic equilibrium and may provide enough potential energy to drive horizontal movements of the lithospheric plates (Ma XY et al., 1987). This hypothesis connects the vertical movements of the Earth's crust with the horizontal ones. However, large-scale surface horizontal movements are not induced by gravitational in-equilibrium of the lithosphere and asthenosphere, because the amounts of horizontal movements on the surface of Earth are much greater than that of vertical movements. It is not proper to over-emphasize the vertical function, while it is reasonable to explain local horizontal displacement and rock deformation by gravitational in-equilibrium.

Surge tectonics. Meyerhoff et al. (1992, 1996) proposed a new hypothesis, opposing the theory of mobilism. Their hypothesis is that surge channels exist beneath oceanic ridges and continental rifts, as channels for the flow of shallow magma, and are linked to the asthenosphere, spreading throughout the globe beneath the continents and oceanic basins. Episodic tectonic surges are suggested to be the cause of rock deformation throughout the globe. The hypothesis emphasizes the role of extension tectonics in deformation, while downplaying the role of subduction zones. Meyerhoff et al. (1992, 1996) were not able to propose a cause for these episodes of surge tectonics and giant migrations of lithosphere plates.

(3) Hypothesis of Mantle Convection

Since the development of the plate tectonic theory the mantle convection-transmission model has been the most favored explanation for the dynamic mechanism responsible for Earth movements and rock deformation. The hypothesis of mantle convection was first proposed by Holmes (1928, 1944) and Griggs (1939) and was generally accepted as an explanation for the process of mountain building or orogeny before the end of 1960's. The originators of the plate tectonic theory (Wilson, 1970; Le Pichon et al., 1973) combined evidence of plate movements with the mantle convection hypothesis to suggest that the plate transmission model was the driving mechanism for plate tectonics. They suggested that movements of the lithospheric plates set up convection currents in the deep mantle. The hypothesis is that cool and heavy lithosphere is subducted into the mantle, driving the downward movement in a convection cell, while the rise of hot, light mantle material drives the upward movement in a convection cell, and produces areas of extension in the mid-ocean ridges; areas of subduction and extension are connected by the horizontal movement of the plate between them. This model was immediately accepted as the dominant driving mechanism for plate tectonics, and at first glance is highly satisfactory.

The phenomenon of "hot spots" was discovered a long time before the development of the transmission hypothesis. Wilson (1963) from his research on the Hawaiian volcanic chain proposed that the ocean island volcano was a hot spot (Fig. 15.1), marking the upward movement of mantle material which was partially melted to produce basaltic magmatism. The volcanic rocks forming the Hawaiian volcanic chain are younger in the east and older in the west. He explained this observation by suggesting that the lithospheric plate had moved from east to west over a stationary active hot spot; the hot spot provided a reference system, recording the movement of the overlying plate. The volcanic chain traces the movement of the lithosphere relative to the hot spot over a period of a hundred million years. This explanation has been generally accepted. The inference is that movement of the mantle, marked by the hot spot, is exceedingly slow, amounting to virtually zero, while the lithospheric plate has moved at velocities of several or dozens of centimeters per year. The question then becomes: How can the mantle

drive the movement of the plates, if the mantle moves more slowly than the lithosphere? This recognition is a death blow for the transmission model originally proposed (Bott and Kusznir, 1984; 1992). In the early 1990s, the IUGG (International Union of Geodesy and Geophysics) said that the problem of establishing the dynamic mechanism driving plate movements would be solved in twenty or thirty years, implicitly acknowledging that there is something fundamentally wrong with the transmission model of plate tectonics.

The dynamic mechanism of lithosphere plate tectonics has not yet been solved; none of the present hypotheses can satisfactorily explain all the characteristics of global plate tectonics.

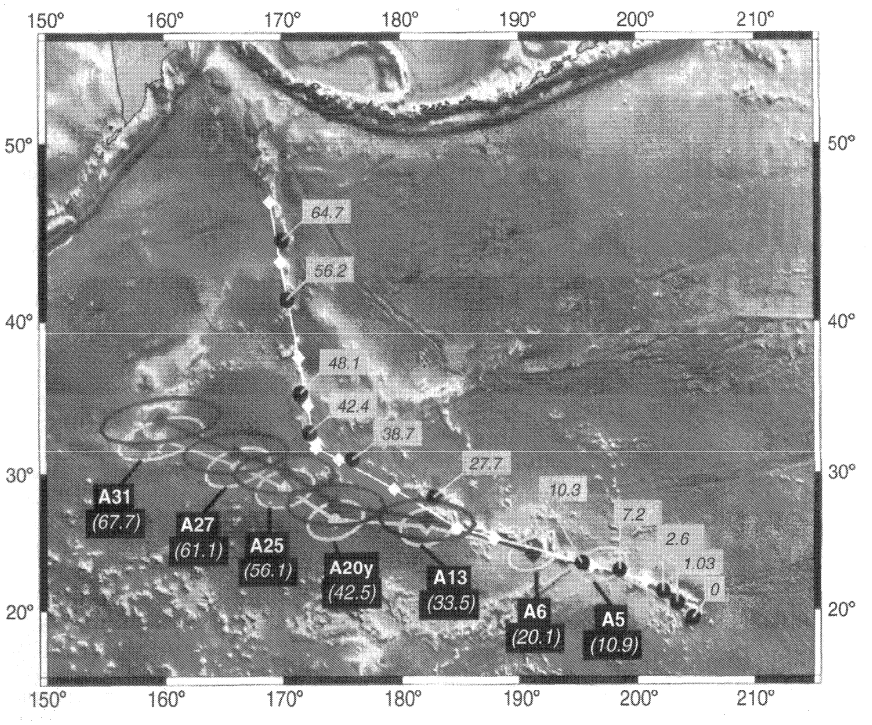

Fig. 15.1 The Hawaii-Emperor seamount chain in the Pacific (ETOPO5 bathymetry image).

The track with diamonds, which closely follows the observed one, is for the best-fit Pacific plate motion. Two reconstructed tracks of Pacific-hotspot motion in the Indo-Atlantic reference frame are also shown with quantitative plate reconstruction error ellipses. The reconstructed track, which is closer to the observed one, includes East-West Antarctic motion. Chrons and ages (in Ma) are shown (after Raymond et al., 2000).

15.2 Progress of Plate Tectonics

In recent decade, various opinions, papers and monographs have appeared, opposing the theory of plate tectonics, because none of the proposed dynamic mechanisms provide a satisfactory driving force. The result is that many non-plate tectonics studies have commenced, and some geoscientists have proposed

a "period of post-plate tectonics" (Zhang GW et al., 2006). But if their papers and monographs are read carefully, it can be found that many of them criticize the hypotheses and data of 1960s–1970s and do not confront the new data and new viewpoints in plate tectonics which have been developed during the past two decades. It is necessary to discuss new advances in plate tectonic theory, in order to reassess the theory objectively and also to further research into the dynamic mechanisms controlling the movements of the lithosphere.

(1) Periods of Tectonic Evolution

For a long time after the development of the theory of plate tectonics, it was believed that extension since 180 Ma, with the spreading of the global plates, was continuous throughout the Mesozoic. This was recognized as the important new concept of "mobilism" (Sengör, 1982, 1991; Hsu et al., 1987, 1989; Li JL, 1991). Belief in the periodicity of tectonic events was taken as evidence that the concepts of "fixism" still persisted in the geoscientific community. At about this time, the third magnetic anomaly map of the ocean floor was published (Cande et al., 1989, 1992; Ma ZJ et al., 1996), which demonstrated that the three main oceans, Pacific, Atlantic and Indian, had undergone six periods of expansion, with different directions and different rates of movement at each period (Fig. 1.1, Table 1.1).

Later, as the result of research into Mesozoic and Cenozoic intra-continental plate deformation in China (Wan TF, 1994), five to six different tectonic events were identified, with each having individual characteristics. Similar tectonic events have been recognized in the Mesozoic and Cenozoic of western North America (Burchfiel et al., 1992) and in the sedimentary basins of western Europe (Hibsch et al., 1995). It is evident that there have been quasi-contemporaneous periods of tectonic evolution in all the continents.

In addition, the study of plate movements and tectonic evolution shows that those periods of activity or catastrophic episodes have alternated with periods of stability in uniform change. It has been recognized that tectonic events in different paleocontinental plates and the periods of convergence or divergence are quasi-contemporaneous over the whole Earth.

At 1,100 Ma most of the plates on the globe were assembled in the super-continent of Rodinia (McMenamin et al., 1990; Hoffman, 1991) (Fig. 3.10); at 800 Ma Rodinia broke up (Fig. 3.11). In the Late Neoproterozoic–Earliest Paleozoic (680–513 Ma) there was the widespread Pan-African tectonic event to form the Gondwana (Unrug, 1996) (Fig. 3.12). At the end of Late Paleozoic (before 260 Ma) most of continental plates were re-assembled to form the super-continent of Pangea (Smith et al., 1981; Sengör, 1989; Yang ZY et al., 1998; Liu BP et al., 2002) (Fig. 5.9). However, the major part of the Chinese continent and its adjacent continental blocks did not take part in the amalgamation or dispersion of the three supercontinents. However, when carefully researched it is found that tectonic events are really asynchronous, or only quasi-synchronous, in each major continental region. It is obviously the result of that function for inter-plates and intra-plates, the formation periods of strong rock deformation are transmitted very slowly (about 0.65 m/yr) (Chapter 9). It is a big harvest nowadays to know the quasi-synchronization or difference of tectonic event period in each continental plate.

(2) Directions and Rates of Plate Movements

From the study of terrestrial paleo-magnetism and intraplate deformation over the whole of geological time, it is now generally understood that lithospheric plates have moved in different directions at different periods of time, and that during the same period of time other plates have been moving in different directions. Plates have been able to move freely across the equator; evidently the movements of the plates have not been restricted by the presence of the equator indicating that the rotation of the Earth does not influence the movements of the plates. Plates have been rotated to certain degree, and are able to be separated and move apart radially (Figs. 7.3, 15.4, 15.5 and 15.6).

There are great differences in the rates of movement of the plates. As is generally known, during the Mesozoic, the Indian Plate moved at the fastest rate northwards at the rate of 17 cm/yr in the Late Cretaceous. Generally, small and thin lithospheric plates were able to move most rapidly, while large,

thick lithospheric plates moved more slowly (such as Baltic Plate). At the present time the most rapid rate of extension, 13 cm/yr, is taking place across the East Pacific Rise, while the rate of extension across the Atlantic Mid-ocean Ridge is only 1–2 cm/yr, and the rate of intra-continental extension is even lower than 1 cm/yr in Chinese continent.

Plates have moved in different directions and at different rates: the Baltic Plate has remained stable throughout geological time, while the Siberian (Angaran) Plate moved from a low latitude in the southern hemisphere to a high latitude in the northern hemisphere during Paleozoic, and the Indian Plate moved from a low to a high latitude in the southern hemisphere in the period between the Paleozoic and Jurassic; since the Cretaceous India Plate has moved from a high latitude in the southern hemisphere to a low latitude in the northern hemisphere. It has been demonstrated by paleo-magnetic determinations, by DSDP and ODP ocean-floor drilling, and from other geological data, that plates have moved over thousands of kilometers over tens of million years. The earlier view that plates have remained in their original places, or have moved for only short distances is no longer tenable.

Recent research has shown that the plates have moved much faster than the underlying mantle. Hotspots have usually been regarded as providing a reference system to determine plate movements (Fig. 15.1). Later studies (Minster and Jordan, 1978) proved that the hotspots themselves have moved, at rates of only several mm/yr. Rates of displacement of some active hotspots have reached 2 cm/yr. It has been realized that the movements of the hotspot reference system, reflecting rates of convection in the deep mantle, are very slow, compared with the rapid movement of most lithosphere plates; this difference amounts to an order of magnitude. From this observation, Bott and Kusznir (1984) deduced that the movements of the lithospheric plates drive the movements of the mantle, rather than the mantle driving the movements of the plates.

(3) What is the Dominant Cause of Plate Movements?

Is subduction or extension the dominant factor driving plate movements? In 1980s–1990s this point was intensely debated? Initially, many geophysicists emphasized the importance of the subduction process (Forsyth and Uyeda, 1975; Turcotte and Schubet, 1982). They considered that the values of tectonic stress driving subduction and plate extension are commonly of the order of 20–30 MPa, but at the margins of a subducting plate could increase to 1,000 MPa. A subducting plate has huge negative buoyancy and this is the major driving force for plate movements. The above data obviously are too bigger than reality. Further factors should be considered in estimating the density of the downgoing plate and therefore the values of negative buoyancy, such as the changing physical parameters of pressure and temperature with depth, differences in subduction velocities, different thickness of plates and various conditions of subduction processes, etc. Taking these factors into account the estimated values of stress at the margins of a subducting plate could be much less, between 40 and 290 MPa (Zang SX et al., 1994).

More recently researches have emphasized plate extension as the dominant process in driving the movement of the plates, especially with relationship to the emplacement of mantle plumes. This model will be discussed in detail in later section.

(4) State of Tectonic Stress

According to the research carried out during the last three decades, the direction of maximum principal compression stress is parallel to the movement direction of the plates. Rock deformation caused by tectonic stress is concentrated in the upper part of the lithosphere, especially in the crust. During geological history, the differential stresses in the crust could be between 100–200 MPa, decreasing to 8 MPa at a depth of 50–60 km below continental rift zones. Beneath continental extension zones the differential stress may decrease from 45 MPa to 5 MPa. The differential stress value commonly decreases to 15–5 MPa at the depth of 100–200 km in the lower part of the continental lithosphere (Mercier, 1980; England and Molnar, 1991). Differential stress is almost negligible in the lower part of lithosphere, where the average confining pressure reaches 2,700–5,500 MPa. Here the density of the rocks is increased and there is little deformation. At present, the value of tectonic stress in the interior of the plates, near the

Earth's surface, determined by many methods, is commonly between 20–30 MPa, (Bott and Kusznir, 1984; Forsyth and Uyeda, 1975; Zoback and Magee, 1991).

It has not been possible so far to obtain samples from the middle and lower parts of the mantle, below the base of the lithosphere. From the isostatic nature of the global gravity field and from experiments on rock materials at high temperatures and pressures, it has been deduced that the strength of mantle materials is very small, and that crystal symmetry is more perfect. In the central and lower parts of the solid mantle, the differential stress is almost zero, i.e. the global stress system is also isostatic.

(5) On Mantle Convection

Based on the maximum depths in the Earth at which earthquake foci are recorded, it was considered, twenty years ago, that lithospheric plates usually could be subducted and penetrate the asthenosphere to a depth of 600–700 km. Part of west Pacific Plate penetrates beneath the east Asian continent to a depth of 600 km (Grand et al., 1997; Van der Hilst et al., 1997; Van der Voo et al., 1999). The subduction of other plates also evidently ceased at depths of ~600 km, for example, the Indian Plate penetrated beneath the Qinghai–Xizang (Tibet) plateau, but at a depth of 600–800 km inverted and crimped to the south. Subducted plates in Saudi Arabia and the Mediterranean region (Maruyama, 1994; Cavazza et al., 2004), and many other examples suggest that there is a zone of detachment in the mantle at a depth of about 600 km (Bigwaard et al., 1998; Van der Voo et al., 1999). However, recent seismic tomographic data, recording variations in seismic velocity within the mantle, have shown that the cool Farallon Plate penetrates very nearly to the boundary between the mantle and core, at a depth of 2,891 km beneath the North American Plate. The subducting rate of plates is about 1–1.5 cm/yr only, much less than the rates of the horizontal movement of the plates across the Earth's surface (Grand et al., 1997).

While plates are continuously subducted and penetrating into the mantle, the hot mantle materials are rising up from the boundary between mantle and core to form the mantle plumes. Subduction of cold lithospheric plates, penetrating into the deep mantle asthenosphere on one hand, and rising hot mantle material on the other, constitutes a huge mantle convection system (Mattauer, 1999; Condie, 2001; Xu ZQ et al., 2003) (Fig. 15.3). An earlier view that the convection systems did not involve the whole mantle, but could occur only within restricted layers must be abandoned.

Although convection in the mantle has been demonstrated, movements of the mantle cannot be held responsible for transporting the lithospheric plates like a transmission belt, because there is no evidence of movement rates in the mantle exceeding 2 cm/yr. A "transmission belt" moving at a slow speed is not able to transport the "goods" at a faster rate. Therefore, the hypothesis that mantle convection acts as a transmission belt to drive the movement of the lithospheric plates is no longer tenable.

Among active extension zones in the present plate system, only the deeper part of the mid-Atlantic Ridge can be demonstrated to be the site of the ascent of hot mantle material from the core/mantle boundary; other ocean ridges have only shallow earthquake foci. Most of the hotspots, which are the surface expressions of mantle diapirs, occur within oceanic or continental plates rather than at oceanic ridges (Figs. 15.1 and 15.2).

(6) Layer Detachments Within Continental Lithospheric Plates

Earlier plate theories assumed that the lithospheric plates were rigid (Wilson, 1970; Le Pichon et al., 1973). However, further research on continental plates has shown that there are detachments (sliding) or ductile shear zones within the continental lithosphere, such as the discontinuities between the sedimentary cover and the crystalline basement, the low seismic velocity / high electric conductivity layer in the middle crust and the Mohorovĭcíc discontinuity. Detachments are usually connected to high angle normal faults or thrust faults in the shallower part of the crust, becoming low angle slides, over-thrusts or ductile shear zones at depth in the crust or in the lithosphere. These discontinuities become the foci of intra-continental earthquakes and give rise to igneous magmas. In transitional areas oceanic and continental lithospheres may become detached along these discontinuities and are able to interpenetrate each other. Active magmatism may be generated where continental crust becomes detached and slides

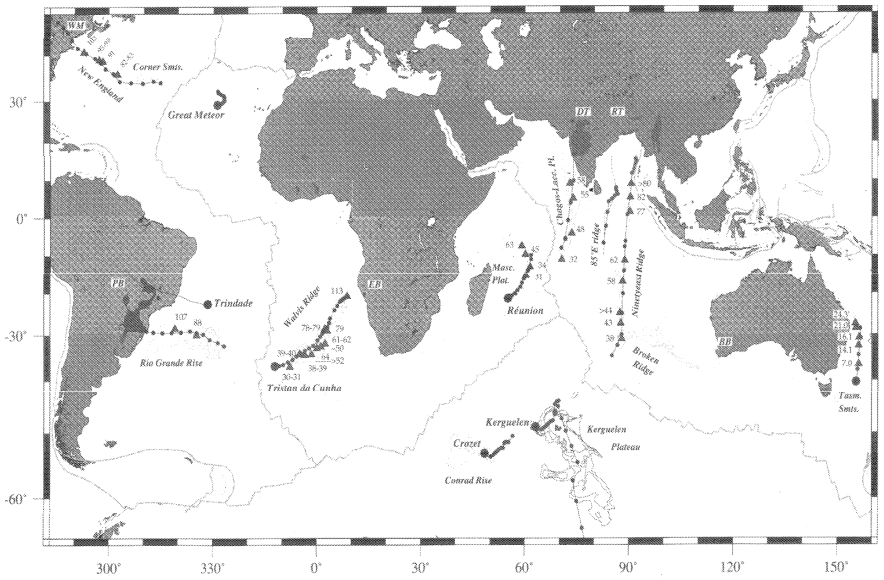

Fig. 15.2 Hotspot traces in the Atlantic and the Indian Ocean (Condie, 2001, with permission of Condie CK).

Large black spots mark the location of present day hotspots; the black triangles give the age of volcanic rock; black lines show the reconstructed trace of the hotspots; number is the isotopic age in Ma (the interval between two spots is 5 Ma);

WM (White Mountains), DT (Deccan traps), RT (Rajmahal traps), PB (Parana flood basalts), EB (Etendeka flood basalts), BB (Bunbury basalts).

Present hotspots: New England-Corner sea mounts, Great Meteor, Trinidade, Rio Grande Rise, Tristan da Cunha, Reunion, Conrad Rise, Kerguelen, Ninetyeast Ridge, Tasmanian sea mounts.

over oceanic mantle, such as in eastern China and in the east Alps (Melcher et al. 2002), discussed in Chapters 7 and 13. It is well known that oceanic lithosphere passes beneath continental lithosphere in subduction zones.

(7) Rapid Rotation of Inner core

The passage of seismic waves shows that the Earth's inner core is not homogeneous (Song XD and Richards, 1996). There is a small systematic drift in the orientation of the axis of rotation of the inner core towards the east, 1.1°/yr. Later, this value was revised to 2–3°/yr (Su WJ et al., 1996). It is found that the maximum rate of rotation on the surface of the inner core at the equator is more than 20 km/yr, hundreds of thousands of times faster than the rate of rotation of the crust and mantle. Several Chinese geoscientists have suggested that this differential movement must influence tectonic activity near the surface of the Earth. This seems very unlikely, because the large massive mantle is rather stable. However, friction and turbulence may be generated in the more rapidly rotating solid inner core and the liquid outer core, against the base of the more slowly rotating solid mantle. This turbulence may influence the magnetic field as recorded near the Earth's surface and might be responsible for the initiation of mantle plumes. This important research is still at a preliminary stage.

In summary, the theory of plate tectonics has been very successful and has generated many new ideas concerning the geometry and kinematics of the movement of lithospheric plates. It is no longer

a hypothesis, but a theory. However, the problem of controlling dynamic mechanisms has not yet been satisfactorily resolved.

15.3 On the Hypothesis of Mantle Plume

In order to discuss mantle plumes, it is necessary to clarify the terminology. A mantle plume is commonly considered to be a mass of relatively hot mantle material with a low density, which rises towards the Earth's surface due to its buoyancy. Wilson (1963) first used this term to account for the gradual displacement of the volcanic edifices forming the Hawaii-Emperor Ridge relative to a stationary hotspot. The implication is that the hotspot marked the top of a rising mantle plume. Although this phenomenon has been thoroughly researched, it must still be regarded as a hypothesis.

Condie (2001) integrated the various suggestions which had put forward, and discussed the definition of mantle plumes systemically. He used the common observation that convection in fluids results from differences in buoyancy to cause light materials to rise and denser materials to sink. A mantle plume is formed when material near the base of the mantle is reduced in density by heating in contact with the liquid core, and rises towards the surface. When the plume reaches the base of the lithosphere it spreads out to form a pancake-like plume head, with a diameter, estimated from the distribution of flood basalt formed by the plume with rich fluid, being of the order of 500–3,000 km (Hill et al., 1992). The diameter of the underlying plume tail is typically only 100–200 km (Fig. 15.3).

Hotspots indicated by basaltic volcanism mark the position of the plume head below the Earth's surface, where magma has been generated by the partial melting of rising mantle material. The main characteristics of present day hotspots are the concentration of volcanic activity and high values of heat flow. The altitude of the landforms above the plume depends on whether it rises beneath an oceanic or continental plate, by the depth of the plume and by the intensity of active volcanism. Superplumes have plume heads with diameters of 1,500–3,000 km, and the volume of flood basalt erupted above a superplume may reach 0.5×10^6 km^3. Mantle diapirs are small-scale plumes, with a plume head less than 300 km in diameter, with no plume tail, and are no longer developing (Herrick, 1999). Though a plume is commonly a large-scale structure, it raises the surface by only several hundred meters forming a widespread and rounded swell. Because the oceanic lithosphere is thin, this surface swell may be very large, with a diameter of 2,000 km and a relief of 500–1,000 m (Crough, 1983; McNutt, 1998). The top of the plume may actually reach the Earth's surface due to the rise of the partially melted base of the lithosphere.

It should be emphasized that plumes are composed of crystals of silicate minerals with an interstitial fluid, full of active components, such as K, LREE, C, water vapor and volatile elements. The passage of seismic waves indicates that mantle plumes are essentially solid, apart from the plume head, where mantle material has undergone partial melting. Hot interstitial fluids rise along fractures and along crystal grain boundaries in the mantle rocks to accumulate in magma reservoirs, before being erupted at the surface (Morgan, 1971). The term "mantle plume" is more appropriate than "mantle column". The concept of the mantle plume is completely different from the convection currents in the solid mantle due to rheology, as visualized by Holmes (1944) and Griggs (1939). Within the plume temperatures in the mantle may exceed normal values by 100–200°C, reducing the viscosity of the mantle rock, the density and the velocity of seismic waves (But, no quantitative data are examined now) (Teng JW, 2001). All of these features indicate the presence of a mantle plume. According to the data from seismic tomography, mantle plumes are generated in the D″ layer, near the core/mantle boundary.

In the hypothesis that mantle plumes drive the movement of the lithospheric plates, it is suggested that the rise of the plume head causes the uplift of the upper lithosphere, causing extension and the formation of radial cracks. As the mantle material rises, reduction in pressure causes adiabatic partial melting and the resulting basaltic fluids are intruded into cracks and fissures to form radial dyke swarms in the lithosphere, or are intruded along horizontal discontinuities near the surface to form sills over

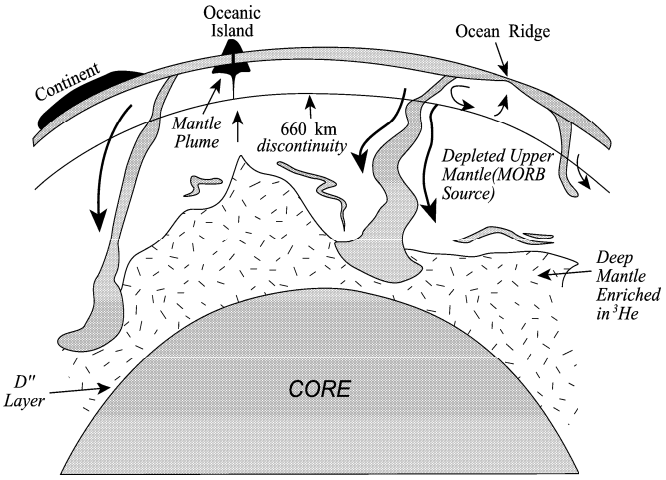

Fig. 15.3 Model of mantle plumes and mantle convection (Condie, 2001, with permission of Condie KC).

wide areas. Magma erupted at the surface forms extensive areas of flood basalt. All of these large-scale magmatic effects are controlled by the plume and occur almost synchronously, yielding rock isotopic ages which differ by less than 1 Ma (Condie, 2001). If these processes continue over a long period of time the lithospheric plate may be extended and broken into several plates, which move away from the area of uplift above the plume head, and become increasingly separated as they are pushed away by continual injections of magma to form new areas of basaltic oceanic crust.

The study of ancient mantle plumes is often very difficult, as evidence for their previous existence is rare, and may have been destroyed. In the North American continent, dike swarms with a fanlike distribution, converging northwestwards, were intruded at 1267 Ma (Ernst et al., 1992). It is reasonable to assume that an ancient mantle plume was located in the northwestern part of the Canadian Shield near Arctic Circle at that time, but other evidence is lacking. A large-scale flood basalt province was formed in Siberia at 250 Ma (Sharma et al., 1997). However, there are still different opinions concerning the location of the center of the mantle plume responsible for this eruption. The Emeishan flood-basalt province in southwestern China (described in Chapter 5) was erupted in the Late Permian, suggesting that an ancient mantle plume was developed at that time beneath the Yangtze Plate and the Gangdise and Qiangtang blocks; further research into this possibility is required.

There is a great more evidence for the occurrence of superplumes since the Mesozoic. Condie (2001) proposed that there was a superplume between North and South America and Africa, which was responsible for the breakup of the Pangean supercontinent (Fig. 15.4). He arrived at this conclusion from the distribution of active volcanic centers, sills and radial dike swarms of forming the Early Jurassic (200 Ma) Central Atlantic Magmatic Province among these three continents (Fig. 15.4). The ages of these rocks determined by $^{40}Ar/^{39}Ar$ dating show that they were formed over a period of less than 1 Myr. The volume of flood-basalt exceeds 7×10^6 km^3(Marzoli et al., 1999; Hames et al., 2000), but no evidence of the deeper structure of this superplume can be recognized at the present time.

From contrasting swells in the geoid and relief on the core-mantle boundary (D″ Layer) estimated from seismic waves, and the distribution of zones of oceanic crustal accretion indicated by magnetic anomalies on the oceanic floor, Pavoni (1997) proposed that there have been mantle superplumes below the African and Pacific plates in the past 180 Ma, since the Middle Jurassic. He proposed that there is a geotectonic bipolarity of two mantle plumes (Fig. 15.5).

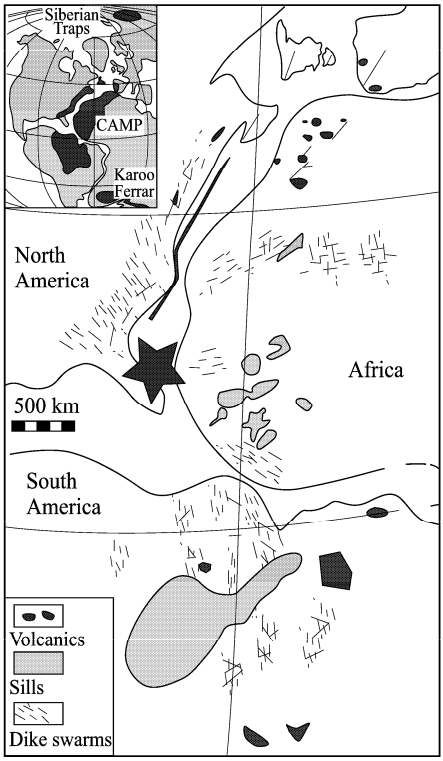

Fig. 15.4 The mantle plume at the junction of the North American, South American and African plates in the Triassic (Condie, 2001, with permission of Condie KC). CAMP = Central Atlantic Magmatic Province; the black star shows the location of the superplume.

The rise of these mantle plumes caused the horizontal displacement of the lithospheric plates and the upper mantle. The anomalous swells in the geoid, with a maximum uplift of 800 m in central Africa, and 1,200 m in the central Pacific, correspond to elevations in the core/mantle boundary of 3,500 m below Africa and 3,000 m below the Pacific. It is generally accepted that mantle plumes arise from core/mantle boundary, and may be caused by differences in the rate of movement of the liquid outer core and the solid mantle, with the resulting turbulence causing the core/mantle boundary swell and the formation of the mantle plumes.

The large Karoo flood-basalt province in South Africa covering an area of 3×10^6 km^2 was erupted between 195 Ma and 177 Ma and corresponds with the Ferrar basaltic province of mafic lavas, sills and dike swarms extending along the eastern boundary of Antarctica, giving isotopic ages of 193–170 Ma, and also the Chon Aike province in southern Argentina in South America (Storey, 1995, 1997) (Fig. 15.6). These three basaltic provinces are centered on the Falkland Islands. It is suggested that a superplume might occupy this position in the Middle Jurassic. The rise of this mantle plume formed the three flood basalt provinces with a rifted triple junction, which led to extension and the breakup of Gondwana. The deep structure of this proposed mantle plume has not yet been explored geophysically.

The mantle plume hypothesis can explain the movement of plates in various directions and their horizontal and radial displacements since the Mesozoic. The mantle plume hypothesis can also explain why the Earth has remained in a stable tectonic state for the last four billions years. It explains how hori-

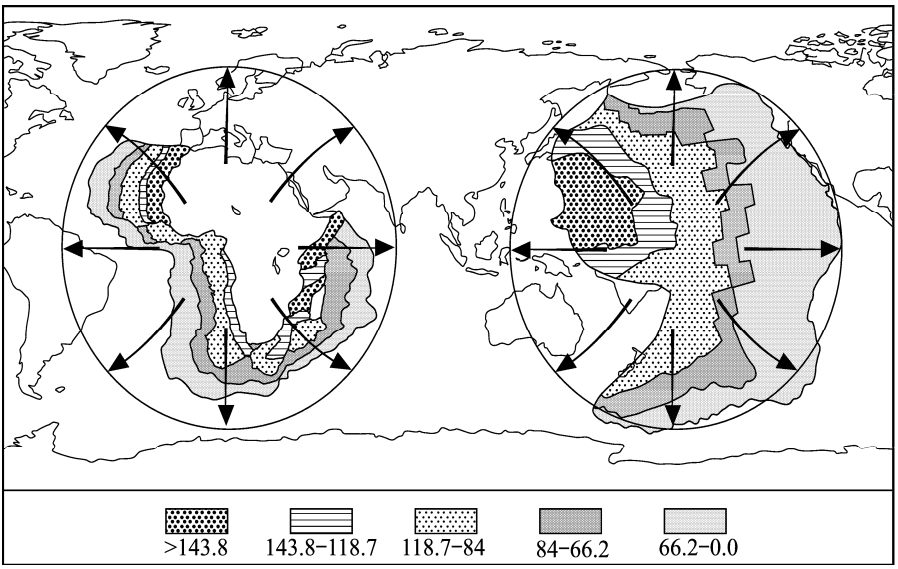

Fig. 15.5 Superplumes in the ancient Pacific and below Africa since the Middle Jurassic (Pavoni, 1997). Different ornaments indicate oceanic crust of different ages, deduced from magnetic anomalies on the ocean floor. The arrows show the directions of horizontal mantle movement beneath the lithospheric plates.

zontal movements of the lithospheric plates can take place, being independent of the rate of convection in the underlying mantle. It is recognized that this hypothesis is more reasonable than the alternatives. However, because of the absence of supporting data this hypothesis cannot explain pre-Mesozoic plate movements, which must have occurred throughout geological history. In addition, it is difficult to explain sudden changes in directions of plate movement over periods of only tens of millions of years, as the evolution of mantle plumes from the mantle-core boundary and their rise to the surface are likely to take hundreds of millions of years. The suggestion that mantle plumes may arise at different depths in the mantle also requires further research.

Maruyama (1994) has divided the evolution of the planets of the solar system into five tectonic periods: "growth tectonics, mantle plume tectonics, plate tectonics, contraction tectonics and terminal tectonics". All the planets have passed through a growth tectonic period in which they accreted from protoplanets, asteroids, comets and meteorites and underwent partial or complete melting, and were then differentiated by gravity into a series of concentric spheres of reducing density. In the mantle plume tectonic period, partial melting occurred at the top and base of the mantle, initiating the process of mantle convection in which no lithospheric plates can be formed. At this period the Earth was similar to Venus at the present day. The current period of Earth's evolution is the plate tectonic period, many spheres have formed, some mantle plumes are still operating, lithospheric plates are still being subducted into the mantle, the upper mantle is differentiating and the material of lower mantle is mixing. In the contraction tectonic period, the outer layer of the Earth's surface becomes thicker, a few craters remain, macro-shield volcanoes are formed, the globe contracts and will be compressed, like Mars and Mercury at the present day. In the terminal tectonic period, the crust and mantle are colder and undergo contraction, with increased rigidity, lithospheric plate movement has ceased and gases are emitted through fractures in the crust and mantle. Eventually the Earth will become similar to the Moon and some other asteroids at the present day. Maruyama's (1994) speculations are helpful to understanding the evolution of the Earth and the other terrestrial planets of the solar system.

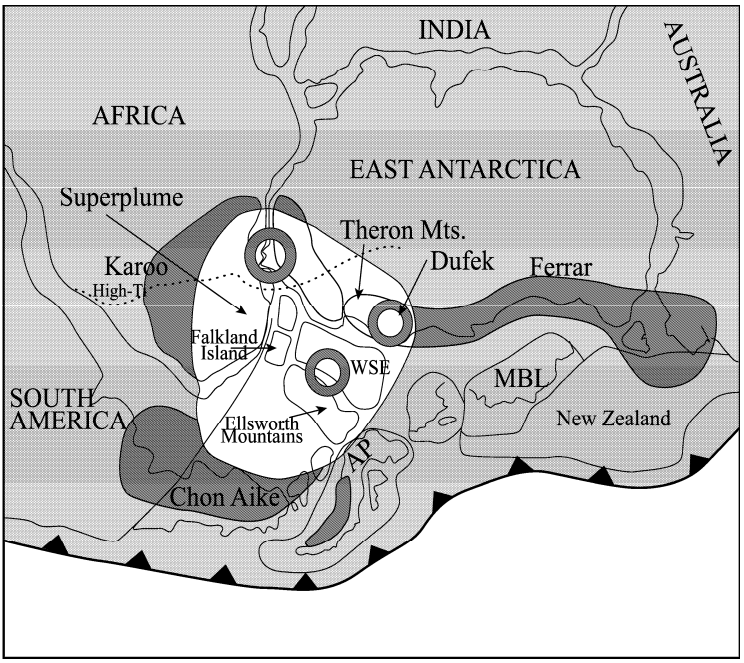

Fig. 15.6 The Middle Jurassic mantle plume in the southern Atlantic and the breakup of Gondwana (Storey, 1995).

15.4 On the Hypothesis of Meteorite Impact

Asteroids and comets, which are abundant in the solar system, impact the Earth's surface periodically. More than 170 meteorite impact craters have been identified, ranging in ages from 2 billion years to the 50,000 year old. Barringer Crater discovered in Arizona, U.S.A. ranges in size from dozens of meters to 300 m. The majority of meteorite impact craters have been found on the continents, as they are much more difficult to identify on the ocean floors, and any craters older than 200 Ma will have been subducted together with the ocean floor. During the last three decades, there has been increasing support for the hypothesis that meteorite impacts may change the direction and rate, and may be responsible for initiating plate movements (Oberbeck et al., 1993; Wan TF et al., 1997).

The outline of this hypothesis is that macro-meteorites impact the Earth with a periodicity of 33 ± 3 Myr (Rampino and Stothers, 1984, 1988) and form huge meteorite craters (Fig. 15.7). A meteorite with a diameter less than 200 meters vaporises on impact and scarcely makes a crater on the Earth's surface, but a major meteorite impact may alter the course of geological events:

(1) When a meteorite, with a diameter greater than 1 km, impacts the Earth's surface, it makes a giant crater of hundreds of kilometers in diameter and more than twenty kilometers deep (Fig. 15.7). Circular and radial fractures extend over thousands of kilometers (Grieve, 1990). Meteorite impacts fracture the surface layers of the Earth and produce a huge mass deficit. Mantle material rises to maintain isostatic equilibrium, forming a mantle diapir in the upper part of the mantle, causing large-scale magmatism with the eruption of flood basalts covering areas of up to 10^6 km^2. The impact produces circular and radial extension fractures. These fractures become filled with magma and develop as triple junctions within the lithospheric plates. The separated plate fragments are pushed apart horizontally and move

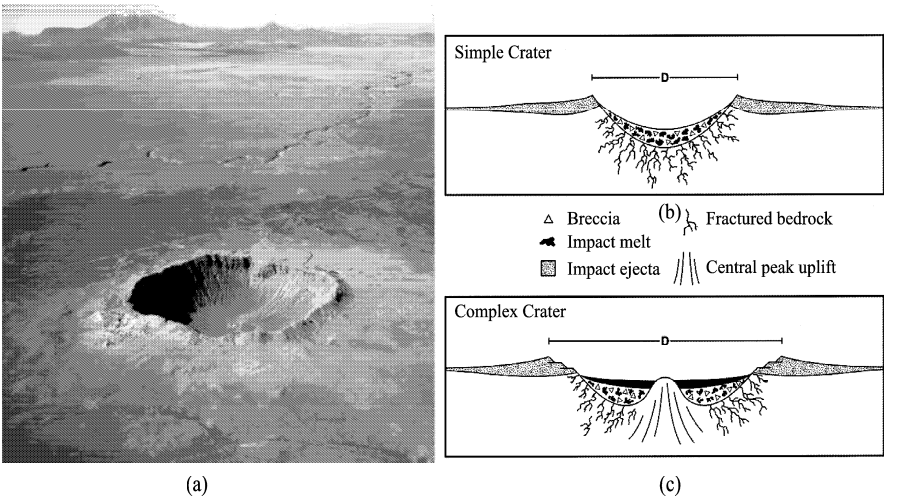

Fig. 15.7 Sketch to illustrate the formation of a meteorite crater (http://craters.gsfc.nasa.gov).

(a) A giant meteorite impact forms a crater, and rock materials (i.e. mixed and crushed meteorites and rocks of the Earth surface) are ejected over a wide area; (b) as the result of high temperature, crushed rock and mass deficit near the surface, deep materials are uplifted and surge over the surrounding area, volcanism may be induced, forming fractures and more crushed rock. (c) ejected impact materials and lava may completely cover the meteorite crater. This impact process refers to that on the Moon.

away from the site of the impact in different directions (Wan TF et al., 1997). (2) The energy of a violent impact at a velocity of 30–50 km/s causes the meteorite and the rocks immediately adjacent to the impact to vaporize, while rocks further away are melted or shattered. Powdered rock and gas form a plume rising up into the atmosphere, spreading out to form black clouds blocking the sun and causing a drop in temperature over a large part of the Earth, perhaps for several months. Where the target rocks, included limestones or evaporates, the greenhouse gases carbon dioxide, hydrogen sulphide and water are emitted by the shattered rock. The period of low temperatures is followed by a period of high temperatures causing wildfires (Alvarez et al., 1980; Wolbach et al., 1985; Rampino and Volk, 1988). Hydrogen sulphide combines with water to form acid rain. (3) High temperatures near the impact site ignite fires killing off all the plants and animals in the immediate area. If the clouds of dust block out the sunlight for a long period of time plants are unable to photosynthesize, in consequence, the plants wither and die. First the herbivores die of starvation followed by the carnivores. If these subsequent effects of the impact cover a very large area and last for a long time, many species of plants and animals will become extinct. Acid rain will also kill the vegetation, contaminate fresh water and inhibit the formation of calcareous shells in marine and fresh water environments, many microorganisms will become extinct, destroying food chains. Many scientists believe that all the mass extinction recorded in the fossil record may have been caused by meteorite impacts (Alvarez et al., 1980; Prinn and Fegley, 1987). (4) If the impact occurred in the ocean, a giant tsunami (seismic sea wave) would attack the adjacent coasts and in low-lying areas extend far inland depositing chaotic tempestites (tsunamites) and the trace elements also changed a lot (Erickson and Dickson, 1987; Hsu, 1990). (5) It is possible that a major impact event could cause reversal of the polarity of the Earth's magnetic field. Although many such reversals are recorded in the rocks during the Earth's history none have been linked to a specific impact event. (6) Macro-meteorite impacts fracture rocks over a large area, and produce a material deficit around the crater. Gravitational isostatic compensation may induce the formation of the shallow mantle plumes (i.e.

mantle diapir), with large-scale magmatism, rupturing the lithospheric plates with radial and circular extension fractures, developing triple junctions, and slowly pushing the segments apart.

Evidently major meteorite impact events will affect the atmosphere, hydrosphere, biosphere, lithosphere and the magnetic field of the Earth.

According to data accumulated by Rampino and Stothers (1984, 1988) and Yin HF et al. (1988), there is a close relationship between periodicity in the tectonic evolution of the Earth and the occurrence of giant meteorite impacts. There are two periodicities in the movement of the solar system around the galaxy: one of 33±3 Ma and another of 265±60 Ma. The former is related to periods when the solar system crosses the galactic disk, where interstellar matter is dense. The resulting changes in the gravitational field may eject asteroids from their orbits to impact the Earth. The latter period is the length of the galactic year, the time when solar system takes to traveling around the galaxy; in one galactic year the solar system crosses the galactic disk eight times.

From our present data, during the last galactic year there were probably a series of catastrophic meteorite impact events at intervals of 33±3 Ma:

(1) At ~ 0.78 Ma, between the Early and Middle Pleistocene, there was the Australasian microtektite impact event (Glass, 1982) (Fig. 15.8, A). Microtektites, with a diameter less than 1 mm, were strewn over a wide area and are preserved as a layer up to 10 m thick in the Australia, Indian Ocean, and nearby Southeast Asia. The microtektites extend over an elliptical area, covering nearly one tenth of the Earth's surface. The age of formation of this tektite field, determined by K-Ar and fission track methods is 0.9–0.7 Ma, and it has been suggested that it represents two separate meteorite impact events. The amount of material thrown out by the impact is estimated to be a hundred million tons. The site of the impact was located near the triple junctions of three lithospheric plates in the Indian Ocean (Fig. 15.8, A) and the impact may have increased the rate of extension among the African, Australian, Eurasian-Indian and Antarctic plates. Its influence on Chinese continent is that Indian Plate moved more rapidly northwards, intensifying the effects of the collision with Asia and producing ~30 kilometers shortening in the Himalaya and Tibet, causing a greater amount of uplift. These effects are represented in West China by an angular unconformity between the Early and Middle Pleistocene (Wan TF et al., 1992, 1994; Ge XH, 2002); in East China, the impact is represented only by a scattering of microtektites.

(2) At ~35 Ma (Oligocene), there was an impact event in North America marked by the widespread occurrence of microtektites (Glass, 1982) (Fig. 15.8, B). The area covered by the microtektites forms an elliptical field with a long axis extending from ENE-WSW (70°–250°), across the southern part of North America, the Caribbean Sea, the central Pacific and Southeast Asia, forming a layer down to 400 m depth below ocean floor. The isotopic age of these microtektites is 34.6–37.5 Ma at the boundary between the Eocene and Oligocene. It is estimated that the weight of the microtektites amounts to $(1–10)\times10^9$ tons and the diameter of the meteorite zone is estimated to be 0.9–2.5 km. It is probable that the meteorite impacted the Earth at very low angle so that material ejected from California extended as far away as Southeast Asia. At about the same time there were mass extinction, unconformities and a major change in geochemical elements in the boundary clay. Evidence from the oceans shows that that was a transitional period from a greenhouse to an icehouse environment (Prothero et al., 2002). Arc fractures are found in the ocean floor west of Baja California to the southwest of the North American continent. The diameter of the circular fractures is ~1,000 km, two thirds of this area lies underneath the North America continent. The centre of the circles, representing the site of meteorite impact, lies near the triple junction of the Pacific, North America and Cocos plates around the East Pacific Rise (Fig. 15.8, B). The distribution of the microtektites suggests that before impact the meteorite was travelling towards SW 250° at a small angle with the Earth's surface. Yin YH et al. (1996) have suggested that this impact may have been responsible for altering the direction and rate of movement of the Pacific Plate. In the Eocene the Pacific Plate moved towards NW 340° with velocity of 7.1 cm/yr; in Oligocene towards WNW 285° with velocity of 10.6 cm/yr; but after the impact, the Pacific Plate has moved at the rate of 8.7 cm/yr obliquely towards SW 245°. The evidence for this event is seen clearly in the Pacific, but not elsewhere.

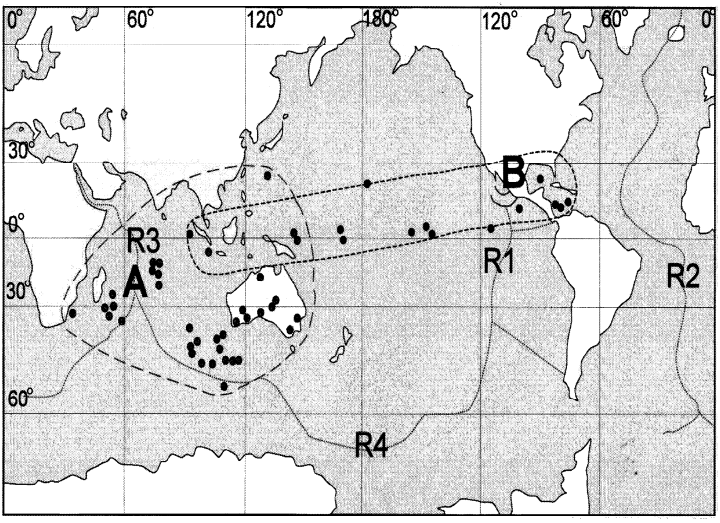

Fig. 15.8 Distribution of microtektites related to the Australasian and North American-Caribbean meteor impact events (revised after Glass, 1982, with permission of Glass BP). A. Area covered by microtektites from the Australasian event; B. Area covered by microtektites from the North American-Caribbean event; the arcuate dash lines offshore Baja California represent circular fractures in the ocean floor. R1= East Pacific Rise; R2= Mid-Atlantic Ridge; R3= Carlsburg Ridge; R4= Circum-Antarctic Ridge. Small circles are DSDP well locations.

At 65 Ma (latest Cretaceous) a large number of Mesozoic organisms, represented by the dinosaurs, became extinct. Nearly thirty years ago this extinction event was attributed to a meteorite impact event (Alvarez et al., 1980). A meteorite impact crater ~200 km in diameter was recognized by Sharpton et al. (1992), at 1100 meters below sea level in the Chicxulub area in the northern part of the Yucatan Peninsula, Mexico, and its adjacent offshore area. The age of the crystallization of the melted rocks in the crater is 65.2±0.4 Ma, determined by $^{40}Ar/^{39}Ar$ analysis. At that time it was generally assumed that the meteorite impact was the main cause of the major extinction event at the end of the Mesozoic. Recently, Keller et al. (2007) recognized that Chicxulub impact predates 300,000 yrs before occurrence of K-T boundary. At that time all the lithospheric plates were moving northwards (Moore, 1989) (Fig. 7.7 right upper). If the influence meteorite impacts have on plate movement described above is correct, an impact site or a mantle plume should be looked for near the Antarctic continent. The existing borehole data from this area are unsatisfactory due to technical problems in drilling, nevertheless more than 100 DSDP and ODP wells were drilled in the K-T boundary layer. However, Norris et al. (1998) obtained three complete cores across the K-T boundary (ODP line 171B, hole site 1049;) in the central Atlantic Ocean using a piston corer. A microtektite layer was found beneath the layer representing the K-T boundary (Keller et al., 2007). Further drilling and sampling should be carried out in the ocean floor around the Antarctic continent, to establish with certainty the location of the Late Cretaceous meteorite impact site.

At about 100 Ma (Mid-Cretaceous), there was an important worldwide oceanic anoxic event (OAE) (Schlanger and Jenkyns, 1976; Hay, 1988) with the deposition of hydrocarbon-rich rocks, associated with the extinction of many species. At this time there was also a long period when there were no inversions of the Earth's magnetic field, known as the "Cretaceous Quiet Period" or the Cretaceous Normal Superchron (CNS; Prevot et al., 1990; Pick and Tauxe, 1993). It was inferred that the D" layer, near the boundary between the core and mantle, thickened (became more viscous?) stabilizing the mantle and weakening convection in the liquid outer core, so that there were no inversions of the magnetic pole, the

intensity of magnetism was reduced, and the rates of migration of the true pole and the magnetic pole were also reduced. At that time most of the lithospheric plates were moving towards the north, but in different directions. Tectono-magmatism was common, before and after this period, but no evidence of a giant meteorite impact has yet been found around 100 Ma, and the causes of the global oceanic anoxic event and the mass extinction have not been determined. However, it may be possible to explain all these events in Middle Cretaceous by changes in deep mantle convection.

An important tectonic event in the period of 138–140 Ma was the radial migration of lithospheric plates in the area of the Pacific (Moore, 1988) (Fig. 7.7 left upper). Pavoni (1997) proposed that two super mantle plumes formed beneath African and Pacific plates at ~180 Ma. However, radial movements with relation to the African Plate began at ~138 Ma, while the radial movements of the plates in the Pacific area occurred at the end of the Jurassic (~140Ma) so that these plumes are likely to be related to each other.

At about 170 Ma, a super mantle plume developed in the area of the south Atlantic near Antarctica, and caused the breakup of Gondwana (Storey, 1995; Fig. 15.6). At the same time, many events occurred in the ancient Pacific area: reorganization of the plates; gaps in deposition; sudden changes in climate with the northward movement of the northern boundary of the bio-stratigraphic zones in the Eurasian continent; changes in the pattern of the Pacific ocean currents, so that warm currents extended to more than latitude 60° N (Liu BP and Chen F, 1995). During this time (180–170 Ma), the global magnetic field was very weak, with only one third of its strength in the Cenozoic; this is the MDL (Mesozoic Dipole Low). It was also a stable time for mantle convection (Prevot et al., 1990). There is no evidence that the super mantle plume at this time was related to processes in the deep mantle, or at the boundary between the mantle and core. It is possible that the super mantle plume in the South Atlantic–Antarctica and the breakup of Gondwana were caused by a giant meteorite impact near Antarctica.

At about 205 Ma, at the boundary between the Jurassic and Triassic, the Central Atlantic super mantle plume formed and caused the breakup of the Pangea super continent (Condie, 2001) (Fig. 15.4). Again, at present, there is no evidence to show that this super mantle plume was related to processes in the mantle. It is possible that these events were caused by a giant meteorite impact in the central Atlantic, forming a super mantle plume and initiating the breakup of the Pangea super continent.

The transitional period of the Paleozoic and Mesozoic, between the Permian and Triassic at 250 Ma, was a time of great catastrophe when more than 90% of species on Earth became extinct, the magnetic field was reversed, the climate and the composition of the atmosphere suddenly changed. Anomalous microelements occur in the boundary clay between the Permian and Triassic successions in South China (Yin HF et al., 1988; Peng YQ et al., 2002). Yang ZY et al. (1991) found ferruginous spherules in the boundary clay in several places, but the spherules were explained as due to a volcanic eruption. However, the spherules have not been subjected to detailed chemical analysis. If the spherules were analyzed using NTIMS (negative thermal ionization mass spectrometry) the ratio of rhenium to osmium could be determined to establish whether they were of terrestrial or meteoric origin. Again it has been suggested that this global catastrophe was related to a giant meteorite impact event. However, so far there is no evidence for the site of the impact. Oberbeck et al. (1993) speculated that "tillites", distributed at low latitudes on Gondwana, were in fact materials ejected by a meteorite impact. Although this interpretation has been much discussed, it has not been generally accepted (Young, 1993; Le Roux, 1994; Zhang SX, 1996).

During the last galactic year, as the solar system rotated around the galactic disk, there have been eight catastrophic tectonic events which could be ascribed to major meteorite impacts.

Periodicity of the galactic year is amazingly similar to the periodicity of major events in the tectonic evolution of the Earth, and corresponds to the convergence and divergence of the lithospheric plates as described in the "Wilson Cycle" (Wilson, 1970). The super-continent of Pangea was formed one galactic year ago, at ~250 Ma, between the Paleozoic and Mesozoic Eras. The super continent of Gondwana was formed two galactic years ago, at ~543Ma, between the Neoproterozoic and Paleozoic Eras. The super continent of Rodinia broke up and many of the continental blocks in China converged three galactic years ago, at ~800 Ma, between the Tonian and Cryogenian Eras, this was at the end of the Jinning

Period in the Chinese continent. The super continent of Rodinia formed four galactic years ago, at ~1,050 Ma, between the Mesoproterozoic and Neoproterozoic. It appears that periodically, for the last one billion years, astronomical events have influenced the tectonic evolution of the Earth. Further back to geological time evidence of earlier events has not yet been recognized, and perhaps is no longer available, was probably destroyed during later tectonic events. Further discussion may be expected on the causes and effects of this periodicity.

Finally, the author offers some speculations about tectonic dynamic mechanisms controlling the movements of the lithosphere.

A very thin surface layer, the lithospheric plates with an average thickness of one sixtieth of the radius of the solid Earth, moves over the Earth's surface, in response to variations in differential stress causing extension, subduction, collision of continents and violent rock deformation, with the formation of mountain ranges. These movements are generated by the thermal and compositional evolution of the Earth's interior, influenced by reactions with the enveloping atmosphere, hydrosphere and biosphere, and probably by periodic meteorite impacts. Super mantle plumes, rising from the boundary between the mantle and core, drive the lithospheric plates, causing radial movement of the plates over long periods of time, being usually of the order of a hundred million years. Rootless mantle diapirs may be caused by meteorite impacts, explaining many short-term changes in the directions and rates of movement of the plates, being of the order of tens of millions of years. The mantle plume hypothesis as the motive force driving plate tectonics does not conflict with the meteorite impact hypothesis, both hypotheses complement each other. Great progress in geodynamics may be expected in the future, based on the systematic accumulation and study of geological, geophysical, geochemical, and possibly astronomical data, which will lead to a better understanding of dynamic mechanisms responsible for the tectonic development of the Earth.

Geodynamics should prove of immense benefit to human society in the exploration and exploitation of energy and mineral resources and the prediction and mitigation of earthquake and geological hazards. Progress will be made only by careful observation, with the accumulation and assessment of the data to develop new theories which can be tested against further observations. Complete success is unlikely to be achieved quickly or easily. Fellow geoscientists are urged to continue their efforts to accumulate reliable tectonic and structural data and to provide new insights into understanding the evolution of the Earth.

References

Allègre CJ (1985) De la Pierre àÍ Etoile. Librairie Arthème Fayard.

Alvarez LW, Alvarez W, Asaro F et al (1980) Extraterrestrial cause for the Cretaceous-Tertiary extinction. Science 208: 1095–1108.

Bigwaard H, Spakman W, Engdahl E (1998) Closing the gap between regional and global travel tomography. J. Geophys. Res. B 103: 30055–30078.

Bott MHP, Kusznir NJ (1984) The origin of tectonic stress in the lithosphere. Tectonophysics 105: 1–13.

Bott MHP, Kusznir NJ (1991) Sublithospheric loading and plate-boundary forces. Phil. Trans. R. Soc. Lond. A 337: 83–93.

Bucher WH (1933) The Deformation of the Earth's Crust. Princeton University Press, Princeton.

Burchfiel BC, Chen ZL, Hodges KV et al (1992) The south Tibetan detachment system, Himalayan Orogen: extension contemporaneous with and parallel to shortening in a collisional mountain belt. Special Paper-GSA, 269: 41.

Cande SC, La Brecque JL, Larson RL et al (1989) Magnetic lineations of the world's ocean basins. AAPG, Tulsa, Oklahoma.

Cande SC, Kent DV (1992) A new geomagnetic polarity time scale for the Late Cretaceous and Cenozoic. J. Geophys. Res. B 97(10): 13917–13951.

Cavazza W, Roure FM, Spakman W et al (2004) The TA Atlas—the Mediterranean Region from Crust to Mantle. Springer, Heidelberg.
Condie KC (2001) Mantle Plumes and Their Record in Earth History. Cambridge University Press, Cambridge.
Crough TS (1983) Hotspot swells. Annu. Rev. Earth Planet. Sci. 11: 165–193.
Dirac PAM (1974) Cosmological models and the large numbers hypothesis. Proc. R. Soc. 338 A: 439–446.
England P, Molnar P (1991) Inferences of deviation stress in actively deforming belts from simple physical models. Phil. Trans. R. Soc. Lond. A 337: 151–164.
Erickson DJ, Dickson SM (1987) Global trace element biogeochemistry at the K/T boundary: Oceanic and biotic response to a hypothetical meteorite impact. Geology 15: 1014–1017.
Ernst RE, Baragar WRA (1992) Evidence from magnetic fabric for the flow pattern of magma in the Mackenzie giant radiating dyke swarm. Nature 356: 511–513.
Forsyth D, Uyeda S (1975) On the relative importance of the driving forces of plate motion. Geophys. J. R. Astron. Soc. 43: 163–200.
Ge XH, Liu YJ, Ren SN (2002) Uplift dynamics of the Qinghai-Tibet plateau and Altun fault. Geology in China, 29(4): 346–350 (in Chinese with English abstract).
Glass BP (1982) Introduction to Planetary Geology. Cambridge University Press, Cambridge.
Glikson A (1980) Precambrian sial-sima relation, evidence for earth expansion. Tectonophysics 6(3): 193–234
Grabau AW (1940) The Rhythm of the Ages. Henri Vetch, Peking.
Grand SP, Van der Hilst RD, Widiyantoro S (1997) Global seismic tomography: a snapshot of convection in the Earth. GSA Today 7(4): 1–7.
Grieve RAF (1990) Terrestrial impact: the record in the rocks. Meteoritics 26: 175–194.
Griggs DT (1939) Creep of rock. J. Geol. 47: 225–251.
Hames WE, Renne PR, Ruppel C (2000) New evidence for geologically instantaneous emplacement of earliest Jurassic Central Atlantic magmatic province basalts on the North American margin. Geology 28: 859–862.
Hay WW (1988) Paleoceanography: a review of the GSA centennial. GSA Bulletin 100: 1934–1956.
Herrick RR (1999) Small mantle upwellings are pervasive on Venus and Earth. Geophys. Res. Lett. 26: 803–806.
Hibsch C, Jarrige JJ, Cushing EM et al (1995) Paleostress analysis, a contribution to the understand-ing of basin tectonics and geodynamic evolution: example of the Permian-Cenozoic tectonics of Great Britain and geodynamic implications in Western Europe. Tectonophysics 252: 103–136.
Hill RI, Campbell IH, Davies GF et al (1992) Mantle plumes and continental tectonics. Science 256: 186–193.
Hoffman PF (1991) Did the breakout of Laurentia turn Gondwanaland inside-out? Science 252: 1409–1412.
Holmes A (1944) Principles of Physical Geology. Thomas Nelson and Sons, London.
Hoyle F, Narliker JV (1971) On the nature of mass. Nature 233: 41–44.
Hsu KJ, Sun S, Li JL (1987) Been South China orogenic zone, but not South China platform. Science in China B 10: 1107–1115 (in Chinese).
Hsu KJ (1989) Time and place in Alpine orogenesis. Geol. Soc. London Spec. Pub. 45: 421–443.
Hsu KJ, Li J, Chen H et al (1990) Tectonics of South China: key to understanding West Pacific geology. Tectonophysics 183: 9–39.
Jeffreys H (1929) The Earth, 2nd edn. Cambridge University Press, London.
Keller G et al (2007) Chicxulub impact predates K-T boundary: New evidence from Brazos, Texas. Earth & Planetary Science Letters 255: 339–356.
Le Pichon S, Francheteau J, Bonin J (1973) Plate tectonics. Elsevier Publishing Company, New York.
Le Roux JP (1994) Impacts, tillites, and the breakup of Gondwanaland: a second discussion. J. Geology, 102: 483–485.

Li JL (1991) Time and special problems of lithospheric tectonic evolution in orogenic belts. In: Annual Report (1989—1990) of Open Laboratory of Lithosphere Tectonic Evolution, Institute of Geology, Chinese Academy of Sciences. China Science and Technology Press, Beijing (in Chinese).

Li SG (Lee JS) (1947) Fundaments and methods of geological mechanics. In: Geological mechanics methods. Science Press, Beijing (in Chinese).

Li SG (1962) An Introduction to Geomechanics. Geological Publishing House, Beijing (in Chinese).

Liu BP, Chen F (1995) Mid-Jurassic bio-climate events and their dynamic significance of the spheres of the Earth. In: Annual Report of the Laboratory of Lithosphere Tectonics and Its Dynamics (MGMR), 1994. Seismological Press, Beijing.

Liu BP, Feng QL, Chonglakmain C et al (2002) Framework of paleotethyan archipelago ocean of western Yunnan and its elongation towards north and south. Earth Science Frontiers 9(3): 161–171 (in Chinese with English abstract).

Ma XY (chief editor, Editorial Board for Lithospheric Dynamics Atlas of China, State Seismological Bureau) (1989) Lithospheric Dynamics Atlas of China. SinoMaps Press, Beijing (in Chinese).

Ma ZJ, Li CT, Gao XL (1996) Global Ceno-Mesozoic tectonic basin characteristics. Geological Science & Technology Information 15(4): 21–25 (in Chinese with English abstract).

Maruyama S (1994) Plume tectonics. Journal of the Geological Society of Japan 100(1): 24–49.

Marzoli A et al (1999) Extensive 200-million-year-old continental flood basalts of the Central Atlantic magmatic province. Science 284 (5,414): 616–618.

Mattauer M (1999) Seismique et tectonique. Pour la Science (265): 28–31.

McMenamin MAS, McMenamin DLS (1990) The Emergence of Animals–The Cambrian Breakthrough. Columbia University Press, New York.

McNutt MK (1998) Superswells. Rev. Geophys. 36(2): 211–244.

Melcher F, Meisel T, Puhl J et al (2002) Petrogenesis and geotectonic setting of ultramafic rocks in the Eastern Alps: constraints from geochemistry. Lithos 65(1–2): 69–112.

Mercier JCC (1980) Magnitude of the continental lithospheric stresses inferred from rheomorphic petrology. Jour. Geophys. Res. B 85(11): 6293–6303.

Meyerhoff AA, Agocs WB, Taner I et al (1992) Origin of midocean ridges. In: Chatterjee S, Horton N Ⅲ (eds) New Concepts in Global Tectonics, 151–178. Texas Tech University Press, Lubbock.

Meyerhoff AA, Taner I, Morris AEL et al (1996) Surge tectonics: a new hypothesis of global geodynamics. 323pp. Kluwer Academic Publishers, Dordrecht-Boston-London.

Milanovsky EE (1980) Problems in the tectonic development of the earth in the light of concepts on its pulsation and expansion. Rev. Geol. Dynam. Geol. Physique, 22(1): 15–27.

Minster JB, Jordan TH (1978) Present-day plate motions. J. Geophys. Res., A, Space Physics 83(B11): 5331–5354.

Moore GW (1989) Mesozoic and Cenozoic paleogeographic development of the Pacific region. Abstracts, of 28th International Geological Congress, 2–455–456. Washington DC, USA.

Morgan WJ (1971) Convection plumes in the lower mantle. Nature 230(5,288): 42–43.

NASA (2010) Finding impact craters. http:// Craters.gsfc.nasa.gov. Accessed 10 May 2010.

Norris RD, Kroon D et al (1998) Proceedings of the Ocean Drilling Program, Initial Report, vol. 171 B, College Station, TX (Ocean Drilling Program)

Oberbeck VR, Marshall JR, Aggarwal H (1993) Impact, tillites, and the breakup of Gondwanaland. J. Geology 101: 1–19.

Owen HG (1992) Has the Earth increased in size? In: Chatterjee S, Horton N Ⅲ (eds) New Concepts in Global Tectonics. Texas Tech University Press, Lubbock.

Pavoni N (1997) Geotectonic bipolarity: evidence of bicellular convection in the Earth's mantle. S. Afr. J. Geol. 100(4): 291–299.

Peng YQ, Yin HF (2002) The global changes and bio-effects across the Paleozoic–Mesozoic transition. Earth Science Frontiers 9(3): 85–93 (in Chinese with English abstract).

Pick T, Tauxe L (1993) Geomagnetic paleointensities during the Cretaceous normal superchron measured using submarine basaltic glass. Nature 266: 238–242.

Press F, Siever R (1974) Earth, 1st edn. W. H. Freeman and Company, New York.
Prevot M, Derder ME, Mcwilliams M et al (1990) Intensity of the Earth's magnetic field: evidence for a Mesozoic dipole low. Earth and Planetary Science Letters 97: 129–139.
Prinn RG, Fegley B (1987) Bolide impacts, acid rain, and biospheric traumas at the Cretaceous-Tertiary boundary. Earth and Planetary Science Letters 83: 1–15.
Prothero DR, Ivany LC, Nesbitt EA (2002) From Greenhouse to Icehouse—The Marine Eocene–Oligocene Transition. Columbia University Press, New York.
Rampino MR, Stothers RB (1984) Geological rhythm and cometary impacts. Sciences 226(4681): 1427–1431.
Rampino MR, Stothers RB (1984) Terrestrial mass extinctions: cometary impacts and the Sun's motion perpendicular to the galactic plane. Nature 308(5961): 709–712.
Rampino MR, Stothers RB (1988) Flood basalt volcanism during the past 250 million years. Science 241(4,866): 663–668.
Rampino MR, Volk T (1988) DMS and the K/T boundary: phytoplankton extinctions, reduction in cloud albedo, and climatic warming. Nature 322: 63–65.
Raymond CA, Stock JM, Cande SC (2000) Fast Paleogene motion of Pacific hotspots from revised global plate circuit constraints. The History and Dynamics of Global Plate Motions. Geophysical Monographys, 121: 359–375.
Scheidegger AE (1963) Principles of Geodynamics, 2nd edn. Springer-Verlag, Berlin.
Scheidegger AE (1982) Principles of Geodynamics, 3rd edn. Springer-Verlag, Berlin.
Schlanger SO, Jenkyns HC (1976) Cretaceous anoxic events: causes and consequences. Geol. Mijnhouw 55: 179–184
Sengör AMC (1982) Edward Suess' relations to the pre-1950 schools of thought in global tectonics. Geol. Rundsch. 71(2): 381–420.
Sengör AMC (1989) Tectonic Evolution of the Tethyan Region. Kluwer Academic Publishers, Dordrecht.
Sengör AMC (1991) Timing of orogenic events: A persistent geological controversy. In: Muller DW, McKenzie JA, Weissert H (eds) Controversies in Modern Geology: Evolution of Geological Theories in Sedimentology, Earth History and Tectonics. Academic Press, London.
Sharma M (1997) Siberian traps. In: Mahoney JJ, Coffin MF (eds) Large igneous provinces: continental, oceanic, and planetary flood volcanism. Geophysical Monograph 100: 273–295. American Geophysical Union, Washington DC.
Sharpton VL, Dalrymple GB, Marin LE et al (1992) New links between the Chicxulub impact structure and the Cretaceous / Tertiary boundary. Nature 359 (6398): 819–821.
Shi YL (1976) Preliminary analysis on the ε type tectonic stress field. Geomechanis Communication (1): 39–54 (in Chinese).
Smith AG, Hurley AM, Briden JC (1981) Phanerozoic Paleocontinental World Maps. Cambridge University Press, Cambridge.
Song XD, Richards PG (1996) Seismological evidence for differential rotation of the Earth's inner core. Nature 382(6,588): 221–224.
Storey BC (1995) The role of mantle plumes in continental breakup: case histories from Gondwanaland. Nature 377: 301–308.
Storey BC, Kyle PR (1997) An active mantle mechanism for Gondwana breakup. S. Afr. J. Geol. 100(4): 283–290.
Su WJ, Dziewenski AM, Jeanloz R (1996) Planet within a planet: Rotation of the inner core of the Earth. Science 274(5,294): 1883–1887.
Teng JW (2001) The exchange of substance and energy, different sphere coupling and deep dynamical process within the Earth. Earth Science Frontiers 8(3): 1–8 (in Chinese with English abstract).
Turcotte DL, Schubet G (1982) Geodynamics: Applications of Continuum Physics to Geophysical Problems. John Wiley & Sons, New York.
Umbgrove JHF (1947) The Pulse of the Earth. The Hague, Nihoff.

Unrug R (1996) The assembly of Gondwanaland-Scientific results of IGCP Project 288: Gondwanaland suture and mobil belts. Episodes 19(1–2): 11–20.
Van der Hilst RD, Widiyantoro S, Engdahl ER (1997) Evidence for deep mantle circulation from global tomography. Nature 386 (6,625): 578–584.
Van der Voo R, Spakman W, Bijwaard H (1999) Mesozoic subducted slabs under Siberia. Nature 397(6716): 246–249.
Wan TF, Cao RP (1992) Tectonic events and stress fields of Middle Eocene-Early Pleistocene in China. Geoscience 6(3): 275–285 (in Chinese with English abstract).
Wan TF (1994) Intraplate Deformation, Tectonic Stress and Their Application for Eastern China in Meso-Cenozoic. China University of Geosciences Press, Wuhan.
Wan TF, Cao XH (1997) Estimation of differential stress magnitude in Middle-Late Triassic to Early Pleistocene for China. Earth Science 22(2): 145–152 (in Chinese with English abstract).
Wan TF (1997) On the accretion of Eastern Asian continental blocks since Triassic. Journal of China University of Geosciences 8(2): 114–120.
Wang HZ, Mo XX (1995) An outline of the tectonic evolution of China. Episodes 18(1–2): 6–16.
Wang HZ (1995) Retrospect of the study on global tectonics. Earth Science Frontiers 2(1): 37–42, 66 (in Chinese with English abstract).
Wang R, He GQ (1979) Rate change of Earth and the global stress field caused by its tide-drawing force under the condition of axial symmetry. In: Astronomical Observatory of Shanghai, Astronomical Geodynamics Memoirs, 8–21. Science Press, Beijing (in Chinese).
Wilson JT (1963) A possible origin of the Hawaiian Island. Can. J. Physics 41: 863–868.
Wilson JT (1970) Continents Adrift: Readings From Scientific American. W. H. Freeman and Company, San Francisco.
Wolbach WS, Lewis RS, Anders E (1985) Cretaceous extinctions: evidence for wildfires and search for meteoric material. Science 230(4,722): 167–170.
Xu ZQ, Zhao ZX, Yang JS et al (2003) Tectonics beneath plates and mantle dynamics. Geological Bulletin of China 22(3): 149–159 (in Chinese with English abstract).
Yang ZY, Ma XH, Huang BC et al (1998) Polar wander paths of magnetism and block migration of north China in Phanerozoic. Science in China B 28 (suppl.): 44–56 (in Chinese).
Yang ZY, Wu SB, Yin HF et al (1991) Geological Events of Permo-Triassic Transitional Period in South China. Geological Publishing House, Beijing (in Chinese with English abstract).
Yin YH, Wan TF (1996) The possibility and dynamics of a microtektite impacted the Pacific plate and caused the change of its moving direction in the end of Eocene. In: 1995 Annual Report, The Laboratory of Lithosphere Tectonics and Its Dynamics (MGMR China), pp.122–132. Geological Publishing House, Beijing.
Yin HF, Xu DY, Wu RT (1988) Catastrophism of Geological Evolution. China University of Geosciences Press, Wuhan (in Chinese).
Young GM (1993) Impacts, tillites, and the breakup of Gondwanaland: discussion and reply. J. Geology 101(5): 675–683.
Zang SX, Ning YJ (1994) Advanced and problems of global dynamics research. In: Contribution to Proseminar of Modern Geodynamics. Seismological Press, Beijing (in Chinese).
Zhang GW, Zhang BR, Yuan XC (1996) Orogenic Process of Qinling Orogenic Belt and Three Dimensional Structural Map Series of Lithosphere. Science Press, Beijing (in Chinese).
Zhang GW, Guo AL, Yao AP (2006) Considering on research of Chinese continental geology and tectonics. Progress of Natural Science (10): 12–17.
Zhang SX (1996) Did the impact result in the breakup of Gondwanaland? In: 1995 Annual Report, The Laboratory of Lithosphere Tectonics and its Dynamics (MGMR), pp.95–104. Geological Publishing House, Beijing (in Chinese).
Zhang WY et al (1959) An Outline of Tectonics of China. Science Press, Beijing(in Chinese).
Zoback ML, Magee M (1991) Stress magnitudes in the crust: constraints from stress orientation and relative magnitude data. Phil. Trans. R. Soc. Lond. A 337(1,645): 181–194.

Appendices

Appendix 1 Tectonic Data about Archaen and Paleoproterozoic

Appendix 1.1 Rock formation time, temperature, pressure, depth and geothermal gradient in Archaen

Area	Lithofacies	Isotopic age (Ma)	Temperature (℃)	Pressure (GPa)	Formation depth (km)	Geothermal gradient (℃/km)	Sources
Qingyuan, Liaoji continental nucleus	granulite	2,924	800	1.0	36.7	18.3	Shen BF et al., 1994
Anshan, Liaoji continental nucleus	granulite	> 2,900	800	1.1	36.7	18.3	Cheng YQ et al., 1994
Huadian, Liaoji continental nucleus	granulite	2,950	750	0.7	23 – 25	25.8	Shen QH et al., 1992
South of Chifeng continental nucleus	granulite	2,846	990	1.1	36.7	23.4	Cui WY et al., 1991
Jining, Dongsheng continental nucleus	granulite	> 2,900	860	1	36	20.3	Cheng YQ et al., 1994
Qian'an, Bohai continental nucleus	amphibolite	3,561	900	1	33	23.3	Shen QH et al., 1992
Xishui, Bohai continental nucleus	granulite	> 2,900	800	0.75	25	26.8	Cheng YQ et al., 1994
Gongdanshan, Yishui, Shandong	granulite	> 3,000	900	0.95	1.7	24.3	Su SG et al., 1997
Qianxi, Bohai continental nucleus	granulite	3,300	800	1.2	40	16.8	Dong SB et al., 1986
Linfen continental nucleus	granulite	> 2,800	900	1	33	23.3	Wu JS et al., 1989
Jining continental nucleus	amphibolite	2,788	600	0.6	20	23.5	Xu HF et al., 1992
Above 11 areas	Average	MA	827	0.95	32	22.2	
Qingyuan, Jiliao continental nucleus	amphibolite	2,624	610	0.61	20	25.5	Shen QH et al., 1992
Jiapigou, Jiliao continent nucleus	amphibolite	2,525	600	0.6	20	25	Shen QH et al., 1992

Continued

Area	Lithofacies	Isotopic age (Ma)	Temperature (℃)	Pressure (GPa)	Formation depth (km)	Geothermal gradient (℃/km)	Sources
Huadian, Jiliao continental nucleus	granulite	~2,500	830	0.6 – 1	30	24.3	Bureau of Geology of Jilin, 1988
Tonghua, Jiliao continental nucleus	granulite	~2,560	750	0.62	27	24	
Qingyuan, Jiliao continent nucleus	granulite	~2,630	1000	0.75	33	27.3	Cheng YQ et al., 1994
Anshan, Jiliao continent nucleus	greenschist	~2,630	570	0.6	20	23.5	Cheng YQ et al., 1994
East of Fushun, Liaoning	blueamphiboleschist	2,484	510	1.0	33	12.4	Liu YX et al., 1995
Jiapigou, Jilin	granulite	>2,500	850	1.3	43	17.4	Sun XM et al.,1992
Chongli, Chifeng continent nucleus	amphibolite	2,470	730	0.91	30	21	Chen QA et al., 1992
Pingquan, Chifeng continental nucleus	granulite	2,650	790	0.8	26.7	25.8	Tan YJ et al., 1991
Pingquan, Chifeng continental nucleus	amphibolite	2,505	670	0.7	23	24.8	Tan YJ et al., 1991
Chongli, Chifeng continental nucleus	granulite	2,454	868	0.9	33	23.3	Wang RM et al., 1994
West Liaoning, Chifeng nucleus	granulite	2,494	800	1	40	17.5	Dong SB et al., 1986
West Liaoning	granulite	2,575	860	1.25	41.7	18.2	Ji JQ et al., 1998
Jianping, West Liaoning	granulite	2,490	820	1.17	39	18.5	Wei CJ et al., 2001
Jianping, West Liaoning	granulite	2,487	850	1.05	35	21.4	Wang CQ et al.,1999
Jianping, West Liaoning	granulite	2,575	860	1.25	42	20.6	Ji JQ et al., 1998
Ruanping, Chengde, North Hebei	granulite	>2,500	800	1.20	40	17.5	Li JH, 1998
Huai'an, Northwest Hebei	granulite	>2,600	860	0.92	31	24.5	Geng YS et al., 2000
Sanggan area, Northwest Hebei	granulite	2,530	830	1.25	42	17.4	Guo JH et al., 1998
Dongsheng continental nucleus	amphibolite	2,625	880	0.8	26.7	33	Jin Wet al., 1991
Wulashan, Dongsheng continental nucleus	granulite	~2,500	710	0.84	28	21.8	Cheng YQ et al., 1994
Daqingshan, Dongsheng continent nucleus	greenschist	~2,550	500	0.4	13.3	30	Cheng YQ et al.,1994
Bohai continent nucleus	amphibolite	2,663	680	0.5	16.7	34.7	Shen QH et al., 1992
Miyun, Bohai continental nucleus	granulite	2,523	900	1	36	22.2	Dong SB et al.,1986
Miyun, Beijing	granulite	>2,500	900	1.02	34	23.5	He GP et al., 1994.
Zunhua, Qian'an, East Hebei	granulite	>2,500	920	1.14	38	21.6	Chen MY et al., 1996

Continued

Area	Lithofacies	Isotopic age (Ma)	Temperature (℃)	Pressure (GPa)	Formation depth (km)	Geothermal gradient (℃/km)	Sources
Qianxi group, East Hebei	granulite	$<2,700$	940	1.1	37	22.7	He GP et al., 1992
Jiaodong, Bohai continental nucleus	granulite	$\sim 2,800$	700	0.65	20 – 23	27.9	Yang ZF et al., 1998
Jiaodong Group, Bohai nucleus	amphibolite	$\sim 2,500$	655	0.65	20 – 23	25.8	Yang ZF et al., 1998
Linfen nucleus	amphibolite	$>2,500$	670	0.8	26.7	21.3	Wu JS et al., 1989
Wutai, Linfen continental nucleus	amphibolite	$\sim 2,550$	690	0.8	26.7	22	Cheng YQ et al., 1994
Yanggao, Linfen continental nucleus	granulite	2,440	900	1.4	41	19.5	Dong SB et al., 1986
Dengfeng, Linfen continental nucleus	amphibolite	$\sim 2,500$	450	0.35	11.7	30	Cheng YQ et al., 1994
Luonan, Linfen continental nucleus	granulite	$\sim 2,500$	650	0.6	20	27.5	Cheng YQ et al., 1994
Wutai-Taihang area	gneiss	$>2,500$	700	0.6	13 – 20	36.4	Wang KY et al., 1991
Taihangshan	rich aluminium gneiss	$>2,600$	800	0.8	26.7	26.2	Liu SW et al., 1997
Jining continental nucleus	amphibolite	2,500	450	0.5	16.7	21	Xu HF et al., 1992
Taishan, Jining continental nucleus	granulite	$>2,626$	700	1	33	18.2	Bureau of Geology of Shandong, 1991
Taishan, Jining continental nucleus	amphibolite	$>2,626$	660	0.8	26.7	21	
Huoqiu, Jining continental nucleus	amphibolite	2,681	600	0.5	20	25	Dong SB et al., 1986
North slope, east Qinling	amphibolite	2,600	600	0.7	23.3	21.5	Qi JY, 1992
Huabei	eclogite	$<2,500$	900	1.2	40	20	Zhai MG et al., 1995
Jiamusi continental nucleus	amphibolite	2,539	690	0.55	18.3	32.2	Cheng YQ et al., 1994
Helanshan, Alaxa	granulite	$\sim 2,500$	800	0.65	21.7	32.2	Cheng YQ et al., 1994
Middle Kangdian greenstone belt	amphibolite	$>2,400$	600	0.41	14	35.7	Lu MJ, 1986
South of Kangdian greenstone belt	greenschist	$>2,400$	550	0.53	17.7	25.4	Lu MJ, 1986
Above 47 areas	Average	NA	714	0.81	27.5	24.2	
World (average)	granulite	Arch.	>750	0.41	14	54	Grambling, 1981

Appendix 1.2 Block motion velocity in the Chinese continent of Archean (3.2–2.5 Ga)

Area	Rock	Sample amount	Isotopic age (Ga)	Deformation velocity (cm/yr)
Xin'antun, Jilin	granitoid	8	3.2 – 2.8	5.2
Anshan, Liaoning	harzburgite	4	> 2.5	–0.88
Raobazhai, Anhui	ultrabasic rock	29	about 2.8 – 2.7	–0.87
Wutaishan, Shanxi	basic lava	80	about 2.8 – 2.7	–0.72
Sihong, Jiangsu	ultrabasic rock	2	about 2.8 – 2.7	–0.83
Wutaishan, Shanxi	basic lava	79	about 2.7 – 2.6	–0.67
Lüliangshan, Shanxi	basic lava	25	about 2.7 – 2.6	–0.85
Tonghua, Jilin	dioritoid	2	about 2.8 – 2.5	4.3
Wutaishan, Shanxi	acidic lava	4	about 2.7 – 2.6	5.3
North of Altun	basic lava	2	2.46	–0.78
North of Altun	acidic lava	4	2.50	5.4
Lüliangshan, Shanxi	basic lava	12	about 2.6 – 2.5	–0.56
Zhongtiaoshan, Shanxi	basic lava	11	about 2.6 – 2.5	–0.48
Jilin	granitoid	8	about 2.6 – 2.5	5.4
Baotou, Inner Mongolia	granitoid	2	about 2.6 – 2.5	5.8
Lüliangshan, Shanxi	acidic lava	27	about 2.6 – 2.5	4.2
Zhongtiaoshan, Shanxi	acidic lava	15	about 2.6 – 2.5	5.9
Wutaishan, Shanxi	granitoid	86	about 2.8 – 2.5	5.7
Taishan, Yishan, Shandong	granitoid	10	about 2.8 – 2.5	4.87
Taishan, Zouxian, Shandong	granodiorite	6	about 2.8 – 2.5	4.5
Bengbu, Anhui	granitoid	1	about 2.6 – 2.5	4.1

Note: "–" is extension velocity, others are shortening velocities.
The rock chemical data got from 1:200,000 regional geological survey reports in those areas and regional geology about those provinces.

Appendix 1.3 Rock formation age, temperature, pressure, depth and geothermal gradient in Paleoproterozoic

Area	Lithofacies	Isotopic age (Ma)	Temperature (℃)	Pressure (GPa)	Formation depth (km)	Geothermal gradient (℃/km)	Sources
East of Hingganling, Heilongjiang	amphibolite	~ 1,900	625	0.25	8.3	66.9	Cheng YQ et al., 1994
Mashan Group, Heilongjiang	gneiss	> 1,900	850	0.47	15.7	49.7	Jiang JS et al., 1993
East of Liaoning-South of Jilin	amphibolite	~ 1920	660	0.8	26.7	22.1	Cheng YQ et al., 1994
Liaohe Group, North Liaoning	amphibolite	> 1,900	630	0.8	26.7	20.1	Li SZ et al., 2001
Liaohe Group, South Liaoning	amphibolite	> 1,900	600	0.7	23	23	Li SZ et al., 2001
East of Liaoning-South of Jilin	low grade amphibolite	< 1,900	640	0.73	24.3	23.5	He GP et al., 1998
Jianping, West of Liaoning	granulite	2,490	820	1.17	39	19.2	Wei CJ et al., 2001

Continued

Area	Lithofacies	Isotopic age (Ma)	Temperature (℃)	Pressure (GPa)	Formation depth (km)	Geothermal gradient (℃/km)	Sources
Shuangshanzi, East Hebei	amphibolite	2,193	548	0.63	20 – 25	21.2	Dong SB et al., 1986
Xinghe, Inner Mengolia	granulite	~ 1,900	850	1	33	23.6	Mei HL et al., 1998
Lüliangshan, Shanxi	greenschist	~ 2,100	400	0.5	18 – 19	17.8	Dong SB et al., 1986
Wutaishan, Shanxi	greenschist	~ 2,129	400	0.33	11	30	Dong SB et al., 1986
Shanxi–Inner Mongolia	khondalite	1,800	750	0.6	20	34	Wu CH et al., 1997
Haiyangsuo, Jiaodong, Shandong	granulite	> 1,900	1,050	1.24	41	23.9	Su SG et al., 1996
Gejiaji, Jiaodong, Shandong	granulite	> 1,900	700	0.9	30	21	Su SG et al., 1996
Jingshan, Jiaodong, Shandong	amphibolite	~ 1,800	600	0.45	16.7	31.7	Yang ZF et al., 1998
Jiaodong–Laixi–Laiyang	gneiss	< 1,900	750	0.7	23.3	29.2	Lu LZ et al., 1998.
Jiaonan Group, Shandong	eclogite	> 1,901	810	1.2	40	18.5	Bureau of Geology of Shandong, 1991
Jiaonan Group, Shandong	amphibolite	> 1,901	580	0.65	21.7	23.5	
Songshan, Henan	greenschist	~ 2,071	400	0.2	6.7	49.5	Cheng YQ et al., 1994
Beishan, Gansu	amphibolite	2,150	620	0.55	18.3	30	Cheng YQ et al., 1994
Dunhuang, Gansu	amphibolite	~ 1,900	660	0.55	17 – 20	31.9	Gansu Geology Bureau, 1989
Qilianshan	amphibolite	2,205	540	0.5	16.7	28.1	Cheng YQ et al., 1994
Mid-Qilianshan Qinghai	amphibolite	2,205	900	0.9	30	27.7	Qinghai Geology Bureau, 1991
Northern Qaidam	amphibolite	> 1,900	800	0.9	30	24.3	
Southeastern Qaidam	amphibolite	1,846	800	0.85	28	26	
Middle part in south margin of Qaidam	amphibolite	1,846	750	0.75	25	27.2	
West part in south margin of Caidam	amphibolite	1,846	700	0.4	13.3	47	
Badu, Zhejiang	amphibolite	~ 1,900	680	0.7	23.3	26.2	Cheng YQ et al., 1994
Maoji, Tongbaishan	granulite	> 1,967	650	0.8	17 – 27	26.4	Liu GH et al., 1993
Dabieshan, Henan	amphibolite	1,982	715	0.4	13.3	48.5	Cheng YQ et al., 1994
Luotian-Huilan, Dabieshan	granulite	> 1,900	880	1.29	43	18.8	You ZD et al., 1995
Ailaoshan Group, Yunnan	amphibolite	~ 1,900	650	0.49	16.3	35.6	Zhong DL, 1998
Dahongshan, Yunnan	hornblende	> 1,900	533	0.94	31	15	Qin DX et al., 2000
Diancangshan Group, Yunnan	amphibolite	~ 1,900	780	0.82	27.3	26	Zhong DL, 1998
Average of 28 areas	amphibolite		681	0.78	28.5	24.6	

Appendix 1.4 Deformation velocity in continental plate During Lüliang period (2.5–1.8 Ga), Paleoproterozoic

Area	Rock	Sample amount	Age (Ga)	Deformation velocity (cm/yr)
Huma,Shuangyashan, Heilongjiang	gabbro	4	2.5 – 2.4	−0.9
Taihang, Lüliang, Shanxi	basalt	36	2.5 – 2.4	−0.55
Chaoyanggou, Liaoning	gabbro	2	2.5 – 2.4	−0.75
NW Jilantai, Inner Mongolia	gabbro	2	2.5 – 2.4	−0.65
Taihang, Lüliang, Shanxi	basalt	57	2.5 – 2.4	−0.45
Jiaobei, Shandong	ultrabasic-basic	55	2.5 – 2.4	−0.8
Taipingxi, Hubei	ultrabasic-basic	25	2.5 – 2.4	−0.8
Cangshan, Yunnan	ultrabasic-basic	2	2.5 – 2.4	−0.7
Ailaoshan, Yunnan	ultrabasic-basic	2	2.5 – 2.4	−1
Liaoning	intermediate-basic rock	6	> 1,900	5.6
West of Shandong	granodiorite	20	2.075 – 1.754	4.6
West of Shandong	metamorphic gabbro	8	2.075 – 1.754	6
Taihang, Shanxi	granitoid	67	2.5 – 2.4	5.5
Qilianshan-Beishan, Gansu	dacite	2	2.5 – 2.4	5.3
Tongshan-Pixian, Jiangsu	ultrabasic rock	1	2.0 – 1.8	−0.9
Cangshan Group, Yunnan	basic volcanic rock	2	~ 1.9	−0.7
Ailaoshan Group, Yunnan	basic volcanic rock	3	~ 1.9	−0.8
Lapeiquan, Altun	basic volcanic rock	13	~ 1.793	−0.5
Lapeiquan, Altun	silicic volcanic rock	5	~ 1.793	8.5
Erguna, Jiamusi, Yichun	granitoid	30	2.0 – 1.8, 1.705	4.7
Budargan, Mayatu, Inner Mongolia	granitoid	3	2.0 – 1.8	6
Miaohe, Jiliao active belt	granitoid	5	2.0 – 1.8	5.8
North Hebei - Liaoning active belt	granitoid	1	2.0 – 1.8	5.8
Post-tectonic stage, North Hebei–Liaoning active belt	granitoid	1	2.0 – 1.8	4.8
Jilin	granitoid	2	1.955 – 1.781	5.8
Wutaishan, Shanxi	granitoid	1	2.0 – 1.8	6.4
Taihangshan, Shanxi	granitoid	2	2.0 – 1.8	5.9
Guandishan, Lüliangshan	granitoid	1	2.0 – 1.8	5.6
Dabieshan, Henan	granitoid	16	2.005	6.0
Middle part of Helanshan	granitoid	16	1.84	7.1
Huoyanshan, Gansu	granitoid	16	2.0 – 1.8	4.9
Kuruktag	granitoid	22	1.9 – 1.8	6.9
East of Kunlun	granitoid	5	1.9 – 1.8	6.5
Tiantangzhai, Hubei	granitoid	14	2.0 – 1.8	5.8
Jiaonan, Shandong	granitoid	11	2.0 – 1.8	6.3
Donghai xian, Jiangsu	meta. volcanite	1	2.0 – 1.8	5.1
Jiangsu	granitoid	10	1.928	5.7

Note: "−" is extension velocity, others are shortening velocities.
Rock chemical data are quoted form the report of 1:200,000 regional geological survey in these areas and regional geology in provinces.

Appendix 1.5 Estimated thickness for Archean–Paleoproterozoic continental crust in Chinese plate

Location	Geological age	Rock	Sample amount	*w*(K60) (%)	Thickness of crust (km)
Qianxi, Hebei	3800 Ma	charnockite	1	1.02	19.01
Qianxi, Hebei	Paleo- & Meso-Archean	tonalite	1	1.05	19.56
Qian'an, Hebei	Paleo- & Meso-Archean	tonalite	9	2.17	39.9
Anshan Group	Neoarchean	amphibolite	1	1.13	21
Molijiang, Liaoning	Neoarchean	plagiogranite	1	1.07	19.9
Wutai, Shizui	Neoarchean	amphibolite	13	0.8	15.08
Wutaishan, Shanxi	Early of Neoarchean	meta. basalt	77	0.99	18.5
Wutaishan, Shanxi	Middle of Neoarchean	meta. basalt	45	0.84	15.8
Lüliangshan	Late of Neoarchean	meta. basalt	37	1.49	27.6
Wulashan Group	Neoarchean	plagiogneiss	1	1.62	29.93
Culaishan, Shandong	Neoarchean	epidiorite	24	1.66	30.6
North of Arjinshan	Neoarchean	plagiogneiss	2	0.76	14.28
Cangshan, Yunnan	Neoarchean	meta. basalt	2	0.88	16.5
Ailaoshan, Yunnan	Neoarchean	meta. basalt	2	0.43	8.3
Above areas	Neoarchean	basic rock	205		21.5
Dantazi Group	Neoarchean	plagiogranite	1	2.98	54.69
E Anshan, Liaoning	Neoarchean	trondhjemite	1	3.54	64.9
Lishan, Liaoning	Neoarchean	trondhjemite	1	3.4	62
Chentaigou, Liaoning	Neoarchean	trondhjemite	1	3.59	65.8
Tiejiashan, Liaoning	Neoarchean	granitoid	1	4.98	91.1
Xin'antun, Jilin	Neoarchean	granitoid	8	3.39	62.2
Taishan, Shandong	Neoarchean	migmatite	31	2.81	51.55
Shigujian, Anhui	Neoarchean	epidiorite	2	3.5	64.15
North Altun	Neoarchean	granite gneiss	4	4.25	77.8
Above areas	Neoarchean	granitoid	50		66.02
National average	Archean	(Cheng YG, 1994)	52	3.54	64.89
Huma, Heilongjiang	Paleoproterozoic	meta. gabbro	10	1.6	29.6
Gaoli Duntai, Liaoning	Paleoproterozoic	monzonitic granite	1	1.1	20.5
Tonghua, Jilin	Paleoproterozoic	diorite	2	1.7	31.4
Jilantai, Inner Mongolia	Paleoproterozoic	meta. gabbro	2	1.21	22.5
Taihangshan, Lüliang, Shanxi	Early stage of Paleoproterozoic	meta. basalt	57	1.78	32.8
Taoke, Shandong	Paleoproterozoic	meta. gabbro	24	1.79	32.95
Kuruktag	Paleoproterozoic	amphibolite	5	1.74	32.1
Kuruktag	Paleoproterozoic	plagiogranite	7	2.05	37.7
North Altunshan	Paleoproterozoic	granodiorite	9	2.02	37.2
East Kunlunshan	Paleoproterozoic	quartz diorite	5	1.4	25.9
Qilian, Gansu	Paleoproterozoic	meta. dacite	1	1.6	29.6
Above areas	Paleoproterozoic	inter. basic rock	123		30.2
Beishan, Gansu	Paleoproterozoic	meta. dacite	1	2.9	53.2
Huoyanshan, Gansu	Late of PP	granitoid	16	4.13	75.7
Gaoliduntai, Liaoning	Late of PP	granitoid	5	2.5	46
Huapigou, Heilongjiang	Late of PP	granitoid	30	2.43	44.8
De'er, Tongte, Inner Mongolia	Late of PP	granitoid	4	2.27	41.7

Continued

Location	Geological age	Rock	Sample amount	w(K60) (%)	Thickness of crust (km)
West Kunlunshan	Paleoproterozoic	quartz diorite	1	2.33	42.8
Taihang, Lüliang	Late of PP	granitoid	88	4.14	75.8
Taoke, Shandong	Paleoproterozoic	quartz diorite	20	2.91	53.4
Zouxian, Shandong	Paleoproterozoic	granodiorite	11	2.87	52.75
Kuluketag	Paleoproterozoic	migmatite	3	2.87	52.84
Liaohe Group	Paleoproterozoic	leptite	1	4.16	76.2
Above areas	Paleoproterozoic	granitoid	180		55.9
National average	Paleoproterozoic	(Cheng YQ, 1994)	361	3.4	62.33

Note: Chemical analysis data were quoted from Cheng YQ (1994) and geology of provinces (1984–1993).

References for Appendix 1

Bureau of Geology and Mineral Resources of Provinces (1984—1993) Regional Geology of Provinces. Geological Publishing House, Beijing (in Chinese with English abstract, as shown in Reference for Chapter 1).

Chen MY, Li SX (1996) The evolution of granulite facies metamorphism in eastern Hebei Province. Acta Petrologica Sinica 12(2): 343–358 (in Chinese with English abstract).

Chen QA, Wang FZ (1992) The thermal history and tectonic setting of the granulites in Chongli Group in Archean of northwestern Hebei Province. In: The 40th Anniversary of China University of Geosciences (Contribution to Petrology), pp.206-216. China University of Geosciences Press, Wuhan (in Chinese).

Cheng YQ (1994) An Introduction to Regional Geology of China. 517pp. Geological Publishing House, Beijing (in Chinese).

Cui WY, Wang CQ, Wang SQ (1991) Geochemistry and metamorphism P-T-t path of the Archean Jianping metamorphic complex in western Liaoning Province. Acta Petrologica Sinica 7(4): 13–26 (in Chinese with English abstract).

Dong SB (1986) Metamorphism of China and its Relationship with Crustal Evolution. 233pp. Geological Publishing House, Beijing (in Chinese with English abstract).

Geng YS, Shen QH (2000) Mineral evolution of pyroxenes of garnet mafic granulites in northwestern Hebei Province. Acta Petrologica Sinica 16(1): 29–38 (in Chinese with English abstract).

Grambling JA (1981) Pressure and temperature in Precambrian metamorphic rocks. Earth Planet. Sci. Lett. 53: 63–68.

Guo JH, Zhai MG, Li YG et al (1998) Contrasting metamorphic P-T paths of Archean highpressure granulites from the North China Craton: Metamorphism and tectonic significance. Acta Petrologica Sinica 14(4): 430–448 (in Chinese with English abstract).

He GP, Ye HW (1992) The evolution of metamorphism in granulite facies terrane, eastern Hebei Province. Acta Petrologica Sinica 8(2): 128–135 (in Chinese with English abstract).

He GP, Ye HW, Xia SL (1994) The evolution of metamorphism and PTt paths of granulite facies terrane in Miyun, Beijing. Acta Petrologica Sinica 10(1): 14–26 (in Chinese with English abstract).

He GP, Ye HW (1998) Two types of Early Proterozoic metamorphism and its tectonic significance in eastern Liaoning and southern Jilin areas. Acta Petrologica Sinica 14(2): 152–162 (in Chinese with English abstract).

Ji JQ, Zhong DL, Chen MY et al (1998) The Semugou transpressional shear zone in Jianping metamorphic complex area, west Liaoning Province, China: Implications for the Proterozoic intracontinental deformation. Scientia Geologica Sinica 33(3): 338–348 (in Chinese with English abstract).

Jiang JS, Chen YQ (1993) Cordierite gneisses in Mashan khondalite series, Northeast China. Acta Petrologica Sinica 9(4): 401–410 (in Chinese with English abstract).

Jin W, Li SX, Liu XS (1991) A study of characteristics of Early Precambrian high-grade metamorphic rock series and their metamorphic dynamics in Daqinshan, Inner Mongolia. Acta Petrologica Sinica 7(4): 27–35 (in Chinese with English abstract).

Li SZ, Han ZZ, Liu YJ et al (2001) Regional metamorphic features of Liaohe Group and its geodynamic significance. Geological Review 47(1): 9–18 (in Chinese with English abstract).

Liu GH, Zhang SG, You ZD et al (1993) Main Metamorphic Rock Groups and Metamorphic Evolution of Qinling Orogenic Belt. 191pp. Geological Publishing House, Beijing.

Liu SW, Liang HH (1997) Metamorphism of Al-rich gneisses in Taihang Mountain Archean metamorphic complex. Acta Petrologica Sinica 13(3): 303–312 (in Chinese with English abstract).

Liu YX, Sun DY, Liu PJ (1995) The upper Archean enslavement of magnesioriebechites-bearing gneiss in Liaoning province: Old glaucophane-schist relict. Acta Petrologica Sinica 11(1): 83–92 (in Chinese with English abstract).
Lu LZ, Dong YS (1998) The P-T-X phase relations and their evolution for the equilibrium assemblages of Al-rich gneisses from Early Proterozoic Jingshan Group in east Shandong. Acta Petrologica Sinica 14(2): 140–151 (in Chinese with English abstract).
Lu MJ (1986) Early Proterozoic metamorphic rock series, west Sichuan and east Yunnan, China. Journal of Changchun College of Geology 45(3): 12–22 (in Chinese with English abstract).
Mei HL, Yu HF, Li Q et al (1998) The first discovery of eclogite and Paleoproterozoic granitoids in the Beishan area, northwestern Gansu Province, China. Chinese Science Bulletin 44(4): 356–361.
Qi JY (1992) Metamorphic rock series of Taihua Group and conditions for its formation in eastern Qingling. Scientia Geologica Sinica (suppl.): 94–107 (in Chinese with English abstract).
Qin DX, Yan YF, Tian YL et al (2000) Geological characteristics and ore-forming evolution of Dahongshan copper deposit. Scientia Geologica Sinica 35(2): 129–139 (in Chinese with English abstract).
Shen BF, Luo H, Han GG et al (1994) Archean Geology and Metallization in Northern Liaoning Province and Southern Jilin Province. Geological Publishing House, Beijing (in Chinese with English abstract).
Shen QH, Xu HF, Zhang ZQ et al (1992) Early Precambrian Granulites of China. 237pp. Geological Publishing House, Beijing (in Chinese).
Su SG, Lai XY, Zhang CL (1996) P-T evolution of granulites and their petrogenetic significance in Haiyangsuo and Gejiaji areas, Jiaodong. Geosciences 10(4): 455–460 (in Chinese with English abstract).
Su SG, Gu DL, Zhu GX (1997) The P-T diagram and its tectonic significance of granulite facies metamorphism in the Yishui area, Shandong Province. Acta Petrologica Sinica 13(3): 331–345 (in Chinese with English abstract).
Sun XM, Xu KQ, Ren QJ et al (1992) Confirmation of the Jiapigou Archaean high grade metamorphic terrain and its geological significance. Chinese Science Bulletin 37(10): 847–850.
Tan YJ, Wang GC, Li SX (1991) Archaean Geology and Its Constraints to Gold Prospecting in Pingquan-Chengde Area, North Hebei Province. 80pp. China University of Geosciences Press, Wuhan (in Chinese with English abstract).
Wang CQ, Cui WY, Kröner A et al (2000) Zircon isotopic ages from magnetite quartzites of the Jianping metamorphic complex, western Liaoning Province. Chinese Science Bulletin 45(6): 547-551.
Wang KY, Li JL, Lin RQ (1991) Origin of the Fuping gneisses. Scientia Geologica Sinica (3): 254–267 (in Chinese with English abstract).
Wang RM, Lai XY, Dong WD et al (1994) Some proof of Neoarchean collisional belt in northwestern Hebei Province. In: Qian XL, Wang RM (eds) Geological Evolution of Granulite Belt in North Part of North China. pp.7-20. Seismological Press, Beijing (in Chinese).
Wei CJ, Zhang CG, Zhang AL et al (2001) Metamorphic P-T conditions and geological significance of high-pressure granulite from the Jianping complex, western Liaoning Province. Acta Petrologica Sinica 17(2): 269–282 (in Chinese with English abstract).
Wu CH, Zhong CT, Chen QA (1997) Discussion on the age of khondalite in Jin-Meng (Shanxi-Nei Mongol) high grade terrain. Acta Petrologica Sinica 13(3): 289–302 (in Chinese with English abstract).
Wu JS, Geng YS, Xu HF (1989) Metamorphic geology of Fuping Group. Journal of Institute of Geology, Chinese Academy of Geological Sciences, (19): 213.
Xu HF, Dong YJ, Shi YH et al (1992) Granite-Greenstone Belt in West Shandong Province. 84pp. Geological Publishing House, Beijing (in Chinese).
Yang ZF et al (1998) The Evolution of Regional Crust and the Geochemistry on Gold Mineralization in Jiaodong. 157pp. Geological Publishing House, Beijing (in Chinese with English abstract).
You ZD, Chen NS, Christopher IC (1995) The metamorphism of deeper crust in the Dabie Mountains: as evidenced by the study of granulites near Huilanshan, Luotian. Acta Petrologica Sinica 11(2): 137-147 (in Chinese with English abstract).
Zhai MG, Guo JH, Li JH et al (1995) Discovery the retrogressive metamorphic eclogite in Archean of North China and its significance. Chinese Science Bulletin 40(17): 1590–1594.
Zhong DL (1998) Paleo-Tethyan Orogenic Belt in Western Yunnan and Sichuan. 231pp. Science Press, Beijing (in Chinese).

Appendix 2 Thickness and Forming Velocity of Sedimentary Strata of Chinese Continent

No.	Area	Thickness of sedimentary rocks (m)					Forming velociety of strata (m/Myr)			
		Meso- & Neoprot.	Paleo-zoic	Meso-zoic	Ceno-zoic	Total thickness	Meso- & Neoprot.	Paleo-zoic	Meso-zoic	Ceno-zoic
1	Hingganling, Heilongjiang	10,692	21,508	22,479	3,158	57,832	8.5	73.4	121.5	48.5
2	Jiamusi, Heilongjiang	6,357	20,609	20,286	696	47,948	0.2	70.3	109.6	10.7
3	Yanbian, Jilin		22,043	16,805	2,996	41,844		75.2	91	46
4	Hingganling, Inner Mongolia	2,064	22,319	10,249	520	35,152	1.6	76.2	55.4	8
5	Yinshan, Inner Mongolia	1,281	3,721	13,573	4,957	23,532	9.4	12.7	73.4	76.3
6	Beishan, Inner Mongolia	8,880	27,189	4,300	731	41,100	7.1	92.8	23.2	11.2
7	Altay-Junggar	9,241	41,110	6,770	4,224	61,345	7.4	140.3	36.6	65
8	Tianshan	7,195	23,743	5,454	3,635	40,029	5.7	81	29.5	56
9	Southeast Jilin	19,053	4,237	10,700	1,786	35,776	15.2	14.5	58	27.5
10	East Liaoning	4,214	5,006	8,660	2,009	19,889	3.4	17.1	47	31
11	West Liaoning	11,718	2,285	13,891	5,453	33,347	9.3	7.8	75	83.9
12	Yanshan	9,200	1,733	35,435	125	46,333	7.3	3.7	191.5	9.6
13	Taihangshan	3,126	2,210	2,766	1,130	9,232	2.5	7.5	15	17.4
14	Plain of Heibei	2,183	2,266	2,766	13,000	20,215	1.7	7.7	15	200
15	East Shandong	1,200	1,349	4,781	2,619	9,949	2.6	4.6	25.8	40
16	West Shandong	4,103	—	3,640	1,733	9,476	14	—	20	27
17	North Henan	19,206	2,452	6,152	4,607	32,417	15.3	8.4	33.3	70.9
18	North Anhui	4,285	3,559	7,377	1,111	16,332	9.4	12	39.9	17
19	North Jiangsu (in Sino-Korean–Plate)	5,207	1,597	3,326	1,889	12,306	11.7	5.9	18	29
20	Northeast Shanxi	1,342	1,007	6,052	1,224	9,625	1.1	3.4	33	19
21	Southeast Shanxi	6,789	1,255	2,563	3,777	14,384	5.4	4.3	14	58
22	West Shanxi	875	874	4,055	183	5,987	0.7	3	22	2.8
23	Erdos	14,156	944	5,405	543	21,048	11.3	3.2	29.2	8.4
24	East Ningxia (Qingyang)	1,571	2,573	3,975	2,899	11,018	1.2	9	21.5	44.6
25	Dabie, Hubei	27,719	3,619	800	2,922	35,060	22.1	12.3	4	45
26	East Qinling	18,124	11,394	9,721	3,363	42,602	14.4	38.9	52.5	51.7
27	Qinling-Wudang, Hubei	11,487	12,950	800	2,469	27,706	9.1	44.2	4	38
28	Middle Qinling	23,592	15,152	8,224	1,051	48,019	37	51.7	44.5	16.2
29	West Qinling, Gansu	26,284	18,507	8,087	2,155	55,033	20.9	63.2	43.7	33.2
30	Jiangsu (in Yangtze plate)	1,763	8,893	8,436	7,461	26,553	3.9	30.3	45.6	114.8
31	South Anhui	4,785	7,019	20,093	2,000	20,543	10.5	23.9	109	30.8
32	Northwest Zhejiang	1,235	9,311	11,410	1,771	24,056	4.8	24.2	61.7	32.3
33	North Jiangxi	22,778	10,556	10,165	1,879	45,378	18	36	54.9	28.9
34	South Hubei	639	4,524	11,873	1,015	18,051	3.1	15.4	64.2	15.6
35	North and Middle Hunan	774	4,544	7,928	1,264	14,510	3	15.5	43	19.4
36	Middle Guangxi	—	6,577	3,861	764	11,202	—	22.5	21	11.8
37	Southeast Guangxi	—	42,755	33,342	6,315	82,412	—	146	180.2	97.2
38	North Guangxi	16,261	—	—	—	16,261	12.9	—	—	—
39	Dabashan, Sichuan	10,490	3,402	3,876	4,035	21,803	8.3	11.6	21	62
40	Chengdu–Xichang	14,436	7,838	10,710	2,332	35,216	56.2	27	58	35.9
41	Chongqing–Chengkou	1,802	4,330	5,600	265	11,997	7	14.8	30	4.1
42	Middle& West Guizhou	4,607	9,842	6,248	1,016	21,760	7.4	33.6	33.8	15.6
43	Southeast Guizhou	—	4,223	4,000	150	8,373	—	14.4	21.6	2.3
44	Kunming	1,454	8,664	11,071	1,548	22,737	5.7	29.6	59.8	24
45	Southeast Yunnan	5,092	11,177	12,225	1,508	30,002	19.8	38	66	23
46	Southeast Zhejiang	> 3,000		12,220	378	15,598	11.7	—	66.1	5.8
47	East Fujian	13,453	3,523	5,410	857	23,243	29.4	12	29	13
48	West Fujian	18,929	11,078	18,636	315	39,789	37	37.8	101	4.8
49	East Taiwan	—	—	—	7,350	7,350	—	—	—	113
50	West Taiwan	—	—	—	14,610	14,610	—	—	—	224.8
51	South Jiangxi	6,428	17,050	22,389	1,320	40,759	14	58	121	20.3
52	Southeast Hunan	4,277	13,082	7,004	920	25,283	16.6	44.6	38	14.2

Continued

No.	Area	Thickness of sedimentary rocks (m)					Forming velociety of strata (m/Myr)			
		Meso- & Neoprot.	Paleo-zoic	Meso-zoic	Ceno-zoic	Total thickness	Meso- & Neoprot.	Paleo-zoic	Meso-zoic	Ceno-zoic
53	West & North Guangdong	5,501	17,433	7,142	1,553	31,629	21.4	59.5	38.6	24
54	Middle Guangdong	3,065	8,668	4,663	2,581	18,977	11.9	29.6	25.2	44.4
55	Northeast Guangdong	3,900	2,811	8,979	2,030	17,720	15.2	9.6	48.5	31.2
56	Hainan	1,840	8,590	2,612	1,671	14,713	7.2	29.3	14.1	25.7
57	Kangding–Zoige	11,651	22,205	23,362	2,443	59,661	45	76	126	37.6
58	Zhongdian	> 7,900	17,247	17,922	5,256	48,325	30.7	59	97	81
59	Lanping–Simao	> 7,900	12,588	11,201	7,953	39,642	30.7	43	60.5	122.3
60	Baoshan–Lancang	> 10,230	19,190	7,463	2,551	39,434	39.8	65.5	40.3	39.2
61	Ningxia	1,571	12,729	4,778	3,653	22,731	1.2	43.4	26	56.2
62	Alxa–Longshoushan	9,662	2,356	8,656	493	21,167	7.7	8	46.8	7.6
63	Dunhuang–Alxa	14,525	19,801	9,743	663	44,732	11.6	67.6	52.7	10.2
64	Qilianshan, Gansu	18,543	27,430	7,988	2,298	56,259	14.8	93.6	43.2	35.4
65	Qilianshan, Qinghai	3,547	23,347	4,543	5,308	36,745	2.8	80	24.6	82
66	Qaidam	8,354	16,327	7,412	6,803	38,896	6.6	56	40	105
67	Tarim	5,879	22,451	4,910	13,782	47,022	4.6	76.6	26.5	212
68	Kunlunshan	24,781	19,846	9,039	8,046	61,712	19.7	67.7	49	124
69	East Kunlun	6,073	11,531	13,034	—	30,638	4.8	39.4	70.5	—
70	Bayan Har Shan	—	6,835	10,811	2,687	20,333	—	23.3	58	4.1
71	Tanggula Shan	—	7,424	19,248	5,383	32,055	—	25.3	104	83
72	Karakorum Shan	—	3,904	10,263	2,108	16,275	—	13.3	55.5	32.4
73	Qiangtang–Qamdo	—	11,409	16,587	6,230	34,226	—	38.9	89.7	95.8
74	Gandise–Nyainqentanglha	—	5,607	11,024	2,203	19,474	—	19	59.6	11
75	Himalaya	—	8,107	17,917	2,912	31,521	—	27.7	96.8	44.8

References for Appendix 2

Bureau of Geology and Mineral Resources of Provinces (1984–1993) Regional Geology of Provinces. Geological Publishing House, Beijing (in Chinese with English abstract, as shown in References for Chapter 1).

Appendix 3 Data of Folding and Principal Stress Axes of Chinese Continental Tectonic Events

Appendix 3.1 Data of folding and principal stress axes of Qingbaikou Period (1,000–800 Ma)

Location		Area	Fold amount		Axes	Limb	σ_1(°)	σ_2(°)	σ_3(°)
Long. (°)	Lat. (°)		Antic.	Sync.	Orien. (°)	Angle (°)			
104.5	32.3	Pingwu	6	6	80	40–60	350∠5	80∠1	170∠85
106.5	32.3	Nanjiang	1	1	70	50–75	340∠12	70∠3	160∠78
107.5	32.3	Zhengba*	1	1	50	65–75	320∠5	50∠2	140∠85
110.5	32.3	Zhushan	1	1	100	40–60	190∠10	100∠4	10∠80
103.5	31.3	Maowen*	1	1	340	50–70	70∠10	340∠5	160∠80
110.5	31.7	Shennongjia	1	1	90	30–85	2∠22	90∠10	181∠68
112.5	31.7	Yicheng	5	4	90	20–40	0∠10	90∠3	180∠80
113.5	31.7	Shuixian*	16	16	300	40–60	30∠9	300∠5	210∠81
114.5	31.7	Xinxian*	13	12	319	35–55	49∠11	319∠6	229∠79
115.5	31.7	shancheng	4	6	115	40–70	25∠9	117∠9	251∠77
116.5	31.3	Lu'an, Yuexi	2	1	90	30–55	0∠8	90∠1	180∠82
114.5	31	Huangpi*	7	5	310	30–65	41∠5	310∠2	220∠85
115.5	31	Luotian*	3	1	300	50–30	30∠11	301∠3	211∠79
102.5	30.3	Baoxing*	1	1	0	50–70	89∠9	1∠4	270∠80
103.5	30.3	Qionglai*	1	1	65	40–70	155∠15	65∠8	335∠75
114.5	30.3	Wuhan*	1	1	136	40–65	227∠1	137∠11	317∠78
115.5	30.3	Qichun*	7	6	300	32–58	206∠4	295∠2	30∠85
116.5	30.3	Taihu	1	1	280	50–70	11∠31	280∠3	192∠60
117.5	30.3	Anqing	2	0	76	60–80	345∠6	75∠5	165∠85
118.5	30.3	Jingde	1	0	92	50–80	1∠15	92∠2	181∠75
103.5	29.7	Emei	1	0	280	70–85	192∠7	280∠3	10∠83
112.5	29.7	Huarong	1	1	99	40–50	183∠3	269∠14	75∠76
113.5	29.7	Puqi	2	2	285	40–85	195∠23	285∠9	15∠67
114.5	29.7	Tongshan	3	4	80	50–60	177∠4	80∠21	266∠73
115.5	29.7	Ruichang	2	1	280	35–70	10∠4	280∠1	190∠86
116.5	29.7	Hukou	7	7	86	30–65	356∠20	86∠1	176∠72
118	29.7	Qimen-Tunxi	7	6	85	36–72	350∠29	85∠1	175∠70
120.5	29.7	Zhuji*	1	0	40	50–60	130∠10	41∠9	310∠82
102.5	29	Shimian	1	0	90	60–65	182∠2	90∠2	1∠88
103.5	29	Mabian	9	9	80	60	350∠5	80∠5	171∠85
112.5	29	Yuanjiang	2	1	95	50–70	185∠9	95∠4	5∠82
113.5	29	Pingjiang	8	7	294	40–60	25∠10	295∠4	204∠79
114.5	29	Xiushui	4	4	85	60–70	175∠5	84∠5	355∠86
115.5	29	Yongxiu	5	3	274	25–45	359∠13	275∠15	197∠76
116.5	29	Boyang	2	1	90	40–80	1∠20	90∠5	181∠69
117.5	29	Leping	2	3	85	50–70	175∠9	85∠11	355∠81
118.5	29	Quxian	2	2	100	52–65	0∠5	91∠6	181∠85
119.5	29	Jinghua	1	1	92	20–35	1∠9	90∠4	182∠81
111.5	28.3	Anhua	6	5	91	50–85	182∠13	89∠6	0∠77
112.5	28.3	Changsha	4	3	110	50–60	20∠5	110∠2	201∠86
113.5	28.3	Liuyang	2	3	90	25–40	182∠4	89∠1	1∠86
114.5	28.3	Tonggu	8	8	93	40–85	4∠3	94∠8	273∠84
115.5	28.3	Gaoan	4	2	78	38–70	347∠9	78∠1	177∠81
116.5	28.3	Dongxiang	11	12	90	45–75	182∠14	90∠10	1∠75
102.5	27.7	Xichang	1	1	80	45	171∠2	80∠2	350∠88
103.5	27.7	Zhaotong*	1	1	5	70–80	275∠6	5∠2	95∠85
108.5	27.7	Jiangkou*	1	1	31	60–80	121∠5	30∠0	300∠84
109.5	27.7	Zhijiang	1	1	80	30–75	170∠23	80∠10	350∠77
112.5	27.7	Shaoshan	2	2	92	45–70	179∠18	90∠12	0∠72
114.5	27.7	Yichun	1	1	81	60–70	351∠10	80∠2	170∠80

Continued

Location		Area	Fold amount		Axes	Limb	σ_1(°)	σ_2(°)	σ_3(°)
Long. (°)	Lat. (°)		Antic.	Sync.	Orien. (°)	Angle (°)			
116.5	27.7	Nancheng	2	2	100	30–70	10∠20	100∠10	191∠72
117.5	27.7	Guangze	1	2	98	55–80	6∠8	98∠15	280∠74
101.5	27	Yanbian	1	2	80	70–85	170∠9	80∠4	351∠73
102.5	27	Miyi	7	5	280	50–60	190∠5	280∠2	10∠85
109.5	27	Huitong	1	1	70	25–45	180∠11	92∠5	2∠81
117.5	27	Shunchang	3	3	87	40–60	357∠1	87∠5	261∠85
99.5	26.3	Lanping*	1	1	350	30–40	260∠5	350∠3	80∠86
101.5	26.3	Yongren*	5	4	40	40–50	310∠5	40∠2	130∠84
102.5	26.3	Huili	2	2	80	55–75	171∠10	80∠5	351∠80
103.5	26.3	Dongchuan*	2	2	2	10–88	271∠15	0∠10	90∠75
117.5	26.3	Sanming	3	1	82	60–70	165∠4	82∠5	344∠84
101.5	25.7	Dahao*	1	2	60	40–50	330∠5	60∠4	151∠85
102.5	25.7	Wuding*	2	3	45	35–50	135∠7	45∠6	315∠83
116.5	25.7	Dingchang	0	1	116	30–35	26∠3	116∠3	252∠86
101.5	25	Chuxiong*	1	0	1	36–45	91∠9	1∠3	271∠82
102.5	25	Kunming*	7	6	15	45–65	105∠10	15∠5	285∠80
103.5	25	Yiliang*	10	10	20	40–50	290∠6	20∠2	110∠84
108.5	25	Luocheng	6	5	280	50–75	10∠13	280∠7	190∠77
116.5	25	Shanghang	1	0	95	40–76	5∠10	95∠5	185∠79
102.5	24.3	Yuxi*	6	6	0	47–78	270∠9	0∠4	92∠81
102.5	23.7	Jianshui	4	4	290	40–60	20∠11	290∠3	202∠80
112.5	23.7	Huaiji	1	1	270	30–72	180∠19	90∠10	0∠71
103.5	22.7	Jinping*	3	4	310	40–50	220∠5	310∠3	40∠85
100.5	22.3	Jinghong*	4	3	10	30–60	100∠15	10∠12	280∠74
100.5	21.7	Menghai*	4	5	30	30–50	330∠10	30∠6	120∠80
* Re-deformation folds by later tectonics.			234	229					

Appendix 3.2 Data of folding and principal stress axis of Qilianian Period (513–397 Ma)

Location		Area	Fold amount		Axes	Limb	σ_1(°)	σ_2(°)	σ_3(°)
Long. (°)	Lat. (°)		Antic.	Sync.	Orien. (°)	Angle (°)			
109	19.3	Hainan Island	1	2	40	45–60	130∠15	40∠10	310∠75
112	21.6	Yangjiang, Guanghai	1	3	0	35–75	90∠5	0∠10	270∠85
109.5	22.3	Lingshan	4	4	85	40–70	175∠15	85∠12	355∠75
110.5	22.3	Yulin	5	3	19	30–70	109∠8	19∠5	289∠82
112	22.3	Yangchun, Kaiping	4	5	5	30–70	95∠15	5∠16	275∠75
107.5	23	Daxin	5	4	90	40–60	180∠10	90∠5	0∠80
109.5	23	Nanning, Guixian	26	27	76	20–70	166∠15	76∠5	346∠75
114.5	22.7	Baoan, Huiyang		3	0	20–80	90∠10	0∠5	270∠80
105.5	23.7	Funing	1, arc type		80	35–45	170∠10	80∠7	350∠80
108	23.3	Baise, Laibin	8	8	90	30–60	180∠7	90∠5	0∠83
111	23.7	Guiping, Wuzhou	6	5	92	35–80	2∠12	92∠8	182∠78
113	23.7	Huaiji, Chonghua	5	6	51	30–85	141∠15	51∠10	321∠75
114.5	23.7	Heyuan	2	2	357	30–65	267∠7	357∠20	170∠80
111	24.3	Lipu, Hexian	23	21	87	40–75	177∠15	87∠12	357∠75
112.5	24.3	Yangshan	2	2	33	45–70	123∠12	33∠11	303∠78
114	24.3	Yingde, Lianping	3	3	15	45–80	105∠10	15∠8	285∠80
115.5	24.3	Xingning	4	4	20	60–85	110∠13	20∠10	290∠77
116.5	24.3	Meixian	3	1	0	30–80	90∠18	0∠5	270∠72
110.5	24.7	Guilin	2	1	256	42–72	163∠12	256∠24	44∠63
111.5	25	Jiangyong	8	7	40	50–60	130∠53	40∠10	10∠85
112.5	25	Lianxian	11,arc	11,arc	90	50–80	0∠10	90∠8	180∠80
113.5	25	Shaoguan	6	6	357	43–60	267∠8	357∠5	87∠82
114.5	25	Longnan	11	5	10	50–80	100∠5	10∠5	280∠85
116	25	Xunwu, Shanghang	8	8	10	30–80	100∠12	10∠5	280∠78

Continued

Location		Area	Fold amount		Axes	Limb	$\sigma_1(°)$	$\sigma_2(°)$	$\sigma_3(°)$
Long. (°)	Lat. (°)		Antic.	Sync.	Orien. (°)	Angle (°)			
117.5	25	Longyan	1		0	30–50	90∠10	0∠5	270∠80
113	25.7	Guiyang, Chenxian	37	36	110	32–85	20∠11	110∠10	200∠79
114.5	25.7	Ganzhou	20	20	355	40–80	85∠20	355∠10	265∠70
116	25.7	Yudu-Changding	10	4	180	30–60	90∠5	180∠10	270∠85
118.5	25.7	Dehua		1	182	60–70	91∠5	182∠8	1∠80
112	26	Yangmingshan	1	1	90	30–40	0∠5	90∠2	180∠85
114.5	26.3	Jinggangshan	15	14	350	35–85	260∠20	350∠15	80∠70
116	26.3	Xingguo, Ninghua	7	5	4	35–80	271∠18	4∠7	103∠71
118	26.3	Sanming, Nanping	5	5	197	25–62	106∠7	197∠10	342∠78
112.5	27	Hengyang	2	3	110	43–69	200∠13	110∠9	290∠77
114.5	27	Youxian, Yongxin	9	8	5	30–70	95∠5	5∠10	275∠85
117.5	27	Guangchang, Jianou	11	10	3	45–61	93∠8	3∠5	273∠82
118	27.7	Guangze, Pucheng	6	6	10	30–80	100∠25	10∠10	280∠65
119.5	28	Lishui, Taishun	3		48	30–80	138∠20	48∠15	318∠70
105.7	26.7	Nayong, Zhijin	1		87	14–20	177∠5	87∠3	356∠86
101	28.2	Muli	3	2	95	30–40	5∠5	95∠0	185∠84
122.2	43	Wafanggou	1	3	55	70–75	144∠5	55∠2	325∠86
125.1	43.5	Gongzhuling	1	2	290	45–60	200∠10	290∠6	110∠80
126.2	44.4	Jiutai	1	0	300	40–60	211∠4	300∠4	121∠85
126.4	42.9	Hulan	2	2	330	45–70	60∠5	330∠4	121∠85
127.2	43.1	South Jiaohe	1	1	20	50–70	110∠5	20∠5	200∠85
128.6	43.9	North sunhua	1	1	0	62–75	91∠4	0∠6	271∠84
128.4	43.6	Guandi	1	1	0	40–75	89∠3	0∠7	269∠86
128.5	43.1	Antu	1	2	320	50–60	51∠3	320∠2	231∠88
128.5	43	Hanchonggou	0	1	320	55–70	51∠5	320∠6	230∠85
128.6	43	North Shuguang	1	0	320	40–70	50∠4	320∠4	230∠86
129	42.7	West Longjing	2	1	340	40–60	70∠5	340∠5	250∠85
129	42.8	Yanji	0	1	330	60–70	62∠2	330∠2	241∠88
131.9	43.1	Hunchun	0	1	0	40–65	90∠4	0∠6	270∠85
100	38	North Qilian	3	3	310	60–70	41∠4	310∠5	221∠85
102.2	36.2	Lajishan	1	1	280	50–70	192∠5	280∠3	12∠84
98.4	36.5	North Qaidam	0	1	290	60–70	200∠6	290∠10	20∠83
100	38.2	South Qilian	6	6	292	40–50	202∠4	292∠5	22∠86
96	38.6	Yueyashan, South Qilian	4	5	270	60–70	180∠3	270∠2	0∠87
91	37.5	Qimantag	5	5	90	60	180∠4	90∠2	0∠88
98	39.3	North Qilian	6	6	300	50–70	32∠6	300∠10	211∠82
98	39	Middle Qilian	11	11	300	60–70	30∠8	302∠5	209∠83
96	38.7	South Qilian	3	2	292	60–70	203∠5	292∠6	22∠85
87.8	48.5	Kasna	6	5	178	70–80	88∠6	178∠10	268∠84
90	47	Kokrokay	4	4	305	70–80	35∠5	305∠8	215∠82
82	42.6	Hark, Tianshan	10	9	70	60–80	340∠7	250∠10	160∠84
86.2	43	Chaganor, Tianshan	7	6	110	40–70	202∠6	110∠9	21∠81
89	41.3	Kuruktag	17	16	98	40–75	8∠10	98∠8	188∠80
93	41	Xingxingxia	6	5	128	50–70	37∠9	128∠12	217∠81
89	38.5	Altun Shan	10	9	100	60–80	191∠7	100∠10	11∠82
88	37.5	East Kunlun	5	6	95	40–75	7∠5	96∠6	187∠85
80	36	Middle Kunlun	4	3	91	55–70	182∠6	91∠2	2∠84
75	38	West Kunlun	18	16	125	50–75	34∠8	125∠7	215∠81
			420	381					

Appendix 3.3 Data of folding and principal stress axis of Tianshanian Period (297–260 Ma)

Location		Area	Fold amount		Axes	Limb	σ_1(°)	σ_2(°)	σ_3(°)
Long. (°)	Lat. (°)		Antic.	Sync.	Orien. (°)	Angle (°)			
90	47.7	Nort	3	2	310	50–60	40∠10	310∠7	221∠80
89	47	Kelan	6	7	306	50–60	36∠5	306∠10	216∠82
90	46.2	Ertix River	4	5	300	50–75	210∠7	300∠5	32∠80
85.7	47	West Junggar	23	21	285	40–75	16∠8	285∠8	195∠82
90	45.8	East Junggar	21	20	302	50–80	32∠10	302∠9	212∠80
86	43.5	North Tianshan	12	10	290	60–80	200∠4	290∠6	20∠86
82	43	Tekes, Tianshan	13	12	86	55–75	356∠3	86∠6	176∠87
86.2	43	Bostenhu, Tianshan	16	17	100	40–70	9∠4	100∠10	190∠86
89	41.3	Kuruktag	12	11	88	45–70	358∠8	88∠7	178∠82
93	41	Xingxingxia	6	5	80	40–65	350∠5	80∠8	170∠85
88	37.5	East Kunlun	14	13	87	50–80	176∠6	87∠9	356∠84
80	36	Middle Kunlun	10	11	122	50–70	202∠5	292∠7	22∠85
75	39	West Kunlun	7	6	130	60–80	40∠4	310∠10	220∠86
97	37.3	JunUl Shan	4	5	90	60–80	180∠4	270∠5	0∠86
92	36.2	Erdaogou	6	5	300	64–75	30∠3	300∠10	210∠87
96	35.6	Burhan Budai	4	3	290	60–75	200∠4	290∠6	20∠86
99	34.5	Anyemaqen	2	2	300	55–80	210∠6	300∠5	30∠84
96.2	41.8	Beishan	15	14	270	40–70	357∠12	268∠15	178∠80
106	34	Tianshui, Huixian	6	6	88	30–70	177∠4	88∠5	358∠85
104.8	33.3	Wudu	8	8	280	40–80	190∠8	280∠10	10∠80
95.5	39.7	Dunhuang	4	4	82	60–70	356∠8	82∠6	174∠82
103.5	39.5	Alxa	4	5	85	50–60	174∠3	85∠6	355∠86
108	42	North Badain Jaran	6	7	90	40–70	1∠8	91∠5	180∠82
114	44	Sonid Zuo Qi	8	7	80	35–65	350∠6	260∠8	172∠84
117	45	Ujimqin	11	12	65	35–60	336∠5	65∠7	155∠85
121	48	Songling	9	8	60	40–60	150∠4	60∠10	331∠86
126	51	Huma	6	6	50	35–55	141∠6	235∠8	325∠84
126	43.3	Shuangyang	8	7	55	30–60	145∠6	235∠8	325∠84
129.7	43.4	Wangqing	2	3	52	30–60	322∠5	52∠9	142∠85
			250	242					

Appendix 3.4 Data of folding and principal stress axis of Indochina Period (260–200 Ma)

Location		Area	Fold amount		Axes	Limb	σ_1(°)	σ_2(°)	σ_3(°)
Long. (°)	Lat. (°)		Antic.	Sync.	Orien. (°)	Angle (°)			
97.8	33.7	Tongtianhe	6	5	290	75–85	20∠3	290∠5	200∠87
100	36.5	Qinghai Nanshan	0	1	292	40–65	202∠5	292∠3	22∠85
101	35	Zeku, Tongde	4	3	282	40–60	12∠3	282∠4	193∠87
100	34.5	Maqen	8	8	290	40–60	201∠6	290∠10	21∠83
93	35.8	East Kunlun	4	6	280	50–70	10∠2	280∠6	191∠88
98	34	Bayn Har Shan	6	6	295	45–65	205∠5	295∠8	25∠85
99.5	33	Baima	2	2	302	40–50	212∠6	302∠5	32∠84
101	37.9	North Qilian	10	9	280	39–60	11∠6	280∠5	190∠83
99.5	37.8	Middle Qilian	7	8	290	50–70	22∠7	290∠4	203∠83
99	37.5	South Qilian	10	9	282	20–60	22∠5	292∠10	202∠85
93.7	38.8	Olunbluk	1	0	285	40–50	195∠2	285∠6	15∠87
94.4	38.3	Maoniushan	0	1	280	30–50	191∠5	280∠8	10∠85
91	37.7	South Qimantag	0	1	284	20–30	13∠3	282∠7	192∠86
91.6	36	East Kunlun	1	2	300	30–64	210∠10	300∠5	30∠80
94	33.5	Tanggula Shan	12	13	290	35–60	20∠4	290∠10	202∠84
101.9	37.3	Menyuan	3	2	300	45–75	208∠3	300∠8	28∠85

Continued

Location		Area	Fold amount		Axes	Limb	σ_1(°)	σ_2(°)	σ_3(°)
Long. (°)	Lat. (°)		Antic.	Sync.	Orien. (°)	Angle (°)			
106	34	Tianshui–Huixian	6	6	88	30–70	177∠4	88∠5	358∠85
104.8	33.3	Wudu	8	8	208	40–80	190∠8	280∠10	10∠80
95.5	39.7	Dunhuang–Batushan	4	4	82	60–70	356∠8	82∠6	174∠82
103.8	36.1	Tianzhu–Jingtai	1	1	100	13–25	190∠2	100∠8	10∠88
79	35.8	Karakorum	14	10	280	35–70	192∠4	280∠7	12∠86
87.5	36.5	East Kunlun	8	7	86	35–70	355∠7	86∠9	175∠83
98	29	Zogang	6	6	335	50–70	65∠5	335∠6	235∠85
97.8	31	Qamdo	17	18	150	40–65	61∠6	150∠10	240∠84
91	32.5	Tanggula Shan	10	12	100	40–60	10∠5	100∠8	190∠85
88.2	34	West Tanggula	7	7	125	40–65	35∠3	125∠6	215∠87
88	35.8	Hohxil Shan	2	2	89	30–60	358∠4	89∠7	179∠86
126.5	50.3	Jadaqi	4	5	90	30–60	1∠7	91∠2	180∠82
126.5	49.3	Longzhen	11	10	41	25–65	132∠15	40∠3	311∠74
128.5	47	Tieli	3	4	45	30–65	135∠10	45∠5	314∠80
129.5	46.3	Hesgula	6	6	60	32–60	329∠6	59∠1	148∠84
132.5	46.3	Baoqing	1	1	46	30–50	136∠8	46∠4	317∠82
122	45.5	Tuquan	8	8	80	28–48	170∠15	80∠3	350∠75
128.5	45.3	Bingxian	8	3	300	32–52	30∠10	300∠5	210∠81
119.5	44	Balin Zuoqi	6	11	75	20–55	345∠14	75∠2	165∠84
126	44	Jilin city 10	9	10	45	35–55	135∠9	45∠3	315∠81
131	43.7	Shuangchengzi	9	4	80	30–50	350∠6	80∠1	170∠84
129.5	43	Yanji	8	6	45	40–57	134∠5	45∠5	315∠85
118	42.7	Chifeng	2	1	70	38–65	160∠10	70∠7	340∠80
120.5	42.3	Xiawa	7	6	81	30–66	352∠7	81∠2	171∠83
126	42	Tonghua	3	8	67	30–62	157∠9	67∠3	338∠81
104.5	41	Uliji	3	4	88	28–58	178∠15	88∠4	358∠75
118	41	Chengde	11	3	83	40–60	173∠8	83∠2	353∠82
110.5	40.3	Baotou	3	4	86	42–62	356∠7	86∠1	176∠83
118	40	Tangshan	8	11	93	30–50	4∠8	93∠2	183∠82
110.2	39.6	Dongsheng	11	0	85	32–48	355∠3	85∠1	175∠87
115.6	39.7	Laishui 25	6	5	85	28–40	175∠18	85∠5	355∠72
109.5	37	Yan'an	5	0	80	13–20	170∠2	80∠1	350∠88
109	34	Qinling	12	5	92	40–60	192∠5	92∠1	42∠85
117.5	34.3	Xuzhou	37	36	44	42–65	314∠6	44∠0	134∠84
102	33	Hongyuan	10	8	90	30–45	180∠15	90∠0	0∠75
103.5	33	Zhangla	5	2	100	35–55	190∠10	100∠5	10∠80
109	33.3	Dabashan	9	7	290	35–65	20∠10	290∠1	200∠80
118	33	Bengbu	5	3	260	30–52	350∠7	260∠1	170∠83
104.5	32.3	Pingwu	21	24	75	36–65	165∠10	75∠6	345∠80
106.5	32.3	Nanjiang	16	0	82	30–60	172∠5	82∠4	351∠86
119	32.3	Nanjing	56	51	72	30–65	162∠5	72∠3	342∠84
103.5	31.7	Maowen	17	17	90	28–66	0∠4	90∠2	180∠86
113.5	31.7	Shuixian	27	27	300	31–55	30∠16	300∠10	210∠74
118.5	31.7	Maanshan 25	17	16	51	29–54	321∠6	51∠0	141∠84
109	31.5	Chengkou	12	11	288	30–50	18∠4	288∠5	199∠85
101	30.7	Kangding	14	12	90	29–55	0∠5	90∠4	180∠85
114	31	Huangbi	18	19	29	30–60	20∠16	290∠7	200∠6
118	31	Xuancheng	24	26	47	29–65	317∠8	47∠1	137∠82
120.5	31.3	Suzhou	15	11	53	28–60	323∠5	53∠1	143∠85
102.5	30.3	Baoxing	8	8	100	20–50	10∠5	100∠2	190∠85
115	30	Tongshan 23	62	61	90	30–60	180∠14	90∠7	0∠76
117	29.7	Qimen	40	46	85	29–55	176∠7	85∠6	355∠82
120.5	29.7	Zhuji	49	37	58	35–60	328∠5	58∠10	148∠85
101	28	Yongning	29	31	85	34–65	175∠5	85∠5	355∠85
112.5	27.5	Hunan	48	54	88	30–65	176∠7	88∠4	356∠83
115	27.3	Jiangxi	46	47	87	28–66	357∠8	87∠7	177∠83
117.5	26.7	Fujian	14	28	95	20–55	185∠5	95∠5	5∠85

Continued

Location		Area	Fold amount		Axes	Limb	σ_1(°)	σ_2(°)	σ_3(°)
Long. (°)	Lat. (°)		Antic.	Sync.	Orien. (°)	Angle (°)			
107	26	Guizhou	28	30	97	20–45	187∠2	97∠1	7∠88
107	23.3	Guangxi	100	91	85	32–50	175∠10	85∠8	355∠80
114	23.5	Guangdong	49	65	89	30–48	359∠15	89∠9	179∠75
100.5	24	Jinggu	42	43	1	40–60	91∠15	1∠6	271∠75
105.5	19	Hainan	0	3	90	35–64	180∠10	90∠5	0∠80
		Joint observation points 83	1,109	1,086					

Appendix 3.5 Data of folding and principal stress axis of Yanshanian Period (200–135 Ma)

Location		Area	Fold amount		Axes	Limb	σ_1(°)	σ_2(°)	σ_3(°)
Long. (°)	Lat. (°)		Antic.	Sync.	Orien. (°)	Angle (°)			
126	50	Longzhen	8	15	24	25–50	294∠5	24∠3	114∠85
128.5	47	Tieli	0	3	30	30–55	120∠3	30∠6	300∠87
132.5	46.3	Baoqing	0	1	25	30–50	115∠6	25∠5	295∠84
119.5	46.3	Hesgula	3	2	14	28–52	284∠5	14∠3	104∠83
121	45.7	Tuquan	17	20	35	25–54	305∠5	35∠4	125∠84
127.5	45.3	Binxian	10	10	27	20–50	117∠9	27∠7	298∠81
118.5	43.3	Wufendi	15	16	200	30–55	110∠9	200∠6	290∠81
130	43.3	Yanji	10	10	28	30–60	118∠5	208∠4	297∠86
120	42.3	Aohan Qi	4	13	29	30–55	299∠3	29∠5	119∠87
117	41.3	Xinglong	36	37	30	25–60	300∠3	30∠2	120∠87
115	39.7	Dongsheng	8	1	28	28–45	118∠1	28∠1	298∠89
115	39.7	Laishui 60	8	11	41	30–63	131∠8	41∠7	312∠81
119	39.7	Qinhuangdao	3	5	23	32–60	113∠7	203∠1	293∠83
107	38.7	Helanshan	14	10	19	30–55	109∠2	199∠1	289∠88
111.5	39	Wuzhai	39	40	32	14–28	122∠4	32∠0	210∠87
114	39	Wutaishan	39	38	45	30–55	315∠4	45∠0	135∠86
111	37	Jiaokou	114	103	25	32–56	115∠4	25∠1	292∠86
113	37	Yushe	129	121	29	31–60	119∠0	29∠0	∠90
107.2	36.7	Huanxian	5	0	2	15–30	92∠3	2∠2	272∠88
109.5	36.7	Yan'an	18	0	22	∼5	292∠1	202∠1	112∠89
114.5	37	Xingtai	7	10	5	30–50	95∠8	5∠6	275∠81
118.5	36	Shandong 29	9	8	24	10–35	294∠7	24∠3	193∠82
111.5	35	Houma	20	18	32	15–50	122∠4	32∠2	301∠86
118	33.3	Bengbu	70	66	25	25–60	294∠9	25∠1	114∠81
110	30	West Hubei	90	88	37	30–60	127∠19	37∠9	307∠71
115	30.3	Wuhan 31	15	10	34	25–60	304∠4	34∠3	124∠87
119.5	30.3	Zhejiang–Anhui	114	106	28	30–60	298∠10	208∠8	118∠80
111	27.7	Hunan 18	208	204	30	30–65	120∠20	30∠12	300∠70
102	27.7	Xichang	36	31	25	32–66	115∠5	25∠1	295∠85
106.5	26.7	Liupanshui	79	78	17	25–55	107∠7	17∠5	286∠83
117	26	Fujian–Jiangxi 30	102	126	22	33–65	293∠9	202∠15	113∠80
103	24.3	Kunming	90	90	39	25–60	129∠8	39∠2	309∠82
110	25	Guilin	130	121	16	26–56	106∠9	16∠3	286∠81
115	24.7	Xunwu	23	47	18	30–50	108∠13	198∠23	345∠63
109.5	23	Nanning	51	66	21	32–60	291∠17	21∠8	111∠73
113.5	23.3	Guangzhou	41	77	29	30–65	119∠18	29∠10	308∠72
85.7	46	Kramay	1	1	50	20–30	140∠20	50∠5	320∠70
		Joint observation points 168	1,566	1,603					

Appendix 3.6 Data of folding and principal stress axis of Sichuanian Period (135–56 Ma)

Location		Area	Fold amount		Axes	Limb	σ_1(°)	σ_2(°)	σ_3(°)
Long. (°)	Lat. (°)		Antic.	Sync.	Orien. (°)	Angle (°)			
90.8	38.6	Xorkuli	8	8	90	60–85	2∠2	90∠85	271∠3
99.1	38.1	Muli	2	2	280	25–52	190∠6	280∠10	10∠82
91	34	upper Tuotuo River	2	2	285	30–60	195∠3	285∠5	10∠85
92	33.3	Wenquan	6	6	290	40–60	200∠8	290∠4	20∠85
94.2	33.3	Moyun	7	7	294	30–50	24∠6	294∠4	204∠84
103.2	36.3	Minhe–Hekou	10	7	288	20–30	19∠7	288∠10	199∠82
104.2	35.1	Weiyuan	1	1	290	20–30	20∠3	290∠5	200∠87
91	32.5	Tanggula	7	8	100	40–65	10∠5	100∠8	190∠85
85	33	Dinggu	3	3	93	40–60	183∠2	93∠6	3∠88
81	34	Zapug	19	18	90	40–60	1∠6	90∠5	181∠84
93	31	Nyainqentanglha	17	18	93	30–70	3∠4	93∠7	183∠86
85	31	Coqen	15	15	92	30–70	2∠6	92∠5	182∠84
124.5	51	Songling	1	6	83	10–35	353∠11	83∠4	173∠78
120.5	45.7	Tulemaotu 3					355∠1	85∠2	175∠85
125	46	Songhuajiang–Liaohe	11	0	296	0.5–5	26∠2	296∠1	206∠89
119.5	44	Balin Zuoqi	4	5	102	1–32	12∠3	102∠2	192∠87
130	43.5	Yanbian	0	9	112	5–33	22∠9	112∠2	202∠81
115	43	Liaoyuan	7	0	315	4–32	225∠6	315∠6	45∠83
118.5	43	Wufendi	3	5	290	2–32	20∠15	290∠6	200∠75
125	43	Siping 12	4	0	318	4–32	48∠3	318∠2	228∠87
121.8	42	Fuxin 16	2	2	162	10–32	252∠10	162∠1	72∠80
118.5	41.7	Harqin Qi	2	1	115	10–32	25∠3	115∠1	205∠87
104.5	40.5	Uliji	4	6	111	12–32	221∠2	111∠1	21∠88
115.5	40.7	Longguan 17	6	7	308	12–32	38∠1	308∠1	216∠88
109.5	39.7	Dongsheng	40	19	98	15–30	8∠2	98∠4	186∠86
119	40	Qinhuangdao	6	7	295	20–40	25∠15	295∠7	206∠80
108.5	38.7	Urad Qianqi	20	4	310	20–40	40∠6	310∠2	220∠87
112	38	Shanxi	3	3	284	20–30	196∠1	284∠2	102∠87
120.2	37	Zhaoyuan–Yexian 14	1	1	122	15–30	30∠18	122∠10	240∠70
103	36.4	Lanzhou	5	7	112	20–36	23∠1	112∠1	296∠88
107.5	35.1	Huanxian	18	1	308	20–30	218∠4	308∠4	38∠85
118.5	36	Middle Shandong 82	12	12	299	10–32	29∠6	299∠3	206∠82
113	34	Henan 10	4	3	106	15–30	196∠12	106∠3	16∠77
117.5	33.5	Bengbu	6	8	321	10–35	51∠3	321∠1	231∠87
102	32	Markam	48	42	310	25–40	40∠6	310∠1	220∠85
106	32	Yilong	85	43	292	20–40	202∠5	292∠1	22∠85
109	32	Dabashan 13	84	76	285	20–40	15∠14	285∠3	195∠76
111	31.5	Hubei 31	120	105	288	22–45	18∠2	288∠3	108∠87
117.5	31.3	Jiangsu–Anhui 25	77	65	115	20–35	205∠2	115∠2	205∠88
103.5	29.3	West Sichuan	83	52	107	22–36	17∠3	107∠1	197∠87
120	29	Zhejiang 29	21	36	295	20–34	25∠3	295∠5	205∠87
102.3	26.7	Yanbian	69	80	302	25–40	210∠6	302∠2	30∠83
105.3	25.3	Liupanshui	15	13	310	25–44	220∠5	310∠2	40∠86
112	27.5	Hunan 18	7	12	123	20–50	213∠2	123∠9	315∠80
115.7	26.3	Jiangxi	12	33	120	20–50	220∠3	120∠12	40∠87
117.5	26.3	Fujian 11	6	27	122	20–54	31∠6	122∠5	262∠82
102	23.7	Yuxi	122	137	301	30–60	211∠10	301∠4	31∠80
114	23.7	Guangdong	10	22	295	20–50	205∠11	295∠3	26∠78
109.2	22.5	Guixian	12	31	121	24–50	31∠4	121∠3	212∠86
109.3	19.5	Hainan	1	1	335	25–50	241∠1	335∠25	150∠65
		281	1,032	976					

* Joint observation points

Appendix 3.7 Data of folding and principal stress axis of North Sinian Period (56–23 Ma)

Location		Area	Fold amount		Axes	Limb	σ_1(°)	σ_2(°)	σ_3(°)
Long. (°)	Lat. (°)		Antic.	Sync.	Orien. (°)	Angle (°)			
128	48	Heilongjiang	2	8	28	0.5–10	118∠8	28∠5	298∠81
124	46	Songhuajiang-Nenjiang	116	110	10	0.5–6	100∠1	10∠2	280∠88
127	43	Jilin	12	21	205	2–32	295∠8	205∠4	25∠82
122	41	Lower Liao River 19	12	10	27	2–33	297∠3	27∠2	117∠87
108	40	Hanggin Qi	8	5	4	0.5–18	94∠3	184∠1	274∠87
106	37	Ningxia	22	20	5	0.5–20	96∠2	5∠2	275∠88
103.9	35.9	South Lanzhou	1	0	178	20–30	86∠4	175∠7	265∠85
104.2	36.3	East Liuhuangshan	0	1	15	20–30	106∠6	15∠10	285∠82
96.9	39	East Yemashan	1	0	183	20–30	274∠4	183∠6	94∠84
97.2	39.6	Yumenhanxia	1	0	180	30–40	0∠5	180∠4	92∠80
118.5	36.5	Shandong 24	6	5	26	10–50	115∠12	26∠3	298∠78
121.5	34	South Huanghai	39	30	9	0.5–28	99∠1	189∠3	279∠88
120	33	North Jiangsu	49	45	175	0.5–30	85∠2	175∠2	265∠87
105	32.5	Guangyuan	33	28	25	2–30	115∠10	25∠4	295∠80
103	31	Guanxian	82	77	40	2–33	130∠9	40∠3	310∠80
112.5	31.2	Hubei 12	4	3	9	5–35	279∠5	9∠3	99∠85
119	32	Nanjing 25	2	5	20	4–33	110∠5	20∠4	290∠85
101.5	30	Kangding	78	82	8	6–32	98∠12	188∠5	278∠78
107.5	30	Daxian	86	72	28	6–32	298∠14	28∠6	118∠75
102	29	Mianning	107	110	1	2–34	91∠10	181∠4	271∠80
120	29	Zhejiang 35	4	3	17	2–31	287∠4	197∠5	107∠86
102	26.3	Huili	110	132	2	2–36	272∠9	182∠5	92∠80
113	27	Hunan	6	15	19	10–32	109∠7	199∠4	289∠82
116	27	Jiangxi-Fujian	6	6	184	6–32	94∠6	184∠4	274∠83
99.5	24	Fengqing	133	142	7	10–40	277∠10	7∠2	97∠80
102.5	24.3	Yuxi	48	45	356	14–44	86∠7	356∠3	266∠83
100.5	22	Jinghong	55	55	8	12–46	278∠11	188∠4	98∠78
113	23	Guangdong-Guangxi	10	17	5	10–36	95∠6	5∠1	275∠84
114	20.5	Mouth of Zhujiang	10	36	170	2–32	80∠1	170∠1	260∠89
		Joint observation points 115	1,043	1,083					

Appendix 3.8 Data of folding and principal stress axis of Himalayan Period (23–0.78 Ma)

Location		Area	Fold amount		Axes	Limb	σ_1(°)	σ_2(°)	σ_3(°)
Long. (°)	Lat. (°)		Antic.	Sync.	Orien. (°)	Angle (°)			
98.4	37	Ulan	1	0	300	0.5–22	30∠5	300∠5	210∠85
100.5	37.7	Middle Qilian	0	1	280	10–32	190∠4	280∠6	10∠86
97.5	39.7	Yumen	4	0	300	10–40	32∠6	302∠4	210∠84
104.2	35.5	Dingxi	1	1	305	10–32	35∠5	305∠3	215∠85
106	33.8	Huixian	0	1	70	20–40	340∠4	70∠5	160∠86
102.7	38.3	Jinchang	0	4	280	0.5–20	10∠6	280∠6	190∠82
79	40.5	Keping	6	5	60–110	10–70	175∠3	85∠5	355∠87
75	39.5	Wuqia	5	4	70–112	10–75	181∠5	91∠8	1∠85
82	41.6	Kuqa	3	2	80	10–70	170∠6	80∠4	350∠85
78	37.4	Yecheng	2	1	115	12–68	195∠4	115∠6	15∠86
82.2	37.7	Minfeng	1	2	86	10–65	176∠4	86∠4	356∠85
89	37	East Kunlun	2	4	100	16–60	180∠5	100∠5	0∠85
93	41	Xingxingxia	5	6	80–100	15–50	178∠3	88∠6	358∠87
91	28.3	East Himalaya	6	6	95	40–50	186∠6	95∠7	5∠84
86	29	Middle Himalaya	8	7	102	40–60	192∠4	102∠5	12∠86

Continued

Location		Area	Fold amount		Axes	Limb	σ_1(°)	σ_2(°)	σ_3(°)
Long. (°)	Lat. (°)		Antic.	Sync.	Orien. (°)	Angle (°)			
80	31	West Himalaya	7	7	150	40–70	240∠5	150∠6	60∠85
81	32	Gegyai	4	3	118	40–60	208∠7	118∠6	28∠82
85	31	Coqen	15	15	92	30–70	2∠7	92∠5	182∠84
93	31	Nyainqentangulha	17	18	93	30–70	3∠4	93∠7	183∠86
81	34	Zapug	19	18	90	40–60	1∠6	90∠5	181∠84
85	33	Dinggu	3	3	93	42–60	183∠2	93∠6	3∠88
91	32.5	Tanggula	7	8	100	40–65	10∠5	100∠8	190∠85
122.3	41.2	Liaoning	4	2	257	14–20	166∠30	257∠3	352∠60
106	37	Ningxia	9	5	292	0.5–20	202∠3	292∠2	22∠87
116.5	38.7	Huanghua	6	5	100	0.5–12	10∠2	100∠1	280∠88
118.5	35.8	Middle Shandong 40					174∠10	85∠10	297∠75
118	37.2	Guangji	8	6	77	0.5–15	167∠3	77∠1	346∠88
105.5	29	Sichuan–Guizhou	11	10	90	0.5–20	180∠6	90∠4	0∠85
113.5	31	Hubei	3	2	277	0.5–16	188∠8	277∠1	91∠82
117.5	32	Anhui	0	3	91	0.5–19	0∠5	91∠2	182∠85
122.5	32.5	South Huanghai	41	30	85	0.5–20	175∠2	85∠1	356∠88
119.5	33.5	North Jiangsu	19	17	90	0.5–20	0∠3	90∠3	180∠87
119.5	29	Zhejiang	2	1	273	0.5–14	3∠4	273∠1	98∠86
112	28.5	Hunan	7	8	94	0.5–20	4∠2	94∠12	273∠78
115.5	27.5	Jiangxi	6	6	269	0.5–16	359∠4	269∠5	178∠83
118	25.5	Fujian 9					181∠7	272∠12	356∠74
102	25	Yunnan 9	14	16	110	0.5–26	201∠8	110∠1	291∠82
108	23	Guangxi	0	7	262	0.5–20	352∠4	262∠2	82∠89
113	23	Guangdong	1	4	85	0.5–20	175∠5	85∠2	355∠87
		Joint observation points 58	247	222					

References for Appendix 3

Bureau of Geology and Mineral Resources of Provinces (1984–1993) Regional Geology of Provinces. Geological Publishing House, Beijing (in Chinese with English abstract, as shown in References for Chapter 1).

Appendix 4 Differential Stress Magnitude of Chinese Continent in Mesozoic–Cenozoic

Appendix 4.1 Indochina Tectonic Period

average value of differential stress ($\Delta\sigma$) (111) 105.5 MPa

Tectonic Period	Area	Long. °E	Lat. °N	Rock	Determined Mineral	Sample	$\Delta\sigma$ (MPa)	Sources
Indochina	Lower & Middle Yangtze	116	30	granitoid	quartz	20	113.2	Wan TF et al.,1997
Indochina	Jiaonan, Shandong	119.5	35.5	mylonite	quartz	5	104.5	Zhang CH etal., 1993
Indochina	North Huaiyang	114.5	32	mylonite	quartz	16	147	Xiong CY et al., 1992
Indochina	Xincheng-Huangpi	114.5	31	mylonite	quartz	6	125.3	Xiong CY et al., 1992
Indochina	Fengxian, Shaanxi	106.5	34	mylonite	quartz	4	142	Wang GH, 1993
Indochina	Jiuling, Jiangxi	115	28.5	fault rock	quartz	41	83.6	Li DW, 1985
Indochina	Hetai, Guangdong	112.5	23.5	mylonite	quartz	2	59	Zhang BY et al.,1994
Indochina	Ailaoshan, Cangyuan	101.5	24	granitoid	quartz	2	94	Wan TF et al., 1997
Indochina	East Gansu	105.5	33.5	granitoid	quartz	9	69.3	Wan TF et al.,1997
Indochina	Altun	92	37	granitoid	quartz	1	125.8	Wan TF et al.,1997
Indochina	Eest Kunlun	94	35.7	granitoid	quartz	2	84.6	Wan TF et al.,1997
Indochina	Burang	81.3	30.2	ultramafic rock	olivine	3	118	Zhao CH (unpublished)

Appendix 4.2 Yanshanian Tectonic Period

average value of differential stress ($\Delta\sigma$) (70) 99.4 MPa

Tectonic Period	Area	Long. °E	Lat. °N	Rock	Determined Mineral	Sample	$\Delta\sigma$ (MPa)	Sources
Yanshanian	Nandazhai, Beijing	116	39.8	mylonite	quartz	4	101.8	Wan TF et al., 1997
Yanshanian	Daheishan, Jilin	125	43.6	granitoid	quartz	3	112.5	Lin JP et al., 1994
Yanshanian	Zhaoyuan–Yexian, shandong	120.3	37.2	granitoid	quartz	3	82.5	Wan TF, 1992
Yanshanian	Mengyin, Shandong	118	35.7	method of conjugate	angle	15	82.6	Yin XH, 1987
Yanshanian	Lower & Middle Yangtze	116	30	granitoid	quartz	14	93.6	Wan TF, 1993
Yanshanian	Fujian	118	26	granitoid	quartz	12	94.6	Lin JP et al., 1990
Yanshanian	Nandan, Guangxi	107.5	25	granitoid	quartz	5	87.7	Wan TF et al., 1997
Yanshanian	East Gansu	105.5	33.5	granitoid	quartz	4	71.6	Wan TF et al., 1997
Yanshanian	East Qinghai	101	36	granitoid	quartz	3	73.8	Wan TF et al., 1997
Yanshanian	Altun	92	37	granitoid	quartz	2	79.5	Wan TF et al., 1997
Yanshanian	West Kunlun	75.5	37	granitoid	quartz	1	81.5	Wan TF et al., 1997
Yanshanian	East Xizang	96	31	schist	quartz	2	135.6	Wang GH(unpublished)
Yanshanian	South Xizang	89	29	meta. sandstone	quartz	2	130.4	Guo TY et al., 1988

Appendix 4.3 Sichuanian Tectonic Period

average value of differential stress ($\Delta\sigma$) (176) 107.4 MPa

Tectonic Period	Area	Long. °E	Lat. °N	Rock	Determined Mineral	Sample	$\Delta\sigma$ (MPa)	Sources
Sichuanian	Daheishan, Jilin	125	43.6	granitoid	quartz	19	102.1	Lin JP et al., 1994
Sichuanian	Nandazhai, Beijing	116	39.8	method of		17	98.3	Wan TF, 1981
	Fuxin, Liaoning	122	42	conjugate angle		16	94.2	Wu CL et al.,1984
	Xikuangshan Hunan	111.5	27.8			28	120.2	Wan CL, 1993

Continued

Tectonic Period	Area	Long. °E	Lat. °N	Rock	Determined Mineral	Sample	Δσ (MPa)	Sources
Sichuanian	North Hebei	116	41.7	granitoid	quartz	2	88.1	Wan TF et al., 1997
Sichuanian	East Shandong	121	37	granitoid	quartz	7	81.8	Wan TF, 1992
Sichuanian	Tan–Lu Fault	118.7	36	Fault rock	Quartz	4	113.5	Wan TF et al., 1997
Sichuanian	West Shandong	117.7	36.2	granitoid	quartz	14	77.8	Wan TF, 1992
Sichuanian	Lower & Middle Yangtze	116	30	granitoid	quartz	16	90.3	Wan TF, 1993
Sichuanian	Linhai, Zhejiang	121	28.8	granitoid	quartz	17	81.7	Chu MJ et al., 1988
Sichuanian	Fujian	118	26	granitoid	quartz	9	86.3	Wan TF, 1993
Sichuanian	Tongbaishan	113.7	32.3	mylonite	quartz	3	140.5	Xiong CY et al., 1992
Sichuanian	Xiongershan	111.7	34.4	vien	quartz	2	121.1	Wan TF et al., 1997
Sichuanian	Mangling, Qinling	108.7	33.7	granitoid	quartz	2	147	Chai YC, 1986
Sichuanian	Deyang, Sichuan	104.4	31.2	sanstone	secendary quartz	9	60.8	Zhang SR et al., 2003
Sichuanian	West Yunnan	98.5	25	granitoid	quartz	4	121.5	Wan TF et al., 1997
Sichuanian	Altun	92.5	39	granitoid	quartz	1	102.5	Wan TF et al., 1997
Sichuanian	West Kunlun	75.5	37	granitoid	quartz	4	92.5	Wan TF et al., 1997
Sichuanian	Ali & Yarlung zangbo	83	31	sandstone	secondary quartz	5	183.5	Wan TF et al., 1997
Sichuanian	Southeast Xizang	91	29	peridotite xenolith	olivine	6	103.7	Zhao CH(unpublished)

Appendix 4.4 North Sinian Tectonic Period

average value of differential stress ($\Delta\sigma$) (47) 81.9 MPa

Tectonic Period	Area	Long. °E	Lat. °N	Rock	Determined Mineral	Sample	Δσ (MPa)	Sources
North Sinian	East Hebei	118.6	39.1	sandstone	secondary quartz	4	74.4	Wang MM, 2003
North Sinian	Daqing Oil Field	124.1	46.7			6	77.3	Chen ZD et al., 2002
North Sinian	Liaohe Oil Field	122.3	41.1	sandstone	secondary quartz	5	72.8	Wang MM, 2003
North Sinian	Kuocangshan	121	28.8	granitoid	quartz	17	45.7	Chu MJ et al., 1988
North Sinian	West Yunnan	98.5	25			4	73.6	Wan TF et al., 1997
North Sinian	Hohxil shan	91	35.5	rhyolite	quartz	1	71.7	Wan TF et al., 1997
North Sinian	West Kunlun	75.5	37	granitoid	quartz	1	71.7	Wan TF et al., 1997
North Sinian	East Xizang	96	31	schist	quartz	3	115.5	Wang GH(unpublished)
North Sinian	South Xizang	89	29	granitoid	quartz	12	81.9	Zhao CH(unpublished)
North Sinian	Burang, Xizang	81.3	30.2	ultramafic rock	olivine	3	118	Zhao CH(unpublished)

Appendix 4.5 Himalayan Tectonic Period

average value of differential stress ($\Delta\sigma$) **in upper crust** (18) 92.6 MPa

Tectonic Period	Area	Long. °E	Lat. °N	Rock	Determined Mineral	Sample	Δσ (MPa)	Sources
Himalayan	Kuocangshan	121	28.8	Intermediate-acid magmatite	quartz	2	89.4	Chu MJ et al., 1988
Himalayan	Tengchong	98.5	25	granitoid	quartz	2	84.7	Yan DP, 1991
Himalayan	Malanshan Qinghai	91	35.8	rhyolite	quartz	1	105.3	Wan TF et al., 1997
Himalayan	West Kunlun	75.5	37	granitoid	quartz	2	82.7	Wan TF et al., 1997
Himalayan	South Xizang	89	29	granitoid	quartz	7	83.8	Zhao CH(unpublished)
Himalayan	Ali	80	32	granitoid	quartz	4	109.8	Guo TY et al.,1988

Appendix 4.6 Following data are the diferentail stresses determined from the inclusion of mantle in Himalayan Period

average value of differential stress ($\Delta\sigma$) in mantel (24) 21.5 MPa

Tectonic Period	Area	Long. °E	Lat. °N	Rock	Determined Mineral	Sample	$\Delta\sigma$ (MPa)	Sources
Himalayan	Damaping, Hebei	114.5	41	iherzolite	olivine	5	21.4	Pan SA, 1989
Himalayan	Shanwang, Shandong	119	36.5	iherzolite	olivine	2	29.5	Pan SA, 1989
Himalayan	Nvshan, Anhui	118.8	32.2	iherzolite	olivine	5	17.8	Pan SA, 1989
Himalayan	Dangtu, Anhui	118.5	31.6	iherzolite	olivine	1	11.5	Sun P et al., 1994
Himalayan	Liuhe, Jiangsu	119	32.2	iherzolite	olivine	1	10.9	Sun P et al., 1994
Himalayan	Mingxi, Fujian	117.2	26.3	iherzolite	olivine	5	29.7	Peng SB et al., 1990
Himalayan	Changle, Fujian	119.5	26	iherzolite	olivine	3	16	Peng SB et al., 1990
Himalayan	Leizhou penensula	110	21	iherzolite	olivine	4	14.5	Peng SB et al., 1990

Appendix 4.7 Following data are the recent diferential stresses determined by hydrofracturing test

15 areas average differential stress ($\Delta\sigma$) 20.9 MPa

Tectonic Period	Area	Determined Depth	No.	$\Delta\sigma$ (MPa)	Sources
Neotectonic	Daqing Oil Field	2,000 m±	7	12.5	Chen ZD et al., 2002
Neotectonic	Fuyu Jilin	2,000 m±		14.8	CNC, IUGG, 1983
Neotectonic	Yingkou Liaoning	2,000 m±		22	CNC, IUGG, 1983
Neotectonic	Dagang Tianjin	2,000 m±		18.2	CNC, IUGG, 1983
Neotectonic	Shengli Oil Field	2,000 m±		12.6	CNC, IUGG, 1983
Neotectonic	Dashuikeng, Ningxia	2,000 m±		19.7	CNC, IUGG, 1983
Neotectonic	Qingyang, Ningxia	2,000 m±		25	CNC, IUGG, 1983
Neotectonic	Jiangdu, Jiangsu	2,000 m±		24.1	CNC, IUGG, 1983
Neotectonic	Qingjiang, Hubei	2,000 m±		22.8	CNC, IUGG, 1983
Neotectonic	Zigong, Sichuan	2,000 m±		32.6	CNC, IUGG, 1983
Neotectonic	Deyang, Sichuan	2,000 m±	12	11.9	Wu ZJ, 2002
Neotectonic	Baise, Guangxi	2,000 m±		25.8	CNC, IUGG, 1983
Neotectonic	Sanshui, Guangdong	2,000 m±		40	CNC, IUGG, 1983
Neotectonic	Yumen, Gansu	2,000 m±		22.4	CNC, IUGG, 1983
Neotectonic	Karamay	2,000 m±		8.8	CNC, IUGG, 1983

References for Appendix 4

Chai YC (1986) The Nappe Structure of Qinling Area. The Master Thesis of Beijing Graduate School, Wuhan College of Geology (in Chinese with English abstract).

Chen ZD, Meng QA, Wan TF et al (2002) Numerical simulation of tectonic stress field in Gulong depression in Songliao basin using elastic-plastic increment method. Earth Science Frontiers 9(2): 483–492 (in Chinese with English abstract).

China National Committee, IUGG (1983) National Report on Seismology and Physics of the Earth Interior. 74pp.

Chu MJ, Wan TF, Li SB (1988) Tectonic Stress Field, Paleogeothermal and Metallogeny near Kuocangshan area, Linhai, Zhejiang Province. China University of Geosciences, an unpublished report.

Guo TY, Wan TF (1988) Estimations of paleotectonic stress magnitude in Rutog-Burang area, Western Xizang-Qinghai Plateau, China. Geoscience 12(1): 57–66 (in Chinese with English abstract).

Li DW (1985) The Structure Features of Yifeng Thrust Belt and its Rock Deformation. The Master Thesis of Wuhan College of Geology (in Chinese with English abstract).

Lin JP, Wan TF, Chu MJ (1990) Semi-quantitative research on tectonic stress field of Mesozoic-Cenozoic in Fujian province. In: Division of Structural Geology and Tectonics, Geological Society of China, Proceedings of International Continental Lithosphere Tectonic Evolution and Dynamics, (1), pp.160–166. Geological Publishing House, Beijing (in Chinese).

Lin JP, Wan TF, Feng M (1994) Tectonic evolution of Late Paleozoic-Mesozoic in the southern Daheishan horst, Jilin Province. Geoscience 8(4): 467–473 (in Chinese with English abstract).

Pan SA (1989) Research on mantle-derived ultra-mafic xenoliths in mid-Tanlu Fault Zone and Damaping, Hebei. Dissertation, China University of Geosciences, Wuhan.

Peng SB, Jin ZM, Zheng BR (1990) Study on the microstructure features of deep-seated xenoliths and their rheological significance of the upper mantle in Cenozoic basaltic rocks from southeastern coastal region of China. In: Division of Mineralogy, Petrology and Geochemistry, Geological Society of China. Contribution to the Features of Upper Mantle and Dynamics in China, pp.112–123. Seismological Press, Beijing (in Chinese).

Sun P, Lu FX (1994) Microstructures of some peridotites from upper mantle in low Yangtze area. Geoscience 8(1): 57–64 (in Chinese with English abstract).

Wan TF (1981) Research on the structural features and mechanism of Nandazhai-Babaoshan fault zone, the Western Mountains, Beijing. Collection of Structural Geology (1): 152–164 (in Chinese with English abstract).

Wan TF, Cao RP (1992) Tectonic events and stress fields of Middle Eocene-Early Pleistocene in China. Geoscience 6(3): 275–285 (in Chinese with English abstract).

Wan TF (1994) Intraplate Deformation, Tectonic Stress and Their Application for Eastern China in Meso-Cenozoic. 156pp. China University of Geosciences Press, Wuhan.

Wan TF, Cao XH (1997) Estimation of differential stress magnitude in Middle-Late Triassic to Early Pleistocene for China. Earth Science 22(2): 145–152 (in Chinese with English abstract).

Wang GH (1993) Research on Tangzang-Huangboyuan ductile shear zone of Fengxian-Taibai area, Shaanxi Province. Dissertation, China University of Geosciences (Beijing).

Wang MM et al (2003) Petroleum Prospecting Region and Target Assessment Around Bohai Bay Areas. An unpublished report for Exploration and Research Institute of China National Petroleum Corporation.

Wu CL (1984) The study of the stress field of paleotectonics in Fuxin basin. Earth Sciences—Journal of Wuhan College of Geology (2): 43–52 (in Chinese with English abstract).

Wu ZJ (2002) Fissures influenced for gas reservoir with low permeability–as a sample for Shangshaximiao formation gas reservoir in Xinchang gas field. Dissertation, Science and Technology University of Chengdu.

Xiong CY, Zhang YM, Wei CS et al (1992) Structural evolution of Tongbai-Dabie area and its influences on mineral deposits. Research Report of Yichang Institute of Geological Minerals Product (an unpublished report in Chinese).

Yan DP (1991) Paleogene-Neogene tectonics in Baoshan-Tengchong area, western Yunnan. Dissertation, China University of Geosciences (in Chinese with English abstract).

Yin YH (1987) The Mesozoic and Cenozoic tectonic stress field of Mengyin basin in Shandong Province. Collection of Structural Geology (7): 107–121. Geological Publishing House, Beijing (in Chinese with English abstract).

Zhang BY, Yu HN (1994) Deep-seated nappe structure of Hercynian-Indochina Collision Zone in West Guangdong. Geological Publishing House, Beijing.

Zhang CH, Gu DL, Song HL (1993) A study of the left-lateral normal slip ductile shear zone in the north margin of Jiaonan uplift. Geoscience 7(4): 435–443 (in Chinese with English abstract).

Zhang ML (1998) Studies on the Tectonic Evolution and the Stress Field of the Qaidam Basin in Meso-Cenozoic Era. The PhD thesis of China University of Geosciences, Beijing (in Chinese with English abstract).

Zhang SR, Wan TF (2003) Research on Tectonic Stress Field and Prediction of Fissure Zone at Upper Triassic system, in Xiaoquan-Xinchang, Sichuan. China University of Geosciences (an unpublished report in Chinese).

Appendix 5 Intraplate Deformation Velocity of Tectonic Periods in Chinese Continent Since Mesoproterozoic

The rock chemistry data are collected from regional geology of provinces and regional geological survey (1:200,000), for calculation of the deformation (extension or shortening) velocity.

Appendix 5.1 Intraplate deformation velocity of Mesoproterozoic (1.8–1.0 Ga)

Area	Rock	Sample amount	Period or Age (Ma)	Deformation velociety (" − " is extension, others are shortening) (cm/yr)
Tangshan, Hebei	Basic volcanic	2	Early Mesoproterozoic	−0.12
Jixian, Hebei	Basic volcanic	3	Early Mesoproterozoic	−0.17
Damiao, Hebei	Anorthosite	37	Early Mesoproterozoic	−0.23
Liaoning	Gabbro	5	Early Mesoproterozoic	−0.45
Bayan Obo rift, Inner Mongolia	Basic volcanic	13	> 1,600	−0.5
West Qinling, Gansu	Basic volcanic	6	Early Mesoproterozoic	−0.73
Qilian, Gansu	Basic volcanic	6	Early Mesoproterozoic	−0.46
Xiongershan–Kuanping, Shanxi	Basalt	22	Early Mesoproterozoic	−0.64
Fangcheng, Henan	Basic volcanic	2	1,489	−0.7
Dabieshan, Hubei	Ultramafic	3	Early Mesoproterozoic	−0.9
Yunyang–Wudangshan, Hubei	Ultramafic	5	Early Mesoproterozoic	−0.9
Shennongjia–Dahongshan, Hubei	Ultramafic	2	Early Mesoproterozoic	−0.6
Baotan, Guangxi	Ultramafic	16	Early Mesoproterozoic	−0.7
Guangxi	Basic volcanic	4	Early Mesoproterozoic	−0.7
Zhuji, Zhejiang	Hornblendite	8	Early Mesoproterozoic	−1.1
Altun	Basic volcanic	7	Early Mesoproterozoic	−0.3
Hark, Tianshan	Basic volcanic	1	Early Mesoproterozoic	−0.2
Kuruktag, Xinjiang	Basic volcanic	2	Early Mesoproterozoic	−0.4
Kangbao, Hebei	Granitoid	5	1,468	2.9
Miyun, Beijing	Granitoid	10	1,588	6
Liaoning	Granitoid	10	1,565–1,305	6.3
Shimengou, Liaoning	Granitoid	1	Early Mesoproterozoic	6.2
Sandaoqiao, Inner Mongolia	Granitoid	5	Early Mesoproterozoic	8.7
Dengkou, Inner Mongolia	Rhyolite	5	Early Mesoproterozoic	8.2
Wuhai, Inner Mongolia	Granitoid	16	1,500–1,714	6.5
Bayan Bieli, Inner Mongolia	Granitoid	4	1,681–1,696	5.8
Zartay Rift, Inner Mongolia	Andesite-rhyolite	8	> 1,600	2.7
Bayan Obo rift, Inner Mongolia	Granitoid	8	> 1,600	2.7
Alxa Zuoqi	Granitoid	6	1,689	7.8
Songji–Lushi, Henan	Granitoid	14	1,508–1,631	4.5
Zhongtiaoshan, Henan	Andesite in land	23	Early Mesoproterozoic	3.3
Xiongershan, Henan	Andesite in sea	48	Early Mesoproterozoic	4.8
South Shaanxi	Granitoid	12	Early Mesoproterozoic	5.2
Huangling, Hubei	Granitoid	8	Early Mesoproterozoic	5.2
Jiuling, Jiangxi	Granitoid	7	Early Mesoproterozoic	7.8
Gate of Qaidam, Altun	Diorite	3	1,474	3
Kongurshan, West Kunlun	Andesite-rhyolite	6	Early Mesoproterozoic	7.4
Qinling, Shaanxi	Basalt	34	1,400–1,000	−0.6
Inner Mongolia	Gabbroid	4	Late Mesoproterozoic	−0.9
Altun	Basic volcanic	7	Late Mesoproterozoic	−0.4
Kongurshan, West Kunlun	Basic volcanic	5	Late Mesoproterozoic	−0.7
North Hunan	Gabbroid	16	Late Mesoproterozoic	−0.7
Inner Mongolia	Diorite	3	Late Mesoproterozoic	6.5
Haizhou, Jiangsu	Andesite-rhyolite	4	Late Mesoproterozoic	4.4

Continued

Area	Rock	Sample amount	Period or Age (Ma)	Deformation velociety (" − " is extension, others are shortening) (cm/yr)
Dabieshan, Hubei	Granitoid	8	Late Mesoproterozoic	5.2
Hannan–Tiechuanshan, Shaanxi	Granitoid	32	1,400–1,000	6.8
South Shaanxi	Dacite	2	1,400–1,000	7.9
Dunhuang, Gansu	Granitoid	2	1,079	5.1
Kongurshan, West Kunlun	Andesite-rhyolite	4	Late Mesoproterozoic	7.6
North Sichuan	Alkalite	13	1,400–1,000	2.8
Fanjingshan, Guizhou	Granitoid	54	1,400–1,000	7.3
Fanjingshan, Guizhou	Andesite-rhyolite	17	1,400–1,000	4.7
Motianling, Northern Guangxi	Granitoid	44	1,400–1,000	7.8
Guangxi	Andesite-rhyolite	2	Late Mesoproterozoic	8
Guangxi	Granitoid	3	Late Mesoproterozoic	7.8
North Hunan	Granitoid	3	Late Mesoproterozoic	7.9
Yifeng Jiangxi	Andesite-rhyolite	1	Late Mesoproterozoic	6.6
		552		

Appendix 5.2 Intraplate deformation velocity of Neoproterozoic–Early Cambrian (1.0 Ga–513 Ma)

Area	Rock	Sample amount	Period or Age (Ma)	Deformation velociety (" − " is extension, others are shortening) (cm/yr)
Yilan-Zhangguangcailing, Heilongjiang	Serpentinite	11	Early Qingbaikou	−0.94
Alatan, Inner Mongolia	Andesite	4	1,056–899	−0.8
Lüliangshan, Shanxi	Basalt-andesite	2	Early Qingbaikou	−0.49
Xixiang, Shaanxi	Basalt	16	1,000–800	−0.56
Fanjingshan, Guizhou	Basalt	25	~ 1,000	−1.1
Sanmen, Guangxi	Basalt	3	1,000–800	−0.59
Sanmen Guangxi	Ultramafic	19	1,000–800	−0.93
Dabieshan, Hubei	Basalt	80	1,000–800	−0.5
Bouder among Anhui, Zhejiang and Jiangxi	Basalt	5	916	−0.55
Fengcheng, Jiangxi	Basic volcanic	56	Early Qingbaikou	−0.3
Gate of Qaidam, Altun	Granitoid	26	Early Qingbaikou	4
Daluomizhen, Heilongjiang	Granitoid	8	Early Qingbaikou	7.1
Mudanjiang, Heilongjiang	Granitoid	5	930	5.1
Shuanghe, Heilongjiang	Granitoid	10	Early Qingbaikou	4.6
Zhongtiaoshan, Shanxi	Andesite	40	Early Qingbaikou	5.8
Shuanyazitun, Heilongjiang	Granitoid	6	Late Qingbaikou	6.8
Shenxianling, Shanxi	Granitoid	6	Late Qingbaikou	6.4
Dabieshan, Hubei	Granitoid	17	1,000–800	7.8
Xixiang, Shaanxi	Rhyolite	11	1,000–800	6.3
Erlangping, Shaanxi	Acid volcanic	33	Late Qingbaikou	6.4
Maodang, Shaanxi	Acid volcanic	39	1,000–800	5.6
Dunhuang, Gansu	Granitoid	1	790	4.8
Altun, Xinjiang	Granitoid	41	1,000–800	6.3
West Kunlun, Xinjiang	Granitoid	19	1,000–800	6.5
Kuruktag, Xinjiang	Granitoid	17	1,000–800	5.5
Tianshan, Xinjiang	Granitoid	4	1,000–800	6.2
Pengcheng-Guanxian, Sichuan	Granitoid	14	1,043–808	5.2
Huangling, Hubei	Granitoid	6	847–879	6.7
Southeast Guizhou	Granitoid	44	Qingbaikou	7.4

Continued

Area	Rock	Sample amount	Period or Age (Ma)	Deformation velociety (" − " is extension, others are shortening) (cm/yr)
Fanjingshan, Guizhou	Alaskite	54	966	7.2
Yuanbaoshan, Guangxi	Granitoid	5	Qingbaikou	7.6
Sanmen, Guangxi	Acid volcanic	8	Qingbaikou	5.9
Jiuling, Jiangxi	Granitoid	19	838–844	6.9
Bouder among Anhui, Zhejiang and Jiangxi	Rhyolite	15	818	3.2
Xiuning, Anhui	Granitoid	17	913	7.1
Northwest Zhejiang	Granitoid	8	1,000–800	6.5
Mayuan, Fujian	Rhyolite	24	Qingbaikou	6.9
Huma-Jixi, Heilongjiang	Ultramafic	54	Nanhua	−0.45
Zhangguangcailing, Heilongjiang	Ultramafic	46	Nanhua	−0.88
Subei, Gansu	Basalt	1	Nanhua	−0.34
Yaolinghe, West Hubei–South Shaanxi	Basalt	13	800–700	−0.55
Hunan	Basalt	4	Nanhua	−0.9
West Guangdong–Hainan	Basalt	2	Nanhua	−0.6
Fujian	Basalt	22	Nanhua	−0.52
Pingxiang–Guangfeng, Jiangxi	Basalt	1	Nanhua	−0.75
Yinyangguan, Guangxi	Basic volcanic	4	Nanhua	−0.22
Qinling, Henan	Granitoid	24	747–606	5.8
Zhejiang	Granitoid	8	844–766	6.9
Rongshui–Sanfang, Guangxi	Granitoid	39	730–712	6.1
Xiuning, Anhui	Granitoid	4	Sinian	6.4
Hutieling, Heilongjiang	Granitoid	68	Sinian	6.4
Yanchangbeishan, Altun	Diorite	3	674.6	7
Yaolinghe, West Hubei–South Shaanxi	Rhyolite	24	800–540	5.3
Henan	Granitoid	7	593–541	5.7
Fujian	Rhyolite	47	Sinian	4.4
Jiangxi	Decite-rhyolite	4	Sinian	4.7
Yingyangguan, Guangxi	Decite-rhyolite	10	Sinian	4.7
Guangdong	Decite-rhyolite	1	Sinian	5.03
		1,100		

Appendix 5.3 Intraplate deformation velocity of Qilianian Period (513–397 Ma)

Area	Rock	Sample amount	Period or Age (Ma)	Deformation velociety (" − " is extension, others are shortening) (cm/yr)
Xinglonggou–Qingshankou, Heilongjiang	Gabbro	22	Cambrian	−0.72
Kedanshan–Xiaosongshan, Inner Mongolia	Ultramafic	11	Cambrian	−1.1
Tongziba, North Qilian	Ultramafic	1	Cambrian	−0.73
Baijingsi, North Qilian	Ultramafic	12	Cambrian	−0.78
Yushigou, North Qilian	Ultramafic	10	Cambrian	−0.86
Lajishan, Qinghai	Ultramafic	12	Cambrian	−0.75
Baiyinchang, North Qilian	Mafic volcanic	10	M. Cambrian	−0.57
Zhongwei, Ningxia	Mafic volcanic	5	M. Cambrian	−0.9
Danfeng, North Qinling	Basalt	5	543–500	−0.28
Heihe, North Qinling	Basalt	6	543–500	−0.23
Erlangping, North Qinling	Basalt	4	543–500	−0.23

Continued

Area	Rock	Sample amount	Period or Age (Ma)	Deformation velociety ("−" is extension, others are shortening) (cm/yr)
Yunjiashan, North Qinling	Basalt	3	543–500	−0.2
Fengxian, Shaanxi	Basalt	15	Ordovician	−0.5
North Qinling, Gansu	Mafic volcanic	3	E.Ordovician	−0.26
North Qinling, Gansu	Mafic volcanic	8	M. Ordovician	−0.49
North Qinling, Gansu	Mafic volcanic	1	E. Silurian	−0.77
Baijiazui, Qinling, Gansu	Ultramafic	4	Ordovician	−0.83
NE border of Qiadam	Ultramafic	22	Ordovician	−1.03
Qingshuiquan, Qinghai	Ultramafic	10	Ordovician	−0.68
Anyemaqen, Qinghai	Ultramafic	17	Ordovician	−0.75
Donghe, Hubei	Ultramafic	4	Ordovician	−0.5
Damingshan, Guangxi	Mafic volcanic	1	Ordovician	−0.4
Dexing, Jiangxi	Mafic volcanic	2	Ordovician	−0.84
Southeast Zhejiang	Ultramafic	6	Ordovician	−0.8
Fujian	Mafic volcanic	6	Ordovician	−0.3
Fujian	Ultramafic	14	Ordovician	−0.9
Guangdong	Ultramafic	2	Ordovician	−0.8
Hainan	Mafic volcanic	1	Ordovician–Silurian	−0.7
Dabieshan	Granitoid	2	515	4.4
Danfeng, North Qinling	Andesite	6	500–435	3.5
Heihe, North Qinling	Andesite	4	500–435	4.8
Erlangping, North Qinling	Andesite	3	500–435	4.5
Yunjiashan, North Qinling	Andesite	2	500–435	5
East Qinling, Henan	Granitoid	7	485–455	2.7
Baoji, Shaanxi	Rhyolite	19	Ordovician	7.1
South Shaanxi	Granitoid	7	Ordovician	5.3
Yichun–Jiling, Heilongjiang	Granitoid	53	Ordovician	6.2
Baiqing–Mishan Heilongjiang	Granitoid	15	Ordovician	5
Bainaimiao–Barde Obo, Inner Mongolia	Diorite	13	Ordovician	9.2
Huawendong, Inner Mongolia	Diorite	7	Ordovician	6.9
Jishishan, Qinghai	Diorite	19	Ordovician	4.9
Lajishan, Qinghai	Granitoid	16	Middld Ordovician	5.5
Qaidanor, Qinghai	Granitoid	11	460	5.6
North Qilian, Gansu	Andesite	1	Late Ordovician	4.4
Beishan, Gansu	Diorite	1	Ordovician	7.5
Yichun, Heilongjiang	Rhyolite	5	Early Ordovician	6
XiaoHingganling,Heilongjiang	Rhyolite	8	Early Ordovician	6.1
XiaoHingganling,Heilongjiang	Rhyolite	80	Middle Ordovician	5.3
Yichun, Heilongjiang	Andesite	23	Middle Ordovician	6.2
Jilin	Gabbro	6	Silurian	−0.52
Jilin	Diorite	7	Silurian	−0.65
Alxan Obo, Inner Mongolia	Ultramafic	7	~417	−0.9
Dengkou, Inner Mongolia	Ultramafic	8	Silurian	−0.7
Xiaosongshan, Inner Mongolia	Ultramafic	5	384	−0.9
Alxa Zuoqi, Inner Mongolia	Mafic volcanic	12	385	−0.6
Altay, Xinjiang	Ultramafic	16	Silurian	−0.84
Altay, Xinjiang	Ultramafic	2	408–396	−0.6
Annanba, Gansu	Ultramafic	1	Silurian	−0.63
East Qiling, Henan	Ultramafic	55	427–370	−0.8
Ankang–Xunyang, Shaanxi	Basalt	9	Early Silurian	−0.45
Alxan Obo, Inner Mongolia	Granitoid	11	Silurian	6.1
Ulan Obo, Inner Mongolia	Granitoid	8	Silurian	6.6
Oagan Nur, Inner Mongolia	Granitoid	6	Silurian	5.6
Sandaoqiao, Inner Mongolia	Granitoid	4	417	4.9
Jilantai, Inner Mongolia	Granitoid	11	Silurian	6.2

Continued

Area	Rock	Sample amount	Period or Age (Ma)	Deformation velociety ("−" is extension, others are shortening) (cm/yr)
South Nigxia	Granitoid	19	~ 391	4.7
Jilin	Granitoid	34	408–360	5.3
Kangbao, Hebei	Granitoid	1	Silurian	4.8
Kangbao, Hebei	Diorite	1	Silurian	7.1
Dabieshan	Granitoid	4	426	4.7
Huichizi., South Shaanxi	Granitoid	40	Silurian	6.1
Ankang–Xunyang, Shaanxi	Rhyolite	4	Early Silurian	7.1
South Qilian, Qinghai	Diorite	20	Silurian	6.7
Dangjinshan, Qinghai	Granitoid	18	Silurian	6.5
Altay, Xinjiang	Granitoid	34	408–396	8.5
East Junggar, Xijiang	Granitoid	12	408–396	5.3
Altun, Xinjiang	Granitoid	5	~ 400	5.8
Tianshan, Xinjiang	Granitoid	12	~ 400	5.7
West Kunlun, Xinjiang	Granitoid	7	~ 400	4.9
East Kunlun, Xinjiang	Granitoid	5	~ 400	5.9
East Qinling, Henan	Granitoid	19	427–370	7
Fujian	Granitoid	11	Silurian	5.6
Jianou, Fujian	Granitoid	5	Silurian	6.5
Ninggang, Jiangxi	Granitoid	1	Silurian	5
Changtan, Jiangxi	Granitoid	4	Silurian	6.3
Wanzai, Jiangxi	Granitoid	3	394	5.7
Lean, Jiangxi	Granitoid	2	450	6
Xunwu, Jiangxi	Granitoid	10	Silurian	5.9
Hubei	Trachyte	15	Silurian	3.2
Hunan	Granitoid	21	Silurian	7.6
Dongkou, Hunan	Granitoid	12	421–360	7.9
Hengshan, Hunan	Granitoid	1	364	5.6
Hainan	Granitoid	19	Silurian	7.5
Hainan	Rhyolite	2	Late Silurian	8
Zhanxian, Guangdong	Granitoid	18	Silurian	7.3
Guangdong	Rhyolite	19	Silurian	6.5
West Guangxi	Granitoid	18	Silurian	7.7
Chenxi, Guangxi	Keratophyre	2	Early Silurian	5
Southeast Guangxi	Granitoid	8	Silurian	6.4
Northeast Guangxi	Granitoid	24	Silurian	6
Yulin, Guangxi	Granitoid	3	Silurian	6.1
Jingxi, Guangxi	Granitoid	1	Silurian	6.1
Wuzhou, Guangxi	Granitoid	1	Silurian	5.2
Lipu, Guangxi	Granitoid	2	Silurian	7.2
		1,124		

Appendix 5.4 Intraplate deformation velocity of Tianshanian Period (397–260 Ma)

Area	Rock	Sample amount	Period or Age (Ma)	Deformation velociety ("−" is extension, others are shortening) (cm/yr)
Xinkailing, Heilongjiang	Ophiolite	12	Devonian	−0.3
Baoqing, Heilongjiang	Ultramafic	22	Devonian	−0.64
Hegenshan, Inner Mongolia	Ultramafic	18	Devonian	−0.8
Badu, Guangxi	Basalt	1	Early Devonian	−0.4
Wude, Guangxi	Basalt	1	Middle Devonian	−0.4
Napo, Guangxi	Trachyte	1	Late Devonian	−0.2

Continued

Area	Rock	Sample amount	Period or Age (Ma)	Deformation velociety (" − " is extension, others are shortening) (cm/yr)
Dakang, Fujian	Ultramafic	2	350	−0.5
Sunke–Fulao, Heilongjiang	Granitoid	13	322	5.6
Mudanjiang, Heilongjiang	Granitoid	4	Devonian	7.6
Woduke–Meishan, Inner Mongolia	Granitoid	5	Devonian	6.3
Daheishan, Heilongjiang	Granitoid	34	Devonian	4.6
Bikou, West Qinling	Diorite	1	Devonian	4.7
Beishan, Gansu	Rhyolite	2	Late Devonian	5.8
North Qiadam, Qinghai	Diorite	4	Devonian	5
South Qiadam, Qinghai	Diorite	21	Devonian	5.5
South Qiadam, Qinghai	Granitoid	9	Devonian	6.9
Altay, Xinjiang	Granitoid	112	377	7.3
Tianshan, Xinjiang	Granitoid	161	377	6.1
Xinxinxia, Xinjiang	Granitoid	11	377	6.6
East Kunlun, Xinjiang	Granitoid	62	377	6.2
Dabieshan	Granitoid	2	376–370	4.1
Jilin	Granitoid	3	Devonian	3.9
Uliji, Inner Mongolia	Basalt	16	Carboniferous	−0.53
Solon, Inner Mongolia	Ultramafic	22	Carboniferous	−0.7
Fujian	Basalt	6	E. Carboniferous	−0.4
Jingxi, Guangxi	Basalt	1	E. Carboniferous	−0.4
Lancangjiang Paleo-ocean	Basalt		E. Carboniferous	−0.67 (after Mo XX)
Jinshajiang Paleo-ocean	Basalt		E. Carboniferous	−0.9 (after Mo XX)
Duobaoshan, Heilongjiang	Granitoid	38	Carboniferous	5
Jilin	Granitoid	3	Carboniferous	4.3
Jingxi, Liaoning	Granitoid	6	312	6.3
Inner Mongolia (active area)	Diorite	8	Carboniferous	6.5
Inner Mongolia (stable area)	Diorite	4	Carboniferous	4.9
Inner Mongolia (active area)	Granitoid	23	Carboniferous	6.5
Inner Mongolia (stable area)	Granitoid	13	Carboniferous	5.9
Beishan, Gansu	Rhyolite	1	E. Carboniferous	7.1
Beishan, Gansu	Dacite	1	M. Carboniferous	4.7
Qilianxian, Gansu	Diorite	1	Carboniferous	6.5
Xinxinxia-Tianshan	Granitoid	174	~ 300	6.2
North Tianshan	Granitoid	238	300–295	6.3
Altay, Xinjiang	Granitoid	160	300–295	6.1
West Junggar	Granitoid	126	300–295	5.8
East Junggar	Granitoid	212	300–295	5.2
Guangdong	Granitoid	5	Carboniferous	6.7
Guangxi	Granitoid	8	Carboniferous	6.4
Piaotang, Jiangxi	Quartz diorite	1	Carboniferous	5.9
Laoheishan, Heilongjiang	Basic volcanic	6	Early Permian	−0.75
Jianping-Xifeng, Liaoning	Ultramafic	6	Early Permian	−0.86
Qilianxian, Gansu	Serpentinite	1	Early Permian	−0.79
Jingxi, Guangxi	Diabase	1	Early Permian	−0.3
Tangma, Guangxi	Basalt	3	Early Permian	−0.6
Xichang, Sichuan	Basalt	5	Late Permian	−0.56
Dukou, Sichuan	Basalt	7	Late Permian	−0.4
Dongchuan, Yunnan	Basalt	3	Late Permian	−0.3
Lufeng, Yunnan	Basalt	9	Late Permian	−0.2
West Guizhou	Basalt	48	Late Permian	−0.5
Border between Yunnan & Guangxi	Basalt	10	Early Permian	−0.6
Lanping-Simao, Yunnan	Basalt	3	Early Permian	−0.5
Ganzi-Litang Paleo-ocean	Basalt		E. Permian–E. Triassic	−0.8 (after Mo XX)

Continued

Area	Rock	Sample amount	Period or Age (Ma)	Deformation velociety (" − " is extension, others are shortening) (cm/yr)
Uliji, Heilongjiang	Granitoid	27	> 203	5.2
Sunke–Furao, Heilongjiang	Granitoid	103	Permian	5
Baoqing–Mishan, Heilongjiang	Dacite	7	Early Permian	7.2
Maanshan, Heilongjiang	Granitoid	9	Early Permian	6.6
Tieli, Heilongjiang	Granitoid	47	Early Permian	4.8
Muhetun, Heilongjiang	Granitoid	41	Early Permian	6.3
Handaqi, Heilongjiang	Granitoid	2	310–308	5.7
Songling Area, Heilongjiang	Granitoid	33	Early Permian	4.7
Longzhen, Heilongjiang	Granitoid	38	Early Permian	5.5
Baoqing, Heilongjiang	Granitoid	14	Early Permian	7.3
Daluomizhen, Heilongjiang	Granitoid	36	Early Permian	5.3
Binxian, Heilongjiang	Granitoid	58	Early Permian	4.2
Mudanjiang, Heilongjiang	Granitoid	5	Early Permian	8.2
Shuangchengzi, Heilongjiang	Granitoid	51	Early Permian	7.5
Jilin	Dacite	62	Permian	6
Jilin	Granitoid	232	302–254	5.5
Tule Mod, Inner Mongolia	Granitoid	11	Early Permian	6.3
Liujiayingzi, Inner Mongolia	Granitoid	5	Early Permian	7.6
Aohanqi, Inner Mongolia	Granitoid	4	Early Permian	5
Sandaoqiao, Inner Mongolia	Granitoid	10	288–279	6.7
Inner Mongolia (active area)	Granitoid	17	Early Permian	5.2
Inner Mongolia (stable area)	Granitoid	27	Early Permian	5.2
Alatan Abo, Inner Mongolia	Granitoid	12	289–252	7.7
Liaoning	Granitoid	14	270–269	5.8
Liaoning	Granitoid	12	~ 240	5.8
116.5°E, 41.7°N	Granitoid	4	Permian	5.3
117.5°E, 42.3°N	Granitoid	1	Late Permian	4.7
Kangbao-Weichang, Hebei	Salic volcanic	6	Early Permian	5.1
Kangbao-Weichang, Hebei	Granitoid	20	266–250	4.7
Kangbao-Weichang, Hebei	Andesite	13	266–250	4.2
Kangbao, Hebei	Granitoid	20	266–250	4.7
Shanghuangqi, Hebei	Granitoid	4	Early Permian	5.3
Qipanshan, Hebei	Granitoid	1	Early Permian	4.7
South Shaanxi	Granitoid	7	Early Permian	7
Beishan, Gansu	Andesite	1	Early Permian	5.6
Beishan, Gansu	Rhyolite	2	Late Permian	7
Northern Qaidam, Qinghai	Granitoid	5	Early Permian	6.1
Southern Qaidam, Qinghai	Granitoid	7	Early Permian	8
Gate of Qaidam, Qinghai	Granitoid	2	Early Permian	6.8
South of Eastern Kunlun,	Granitoid	6	259	5.9
Fujian	Quartz Diorite	6	Early Permian	7.4
Ganfang, Jiangxi	Granitoid	1	Permian	6
Yunkaidashan, Guangdong	Schist	1	Early Permian	10
Liuzhou, Guangxi	Tuff	1	Late Permian	8.7
Darongshan, Guangxi	Granitoid	90	Early Permian	6.3
Lanping-Simao, Yunnan	Dacite	4	Early Permian	5.3
		2,548		

Appendix 5.5 Intraplate deformation velocity of Indosinian Period (260–200 Ma)

Area	Rock	Sample amount	Period or Age (Ma)	Deformation velociety ("−" are extension, others are shortening) (cm/yr)
Bangong Co-Domar, Xizang	Basalt	4	Early Triassic	−0.2
East Hohxilshan	Diabase	3	E.&M. Triassic	−0.2
Bayan Har Shan	Basalt	6	E.&M. Triassic	−1.2
Tanggula Shan	Basalt	8	E.&M. Triassic	−0.4
Paleo–Jinshajiang Ocean (Closing)	Granitoid		E.Permian–E.Triassic	4.69 (after Mo XX)
North Tianshan	Granitoid	61	~ 239	4.7
Alatan Abo, 104.5 °E, 40.3 °N	Granitoid	25	~ 235	5.8
Ela shan, Qinghai	Acid volcanic	9	~ 240	5.4
East Kunlun	Granitoid	101	~ 235	5.5
East Kunlun	Acid volcanic	7	~ 240	5.6
Mingshan–Lixian, North Qinling	Granitoid	132	~ 233	5.4
West Qinling	Rhyolite	4	Early Triassic	6.8
Northwest Qiangtang	Granitoid	1	239.8	5.9
Baosahn, Yunnnan	Granitoid	44	~ 230	6.1
Lincang, Yunnan	Granitoid	300	~ 235	6.1
Nyalam–Yadong, Xizang	Granitoid	1	235.8	5.5
Yarlung Zangbo Jiang	Basalt	7	Late Triassic	−0.2
Burang–Daba	Ophyolite	5	Late Triassic	−1.6
Altay, Xinjiang	Granitoid	4	~ 228	4.9
Hami, Xinjiang	Granitoid	13	~ 230	4.9
Raohe–Baoqing, Heilongjiang	Ultramafic	81	Triassic	−0.61
Wandashan, Heilongjiang	Ultramafic	53	Late Triassic	−0.48
Baoqing, Heilongjiang	Acid volcanic	105	Late Triassic	5.5
Hingganling, Heilongjiang	Granitoid	355	~ 229	4.2
Tieli, Heilongjiang 128.5 °E, 47 °N	Granitoid	47	Triassic	4.8
Jilin	Granitoid	18	~ 223	5.7
Hetao, Inner Mongolia	Granitoid	58	~ 225	4.5
Jilantai, 105.5 °E, 39.6 °N	Granitoid	7	223	4.9
North Shanxi	Granitoid	12	~ 227	4.9
North Hebei	Granitoid	15	~ 226	5
West Shanxi	Tuff	8	Triassic	1.6
Tianzhen–Yangyuan, Shanxi	Nepheline-syenite	6	Triassic	1.5
Hezuo, North Qinling	Granitoid	75	~ 227	6.6
Qinling	Granitoid	213	~ 226	5.5
Henan	Granitoid	6	~ 224	4.9
Anhui	Granitoid	12	220–230	5.5
Jiangxi	Granitoid	29	~ 235	5.2
Hunan	Granitoid	40	~ 224	6
Zhuji, Zhejiang	Granitoid	5	Triassic	4.8
Quxian, Zhejiang	Granitoid	7	Triassic	5
Fujian	Granitoid	13	~ 226	5.6
Guangxi	Granitoid	86	~ 226	6.5
Guangdong	Granitoid	12	~ 225	5.1
Panzhihua–Xichang	Granitoid	15	~ 230	6.3
Lancangjiang Paleo-ocean (closing)	Granitoid		~ 230	5.3 (after Mo XX)
Jomda–Qamdo, Xizang	Dacite	22	E. – M. Triassic	5.8
Yalongjiang, West Sichuan	Granitoid	81	~ 229	7
Dawu, West Sichuan	Granitoid	31	~ 221	6.9
Lanping–Simao, Yunnnan	Granitoid	111	~ 225	5.2
Laoyeling, Heilongjiang	Granitoid	215	~ 219	5.4
Dengkou, 106.5°E, 40.7°N	Granitoid	22	~ 218	5.7

Continued

Area	Rock	Sample amount	Period or Age (Ma)	Deformation velociety (" − " is extension, others are shortening) (cm/yr)
Baotou, 110°E, 40.3 °N	Granitoid	1	~ 217	4.7
Liaoning	Granitoid	51	~ 213	5.4
Kuruktag, Xinjiang	Granitoid	2	Triassic	6.6
South Tianshan	Granitoid	5	~ 215	5.3
Qimantag, Xijiang	Granitoid	21	Triassic	5.1
Qimantag, Xijiang	Tuff	2	~ 211	5.8
Karakorun Shan	Granitoid	18	~ 211	6.9
Tianshui, north Qinling	Granitoid	101	~ 217	5.4
South Qinling	Granitoid	9	~ 217	5.3
West Qinling, Qinghai	Granitoid	15	~ 219	6.2
Beishan, Gansu	Granitoid	32	~ 219	6
Middle Qilian	Granitoid	75	~ 218	5.5
Barkam, Sichuan	Granitoid	70	~ 219	6.5
Yidun, West Sichuan	Granitoid	45	~ 218	7.2
North Qiangtang	Diacite	2	Late Triassic	6.8
Yushu, Qinghai	Acid volcanic	63	Late Triassic	5.5
Tanggulashan	Acid volcanic	41	Late Triassic	5.3
Taniantaweng Shan	Granitoid	16	219.6	5.8
Jomda–Markam, East Xizang	Acid volcanic	50	Late Triassic	7
Jomda–Markam, East Xizang	Granitoid	17	215	5.3
Uliji, 104.5 °E, 41 °N	Granitoid	3	~ 203	5.6
North Border of Qaidam	Granitoid	128	~ 205	5.9
		3,284		

Appendix 5.6 Intraplate deformation velocity of Yanshanian Period (200–135 Ma)

Area	Rock	Sample amount	Period or Age (Ma)	Deformation velociety ("−" is extension, others are shortening) (cm/yr)
East to Harbin	Granitoid	56	~ 170	5.7
North Hingganling	Granitoid	63	~ 170	5.7
South Hingganling	Granitoid	19	~ 166	5.2
Laoyeling	Granitoid	86	~ 167	4.7
Jilin	Granitoid	109	~ 169	5.2
Liaoning	Granitoid	79	~ 180	5
West Liaoning	Acid volcanic	137	M.& E.Jurassic	5.3
Chifeng	Granitoid	6	169	3.5
Wuhai, Inner Mongolia	Syenite	1	187	2.1
Nandaling Formtion, Yanshan	Basalt	21	~ 178	4.2
Tiaojishan Formtion, Yanshan	Andesite	30	~ 165	4.5
Zhangjiakou Formtion,Yanshan	Rhyolite	118	~ 150	6
Helanshan	Granitoid	7	~ 173	4.8
Shanxi	Granitoid	73	~ 170	4
Handan, Hebei	Granitoid	16	~ 148	5.2
East Shandong	Granitoid	127	~ 159	5.1
Qinling	Granitoid	90	~ 158	4.8
North Hebei	Granitoid	20	~ 157	5
Southwest Henan	Granitoid	84	~ 158	4.1
North Huaiyang	Acid volcanic	7	> 144	4.7
Jiangsu	Granitoid	2	Jurassic	4.9
South Anhui	Granitoid	52	~ 153	5.7
Southeast Hubei	Granitoid	199	~ 166	5.1

Continued

Area	Rock	Sample amount	Period or Age (Ma)	Deformation velociety ("−" is extension, others are shortening) (cm/yr)
West Zhejiang	Rhyolite-andesite	7	~ 190	6.2
Northwest Zhejiang	Granitoid	108	~ 157	5.3
East Zhejiang	Granitoid	126	~ 156	5.5
Fujian	Granitoid	20	~ 167	5.2
Fujian	Granitoid	31	~ 149	5.6
Jiangxi	Granitoid	24	~ 190	5.9
Jiangxi	Granitoid	38	~ 164	6.3
Jiangxi	Granitoid	25	~ 148	5.7
Northeast Hunan	Granitoid	21	~ 161	6.5
Middle Hunan	Granitoid	35	~ 161	6.5
Guangxi	Granitoid	41	~ 178	6
Guangxi	Granitoid	94	~ 149	6.1
Guangdong	Granitoid	62	~ 180	7.1
Guangdong	Granitoid	20	~ 158	6.2
Guangdong	Granitoid	183	~ 144	6.2
Southeast Yunnan	Granitoid	34	~ 167	5.2
Tengchong, West Yunnan	Granitoid	19	~ 160	5.9
Panzhihua–Xichang	Granitoid	9	~ 167	4
Aba, West Sichuan	Granitoid	17	~ 137.3	6.1
Markam, West Sichuan	Granitoid	18	~ 157	6
Dafu, West Sichuan	Granitoid	35	~ 154	5.7
Yalongjiang, West Sichuan	Granitoid	5	~ 187	6.2
Yidun, West Sichuan	Granitoid	46	~ 176	6.4
East Bayanhar, Qinghai	Acid volcanic	17	Early Jurassic	7.3
Bayanhar, Qinghai	Granitoid	21	~ 192	6
Qaidam, Qinghai	Granitoid	29	~ 152	6.1
Qaidamshan, Qinghai	Granitoid	2	~ 182	6.4
Northeast, Qinghai	Granitoid	54	~ 187	6.9
Langmusi, West Qinling	Andesite	3	Middle Jurassic	7.3
Tianshui, North Qinling	Granitoid	92	~ 180	5.3
Altay	Granitoid	24	~ 171	5.6
Altun	Granitoid	3	Jurassic	5.6
West Karakorum	Dacite	3	~ 167	6.2
Qarlong	Baslte	6	E.&M.Jurassic	−0.3
Qarlong	Andesite	4	E.&M. Jurassic	5
Kunlun, Xijiang	Granitoid	11	Jurassic	6.4
North Qiangtang	Granitoid	1	Jurassic	7
Luma Co – Doma, Xizang	Granitoid	8	~ 167	6.4
Jomda, Xizang	Granitoid	4	~ 143	6.3
Qiangtang–Qamdo, Xizang	Rhyolite-andesite	8	Jurassic	5.4
Tanggula, Xizang	Granitoid	4	Jurassic	6.3
Amdo–Nyainrong, Xizang	Granitoid	10	~ 163	5.5
Naggqu–Baile, Xizang	Ophyolite	1	Late Jurassic	−1.5
Bangongco–Nujiang, Xizang	Ophyolite	81	Late Jurassic	−4
Bangongco–Dengqen, Xizang	Ophyolite	64	Jurassic	−1.1
Bangongco–Dengqen, Xizang	Basalt	17	Jurassic	4.3
Ngari, Xizang	Granitoid	13	~ 165	6.4
North Nyainqentanglha Xizang	Basalt	8	M.&L. Jurassic	−0.4
North Nyainqentanglha Xizang	dacite	54	M.&L. Jurassic	6.6
Shiquanhe, Xizang	Ophyolite	11	M.&L. Jurassic	−3.2
South Nyainqentanglha Xizang	dacite	6	M.&L. Jurassic	6
Laguigangri, Xizang	Basalt	5	M.&L. Jurassic	−0.4
		2,984		

Appendix 5.7 Intraplate deformation velocity of Sichuanian Period (135–56 Ma)

Area	Rock	Sample amount	Period or Age (Ma)	Deformation velociety ("−" is extension, others are shortening) (cm/yr)
SE Yarlung Zangbo Jiang	Basalt	18	Early Cretaceous	−0.7
SW Yarlung Zangbo Jiang	Basalt	88	Early Cretaceous	−0.5
Ngari–Shiquanhe, Xizang	Basalt	13	Early Cretaceous	−0.9
Ngari–Rutog, Xizang	Basalt	6	Early Cretaceous	−0.5
East Nyainqentangulha	Granitoid	25	~ 128	6.5
Luobusha, Xizang	Ophyolite	85	Cretaceous	−3.3
Coqen–Namco, Xizang	Ophyolite	20	Cretaceous	−3.1
South Yarlung Zangbo Jiang	Gabbro	5	Late Cretaceous	−1.8
Yamzho Yumco	Diabase	1	Late Cretaceous	−1.1
Yarlung Zangbo Jiang	Gabbro	7	Late Cretaceous	−0.3
Yarlung Zangbo Jiang	Dacite	24	Late Cretaceous	5.1
Yangbajing, Xizang	Granitoid	49	~ 76	6
Nyainqentangulha	Dacite	78	Late Cretaceous–Eocene	5.2
West Lancangjiang	Granitoid	1	~ 76	6.1
North Nyainqentangulha	Granitoid	18	~ 104	5.6
Ngari–Shiquanhe, Xizang	Andesite	31	Late Cretaceous–Eocene	5.2
Shiquanhe–Bomi	Granitoid	8	~ 108	6.5
Gegyai, Ngari	Dacite	25	Late Cretaceous–Paleocene	5.5
West Qiangtang	Granitoid	1	~ 90.4	6.4
82°E, 36°N	Basalt	2	Paleocene-Eocene	−0.3
79°E, 35°N	Dacite	1	Late Cretaceous	6.6
Karakorum	Granitoid	10	~ 95	6.4
Tanggula, Qinghai	Basalt	12	Cretaceous	4.2
Tanggula, Qinghai	Granitoid	8	~ 85	5.5
Tongren, Qinghai	Basalt	2	Cretaceous	−0.5
Jiuquan, Gansu	Latite	5	83	2.7
Garze–Litang Paleo-ocean (closing)	Granitoid	42	Cretaceous	6.2
Biluoxueshan	Granitoid	14	100–52	6.2
Nujiang Paleoocean(closing)	Granitoid	78	138–51	6.4
Dawu, West Sichuan	Granitoid	18	139–52	6.5
Panzhihua–Xichang	Granitoid	14	~ 123	5.9
Southeast Yunnan	Granitoid	162	102–78	5.3
Guangxi	Granitoid	143	132–68	6
Southeast Guangxi	Acid volcanic	66	100–67	4.9
Guangdong	Granitoid	123	135–90	5.7
Guangdong	Granitoid	84	90–55	5.9
Hunan	Granitoid	10	131–65	6.4
Jiangxi	Granitoid	19	135–70	5.8
Fujian	Granitoid	187	127–70	6.1
Fujian	Acid volcanic	475	127–125	6
Zhejiang	Granitoid	22	125–70	5.3
Shanghai	Acid volcanic	42	136–84	4.6
Nanjing–Wuhu	Granitoid	41	137–91	5.2
South Anhui	Granitoid	14	136–115	5.1
Lujiang–Zongyang, Anhui	Acid volcanic	62	133–108	3.6
Dabie–Qinling	Granitoid	98	121–105	6
Southeast Hubei	Acid volcanic	153	132–102	4.6
Henan	Acid volcanic	218	135–87	4.8

Continued

Area	Rock	Sample amount	Period or Age (Ma)	Deformation velociety ("−" is extension, others are shortening) (cm/yr)
South Gansu,	Tuff	3	Late Cretaceous	5.6
Tianshui, North Qinling	Granitoid	11	127–104	5.3
Mingshan–Lixian, North Qinling	Granitoid	5	Cretaceous	5.3
Helanshan	Acid volcanic	27	71–66	4
104.5°E, 40.3°N	Basalt	1	Late Cretaceous	4
104.5°E, 41°N	Acid volcanic	23	Early Cretaceous	4.7
Shanxi	Granitoid	23	135–74	5.4
Handan, Hebei	Alkali rock	6	110–52	2.7
West Shandong	Acid volcanic	337	133–78	4.7
East Shandong	Acid volcanic	285	136–90	5.7
Yanshan	Granitoid	52	140–110	3.4
West Liaoning	Acid volcanic	369	135–70	4.2
Liaoning	Acid volcanic	74	135–70	5
Liaoning	Granitoid	70	132–80	4.9
Jilin	Granitoid	34	104–76	5
South Hingganling	Granitoid	74	132–91	4.9
Laoyeling	Granitoid	18	128–76	77
North Hingganling	Granitoid	30	132–105	5.2
Japan Sea	Rhyolite	11	127	5.1
West Pacific Ocean			90–80	Magnetic anomalies, 8
		4,081		

Appendix 5.8 Intraplate deformation velocity of North Sinian Period (56–23 Ma)

Area	Rock	Sample amount	Period or Age (Ma)	Deformation velociety ("−" is extension, others are shortening) (cm/yr)
West Pacific Ocean			40–30	Magnetic anomalies, 9
Baitoushan, Jilin	Trachyte-rhyolite	1	Eocene–Oligocene	5.4
Jilin	Basalt	7	32.9	4.2
Lower Liaohe	Basalt	54	Eocene–Oligocene	3.2
Hebei Plain	Basalt	26	49–37	5.4
Fansi, Shanxi	Basalt	2	Eocene–Oligocene	4.9
Mouth of Yellow River	Basalt	6	45–39	6.4
South Huanghai–North Jiangsu	Basalt	8	47–42	4.2
North Anhui	Basalt	4	Eocene–Oligocene	5.7
Hefei, Anhui	Basalt	4	Eocene–Oligocene	5.4
Southeast Hubei	Basalt	2	52	4
South Anhui	Basalt	1	42.6	2.2
Coastal Mountians, Taiwan	Basalt	20	Paleogene	7.1
Fujian	Basalt	10	Paleogene	3.6
Jiangxi	Basalt	2	32–20	5.4
Sanshui, Guangdong	Basalt	7	51–45	3.3
Guangxi	Basalt	4	47–33	3
Eastern Nanhai			52–25	Magnetic anomalies, −4.9
Jinshajiang–Red River			44–23	Sinistral slip, 0.45
Middle Yunnan	Basalt	9	52–34	2.9
West Yunnan	Basalt	2	38	6.6
Panzhihua–Xichang	Basalt	2	31	1.9
Jomda-Yulong	Granitoid	128	55–34	5.7
Tianshan	Granitoid	1	Paleogene	3

Continued

Area	Rock	Sample amount	Period or Age (Ma)	Deformation velociety ("−" is extension, others are shortening) (cm/yr)
North Tanggula	Granitoid	17	46–36	4.5
South Yushu area	Trachyandensite	19	Paleogene	0.75
West Karakorum	Granitoid	1	33.6	4.5
Nyainqentanglha	Granitoid	5	53–31	5.8
Nyainqentanglha	Dacite	17	Oligocene	5.4
Yamzho Yumco (NWW)	Diabase	3	Paleogene	−1.1
Yarlung Zangbo Paleo-ocean (closing)	Granitoid	5	43–32	6.3
East end of Himalaya Shan	Basalt	10	Eocene	−0.2
		377		

Sources of rock chemistry data: Data of Lower Liaohe, Mouth of Yellow River and Taiwan, after E ML and Zhao DS(1987); Panzhihua and Xichang, after LuoYN (1985); Jinshajiang-Red River, after Wu HW (1989); Nanhai, after Liu ZS (1988); Japan Sea, after Uyeda et al., (1974); Data of West Yunnan are sent by Prof. Zhao CH (personal communication); others collected from geological survey.

Appendix 5.9 Intraplate deformation velocity of Himalayan Period (23–0.78 Ma)

Area	Rock	Sample amount	Period or Age (Ma)	Deformation velociety ("−" is extension, others are shortening) (cm/yr)
Zayu, Southeast Xizang	Granitoid	16	20–16	6
High Himalaya	Granitoid	30	21–10	5.8
Nyainqentanglha	Granitoid	19	23–12	6
Nyainqentanglha	Dacite	6	Neogene	5.7
Qamdo, Xizang	Dacite	2	Neogene	6
Qiangtang	Dacite	31	Neogene	5.6
90°E, 34.6°N	Andesite	25	Neogene	4.9
90°E, 36°N	Trachyandensite	9	Neogene	5.1
86.5°E, 36°N	Dacite	6	Neogene	4.8
82°E, 36°N	Trachyandensite	13	28–20	4.4
75°E, 38.5°N	Trachyandensite	13	1.4–1.2	4.1
West Karakorum	Granitoid	3	17–10	4.9
87°E, 36.3°N	Andesite	15	10.5–5	4.7
Tanggula Shan	Rhyolite	14	26–10	4.7
Urad Houqi	Basalt	1	1.19	−0.1
Xilingol Meng	Basalt	36	∼14	−0.14
Northwest Shanxi	Basalt	21	26–7	−0.24
Hannuoba, Hebei	Basalt	72	∼18	−0.23
West Henan	Basalt	2	11–3.5	−0.15
Mudanjiang	Basalt	11	16–1.1	−0.53
Nearby Changbaishan	Basalt	154	14–1.2	−0.2
East Liaodong	Basalt	6	9.8–0.9	−0.29
Shandong	Basalt	86	21–0.86	−0.28
Tancheng–Lujiang fault	Basalt	85	16.5–9	−0.25
East Yunnnan	Basalt	18	Neogene	−0.33
Southeast Guangxi	Basalt	7	Neogene	−0.34
Baiyu, Sichuan	Basalt	3	Neogene	−0.23
Tengchong, Yunnan	Basalt	5	23–2	−0.37
Tengchong, Yunnan	Basalt	13	2–0.78	5.6
Middle Zhejiang	Basalt	50	Pliocene	−0.25
West Fujian	Basalt	37	Neogene	−0.14

Continued

Area	Rock	Sample amount	Period or Age (Ma)	Deformation velociety ("−" is extension, others are shortening) (cm/yr)
Coastal area of Fujian & Guangdong	Basalt	128	20–1.8	−0.43
Ocean crust of Japan Sea	Basalt	1	7–1.8	−0.35
West Honshu, Japan	Basalt	2	6–0.8	−0.24
Ryukyu Trough	Basalt	2	11–1	−0.9
East Taiwan rift	Basalt	66	25–1.85	−0.68
Penhu Islands	Basalt	48	~ 2	−0.47
117.5°E, 17.5 °N	Basalt	1	14.1	−0.63
115.5°E,14 °N	Basalt	1	3.49	−0.28
Philippine Sea Plate			17	Magnetic anomalies, 8
Philippine Sea Plate			4	Magnetic anomalies, 4
		1,076		

Sources of rock chemistry data: Data of Fujian, Guangdong, Taiwan, Tancheng–Lujiang, after E ML and Zhao DS (1987); Changbaishan, after Jin BL et al., (1994); Nanhai, after Liu ZS (1988); Japan Sea, after Harumoto (1970), Aoki (1987); Xilingol, after Chi JS et al.,(1988); Tengchong, after Liao ZJ (1988); Penghu Islands, after Chen (1973); Ryukyu Trough, after Liu CB (1989), Philippine Sea Plate, after Seno and Maruyama (1977, 1984); others collected from geological survey.

Appendix 5.10 Intraplate deformation velocity of Neotectonic Period (since 0.78 Ma)

Area	Rock	Sample amount	Period or Age (Ma)	Deformation velociety ("−" is extension, others are shortening) (cm/yr)
North Qiangtang	Trachyte-andesite	7	0.067	4.5
87°E, 36.3°N	Trachyte	2	Late Pleistocene	4
75 °E, 38.5°N	Trachyte-andesite	1	Late Pleistocene	4
81.6°E, 35.8°N	Rhyolite	3	Holocene	4.4
Tengchong, Yunnan	Andesite-basalt	26	Late Pleistocene & Holocene	4.6
Qiongshan Hainan	Basalt	3	0.319	−0.5
Leizhou Peninsula	Basalt	36	Holocene	−0.6
Nvshan–Fushan, Anhui	Basalt	16	0.73~0.5	−0.18
Hannuoba–Datong, Shanxi	Basalt	72	0.73~0.2	−0.18
Lower Liaohe, Liaoning	Basalt	14	0.12	−0.16
Changbaishan	Trachyte	69	Mid–Late Pleistocene	3
Changbaishan	Trachyte	21	Holocene	2.9
Longgang, Jilin	Basalt	31	0.07	−0.14
Wudalianchi, Heilongjiang	Basalt	113	0.39	−0.12
Mudanjiang, Heilongjiang	Basalt	15	Mid Pleistocene–Holocene	−0.21
Daxiongshan, Heilongjiang	Basalt	10	Mid Pleistocene–Holocene	−0.5
Hakone, Japan	Trachyte-andesite	1	Holocene	9
Ryukyu Trough	Rhyolite	6	Mid Pleistocene–Holocene	5.2
Datun, Taiwan	Andesite	9	Mid Pleistocene–Holocene	8.3
		455		

Sources of rock chemistry data: Data of Taiwan, after E ML and Zhao DS (1987); Tengchong, after Liao ZJ (1988); Changbaishan, after Jin BL et al., (1994); Nanhai, after Liu ZS (1988); Japan Sea, after Harumoto (1970), Aoki (1987); Xilingol, after Chi JS et al., (1988); Ryukyu Trough, after Liu CB (1989), Philippine Sea Plate, after Seno and Maruyama (1977, 1984); others collected from geological survey.

Appendix 5.11 Plate deformation velocity (cm/yr) in recent, according to the data of GPS (362 stations) and earthquake moment (after Zhang PZ et al., 2002)

Area	Deformation velocity	Area	Deformation velocity
Indian Plate	4.1	Ordos	0.8
High Himalaya	1.5	North China	0.3
Gandise	2.85	Yanshan–West Liaoning	0.45
East Qiangtang	2.8	Northeast China	0.35
Bayanhar Shan	2.1	North Northeast China	0.08
Qaidam	1.3	North Jiangsu	0.7
Altun	0.8	Kazakhstan	0.4
North Qilian	1	Shanghai	1.1
West Tarim	1.3	Sichuan–Yunnan	1.3
West Tianshan	2	Baoshan, West Yunnan	0.55
Middle Tianshan	0.7	Red River	0.7
Bogda Shan, Xinjiang	0.2	Xiaojiang, West Sichuan	1.25
West Junggar	0.1	East Yunnan	0.9
Altay, Xinjiang	0.22	South China	1
Alxa	0.5	Philippine Sea Plate	4.1

References for Appendix 5

Aoki K (1970) Japanese Island arc: Xenoliths in alkali basalts, high-alumina basalts and calc-alkaline andesites and decites. In: Nixon PH (ed) Mantle Xenoliths. pp.319–334. John Wiley & Sons, New York.

Bureau of Geology and Mineral Resources of Provinces (1984—1993) Regional Geology of Provinces. Geological Publishing House, Beijing (in Chinese with English abstract, as shown in References for Chapter 1).

Chi JS (chief editor) (1988) The Study of Cenozoic Basalts and Upper Mantle Beneath Eastern China (Attachment Kimberlites). 277pp. China University of Geosciences Press, Wuhan (in Chinese with English abstract).

E ML, Zhao DS (1987) The Cenozoic Basalts and Deep-derived Rock Xenoliths of Eastern China. 490pp. Science Press, Beijing (in Chinese).

Harumoto A (1970) Volcanic rocks and associated rocks of Utsuryoto Island (Japan Sea). Geol. Surv. Japan, 15.

Jin BL, Zhang XY (1994) Research on Volcanic Geology of Changbai Mountains. 223pp. Northeastern Korean Nationality Education Publishing House, Yanji (in Chinese).

Liao ZJ (1988) Late Cenozoic Volcano of Tengchong. In: Tong W, Zhang MT, Geothermal of Tengchong, pp.1–19. Science Press, Beijing (in Chinese).

Liu CB (1989) The pumice in Okinawa trough. Acta Petrological et Mineralogical 8(3): 193–202 (in Chinese with English abstract).

Seno T (1977) The instantaneous rotation vector of the Philippine Sea Plate relative to the Eurasian Plate. Tectonophysics 42(2–4): 209–226.

Seno T, Maruyama S (1984) Paleogeographic reconstruction and origin of the Philippine Sea. Tectonophysics 102(1–4): 53–84.

Zhang PZ, Wang Q, Ma ZJ (2002) GPS velocity field and active crustal blocks of contemporary tectonic deformation in continental China. Earth Science Frontiers 9(2): 430–441 (in Chinese with English abstract).

Appendix 6 Paleomagnetic Data of Chinese Continent and Its Adjacent Area

Strata symbols refer to that of international stratigraphic chart (UNESCO and IUGS, 2000); N is the amount of samples or sites used in statistical analysis; $\phi_P(^\circ)$ are the degrees of longitude of virtual geomagnetic pole; $\lambda_P(^\circ)$ are the degrees of north latitude of virtual geomagnetic pole ("−" is south latitude); α_{95} is radius (degrees) of circle of 95% confidence about the mean direction; $D(^\circ)$ is mean paleomagnetic declination in degree; $P(^\circ)$ is mean north paleolatitude in degree ("−" is south latitude). The data of D and P recalculated according to central reference point of block, based on the original data from sources. The symbols of plates or blocks are the same as in the paleotectonic reconstruction figures.

1. Sino-Korean Plate (SK)

(central reference point: before Late Jurassic is 112°E, 38°N; after Early Cretaceous is 115°E, 37°N)

Strata	N	$\phi_P(^\circ)$	$\lambda_P(^\circ)$	α_{95}	$D(^\circ)$	$P(^\circ)$	Sources
$Q_{2.5-0Ma}$	8	25.2	84.9	4	353.6	36.8	Liu C et al., 1983
$N_{23-2.6}$	9	208	86.2	4.4	4.7	36.7	Lin JL et al., 1985; Cheng GL et al., 1991
E_{65-24}	4	203.5	79.7	9.1	12.9	36.6	Cheng GL et al., 1991
$K_{2\ 100-66}$	1	170.7	79.6	5.5	11.6	42.3	Zheng Z & Kono, 1991
$K_{1\ 137-101}$	1	210.8	75.9	9.7	17.1	34.3	Ma XH et al., 1993
$J_{3\ 165-137}$	2	221.8	69.4	15.4	22.2	28	Fang DJ et al., 1988
$J_{2\ 190-166}$	5	229.7	76.8	5.6	3.6	31	Ma XH et al., 1993; Cheng GL et al., 1988
$J_{1\ 205-191}$	1	286	82.4	6.8	0.9	30.4	Ma XH et al., 1993
$T_{3\ 227-206}$	1	7.7	62.3	3.8	30	27	Ma XH et al., 1993
$T_{2\ 241-228}$	7	2	61	2.9	330.1	24.1	Fang DJ et al., 1988; Ma XH et al., 1993
$T_{1\ 250-242}$	6	353.7	56.9	4.6	329.6	18.2	Fang DJ et al., 1988; Ma XH et al., 1993
$P_{2\ 277-251}$	11	355.1	50.3	5.7	324	14.2	Zhao XX et al., 1990; Ma XH et al., 1993
$P_{1\ 295-278}$	1	359.2	47	4.5	319.7	13.9	Ma XH et al., 1993
$C_{354-296}$	3	333.3	56.5	6	338.2	10.8	Lin JL et al., 1985; Wu HN, 1991
$O_{1-2\ 490-455}$	6	323.4	33.4	8.5	333.5	−12.9	Huang BC et al., 1999; Yang ZY et al., 1998
$\in_{3\ 500-491}$	11	323	28.3	7.3	331.6	−17.6	Huang BC et al., 1999;
$\in_{2\ 513-501}$	17	324.1	30.6	7.4	331.7	−15.1	Huang BC et al., 1999;
$\in_{1\ 543-514}$	8	332.4	20.6	10.3	319.7	−20.2	Huang BC et al., 1999;
North Korean Peninsula (KN)						(central reference point: 128°E, 41°N)	
Q	1	335.3	85.2	4.3	357.5	36.5	Sasajima, 1981
E_2	1	26	75.6	7.1	342.2	36.5	Sasajima, 1981
E_1	1	315.9	81.8	4.4	358.9	33.3	Sasajima, 1981
K_{2-3}	7	194.9	66.5	9.8	30.9	43.4	Sasajima, 1981
K_1	2	205.7	22.6	10	77.7	21.5	Sasajima, 1981
J	4	212.9	54.4	17.4	43.5	34.9	Sasajima, 1981
South Korean Peninsula (KS)						(central reference point: 128°E, 36°N)	
$K_{2-3\ 65-90}$	1	191	69	8	25.8	42.9	Van der Voo, 1993
K_{65-144}	1	195	64	6	32.8	41.8	Van der Voo, 1993
$K_{1\ 98-144}$	1	183	76	3	15.7	43	Van der Voo, 1993
$J_{144-178}$	1	174	63	9	31.2	51.2	Van der Voo, 1993
$J_{133-178}$	1	176	63	9	31.9	50.3	Kim & Van der Voo, 1990
$J_{157-202}$	1	213	54	17	43.2	31.1	Kim & Van der Voo, 1990
$T_{208-245}$	1	216	34	15	63	21	Kim & Van der Voo, 1990

2. Yangtze Plate (YZ)

(central reference point: before Jurassic is 105°E, 30°N; after Early Cretaceous is 106.5°E, 29.5°N)

$Q_{2.5-0Ma}$	4	222.6	87.5	11.3	2.6	28.4	Zhai YJ, 1989
$N_{23-2.6}$	8	18.8	85.7	9.8	355.1	29.6	Liu C, 1976; Lin JL, 1987
E_{65-24}	8	200.2	81.1	7.5	10	28.5	Li HM et al., 1965; Liang QZ, 1986; Zhuang ZH, 1988
$K_{2\ 100-66}$	4	185.4	75.1	5.9	17.2	31.3	Kent et al., 1986; Huang KN et al., 1993; Zhu ZW et al., 1988

Continued

Strata	N	$\phi_P(^\circ)$	$\lambda_P(^\circ)$	α_{95}	$D(^\circ)$	$P(^\circ)$	Sources
$K_{1\ 137-101}$	4	219.3	77.1	5	13	23.9	Kent et al., 1986; Huang KN et al., 1993; Zhu ZW et al., 1988
$J_{3\ 165-138}$	2	214.9	65.7	9.1	24.2	19.5	Liang QZ, 1990; Cheng GL, 1996
$J_{2\ 190-166}$	5	205.7	70.8	7.6	20.9	24.8	Liang QZ, 1990;Zhu ZW et al., 1988; Enkin et al., 1992a
$J_{1\ 205-191}$	1	190.9	65.5	5.3	28.1	28.7	Huang KN et al., 1993
$T_{3\ 227-206}$	23	190.2	55.8	6.5	39	27	Liang QZ, 1990; Zhu ZW et al., 1988; Cheng GL et al., 1996; Zhou YX et al., 1988
$T_{2\ 241-228}$	4	228.6	69.8	16.8	17.6	17.7	Zhu ZW et al., 1988;Opdyke et al., 1986; Chan et al., 1984
$T_{1\ 250-242}$	9	218.3	52	5.6	35.1	10.6	Enkin et al., 1992; Zhu ZW et al., 1988; Opdyke et al., 1986
$P_{2\ 257-251}$	13	243.6	55.3	5.2	22.1	2.4	Liu C, 1987; Zhao XX et al., 1996; Wu HN et al., 1999; Huang KN, 1986; Ma XH et al., 1989
$P_{1\ 295-258}$	1	228.8	48.7	12.3	33.3	3.3	Wu HN et al., 1999; Liu BJ et al., 1993
$C_{2-3\ 320-296}$	1	229.9	53.5	24	29.4	6.2	Zhang SH et al., 2001
$C_{1\ 354-321}$	1	229.1	47.5	9.6	34	2.3	Zhang SH et al., 2001
$D_{3\ 372-355}$	1	234.1	45.4	6.6	33	−1.6	Zhang SH et al., 2001
$D_{1-2\ 410-373}$	1	231.4	36.1	12.1	40.9	−6.9	Zhang SH et al., 2001
$S_{2-3\ 420-411}$	1	195.7	6.8	5.3	83.8	2.8	Opdyke et al., 1987
$S_{1-2\ 438-420}$	1	157	−55.7	7.9	153.5	−6.5	Wu HN et al., 1999
$O_{1-2\ 490-460}$	1	154.9	−38.4	13.7	144.6	−8.8	Wu HN et al., 1999
$\in_{2\ 513-500}$	1	185.1	−39.5	7.8	129.1	−11.7	Bai LX et al., 1998

3. Cathaysian Plate (CA)

(central reference point: 113.6°E, 25°N)

T_1	1	209.2	−1	9.1	88.5	−5.5	Chen HH et al., 1991
C_1	1	227.7	22.6	19.7	58.9	−10.3	Chen HH et al., 1991
D_3	1	351.1	33.5	10.4	314.4	−10	Chen HH et al., 1991
D_2	1	205.4	−24.9	14.8	111.2	−11.8	Chen HH et al., 1991
$\in_3$	1	54.5	−65.5	6.1	201.3	−11	Liu BJ et al., 1993
$\in_2$	1	51.5	−65.5	4.8	202	−12	Liu BJ et al., 1993
$\in_1$	1	49.8	−62.2	8.4	205.4	−10.8	Liu BJ et al., 1993
Taiwan block (TW)					(central reference point: 121.5°E, 23.5°N)		
1–5 Ma	1	256	82	8	6	17.8	Van der Voo, 1993
5–24 Ma	1	294	82	13	1.1	15.6	Van der Voo, 1993
$N_1^1 - N_2^1$	8	268.9	65.9	10.8	12.7	2.8	Li DG et al., 1991

4. Blocks in the Hingganling-Mongolia collision zone (XM)

K_1	2	358	81.6	4.8	349.7	44.3	Manzhouli, 117°E, 48.9°N; Zhao XX et al., 1990
J_3	7	192.6	69.2	4.4	31.3	50.2	Huaan, 123.1°E, 47°N; Zhao XX et al., 1990
J_3	2	185	56	7.8	49.2	47.5	Balin Zuoqi, 118.9°E, 43.8°N; Zhao XX et al., 1990
T	7	47.7	84.5	4.9	353.1	43	Jining, 113.2°E, 40.9°N; Zhao XX et al., 1990
P_2	4	56.7	−8	7.1	244.4	13.7	Balin Zuoqi, 118.9°E, 43.8°N; Zhao XX et al., 1990
P_2	7	327.5	63.5	8.2	347	18.6	Wudan, 118.9°E, 42.7°N; Zhao XX et al., 1990
C_3	3	31.6	77.7	6.6	343	43.1	Balin Zuoqi, 118.9°E, 43.8°N; Zhao XX et al., 1990

Continued

Strata	N	$\phi_P(^\circ)$	$\lambda_P(^\circ)$	α_{95}	$D(^\circ)$	$P(^\circ)$	Sources
C_2	4	304.5	77	5.5	358.7	36.2	Hailar, 119.8°E, 49.2°N; Zhao XX et al., 1990
C_2	5	231.2	46.9	8.9	43.7	23	Ming'an Obo, 113.2°E, 43.1°N; Zhao XX et al., 1990
Wandashan block (ND)					(central reference point: 133°E, 46.3°N)		
K_1	1	224.1	51	2.9	49.1	33.6	Shao JA et al., 1991
T_3	1	47	−0.4	5	266.8	2.5	Shao JA et al., 1991
P_1	1	214.1	−22.6	4.1	112	−10.3	Shao JA et al., 1991
C_3	1	251.6	0	23.2	68.5	−19.4	Shao JA et al., 1991
Jiamusi block (JM)					(central reference point: Qitaihe, 131.1°E, 45.8°N)		
K_2	1	57.9	79.3	12.1	344.6	48.2	Zhang SH, 1996
K_1	1	63.7	64.4	5	322	49.7	Zhang SH, 1996
J_3	1	59.6	71.3	15.7	332.7	48.6	Zhang SH, 1996
Yagan block (YG)					(central reference point: 102.6°E, 41.7°N)		
P_1	1	246.8	64.3	9.5	15.6	19.7	Zhu H et al., 1987
D	1	296	65.3	10.2	354.1	17.5	Zhu H et al., 1987
S_3	1	205.9	−25.7	12.4	102	−26.4	Zhu H et al., 1987, Polar re-correction
O_3	1	216.1	−17.8	7.1	88.4	−29.1	Zhu H et al., 1987, Polar re-correction
$\in_3$	1	206.6	−15.7	4.1	92.9	−20.7	Zhu H et al., 1987, Polar re-correction

5. Siberian Plate (SB)

(central reference point: 80°E, 60°N)

Q_{2Ma}	13	157	86	4	8	60.1	Khramov et al., 1981
$N_{2\ 5}$	5	152	83	3	14	61.4	Khramov et al., 1981
$N_{1\ 15}$	9	156	80	7	22	60.9	Khramov et al., 1981
$E_{3\ 25}$	3	137	72	14	38	65.2	Khramov et al., 1981
$E_{1-2\ 45}$	19	161	76	3	28	59.2	Khramov et al., 1981
$K_{3\ 65}$	3	152	74	13	33	61.1	Khramov et al., 1981
$K_{2\ 100}$	6	167.4	69.5	8.7	38	55	Khramov et al., 1981
$K_{1\ 121}$	5	166	70	4	37	55.7	Khramov et al., 1981
$J_{3\ 142}$	6	150	70	9	41.1	60.7	Khramov et al., 1981
$J_{2\ 173}$	6	132	63	11	60.4	65.7	Khramov et al., 1981
$J_{1\ 195}$	4	130	69	15	46	67.5	Khramov et al., 1981
$T_{3\ 207}$	6	129	56	8	77.3	64.2	Khramov et al., 1981
$T_{2\ 238}$	7	150	52	7	69.9	52	Khramov et al., 1981
$T_{1\ 245}$	9	156	52	4	66.1	49.2	Khramov et al., 1981
$P_{2\ 253}$	6	161	42	7	72.3	39.6	Khramov et al., 1981
$P_{1\ 268}$	5	159	38	9	77.1	37.5	Khramov et al., 1981
$C_{3\ 288}$	5	158	34	11	80.9	34.8	Khramov et al., 1981
D_{360}	7	151	28	8	91	33.4	Khramov et al., 1981
S_{420}	8	121	−4	19	136.4	18.4	Khramov et al., 1981
$O_{2\ 460}$	11	130	−22	4	134.7	−1.5	Khramov et al., 1981
$O_{1\ 490}$	12	132	−40	7	140.4	−18.7	Khramov et al., 1981
$\in_{1\ 530}$	4	157	−44	12	124.8	−31.4	Khramov et al., 1981

6. Junggar Plate (JG)

(central reference point: 86°E, 46°N)

K	1	83	−14.1		183.4	29.8	Li YA et al., 1992
J	1	180.5	59.3	17.9	39.1	36.2	Li YA et al., 1992
T	1	179.2	45.3	27.7	52.7	28.2	Li YA et al., 1992
P	1	175.6	40.9	27.4	59.4	28.3	Li YA et al., 1992
C	1	200.6	59.5	11	31.6	28.2	Li YA et al., 1992
D	1	312.4	68.7	25	342.4	29.7	Li YA et al., 1992

Continued

Strata	N	$\phi_P(^\circ)$	$\lambda_P(^\circ)$	α_{95}	$D(^\circ)$	$P(^\circ)$	Sources
S	1	17.5	−60.8	18.6	211.7	−30.2	Li YA et al., 1992

7. Kazakstan Plate (KZ)

(central reference point: 77°E, 50°N)

E_3	2	269	78	6	357	38.2	Khramov et al., 1981
E_1	2	196	76	11	16	41.3	Khramov et al., 1981
K_2	4	180.2	68.4	16	28	41.2	Khramov et al., 1981
K_1	2	192.5	65	4	28	35.3	Khramov et al., 1981
J_{1-2}	3	233.2	62.5	19	12	24.1	Khramov et al., 1981
T_1	2	323.5	32	11	308	10.9	Khramov et al., 1981

8. Xiyu Plate (XY)

(1) Tarim block (TR)						(central reference point: 83°E, 39.5°N)	
$N_{20\,Ma}$	3	268.3	79.2	1.5	358.9	28.9	Li YA et al., 1989
E_{40}	3	223.7	75.5	10.6	10.3	27.8	LiYA et al., 1989
K_{105}	1	211.6	69.7	8	17.5	25.4	Li YP et al., 1988
K_{134}	3	217.1	68.1	15.7	16.9	22.9	Li YP et al., 1988; Meng ZF, 1990; Zhang ZK, 1989
J_{150}	1	219.9	65.6	14	17.5	20.3	Li et al., 1989
J_{172}	1	185.9	62.7	13.5	30.8	29.1	Fang DJ et al., 1992
T_{238}	4	181.5	63.7	10.7	30.9	31.3	Fang DJ et al., 1992; Li YA et al., 1989
P_{250}	4	193.1	70.8	6.3	21.1	30.9	Fang DJ et al., 1992; Bai YH et al., 1985
C_{306}	5	171.3	51.9	9	46	31	Fang DJ et al., 1992
D_{390}	2	153.7	10	1.9	94.5	21.2	Fang DJ et al., 1996; Li YR et al., 1990
$S_{1\,427}$	3	215.7	25.1	4	79.3	−12	Meng ZF, 1990
O_{481}	1	4.0	−45.7	15.4	227.1	−18.4	Li YA et al., 1995
$\in_{520}$	1	44.7	−46.7	9.8	208.2	−6.3	Li YA et al., 1995
(2) Alxa block (AL)						(central reference point: 105.9°E, 37.2°N)	
P_2	1	355.2	50.3	5.7	327.5	8.6	Huang BC et al., 2000
C	3	2.9	23.6	11.1	296.4	4.5	He ZX et al., 1988; Huang BC et al., 2000
D_{2-3}	2	343.3	30.7	9.2	313.5	−3.5	He ZX et al., 1988; Huang BC et al., 2000
S	2	289.1	38.3	13.2	357.4	−14.4	He ZX et al., 1988; Huang BC et al., 2000
O	3	187.5	−20.2	11.3	111.1	−5.7	He ZX et al., 1988; Huang BC et al., 2000
$\in_3$	1	38.6	−48	14.4	219.5	−14	He ZX et al., 1988, Polar re-correction
(3) Qaidam block (QD)						(central reference point: 96°E, 37.5°N)	
N_2	1	189.4	72.9	11.8	20.9	34.6	Ge XH et al., 1990
J_3	1	212	55.5	7.1	32.3	17.7	Ge XH et al., 1990
J_{1-2}	1	215	47	4.5	37.4	10.5	Ge XH et al., 1990
C_1	1	246.7	54.3	3.4	16.7	5.2	Ge XH et al., 1990
O_1	2	43.2	−57	11.6	206.6	−14.4	Ge XH et al., 1990
(4) West Kunlun block (Kudi block) (KX)						(central reference point: 77°E, 36.5°N)	
J_{1-2}	2	77.2	−27.1	15.3	179.8	26.4	Li YA et al., 1998
T_1	1	165.9	41.7	24.5	54.8	24	Li YA et al., 1998
P_1	1	188	60.6	19.6	29.7	22.1	Li YA et al., 1998
$\in -O$	1	344.3	−31	18.5	245.5	−19.8	Li YA et al., 1998; 480–510 Ma
816 Ma	1	18.4	−71.5	13.7	18.4	−25.5	Li YA et al., 1998

9. East Kunlun Block (KD)

(central reference point: 94.6°E, 35.9°N)

K_2	1	209.3	60	18.9	28.9	19.8	Lin JL & Watts, 1990
J_1	1	313.3	53.4	4.5	339	5.5	Wu GJ et al., 1998

Continued

Strata	N	$\phi_P(^\circ)$	$\lambda_P(^\circ)$	α_{95}	$D(^\circ)$	$P(^\circ)$	Sources
T_3	1	256.1	42.3	3.8	15.1	−9.2	Wu GJ et al., 1998
T_2	1	266.2	38.5	11.7	6.8	−15.2	Dong XB et al., 1991
T_1	1	229.3	30.2	5.6	38.8	−11.4	Dong XB et al., 1991
P_1	1	288.3	41.4	8.1	349.5	−11.7	Dong XB et al., 1991
C	1	223.9	13	10.7	54.2	−21.6	Lin JL & Watts, 1990
D	1	17.5	−64	13.8	208.5	−26.6	Lin JL & Watts, 1990

10. Qiangtang Block (QT)

(central reference point: 92°E, 33.8°N)

Q_1	2	126.27	−76.6	2.05	51.44	32.1	Qian F et al., 1997 (recent latitude of sample, 35.69°)
N_2	1	309.7	79.3	2.9	352.8	25.1	Ye XH et al., 1987
E	1	202.4	55.1	8.8	34.1	16.9	Lin JL & Watts, 1990
K_2	3	328.5	67.4	10.6	340.1	19.7	Zhou YX et al., 1984
J_2	2	333.3	57.1	7.7	330.5	14.5	Dong XB et al., 1991
T_{2-3}	3	232.9	41.1	15.6	28.6	−6.9	Lin JL & Watts, 1990; Li YA et al., 1995
P_1	3	318.5	27.1	5.6	318.1	−14.8	Ye XH et al., 1987; Dong XB et al., 1991
C_3	5	312.5	22.5	13.4	319.8	−21.8	Ye XH et al., 1987
D_2	1	328.7	7.3	9.4	296.2	−22.4	Ye XH et al., 1987

11. Gandise Block (GD)

(central reference point: 91.2°E, 29.7°N)

E_1	1	299.4	71.8	11	351.3	13.4	Allegre et al., 1984
K_2	10	321.3	64.3	7.5	340	11.8	Ye XH et al., 1987; Lin JL & Watts, 1990; Zhou YX et al., 1984; Achache, 1989; Dong XB et al., 1991; Zhu ZW, 1985
K_1	1	17.9	−10.5	13.6	252	8.9	Dong XB et al., 1991
J_3	5	295.3	45.4	13.6	343	−11.8	Ye XH et al., 1987; Dong XB et al.1991; Zhu ZW et al., 1985
T_3	1	211.6	8.2	6	66.5	−21.4	Dong XB et al., 1991
P_1	1	271.2	36.8	9.7	359	−23.5	Dong XB et al., 1991
C_3	1	288.7	41.1	6.8	346.3	−17.4	Dong XB et al., 1991
C_{1-2}	2	282.8	33	13.4	349	−26.1	Dong XB et al., 1991
D_2	1	290	35.5	4.2	343.5	−22.4	Dong XB et al., 1991
S	1	263	24.3	4	9.2	−35.4	Dong XB et al., 1991

12. Himalayan Block (HM)

(central reference point: 89.5°E, 28.7°N)

Q_{2-3}	14	170.96	78.42		13.49	30.5	Qian F, 1990 (recent latitude of sample, 31.5°)
Q_1	14	114.87	84.56		356.47	27.2	Qian F, 1990 (recent latitude of sample, 31.5°)
N_2-Q	1	161.5	85.5	9.9	4.9	30	Zhu ZW et al., 1984
N_2	1	208	82.7	8.8	7	25	Zhu ZW et al., 1984
E	1	334.5	42.6	11	318.1	3	Zhu ZW et al., 1984
K_2	3	312.4	47.9	6.5	332.8	−4.3	Dong XB et al., 1991; Lin JL & Watts, 1990
J_3	2	329.4	5.8	12.6	290.9	−22.9	Ye XH et al., 1987; Zhu ZW et al., 1985
J_2	1	326.5	3	11.3	290	−26.9	Ye XH et al., 1987; Zhu ZW et al., 1985
T_{1-2}	1	308	22.7	6.3	320	−26.6	Zhu ZW et al., 1985
C	2	321.4	0.8	16.5	291.4	−32.3	Zhu ZW et al., 1985
D	2	335.4	−18.8	12.4	263.6	−29.6	Zhu ZW et al., 1985
S	1	283.7	28.3	5.8	345.3	−31.4	Zhu ZW et al., 1985
O_1	1	289.1	26.3	16	339.3	−31.9	Zhu ZW et al., 1985

Continued

Strata	N	$\phi_P(^\circ)$	$\lambda_P(^\circ)$	α_{95}	$D(^\circ)$	$P(^\circ)$	Sources
$\in_1$	1	334.8	-30.9	6	250	−34	Zhu ZW et al., 1985

13. Indian Plate (ID) (central reference point: 79°E, 21°N)

5–22.5 Ma	1	114.5	−78.5	2.3	353	11.5	Klootwijk, Radhakriehnamurty, 1981
25–35	1	136	−72.5	3.5	345.1	10.9	Klootwijk, Radhakriehnamurty, 1981
35–45	1	132	−67.5	12	342	6.7	Klootwijk, Radhakriehnamurty, 1981
45–55	1	121.5	−57.5	9	158.7	3.9	Klootwijk, Radhakriehnamurty, 1981
60–65	4	286.1	34.1	16.6	334.4	−29.2	Klootwijk, Radhakriehnamurty, 1981
$K_{2\ 100-66}$	17	294.7	21.4	5	318	−35.1	Klootwijk, Radhakriehnamurty, 1981
$K_{1\ 137-101}$	7	295.7	7.9	3.6	305	−43.8	Klootwijk, Radhakriehnamurty, 1981
$J_{2\ 190-166}$	2	288.7	16.5	18.2	320	−42.5	Klootwijk, Radhakriehnamurty, 1981
$T_{1-2\ 250-228}$	2	306	13	19.5	302	−32.7	Klootwijk, Radhakriehnamurty, 1981
$P_{2\ 257-251}$	11	310	−16.4	7.2	266	−41.6	Klootwijk, Radhakriehnamurty, 1981
$P_{1\ 295-258}$	1	317	−13	7.3	268	−34	Klootwijk, Radhakriehnamurty, 1981
$C_{3\ 310-296}$	1	316	−22.3		257	−37.3	Klootwijk, Radhakriehnamurty, 1981
$C_{2\ 331-311}$	1	212	22		49.6	−27.1	Klootwijk, Radhakriehnamurty, 1981
$C_{1\ 365-330}$	1	218	28.5		40.2	−26.6	Klootwijk, Radhakriehnamurty, 1981
$D_{3\ 378-366}$	1	243	22		20.9	−44.3	Klootwijk, Radhakriehnamurty, 1981
$D_{1\ 393-379}$	1	281	37		340	−28.4	Klootwijk, Radhakriehnamurty, 1981
$S_{2\ 429-415}$	1	238	37		19	−28.7	Klootwijk, Radhakriehnamurty, 1981
$O_{3\ 467-430}$	1	187	−14		97.3	−21.5	Klootwijk, Radhakriehnamurty, 1981
$O_{1\ 505-468}$	1	200	3		74.8	−27.5	Klootwijk, Radhakriehnamurty, 1981
$\in_{1\ 543-506}$	1	199	6		72.2	−25.3	Klootwijk, Radhakriehnamurty, 1981
$Z_{575-544}$	1	212	35	15	39.2	−18.4	Klootwijk, Radhakriehnamurty, 1981

14. Baoshan–Sibumasu Plate (BS) (central reference point: 99.1°E, 25.2°N)

J_2	5	168.2	15.7	5	83.7	25.2	Liang, 1990; Zhuang ZH, 1995
T_3	2	174.5	−12	11.7	107.2	7.7	Zhuang ZH, 1995
T_2	1	167.6	−2.4	15.1	101.8	18.3	Zhuang ZH, 1995
C_3	6	317	33.4	13.6	326.6	−21.2	Liang QZ, 1990; Zhuang ZH, 1995
C_1	1	296.3	33.1	12.7	343.5	−29.4	Zhuang ZH, 1995
D_3	1	357.3	−57.5	11.1	216.3	−27.3	Zhuang ZH, 1995
D_1	5	356.3	−55.8	8.6	218.2	−27.7	Liang QZ, 1990; Zhuang ZH, 1995
S_3	1	0.8	−68.3	9	204.1	−26.4	Zhuang ZH, 1995
S_1	1	242	31.5		34	−23.1	Liang QZ, 1990
O_3	5	2.6	−46.1	12	228.1	−22.2	Liang QZ, 1990; Zhuang ZH, 1995
O_1	5	2.6	−36.7	20	237.8	−19.7	Liang QZ, 1990; Zhuang ZH, 1995

15. Lanping–Simao–Indochina Plate (LI) (central reference point: 101.4°E, 22.5°N)

E	1	70.8	85.5	9.6	358	30.5	Liang QZ, 1990
K_2	2	171.1	40	7.9	56	29.4	Liang QZ, 1990
K_1	3	171.9	37.1	10.4	59	28.8	Liang QZ, 1990
J_2	1	170.1	4.9	10.4	94	20.5	Liang QZ, 1990
T_3	3	171.5	−5	21.8	103	16.2	Liang QZ, 1990
C_3	1	216.9	31.6	10	50.9	−7.9	Liang QZ, 1990
S_2	2	347.7	30.3	15.8	307.1	−7.3	Liang QZ, 1990
Nakhon Plateau (IC)					(central reference point: 102.5°E, 16.5°N)		
11–0 Ma	1	171	86	5	4	17.9	Van der Voo, 1993; Yang & Besse, 1993
K	1	176	79	8	11.2	19.3	Van der Voo, 1993; Yang & Besse, 1993
J_3	1	177	60	14	31.3	22.8	Van der Voo, 1993; Yang & Besse, 1993

Continued

Strata	N	$\phi_P(^\circ)$	$\lambda_P(^\circ)$	α_{95}	$D(^\circ)$	$P(^\circ)$	Sources
J_2	1	178.5	62.1	7.7	29.1	21.1	Van der Voo, 1993; Yang & Besse, 1993
T_3–J_1	1	181.6	57.4	5	34.2	19.7	Van der Voo, 1993; Yang & Besse, 1993
T_3	1	180	53	9	38.6	20.6	Van der Voo, 1993; Yang & Besse, 1993
T_1	1	172	49	8	43	25.8	Van der Voo, 1993; Yang & Besse, 1993
P_2	1	356.2	−58.4	6	213	−22.5	Yang & Besse, 1993
P_2–T_1	1	332	−57	10.7	207.2	−22.9	Haile, 1981 (101.5°E, 3°N)
C_2–P_1	1	344	−55	11.2	212.3	−17.8	Haile, 1981 (101.5°E, 3°N)
C_1	1	2	−57	9.2	212.1	−7.6	Haile, 1981 (101.5°E, 3°N)
O	1	256	−46	6.3	156.5	−41.6	Haile, 1981 (101.5°E, 3°N)

16. Australia Plate (AU)

(central reference point: 135°E, 25°S)

$E_{1\,37-66\,Ma}$	1	301	61	10	11.2	−52.7	Van der Voo, 1993
$K_{2\,67-96}$	1	318	56		356.7	−58.9	Van der Voo, 1993
$K_{1\,98-144}$	1	338	41	17	315.6	−65.1	Van der Voo, 1993
$J_{3\,145-176}$	1	349	48	13	319.6	−54.8	Van der Voo, 1993
$J_{1\,177-195}$	1	357	48	5	316	−49.9	Van der Voo, 1993
$T_{3\,216-232}$	1	350	32		291	−58.6	Van der Voo, 1993
$T_{1\,233-245}$	1	342	42		314.1	−62	Van der Voo, 1993
$P_{2\,246-266}$	1	320	43		348.4	−71.5	Van der Voo, 1993
$P_{1\,267-281}$	1	302	46		23.1	−66.6	Van der Voo, 1993
$C_{2\,282-308}$	1	322	62		354.6	−52.7	Van der Voo, 1993
$C_{1\,309-365}$	1	141	84		0.7	−19	Van der Voo, 1993
$D_{3\,366-378}$	1	203	62	16	26.5	−12.3	Van der Voo, 1993
$D_{2\,379-397}$	1	80	77		348.9	−17.1	Van der Voo, 1993
$S_{2\,415-429}$	1	318	−53.9	14.4	181.8	−11.1	Van der Voo, 1993
$O_{1\,468-505}$	1	20.6	−17	17	243.6	−13.6	Van der Voo, 1993
$\in_{506-543}$	1	20.3	−18	16	242.6	−13.3	Van der Voo, 1993

17. Southwest Japan (JP)

(central reference point: 133°E, 35°N)

N_1	5	222.5	73.6	11.9	19.8	33.5	Sasajima, 1981
E_1	7	216.4	56.7	6.7	40.1	32.1	Sasajima, 1981
K_2	8	207.5	46	8.6	54.2	34.4	Sasajima, 1981
K_1	5	195	47.5	12.9	54.7	43.1	Sasajima, 1981
J_3	1	17	49.6	20	323.5	11.8	Sasajima, 1981
T_3	2	347.2	58.8	13.5	342.9	8	Sasajima, 1981
P_{1-2}	1	295.4	55.6	7.4	9.8	1.8	Sasajima, 1981
C_3	1	202.9	−21.3	8	118.8	3.1	Sasajima, 1981

References for Appendix 6

Achache J, Courtillot V, Zhou YX (1984) Paleomagnetic and tectonic evolution of southern Tibet since Middle Cretaceous time: New paleomagnetic data and synthesis. J. Geophys. Res. 89(B12): 10311–10339.

Allègre CJ, Courtillot V, Tapponnier P et al (1984) Structure and evolution of the Himalaya-Tibet orogenic belt. Nature 307: 17–22.

Bai LX, Wu HN, Zhu RX et al (1998) New results of Middle Cambrian paleomagnetism in Yangtze block Science in China D 28 (suppl.): 57–62 (in Chinese).

Bai YH, Cheng GL, Sun QG et al (1985) Late Paleozoic polar wander path for the Tarim block and tectonic significance. Seismology and Geology 7(1): 71–80 (in Chinese with English abstract).

Chan LS, Wang CY, Wu XY et al (1984) Paleomagnetic results of some Permian-Triassic from Southwest China. Geophys. Res. Lett. 11(11): 1157–1160.
Chen HH, Sun S, Li JL, Xu JH et al (1991) New results of paleo-geomagnetism of South China plate In: Annual Reports (1989—1990) of Open Laboratory of Lithosphere Tectonic Evolution, Institute of Geology, China Academy of Sciences, pp.102–106. Science Press, Beijing (in Chinese).
Cheng GL, Bai YH, Sun YH (1988) Paleomagnetic study on the tectonic evolution of the Ordos Block, North China. Seismology and Geology 10(2): 81–87 (in Chinese with English abstract).
Cheng GL, Sun YH, Li SL (1991) China paleomagnetic data list for Cenozoic. Seismology and Geology 13(2): 184–186 (in Chinese with English abstract).
Cheng GL, Sun YH, Sun QG et al (1995) Paleomagnetic research on the Phanerozoic tectonic evolution of China. Seismology and Geology, 17(1): 69–78 (in Chinese with English abstract).
Cheng GL, Sun YH, Sun QG et al (1996) Phanerozoic paleomagnetic data for the main blocks of China. Seismology and Geology 18(2): 182–192 (in Chinese with English abstract).
Dong XB, Wang ZM, Tan CZ et al (1991) New results of paleomagnetism of the Qinghai- Tibet plateau Geological Review 37(2): 160–164 (in Chinese with English abstract).
Enkin RJ, Yang ZY, Chen Y, Courtilot V (1992) Paleomagnetic constrains on the geodynamic history of the major blocks of China from the Permian to the present. J. Geophys. Res. 97: 13953–13989.
Enkin RJ, Courtilot V, Letoup P et al (1992) The Upper Permian record of Uppermost Permian, Lower Triassic rocks from the South China block. Geophys. Res. Lett. 19: 2147–2150.
Fang DJ, Guo YB, Wang ZL et al (1988) Tectonic significance of paleomagnetic study on the Triassic and Jurassic systems in Ningwu basin, Shanxi. Chinese Science Bulletin, 33(24): 2057–2059.
Fang DJ, Jin GH, Chen HL et al (1992) Preliminary approach to Late Paleozoic-Mesozoic geomag- netism and tectonic evolution in north margin of Tarim plate. In: Jia RX (ed) Research of Petroleum Geology of Northern Tarim Basin in China: Structural and Petroleum Geology (2), pp.96–104. China University of Geosciences Press, Wuhan (in Chinese).
Fang DJ, Jin GH, Jiang LP et al (1996) Paleozoic paleomagnetic results and the tectonic significance of Tarim Plate. Acta Geophysica Sinica 39(4): 522–532 (in Chinese with English abstract).
Ge XH, Duan JY, Li C et al (1990) Formation and Evolution of Qaidam Basin. 151pp. Petroleum Bureau of Qinghai & Changchun College of Geology (an unpublished report in Chinese).
Haile NS (1981) Palaeomagnetism of Southeast and East Asia. In: McElihnny MW, Valencio DA (eds) Palaeoreconstruction of the Continents. Geodynamics Series 2, pp.129–135. American Geophysical Union.
He ZX, Zheng ZC, Zhu H (1998) A preliminary research on paleomagnetism of Paleozoic strata in the Hexizoulang massif. Geoscience 2(2): 186–193 (in Chinese with English abstract).
Huang KN, Opdyke ND, Kent DV et al (1986) Further paleomagnetic results from the Permian Emeishan basalt in SW China. Chinese Science Bulletin 31(17): 1195–1201.
Huang KN, Opdyke ND (1993) Paleomagnetic results from Cretaceous and Jurassic rocks of South and Southwest Yunnan: evidence for large clockwise rotations in the Indochina and Shan-Thai-Malay terranes. Earth Planet. Sci. Lett. 117: 507–524.
Huang BC, Zhu RX, Yang ZY (1999) Study of Paleozoic kinematics features of the North China block Geoscience 13(suppl.): 1–7 (in Chinese with English abstract).
Huang BC, Yang ZY, Otofuji Y, Zhu RX (1999) Early Paleozoic paleomagnetic poles from the western part of the North China Block and their implications. Tectonophysics 308: 377–402.
Huang BC, Otofuji Y, Yang ZY, Zhu RX (2000) New Silurian and Devonian paleomagnetic results from the Hexi Corrider terrane, northwest China and their tectonic implications. Geophy. Jour. Inter. 140: 132–146.
Kent DV, Xu G, Huang K et al (1986) Paleomagnetism of Upper Cretaceous rocks from South China. Earth Planet. Sci. Lett. 79: 179–184.
Khramov AN, Petrova GN, Peckersky DM (1981) Paleomagnetism of Soviet Union. In: McElhinny MW, Valencio DA (eds) Paleoconstruction of the Continents, Geodynamic Series. pp.177–194. Boulder, Colorado: Geological Society of America.
Kim KH, Van der Voo R (1990) Jurassic and Triassic paleomagnetism of South Korea. Tectonics 9(4): 699–717.
Klootwijk CT, Radhakrishnamurty C (1981) Phanerozoic paleomagnetism of the Indian plate and India-Asia collision. In: McElhinny MW, Valencio DA (eds) Paleoconstruction of the Continents. Geodynamics Series, 93–105. Boulder, Colorado: Geological Society of America.
Li DG, Ji WR, Kissel C, Barrie E (1991) Paleomagnetic strata of sedimentary rock systems in the middle and southern part of coastal mountains in eastern Taiwan. Petroleum Communication of Taiwan 8(1): 55–61 (in Chinese).
Li HM (1965) Paleo-magnetic research on the red layers in Yichang, Hubei and in Hengyang, Hunan In: Institute of Geology, China Academy of Sciences, Problems on Tectonics, p.150–163. Science Press, Beijing (in Chinese).
Li PW, Zhang SH, Shen NH (1999) Mesozoic paleomagnetic results from Jiamusi terrane. Geoscience 13 (suppl.): 41–44 (in Chinese with English abstract).
Li YP, McWilliams M, Sharps R et al (1988) Mesozoic paleomagnetic results of the Tarim Craton: Tertiary relative motion between China and Siberia. Geophysical Research Letters 15(3): 217–220.

Li YP, Cox A, Li YA et al (1990) A Devonian paleomagnetic pole from red beds of the Tarim block, China. J.G. R. 95(12): 19185–19198.
Li YA, Li Q, Zhang ZK et al (1989) Study on palaeomagnetism of Tarim craton since Late Palaeozoic. Xinjiang Geology 7(3): 1–77 (in Chinese with English abstract).
Li YA, Cheng GL, Li Q et al (1992) Paleomagnetic study of the eastern Xinjiang. Xinjiang Geology 10(4): 329–371 (in Chinese with English abstract).
Li YA, Li Q, Zhang H et al (1995) Palaeomagnetic study of Tarim and its adjacent area as well as the formation and evolution of Tarim basin. Xinjiang Geology 13(4): 293–376 (in Chinese with English abstract).
Li YA (1998) Discussion on paleomagnetism and tectonic evolution along the Qinghai-Xizang road and adjacent areas. Science in China D 27(3): 200–206 (in Chinese).
Liang QZ, Ding S, Yu RY et al (1986) A case study of the Paleogene paleomagnetic pole sites and characteristics of magnetic strata in eastern Yunnan, China. Geological Review 32(2): 144–149 (in Chinese with English abstract).
Liang QZ (1990) Paleo-magnetic Research on Petrological Phase Paleogeography and Sedimentation. An unpublished report of Institute of Scientific Research, Geological Bureau of Yunnan (in Chinese).
Lin JL, Fuller M, Zhang WY (1985) Preliminary Phanerozoic polar wander paths for the North and South China blocks. Nature 313: 444–449.
Lin JL (1987) China paleomagnetic data list (1). Scientia Geologica Sinica (2): 184–187 (in Chinese with English abstract).
Lin JL, Watts DR (1988) Paleomagnetic results from the Tibetian Plateau. Philos. Trans. R. Soc. London A 327: 239–262.
Lin JL (1989) China paleomagnetic data list (2). Scientia Geologica Sinica, (4): 400–404 (in Chinese with English abstract).
Lin JL, Watts DR (1990) Paleomagnetic results from the Tibetan Plateau. In: Comprehensive Geological Bregade in Qinghai-Xizang Cooperation with China and United Kingdon, The Geological Evolution of Tibetan Plateau, pp.242–281. Science Press, Beijing (in Chinese).
Liu C, Cheng GL, Ye SJ et al (1976) The paleomagnetic study on some Cenozoic basalt groups in vicinity of Nanking and the preliminary determination of its geological ages. Acta Geophysica Sinica 19(2): 125–137 (in Chinese with English abstract).
Liu C (1983) Paleomagnetic study of some Late Cenozoic basalt group from Datong region, Shanxi Province. Scientia Sinica (Series B) 26(2): 196–203.
Liu C, Zhu RX, Jin ZX (1987) Paleomagnetism of Late-Precambrian Emeishan basalts from Panxi and its neighboring area. In: Zhang YX, Liu BG (eds) Contribution to Panzhihua-Xichang Rift, China. No.2, pp.194–200. Geological Publishing House, Beijing (in Chinese with English abstract).
Liu ZQ, Li XZ, Ye QT et al (1993) Division of Tectonic Magma Belt in Sanjiang Area (Hengduanshan) and its Distribution of Mineral Resources. 246pp. Geological Publishing House, Beijing (in Chinese).
Ma XH, Zhang ZK, McElhinny MW et al (1989) Paleomagnetic research of Permian in Emei, Sichuan Province and Taiyuan, Shanxi Pprovince. Acta Gephysica Sinica 32: 451–465 (in Chinese with English abstract).
Ma XH, Xing LS, Yang ZY et al (1992) Paleomagnetic Study since Late Paleozoic in Ordos Basin 74pp. Seismological Press, Beijing (in Chinese with English abstract).
Ma XH, Yang ZY (1993) The collision and suturing of the three major blocks in China and the reconstruction of the Paleo-Eurasian continent. Acta Geophysica Sinica 36(4): 476–488 (in Chinese with English abstract).
Meng ZF (1990) Paleomagnetic research on polar wander paths and relative movement of sub-tectonic units. In: Zhou QJ, Zheng JZ (ed) Tarim Tectonic Analysis, Oil and Gas Geology of Tarim (3): 50–87. Science Press, Beijing.
Opdyke ND, Huang K, Xu G et al (1986) Paleomagnetic results from the Triassic of the Yangtze Platform. J. Geophys. Res. B 91(9): 9553–9568.
Opdyke ND, Huang K, Xu G et al (1987) Paleomagnetic results from the Silurian of the Yangtze Paraplatform. Tectonophysics 139(1–2): 123–132.
Qian F (1990) Preliminary study of horizontal movement since Late Pliocene by paleomagnetic method in all area, Xizang (Tibet). In: Chinese Academy of Geological Sciences, Tectonic Evolution of Lithosphere of the Himalayas-Contribution to the Geophysics of Xizang (Tibet) pp.198–206. Geological Publishing House, Beijing (in Chinese with English abstract).
Qian F, Zhang JQ (1997) Study on the magnetic stratigraphy of the Qiangtang formation and the neotectonism at Kunlun Mountain pass. Journal of Geomechanics 3(1): 50–56 (in Chinese with English abstract).
Sasajima S (1981) Pre-Neogene paleomagnetism of Japanese Islands and vicinities. In: McElhinny MW, Valencio DA (eds) Paleoreconstruction of the Continents. Geodynamics Series 2: 115–128. American Geophysics Union.
Shao JA, Wang CY, Tang KD (1992) A new approach to the tectonics in the Ussuri (Wusuli) region. Geological Review 38(1): 33–39 (in Chinese with English abstract).
Van der Voo R (1993) Paleomagnetism of the Atlantic, Tethys and Iapetus Oceans. 273pp. Cambridge University Press, Cambridge.
Wu HN, Chang CF, Liu C et al (1991) Revised and synthetic apparent polar wander paths of the north and south China blocks from the Cambrian to Cretaceous Journal of Northwest University 21(3): 99–105 (in Chinese with English abstract).

Wu HN, Zhu RX, Bai LX et al (1998) Revised apparent polar wander path of the Yangtze Block and its tectonic implications Science in China D 41(2): 182–194.
Wu HN, Zhu RX, Bai LX et al (1999) Paleomagnetic results of Paleozoic and Mesozoic rocks from Xingshan-Zigui section in Hubei Province, South China. Science in China D 42(2): 144–154.
Yang ZY, Besse J (1993) Paleomagnetic study of Permian and Mesozoic sedimentary rocks from North Thailand supports the extrusion model for Indochina. Earth and Planetary Science Letters 117(3–4):525–552
Yang ZY, Ma XH, Sun ZM et al (1996) Preliminary result of Early Paleozoic paleomagnetism in Northern Henan and its significance. Chinese Science Bulletin 42(4): 401–406.
Yang ZY, Otofuji Y, Sun ZM et al (1998) Geomagnetic pole series of boundary between Cambrian and Ordovician in Tangshan, Hebei. Chinese Science Bulletin 43(17): 1881–1885.
Ye XH, Li JF (1987) Paleomagnetism and evolution of Tibet plates and Tethys Journal of Chengdu College of Geology 14(1): 65–79 (in Chinese with English abstract).
Zhai Yongjian, Zhou Yaoxiu (1989) Paleomagnetism and tectonic evolution of North and South China Blocks since the Phanerozoic. Acta Geophysica Sinica 32(3): 292–307 (in Chinese with English abstract).
Zhang SH, Yang HX (1996) Paleomagnetism of the Jiamusi terrane in the late Jurassic epoch and cretaceous period and its tectonic significance, NE China Journal of Changchun University of Earth Sciences 26(2): 206–210 (in Chinese with English abstract).
Zhang SH, Zhu H, Meng XH (2001) New results of paleomagnetism of Devonian-Carboniferous in Yangtze block and their paleogeographical implications. Acta Geologica Sinica 75(3): 303–313 (in Chinese with English abstract).
Zhao XX, Coe RS (1987) Paleomagnetic constraints on the collision and rotation of North and South China. Nature 327: 142–144.
Zhao XX, Coe RS, Zhou YX et al (1990) New paleomagnetic results from northern China: collision and suturing with Siberia and Kazakhstan. Tectonophysics 181(1–4): 43–81.
Zhao XX, Coe RS, Gilder SA et al (1996) Paleomagnetic constraints on the paleogeography of China: implications for Gondwanaland. Austra. J. Earth Sci. 43(6): 643–672.
Zheng Z, Kono M et al (1991) The apparent polar wander path for the North China block since the Jurassic. Geophys. Jour. Int. 104(1): 29–40.
Zhou YX, Lu LZ, Yuan XG et al (1984) Donnees paleomagnetiques nouvelles au Tibet-connaissance fundamental pour le mouvement du bloc de Lhasa. In: Himalayan Geology, II. pp.279–297. Geological Publishing House, Beijing (in Chinese with English abstract).
Zhou YX, Lu LZ, Zhang BM (1988) Preliminary paleomagnetic research for Panxi region. In: Zhang YX, Yuan XC (eds) Contribution to Panzhihua-Xichang Rift, China. No.3. pp.212–230. Geological Publishing House, Beijing (in Chinese with English abstract).
Zhu H, Zheng ZC, He XY (1987) Paleozoic Biostratigraphy and Tectonic Evolution of the Alxa Massif Margin 159pp. Wuhan College of Geology Press, Wuhan (in Chinese with English abstract).
Zhu RX, Tschu KK (2001) Studies on Paleomagnetism and Reversals of Geomagnetic Field in China. 168pp. Science Press, Beijing.
Zhu ZW, Teng JW (1984) Paleomagnetic proof of Indian Plate's dispersal toward north after the splitting of Gondwana continent and its collision with Eurasia Plate. In: Products of Cooperative Inspection of Himalaya between China and France, pp.17–23. Geological Publishing House, Beijing (in Chinese).
Zhu ZW (1985) Comparative significance of apparent polar wander path of Xizang and its adjacent regions from Phanerozoic. Acta Geophysica Sinica 28(suppl.): 219–225.
Zhu ZW, Hao TY, Zhao HS (1988) Paleomagnetism and its implication of Pan-Xi region in Mesozoic. In: Zhang YX, Yuan XC (eds) Collection of Pan-Xi Rift, China, (3): 199–211. Geological Publishing House, Beijing (in Chinese with English abstract).
Zhuang ZH, Tian DX, Ma XH et al (1988) A paleomagnetic study along the Ya'an-Tianquan Cretaceous-Eogene section in Sichuan basin. Geophysical & Geochemical Exploration 12(3): 224–228 (in Chinese with English abstract).
Zhuang ZH (1995) Research on plaeomagnetism of Hengduan Mountains and its adjacent areas. Chengdu Institute of Geological Mineral Products, Ministry of Geology and Mineral Resources (in Chinese).

Appendix 7 Temperature, Pressure, Depth and Thermal Gradient in Rock Forming Stages of Chinese Continent

The calculating method of thermal gradient in crust showed in Chapter13. In the table, M is the depth of Mohorovĭcíc discontinuity, according to the determined data, C is the depth of crust, L is the depth of lithosphere bottom FT-Fission Track method; TL-Thermoluminescence technique.

Area	Rock	Isotopic age (Ma)	Temperature (℃)	Pressure (GPa)	Forming depth (km)	Thermal gradient (℃/km)	Sources
Early Mesoproterozoic Changcheng Period 1,800–1,400 Ma							
Laixi-Laiyang, Shandong	Granulite	1,752	860	> 1.4	46.7	21	Liu et al., 1998
West Miyun, Beijing	Granet	> 1,717	774	0.957	31.9	24.2	Chen et al., 1994
East Miyun, Beijing	inclusion	> 1,717	856	1.23	41	22.7	Chen et al., 1994
South Jilin	Green schist	~ 1,400	660	0.8	26.7	25	Cheng et al., 1994
Late Mesoproterozoic Jixian Period 1,400–1,000 Ma							
Mudanjiang, Heilongjiang	Amphibolite	~ 1,100	370	0.7	23.3	15.9	Cheng et al., 1994
Kuanping Group, Qinling	Green schist	1,400–1,000	550–650	0.4–0.6	13–20	13–30	Liu et al., 1993
Kuanping Group, Qinling	Green schist	1,400–1,000	650	0.6	20	33	Zhang et al., 1991
Kuanping Group, Qinling	Green schist	1,393	550	0.5	16.7	33	Cheng et al., 1994
Hong'an Group, Dabie	Green schist	> 1,000	600	0.63	21	28.6	Hubei Geological Survey, 1990
Wudang Group	Green schist	1,304–965	350	0.6	20	17.5	Liu et al., 1993
Wudang Group	Mylonite	1,304–965	300	0.2	10	30	Liu et al., 1993
Xilingol, Inner Mongolia	Amphibolite	Jixian	550	0.6	20	27.5	Zhao et al., 2002
South Dulan, Qinghai	Eclogite	1,160–900	913	> 2.0	66.7	34	Yang et al., 2000
Sibao Group, Jiangnan	Green schist	~ 1,063	250	0.2	6.7	37	Cheng et al., 1994
Songshugou, Qinling	Granulite	~ 1,030 ± 46	800–900	1.3–1.6	43–53	18–20.6	Zhang et al., 2001
Yanggao, Shanxi	Kimberlite	1,183 (?)	1200	2.5–3.5	82–115	10.4–15	Chi et al., 1996
Tieling, Liaoning	Kimberlite	701–1,181			150 L		Chi et al., 1996
Early Neoproterozoic Qingbaikou Period 1,000–800 Ma							
Hong'an Group, Dabie	Eclogite	1,000–800	683	1.27	42	18	Liu et al., 1993
Qinling Group, Qinling	Anphibolite	990–800	720	0.9	30	24	Liu et al., 1993
Songshugou, Qinling	Pyroxenolite	983	828–887	1.4–1.6	50	21	Liu et al., 1994
Songshugou, Qinling	Granulite	983	765–825	1.03	34.3	24	Liu et al., 1994
Songshugou, Qinling	Anphibolite	983	~ 625	~ 0.9	30	19–28	Zhang, 2001
Hong'an Group, Dabie	Green schist	~ 800	500	0.55	22	23	Liu et al., 1993

Continued

Area	Rock	Isotopic age (Ma)	Temperature (℃)	Pressure (GPa)	Forming depth (km)	Thermal gradient (℃/km)	Sources
Jiaonan Group. Shandong	Eclogite	~ 800	650	1.6	53.3	13.3	Su et al., 1994
Su-Lu collision zone	Eclogite	900–720	1,100	3.1	103	12	Zhang et al., 2002
Yukahe, North Qaidam	Eclogite	950–850	> 732	2.8	80	9.2	Liet al., 1999
Dikou formation, Fujian	Anphibolite	~ 800	625	0.4	13.3	47	Fujian Geological Survey, 1985
Yunkaidashan, Guangdong	Granulite	950	650	0.52	17.5	54	Zhou et al., 1997
Yunkaidashan	Granulite	813–638	883	0.71	23.7	37	Du et al., 1999
Yuanmou, Yunnan	Anphibolite	1,000–820	630	0.8	26.7	23.6	Deng et al., 2001
North Qaidam	Eclogite	NP	722	2.2	73.3	9.8	Yang et al., 1998
Beishan, Gansu	Eclogite	NP	800	> 1.6	53.3	17.6	Mei et al., 1998
Bixiling, Dabieshan	Eclogite	NP	775	4.76	159	4.9	Liu et al., 1995
Border among Shaanxi, Gansu and Sichuan	Glaucophane	1,000–800	400	0.6	20	20	Wei et al., 1994
	Green schist	1,000–800	400	0.4	13.3	30	
South Dabieshan	Migmatization	848	580	1.4	46.7	12.4	Wei et al., 1997
East of East Kunlun	Gneiss	NP	820	1	33	24.8	Chen et al., 1999
Gangbian, Jiangxi	Monzonite	~ 847	750	1	30	25	Li et al., 1997
Gangbian, Jiangxi	Basalt	~ 847	1,000	0.7	55	23	Li et al., 1997
Lushan, Jiangxi	Granite	823	565	0.57	19	24	Li et al., 1998
Late Neoproterozoic–Early Cambrian Period (Nanhua-Sinian–Early Cambrian) 800–513 Ma							
Rizhao, Shandong	Eclogite	613.3	981	2.95	98.3	10	Zhang et al., 1999
Jiaonan, Shandong	Green schist	> 574	458	0.73	24.3	18.8	Su et al., 1994
Middle Altun	Metam. shale	> 570	550	2	66.7	8.2	Liu et al., 1999
South Altun	Eclogite	> 519	830	1.85	61.7	16	Liu et al., 1999
Altun	Mylonite	574.68	550	2	66.7	8.2	Che et al., 1995
East Dabieshan	Gneiss	772	515	0.75	25	20.6	Dong et al., 2002
Kudi, Southwest Xinjiang	Anphibolite	Sinian	993	1.66	55.3	22.6	Sheng et al., 1996
Kudi, Southwest Xinjiang	Peridotite	Sinian	993.2	2.39	62.3	20.6	Sheng et al., 1996
Ulausu, Inner Mongolia	Anphibolite	638–607	670	0.3	11	61	Zhang et al., 1996
Ondors Inner Mongolia	Basalt	624	400	0.7	23.3	17	Zhang et al., 1998
Early Paleozoic Qilianian Period 513–397 Ma							
Ondor Sum Group, Inner Mongolia	Green schist	~ 400	450	0.8	26.7	19	Inner Mongolia Geological. Survey, 1991
Harkshan, Xinjiang	Anphibolite	456–415	425	0.8	26.7	16	Cheng et al., 1994
Xitieshan, Qinghai	Eclogite	E. Paleozoic	830	> 1.4	46.7	20.4	Zhang et al., 2002
Da Qaidam	Eclogite	E. Paleozoic	730	2.8	93	8	Zhang et al., 2002

Continued

Area	Rock	Isotopic age (Ma)	Temperature (℃)	Pressure (GPa)	Forming depth (km)	Thermal gradient (℃/km)	Sources
Qinling Group,	Anphibolite	425	760	0.6	20	38	Liu et al., 1993
North Qinling	Anphibolite	450–380	767	0.7	23	31	Zhang et al., 2001
North of East Qinling	Basalt	403.5	1190	1.36	45.3	31	Wang et al., 1991
Maoji, Tongbaishan	Anphibolite	575–434	600	0.7	23.3	26	Liu et al., 1993
Maoji, Tongbaishan	Green schist	467–411	520	0.6	20	26	Liu et al., 1993
North Qilian	Anphibolite	~ 400	550	0.8	26.7	20.6	Cheng et al., 1994
North Qilian	Glaucophane	460–440	150–250	0.4–0.7	13–23	11	Wu et al.1993
North Qilian	Glaucophane	460–440	> 380	0.6–0.7	20–23	16–19	Wu et al.1993
North Qilian	Eclogite	460–440	340	0.8	26.7	13	Wu et al.1993
North Qilian	Phengite	455–440	350	0.75	25	12.5	Zhang et al., 1998
Middle of North Qilian	Garnet	> 462	400	0.65	21.7	18.4	Zhang et al., 1998
North border of Qaidan	Eclogite	465	850	2.5	83	10.2	Lai et al., 1996
North border of Qaidan	Anphibolite	465	520	0.52	17.3	30	Lai et al., 1996
North border of Qaidan	Eclogite	466	730	2.8	93	8	Yang et al., 1998
West Altun	Eclogite	503–500	860	3	100	8.6	Zhang et al., 1999
West Altun	Granulite	447–462	850	1.2	40	21.3	Zhang et al., 1999
West Altun	Eclogite	503–500	850	3	100	8.5	Zhang et al., 2002
Altun	Peridotite	494.6	970	5.1	> 100	9.7	Liu et al., 2002
West Altun	Peridotite	519	500	0.5	18.5	27	Liu et al., 1996
South Tianshan	Ophyolite	440	964	1.42	47.3	24	Wang et al., 1999
South Tianshan	Granulite	452–402	813	1.5	50	19	Su et al., 1996
South Tianshan	Glaucophane	450–350	375	0.65	21.7	17.3	Gao et al., 1996
Jianglang,West Sichuan	Anphibolite	525	555	0.38	13	43	Yan et al., 1997
Yunlu,West Guangdong	Granulite	E. Paleozoic	836	0.69	23	36	Chen et al., 1994
Jianyang–Changping	Anphibolite	~ 400	650	0.28	9.3	70	Fujian Geological
Chong'an–Shicheng	Anphibolite	~ 400	575	0.3	10	57.5	Survey, 1985
Kalpin, Xinjiang	Sandstone-shale	Cambrian				24–22	Wei, 1989
Kalpin, Xinjiang	Sandstone-shale	Ordovician				22–21	Wei, 1989
Erdos basin	Sandstone-shale	E.Paleozoic				25–30	Ren, 1996
Mengying, Shandong	Kimberlite	457±7	1,184	6.75	222.7 L	5.3	Chi et al., 1996
Fuxian, Liaoning	Kimberlite	462.7±4.8	1,123	6.3	208 L	5.4	Chi et al., 1996
Yingxian, Shanxi	Kimberlite	E. Paleozic	1,113	5.2	172 L	6.5	Chi et al., 1996
Langao, Shaanxi	Pyroxenite	431.9	1,350	3	100 L	20	Huang, 1993
North Qilian	Peridotite	495–522	1,093	4.28	132 L	8.3	Song and Su, 1998
North Qilian	Peridotite	495–522	1,100	4.2	140 L	8	Su et al., 1999
Xiawan, Zhejiang	Admellite	E. Paleozic				20	Yang et al., 1996

Continued

Area	Rock	Isotopic age (Ma)	Temperature (℃)	Pressure (GPa)	Forming depth (km)	Thermal gradient (℃/km)	Sources
Zhuzhou, Fujian	Admellite	E. Paleozic				21.5	Yang et al., 1996
Ninghua, Fujian	Admellite	E. Paleozic				29.5	Yang et al., 1996
East Qinling–Tongbai	Tholeiite	403.5	1,190	1.36	45	31	Wang et al., 1991
Late Paleozoic Tianshanian Period 397–260 Ma							
Altay, Xinjiang	Basalt	M. Devonian	1,300	0.5	18.5	70.3	Niu et al., 1999
West Junggar	Lherzolite	L. Paleozoic	1,100	1.6	53.3	26	Zhao et al., 1993
West Tianshan	Eclogite	Devonian	530	1.9	63.3	8.4	Zhang et al., 2000
South Tianshan	Pyroxenite	315	964	1.4	47.3	24	Wang et al., 1999
South Tianshan	Glaucoph.	345	375	0.65	21.7	17.3	Gao et al., 1996
Longmenshan, Sichuan	Anphibolite	E. Permian	500	0.5	16.7	30	Sichuan Geolo.
Jinshajiang, Sichuan	Anphibolite	E. Permian	600	0.48	16	37	Survey, 1991
Lancangjiang	Anphibolite	Permian	735	0.5	16.7	44	Zhong, 1998
West Tianshan	Eclogite	Devonian	530	1.6–1.9	53–63	10	Zhang et al., 2000
West Junggar	Granulite	> 320	1,100	1	33	33	Zhang et al., 1998
Fuping, South Qinling	Anphibolite	285–240	688–693	0.6	20	34	Zhang et al., 1998
Fuping, South Qinling	Anphibolite	260	570–598	0.7–1	23–33.3	18–26	Zhang et al., 1998
North China	Sandstone-shale	Carbon.-Permian	reflectivity			25∼30	Ren et al., 2000
Tarim basin	Sandstone-shale	Carbon.-Permian	of coal			32∼29	Pan et al., 1996
Shiwandashan	Sandstone-shale	Carbon.-Permian				40∼50	Wang, 1998
NW Junggar	Sandstone-shale	Permian	reflectivity			20∼25	Zhang et al. 1999
Tarim basin	Sandstone-shale	Carbon.-Permian	of coal			30	Fan et al., 1990
Erdos basin	Sandstone-shale	Carbon.-Permian				22∼24	Ren, 1996
Zhenyuan, Hunan	Garnet	∼ 360	1,250	5.2	172 L	7.3	Lu et al., 1997
Yuanshui, Hunan	Daimond	∼ 360 (?)	1,350	5.8	192 L	7	Lu et al., 1997
Dahongshan, Hubei	Peridotite	326–352	1,150	3.39	120 L	9.6	Liu et al., 1991
Minggang, Qinling	Peridotite	Carboni.	870	1.3	43	22.6	Lu et al., 1997
Wuyueshan, Dabieshan	Granitoid	376		0.56	18.6		Ma et al., 1995
Muojiang, Yunnan	Pyroxene-	Carboni.	1,212	<1	<33.3	36.4	Zhou et al., 1992
Muojiang, Yunnan	Plagioclase	Permi.	1,276	< 1	< 33.3	38.5	Zhou et al., 1992
Darongshan, Guangxi	Granite	265	700	0.4	13.3	52.6	Wang, 1990

Continued

Area	Rock	Isotopic age (Ma)	Temperature (℃)	Pressure (GPa)	Forming depth (km)	Thermal gradient (℃/km)	Sources
Shiwandashan	Granite	265	693	0.43	14	49	Xu et al., 2001
Indosinian Period 260–200 Ma							
Dabieshan	Eclogite	243–221	750	1	33	~ 23	Chen et al., 1994
Dabieshan	Eclogite	243–221	1,000	4	133	7.5	Chen et al., 1994
Dabieshan	Eclogite	243–221	896	2.05	68	16	You et al., 1997
Luotian, Dabieshan	Migmatite	Triassic	800	0.5	16.7	48	You et al., 1997
Shuanghe, Dabieshan	Jadeite-quartz	Triassic	800	1.31	43.6	20.4	Han et al., 1997
Shima, Dabieshan	Eclogite	243	850	2.8	93	9	Xiao et al., 1993
Shima, Dabieshan	Eclogite	217	650	1.4	47	14	Xiao et al., 1993
East Dabieshan	Anphibolite	243–221	850	2.8	93	9	Xiao et al., 1993
Dawu, Dabieshan	Eclogite	243–221	500	1.6	53	9.4	Ma et al., 1995
Bixiling, Dabieshan	Eclogite	250–230	700	2.7	90	7.8	Zhang et al., 1995
Dabieshan	Clinohumite	250–230	800	6.7	223	3.5	Zhang et al., 1995
Hong'an, Dabieshan	Glaucophane	243–221	500	0.7	23	22	Liu et al., 1993
Dabieshan–Sulu	Marble	Triassic	660	3.5	116.7	5.7	Cong et al., 1999
South Dabieshan	Zoisite	220–210	600	1.1	36.7	16.3	Jiang et al., 1999
Tongbaishan	Eclogite	250–210	780	1.4	47	19	Suo et al., 2001
Dabieshan Collision	Eclogite	Triassic	800	> 2.8	> 93.3	8.6	Zhong et al., 2001
Fuping, Qinling	Granulite	220	720–770	0.6	20	36–38.5	Zhang et al., 1998
Rongcheng	Eclogite	232	797	1.8	60	15.6	Ye et al., 1992
Dabieshan, Anhui	Daimond inclu.	Triassic	> 900	> 4.0	> 133 L	6.8	Xu et al., 1991
Huashanzhai, Hubei	Alkali rock	215	1,120	0.7	23.3	48	Li et al., 1991
Xinxian, Henan	Eclogite	240–210	650	3	100	6.5	Zhang et al., 1993
Dabieshan, Anhui	Eclogite	250–210	> 600	> 2.5	83.3	7.2	Du et al., 1998
East Dabieshan	Mica schist	Triassic	630	2.4	80	7.9	Jiang et al., 1998
Dahingganling–Yanshan	Granulite	229	900	1	33.3	27	Shao et al., 2002
Ninghua,West Fujian	coal metamorph.	E. Triassic	923		33 M	28	Yang et al., 1996
Datian, Middle Fujian	coal metamorph.	E. Triassic	849		37 M	22.9	Yang et al., 1996
Nan'an, East Fujian	coal metamorph.	E. Triassic	887		43 M	23	Yang et al., 1996
Qiangtang, Xizang	Glaucophane	222.5	420	0.72	24	17.5	Li, 1997
Shuanghu, NorthXizang	Glaucophane	222.5	460	0.75	25	18.4	Bao et al., 1999
Santanghu Basin	Sandstone-shale	Triassic				35	Zhou et al., 1998
Youjiang Basin	Sandstone-shale	Triassic	reflectivity			40–43	Suo et al., 1999
Shiwandashan,Guangxi	Sandstone-shale	E.-M. Trias.	of coal			40–45	Wang et al. 1998
Jinhua, Zhejiang	Granitoid	Triassic				28	Yang et al., 1996

Continued

Area	Rock	Isotopic age (Ma)	Temperature (℃)	Pressure (GPa)	Forming depth (km)	Thermal gradient (℃/km)	Sources
Shaoxing, Zhejiang	Granitoid	Triassic	reflectivity			15	Yang et al., 1996
West Fujian	Granitoid	Triassic	of coal			60	Yang et al., 1996
East Fujian	Granitoid	Triassic				22	Yang et al., 1996
Rongcheng, Shandong	Peridotite	232	1,033	5.27	175 L	6	Ye et al., 1992
Horqin, Inner Mongolia	Granulite	Triassic	900	1	33.3	27	Han et al., 2000
Yanshanian Period 200–135 Ma							
Bixiling, Dabieshan	Anphibolite	179	450	0.7	23	19.6	Suo, 2001
North Dabieshan	Gneiss	151–133	700	0.76	25.3	27.7	Sun et al., 1994
Dabieshan	Anphibolite	180–140	560	0.7	23.3	24	Zhao et al., 1999
East Dabieshan	Metam. granite	190	650	1	33.3	19.5	Xu et al., 1998
Luotian Dabieshan	Granulite	Jurassic	900	1.1	> 30	30	Jin, 1997
Dabieshan		200–170	600	0.6	20	30	Zhong et al. 1998
Xiaoqinling	Epidote	160–135	498	1.03	34.2	14.6	Liu et al., 1998
Xiaoqinling	Epidote	160–135	652	0.476	15.9	41	Liu et al., 1998
Lancangjiang	Glaucophane	193	390	0.67	22.3	17.5	Zhang et al. 1990
Pingdang-Dongshan	Mica Schist	202–166	717	0.62	20.7	34.6	Chen et al., 1997
Ninghua, Fujian	Coal metam.	M. Jurassic	905		32	28.3	Yang et al., 1996
Datian, Fujian	Coal metam.	M. Jurassic	809		31	26.1	Yang et al., 1996
Nan'an, Fujian	Coal metam.	M. Jurassic	863		34.3	25.2	Yang et al., 1996
North Hubei	Glaucophane	185.1	450	0.7	23.3	19.3	Niu et al., 1993
East Guangdong	Green schist	L. Jurassic	600	0.7	23.3	25.8	Chen et al., 1994
Changle–Nan'ao	Green schist	178–165	800	0.86	28.7	27.9	Chen et al., 1994
Daqing oil field	Coal metam.	L. Jurassic				33	Wu et al., 1991
Santanghu basin	Sandstone-shale	Jurassic	Reflectivity of coal			27–28	Zhou et al, 1998
Jiuquan basin	Sandstone-shale	Jurassic				37.5–45	Ren et al., 2000
Xinshuai basin	Sandstone-shale	Jurassic				47.3–61	Ren et al., 1999
Junggar basin	Sandstone-shale	Jurassic	Reflectivity of coal			30–20	Zhou et al., 1989
Erenhot basin	Sandstone-shale	Jurassic				35–55	Ren et al., 2000
Erdos basin	Sandstone-shale	Jurassic	Reflectivity of coal			36–41	Ren et al., 1994
Turpan–Hami basin	Sandstone-shale	Jurassic				~30	Ren et al., 2000
Tarim basin	Sandstone-shale	Jurassic	Reflectivity of coal			~25	Ren et al., 2000
Tarim basin	Sandstone-shale	Jurassic				26–29	Pan et al., 1996
Shiwandashan	Sandstone-shale	E.-M. Jurassic				20–30	Wang, 1998
Daqing oil field, Heilongjiang	Granite in NE and S-N	Jurassic	Reflectivity of coal		C		Compiling Group of Petrole. Geo. 1993

Continued

Area	Rock	Isotopic age (Ma)	Temperature (℃)	Pressure (GPa)	Forming depth (km)	Thermal gradient (℃/km)	Sources
Daqing oil field, Heilongjiang	Dacite in NE, NNE trend	M.-L Jurassic			C		Compiling Group of Petrole. Geo. 1993
Daqing oil field, Heilongjiang	Dacite in NE, NNE trend	Earliest Cret.			C		Compiling Group of Petrole. Geo. 1993
Mingyuegou Basin, Yanbian, Jilin	Pyroxenite inclusion	M. Jurassic	991–1,158	0.55–0.96	32–37	~30	Wang et al., 2005
Yanbian, Jilin	Pyroxenite inclusion	M. Jurassic			25–37		Zhao et al., 2005
Baishishan, Zhangguangcailing, Jilin	Granitoid	196			C-M		Sun et al., 2001
Dahingganling	Granitoid	Jurassic			C-M		Lin et al., 2004
Northern Dahingganling	Alkalic volcanic rock	L. Jurassic			C-M		Yin et al., 2006
Jiulianzhuang, Dahingganling	Syenite	137.5			C-M		Xue et al., 2006
Hatumo River, Dahingganling	Dacite	154–147.3			C-M		Xue et al., 2006
Baiyinnu ore field, Dahingganling	Ignimbrite	160.3			C-M		Xue et al., 2006
Manituxi Mount, Dahingganling	Dacite	149			C-M		Xue et al., 2006
Wudan, Middle Dahingganling	Tuff	152.3			C-M		Xue et al., 2006
Du'erki, middle Dahingganling	Granitoid in NE trend	E. Jurassic			C-M		Xiao et al., 2004
Ma'anzi, southern Dahingganling	Granitoid in NE trend	L. Jurassic			C-M		Xiao et al., 2004
Huangganglianq, southern Dahingganling	Plagio granite	142			C-M		Xue et al., 2006
Gedenghua, southern Dahingganling	Admellite	185			C-M		Xue et al., 2006
Haisuba, southern Dahingganling	Hornblendite	202			C-M		Xue et al., 2006
Baiyinnuo, eastern Inner Mongolia	Granodiorite in NE trend	E. Jurassic			C-M		Xiao et al., 2004
Taibudai, eastern Inner Mongolia	Granite in NE trend	E. Jurassic			C-M		Xiao et al., 2004
Baishilazi, eastern Inner Mongolia	Granitoid in NE trend	E. Jurassic			C-M		Xiao et al., 2004
Mogutu, eastern Inner Mongolia	Granitoid in NE trend	E. Jurassic			C-M		Xiao et al., 2004
Wulantao, eastern Inner Mongolia	Granitoid in NE trend	E. Jurassic			C-M		Xiao et al., 2004
Chabuganshan, Tianshanxian	Rhyolite	164			C		Chen et al., 1997
Lubeixian, Inner Mongolia	Andesite, ignimbrite	167.2			C		Chen et al., 1997
Duijiugou, Fengzhen, Inner Mongolia	Minette and Gabbro	144–146.6			L		Shao et al., 2005a
Uliji, 104°23.1′E, 40°54.8′N	Granodiorite	207.7,U-Pb			C-M		Hong et al., 2003
East Baotou, Inner Mongolia	Shonkinite	198±6			C-M		Yan et al., 2000
Liangcheng, Inner Mongolia	Shonkinite	190±7			C-M		Yan et al., 2000
Well Kacan-1, Jianchang, Liaoning	Trachyandesite and tuff	146–165.6			C-M		Chen et al., 1997
Xinglonggou Formation, Liaoning	Dacite in ENE trend	199–189			C		Lu et al., 2005
Wulong, eastern Liaoning	Granite	136			C		Wei et al., 2003
Wulahada, west Liaoning	Andesite in NNE	142.4			C-M		Zhang et al., 2001
Guancaishan, Liaoning	Andesite	134.6			C-M		Zhang et al., 2001

Continued

Area	Rock	Isotopic age (Ma)	Temperature (℃)	Pressure (GPa)	Forming depth (km)	Thermal gradient (℃/km)	Sources
Haifanggou, Beipiao, Liaoning	Rhyolitic tuff	140			C-M		Chen et al., 1997
Lanqidonggou, Beipiao, Liaoning	Andesite	141.6			C-M		Chen et al., 1997
Huaziyu Magnesite Mining, Liaoning	Lamprophyre	155			L		Jiang et al., 2005
Da'ertaizi, Songlingmen, Chaoyang	Andesite	166			C-M		Chen et al., 1997
Yanshan	Granitoid	170–135	⩽ 900	0.9–1.7	30–56 C-M	30–16	Wang, 2002
Badaling, Beijing	Granitoid	Jurassic			C		Zhang, 2001
Chahe, Zhulu, Hebei	Diabase	153.6			L		Shao et al., 2005a
Fengning, Hebei	Granitoid	125.2–157.4			C		Wu et al., 1984
Kuancheng, Hebei	Granodiorite	162			C		Wu et al., 1984
Beichagoumen, Northern Hebei	Diorite, quartz, syenite, granodiorite	146.2–147.6			C		Chen et al., 2004
Tiaojishan Formation, Luanping, Hebei	Andesite	162.8			C		Zhang, 2006
Zhangjiakou Formation, Luanping, Hebei	Rhyolite	135.7–135.2			C		Zhang, 2006
Handan, Hebei	Peridotite inclusion	E. Jurassic	1,008	1.7	57.7	18	Xu et al., 1991
Xiabancheng, north Hebei	Trachyandesite in NE	171–186			C-M		Li et al., 2004
Shexian, south Hebei	Gabbro in NNE	150			C-M		Hong et al., 2003
Laiyuan, Hebei	Gabbro in NNE	140			C-M		Hong et al., 2003
South Taihang Mts.	Peridotite inclusion	~ 170	1,000	2.7	90 L	11	Xu et al., 1993
South Taihang Mts.	Mafic inclusion	~ 170	1,000	2.1	70 L	14	Niu et al., 1994
Linglong Shandong	Granitoid with foliation	166–153	750	0.45	20 C	37.5	Wan et al., 2001
Linglong, Shandong	Granitoid with foliation	155–160			C		Luo et al., 2002
Luanjiahe, east Shandong	Granitoid with foliation	155–160			C		Luo et al., 2002
Wendeng, east Shandong	Admellite	159.8			C-M		Guo et al., 2005
Dougushan, Shandong	Granodiorite	160.7			C-M		Guo et al., 2005
Sanshandao, Jiaojia, Shandong	Granite	M. Jura.			11–15		Sun, 1994
Western Shandong	granodiorite				7.4–11		Sun, 1994
Guojialing, Shandong	Granodiorite in WNW	148–134	700	0.5–0.28	34 C-M	21	Chen et al., 1993
Gudao, Zhuangxi 5 area, Jiyang, Shandong	Andesite, basalt	Mesozoic			C-M		Compiling Group of Petrol. Geo., 1993
Binnan, Gudao, Jiyang, Shandong	Diorite porphyry	Jurassic			C-M		Compiling Group of Petrol. Geo., 1993
Jiyang, Shandong	Lamprophyre	Jurassic			C-M		Compiling Group of Petrol. Geo., 1993
Ta'ershan, south Shanxi	Monzonite-diorite	Jurassic			C-M		Zeng et al., 1997
Laoshan, south Shanxi	Quartz syenite	Jurassic			C-M		Zeng et al., 1997
Jiaojieshan, south Shanxi	Aegirine-augite syenite	Jurassic			C-M		Zeng et al., 1997
Wutaishan–Hengshan, Shanxi	Granite-porphyry	Jurassic			C-M		Zhen, 2004

Continued

Area	Rock	Isotopic age (Ma)	Temperature (℃)	Pressure (GPa)	Forming depth (km)	Thermal gradient (℃/km)	Sources
Pingshun–Huguan, south Shanxi	Diorite	154–158			C-M		Shanxi Geological Survey, 1989
Zhujiagou, Tianzhen, Shanxi	Diorite	140.4			C		Shao et al., 2005a
Qixian, Middle Shanxi	Alkali quartz syenite	141.8			C		Shanxi Geological Survey, 1989
Zijinshan, Dadushan, Jiaopaishan, Linxian	Alkali complex	Jurassic			C		Shanxi Geological Survey, 1989
Huyanshan, Gujiao-Jiaocheng, Shanxi	Syenite	Jurassic			C		Shanxi Geological Survey, 1989
Gudongdao-Ximaling, Jiaocheng, Shanxi	Syenite	Jurassic			C		Shanxi Geological Survey, 1989
Xixianding-Xiye, Gujiao-Jiaocheng	Syenite	Jurassic			C		Shanxi Geological Survey, 1989
Dongxianding-Shangbai-quan, Gujiao-Jiaocheng, Shanxi	Syenite	Jurassic			C		Shanxi Geological Survey, 1989
Mulianpo-Kuangquan, Gujiao-Jiaocheng	Syenite	Jurassic			C		Shanxi Geological Survey, 1989
Longzhuanggou, Heishanya Zhuanger-shang, Jiaocheng, Shanxi	Quartz syenite porphyry	Jurassic			C		Shanxi Geological Survey, 1989
NW Huyanshan, Gujiao-Jiaocheng, Shanxi	Aegirine-augite Syenite	Jurassic			C		Shanxi Geological Survey, 1989
Longzhuanggou-Ketoudongtacun, Gujiao-Jiaocheng, Shanxi	Aegirine-augite Syenite	Jurassic			C		Shanxi Geological. Survey, 1989
Longwangmiao-Yichengxian, Shanxi	Quartz monzonite	Jurassic			C		Shanxi Geological Survey, 1989
Laoshan-Qiao'erjiao-Yutuling, Xiangfen	Quartz monzonite	Jurassic			C		Shanxi Geological Survey, 1989
Ta'ershan, Xiangfen-Quwo-Yicheng Shanxi	Quartz–monzonite dior-ite	Jurassic			C		Shanxi Geological Survey, 1989
Hanjiayan- Heilaoding, Xiangfen, Shanxi	Quartz–monzonite dior-ite	Jurassic			C		Shanxi Geological Survey, 1989
Shengwangshan-Shanchahe-Jiaojie-shan, Shanxi	Quartz–monzonite dior-ite	Jurassic			C		Shanxi Geological Survey, 1989
Yanwowa, Northwest Yicheng, Shanxi	Quartz–monzonite dior-ite	Jurassic			C		Shanxi Geological Survey, 1989
South Ta'ershan, Shanxi	Monzonite	Jurassic			C		Shanxi Geological Survey, 1989
Guniangshan, Northwest Yicheng, Shanxi	Granite porphyry	Jurassic			C		Shanxi Geological Survey, 1989
Dagushan-Zimashan, Fushan-Xiangfen-Yicheng	Syenite	Jurassic			C		Shanxi Geological Survey, 1989
Longwangmiao-Hanjia-Yan, Xiangfen, Shanxi	Syenite	Jurassic			C		Shanxi Geological Survey, 1989
Zhoujiazhuang-Cijiao-cun, east Xiangfen, Shanxi	Sodium Syenite	Jurassic			C		Shanxi Geological Survey, 1989

Continued

Area	Rock	Isotopic age (Ma)	Temperature (℃)	Pressure (GPa)	Forming depth (km)	Thermal gradient (℃/km)	Sources
East to Zhoujiazhuang, east Xiangfen, Shanxi	Aegirine-augite Syenite	Jurassic			C		Shanxi Geological Survey, 1989
South Ludingshan, Quwo, Shanxi	Quartz Syenite diorite	Jurassic			C		Shanxi Geological Survey, 1989
Qiaoshan, north Quwo, Shanxi	Quartz Syenite diorite	Jurassic			C		Shanxi Geological Survey, 1989
Yangtancun, North Quwo, Shanxi	Quartz Syenite diorite	Jurassic			C		Shanxi Geological Survey, 1989
Heshangwengduishan, Yicheng, Shanxi	Quartz monzonite	Jurassic			C		Shanxi Geological Survey, 1989
Erfengshan, south Fushan, Shanxi	Syenite diorite	Jurassic			C		Shanxi Geological Survey, 1989
Sikongshan, south Fushan, Shanxi	Monzonite	Jurassic			C		Shanxi Geological Survey, 1989
Tiantanshan-Shiliyuan, East Fushan, Shanxi	Syenite diorite	Jurassic			C		Shanxi Geological Survey, 1989
Xincun-Beiye, Yicheng, Shanxi	Syenite diorite	Jurassic			C		Shanxi Geological Survey, 1989
Shitancun, NE Yicheng, Shanxi	Syenite diorite	Jurassic			C		Shanxi Geological Survey, 1989
Xincun-Beiye, Yicheng, Shanxi	Syenite diorite	Jurassic			C		Shanxi Geological Survey, 1989
Southeast Linfen, Shanxi	Aegirine-augite Syenite	Jurassic			C		Shanxi Geological Survey, 1989
Hejiazhuang-Shicunshan, southeast Linfen, Shanxi	Aegirine-augite Syenite	Jurassic			C		Shanxi Geological Survey, 1989
Guanquecun-Liangjiapo, east Linfen, Shanxi	Aegirine-augite Syenite	Jurassic			C		Shanxi Geological Survey, 1989
Qingyangling southeast Xiangfen, Shanxi	Syenite diorite	Jurassic			C		Shanxi Geological Survey, 1989
Songcun, east Xiangfen, Shanxi	Syenite diorite	Jurassic			C		Shanxi Geological Survey, 1989
Dapocun, southeast Xiangfen, Shanxi	Syenite diorite	Jurassic			C		Shanxi Geological Survey, 1989
Pandao,Xiangfen, Shanxi	Diorite porphyry	Jurassic			C		Shanxi Geological Survey, 1989
Dongzhangcun-Xiangfen, Shanxi	Syenite diorite	Jurassic			C		Shanxi Geological Survey, 1989
Xihaicun, east Quwo, Shanxi	Syenite diorite	Jurassic			C		Shanxi Geological Survey, 1989
Ganjuncun, Yicheng, Shanxi	Syenite diorite	Jurassic			C		Shanxi Geological Survey, 1989
Pingshun-Lingchuan, SE Shanxi	Diorite	Jurassic			C		Shanxi Geological Survey, 1989
East Pingshun, SE Shanxi	Syenite diorite	Jurassic			C		Shanxi Geological Survey, 1989
Xingcheng-Pushuicun, southeast Shanxi	Diorite	Jurassic			C		
Yetou-Zheshuicun, Lingchuan, Shanxi	Syenite diorite	Jurassic			C		Shanxi Geological Survey, 1989
Liuquan,;Lingchuan, Shanxi	Syenite diorite	Jurassic			C		Shanxi Geological Survey, 1989
Tongguxia-Xibanshan, Lingchuan, Shanxi	Syenite diorite	Jurassic			C		Shanxi Geological Survey, 1989

Continued

Area	Rock	Isotopic age (Ma)	Temperature (℃)	Pressure (GPa)	Forming depth (km)	Thermal gradient (℃/km)	Sources
East Longzhen, Pingshun–NE Huguan, Shanxi	Syenite diorite	Jurassic			C		Shanxi Geological Survey, 1989
NE Pingshun, Shanxi	Syenite diorite	Jurassic			C		Shanxi Geological Survey, 1989
Southeast Pingshun, Shanxi	Syenite diorite	Jurassic			C		Shanxi Geological Survey, 1989
Shuzhangzhen, Huguan, Shanxi	Syenite diorite	Jurassic			C		Shanxi Geological Survey, 1989
Dabieshan	Quartz monzonite	170			C		Li et al., 2001
Baimajian,Dahuaping- Dabieshan	91 granite bodies	Jurassic			C-M		Guan et al., 1997
Huangshan, Taiping, Anhui	Granite	178–143			C-M		Nanjing University, 1981
Jingde, Anhui	Granite	147–138			C-M		Nanjing University, 1981
Langheqiao, Jingxian, Anhui	Granite	140			C-M		Nanjing University, 1981
Fuling, Jixi, Anhui	Granite	148			C-M		Nanjing University, 1981
Caoshan, Tongling, Anhui	Diorite	136.6	880–1,240		28–33C	31–37	Du et al., 2004
Jiguanshan, Tongling, Anhui	Granodiorite	139.8	1,270–1,290		42–48	30–27	Du et al., 2004
Tongling, Anhui	Alkali-granodiorite	L. Jurassic			C-M		Wang, 2004
Fanchang-Tongling Anhui	Quartz-monzonite	Jurassic			C-M		Lou et al., 2006
Tongling, Anhui	Pyroxene diorite	142.9			C-M		Wang et al., 2004
Jingshan, Huaiyuan, Anhui	Foliation Granite	160.2			C-M		Xu et al., 2004
Tongguanshan, Anhui	Diorite in WNW	150			C-M		Zhai et al., 1992
Jinkouling, Tongling, Anhui	Granite	136			C		Zhou, 1989
Tongguanshan, Anhui	Quartz diorite	Jurassic			C-M		Wang et al., 2002
Xihu, Tongling, Anhui	Quartz diorite	Jurassic			C-M		Wang et al., 2002
Hushan, Tongling, Anhui	Quartz diorite	Jurassic			C-M		Wang et al., 2002
Shizishan, Tongling, Anhui	Quartz diorite	Jurassic			C-M		Wang et al., 2002
Dalongshan, Anqing, Anhui	Alkali-biotite granite	Jurassic			C		Jiangxi Geological Survey, 1983
E'cheng, Hubei	Granite in WNW trend	157.9			C-M		Zhai et al., 1992
Tongshankou, Daye, Hubei	Diorite in WNW trend	183.2			C-M		Zhai et al., 1992
Jinshandian, Daye, Hubei	Quartz diorite in WNW	138			C-M		Zhai et al., 1992
Yinzhu, Daye, Hubei	Quartz diorite in WNW	189			C-M		Zhai et al., 1992
Yangxin, Hubei	Granodiorite in WNW	157–153			C-M		Zhai et al., 1992
Ruannitu, Yangxin, Hubei	Diorite in WNW trend	154			C-M		Zhai et al., 1992
Fengshandong, Hubei	Diorite in WNW trend	138			C-M		Zhai et al., 1992
Jiuliping, Yichang, Hubei	Rhyolite	Late Jurassic			C		Gao et al., 1999
Caoguan, west Qinling	Quartz-diorite	205			C		Li et al., 2004
Donghe, west Qinling	Pyroxene diorite	195.1			C		Li et al., 2004
Waquanshan, west Qinling	Gabbro	184			C-M		Li et al., 2004
Muhuguan, north Qinling	Granite	Jurassic			C-M		Liu et al., 1996

Continued

Area	Rock	Isotopic age (Ma)	Temperature (℃)	Pressure (GPa)	Forming depth (km)	Thermal gradient (℃/km)	Sources
Yuku, Luanchuan, Henan	Granitoid	204			C		Shang et al., 1988
Yinjiagou, Lingbao, Henan	Granitoid	152			C		Shang et al., 1988
Nannihu, Luanchuan, Henan	Granitoid	141			C		Shang et al., 1988
Shangfanggou,Luanchuan, Henan	Granitoid	134			C		Shang et al., 1988
Babaoshan, Lushi, Henan	Granitoid	Jurassic			C		Shang et al., 1988
Xiong'ershan, West Henan	Granite	Jurassic			C		Hu et al., 2006
Fengshandong, Yangxin, Hubei	Granodiorite porphyry	Jurassic			C-M		Jiangxi Geological Survey, 1983
Jinduicheng,Xiaoqinling, Shaanxi	Granite	148			C-M		Yan et al., 1985
Shanyang-Zhashui, Shaanxi	Granite-diorite porphyry	148			C-M		Yan et al., 1985
Baoji–Longxian, Shaanxi	Quartz diorite, granite	187			C		Yan et al., 1985
Luonan, Shangxian, Shaanxi	Grano-quartz porphyry	148			C		Shang et al., 1988
Dongjiangkou, Shaanxi	Quartz dioritegranite	189			C		Yan et al., 1985
Luonan-Danfeng, Shaanxi , Lushi,Henan	Diorite, admellite	173			C		Yan et al., 1985
Shihuichang, Lantian, Shaanxi	Admellite	173			C		Yan et al., 1985
Huashan, Shaanxi	Admellite granite	166			C		Yan et al., 1985
Mulonggou, Heishan, Luonan Shaanxi	Diorite	142			C		Shang et al., 1988
Poxianggou, Shaanxi	Quartz diorite	142			C-M		Shang et al., 1988
Heishan, Luonan, Shaanxi	Granodiorite	142			C-M		Shang et al., 1988
Baijiazhuang, Minxian, Gansu	Admellite	190			C-M		Shang et al., 1988
Dongchagou, Gansu	Alkali granite	196			C-M		Shang et al., 1988
Shaoxing Zhejiang	Granitoid	Jurassic			C		Yang et al., 1996
West Zhejiang	Granitoid	Jurassic			C		Yang et al., 1996
North to Changhua, Zhejiang	Granite	147			C-M		Nanjing University, 1981
Lixi , Wuxing, Zhejiang	Granite	145			C-M		Nanjing University, 1981
Fulingxuechuan, Lin'an, Zhejiang	Granite	143			C-M		Nanjing University, 1981
Dazhang, Fuyang, Zhejiang	Granite	140			C		Nanjing University, 1981
Houzhai, Yiwu, Zhejiang	Granite	171			C		Nanjing University, 1981
Lishui, Zhejiang	Granite	163–174			C-M		Nanjing University, 1981
Shaoxing-Zhuji, Zhejiang	Granitoid in NE	Jurassic			C		Yang, 1996
Western Zhejiang	Granitoid in NE	Jurassic			C		Yang, 1996
Jiande, Lin'an, Jinhua, Zhejiang	Granitoid in NE trend	Jurassic			C		Zhu et al., 2005
Coastal areas of Zhejiang-Fujian-Guangdong	Calc-Alkali bimodal Volcanic	155–139			C		Gao et al., 1999
Chujia, Ninghai, Zhejiang	Rhyolite	L. Jurassic			C		Gao et al., 1999
Hutanggang, Zhuji, Zhejiang	Tuff and ignimbrite	L. Jurassic			C		Gao et al., 1999

Continued

Area	Rock	Isotopic age (Ma)	Temperature (℃)	Pressure (GPa)	Forming depth (km)	Thermal gradient (℃/km)	Sources
Zhoucun, Jinhua, Zhejiang	Tuff and ignimbrite	L. Jurassic			C		Gao et al., 1999
South Anhui–West Zhejiang	Granitoid	< 145			C		Zhou et al., 2004
Furongling, Zhejiang–Xiangshan Jiangxi	Calc-Alkali bimodal volcanic	155–141			C		Gao et al., 1999
Longyou, Zhejiang	Quartz-monzonite	L. Jurassic			C		Gao et al., 1999
Dayang, Jiande, Zhejiang	Granite	L. Jurassic			C		Gao et al., 1999
Suzhou, Jiangsu	Granite in WNW	155–141			C		Zhai et al., 1992
Chengtou, Ganyu, Jiangsu	A type granite in NE	L. Jurassic			C-M		Li et al., 1999
Suzhou, Jiangsu	A type granite	L. Jurassic			C-M		Zhou et al., 1997
Wushan, NW Jiangxi	Diorite in WNW	140.1			C-M		Zhai et al., 1992
Northeast Jiangxi	Granite porphyry	160–170			C-M		Zhou et al., 2004
Dajishan, Jiangxi	Mica granite	Jurassic	740		C		Jiang et al., 2005
Potouzhen, Quannan, Jiangxi	A type granite	178			C		Chen et al., 2004
Zhaibei, Dingnan, Jiangxi	A type granite	171			C		Li et al., 2003
Quannan, Jiangxi	A type granite	164			C		Li et al., 2003
Xiangshan, Fuzhou, Jiangxi	A type granite	135–137			C		Chen et al., 1999
Luoqiao, Shangrao, Jiangxi	Ignimbrite	L. Jurassic			C		Gao et al., 1999
Jiujiang–Ruichang–Dexing	Diorite in WNW trend	204–146			C-M		Zhai et al., 1992
Luxi, Pingxiang, Jiangxi	Granodiorite porphyry	135			C-M		Jiangxi Geological Survey, 1983
Yangchuling, Duchang, Jiangxi	Granodiorite	142.3–150.6			C-M		Jiangxi Geological Survey, 1983
Dawangmiao, Pingxiang, Jiangxi	Quartz diorite porphyry	143			C-M		Jiangxi Geological Survey, 1983
Tongling, Ruichang, Jiangxi	granodiorite porphyry	153			C-M		Jiangxi Geological Survey, 1983
Dingjiashan, Jiujiang, Jiangxi	Granodiorite porphyry	153			C-M		Jiangxi Geological Survey, 1983
Chengmengshan, North Jiangxi	Granodiorite porphyry	148–155			C-M		Jiangxi Geological Survey, 1983
Fenglincun, Dongxiang, Jiangxi	Granite porphyry	161			C		Jiangxi Geological Survey, 1983
Fujiawu, Dexing, Jiangxi	Granodiorite porphyry	157			C-M		Jiangxi Geological Survey, 1983
Yongping, Qianshan, Jiangxi	Granite porphyry	161			C-M		Jiangxi Geological Survey, 1983
Wushan, Ruichang, Jiangxi	Granodiorite porphyry	165			C-M		Jiangxi Geological Survey, 1983
Bangyankeng, Wuyuan, Jiangxi	Granodiorite porphyry	155.4			C-M		Jiangxi Geological Survey, 1983
Tongchang, Dexing, Jiangxi	Granodiorite porphyry	170			C-M		Jiangxi Geological Survey, 1983
Baoshan, Wan'an, Jiangxi	Granodiorite porphyry	176			C-M		Jiangxi Geological Survey, 1983
Nanmuxiang, Yichun, Jiangxi	Granodiorite	184			C-M		Jiangxi Geological Survey, 1983
Qibaoshan, Shanggao, Jiangxi	Granite porphyry	184			C-M		Jiangxi Geological Survey, 1983
Dongleiwan, Ruichang, Jiangxi	Granodiorite porphyry	Jurassic			C-M		Jiangxi Geological Survey, 1983
Yongping, Qianshan, Jiangxi	Biotite admellite	Jurassic			C-M		Jiangxi Geological Survey, 1983
Taqian, Leping, Jiangxi	Granodiorite porphyry	Jurassic			C-M		Jiangxi Geological Survey, 1983

Continued

Area	Rock	Isotopic age (Ma)	Temperature (℃)	Pressure (GPa)	Forming depth (km)	Thermal gradient (℃/km)	Sources
Xihuashan, Dayu, Jiangxi	Alkali granite	184–148			C		Jiangxi Geological Survey, 1983
Huangsha, Yudu, Jiangxi	Alkali granite	Jurassic			C		Jiangxi Geological Survey, 1983
Tieshanlong, Yudu, Jiangxi	Admellite porphyry, Alkali granite	Jurassic			C		Jiangxi Geological Survey, 1983
Qianshan, Chongyi, Jiangxi	Admellite, Alkali granite	Jurassic			C		Jiangxi Geological Survey, 1983
Zhulanmeng, Yudu, Jiangxi	Admellite	Jurassic			C		Jiangxi Geological Survey, 1983
Dajishan, Quannan, Jiangxi	Admellite	Jurassic			C		Jiangxi Geological Survey, 1983
Hukeng, Anfu, Jiangxi	Muscovite granite	183			C		Jiangxi Geological Survey, 1983
Xiatongling, Fenyi, Jiangxi	Muscovite granite, Granite porphyry	Jurassic			C		Jiangxi Geological Survey, 1983
Xiaolong, Taihe, Jiangxi	Biotite granite, Dacite porphyry	Jurassic			C		Jiangxi Geological Survey, 1983
Baishuidong, Jing'an, Jiangxi	Biotite- muscovite granite	Jurassic			C		Jiangxi Geological Survey, 1983
Xiangshan, Chongren, Jiangxi	Granite and rhyolite porphyry	Jurassic			C		Jiangxi Geological Survey, 1983
Dongjiang, Longnan, Jiangxi	Biotite -muscovite granite	Jurassic			C		Jiangxi Geological Survey, 1983
Heling, Qingshanzhen, NW Jiangxi	Alkali granite	Jurassic			C		Jiangxi Geological Survey, 1983
Da'anfenshuiguan, Jiangxi	Granite	139			C		Ling et al., 1999
Wushan, Jiujiang- Ruichang, Jiangxi	Granodiorite porphyry in NWW	140			C-M		Luo, 2006
Chengmengshan, Jiujiang-Ruichang,	Granodiorite porphyry in NWW	148			C-M		Luo, 2006
Dongleiwan, Jiujiang- Ruichang, Jiangxi	Granodiorite porphyry in NWW	196			C-M		Luo, 2006
Baoshan, Jiujiang- Ruichang, Jiangxi	Granodiorite porphyry in NWW	176			C-M		Luo, 2006
Niuling'ao, Ganxian, Jiangxi	Granite	Jurassic			C		Jiangxi Geological Survey, 1983
Chunyashan, Yichun, Jiangxi	Biotite and Alkali Granite	Jurassic			C		Jiangxi Geological Survey, 1983
Mengshan, Shanggao, Jiangxi	Biotite Granite, Rapakivi	Jurassic			C		Jiangxi Geological Survey, 1983
Benggangshan-Xinkaishan, Dayu,	Biotite Granite	Jurassic			C		Jiangxi Geological Survey, 1983

Continued

Area	Rock	Isotopic age (Ma)	Temperature (℃)	Pressure (GPa)	Forming depth (km)	Thermal gradient (℃/km)	Sources
Zengjialong, De'an, Jiangxi	Biotite Granite	Jurassic			C		Jiangxi Geological Survey., 1983
Xingluokeng, Ninghua, west Fujian	Biotite Granite, Muscovite granite	Jurassic			C		Jiangxi Geological Survey. , 1983
Lingshan, NE Shangrao, Jiangxi	Granite	168			C		Nanjing University, 1981
Fujiawu, Dexing, Jiangxi	Granite	161, 157			C		Nanjing University, 1981
Donghengshan, Jiujiang, Jiangxi	Granite	176			C		Nanjing University, 1981
Five intrusions at West to Jiujiang	Granite	143, 148, 155			C		Nanjing University, 1981
Mengshan, Shanggao, Jiangxi	Granite	170			C		Nanjing University, 1981
Southwest Wanzai intrusion, Yichun,	Granite	182			C		Nanjing University, 1981
West to Yihuang, Jiangxi	Granite	155,158			C		Nanjing University, 1981
Nanzhaoxie, Le'an, Jiangxi	Granite	183,158			C		Nanjing University, 1981
Huangpi, West Guangchang, Jiangxi	Granite	164,177			C		Nanjing University, 1981
Jiangbei, west Ningdu, Jiangxi	Granite	137,155, 175			C		Nanjing University, 1981
Nan'ebo, Ningdu, Jiangxi	Granite	175			C		Nanjing University, 1981
Xingguo, Jiangxi	Granite	154			C		Nanjing University, 1981
Zhulanpu, Huichang, Jiangxi	Granite	136,153, 175			C		Nanjing University, 1981
Zhangtiantang, Shangyou, Jiangxi	Granite	Jurassic			C		Nanjing University, 1981
Hongtaoling, Chongyi-Shangyou,	Granite	Jurassic			C		Nanjing University, 1981
Xialong, Chongyi- Shangyou, Jiangxi	Granite	Jurassic			C		Nanjing University, 1981
Tianmenshang, SE Chongyi, Jiangxi	Granite	Jurassic			C		Nanjing University, 1981
Piaotang, north Dayu, Jiangxi	Granite	161			C		Nanjing University, 1981
Bai'e, south Yudu, Jiangxi	Granite	Jurassic			C		Nanjing University, 1981
Tieshikou, south Xinfeng, Jiangxi	Granite	Jurassic			C		Nanjing University, 1981
South Longnan, Jiangxi	Granite	Jurassic			C		Nanjing University, 1981
Wuliting, Dajishan, Quannan, Jiangxi	Granite	158,180			C		Nanjing University, 1981
Youshan, SE Dayu, Jiangxi	Granite	177			C		Nanjing University, 1981
West Xunwu, Jiangxi	Granite	164, 189			C		Nanjing University, 1981
No.414 Mining, Wugongshan, Jiangxi	Granite	165,136			C		Nanjing University, 1981
Hongshuizhai, Chongyi, Jiangxi	Granite	188–140			C		Nanjing University, 1981
Yushan,Gulonggang, Xingguo, Jiangxi	Granite	146–175			C		Nanjing University, 1981
76 intrusions in Shangrao, Jiangxi	Granitoid in NE trend	Jurassic			C		Zhu et al., 2005
Nanxi, Jitai, Jiangxi	Alkali basalt	139–143			C-M		Yu, 2005
Shangqinggong, Guixi, Jiangxi	Daguling Formation, Volcanic rock	L. Jurassic			C		Gao et al., 1999
Xiangshan, Chongren, Jiangxi	Ehuling Formation, Volcanic rock	L. Jurassic			C		Gao et al., 1999

Continued

Area	Rock	Isotopic age (Ma)	Temperature (℃)	Pressure (GPa)	Forming depth (km)	Thermal gradient (℃/km)	Sources
Southern Jiangxi	Changpu and Jilongzhang Formation, volcanic	Jurassic			C-M		Lai et al., 1996
398 bodies in Cathysian plate	Granitoid in NE trend	L. Jurassic			C		Zhu et al., 2005
Zhenghe, Fujian	Granitoid	Jurassic			C		Yang et al., 1996
Fangken,Yongding, Fujian	A type Basalt	M. Jurassic			C-M		Zhou et al., 2005
Guangze, Fujian	Granite	180			C		Ling et al., 1999
Wuping, Fujian	Granite	166			C		Ling et al., 1999
Xiaotao,Yong'an, Fujian	Granite	180			C-M		Ling et al., 1999
Yongding, Fujian	Granite	145			C-M		Ling et al., 1999
Hukeng,Yongding, Fujian	Admellite	165			C		Ling et al., 1999
Bailian, Jiangle, Fujian	Granite	140			C-M		Ling et al., 1999
Guiyang, Yongchun, Fujian	Admellite	201			C-M		Ling et al., 1999
Zhenghe, Fujian	Granite	140			C-M		Ling et al., 1999
Youxi, Fujian	Granite	140			C-M		Ling et al., 1999
Zhongteng,Pinghe,Fujian	Monzonite-diorite	136			C-M		Ling et al., 1999
Maotiling,Songxi, Fujian	Andesite	L. Jurassic			C		Gao et al., 1999
Huyang, Shanghang, Fujian	Granite	L. Jurassic			C		Gao et al., 1999
Longmen, Anxi, Fujian	Granite	L. Jurassic			C		Gao et al., 1999
Damaoshan, Longhai, Fujian	Granite-admellite	L. Jurassic			C		Gao et al., 1999
Jinshan, Anxi, Fujian	Granite-admellite	L. Jurassic			C		Gao et al., 1999
Gaide, Dehua, Fujian	Granite	L. Jurassic			C		Gao et al., 1999
Yongfu,Zhangping, Fujian	Granite	L. Jurassic			C		Gao et al., 1999
Gumeishan,Fuqing, Fujian	Admellite	L. Jurassic			C		Gao et al., 1999
Longsandong, Shao'an, Fujian	Granite-admellite	L. Jurassic			C		Gao et al., 1999
Hufang, Mingxi, Fujian	Granite	L. Jurassic			C		Gao et al., 1999
Caixi, Shanghang, Fujian	Admellite	L. Jurassic			C		Gao et al., 1999
Dabugang,Shaowu, Fujian	Granite	L. Jurassic			C		Gao et al., 1999
Southeast Pucheng, Fujian	Granite	Jurassic			C		Nanjing University, 1981
Southeast Nanping, Fujian	Granite	Jurassic			C		Nanjing University, 1981
North to Shaxian, Fujian	Granite	Jurassic			C		Nanjing University, 1981
Xingluoken, Qingliu, Fujian	Biotite Granite	155			C		Nanjing University, 1981
North to Qingliu, Fujian	Granite	Jurassic			C		Nanjing University, 1981
Gutian,Longquan-Liancheng,	Granite	173–146			C		Nanjing University, 1981
Hetian, SE Changting, Fujian	Granite	148			C		Nanjing University, 1981
Guobao, Dehua, Fujian	Granite	157–160			C-M		Nanjing University, 1981

Continued

Area	Rock	Isotopic age (Ma)	Temperature (℃)	Pressure (GPa)	Forming depth (km)	Thermal gradient (℃/km)	Sources
Zhongteng, Pinghe, Fujian	Granite	Jurassic			C-M		Nanjing University, 1981
Nandayang, Longyan, Fujian	Granite	158			C		Nanjing University, 1981
Zhenghe, Fujian	Granitoid in NNE trend	Jurassic			C		Yang, 1996
Coastal zone of Fujian	Andesite-rhyolite	L. Jurassic			C-M		Jiang, 2001
Lingdai, Xianxia, Fujian	Trachyte-rhyolite	L. Jurassic			C-M		Jiang, 2001
Yongding, Fujian	Bimodal volcanic rocks	188–179			C-M		Gao et al., 1999
Gutianxian, Fujian	Granoid	164–143			C-M		Gao et al., 1999
Xingluokeng, Ninghua, Fujian	Granoid	164–143			C-M		Gao et al., 1999
Longsandong, Shao'an, Fujian	Granitoid	164–143			C-M		Gao et al., 1999
South Wuyishan, Fujian	Granitoid	164–143			C-M		Gao et al., 1999
Dawangshan, Pinghe, Fujian	Granitoid	164–143			C		Gao et al., 1999
Hongshan, Fuzhou, Fujian	Quartz syenite	135			C		Gao et al., 1999
Daiyunshan, Dehua, Fujian	Ignimbrite	L. Jurassic			C		Gao et al., 1999
Lianhuashan, Anxi, Fujian	Tuff and Andesite	L. Jurassic			C		Gao et al., 1999
Meilin, Nanjing, Fujian	Ignimbrite	L. Jurassic			C		Gao et al., 1999
Shiping, Changle, Fujian	Ignimbrite	L. Jurassic			C		Gao et al., 1999
Buling, Minhou, Fujian	Ignimbrite	L. Jurassic			C		Gao et al., 1999
Yangzhong, Ningde, Fujian	Ignimbrite	L. Jurassic			C		Gao et al., 1999
Nankou, Jiangle, Fujian	Diorite- admellite	187–183			C-M		Gao et al., 1999
Jiufeng, Pinghe, Fujian	Dacite	L. Jurassic			C		Gao et al., 1999
Yangmingshan, Taibei, Taiwan	Granite-porphyry	L. Jurassic			C		Gao et al., 1999
Tianzhushan, between Chong'an, Fujian and Qianshan, Jiangxi	Granite	168			C		Nanjing University, 1981
Dajishan, Jiangxi	Granite	151.7–144			C		Zhang et al., 2006
Qingzhang, South Nanxiong, Guangdong	Granite	185			C		Nanjing University, 1981
Lianhuashan, Raoping, Guangdong	Granite-porphyry	L. Jurassic			C		Gao et al., 1999
Beidiaogong,Haifeng, Guangdong	Granite	157			C-M		Nanjing University, 1981
Dongzhongba, Zijin, Guangdong	Granite	157–145			C-M		Nanjing University, 1981
Beitouwo, Puning, Guangdong	Granite	143–147			C-M		Nanjing University, 1981
Nangudoushan, Taishan, Guangdong	Granite	148			C-M		Nanjing University, 1981
Guanghai, Taishan,Guangdong	Granite	166–167					Nanjing University, 1981
Shanbeishan, Taishan, Guangdong	Granite	136–139			C-M		Nanjing University, 1981
Putang, Yangjiang, Guangdong	Granite	157–162			C-M		Nanjing University, 1981
Dianbaitangkou, Yangjiang	Granite	140–148			C-M		Nanjing University, 1981
Guling, West Heyuan, Guangdong	Granite	143–163			C-M		Nanjing University, 1981
Northwest Xinfeng, Guangdong	Granite	160			C-M		Nanjing University, 1981

Continued

Area	Rock	Isotopic age (Ma)	Temperature (℃)	Pressure (GPa)	Forming depth (km)	Thermal gradient (℃/km)	Sources
W Heyuan, S Yingde, Guangdong	Granite	165			C-M		Nanjing University, 1981
Lianhe, Hetai, Guangdong	Biotite granite	186	942.6–953		C		Wu, 1986
Gaocun, Hetai, Guangdong	Pegmatite	194			C		Ye, 1989
Zacun, Hetai, Guangdong	Biotite admellite	157.5			C-M		Cui , 1989
Tangkou, Guangdong	Granite	135–161			C		Wang et al., 2003
Xituokou, Guangdong	Granite	150			C		Wang et al., 2003
Mashan,west Guangdong	Granite	201			C-M		Wang et al., 2003
Gangmei, Guangdong	Granite	172–186			C-M		Wang et al., 2003
Fougang, Guangdong	Granite	141			C		Nanjing University,1981
Guidong, Guangdong	Granite	143			C		Nanjing University, 1981
Shibei, Lianping, Guangdong	Granite	165			C-M		Nanjing University, 1981
West to Liannan, Northwest to Taibao	Granite	168			C		Nanjing University, 1981
Shantou, Guangdong	Granitoid in NE	Jurassic			C		Yang, 1996
Zhenjiang,Shaoguan City, Guangdong	Granite	L. Jurassic			C		Gao et al., 1999
Nanling, west Guangdong	Granite	160			C		Geng et al., 2006
Nanling, south China	Admellite	170–150			C		Hua, 2005
East to Ganjiang, Nanling	Acid volcanic	139			C		Hua, 2005
Eastern Nanling	Basalt Lava	157.8–179			L		Zhang, 2004
Eastern Nanling	dyke	142.6			L		Zhang, 2004
Zhuguangshan, Nanling	admellite	L. Jurassic			C-M		Ma et al., 2006
Tabei, Eastern Nanling	A type syenite	188.6			C-M		Chen et al., 2004
Potou, Eastern Nanling	granitoid	186.3			L		Chen et al., 2004
Fogang, west Guangdong	A type granite and syenite	140			C-M		Geng et al., 2006
Nanling, Southeast Hunan	Granodiorite	170			C-M		Geng et al., 2006
Shizhuyuan, Chengzhou, Hunan	Biotite admellite, Granite porphyry	Jurassic			C		Jiangxi Geological Survey, 1983
Baofengxian, southeast Hunan	Biotite admellite	156.8			C		Jiangxi Geological Survey, 1983
Shaziling, Xiangtan, Hunan	A type granite	184			C		Gilder et al., 1996
Jinjiling, Lanshan, Hunan	A type granite	156			C		Fu et al., 2005
Qianlishan, Chenzhou, Hunan	A type granite	152			C		Li et al., 2004
Huziyan, Daoxian, Hunan	lherzolite in basalt	132—151			85–38, L		Kong et al., 2001
Liujiazui, Huarong, Hunan	Granite	165			C-M		Nanjing University, 1981
Mufushan, boundary of Hunan, Hubei	Granite	138–140			C		Nanjing University, 1981
Jiuningshan, SW Lanshan, Hunan	Granite	157			C		Nanjing University, 1981
Xianghualing, north Linwu, Hunan	Granite	155			C		Nanjing University, 1981

Continued

Area	Rock	Isotopic age (Ma)	Temperature (℃)	Pressure (GPa)	Forming depth (km)	Thermal gradient (℃/km)	Sources
Yaogangxian, south Zixing, Hunan	Granite	177–178			C		Nanjing University, 1981
Qianlishan, Dongpo, Hunan	Granite	139–172			C		Nanjing University, 1981
Tongshanling, Jiang- yong, Hunan	Granite	176			C		Nanjing University, 1981
Ziyunshan, Xiangxiang, Hunan	Granite	147			C		Nanjing University, 1981
Nanyue, Hengyang, Hunan	Granite	178–153			C		Nanjing University, 1981
Dengbuxian, north Chaling, Hunan	Granite	Jurassic			C		Nanjing University, 1981
Zhuguangshan. Rucheng, Hunan	Granite	172			C		Nanjing University, 1981
North Zhuguangshan, Xitian, Hunan	Granite	177			C		Nanjing University, 1981
Guidong, SE Zhuguangshan, Hunan	Granite	170–175			C		Nanjing University, 1981
NE Dupangling, Daoxian, Hunan	Granite	170–175			C		Nanjing University, 1981
Jinjing, SE Pingjiang, Hunan	Granite	168			C		Nanjing University, 1981
Taiyangshan, Ningyuan, Hunan	Iherzolite in basalt	Jurassic			C-M		Chen et al., 2004
NW Guposhan, Hezhou, Guangxi	Granite	164–160			C		Gu et al., 2006
East of NW Guposhan, Hezhou	Granite	150–146			C		Gu et al., 2006
West of NW Guposhan, Hezhou	Granite	150–146			C-M		Gu et al., 2006
Huashan, Nanning, Guangxi	A type granite	161–165			C		Li et al., 2004a
Yangmei, Rongxian, Guangxi	A type granite	161.6			C		Li et al., 2004a
Lisong, Hexian, Guangxi	A type granite	160			C		Li et al., 2004a
Qinghu, Luchuan, Guangxi	A type granite	158			C		Li et al., 2004a
Yuanshishan, north to Pingle, Guangxi	Granite	153			C		Nanjing University, 1981
Limu, southeast Guilin, Guangxi	Granite	185–172			C		Nanjing University, 1981
South Miao'ershan, Guangxi	Granite	160–180			C		Nanjing University, 1981
Luorong, Southeast Guangxi	Gabbro-diorite-mo-nzonite-syenite	Jurassic			C-M		Guo et al., 2001
Mashan, Southeast Guangxi	Alkalic Gabbro–syenite-Granite	Jurassic			C		Guo et al., 2001
Yuxi, Yulin City, Guangxi	Rhyorite	L. Jurassic			C		Gao et al., 1999
Guposhan, Guangxi	Granitoid	L. Jurassic			C - M		Wang et al., 2006
Sichuanian Period 135–56 Ma							
North Dabieshan	coal metamorph.	129	191		5.8	32.7	Zhang, 2001
Shan-DanQinling	Mylonite	126	530	0.65	21.7	24.4	Zhou et al., 1996
Chifeng	Anphibolite	133	550	0.54	20	27.5	Zhang et al., 2002
Yuli, Taiwan	Green schist	Cretaceous	500	0.8	26.7	18.7	Chen et al., 1994
Tailuge, Taiwan	Anphibolite	87	600	0.6	20	30	Chen et al., 1994
Tailuge, Taiwan	Sillimanite	87	600	0.5	16.7	35.9	Cao et al., 1990

Continued

Area	Rock	Isotopic age (Ma)	Temperature (℃)	Pressure (GPa)	Forming depth (km)	Thermal gradient (℃/km)	Sources
Tengchong	Granulite	60-75	860	1	33.3	25.8	Ji, 1998
West Yunnan	Granulite	75	860	1	33.3	25.8	Zhong et al., 1999
Nyainqentanglha	Green schist	~ 65	610	0.5	16.7	~ 36	Xizang Geologicel
Nyainqentanglha	Green schist	~ 65	650	0.51	17	~ 38	Survey, 1993
Daqing oil field	coal metamorph.	E.Cretaceous	reflectivity			60–30	Wu et al., 1991
Songhuajiang-Liaohe basin	Sandstone-shale	L.Cretaceous	of coal			42–48	Ren et al., 2001
Santanghu basin	Sandstone-shale	Cretaceous	reflectivity			~22	Zhou et al., 1998
Hongze, Jiangsu	Sandstone-shale	Paleocene	of coal			36–40	Zhou et al., 1998
Erenhot basin	Sandstone-shale	E.Cretaceous	reflectivity			~49.6	Ren et al., 2000
West Sichuan	Sandstone-shale	~ 60	of coal			~ 25	Liu et al., 1995
Kalpin, Xinjiang	Sandstone-shale	Cretaceous				15–17.7	Wei et al., 1989
Tarim basin	Sandstone-shale	Cretaceous	reflectivity			25	Fan et al., 1990
Song-Liao basin	Sandstone-shale	Cretaceous	of coal			~ 38	Wang et al., 1989
Erdos basin	Sandstone-shale	Cretaceous				33–45	Ren et al., 1996
Huanggangliang–Ganzhue rmiao, Dahing-ganling	Granoid in NNE trend	Cretaceous			C-M		Xiao et al., 2004
Northern Dahingganling	High potassium calc-alkali series	L. Cretaceous			C		Yin et al., 2006
Northern Dahingganling	Alkali-subalkali	E. Cretaceous			C-M		Yin et al., 2006
Balinzuoqi, Mid.–S. Dahingganling	Granite	115–117			C-M		Xue et al., 2006
Shuanfatun, Mid.–S.	Basalt	121.9			C-M		
Laofangshen, Wushijiazi, middle Dahing-ganling	Granite	127–136			C-M		Xue et al., 2006
Haolaibao, Baoridongshan, Inner Mongolia	Granoid in NNE trend	Cretaceous			C		Xiao et al., 2004
Gongnongbing, Lubei, Inner Mongolia	Rhyolite	114.2			C		Chen et al., 1997
Baiyinbaolihao, Lubei, Inner Mongolia	Tuff, rhyolite and andesite	121.3			C		Chen et al., 1997
Chabugan, Tianshanxian, Inner Mongolia	rhyolite	124			C		Chen et al., 1997
Chabugan quarry, Tian-shanxian, Inner Mongolia	Tuff and trachyandesite	126.5			C		Chen et al., 1997
Heilongtan, Karaqin, Inner Mongolia	Olivine minette	124			C-M		Shao et al., 2003
Chifeng, Inner Mongolia	Basalt in NNE	107.3			C-M		Zhang et al., 2003
Qingshankou Formation, Songliao basin	Tholeiite in NNE trend	E. Cretaceous			C-M		Lu et al., 1997
Jiutai, Jilin	Dacite	Cretaceous	1,276	1.27	42 C-M		Lu et al., 1996

Continued

Area	Rock	Isotopic age (Ma)	Temperature (℃)	Pressure (GPa)	Forming depth (km)	Thermal gradient (℃/km)	Sources
Jiutai, Jilin	Dacite in NNE	Cretaceous			70–80 L		Lu et al., 1996
Hafucun, Siping, Jilin	Rhyolite	122			C-M		Chen et al., 1997
Changchundatun Yitong-Datun, Jilin	Basalt	92.5			C-M		Zhang et al., 2006
Fufengshan, Changchun, Jilin	Alkali olivine basalt and tholeiite	82.5–83.5			L		Liu , 1992
Siziwangqi, Inner Mongolia	Granulite	108.6–128.4			C-M		Xu et al., 2004
Sanmen, Siping, Jilin	Mantle inclusion in Rhyolite	110.1	1,100	4.5–9.1	150–300 L	7-4	Zhang, 2001
Fuxin, Liaoning	Peridotite	84.8	1,272	2.93	97.7	13	Zheng, 1999
Jianguo, Fuxin, Liaoning	Mantle intrusion in A type granoid	109–93			C-M		Zhang et al., 2003; Shao et al., 2004
Yemaotai, Zhangwu, Liaoning	Trachyandesite andesite	124.8			L		Chen et al., 1997
Dingjiafang,Zhangwu, Liaoning	Dacite	125.9			L		Chen et al., 1997
Yingzi, Huide, Liaoning	Trachyandesite dacite	123.7			L		Chen et al., 1997
Maoniuhai, Zhangwu, Liaoning	Andesite	125.5			L		Chen et al., 1997
Daheishan, Beipiao, Liaoning	Dacite, rhyolite trachyandesite	88.2			L		Chen et al., 1997
Hejiagou, Yixian, Liaoning	Andesite	119			L		Chen et al., 1997
Zhujiagou,Yixian, Liaoning	Andesite	124.5			L		Chen et al., 1997
Sanbailong,Yixian, Liaoning	Andesite	125.5			L		Chen et al., 1997
Zhuanchengzi, Yixian, Liaoning	Andesite	129			L		Chen et al., 1997
Shangdijiagou, Yixian, Liaoning	Andesite	133			L		Chen et al., 1997
Yixian, Liaoning	Basalt-andesite	Cretac.	1,117	0.002	67 L	17	Zhang et al., 1994
Damintun, Lower Liaohe	Basalt in NNE	74.4			C-M		Liu , 1992
Fuxin, Liaoning	Basalt in NNE	94.2			C-M		Zhang et al., 2003
Zhangwu, Liaoning	Trachyandesite in NNE trend	124–117			C-M		Hong et al., 2003
Yixian, Liaoning	Basalt in NNE	Cretac.			C-M		Hong et al., 2003
Fushun, Liaoning	Tholeiite	52.09–72.02			L		Liu , 1992
Yangmaying, Tieling, Liaoning	Andesite, rhyolite	135			C-M		Chen et al., 1997
Nankou, Beijing	Olivine basalt	128			C-M		Hong et al., 2003
Nankou, Beijing	Alkali Basalt and granite dyke in NNW trend	119–114			M		Shao et al., 2001
Xuejiashiliang, North Beijing	Gabbro and syenite	132.8–123.3			C-M		Su et al., 2006
Fangshan, Beijing	Grano-diorite	130.7			M		Cai et al., 2005

Continued

Area	Rock	Isotopic age (Ma)	Temperature (℃)	Pressure (GPa)	Forming depth (km)	Thermal gradient (℃/km)	Sources
Nankou, Beijing	lamprophyre and diabase	119–114			C-M		Shao et al., 2001
Kongdian-Huanghua, Dagang Oil Field	Trachyandesite	65–75			C-M		Compiling Group of Petrol. Geol., 1993
Section 1-2, Kongdian Formation, Dagang oil field	Lamprophyre in NE trend	Eocene			L		Compiling Group of Petrol. Geol., 1993
Taihangshan	Quartz Syenite NNE	127–133			C-M		Chen et al., 2006
Well Bai 4, Zhangqiang	Trachyandesite	98.2			C-M		Chen et al., 1997
Well Bai 5, Zhangqiang	Trachyandesite	109.1			C-M		Chen et al., 1997
Well Bai 8, Zhangqiang	Trachyandesite	80.4			C-M		Chen et al., 1997
Well Bai 10, Zhangqiang	Trachyandesite	105.2			C-M		Chen et al., 1997
Haoying, Luanping, Hebei	Andesite	116.2			20–40C		Wu, 1984
North to Changli, Hebei	Granite	134.1			C		Wu, 1984
Pingquan, Hebei	Andesite	96.8–113			20–40C		Wu, 1984
Shimengou, Chengde, Hebei	Andesite	113–114			20–40C		Wu, 1984
Manziying, Qian'an Hebei	Andesite	109.8			20–40C		Wu, 1984
Lingyuan-Jianchang, North Hebei	Basalte-andesite in NNE trend	120–135			C		Lu et al., 2005
Taihangshan, north China	Lamprophyre	L. Mesozoic			M		Zhang et al., 2003
Weideshan-Haiyang,E Shangdong	Granite	L. Cretac.			C-M		Sun, 1994
Cuokou-Laoshan,East Shangdong	Granite	L. Cretac.			C-M		Sun, 1994
Denggezhuang ore deposit, East Shangdong	Kylite inclusion in Trachyte and alkali-basalt	80–149			C-M		Chen et al., 1993
Zhucheng, East Shangdong	alkali-basalt	76			L		Meng et al., 2006
Jiaozhou, East Shangdong	alkali-basalt	72			C-M		Meng et al., 2006
Daxizhuang, East Shangdong	Basalt with lherzolite	73.2	1,010–1,140	2	50-70 L	18.5	Yan et al., 2005 b
Eastern Shandong	Lamprophyre dyke in NNE	110–105			C-M		Chen et al., 1993
Eastern Shandong	Basic dyke in NNE	120–130			C-M		Zhang et al., 2002
Qingshanzhu in Shandong	Andesite in NNE	127			C-M		Chen et al., 1993
Fangcheng, Shandong	Basalt in NNE	124.9			C-M		Zhang et al., 2003
Zouping, Shandong	Gabbro in NNE	115			C-M		Hong et al., 2003
Zhucheng, Shandong	Olivine basalt in NNE trend	111.4			C-M		Hong et al., 2003
Daxizhuang, northeast Jiaozhou, Shandong	Lherzolite inclusion	Cretac.	970–1,140	2.0	65 L	17	Yan et al., 2003
Daxizhuang, NE Jiaozhou, Shandong	Basalt	73.5			65-95 L		Yan et al., 2003

Continued

Area	Rock	Isotopic age (Ma)	Temperature (℃)	Pressure (GPa)	Forming depth (km)	Thermal gradient (℃/km)	Sources
Hanqiao, Qixia, Shandong	Andesite	119.4			20–40 C		Wu et al., 1984
Chenjiayu, Laiwu, Shandong	Andesite	121			20–40 C		Wu et al., 1984
Xidong, Zouping, Shandong	Andesite	106.5			20–40 C		Wu et al., 1984
Guojialing, Zhaoyuan, Shandong	Grano-diorite	130–126			C-M		Liu, 2006
Mengyin, Shandong	Alkali basalt in NNE trend	124–115			C-M		Zhang et al., 2003
Jinan, Shandong	Gabbro in NNE	115			C-M		Hong et al., 2003
Dongliujing, Zaozhuang, SW Shandong	Grano-diorite	127			C-M		Xu et al., 2004
Tietonggou, Laiwu, Shandong	Dunite in dorite	119–132			L		Xu et al., 1993
Jinling, Zibo, Shandong	Dunite in diorite	119–132			L		Xu et al., 1993
Feixian, Shandong	Mantle source relict crystal	119			L		Pei et al., 2004
Western Shandong	Pyroxene inclusion in gabbro-diorite	Cretaceous			L		Wang et al., 2004
Aishan-Huashan, Shangdong	Granite in SN	L. Cretaceous		< 0.1	C-M		Sun, 1994
Yuangezhuang-Yashan, E. Shangdong	Granite	L. Cretaceous			C-M		Sun, 1994
Tongjing, Yinan, Middle Shandong	Diorite porphyry in NNE trend	125–117.5			C-M		Wan et al., 1992
Jinchang, Yinan, Middle Shandong	Granite porphyry in NNE trend	105.4			C		Wan et al., 1992
South Pingshun, Shanxi	Syenite-diorite	123–126			C		Shanxi Geological Survey, 1983
Luoting coal field, Guangling, Shanxi	diabase	134.5			C		Shao et al., 2005a
Julepu, Datong, Shanxi	diabase	116.3			C		Shao et al., 2005a
Northeast Yetou, Linchuan, Shanxi	Syenite-diorite	Early Cretac.			C-M		Shanxi Geological Survey, 1983
West to Liuquan, Linchuan, Shanxi	Syenite-diorite	Early Cretac.			C-M		Shanxi Geological Survey, 1983
Tonggujiacun, northeast Linchuan, Shanxi	Syenite-diorite	Early Cretac.			C-M		Shanxi Geological Survey, 1983
Shadizhan–Dongqiao, south to Pingshun, Shanxi	Syenite-diorite	123–126			C-M		Shanxi Geological Survey, 1983
East to Longzhen, Pingshun, Shanxi	Syenite-diorite	Early Cretac.			C-M		Shanxi Geological Survey, 1983
Northeast 5 km to Pingshun, Shanxi	Syenite-diorite	Early Cretac.			C-M		Shanxi Geological Survey, 1983
Southeast Pingshun, Shanxi	Syenite-diorite	Early Cretac.			C-M		Shanxi Geological Survey, 1983
Shuzhangzhen, southeast Huguan, Shanxi	Syenite-diorite	Early Cretac.			C-M		Shanxi Geological Survey, 1983
Xigou, Luonan, Shaanxi	Granite	124.5			C		Yan et al., 1985
Daijiatan, Ziyang, Shaanxi	Granite, Rhyolite porphyry	129			C		Yan et al., 1985
Jinduicheng, Huaxian, Shaanxi	Granite-porphyry	132			C		Shang et al., 1988

Continued

Area	Rock	Isotopic age (Ma)	Temperature (℃)	Pressure (GPa)	Forming depth (km)	Thermal gradient (℃/km)	Sources
Shangxian, Shaanxi	Quartz diorite, Granite	114–133			C		Yan et al., 1985
Huashan Mount, Huayin, Shaanxi	Granite	100–113			C-M		Yan et al., 1985
West Qinling	Basalt, A type	L. Mesozoic			C-M		Li et al., 2006
Heyu, Luanchuan, Henan	Granite	110			C		Shang et al., 1988
Laojunshan.Luanchuan, Henan	Granite	105			C		Shang et al., 1988
Jinzhai-Suxianshi, North Dabieshan	Diorite, granitemonzonite	140–97	866–1,150	0.1–0.2	30	29–38	Li et al., 1997
North Dabieshan	A type TTG gniess	130–120			C-M		Li et al., 2001
North Dabieshan	Pyroxene gabbro	130–120			C-M		Li et al., 2001
Tiantangzhai, Dabieshan	Granitoid	131	830	0.54	18 C	46	Wang et al., 2000
North Huaiyang	Basalt in WNW	Early Cretaceous			C-M		Lu et al., 2005
North Huaiyang	Trachyandesite in WNW trend	Early Cretaceous			C-M		Lu et al., 2005
Dabieshan	Granitoid	125–95			C		Ma et al., 1999
Mingguang, Jiashan, Anhui	Olivine basalt	72.2			L		Liu , 1992
Tieshan, East Hubei	Diorite in NNE	117±10			C-M		Zhai et al., 1992
Jiangling, Hubei	Tholeiite	57–79			L		Liu , 1992
Guangqi-Huangmei Eastern Hubei	Syenite-Alkali granite	125			C-M		Zhai, 1989
Lingxiang, Daye, Hubei	Rhyolite	115–90			C		Wu et al., 1984
Taihezhen, E'cheng, Hubei	Rhyolite and pearlite	96–132			C		Wu et al., 1984
Lingxiangzhen, Daye, Hubei	Basalt	114–127			L		Wu et al., 1984
Jiuhuashan, south Anhui	Admellite	123			C		Zhang et al., 2002
Huangshan, south Anhu	Admellite	125			C		Zhang et al., 2002
Tanshan, south Anhui	Granite	124			C		Zhang et al., 2002
Wuling, south Anhui	Granite	129			C		Zhang et al., 2002
Tongxinguo, south Anhui	Quartz Syenite	127			C		Zhang et al., 2002
Fuling, south Anhui	Granite	121			C		Zhang et al., 2002
Yanghutang, Anhui	Gabbro	125			C-M		Xing et al., 1994
Huoli, Anhui	Granite	123			C-M		Xing et al., 1995
Longwangshan, Nanjing-Wuhu	Trachyte-andesite	126.1			C-M		Li et al., 1998
Niangniangshan, Nanjing-Wuhu	Phonolite	99.8			C		Wu et al., 1984
Meishan, Nanjing-Wuhu	Andesite and trachyte	91–114			C		Wu et al., 1984
Tongjing, Nanjing-Wuhu	Lamprophyte	105			C		Wu et al., 1984
Yueshan, Anhui	Diorite in NNE	80 ± 7			C-M		Zhai et al., 1992
Hongzhen, Anhui	Granite in NNE	124			C-M		Zhai et al., 1992

Continued

Area	Rock	Isotopic age (Ma)	Temperature (℃)	Pressure (GPa)	Forming depth (km)	Thermal gradient (℃/km)	Sources
Gushan, Nanjing-Wuhu	Andesite	115.7			C		Wu et al., 1984
Fenghuangshan, Anhui	Grano-diorite in NNE trend	133			C-M		Zhai et al., 1992
Washan, Ma'anshan, Anhui	Diorite porphyry dyke in NNE	120			C-M		Zhai et al., 1992
Huaiguang, Benbu, Anhui	Grano-diorite	130			C		Jin et al., 2003
Nvshan and Lushan, Benbu, Anhui	Granite	129–130			C		Yang, 2005
Dongguandian, Benbu, Anhui	Grano-diorite	126.9			C-M		Xu et al., 2004
Jiaohuashan,Huangshan, Anhui	Granite	125			C-M		Wang et al., 2005
Zhangbaling, Anhui	Andesite	126			C-M		Niu, 2006
Niangniangshan, Anhui	A type granite	97			C		Xing et al., 1999
Lishui, Jiangsu	Diorite porphyry dyke in NNE	124–99			C-M		Zhai et al., 1992
Maotan, Guichi, Anhui	A type granite	99	680–850		L		Wu et al., 1998
Huangmeijian, Congyang, Anhui	A type granite	133			C		Zhang et al., 1988
Kedoushan, Fanchang, Anhui	Basalt	Late Cretaceous			L		Yan et al., 2005 a
Fanchang, Nanjing-Wuhu	Diorite-alkaligranite-basalt-rhyolite	120–110			C-M		Qi et al., 2002
Lujiang-Zongyang, Anhui		120–110			C-M		Qi et al., 2002
Tiantangzhai, Dabieshan	Granotoid in NNE	131	830	0.54	18 C	46	Wang et al., 2000
Dabieshan	Granotoid	125–95			C		Ma, 1999
Liguo, north Xuzhou, Jiangsu	Diorite porphyry	131			C-M		Xu et al., 2004
Northwest Suzhou	Diorite porphyry	132			C-M		Xu et al., 2004
Nanjing-Wuhu	Diorite porphyry dyke in NNE	136–91			C-M		Zhai et al., 1992
Suzhou, Jiangsu	A type granite	E. Cretac			C		Zhou et al., 1997
Suzhou, Jiangsu	A type granite	133–123			C		Chen et al., 1993
Jiashan, Chengtou, Ganyu	I type granite in NE	E. Cretaceous			C-M		Li et al., 1999
Funiushan, Zhengjiang, Jiangsu	Grano-diorite	111			C-M		Ye et al., 1999
Shima, Jiangsu	Diorite in NNE	95.5			C-M		Zhai et al., 1992
Yongjia-Leqing, Zhejiang	Rhyolite	91.4–113.1			C		Gong et al., 1998
Yongjia–Leqing, Zhejiang	Rhyolite, trachyte, andesite, basalt	Early Cretaceous			C-M		Gong et al., 1998
Luannitan, Coast of SE China	Granite	124			C-M		Li et al., 1998
Honggong, Zhejiang	Quartz Syenite	123			C-M		Chen, 1991
Tiantaishan, NW Zhejiang	Alkali Granite	114			C		Zhang et al., 2002

Continued

Area	Rock	Isotopic age (Ma)	Temperature (℃)	Pressure (GPa)	Forming depth (km)	Thermal gradient (℃/km)	Sources
Dalishan, Northwest Zhejiang	Alkali Granite	Early Cretaceous			C		Zhang et al., 2002
Bashan, Northwest Zhejiang	Alkali Granite	110			C		Zhang et al., 2002
Sucun, Suichang, Zhejiang	Alkali Granite	86			C-M		Wang et al., 2005
East Zhejiang	Tuff	130–100	866	0.6	20 C	43	Wang, 1987
West Zhejiang	Tuff in NE trend	130–100	707	0.6	20 C	35	Wang, 1987
West Zhejiang	Granite in NE	Cretaceous			C		Yang et al., 1996
Changshan, Zhejiang	Rhyolite porphyry	124			C		Wu et al., 1984
Chayuan, Zhejiang	Rhyolite porphyry	133			C		Wu et al., 1984
Jinhua, Zhejiang	Rhyolite porphyry	133			C		Wu et al., 1984
Changle, Chenxian, Zhejiang	Granite	132			C-M		Nanjing University, 1981
Qingjubao,Shuichang	Granite	120			C-M		Nanjing University, 1981
Wuxi, Yunhe, Zhejiang	Granite	124–95			C-M		Nanjing University, 1981
Quanyantou, Wenzhou	Granite	90			C-M		Nanjing University, 1981
West Pingyang, Zhejiang	Granite	72			C-M		Nanjing University, 1981
Qingjie, Pingyang, Zhejiang	Granite	76			C-M		Nanjing University, 1981
Tangyuankou, Jiangshan, Zhejiang	A type granite	124			C		Chen et al., 1991
Qingtian, Zhejiang	A type granite	101			C-M		Qiu et al., 1999 b
Putuo, Zhoushan, Zhejiang	A type granite	94			C-M		Qiu et al., 1999 b
Taohua, Putuo, Zhejiang	A type granite	93			C-M		Qiu et al., 1999 b
Putuo, Zhoushan, Zhejiang	Diorite and alkali granite	92–111.8			C-M		Qiu et al., 1999 b
Taohua Island, Coastalof Zhejiang	Alkali granite	90.53–142.4			C-M		Qiu et al., 1999 b
Qingtian, Zhejiang	Alkali granite	100.7–114.3			C-M		Qiu et al., 1999 b
Zhejiang-Fujian-Guangdong	A type granite in NE	100–70			C-M		Hong et al., 2002
Liangnong, Yuyao, Zhejiang	Granite-syenite porphyry-gabbro	128–103			L		Gao et al., 1999
Beijie, Shuichang, Zhejiang	Alkali granite	86			C-M		Wang et al., 2005
North Changpu, Fujian	Granite	Cretaceous			C-M		Nanjing University, 1981
Shao'an, Changpu, Fujian	Granite	Cretaceous			C-M		Nanjing University, 1981
Yunxiao, Fujian	Granite with amazonite	100–112			C-M		Nanjing University, 1981
Dongshan Island, Fujian	Granite	66.8–62.4			C-M		Nanjing University, 1981
Jiangmukeng, Shao'an, Fujian	Granite	51.9			C-M		Nanjing University, 1981
Shiwatou, Yunxiao, Fujian	Admellite	106.9			C-M		Nanjing University, 1981
Southeast Pinghe, Fujian	Granite	Cretaceous			C-M		Nanjing University, 1981
Coastal of Fujian	Alkali Granite	Cretaceous			C-M		Lin et al., 1999

Continued

Area	Rock	Isotopic age (Ma)	Temperature (℃)	Pressure (GPa)	Forming depth (km)	Thermal gradient (℃/km)	Sources
Dalishan, Northwest Zhejiang	Alkali Granite	Early Cretaceous			C		Zhang et al., 2002
Bashan, Northwest Zhejiang	Alkali Granite	110			C		Zhang et al., 2002
Sucun, Suichang, Zhejiang	Alkali Granite	86			C-M		Wang et al., 2005
East Zhejiang	Tuff	130–100	866	0.6	20 C	43	Wang, 1987
West Zhejiang	Tuff in NE trend	130–100	707	0.6	20 C	35	Wang, 1987
West Zhejiang	Granite in NE	Cretaceous			C		Yang et al., 1996
Changshan, Zhejiang	Rhyolite porphyry	124			C		Wu et al., 1984
Chayuan, Zhejiang	Rhyolite porphyry	133			C		Wu et al., 1984
Jinhua, Zhejiang	Rhyolite porphyry	133			C		Wu et al., 1984
Changle, Chenxian, Zhejiang	Granite	132			C-M		Nanjing University, 1981
Qingjubao,Shuichang	Granite	120			C-M		Nanjing University, 1981
Wuxi, Yunhe, Zhejiang	Granite	124–95			C-M		Nanjing University, 1981
Quanyantou, Wenzhou	Granite	90			C-M		Nanjing University, 1981
West Pingyang, Zhejiang	Granite	72			C-M		Nanjing University, 1981
Qingjie, Pingyang, Zhejiang	Granite	76			C-M		Nanjing University, 1981
Tangyuankou, Jiangshan, Zhejiang	A type granite	124			C		Chen et al., 1991
Qingtian, Zhejiang	A type granite	101			C-M		Qiu et al., 1999 b
Putuo, Zhoushan, Zhejiang	A type granite	94			C-M		Qiu et al., 1999 b
Taohua, Putuo, Zhejiang	A type granite	93			C-M		Qiu et al., 1999 b
Putuo, Zhoushan, Zhejiang	Diorite and alkali granite	92–111.8			C-M		Qiu et al., 1999 b
Taohua Island, Coastalof Zhejiang	Alkali granite	90.53–142.4			C-M		Qiu et al., 1999 b
Qingtian, Zhejiang	Alkali granite	100.7–114.3			C-M		Qiu et al., 1999 b
Zhejiang-Fujian-Guangdong	A type granite in NE	100–70			C-M		Hong et al., 2002
Liangnong, Yuyao, Zhejiang	Granite-syenite porphyry-gabbro	128–103			L		Gao et al., 1999
Beijie, Shuichang, Zhejiang	Alkali granite	86			C-M		Wang et al., 2005
North Changpu, Fujian	Granite	Cretaceous			C-M		Nanjing University, 1981
Shao'an, Changpu, Fujian	Granite	Cretaceous			C-M		Nanjing University, 1981
Yunxiao, Fujian	Granite with amazonite	100–112			C-M		Nanjing University, 1981
Dongshan Island, Fujian	Granite	66.8–62.4			C-M		Nanjing University, 1981
Jiangmukeng, Shao'an, Fujian	Granite	51.9			C-M		Nanjing University, 1981
Shiwatou, Yunxiao, Fujian	Admellite	106.9			C-M		Nanjing University, 1981
Southeast Pinghe, Fujian	Granite	Cretaceous			C-M		Nanjing University, 1981
Coastal of Fujian	Alkali Granite	Cretaceous			C-M		Lin et al., 1999

Continued

Area	Rock	Isotopic age (Ma)	Temperature (℃)	Pressure (GPa)	Forming depth (km)	Thermal gradient (℃/km)	Sources
Zhangzhou City, Fujian		128–103			C-M		Gao et al., 1999
Xianglushan, Guangze, Fujian	bimodal volcanic	138–102			C-M		Gao et al., 1999
Yunshan, Yongtai, Fujian	bimodal volcanic	138–102			C-M		Gao et al., 1999
Lingtongshan, Daxi, Pinghe, Fujian	bimodal volcanic	138–102			C-M		Gao et al., 1999
Dayoushan, Sanming City, Fujian	bimodal volcanic	138–102			C-M		Gao et al., 1999
Sukeng,Yunxiaonanshan, Fujian	Gabbro	65			C-M		Gao et al., 1999
Xiahebian, Yunxiao, Fujian	Gabbro porphyry	70			C-M		Gao et al., 1999
Longhai-Shen'ao, Fujian	Diorite porphyry	77			C-M		Ling et al., 1999
Dayuancun, Fujian	Aegirine-augite riebeckite granite	95			C-M		Wang et al., 2005
Sukeng, Pingwu and Yongcun	Diabase gabbro	69			C-M		Gao et al., 1999
Hongshan, Fuzhou	A type granite	99			C		Huang et al., 1998
Guizhi, Gushan, Fuzhou	A type granite	95			C-M		Qiu et al., 1999 b
Wushan, Fuzhou	A type granite in NE	95	> 800		C-M		Qiu et al., 2000
Jingangshan, Southeast Fujian	A type granite in NE	92	> 800		C-M		Qiu et al., 2000
Xincun, SE Fujian	A type granite in NE	92	> 800		C-M		Qiu et al., 2000
Shimaoshan, Yuanshan, Yongtai	Basalt	113.2			L		Qiu et al., 1999 a
Shimaoshan, Yuanshan, Yongtai	Rhyolite	106.8			C-M		Qiu et al., 1999 a
Baishiding, Jianning, Fujian	Granite	103			C-M		Ling et al., 1999
Tailaoshan, Fuding, Fujian	Alkali granite	100			C-M		Ling et al., 1999
Yongchun, Fujian	Granite-diorite	120			C-M		Ling et al., 1999
Zhouning, Fujian	Granite	120			C-M		Ling et al., 1999
Zijinshan, Fujian	Mantle inclusion in NW trend	128–94	800	3.6	86.6 L	9	Zhang et al., 2001
Yuanshan, Yongtai, Fujian	Basalt	E. Cretaceous			C-M		Qiu et al., 1999 a
Youxi, Fujian	Rhyolitic pyroclastic	130			C		Wu et al., 1984
Yongtai, Fujian		86.7			C		Wu et al., 1984
Guanshan, Gushan, Fujian	Gabbro	90–106			C-M		Hong et al., 1987
Nanyu, Gushan, Fujian	Diorite	90–106			C-M		Hong et al., 1987
Jiantian, Gushan, Fujian	Grano-diorite	90–106			C-M		Hong et al., 1987
Danyang, Gushan, Fujian	Monzonite	90–106			C-M		Hong et al., 1987
Fuzhou, Gushan, Fujian	Alkali granite	90–106			C-M		Hong et al., 1987
Qianyang, Gushan, Fujian	Alkali granite	90–106			C-M		Hong et al., 1987
Guizhi, Gushan, Fujian	Granite	90–106			C-M		Hong et al., 1987
Bijiashan, Gushan, Fujian	granitic porphyry	90–106			C-M		Hong et al., 1987
Shangfangcun, Zhangzhou	Pyroxene diorite	90–106			C-M		Hong et al., 1987

Continued

Area	Rock	Isotopic age (Ma)	Temperature (℃)	Pressure (GPa)	Forming depth (km)	Thermal gradient (℃/km)	Sources
Dongjiucun,Zhangzhou, Fujian	Diorite	90–106			C-M		Hong et al., 1987
Changtai, Zhangzhou, Fujian	Grano-diorite	90–106			C-M		Hong et al., 1987
Gunong, Zhangzhou, Fujian	Monzonite	90–106			C-M		Hong et al., 1987
Xincun, Zhangzhou, Fujian	Granite	90–106			C-M		Hong et al., 1987
Baishishan, coast of Fujian	Grano-diorite	90–106			C-M		Hong et al., 1987
Jingangshan, Fujian	Alkali granite	Cretaceous			C-M		Hong et al., 1987
Xiadashanjia, Yongcun, Fujian	Granite porphyry	Cretaceous			C-M		Gao et al., 1999
Huayu, Penghu Islands	Quartz dioritic porphyry	> 61			C-M		Gao et al., 1999
Huayu, Penghu Islands	Andesite	> 65			L		Gao et al., 1999
Western Fujian	Granite in NE	Cretaceous			C		Yang et al., 1996
Sifang, southwest Fujian	Grano-diorite	104–108			C-M		Mao et al., 2002
Huatuangong, Coast of SE China	Granite	126			C-M		Li W D et al., 1998
Jiangmiao, Coast of SE China	Gabbro	125			C-M		Li W D et al., 1998
Zhuanqiao, Coast of SE China	Trachyte-andesite	126.6			C-M		Li W D et al., 1998
Shangfang, Fujian	Gabbro-norite	123			C-M		Zhou et al., 1994
Changtai, Fujian	Grano-diorite	123			C-M		Zhou et al., 1994
Yangchunshi, Fujian	Grano-diorite	122			C-M		Li W D et al., 1998
Lingshan,Shangrao, Jiangxi	Granite	95			C		Nanjing University, 1981
Xingzi, Jiujiang, N. Jiangxi	Granite	133, 107			C		Nanjing University, 1981
Yunshan, De'an , Jiangxi	Granite	114			C		Nanjing University, 1981
South to Guixi, Jiangxi	Granite porphyry	90			C		Nanjing University, 1981
Shangjia, SE Xunwu, Jiangxi	Granitoid	114			C		Nanjing University, 1981
Northern Jiangxi	Granitoid in NE	Cretaceous			C		Zhu et al., 2005
Wushan, Jiujiang-Ruichang, Jiangxi	Lamprophyre in NNE trend	107			C-M		Luo, 2006
Chengmenshan, Ruichang, Jiangxi	Quartz keratophyre in NNE trend	103			C-M		Luo, 2006
Ganjiang, Jiujiang-Ruichang, Jiangxi	Granite in NNE trend	100			C-M		Luo, 2006
Chengmengshan, Jiujiang	Quartz porphyry	Cretaceous			C-M		Jiangxi Geological Survey, 1983
Guangfeng-Shangrao, Jiangxi	Tholeiite	E. Cretaceous			56		Liao et al., 1999
Guangfeng-Shangrao, Jiangxi	Alkali basalt	L.Cretaceous			83		Liao et al., 1999
Southern Jiangxi	Kimberlite conglomer-ate	Cretaceous			L		Lai et al., 1996
Northeastern Jiangxi	Intermediate-acid	E. Cretaceous			C-M		Wang et al., 2000
Jiangshan, Zhejiang-Guangfeng, Jiangxi	Tholeiite, Alkali basalt	98–105			C-M		Yu et al., 2004
Jiazi, Lufeng , Guangdong	Granite	99–100–126			C-M		Nanjing University, 1981

Continued

Area	Rock	Isotopic age (Ma)	Temperature (℃)	Pressure (GPa)	Forming depth (km)	Thermal gradient (℃/km)	Sources
Shanwei, south Haifeng,Guangdong	Granite	112			C-M		Nanjing University, 1981
Qiniangtan, NW Huiyang,Guangdong	Granite	136–132			C-M		Nanjing University, 1981
North Boluo, Guangdong	Granite	91–127			C-M		Nanjing University, 1981
Kunshan, Zengcheng, Guangdong	Granite	132			C-M		Nanjing University, 1981
Tangkou, Yangchun, Guangdong	Granite	119			C-M		Nanjing University, 1981
Liantang,Chenhai, Guangdong	Granite	90			C-M		Nanjing University, 1981
Tangkou, Dianbai, Guangdong	Granite	108			C-M		Nanjing University, 1981
Southeast Zijin, Guangdong	Granite	100			C-M		Nanjing University, 1981
NE Yangchun, Guangdong	Granite	125			C-M		Nanjing University, 1981
Huangtian, Hetai, Guangdong	Alkali granite	84.8			C-M		Cui, 1989
Yingqiao, Lianjiang, Guangdong	Granite	Cretaceous			C-M		Wang et al., 1999
East Guangdong	Granitoid	Cretaceous			C		Yang et al., 1996
Naqing, South Anping, Guangdong	Granite	130–136			C		Nanjing University, 1981
Yangchun, west Guangdong	Granite diorite	125			C-M		Geng et al., 2006
Western Guangdong	Granite diorite, Monzonite Rhyolite dacite	100			C		Geng et al., 2006
Xinpeng, Western Guangdong	Granite	116			C		Wang et al., 2003
Yingwuling, Western Guangdong	Granite	67			C		Wang et al., 2003
Xishan, Western Guangdong	Granite	81			C		Wang et al., 2003
Xiaonanshan, Western Guangdong	Granite	55–82			C		Wang et al., 2003
Yinyan, Western Guangdong	Granite	80.5–92.3			C		Wang et al., 2003
Xiping, Western Guangdong	Granite	81–119			C		Wang et al., 2003
Shilu, Western Guangdong	Granite	122			C-M		Wang et al., 2003
Tangpeng, Western Guangdong	Granite	132	777.7	0.848	32	24	Wang et al., 2003
Tongzigen, Western Guangdong	Granite	98			C-M		Wang et al., 2003
Baiyunzhang, East Guangdong	Alkali rhyolite, trachyte	140–129			C		Zhang, 2001
Liangkou, Conghua, Guangdong	Syenite	137–86			C-M		Wang et al., 2005
Qilin, Shantou, Guangdong	Granulite in Basalt	112			C-M		Xu et al., 1999
Huichang, Jiangxi, Rencha,Guangdong	Basaltic dyke	93–119			L		Zhang et al., 2004
Zhuguangshan and Guidong,Guangdong	Acid rock dyke	85.9–92.7			C-M		Zhang et al., 2004
Yaji, Fogang, Guangdong	Alkali rock	127			C-M		Li et al., 1998
Longmenshan, Emanzhen, Hainan	Basic–acid bimodal volcanic	138–102			L		Gao et al., 1999
Dachang, Nandan, Guangxi	Granite	91			C		Nanjing University, 1981
Kunlunguan, SE Pinyang, Guangxi	Granite	108–129			C		Nanjing University, 1981
Daming, South Mashang, Guangxi	Granite	86–88			C		Nanjing University, 1981

Continued

Area	Rock	Isotopic age (Ma)	Temperature (℃)	Pressure (GPa)	Forming depth (km)	Thermal gradient (℃/km)	Sources
Huarong, Hunan	Granite	110			C-M		Nanjing University, 1981
Tianjingshan, East Huarong, Hunan	Granite	119–127			C-M		Nanjing University, 1981
Northeast Pingjiang, Hunan	Granite	110			C		Nanjing University, 1981
South Mufushan, Hunan and Hubei	Granite	127–100			C		Nanjing University, 1981
Wangxiang, Changsha, Hunan	Granite	127			C		Nanjing University, 1981
Tongshanling,Jiangyong, Hunan	Granite	91–110			C		Nanjing University, 1981
Shuikoushan, Changning, Hunan	Granite	106			C		Nanjing University, 1981
Baimashan, East Qianyang, Hunan	Granite	107			C		Nanjing University, 1981
Northwest Xitian, Hunan	Granite	128–130			C		Nanjing University, 1981
Ningyuan-Daoxian-Shiwandashan	Basalt in NE trend	132–135	1,083	2.2	70–85	14	Zhu et al., 2005
Rucheng, Southeast Hunan	Diabase, basalt	112–128			C-M		Jia, 2003
Northeast Hunan	Basalt	85–95			L		Xu et al., 2006
Yingjiashan, Northeast Hubei	Alkali Basalt	62.1			L		Peng et al., 2006
Tiantangzhai Dabieshan	Granitoid	131	830	0.54	18	46	Wang et al., 2000
Jiutai, Jilin	Dacite	Cretaceous	1,276	1.27	42 M	30.4	Lu et al., 1996
Jiutai, Jilin	Dacite	Cretaceous			70–80		Lu et al., 1996
East Zhejiang	Tuff	130–100	866	0.6	20	43	Wang, 1986
West Zhejiang	Tuff	130–100	707	0.6	20	35	Wang, 1986
West Zhejiang	Granitoid	Cretaceous				<22	Yang et al., 1996
West Fujian	Granitoid	Cretaceous				<25	Yang et al., 1996
Zijinshan, Fujian	Granitoid	128–94	800	2.6	86.6	9.2	Zhang et al., 2001
East Guangdong	Granitoid	Cretaceous				75	Yang et al., 1996
Fuxin, Liaoning	Peridotite	84.8	1272	2.93	97.7	18.4	Zheng, 1999
North Sinian Period 56–23 Ma							
Fushun, Liaoning	coal metamorph.	Paleogene				29	Yang et al., 1996
Hannuoba, Hebei	Granulite	Paleogene	900	1.1	36.7	24.5	Chen et al., 1998
West Tengchong	Granulite	27–17	720	0.8	26.7	27	Ji et al., 1998
Labieshan, Yunnan	Anphibolite	23.1	720	0.8	26.7	27	Ji et al., 1998
South east Xizang	Eclogite	49	650	2.6	86.7	7.5	Zheng et al., 2001
Beibuwan	Sandstone-shale	Eocene	TL			36.7	Wang et al., 1995
Beibuwan	Sandstone-shale	Oligocene	TL			34.6	Wang et al., 1995
Zhujiang-Sanshui	Sandstone-shale	Eocene	TL			39.4	Wang et al., 1995
Beibuwan	Sandstone-shale	Oligocene	TL			38.9	Wang et al., 1995
Yinggehai basin	Sandstone-shale	Oligocene	TL			43.7	Wang et al., 1995

Continued

Area	Rock	Isotopic age (Ma)	Temperature (℃)	Pressure (GPa)	Forming depth (km)	Thermal gradient (℃/km)	Sources
West Qaidam	Sandstone-shale	Eocene	reflectivity of coal			24	Zhou et al., 1998
Liaohe basin	Sandstone-shale	Eocene				45	Zhou et al., 1998
Liaohe basin	Sandstone-shale	Paleogene	FT			42.3	Zhou et al., 1998
Xihu basin, Donghai	Sandstone-shale	40–20	FT			28	Jiang et al., 2001
Dongying basin	Sandstone-shale	Paleogene				48.2	Zeng et al., 2000
Tarim basin	Sandstone-shale	Paleogene				26–20	Pan et al., 1996
Shiwandashan	Sandstone-shale	Paleogene				~ 21	Wang, 1998
North Jiangsu	Sandstone-shale	Paleogene				~ 30	Wang et al., 1989
Liaohe basin	Sandstone-shale	Paleogene				~ 34	Wang et al., 1989
Bohaiwan	Sandstone-shale	Paleogene				~ 36	Wang et al., 1989
Yitong Volcanic area, Jilin	Tholeiite	31			M		Zhang et al., 2006
Hengshantou, Yitong	Alkali olivine basalt	31			L		Liu et al., 1992
Sifangtingzi, Huinan, Jilin	Alkali olivine basalt	27.3			L		Liu et al., 1992
Malugou, Dunhua, Jilin	Alkali olivine basalt	27.9			L		Liu et al., 1992
Yongshen, South Jilin	Syenite	31			L		Yuan et al., 2003
Huanghua, Mudanjiang, Heilongjiang	Tholeiite	44.9			L		Liu et al., 1992
Chifeng, Inner Mongolia	Quartz and olivine tholeiite	33–24			L		Jia et al., 2002
Jining, Inner Mongolia	Tholeiite, olivine basalt, basanite, alkali basalt	33			M		Zhang et al., 2005, 2006
Panjing, Liaoning	Alkali olivine basalt	24.8–31.4			L		Liu et al., 1992
Yingmawan, Eastern Liaoning	Gabbro	32			L		Yuan et al., 2003
Oulituozi, Liaohe Basin	Trachyte	38–43			L		Zhang et al., 2006
Dongying Formation, Lower Liaohe Depression	Tholeiite, pyroxene basalt	Oligocene			L		Compiling Group of Petrol. Geol., 1993
Fangshenpao, Lower Liaohe Depression	Alkali olivine basalt	Oligocene			L		
Lower Liaohe Depression	Basalt in NNE trend	35.9–56			M		Liu et al., 1992
Shuiquanzhen, Weixian, Hebei	Alkali olivine basalt	29.3			L		Liu et al., 1992
Hannuoba, Hebei	Granulite in basalt	Eogene	900	1.1	36.7 C		Chen et al., 1998
Yangyuan, Hebei	Peridotite and pyroxenite in basalt	29.3–32.2			L		Ma et al., 2006
Shayiduan, Huanghua, Hebei	Diabase	Oligocene			L		Compile Group of Petrol. Geol., 1993
Sha'erduan, Huanghua, Hebei	Basalt	Oligocene			L		Compile Group of Petrol. Geol., 1993
Shayiduan-Shasanduan, North Huanghua	Gabbro and Diabase	Oligocene			L		Compile Group of Petrol. Geol., 1993

Continued

Area	Rock	Isotopic age (Ma)	Temperature (℃)	Pressure (GPa)	Forming depth (km)	Thermal gradient (℃/km)	Sources
Shayiduan, Huanghua	Diabase	Oligocene			L		Compile Group of Petrol. Geol., 1993
Dongying Formation, Qikou, Nanpu,	Diabase in NE trend	Upper Oligocene			L		Compile Group of Petrol. Geol., 1993
Western Qikou-Nanpu	Tholeiite, in NNE trend	Upper Oligocene			L		Compile Group of Petrol. Geol., 1993
Shayiduan, Zhanhua, Shenli	Basalt	Eogene			L		Compile Group of Petrol. Geol., 1993
Shasanduan, Huiming	Olivine Basalt	Eogene			L		Compile Group of Petrol. Geol., 1993
Dongtai, Wutaishan, Shanxi	Diabase	51.9			L		Shao et al., 2005a
Shuiyao, Zuoyun, Shanxi	Alkali olivine basalt	47.5			L		Shao et al., 2005a
Fanshi, Shanxi	Tholeiite, Alkali olivine basalt	26–36			L		Liu et al., 1992
Yingxian, Shanxi	Kimberlite	Eogene			A		Dong,1994
Nvshan, Anhui	Basalt in NNE trend	36–5.9			M		E and Zhao, 1987
Tuanshanbao, Guangde, Anhui	Basalt	42.6			L		E and Zhao, 1987
Northern Jiangsu Basin	Tholeiite, Alkali olivine basalt	46–65			L		Liu et al., 1992
Nanhui, Shanghai	Alkali olivine basalt	26.7			L		Liu et al., 1992
Gaoyou, Jiangsu	Alkali olivine basalt	46.3			L		Liu et al., 1992
Northern Jiangsu Basin	Tholeiite	Eogene			L		E and Zhao, 1987
Jintan Basin, Jiangsu	Tholeiite	Eogene			L		E and Zhao, 1987
Zhaomingshan, Anhui	Tholeiite	Eogene			L		E and Zhao, 1987
Wuyuanshan, Anhui	Tholeiite	Eogene			L		E and Zhao, 1987
Tuanshan, Guangde, Anhui	Olivine tholeiite	42.6			40–50		Wu et al, 1984
Balinshan, Jianglin, Hubei	Tholeiite	52			L		Liu et al., 1992
Baishe, Nanfeng, Jiangxi	Mafic-ultramafic rocks	37			L		Gao et al., 1999
Southeastern Coastal Area	Tholeiite	50			L		Li et al., 1998
Sanshui-Heyuan-Lianping, Guangdong	Olivine basalt in E-W trend	61–45			L		Zhu et al., 2005
Leizhou,Paninsula, Guangdong	Olivine basalt in E-W	61–45	1,100–1,200	1.5–2.0	77	16	Zhu et al., 2005
Mashan, Guangxi	Olivine basalt in E-W	61–45			L		Zhu et al., 2005
Maguan, Yunnan	Olivine basalt in E-W	61–45	1,337	4.1–4.7	> 60	22	Zhu et al., 2005
Hamalayan Period 23–0.78 Ma							
Yarlung Zangbo	Glaucophane	<23	350	0.8–0.96	26.7–32	~ 10	Xizang Geological
Nyalum, Xizang	Anphibolite	<20	650	0.72	24	~ 24	Survey, 1993

Continued

Area	Rock	Isotopic age (Ma)	Temperature (℃)	Pressure (GPa)	Forming depth (km)	Thermal gradient (℃/km)	Sources
Yadong, Xizang	Anphibolite	<20	670	0.8	28.5	~ 23	Survey, 1993
Gamba, Xizang	Anphibolite	21–13	560	0.7	23.3	~ 24	Survey, 1993
Southeast Xizang	Granulite	17–14	850	1.8	60	~ 17	Zhai, 1998
Dabieshan	Mylonite	Neogene	350	0.6	20	17.5	Liu et al., 1990
Central mountains of Taiwan	Green schist	Miocene	300	0.4	13.3	22–23	Chen et al., 1994
Yuli, Taiwan	Green schist	L. Miocene	350	0.6	20	17–18	Chen et al., 1994
Tailuge, Taiwan	Green schist	35–2.66	475	0.5	16.7	28–29	Chen et al., 1994
North Nanhai	Apatite	> 10	FT			34	Deng et al., 1997
Leizhou, Guangdong	Granulite	Cenozoic	1,160	1.7	56.7	27	Yu et al., 1998
Beibuwan	Sandstone-shale	Neogene	TL			31.1	Wang et al, 1995
Zhujiang-Sanshui	Sandstone-shale	Neogene	TL			37.2	Wang et al, 1995
Yinggehai basin	Sandstone-shale	Neogene	TL			38.7	Wang et al, 1995
Kalpin, Xinjiang	Sandstone-shale	Neogene				7~21.3	Wei et al., 1989
Tarim basin	Sandstone-shale	Neogene	reflectivity of coal			20	Fan et al., 1990
Erdos basin	Sandstone-shale	Neogene				28	Ren et al., 1996
Keluo, Nenghe, Heil ongjiang	Peridotite inclusion	5.4–2.5	1,100	2.6	85.6	13	Chi et al., 1988
Ludao, Heilongjiang	Iherzolite	Neogene			L		E and Zhao, 1987
Shangzhi,Yuanbao, Heilongjiang	Iherzolite	Neogene			L		Chi et al., 1988
Jingpohu-Beihutou Heilongjiang	Iherzolite, dunite, harzburgite	Neogene			L		E and Zhao, 1987
Jingpohu, Heilongjiang		Neogene			L		E and Zhao, 1987
Mudanfeng, Mudanjiangshi	Iherzolite, dunite	Neogene			L		E and Zhao, 1987
Kedong, Heilongjiang	Iherzolite, dunite	Neogene			L		Liu, 1983
Wudalianchi, Heilongjiang	Spinel Iherzolite	Neogene			L		Qiu et al., 1997
Shangzhi, Heilongjiang	Alkali basalt in NNE	18.9–17.7	1,412	2.2	73	19	Liu et al., 1992
Nengjiangxian, Heilongjiang	Alkali olivine basalt	2.5			L		Compiling Group of Petrol. Geol., 1993
Shifenggou, Ning'anxian	Basalt	6.35			L		
Ning'anxian, Heilongjiang	Alkali olivine basalt	7.59			L		
Wuchagou, Daqing Oil field	Basalt	Neogene			L		
Daluomi, Daqing Oil field	Basalt	Neogene					
Jidong-Dongning, Daqing	Basalt	Neogene					
Huanghua, Daqing Oil field	Basalt	Neogene					
Donghua Formation, Daqing	Basalt	E. Quart.					
Jingpohu, Heilongjiang	Basalt	E. Quart.					

Continued

Area	Rock	Isotopic age (Ma)	Temperature (℃)	Pressure (GPa)	Forming depth (km)	Thermal gradient (℃/km)	Sources
Wangtianhe, Changbaishan, Jilin	Trachyte basalt, andesite	2.12–2.87			M		Fan et al., 1998
Jingyu, Jilin	Peridotite inclusion in NNE trend	15–1.48	1,450	2.8	91.8	16	Chi et al., 1988
Wangqing, Jilin		6.2–2.1	1,320	1.9	62.5	21	Chi et al., 1988
Wangqing, Jilin		6.3–2.1	880–1,100	1.4–2.3	52–70	17–16	Wang et al., 2000
Yitong, Jilin		21–7.8	1,410	2	67	21	Chi et al., 1988
Huinan, Jilin		15–1.48	1,252	2.1	71	18	Chi et al., 1988
Changbaishan, Jilin		6.4–3.1	1,460	2.5	85	17	Chi et al., 1988
Da-Xiaogusha, Ma'anshan,Yitong	Iherzolite, and pyroxenite Spinel	Neogene			L		Wu, 1984
Jiaohe, Jilin		Neogene			L		Wu, 1984
Erdaobaihe, Antu, Jilin	Iherzolite	Neogene			L		Liu, 1983
Dayishan, Huinan, Jilin	Iherzolite, harzburgite, dunite, websterite	Neogene			L		Luo, 1984
Dalongwan, Huinan, Jilin		Neogene			L		Wu, 1984
Laomiao, Jilin	Iherzolite inclusion	Neogene			L		E and Zhao, 1987
Qixingshan, Shuangliao, Jilin	Iherzolite, pyroxenite	Neogene			L		E and Zhao, 1987
Houtuanshan, Yongji, Jilin	Peridotite	Neogene			L		Chi et al., 1988
Fengmang, Jilin	Basalt, Alkali olivine basalt	4.9–5.3			L		Liu et al., 1992
Houtuanshan, Jilinshi, Jilin		13.2–22.3			L		Compiling Group of Petrol. Geol., 1993
Wangqing, Jilin	Basalt	2.13			L		Compiling Group of Petrol. Geol., 1993
Dunhua, Jilin	Alkali olivine basalt	23.9			L		Compiling Group of Petrol. Geol., 1993
Dagushan, Yitong, Jilin	Basalt	12.8			L		Compiling Group of Petrol. Geol., 1993
Xiaogushan, Yitong, Jilin	Basalt	10.4			L		Compiling Group of Petrol. Geol., 1993
Dongjianshan, Yitong, Jilin	Basalt	9.74			L		Compiling Group of Petrol. Geol., 1993
Sulan, Jilin	Alkali olivine basalt	12.4			L		Compiling Group of Petrol. Geol., 1993
Yongjixian, Jilin	Basalt	Miocene			L		Compiling Group of Petrol. Geol., 1993
Chandishan, Huadian, Jilin	Basalt	Miocene			L		Compiling Group of Petrol. Geol., 1993
Junjianshan, Helong, Jilin	Basalt	13.5–28.4			L		Compiling Group of Petrol. Geol., 1993
Wangqing, Jilin	Basalt	Neogene	1,310–1,330	1.5–2.2	53–70	23–19	Liu et al., 1992
Tianchi, Changbaishan, Jilin	Trachyte-basalt	2–0.1			L		Fan et al., 2006

Continued

Area	Rock	Isotopic age (Ma)	Temperature (℃)	Pressure (GPa)	Forming depth (km)	Thermal gradient (℃/km)	Sources
Yitong, Jilin	Basalt	9–15			A		Zhang et al., 2006
Malianshan, Qingyuan, Liaoning	Alkali olivine basalt	5.5–7			L		E and Zhao, 1987
Guantao, Xialiaohe	Basalt	Neogene			L		Compiling Group of Petrol. Geol., 1993
East basin, Xialiaohe	Basalt in NE trend	Miocene			L		
Fuxian, Liaoning	Eclogite in NNE trend	Neogene	1,150	2.5	83.3 L		Zhou, 1996
Kuandian, Liaoning	Olivine tholeiite, Alkali olivine basalt	Neogene	1,390–1,430	1.8–2.5	60–80	23–18	Lu et al., 1981
Kuandian, Liaoning	Websterite	Neogene	1,675	4.35	143	12	Lu et al., 1981
Huangyishan, Kuandian, Liaoning	harzburgite、websterite	Neogene			L		Lu et al., 1981
Huashan, Shenyang, Liaoning	Alkali olivine basalt	9.76			L		Liu et al., 1992
Qingyishan, Kuandian, Liaoning	Iherzolite	Neogene			L		Liu et al., 1981
Liujia, Kuandian, Liaoning	Iherzolite	Neogene			L		Liu et al., 1981
Zhen'an, Beining, Liaoning	Peridotite	Neogene			L		Chi et al., 1988
Longgang, Liaoning	Spinel iherzolite websterite	Neogene			L		Yang et al., 1994
Dayishan, Kuandian, Liaoning	Alkali olivine basalt	Neogene	1,129–1,330	1.7–2.1	55–70	21–19	Luo, 1984
Northeast China	Peridotite in NNE trend	Neogene	1,118	2.76	80–91	14–12	Qiu et al., 1997
Hexigtun, Inner Mongolia	Shoshonite	0.89–1.74			L		Liu et al., 1992
Xilingol, Inner Mongolia	Peridotite in NNE trend	15.6–3.9	1,450	2.2	73.3	20	Chi et al., 1988
Siziwang, Inner Mongolia	Spinel Iherzolite	Miocene	1,100–1,250	1.7–2.0	77	14–16	Chen et al., 2004
Sanyitang, Jining, Inner Mongolia	Pyroxene macro-crystal in Spinel iherzolite	Neogene	950	1.5	50–60	19–16	Du et al., 2005
Jining, Inner Mongolia	Continental flood basalt	Miocene			L		Liu et al., 1992
Zuoyun, Inner Mongolia	Continental flood basalt	Miocene			L		Liu et al., 1992
Weichang, Inner Mongolia	Continental flood basalt	Miocene			L		Liu et al., 1992
Chifeng, Inner Mongolia	Basalt	10–6			L		Jia et al., 2002
South to Xarmoron River	Basalt	4.8			L		Jia et al., 2002
Hexigten, Inner Mongolia	Basalt	0.89–0.16			L		Jia et al., 2002
Jining, Inner Mongolia	Tholeiite, olivine basalt, basanite	22.8–22.1, 12.2–9.4			M		Zhang et al., 2005, 2006
Arxan, Inner Mongolia	Mantle source inclusion	Neogene			L		Yu et al., 2006
Abag Qi, Inner Mongolia	Alkali olivine basalt	5.44			L		Liu et al., 1992
Fengzhen, Inner Mongolia	Tholeiite	8.84			L		Liu et al., 1992
Dawang, Fengzhen, Inner Mongolia	Tholeiite	7.48			L		Liu et al., 1992
Hanuoba, Hebei	Peridotite in NNE trend	Neogene	1,110	2.16	70	16	Li et al., 1999

Continued

Area	Rock	Isotopic age (Ma)	Temperature (℃)	Pressure (GPa)	Forming depth (km)	Thermal gradient (℃/km)	Sources
Hanuoba, Hebei	Granulite inclusion	Neogene	800–950	1.11	43	19–22	Chen et al., 1998
Zhangjiakou, Hebei	Continental flood basalt	Miocene			L		Liu et al., 1992
Damaping, Hebei	Peridotite in NNE trend	24.3–3.9	1,380	3.2	105	13	Chi et al. 1988
Pingquan, Hebei		24.5	1,400	2.3	76.4	18	
Chongli, Hebei	Garnet Iherzolite in basalt	Neogene					Liu et al., 1985
Shexian, Hebei	Eclogite in kimberite	Neogene		1.0	L		Dong, 1994
Shizijie, Zhangbei, Hebei	Tholeiite	13.7			L		Liu et al., 1992
Zhangbei, Hebei	Alkali olivine basalt	17.8			L		Liu et al., 1992
Damaping, Wanquan, Hebei	Basanite	21			L		Liu et al., 1992
Wuluogongshan, Weichang, Hebei	Alkali olivine basalt	26			L		Liu et al., 1992
Qipanshan, Weichang, Hebei	Alkali olivine basalt	7.26			L		Liu et al., 1992
Zhouba, Zhangbei, Hebei	Tholeiite	22.8			L		Liu et al., 1992
Xiaosuangou, Shangyi, Hebei	Tholeiite	4.38			L		Liu et al., 1992
Luotuofeng, Pingquan, Hebei	Tholeiite	24.3			L		Liu et al., 1992
Yangyuan, Hebei	Peridotite in basalt	Neogene	975–1,054	1.1–2.2	35–68	28–16	Liu et al., 2006
Baigezhuang, Beijing	Tholeiite	15.9			L		Liu et al., 1992
Baicaoping, Wu'an, Hebei	Olivine basalt	3.52–4.3			L		Liu et al., 1992
Jingxing, Hebei	Alkali olivine basalt	6.31			L		Liu et al., 1992
Center-North Dagang Oil Field	Basalt in NNE trend	Miocene			L		Compiling Group of Petrol. Geol., 1991
Gangdong, Dagang Oil Field	Basalt	Pliocene			L		Compiling Group of Petrol. Geol., 1991
Qikou, Well Qinan 1, Dagang Oil Field	Basalt	Pliocene			L		Compiling Group of Petrol. Geol., 1991
Gaoshangbao, Dagang Oil Field	Olivine basalt	22.1			L		Liu et al., 1992
Huangjiawa-Datong Shanxi	Spinel Iherzolite	E.Quart.	900–1,050	1.1–1.7	40–60	23–18	Chen et al., 1997
Dongtaigou, Wutaishan, Shanxi	Spinel Iherzolite	Neogene			L		He et al., 1983
Fenghuangshan, Xiyang, Shanxi	Alkali olivine basalt	7.25			L		Liu et al., 1992
Jiaoyanshan, Linju, Shandong	Alkali olivine basalt	14.3–20.7			L		Liu et al., 1992
Xiaoshanwan, Linju, Shandong	Alkali olivine basalt	13.2–14.2			L		Liu et al., 1992
Dafangshan, Qixia, Shandong	Olivine nephelinite	8.13			L		Liu et al., 1992
Daheishan Island, Penglai	Alkali olivine basalt	8.08			L		Liu et al., 1992
Fushan, Pingdu, Shandong	Basanite	7.99			L		Liu et al., 1992
Linju, Shandong	Monoclinic in basalt	4–14			L		Zhang et al., 2006
Qijiadian, Shandong	Peridotite inclusion in NNE trend	Neogene	875	4.1	136	7	You, 1998

Continued

Area	Rock	Isotopic age (Ma)	Temperature (℃)	Pressure (GPa)	Forming depth (km)	Thermal gradient (℃/km)	Sources
Shanwan-Changle, Shan dong	Spinel Iherzolite, pyroxenite	Neogene			L		Zhao et al., 1982
Qixia-Penglai, Shandong	Iherzolite, spinel harzburgite, pyroxenite, diallage-peridotite	Neogene			L		Zhao et al., 1982; Liu et al., 1981; Zhang, 1982; Jin, 1982
Shanwan, Linju, Shandong	Alkali olivine basalt	Neogene			50–80		Wu et al., 1984
Huashan-Daxiao-Fangshan, Qixia	Iherzolite inclusion	E Quart.			L		Wu et al., 1984
Chishan-Xishan, Penglai	Basanite, phonolite	Neogene			L		Wu et al., 1984
Guantao Formation, Huiming Shengli Field	Olivine basalt	Neogene			L		Compiling Group of Petrol. Geol., 1993
Shangyu, Hebi, Henan	Spinel Iherzolite, Spinel harzburgite	E. Quart.			L		Yang et al., 1976 Liu et al., 1981
Hebi, Henan	Kimberite	E. Quart.			A		Dong,1994
Pangcun, Hebi, Henan	Alkali olivine basalt	4.32			L		Liu et al., 1992
Heishantou, Pangcun, Henan	Alkali olivine basalt	3.99			L		Liu et al., 1992
Da'ancun, Ruyang, Henan	tholeiite	6.83			L		Liu et al., 1992
Liuhe, Jiangsu	Peridotite in NNE trend	Neogene	1,193	1.5	50	24	Zhi et al., 1996
Liuhe, Jiangsu		Pliocene	1,052	2.06	68.7	15	Dong et al., 1993
Liuhe, Jiangsu		16.3–8.6	1,061	2.2	74	14	Sun et al., 1994
Liuhe, Jiangsu		16.3–8.6	909–982	1.2–1.6	46–52	19	Wang et al., 2000
Nalianshan, Liuhe, Jiangsu	Spinel Iherzolite	4	1,032–1,080	1.7–1.9	56–63	17	Chen et al, 1994; Zhi et al, 2001
Fangshan, Liuhe, Jiangsu	Spinel Iherzolite	Neogene	1,084–1,178	2.3–2.6	75–85	14	E and Zhao, 1987
Guafushan, Liuhe, Jiangsu	Spinel Iherzolite	Neogene	1,113–1,237	2.25–3.2	74–100	15–12	E and Zhao, 1987
Fushan, Liuhe, Jiangsu	Spinel Iherzolite	Neogene	1,134–1,216	2.5–3.2	80–100	14–12	E and Zhao, 1987
Pingmingshan, Donghai Jiangsu	Spinel Iherzolite、harzburgite, websterite	4.02–6.38	830–900	1.5–1.7	56–65	15–14	Zhao, 1982 Jin et al., 2003
Nvshan, Mingguan, Anhui	Peridotite in NNE trend	E.Quart.	1,100	1.9	63.3	17	Jin et al., 1998
Nvshan, Mingguan, Anhui	Spinel iherzolite, spinel olivine websterite	16.5–1.4	1,029	1.9	62	17	Sun et al., 1994
Nvshan, Mingguan, Anhui		16.5–15.4	900–1,128	1.1–2.0	38–65	24–17	Wang et al., 2000
Dangtu,Anhui		16.5–1.4	1,174	2.9	92	13	Sun et al., 1994
Jingong, Huaining, Anhui		Neogene			L		E and Zhao, 1987
Xishanqiao, Nanjing	Alkali olivine basalt, olivine tholeiites	Pliocene			40–80		Liu et al., 1992
Yaomai, Nanjing		Pliocene			40–80		Liu et al., 1992

Continued

Area	Rock	Isotopic age (Ma)	Temperature (℃)	Pressure (GPa)	Forming depth (km)	Thermal gradient (℃/km)	Sources
Chishan, Jurong, Nanjing		Pliocene			40–80		Liu et al., 1992
Pingmingshan, Donghai, Jiangsu	basanite	6.10			L		Liu et al., 1992
Guafushan, Liuhe, Jiangsu	Alkali olivine basalt	9.35			L		E and Zhao, 1987
Fangshan, Liuhe, Jiangsu	Alkali olivine basalt	8.60			L		E and Zhao, 1987
Chishan, Jurong, Jiangsu	Olivine basalt	13.9			L		E and Zhao, 1987
Liyang, Jiangsu	Alkali olivine basalt	20.7			L		E and Zhao, 1987
Shangxing, Liyang, Jiangsu	Alkali olivine basalt	15			L		E and Zhao, 1987
Chuansha, Shanghai	Alkali olivine basalt	18.7			L		E and Zhao, 1987
North Jiangsu Basin	tholeiite	9.18			L		E and Zhao, 1987
Tushan, Anhui	Spinel iherzolite	Neogene	1,106–1,168	5.2	82	14	E and Zhao, 1987
Dashushan, Hefei, Anhui		Neogene	1,118–1,159	2.9	90	13	E and Zhao, 1987
Xinchang, Zhejiang	Iherzolite in NNE	Neogene	1,210	2.4	80	15	Lin et al., 1995
Xinchang, Zhejiang	Basalt	Neogene	1,460–1,500	2.0–2.5	96	16	Zhao, 1990
Xilong, Quxian, Zhejiang	Spinel Iherzolite harzburgite	Neogene			L		E and Zhao, 1987
Quxian, Zhejiang	Nephelinite	Neogene	1,540	2.9	80.5	19	Zhao, 1990
Jinyun, Zhejiang	Spinel Iherzolite pyroxenite	Neogene			L		E and Zhao, 1987
Zhongfu, Longyou, Zhejiang	Peridotite	Neogene			L		E and Zhao, 1987
Talong, Longyou, Zhejiang	Peridotite	Neogene			L		E and Zhao, 1987
Huangyan, Zhejiang	Spinel Iherzolite	Neogene			L		E and Zhao, 1987
Xinchang-Tiantai, Zhejiang	tholeiite, Alkali olivine basalt	6–7			L		Liu et al., 1992
Mingxi, Fujian	Peridotite in NNE trend	Neogene	1,115	1.84–2.6	59–79	16	Peng et al., 1990
Mingxi, Fujian	Basanite	Neogene	1,490–1,510	2.5	112	14	Zhao, 1990
Mingxi, Fujian	Nephelinite	Neogene	1,515–1,550	2.7–2.9	108	14	Zhao, 1990
Mingxi, Fujian	Basalt	Neogene	1,500	3.5	135	11	Zhao, 1990
Xilong, Fujian	Garnet Iherzolite	Neogene			L		E and Zhao, 1987
Longhai, Fujian	Peridotite in NNE trend	Neogene	1,016	1.7	56	18	Peng et al., 1990
Minqing, Fujian		Neogene	1,270	3.7–4.5	130	10	Xu et al., 1995
Minqing, Fujian		Neogene	1,400–1,430	1.5–2.0	77	19	Zhao, 1990
Niutoushan, Shouning, Fujian	Spinel Iherzolite in Alkali basalt	Neogene			L		Yue et al, 2005
Niutoushan, Shouning, Fujian	Basalt	Neogene	1,350	1.2–1.6	61	22	Zhao, 1990
Dayang, Mingxi, Fujian	Garnet spinel Iherzolite, harzburgite	Neogene			L		Sun and Lai, 1980

Continued

Area	Rock	Isotopic age (Ma)	Temperature (℃)	Pressure (GPa)	Forming depth (km)	Thermal gradient (℃/km)	Sources
Shiheng, Mingxi, Fujian	Spinel Iherzolite dunite harburgite	Neogene			L		Sun and Lai, 1980
Mingxi, Fujian	tholeiite. Alkali basalt, andesite	0.1–25.1			L		Gao et al., 1999
Minqing, Fujian		0.1–25.1			L		Gao et al., 1999
Changpu, Fujian		0.1–25.1			L		Gao et al., 1999
Liuhui, Longhai, Fujian	Tholeiite	17.6–18.1			L		Liu et al., 1992
Xiangshan, Longhai, Fujian	Tholeiite	17.5–17.7			L		Liu et al., 1992
Niutoushan, Longhai, Fujian	Tholeiite, Alkali olivine basalt	11.7–16.7			L		Zhou, 1981
Penghu Islands	Basalt, in NNE trend	2			L		Chen, 1973
Penghu Islands	Tholeiite, Alkali basalt	16.2–8.2			C-M		Liu, 1999
Penghu Islands	Tholeiite, Alkali basalt, andesite	0.8–25.1			L		Gao et al., 1999
Taiwan		0.8–25.1			L		Gao et al., 1999
Pengjiayu, North Taiwan	Andesite, basalt	3.6–1.6			L		Liu, 1999
Datun volcano, North Taiwan	Andesite, basalt	2.8–0.8			C-M		Liu, 1999
Jilong volcano, North Taiwan	Andesite, basalt	1.7–0.81			C-M		Liu, 1999
Lanyu, Southeast Taiwan	Andesite	13.5–2			L		Liu, 1999
East Taiwan longitude valley	Basalt in NNE trend	25–1.85			L		E and Zhao, 1987
Puning, Shantou, Guangdong	Peridotite in NNE trend	Neogene	1,380	1.7	55.5	25	Chi et al., 1988
Puning, Shantou, Guangdong	Alkali basalt	Neogene	1,300–1,380	1.4–1.65	46	28	Zhao, 1990
Puning, Shantou, Guangdong	Pyroxenite	Neogene	1,490–1,570	2.2–2.7	100	15	Zhao, 1990
Coast of Fujian and Guangdong	Pyroxenite in NE trend	20–1.8	1,050	1.7–2.3	50–80	21–13	E and Zhao, 1987
Tianyang-Yingfeng, Xuwen, Guangdong	Spinel Iherzolite, harzburgite, Pyroxenite	Neogene			L		Hu and Zhong, 1982
Wenchang-Anding, Hainan		Neogene			L		Hu and Zhong, 1982
Qilin, Puning, Guangdong	Peridotite in NNE trend	Neogene	1,150	1.6	53.3	22	Xu et al., 1995
Qilin, Puning, Guangdong		Neogene	1,380	1.7	55.5	25	Chi et al., 1988
Leizhou, Guangdong		Neogene	1,044	1.85	60	17	Peng et al., 1990
Wenchang, Penglai, Hainan	Peridotite in NNE trend	N–Q	1,031	1.6	53	19	Peng et al, 1990

References for Appendix 7

Aoki K (1970) Japanese Island arc: Xenoliths in alkali basalts, high-alumina basalts and calc-alkaline andesites and decites. In: Nixon PH (ed) Mantle Xenoliths. John Wiley & Sons, New York

Bai J, Huang XG, Wang HC et al (1996) The Precambrian Crustal Evolution of China. (2^{nd} edition). Geological Publishing House, Beijing (in Chinese with English abstract).

Bai WJ, Robinson P, Yang JS et al (1995) The Ophiolites in different stages and its tectonic evolution of the western Junggar, Xinjiang. Acta Petrologica Sinica 11(suppl.): 62–72 (in Chinese with English abstract).

Bao PS, Xiao XC, Wang J (1999) The blueschist belt and its tectonic implication in the Shuanghu region, Central-Northern Tibet. Acta Geologica Sinica 73(4): 302–314 (in Chinese with English abstract).

Bao YG, Bai ZM, Ge SW et al (1995) Volcano-geology and rocks of Beijing in Yanshanian Period. Geological Publishing House, Beijing (in Chinese).

Bi H, Wang ZG, Wang YL et al (1999) History of tectono-magmatic evolution in the Western Kunlun Orogen. Science in China D 42(6): 604–619.

Bian QT, Zheng XS, Li HS et al (1997) Age and tectonic setting of ophiolite in the Hoh Xil region, Qinghai province. Geological Review 43(4): 347–355 (in Chinese with English abstract).

Burchfiel BC, King R, Royden LH et al (1998) Tectonic interpretation of GPS results from the SE part of the Tibetan Plateau and within the European-Asian framework. Abstracts with Programs–GSA, 30(7): 108.

Bureau of Geology and Mineral Resources of Provinces (1984—1993) Regional Geology of Provinces. Geological Publishing House, Beijing (in Chinese with English abstract, as shown in Reference for Chapter 1).

Cai JH, Yan GH, Mu BL et al (2005) Zercon U-Pb age, Sr, Nd, Pb isotopic, trace elements and discussion on its origin in Fangshan intrusion, Beijing. Acta Petrlogica Sinica 21(3): 776–788 (in Chinese with English abstract).

Cai MH (2001) The Study on Metallogenic Regularity and Dynamics of Mesozoic Colored Metal and Noble Metal Deposits in Eastern Guangxi-Western Guangdong Provinces. Dissertation, China Academy of Geological Sciences (in Chinese with English abstract).

Che ZC, Liu L, Liu HF et al (1995) Discovery high-pressure metamorphic mud rocks and its produced environment in Altun area. Science Bulletin 40(14): 1,298–1,300.

Chen BH, Jia BH, Liu YR et al (2004) Sm-Nd isochron age of spinel lherzolite inclusion in Mesozoic volcanic rocks of South Hunan. Geological Review (2): 180–183 (in Chinese with English abstract).

Chen B, Zhuang YX (1994) The petrology and petrogenesis of Yunlu chamockite and its granulite inclusion, west Guangdong, South China. Acta Petrologica Sinica 10(2): 139–150 (in Chinese with English abstract).

Chen B (1997) Petrographic evidences and tectonic significance for two phases of metamorphism in sillmanite-and garnet-bearing mica schists of Pintan-Dongshan metamorphic zone of eastern Fujian, China. Acta Petrologica Sinica 13(3): 380–394 (in Chinese with English abstract).

Chen B, Liu CQ, Tian W (2006) Crust-Mantle magma migmatization during Mesozoic in Taihangshan: evidences of petrology and geochemistry. Earth Science Frontiers 13(2): 140–147 (in Chinese with English abstract).

Chen DG, Yang RY (1994) Mineral chemistry, composition of rare earth element and their significance in peridotite inclusion of Liuhe, Jiangsu. Acta Petrologica Sinica 10(1): 68–80.

Chen FJ, Wang XW, Zhang GY et al (1992) Structure and geodynamic setting of oil and gas basins in the People's Republic of China. Geoscience 6(3): 317–327 (in Chinese with English abstract).

Chen GY, Sun DS et al (1993) Genetic Mineralogy and Gold Mineralization of Guojialing Granodiorite in Jiaodong Region. Press of China University of Geosciences, Wuhan (in Chinese with English abstract).

Chen HJ, Ji Y (1993) Preliminary research on the time of Yunkai Group and thrust at Naluoxihe, south to Fenjiezhen, Luoding, Guangxi province. In: Collection of Structural Geology in Yunkaidashan and its adjacent area, Geological Publishing House, Beijing (in Chinese).

Chen H, Shao JA (1987) Formation pattern and tectonic background of carbonate in Bayan'obo. In: Contributions to the Project of Plate Tectonic in Northern China. (2): 73–79. Geological Publishing House, Beijing (in Chinese with English abstract).

Chen JF, Zhou TX, Yin CS et al (1991) $^{40}Ar/^{39}Ar$ age dating of some Mesozoic intrusions in Southeast Zhejiang. Acta Petrologica Sinica 7(3): 37–44 (in Chinese with English abstract).

Chen JF, Foland K A, Liu YM (1993) Accurate $^{40}Ar/^{39}Ar$ age dating of granite complex in Suzhou. Acta Geologica Sinica 9(1): 77–85 (in Chinese with English abstract).

Chen JC (1973) Geochemistry of basalts from Penghu islands. Proc. Geol. Soc. China (Taiwan) 16: 23–36

Chen JY, Wang JY, Pang SY et al (2001) On the earth crust movement of Qomolangma area. Science in China 31(4): 265–271 (in Chinese).

Chen MY, Li SX (1996) The evolution of granulite facies metamorphism in eastern Hebei Province. Acta Petrologica Sinica 12(2): 343–358 (in Chinese with English abstract).

Chen NS, Wang RJ, Shan WR et al (1994) Isobaric cooling (IBC) P-T-t path for the western portion of Archean Miyun complex, Beijing: Constraints and its geodynamic genesis. Scientia Geologica Sinica 29(4): 355–365 (in Chinese with English abstract).

Chen NS, You ZD, Sun M (1998) Decompression metamorphism of Dabie Complex and rapid tectonic-uplift from deep level of the orogenic belt. Science in China D41(2): 144–150.
Chen NS, Zhu J, Wang GC et al (1999) Metamorphic petrological features of high-grade metamorphic microlithons in Qingshuiquan region, eastern section of eastern Kunlun orogenic zone. Earth Science 24(2): 116–120 (in Chinese with English abstract).
Chen PR, Hua RM, Zhang BT et al (2002) Early Yanshanian post-orogenic granitoids in the Nanling region: Petrological constraints and geodynamic settings. Science in China D 45(8): 755–768.
Chen PR, Zhou XM, Zhang WL et al (2004) Origin and significance of syenite-granite complex of Early Yanshanian at eastern part of Nanling. Science in China D 34(6): 493–503 (in Chinese).
Chen QA, Wang FZ (1992) The thermal history and tectonic setting of the granulites in Chongli Group in Archean of northwestern Hebei province. In: The 40th Anniversary of China University of Geosciences (Contribution to Petrology), China University of Geosciences Press, Wuhan (in Chinese).
Chen QH, Chen ZB, Chen ZY et al (1998) Mesozoic Extension Tectonics and Uranium Minerali-zation in Southeastern China. Geological Publishing House, Beijing (in Chinese).
Chen SH, Zhang GH, Zhou XH et al (1998) Petrological investigations on the granulite xenoliths from Hannuoba basalts, Northern Sino-Korean carton. Acta Petrologica Sinica 14(3): 366–380 (in Chinese with English abstract).
Chen WJ, Ge TM, Li DM et al (1992) The K-Ar magnetostratigraphic chronology of Cenozoic basalt in Hainan Island and Leizhou Peninsula. In: Liu RX (ed) The Age and Geochemistry of Cenozoic Volcanic Rock in China, Seismological Press, Beijing (in Chinese).
Chen WJ, Li Q, Hao J et al (1999) Postcrystallization thermal evolution history of Gangdise batholithic zone and its tectonic implication. Science in China D 42(1): 37–44.
Chen X, Xiao L (1999) Geochemistry research of Erentaolegai silver ore deposit, Inner Mongolia. Noble Metal Geology 8(3): 171–178 (in Chinese).
Chen XD, Lin CY (1997) Deformation characteristics of mantle inclusion and rhyological significance of upper mantle in Quaternary volcanic rock at Datong, Shanxi Seismology and Geology, 19(4): 313–320 (in Chinese with English abstract).
Chen XM, Lu JJ, Liu CS et al (1999) Single zircon U-Pb age in Tonglu–Xiangshan volcanic–intrusion complex. Acta Petrologica Sinica 15(2): 272–278 (in Chinese with English abstract).
Chen Y, Wu TR, Xu X et al (2004) Discovery and significance of Miocene ultra-potassium olivine basalt with deep source inclusion in Dongbahao, Siziwangqi, Inner Mongolia. Journal of Geology of Universities 10(4): 586–593 (in Chinese with English abstract).
Chen YX, Chen WJ, Zhou XH (1997) Mesozoic volcanic rock in western Liaoning and adjacent area. Seismological Press, Beijing (in Chinese with English abstract).
Chen YH et al (1998) Meso-Cenozoic Extensional Tectonics and Uranium Metallogenesis in Southeast China. Atomic Energy Press, Beijing (in Chinese).
Chen ZH, Mao DB, Zuo YC et al (2004) Mesozoic magmatic intrusion–mineralization system in Beichagoumen. Journal of Earth 23(4): 224–228 (in Chinese with English abstract).
Cheng YQ (1994) An Introduction to Regional Geology of China. Geological Publishing House, Beijing (in Chinese).
Chi JS (1988) The Study of Cenozoic Basalts and Upper Mantle Beneath Eastern China (Attachment Kimberlites). China University of Geosciences Press, Wuhan (in Chinese with English abstract).
Chi JS, Lu FX, Zhao L et al (1996) The Kimberlites and Paleozoic Features of Lithospheric Mantle of North China Platform. Science Press, Beijing (in Chinese).
Chi XG, Li C, Jin W et al (1999) Cenozoic volcanic evolution and plateau uplift in Northern Xizang. Geological Review 45(Supplement): 978–986 (in Chinese).
Chu MJ, Wan TF, Li SB (1988) Tectonic Stress Field, Paleogeothermal and Metallogeny near Guacangshan area, Linhai, Zhejiang province. China University of Geosciences, unpublished report.
Compiling Group of Petroleum Geology (1991) Dagang Oil Field. Zhai et al. Petroleum Geology, Vol. 4, 92–95. Petroleum Industry Press, Beijing (in Chinese).
Compiling Group of Petroleum Geology (1993) Daqing Oil Field. Zhai et al. Petroleum Geology, Vol. 4 (A), 34–40. Petroleum Industry Press, Beijing (in Chinese).
Compiling Group of Petroleum Geology (1993) Jilin Oil Field. Zhai et al. Petroleum Geology, Vol. 2 (B), 12–15. Petroleum Industry Press, Beijing (in Chinese).
Compiling Group of Petroleum Geology (1993) Liaohe Oil Field. Zhai et al. Petroleum Geology, Vol. 3, 80–83. Petroleum Industry Press, Beijing (in Chinese).
Compiling Group of Petroleum Geology, Qinghai–Xizang Oil Province (1993) Petroleum Geology, Vol.14, 72–78. Petroleum Industry Press, Beijing (in Chinese).
Compiling Group of Petroleum Geology (1993) Shengli Oil Field. Zhai et al. Petroleum Geology, Vol. 6, Petroleum Industry Press, Beijing (in Chinese).
Compiling Group of Petroleum Geology, Coastal and Sea Areas (1993) Zhai et al. Petroleum Geology, Vol.16 (A), 175–176. Petroleum Industry Press, Beijing (in Chinese).

Cong BL, Zhang WH, Ye DN (1979) Research on Cenozoic basalt in North China fault-block. Acta Geologica Sinica 2: 112–124.
Cong BL, Wang QC (1994) Review of researches on ultrahigh-pressure metamorphic rocks in China Chinese Science Bulletin 39(24): 2068–2075.
Cong BL, Wang QC (1999) The Dabie-Sulu UHP rocks belt: review and prospect. Chinese Science Bulletin 44(12): 1074–1086.
Cui WY, Wang CQ, Wang SQ (1991) Geochemistry and metamorphism P-T-t path of the Archean Jianping metamorphic complex in western Liaoning province. Acta Petrologica Sinica 7(4): 13–26 (in Chinese with English abstract).
Cui Y (1989) Isotopic chronology and origin evolution of Hetai granite. Proceedings of 4th China Isotopic Conference, 58–59 (in Chinese).
Deng SX, Wang JH, Zhu BQ (2001) P-T-t path of metamorphism for the Julin Group and its geodynamical implications in Yuanmou, Yunnan Science in China D 44(7): 609–620 (in Chinese).
Deng WM (1995) Geological features of ophiolite and tectonic significance in the Karakorum-west Kunlun Mts Acta Petrologica Sinica 11(suppl.): 98–111 (in Chinese with English abstract).
Deng WM (1998) Cenozoic Intraplate Volcanic Rocks in the Northern Qinghai–Xizang Plateau. Geological Publishing House, Beijing (in Chinese).
Deng WM, Huang X, Zhong DL (1998) Alkali-rich porphyry and its relation with intraplate deformation of north part of Jinsha River belt in western Yunnan, China Science in China D 41(3): 297–305 (in Chinese with English abstract).
Deng WM, Sun HJ, Zhang YQ (2001) Petrogenesis of Cenozoic potassic volcanic rocks in Nangqen Basin. Scientia Geologica Sinica 36(3): 304–318 (in Chinese with English abstract).
Deng X, Chen MX, Wang JA et al (1997) Apatite fission-track analysis in the west region of north shelf in South China Sea. Acta Petrologica Sinica 13(4): 507–514 (in Chinese with English abstract).
Deng XG, Ting L, Liu XH et al (2000) Blueschist and its $^{40}Ar/^{39}Ar$ chronology in Gangmuri area, Middle Qiangtang, Qingzang Plateau. Chinese Science Bulletin, 45(21): 2322–2326 (in Chinese).
Department of Geology, Nanjing University (1981) South China Granitoids in different periods and their Mineralizations. Science Press, Beijing.
Ding L, Zhong DL (1999) Metamorphic characteristics and geotectonic implications of the high–pressure granulites from Namjagbarwa, eastern Tibet. Science in China D 42(5): 491–505.
Ding L, Zhong DL, Yin A et al (2001) Cenozoic structural and metamorphic evolution of the eastern Himalayan syntaxis (Namche Barwa). Earth and Planetary Science Letters, 192: 423–438.
Dong CW, Zhou XM, Li HM et al (1997) Mesozoic crust and mantle migmatization in Southeast Fujian: isotopic evidence of magmatic complex in Pingtan. Chinese Science Bulletin 42(9): 960–962.
Dong HG, Ming MZ, Zhang FS et al (1993) Research on olivine dislocation of mantle inclusion in Fanshan, Liuhe of Jiangsu. Geological Review 39(5): 459–464.
Dong SB (1986) Metamorphism of China and its Relationship with Crustal Evolution Geological Publishing House, Beijing (in Chinese).
Dong SW, Qiu RL (1993) Tectonism and Magmatism in Anqing–Yueshan Area Geological Publishing House, Beijing (in Chinese).
Dong SW, Liu XC (2002) Zercon U-Pb ages in granitic gneiss of eastern Dabieshan Geologica Scientica 37(2): 165–173 (in Chinese with English abstract).
Dong XB, Wang ZM, Tan CZ et al (1990) New paleomagnetic results from Yadong-Golmud geoscience transect and a preliminary study on the model of terranes evolution in Qinghai-Xizang plateau Bulletin of the Chinese Academy of Geological Sciences 21: 139–148 (in Chinese with English abstract).
Dong YP, Zhang GW, Lai SC et al (1999) An ophiolitic tectonic melange first discovered in Huashan area, south margin of Qinling Orogenic Belt and its tectonic implications. Science in China D 42(3): 292–302.
Dong ZX (1994) Kimberlite in China. Science Press, Beijing (in Chinese with English abstract).
Dorsett BH, Wilde SA, Liu JL (1996) A Pan-African granulite facies event in northeastern China: SHRIMP U-Pb zircon dating of the Mashan Group of Liumao, Heilongjiang Province. 30th IGC, Abstracts, 2: 552.
Du JG, Zhang JZ, Sun ML et al (1998) Isotopic composition of Helium in eclogite from the Dabie Mountains, central China and its geological significance. Chinese Science Bulletin 43(16): 1362–1366 (in Chinese with English abstract).
Du W, Han BF, Zhang WH et al (2005) Discovery and significance of peridotite inclusion and mega-crystal in Cenozoic basalt. Journal of Mineralogy and Petrology 25(1): 13–24 (in Chinese with English abstract).
Du YS, Collerson KD, Zhao JX et al (1999) Characteristics and petrogenesis of granulite enclaves in S-type granites in the junction of Guangdong and Guangxi provinces. Acta Petrologica Sinica 15(2): 309–314 (in Chinese with English abstract).
Du YS, Che QJ, Qin XL et al (2003) A review of progresses in research of xenoliths in granitoids. Bulletin of Mineralogy Petrology & Geochemistry, 22(4): 334–339 (in Chinese with English abstract).
Du YS, Qing XL, Li XJ (2004) Mesozoic mantle source magmatic underplating of Tonglin, Anhui–Evidences from great crystal and rock inclusion Journal of Petrology and Mineralogy 23(2): 109–116 (in Chinese with English abstract).
E ML, Zhao DS (1987) The Cenozoic Basalts and Deep-derived Rock Xenoliths of Eastern China. Science Press Beijing (in Chinese).

Fan QC, Liu RX, Zhang GH et al (1998) Original Evolution of Bimodal Volcanic Rock at Wangtian'e, Changbaishan. Acta Petrologica Sinica 14(3): 305–317 (in Chinese with English abstract).
Fan QC, Shui JL, Liu RX (2001) Sr, Nd isotopic geochemistry characteristics and magmatic evolution in Wudalianchi, Tianchi and Tengchong volcanic rocks. Journal of Mineralogy and Petrology 20(3): 233–238 (in Chinese with English abstract).
Fan QC, Sun Q, Li N et al (2004) Volcanism by stages and Holocene magmatic evolution in North Hainan Island. Acta Petrologica Sinica 20(3): 533–544 (in Chinese with English abstract).
Fan QC, Shui JL, Wang TH et al (2006) Eruption history and evolution of trachyte-basalt in Tianchi volcano, Changbaishan. Acta Petrologica Sinica 22(6): 1449–1457 (in Chinese with English abstract).
Fan SF, Zhou ZY, (1990) Paleo-geotemperature, Oil and Gas of Tarim. Science Press, Beijing (in Chinese).
Fang QH et al (1987) S-type granitic suite in Darongshan, Guangxi. Acta Petrologica Sinica 3: 23–34 (in Chinese with English abstract).
Fang QH, He SY (1988) Rare-earth elements geochemistry of granitic suite in Darongshan, Guangxi Journal of Guilin College of Metallurgical Geology, 8(3): 255–262 (in Chinese).
Fei GC, Li YG, Chen X et al (2006) Petrological chemistry characteristics of shallow source granite and discussion on mineralization Xinjiang Geology 24(3): 305–309 (in Chinese).
Feng YM, He SP (1995) Research for geology and geochemistry of several ophiolites in the north Qilian Mountains, China Acta Petrologica Sinica, 11(suppl.): 125–146 (in Chinese with English abstract).
Feng ZZ, Zhang QR, Huang SX et al (1991) Volcanic geology and its mineralization in Yongtai–Dehua areas of Fujian Journal of Nanjing Institute of Geology and Resources 9 (supplement): 1–100 (in Chinese with English abstract).
Fu JM, Ma CQ, Xie CF et al (2005) Determined A type aluvine granite and tectonic environment analysis in Jinjiling of Hunan. Geochemistry, 34 (3): 215–226 (in Chinese with English abstract).
Gao J, He GQ, Li MS et al (1996) Uplift mechanism of high–pressure metamorphic rocks, South Tianshan, Xinjiang Scientia Geologica Sinica 31(4): 365–374 (in Chinese with English abstract).
Gao TJ, Wang ZM, Wu KL et al (1999) Tectono-Magmatic Evolution and Metallogeny of Taiwan Strait and Its Adjacent Areas. Geological Publishing House, Beijing (in Chinese).
Gao TS, Tang JF, Zhou CT et al (1997) The discovery of eclogite dikes in low-greenschist facies volcaniclastic rocks of the Dabie Mountains. Chinese Science Bulletin 42(20): 1726–1729 (in Chinese with English abstract).
Gao YL, Wu XN, Zuo GC (1988) Ophiolitic features of Qingshuiquan in east Kunlun and their tectonic significances. Journal of Xi'an Institute of Geology and Mineral Resources, Chinese Academy of Geological Sciences (21): 17–28 (in Chinese).
Ge LS, Zhou YL, Li ZH et al (2003) Geochemistry characteristics and origin of Granite in Banazangbu and Jiagangxueshan areas, Tibet. Mineralogy and Petrology 23(2): 55–61 (in Chinese).
Ge LS, Deng J, Yang LQ et al (2006) Meso-Cenozoic intermediate-acid intrusion magmatism and tectonic evolution in Gangdise block of Tibet. Geology and Resource 15(1): 1–10 (in Chinese with English abstract).
Geng HY, Xu XS, O'Reilly SY et al (2006) Cretaceous volcanic-intrusion in western Guangdong and its geological significance. Science in China, D 36(7): 601–617 (in Chinese).
Geng YS, Shen QH (2000) Mineral evolution of pyroxenes of garnet mafic granulites in northwestern Hebei province. Acta Petrologica Sinica 16(1): 29–38 (in Chinese with English abstract).
Gong XF, Guan JQ (1998) Volcanic geological characteristics and evolution in lower and middle reaches of Nanxijiang, Southeast Zhejiang. Zhejiang Geology 14(1): 11–17 (in Chinese).
Gu CY, Hua RM, Qi HW (2006) Single zircon LA-ICP-MS U-Pb dating and whole rock Sr-Nd isotopic of Guposhan granite in Guangxi. Acta Geologica Sinica 80(4): 543–553 (in Chinese).
Guan YC, Wu HQ (1997) Characteristics of Baimajian ultra-unite and its origin. Anhui Geology 7(2): 26–35 (in Chinese).
Guo JH, Chen FK, Zhang XM et al (2005) Mesozoic magmatic intrusion and syn-collision–post-collision tectonics in Northern Sulu UHP belt, eastern China: Implications for SHRIMP zircon U-Pb dating. Acta Petrologica Sinica 21(4): 1281–1301.
Guo JH, Zhai MG, Li YG et al (1998) Contrasting metamorphic P-T paths of Archean highpressure granulites from the North China Craton: Metamorphism and tectonic significance. Acta Petrologica Sinica 14(4): 430–448 (in Chinese with English abstract).
Guo TY, Liang DY, Zhang YZ et al (1991) Geology of Ngari Tibet (Xizang). China University of Geosciences Press, Wuhan (in Chinese with English abstract).
Guo XS, Chen JF, Zhang X et al (2001) Nd isotopic composition of alkali magmatic complex in southeast Guangxi: South China Mesozoic mantle material uplift event. Acta Petrologica Sinica 17 (1): 19–27 (in Chinese with English abstract).
Guo ZJ, Zhang ZC, Wang JJ (1999) Sm-Nd isochron age of ophiolite along northern margin of Altun Tagh Mountains and its tectonic significance. Chinese Science Bulletin 44(5): 456–458.
Han BF, He GQ, Wang SG et al (1998) Postcollisional mantle-derived magmatism and vertical growth of the continental crust in north Xinjiang. Geological Review 44(4): 396–406 (in Chinese with English abstract).
Han BF, He GQ Wang SG (1999) Postcollisional mantle-derived magmatism, underplating and implications for basement of the Junggar Basin. Science in China D42 (2): 113–119 (in Chinese).

Han QJ, Shao JA (2000) Mineral chemistry and metamorphic p-t conditions of granulite xenoliths in Early Mesozoic diorite in Harkin region, eastern Inner Mongolia Autonomous Region, China. Earth Science 25(1): 21–27 (in Chinese with English abstract).

Han YJ, Zhang ZM, Liu Rong (1997) Fluid inclusions in coesite-bearing jadeite quartzite from Shuanghe, Anhui province. Earth Science 22(3): 322–326 (in Chinese with English abstract).

Harumoto A (1970) Volcanic rocks and associated rocks of Utsuryoto Island (Japan Sea). Geol. Surv. Japan, 15.

He GP, Ye HW (1992) The evolution of metamorphism in granulite facies terrane, eastern Hebei province Acta Petrologica Sinica 8(2): 128–135 (in Chinese with English abstract).

He GP, Ye HW, Xia SL (1994) The evolution of metamorphism and PTt paths of granulite facies terrane in Miyun, Beijing. Acta Petrologica Sinica, 10(1): 14–26 (in Chinese with English abstract).

He GP, Ye HW (1998) Two types of Early Proterozoic metamorphism and its tectonic significance in eastern Liaoning and southern Jilin areas. Acta Petrologica Sinica 14(2): 152–162 (in Chinese with English abstract).

He GQ, Shao JA (1983) Determination of Early Paleozoic ophiolite in southeastern Nei Mongol and their geotectonic significance. In: Contributions to the Project of Plate Tectonic in Northern China. (1): 243–250. Geological Publishing House, Beijing (in Chinese with English abstract).

He GQ, Li MS, Liu DQ et al (1994) Paleozoic Crustal Evolution and Mineralization in Xinjiang of China. People's Publishing House of Xinjiang, Xinjiang & Cultural Education Publishing House of Hongkong, Hongkong (in Chinese with English abstract).

He YN, Lin CY, Chen XD et al (1983) Research on Olivine dislocation in deep source inclusion of Dongtaigou, Wutaishan. Research on Petrology. Vol.3, 67–76. Geological Publishing House, Beijing.

He ZX, Zheng ZC, Zhu H (1998) A preliminary research on paleomagnetism of Paleozoic strata in the Hexizoulang massif. Geoscience 2(2): 186–193 (in Chinese with English abstract).

Hong DW, Guo WQ, Li GJ et al (1987) Miarolitic granite petrology and original evolution at coastal of Fujian. Beijing Science and Technology Press, Beijing (in Chinese with English abstract).

Hong DW, Xie XL, Zhang JS (2002) Geological significance of the Hangzhou–Zhuguangshan-Huashan high-ε_{Nd} granite belt. Geological Bulletin of China 21(6): 348–354 (in Chinese with English abstract).

Hong L, Xu ZB (1997) Magmatic series and tectonic evolution of Northern Qaidam. Tectonics and Mineralization 21(1): 41–50.

Hou ZQ, Qu XM, Wang SX et al (2003) Re-Os age of molybdenite in Gangdise porphyry copper zone of Xizang: timing of metallogenesis and dynamic background. Science in China D 33(7): 609–618.

Hu CQ, Zhong ZY (1982) Alkali olivine basalt and its mantle source inclusion at Qiong-Lei areas of Guangdong (an unpublished paper in Chinese).

Hu HZ, Li Y (2006) Restrict factor of Yanshanian magmatism to gold and silver mineralization in Xiong'ershan, western Henan. Mineralization and Geology 20(4–5): 427–429 (in Chinese with English abstract).

Hua RM (2005) Differential time between continental crust remeld granite and mineralization, and their geological influence. Geological Review 51(6): 27–33 (in Chinese).

Huang H, Li RA, Yang CX (1990) Geochronologic study for the metamorphic belt along the coast of Fujian province and its tectonic significance. Chinese Science Bulletin 35(9): 751–754.

Huang KN, Yang RY, Wang XC et al (1988) Preliminary research on trace element geochemistry of basalts in Emei Mountain, southwestern China. Acta Petrologica Sinica 4 (1): 49–60 (in Chinese).

Huang YH (1993) Mineralogical characteristics of phlogopite-amphibole-pyroxenite mantle xenoliths included in the alkali mafic-ultramafic subvolcanic complex from Langao County, China. Acta Petrologica Sinica 9(4): 367–378 (in Chinese with English abstract).

Huang ZL (1997) Magma process modelling of alkali ultrabasic complex in Jijia Yunnan. Tectonics and Mineralization 21(1): 24–31 (in Chinese with English abstract).

Jahn BM, Martineau F, Percat JJ et al (1986) Geochronology of the Tananao schist complex, Taiwan and its regional tectonic significance. Tectonophysics 125: 103–124.

Jahn BM (2004) The central Asian Orogenic Belt and growth of the continental crust in the Phanerozoic. In Malpas J et al (eds) Aspects of the Tectonic Evolution of China. 73–100. London: The Geological Society. Special Publication 226.

Ji JQ, Zhong DL, Chen MY et al (1998) The Semugou transpressional shear zone in Jianping metamorphic complex area, west Liaoning province, China: Implications for the Proterozoic intracontinental deformation. Scientia Geologica Sinica 33(3): 338–348 (in Chinese with English abstract).

Ji JQ, Zhong DL, DL et al (1998) Study on metamorphism of granulite-facies metamorphic rocks discovered in the Nabang area on the border between China and Burma. Acta Petrologica Sinica 14(2): 163–175 (in Chinese with English abstract).

Jia DC, Hu RZ, Lu Y (2003) Element geochemistry of volcanic rock and discussion on source characteristics in Rucheng basin, Southeast Hunan. Geoscience 17(2): 131–136 (in Chinese with English abstract).

Jia W, Zhu HZ, Shao JA (2002) The time and space distribution of Cenozoic basalts in Chifeng area, Inner Mongolia. Geological Review 48(3): 267–272 (in Chinese with English abstract).

Jiang GH, Hu RZ, Xie GQ et al (2005) Biotite geochemistry characteristics and influences of rock and ore deposit formation in Dajishan granite. Mineralogy and Petrology 25(5): 58–61 (in Chinese).

Jiang JL (2001) Two distinguish macro-volcanic zones of Late Jurassic in Fujian. Fujian Geology 20(4): 171–176 (in Chinese with English abstract).
Jiang JS, Chen YQ (1993) Cordierite gneisses in Mashan khondalite series, Northeast China. Acta Petrologica Sinica 9(4): 401–410 (in Chinese with English abstract).
Jiang LL, Xu ST, Wu WP et al (1998) The white schist assemblage in kyanite quartzite from the ultrahigh-pressure metamorphic belt, eastern Dabie Mountains. Chinese Science Bulletin 43(19): 1651–1655.
Jiang LL, Liu YC, Wu WP et al (1999) The deformation history and exhumation process of the UHPM rocks in the Dabieshan. Scientia Geologica Sinica 34(4): 432–441 (in Chinese with English abstract).
Jiang L, Zhou XH, Jin Q (2001) Estimation of ancient subsurface temperatures in Xihu depression with apatite fission tracks. Journal of the University of Petroleum (Edition of Science) 25(1): 30–33 (in Chinese with English abstract).
Jiang SH, Nie FJ, Chen WS et al (2006) ^{40}Ar–^{39}Ar isotopic chronology and fluid inclusion characteristics in Nanjinshan gold deposit of Beishan area. Geological Review 52(2): 124–133 (in Chinese with English abstract).
Jiang YH, Jiang SY, Zhao KD et al (2005) SHRIMP zircon U-Pb age of lamprophyre at East Liaoning Peninsula and restriction of beginning time for lithosphere thinning of Eastern China. Chinese Science Bulletin 50(19): 2161–2168 (in Chinese).
Jiangxi Geological Survey (1983) Basic characteristics of Granitoid and Relation to Tungsten Mineralization in Jiangxi Province (an unpublished paper in Chinese).
Jin BL, Zhang XY (1994) Research on Volcanic Geology of Changbai Mountains. Northeastern Korean Nationality Education Publishing House, Yanji (in Chinese).
Jin K, Xu WL, Wang QH et al (2003) Formation time and source area of grano-diorite in Huaiguang, Benfu: Zircon SHRIMP U-Pb chronology evidence. Journal of Earth 24(4): 331–335 (in Chinese with English abstract).
Jin SY, Pan SA (1998) Mantle-derived xenoliths of spinel-garnet iherzolite from Nushan and their implications for lithophysics. Earth Science 23(5): 475–479 (in Chinese with English abstract).
Jin W, Li SX, Liu XS (1991) A study of characteristics of Early Precambrian high-grade metamorphic rock series and their metamorphic dynamics in Daqinshan, Inner Mongolia Acta Petrologica Sinica 7(4): 27–35 (in Chinese with English abstract).
Jin WJ, Song HL, Ma WP (1997) Eclogites of the metamorphic mélange in Tongbai-western Dabie orogen. Scientia Geologica Sinica 6(2): 155–163.
Jin ZM, Yu RD, Yang WC et al (2003) Mantle source olivine inclusion in Donghaixian Jiangsu and its deep tectonic significance. Acta Geologica Sinica 77(4): 451–462 (in Chinese).
Jing LZ, Guo YJ, Ding CX (1995) Chronology of alkali rock and formation of alkali magma in Saima, Liaoning. Liaoning Geology 4: 257–271 (in Chinese with English abstract).
Kong H, Ma F, Huang DZ (2001) Deep rock section in Hunan area: Evidence from deep source inclusions. Journal of Institute of Technology of Guilin 21(3): 195–201 (in Chinese with English abstract).
Kong H, Ma F, Jin ZM et al (2001) Olivine microstructures from mantle-derived xenolith in Pingnan county, Guangxi. Earth Science 26(1): 7–12 (in Chinese with English abstract).
Lai SC, Deng JF, Zhao HL (1996) Volcanism and tectonic setting during Ordovician period on north margin of Qaidam. Journal of Xi'an College of Geology 18(3): 8–14 (in Chinese with English abstract).
Lai SC, Deng JF, Zhao HL (1996) Paleozoic ophiolites and its tectonic significance on the north margin of Qaidam basin. Geoscience 10(1): 18–28 (in Chinese with English abstract).
Lai SC (1999) Petrogenesis of the Cenozoic volcanic rocks from the northern part of the Qinghai-Tibet Plateau. Acta Petrologica Sinica 15(1): 98–104 (in Chinese with English abstract).
Lai ZZ, Wang AC (1996) The Mesozoic volcanic ages and the source of magma in south Jiangxi. Geology of Jiangxi 10(2): 111–118 (in Chinese with English abstract).
Li C (1997) The $^{40}Ar/^{39}Ar$ age and its significance of the crosstie from blueschists in the mid-Qiangtang Area, Tibet. Chinese Science Bulletin, 42(1): 88 (in Chinese).
Li CN, Wang FZ, Zhong CS (2005) Geochemistry of Quaternary basaltic volcanic rocks and its characteristics of source area in Weizhou Island, Beihai, Guangxi. Journal of Mineralogy and Petrology 24(1): 1–11 (in Chinese with English abstract).
Li GM, Rui ZY (2004) The ages of metallogenesis and petrogenesis of porphyry copper deposits in Gangdise metallogenic zone of Xizang. Tectonics and Metallogeny 28(2): 165–170 (in Chinese with English abstract).
Li HK, Lu SN, Zhao FQ et al (1999) Determination and significance of the coesite eclogite on the Yuqia River on the north margin of the Qaidam basin. Geoscience 13(1): 43–50 (in Chinese with English abstract).
Li HM, Mao JW, Zhang G et al (2006) Alternation zoning of basaltic copper deposits, hydrocarbon inclusion characteristics, and their geological significance at boundary between Yunnan and Guizhou. Acta Geologica Sinica 80(7): 1026–1034.
Li JZ, Zhang AM (1997) Original type and magmatic evolution characteristics of Mesozoic granite in Jinzhai-Suxian area of Northern Huaiyang. Geoscience 11(2): 253–260 (in Chinese with English abstract).
Li JH, Zhai MG, Li YG et al (1998) The discovery of Mesoarchean high-pressure granulites in Luanping-Chengde area, Northern Hebei, and their tectonic implication. Acta Petrologica Sinica 14(1): 34–41 (in Chinese with English abstract).

Li JY (1995) Main characteristics and emplacement processes of the east Junggar ophiolites, Xinjiang, China. Acta Petrologica Sinica 11(suppl.): 73–84 (in Chinese with English abstract).
Li JY (1996) The timing and special distribution of ophiolites in China. In: Zhang Q (ed) Study on the Ophiolites and Geodynamics. Geological Publishing House, Beijing (in Chinese with English abstract).
Li JJ, Shen BF, Li HM et al (2004) Single grain zircon U-Pb age of granitodioritic gneiss in Bayan'ula Shan area,Western Inner Mongolia Geological Bulletin 23(12): 1243–1245.
Li SZ, Han ZZ, Liu Yongjiang et al (2001) Regional metamorphic features of Liaohe Group and its geodynamic significance. Geological Review 47(1): 9–18 (in Chinese with English abstract).
Li S (1990) Discussion on genetic type of Tiantangzhai granite from Dabie Mountains, Hubei province. Acta Petrologica Sinica 6(3): 65–71 (in Chinese with English abstract).
Li S (1991) Age and genesis of the alkaline rocks in northern Hubei province. Acta Petrologica Sinica 7(3): 27–36 (in Chinese with English abstract).
Li SG, Chen YZ, Zhang GW et al (1991) A 1Ga Alpine peridotite body emplaced into the Qinling group: evidence for the existence of the Neoproterozoic plate tectonics in the north Qinling area. Geological Review 37(3): 235–242 (in Chinese with English abstract).
Li SG, Zhang ZM, Zhang QD et al (1993) The zircon U-Pb ages of Qingdao eclogite and gneiss in Jiaonan Group–evidence of magmatic event of Jinning stage in Jiaonan Group. Chinese Science Bulletin 38(19): 1773–1777.
Li TF, Ma HW, Bai ZM (1999) Temperature and pressure states of spinel-garnet transition zone beneath Hannuoba area. Geoscience 13(1): 66–72 (in Chinese with English abstract).
Li WD, Mao JR, Zhu YH et al (1998) Mesozoic magmatism and Ore Deposits of Southeast China. Seismological Press, Beijing (in Chinese with English abstract).
Li WP, Li XH (2004) Origin and its significance of Middle-Late Jurassic intermediate-acid volcanic rocks, in middle Yanshan orogenic zone Acta Petrologica Sinica 20(3): 247–254 (in Chinese with English abstract).
Li WX, Xu XS, Zhou XM et al (1998) Epidote granite in the "Xingzi Complex"of Lushan mountain: dating and genesis. Geological Review 44(2): 143–148 (in Chinese with English abstract).
Li XH, Chen ZG, Liu DY et al (2003) Jurassic gabbro-granite-syenite suites from southern Jiangxi Province, SE China: Age, origin and tectonic significance. Int. Geol. Rev. 45: 898–921.
Li XH, Chung SL, Zhou HW et al (2004) Jurassic intraplate magmatism in southern Hunan-eastern Guangxi: ^{40}Ar / ^{39}Ar dating, geochemistry, Sr-Nd isotopes and implications for tectonic evolution of SE China. In: Malpas J, Fletcher CJ, Aitchison JC et al (eds) Aspects of the Tectonic Evolution of China. Geological Society, London, Special Publications, 226: 193–216.
Li XD, Wang QM, Wang KZ (1998) New information of post-collisional evolution of the Tianshan mountains-evidence from dynamic metamorphic rocks from the middle sector of Awulale range. Geological Review 44(4): 443–448 (in Chinese with English abstract).
Li XQ, Chen JD, Pan MB et al (1999) Petrological suits of Mesozoic intrusion in Chengtou area, Ganyu, Jiangsu. Jiangsu Geology (2): 80–83 (in Chinese with English abstract).
Li XY, Fan LY (2006) Discovery and its significance of Late Mesozoic OIB type basalt in Western Qinling. Journal of Zhongshan University (Science) 45(3): 127–128 (in Chinese with English abstract).
Li YH, Li JC, Song HB et al (2001) Helium isotopic research of mantle inclusion and high pressure giant crystal in Cenozoic basalt of Eastern China. Science in China D 31(8): 641–647.
Li YS, Qin DX, Dang YT et al (2006) Basaltic mineralization of Gejiu tin deposit, Yunnan. Journal of Jilin University (Earth Science) 36(3): 326–335.
Li YJ, Xie QS, Luan XD et al (2004) Origin and tectonic significance of West Qinling Michuling magma belt. Xinjiang Geology 22(4): 374–377 (in Chinese with English abstract).
Li YZ (1995) Some common pattern for geological characters of Cenozoic volcanic rocks and development of volcanism in Eastern China. Mineralogy and Petrology 15(3): 1–7.
Liao QK (1991) Formation time of Darongshan-Shiwandashan granite batholith in Guangxi. Geology of Guangxi 4(4): 59–68 (in Chinese with English abstract).
Liao QA, Wang JN, Xue ZS et al (1999) Characteristics of two type basalts in Cretaceous Basins of Guangfeng, Jiangxi and its relationship of basin evolution. Acta Petrologica Sinica 15(1): 116–123 (in Chinese with English abstract).
Liao ZJ (1988) Late Cenozoic Volcano of Tengchong. In: Tong W, Zhang MT (eds) Geothermal of Tengchong. Science Press, Beijing (in Chinese).
Liao ZL, Mo XX, Pan GT et al (2003) Distribution of ultra-alumina granite and its significance in south Tibet Sedimentary and Tethys Geology 23(3): 12–20 (in Chinese with English abstract).
Lin CY, Shi LB, Chen XD et al (1995) Rheological features of garnet lherzolite xenoliths from Xinchang, Zhejiang province, China and their geological implications. Acta Petrologica Sinica 11(1): 55–64 (in Chinese with English abstract).
Lin HF, Shen WC, Huang XL (1999) Nd-Sr isotopic characteristics of granitoid and their significances in Fujian. Acta Petrologica Sinica 15(2): 255–262 (in Chinese with English abstract).
Lin Q, Ge WC, Wu FY et al (2004) Granitoid geochemistry of Mesozoic in Dahingganling. Acta Petrologica Sinica 20(3): 403–412 (in Chinese with English abstract).

Ling HF, Shen WC, Huang XL (1999) Nd-Sr isotopic characteristics of granitoid and their significances in Fujian. Acta Petrologica Sinica 15(2): 255–262 (in Chinese with English abstract).
Liu AP, Jin JF (1996) Research on zircon typomorphic characteristics in Muhuguan granite. Geology and Geochemistry 4: 15–20 (in Chinese with English abstract).
Liu BJ, Xu XS, Pan XN et al (1993) Sedimentation, Crustal Evolution and Metallogenesis of Paleo-continent in South China. Science Press, Beijing (in Chinese).
Liu BG, Zheng GC, Chen SM et al (1995) The zircon U-Pb isotopic dating and its significance for pre-Cambrian volcanic rocks, western Zhejiang. Chinese Science Bulletin 40(21): 2015–2016 (in Chinese).
Liu CS, Chu XJ, Shen WZ et al (1992) The discovery and genetic significance of Al-rich minerals in Mesozoic volcanic rocks of Dongxiang-Xiangshan, Jiangxi province. Geological Review 38(2): 157–163 (in Chinese with English abstract).
Liu GH, Zhang SG, You ZD et al (1993) Main Metamorphic Rock Groups and Metamorphic Evolution of Qinling Orogenic Belt. Geological Publishing House, Beijing (in Chinese).
Liu HF, Xu YG (2006) Mineralogy and geochemistry characteristics of two kinds of pyroxene inclusion in Cenozoic basalt at Yangyuan, Hebei. Tectonics and Mineralization 30(1): 52–62 (in Chinese with English abstract).
Liu JB, Ye K, Cong BL et al (2001) Coesite inclusions in zircon from gneisses identified by laser raman microspectrometer in ultra-high pressure zone of Dabie Mountains, China. Chinese Science Bulletin 46(22): 1912–1916.
Liu JQ (1983) Research on Cenozoic volcanism at Changbaishan area. Institute of Geology, Academic of China, Proceedings of Master Thesis, 1981. Beijing Science and Technology Press, Beijing (in Chinese with English abstract).
Liu JQ (1999) China Volcano. Science Press, Beijing (in Chinese).
Liu L, Zhou DW (1994) Discovery and preliminary study on highpressure basic granulite at Songshugou, Shannan, East Qinling Chinese Science Bulletin 39(17): 1599–1601 (in Chinese).
Liu L, Che ZC, Luo JH et al (1997) Recognition and implication of eclogite in the western Altun Mountains, Xinjiang. Chinese Science Bulletin 42(11): 931–934.
Liu L, Che ZC, Wang Y et al (1998) The evidence of Sm-Nd isochron age for the Early Paleozoic ophiolite in Mangya area, Altun Mountains. Chinese Science Bulletin 43(9): 754–756.
Liu L, Che ZC, Wang Y et al (1999) The petrological characters and geotectonic setting of high-pressure metamorphic rock belts in Altun Mountains. Acta Petrologica Sinica 15(1): 57–64 (in Chinese with English abstract).
Liu L, Sun Y, Xiao PX et al (2002) Discovery of ultrahigh-pressure magnesite-bearing garnet lherzolite (>3.8GPa) in the Altun Tagh, Northwest China. Chinese Science Bulletin 47(11): 881–886.
Liu RX, Yang ME, Xu HJ et al (1981) Primary research of ultramafic inclusion in Cenozoic alkali basalt for North China. Seismology and Geology 3(3, 4): 1–16, 39–48 (in Chinese with English abstract).
Liu RX, Chen WJ, Xie GX et al (1992) The Chronology and Geochemistry of Cenozoic Volcanic Rock in China. Seismological Press, Beijing (in Chinese).
Liu RX, Fan QC, Li HM et al (1995) Chronology research for highpressue metamorphism of garnet peridotite-eclogite in Bixiling, Dabieshan. Chinese Science Bulletin 40(14): 1304–1306 (in Chinese).
Liu SG, Luo ZL, Dai SL et al (1995) The uplift of the Longmenshan thrust belt and subsidence of the western Sichuan foreland basin. Acta Geologica Sinica 69(3): 205–214 (in Chinese with English abstract).
Liu SW, Liang HH (1997) Metamorphism of Al-rich gneisses in Taihang Mountain Archean metamorphic complex. Acta Petrologica Sinica 13(3): 303–312 (in Chinese with English abstract).
Liu SW, Zhang JJ, Zheng YD (1998) Syn-deformation P-T paths of Xiaoqinling metamorphic core complex. Chinese Science Bulletin 43(22): 1927–1934.
Liu SW, Guo ZJ, Zhang ZC et al (2004) Characteristics of Pre-Cambrian metamorphic block in eastern part of Middle Tianshan: the restrain of geochronology and Nb isotopic geochemistry. Science in China D 34(5): 395–403 (in Chinese).
Liu WJ, Zhai MG, Li YG (1998) Metamorphism of the high-pressure basic granulites in Laixi, eastern Shandong, China. Acta Petrologica Sinica 14(4): 449–459 (in Chinese with English abstract).
Liu X (1999) Cenozoic volcanic structural controlling and volcanic hazard. World Geology 2: 23–29.
Liu XH (1990) Researches of Miocene potassium basalts of Shangzhi area, Heilongjiang province. Acta Petrologica Sinica 6(3): 53–64 (in Chinese with English abstract).
Liu XH, Wang JR, Sun XL et al (2006) Research on granite and gold mineralization in Zhaoyuan-Yexian ore fields. Color Metal 58(4): 15–20 (in Chinese).
Liu Y, Yang ZQ, Wang M (2007) History of zircon growth in a high-pressure granulite within the Eastern Himalayan syntaxis, and tectonic implications. International Geology Review 49: 861–872.
Liu YC, Xu ST, Li SG et al (2003) Tectonic setting and cooling history of eclogites from Northern Dabie Mountains. Earth Science 28(1): 11–16 (in Chinese with English abstract).
Liu YJ, Ye HW, Ge XH et al (2001) Laser probe $^{40}Ar/^{39}Ar$ dating of mica on the deformed rocks from Altun Fault and its tectonic implication, western China. Chinese Science Bulletin 46(4): 322–325.
Liu YS, Zhao CH (1991) Discovery of fresh garnet lherzolite xenolith in Penjiabang kimberlite pipe in Dahongshan area, Hubei province. Geological Science & Technology Information 10(suppl): 109–116 (in Chinese with English abstract).
Liu YX, Sun DY, Liu PJ (1995) The upper Archean enslavement of magnesioriebechites-bearing gneiss in Liaoning province: Old glaucophane-schist relict. Acta Petrologica Sinica 11(1): 83–92 (in Chinese with English abstract).

Liu ZQ, Li XZ, Ye QT et al (1993) Division of Tectonic Magma Belt in Sanjiang Area (Hengduanshan) and its Distribution of Mineral Resources. Geological Publishing House, Beijing (in Chinese).
Lou YE, Du YS (2006) Characteristics and original discussion of biotite in Mesozoic intrusion of Fanchang-Tongling, Anhui. Journal of Mineralogy 26(2): 175–180 (in Chinese).
Lu FX, Deng JF, E ML (1981) Discussion on magma original problem of alkali basalt in Huangyishan, Guandian, Liaoning. Geochemistry 1: 183–196 (in Chinese with English abstract).
Lu FX, E ML, Deng JF (1983) Ultramafic inclusion and mega-crystal in alkali basalt of Huangyishan, Guandian, Liaoning. Research on Petrology, No.3. Geological Publishing House, Beijing (in Chinese with English abstract).
Lu FX, Zhu QW, Xie YH et al (1996) Discovery of highpressure pyroxene megacrystal in dacite and their significance. Earth Science 21(5): 541–545 (in Chinese with English abstract).
Lu FX, Zhu QW, Li ST et al (1997) Mesozoic volcanism surrounding Songliao basin, China: implication for the relationship with evolution of basin. Journal of China University of Geosciences 8(1): 72–77.
Lu FX, Zheng JP, Wang FZ et al (1997) The comparison of composition and thermal condition of paleo-mantle in North China Craton, Yangtze Craton and Qinling orogenic belt. Earth Science 22(3): 247–251 (in Chinese with English abstract).
Lu FX, Wang CY, Zheng JP et al (2004) Lithospheric composition and structure beneath the northern margin of the Qinling orogenic belt-on deep-seated xenoliths in Mingguang region of Henan province. Science in China D 47(1): 13–22.
Lu LZ, Dong YS (1998) The P-T-X phase relations and their evolution for the equilibrium assemblages of Al-rich gneisses from Early Proterozoic Jingshan Group in east Shandong. Acta Petrologica Sinica 14(2): 140–151 (in Chinese with English abstract).
Lu MJ (1986) Early Proterozoic metamorphic rock series, west Sichuan and east Yunnan, China. Journal of Changchun College of Geology 45(3): 12–22 (in Chinese with English abstract).
Luo XH (2006) Mesozoic magmatism and its tectonic significance in Jiujiang–Ruichang areas. Journal of Technology Institute of East China 29(2): 121–126 (in Chinese with English abstract).
Luo ZH (1984) Research on Ultramafic rock inclusion in Dayishan basalt of Huinan, Jilin. Earth Science 1: 73–80 (in Chinese with English abstract).
Luo ZH, Xiao XC, Cao YQ et al (2001) The Cenozoic mantle magmatism and motion of lithosphere on the north margin of the Tibetan Plateau. Science in China D 44(suppl.): 10–17.
Luo ZK, Miao LC (2002) Granites and Gold Deposits in Zhaoyuan-Laizhou Area, Eastern Shandong Province. Metallurgical Industry Press, Beijing (in Chinese).
Ma CQ, Yang KG, Tang ZH et al (1995) Formation and differential rock uplift—exhumation of high-pressure metamorphic terrane in Dabie mountains, Central China: evidence from igneous rocks. Earth Science 20(5): 515–520 (in Chinese with English abstract).
Ma CQ, Ming HL, Yang KG (2004) Ordovician magmatic arc in north margin of Dabieshan : Chronology and geochemistry evidence of intrusion. Acta Petrologica Sinica 20(3): 393–402 (in Chinese with English abstract).
Ma HW (1990) Petrology and Mineralization of Granites in Yulong Porphyry Copper Belt, Tebet. China University of Geosciences Press, Wuhan (in Chinese with English abstract).
Ma JL, Xu YG (2006) Sr-Nd isotopic characteristics of mantle source inclusion in Yangyuan, Hebei indicated the existing of EMI type paleo-rich mantle in central North China craton. Chinese Science Bulletin 51(10): 1190–1196 (in Chinese).
Ma TQ, Kuang J, Bo DY et al (2006) Granite geochemistry characteristics and their analysis of formation tectono-environment at south Zhuguangshan of Middle Nanling. China Geology 33(1): 119–131 (in Chinese).
Mao JR (1994) The Mesozoic-Cenozoic magmatism and geodynamics of crustal and mantle evolution in southeast China. Volcanology & Mineral Resources 15(2): 1–11 (in Chinese with English abstract).
Mao JR, Tao KY, Li JY et al (2002) Mesozoic grano-diorite characteristics and its tectonic evolution in Southwest Fujian. Journal of Petrology and Mineralogy 21(2): 135–142 (in Chinese with English abstract).
Mei HL, Yu HF, Li Q et al (1998) The first discovery of eclogite and Paleoproterozoic granitoids in the Beishan area, northwestern Gansu Province, China. Chinese Science Bulletin 44(4): 356–361.
Mei HL, Li HM, Lu SN et al (1999) The age and origin of the Liuyuan granitoid, northwestern, Gansu. Acta Petrological et Mineralogical 18(1): 14–17 (in Chinese with English abstract).
Meng FC, Li TF, Xue HM et al (2006) Contrast with two Late Cretaceous basic magma (Zhucheng and Jiaozhou basalts, in Jiaolai Basin) formed in different mantle sources. Acta Petrologica Sinica 22(6): 1644–1656 (in Chinese with English abstract).
Mo XX (1991) Volcanism and the evolution of Tethys in Sanjiang area, southwestern China. In: Proceedings of 1st International Symposium on Gondwana Dispersion and Asian Accretion, 51–56. Kunming, China.
Mo XX, Lu FX, Sheng SY et al (1993) Sanjiang Tethyan Volcanism and Related Minerali-zation. Geological Memoirs (20): 267. Geological Publishing House, Beijing (in Chinese).
Mo XX, Sheng SY, Zhu QW et al (1998) Volcanic-Ophiolite and Mineralization of Middle-Southern Part in Sanjiang Area of Southeast China. Geological Publishing House, Beijing (in Chinese with English abstract).
Niu BG, Fu YL, Liu ZG et al (1993) $^{40}Ar/^{39}Ar$ dating of glaucophane and its geological significance of North Hubei. Chinese Science Bulletin 38(14): 1309–1313 (in Chinese).

Niu HC, Xu JF, Yu XY et al (1999) Discovery of Mg-rich volcanic rock series in western Altay area, Xinjiang. Chinese Science Bulletin 47(18): 1685–1688 (in Chinese with English abstract).
Niu ML, Zhu G, Song ZZ et al (2001) Mantle characteristis and its evolution of Cenozoic basalt source area at middle and southern sections of Tancheng–Lujiang fault zone. Geosciences 15(4): 383–390 (in Chinese with English abstract).
Niu ML (2006) Compare research on rare earth elements of Early Cretaceous volcanic rock in south margin of Zhangbaling uplift area. Journal of Rare Earth Element in China 24(6): 739–744 (in Chinese with English abstract).
Niu SY, Chen L, Xu CS et al (1994) The Crustal Evolution and Metallogenic Regularity of the Taihangshan Area. Seismological Press, Beijing (in Chinese with English abstract).
Pan CC, Zhou ZY, Fan SF et al (1996) Thermal history of Tarim basin. Bulletin of Mineralogy Petrology & Geochemistry 15(3): 150–152, 177 (in Chinese with English abstract).
Pan GT, Chen ZL, Li XZ et al (1997) Geological-Tectonic Evolution in the Eastern Tethys. Geological Publishing House, Beijing (in Chinese with English abstract).
Pan SA (1989) Research on Mantle-derived ultra-mafic xenoliths in Mid-Tanlu Fault Zone and Damaping, Hebei. Dissertation, China University of Geosciences, Wuhan (in Chinese with English abstract).
Pei FP (2004) Mesozoic basalt and mineral-chemistry of crystal inclusion of mantle source: restrict to character of lithosphere mantle. Journal of Geology of Universities 10(1): 88–97 (in Chinese with English abstract).
Peng LG, Liu RX, Fan QC (1994) Fluid and melt inclusion researches of pyrolite xenoliths from the shore of southeastern China. Acta Petrologica Sinica 10(4): 440–448 (in Chinese with English abstract).
Peng LH (1984) Geological time of Ophiolite suite at south zone of Udormiao Group, Inner Mongolia and its tectonic significance. Chinese Science Bulletin 29: 104–107 (in Chinese).
Peng PT, Wang YJ, Peng BX et al (2006) Geochemistry characteristics and its original significance of Paleogene basalt in Yingjiashan, Northeast Hubei. Geochemistry 35(4): 395–404 (in Chinese with English abstract).
Peng SB, Jin ZM, Zheng BR (1990) Study on the microstructure features of deep-seated xenoliths and their rheological significance of the upper mantle in Cenozoic basaltic rocks from southeastern coastal region of China. In: Division of Mineralogy, Petrology and Geochemistry, Geological Society of China. Contribution to the Features of Upper Mantle and Dynamics in China, 112–123. Seismological Press, Beijing (in Chinese).
Qi JY (1992) Metamorphic rock series of Taihua Group and conditions for its formation in eastern Qingling. Scientia Geologica Sinica (suppl.): 94–107 (in Chinese with English abstract).
Qi JZ (2001) Metallogenesis research on gold deposit at Qiyugou, Henan province. Dissertation, China University of Geosciences, Beijing (in Chinese with English abstract).
Qi XX, Kuang HW, Chen PL et al (2002) Geochemistry characteristics and its geological significance of Yanshanian intrusion in lower and middle reaches of Yangtze River. Resource Survey and Environment 23(1): 52–59 (in Chinese with English abstract).
Qian XL, Wang RM (1994) Geological Evolution of Granulite Belt in North Part of North China. Seismological Press, Beijing (in Chinese).
Qin DX, Yan YF, Tian YL et al (2000) Geological characteristics and ore-forming evolution of Dahongshan copper deposit. Scientia Geologica Sinica 35(2): 129–139 (in Chinese with English abstract).
Qin JF, Lai SC, Bai L (2006) Rock origin and interaction between crust and mantle in Yangba body of Kangxian, Gansu. Journal of Earth Science and Environment 28(2): 11–18 (in Chinese with English abstract).
Qiu JS, Wang DZ, McInnes BIA (1999) Geochemistry and origin of I and A types granite complex in Coastal of Zhejiang and Fujian. Acta Petrologica Sinica 15(2): 237–246 (in Chinese with English abstract).
Qiu JS, Wang DZ, Zhou JC (1999) Geochemistry and rock origin of bimodal volcanic rocks during Late Mesozoic in Yunshan, Yongtai, Fujian. Journal of Petrology and Mineralogy 18(2): 97–107 (in Chinese with English abstract).
Qiu JS, Wang DZ, McInnes BIA (2000) Geochemistry and origin of aluminum A type granite in Coastal of Fujian. Geochemistry 29(4): 313–321 (in Chinese with English abstract).
Qiu JX, Zeng GC, Wang SY et al (1995) Early Paleozoic volcanic rocks in Lajishan orogenic zone of Qinghai. Geological Science of Northwest China 16(1): 70–82 (in Chinese with English abstract).
Qiu JX, Wang RJ, Li CN et al (1997) Potassium-rich Volcanic Rocks in Wudalianchi-Keluo–Erkeshan. China University of Geosciences Press, Wuhan (in Chinese with English abstract).
Qiu JX, Zhang ZF (1997) Experiment, composition and tectonic opening-closing of Early Palaeozoic marine volcanic rocks from northern Qinling Mountains, China. Earth Science 22(3): 233–239 (in Chinese with English abstract).
Qiu YX, Chen HJ (1993) Professional Papers for the Geological Structure of Yunkaidashan and Its Adjacent Areas. Geological Publishing House, Beijing (in Chinese with English abstract).
Ren ZL, Zhao ZY, Zhang J et al (1994) Research on paleotemperatures in the Ordos basin. Acta Sedimentologica Sinica 12(1): 56–65 (in Chinese with English abstract).
Ren ZL (1996) Research on the relations between geothermal history and oil-gas accumulation in the Ordos basin. Acta Petrologica Sinica 17(1): 17–24 (in Chinese with English abstract).
Ren ZL, Zhao ZY, Chen G et al (1999) Tectonic thermal events of Late Mesozoic in Qinshui basin. Oil & Gas Geology 20(1): 46–48 (in Chinese with English abstract).
Ren ZL, Liu CY, Zhang XH et al (2000) Recovery and comparative research of thermal history on Jiuquan basin group. Chinese Journal of Geophysics 43(5): 635–645 (in Chinese with English abstract).

Ren ZL, Liu CY, Feng JH et al (2000) Research on geothermal history of Bayindulan depression in Erlian basin. Acta Petrolei Sinica 21(4): 42–45 (in Chinese with English abstract).
Ren ZL (2000) Comparison of thermal evolution history in sedimentary basins, north China. Oil & Gas Geology 21(1): 33–37 (in Chinese with English abstract).
Ren ZL, Xiao DM, Chi YL (2001) Restoration of the palaeogeothermal in Songliao basin. Petroleum Geology & Oilfield Development in Daqing 20(1): 13–14 (in Chinese with English abstract).
Seno T (1977) The instantaneous rotation vector of the Philippine Sea Plate relative to the Eurasian Plate. Tectonophysics 42(2–4): 209–226.
Seno T, Maruyama S (1984) Paleogeographic reconstruction and origin of the Philippine Sea. Tectonophysics 102(1–4): 53–84.
Shang RJ, Yan Z, Huang YY et al (1988) Granite in Qinling and Dabashan. China University of Geosciences Press, Wuhan (in Chinese).
Shao JA, Zhang LQ, Mou BL (1998) Tectono-thermal evolution of middle-south section of the Da Hinggan Mountains. Science in China D 41(6): 570–579.
Shao JA, Zhang LQ, Wei CJ et al (2001) The composition and its characteristics of bimodal dyke swarm of Mesozoic at Nankou, Beijing. Acta Geologica Sinica 75(2): 205–212 (in Chinese with English abstract).
Shao JA, Li XH, Zhang LQ (2001) Geochemical condition for genetic mechanism of the Mesozoic bimodal dike swarms in Nankou-Guyaju. Geochimica 30(6): 517–524 (in Chinese with English abstract).
Shao JA, Jia W, Chu ZY et al (2003) Early Cretaceous olivine–pyroxene minette volcanic pipe in Karaxin, Inner Mongolia. Acta Petrologica Sinica 19(3): 429–434 (in Chinese with English abstract).
Shao J, Li ZD, Zhang LQ (2004) Time and space symmetry distribution and significance of Mesozoic–Cenozoic volcanic rocks in western Liaoning and its adjacent areas. Geologica Scientia 39(1): 98–106 (in Chinese with English abstract).
She HQ, Wang YW, Li QH et al (2006) Characteristics of basic granulite inclusion and significance of mineralization dynamics in Caihulanzi Gold deposit of Chifeng, Inner Mongolia. Acta Geologica Sinica 80(6): 863–875.
Shen BF, Luo H, Han GG et al (1994) Archean Geology and Metallization in Northern Liaoning Province and Southern Jilin Province. Geological Publishing House, Beijing (in Chinese with English abstract).
Shen BM, Zhou YS, Deng WM et al (1996) Mantle-genetic tremolite in metamorphic perodotite from Kuda, China. Chinese Science Bulletin 41(18): 1,538–1,541 (in Chinese with English abstract).
Shen BM, Deng WM, Han XL et al (1996) The texture, mineral assemblage and genesis of metamorphic peridotite from Kuda ophiolite, Xinjiang with correct expression on partial melting of upper mantle and its product. Acta Petrologica Sinica 12(4): 499–513 (in Chinese with English abstract).
Shen GF, Lü BX (2000) Formation of Rocks and Ore Deposits of Cenozoic Intrusion in Hengduanshan Areas, Southwest China. Geological Publishing House, Beijing (in Chinese).
Shen QH, Xu HF, Zhang ZQ et al (1992) Early Precambrian Granulites of China. Geological Publishing House, Beijing (in Chinese).
Shen QH, Qian XL (1995) Assemblages, episodes and tectonic evolution in the Archaean of China. Episodes 18(1–2): 44–48.
Shen SY, Zhang BM et al (1994) Research on the volcanic characteristics of oceanic ridge-quasi ridge of Jinshajiang. Tethys Geology (18). Geological Publishing House, Beijing (in Chinese).
Shen WC, Zou HB, Chu XJ et al (1992) Nd, Sr and O isotopic study on Fuchuan ophiolite suite in Anhui province. Scientia Geologica Sinica (4): 333–341 (in Chinese with English abstract).
Shi RD, Yang JG, Wu CL et al (2004) First SHRIMP dating for formation of Late Sinian at Yushigou ophiolite, North Qilian Mountains. Acta Geologica Sinica 78(5): 649–657 (in Chinese).
Song B, Li JY, Niu BG et al (1997) Single-grain zircon ages and its implications in biotite-plagioclase gneiss in Mashan group in the eastern Heilongjiang. Acta Geoscientia Sinica 18(3): 306–312 (in Chinese with English abstract).
Su L, Song SG, Wang ZH (1999) CH_4-rich fluid inclusions in the Yushigou mantle peridotite and their implications, North Qilian Mountains, China. Chinese Science Bulletin 44(21): 1992–1995.
Su LS, Deng GH et al (2005) Geochemistry characteristics and its tectonic significance of alkali basalt in Jitai Basin, Jiangxi. Geoscience 19: 133–140 (in Chinese with English abstract).
Su SG, Wang RM, Gu Delin et al (1994) High-pressure metamorphism of eclogite country rocks, Jiaonan Group, Zhucheng district, Shandong province. Geoscience 8(1): 65–72 (in Chinese with English abstract).
Su SG, Lai XY, Zhang CL (1996) P-T evolution of granulites and their petrogenetic significance in Haiyangsuo and Gejiaji areas, Jiaodong. Geosciences 10(4): 455–460 (in Chinese with English abstract).
Su SG, Gu DL, Zhu GX (1997) The P-T diagram and its tectonic significance of granulite facies metamorphism in the Yishui area, Shandong province. Acta Petrologica Sinica 13(3): 331–345 (in Chinese with English abstract).
Su SG, Deng JF, Zhao GC (2006) Characteristics, origin, source region and thinning type of lithosphere Xuejiashiliang complex. Earth Science Frontier 13(2): 148–157 (in Chinese with English abstract).
Sun DY, Wu FY, Lin Q et al (2001) Origin of Baishishan intrusion and interaction between crust and mantle during Early Yashanian in Zhangguangcailing. Acta Petrologica Sinica 17(2): 227–235 (in Chinese with English abstract).
Sun FY (1994) Mesozoic-Cenozoic regional tectonic evolution and mineralization in Eastern Shandong. Journal of Changchun Institute of Geology 24(4): 378–384 (in Chinese with English abstract).

Sun MZ, Xu KQ (1990) On the Caledonian granitoids and their geotectonic environments of south China. Journal of Nanjing University (4): 10–22 (in Chinese with English abstract).
Sun WH, Lai ZM (1980) On the relationship of Cenozoic volcanic rock lithochemistry characteristics and structure in Fujian Province. Geochemistry 2: 134–147.
Sun XR, Zhou ZZ (1994) Petrogenesis of red corundum rocks from the northern Dabie Mountain, Anhui. Acta Petrologica Sinica 10 (3): 275–289 (in Chinese with English abstract).
Sun XM, Nie ZT, Liang DY (1994) On the time and tectonic significance of ophiolite melange in Jinsha River belt, northwest Yunnan. Geoscience 8(3): 241–245 (in Chinese with English abstract).
Sun XM, Zhang BM, Nie ZT et al (1997) Formation age and environment of ophiolite and ophiolitic mélange in the Jinshajiang belt, northwestern Yunnan. Geological Review 43(2): 113–120 (in Chinese with English abstract).
Sun XM, Xu KQ, Ren QJ et al (1992) Confirmation of the Jiapigou Archaean high grade metamorphic terrain and its geological significance. Chinese Science Bulletin 37(10): 847–850.
Sun XM, Wang PJ, Hao FJ et al (2005) Time–space distribution, migration and origin type of Mesozoic–Cenozoic regional fault system at middle area of continental margin of Eastern China. Journal of Jilin University (Geosciences) 35(5): 554–563 (in Chinese with English abstract).
Sun Y, Liu CY, Che ZC (1997) The Proterozoic rift volcanic series in the Lapeiquan area,the Altun mountains and its tectonic significance. Geological Review 43(1): 17–24 (in Chinese with English abstract).
Sun YF (1994) Mesozoic-Cenozoic regional tectonic evolution and mineralization in Eastern Shandong. Journal of Changchun Institute of Geology 24(4): 378–384 (in Chinese with English abstract).
Suo ST, Sang LK, Han YJ et al (1993) The Petrology and Tectonics in Dabie Precambrian Metamorphic Terranes, Central China. China University of Geosciences Press, Wuhan (in Chinese with English abstract).
Suo ST, Zhong ZQ, Zhang HF et al (2001) High-pressure metamorphic belt and its tectonic pattern in Tongbai Mountains, Central China. Earth Science 26(6): 551–559 (in Chinese with English abstract).
Suo ST, Zhong ZQ, Zhou HW et al (2003) Kanfenggou UHP metamorphic fragment in eastern Qinling orogen and its relationship to Dabie-Sulu UHP and HP metamorphic belts, Central China. J. China University of Geosciences 14(2): 95–102.
Tamaki K, Suyehiro K, Allan J et al (1992) Tectonic synthesis and implications of Japan Sea ODP drilling. Proc. Ocean Drill. Program Sci. Results 127–128: 1333–1348.
Tang HF, Zhou XM (1997) Geochemical constraints on the petrogenesis of basalts from eastern Jiangnan orogen, South China. Science in China D 40(6): 627–633.
Tang JF, Gao TS, Li HK (2004) Meso-Cenozoic tectonic framework, formation and evolution of Magmatic zone in Eastern China. Geological Survey and Research 27(2): 65–74 (in Chinese with).
Tao GY, Gao TJ, Lu ZG et al (1998) Basement Tectonics of Volcanic Rock and Volcanic-Intrusion Related to Mineralization of Coastal Area in Southeast China. Geological Publishing House, Beijing (in Chinese with English abstract).
Tian N, Yang YQ (1991) Geology, Geochemistry and genesis of gold deposits in ophiolitic mélange in northern Ailao Mountain, Yunnan. In: Contribution to the Geology of the Qinghai–Xizang (Tibet) Plateau. 21: 84–97. Geological Publishing House, Beijing (in Chinese with English abstract).
Wan TF (1984) Recent tectonic stress field, active faults and geothermal fields (hot water type) in China. Journal of Volcanology and Geothermal Research 22(3–4): 287–300.
Wan TF, Chu MJ, Chen MY, 1988. Thermal regimes of lithosphere and geothermal resources potential in Fujian province, China. Acta Geologica Sinica 62(2): 178–189.
Wan TF (1988) Silica heat flow in South China. Chinese Science Bulletin 33(8): 655–657.
Wan TF, Tong YF, Zheng WW (1989) Thermal structure of the lithosphere in Fujian, China. Journal of Geophysical Research B 94(2): 1888–1894.
Wan TF (1994) Intraplate deformation, tectonic stress and their application for Eastern China in Meso-Cenozoic. China University of Geosciences Press, Wuhan.
Wan TF, Teyssier C, Zeng HL et al (2001) Emplacement mechanism of Linglong granitoid complex, Shandong Peninsula, China. Science in China D 44(6): 535–544.
Wan TF, Wang YM, Liu JL (2008) Detachment and magmatic source depth in lithosphere of Eastern China during Yanshanian and Sichuanian stages. Earth Science Frontiers 15(3): 1–35 (in Chinese with English abstract).
Wang CQ, Cui WY, Kröner A et al (2000) Zircon isotopic ages from magnetite quartzites of the Jianping metamorphic complex, western Liaoning Province. Chinese Science Bulletin 45(6): 547–551.
Wang DZ, Zhou XM, Su LS et al (2002) Origin of Granitic volcanic-intrusion complex and crustal evolution during Late Mesozoic in Southeast China. Science Press, Beijing (in Chinese with English abstract).
Wang DY, Xu WL, Lan X et al (2004) Origin of pyroxenite inclusion in Mesozoic Gabbro-Diorite of Western Shandong. Journal of Jilin University (Earth Science) 34(2): 167–173 (in Chinese with English abstract).
Wang J, Li SQ (1987) The Langshan-Bayanobo rifting and its metallogenesis. In: Contributions on the Project of Plate Tectonic in Northern China, 2: 59–72. Geological Publishing House, Beijing (in Chinese with English abstract).
Wang J, Li SQ, Wang BL et al (1999) The Langshan-Baiyunebo Rift System. Peking University Press, Beijing (in Chinese with English abstract).

Wang JA, Deng X, Chen MX (1995) Analyses on Cenozoic thermal history and its features in west sector shelf of northern South China Sea. Scientia Geologica Sinica 30(3): 220–232 (in Chinese with English abstract).
Wang JH, Jiang BC, Kong XW et al (2006) Basic characteristics of Guposhan complex intrusion and relationship with mineralization. Mineralization and Geology 20(1): 47–53 (in Chinese with English abstract).
Wang JC (1994) A study on the time and tectonics of metamorphic rock in Yunkai Mountains. Journal of Nanjing University 6(1): 59–68 (in Chinese with English abstract).
Wang J, Huang SY, Huang GS et al (1990) Basic Characteristics of the Earth's Temperature Distribution in China. Seismological Press, Beijing (in Chinese with English abstract).
Wang J (1998) Uplift of the Karibasheng and Kuzigan granite in the west Kunlun mountains-evidence from apatite fission track analysis. Geological Review 44(4): 435–442 (in Chinese with English abstract).
Wang KH, Pei FP, Feng YS et al (2005) Discovered deep source inclusion and inclusion crystal and their mineral-chemistry of Mesozoic volcanic rocks in Mingyuegou Basin, Yanbian. Jilin Geology 24(2): 21–27 (in Chinese).
Wang KY, Li JL, Lin RQ (1991) Origin of the Fuping gneisses. Scientia Geologica Sinica (3): 254–267 (in Chinese with English abstract).
Wang KF (1991) Metamorphic event research of gold-bearing metamorphic rocks of Baoban Group in Hainan province. Hainan Geology and Geography (1): 9–12 (in Chinese).
Wang LS, Shi YS (1989) Geothermal Study on the Oil and Gas Basin-Tectonic and Thermal Evolution in Northern Jiangsu Basin and Its Evolution of Oil and Gas Resources. Nanjing University Press, Nanjing (in Chinese with English abstract).
Wang M, Dai CG, Mu SY et al (2006) Granite major elements characteristics and distinguish of tectonic environment in Yunwuling area, Xinjiang. Guizhou Geology 23(1): 5–11 (in Chinese with English abstract).
Wang Q, Zhao ZH, Jianping et al (2005) Chronology of Cretaceous A type granitoid or alkali intrusion in inland of South China and restrain for Late Mesozoic tectonic evolution in South China. Acta Petrologica Sinica 21(3): 795–808 (in Chinese with English abstract).
Wang QQ, Wang LK (1989) Physicochemical conditions for the formation of peraluminous granites at Darongshan Guangxi, China. Geochenica (4): 287–296 (in Chinese with English abstract).
Wang RM, Lai XY, Dong WD et al (1994) Some proof of Neoarchean collisional belt in northwestern Hebei province. In: Qian XL, Wang RM (eds) Geological Evolution of Granulite Belt in North Part of North China. Seismological Press, Beijing (in Chinese).
Wang RS, Zhou DW, Wang JL et al (1999) Variscan terrane of deep-crustal granulite facies in Yushugou area, southern Tianshan. Science in China D 42(5): 306–313.
Wang TG, Bao JP, Simoneit BRT (2002) Organic geochemical evidence for a regional stratigraphic thermal event in East China. Journal of Asian Earth Sciences 20(8): 913–920.
Wang YM, Wan TF (2008) Lithosphere Tectonic Detachments in Eastern China Control of Cenozoic Magmatism and Earthquake. Geoscience 22(2): 207–229.
Wang YB, Liu DY, Zeng PS et al (2004) Underplating chronology of mantle magma in Tongling, Anhui-Zircon SHRIMP dating in Chaoshan pyroxene diorite. Journal of Earth 25(4): 423–427 (in Chinese with English abstract).
Wang Y, Deng JF (2002) Petrochemical characteristics and geodynamic significance of the Yanshanian strongly per aluminous intrusive rocks in the Hebei-Shanxi-Liaoning area. Geological Bulletin of China 21(4–5): 270–276 (in Chinese with English abstract).
Wang YF, Xu GZ (1991) The characteristics of the metavolcanic rock series of Early Paleozoic era and the structural environment of their genesis in the northern part of the east Qingling-Tongbai-Dabie collision type orogenic belt. Acta Petrologica Sinica 7(1): 44–53 (in Chinese with English abstract).
Wang Y, Yu DG (2000) Trace elements geochemistry characteristics and origin of intermediate-acid volcano-intrusion complex of Early Cretaceous in Northeast Jiangxi. Jiangxi Geology 14(4): 251–255 (in Chinese with English abstract).
Wang YL, Wang X, Zhang Q (2004) Geochemistry characteristics and their mineralization–geodyna-mic influence of Mesozoic intermediate-acid intrusions in Tonglin area. Acta Petrologica Sinica 20(2): 325–338 (in Chinese).
Wang YS, Chen JN (1987) Metamorphic belts and metamorphism of Qinghai province and adjacent areas. Geological Memoirs. no.6. Geological Publishing House, Beijing (in Chinese).
Wang ZH, Lu HF (1997) $^{40}Ar/^{39}Ar$ geochronology and exhumation of mylonitized metamorphic complex in Changle-Nan'ao ductile shear zone. Science in China D 40(6): 641–647.
Wang ZJ, Yang QF, Yuan HH et al (1987) Some Basic Problems of Mesozoic Volcanic Geology in Zhejiang–Fujian–Jiangxi. Journal of Institute of Geology and Resources of Nanjing 8(3): 1–14 (in Chinese).
Wang ZW, Zhou YZ, Zhang HH et al (1999) Rare earth elements geochemistry of Silver deposit in Panxidong, western Guangdong. Gold Geology 5(2): 52–54 (in Chinese).
Wei CJ (1994) Metamorphism and its geological significance of the Bikou group in the Shanxi–Gansu-Sichuan border region. Acta Geologica Sinica 68(3): 241–254 (in Chinese with English abstract).
Wei CJ, Shan ZG (1997) Metamorphism of the Susong complex from the southern Dabie mountains, Anhui province. Acta Petrologica Sinica 13(3): 356–368 (in Chinese with English abstract).
Wei CJ, Wu YX, Ni YY et al (1999) Characteristics and geological significance of the eclogites from the Tongbai Mountains, Henan. Chinese Science Bulletin 47(22): 2076–2080 (in Chinese).

Wei CJ, Zhang CG, Zhang AL et al (2001) Metamorphic P-T conditions and geological significance of high-pressure granulite from the Jianping complex, western Liaoning province. Acta Petrologica Sinica 17(2): 269–282 (in Chinese with English abstract).
Wei DW (1989) Evolution of Paleogeothermal of Northeast Part of Tarim Basin, Xinjiang. Institute of Geomechanics. Geological Minerals Department of the People's Republic of China (an unpublished report in Chinese).
Wei JH, Liu CQ, Tang HF (2003) Trace element, isotopic evidence in syn-original magmatism of Yanshanian intrusions and gold mineralization at Wulong area of Liaoning. Geological Review 49(3): 265–271 (in Chinese).
Wu CL, Zhou XR, Huang XC et al (1998) Research on A type granite in Maotan, Anhui. Acta Geologica Sinica 72(3): 237–247 (in Chinese).
Wu CL, Yang JS, Xu ZQ et al (2001) The mineral chemistries of pyroxenite xenoliths in the volcanic rocks for Hoh Xil, and their significance. Science in China D44(suppl.): 128–138.
Wu CH, Zhong CT, Chen QA (1997) Discussion on the age of khondalite in Jin-Meng (Shanxi-Nei Mongol) high grade terrain. Acta Petrologica Sinica 13(3): 289–302 (in Chinese with English abstract).
Wu CH, Li HM, Zhong CT et al (2000) Timing U-Pb single zircon ages for the orthogneiss and the paragneiss of Fuping complex: implications for existence of the Palaeoproterozoic supracristal rocks in the central basement of north China craton. Progress in Precambrian Research 23(3): 129–139 (in Chinese with English abstract).
Wu GY (1986) Research on chronology of Guangning granite complex. Guangdong Geology 1: 1–22 (in Chinese).
Wu JS, Geng YS, Xu HF (1989) Metamorphic geology of Fuping Group. Journal of Institute of Geology, Chinese Academy of Geological Sciences 19: 213 (in Chinese).
Wu LR (1984) Meso-Cenozoic Volcanic Rocks in East China and Adjacent Areas. Science Press, Beijing (in Chinese).
Xia LQ, Xia ZC, Xu XY (1995) Dynamics of tectono-volcano-magmatic evolution from North Qilian Mountains, China. Northwest Geoscience 16(1): 1–28 (in Chinese with English abstract).
Xia ZC, Xu XY, Xia LX et al., 2005. Petrology geochemistry study for post-collision granitoid during Carboniferous–Permian in Tianshan. Northwest China Geology 38(1): 1–14 (in Chinese).
Xiao CD, Zhang ZL, Zhao LQ (2004) Nd, Sr, Pb isotope and rock origin of Yanshanian granite in eastern Inner Mongolia. China Geology 31(1): 57–63 (in Chinese with English abstract).
Xiao YL, Li SG (1993) P-T-t paths and its tectonic significance of eclogites from Shima, Dabie Mountains. Geotectonica et Metallogenia 17(3): 239–250 (in Chinese with English abstract).
Xiao YF, Ma RZ, Wei XG et al (1998) The Characteristics and genesis of the basic intrusive complex in Chengjiang Period, Micangshan, Sichuan. Journal of Chengdu University of Technology (4): 68–73 (in Chinese with English abstract).
Xing FM, Xu X (1994) Two A type granite zones in Anhui. Acta Petrologica Sinica 10(4): 357–369.
Xing FM (1995) Basic characteristics of Mesozoic magma along Yangtze River in Anhui. Acta Petrologica Sinica 11(4): 409–422.
Xing FM, Xu X (1999) Magma Rock Zone and Mineralization in Yangtze of Anhui. People's Publishing House of Anhui, Hefei (in Chinese with English abstract).
Xu B, Guo LZ, Shi YS (1992) Proterozoic Terranes and Multiphase Collision Orogenesis in Anhui-Zhejiang Area. Geological Publishing House, Beijing (in Chinese with English abstract).
Xu B Grove M, Wang CQ et al (2000) $^{40}Ar/^{39}Ar$ thermochronology from the northwestern Dabie Shan: constrains on the evolution of Qinling-Dabie orogenic belt, east-central China. Tectonophysics 322(3–4): 279–301.
Xu DR, He ZL, Li PC et al (2006) Discovery of Late Yanshanian spilitic basalt and its geological significance in Northeast Hunan. Geological Scientia Sinica 41(2): 311–332 (in Chinese with English abstract).
Xu HF, Dong YJ, Shi YH et al (1992) Granite-Greenstone Belt in West Shandong Province. Geological Publishing House, Beijing (in Chinese).
Xu WL, Lin JQ (1991) The discovery and study of mantle-derived dunite inclusions in hornblende-diorite in the Handan-Xingtai area, Hebei. Acta Geologica Sinica 65(1): 33–41 (in Chinese with English abstract).
Xu WL, Chi XG, Yuan C et al (1993) Mesozoic Diorite Rocks and Deep-derived Xenoliths in Central Part of North China Platform. Geological Publishing House, Beijing (in Chinese).
Xu WL, Wang QH, Wang DY et al (2004) Mesozoic lithosphere thinning and mechanism of eastern North China Craton: Evidences of deep inclusion of Mesozoic magmatic rocks. Earth Science Frontier, 11(3): 309–317 (in Chinese with English abstract).
Xu WL, Wang QH, Liu XC et al (2004) Chronology and sources of Mesozoic intrusive complex in Xu-Huai region, central China: Constraints from SHRIMP zircon U-Pb dating. Acta Geologica Sinica 78(1): 96–106.
Xu WL, Ge WC, Pei FP et al (2008) Chronology of Mesozoic volcanism and its tectonic significance in Northeast China. Proceedings of China Geochemistry Conference (an unpublished paper in Chinese).
Xu XS, Zhou XM (1995) The xenoliths from Qilin Cenozoic basaltic pipe, Guangdong. Acta Petrologica Sinica 11(4): 441–448 (in Chinese with English abstract).
Xu XS, Zhou XM, Reillysy O et al (1999) Lower crust material and granite origin in Southeast China. Acta Petrologica Sinica 15(2): 217–223 (in Chinese with English abstract).
Xu YG (1999) Continental basaltic magmatism in extension: characteristics and dynamics. In: Zheng YF (ed), Chemical Geodynamics. Science Press, Beijing (in Chinese).

Xue G, Luo JY, Liu JY et al (2006) Mesozoic volcanic rock characteristics and origin in middle–southern Dahingganling. Science, Technology and Economy of Inner Mongolia, 4: 100–102 (in Chinese).
Xue HM, Dong SW, Liu XC (2002) U-Pb zircon dating of granitic gneisses in eastern Dabie Mountains, Central China. Chinese Journal of Geology 37(2): 165–173 (in Chinese with English abstract).
Xue JS, Li ST (1982) A discussion on the forming time of Shandong Yishu fault belt. Journal of Shandong College of Oceanology 12(4): 51–59 (in Chinese with English abstract).
Yan DP (1991) Paleogene-Neogene tectonics in Baoshan-Tengchong area, western Yunnan. Dissertation, China University of Geosciences (in Chinese with English abstract).
Yan DP, Song HL, Fu ZR et al (1997) Metamorphic Core Complexes in the Western Margin of Yangtze Platform. Geological Publishing House, Beijing (in Chinese with English abstract).
Yan GH, Xu BL, Mu BL et al (2000) Alkaline intrusion at the east foot of the Taihang-Dahinggan Mountains: Chronology, Sr, Nd and Pb isotopic characteristics and their implications. Acta Geologica Sinica, 74(4): 774–781.
Yan J, Chen JF, Xie Z et al (2003) Mantle source inclusion of Late Cretaceous basalt in East Shandong: New evidence for time restrain of Eastern China lithosphere thinning. Chinese Science Bulletin 48(14): 1570–1574 (in Chinese).
Yan J, Chen JF, Xie Z et al (2005) Research on petrology and geochemistry of Late Cretaceous Basalt and mantle inclusion in East Shandong. Acta Petrologica Sinica 21(1): 99–110 (in Chinese with English abstract).
Yan J, Chen JF, Xie Z et al (2005) Geochemistry research of Late Mesozoic basalt in Kedoushan, lower and middle reaches of Yangtze River: Mantle feature of lithosphere and evolution restrain. Geochemistry 34(5): 455–469 (in Chinese with English abstract).
Yan YX, Zhang CL (2005) Geochemistry characteristics and formation environment of Zhangjiaba and Xinyuan bodies in South Qinling. Geological Journal of Universities 11(3): 425–433.
Yan Z, Xu QC, Zhang HJ et al (1985) Granite in Shaanxi Province. Xi'an Communication University Press, Xi'an (in Chinese with English abstract).
Yang DB, Xu WL, Pei FP et al (2005) Granite formation age and feature of magma source area for Benfu area: Zircon LA-ICPMS U-Pb age dating and tracing. Geochemistry 34(5): 443–454 (in Chinese with English abstract).
Yang JS, Xu ZQ, Li HB et al (1998) Discovery of eclogite at northern margin of Qaidam Basin, NW China. Chinese Science Bulletin 43(20): 1755–1760.
Yang JS, Xu ZQ, Song SG et al (2000) Discovery of eclogite in Dulan, Qinghai province and its significance for studying the HP-UHP metamorphic belt along the central orogenic belt of China. Acta Geologica Sinica 74(2): 156–168 (in Chinese with English abstract).
Yang JS, Meng FC, Zhang JX et al (2001) The shoshonitic volcanic rocks at Hongliuxia: Pulses of the Altyn Tagh fault in Cretaceous? Science in China D 44(suppl.): 94–102.
Yang JS, Song SG, Xu ZQ et al (2002) Discovery typical UHP mineral–eclogite in Early Paleozoic HP-UHP metamorphic zone of north border of Qaidam Basin. Acta Geologica Sinica 75(2): 175–179 (in Chinese with English abstract).
Yang KH (1998) A plate reconstruction of the eastern Tethyan orogen in southwestern China. In: Flower MFJ et al (eds) Mantle Dynamics and Plate interactions in East Asia, Geodynamics Series 27, 269–288, Washington DC: AGU.
Yang QJ, Xu YQ, Huang XL et al (2006) Chronology and geochemistry of granite in Gaoligong tectonic zone and their tectonic significance. Acta Petrologica Sinica 22(4): 817–834 (in Chinese with English abstract).
Yang RH, Dong JL, Li C et al (2002) Major mineral characteristics and temperature-pressure conditions of the minerals in Cenozoic volcanic rocks in the Northern Tibetan Plateau. Geoscience 16(2): 153–158 (in Chinese with English abstract).
Yang RY, Yuan C (1994) Rare elements geochemistry characteristics in ultra-mafic inclusion in Liaoning and Eastern Jilin. Nuclear Technology 17(3): 176–181 (in Chinese).
Yang WR, Jian P, Han YJ (2002) Determination and significance of Caledonian high-pressure and ultrahigh-pressure metamorphism in Dabie orogen. Earth Science Frontiers 9(4): 273–283 (in Chinese with English abstract).
Yang ZF et al (1998) The Evolution of Regional Crust and the Geochemistry on Gold Mineralization in Jiaodong. Geological Publishing House, Beijing (in Chinese with English abstract).
Ye BD (1989) Isotopic ages and its geological significance in Yunkai area of Guangdong and Guangxi. Guangdong Geology 3: 39–55 (in Chinese).
Ye HW, Zhang XZ, Zhou YW (1994) ^{40}Ar–^{39}Ar age and its geologic significance of vein crossite in glaucophane-schist, Mudanjiang area. Journal of Changchun University of Earth Sciences 24(4): 369–372 (in Chinese with English abstract).
Ye K, Xu P (1992) Petrogenesis of eclogite and related peridotite rocks in Datuan area of Rongcheng county, Shandong province. Acta Petrologica Sinica 8(1): 27–39 (in Chinese with English abstract).
Ye SQ (1999) Rb-Sr isochronal age of Funiushan intrusion in Nanjing-Zhenjiang, Jiangsu. Jiangsu Geology 23(3): 148–150 (in Chinese with English abstract).
Ye S, Yang M, Ye DL et al (2001) Rb-Sr isotopic dating and geological significance of kimberlitic lamprophyre pipe from Lujing, Anyuan, Jiangxi province. Geological Science & Technology Information 20(2): 27–29 (in Chinese with English abstract).
Yin ZG, Zhang YL, Yang XP et al (2006) Characteristics and magmatic evolution of Mesozoic volcanic rocks at northern Dahingganling. World Geology 25(2): 120–128 (in Chinese).

You ZD, Chen NS, Christopher IC (1995) The metamorphism of deeper crust in the Dabie Mountains: as evidenced by the study of granulites near Huilanshan, Luotian. Acta Petrologica Sinica 11(2): 137–147 (in Chinese with English abstract).
You ZD, Zhong ZQ, Han YJ et al (1997) Metamorphic evidences for the uplift of the root zone crystalline complex of Qinling–Dabie collisional orogen, Central China. Earth Science 22(3): 305–310 (in Chinese with English abstract).
Yu FS, Chong LM (2006) Rare elements characteristics of Cenozoic basalt and its mantle inclusion in Arxan, Inner Mongolia. Mineralogy and Petrology 26(1): 29–34 (in Chinese with English abstract).
Yu HF, Mei HL, Li Q (1998) The characteristics of Archean khondalite series in Dunhuang, Gansu province. Progress in Precambrian Research 21(1): 19–25 (in Chinese with English abstract).
Yu JH, Fang Z, Lai MY et al (1998) Garnet granulite facies xenoliths from Yingfengling Cenozoic basalt in Leizhou, Guangdong Province. Chinese Science Bulletin 43(23): 2013–2018.
Yu XQ, Su LS, Yan TZ et al (2004) Rock geochemistry and its tectonic significance of Early Cretaceous basalt in Jiangshan-Guangfeng areas. Geochemistry 33(5): 465–474 (in Chinese with English abstract).
Yu XQ, Su LS, Deng GH et al (2005) Geochemistry characteristics and its tectonic significance of alkali basalt in Jitai basin, Jiangxi. Geoscience 19: 133–140 (in Chinese with English abstract).
Yu XH, Mo XX, Liao ZL et al (2001) Temperature and pressure condition of garnet lherzolite and websterite from west Qinling, China. Science in China D 44(suppl.): 155–161 (in Chinese).
Yu YW, Zhou TX, Chen JF (1993) The characteristics and origin of the Xuantandi Bimodal volcanic rocks of the late stage of Early Cretaceous, Zhejiang. Journal of Nanjing University 5(4): 420–429 (in Chinese with English abstract).
Yuan C, Sun M, Li JL. 1999. Ages of two granite bodies and perhaps source areas in Middle Western Kunlun. Chinese Science Bulletin 44(5): 534–538.
Yuan F, Zhou TF, Yue SC (2002) Tectonic environment of magmatic formation and its significance in Nort area of Xinjiang. Tectonics and Mineralization 26(2): 148–155 (in Chinese).
Yuan HL, Wu FY, Gao S et al (2003) SHRIMP zircon U-Pb dating of Cenozoic intrusions and rare earth elements analysis in Northeastern China. Chinese Science Bulletin 48(14): 1511–1520 (in Chinese).
Yue KF, He Y, Liu WF (2005) Research on sulphite of mantle inclusion in Neogene alkali basalt in Niutoushan, Fujian. Geologica Scientica 40(1): 114–119 (in Chinese with English abstract).
Yun P, Lei YH, Lü CY (2005) Sr and Nb isotopic restrict and its significance in Triassic granite source area of central and northern Hainan Island. Tectonics and Mineralization 29(2): 234–241 (in Chinese with English abstract).
Zeng GC, Wang FZ, Zheng HR et al (1997) Cenozoic volcanic rocks and its relations to basin evolution and oil accumulation in Dongying sag. Earth Science 22(2): 157–164 (in Chinese with English abstract).
Zeng JH (2000) Prediction of pore-fluid pressure in deep strata of Songliao basin. Earth Science 25(2): 132–136 (in Chinese with English abstract).
Zeng JN, Zuo DH, Ma X (1997) Yanshanian magmatic evolution and its influence to metal minerali-zation in Ta'ershan, Shanxi. Journal of Geology and Mineral Resources of North China 12(1): 33–43 (in Chinese with English abstract).
Zhai JP (1989) Sr isotopic characteristics and origin research of Kunshan, Chengshan and Dalongshan intrusions. Geochemistry 3: 202–209 (in Chinese with English abstract).
Zhai MG, Guo JH, Li JH et al (1995) Discovery the retrogressive metamorphic eclogite in Archean of North China and its significance. Chinese Science Bulletin 40(17): 1590–1594 (in Chinese).
Zhai MG (1998) Three important high-pressure and high-temperature metamorphic zones in China and their geotectonic significance. Acta Petrologica Sinica 14(4): 419–429 (in Chinese with English abstract).
Zhai MG, Cong BL, Guo JH et al (1999) Sm-Nd geochronology and petrography of garnet pyroxene granulite in the northern Sulu region and their geotectonic implication. Scientia Geologica Sinica 34(3): 301–310 (in Chinese with English abstract).
Zhai MG (2004) Precambrian tectonic evolution of the North China Craton. In: Malpas J et al (eds) Aspects of the Tectonic Evolution of China. London: The Geological Society. Special Publication 226.
Zhai QG, Li C, Cheng LR et al (2004) Geological features of Permian ophiolite in the Jiaomuri area, Qiangtang, Tibet, and its tectonic significance. Geological Bulletin of China 23(12): 1228–1230 (in Chinese with English abstract).
Zhai XM, Day HW, Hacker BR et al (1998) Paleozoic metamorphism in the Qinling Orogen, Tongbai Mountains, Central China. Geology 26(4): 371–374.
Zhai YS, Yao SZ et al (1992) Metallogeny of Ion, Copper and Gold in Lower and Middle Reaches of Yangtze River. Geological Publishing House, Beijing (in Chinese).
Zhang BT, Zhang FS, Ni QS et al (1988) Discussion on geology and geochemistry characteristics and origin in quartz syenite zone of Anqing–Lujiang area. Acta Petrologica Sinica 4(3): 1–12 (in Chinese with English abstract).
Zhang BT, Chen PR, Kong XG (2002) Rb-Sr chronology of bimodal volcanic rocks of Yutian Group in the Linjiang basin, Southern Jiangxi. Geology in China 29(4): 351–354 (in Chinese).
Zhang BY, Yu HN (1994) Deep-seated Nappe Structure of Hercynian-Indochina Collisional Zone in West Guangdong. Geological Publishing House, Beijing (in Chinese).
Zhang C, Li MS, He GQ et al (1996) Age of Sm-Nd isotopic isochron of amphibolite facies metamorphic zone and its significance in Wulawusu-Deyanqimiao area of Inner Mongolia. Scientia Geologica Sinica 31(1): 65–70 (in Chinese with English abstract).

Zhang C, Wu TR (1998) Sm-Nd, Rb-Sr isotopic isochron of metamorphic volcanic rocks of Ondor sum Group, Inner Mongolia. Scientia Geologica Sinica 33(1): 25–30 (in Chinese with English abstract).
Zhang DQ, Zhou JA, Sun GY (1982) Research on distribution and composition of Cenozoic basalts and their lherzolite inclusion in Eastern China. Journal of Geological Institute of China Geological Science Academy (4): 15–31 (in Chinese with English abstract).
Zhang DQ, Sun GY (1988) Granites of Eastern China. China University of Geosciences Press, Wuhan (in Chinese with English abstract).
Zhang DQ, She HQ, Yan KH et al (2001) Magmatic geochemistry evidences for Mesozoic tectonic environments change at Zijinshan area of Fujian. Geological Review 47(6): 608–616 (in Chinese with English abstract).
Zhang DQ, Xu HL (2002) Compare research on geology-geochemistry of granitoid in lower and middle reaches of Yangtze River. South China Geology and Resources 3: 66–77 (in Chinese with English abstract).
Zhang H, Yuan HL, Hu ZC et al (2006) Rare earth element characteristics and its significance of single zircon in Mesozoic volcanic rocks, in Luanping of Hebei. Journal of Rare Earth Element in China 24(2): 227–234 (in Chinese).
Zhang HF, Sun M (2002) Geochemistry of Mesozoic basalts and mafic dikes, southeastern north china craton and tectonic implications. International Geological Review 44: 370–382.
Zhang HF, Sun M, Zhou XH et al (2003) Secular evolution of the lithosphere beneath the eastern North China Craton: Evidence from Mesozoic basalts and high-Mg andesites. Geochimica et Cismochimica Acta 67(22): 4373–4387 (in Chinese with English abstract).
Zhang HF, Zheng JP (2003) Geochemistry characteristics and rock origin for Mesozoic basalt in North China–case of Fuxin, Liaoning. Chinese Science Bulletin 48(6): 603–609 (in Chinese).
Zhang HF, Nakamura E, Zhang J et al (2006) Glass melted inclusion in monoclinic crystal of Cenozoic basalt at Linju, Shandong. Chinese Science Bulletin 51(13): 1558–1564 (in Chinese).
Zhang HH, Xu YG, Ge WC et al (2006) Basalt geochemistry characteristic and its significance during Late Mesozoic–Cenozoic in Yitong–Datun areas, Jilin. Acta Petrologica Sinica 22(6): 1579–1596 (in Chinese with English abstract).
Zhang JX, Xu ZQ, Chen W et al (1997) A tentative discussion on the ages of the subduction-accretionary complex/volcanic arcs in the middle sector of north Qilian Mountains. Acta Petrological et Mineralogical 16(2): 112–119 (in Chinese with English abstract).
Zhang JX, Zhang ZM, Xu ZQ et al (1999) The age of U-Pb and Sm-Nd for eclogite from the western segment of Altun Tagh tectonic belt-Evidence for existence of Caledonian orogenic root. Chinese Science Bulletin 44(24): 2256–2259.
Zhang JX, Zhang ZM, Xu ZQ et al (2000) Discovery of khondalite series from the western segment of Altun Tagh and their petrological and geochronological studies. Science in China D 43(3): 308–316.
Zhang JX, Meng FC, Qi XX (2002) Comparison of garnet zoning between edlogites in Da Qaidam and Xitieshan on the northern margin of the Qaidam basin. Geological Bulletin of China 21(3): 123–129 (in Chinese with English abstract).
Zhang JS, Xu J, Wan JL et al (2002) Meso-Cenozoic detachment zones in the front of the Taihang Mountains and their fission-track ages. Geological Bulletin of China 21(4–5): 207–210 (in Chinese with English abstract).
Zhang LF, Sun M, Xian WS (1998) The discovering of charnockites and their granulite xenoliths in west Junggar, Xinjiang. Earth Science Frontiers, 5(3): 132 (in Chinese with English abstract).
Zhang LF, Gao J, Ekebair S et al (2001) Low temperature eclogite facies metamorphism in Western Tianshan, Xinjiang. Science in China D 44(1): 85–96 (in Chinese).
Zhang Q (1992) The Mafic-Ultramafic Rocks in Hengduan Mountains. In: Comprehensive Geological Bregade of Qinghai-Tibet Plateau, China Acadamy of Science, Zhang KW, Li DZ (eds) The Series of the Scientific Expedition to the Hengduan Mountains of the Qinghai-Xizang Plateau. Science Press, Beijing (in Chinese).
Zhang Q, Chen Y, Zhou DJ et al (1998) Geochemical characteristics and genesis of Dachadaban ophiolite in North Qilian area. Science in China D 41(3): 277–281 (in Chinese).
Zhang RY, Liu ZG, Wang XM (1993) Discovery of coesite eclogite in Henan province, Central China and its tectonic signification. Acta Petrologica Sinica, 9(2): 186–191 (in Chinese with English abstract).
Zhang RY, Liou JG, Cong BL (1995) Talc-magnesite and Ti-clinohumite-bearing ultrahigh-pressure meta-mafic and ultramafic complex in the Dabie Mountians China. Journal of Petrology 36(4): 1011–1037.
Zhang SG, Wan YS, Liu GH et al (1991) Metamorphic Geology of the Kuanping Group in the Northern Qinling Mountains. Beijing Scientific and Technical Press, Beijing (in Chinese with English abstract).
Zhang SG, Wei CY, Yang CH (1998) Metamorphism of east part of South Qinling orogenic belt. Earth Science Frontiers 5(4): 210 (in Chinese).
Zhang SM, Wu JH, Zhou WX et al (2004) Nd-Sr isotopic study for mafic rocks of Yanshanian at eastern Nanling. Journal of Institute of Technology of East China 27(2): 129–135 (in Chinese with English abstract).
Zhang SY, Hu K, Liu XC (1989) The glaucophane–mica schist-eclogite zone of Proterozoic at central China. Journal of Changchun College of Geology, Monography of glaucophane zone at Hubei and Anhui, 158–162 (in Chinese).
Zhang SY, Hu K, Liu XC (1990) The rock sequences and origins of highpressure metamorphic zone at central China. Collections of Qinling–Dabie Geology (1): 221–229. Beijing Science and Technology Press, Beijing (in Chinese).
Zhang WH, Han BF, Du H et al (2005) Characteristics of mantle source area of Cenozoic basalt at Jining, Inner Mongolia: elements and Sr-Nd-Pb isotopic geochemistry evidences. Acta Petrologica Sinica 21(6): 1569–1582 (in Chinese with English abstract).

Zhang WH, Han BF (2006) K-Ar chronology and geochemistry of Cenozoic basalt and deep dynamic significance at Jining, Inner Mongolia. Acta Petrologica Sinica 22(6): 1597–1607 (in Chinese with English abstract).
Zhang WL, Hua RM, Wang RC et al (2006) Research on formation of granite and forming age of Tungsten ore deposit at Dajishan, South Jiangxi. Acta Geologica Sinica 80(7): 956–962 (in Chinese).
Zhang XD, Wang SG, Li JW et al (1999) PTt path of metamorphism of Lanshantou eclogite in southeastern Shandong and its geological significance. Acta Petrologica Sinica 15(1): 37–47 (in Chinese with English abstract).
Zhang X (2001) Geological characteristics of Early Cretaceous rhyolite in Shanmen, Siping, Jilin. Jilin Geology 20(3): 30–34 (in Chinese with English abstract).
Zhang XC (1995) The Volcanism of Kang-Dian rift zone and characteristics of its alkalic (sodic) volcanic rocks series. Yunnan Geology (2): 81–98 (in Chinese with English abstract).
Zhang YJ, Zhang HB, Liu B (2003) Basic volcanic characteristics and their origin in Huluhe, Qin'an. Journal of Gansu Geology 12(2): 18–24 (in Chinese with English abstract).
Zhang YJ, Deng YP, Zhang HB (2005) Granite bodies characteristics and their origin in eastern Qilian oroginic belt. Journal of Gansu Geology 14(2): 23–29 (in Chinese with English abstract).
Zhang Y, Chen B, Shao JA (2003) Geochemistry characteristics and discussion on origin for Late Mesozoic lamprophyre in Taihangshan, North China. Journal of Mineralogy and Petrology 22(1): 29–33 (in Chinese with English abstract).
Zhang YQ, Xie YW (1997) Geochronology of Ailaoshan-Jinshajiang alkali-rich intrusive rocks and their Sr and Nd isotopic characteristics. Science in China D 40(5): 524–529.
Zhang ZC, Li ZN, Wang FB (1994) Basic characteristic of volcanic rock and its origin in Yixian Basin, western Liaoning. Geosciences 8(4): 441–451 (in Chinese with English abstract).
Zhang ZC, Xiao XC, Wang J et al (2002) Discovery of enclaves from Cenozoic Pulu volcanic rocks in West Kunlun Mountains and their geological implications. Earth Science 27(4): 386–390 (in Chinese with English abstract).
Zhang ZC, Mahoney JJ, Wang FS et al (2006) Geochemistry of picrite and its paragenetic basalt at western Emeishan large igneous province: melt evidence of mantle head. Acta Petrologica Sinica 22(6): 1538–1552 (in Chinese with English abstract).
Zhang ZS (2001) Basic characteristics and formation environment of Late Mesozoic alkali volcanic rock in Baiyunzhang. Guangdong Geology 16(4): 22–28 (in Chinese with English abstract).
Zhao DS, Xiao ZY, Wang YW (1982) Research on Cenozoic basaltic rocks with deep source inclusion in Jiangsu, Shandong and Anhui areas. Research on Petrology. 1: 54–64. Geological Publishing House, Beijing (in Chinese).
Zhao G, Zhu YF, Zhang Y (2002) Petrology and metamorphic P-T condition of Xilin Gol complex, Inner Mongolia, China. Acta Petrological et Mineralogical 21(1): 40–48 (in Chinese with English abstract).
Zhao GC, Wilde SA, Cawwod PA et al (1998) Thermal evolution of Archaean basement rocks from the eastern part of the North China Craton and its bearing on tectonic setting. International Geological Review 40: 706–721.
Zhao GC (2001) Paleoproterozoic assembly of the North China craton. Geological Magazine 138: 87–91.
Zhao GC, Sun M, Widle SA et al (2004) Late Archaean to Paleoproterozoic evolution of the Trans-North China Orogen: In slights from synthesis of existing data of the Hengshan-Wutai-Fuping belt. In: Malpas J et al (eds) Aspects of the Tectonic Evolution of China. London: The Geological Society. Special Publication 226.
Zhao HL (1990) Continental rift volcanism and deep processes of Neogene-Quaternary in Southeastern China coastal area. China University of Geosciences Press, Wuhan (in Chinese with English abstract).
Zhao HL, Deng JF, Chen FJ et al (1996) Petrology and tectonic setting of Mesozoic volcanic rocks along southeastern margin of Songliao basin. Earth Science 21(4): 421–427 (in Chinese with English abstract).
Zhao JX, Li XH, Mcculloch MT et al (1995) Petrogenesis of ophiolites from south Anhui and northeast Jiangxi, and their tectonic implications: chemical and Sm-Nd isotopic constraints. Geochemica, 24(4): 311–326 (in Chinese with English abstract).
Zhao J, Zhong DL, Wang Y (1994) Metamorphism of Lanchang metamorphic belt, the western Yunnan and its relation to deformation. Acta Petrologica Sinica 10(1): 27–40 (in Chinese with English abstract).
Zhao QG, Xu WL, Jin K et al (2005) Magmatic source area of Mesozoic volcanic rocks in Yanbian area: evidences form Sr—Nd isotope and deep source inclusion. Journal of Jilin University (Earth Science) 35(4): 416–422 (in Chinese).
Zhao ZY (1993) Dislocation structures in olivine from spinel lherzolite of Sartokay ophiolite and their significance in upper mantle rheology. Scientia Geologica Sinica 28(3): 279–282 (in Chinese with English abstract).
Zhen YQ (2004) Isotopic geochemistry and its mineralization model of gold, silver, multi-metal ore deposits in Wutaishan–Hengshan. Journal of Technology Institute of Guilin 24(2): 127–136 (in Chinese with English abstract).
Zheng CQ, Xu WL, Wang DY (1999) The petrology and mineral chemistry of deep-seated xenoliths in Mesozoic basalt in Fuxin district from western Liaoning. Acta Petrologica Sinica 15(4): 616–622 (in Chinese with English abstract).
Zheng JP (1999) Mantle Replacement of Eastern China and Lithosphere Thinning in Meso-Cenozoic. China University of Geoscience Press, Wuhan.
Zheng Z, Kono M, Shao JA (1990) The amalgamative history of Eastern Asia inferred from paleomag-netism of the North China. Rock Magneitism and Paleogeophysics 17: 86–93.
Zhi XC, Li BX, Yang J et al (1996) Calculation of temperature and pressure for peridotite xenoliths from eastern Yangtze Block, eastern China. Acta Petrologica Sinica 12(3): 446–454 (in Chinese with English abstract).

Zhi XC, Peng ZC, Chen DD et al (2001) Osmium isotopic model age of long time-peridotite inclusion in continental lithosphere mantle at Jiangsu and Anhui areas. Science in China D 31(6): 464–470.
Zhong H, Hu RZ, Ye ZJ et al (2000) Isotope geochronology of Dapingzhang spilite-keratophyre formation in Yunnan Province and its geological significance. Science in China D 43(2): 200–207 (in Chinese).
Zhong HM, Tong JS, Lu RK et al (2006) Geochemistry characteristics and tectonic background of Aluminum granite in Songxi area, Rutog, Tibet. Bulletin of Geology 25(1–2): 183–188 (in Chinese with English abstract).
Zhong ZQ, You ZD, Zhou HW et al (1996) The evolution and basic structural framework of the basement of the Yunkai uplift in Gunagdong and Guangxi. Regional Geology of China (1): 36–43 (in Chinese with English abstract).
Zhong ZQ, Suo ST, Zhang HF et al (2001) Major constitutents and texture of the Tongbai-Dabie collisional orogenic belt. Earth Science 26(6): 560–567 (in Chinese with English abstract).
Zhou DJ, Zhou YS, Xu P (1992) Carboniferous and Late Permian volcanic rocks of western Mojiang, Yunnan. Scientia Geologica Sinica (3): 249–259 (in Chinese with English abstract).
Zhou HW, You ZD, Zhong ZQ et al (1997) Origin of thermal center type of migmatites in the Yunkai uplift. Earth Science 22(3): 332–338 (in Chinese with English abstract).
Zhou JC, Zhang HJ, Yu YW (1994) Magma migmatization in complex flow of Early Cretaceous in Xinchang, Zhejiang. Acta Petrologica Sinica 10(3): 236–247 (in Chinese with English abstract).
Zhou JC, Jiang SY, Wang XL et al (2005) Petrological-geochemistry for Middle Jurassic in South China–example to basalt of Fanken in Fujian. Science in China D 35(10): 927–936 (in Chinese).
Zhou MF, Yan DP, Kennedy AK et al (2002) SHRIMP U-Pb zircon geochronological and geochemical evidence for Neoproterozoic arc-magmatism along the western margin of the Yangtze Block, South China. Earth Planet. Scie. Lett. 196: 51–67.
Zhou TX, Chen JF, Li XM et al (1988) Query the Indosinian magmatism in Anhui. Acta Petrologica Sinica (3): 46–53 (in Chinese with English abstract).
Zhou TF, Yuan F, Hou MJ et al (2004) Origin of Yanshanian granite and geodynamic background in the boundary between Anhui and Jiangxi of Jiangnan Uplift area. Mineralogy and Petrology 24(3): 65–71 (in Chinese).
Zhou XM (1981) Research on two series of basalts and their inclusions in Niutoushan, Fujian. Journal of Nanjing University (Natural Science) 3: 382–391 (in Chinese with English abstract).
Zhou XM, Zhou HB, Yang JD et al (1989) Sm-Nd isochron age of ophiolite suite and its geological significance in Fuchuan, Xixian, Anhui province. Chinese Science Bulletin 34(16): 1243–1245 (in Chinese).
Zhou XZ (1996) The Discovery of phlogopite exsolution lamellae in garnets of eclogite enclaves, Liaoning province. Acta Geologica Sinica 70(3): 223–231 (in Chinese with English abstract).
Zhou XR, Yang J, Ren J (1997) Comparative study on the characteristics and genesis between I-and A-type granite of Suzhou area. Earth Science 22(3): 240–246 (in Chinese with English abstract).
Zhou XR, Ren J (1997) Mesozoic Granite in Lower and Middle Reaches of Yangtze River. Geological Publishing House, Beijing (in Chinese with English abstract).
Zhou XR, Wu KL (1994) I-A Type Granite in Zhangzhou. Science Press, Beijing (in Chinese with English abstract).
Zhou ZY, Pan CC, Fan SF et al (1989) Geothermal characteristics of the Junggar basin and its significance to oil searching. Xinjiang Petroleum Geology 10(3): 67–74 (in Chinese with English abstract).
Zou HY, Wu ZY (1998) Application of vitrinite reflectance in reconstruction of paleotemperature: evolution of paleotemperature in the eastern and western Mesozoic-Cenozoic sedimentary basin, China. Acta Sedimentologica Sinica 16(1): 112–119 (in Chinese with English abstract).

Index

D

E

F

G

H

I

J

K

L

M

N

O

P

Q

R

S

T